DOE/NASA/0153-2
NASA CR-174735
84AEPD004

Mod-5A Wind Turbine Generator Program Design Report

Volume II—Conceptual and Preliminary Design
Book 2

General Electric Company
(Advanced Energy Programs Department)

August 1984

Prepared for
NATIONAL AERONAUTICS AND SPACE ADMINISTRATION
Lewis Research Center
Under Contract DEN 3-153

for
U.S. DEPARTMENT OF ENERGY
Conservation and Renewable Energy
Division of Wind Energy Technology

DOE/NASA/0153-2
NASA CR-174735
84AEPD004

Mod-5A Wind Turbine Generator Program Design Report

Volume II—Conceptual and Preliminary Design
Book 2

General Electric Company
(Advanced Energy Programs Department)

August 1984

Prepared for
National Aeronautics and Space Administration
Lewis Research Center
Cleveland, Ohio 44135
Under Contract DEN 3-153

for
U.S. DEPARTMENT OF ENERGY
Conservation and Renewable Energy
Division of Wind Energy Technology
Washington, D.C. 20545
Under Interagency Agreement DE-AI01-79ET20305

DISCLAIMER

Printed in the United States of America
Available from:
National Technical Information Service
U.S. Department of Commerce
5285 Port Royal Road
Springfield, VA 22161

Volume I, Executive Summary

Volume I contains an overview of the MOD-5A Program. These topics are covered:

- Objectives of the MOD-5A Program
- Description of the Final Design (Model 304.2)
- Cost of Energy
- Power Output
- Trade-Off Studies
- Development Tests
- Analyses of Loads and Dynamics
- Manufacturing and Quality Assurance and Safety Plans

Volume II, Conceptual and Preliminary Design

These sections comprise Volume II, which is divided into two books, as follows:

Book 1

- 1.0 Summary
- 2.0 Introduction
- 3.0 Design Requirements
- 4.0 Conceptual Design Studies
- 5.0 Design, Development, and Optimization
- 6.0 System Dynamics Analysis
- 7.0 System Loads Analysis

Book 2

- 8.0 Development Tests
- 9.0 Design Criteria
- Appendix A System Specification
- Appendix B Design Load Tables

Volume III, Final Design and System Description

These sections comprise Volume III, which is divided into two books, as follows:

Book 1

- 1.0 Summary
- 2.0 Introduction
- 3.0 System Description - Model 304.2
- 4.0 Rotor Subsystem
- 5.0 Drivetrain Subsystem
- 6.0 Nacelle Subsystem
- 7.0 Tower and Foundation Subsystems

Book 2	8.0	Power Generation Subsystem
	9.0	Control and Instrumentation Subsystems
	10.0	Manufacturing
	11.0	Site and Erection
	12.0	Quality Assurance and Safety
	13.0	FMEA, RAM and Maintenance
	Appendix A	C.F. Braun & Company - Foundation Design Criteria
	Appendix B	GE - Product Assurance Program Plan for the MOD-5A WTG Program
	Appendix C	GE - System Safety Plan for the MOD-5A Program
	Appendix D	GE - MOD-5A Configuration Management Plan
	Appendix E	GE - MOD-5A Defect Reports for Development Hardware
	Appendix F	GE - MOD-5A Program Quality Assurance Requirements for the Control of Raw Materials and the Blade Fabrication Process
	Appendix G	GE - Statement of Work for the Erection of the MOD-5A WTG Yaw, Nacelle and Blade Subsystems

Volume IV, Drawings and Specifications

This volume contains the numbered drawings and specifications for the final design of the MOD-5A wind turbine. The volume is divided into five books, as follows:

Book 1	47A380002 through 47A380030
Book 2	47A380031 through 47A380068
Book 3	47A380074 through 47A380126
Book 4	47A380128 through 47A387125
Book 5	47D381002 through 47D387130

MOD-5A WIND TURBINE GENERATOR
DESIGN REPORT
VOLUME II, BOOK 2

Section | Page

Section | Page

Section | Page

Section Page

Section Page

Section Page

Section | Page

Section Page

Section Page

LIST OF FIGURES

LIST OF FIGURES (Cont'd)

LIST OF FIGURES (Cont'd)

LIST OF FIGURES (Cont'd)

LIST OF FIGURES (Cont'd)

LIST OF FIGURES (Cont'd)

LIST OF FIGURES (Cont'd)

LIST OF FIGURES (Cont'd)

LIST OF FIGURES (Cont'd)

LIST OF FIGURES (Cont'd)

LIST OF FIGURES (Cont'd)

LIST OF FIGURES (Cont'd)

LIST OF FIGURES (Cont'd)

LIST OF FIGURES (Cont'd)

LIST OF FIGURES (Cont'd)

LIST OF TABLES

LIST OF TABLES (Cont'd)

LIST OF TABLES (Cont'd)

LIST OF TABLES (Cont'd)

LIST OF TABLES (Cont'd)

LIST OF TABLES (Cont'd)

8.0 DEVELOPMENT TESTS

8.0 DEVELOPMENT TESTS

Development tests were made during the design phases to qualify components and determine material properties.

This section describes the configurations and results of tests on material for the blade, made of wood and epoxy, attachments to the blade material, hydraulic components, airfoil and control surface arrangements, and electrical items.

Blade material tests are described in section 8.1. These tests provided data to substantiate the static and fatigue allowable stress values. Tests were also made to examine epoxy fillers, joints, moisture effects, the influence of size, and damping properties. The last subsection in 8.1 is a summary of allowable stresses.

Blade component development tests, section 8.2, evaluated structural attachments, fabrication joints and inserts.

Hydraulic component tests are described in section 8.3. Actuators and valves were tested for qualification in a high acceleration.

Section 8.4 describes wind tunnel and MOD-0/5A wind turbine tests. Tests were made with several airfoil thickness, trailing edge details, and aileron configurations.

Electrical tests in Section 8.5 were conducted on the controller and on a cable twist.

Gougeon Brothers, Inc. (GBI) participated in many of the tests as a subcontractor to GE-AEPD.

8.1 WOOD LAMINAE/EPOXY MATERIAL CHARACTERIZATION

8.1.1 PHASE A STATIC TESTS

The Phase A series of tests included a comprehensive static evaluation of the Douglas fir veneer and West System® epoxy composite. Sliced Douglas fir veneer had been used on small wind turbine blades, up to 60 ft. long.

However, rotary peeling was the method proposed for producing veneer for the MOD-5A blades.

In rotary peeling a layer is pared from the circumference of a prepared log, as shown in Figure 8-1. The tool feed rate is controlled much as a lathe cut is made. Rotary peeling is faster than slicing and results in a higher yield, and a lower cost. The plywood industry now uses this state-of-the-art process. Preliminary studies indicated that rotary-peeled Douglas fir veneer could be graded by non-destructive ultrasonic tests. Rotary-peeled veneer combined the advantages of availability, lower cost and a veneer with predictable strength properties. However, the strength properties of this material had to be demonstrated.

In developing the characteristics of laminated composite material it was assumed that the structural properties, composition and variability were not the same as solid wood. Therefore, comparisons to the strength of solid wood are difficult to make and will be avoided.

The following tests were included in this evaluation:

- Yield of various grades of veneer
- Optimum glue spread, evaluated by block shear testing
- Moisture content, based on six specimen sizes
- Tensile strength parallel to grain and normal to grain in the radial direction
- Parallel and radial compression strength
- Parallel and radial bending strength
- Radial and tangential tensile strength normal to the grain
- Effect of temperature on parallel to the grain compressive strength
- Yield of various grades of sliced birch veneer
- Birch/glass fiber-reinforced plastic (FRP) bond line strength parallel and normal to laminations
- Birch/FRP tension strength parallel and normal to grain in the radial and tangential directions
- Birch/FRP compression strength parallel and normal to grain in the radial and tangential direction

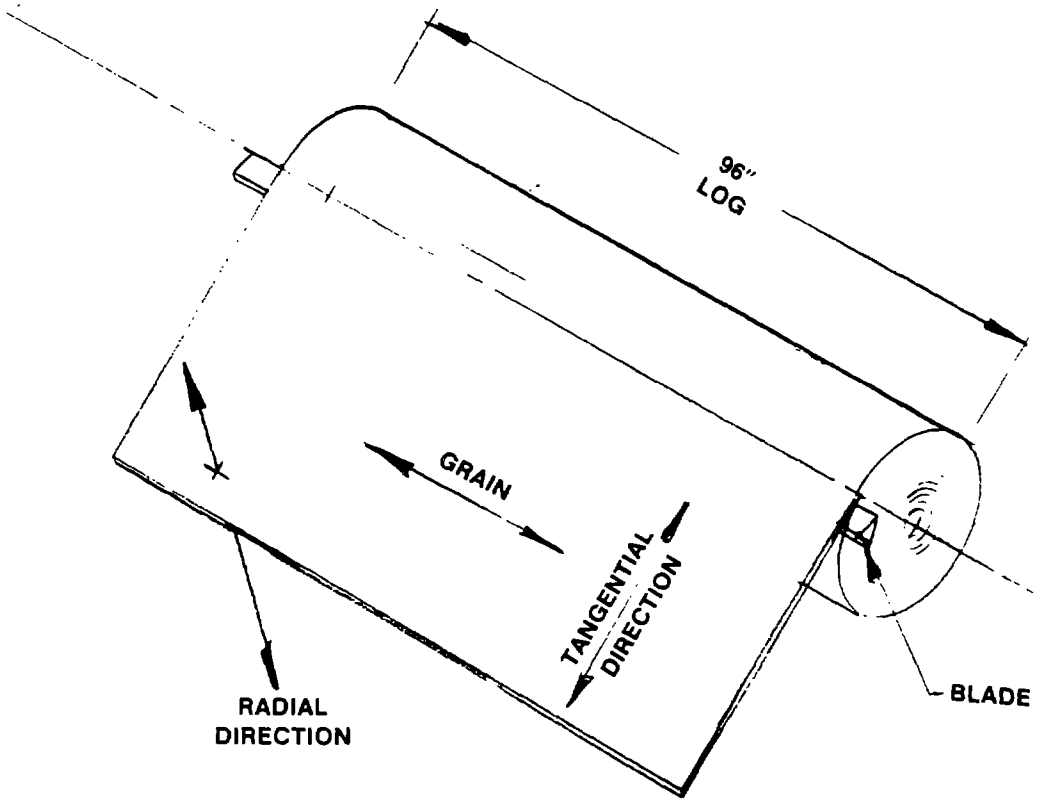

Figure 8-1 Rotary Peeling Veneer From Prepared Log.

The results of these tests provided useful data, and in some cases indicated a need for further investigation. The veneer yield studies led to the selection of Douglas fir veneer for use in the MOD-5A blade, since the cost of birch is much higher. The optimum glue spread tests demonstrated that a double glue line of 60 lbs per thousand square feet, provided the best test results, based on block shear results. This application rate was selected for use throughout the MOD-5A program. The moisture content study demonstrated that unprotected specimens responded to variations in the atmospheric moisture level, and indicated the need to seal edges of specimens. The tension, compression and bending strength tests provided data that was useful in determining allowable stress levels, and also provided useful information on test techniques and specimen design that were used later in the program. Birch veneer yield studies were used to compare with the Douglas fir studies for a relative cost comparison. Tests of birch combined with FRP yielded reasonable results, but the cost comparison ruled out the use of birch in the MOD-5A blade.

A study of the yield of the birch veneer indicated that there is 30% more blade grade 1 and 2 birch than grade 1 and 2 Douglas fir veneer. Most of the increase occurred in blade grade 2. However, birch veneer costs more, and it is supplied in random widths and lengths. Additional handling is required for grading and conversion to uniformly sized, rectangular pieces for the manufacture of the blade.

The FRP and birch combinations had anisotropic strength properties. The epoxy FRP and birch was stronger than the polyester FRP and birch in compression parallel and perpendicular to the grain, and in shear by compressive loading parallel to the laminations. Polyester FRP was stronger than epoxy FRP in tangential tension perpendicular to the grain, and in shear perpendicular to the laminations. There was no difference in tension parallel or radial perpendicular tensile strength. Increasing the temperature to 104°F had no effect in tension or compression, but it significantly lowered shear strength by compressive loading parallel to the laminations for both FRP's. All strength properties, except radial tension perpendicular to the grain, of the birch and FRP, were greater than those of the Douglas fir and epoxy. Across the grain, the strength properties of birch showed outstanding improvement.

8.1.1.1 Veneer Grade Study

A non-destructive grading technique supplemented visual grading of Douglas fir veneer, to guarantee that the quality of the selected material met the stringent requirements for structural material used in the MOD-5A blade. The method measured the propagation time of ultrasonic waves along the length of the sheets to determine the average modulus of elasticity of each piece. Ten to 80 readings for each sheet were assessed, to determine the average stiffness.

8.1.1.1.1 Objectives

The objective of this evaluation was to determine the grades of material from various suppliers. Commercially available grades A/B and C/D, which are determined from visual inspections, were included. The price of grade C/D was approximately half the cost of grade A/B. Since there is excellent correlation between stiffness and strength, this study would optimize the cost of the veneer.

8.1.1.1.2 Description

Approximately 6,000 sheets of grade A/B Douglas fir veneer and 1,500 sheets of grade C/D were obtained from three suppliers. The sheets were 0.1 in. thick, and rotary peeled. The sheets were dried, and ultrasonically graded at the Trus Joist Corp. Micro-lam plant in Eugene, Oregon. The objective was to determine yields, using the ultrasonic grader, and to compare the relative yields of A/B and C/D veneer.

A/B veneer from each supplier was dried separately, graded, and divided into various classes according to the modulus of elasticity (E), which was determined using the ultrasonic grader, to characterize the sample population. A/B veneer fell into two groups: A+, for which E = 2.45 x 10^6 psi or greater, and A, for which E = 2.10 to 2.44 x 10^6 psi. These groups were used to fabricate material for the test program. Veneer not included in these groups was used by Trus Joist in their manufacturing process. The three suppliers for grade A/B veneer were Pope and Talbot, Sun, and Trend.

Grade C/D veneer from the same suppliers were dried and graded, but inadvertently sheets from Pope and Talbot were used in production and sheets

from Mazama were substituted. There were not enough C/D sheets from each supplier to justify separate drying charges so they were dried and graded as a group, consisting of veneer from Mazama, Sun, and Trend. Veneer from the C/D mix were selected for fabricating test samples from only one range, which had $E = 2.10 \times 10^6$ psi or greater.

Moisture detectors evaluated and marked sheets with greater than a maximum average moisture content of 6% and sheets with wet spots. These sheets were removed from the line before they were graded. The discrepancy between the number of sheets used and the number of sheets that were dried and graded represented the number of sheets sent back for redrying.

8.1.1.1.3 Results

The results of frequency distribution by longitudinal stiffness for grades A/B and C/D veneer are shown in Figures 8-2 and 8-3, and data is listed in Table 8-1. A cumulative frequency distribution for the two grades is presented in Figure 8-4. In general, the grade A/B veneer was of better quality than grade C/D veneer. Grade A/B veneer had at higher mean stiffness: 2.09×10^6 psi vs. 1.99×10^6 psi. Since A/B veneer costs about twice as much as C/D, yields of higher quality veneer should match the difference in

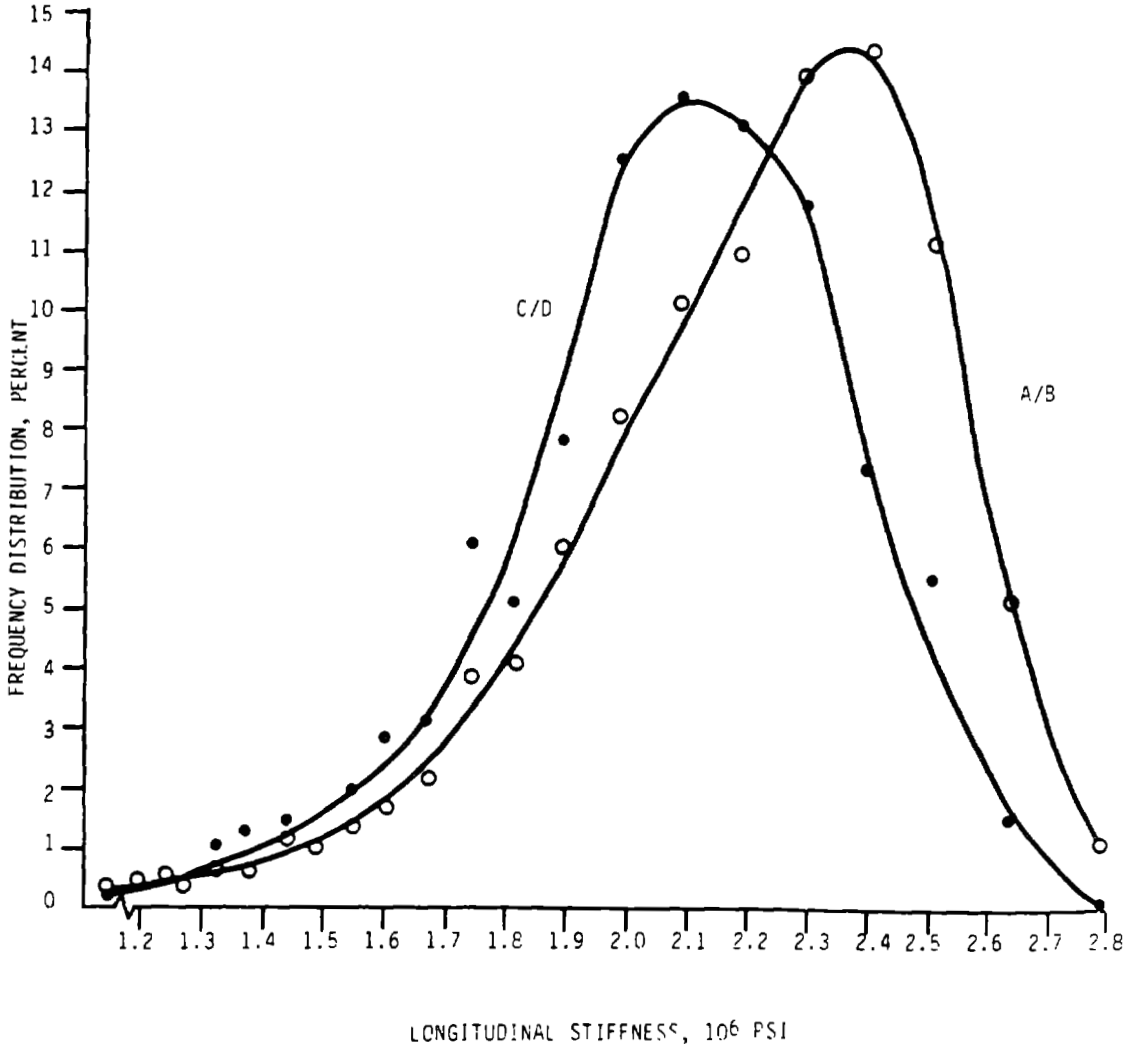

Figure 8-2 Frequency Distribution of Longitudinal Stiffness for Grades A/B and C/D Veneer

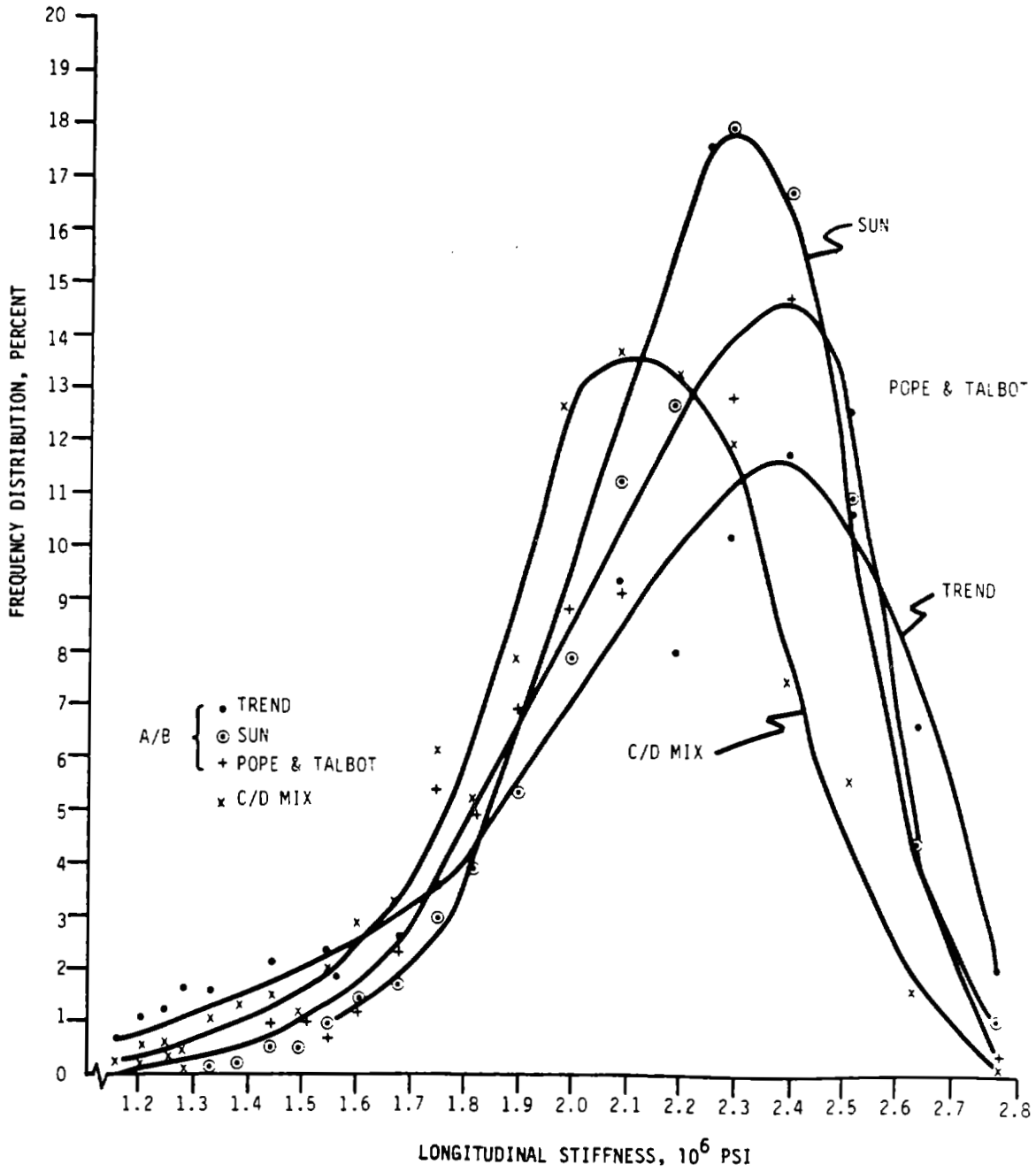

Figure 8-3 Frequency Distribution of Longitudinal Stiffness for Grades A/B and C/D Veneer from Three Suppliers

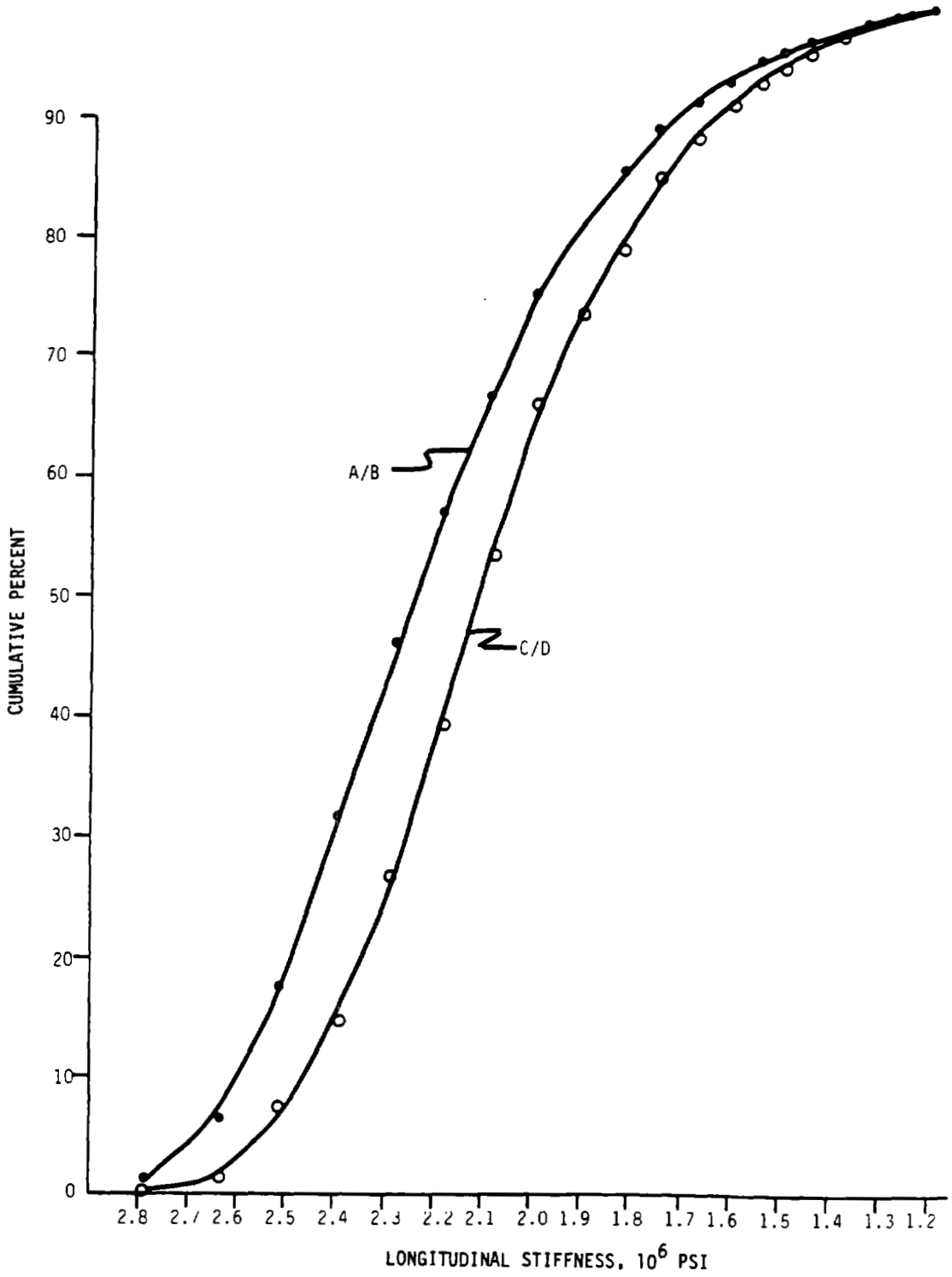

Figure 8-4 Cumulative Frequency Distribution of Longitudinal Stiffness for Grades A/B and C/D Veneer

Table 8-1 Distribution of Longitudinal Stiffness for Grade A/B and C/D Veneer

Longitudinal Stiffness (E) x 10^6 psi	A/B Veneer %	A/B Veneer cum. %	C/D Veneer %	C/D Veneer cum. %
2.71 - 2.84	1.2	1.2	0.2	0.2
2.57 - 2.69	5.2	6.4	1.6	1.8
2.45 - 2.56	11.2	17.6(1)	5.6	7.4(1)
2.33 - 2.44	14.4	32.0	7.5	14.9
2.23 - 2.32	14.0	46.0	11.8	26.7
2.13 - 2.22	11.0	57.0(2)	13.0	39.7(2)
2.03 - 2.12	10.1	67.1	13.6	53.3
1.95 - 2.02	8.0	75.1(3)	12.7	66.0
1.86 - 1.94	6.1	81.2	7.9	73.9
1.79 - 1.85	4.2	85.4	5.2	70.1
1.72 - 1.78	3.8	89.2	6.1	85.2
1.65 - 1.71	2.2	91.2	3.2	88.4
1.58 - 1.64	1.7	93.1	2.8	91.2
1.52 - 1.57	1.4	94.5	1.9	93.1
1.47 - 1.51	1.0	95.5	1.2	94.3
1.41 - 1.46	1.2	96.7	1.5	95.8
1.36 - 1.40	0.6	97.3	1.3	97.1
1.31 - 1.35	0.7	98.0	1.0	98.1
1.27 - 1.30	0.4	98.4	0.4	98.5
1.22 - 1.26	0.5	98.9	0.4	98.9
1.18 - 1.21	0.4	99.3	0.4	99.3
1.14 - 1.17	0.3	99.6	0.2	99.5
less than 1.14	0.4	100.0	0.5	100.0
number of sheets		4,720		1,285
mean E		2.09		1.99
standard deviation (s)		0.19		0.18
coefficient of ariation (%)		9.2		9.0

Notes (1), (2) and (3) refer to veneer yield relationships discussed in section 8.1.1.1.3.

price if A/B is cost competitive. In this study, data for the A+ group tended to support the view that A/B veneer was cost competitive. (See Table 8-2, note 1.)

The ultrasonic grader selected veneers by stiffness. If the stiffest veneer, with $E \geq 2.45 \times 10^6$, is required to meet the structural strength requirements, grade A/B was the logical choice, since it can supply more veneer that meets the requirements than C/D can. Otherwise, grade C/D can supply the veneer at half the cost of A/B. With the class broadened to include veneer with E as low as 2.1×10^6, the two to one relationship of high E to low E tended to break down (see Table 8-2, note 2). The sample also indicated that for an arbitrary range of 2.00×10^6 psi to 2.45×10^6 psi or greater, about 75% of the grade A/B veneer could be used (see Table 8-2, note 3).

Other statistical measures, such as standard deviation and coefficient of variation, identified and quantified the frequency distribution and dispersion of the sample population. The standard deviation, a measure of dispersion about the mean, was remarkably similar, 0.19 and 0.18 for grades A/B and C/D respectively. The coefficient of variability, which measures dispersion in relation to its mean, is the standard deviation divided by the mean, converted to a percentage. These values were also very similar for the two grades.

The distribution of longitudinal stiffness of grade A/B from the three suppliers is shown individually in Table 8-2 and Figure 8-2. Sun and Pope and Talbot veneer were similar in quality. They were characterized by high mean stiffness, small standard deviations of this stiffness, and low coefficients of variation. Veneer from Trend was the poorest in quality. This veneer was quite similar to grade C/D in mean stiffness, it had the most variability of any grade or supplier evaluated in this study. Trend veneer did, however, contain significantly higher percentages of the stiffer veneer, compared to the C/D mix.

8.1.1.2 Optimum Glue Spread Test

The application rate of epoxy can have a significant impact on the cost and weight of a structure as large as the MOD-5A blade. The tests evaluated two

Table 8-2 Distribution of Longitudinal Stiffness in Grade A/B Veneer from Various Suppliers

Longitudinal Stiffness (E)	Trend		Sun		Pope and Talbot	
x 10^6 psi	%	cum. %	%	cum %	%	cum. % *
2.71 - 2.84	2.0	2.0	1.0	1.0	0.3	0.3
2.57 - 2.69	6.6	8.6	4.3	5.3	4.4	4.7
2.45 - 2.56	10.6	19.2	10.9	16.2	12.5	17.2
2.33 - 2.44	11.7	30.9	16.7	32.9	14.7	31.9
2.23 - 2.32	10.2	41.1	17.9	50.8	12.8	44.7
2.13 - 2.22	8.0	49.1	12.7	63.5	12.9	67.6
2.03 - 2.12	9.3	58.4	11.2	74.7	9.1	66.7
1.95 - 2.02	7.7	66.1	7.8	82.5	8.8	75.5
1.86 - 1.94	6.7	72.8	5.3	87.8	6.9	82.4
1.79 - 1.85	4.1	76.9	3.9	91.7	5.0	87.4
1.72 - 1.78	3.6	80.5	3.0	94.7	5.4	92.8
1.65 - 1.71	2.6	83.1	1.7	96.4	2.3	95.1
1.58 - 1.64	2.4	85.5	1.4	97.8	1.3	96.4
1.52 - 1.57	2.3	87.8	0.9	98.7	0.7	97.1
1.47 - 1.51	1.7	89.5	0.5	99.2	0.9	98.0
1.41 - 1.46	2.1	91.6	0.5	99.7	0.9	98.9
1.36 - 1.40	1.2	92.8	0.2	99.9	0.2	99.1
1.31 - 1.35	1.6	94.4	0.1	100.0	0.2	99.3
1.27 - 1.30	1.1	95.5			0.1	99.4
1.22 - 1.26	1.2	96.7			0.3	99.7
1.18 - 1.21	1.1	97.8			0.2	99.9
1.14 - 1.17	0.7	98.5				
less than 1.14	1.5	100.0			0.1	100.0
number of sheets	1776		1939		1005	
mean E	2.00		2.17		2.12	
standard deviation (s)	0.23		0.15		0.16	
coefficient of variation (%)	11.5		6.9		7.7	

* cumulative percent

types of veneer, and included application rates determined to be extreme from previous tests.

8.1.1.2.1 Objectives

The objective of this series of tests was to determine the application rate of epoxy, and to develop the optimum strength of the veneer.

8.1.1.2.2 Description

Three hundred specimens were tested; 275 had the parallel configuration shown in Figure 8-5. Groups of 25 specimens were tested using grade A or C veneer, and application rates varying from 45 to 65 lbs per 1000 square feet of double glue line (lbs/MDGL) in increments of 5 lbs. Samples were loaded in shear, parallel to the grain, at a rate of 0.015 in. per minute. Shear strength, moisture content and completeness of wood vs. epoxy failure were recorded.

8.1.1.2.3 Results

Table 8-3 lists the test results, averaged for each 25 specimens. Figure 8-6 shows a plot of these shear strength values. Grade A veneer proved to be stronger than grade C. There were also significant variations in strength between the application rates. The 60 lbs/MDGL spread rate had the highest strength with either veneer. The estimate of completeness of wood failure was used only as a supplementary factor, since it is influenced greatly by the character of the wood peel surface. Rotary-peeled veneer has cellular variations based on the location of the wood in the growth ring, which deviate from sample to sample. The 60 lbs/mdgl rate was selected for all further MOD-5A fabrication.

The average shear strength decreased 10%, from 1,595 to 1,436 psi, when the veneer was exposed to moisture, as shown in lines 7 and 11 of Table 8-3. The last series of tests was conducted on specimens with laminations perpendicular to the glue line, as shown in Figure 8-5. The average shear strength was 21% higher: 2,018 psi vs. 1,595 psi.

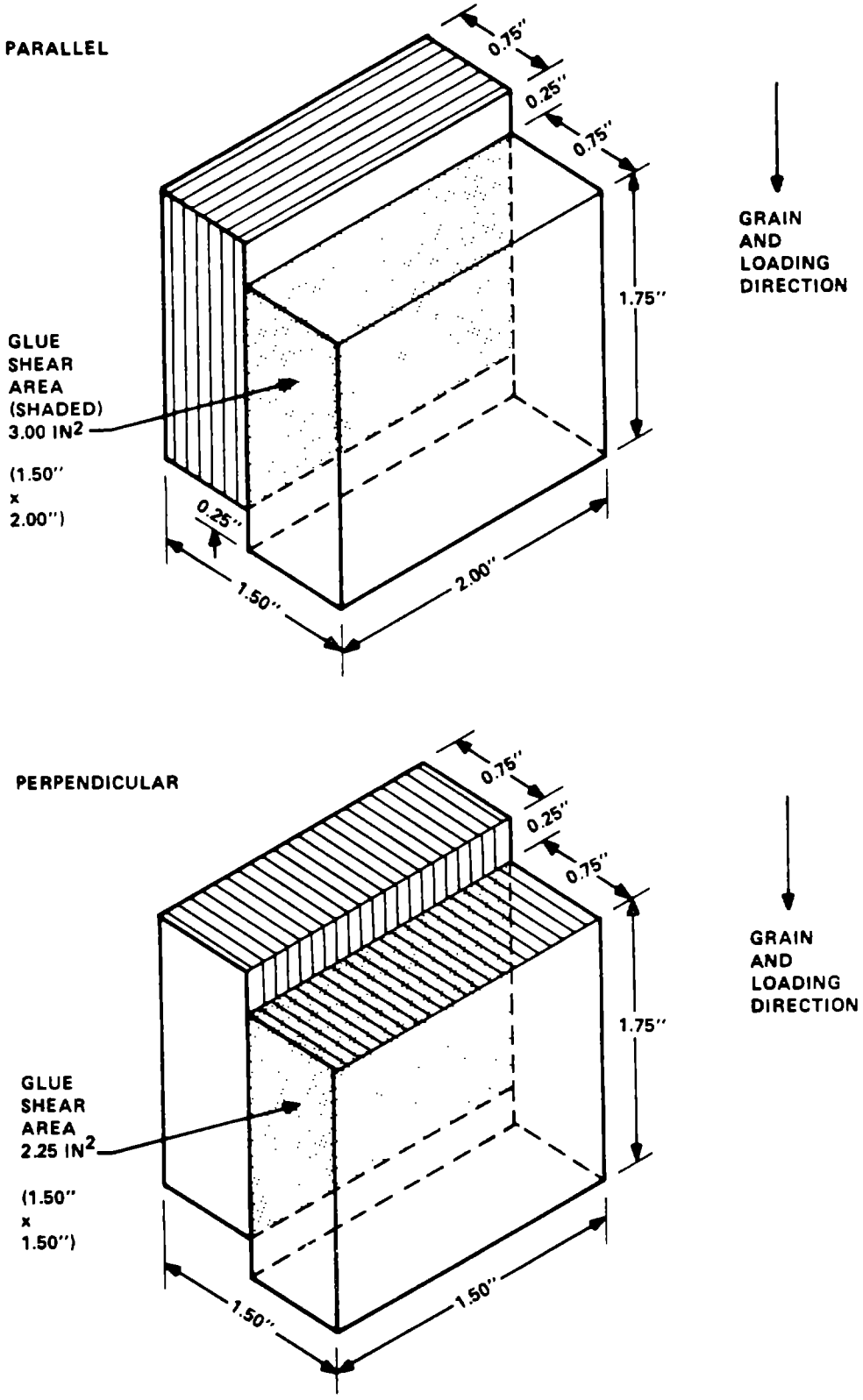

Figure 8-5 Block Shear Specimens Parallel and Perpendicular to Laminations

Table 8-3 Block Shear Strength of Epoxy and Laminated Douglas Fir

Temp. (°F)	Epoxy Spread	No. of Specimens	Veneer Grade	Average Moisture Content %	Average Shear Strength (psi)	Average Wood Failure (%)
RT	65	25	A+	3.0	1,697	96
RT	60	25	A+	2.8	1,824	79
RT	55	25	A+	2.9	1,659	95
RT	50	25	A+	3.1	1,511	89
RT	45	25	A+	3.5	1,056	34
RT	65	25	C	3.5	1,493	86
RT	60	25	C	3.6	1,595	91
RT	55	25	C	3.6	1,406	84
RT	50	25	C	4.1	1,448	87
RT	45	25	C	4.0	1,159	73
90°F	60	25	C	11.5	1,436	89
*76°F	60	25	C	4.2	2,018	100

* Perpendicular to grain samples.

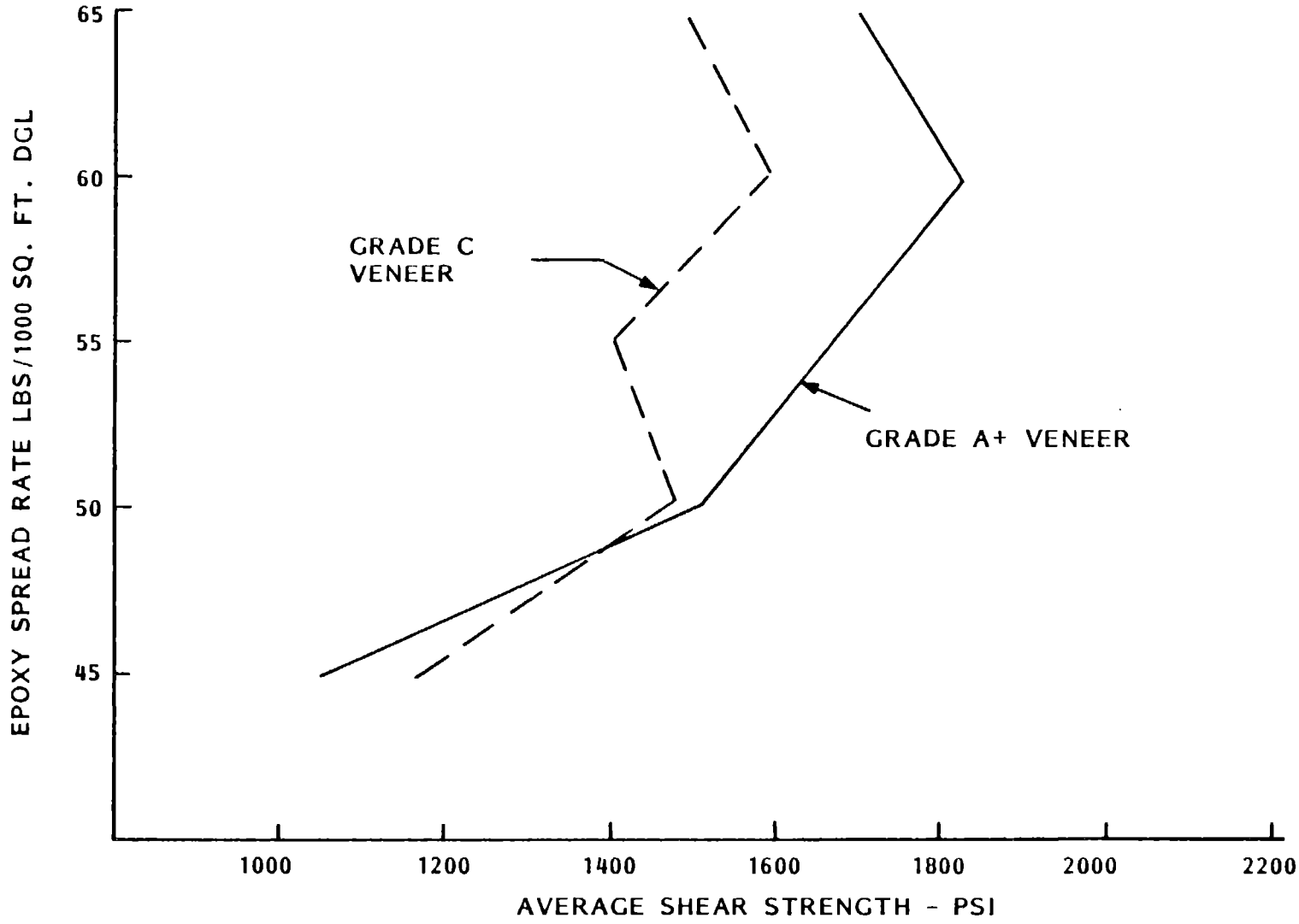

Figure 8-6. Block Shear Strength Vs. Epoxy Spread Rate

8.1.1.3 Moisture Content Variation Tests

The moisture content of wood influences its strength significantly. The range of acceptable moisture content was defined, to permit the design to be analyzed. Controlling the range affords an opportunity to optimize the strength of the wood.

8.1.1.3.1 Objectives

The test was designed to measure the variation in moisture content as a function of time for six differently sized specimens. The moisture sealing capability of the West System® epoxy, used to bond adjacent layers of veneer, was also evaluated.

8.1.1.3.2 Description

Specimens of six sizes used in other phase A static tests were sampled, and the moisture content was determined using the oven drying method. Other samples were exposed for two, four or six weeks 90°F, and 90% relative humidity. This environment is 20% equivalent moisture content (EMC). The specimens that were exposed for six weeks were subsequently stabilized for two weeks at 70°F, 65% relative humidity, and 12% EMC.

8.1.1.3.3 Results

The moisture content measurements are shown in Table 8-4. The first two-week period showed a significant increase in moisture content in all the exposed samples. The moisture content of the larger specimens continued to increase during the following two-week periods, but did not reach the levels attained by the smaller specimens. The conditioning at 12% EMC equalized the moisture throughout the specimen. The smaller specimens responded more dramatically. Since these specimens were not coated with epoxy on edges or ends, they did not represent the moisture characteristics that could be anticipated for the MOD-5A blade, but they indicated the need for sealing. The epoxy used to bond layers of veneer apparently did not penetrate the veneer enough to provide a barrier against moisture.

8.1.1.4 Tensile Strength Parallel and Perpendicular to Grain

A two-part test provided values of tensile strength for laminated Douglas fir loaded parallel or perpendicular to the grain in relatively small cross-sections. The perpendicular loads were applied in the radial direction.

Table 8-4 Moisture Content of Various Test Specimens Exposed to Moisture

Test Specimen	Moisture Content (%) - 20% EMC*				Equalized at 12% EMC**
	Initial	2 wks	4 wks	6 wks	2 wks
Block Shear	6.1	15.4	15.4	15.4	11.6
	5.1	15.7	15.5	15.7	11.6
	5.6	15.1	14.9	15.3	11.4
	4.6	15.1	15.1	15.1	11.3
	4.7	14.5	14.9	14.9	11.5
Tensile Parallel	5.4	10.0	11.3	12.1	10.6
	6.4	11.8	15.0	14.3	11.7
	6.0	10.6	12.1	12.7	10.8
	6.8	11.6	13.2	13.5	11.3
	5.1	10.0	11.6	12.0	9.6
Tensile Perpendicular	5.3	13.5	13.5	13.5	9.9
	4.3	12.5	13.5	12.8	9.6
	5.1	14.0	14.0	13.8	10.4
	4.9	13.9	13.9	13.9	10.6
	4.2	12.8	13.1	12.8	9.6
Compression Parallel	5.8	11.6	12.4	12.0	10.0
	5.1	11.5	12.1	12.0	9.7
	5.1	11.2	12.2	11.9	9.8
	5.7	11.8	12.5	12.3	10.2
	6.0	12.0	12.6	12.5	10.4
Compression Perpendicular	4.8	12.0	12.6	12.3	10.2
	4.6	11.9	12.8	12.4	10.6
	4.4	11.6	12.6	12.2	10.1
	4.7	12.3	13.1	12.7	10.6
	4.8	12.3	13.0	12.6	10.5
Bending	6.0	10.9	12.4	13.3	11.0
	5.8	11.0	12.4	13.2	11.0
	5.9	10.8	12.2	12.9	11.0
	6.3	11.5	13.0	13.7	11.4
	5.8	10.2	11.8	12.6	11.0

* 20% EMC = 90°F and 90% relative humidity.
** 12% EMC = 70°F and 65% relative humidity.

8.1.1.4.1 Objectives

The test was designed to provide a statistically representative baseline for determining the tensile strength of the laminae in two directions. The strength characteristics of laminated wood were expected to be different from those of solid wood. By simulating the materials and processes used in the manufacture of the blade, representative strength properties of the blade sections were determined. This data served as part of the characterization data used to define allowable stresses for the blade design.

8.1.1.4.2 Description

Samples were fabricated from billets constructed of 15 sheets of veneer; each billet was 1.5 in thick. The specimens were cut parallel to the grain, 2.0 in. wide and 92 in. long. Testing was performed on a compression grip tensile testing machine at the University of Oregon. Loading was increased linearly to provide failure parallel to the grain in approximately 5 minutes . In tests in which the loading was normal to the grain, the loading rate was 0.15 in. per minute, on samples with a cross-section of 2 by 2 in. Figure 8-7 snows the specimen's geometry. Metal blocks were bonded to these specimens to interface with the testing machine. They created some problems during testing.

Fifty samples each of grades A+, A and C veneer, with moisture contents between 3.2% and 5.2% were used in the parallel tests. Twenty-five of each grade contained no veneer joints; the remaining samples contained butt joints staggered on 3-in. centers. Twenty-five moisture-conditioned samples of grade A veneer, with an average 10% moisture content were also tested. Perpendicular tests used 25 samples of grade C veneer, at two moisture content levels.

8.1.1.4.3 Results

The results of these tests are summarized in Table 8-5. The tests provided some insight into the significant effect of defects in the veneer on the strength of small samples. The strength decreases with grade; grade A+ had the highest strength. The butt joints decreased strength slightly, except in grade A+ veneer. This anomaly can be attributed to variations in strength within the grade. The large variations in the perpendicular test results are

TENSION PARALLEL TO GRAIN

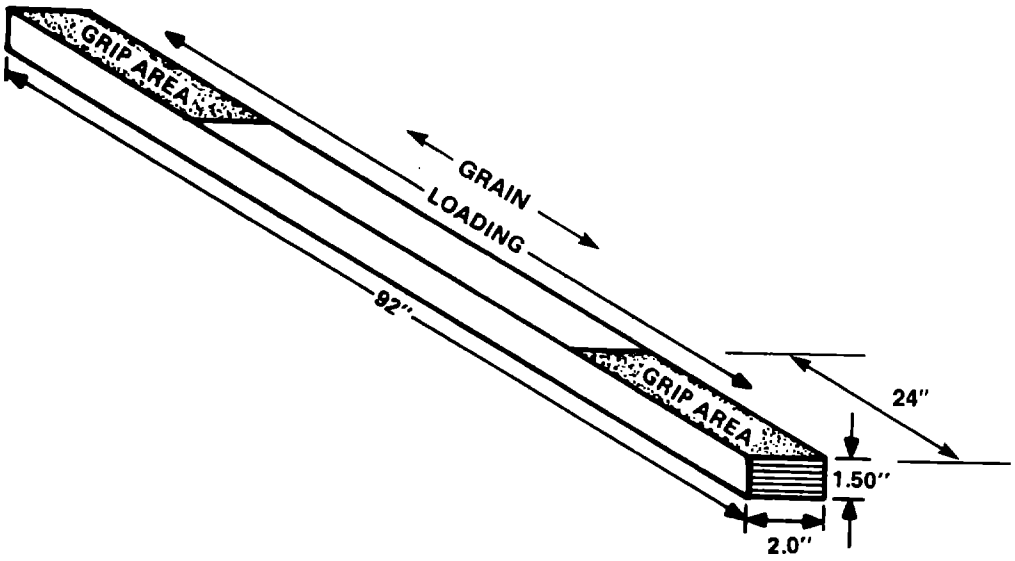

TENSION PERPENDICULAR TO GRAIN (TANGENTIAL)

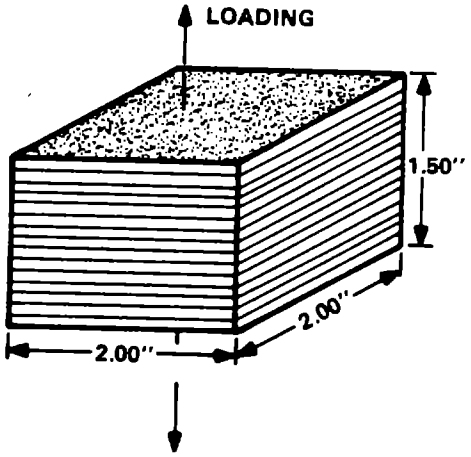

Figure 8-7 Specimens for Tension Parallel and Perpendicular to Grain

Table 8-5 Tension Parallel and Perpendicular to the Grain

Test	Quantity	Veneer Grade	Veneer Joint	Average Moisture Content (%)	Average Stress (psi)	Coefficient of Variation (%)	Maximum/Minimum (psi)
Parallel	25	A+	None	5.0	10,660	17.5	13,940/8,305
Parallel	25	A+	3" Butt	5.0	11,183	17.0	14,194/8,446
Parallel	25	A	None	4.8	11,035	9.6	12,684/9,070
Parallel	25	A	3" Butt	5.2	9,943	10.7	11,236/7,674
Parallel	25	C	None	3.8	10,691	9.1	11,832/8,026
Parallel	25	C	3" Butt	3.2	8,407	10.1	9,890/7,166
Parallel	25	A	None	10.0	10,644*	17.4	13,486/7,344

* Tested at 90°F, 90% relative humidity.

Perpendicular	25	C	None	4.5	217	34.8	359/59
Perpendicular	25	C	None	9.6	156	37.2**	294/54

** 7 specimens failed at the bond to the metal pull block, so the results are probably to be biased low. Also tested at 90°F, 90% relative humidity.

to be expected since the strength depends on the weakest veneer in the specimen, and does not include an averaging effect as the other test samples do. Any discontinuity in the grain or flaw in a sheet greatly influences the strength of the sample.

8.1.1.5 Compression Strength Parallel and Perpendicular to the Grain

A series of tests determined the compression strength of laminated Douglas fir, loaded parallel to the grain and perpendicular to the grain in the tangential direction.

8.1.1.5.1 Objectives

The objective of this test was to provide a statistically representative data base for determining the compression strength in two directions of the laminae. This data was to serve as a part of the characterization data used to define allowable stresses for the blade design.

8.1.1.5.2 Description

The test samples were designed to perform as short columns that would not require lateral support. The specimens for parallel tests were 6.5 in. long, with a 1.5 in. by 2.0 in. cross section. They were made of fifteen 0.1 in. thick laminae. Figure 8-8 shows the specimen's configurations. The testing used stroke control, and a rate of 0.01 in. per minute. Some specimens were built with 2 in. square pads of Teflon®, or a Teflon® disc with a diameter of 1.5 in. in the center lamination, to simulate a defective bond joint.

Perpendicular testing was performed on 2 in. thick samples, 1.5 in. wide and 6 in. long. They were made with fifteen 0.1 in. thick laminae. Laminations were set normal to the loading face with the 2 in. length as a column. Specimens were loaded until a compression deflection of 0.1 in. was reached, and the load was recorded at that time, since the material is spongy in the cross grain direction and does not have a characteristic peak value.

8.1.1.5.3 Results

The results presented in Table 8-6 indicated that compression strength decreases with grade, and is lower for butt-jointed samples. The strength was significantly reduced by high moisture content. The Teflon® imperfections did not affect strength.

COMPRESSION PARALLEL TO GRAIN

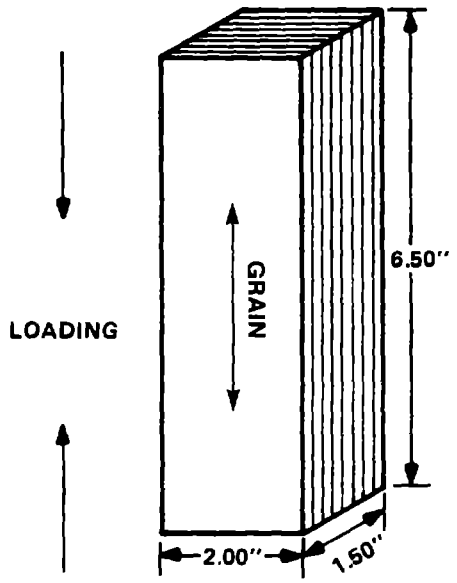

COMPRESSION PERPENDICULAR TO GRAIN

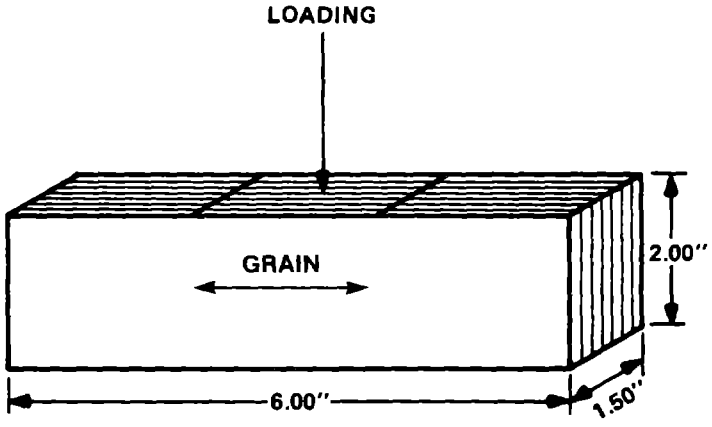

Figure 8-8 Specimens for Compression Parallel and Perpendicular to Grain

Table 8-6 Results from Compression Parallel and Perpendicular to the Grain

Test	Quantity	Veneer Grade	Veneer Joint	Average Moisture Content (%)	Average Stress (psi)	Coefficient of Variation (%)	Maximum/Minimum (psi)
Parallel	20	A+	None	3.4	11,285	3.2	11,790/10,490
Parallel	20	A+	3" Butt	3.5	10,590	5.3	11,479/ 9,339
Parallel	20	A	None	4.4	10,235	6.4	11,343/ 8,923
Parallel	20	A	3" Butt	4.0	9,491	8.3	11,306/ 7,833
Parallel	20	C	None	4.5	9,842	5.6	10,694/ 8,852
Parallel	20	C	3" Butt	4.5	9,503	6.1	10,373/ 8,370
Parallel	20	A	3" Butt	10.0	6,773	2.9	7,184/ 6,352
Parallel	10	A	None	4.3	10,717*	5.7	11,710/ 9,831
Parallel	10	A	None	4.1	10,988**	3.4	11,494/10,387

* These samples contained a delamination disc.

** These samples contained a delamination area.

Perpendicular	20	C	None	4.7	3,013	5.4	3,451/ 2,758
Perpendicular	20	C	None	10.5	2,273***	4.8	2,442/ 2,027

*** Tested at 90°F, 90% relative humidity.

8.1.1.6 Bending Strength

A series of 100 tests was conducted with samples subjected to 4-point bending, to measure bending strength and stiffness for various grades of veneer.

8.1.1.6.1 Objectives

The tests measured flexural strength and stiffness in a 4-point bending system. The tests compared the relative results for various grades. One series used the veneer in a horizontal plane and one series used samples with a high moisture content, which were tested at 90°F.

8.1.1.6.2 Description

The test specimens were 2.0 in. wide and 1.5 in. thick, made from 15 laminations. Vertical lamination specimens were 80 in. long, and horizontal lamination specimens were 66 in. long. Figure 8-9 shows the samples and the loading points. Load and deflection data was plotted during the test, and stress levels and the modulus of elasticity were calculated using standard beam theory. The loading rate was 0.50 in. per minute for vertical laminations and 0.30 in. per minute for horizontal laminations.

8.1.1.6.3 Results

Table 8-7 shows the results of the 100 tests averaging values for groups of 20. In general, failure initiated in the compression side of the beam, since the tensile strength is usually higher.

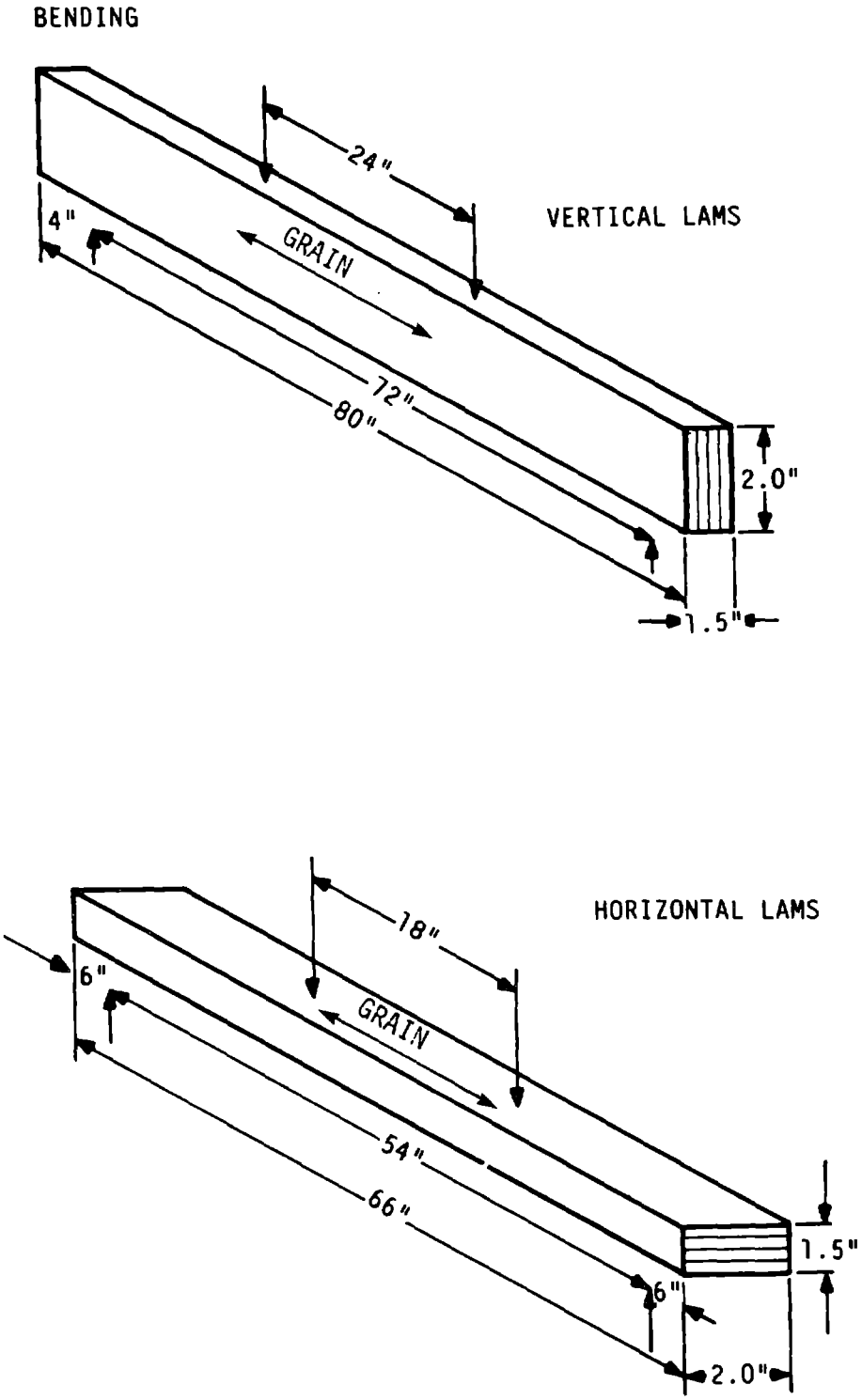

Figure 8-9 Specimens for Bending with Vertical and Horizontal Laminations

Table 8-7 Bending Strength and Stiffness, with 3-in. Butt Joints and Vertical Laminations, Unless Otherwise Noted

Quantity	Veneer Grade	Average Moisture Content (%)	Average Bending Strength (psi)	Maximum/Minimum (psi)	Stiffness (E) x 10^6 psi	Maximum/Minimum (psi)
20	A+	3.7	14,736	13,157/15,727	2.22	2.37/2.04
20	A	4.6	12,418	14,891/ 6,853	1.97	2.35/1.73
20	C	4.7	12,580	14,581/10,843	2.11	2.39/1.93
*20	A	10.0	11,499	12,228/10,175	1.90	2.04/1.77
**20	A	4.4	13,039	15,723/11,685	2.00	2.23/1.82

* Tested at 90°F, 90% relative humidity.

** Vertical laminations.

8.1.1.7 Tensile Strength Properties Perpendicular to the Grain (Radial and Tangential)

This test supplemented previous test results, by using blade grade 2 Douglas fir veneer, which was previously defined as grade A, in a series of tests with tension perpendicular to the grain. The previous tests used grade C veneer, and the increased number and size of allowable defects in those samples yielded lower results than could be obtained with higher quality wood.

8.1.1.7.1 Objectives

The objective of these tests was to measure tension properties in the radial and tangential directions normal to the grain of blade grade 2 Douglas fir veneer bonded with West System® epoxy, at room temperature. There were no joints in any of the samples in this test sequence. The radial direction was defined as normal to the plane of the bond line, and the tangential direction was parallel to the bond line.

8.1.1.7.2 Description

The veneer was 0.10 in. thick. It was bonded into 1.5 in. thick billets of 15 layers, with West System® epoxy between layers. Two types of specimens were prepared. The samples for radial tension had a 2 in. by 2 in. cross section, and metal pull blocks bonded to the faces of the slab, as shown in Figure 8-10. The samples for tangential tension were 2 in. wide and 24 in. long, with a gage length of 8 in., allowing 8 in. for gripping at each end, as shown in Figure 8-11.

The samples for radial tension were tested by interfacing the pull blocks with a matching tension test machine fitting. Tangential tension tests used a compression grip. A loading rate of 0.15 in. per minute was used for radial tension tests, and a ramp of approximately 200 lbs. per minute was applied to the tangential specimens. The breaking load, specimen cross section area, tensile strength and moisture content were determined for each of the 20 specimens of each type tested.

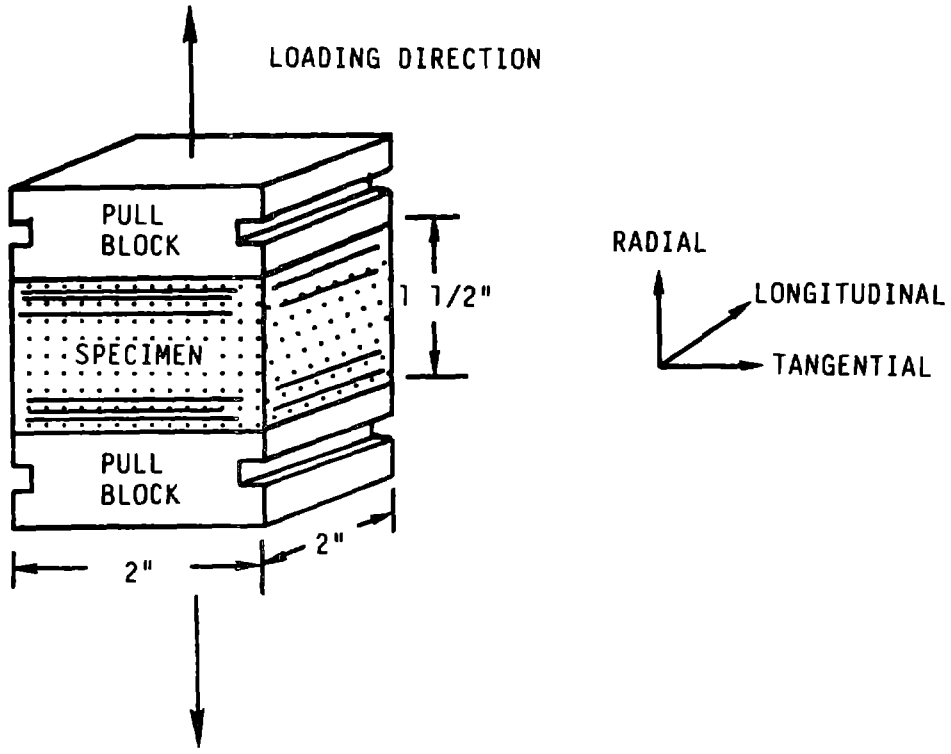

Figure 8-10 Specimen for Tension Perpendicular to Grain Tests (Radial Direction)

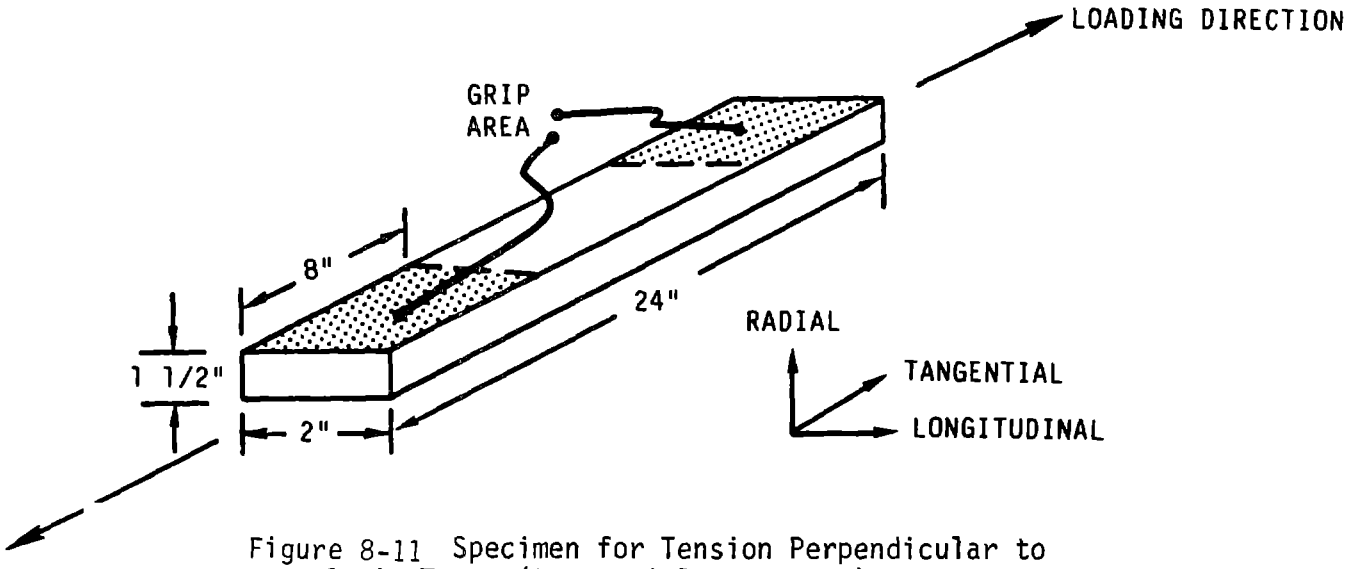

Figure 8-11 Specimen for Tension Perpendicular to Grain Tests (Tangential Direction)

8.1.1.7.3 Results

The radial tension test results are listed in Table 8-8. The average failure stress was 492 psi. Earlier tests, discussed in section 8.1.1.4, showed that grade C veneer had an average failure stress of 217 psi. Specimen #19 failed in the bond interface to the test block, but the load was included in the data.

The tangential tension test results are tabulated in Table 8-9. The average failure stress was 273 psi. Data describing the wood characteristics indicate that the two tension strengths normal to the grain should be nearly equal, and the disparity in this set of data is probably due to lathe checks in the veneer caused by the peeling operation. If this lower strength was significant in the design, the strength could be enhanced by the use of sheets of glass fiber between the layers.

8.1.1.8 Effect of Temperature on Compression Parallel to the Grain

This test program studied the strength of the blade material in compression at temperatures above and below the ambient temperature. Samples with no joints, and samples witn staggered butt joints spaced 3 in. apart were tested.

8.1.1.8.1 Objectives

The objective of the test was to determine the effect of high (120°F) and low (30°F) temperatures on the static compression strength of epoxy-bonded laminated Douglas fir loaded parallel to the grain. Neither the length of time the samples spent at the temperature nor exposure to temperatures beyond the actual test conditions were variables.

8.1.1.8.2 Description

Fifteen layers of grade A Douglas fir veneer, 0.10 in. thick, were bonded with West System® epoxy. Samples without veneer joints and samples with staggered butt joints on 3 in. centers were tested. Ten specimens of each joint type were tested at both temperatures, resulting in a total of 40 tests.

Table 8-8 Tensile Strength Perpendicular to Grain in the Radial Direction for Epoxy and Laminated Douglas Fir

Veneer Grade - Blade Grade 2
Veneer Joint - None
Temperature - 77°F

Specimen #	Moisture Content (%)	Area (in^2)	Failing Load (lbs)	Tensile Strength (psi)
01	5.2	4.04	1345	333
02	4.4	4.04	2203	545
03	4.7	4.00	1317	329
04	4.5	4.04	2417	598
05	4.8	4.02	1322	329
06	4.6	4.05	2265	559
07	4.2	4.05	2396	592
08	4.4	4.04	2035	504
09	4.6	4.02	1795	447
10	5.1	4.02	1465	364
11	4.6	4.04	1866	462
12	5.1	4.01	1873	467
13	4.2	4.02	2228	554
14	4.5	4.04	1615	400
15	4.3	4.05	2173	537
16	4.8	4.01	1727	431
17	4.3	4.04	2719	673
18	4.1	4.05	2402	593
19	4.5	4.03	2289	568*
20	4.9	4.00	2217	554
Average	4.6			492
Standard Deviation				102
Coefficient of Variation (%)				20.7

* Specimen failed at metal pull block/specimen interface.

Table 8-9 Tensile Strength Perpendicular to Grain in the Tangential Direction for Epoxy and Laminated Douglas Fir

Veneer Grade - Turbine Grade 2
Veneer Joint - None
Temperature - 77°F

Specimen #	Moisture Content (%)	Area (in^2)	Failing Load (lbs)	Tensile Strength (psi)
01	5.7	3.10	920	297
02	5.6	3.10	740	239
03	6.0	3.11	920	296
04	5.2	3.04	940	303
05	5.2	3.05	780	256
06	4.9	3.06	800	261
07	5.3	3.03	700	231
08	5.2	3.07	940	306
09	5.1	3.08	680	221
10	5.0	3.05	960	315
11	4.8	3.06	1040	340
12	4.9	3.03	760	251
13	5.0	3.04	1280	421
14	5.2	3.04	1160	382
15	5.2	3.04	560	184
16	5.1	3.04	840	276
17	4.9	3.03	740	244
18	4.7	3.04	580	191
19	5.0	3.05	720	236
20	4.7	3.05	620	203
Average	5.0			273
Standard Deviation				61
Coefficient of Variation (%)				22.5

The specimen's length was 6.5 in. and the cross section was 1.5 by 2 in., resulting in a short column with a slenderness ratio of approximately 15, so there was no need for lateral supports. Loading was applied at a head travel rate of 0.01 in. per minute, until crushing failure occurred.

8.1.1.8.3 Results

Table 8-10 lists the results of ten specimens of each type tested at 30°F. The average strength of the butt-jointed specimens was 5.4% lower than that of the specimens without joints. At 120°F the average strength of the butt-jointed samples was 2.2% below that of the unjointed samples. The strength at 120°F is approximately 30% lower than at 30°F. For purposes of evaluation, the table lists 20 tests each, which were conducted on other samples made from the same billets (see section 8.1.1.5). The average compressive strength was 10,235 psi for unjointed specimens and 9,491 psi for jointed specimens. Figure 8-12 presents a graph. The statistical analysis indicates that the compression strength of the material is reduced when staggered butt joints are included, but the temperature variation affected strength more than the joints. The regression equations, shown in Figure 8-12, indicate that there is a 4% change in compression strength for each 10°F change in temperature. This highly linear relationship agrees well with previous work on similar materials.

8.1.1.9 Birch Veneer Yield Study

This study evaluated the yield of veneer by grade, to determine the relative costs of Douglas fir and birch. Because the yield of blade grade Douglas fir is relatively poor, the feasibility of birch was considered as an alternative, if it was more cost effective. Birch veneer is sliced, so it is only available in random widths, whereas rotary-peeled Douglas fir is available in standard widths.

8.1.1.9.1 Objectives

The objective of the study was to determine whether birch would be feasible for the manufacture of the blade. Since the cost of the material is high, the yield is important.

Table 8-10 Compressive Strength Parallel to Grain of Grade A Veneer

Quantity of Tests	Joint	Test Temp. (°F)	Average Moisture Content (%)	Average Compression Strength (psi.)	Maximum/Minimum (psi.)
10	None	30°	3.9	12,395	13,212/10,839
10	3" Butt	30°	3.6	11,728	12,814/10,444
10	None	120°	3.6	8,614	9,176/ 7,404
10	3" Butt	120°	3.4	8,429	9,304/ 6,779
20	None	69°	4.4	10,235	11,343/ 8,923
20	3" Butt	69°	4.0	9,491	11,306/ 7,833

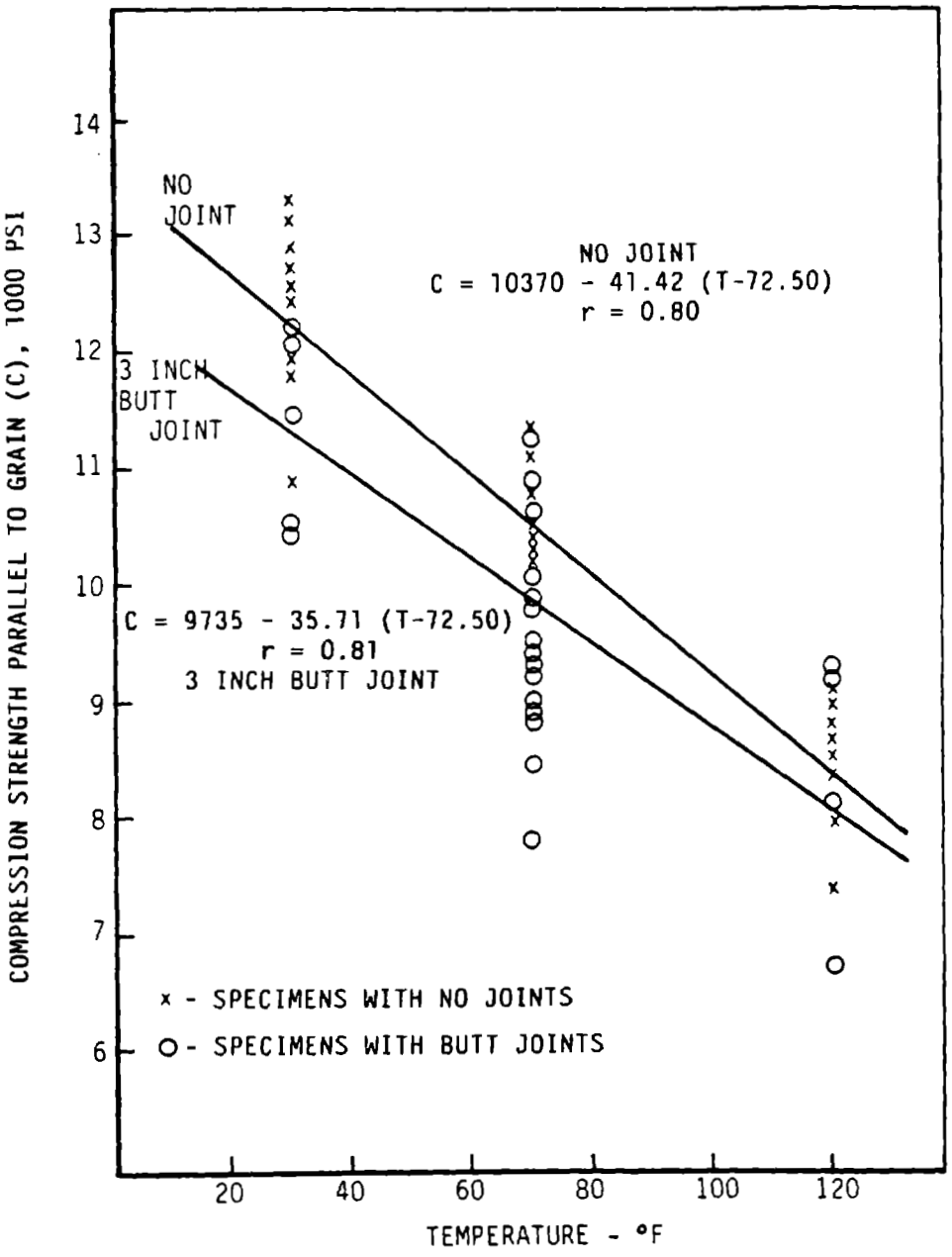

Figure 8-12 Relationship Between Temperature and Compression Strength

8.1.1.9.2 Description

638 pieces of birch veneer, with a total area of 3,031 square ft. were graded into two stiffness groups using ultrasonic inspections. Veneer in grade 1 had moduli of 2.45×10^6 psi or greater. Veneer in grade 2 had moduli between 2.10 and 2.44×10^6 psi. Any veneer with a modulus below 2.10×10^6 psi was rejected.

8.1.1.9.3 Results

638 pieces of sliced, 0.10 in. thick birch veneer with random widths were graded by stress wave evaluation. The longitudinal stiffness distributions are shown in Table 8-11. About 93% of the veneer was usable. Similar procedures in previous studies of Douglas fir yielded about 30% less. In this instance, the increase in yield is due to grade 2 of the birch. 59% of the birch was grade 2, whereas less than 50% of the Douglas fir veneer met the requirements of grade 2. This statistic indicates that the quality of birch logs used for slicing may be higher than that of the Douglas fir logs used for peeling.

8.1.1.10 Birch/FRP Bond Line Strength Parallel and Perpendicular to Laminations

A group of 40 tests studied bond lines parallel to laminations and 20 tests studied the bond line shear normal to the laminations. These tests evaluated a material made of birch veneer, West System® epoxy and glass fiber-reinforced plastic (FRP). The tests used two types of FRP, and took some data at 104°F.

Table 8-11

Distribution of Longitudinal Stiffness of
1/10-in. Thick Sliced Birch Veneer

Longitudinal Stiffness ($E \times 10^6$ psi)	Percent of Total (%)	Cumulative Percent (%)	
2.85 - 2.98	0.1	0.1	
2.71 - 2.84	2.2	2.3	
2.57 - 2.69	5.5	7.8	
2.45 - 2.56	26.3	34.1	(BG 1)
2.33 - 2.44	18.8	52.9	
2.23 - 2.32	17.9	70.8	
2.13 - 2.22	13.5	84.3	
2.03 - 2.12	8.8	93.1	(BG 2)*
1.95 - 2.02	4.2	97.3	
1.86 - 1.94	2.7	100.0	

Total number of pieces graded = 638

Grade Yield

BG 1 = 34.1%
BG 2 = 59.0%
Unusable= 6.9%

* Actual Blade Grade 2 Range Per Gougeon Materials Specification is from 2.1×10^6 to $2.44 \times (10)^6$.

8.1.1.10.1 Objectives

The purpose of these tests was to evaluate the static strength properties of the construction consisting of 0.10-in. thick, grade 2 birch veneer and 0.10-in. thick epoxy or polyester FRP per MIL-P-17549 grade 1. The birch and FRP composite, 1.5-in. thick, consisted of 15 layers: 10 layers of birch and 5 layers of FRP. There were 3 layers of birch on each side, and birch and FRP alternated in the center.

The objective of these tests was to determine the glue line strength at the interface between the birch and the FRP. West System® epoxy, spread at a rate of 60 lbs./MDGL, was the bonding material. Sample block shear specimens were machined to test the glue line closest to the middle of the block.

8.1.1.10.2 Description

Specimen configuration and dimensions for block shear parallel to the laminations is shown in Figure 8-13. The specimens were loaded to failure, at a rate of 0.015 in./min, with each of the following combination of test variables evaluated. A total of 40 specimens were tested.

FRP - epoxy and polyester
Temperature - 70°F and 104°F

After testing, the specimens were oven dried, and the moisture content was determined.

The specimen configuration and dimensions for block shear perpendicular to the laminations are shown in Figure 8-13. For this test each combination of test variables was evaluated as shown below. A total of 20 specimens were tested.

FRP - epoxy and polyester
Temperature - 70°F

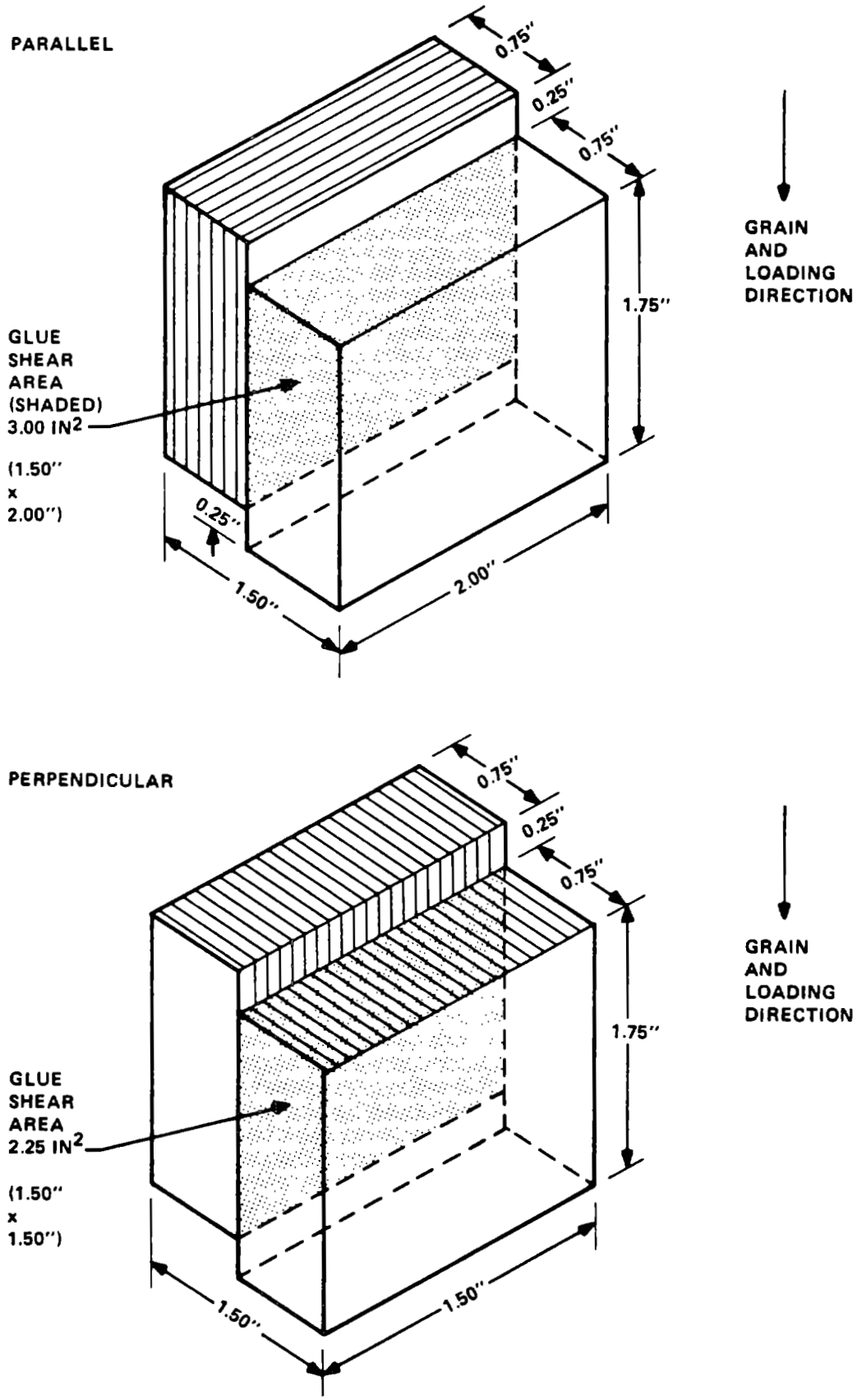

Figure 8-13 Specimens for Block Shear Tests Parallel and Perpendicular to Laminations

Load deformation diagrams were made using an electronic deflectometer to measure head movement.

3.1.1.10.3 Results

Bonds between the birch and the two types of FRP were evaluated using the block shear test at temperatures of 70°F and 104°F. The results of these tests are listed in Table 8-12. The moisture content was determined by the oven drying method.

Statistical analysis of the results indicated the epoxy FRP forms a much stronger bond with birch veneer than polyester FRP. Epoxy FRP is also less affected by higher temperatures. Likewise, epoxy FRP displayed a higher yield point (fiber stress at proportional limit - FSPL) than polyester FRP at both temperatures. In general, the FSPL for epoxy FRP occurred at 90% to 93% of the ultimate, while that of polyester FRP was approximately at 95%.

In addition to generally lower shear values for polyester FRP, some of the specimens had interlaminar shear failures between layers of the polyester material, which may constitute a weak zone in the material. Several specimens failed by interlaminar shear within the FRP. In some cases the interlaminar failure occurred so near the outer layers of cloth, that, unless it was carefully examined, the failure would have been misdiagnosed. The failure would have appeared to have occurred at the interface between the birch and FRP. In several specimens, at 104°F, a slight precure condition was observed, because the imprint of the polyester cloth appears to have been made into the epoxy after it started to polymerize.

Table 8-12 Shear Test Results

Quantity of Specimens	Test Temperature °F	Test Direction	FRP Type	Average Moisture Content (%)	Average Shear Strength (psi)	High/Low (psi)
10	70	Parallel	Epoxy	6.6	3,278	4,214/2,653
9	104	Parallel	Epoxy	6.1	2,742	3,256/2,392
10	70	Parallel	Polyester	6.1	2,775	3,258/1,811
10	104	Parallel	Polyester	6.1	2,067	2,555/1,551
10	70	Perpendicular	Epoxy	6.0	6,060	8,103/5,495
10	70	Perpendicular	Polyester	6.4	6,433	6,976/5,980

8.1.1.11 Birch and FRP Tension Tests, Parallel and Perpendicular to Grain

Tension tests were conducted on the birch and FRP material parallel to the grain, and in the radial and tangential directions normal to the grain.

8.1.1.11.1 Objectives

The objective was to determine the tensile strength of birch reinforced with either epoxy or polyester FRP, at 70°F and at 104°F. This data would provide a basis for determining design allowables.

8.1.1.11.2 Descriptions

The configurations of the test specimen are shown in Figures 8-14, -15, and -16. The loading rate for the test parallel to grain and tangential tests was set to provide failure in approximately 5 minutes. The loading rate for the radial tests was 0.15 in. per minute. The tests were conducted at 70°F and at 104°F.

8.1.1.11.3 Results

Table 8-13 summarizes the average results of the tension tests in the three directions. The results indicated that there is no significant difference in the parallel to grain tensile strength of the two types of FRP at either temperature. The parallel grain specimens contained butt joints on 3 in. staggered centers, and most failures occurred in that area. These materials were approximately 20% stronger than the equivalent Douglas fir.

The results from the radial tension tests show little difference in the strength of birch or Douglas fir. The birch and polyester FRP was slightly stronger. In the tangential direction, the polyester FRP was stronger than the epoxy FRP and approximately 36 times stronger than unreinforced Douglas fir.

Table 8-13 Tension Test Results

Quantity of Specimens	Test Direction	Test Temp. (°F)	Average Moisture Content (%)	Tensile Strength (psi)	Maximum/Minimum	FRP Type
10	Parallel	70	6.3	13,546	14,610/12,128	Epoxy
10	Parallel	104	5.9	13,014	14,184/11,854	Epoxy
10	Parallel	70	6.2	13,460	15,178/12,237	Polyester
10	Parallel	104	6.4	13,384	14,805/12,072	Polyester
9	Radial	70	6.4	540	740/ 317	Epoxy
10	Radial	70	6.2	575	726/ 433	Polyester
10	Tangential	70	6.1	7,852	8,447/ 6,581	Epoxy
10	Tangential	104	6.0	7,538	8,084/ 6,946	Epoxy
10	Tangential	70	6.5	9,763	10,738/ 8,756	Polyester
10	Tangential	104	6.1	9,527	10,257/ 8,851	Polyester

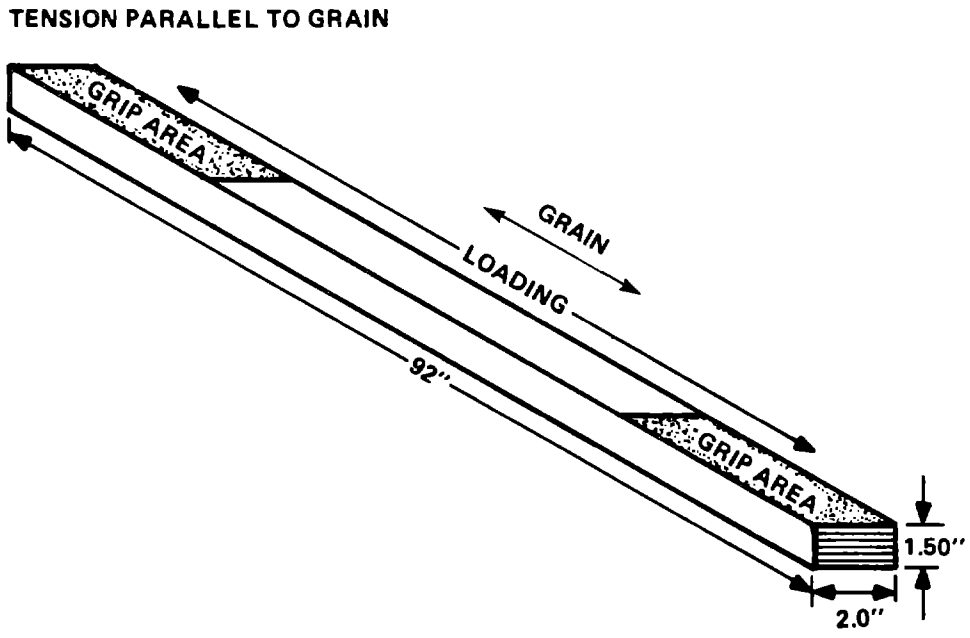

Figure 8-14 Specimen for Tension Parallel to Grain Test

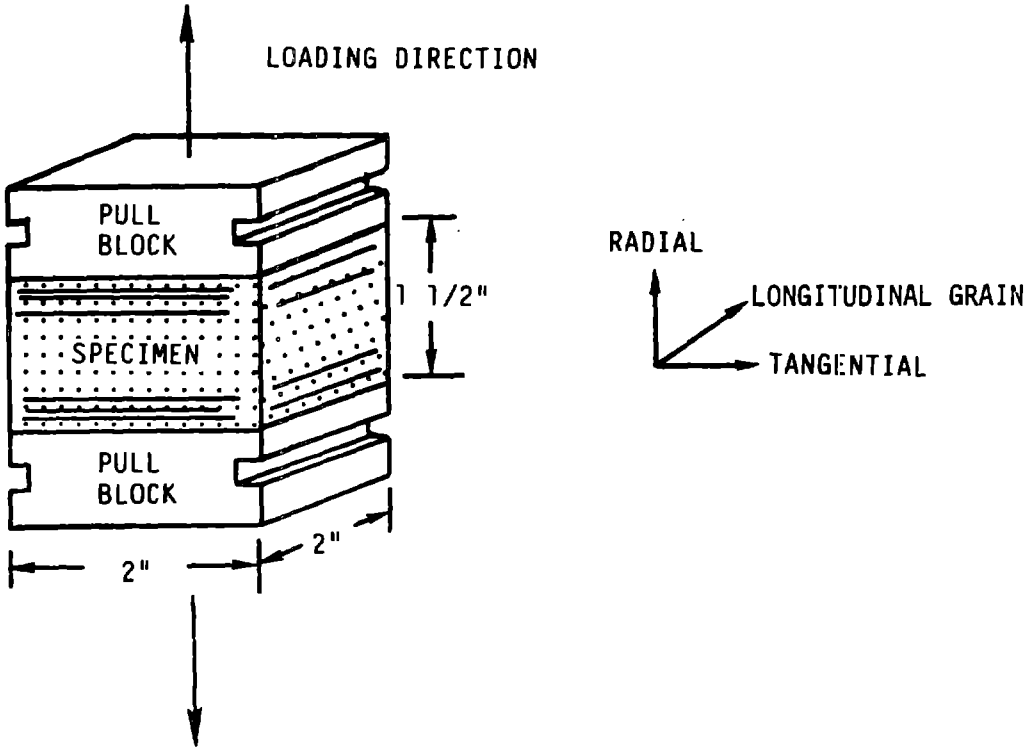

Figure 8-15 Specimen for Tension Perpendicular to Grain in the Radial Direction Tests

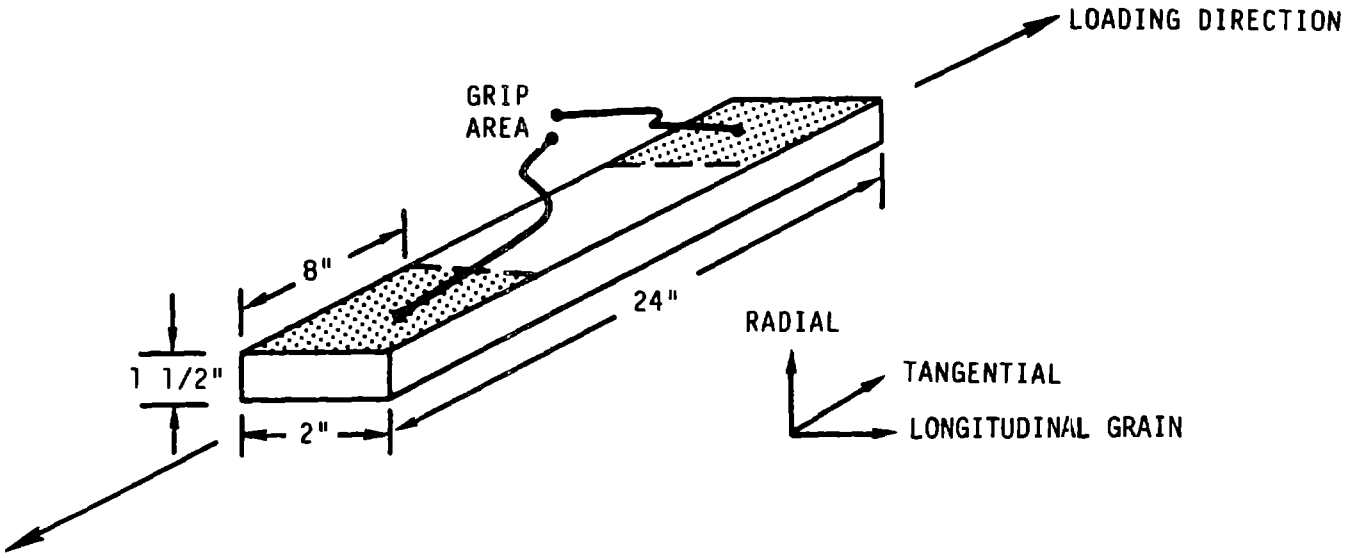

Figure 8-16 Specimen for Tension Perpendicular to Grain in the Tangential Direction Tests

8.1.1.12 Birch and FRP Compression Tests, Parallel and Perpendicular to the Grain

Compression strength tests in two directions were conducted to supplement the data base for birch and FRP.

8.1.1.12.1 Objectives

These tests provided block compression strength data for the two types of birch and FRP at 70°F, 104°F, and 120°F. This data was used to compare these materials with Douglas fir material.

8.1.1.12.2 Description

Five tests of birch augmented with each type of FRP were conducted at 70°F and 104°F, in compression parallel to the grain, and at 70°F, in compression perpendicular to the grain in the tangential direction. Also, five epoxy FRP samples were tested parallel to the grain at 120°F. The configurations of the test specimens are shown in Figure 8-17.

8.1.1.12.3 Results

Table 8-14 lists the results of the 35 compression tests, and indicates that the epoxy FRP was significantly stronger than the polyester FRP parallel to the grain. The test at 120°F showed a marked decrease in strength of the epoxy and indicated a possible temperature limitation on this material. It was noted that the proportional limit was lower in relation to ultimate stress, ranging from 13% to 30% of the latter value. The epoxy FRP was stronger parallel to the grain than the polyester material. The birch reinforced with FRP was 5 to 6 times stronger parallel to the grain than the unreinforced Douglas fir. The use of glass fiber to reinforce wood veneer significantly increases the strength of the composite. The cost effectiveness of the birch and FRP and Douglas fir and FRP laminae must abe evaluated.

COMPRESSION PARALLEL TO GRAIN

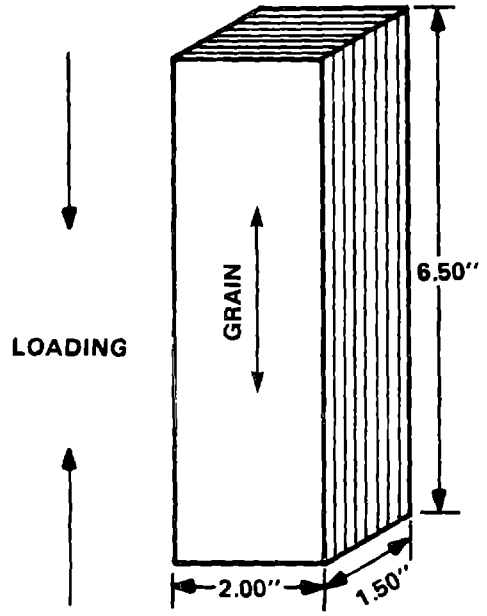

COMPRESSION PERPENDICULAR TO GRAIN

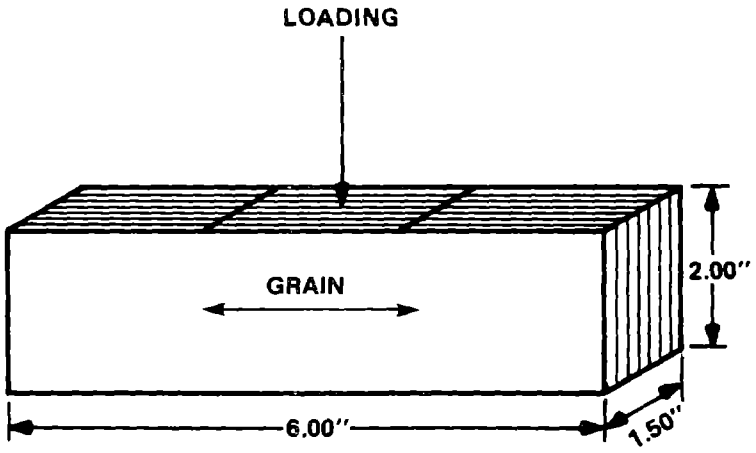

Figure 8-17 Specimens for Compression Parallel and Perpendicular to Grain

Table 8-14 Birch and FRP Compression Test Results

Quantity of Tests	Test Type	Test Temp. (°F)	FRP Type	Average Moisture Content (%)	Average Strength (psi)	Maximum/Minimum
5	Parallel	70	Epoxy	6.7	29,300	30,201/28,397
5	Parallel	104	Epoxy	6.2	28,202	31,294/24,826
5	Parallel	120	Epoxy	5.9	19,503	20,790/18,079
5	Parallel	70	Polyester	6.5	21,982	24,219/17,537
5	Parallel	104	Polyester	6.4	20,908	23,734/18,914
5	Tangential	70	Epoxy	6.1	18,940	19,612/17,914
5	Tangential	70	Polyester	6.0	16,325	16,707/15,964

8.1.2 PHASE B FATIGUE STRENGTH TESTING OF DOUGLAS FIR AND LAMINAE EPOXY

8.1.2.1 Introduction

The fatigue testing of laminated Douglas fir and West System® epoxy laminated material provides cyclic loading capabilities to supplement the static strength data compiled in the Phase A testing effort. The testing includes specimens made from blade grade 1 veneer, formerly known as A+ veneer, with a longitudinal Young's modulus of 2.45 x 10^6 psi or greater, and from blade grade 2 veneer, formerly Grade A/B, with a modulus between $2.1x10^6$ psi and $2.44x10^6$ psi. The testing was completed in two programs. Phase B1 testing was conducted at the GBI's facility in Bay City, MI, during the spring of 1982, and concentrated on low to medium cycle data. Phase B2 work was done at GBI, and at the University of Illinois in Urbana, IIT Research Institute in Chicago, Illinois and the University of Dayton. Phase B2 ran from May, 1982 to August, 1983.

8.1.2.2 Objectives

The Phase B testing program was developed to provide parallel to grain fatigue data in tension, compression and fully reversed loading, to supplement static strength data from the phase A program, described in section 8.1.1. All testing was conducted parallel to the grain and compared the two veneer grades in various load ratio tests. The effect of moisture content on fatigue strength was monitored by measuring each specimen for moisture content.

8.1.2.3 Description

The three basic types of fatigue loading are discussed separately in the following sections.

8.1.2.3.1 Compression Fatigue

The simplest specimens were those tested in compression fatigue, since gripping methods were not required. Each of the 51 samples was an 8 in. long, with a 2.25 in. diameter. The three center veneers had butt joints staggered on 3 in. centers, as shown in Figure 8-18 Four dogbone specimens, shown in Figure 8-19, were also tested in one time compression to failure. Of the 55 cylindrical samples, 30 were statically tested, and 21 were subjected to fatigue loading.

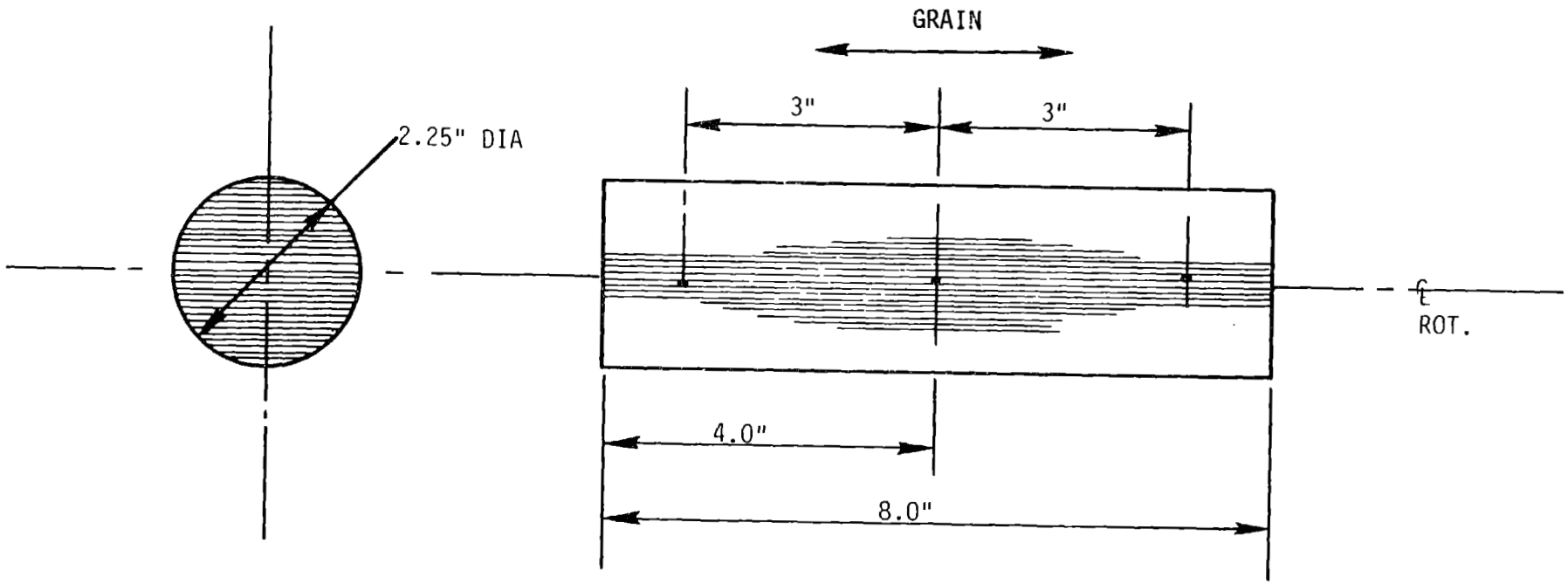

REF G.B.I DWG NO. C-9-054

Figure 8-18 Phase B1 Compression Test Specimen

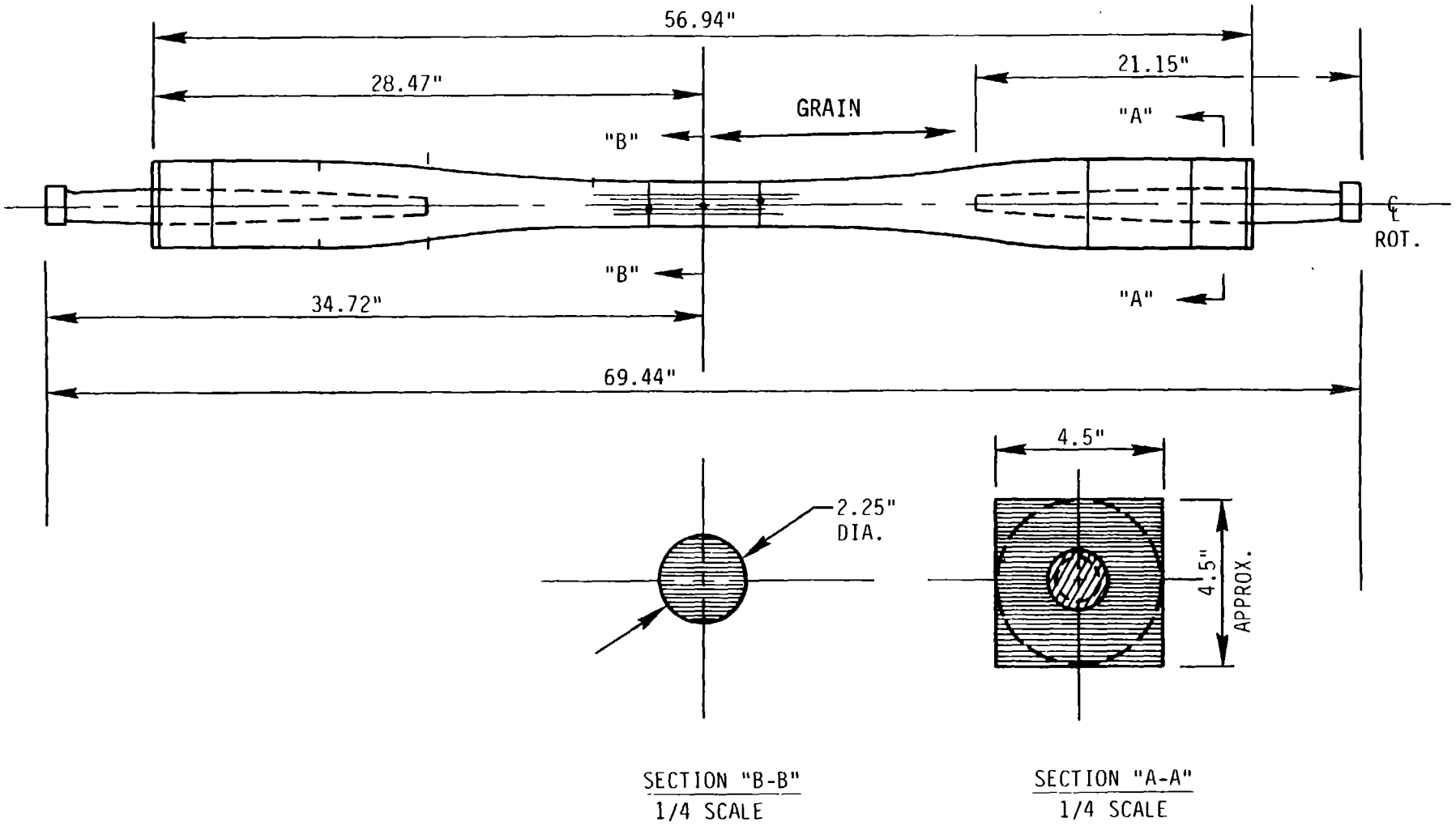

Figure 8-19 Phase B1 Dogbone-Style Test Specimen

The static tests provided information on sample strength, so that levels to be tested could be predicted, to provide representative fatigue life. Five samples were fatigue tested at a load ratio of 0.4 and 16 with a load ratio of 0.1. The load ratio, or R value, is the ratio of the minimum applied load to the maximum applied load. For example, a tension load between 70,000 lb and 7,000 lb. has an R value of 7,000/70,000=+0.1. A compression load load on the minimum side changes the sign: for 70,000 to -7,000 lb, R=-7,000/70,000=-0.1. A compresion-compression test has an R value greater than 1.0: for -7,000 to -70,000 lb, R=-70,000/-7,000 = +10. A fully reversed load test has an R value of -1: +70,000 to -70,000 lb, R=-70,000/70,000 = -1. Table 8-15 shows the summary of samples tested in this series of tests. The compression testing was done at GBI and at IITRI, in both cases using MTS load frames. The loading rate was on static tests and was aimed at achieving failure in five minutes. The test rate in fatigue was 5 Hz.

8.1.2.3.2 Tension Fatigue

The tension samples were the dogbone shown in Figure 8-18. Twenty-six were tested; seven were subjected to one time tension to failure, using a 5-minute load ramp. Table 8-15 shows the breakdown by load ratio.

The dogbone specimens contained a button head stud in each end, which mated with adapters in the test machines. The test section area was 6 in. long and 2.25 in. in diameter, latne cut about tne stud centers. The center section flaired out to a 4.25 in. diameter at each end of the 57 in. long specimen. The tension fatigue tests were conducted at a frequency of approximately 4 Hz.

8.1.2.3.3 Reverse Axial Fatigue

Twenty-two dogbone specimens were tested in reverse axial fatigue. Four braces were used during testing to provide lateral stability and prevent buckling of the specimen when subjected to compression loading. The supports functioned normal to the veneer plane only, because of the orientation of the specimens in the test machine. Testing was conducted at rates between 2.2 and 3 Hz. Sample number 1B5 contained one butt joint with a wide enough gap to allow the insertion of a thermocouple, which would permit measurement of the internal temperature during testing at 3 Hz. The finding was a rise of from 3.5 to 6°C above the ambient temperature (21°C). The test machine travel was limited, to prevent total destruction of the specimens at time of failure. Reverse axial fatigue testing was conducted at GBI and UDRI laboratories.

Table 8-15 Types and Quantities of Samples Tested in Phase B1 and B2 Research

	TENSION			COMPRESSION				
	Static Tension	Fatigue R = 0.1	Fatigue R = 0.4	Static Compression	Fatigue R = 0.1	Fatigue R = 0.4	REVERSE AXIAL Fatigue R = -1.0	Totals:
"Dogbones" Tested:								
BG-1	5	12	--	3	--	--	13	33
BG-2	2	5	2	1	--	--	9	19
Cylinders Tested:								
BG-1	--	--	--	18	13	2	--	33
BG-2	--	--	--	12	3	3	--	18
Column Totals:	7	17	2	34	16	5	22	103

8.1.2.4 Results

The results of the 103 tests that comprised this portion of the program are defined in the next three sections. The sample number indicates the billet with the first digits, and the letter and last digit indicate location. Billets 1 through 4 were a part of Phase B1 testing.

8.1.2.4.1 Compression Test Results

The results of 21 static compression tests on blade grade 1 veneer are shown in Table 8-16. The results indicate an average strength of 7,777 psi after adjusting strength of the laminae moisture content (LMC) to a rated wood moisture content of 12%. Thirteen static compression tests were conducted on blade grade 2 veneer. The results in Table 8-17 indicate a mean strength of 7,540 psi, after the adjustment for the wood moisture content of 12%. The fatigue test results for the two veneer grades are shown in Tables 8-18 and 8-19. This data is plotted in Figure 8-20. The straight line trend line is fitted to the blade grade 1 veneer results, using the least squares method. Table 8-20, and Figure 8-21, summarize the regression data for the three fatigue test groups, and for Douglas fir test data obtained by Kommers, of the Forest Products Laboratory in 1943. This data provided a fatigue trend line, which was previously used as a baseline for the MOD-5A evaluation. The plot of Figure 8-21 shows that it is parallel to the compression data gathered here, but significantly different from the tension and reverse axial trends.

8.1.2.4.2 Tension Test Results

Table 8-21 summarizes the results of seven static tests, which provided a mean strength of 11,065 psi, after the adjustment was made for the 12% moisture content. Table 8-22 presents the results of 13 fatigue tests on blade grade 1 veneer specimens and includes one sample that did not fail, even after 10 million cycles. The results of seven tests on blade grade 2 samples are presented in Table 8-23. The results of both sets of data are plotted in Figure 8-22, and are compared to other data in Figure 8-21 and Table 8-20.

Table 8-16 Static Compression Tests on Blade Grade 1 Veneer

STATIC COMPRESSION TESTS (5-Minute Ramp to Failure)
Test Program: MOD-5A, Phase B1, B2
Material: Laminated, Douglas Fir and Epoxy, Blade Grade 1 Veneer
Construction: 2.25 in. Diameter x 8-in. Long Cylinder, With 3 Transverse Butt Joints in Center Veneers, 3-in. Spacing
Load Direction: Compression Parallel to Grain
Temperature: 70°F

Sample No.	Test Site	Max Stress (psi)	LMC (%)	Max Stress Adjusted to 12% W.M.C. (psi)
1C3	GBI	-10,168	5.3	-7,526
2A6	GBI	-10,224	5.1	-7,468
3A4	GBI	- 9,608	5.7	-7,303
4A4	GBI	- 9,960	5.8	-7,621
3B4**	GBI	-10,332	5.9	-7,958
4B1**	GBI	9,574	6.0	-7,423
11A3	GBI	- 8,317	8.3	-7,511
11A5	GBI	- 8,170	8.6	-7,527
11C2	GBI	- 8,421	10.1	-8,570
11C4	GBI	- 8,371	8.5	-7,661
12A1	GBI	- 7,895	9.2	-7,569
12A2	GBI	- 8,070	8.5	-7,386
12A5	GBI	- 8,070	8.5	-7,386
12C1	GBI	- 8,095	8.8	-7,557
12C4	IITRI	- 8,525	6.3	-6,743
13A1	GBI	- 9,102	8.7	-8,441
13A4	GBI	- 9,296	8.3	-8,396
13C1	GBI	- 9,273	8.0	-8,210
13C2	GBI	- 9,198	8.9	-8,644
13C4	GBI	- 8,747	8.1	-7,796
11B2**	GBI	- 8,413	10.2	-8,619
			Average:	-7,777

** Dogbone Shaped Specimen, With 3 Transverse Butt Joints in Center Veneers, 3 in. Spacing

Table 8-17 Static Compression Tests on Blade Grade 2 Veneer

STATIC COMPRESSION TESTS (5-Minute Ramp to Failure)
Test Program: MOD-5A, Phase B1, B2
Material: Laminated, Douglas Fir and Epoxy, Blade Grade 2 Veneer
Construction: 2.25 in. Diameter x 8-in. Long Cylinder, With 3 Transverse Butt Joints in Center Veneers, 3-in Spacing
Load Direction: Compression Parallel to Grain
Temperature: 70°F

Sample No.	Test Site	Max Stress (psi)	LMC (%)	Max Stress Adjusted to 12% W.M.C. (psi)
8A1**	IITRI	- 7,791	7.6	-6,717
8A2**	IITRI	- 7,975	10.0	-8,062
8A3	GBI	- 8,239	8.3	-7,441
8A5	GBI	- 8,210	8.1	-7,317
9A1	GBI	- 8,500	9.4	-8,258
9A2	GBI	- 8,624	9.3	-8,323
10A3	GBI	- 9,352	7.1	-7,800
10A5	GBI	- 9,426	7.2	-7,914
10B2+	GBI	- 8,513	6.9	-7,007
17A1	GBI	- 9,257	6.7	-7,519
17A3	GBI	- 9,057	6.5	-7,259
17C2	GBI	- 9,089	6.2	-7,141
17C4	GBI	- 9,239	6.2	-7,259
			Average:	-7,540

** Rate, approximately 1.5 times (73 lbf/sec) too fast
+ "Dogbone" shape specimen, with 3 transverse butt joints in center veneers, 3-in. spacing

Table 8-18 Fatigue Tests on Blade Grade 1 Veneer

COMPRESSION FATIGUE TESTS @ 5 Hz ++
Test Program: MOD-5A, Phase B1, B2
Material: Laminated, Douglas Fir and Epoxy, Blade Grade 1 Veneer
Construction: 2.25-in. Diameter x 8-in. Long Cylinder, With 3 Transverse Butt Joints in Center Veneers, 3-in. Spacing
Load Direction: Compression Parallel to Grain
Temperature: 70°F

Sample No.	Test Site	Stress Ratio (R Value)	Min. Stress (psi)	Max. Stress (psi)	Total Cycles	LMC (%)	Max Stress Adjusted to 12% W.M.C.* (psi)	Per Cent of Overall BG-1 Avg Static
1A2	GBI	0.1	- 900	-9,000	14,910	5.6	-6,796	87.4
2A2	GBI	0.1	- 850	-8,500	13,850	5.5	-6,376	82.0
1C4	GBI	0.1	- 850	-8,500	20,930	5.5	-6,376	82.0
1C5	GBI	0.1	- 800	-8,000	153,030	5.3	-5,922	76.1
2C3	GBI	0.1	- 750	-7,500	82,720	5.3	-5,552	71.4
3A5	GBI	0.1	- 750	-7,500	518,430	5.2	-5,515	70.9
1C2	GBI	0.1	- 750	-7,500	549,720	5.4**	-5,552	71.4
4A5	GBI	0.1	- 750	-7,500	2,351,000	4.5	-5,265	67.7
11C3	IITRI	0.1	- 650	-6,500	303,000	5.6	-4,908	63.1
11C5	IITRI	0.1	- 540	-5,400	12,675,200+	5.6**	-4,077	52.4
12A3	IITRI	0.1	- 529	-5,285	10,593,000	6.1	-4,125	53.0
13A3	IITRI	0.1	- 597	-5,930	4,674,600	6.0	-4,598	59.1
13A5	IITRI	0.1	- 547	-5,474	3,031,200	5.5	-4,106	52.8
12C3	IITRI	0.4	-2,569	-6,423	8,751,600	6.2	-5,047	64.9
12C5	IITRI	0.4	-2,760	-6,900	4,019,400	6.3	-5,458	70.2

** Estimated
+ Specimen unfailed as of cycle total listed
++ Samples tested at GBI were run at 10 Hz, except for Sample 1A2 at 8 Hz

Table 8-19 Fatigue Tests on Blade Grade 2 Veneer

COMPRESSION FATIGUE TESTS @ 5 Hz IIT Research Institute, Chicago, IL
Test Program: MOD-5A, Phase B1, B2
Material: Laminated, Douglas Fir and Epoxy, Blade Grade 2 Veneer
Construction: 2.25 in. Diameter x 8-in. Long Cylinder, With 3 Transverse Butt Joints in Center Veneers, 3-in. Spacing
Load Direction: Compression Parallel to Grain
Temperature: 70°F

Sample No.	Test Site	Stress Ratio (R Value)	Min. Stress (psi)	Max. Stress (psi)	Total Cycles	LMC (%)	Max Stress Adjusted to 12% W.M.C. (psi)	Per Cent of Overall BG-2 Avg Static
8A4	IITRI	0.1	- 584	-5,840	304,000	6.6	-4,712	62.5
9A3	IITRI	0.1	- 565	-5,650	1,360,000	6.8	-4,620	61.3
10A2	IITRI	0.1	- 667	-6,666	1,370,000	6.3	-5,273	69.9
10A1	IITRI	0.4	- 742	-7,417	61,200	6.3	-5,867	77.8
10A4	IITRI	0.4	- 742	-7,417	1,120,000	6.1	-5,789	76.8
17A2	IITRI	0.4	- 730	-7,300	4,229,051	5.4	-5,439	72.1

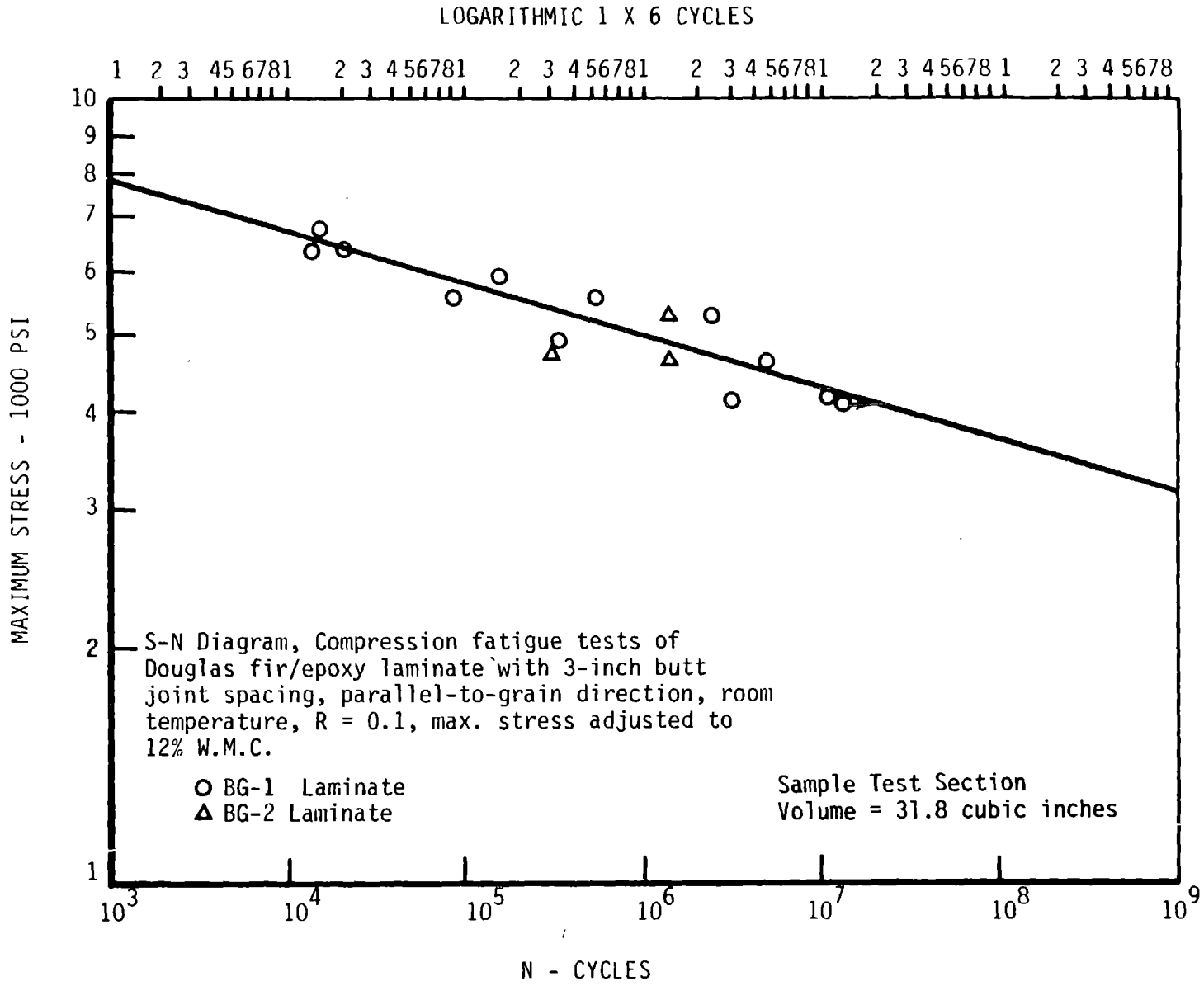

Figure 8-20 S-N Diagram, Compression Fatigue Tests

Table 8-20 Regression of Data from Various Fatigue Tests

	Total BG 1 Data Points	Correlation Coefficient of Linear Regression Line	Equation of Linear Regression Line	Max Stress Intercept of Linear Regression Line @ 10^4 Cycles (psi)	Max Stress Intercept of Linear Regression Line @ 10^9 Cycles (psi)
Tension Fatigue (R=0.1):	11	-0.8012	$S=19,329 \times N^{-0.0840}$	8,919	3,392
Compression Fatigue (R=0.1):	12	-0.9070	$S=12,286 \times N^{-0.0653}$	6,732	3,174
Reverse Axial Fatigue (R=-1):	10	-0.9811	$S=10,361 \times N^{-0.0870}$	4,650	1,708
Kommers (R=-1) Reverse Axial Flexural Fatigue	424*	-0.9600	$S=11,437 \times N^{-0.0692}$	7,100	2,720

*Kommers samples consisted of solid Douglas fir, not laminae

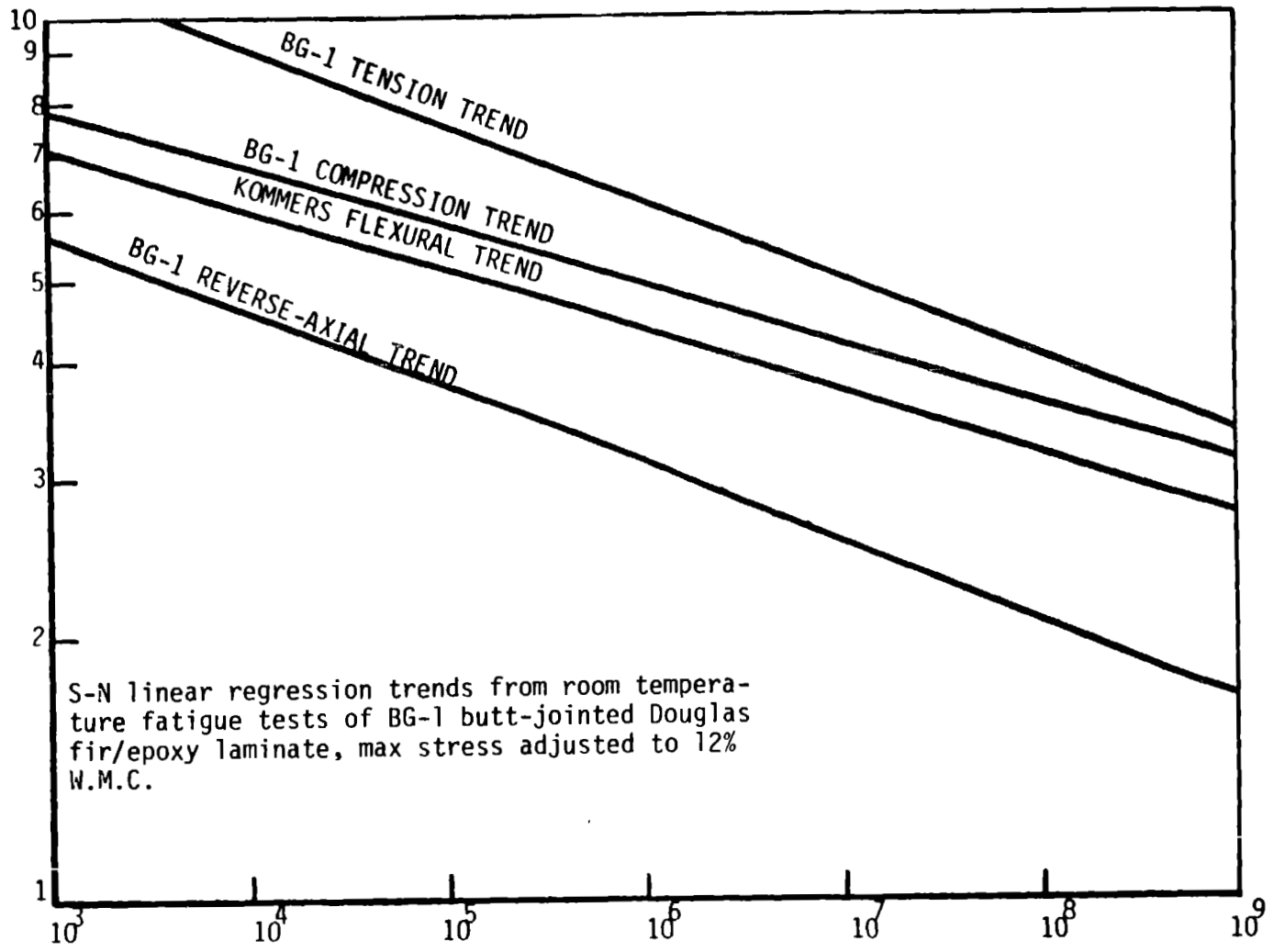

Figure 8-21 S-N Linear Regression Trends

Table 8-21 Summary of Static Tests

Static Tensile Tests (5-minute ramp to failure) Gougeon Brothers, Inc., Bay City, MI
Test Program: MOD-5A Phase B1, B2
Material: Laminated, Douglas Fir and Epoxy
Construction: Dogbone Shaped Specimen, with 3 Transverse Butt Joints in Center Veneers, 3-in Spacing
Load Direction: Tension Parallel to Grain
Temperature: 70°F

Sample No	Test Site	Veneer Grade	Max Stress (psi)	LMC (%)	Max Stress Adjusted to 12% W.M.C. (psi)
1B2	GBI	BG-1	10,841	5.5	9,967
2B3	GBI	BG-1	11,287	5.8	10,438
11B4	GBI	BG-1	12,195	9.2	12,046
12B4	GBI	BG-1	11,267	8.9	11,064
13B3	GBI	BG-1	12,363	6.0	11,477
8B4	GBI	BG-2	10,028	7.4	9,566
9B4	GBI	BG-2	13,187	8.7	12,900
		Average:	11,065		

Table 8-22 Fatigue Tests on Blade Grade 1 Veneer

TENSION FATIGUE TESTS University of Illinois, Urbana, IL
Test Program: MOD-5A, Phase B1, B2
Material: Laminated, Douglas Fir and Epoxy, Blade Grade 1 Veneer
Construction: Dogbone Shaped Specimen with 3 Transverse Butt Joints in Center Veneers, 3-in. Spacing
Load Direction: Tension Parallel to Grain
Temperature: 70°F

Sample No.	Test Site	Stress Ratio (R Value)	Cycle Rate (Hz)	Min Stress (psi)	Max Stress (psi)	Total Cycles	LMC (%)	Max Stress Adjusted to 12% W.M.C. (psi)
1B3	GBI	0.1	4.0	850	8,500	21,450	5.8	7,860
1B1	GBI	0.1	4.0	850	8,500	111,910	5.6	7,830
3B3	GBI	0.1	4.0	800	8,000	429,570	5.7	7,384
4B4	GBI	0.1	4.0	750	7,500	922,390	5.6	6,909
2B2	GBI	0.1	4.5	750	7,500	138,960	6.0	6,963
3B1	GBI	0.1	4.5	750	7,500	1,148,940	6.1	6,976
12B2	U I	0.1	4.0	580	5,800	845,800	6.7**	5,458
12B3	U I	0.1	4.0	710	7,098	206,500	6.5	6,654
12B5	U I	0.1	4.0	473	4,732	6,718,300	5.6	4,359
13B1	U I	0.1	4.0	620	6,200	2,450,000	5.2	5,667
13B2	U I	0.1	4.0	519	5,192	10,000,000+	4.4	4,673
13B2	U I	0.1	4.0	600	6,000	1,470,500	4.4	5,400
13B5	U I	0.1	4.0	779	7,789	59,400	5.5	7,161

** Estimated, caused by error in testing WMC
+ Specimen unfailed as of cycle total listed

Table 8-23 Fatigue Tests on Blade Grade 2 Veneer

TENSION FATIGUE TESTS University of Illinois, Urbana, IL
Test Program: MOD-5A, Phase B1, B2
Material: Laminated, Douglas Fir and Epoxy, Blade Grade 2 Veneer
Construction: Dogbone Shaped Specimen with 3 Transverse Butt Joints in Center Veneers, 3-in. Spacing
Load Direction: Tension Parallel to Grain
Temperature: 70°F

Sample No.	Test Site	Stress Ratio (R Value)	Cycle Rate (Hz)	Min Stress (psi)	Max Stress (psi)	Total Cycles	LMC (%)	Max Stress Adjusted to 12% W.M.C. (psi)
8B5	U I	0.1	4.0	642	6,419	493,000	6.5	6,017
9B1	U I	0.1	4.0	778	7,780	210,600	9.2	7,685
9B2	U I	0.1	4.0	712	7,120	1,285,300	7.6	6,818
9B3	U I	0.1	1.5	850	8,500	97,300	8.6	8,299
9B5	U I	0.1	3.0	850	8,500	67,500	9.4	8,428
8B2	U I	0.4	4.0	2,864	7,160	316,900	6.4	6,699
8B1	U I	0.4	4.0	2,869	7,166	14,200	6.4	6,704

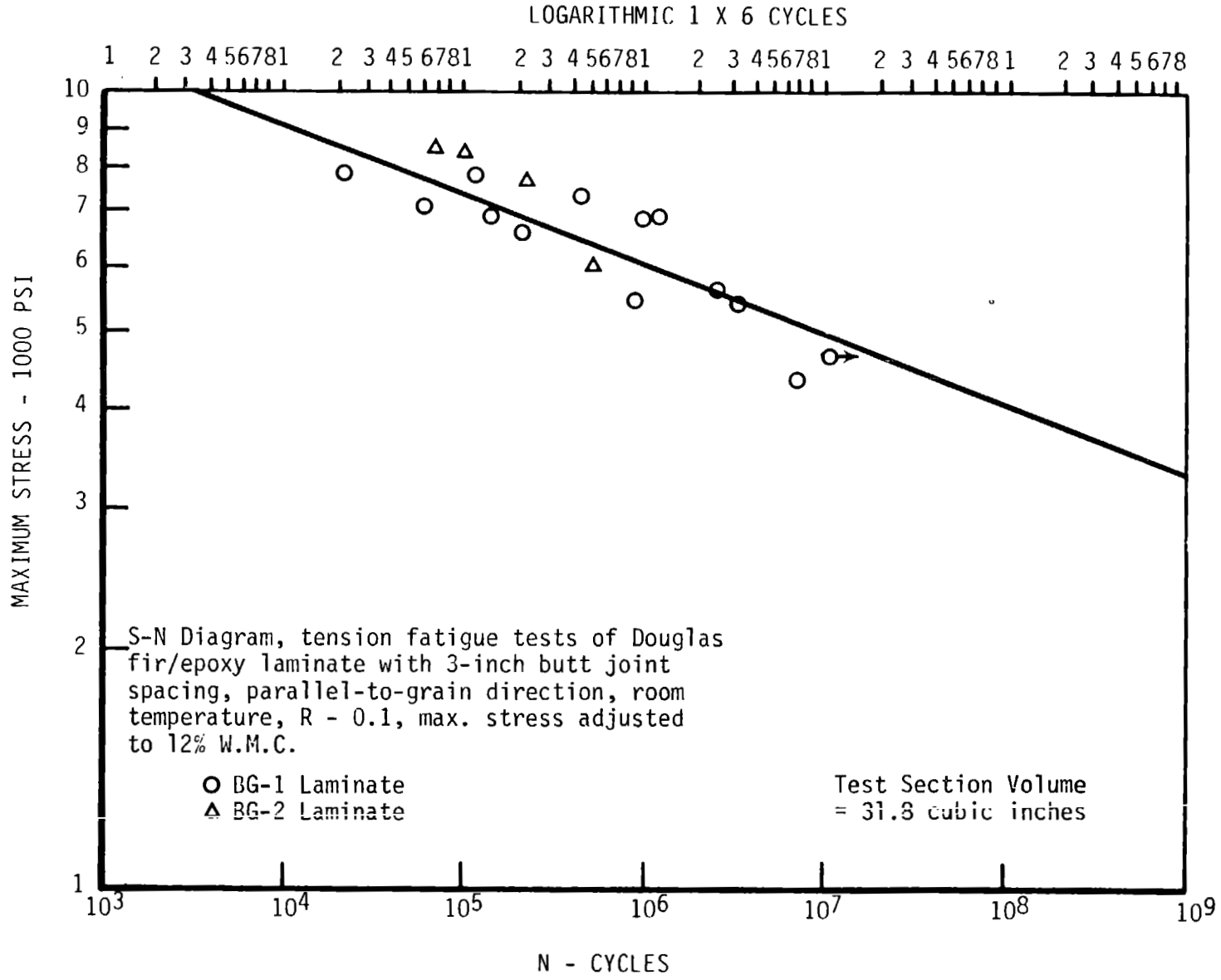

Figure 8-22 S-N Diagram, Tension Fatigue Tests

8.1.2.4.3 Fully Reverse Results

The load levels selected for this set of tests were based on the tension and compression test results. Blade grade 1 testing included 16 samples, seven of which lasted more than one million cycles, and one of which lasted longer than 23 million cycles, as shown in Table 8-24. Table 8-25 presents test results for blade grade 2 veneer samples; five of 15 lasted more than one million cycles. Figure 8-23 shows the trend of the data and Table 8-20 and Figure 8-21 include this data in their comparisons.

Table 8-24 Fully Reversed Loading, Blade Grade 1

REVERSE AXIAL TENSION-COMPRESSION FATIGUE TESTS
Test Program: MOD-5A, Phase B1, B2
Material: Laminated, Douglas Fir and Epoxy, Blade Grade 1 Veneer
Construction: Dogbone Shaped Specimen, With 3 Transverse Butt Joints in Center Veneers, 3-in. Spacing
Load Direction: Reverse Axial Tension-Compression Parallel to Grain
Temperature: 70°F
Stress Ratio (R Value): -1.0

Sample No.	Test Site	(Hertz) Cycle Rate	Max. Tension Stress (psi)	Max. Compression Stress (psi)	Total Cycles	LMC (%)	Max Compressive Stress Adjusted to 12% W.M.C. (psi)	Per Cent of Overall BG-1 Compr Static Avg
4B3	GBI	2.2	7,500	-7,500	2,360	5.2	-5,515	70.9
3B2	GBI	2.2	7,000	-7,000	3,060	6.4	-5,574	71.7
2B1	GBI	2.2	6,000	-6,000	2,450	6.2	-4,714	60.6
1B4	GBI	2.2	5,000	-5,000	227,650	5.3	-3,701	47.6
4B5	GBI	2.2	4,500	-4,500	138,710	5.7	-3,420	44.0
4B2	GBI	2.2	4,500	-4,500	551,940	5.6	-3,398	43.7
3B5	GBI	2.5	4,000	-4,000	632,470	6.3	-3,164	40.7
11B1	UDRI	3.0	3,400	-3,400	8,262,200	5.5	-2,550	32.8
11B5	GBI	3.0	3,500	-3,500	5,926,310	6.3	-2,768	35.6
1B5	GBI	3.0	3,200	-3,200	23,672,280	5.1	-2,337	30.1
11B3	GBI	3.0	2,662	-2,662	10,292,050+	5.7	-2,023	26.0
11B3*	GBI	3.0	3,500	-3,500	4,079,940	5.7	-2,660	34.2
12B1	UDRI	3.0	2,602	-2,602	10,000,000+	5.9	-2,004	25.8
12B1*	UDRI	3.0	4,000	-4,000	895,000	5.9	-3,081	39.6
13B4	GBI	3.0	3,200	-3,200	9,964,820+	4.9	-2,307	29.7
13B4*	UDRI	3.0	4,000	-4,000	728,800	4.9	-2,883	37.1

+ Specimen unfailed as of cycle total listed

* Test extended at higher load levels.

Table 8-25 Fully Reversed Loading, Blade Grade 2

REVERSE AXIAL TENSION-COMPRESSION FATIGUE TESTS
Test Program: MOD-5A, Phase B1, B2
Material: Laminated, Douglas Fir and Epoxy, Blade Grade 2 Veneer
Construction: Dogbone Shaped Specimen, With 3 Transverse Butt Joints in Center Veneer, 3-in. Spacing
Load Direction: Reverse Axial Tension-Compression Parallel to Grain
Temperature: 70°F
Stress Ratio (R Value): -1.0

Sample No.	Test Site	(Hertz) Cycle Rate	Max. Tension Stress (psi)	Max. Compression Stress (psi)	Total Cycles	LMC (%)	Max Compressive Stress Adjusted to 12% W.M.C (psi)	Per Cent of Overall BG-2 Compr Static Avg
10B1	GBI	3.0	3,320	-3,320	698,500	6.9	-2,733	36.2
17B4	UDRI	3.0	3,500	-3,500	4,764,600	5.4	-2,608	34.6
17B1	UDRI	3.0	4,700	-4,700	204,600	6.0	-3,644	48.3
17B5	UDRI	3.0	3,700	-3,700	2,635,700	6.1	-2,888	38.3
10B3**	GBI	2.7	4,500	-4,500	175,030	5.5	-3,375	44.8
10B4**	GBI	3.0	4,000	-4,000	479,280	5.5	-3,000	39.8
10B5**	GBI	2.5	5,000	-5,000	44,620	5.7	-3,801	50.4
17B3	UDRI	3.0	4,700	-4,700	10,000+	5.5	-3,525	46.8
17B3	UDRI*	3.0	3,700	-3,700	100,000+	5.5	-2,775	36.8
17B3	UDRI*	3.0	3,100	-3,100	1,000,000+	5.5	-2,325	30.8
17B3	UDRI	3.0	3,700	-3,700	2,138,300	5.5	-2,775	36.8
17B2	UDRI	3.0	3,100	-3,100	1,000,000+	6.0	-2,404	31.9
17B2	UDRI*	3.0	3,700	-3,700	100,000+	6.0	-2,869	38.1
17B2	UDRI	3.0	4,700	-4,700	150,700	6.0	-3,644	48.3

** Specimen contains only 2 transverse butt joints in center veneers instead of 3 due to machining error
+ Specimen unfailed as of cycle total listed
* Test extended at higher load levels.

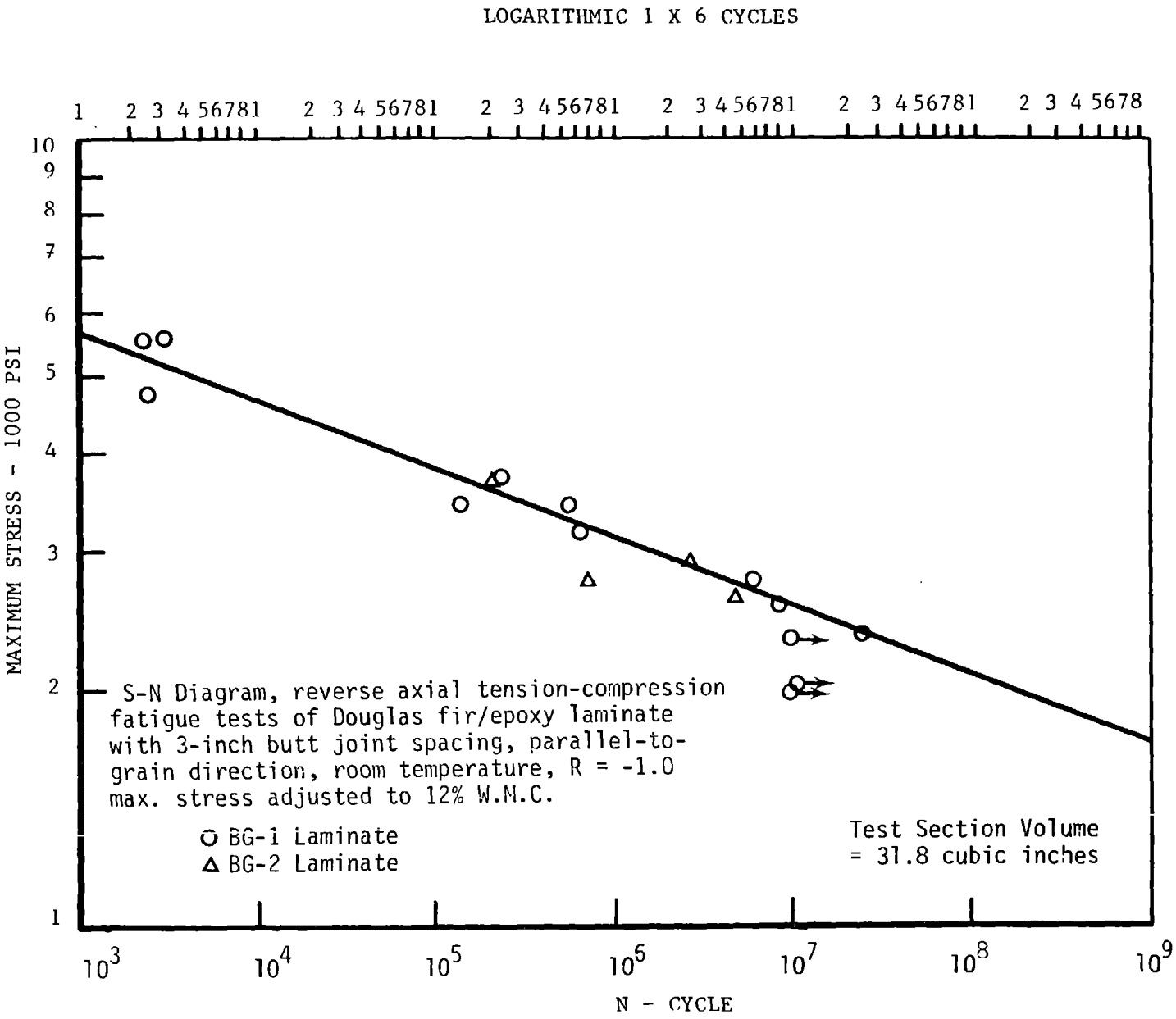

Figure 8-23 S-N Diagram, Reverse Axial Tension-Compression Fatigue Tests

8.1.3 FILLED EPOXY TEST PROGRAM

8.1.3.1 Introduction

Testing was performed on two types of West System® filled epoxy. GBI holds the trademark and distributes the product. The materials are proprietory so formulation data is not available. Based on these tests and on process evaluations, the asbestos-filled thixotropic epoxy (206-ASB) was selected over the carbon-filled thixotropic epoxy (206-CFS) for use in the MOD-5A blade assembly. However, in late 1983 GBI decided that government regulations concerning personnel safety were too stringent to allow the asbestos filler to be used in the MOD-5A. GBI was also concerned that the material would be harder to obtain.

The carbon-filled material was too viscous to be used in applications that required coverage of large surface areas, GBI developed another carbon-filled epoxy that would satisfy all requirements. The tests of this material (X-216-CFW) are not reported here, since it was not funded by GE. The tests were performed on these epoxies:

West System® asbestos-filled thixotropic epoxy 206-ASB

West System® carbon-filled thixotropic epoxy 206-CFS
(The tests of these adhesives are reported in this section.)

West System® modified thixotropic epoxy X-216-CFW
(This epoxy is used in joining finger joints of the finger joint process demonstration unit - see section 8.2.1)

8.1.3.2 Objectives

This test series determined properties of the two thixotropic epoxies for the MOD-5A program. Strength and fatigue capabilities and thermal properties were of interest for applications throughout the blade. Epoxy serves as the adhesive and filler material for bonding the Douglas Fir laminae. Thixotropic epoxy was used as a void filler, a fillet material and as an adhesive for bonding metal parts to the wood structure. These test results played a key role in the selection of asbestos-filled thixotropic epoxy.

The thixotropic materials were tested independently of other blade materials, such as wood, glass fiber and steel, so that the properties of the epoxies could be compared. The unfilled West System® epoxy was tested as a component of the wood composite.

8.1.3.3 Description

The tests described in this report include the determination of density, tension, compression, torsional shear, shear fatigue, heat deflection temperature and thermal expansion. Table 8-26 summarizes the tests.

Table 8-26 Matrix of Tests

	NUMBER OF TEST SPECIMENS								
MATERIAL	ASBESTOS-FILLED EPOXY					CARBON-FILLED EPOXY			
TEST TEMPERATURES (°F)	-40	R.T.	90	100	120	-40	R.T.	90	100
DENSITY	-	3	-	-	-	-	3	-	-
TENSION	10	10	5	5	9	10	10	5	5
COMPRESSION	10	10	5	5	10	10	10	5	5
TORSIONAL SHEAR	9	10	5	5	10	10	10	5	5
SHEAR FATIGUE	-	9	-	-	-	-	8	-	-
HEAT DEFLECTION TEMPERATURE	6 (R.T. TO APPROX. 120°F)					3 (R.T. TO APPROX. 120°F)			
THERMAL EXPANSION	3, APPROX.					4, APPROX.			

R.T. = Room Temperature

A. Static Tests - For the tension, compression and torsional swear tests, the load calibration was checked before testing, or at least daily, by dead weight loading. Strain in the tension and compression tests was measured by extensometers, which were calibrated before use by a precision micrometer calibration device.

1. Tension Tests - The tensile test method was basically that of ASTM-D638-67T and used the "Type I" specimen of that method. The specimen was 8.5 in. long, 2 in. longer than the minimum, to provide better gripping.

   The "Instron" universal test machines, with 10,000 and 20,000 lb. capacities were used in the tension tests. They were operated at a fixed cross-head speed of 0.10 in. per minute.

   For tests above or below room temperature, forced convection test chambers were employed. The temperature of the specimen was checked by a thermocouple taped to its surface. Since room and test chamber humidities were controlled by the building's air-conditioning, the specimens were tested immediately after they were removed from the conditioning chamber. However, the relative humidity in the laboratory was close to 50%.

2. Compression Tests - The compression test method was basically that of ASTM-D695-63T. The test specimens were right circular cylinders, 0.50 in. in diameter and 1.00 in. long. These specimens are one of the preferred specimens, according to ASTM-D695-63T.

   The same Instron universal test machines were used for the compression tests, but they were set up for compressive loading instead of tension. The tests were run at a cross-head speed of 0.05 in. per minute. Both load-strain and lead-time curves were recorded. Tests above or below room temperature were conducted in the same manner as the tension tests.

3. Torsional Shear Tests - There is no satisfactory ASTM method for testing torsional shear properties of polymer or other materials. ASTM-D1043-61T is inadequate. ASTM-E143-61 is better, but can only be used at room temperature. A procedure, which has been used on metals, plastics and composites, is given in USAF Specification No. S-133-1140 (22 November, 1978) for carbon-carbon composites. Although GE wrote this specification, the specimen was developed by the Southern Research Institute (SRI). For the MOD-5A program, the specimen was based on the SRI design, but the heads were 0.25 in. longer than the SRI specimen. The shorter heads of the SRI specimens had created some minor problems, mainly in fatigue testing.

   The rate of twisting the specimen was adjustable. The rate of 2 to 5% shear strain per minute was used. Torque in these tests was measured by a torsional load cell, which was calibrated by dead weights applied to a lever arm of known length. Strain gages were used for strain measurement.

   Torque was recorded as a function of strain. This data was reduced to a shear stress versus shear strain curve. Data analysis assumed linear-elastic behavior, although the assumption is really not valid, except in the early stages of loading. Techniques for handling non-linear behavior are available, however.

   Test temperature and humidity considerations were comparable to those of tension and compression testing, hence, the earlier discussions apply.

B. Torsional Shear Fatigue - An electrohydraulic tester capable of load, strain or deflection control was used in the torsional shear fatigue tests. The hydraulic ram, hydraulic controls and electronics of this machine were made by Instron. The machine was basically for tension and compression, but a fixture that converted ram motion to torsion was built.

Torsional fatigue tests were run at room temperature under load control conditions. The ratio of minimum to maximum torque was C.35. The initial stresses were based upon the static test results. The stresses were less than the static strength of the material, but estimated to be high enough to result in failure in a fairly short time.

In the static torsion tests on the asbestos-filled epoxy, at 120°F, the material was so rubber-like that the specimens did not fail even under high strains. These unfailed specimens were then used to check the operation of the fatigue test set-up. The machines could operate at a frequency of 15 Hz at fairly high loads, so this frequency was adopted for the tests. At least two of the used specimens were fatigued until they failed, to provide data used to choose initial stress conditions. Once a fatigue failure was achieved, test conditions were based on the previous tests, and the static tests.

C. Heat Deflection Temperature - The standard procedure for measuring heat deflection temperature is given in ASTM-D648. This test followed the standard procedure, for the most part, including the use of a mineral oil bath. However, this test used special calibration "T" thermocouples, a temperature recorder and a calibrated linear variable differential transducer to record deflection. The tests were run at a stress of 264 psi. Deflections were recorded and plotted as a function of the mV output of the thermocouple in contact with the specimen.

D. Thermal Expansion Measurements - Thermal expansion measurements in the temperature range of -180°F to +600°F were made in a fused silica dilatometer, which was heated at a rate of about 3.6°F per minute (2.0°C/min) after it was cooled to near liquid nitrogen temperature. Thermal expansion was measured by a Linear Variable Differential Transducer. Temperatures were measured by a T thermocouple in contact with the specimen. An X-Y recorder was used to plot the output of the linear variable differential transducer as a function of the thermocouple output.

The glass transition temperature, T_g, is most often determined by thermal expansion or contraction measurements. Actually, T_g is not a transition at all, but the temperature at which the internal viscosity of the material reaches a particular value. Usually, the material starts at a high temperature and cools slowly. For some polymers, particularly thermosetting types, such as epoxies and phenolics, this set-up is not possible since the apparent T_g is generally above the cure temperature and is affected by temperatures above the cure temperature. In running thermal expansion tests, T_g is indicated by a change in the slope of the thermal strain vs. temperature curve. The expansion measurements started, therefore, at a low temperature (near liquid nitrogen temperature). The temperature was increased at about 3.6°F per minute until the curve showed that the temperature was well above T_g.

When the tests were planned, it was not certain whether this method would yield an accurate measure of T_g. The method did not yield an accurate measurement, but for all practical purposes, the estimated value was probably adequate, and agreed with the heat deflection temperature.

E. Density Measurements - Density measurements were not in the original test matrix, but were requested shortly after the specimens were received. Densities were measured by weighing specimens in air and in water, with a precision balance. The calculation of the density took the water temperature (24.0°C) into consideration, and its density at that temperature. Three specimens of each material were measured.

F. Sampling Procedure - The instructions that accompanied the first specimens of asbestos-filled epoxy indicated that the specimens should not be tested until 14 days after the date on each pack. There were seven dates for torsion specimens, six dates for compression specimens, and eight dates for tension specimens. Presumably the specimens were prepared in a series of small batches, and the date indicated casting date. Since all specimens were cured at room temperature, the 14 days was to complete the cure. Since batch-to-batch variations were expected, each batch of each type of specimen was distributed as evenly as possible across the range of

test temperatures to avoid confusing temperature effects with batch variation effects. Because the number of specimens of a given type from a batch tested at a given temperature was very small, no significant batch-to-batch variation was detected, except in the thermal expansion of carbon-filled epoxy. This case is discussed in the section on thermal expansion.

The following observations resulted from an inspection of the specimens:

Tensile specimens were cast as sheets, approximately 1/8 in. thick, and machined to shape. Only the thin edges were machined surfaces.

Compression specimens were cast as rods with a 0.5 in. diameter. The rods were cut to length and the ends machined flat. Torsion specimens were cast as square rods and were cut to length. The ends, gage section and fillets were machined. These specimens had a much greater area of machined surface, compared to others.

Thermal expansion specimens were cast as rods with a .25 in. diameter. The rods were then cut to length. Only the ends were machined.

Heat deflection temperature specimens were cast as flat sheets, .25 in. thick. There appeared to have been some slight machining of one surface of the sheet (probably to obtain uniform thickness), after which the bars were cut out. This cutting was not particularly clean; the edges of most of these specimens were chipped. Most of the specimens contained voids in a wide range of sizes, apparently because the mix was not deaerated. These voids were not apparent on the cast surfaces, which were very smooth, although close examination of these surfaces sometimes indicated that subsurface voids were present. The voids were obvious on the machined surfaces, and on fracture surfaces of tested specimens. Since the torsion specimens had the greatest percentage of machined surface, the voids were largest and most obvious on these specimens.

8.1.3.4 Test Results

A. Density - The results of density measurements are given in Table 8-27. The density of the asbestos-filled epoxy was about 3.5% higher than that of the carbon-filled epoxy.

The difference in density was caused by the difference in filler densities. The carbon density was about 1.8 g./cm.$^{-3}$, and the asbestos density was about 3.3 g./cm.^{3} . For these densities a volume of filler of about 2.6% for the epoxy density of about 1.096 g. /cm^{-3} would result in the difference in density of the filled epoxies.

On the other hand, if the weight fraction of filler was constant, the asbestos-filled epoxy would have the higher density because of the smaller volume of asbestos for a given weight. If this was the case, then the weight percent of fiber would be near 12% and the density of the epoxy would be roughly 1.06 g./cm^{-3}.

This kind of speculation might seem purposeless. Later, data showed that the carbon-filled epoxy showed greater strength. If the volume fraction of fibers was constant, the greater strength could suggest that the carbon fibers were longer. However, if the weight percent was the same, there would be more carbon fibers, which would have the same result. Since no formulation data was available, this kind of speculation helped to interpret the test results.

Table 8-27 Density (g/cm^3) Measurements

SPECIMEN NUMBER	ASBESTOS FILLED	CARBON FILLED
1	1.1534	1.1144
2	1.1552	1.1134
3	1.1524	1.1150
AVERAGE	1.1537	1.1143
STANDARD DEVIATION (σ)	0.0014	0.0008

B. Heat Deflection Temperature - The results of heat deflection temperature measurements are given in Table 8-28. The average heat deflection temperature for carbon-filled epoxy is 6.7°F higher than that of the asbestos-filled epoxy. The data compares well with the glass transition temperature, determined by thermal expansion methods to be between 110°F and 114°F for the asbestos-filled epoxy and between 113°F and 117°F for the carbon-filled epoxy.

C. Tensile Measurements - The average results of tensile measurements on the two materials are given in Table 8-29 and typical traces are shown in Figures 8-24 and 8-25.

The strengths of the two materials are essentially the same at -40°F, but the variation with temperature is quite different. The strength of the carbon-filled epoxy was less sensitive to temperature. At 100°F the strength of the carbon-filled epoxy was about 71% of the strength at -40°F, whereas the strength of asbestos-filled epoxy dropped to about 26%. In the case of modulus, the carbon-filled epoxy starts with about a 53% higher modulus at -40°F and retains 67% of this modulus at 100°F, while the asbestos-filled epoxy retains about 36%.

Table 8-28

Heat Deflection Temperatures (°F)

(Applied Stress = 264 psi)

SPECIMEN NO.	ASBESTOS FILLED EPOXY	CARBON FILLED EPOXY
1	108.7	115.0
2	105.4	114.6
3	109.0	115.0
4	108.4	-
5	110.5	-
6	107.4	-
AVERAGE	108.2°F	114.9°F
STANDARD DEVIATION	1.7	0.23

Table 8-29 Mean Value Summary of Asbestos and Carbon Filled Epoxy Tests

		TEMPERATURE								
	UNITS	-40°F		RT		90°F		100°F		120°F
FILLER		ASBESTOS	CARBON	ASBESTOS	CARBON	ASBESTOS	CARBON	ASBESTOS	CARBON	ASBESTOS
Density	gm/cm^3	-----	------	1.1537	1.1143	----	----	---	----	----
Heat Deflection	°F	-----	------	108.2	114.9	----	----	----	----	----
Tension										
Max Stress	psi	6,530	6600	4550	5950	3580	5450	1710	4710	776
Max Strain	%	1.21	0.79	1.76	1.03	2.0	1,07	5.0	----	19.6
Modulus	Ksi	590	900	420	740	362	650	212	605	30.9
Compression										
Max Stress	psi	------	18,750	----	8830	6170	7630	2920	5240	----
Yield Stress	psi	19,600	------	7020	----	----	----	----	----	----
Modulus	Ksi	587	562	400	559	293	512	173	418	62.5
2% Strain	psi	------	------	----	----	----	----	----	----	528
5% Strain	psi	------	------	----	----	----	----	----	----	792
10% Strain	psi	------	------	----	----	----	----	----	----	1125
Stress @ 25% Strain	psi	----	----	7100	----	----	----	----	----	----
Yield Strain	%	7.02	6.59	3.29	2.54	3.62	2.41	3.81	2.12	----
Torsional Shear										
Max Stress	psi	4180	4160	4350	4710	3220	4320	3040	3290	----
Max Strain	%	1.8	1.6	4.4	3.7	----	----	----	----	----
2% Strain	psi	----	----	----	----	----	----	----	----	152
5% Strain	psi	----	----	----	----	----	----	----	----	237
10% Strain	psi	----	----	----	----	----	----	----	----	324
Modulus	Ksi	241	274	162	196	127	182	125	162	10.1
Yield Strain	%	----	----	----	----	7.7	4.0	9.2	3.8	----

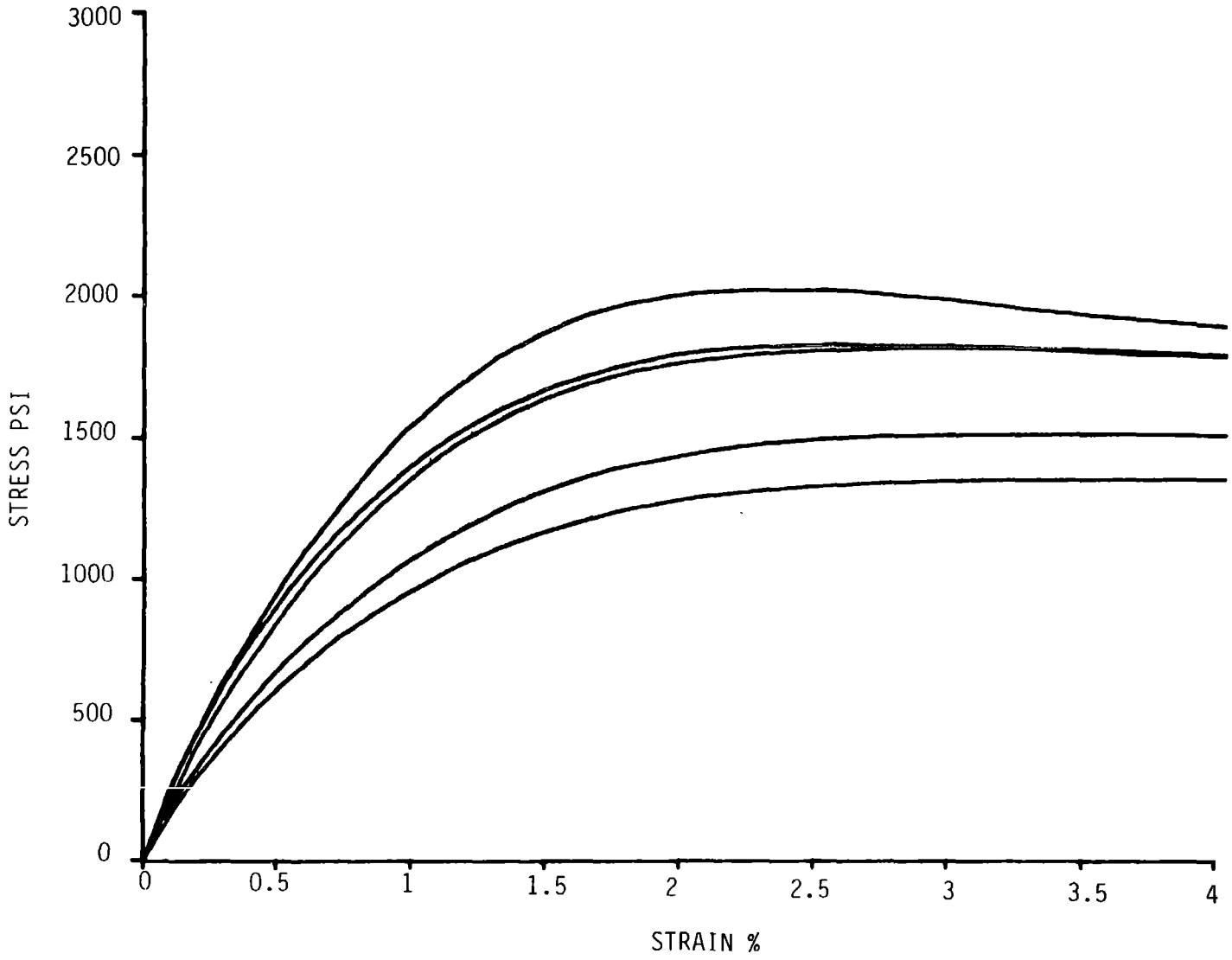

Figure 8-24 Asbestos Epoxy Tensiles at 100°F

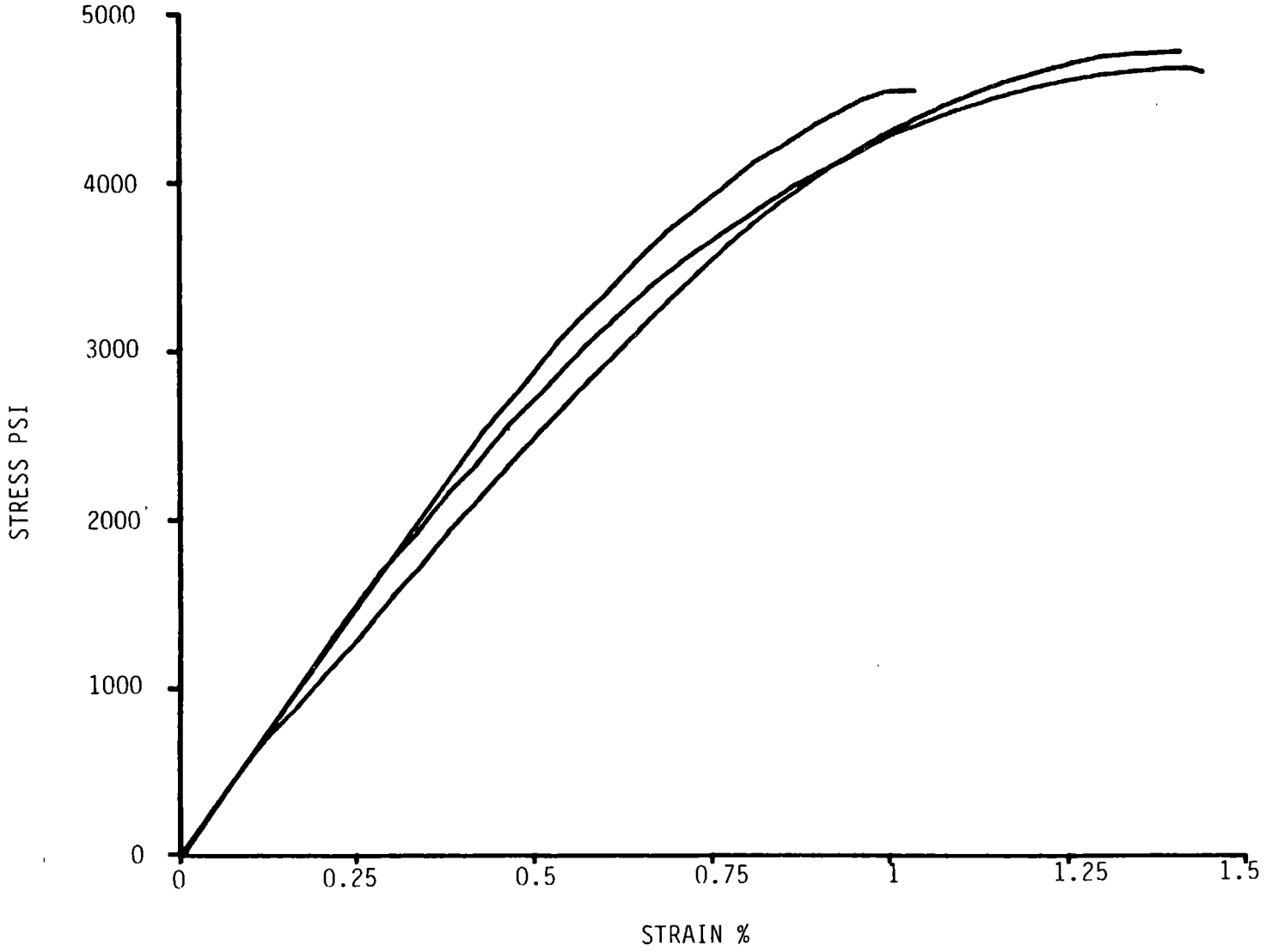

Figure 8-25 Carbon Epoxy Tensile at 100°F

D. Compression Measurements - The average results of compression measurements are given in Table 8-29 and in Figures 8-26 and -27. Except for a few tests at -40°F, the compression specimens did break. Instead, the specimen deformed to strains greater than would be of any interest in most structures. Except for the tests at 120°F on the asbestos-filled epoxy, the specimens showed a yield, (or a maximum, after which the stress decreased with increasing strain. In some cases, as with the asbestos-filled epoxy at room temperature, the load eventually started to increase, and for asbestos-filled epoxy at room temperature, got back up to about the yield stress at about 25% strain. At this high strain, however, the cross-section of the specimen had increased considerably, so that stresses based on the actual cross-section would be considerably less than those based on the initial cross-section.

The specimens withstood higher compressive stresses than tensile stresses, particularly at -40°F. At -40°F the asbestos-filled epoxy was slightly stronger than the carbon-filled epoxy, though in the tensile case they were very nearly the same. As with the tensile case, the carbon-filled epoxy retained its strength better as the temperature was increased, but the difference between the two materials was not as great. For example, in tension at 100°F the strength of the asbestos-filled epoxy was about 36% that of the carbon-filled epoxy, whereas in compression at 100°F it was about 56%.

The modulus of the asbestos epoxy at -40°F is essentially the same under compression and tension. As temperature was increased to 100°F, however, the compression modulus was lower than the tensile modulus. This effect could be a strain rate effect since polymers tend to become more rate sensitive as T_g is approached, and while the strain rates in tension and compression should have been close, based on dimensions and cross-head speeds, there probably was some difference in strain rate. The problem with this hypothesis is that the lower rate would be expected in the tensile test because of the deformation in the specimen fillets and the lower tensile moduli.

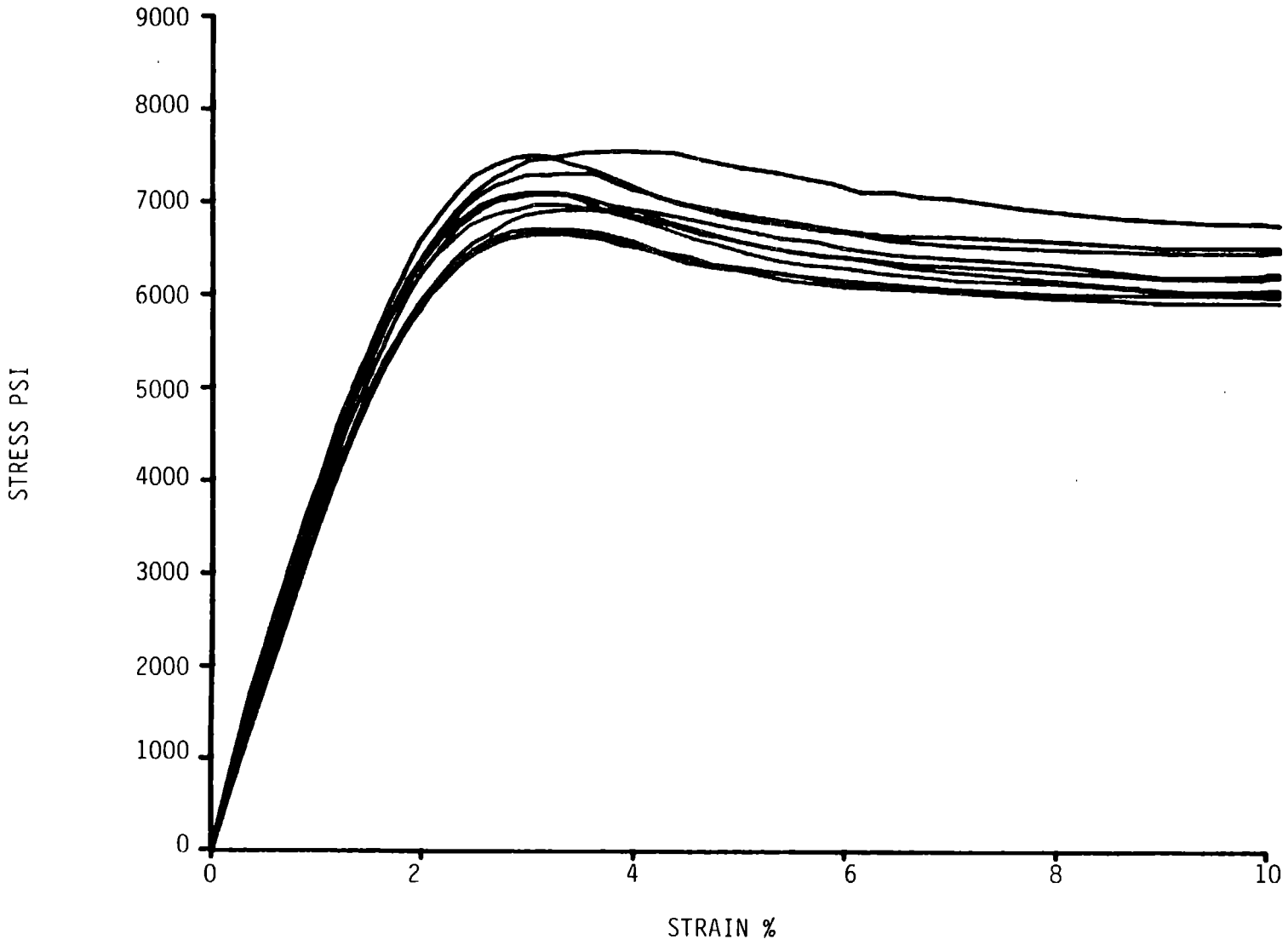

Figure 8-26 Asbestos Epoxy Compression R.T.

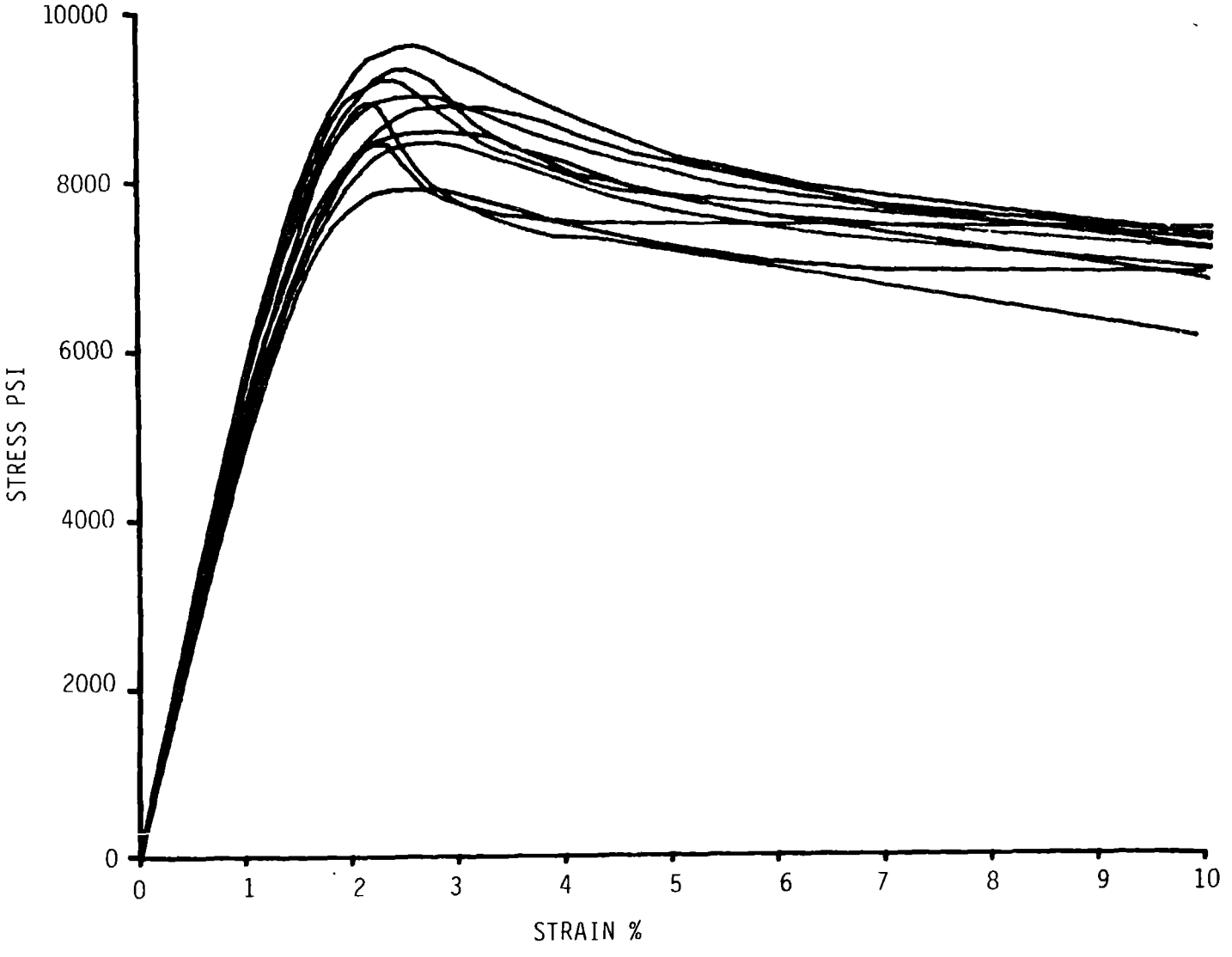

Figure 8-27 Carbon Epoxy Compression R.T.

Considering the carbon-filled epoxy, there was a significant difference between tensile and compressive moduli. This differences suggested that the material is anisotropic, which be expected from a fibrous filler. Again, the fact that it appeared to be much more anisotropic than the asbestos-filled epoxy could be due to a higher volume of fiber or the greater fiber length or both. If so, the degree of anisotropy could differ among specimen types, depending on how the material was cast.

E. Torsional Shear - The average results of torsional shear measurements are given in Table 8-29 and in Figures 8-28 and 8-29. The two materials are similar in strength at -40°F and the carbon-filled epoxy retains its strength better at elevated temperatures. The shear strength was highest at room temperature.

F. Torsional Shear Fatigue - The results of the torsional shear fatigue tests are given in Table 8-30 and in Figures 8-30 and 8-31.

There were small voids in all of the fatigue specimens, and in most cases, probably medium and large voids as well. Fatigue failures generally seemed to originate at a void. The size and distribution of voids affected fatigue life, so considerable scatter could be expected at any stress level. If the materials had been deaerated to eliminate voids, the fatigue performance would undoubtedly have been better.

The data showed that there was little difference between the fatigue performance of the two materials, as shown in Figure 8-32.

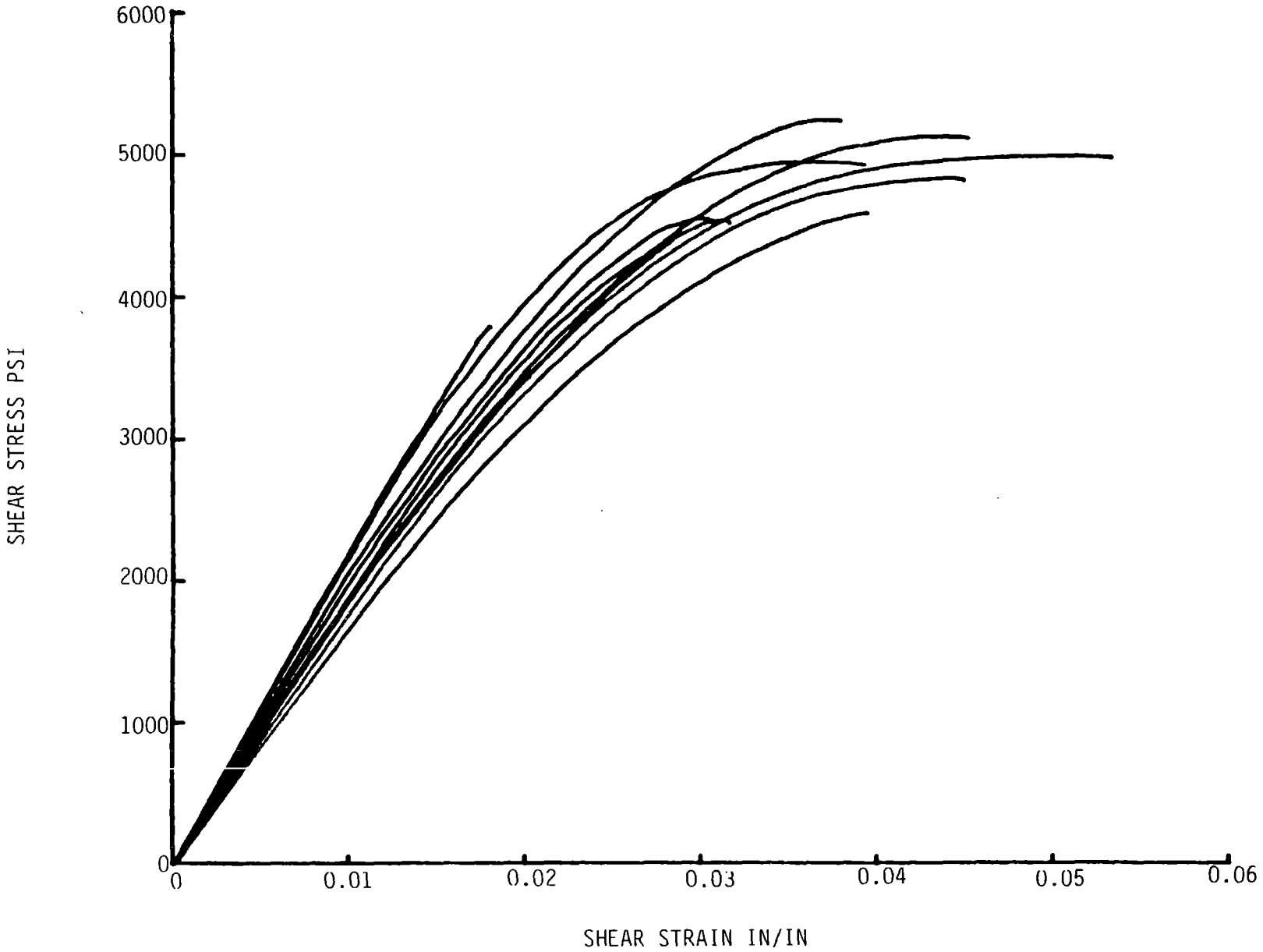

Figure 8-28 Carbon Epoxy Torsional Shear at R.T.

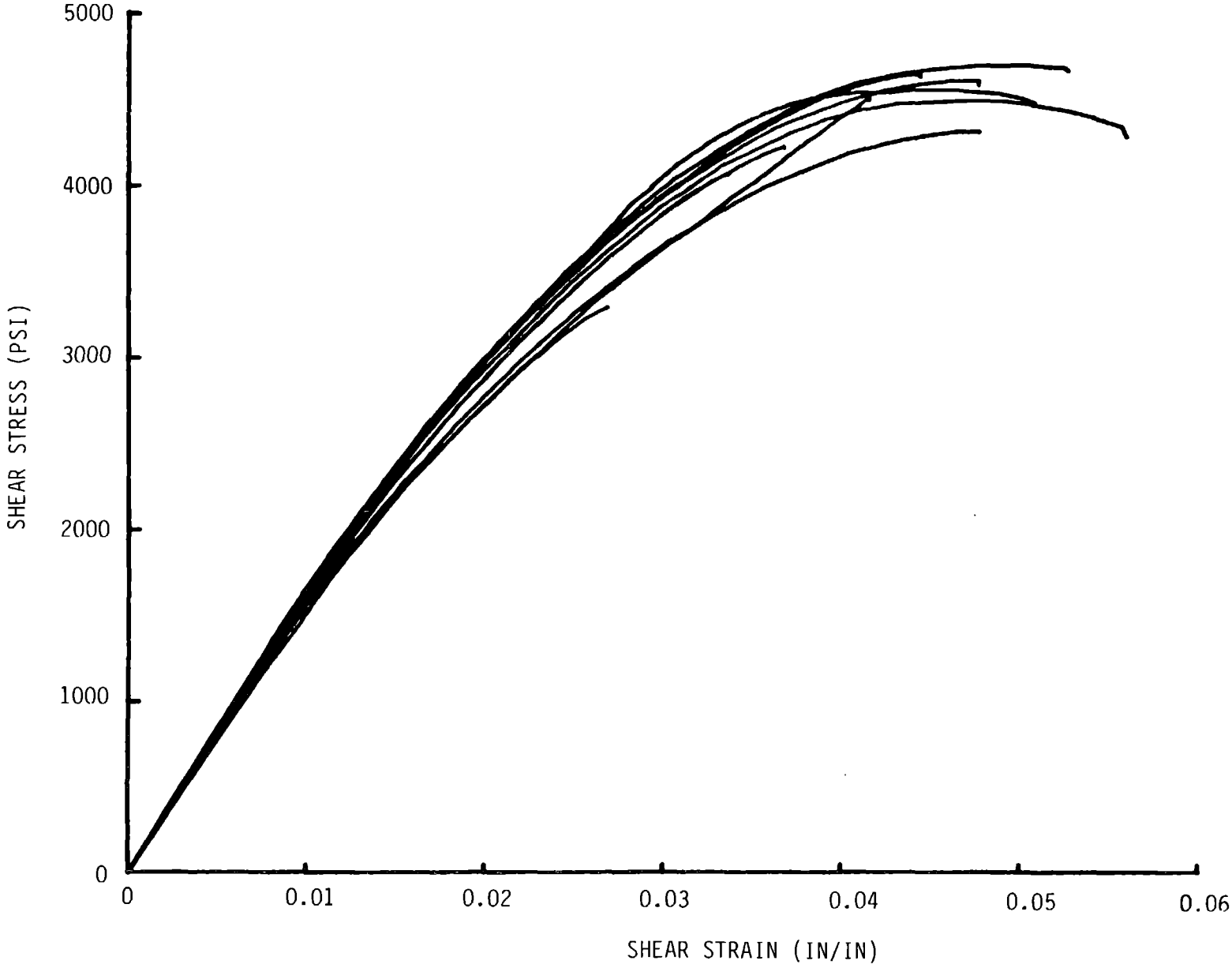

Figure 8-29 Asbestos Epoxy Torsional Shear at R.T.

Table 8-30 Asbestos Epoxy Fatigue

SPECIMEN	PEAK STRESS (PSI)	CYCLES TO FAILURE
33	3024	160
9	3006	26,560
37	2515	5,080
29	2511	91,560
41	1997	786,100
16	1996	1,587,270
25	1806	774,820
18	1703	6,452,140
5	1503	10,000,000

ROOM TEMPERATURE
FREQUENCY = 15 Hz
R = 0.35

CARBON EPOXY FATIGUE

SPECIMEN	PEAK STARESS (PSI)	CYCLES TO FAILURE
15	2872	8,640
32	2700	7,800
40	2613	269,514
7	2401	203,990
16	2390	426,576
24	2250	309,954
23	2100	1,834,200
8	1850	686,292

ROOM TEMPERATURE
FREQUENCY = 15.0 Hz
R = 0.35

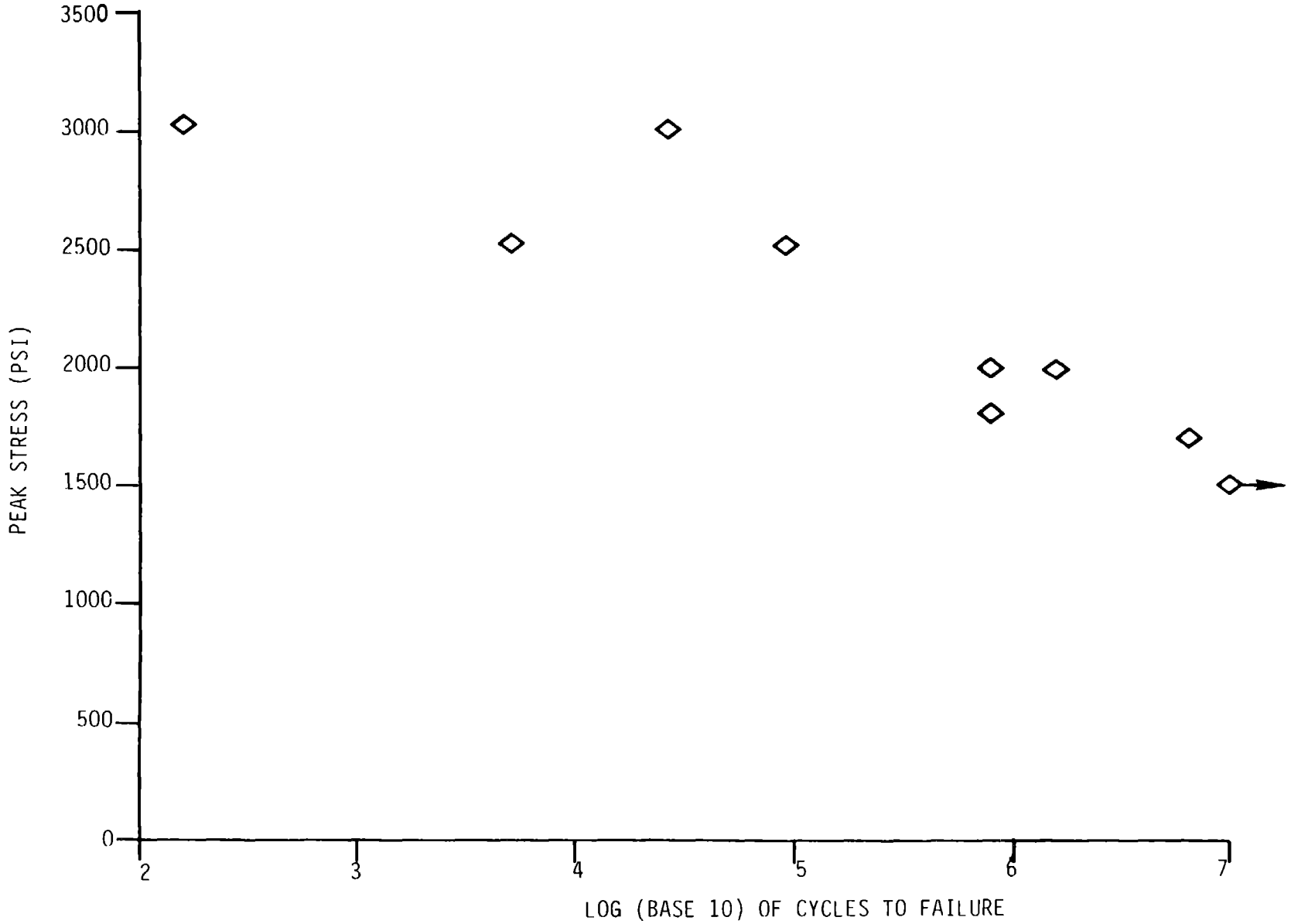

Figure 8-30 Shear Fatigue Asbestos Epoxy R = 0.35

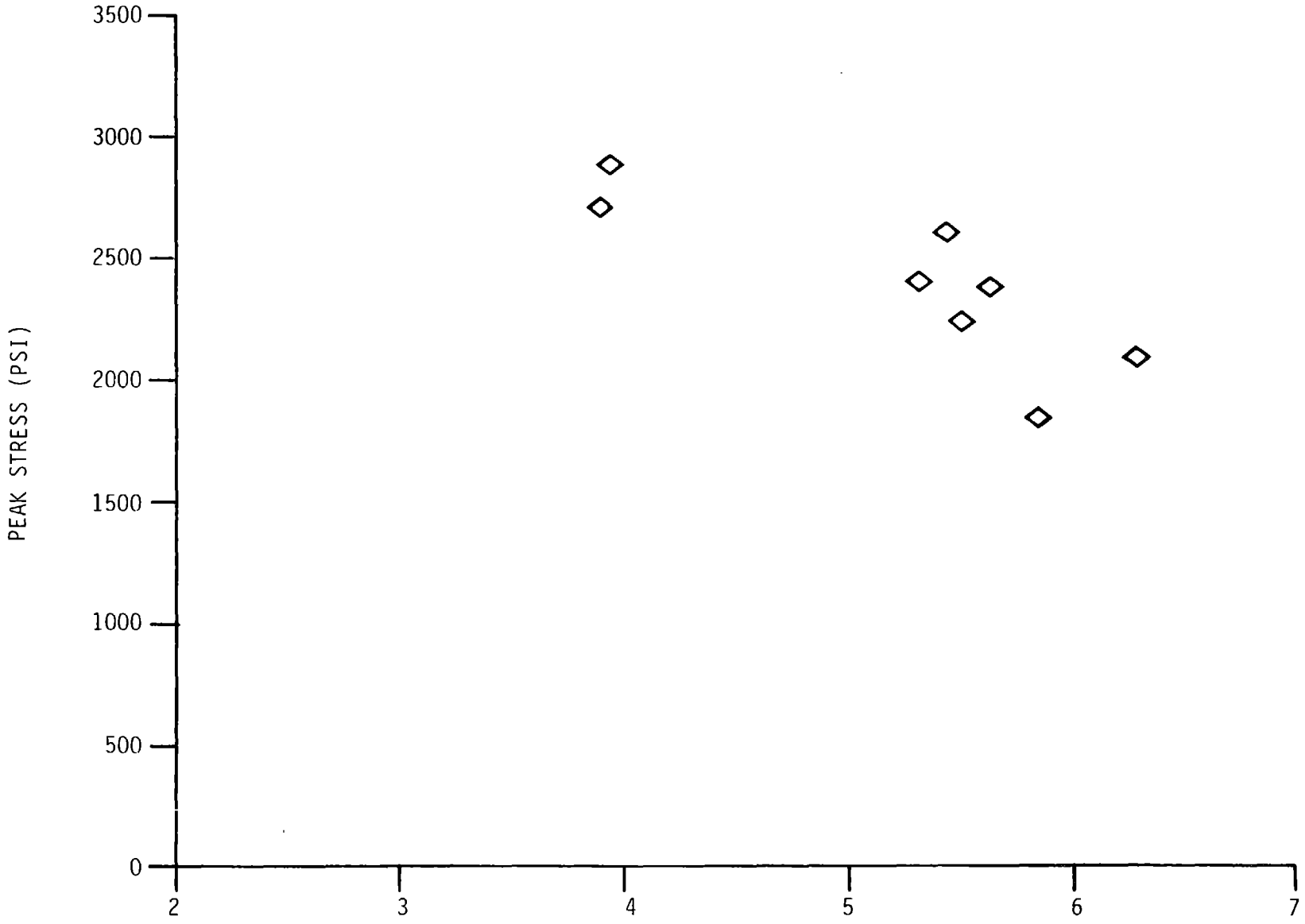

Figure 8-31 Shear Fatigue Carbon Epoxy R = 0.35

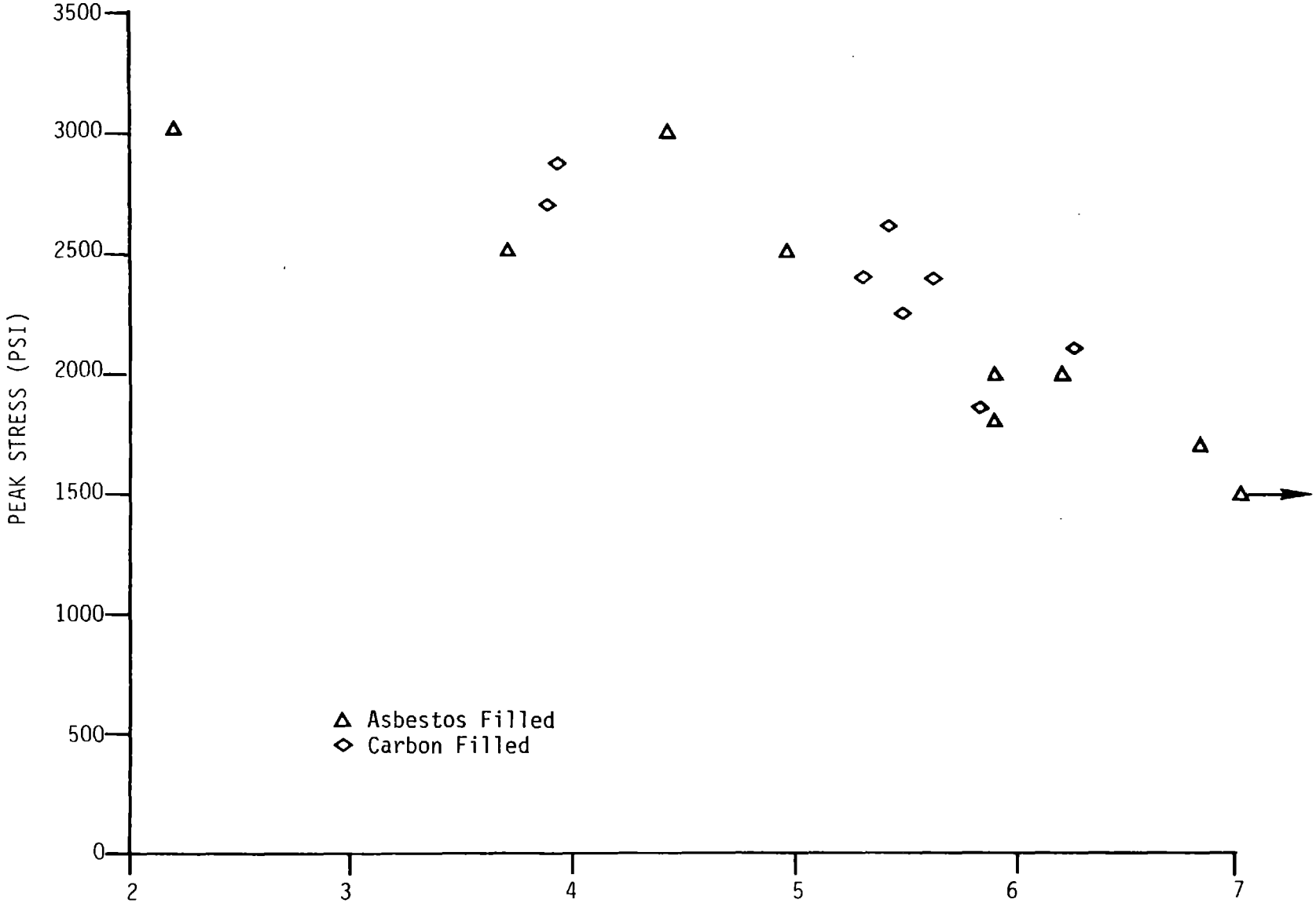

Figure 8-32 Comparison of Fatigue Results

G. Thermal Expansion Measurements - The results of the thermal expansion measurements on the asbestos-filled epoxy are shown in Figure 8-33. Note that the expansion peaked at about 107°F, then contracted slightly, and then there was further expansion. This behavior made it impossible to use the usual method for calculating the T_g. However, the behavior suggested T_g was in the region between 110°F and 115°F.

The results of measurements on the carbon-filled epoxy are shown in Figure 8-34. Of the first three specimens tested, specimens #1 and #2 did not show the same kind of behavior as the asbestos-filled epoxy, but #3 did. This result prompted the testing of Specimen #4, which behaved like #3. It was noted that specimens #1 and #2 were dated 7/6, whereas #3 and #4 were dated 7/2. At first the difference in behavior was attributed to batch-to-batch variation, but additional measurements of material that had been exposed to elevated temperature showed that the behavior of specimens #1 and #2 was typical of material that had been exposed to temperatures of about 110°F to 120°F. Thus, the data for these two specimens did not represent material cured at room temperature.

POST CURE EFFECTS

Several short experiments were conducted to determine whether a post-cure treatment might affect the strength of the asbestos-filled epoxy. Several torsional shear specimens of the asbestos-filled epoxy were still available. They were tested at 120°F, without rupturing, although they experienced rather large strains. Three of these used specimens were tested at room temperature and demonstrated strengths of 3701, 4156 and 4897 psi (average = 4251 psi). Three additional specimens were post-cured overnight at 140°F and then tested at room temperataure. These specimens had strengths of 4555, 4572 and 5002 psi (average = 4710 psi). The virgin material had an average room temperature strength of 4350 psi. The strengths of the virgin material ranged from 3300 to 4710 psi with a standard deviation of 419 psi. This data showed that the post-cure had

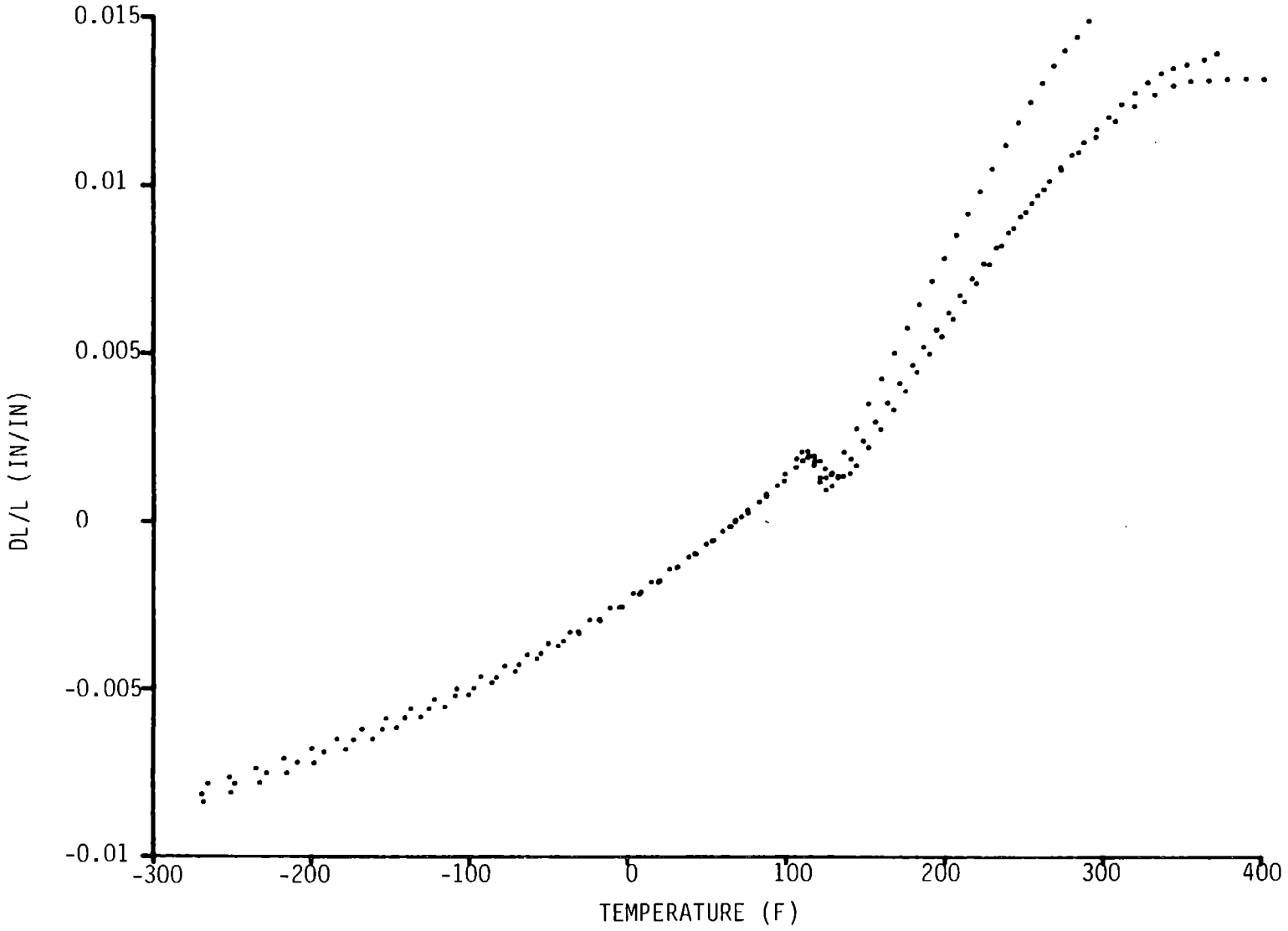

Figure 8-33 Thermal Expansion Asbestos Epoxy

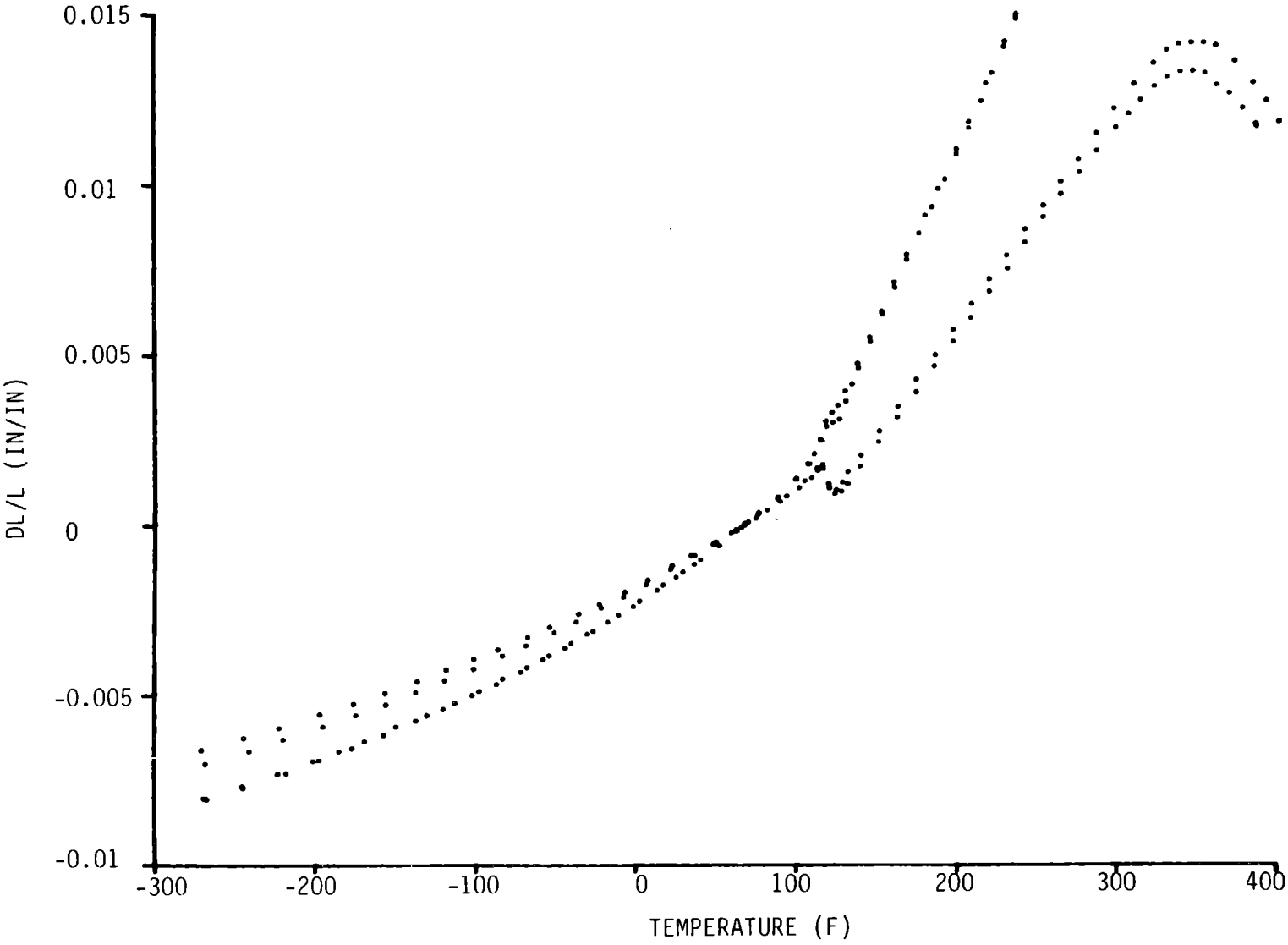

Figure 8-34 Thermal Expansion Carbon Epoxy

little, if any, effect on shear strength. However, the post-cured specimen may have suffered some damage as a result of the original tests, so this data may not be valid.

As a further check, the asbestos-filled bars for the heat deflection temperature tests were post-cured overnight at 140°F and then tested for flexure. These specimens showed strengths of 6660 and 7040 psi, with a mean of 6850 psi. This value is significantly higher than the tensile strength, which was 4550 psi, but this comparison may not be meaningful as the flex can be much less sensitive to internal flaws.

8.1.4 SCARF JOINT TESTING

8.1.4.1 Introduction

In commercially available wood veneer products, two types of joints at veneer ends are common. The ends of the sheets are either overlapped a short distance, or they are butt-jointed. Butt joints almost always result in a small gap at the joint. The overlapping joint is successfully used in products that are bonded under high pressure, so that the increase in thickness at the joint is minimized under pressure during bonding. If these joints are staggered along the length, the finished product functions acceptably. GBI's blade production process does not lend itself to overlapping joints, however. Furthermore, butt joints were used in GBI's previous applications, and early in the MOD-5A program. The butt joint gaps can, at times, exceed 1/8 in., because of sheet end waviness and layering tolerances. In some instances, the epoxy does not fully seal the gap. The butt joint gap interrupts the continuity of the wood fiber and reduces the strength of the wood member. The reduction in strength cannot be determined as easily as it could be for materials of uniform strength, because of wood's imperfect structure and compliance. Previous testing indicated that butt joints reduce the strength of members, so GBI developed a method of scarfing sheet ends so that they could be reversed on each other and overlapped for the length of the scarf joint. The result is a joint that can transfer a load across the angled glue line, and prevent any sharply defined break in continuity.

The scarf joint static test program was conducted on relatively large samples, in order to provide some data on the effects of size, and a comparison of scarf and butt joints. The data presented on static strength was also used in section 8.1.6 to evaluate the affects of size. A scarf joint fatigue test program was conducted on standard dogbone-size samples, for use in the comparison of butt and scarf joints. The static test program evaluated the two joints and two spacings in three phases. The first phase tested 32 butt-jointed specimens, the second tested 32 specimens with butt or scarf joints on 3 in. centers, and the third phase tested 24 specimens with scarf joints on 3 or 6 in. centers.

8.1.4.2 Objectives

The test series provided a comparison of the static strengths of butt and scarf joints with two different staggered spacings, in a range of sizes. The joint is related to panel thickness, since a single ply would be more severely affected by a joint than a thicker panel with offset or staggered joints would be. All static test specimens were 1.5 in. thick, to maintain a consistent base for the comparison of results.

The scarf joints are more expensive because of the cutting operation and because more care in setting the overlap is required. If the strength, and consequently, the allowable stress levels are increased, the wood content could be decreased. The increased cost of the scarf joint would be offset by the decreased cost of wood. The number of tests was selected to be statistically significant for the joint evaluation, and for the study of size effects, defined in section 8.1.6.

8.1.4.3 Description

The butt joint test series was the first of three tests. These tests used 32 specimens manufactured from two billets of blade grade 1 Douglas fir veneer. Six sizes were used, as shown in Table 8-31. These specimens all contained butt joints staggered on 3 in. centers, as shown in Figure 8-35. Each veneer sheet was trimmed to 90 in. long for all billets in this series. The two billets were cut identically, to provide an equal number of samples, so that pallet to pallet variations could be studied. All edges and ends were sealed with West System® epoxy after cutting, and samples were shipped to Washington State University (WSU) in Pullman, Washington, for testing. A timber testing machine with adequate capacity for the 30 ft. length and a force capability of approximately 200,000 lb. was used. The gripping system used 24 in. long, hydraulically actuated jaws at each end of the machine. The jaws were lined with polyurethane sheets. Squeezing force was controlled independently of the axial force exerted. The machine contained an 11 x 17 in. plotter for recording force and displacement, which was read from an LVDT integrator into an extensometer of variable length. The extensometer attaches to the test specimen rather than to the machine heads. WSU also measured moisture content using samples cut from the failure area after the testing.

Table 8-31 Samples from Pallets 1 and 2 (All Butt Joints)

Quantity	Length (ft)	Width (in.)	Thickness (in.)
8	7	2	1.5
8	7	8	1.5
4	15	2	1.5
4	15	8	1.5
4	30	2	1.5
4	30	8	1.5

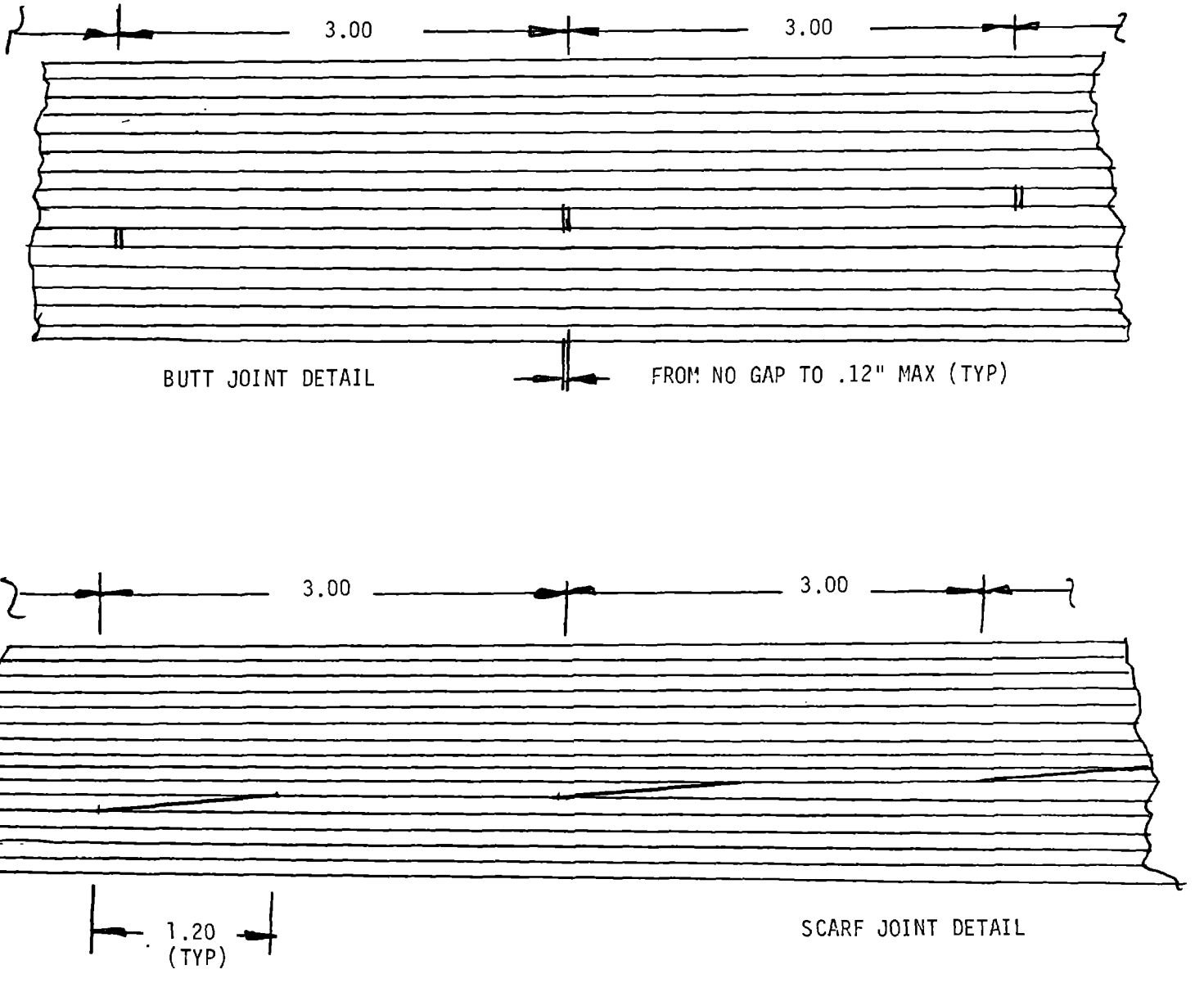

Figure 8-35 **Joint Details**

The second program compared 16 specimens each of butt and scarf joints, all on 3 in. staggered centers, as shown in Figure 8-35 and Table 8-32. The samples were prepared and tested at WSU using the same equipment described previously.

The third phase provided additional data on the scarf joint since the strength of the scarf joint proved to be superior to that of the butt joint in the previous comparison. Billets 4 and 5 were prepared and cut into 24 samples of six sizes, as shown in Table 8-33, and with joints staggered on 3 in. or 6 in. centers. The spacing variation was aimed at gaining additional strength since there was a possibility of linking the joint weaknesses of 3 in. spaced joints.

8.1.4.4 Results

The results of the 80 tests are summarized in Tables 8-34 through 8-36. All tests were run on a 5 minute load ramp to expected failure, and all samples failed in the gage length without an indication of significant involvement of grips. The last columns define results corrected to 10% moisture content, which was the design goal at the time of testing.

Table 8-37 is a compilation of data in various combinations and includes average failure stress and standard deviation, all corrected to 10% wood moisture content. Table 8-38 is similar, but it compares butt joint and scarf joint data. Table 8-39 compares joint spacing results. Figure 8-36 is a plot of the strength of scarf-jointed specimens by spacing versus test volume (exclusive of the volume of wood in grips) for various scarf joint spacings. The decrease in strength with increasing volume is quite apparent, but there is no consistent trend indicating that the increased joint spacing improves strength. Figure 8-37 is a plot comparing butt and scarf joints as a function of test volume. The superiority of the scarf-jointed specimens is noteworthy. Figure 8-38 shows the mean of all samples versus sample size, and shows clearly the decrease in strength with increasing size.

Table 8-32 Pallet 3 Samples

Quantity	Joint Type	Length (ft)	Width (in.)	Thickness (in.)
8	Scarf	7.5	2	1.5
8	Butt	7.5	2	1.5
8	Scarf	7.5	8	1.5
8	Butt	7.5	8	1.5

Table 8-33 Pallet 4 and 5 Samples
(All Scarf Joints)

Quantity	Joint Spacing	Length (ft)	Width (in.)	Thickness (in.)
2	3	7.5	2	1.5
2	3	7.5	8	1.5
3	3	15	2	1.5
2	6	15	2	1.5
3	3	15	8	1.5
2	6	15	8	1.5
4	3	30	2	1.5
1	6	30	2	1.5
4	3	30	8	1.5
1	6	30	8	1.5

Table 8-34 Butt Joint Test Data

TEST SPECIMEN	NO. OF BUTTS BETWEEN JAWS	NO. OF BUTTS IN FAILURE	FACE SHEET SCARF JOINTS	NO. EDGE DEFECTS	(LBS.) WEIGHT	% MOISTURE CONTENT	FAILURE LOAD (LBS.)	AVG AREA (IN^2)	FAILURE STRESS (PSI)	EXTENSO-METER GAGE LENGTH (IN)	FAILURE DEFLECTION (IN)	FAILURE STRAIN	MODULUS (10^6 PSI)	CORRECTED TO 10% MC FAILURE STRESS	CORRECTED TO 10% MC MODULUS
1A2X7L	7	--	0	0	6.25	7.2	29,400	3.0225	9,727	36.0	.1280	.003556	2.735	9318	2.600
1A2X7R	13	13	1	1	6.18	7.1	37,040	3.0368	12,197	36.0	.1704	.004733	2.577	11666	2.466
1B2X7L	13	10	0	1	6.32	6.7	33,920	3.0126	11,259	36.0	.1520	.004222	2.667	10702	2.512
1B2X7R	8	5	2	0	6.27	7.0	30,920	3.0255	10,220	36.0	.1408	.003911	2.613	9760	2.475
2A2X7L	5	1	0	2	6.25	7.0	33,440	2.9933	11,172	36.0	.1498	.004161	2.685	10669	2.543
2A2X7R	0	--	1	1	5.85	7.3	42,480	3.0236	14,049	36.0	.2220	.006167	2.278	13480	2.170
2B2X7L	0	--	2	2	5.97	7.1	35,920	3.0148	11,915	36.0	.1728	.004800	2.482	11397	2.355
2B2X7R	5	5	2	1	5.91	7.0	35,160	3.0193	11,645	36.0	.1776	.004933	2.631	11121	2.492
1A8X7L	7	4	0	0	24.68	7.2	134,600	12.0216	11,196	36.0	.1526	.004222	2.652	10726	2.521
1A8X7R	12	10	0	0	24.45	7.1	119,200	12.0225	9,912	36.0	.1394	.003872	2.560	9481	2.429
1B8X7L	13	13	1	0	24.95	6.7	99,800	12.0300	8,296	36.0	.1088	.003022	2.745	7885	2.586
1B8X7R	7	2	2	0	24.98	7.1	103,200	12.0225	8,504	36.0	.1174	.003261	2.632	8130	2.498
2A8X7L	8	4	0	1	25.03	7.2	124,200	12.0117	10,340	36.0	.1390	.003861	2.672	9906	2.540
2A8X7R	0	--	1	0	23.30	7.2	149,000	11.9985	12,418	36.0	.1848	.005133	2.419	11896	2.300
2B8X7L	0	--	2	1	23.80	7.4	157,800	11.9824	13,169	36.0	.1956	.005433	2.424	12655	2.313
2B8X7R	5	5	2	2	23.40	7.0	123,200	11.9473	10,312	36.0	.1524	.004233	2.437	9848	2.308
1A8X15	21	12	2	1	50.09	7.2	114,000	12.0139	9,489	120.0	.4500	.003750	2.530	9090	2.405
1B8X15	22	10	2	1	49.80	7.1	124,000	12.0235	10,313	120.0	.4600	.003933	2.622	9864	2.488
2A8x15	14	13	2	1	47.10	6.8	113,400	12.003	9,448	120.0	.4800	.00400	2.362	8994	2.229
2B8X15	14	13	4	0	46.90	7.2	125,600	12.0154	10,453	120.0	.5240	.004367	2.394	10014	2.276
2A2X15	13	0	2	2	11.92	6.7	33,600	3.0291	11,092	120.0	.5540	.004617	2.403	10543	2.263
2B2X15	14	9	4	1	11.88	7.0	32,520	3.0062	10,818	120.0	.5280	.004400	2.459	10331	2.329
1A2X15	21	13	2	3	12.77	7.0	27,680	3.0425	9,098	120.0	.4300	.003583	2.539	8689	2.405
1B2X15	22	10	2	2	12.72	7.1	26,160	3.042	8,622	120.0	.3860	.003217	2.680	8247	2.543
2A2X30	39	9	6	0		6.7	29,120	3.0143	9,661	120.0	.5000	.004167	2.318	9183	2.183
2B2X30	39	12	6	2		7.0	30,440	3.0159	10,093	120.0	.5180	.004317	2.338	9639	2.215
1A2X30	45	11	6	4		7.0	29,400	3.0398	9,672	120.0	.4400	.003667	2.637	9237	2.498
1B2X30	46	5	6	1		7.2	27,920	3.0316	9,210	120.0	.4160	.003467	2.656	8823	2.525
1A8X30	46	6	6	4		7.2	112,600	12.0229	9,365	120.0	.4480	.003733	2.509	8972	2.385
1B8X30	46	7	6	1		7.4	98,200	12.0282	8,164	120.0	.3780	.003150	2.592	7846	2.473
2A8X30	39	13	6	2		7.6	108,400	12.0149	9,022	120.0	.4460	.003717	2.427	8697	2.324
2B8X30	39	9	9	8,		7.2	125,200	12.009	10,426	120.0	.5420	.004517	2.308	9988	2.194

Table 8-35 Butt/Scarf Joint Test Data

TEST SPECIMEN	WIDTH (IN.)	NUMBER OF JOINTS BUTT	NUMBER OF JOINTS SCARF	WEIGHT (LBS.)	VOLUME ($IN.^3$)	DENSITY (LB/IN^3)	FAILURE LOAD (LBS.)	STRESS AREA (IN^2)	FAILURE STRESS (PSI)	EXTENSOMETER GAGE LENGTH (IN.)	FAILURE DEFLECTION (IN.)	FAILURE STRAIN	MODULUS (10^6PSI)	NO. BUTTS IN FAILURE	NO. FLAWS	MOISTURE CONTENT %	CORRECTED TO 10% WOOD MOISTURE CONTENT FAILURE STRESS	CORRECTED TO 10% WOOD MOISTURE CONTENT MODULUS
3A1	8	13	--	25.97	1080.36	.02404	110,000	12.012	9,158	36.0	.122	.003389	2.702	13	1	6.9	8734	2.555
3B1	8	--	13	25.63	1078.56	.02376	122,000	12.004	10,163	36.0	.1462	.004061	2.503	--	5	7.1	9722	2.376
3C1	8	13	--	26.30	1078.99	.02437	107,600	12.008	8,961	36.0	.127	.003528	2.540	13	1	7.2	8578	2.412
3D1	8	--	13	25.90	1080.07	.02398	136,000	12.016	11,318	36.0	.157	.004361	2.595	--	2	7.3	10853	2.470
3E1	8	13	--	25.71	1078.99	.02383	124,000	11.996	10,337	36.0	.1473	.004092	2.526	7	0	6.5	9790	2.369
3F1	8	--	13	25.40	1079.64	.02353	125,000	12.012	10,406	36.0	.150	.004167	2.497	--	1	7.3	9981	2.377
3G1	8	13	--	25.46	1077.91	.02362	120,000	11.992	10,007	36.0	.148	.004111	2.434	11	3	6.0	9403	2.330
3H1	8	--	13	25.97	1080.36	.02404	126,000	12.012	10,490	36.0	.170	.004722	2.221	--	1	8.8	10298	2.173
3A2	2	13	--	6.58	271.63	.02422	34,600	3.020	11,457	36.0	.149	.004139	2.768	13	0	7.0	10933	2.619
3B2	2	--	13	6.53	271.65	.02404	40,806	3.020	13,512	36.0	.1844	.005122	2.638	--	2	6.7	12845	2.326
3C2	2	13	--	6.56	271.61	.02415	32,680	3.020	10,821	36.0	.141	.003917	2.763	9	2	6.3	10212	2.581
3D2	2	--	13	6.50	271.50	.02394	31,160	3.016	10,332	36.0	.1422	.003950	2.616	--	2	6.7	9824	2.465
3E2	2	13	--	6.48	270.94	.02392	37,520	3.014	12,449	36.0	.1630	.004528	2.749	12	3	6.6	11805	2.582
3F2	2	--	13	6.46	271.42	.02380	32,000	3.016	10,610	36.0	.1460	.004056	2.616	--	0	7.1	10152	2.483
3G2	2	13	--	6.45	271.69	.02374	30,000	3.019	9,937	36.0	.1414	.003928	2.530	10	1	7.5	9569	2.420
3H2	2	--	13	6.60	272.04	.02426	36,400	3.035	11,993	36.0	.1622	.004506	2.662	--	1	7.3	11514	2.537
3A3	8	13	--	26.15	1080.12	.02421	132,000	12.008	10,993	36.0	.1464	.004067	2.703	13	2	7.1	10516	2.566
3B3	8	--	13	26.11	1080.14	.02497	132,000	12.008	10,993	36.0	.1562	.004339	2.534	--	2	6.7	10442	2.385
3C3	8	13	--	26.12	1079.64	.02419	120,000	12.012	9,990	36.0	.1335	.003708	2.694	13	2	6.2	9425	2.515
3D3	8	--	13	25.95	1079.64	.02404	138,000	12.008	11,492	36.0	.1560	.004333	2.652	--	2	6.8	10932	2.500
3E3	8	13	--	25.65	1080.33	.02374	122,000	12.012	10,157	36.0	.1524	.004233	2.399	13	0	6.6	9639	2.255
3F3	8	--	3	25.92	1080.79	.02398	128,000	12.012	10,656	36.0	.1400	.003889	2.740	--	0	6.7	10121	2.578
3G3	8	13	--	25.90	1078.49	.02402	123,000	12.000	10,250	36.0	.1340	.003722	2.754	9	4	6.7	9738	2.593
3H3	8	--	13	26.65	1079.64	.02468	150,200	12.000	12,517	36.0	.1454	.004039	2.754	--	1	7.4	12036	2.630
3A4	2	13	--	6.51	272.13	.02392	33,600	3.026	11,104	36.0	.1502	.004172	2.662	13	4	6.8	10574	2.513
3B4	2	--	13	6.45	271.84	.02373	36,000	3.022	11,913	36.0	.1682	.004672	2.550	--	4	7.1	11397	2.420
3C4	2	13	--	6.57	271.06	.02424	28,440	3.016	9,430	36.0	.1390	.003861	2.590	13	2	6.4	8921	2.426
3D4	2	--	13	6.46	270.62	.02387	36,800	3.020	12,185	36.0	.1780	.004944	2.465	--	2	6.5	11553	2.315
3E4	2	13	--	6.52	271.11	.02405	36,240	3.028	11,968	36.0	.1684	.004678	2.558	10	3	6.9	11419	2.420
3F4	2	--	13	6.48	272.30	.02380	33,600	3.025	11,107	36.0	.1584	.004400	2.524	--	0	6.9	10589	2.386
3G4	2	13	--	6.43	271.74	.02366	30,080	3.021	9,957	36.0	.1330	.003694	2.695	11	1	6.9	9491	2.547
3H4	2	--	13	6.60	272.73	.02420	36,400	3.032	12,005	36.0	.1584	.004400	2.728	--	1	7.0	11465	2.584

Table 8-36 Scarf Joint Data

TEST SPECIMEN	WIDTH (IN.)	NO. OF EDGE DEFECTS	WEIGHT (LBS.)	% MOISTURE CONTENT	VOLUME (IN^3)	DENSITY (LB/IN^3)	FAILURE LOAD (LBS.)	STRESS AREA (IN^2)	FAILURE STRESS (PSI)	EXTENSO-METER GAGE LENGTH (IN)	FAILURE DEFLECTION (IN)	FAILURE STRAIN	MODULUS (10^6PSI)	CORRECTED TO 10% WOOD MOISTURE CONTENT FAILURE STRESS	MODULUS
4B2X7L	2	0	6.69	6.3	270	.0248	41,160	3.07	13,407	36	.1812	.00503	2.664	12671	2.498
4B2X7R	2	0	6.44	4.4	270	.0239	39,920	3.049	13,093	36	.1806	.00502	2.610	11991	2.610
4B8X7L	8	0	26.5	7.2	1080	.0245	145,800	12.083	12,067	36	.1574	.00437	2.761	11560	2.630
4B8X7R	8	0	25.63	4.5	1080	.0237	116,200	11.833	9,820	36	.1398	.00388	2.529	9011	2.293
4B2X15	2	0	12.75	6.2	540	.0236	35,960	3.004	11,971	120	.558	.00465	2.574	11292	2.409
5B2X15LT	2	0	12.5	4.5	540	.0231	27,560	3.031	9,093	120	.438	.00365	2.491	8344	2.259
5B2X15RT	2	0	12.5	4.9	540	.0231	36,440	3.026	12,042	120	.616	.00513	2.347	11117	2.143
5B2X15LB	2	0	12.5	5.2	540	.0231	26,400	3.026	8,724	120	.432	.0036	2.423	8102	2.227
5B2X15RB	2	0	12.0	5.1	540	.0222	32,400	2.999	10,804	120	.568	.00473	2.284	10013	2.095
4B8X15	8	0	51.25	6.1	2160	.0237	139,600	12.046	11,589	120	.558	.00465	2.492	10915	2.327
5A8X15LT	8	0	51.0	4.4	2160	.0236	119,000	12.1	9,835	120	.454	.00378	2.602	9007	2.354
5A8X15RT	8	0	50.38	4.9	2160	.0233	109,800	12.016	9,138	120	.426	.00355	2.574	8436	2.350
5A8X15LB	8	0	51.0	5.0	2160	.0236	130,000	12.016	10,819	120	.500	.00417	2.594	10008	2.374
5A8X15RB	8	0	51.0	5.0	2160	.0236	119,200	11.954	9,972	120	.460	.00383	2.604	9224	2.383
4A2X30T	2	1	26.0	5.6	1080	.0241	32,520	3.042	10,690	120	.506	.00422	2.533	9986	2.344
4A2X30B	2	0	25.88	6.2	1080	.0240	26,480	3.017	8,777	120	.404	.00337	2.604	8279	2.437
5A2X30	2	0	25.38	6.3	1080	.0235	27,680	2.983	9,279	120	.414	.00345	2.690	8770	2.523
5A2X30T	2	0	25.0	4.6	1080	.0231	29,880	3.032	9,855	120	.464	.00387	2.547	9063	2.315
5A2X30L	2	0	25.0	5.1	1080	.0231	29,200	3.03	9,637	120	.460	.00383	2.516	8932	2.307
4A8X30T	8	0	104.56	5.9	4320	.0242	121,200	12.150	9,975	120	.460	.00383	2.604	9355	2.421
4A8X30B	8	1	105.0	5.9	4320	.0243	120,000	12.053	9,956	120	.460	.00383	2.599	9356	2.529
4A8X30	8	0	102.88	6.6	4320	.0238	119,000	11.916	9,987	120	.444	.00370	2.699	9476	2.543
5B8X30T	8	1	100.5	4.5	4320	.0233	114,000	12.033	9,474	120	.460	.00383	2.474	8694	2.243
5B8X30B	8	0	101.5	4.6	4320	.0235	116,200	11.996	9,687	120	.472	.00393	2.465	8908	2.240

Table 8-37 Combined Butt and Splice Joint Results

DATA FORMAT

Stress Column - Avg. Stress at Failure-PSI

Modulus Column - Avg. Modulus-$(10)^6$PSI

(CORRECTED TO 10% WOOD MOISTURE CONTENT)

SPECIMEN SAMPLE	PANEL 1		PANEL 2		PANEL 3		PANEL 4		PANEL 5		PANELS 4 & 5		PANELS 1 & 2		PANELS 1 THRU 5	
	STRESS	MODULUS	STRESS	MODULUS	STRESS	MODULUS	STRESS	MODULUS	STRESS	MODULUS	STRESS	MODULUS	STRESS	MODULUS	STRESS	MODULUS
	SIGMA	SIGMA	SIGMA	SIGMA	SIGMA	SIGMA	SIGMA	SIGMA	SIGMA	SIGMA	SIGMA	SIGMA	SIGMA	SIGMA	SIGMA	SIGMA
ALL 1-1/2"x2"x7-1/2'	10362	2.513	11667	2.390	10766	2.477	12331	2.430	---	---	12331	2.430	11014	2.454	10963	2.465
	1044	.061	1246	.167	1034	.094	481	.097	---	---	1265	.097	1272	.134	1131	.105
ALL 1-1/2"x8"x7-1/2'	9056	2.509	11001	2.365	10013	2.443	10286	2.462	---	---	10286	2.462	10028	2.437	10070	2.442
	1316	.065	1507	.117	854	.130	1802	.238	---	---	1802	.238	1673	.116	1162	.127
ALL 1-1/2"x2"x15'	8468	2.474	10437	2.296	---	---	11292	2.409	9394	2.181	9774	2.227	9453	2.385	9631	2.297
	313	.098	150	.047	---	---	---	---	1429	.075	1501	.121	1154	.120	1286	.140
ALL 1-1/2"x8"x15'	9477	2.447	9504	2.253	---	---	10911	2.327	9169	2.366	9518	2.358	9491	2.350	9506	2.354
	547	.059	721	.033	---	---	---	---	651	.016	963	.022	523	.119	753	.074
ALL 1-1/2"x2"x30'	9030	2.512	9411	2.199	---	---	9012	2.435	8998	2.311	9006	2.385	9221	2.355	9101	2.372
	293	.019	322	.023	---	---	879	.090	93	.006	623	.093	334	.181	499	.130
ALL 1-1/2"x8"x30'	8409	2.429	9343	2.259	---	---	9396	2.498	8801	2.234	9158	2.395	8876	2.344	9032	2.372
	796	.062	913	.092	---	---	70	.067	151	.013	338	.148	883	.117	610	.130
ALL 2" WIDTH	9555	2.506	10795	2.319	10766	2.477	10948	2.429	9262	2.224	9880	2.327	10175	2.411	10310	2.412
	1132	.057	1304	.139	1034	.094	1775	.072	1126	.089	1557	.132	1343	.140	1326	.134
ALL 8" WIDTH	8999	2.473	10250	2.311	10013	2.443	9945	2.457	9046	2.324	9496	2.391	9606	2.392	9731	2.410
	1021	.066	1357	.103	854	.130	1032	.132	543	.065	916	.121	1325	.118	1065	.123
ALL 7-1/2" LENGTH	9707	2.511	11334	2.378	10390	2.460	11308	2.446	---	---	11308	2.446	9709	2.444	10507	2.453
	1306	.058	1328	.134	1008	.113	1598	.150	---	---	1598	.150	1303	.121	1224	.115
ALL 15' LENGTH	9935	2.460	8986	2.274	---	---	11102	2.368	9282	2.273	9645	2.292	9477	2.367	9568	2.326
	618	.068	751	.042	---	---	269	.058	1035	.111	1196	.107	936	.112	1024	.113
ALL 30' LENGTH	8720	2.470	9377	2.229	---	---	9204	2.466	8899	2.276	9082	2.390	9048	2.350	9060	2.372
	607	.061	560	.065	---	---	596	.079	153	.040	479	.117	645	.141	541	.126
ALL	9277	2.488	10523	2.315	10390	2.460	10222	2.443	1154	2.274	9688	2.359	9922	2.401	10020	2.411
	1080	.062	1316	.119	1008	.113	1414	.103	851	.091	1265	.128	1316	.128	1230	.128

SIGMA = Standard Deviation

Table 8-38 Butt & Scarf Joint Comparison Results

(CORRECTED TO 10% WOOD MOISTURE CONTENT)

SPECIMEN SAMPLE	PANEL 3 BUTT	PANEL 3 JOINTS	PANEL 3 SCARF	PANEL 3 JOINTS	PANELS 1,2,& 3 BUTT	PANELS 1,2,& 3 JOINTS	PANELS 3,4,& 5 SCARF	PANELS 3,4,& 5 JOINTS	PANELS 1 & 2 BUTT	PANELS 1 & 2 JOINTS	PANELS 4 & 5 SCARF	PANELS 4 & 5 JOINTS
1.5"x2"x7-1/2'	10366 1004	2.514 .816	11167 956	2.440 .096	10690 1157	2.483 .112	11400 988	2.438 .091	11014 1272	2.454 .134	12331 1265	2.430 .097
1.5"x8"7-1/2'	9478 614	2.449 .125	10548 728	2.436 .142	9772 1250	2.443 .117	10496 887	2.441 .149	10028 1673	2.437 .116	10286 1802	2.462 .238
1.5"x2"x15"									9453 1154	2.385 .120	9774 1501	2.227 .121
1.5"x8"x15'									9491 523	2.350 .119	9518 963	2.358 .022
1.5"x2"x30'									9221 334	2.355 .181	9006 623	2.385 .093
1.5"x8"x30'									8876 883	2.344 .117	9158 338	2.395 .148
ALL 2" WIDTH					10238 1220	2.411 .140	10395 1470	2.347 .136				
ALL 8" WIDTH					9576 1127	2.411 .121	9917 980	2.409 .129				
ALL 7-1/2' LENGTH	9922 925	2.481 .107	10858 881	2.438 .117	10231 1273	2.463 .114	10948 1025	2.439 .120				
ALL 15' LENGTH					9472 832	2.367 .112	9646 1196	2.281 .105				
ALL 30' LENGTH					9048 645	2.350 .141	9082 479	2.390 .117				
ALL SIZES					9907 1209	2.428 126	10156 1257	2.390 .129				

Table 8-39 Scarf Joint Spacing Comparison

(CORRECTED TO 10% WOOD MOISTURE CONTENT)

SPECIMEN SAMPLE	PANEL 5 6" SCARFS		PANEL 5 3" SCARFS		PANELS 4 & 5 3" SCARFS	
1-1/2"x2"x7-1/2'	--	--	--	--	12331	2.430
	--	--	--	--	480	.097
1-1/2"x8"x7-1/2'	--	--	--	--	10286	2.462
	--	--	--	--	1802	.238
1-1/2"x2"x15'	9058	2.161	9731	2.201	10251	2.27
	1351	.093	1960	.082	1654	.133
1-1/2"x8x15'	9616	2.379	8722	2.352	9453	2.344
	554	.006	404	.003	1298	.014
1-1/2"x2"x30'	8932	2.307	9063	2.315	9025	2.435
	--	--	--	--	1718	.090
1-1/2"x8"x30'	8908	2.240	8694	2.243	9220	2.439
	--	--	--	--	355	.139
2" WIDTH	9016	2.210	9508	2.239	10168	2.365
	958	.107	1439	.088	1652	.119
8" WIDTH	9380	2.332	8712	2.316	9534	2.410
	566	.080	286	.063	1033	.130
7-1/2' LENGTH	--	--	--	--	--	--
15' LENGTH	9337	2.270	9226	2.277	9852	2.307
	903	.137	1294	.099	1400	.094
30' LENGTH	8920	2.274	8920	2.279	9122	2.419
	17	.047	17	.051	535	.111
ALL	9198	2.271	9110	2.277	9273	2.388
	732	.108	1025	.080	2412	.123

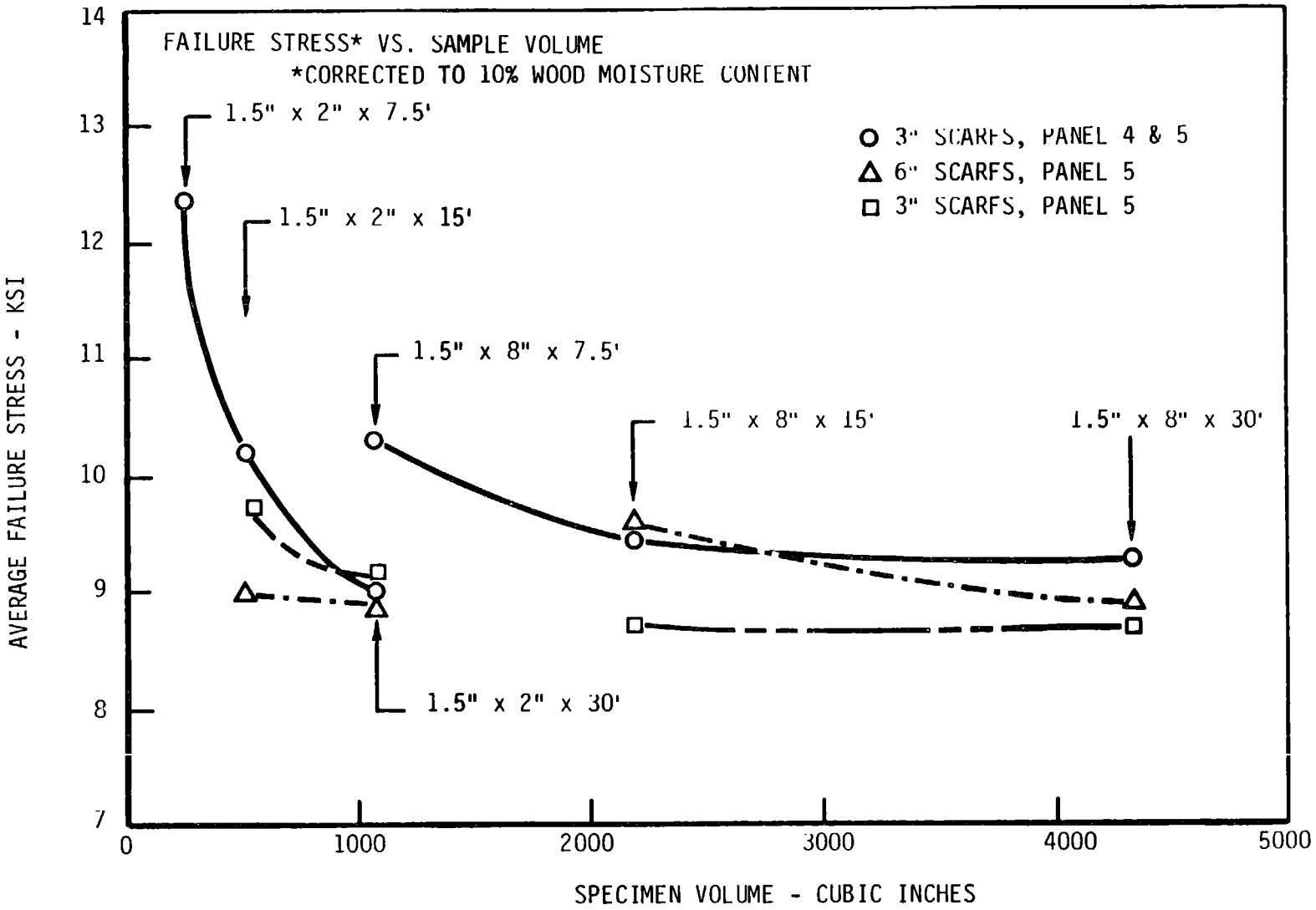

Figure 8-36 Failure Stress vs. Stressed Volume for Various Scarf Joint Spacings

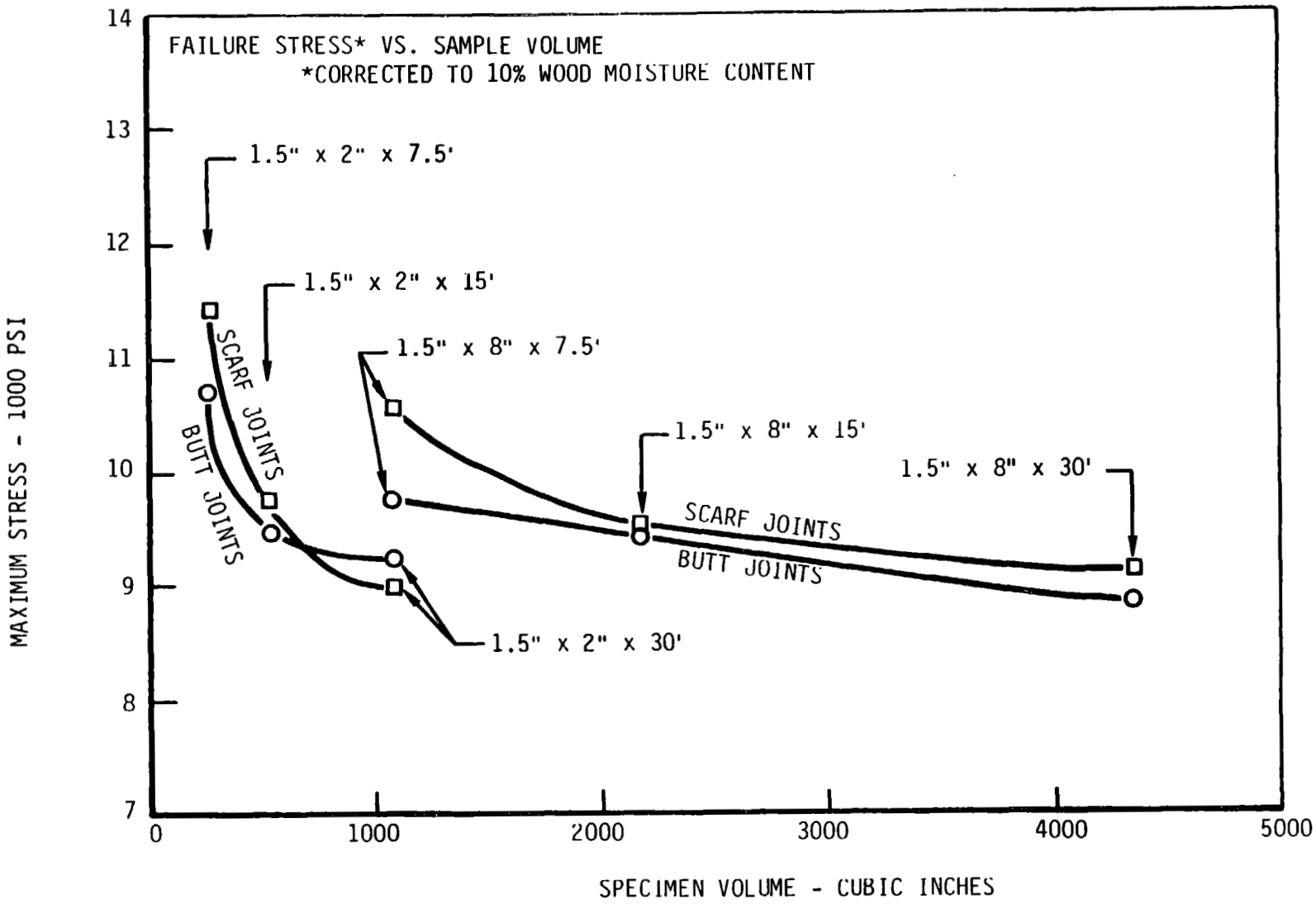

Figure 8-37 Butt/Scarf Joint Comparison

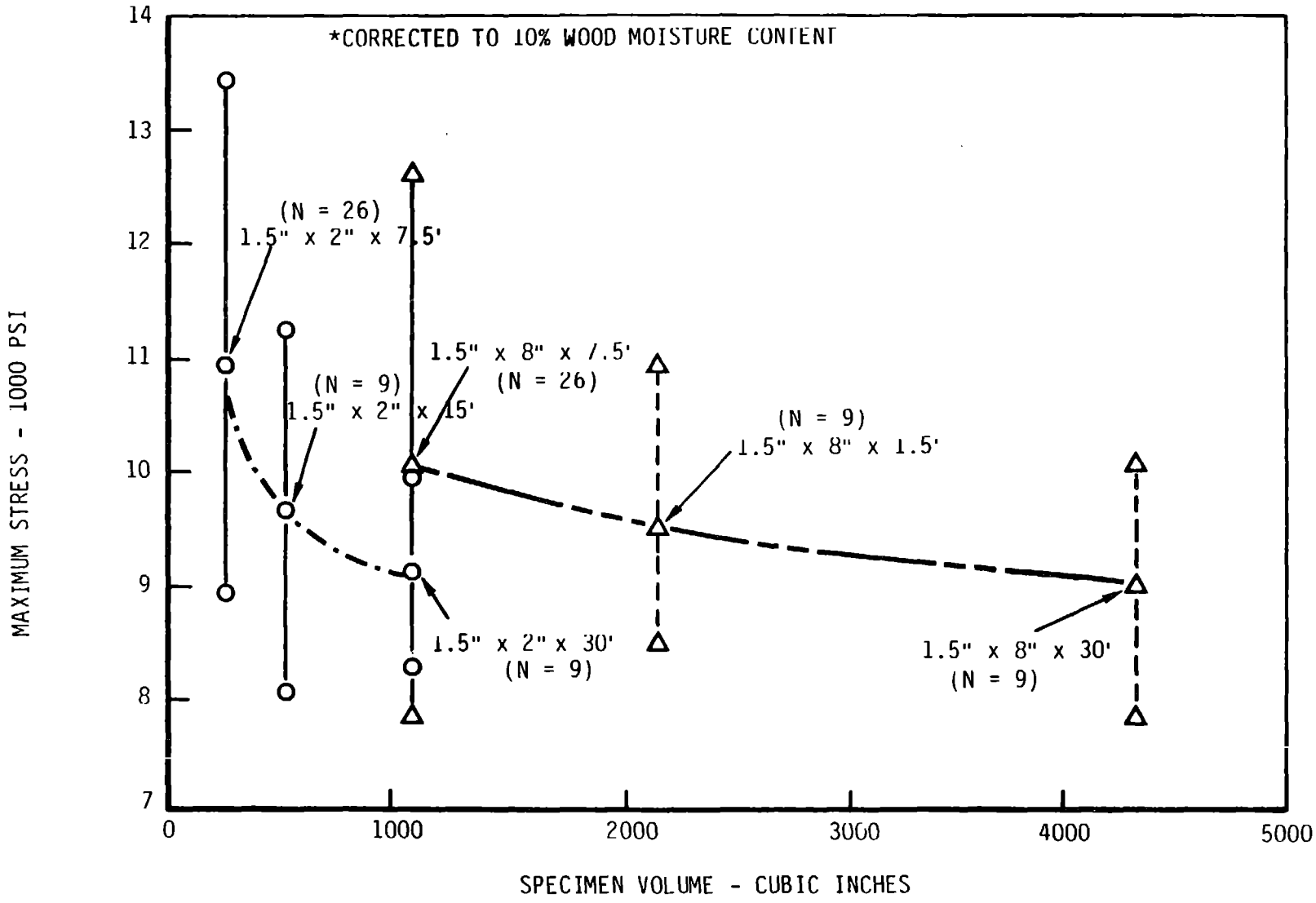

Figure 8-38 **Failure Stress vs. Sample Volume - All Samples**

8.1.5 MOISTURE EFFECTS TESTING

8.1.5.1 Moisture Effect on Fatigue

8.1.5.1.1 Introduction

The available fatigue characterization data on wood did not provide enough information to determine the effects of moisture on fatigue life. Handbooks and other sources contain data on the variation of static strength with moisture, however, none exists for fatigue life. This program fatigue tested a composite of blade grade 1, Douglas fir veneer and West System® epoxy.

8.1.5.1.2 Objective

The objective of this test series was to provide data on fatigue characteristics for forces parallel to the grain of the laminae at various moisture contents, to establish design allowables for a range of moistures. Fatigue data under fully reversing loads, at various load ratios in tension/tension and compression/compression fatigue, were obtained. Samples with scarf joints, or butt joints, were tested to provide a tie with other data bases.

8.1.5.1.3 Description

The test program consisted of 52 samples of various types made from three pallets (#21, 22 and 23) that were fabricated to provide a wood moisture content above the normal moisture content. Thirteen samples were built from pallet number 20, which contained scarf joints that were intentionally built with imperfect fits so that their strength could be evaluated. Pallet 20 was built with a normal moisture content, but the results are useful because they extended the data base. Normal moisture content is defined as between 4.5 and 6.1% wood moisture content (WMC), the equivalent of between 3.7 and 5.0% laminae moisture content (LMC). The high moisture samples were as close to 12% WMC (9.8% LMC) as possible. Emphasis was placed on maintaining a constant moisture content before and during testing, and post test moisture levels were carefully determined. All specimens were treated with a double coating of West System® epoxy after fabrication and were wrapped in plastic sheets before testing. Samples tested for 10^4 cycles were also wrapped during testing. The wrap contained a moisture bearing medium that was kept from direct contact with the sample.

Test specimens were designed to be similar to those described in section 8.1.2, with a 2.25 in. diameter for a cross section of 4.0 square in. The compression cylinders were 8 in. long, to provide a stressed volume of 318 cubic in. The configuration is shown in Figure 8-39. Transverse joints were spaced 3 in. apart in three adjacent laminae at the specimen's centerline. Where scarf joints were used, they had a slope of 12 to 1. Figure 8-40 shows the dogbone geometry, with joints in the three center veneers. Because of the cylindrical shape, the joints in the widest layers create a ratio of joint length per unit volume that is almost double that of a typical blade section. The taper and square end sections of the dogbones were wrapped with five layers of glass or 60 lb test cotton cord to induce some cross grain compression, to reduce sensitivity to crossgrain tension loads. A third type of sample, the static plank, is shown in Figure 8-41. It was tested in static tension to failure. The plank also contains three joints in the three center sheets, but the stressed volume is 216 cubic in.

The veneer scarf joints used in billet number 20 were intentionally mismatched, as shown in Figure 8-42. Figure 8-43 shows joints for billets 21 and 22 and Figure 8-44 shows the reversed angle scarf joints of billet 23. Figures 8-45 through 8-48 describe the locations of test samples within the pallets, and show the portions of billets conditioned to high moisture levels. The following code is used to identify test use:

	TS	=	Tension Static
0.1	TF	=	Tension Fatigue, R = 0.1
	CS	=	Compression Static
0.1	CF	=	Compression Fatigue, R=10
0.4	CF	=	Compression Fatigue, R=2.5
-1.0	TCF	=	Tension-Compression Fatigue, R=-1

Billets 21 and 22 were used to make moisture content samples. They fell short of the 12% goal. The cause was found to be the manufacturing process used, so it was modified for billet 23.

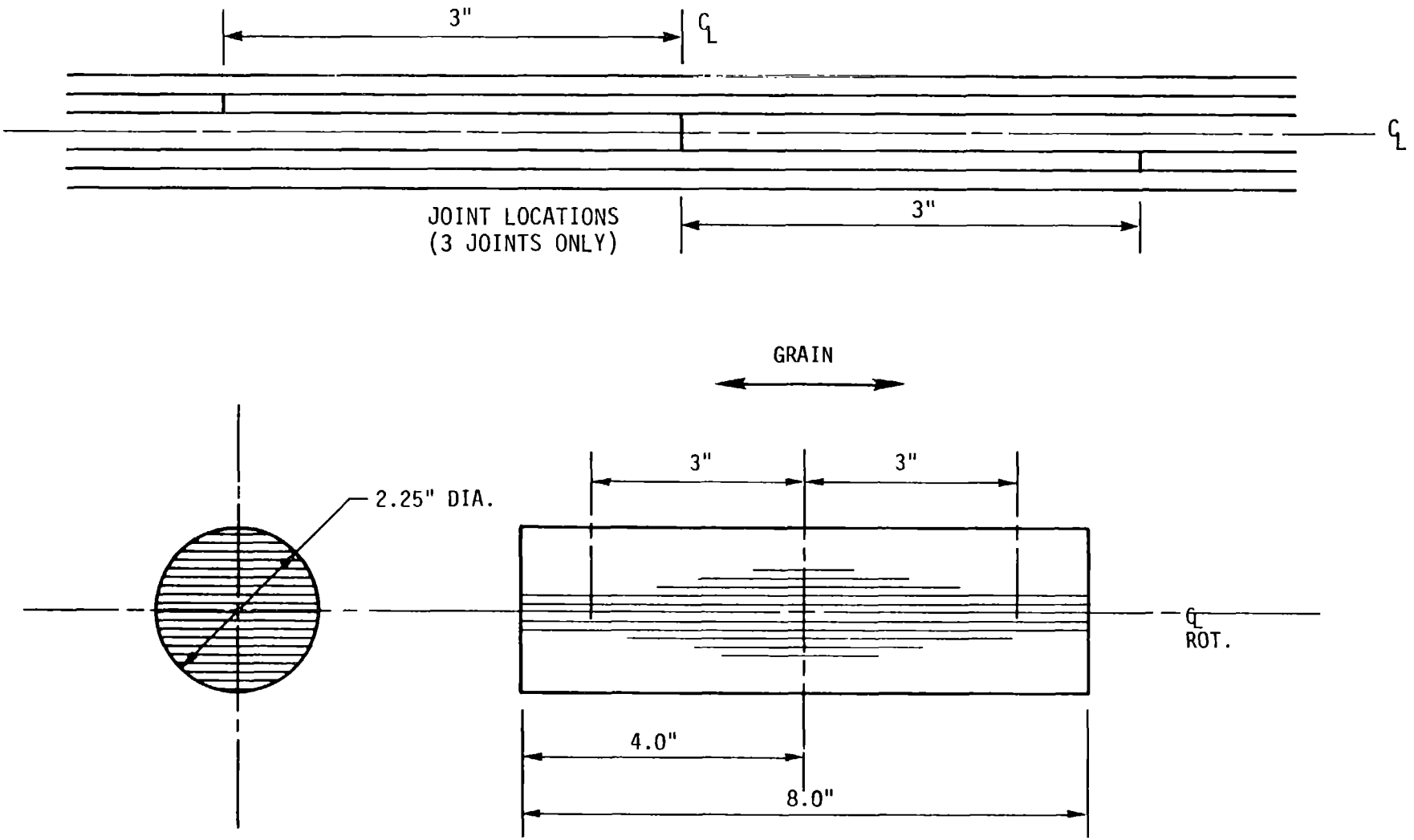

Figure 8-39 Compression Cylinder Configuration

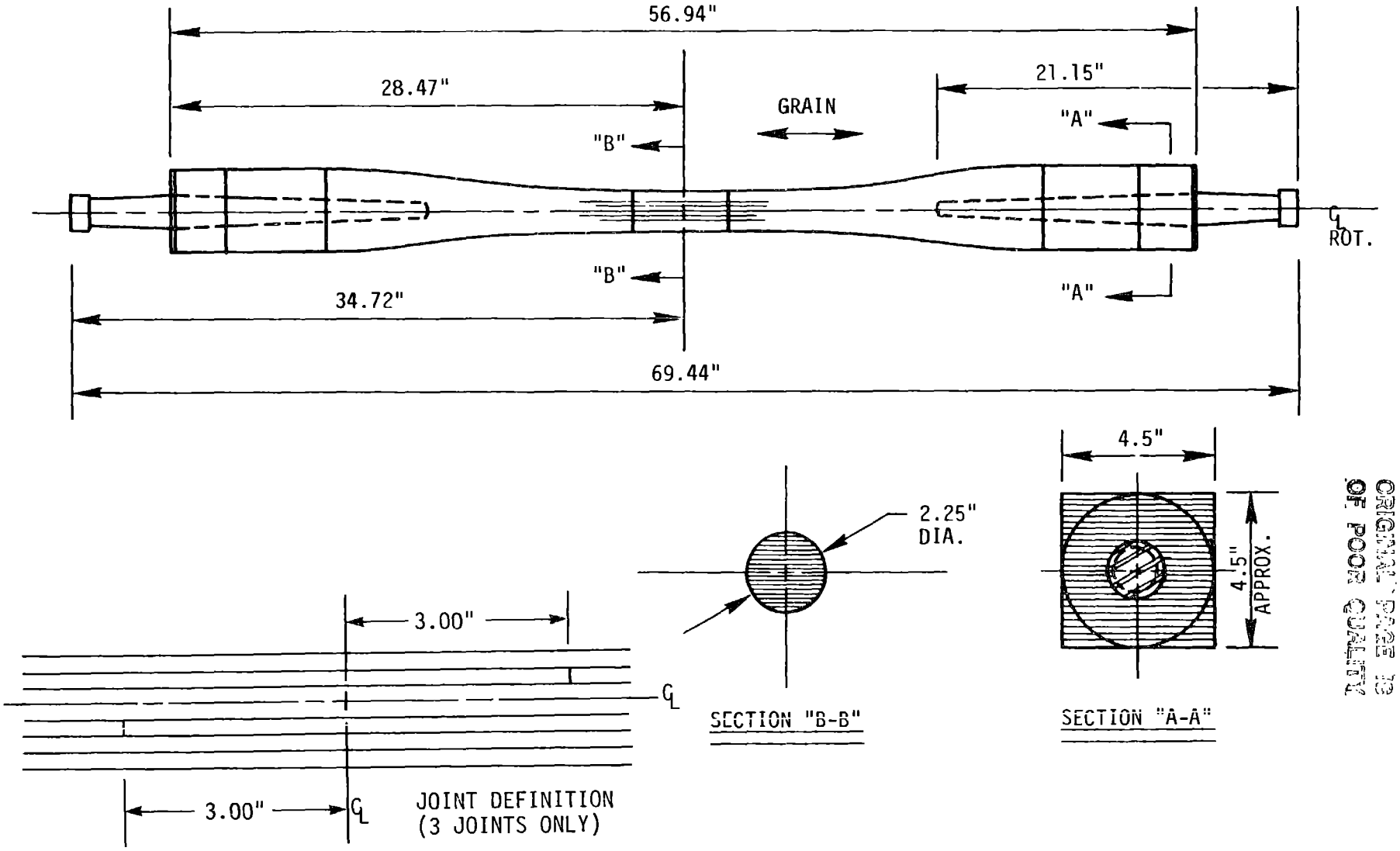

Figure 8-40 "Dogbone" Style Test Specimen

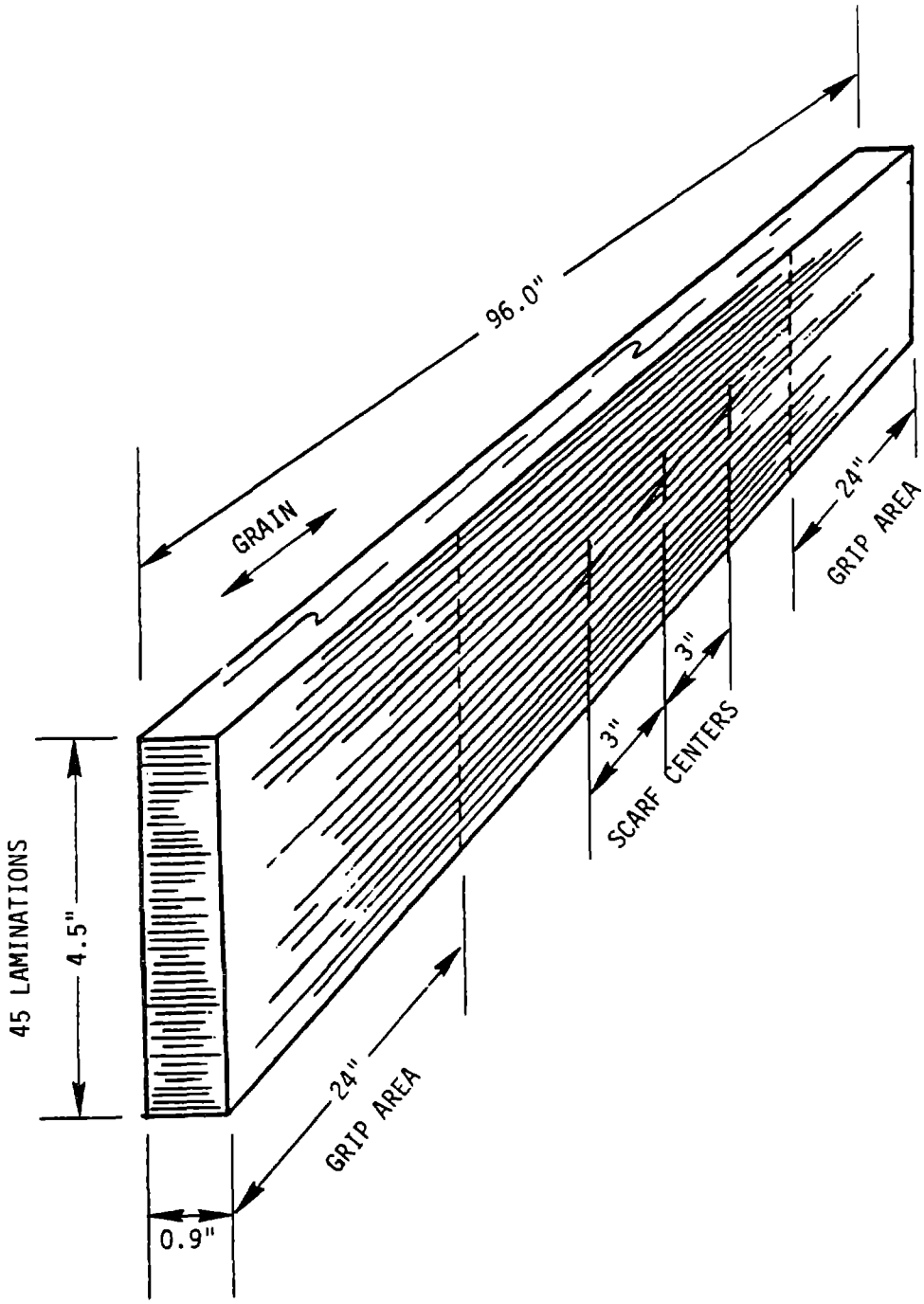

Figure 8-41 "Plank" Style Static Tensile Test Specimen

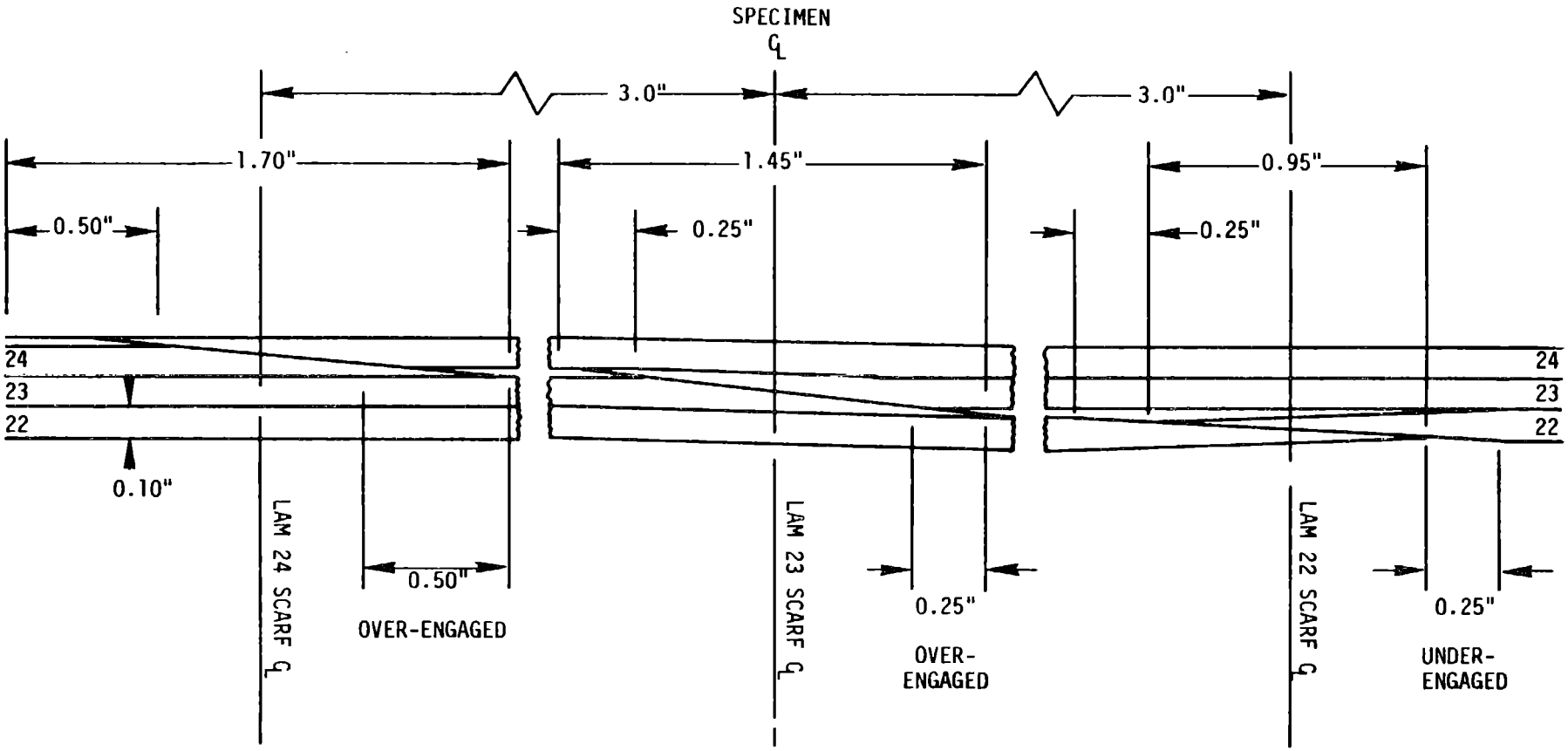

Figure 8-42 Edge View of the Three Central Laminations of Billet 20 Showing the Intentional Scarf Joint Mismatches

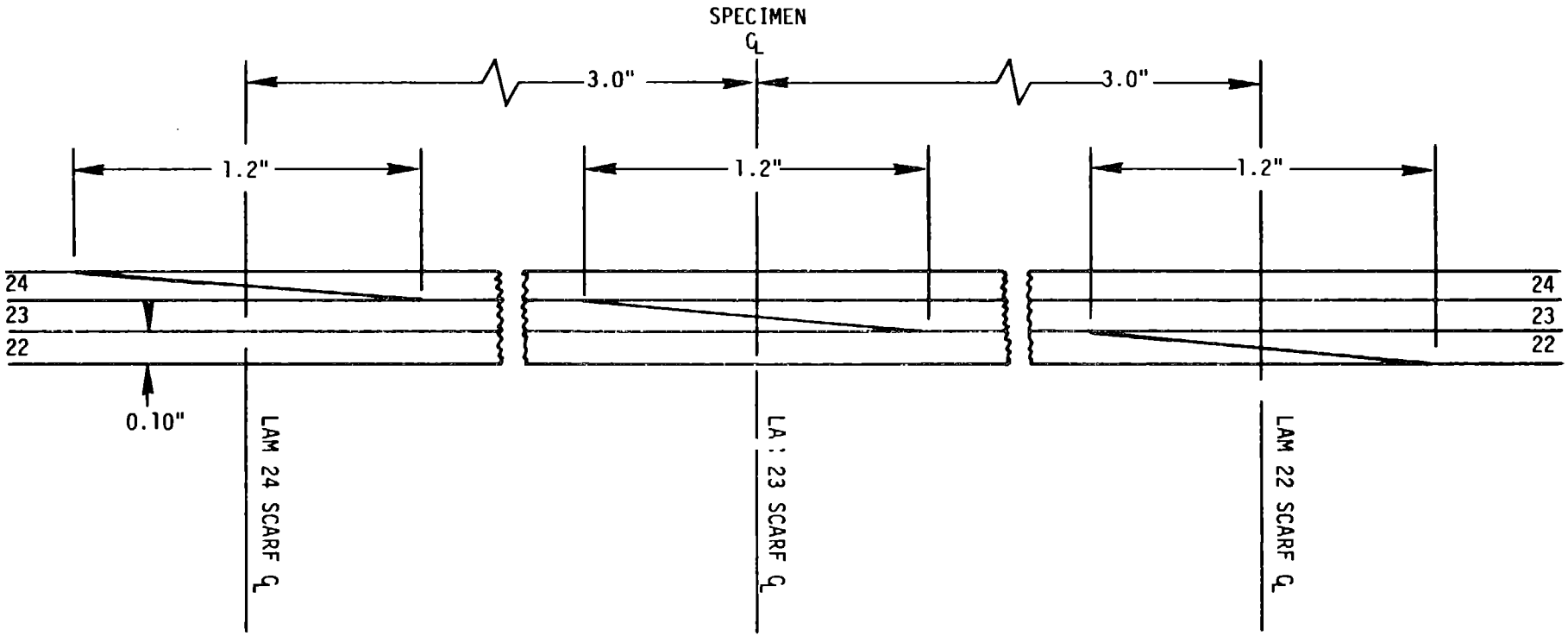

Figure 8-43 Edge View of the Three Central Laminations of Billet 21 and 22 Showing Normal 12:1 Scarf Joint Layout

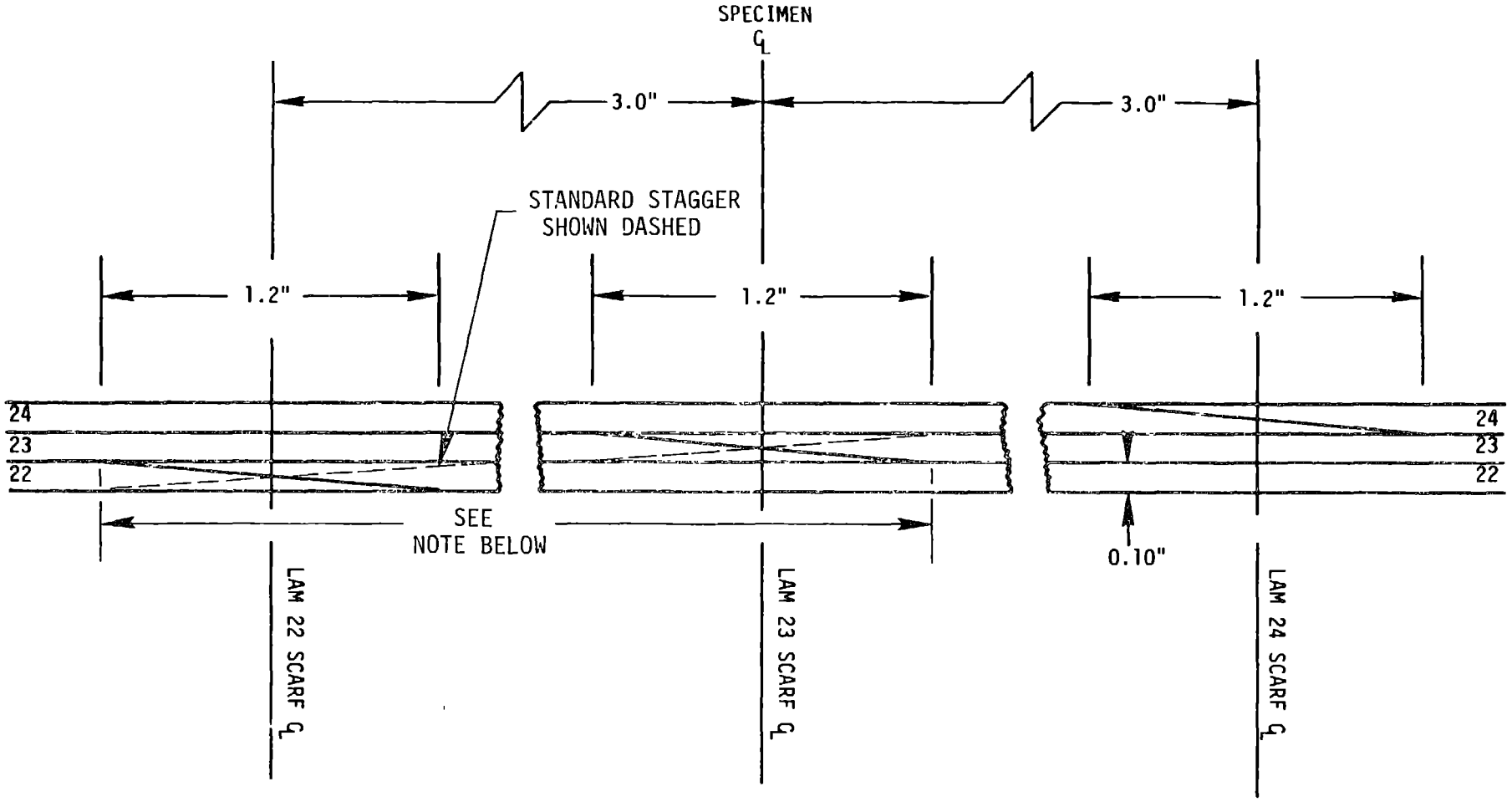

NOTE - WITH STANDARD STAGGER, SPACING BETWEEN JOINT ENDS ON COMMON VENEER PLANE IS 1.8" VS. 4.2" SHOWN HERE.

Figure 8-44 Edge View of the Three Central Laminations of Billet 23 Showing 12:1 Scarf Joint Layout with Reverse Stagger

GRAIN

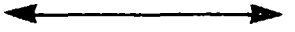

	A CYLINDERS	B "DOGBONES"	C CYLINDERS	
1	20-A-1 BUTT 0.1 CF	20-B-1 BUTT -1.0 TCF	20-C-1 CLEAR SPARE	1
2	20-A-2 SCARF 0.1 CF	20-B-2 SCARF -1.0 TCF	20-C-2 BUTT 0.1 CF	2
3	20-A-3 SCARF 0.1 CF	20-B-3 SCARF -1.0 TCF	20-C-3 BUTT CS	3
4	20-A-4 SCARF 0.1 CF	20-B-4 SCARF -1.0 TCF	20-C-4 BUTT SPARE	4
5	20-A-5 SCARF CS	20-B-5 SCARF TS	20-C-5 BUTT CS	5

NOTE: 0.1 CF SPECIMENS WERE TESTED AT A LOAD RATIO OF 10.

Figure 8-45 Billet #20 Schematic Test Specimen Type, Use, and Billet Location

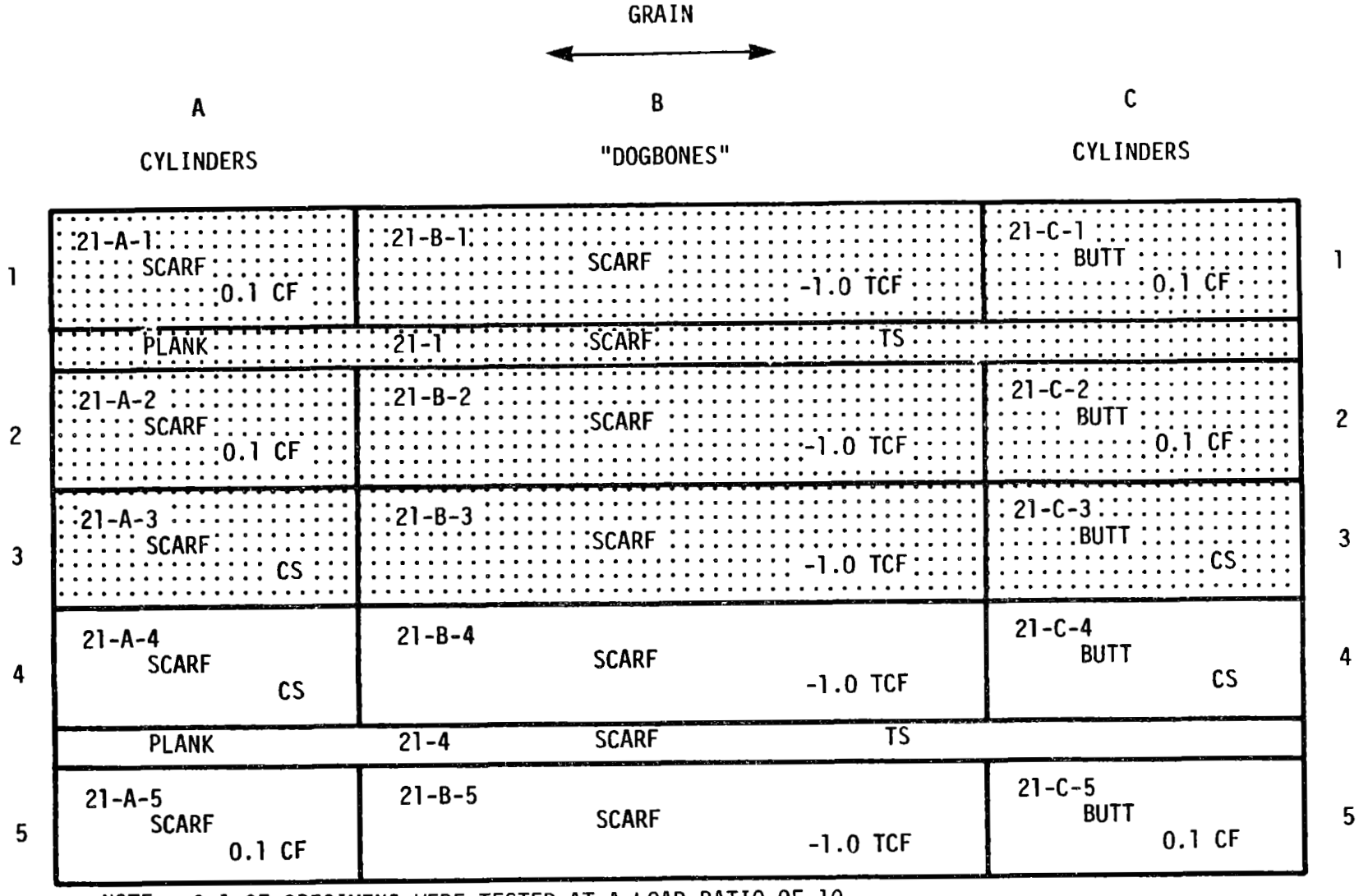

Figure 8-46 Billet #21 Schematic Test Specimen Type, Use, and Billet Location

(Shaded area indicates billet portion conditioned to higher M.C.)

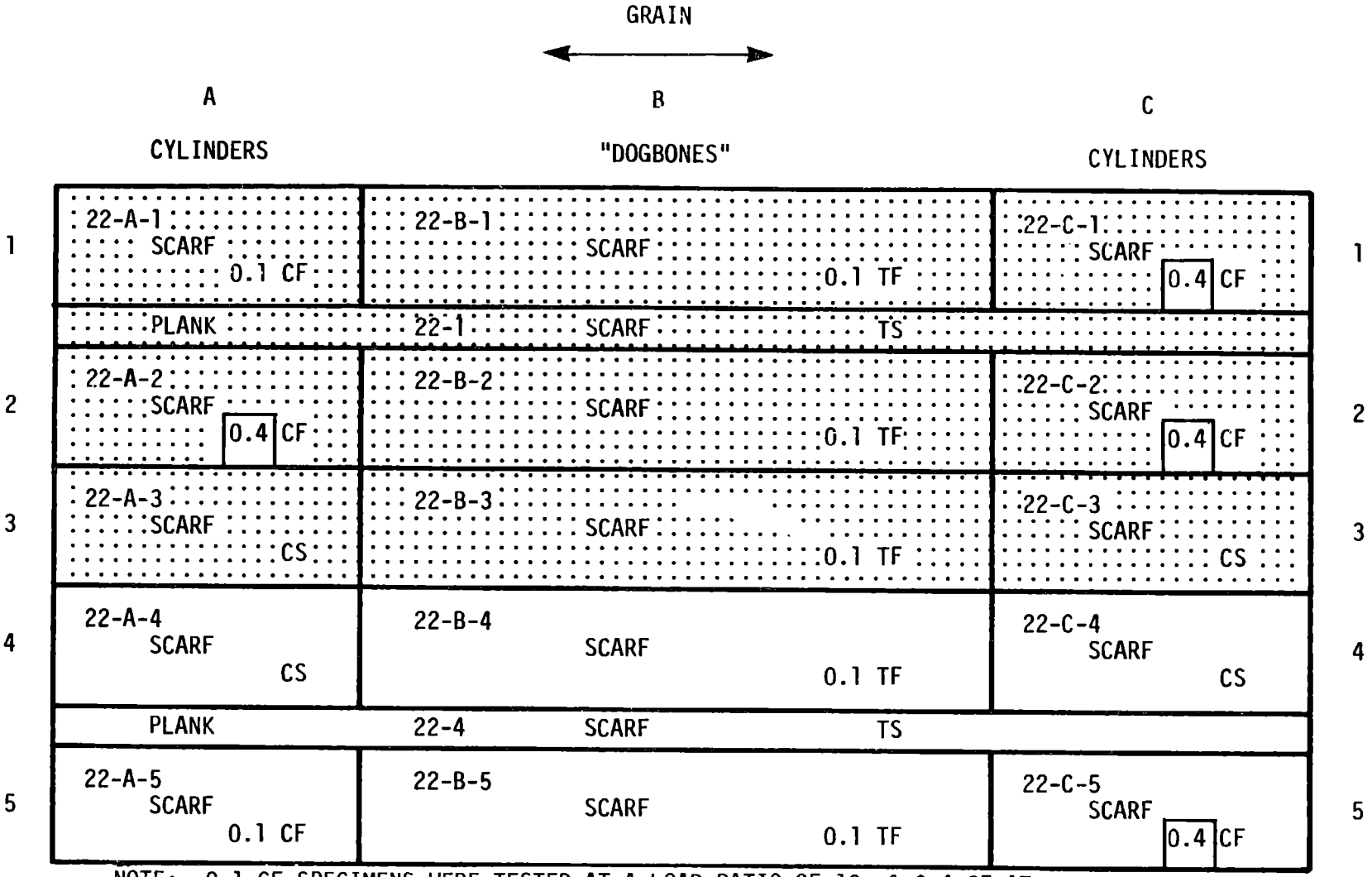

NOTE: 0.1 CF SPECIMENS WERE TESTED AT A LOAD RATIO OF 10, & 0.4 CF AT A LOAD RATIO OF 2.5.

Figure 8-47 Billet #22 Schematic Test Specimen Type, Use, and Billet Location

(Shaded area indicates billet portion conditioned to higher M.C.)

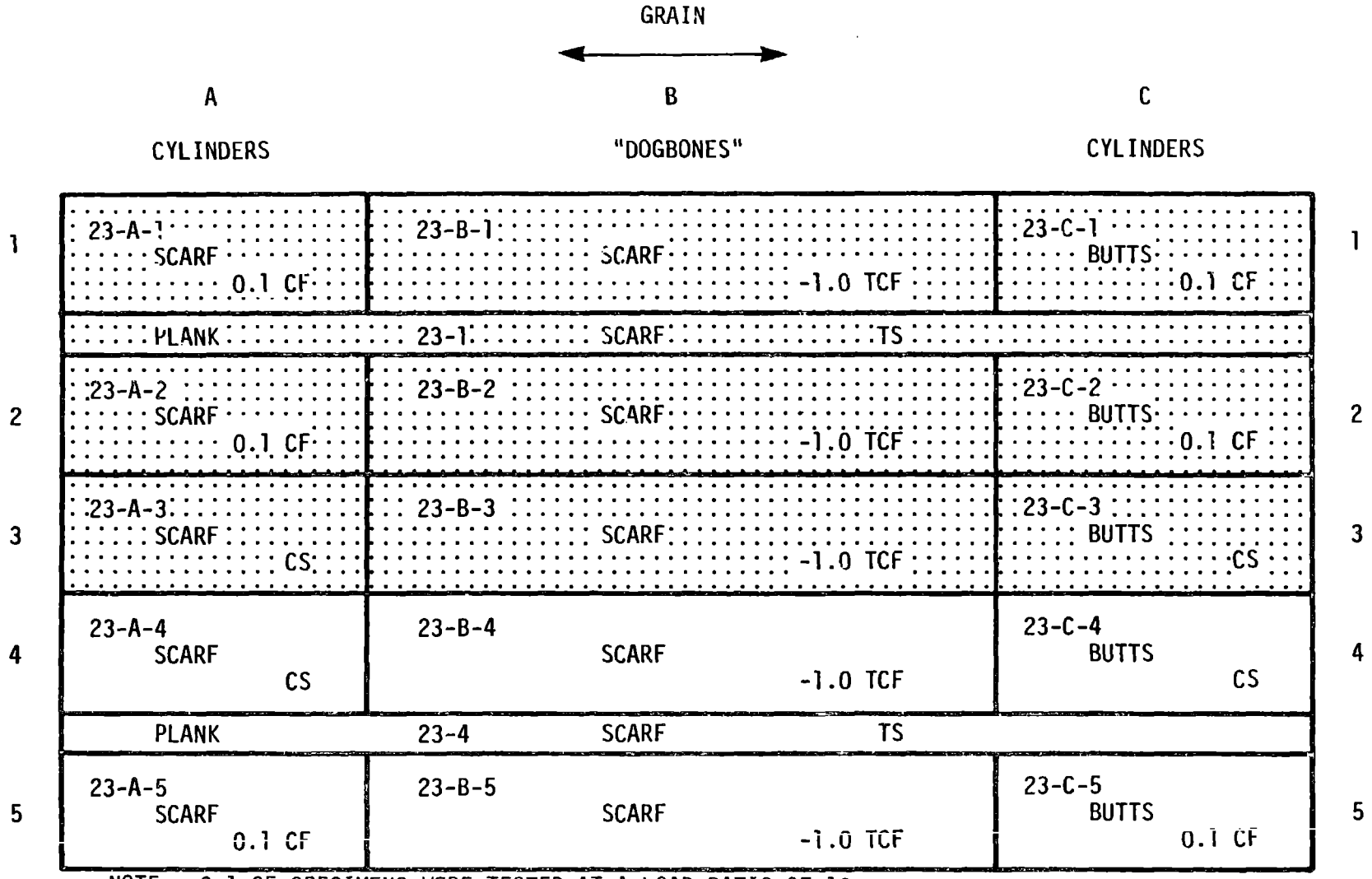

NOTE: 0.1 CF SPECIMENS WERE TESTED AT A LOAD RATIO OF 10.

Figure 8-48 Billet #23 Schematic Test Specimen Type, Use, and Billet Location

(Shaded area indicates billet portion conditioned to higher M.C.)

Table 8-40 lists the use for the 51 samples cut from billets 21 through 23, and also defines the number of high moisture content samples in each group.

8.1.5.1.4 Results

It was very important to determine the moisture level in the test samples, and Table 8-41 lists the pretest and post-test values for the three billets. The subscripts indicate the number of samples used in the averaging.

Tension tests were conducted on eleven specimens, five of them dogbones that were fatigue tested. The other six were statically tested planks. Table 8-42 lists the results of these tension tests, and stress values adjusted to 12% wood moisture content in accordance with static tensile strength factors listed in the Wood Handbook. The average adjusted static strength was 10,600 psi, 4.2% below the equivalent value of 11,065 psi, from seven butt-jointed dogbone samples tested in section 8.1.2. The increased stressed volume, with a factor greater than 6, of the plank samples results in a size effect, which reduces the scarf joint specimen strength. See section 8.1.6.

Compression tests were conducted on a total of 30 specimens. Table 8-45 shows the results of a number of weighings used to determine the changes in moisture content of a sample during testing. Static failures of eight compression cylinders with scarf joints averaged -8,127 lbs. Four butt-jointed cylinders averaged -7,840 psi, both adjusted to 12% wood moisture content. These results are shown in Table 8-43. Table 8-44 lists the results of 12 scarf-jointed and six butt-jointed compression cylinders that were fatigue tested. The static test results for butt joints are consistent with previous test data, but the results on billet 23 are decidedly lower than those of billet 21. The static data on scarf joints also indicates a lower strength for billet 23. The average for scarf joints is about 4.7% higher than previous test results.

Reverse axial testing results of ten samples are tabulated in Table 8-46. All were run at a rate of 3 Hz except specimen 23B4, which had the highest load, ±6500 lb, and was run at 2.2 Hz. The moisture content adjustment to 12% is based on compression rather than tension, since the compression side would dominate in determining failure.

Table 8-40 Types and Quantities of Samples Tested with High Moisture Content Scarf Joint Research*

	TENSION		COMPRESSION			REVERSE AXIAL	
	Static Tension	Fatigue R = 0.1	Static Compression	Fatigue R = 10	Fatigue R = 2.5	Fatigue R = -1.0	Totals:
"Dogbones" Tested							
Scarfs	---	5_3	---	---	---	10_6	15_9
Butts	---	---	---	---	---	---	---
Cylinders Tested:							
Scarfs	---	---	8_4	6_4	4_3	---	20_{12}
Butts	---	---	4_2	6_4	---	---	10_6
Planks Tested:							
0.9" x 4.5" x 96.0"	6_3	---	---	---	---	---	6_3
Column Totals:	6_3	5_3	12_6	14_9	4_3	10_6	51_{30}

* Subscripts indicate the number of specimens from among the total listed which were manufactured from billet portions laid up with veneer conditioned to higher W.M.C. levels.

Table 8-41 Summary of Moisture Data

Billet Number	Region	Average Pre Test W.M.C. (%)	Average Post Test W.M.C. (%)	Highest Post Test W.M.C. (%)	Lowest Post Test W.M.C. (%)	Apparent Greatest Change In W.M.C. (%)
21	Wet	8.6_4	8.1_{10}	8.7	7.6	-1.0
21	Dry	5.5_2	5.6_7	5.9	5.2	+0.4
22	Wet	8.3_4	8.0_{10}	8.5	7.7	-0.6
22	Dry	5.9_2	5.8_7	7.1	5.2	+1.2
23	Wet	11.0_6	10.9_{10}	11.8	8.9	-2.1
23	Dry	5.3_4	5.5_7	6.1	4.5	$\pm$0.8

Table 8-42

TENSION FATIGUE TESTS (R = 0.1)
Test Program: MOD-5A, High-Moisture Scarf Joint Fatigue
Material: Douglas Fir and Epoxy, Blade Grade 1 Veneer
Construction: Dogbone Shaped with 3 Transverse 12:1 Slope Scarf Joints in Center Veneers, 3-in. Stagger
Load Direction: Tension Parallel to Grain
Temperature: 70°F

Sample Number	Test Site	Cycle Rate (Hz)	Minimum Stress (psi)	Maximum Stress (psi)	Total Cycles	LMC (%)	WMC (%)	Maximum Stress Adjusted To 12% W.M.C. (psi)
22B3	UDRI	4	900	9,000	178,500	6.5	7.9	8,437
22B2	UDRI	4	850	8,500	597,900	6.3	7.7	7,937
22B4	GBI	4	850	8,500	305,320+	4.6	5.6	7,680
22B5	GBI	4	800	8,000	1,930,730	4.7	5.7	7,242
22B1	UDRI	4	700	7,000	7,550,000	7.0	8.5	6,626

STATIC TENSILE TESTS 5-Minute Ramp to Failure (K Consulting Company, Boise, Idaho)
Material: Douglas Fir and Epoxy, Blade Grade 1 Veneer
Construction: 0.9" Wide Slice Cut from Billet Lengthwise Full-Depth (Through all 45 Laminations) With 3 Transverse 12:1 Slope Scarf Joints in Center Veneers, 3-in. Stagger, Dimensions 0.9" x 4.5" x 96.0".
Load Direction: Tension Parallel to Grain
Temperature: 70°F

Sample Number	Maximum Stress (psi)	LMC (%)	WMC (%)	Maximum Stress Adjusted To 12% W.M.C. (psi)
21-1	12,937	7.1	8.7	12,269
21-4	10,130	4.6	5.6	9,153
22-1	10,438	6.5	7.9	9,785
22-4	10,990	5.8	7.1	10,163
23-1	11,512	9.0	11.0	11,327
23-4	11,971	5.0	6.1	10.900
			Average:	10,600

+ Premature Failure Due to Accidental Damage.

Table 8-43

STATIC COMPRESSION TESTS (5-Minute Ramp to Failure, 8,696 lbs. per minute)
Test Program: MOD-5A, High Moisture Scarf Joint Fatigue
Material: Douglas Fir and Epoxy, Blade Grade 1 Veneer
Construction: 2.25 in. Diameter x 8 in. Long Cylinder, with 3 Transverse 12:1 Slope Scarf Joints in Center Veneers, 3-in. Stagger
Load Direction: Compression Parallel to Grain
Temperature: 70°F
Test Site: GBI

Sample Number	Maximum Stress (psi)	LMC (%)	WMC (%)	Maximum Stress Adjusted To 12% W.M.C. (psi)
21A3	10,651	6.5	7.9	-8,537
21A4	11,783	4.5	5.5	-8,271
22A3	10,324	6.4	7.8	-8,220
22A4	11,670	4.5	5.5	-8,192
22C3	10,689	6.3	7.7	-8,455
22C4	11,783	5.0	6.1	-8,550
23A3	7,779	8.9	10.9	-7,311
23A4	11,020	4.0	4.9	-7,483
			Average:	-8,127

STATIC COMPRESSION TESTS OF BUTT-JOINTED CONTROL SPECIMENS

21C3	10,438	7.0	8.5	-8,648
21C4	11,519	4.6	5.6	-8,140
23C3	7,719	9.0	11.0	-7,303
23C4	10,920	3.7	4.5	-7,269
			Average:	-7,840

Table 8-44

COMPRESSION FATIGUE TESTS
Test Program: MOD-5A, High-Moisture Scarf Joint Fatigue
Material: Douglas Fir and Epoxy, Blade Grade 1 Veneer
Construction: 2.25 in. Diameter x 8 in. Long Cylinder with 3 Transverse 12:1 Slope Scarf Joints in Center Veneers, 3-in. Stagger
Load Direction: Compression Parallel to Grain
Temperature: 70°F

Sample Number	Test Site	Stress Ratio (R Value)	Cycle Rate (Hz)	Maximum Stress (psi)	Minimum Stress (psi)	Total Cycles	LMC (%)	WMC (%)	Maximum Stress Adjusted To 12% W.M.C. (psi)
23A5	GBI	10	8	-950	-9,500	50,640	5.0	6.1	-6,893
23A2	GBI	10	8	-750	-7,500	71,860	8.1	9.9	-6,684
21A1	UDRI	10	10	-780	-7,800	325,010	6.8	8.3	-6,377
22A5	GBI	10	8	-870	-8,700	316,740	4.6	5.6	-6,148
22A1	UDRI	10	10	-750	-7,500	1,333,400	6.7	8.2	-6,092
21A5	GBI	10	8	-850	-8,500	1,655,890	4.5	5.5	-5,967
21A2	UDRI/GBI	10	10*	-700	-7,000	18,571,520	6.2	7.6	-5,500
23A1	GBI	10	8	-650	-6,500	17,509,310	7.3	8.9	-5,494
22C2	UDRI	2.5	10	-3,600	-9,000	89,500	6.6	8.1	-7,262
22A2	UDRI	2.5	10	-3,600	-9,000	1,036,100	6.5	7.9	-7,214
22C5	GBI	2.5	8	-4,000	-10,000	328,920	4.3	5.2	-6,927
22C1	UDRI/GBI	2.5	10	-3,400	-8,500	10,795,730	6.5	7.9	-6,813
				COMPRESSION FATIGUE TESTS OF BUTT-JOINTED CONTROL SPECIMENS:					
21C1	UDRI	10	10	-780	-7,800	44,990	6.7	8.2	-6,335
21C1	GBI	10	8	-820	-8,200	61,200	4.6	5.6	-5,794
21C2	UDRI	10	10	-700	-7,000	1,024,650	6.3	7.7	-5,537
23C5	GBI	10	8	-750	-7,500	792,690	4.6	5.6	-5,300
23C1	GBI	10	8	-520	-5,200	48,060	9.6	11.7	-5,119
23C2	GBI	10	8	-460	-4,600	1,839,930+	9.7	11.8	-4,559

* Test was completed at GBI at 9 Hz.
\+ Premature failure because of improper storage during interruption of test at 1,835,000 cycles.

Table 8-45 Examples of Apparent Changes in LMC of the Sample That Occurred During Compression Fatigue Testing

Sample Number	Joint Style	R Value	Cycle Rate (Hz)	Total Cycles	Pretest Weight (g)	Post-Test Weight (g)	Delta Weight (g)	Pretest LMC (%)	Post-Test LMC (%)	Delta LMC (%)
23C1	Butts	10	8	48,060	336.25	336.30	+0.05	9.63	9.65	+0.02
23A1	Scarfs	10	8	17,509,310	336.13	339.10	+2.97	6.38	7.32	+0.94
23A2	Scarfs	10	8	71,860	339.10	338.98	-0.12	8.15	8.11	-0.04
23C5	Butts	10	8	792,690	326.18	326.15	-0.03	4.63	4.62	-0.01
23A5	Scarfs	10	8	50,640	327.70	327.23	-0.47	5.13	4.98	-0.15

Table 8-46

REVERSE AXIAL TENSION-COMPRESSION FATIGUE TESTS (R = -1.0)
Test Program: MOD-5A, High-Moisture Scarf Joint Fatigue
Material: Douglas Fir and Epoxy, Blade Grade 1 Veneer
Construction: Dogbone Shape with 3 Transverse 12:1 Slope Scarf Joints in Center Veneers, 3-in. Stagger
Load Direction: Reverse Axial Tension-Compression Parallel to Grain
Temperature: 70°F

Sample Number	Test Site	Cycle Rate (Hz)	Minimum Tension Stress	Maximum Compression Stress	Total Cycles	LMC (%)	WMC (%)	Maximum Compressive Stress Adjusted to 12% W.M.C. (psi)
23B4	GBI	2.2	6,500	-6,500	17,710	4.7	5.73	4,624
21B1	UDRI	3.0	5,500	-5,500	32,400	6.6	8.10	4,438
23B3	GBI	3.0	4,500	-4,500	34,360	9.6	11.71	4,430
23B2*	GBI	3.0	4,500	-4,500	1,323,640	8.8	10.74	4,201
21B3	UDRI	3.0	5,000	-5,000	643,400	6.7	8.17	4,061
21B4	GBI	3.0	5,500	-5,500	486,250	4.8	5.86	3,938
23B1	GBI	3.0	3,750	-3,750	2,592,180**	9.7	11.83	3,716
21B5	GBI	3.0	5,200	-5,200	699,500	4.3	5.25	3,602
23B5	GBI	3.0	5,000	-5,000	355,450	4.5	5.49	3,510
23B2	GBI	3.0	3,500	-3,500	10,260,000+	8.8	10.74	3,268
21B2	UDRI	3.0	4,000	-4,000	10,169,100	6.2	7.56	3,143

* This was the second test of Sample 23B2. The first test did not result in failure at the initial maximum load of 3,500 psi.
** Failure initiated outside the test section caused test to terminate prematurely.
\+ Specimen did not fail, as of cycle total listed.

The results of testing the 13 specimens from billet 20, all of which contained butt joints or imperfect scarf joints, are shown in Table 8-47. These specimens all had relatively low moisture contents, and the adjusted static test values matched previous test results well.

The interpretation of fatigue test results is presented in two versions. S-N curves were plotted with the actual stress levels, and with the stress level adjusted to 12% wood moisture content. The latter results are fitted with straight trend lines on log-log plots, using the least squares fit data contained in Table 8-48.

Figure 8-49 shows the actual fatigue stress level plot for tension fatigue tests with a load ratio of R = 0.1. Figure 8-50 shows the corresponding plot with the adjusted to 12% wood moisture content. The two plots are very similar; the correlation factor was raised only 1.5% when the values were adjusted. In compression fatigue with R = 10, Figure 8-51 shows actual stress levels plotted. Figure 8-52 shows the results adjusted to 12% wood moisture content. The amount of scatter is significantly reduced with the adjustment, and the correlation coefficient trend is 34.8% lower. Figure 8-53 is a repeat of the adjusted data, but with data from section 8.1.2 testing superimposed. The data shown in Figure 8-54 is for the R = 2.5 scarf joint compression fatigue tests, shown with comparable data from the section 8.1.2 results for R = 2.5 butt joint tests and R = 10 scarf and butt joint trends.

Figure 8-55 shows the mismatched scarf joint fatigue data from specimens from billet number 20. The results are superimposed over the normal scarf joint trend from this section, and the butt joint trend from section 8.1.2.

Actual reverse axial fatigue results are shown in Figure 8-56, and Figure 8-57, shows these results adjusted to 12% wood moisture content. The

Table 8-47 Results of Static and Fatigue Tests of Blade Grade 1 Laminae with Imperfect Scarf Joints

Test Program: MOD-5A, High Moisture Scarf Joint Fatigue
Material: Douglas Fir and Epoxy, Blade Grade 1 Veneer
Load Direction: Parallel to Grain
Temperature: 70°F
Test Site: GBI

STATIC TESTS:

Sample Number	Sample Configuration	Joint Type	Loading	Ramp Rate (lbf/min)	Maximum Stress (psi)	LMC (%)	WMC (%)	Maximum Stress Adjusted to 12% WMC (psi)
20B5	Dogbone	Scarf	Tension	7,895	11,917	5.0	6.1	10,851
20A5	Cylinder	Scarf	Compression	8,696	10,262	5.6	6.8	7,749
20C3	Cylinder	Butt	Compression	8,696	10,072	5.5	6.7	7,555
20C5	Cylinder	Butt	Compression	8,696	9,980	6.0	7.3	7,738

COMPRESSION FATIGUE (R = 10):

Sample Number	Sample Configuration	Joint Type	Cycle Rate (Hz)	Minimum Stress (psi)	Maximum Stress (psi)	Total Cycles	LMC (%)	WMC (%)	Maximum Compressive Stress Adjusted to 12% WMC (psi)
20A2	Cylinder	Scarf	10	-750	-7,500	260,100	5.7	6.9	5,701
20A3	Cylinder	Scarf	10	-800	-8,000	48,030	5.3	6.9	5,922
20A4	Cylinder	Scarf	10	-850	-8,500	22,970	5.4	6.6	6,334
20A1	Cylinder	Butt	10	-800	-8,000	13,410	6.5	7.9	6,412
20C2	Cylinder	Butt	10	-800	-8,000	34,040	5.8	7.1	6,121

REVERSE AXIAL TENSION AND COMPRESSION FATIGUE (R = -1.0):

20B2	Dogbone	Scarf	3.0	-4,000	4,000	770,030	4.5	5.5	2,808
20B3	Dogbone	Scarf	3.0	-5,000	5,000	29,890	5.3	6.5	3,701
20B4	Dogbone	Scarf	2.5	-6,000	6,000	8,900	5.7	7.0	4,561
20B1	Dogbone	Butt	3.0	-4,500	4,500	65,090	5.0	6.1	3,265

Table 8-48 Summary of MOD-5A High-Moisture Scarf Joint Fatigue Data Analyses

	Total BG-1 Data Points	Correlation Coefficient of Linear Regression Line	Equation of Linear Regression Line	Maximum Stress Intercept of Linear Regression Line @ 10^4 Cycles (psi)	Maximum Stress Intercept of Linear Regression Line @ $4x10^8$ Cycles (psi)
Tension Fatigue (R = 0.1):	4	-0.9971	$S = 18,832 \times N^{-0.0658}$	10,270	5,112
Compression Fatigue (R = 10):	8	-0.9845	$S = 10,023 \times N^{-0.0361}$	7,191	4,906
Reverse Axial Fatigue (R = -1.0):	8	-0.9230	$S = 8,169 \times N^{-0.0587}$	4,757	2,554
Kommers (R = -1.0) Reverse Axial Flexural Fatigue:	424*	-0.9600	$S = 11,437 \times N^{-0.0692}$	6,047	2,904

* Kommers samples (.375" x 1.25" x 9.0") consisted of solid Douglas fir, not laminae. Kommers tests were not load controlled. "The Fatigue Behavior of Wood & Plywood Subjected to Repeated & Reversed Bending Stresses", Report No. 1327 dated 1943, prepared by W. J. Kommers, Forest Products Laboratory, Madison, WI.

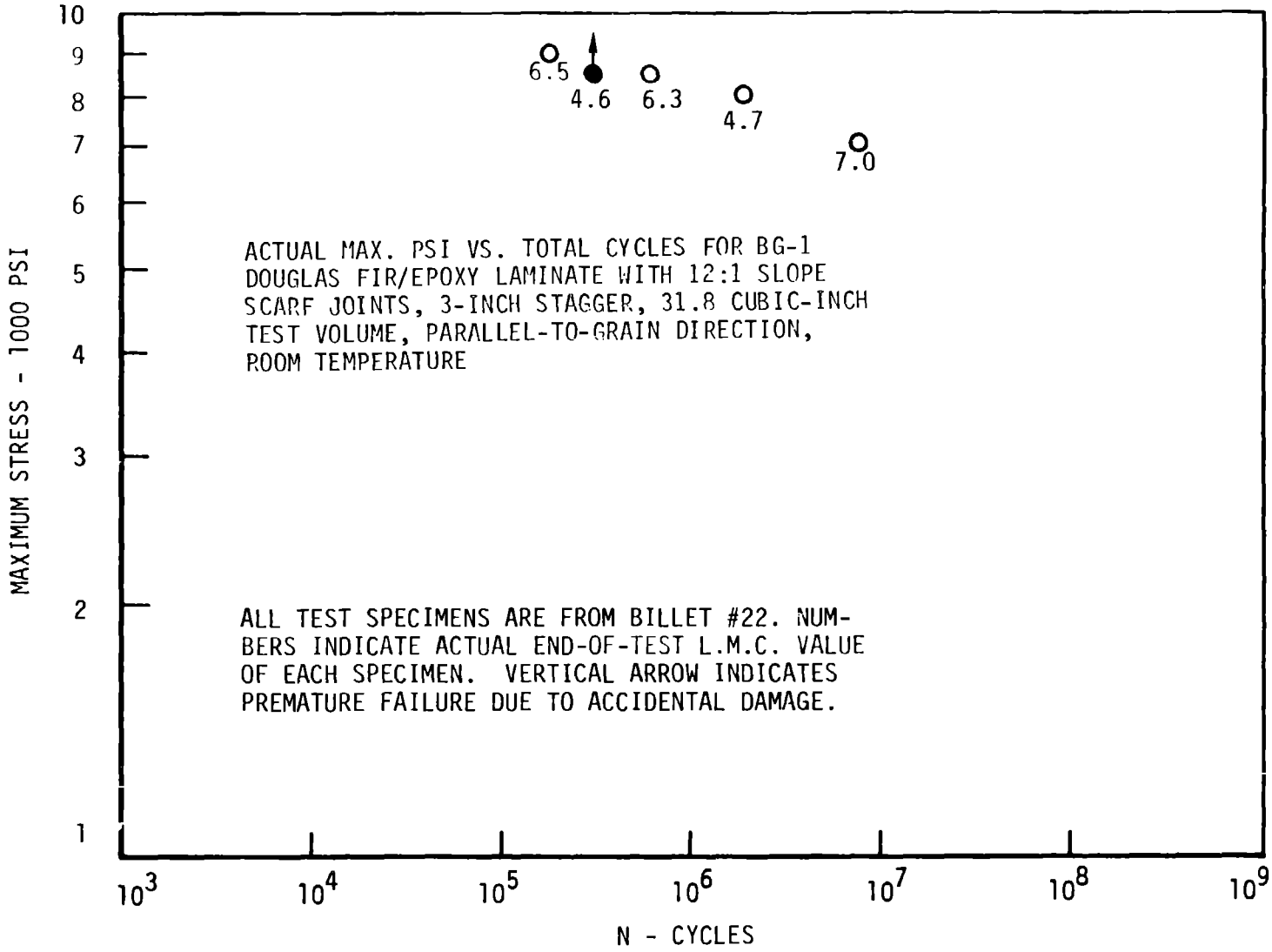

Figure 8-49 Tension Fatigue (R = 0.1) S-N Diagram

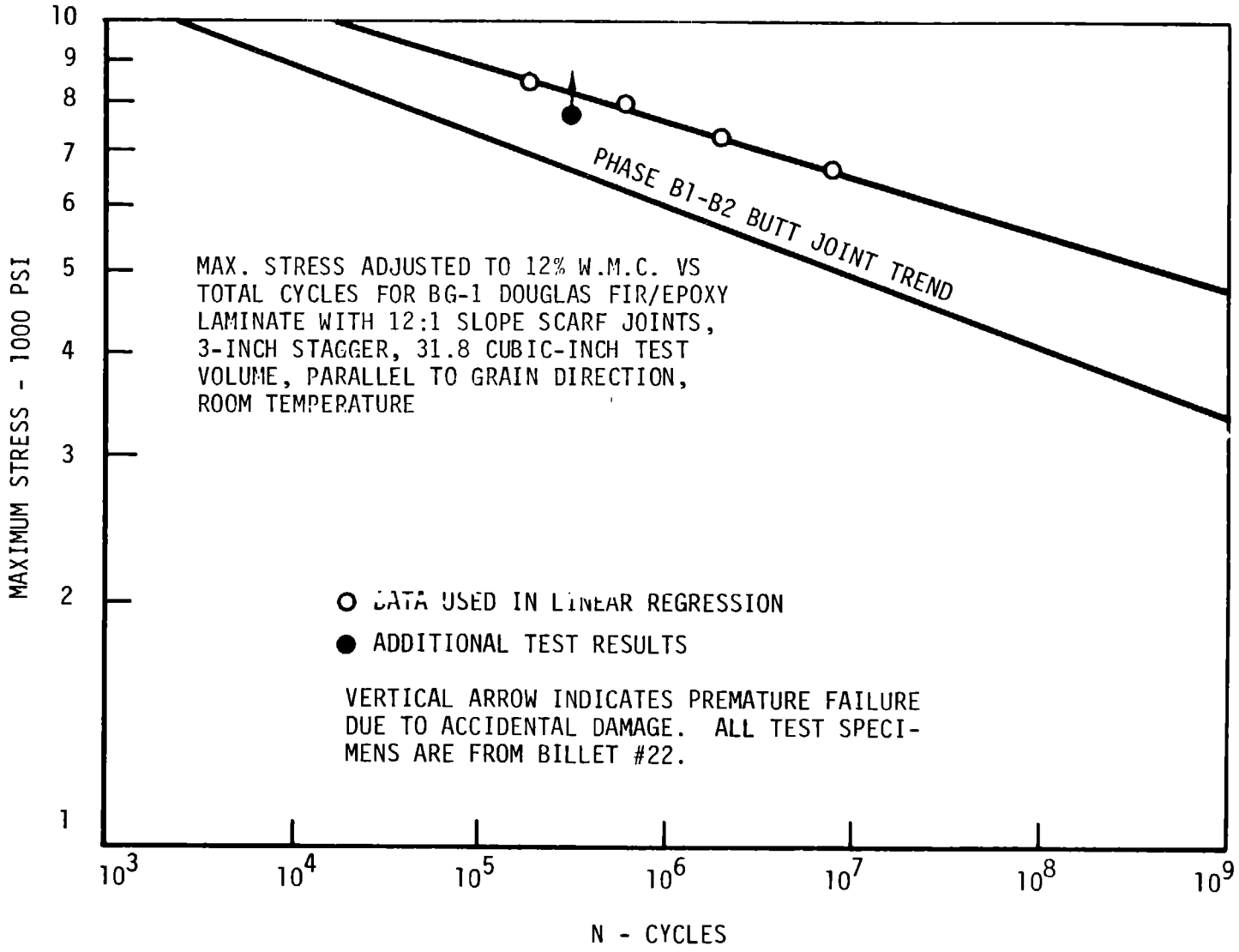

Figure 8-50 Tension Fatigue (R = 0.1) S-N Diagram

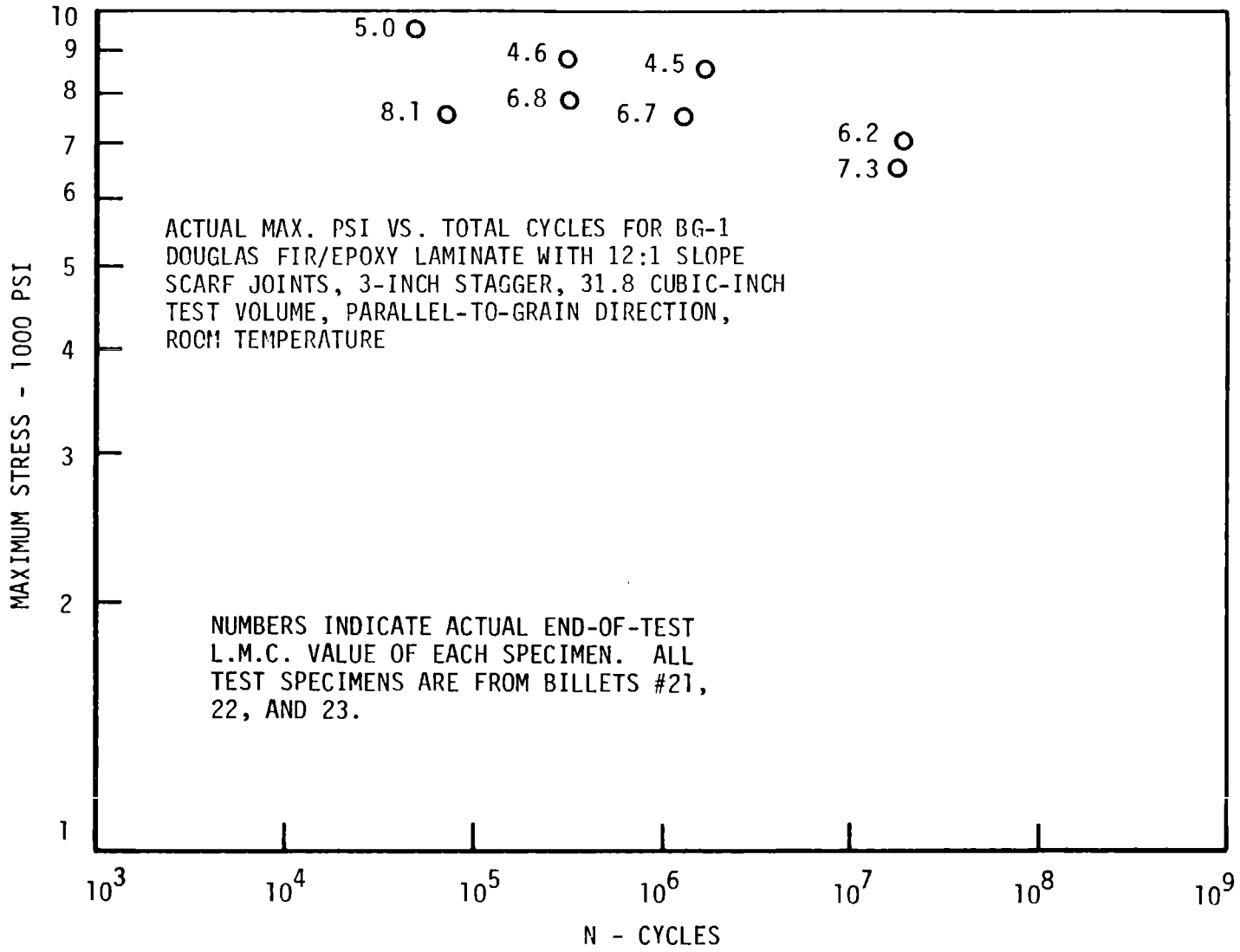

Figure 8-51 Compression Fatigue (R = 10) S-N Diagram

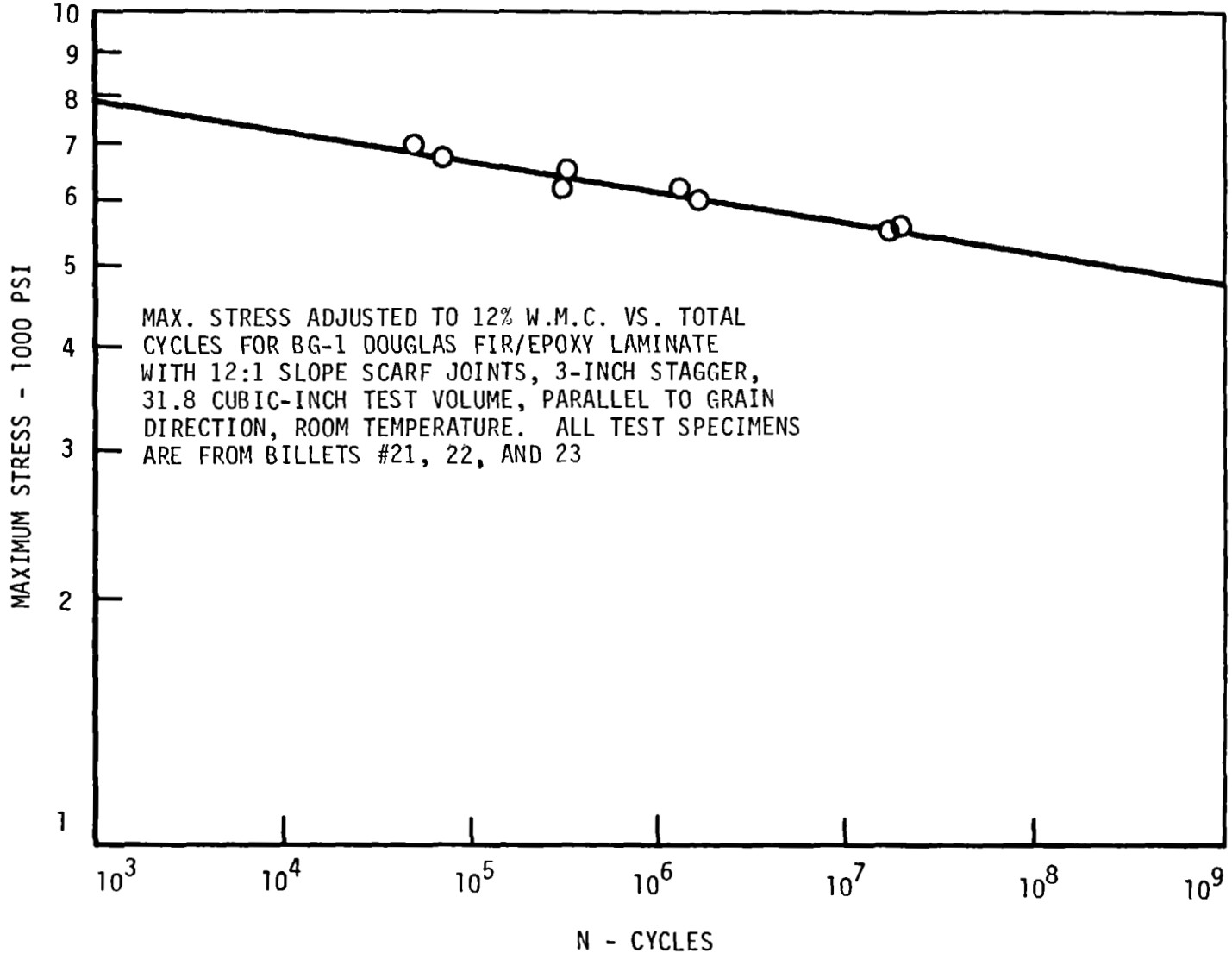

Figure 8-52 Compression Fatigue (R = 10) S-N Diagram

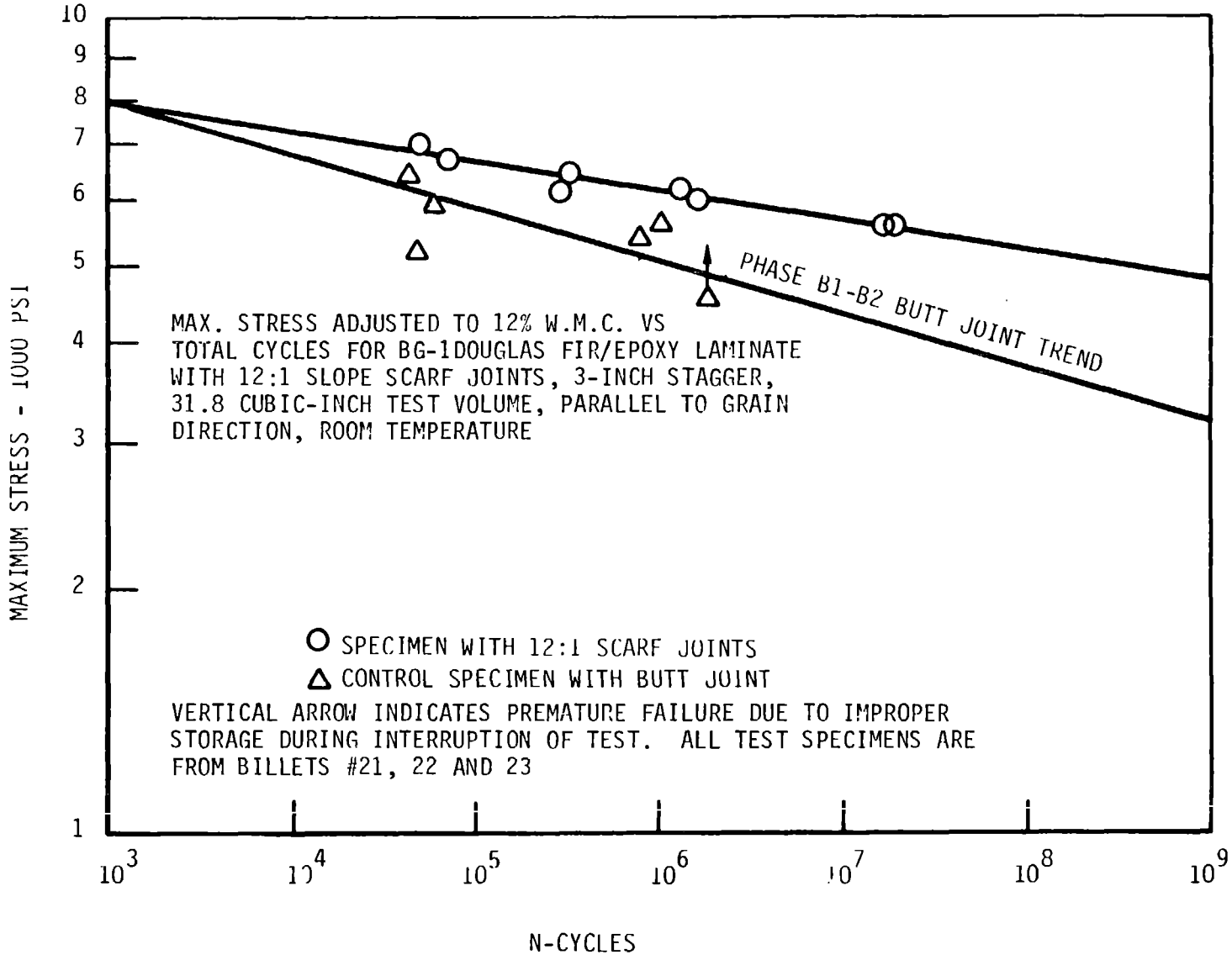

Figure 8-53 Compression Fatigue (R=10) S-N Diagram

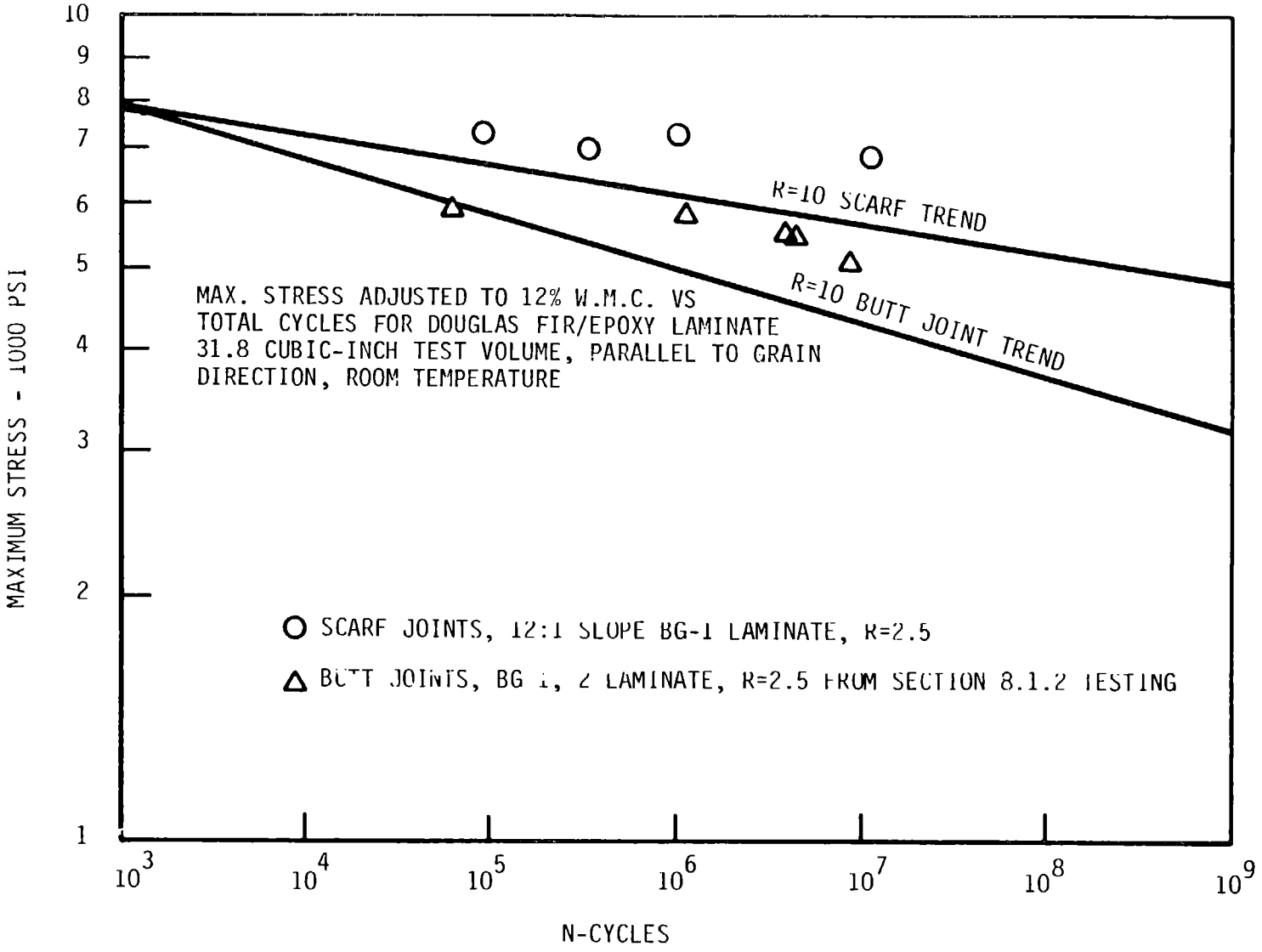

Figure 8-54 Compression Fatigue (R = 2.5) S-N Diagram

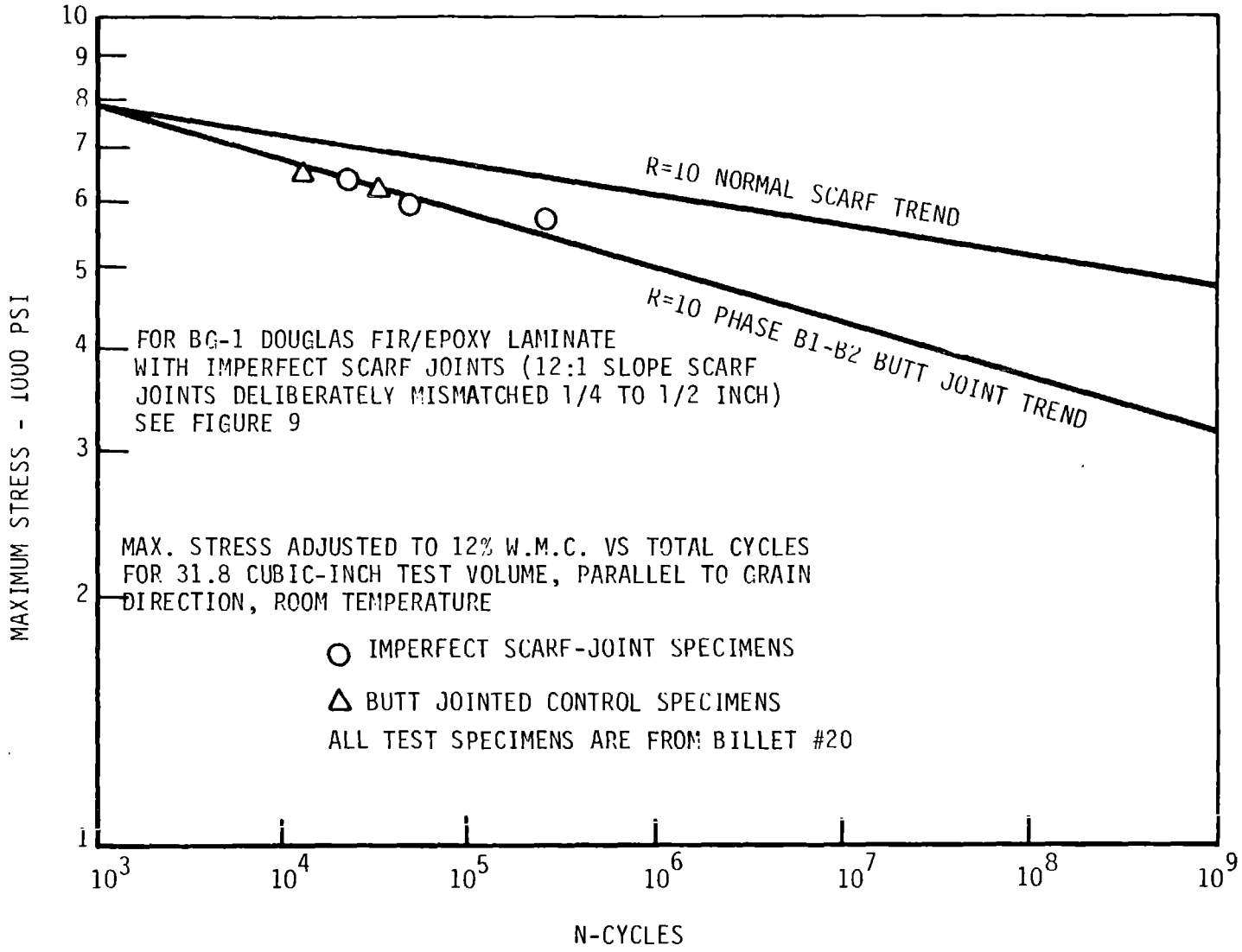

Figure 8-55 Compression Fatigue (R = 10) S-N Diagram

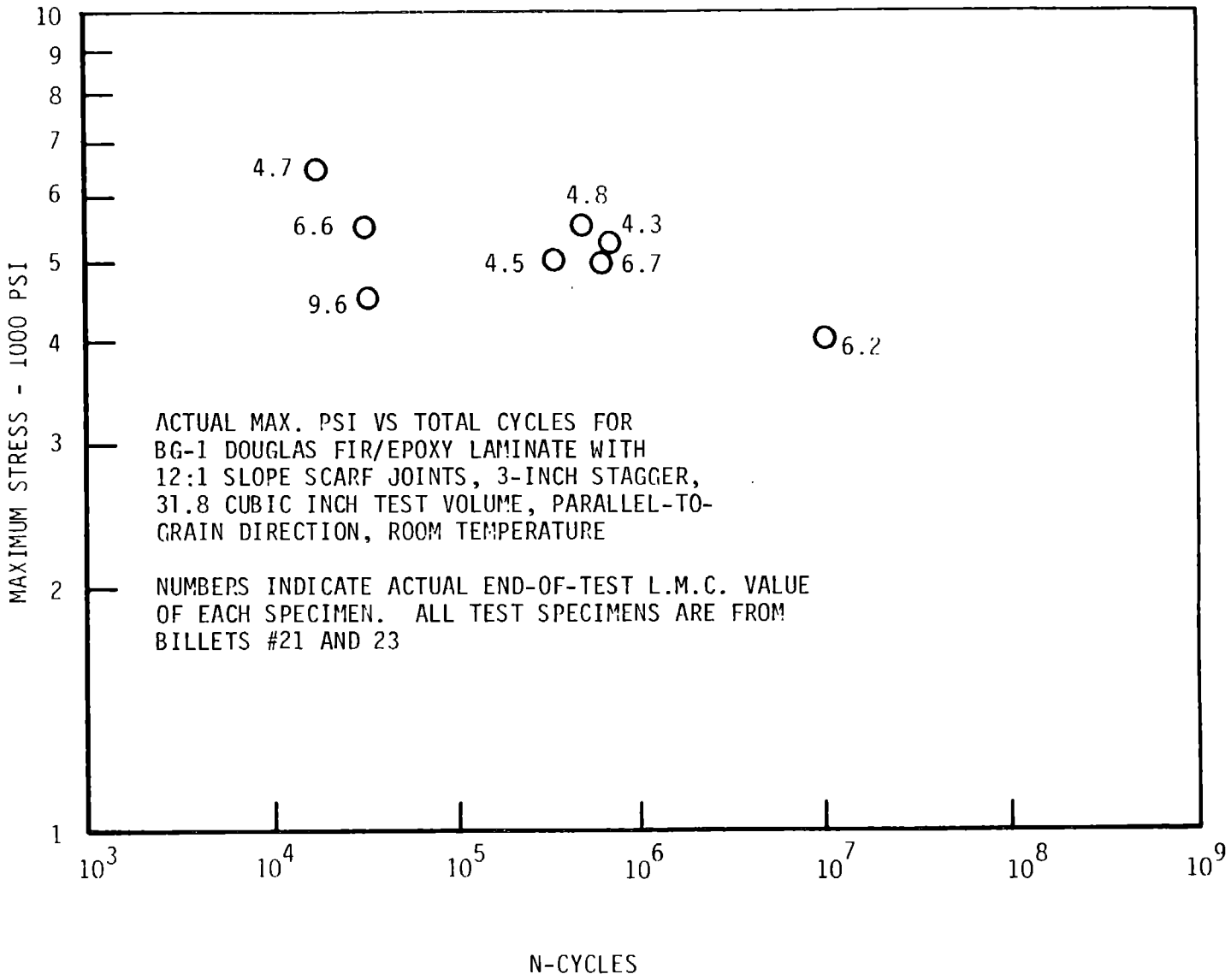

Figure 8-56 Reverse Axial Tension Compression (R = -1.0) S-N Diagram

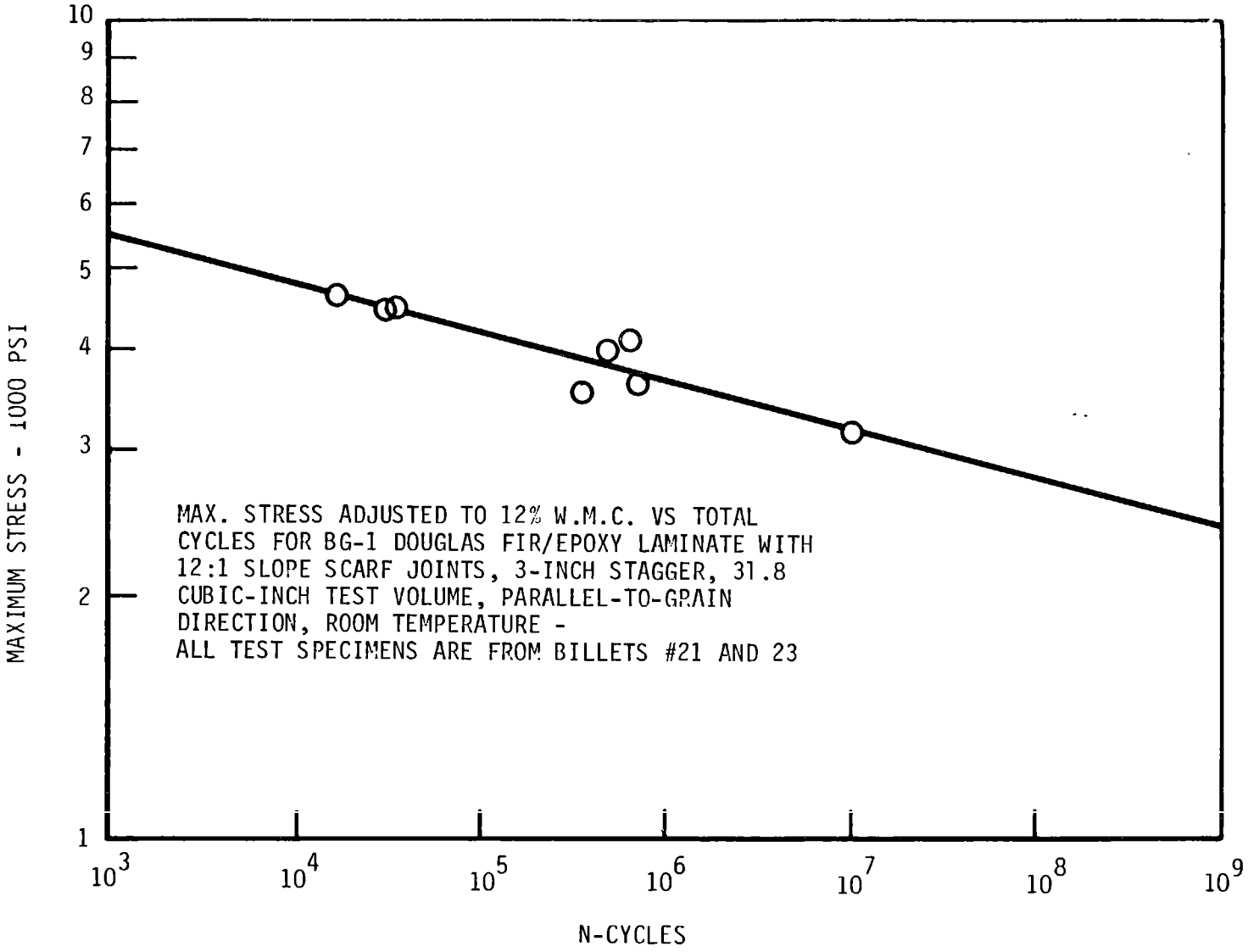

Figure 8-57 Reverse Axial Tension-Compression (R = -1.0) S-N Diagram

latter has an apparent data scatter decrease, and a 40.8% decrease in the correlation coefficient. Figure 8-58 indicates that the compressive wood moisture content adjustment works well for low cycle reverse axial testing. This figure includes more results from billet 23 samples. Sample 23B2 did not fail after testing for 10 million cycles at ± 3,500, but it did fail after another 1.32 million cycles at ± 6,000 psi. The point plotted is for 10.5 million cycles at the original load. This cycle credit was based on using a regression analysis slope based on 8 legitimate points tnat showed an apparent 72.2 cycles at the lower load to be equal to one at the higher load. The performance of 23B2 during the second test phase was well above the trend, as was the abbreviated test of sample 23B1. These two samples had high moisture contents, and indicate that moisture may be beneficial to high cycle R = -1 fatigue performance. Figure 8-59 shows the R=-1 fatigue trend lines for scarf and butt joint and Kommers' data. Figure 8-60 contains imperfect scarf joint test points from billet 20 samples.

Table 8-49 presents a summarized comparison of 12:1 normal scarf joint fatigue performance with butt joint data from section 8.1.2 data at 10^6 and 10^7 cycles. The numbers are based on 12% wood moisture content linear regression trend lines at 12% wood moisture content and reflect the percent increase in load-carrying capability for the lifetime noted.

Table 8-49 Fatigue Performance Improvement of 12:1 Slope Scarf Joints Compared to Phase B1-B2 Butt Joints

Fatigue Mode	10^6 Cycles	10^7 Cycles
R = 0.1 Tension	25.8%	30.0%
R = 10 Compression	22.0%	30.2%
R = 2.5 Compression	20.7%	33.3%
R = -1.0 Reverse Axial	19.4%	25.5%

The S-N diagrams presented in Figures 8-49 through 8-60 suggest that the relationship between fatigue strength and moisture content of Douglas fir

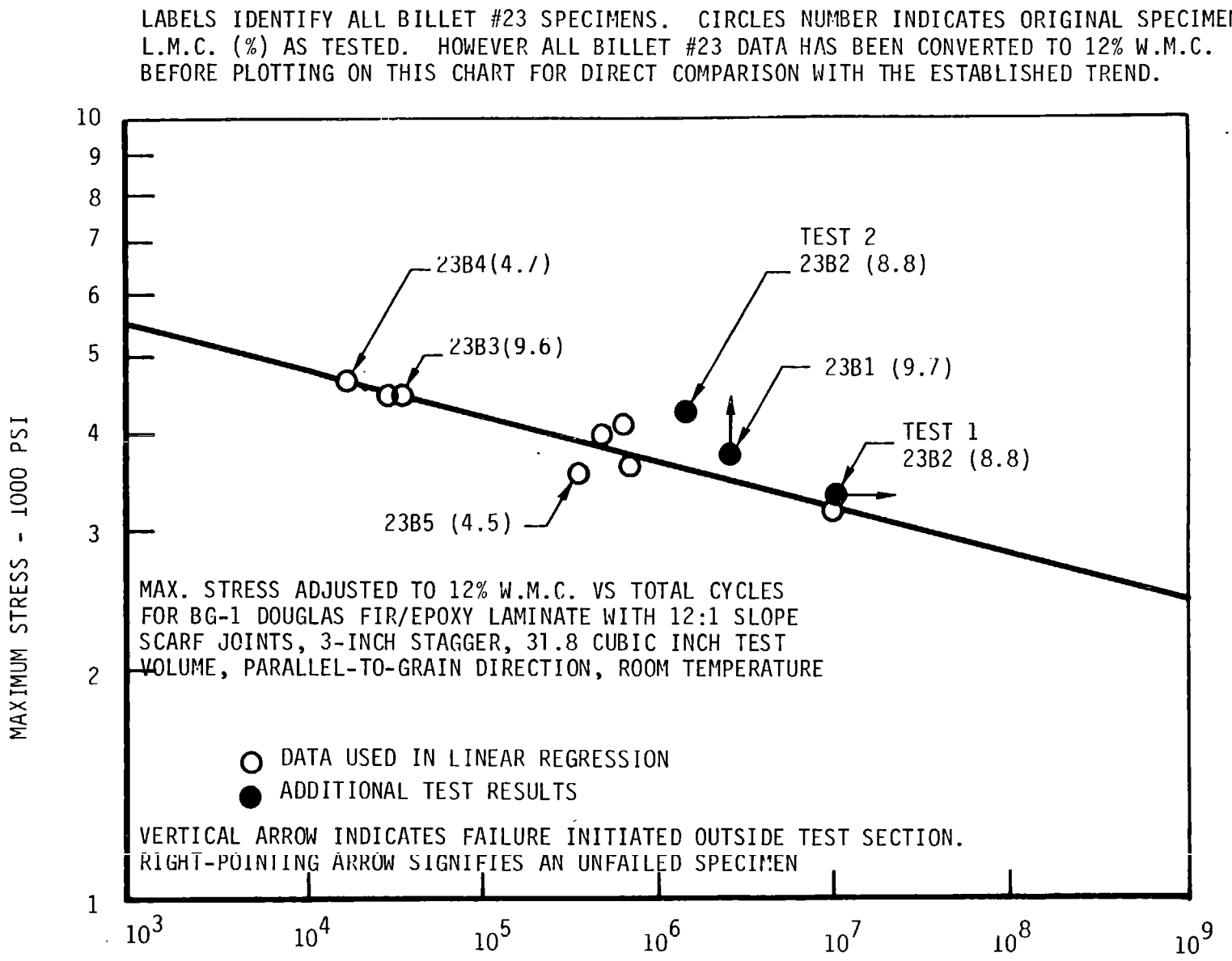

Figure 8-58 Reverse Axial Tension-Compression (R = -1.0) S-N Diagram

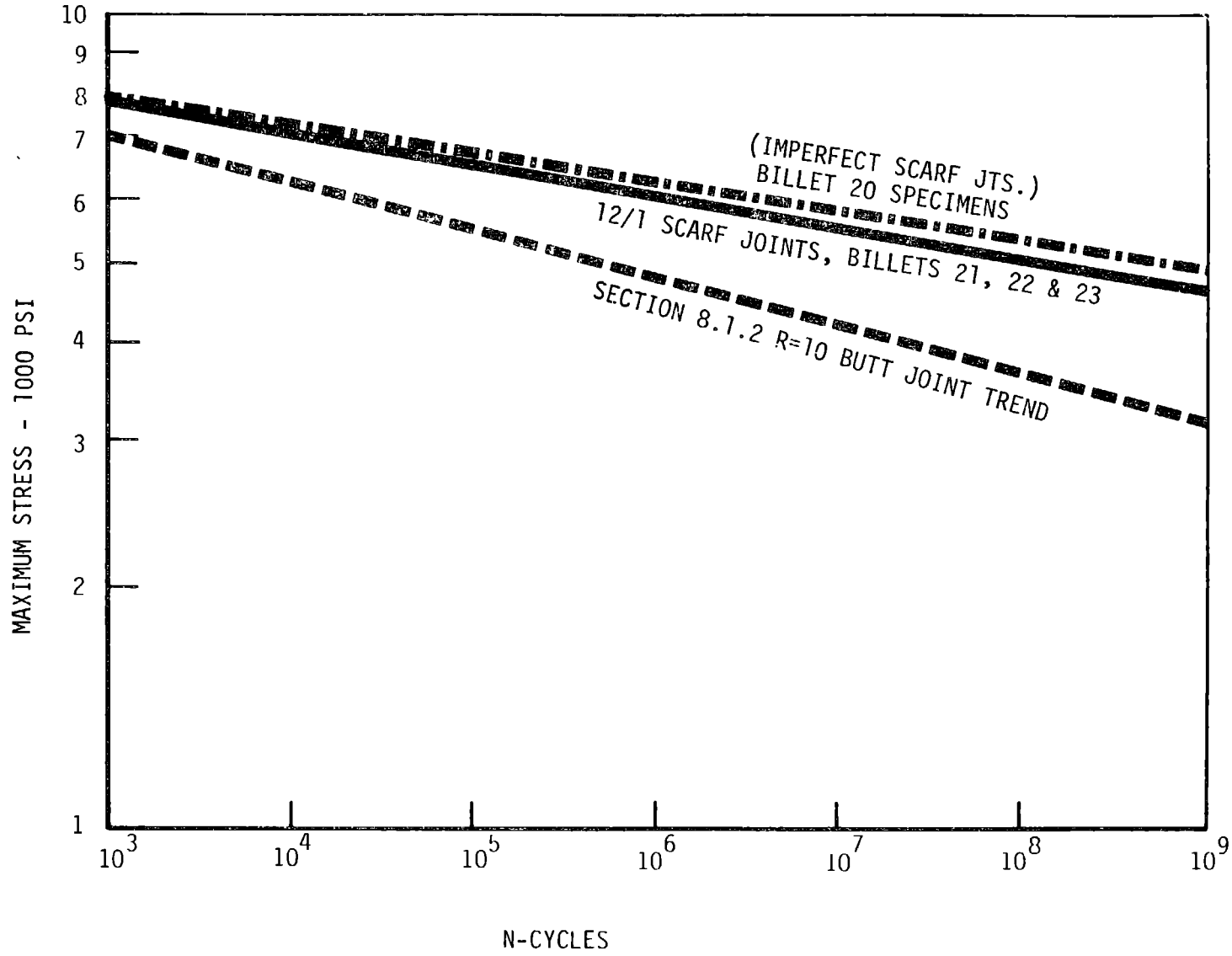

Figure 8-59 Compression/Compression (R=10) Fatigue S-N Trends Adjusted to 12% M.C.

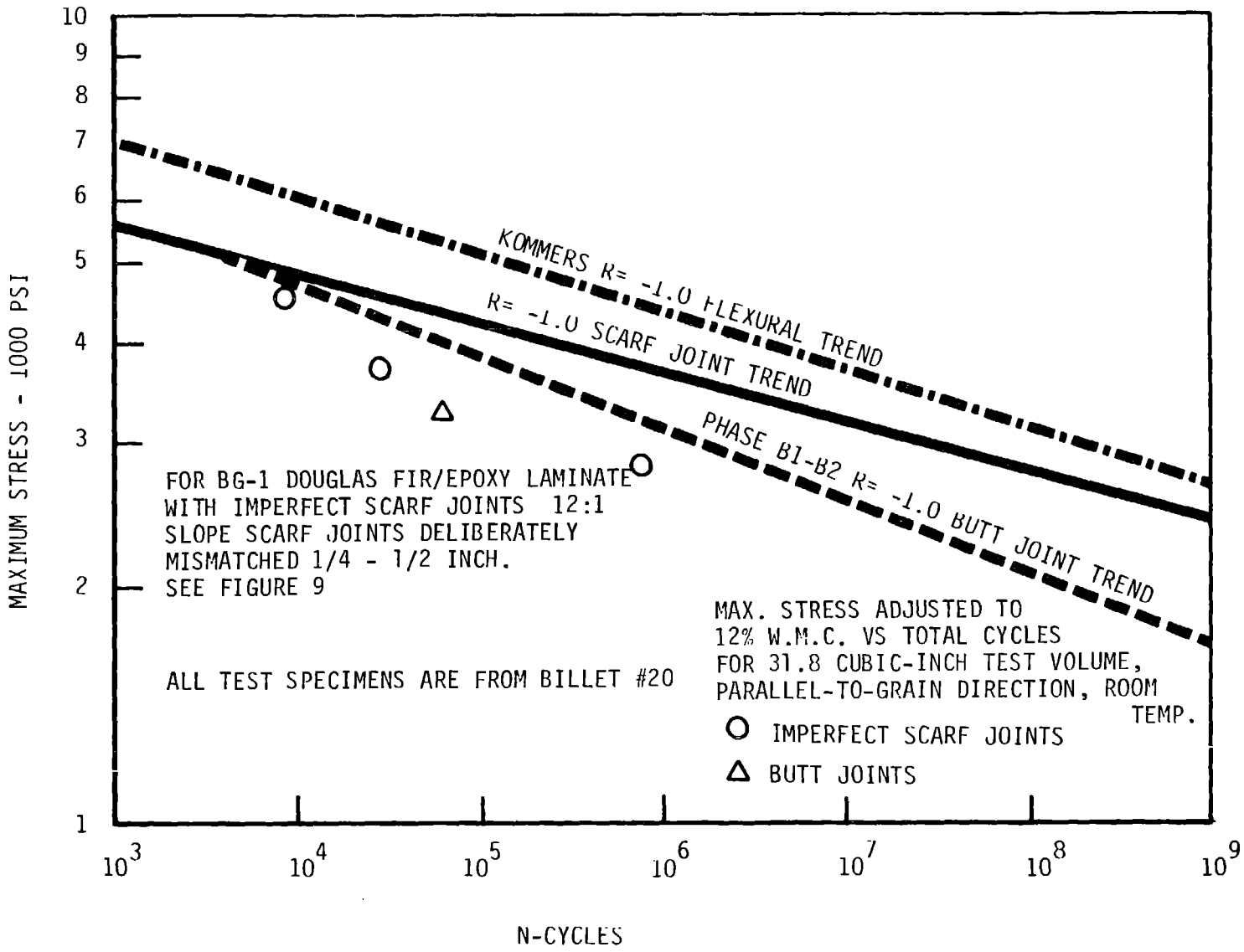

Figure 8-60 Reverse Axial Tension-Compression (R=-1.0) S-N Diagram

laminae with scarf joints is basically the same for low cycles as the relation between the static strength and moisture content of small, straight-grained, clear wood samples. The relationship is the same as the relation upon which the Wood Handbook's (reference 4) method of quality comparison is based. The data tends to indicate that for high cycle life, the trends are overly conservative. However, more high-moisture, high-cycle tests are needed, particularly in the R = -1.0, reverse-axial tension and compression fatigue mode.

8.1.5.2 Outdoor Exposure Moisture Test

8.1.5.2.1 Introduction

The MOD-5A was developed to perform in a vast range of environments. As was shown in section 8.1.5.1 and in previous publications, the strength of wood members varies significantly with the moisture content of the wood. The MOD-5A blade contained a large amount of wood in structural applications, so the cost was influenced strongly by strength allowables and, by moisture content. Precautions were taken to retard the transmittal of moisture from the environment to the blade. However, the long term effect was unproven, especially in high moisture areas such as Hawaii or Houston, Texas, or in a very dry desert condition, such as that in Palm Springs, California.

8.1.5.2.2 Objectives

This test series exposed scaled blade samples to various moisture environments to determine the actual variation in moisture over an extended time. The sites were selected to be either extreme or representative of actual rainfall, humidity and temperature.

8.1.5.2.3 Description

The test article was designed to represent a typical section of the MOD-5A blade. It was a circular section, 11.38 in. in diameter. The section was 5.6 in. thick, made of 56 layers. The section was set in the top of a 12 in. high plexiglass tube leaving a 6.4 in. space between the inner face of the specimen and the bottom of the tube. The configuration is shown in Figure 8-61. A pattern of eight vent holes was provided beneath the specimen. The top surface was prepared with two coats of white urethane paint over an epoxy gel coat, which was over two layers of Burlington, 6 ounce glass cloth wet with West System® epoxy. The lower face was sealed with a coat of West System®

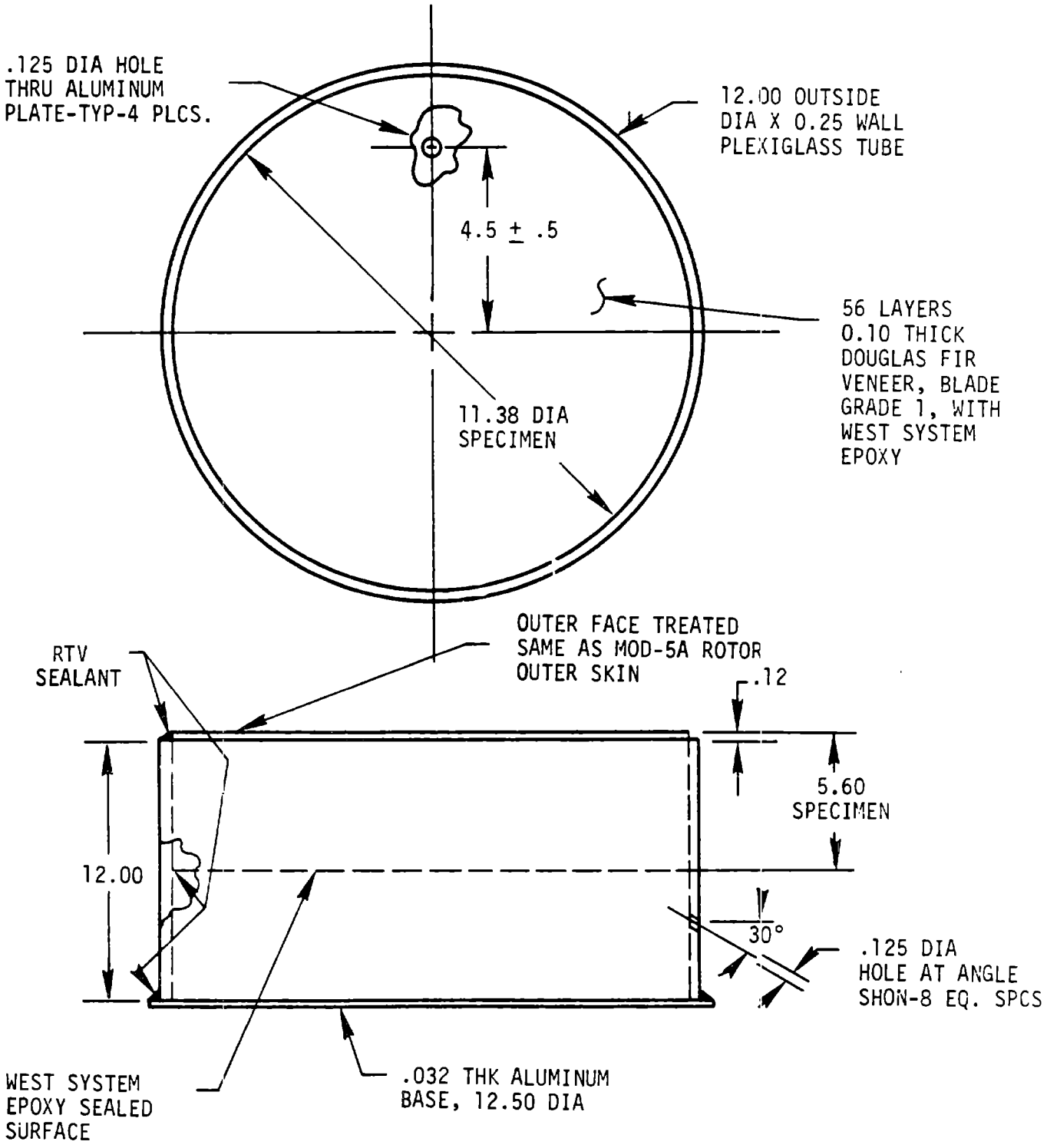

Figure 8-61 Outdoor Moisture Specimen

aluminum-filled epoxy applied over two layers of Burlington, 6 ounce glass fiber cloth wet with West System® epoxy. The design was intended to duplicate the materials of construction and the exposure the two surfaces of the blade would receive. Setting the test section in the tube in this way was required to provide a simulated vented blade cavity on the backside of the wood and providing edges that would be sealed against moisture penetration. To further limit moisture penetration through the end grain the edges were sealed with West System® epoxy under and over a wrap of aluminum foil. This plan was in keeping with the concept of the blades unexposed edge grain surface. Three samples were fabricated by GBI and completed in October, 1983.

Three sites were selected for testing the specimens. Houston, Texas, has a warm, moist climate, so one sample was placed on the roof of a building at the NASA Johnson Space Flight Center. The sample rests on a drain cover, which will prevent immersion of the base in water since it is several inches above the roof surface. The sample was installed on November 9, 1983.

The second sample was located in the desert at Southern California Edison's Deever sub-station, situated outside Palm Springs, California, in the San Gorgonio pass. The specimen is located on the roof of a small storage building. The base will not be immersed in water, although the sample is fully exposed to the environment. It was placed on November 10, 1983.

The third sample is located at the University of Hawaii at Manoa, on the island of Oahu. This site was selected since it had the same general characteristics that would be experienced at the MOD-5A site at Kahuku Point, Oahu. It was placed on location on January 23, 1984.

8.1.5.2.4 Results

Since November of 1983, the Houston and Palm Spring samples have been monitored twice. The results of those readings, and two from the specimen in Hawaii, are shown in Table 8-50. The wood moisture content calculations are based on an average content of 6.87% at fabrication, measured by GBI. The sample weights (laminae only) were as follows at the time of fabrication:

Table 8-50 Moisture Specimen Test Results

Specimen Location	Date	Total Days of Exposure	Weight (grams)	Comments	Weight Difference (grams) From Start	Calculated Wood Moisture Content (%)	Calculated WMC Change (%)
Houston	11/09/83	0	8569.5	Initial Deployment		8.380	
	01/18/84	70	8574.5		+5.0	8.488	+.108
	03/29/84	141	8587.0		+17.5	8.757	+.377
Palm	11/10/83	0	8613.5	Initial Deployment		8.383	
Springs	01/19/84	70	8618.5		+5.0	8.490	+.107
	03/28/84	139	8614.0		+0.5	8.394	+.001
Hawaii	01/23/84	0	18.94 lbs.	Initial Deployment		8.381	
	02/29/84	37	18.95 lbs.*				
	05/31/84	92	18.961 lbs.*				

* Changes are less than scale resolution.

	Laminae Weight (grams)	Water Weight	Wood Weight
Houston Specimen	5671.4	389.6	4649
Palm Springs Specimen	5712.5	392.5	4682
Hawaii Specimen	5687.3	390.7	4662

As shown in Table 8-50, the wood moisture content of the Houston sample increased by 0.377% over 141 days, and that of the Palm Springs sample seemed to rise during the wet season and is now losing some moisture. The Hawaii sample differentials are still within the resolution range of the scale and cannot yet be utilized. The plan calls for the testing to continue, to establish long term trends.

8.1.5.3 Finger Joint Enhancement and Stabilization Test Program

8.1.5.3.1 Introduction

The use of finger joints to join adjacent blade sections requires fairly precise surfaces to be cut on the ends of the large structures. This job is more easily performed at the factory than in the field. However, the possibility that dimensions might change during the shipping and field storage periods was of concern. Precautions, such as wrapping the exposed surfaces in plastic were considered, but the duration and extremes of climate that could be expected when shipping a blade between Michigan and Hawaii over ground and sea, may still be a problem. Augmentating the surfaces adjacent to the ends with Kevlar or glass fiber was considered. The stiffness of these two materials is significantly higher than wood's, and they are only slightly influenced by moisture. However, this plan would increase the cost of the blade. The blade ends could be sealed in plastic filled with wood chips conditioned to the same moisture level as the blade. The effectiveness of these techniques needed to be established.

8.1.5.3.2 Objectives

The primary objective of this test was to demonstrate the feasibility of stabilizing the dimensions of newly prepared finger joints for shipment.

The shipment of the MOD-5A blade between its manufacturing site in Bay City, Michigan to the first construction site at Kahuku Point, Oahu, Hawaii was the main interest.

8.1.5.3.3 Description

A box 42.5 in. high, 46 in. wide and 133 in. long was fabricated and painted white for use in encasing and shipping the test specimens. The crate was vented, and contained four billets, each made of 15 layers of blade grade 1, Douglas fir veneer. They were 120 in. long. They all had finger joints cut along the length of one end. Two of the billets were unaugmented, one had #7500 Burlington glass fiber between all layers, and the fourth was similarly augmented with #5285 Burlington Kelvar cloth. One of the unaugmented billets and the two augmented ones were sealed in a Kevlar bag filled with wood chips conditioned to the same moisture content as the veneer. The fourth billet was placed in the box, but was not protected. Steel rods and measuring tabs were placed with the specimens to allow length variations to be measured using a micrometer. The crate was shipped by truck to the West Coast, by ship to Honolulu, and by truck to the site at Kahuku Point, Oahu, Hawaii. Figure 8-62 shows the crate in place.

8.1.5.3.4 Results

The results to date are shown in Table 8-51 for exposure while the crate was in transit. It left Bay City, Michigan approximately May 12, 1984 and arrived in Hawaii on June 6, 1984. The crate was moved from Kahuku Point to the Waiau Power Station of HECO, located near Pearl City and is presently sitting in an unshaded area.

The Kevlar-augmented specimens had the least variation in length. The glass fiber allowed a growth of two to three times as much. These values were both considerably less than those for the unaugmented control specimens. The protected control grew by a factor of 10 times that of the Kevlar-augmented sample, and the unprotected control factor was greater than 60. Augmentation significantly reduced growth, but the decision to protect joint ends must be evaluated for each case, based on accuracy requirements.

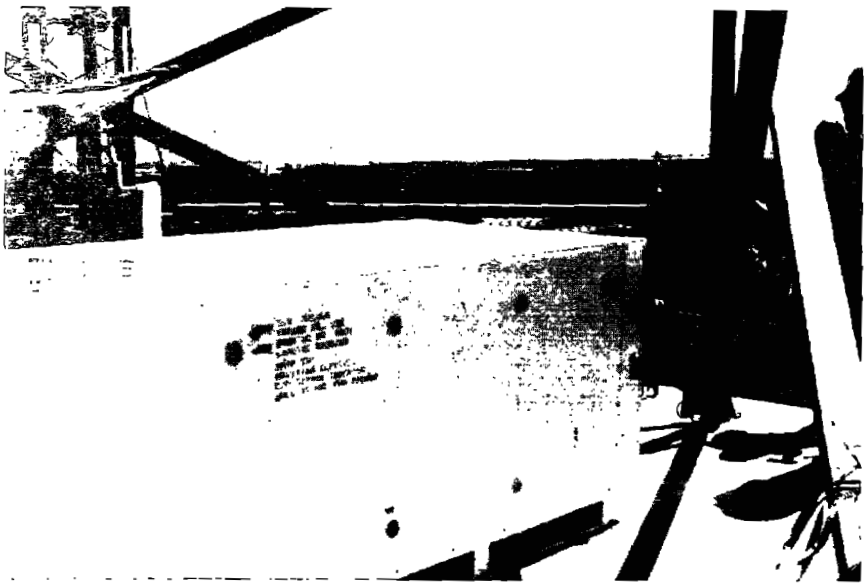

Figure 8-62 Crate on Location at Kahuku Point

C-3

Table 8-51 Finger Joint Enhance and Stability Test Results

Date	Time	Temperature (°C)	Humidity (%)	DIFFERENTIAL GROWTH FROM 5-9-84 (IN.)* Protected Control	Kevlar Augmented	Glass Fiber Augmented	Unprotected Control
05-09-83	14:19	21.0	40.0	0	0	0	0
05-10-83	16:09	20.0	38.0	-.0095	+.0001	-.0001	+.0009
05-11-83	08:15	17.0	51.5	-.0071	+.0013	-.0019	+.0009
05-12-83	08:04	15.0	52.0	-.0048	+.0020	-.0035	+.0027
06-14-83	10:45	27.0	50.0	+.0348	+.0093	+.0272	+.1521
06-23-83	14:30	27.2	55.0	+.0498	+.0156	+.0254	+.2273
07-06-83	10:30	26.7	60.0	+.0519	+.0179	+.0222	+.3130
07-20-83	10:00	27.8	60.0	+.0595	+.0260	+.0242	+.3957
07-27-83	11:15	28.9	50.0	+.0568	+.0121	+.0288	+.4288
08-03-83	14:30	29.4	66.0	+.0719	+.0148	+.0271	+.4900
08-15-83	16:00	29.4	57.0	+.0874	+.0253	+.0466	+.5422
08-22-83	09:30	28.9	63.0	+.0530	+.0083	+.0191	+.5444
08-31-83	14:00	29.4	59.0	+.0695	+.0095	+.0208	+.6033
09-14-83	10:50	28.8	54.0	+.0630	+.0086	+.0200	+.6411
09-28-83	11:07	27.5	71.5	+.0681	+.0081	+.0210	+.6966
10-11-83	12:45	25.0	70.5	+.0562	+.0046	+.0183	+.6879
11-01-83	12:05	26.6	67.6	+.0655	+.0082	+.0231	+.7334
11-15-83	12:15	29.2	54.0	+.0678	+.0054	+.0187	+.7517
11-28-83	09:00	25.0	67.0	+.0630	+.0068	+.0209	+.7626
12-21-83	12:24	25.0	63.0	+.0597	.0001	+.0105	+.7843
01-09-84	12:43	27.8	53.0	+.0746	+.0053	+.0180	+.8497
01-26-84	13:30	29.4	54.0	+.1146	+.0121	+.0319	+.8826
02-11-84	11:20	30.5	51.0	+.0992	+.0117	+.0542	+.8202
03-13-84	08:30	26.6	61.5	+.1022	+.0137	+.0324	+.7602
03-27-84	13:00	29.4	50.0	+.1246	+.0118	+.0329	+.7349
04-13-84	10:30	28.3	62.0	+.1102	+.0118	+.0317	+.7149
04-30-84	11:30	29.44	48.0	+.1180	+.0118	+.0308	+.7356
05-21-84	10:00	28.89	50.0	+.1171	+.0116	+.0322	+.7153

* Over 120 in. width crossgrain specimen.

8.1.6 SIZE EFFECT TESTING

8.1.6.1 Introduction

Most tests conducted on any material use relatively small samples, since they are convenient and inexpensive. For many materials the results can be applied to larger structures without question, but a wood structure is affected by its size. The strength of wood decreases as size increases. There are several theories aimed at explaining this phenomenon. The MOD-5A blade was a very large wood structure, so using strength data from characterization tests on small samples, without considering the size effect, would have been risky. The testing described in section 8.1.4 provided a significant amount of data on static strength versus size for samples with volumes as large as 3744 cubic in. The testing conducted in this section determines the static strength for specimens with volumes of 32,833 cubic in. and fatigue data for specimens with volumes of 7,488 cubic in.

8.1.6.2 Size Effect Static Test Program

8.1.6.2.1 Objectives

The objective of this large scale, static test program was to provide a representative strength data point for a specimen with a volume of 32,832 cubic in. Used with test data from smaller samples, this test will permit test data to be extrapolated out to the point of the MOD-5A blade volume, which is approximately a decade beyond this test volume.

8.1.6.2.2 Description

A search of test facilities was conducted, to identify machines capable of handling specimens large enough to meet the objectives of this test. Four Baldwin test machines that met this criteria were located. One is located in California, one in the Philadelphia Navy Yard (in need of repairs), one in the National Bureau of Standards in Washington, D.C., and one in Lehigh University, Bethlehem, PA. Lehigh University was willing to participate in the project and was selected to do the testing. Their laboratory has a test capacity of 5×10^6 lbs., and is well equipped for handling large specimens. The difficult portion of this test was developing a way to interface the ends of the test specimen and the machine. In order to minimize bending of the test article during loading, machine fittings with spherical self-aligning bearings were selected.

The specimen gage section was 6 by 24 in. and was 228 in. long. Each layer of blade grade 1 Douglas fir veneer was assembled with scarf joints on 3 in. staggered centers, and all were 24 in. wide. The length of the specimen was 334 in.; 53 in. on each end contained a flared section with a 12 by 24 in. cross section. A complement of 18 hollow studs, described in section 8.1.4 is report, were installed in each end of the specimen, using asbestos-filled West System® epoxy. The end sections were wrapped with glass fiber cloth and epoxy to a thickness of 0.10 in. Before the studs were installed, the wood assembly weighed approximately 1,475 lbs. A pair of end fittings was developed to adapt the stud-ended specimen to the test machine. The three rows of six studs each mated with a 4.0 in. thick plate, with upstanding gusset plates, which mated with a 10 in. diameter clevis pin on the test machine. The test specimen is shown in Figure 8-63. Six test specimen assemblies were manufactured, with two sets of end fittings and two full complements of hardware. One group of 18 threaded shanks, which attach the studs to end fittings, was fitted with internal strain gages to evaluate the distribution of load into the specimen end.

8.1.6.2.3 Results

The first specimen subjected to test contained strain gage studs, and was fitted with four LVDT sensors, to measure the elongation of the four sides of the gauge length. The specimen was loaded into the test machine vertically. The upper head of the machine is driven by a pair of power screws, and the lower head contained a load cell. A load ramp of 250,000 lbs. per minute was applied. Strain gages, LVDT's and the load cell output were recorded using a Kaye Digi Strip Data Logger. Specimen number 6 failed at a load of 1,077,000 lbs. Two acoustic reports were emitted. An inspection of the lower end of the specimen indicated that the bolster on the last 53 in. of the specimen had sheared free of the sample on one side and had moved 3.62 in. The 12 studs in the other portion had pulled free. The failure had taken place almost entirely in the end attachment area instead of in the gage length, and had occurred at a gage section stress level of 7,479 psi, although the design goal was more than 10,000 psi. A reduction of test data showed that load introduction into the studs was within 23% of the mean, which was considered reasonable for this configuration. The load pattern was very symmetrical and LVDT readings were all within 5% of each other, a spread within the system

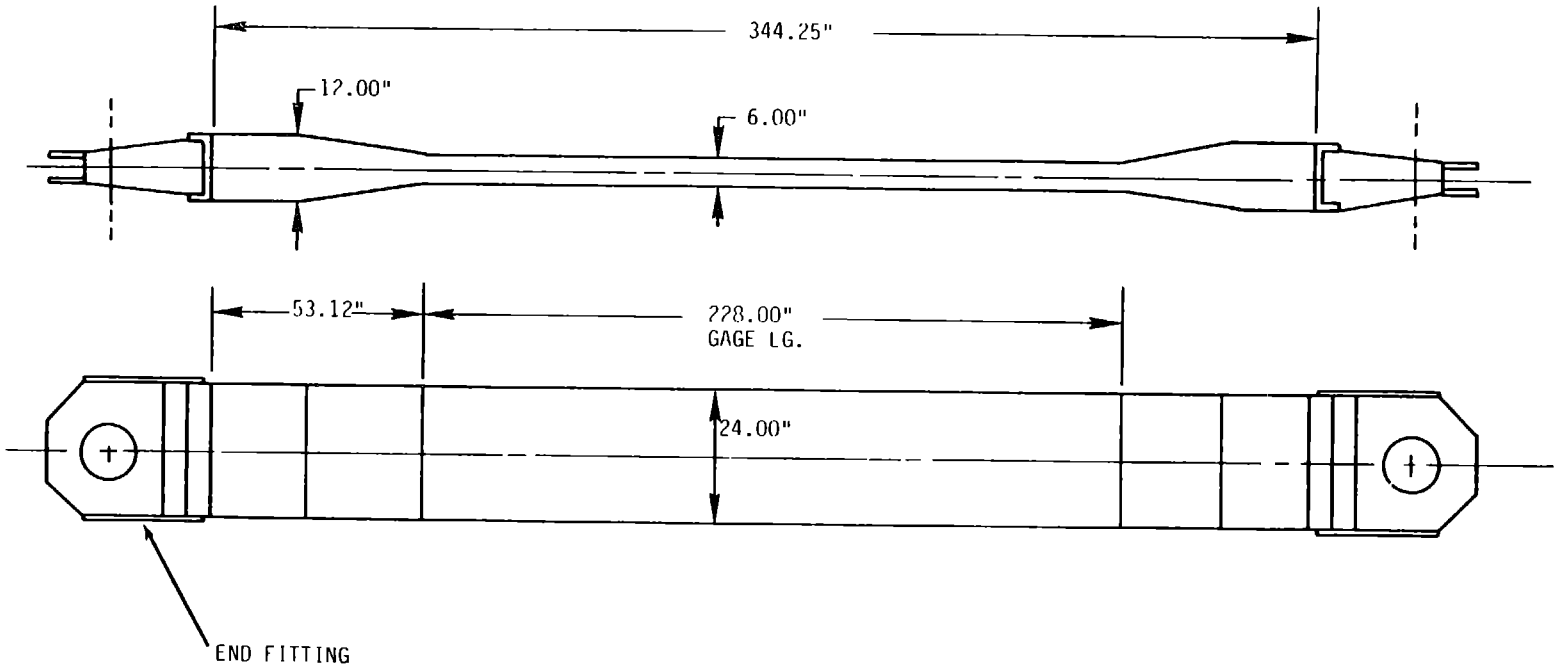

Figure 8-63 Test Specimen, Static

tolerance range. A second sample was tested, to determine if the failure of the first sample was an anomaly. This sample failed at 1.10 million pounds (7,639 psi) in a similar fashion, and further testing was delayed until a solution to the problem could be found. Analysis indicated that the failures were triggered by high combined stress levels in the area of the outside rows of studs. Shear lag from the bolsters into the gage section combined with crossgrain tension and stud loads, and caused failure of the composite near the surfaces of the studs.

Several solutions to the problem were suggested: reducing the gage section area to a value within the predicted capability of the end attachments increasing the width of specimen ends from 24 to 36 in. controlling the temperature of stud areas during testing to enhance strength, and several methods of applying crossgrain compression loads to the attachment area. The test volume would be reduced if the gage section was altered; an undesirable solution. The addition of bolsters would require work on the end fittings to utilize the additional studs, which would result in a lengthy and expensive rework. Temperature influence would yield only a small increase in strength, so this suggestion was not implemented. The use of a crossgrain compressive load was chosen. Several techniques for applying the load to the stud area were considered, and a cylindrical clamping approach was selected. Wood pieces were developed to fit between the clamp and the test article, which has an irregular outer shape. Shims of pressed board and rubber were designed to serve as interfaces, to distribute the load better. An analysis indicated that a radial pressure of 500 psi would enhance the hollow stud interface by a minimum of 15%, a marginal strength, should the wood size effect be small. The clamps were specified to provide this level of compression, and consisted of three individual assemblies at each end, each being 20 in. long, and weighing 625 lbs. Each of the six clamps was built in three radial segments with two sets of hinges and two tee bolt clamps on one joint.

In order to preserve the four remaining test specimens if the clamp scheme did not function properly, the residual sections of specimens 5 and 6 were sent to GBI, to be reconstituted into a single article of full length using a scarf joint reinforced with veneer added to two faces. The retrofit is shown on Figure 8-64, and was the first piece tested with the end reinforcement

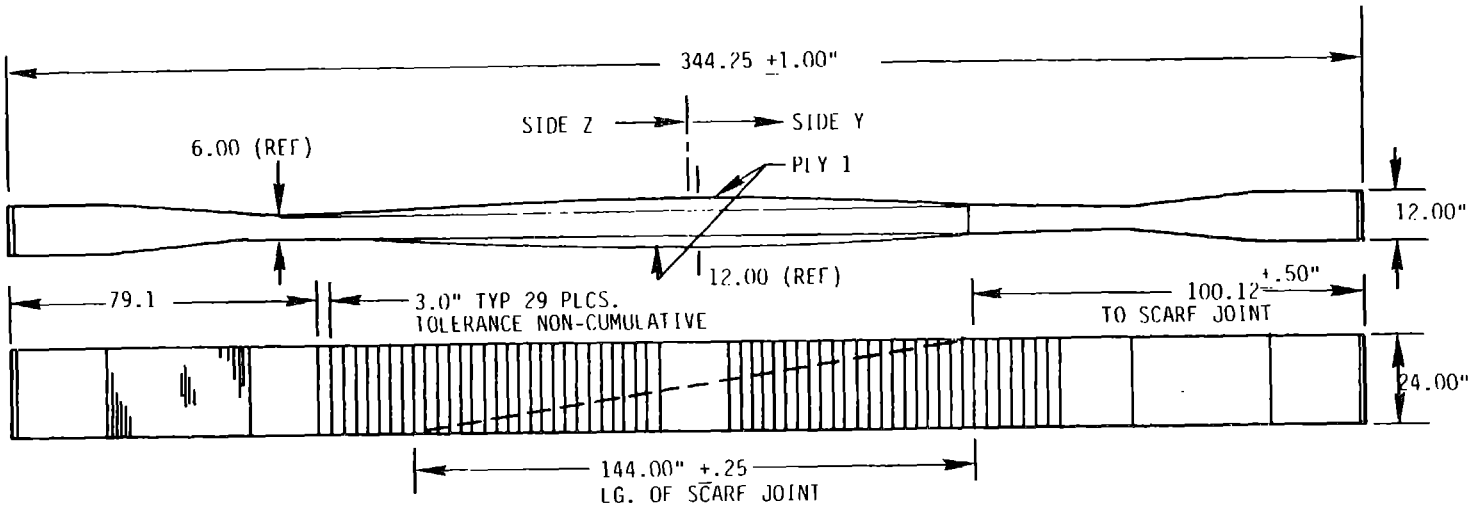

Figure 8-64 Scarf Jointed Specimen

scheme. The six clamps were installed and tightened, and the resulting specimen weighed approximately 8,500 lbs. The specimen was tested and failure occurred at 1.08×10^6, and took place in the gage length. The reinforced splice joint failed sooner than anticipated, but the clamps performed well. During removal of the sample from the test machine it inadvertently fell to the ground, destroying one of the remaining samples. The remaining three specimens were tested using the clamps.

Specimen number 1 was selected for the next test, and was fitted with the end clamps after some minor repair to the clamp tee bolt handles. The clamps were torqued to an internal pressure of 500 psi. The specimen weighed 8,500 lbs. On November 29, 1983, the specimen was tested. Audible cracks occurred at 560,000 lbs. and increased in frequency as load was added. Ultimate failure occurred at 1.264×10^6 lbs., following a relatively loud report at 1.25×10^6 lbs. A post-test inspection showed that the failure had extended throughout the gage section, and that one bolster plane had cracked on the upper end. It is suspected that the report that was heard approximately 8 seconds before failure was caused by the bolster crack. The resulting stress level at failure 18,778 psi was significantly higher than the earlier test results, and was in the range of interest.

Sample number 4 was prepared for testing, and testing commenced on December 1, 1983. Some acoustic outputs were heard beginning at 470,000 lbs, and a single report occurred at the point of ultimate failure, 1.294×10^6 lbs. The resulting stress level of 8,988 psi resulted in a failure that took place throughout the gage length and no end attachment involvement was noticeable.

Specimen number 3 was readied for testing. Indentations in the gage length were deeper than in previous specimens, resulting in a reduction of approximately 3 square in. (2%) at one end. Clamps were torqued as before, and testing took place. A single failure report at 1.230×10^6 lbs occurred, with the 8,542 psi stress level felt to be representative of the sample size. The failure was quite complete, and included most of the gage section. No end attachment failure was noticeable.

The failure of specimens 5 and 6 were not significant since the gage section did not fail, and only reinforced a lower bound. The result of specimens 5 and 6, which had a reinforced gage section, served no useful purpose. The following results were evaluated:

Sample	Failure Stress	Corrected to 10% MC
1	8,778 psi	8,448 psi
4	8,986 psi	8,649 psi
3	8,542 psi	8,222 psi

The unadjusted resulting mean value is 8,769 psi, with a standard deviation of 22.1 psi. If the result is adjusted for a 10% moisture content, the values are 8,440 psi and 213.6 psi.

The objective of this test was to identify the large scale extrapolation point to take into account size effects. The results were combined with results from section 8.1.4. A regression analysis was performed, in which the strength data were corrected for a wood moisture content of 10%. Forty-three data points were used. The Weibull prediction was determined by a least squares fit to a power function of form $Y=A(X)^B$. The hyperbolic function is of form $Y=A+(B/X)$. Both are shown with and without the inclusion of the data points determined in this test series. Figure 8-65 shows the plot based on the analysis of mean data (six data points). As a result, the Weibull curve was selected as the design curve for MOD-5A.

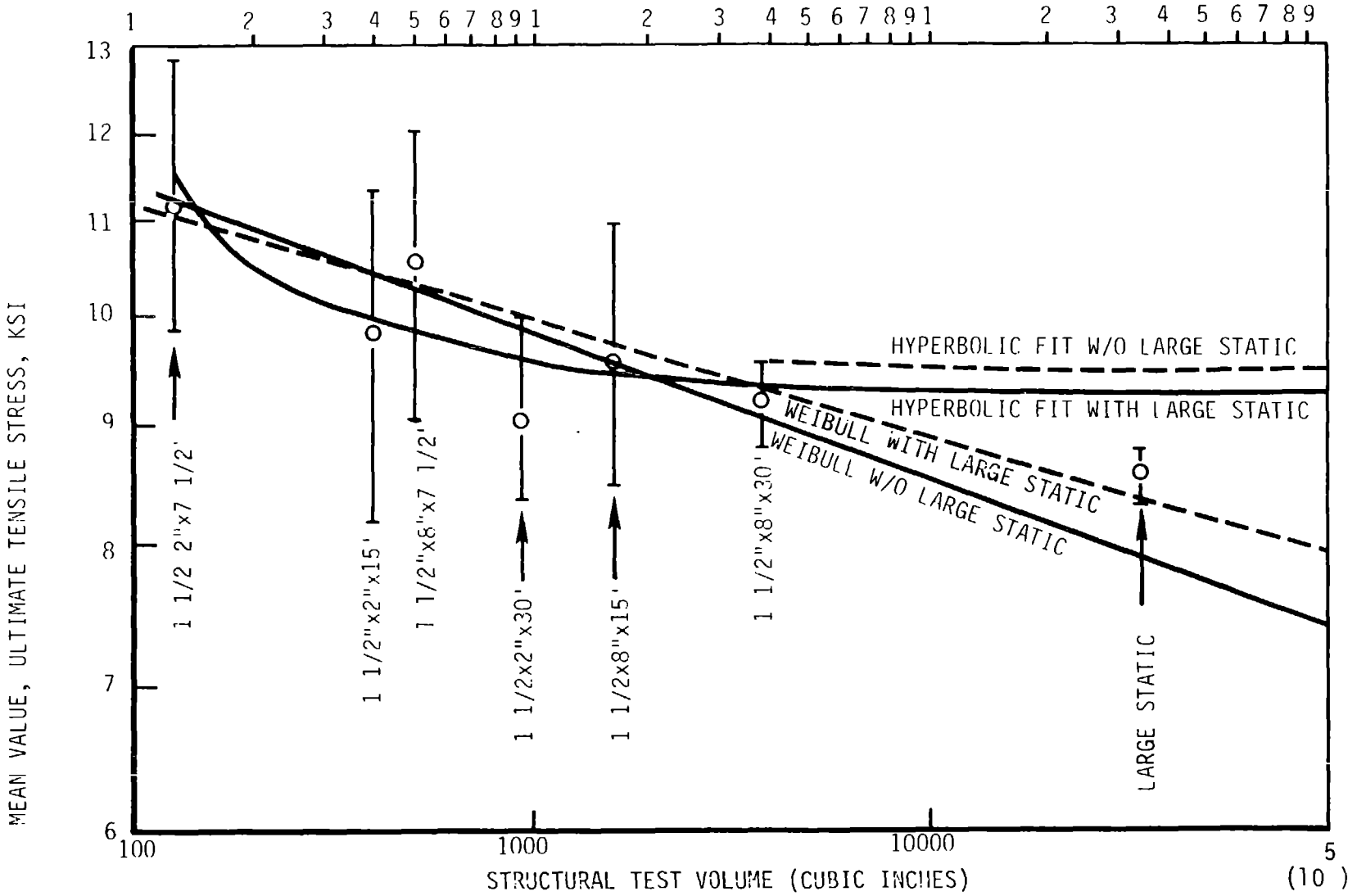

Figure 8-65 Scarf Joint Size Effect Data - Corrected to 10% Moisture Content

8.1.6.3 Size Effect Fatigue Test Program

8.1.6.3.1 Objectives

The large-scale fatigue test evaluated large wood specimens at two load ratios, to determine how the fatigue properties of wood structures vary with size. The available data on wood fatigue is sparse, and consists almost exclusively of results on small samples. By providing a test point for a structure with a large volume, through which an extrapolation could be made, the MOD-5A fatigue allowables could be determined with more confidence.

8.1.6.3.2 Description

The largest test machine with cyclic capability that is compatible with timber is Washington State University's tensile testing machine. The machine was initially frequency limited when used in large amplitude cyclic testing, but was upgraded with a larger hydraulic system to expedite this testing program. During testing many metal parts failed because of the fatigue loading they were subjected to. Several parts were repaired or replaced, some many times. One major problem was the load cell failure, which resulted in a change of test methods. Most testing was conducted at approximately 1 Hz.

Replacing the load cell was very expensive, and manufacturers guarantee the units for a relatively small number of cycles. To preclude additional load cell fatigue, the test was initiated within the load range of interest with the load cell output serving as the servo system input, while load versus deflection traces were made. The load cell was then removed and the testing continued using the stroke limits to drive the servo. Occasional checks were made to verify that the load was being maintained.

The test specimens were the maximum volume that was compatible with the test machine. A load ratio of 0.1 was used for specimens that were 2 in. thick, 8 in. wide, and 30 ft. long. A load ratio of -1.0 was used with specimens that were 3. in. thick, 8 in. wide, and 30 ft. long. Six samples of each size were manufactured in addition to static control specimens that provided an equivalent strength profile of each pallet. The static controls for the R = 0.1 pallets (1, 2 and 3) were made 1.5 in. thick, by placing a plastic sheet between the fifteenth and sixteenth veneers in the static controls area, to provide separation. This arrangement also yielded residual planks that were

0.5 in. thick (veneers 16 through 20). This arrangement was used since the machine's capability of 200,000 lbs. could have been inadequate to fail a plank of the full thickness. The static controls for the R = -1 samples were split at the centerline to provide two 1.5 in. thick specimens.

During testing of the fully reversed specimens, lateral supports were implemented to prevent buckling of the test samples.

8.1.6.3.3 Results

The results of the static tests are shown in Table 8-52. Much of the fatigue test time was devoted to repairing the machine. The tension-tension fatigue tests with a load ratio of 0.1 yielded the data shown in Table 8-53. All failures were deemed valid except for specimen number 2-2. Figure 8-66 is a plot of the data corrected to a 10% moisture content. The fully reversed loading tests (R = -1) yielded the results shown in Table 8-54 and Figure 8-67. Specimen number 4-2 is not included since it was failed during setup, and samples 5-1 and 5-2 were not failed at the conclusion of the test, but had accumulated the number of cycles shown.

The tension-tension tests yielded a less steep trend line, which agreed with Phase B testing on the high cycle end. The fully reversed loading results are higher on the low cycle end, but the slope is steeper than that of Phase B. the results confirmed the allowable stress selection methods used for MOD-5A.

Table 8-52 Fatigue Program R = 0.1 Tension Test Results

Sample Number	Size (TxWxL) (in.)	Test Volume (in^3)	Moisture Content (%)	Failure Stress (psi)	Failure Stress (Corrected to 10% Moisture Content) (psi)
LSF1-3S	1.5 x 7.25 x 360	3393	5.0	9379	8675
LSF2-3S	1.5 x 7.25 x 360	3393	5.0	12094	11163
LSF3-3S	1.5 x 7.25 x 360	3393	5.0	9655	8912
LSF1-3TT	.5 x 7.25 x 360	1131	5.0	9280	8565
LSF2-3TT	.5 x 7.25 x 360	1131	4.9	10229	9421
LSF3-3TT	.5 x 7.25 x 360	1131	5.2	9490	8788
LSF4-3S	1.5 x 7.25 x 360	3393	6.1	10302	9684
LSF4-4S	1.5 x 7.25 x 360	3393	6.0	9050	8498
LSF5-3S	1.5 x 7.25 x 360	3393	5.6	9781	9106
LSF5-4S	1.5 x 7.25 x 360	3393	5.8	9228	8628
LSF6-3S	1.5 x 7.25 x 360	3393	6.2	9638	9069
LSF6-4S	1.5 x 7.25 x 360	3393	6.2	9396	8842

Mean Failure Stress
(Corrected to 10% Moisture Content)

Pallet Number	Number of Tests	Mean Stress (psi)	
1	2	8620	
2	2	10292	Mean = 9254
3	2	8850	
4	2	9091	
5	2	8867	Mean = 8971
6	2	8956	

Table 8-53 Fatigue Program Tension/Tension Test Results

Sample Number	Size (TxWxL) (in.)	Test Volume (in^3)	Moisture Content (%)	Test Range (psi)	Cycles	Test Range (Corrected to 10% Moisture Content)
LSF1-1	2 x 8 x 360	4992	5.0	6500 to 650	20,421	5993 to 599
LSF1-2	2 x 8 x 360	4992	5.0	7000 to 700	49,686	6454 to 645
LSF2-1	2 x 8 x 360	4992	5.2	6500 to 650	5,626	6019 to 602
LSF2-2	2 x 8 x 360	4992	5.1	No Test		
LSF3-1	2 x 8 x 360	4992	5.2	5800 to 580	164,458	5371 to 537
LSF3-2	2 x 8 x 360	4992	5.0	5200 to 520	1,366,128	4794 to 479

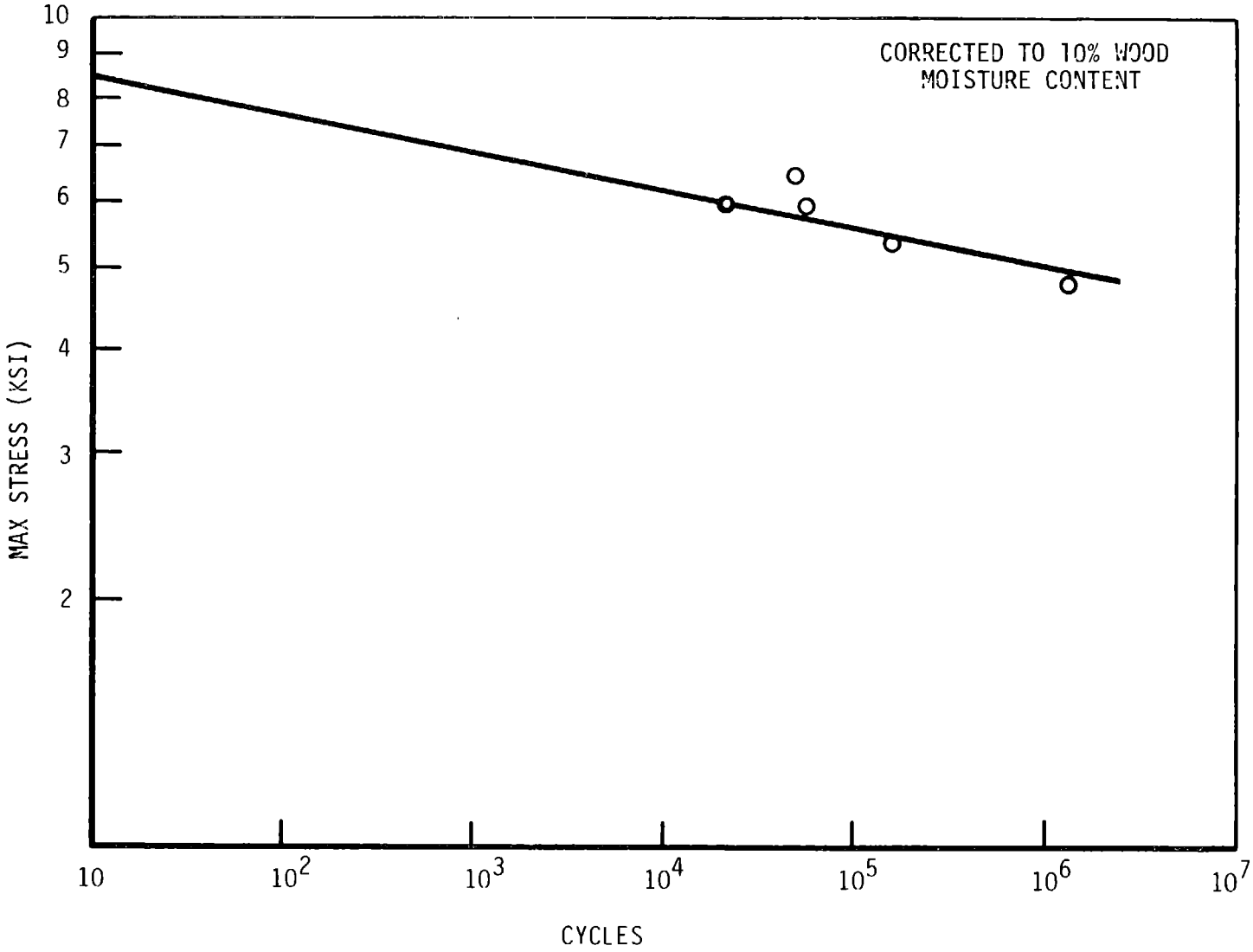

Figure 8-66 Tension-Tension Fatigue Test Data, R = 0.1

Table 8-54 Reverse Axial Fatigue Results

Sample Number	Size (TxWxL) (in.)	Test Volume (in^3)	Moisture Content (%)	Test Range (psi)	Cycles	Test Range (Corrected to 10% Moisture Content)
LSF4-1	3 x 8 x 360	7488	6.3	3750 to -3750	40,654	3534 to -3534
LSF4-2	3 x 8 x 360	7488		No Test		
LSF5-1	3 x 8 x 360	7488	6.2 (est.)	3122 to -3122	$>1.3(10)^6$	2938 to -2938
LSF5-2	3 x 8 x 360	7488	6.2 (est.)	3500 to -3500	>163,000	3294 to -3294
LSF6-1	3 x 8 x 360	7488	6.4	3250 to -3250	303,068	3068 to -3068
LSF6-2	3 x 8 x 360	7488	6.1	3000 to -3000	$1.05(10)^6$	2817 to -2817

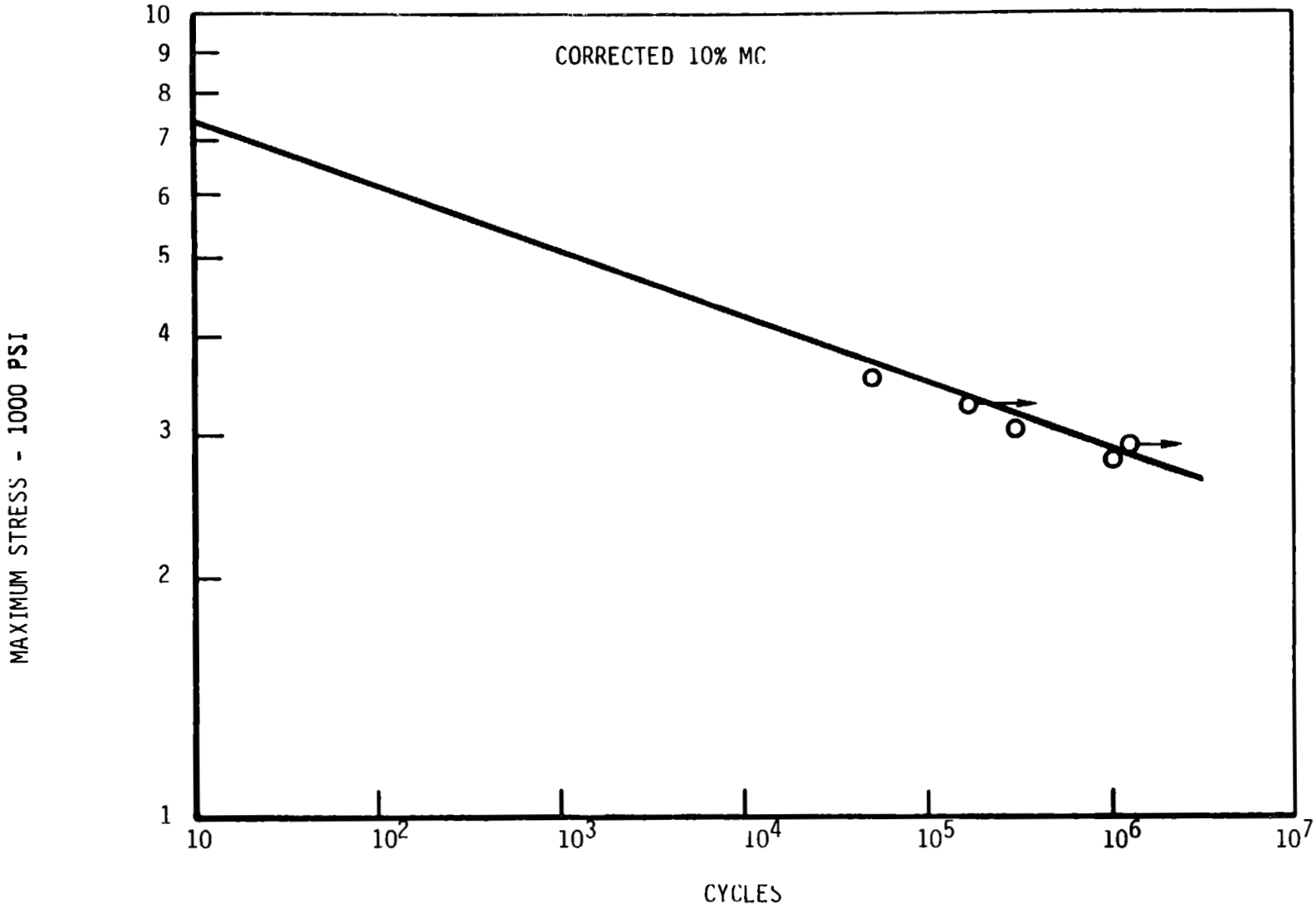

Figure 8-67 Fully Reversed Fatigue Test Data, R = -1

8.1.7 DAMPING COEFFICIENT TEST

8.1.7.1 Introduction

The damping coefficient tests were conducted by Metrigard, Incorporated, a lumber industry test equipment manufacturer located in Pullman, Washington. The testing took place in early 1983. A flexural vibration was induced in a laminated Douglas fir beam, and the test identified the number of vibration cycles required for the amplitude of the vibration to decay to 1/e of the threshold level (e is the base of natural logarithms, and its value is 2.71828). A simple mathematical model analysis determined the damping coefficient.

8.1.7.2 Test Objectives

The test was performed to provide information on the damping characteristics of Douglas fir veneer. The beams were made of 15 layers of wood, each 0.10 in. thick, bonded into a laminated constuction with West System® epoxy. Damping characteristics were needed with the beam loaded both radially and tangentially for use in dynamic analysis models that predict the operational and vibration characteristics of the MOD-5A wind turbine generator. Refining the knowledge of the elastic damping coefficient would optimize the blade configuration and improve confidence in the loads predictions.

8.1.7.3 Test Description and Results

The tests were performed on four specimens, which were remnants of the scarf joint and size effects tests. The cross section of each sample was 1.5 by 2.0 in. The length of the samples ranged from 13.8 ft. to 19.6 ft. The specimen was supported at one end on a pivot blade and at the other end on a load cell, as shown in Figure 8-68. The beam was excited vertically near its center and a harmonic response vibration was transmitted to the load cell. The load cell output was recorded.

The data was processed through a Model 3300 Transverse Vibration E-Computer, a system Metrigard produces and uses in modulus tests. The processed data was stored in a Nicolet Instrument, Model 206 Explorer III Digital Storage Oscilloscope. A Hewlett-Packard Model 7034 X-Y Recorder was used to plot the information to confirm the computed damping coefficient. Typical test results are shown in Figure 8-69.

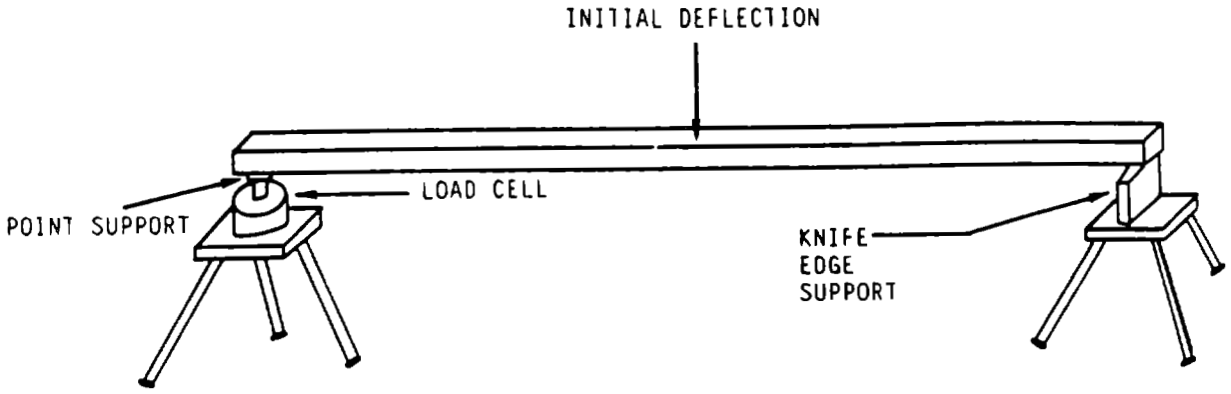

Figure 8-68 Transverse Vibration Test Configuration

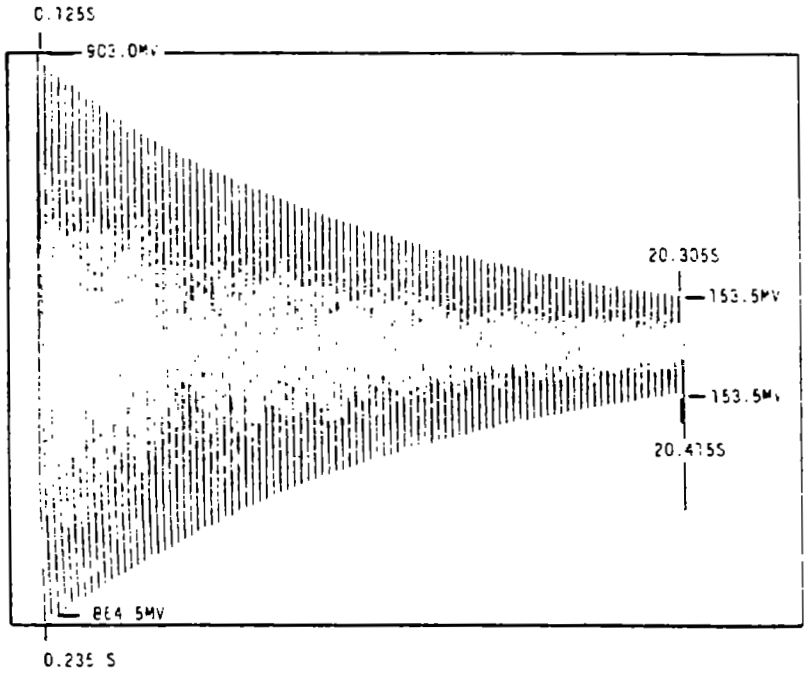

Figure 8-69 Vibration Waveform of Piece 1, Face 1 (F1F1)

The four test pieces are described in Table 8-55. The orientation of the piece during its test was identified by the number on the upward face, as shown in Figure 8-70. For example, a test labeled P2F2 refers to a test on piece 2 with its face 2 up. The test data are shown in Table 8-56. The effective damping ratio is about 0.0025 and the value appears to be independent of the orientation of the laminations.

The lower damping coefficient determined in these tests was used in the loads analysis.

Table 8-55 Test Pieces

Piece #	Length* (Inches)	Thickness (Inches)	Width (Inches)	Weight (lbs)	Density* (lbs/ft^3)	Corrected Density (lbs/ft^3)
P1	178.5	1.51	2.03	13.2	42.2	41.7
P2	166.0	1.49	2.01	10.7	37.6	37.1
P3	223.6	1.53	2.02	15.7	39.6	39.2
P4	235.6	1.50	2.02	15.3	37.4	37.1

* Because one inch was used for overhang on each end at the E-Computer tripods, the span length entered into the E-Computer was 2 inches less than the length shown. Thus the density computed by the E-Computer is based on a length which is two inches less than the actual material length. The column labeled Corrected Density is computed from the actual lumber length.

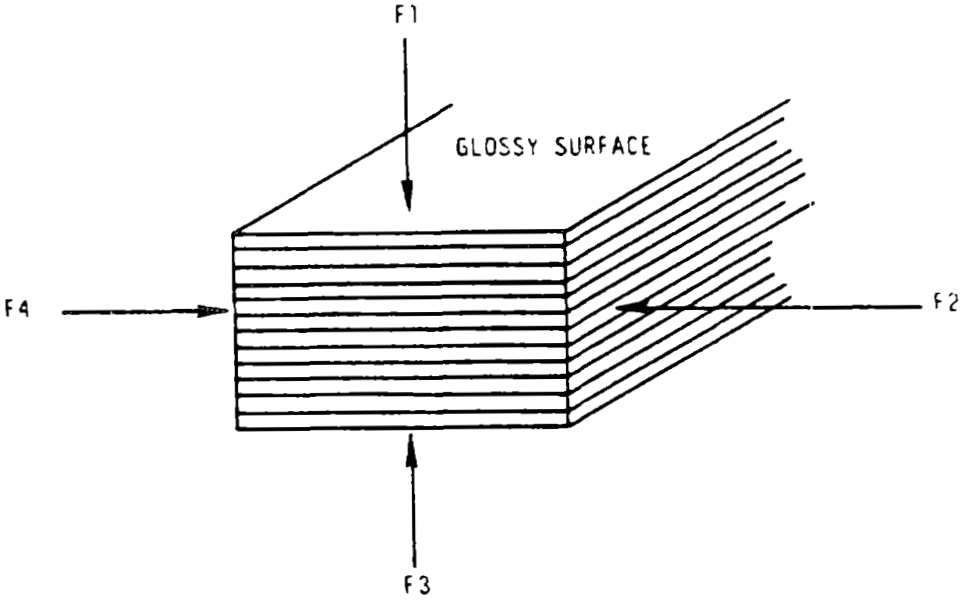

Figure 8-70 Test Piece Face Identification

Table 8-56 Test Results

Piece and Test Face	E (10^6 psi)	E-Computer Measurements				From Vibration Waveform						
		N	$\zeta = 1/(2\pi N)$	Period (sec)	Freq (Hz)	N	Initial Max-Min (mv)	After N Max-Min (mv)	R	$\zeta = \ln R/(2\pi N)$	Period (sec)	Freq (Hz)
P1F1	2.71	56	0.00284	0.218	4.59	93	1767.5	307.0	5.757	0.00300	0.217	4.61
P1F2	2.60	65	0.00245	0.165	6.06	122	1484.5	198.0	7.497	0.00263	0.165	6.07
P1F3	2.71	56	0.00284									
P1F4	2.60	64	0.00249	0.165	6.06							
P2F1	2.33	66	0.00241	0.194	5.15	103	1774.0	325.5	5.450	0.00262	0.195	5.12
P2F2	2.31	68	0.00234	0.144	6.94	139	1583.5	192.0	8.247	0.00242	0.144	6.94
P2F3	2.33	66	0.00241	0.194	5.15							
P2F4	2.30	69	0.00231	0.145	6.90							
P3F1	2.48	64	0.00249	0.344	2.91	57	969.0	398.0	2.435	0.00248	0.342	2.92
P3F2	2.51	72	0.00221	0.259	3.86	77	1175.0	387.5	3.032	0.00229	0.258	3.88
P4F1	2.38	60	0.00265	0.386	2.59	52	983.5	402.5	2.443	0.00273	0.384	2.60
P4F2	2.30	66	0.00241	0.292	3.42	69	1125.0	376.5	2.988	0.00252	0.290	3.44
↓↓ With 8 Pound Mass Load in Span Center ↓↓												
P3F1		70	0.00227	0.487	2.05	40	1061.0	580.0	1.829	0.00240	0.484	2.07
P3F2		74	0.00215	0.368	2.72	54	1145.5	527.5	2.174	0.00229	0.366	2.73
P4F1		64	0.00249	0.547	1.83	*	*	*	*	*	*	*
P4F2		68	0.00234	0.419	2.39	47	1221.5	590.0	2.070	0.00246	0.415	2.41
P4F2						47	1281.5	617.0	2.077	0.00248	0.416	2.41
↓↓ With 2 Instead of 5 msec Waveform Sampling Interval; No Mass Loading ↓↓												
P2F1						40	974.5	515.5	1.890	0.00253	0.193	5.17
P2F2						55	1489.0	627.0	2.375	0.00250	0.144	6.94

* By mistake, the P4F2 waveform experiments were done a second time instead of the P4F1 experiments. The second waveform for P4F2 has some value to demonstrate the degree of repeatability and is included as Figure 7.1.7-14.

8.1.8 SUMMARY AND RECOMMENDED ALLOWABLE STRESSES

The testing discussed previously provided a data base from which static and fatigue allowables for wood could be developed. The static allowables for the wood laminae are shown in Table 8-57. These values were used to establish the requirements for section properties of the blade under frequently occurring limit load conditions. They may be increased by 19% when designing for infrequently occurring limit loads such as hurricane, or overspeed conditions.

The number of samples tested does not always provide statistically representative results. However, the data did provide comparative results. One objective of this test program was to show that the test data correlated with the much larger data base of the Wood Handbook. In this way, the allowables could be established with greater confidence. Furthermore, other Wood Handbook data could be used without being verified. The comparison is shown in Table 8-58. The two sets of data were in close agreement.

The static allowables were derived from the lower 2σ ultimate test data, which implies that the ultimate strength will be higher 97.5% of the time, yielding a data cutoff of 2.5%. This case compares favorably with procedures used by the wood stress grading industry, which specifies a 5% cutoff, and the wood aircraft industry, which specifies a 25% cutoff. The strengths are adjusted to reflect the available strength at a moisture content of 10%, per procedures described in the Wood Handbook. Wood has a proportional limit in compression, which was shown to vary between 85% and 90% of its ultimate strength. Since the structural design criteria do not allow limit loads to cause material yielding, the allowable for compression includes a proportional limit factor of 0.85. In tension, wood is affected by size, which reduces its ultimate strength as described in section 8.1.4. The allowable for tension parallel to the grain incorporates a factor that accounts for the blade stressed volume versus the test sample volume. Figure 8-71 illustrates the relationship between strength and stressed volume. The stressed volume for the blade equals approximately 343,000 in^3, which corresponds to a size effect factor equal to 0.647. The stressed volume is 1% of the tip-to-tip volume of the structural portion of the airfoil. It represents the amount of material that is subjected to the extreme fiber tensile stress produced by

Table 8-57 Static Allowables for Wood Laminae [1]

	Parallel To Grain, psi				Perpendicular to Grain, psi				
	Tension	Compression	Shear		Tension		Compression		Rolling Shear
	L Direction	L Direction	LT Plane	LR Plane	R Direction	T Direction	R Direction	T Direction	RT Plane
Test Ultimate Mean at 12% Moisture Content	11062[2]	- 7583[3]	1546	1961[4]	467[5]	257[5]	- 372[5] [7]	- 732[5] [7]	186[8]
Standard Deviation, σ	$\pm$ 885	$\pm$ 295	$\pm$ 127	$\pm$ 188	$\pm$ 96	$\pm$ 57	$\pm$ 37	$\pm$ 73	$\pm$ 15
Mean - 2σ	9292	- 6993	1292	1585	275	143	- 298	- 586	156
10% Moisture Factor	1.032	1.113	1.040	1.040	1.019	1.019	1.133	1.133	1.049
Proportional Limit Factor	1.0	.85	1.0	1.0	1.0	1.0	1.0	1.0	1.0
Size Effect Factor	.647[2a]	1.0	1.0	1.0	1.0	1.0	1.0	1.0	1.0
Temperature Factor	1.0	1.0	1.0	1.0	1.0	1.0	1.0	1.0	1.0
Load Duration Factor	1.0	1.0	1.0	1.0	1.0	1.0	1.0	1.0	1.0
Factor of Safety	0.67	0.67	0.67	0.67	0.67	0.67	0.67	0.67	0.67
Allowable	4200	- 4400	900	1100	190[6]	100[6]	- 230	- 440	110

(1) Allowables for scarf jointed, blade grade 1 veneer with 10% moisture content at 68°F, unless otherwise noted.

(2) Predicted strength at a stressed volume equal to 32 in^3 based on best fit curve to size effect data.

(2a) Size effect factor corresponding to a stressed volume equal to 343,000 in^3.

(3) Reflects the weighted average at Phase A no-joint data with scarf-joint compression data.

(4) Derived from Phase A blade grade 2 test results.

(5) Blade grade 2 material.

(6) For stressed volumes less than 20 in^3.

(7) Values reported are stresses at proportional limit.

(8) Not tested, assumed 12% of shear parallel to grain value (1546 psi) per wood handbook recommendation.

Table 8-58 Correlation of Static Test Results with Wood Handbook Data

	Average Results at 12% Moisture Content	
	Wood Handbook (psi)	Test Result (psi)
Parallel to Grain		
Tensile Ultimate	12,400	11,363
Compression Ultimate	-7,240	-7,583
Shear Ultimate	1,130	1,546
Perpendicular to Grain		
Tensile Ultimate, R Direction	340	467
Compression P.L., T Direction	-800	-732

R = Radial, through laminae thickness
P.L. = Proportional limit
T = Tangential, through laminae width

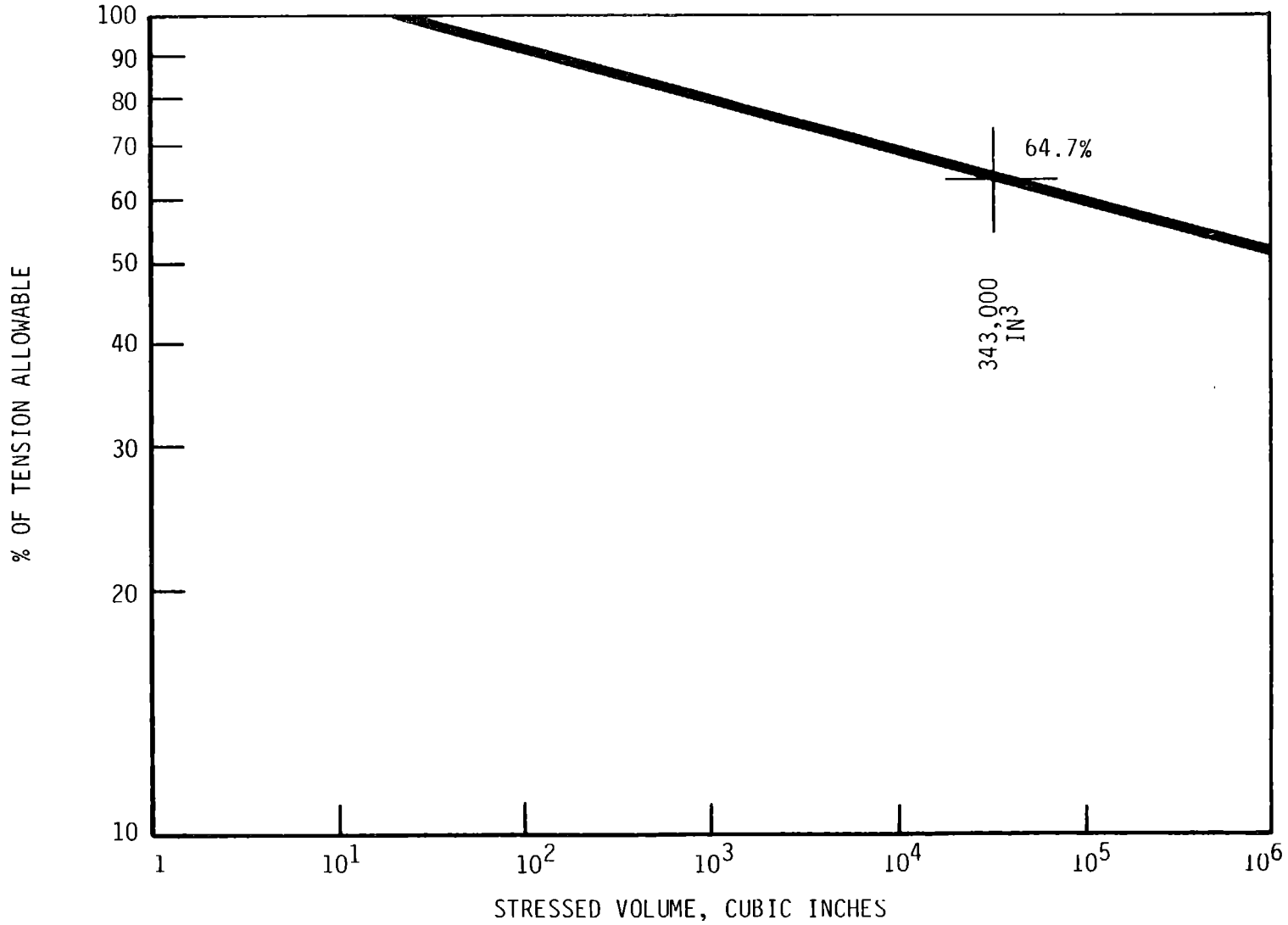

Figure 8-71 Tension Size Effect Factor

the blade bending loads. A temperature factor was not applied to the allowables because the high temperature limit load case would have to occur under extreme temperature conditions. An examination of weather data indicated that this situation is not likely to occur since extreme high temperatures occur when the wind speed is less than 3 mph. Also, low temperature increase the wood's capability so they are not a limiting case. Finally, the wood strength reduces when the wood is subjected to a constant state of stress. The blade is in these conditions when parked, or when it is subjected to either a limit or mean fatigue load. An analysis of the load duration effect caused by parked and limit loads indicated little change in the residual strength of the wood, hence, the static allowables do not include a load duration factor. The load duration effect caused by mean fatigue loads is discussed later.

The fatigue allowables for stresses parallel to the grain are shown in Table 8-59. Most of the effort to characterize fatigue was spent in developing a data base, since it corresponds to the primary direction of blade stress. The test data supporting these allowables at each of the stress ratios is shown in section 8.1.2 for butt-jointed laminae and section 8.1.5.1 for scarf-jointed laminae. In each case the fatigue performance is best represented by a curve with the equation

$$Y = AX^B \quad \text{(straight line on log-log plot)} \qquad [8.1.8\text{-}1]$$

Where:
- Y = failure stress
- X = lifetime (cycles) corresponding to failure stress
- A = a constant describing the level of the curve
- B = a constant describing the slope of the curve

Most of the test data was generated for butt-jointed laminae, reflecting the original blade fabrication plans. The improved performance of scarf-jointed laminae, which represent the current manufacturing plans, was determined by testing a small number of samples. The test did not provide a large enough data base to prevent the derived allowables for scarf-jointed laminae from being either too conservative or too optimistic. To circumvent this problem, the slope in the performance equations for scarf-jointed laminae was modified by weight averaging the results of the butt-jointed data. This modification, was used to find a new coefficient based on the performance of scarf-jointed

Table 8-59 Wood Laminae Fatigue Allowables for Stress Parallel to Grain

	Maximum Allowable Stress, psi				
	Stress Ratio (R)				
Lifetime Cycles	R = 1(T)	R = .1	R = -1	R = 10	R = 1(C)
10^4	5500	4100	2700	4400	6400
10^5	5300	3400	2300	3900	6200
10^6	5200	2800	1900	3600	6000
10^7	4800	2300	1700	3200	5500
4×10^8	3200	1700	1300	2700	3700

(1) Allowables for scarf-jointed, blade grade 1 veneer at a moisture content of 10%, and 90°F.

laminae at 10^6 cycles. The performance at 10^6 cycles was selected as a point on the new performance curve because its lifetime is near the mid-point of the lifetimes of interest, 10^4 cycles and 4×10^8 cycles. A summary of the test data and the resultant weighted average slopes is shown in Table 8-60. The new set of performance equations are shown below, based on weight averaged slopes and scarf joint test failure stress:

Reversed Axial (R = -1)

$$Y = 10307\ X^{-.0704} \qquad [8.1.8\text{-}2]$$

Tension-Tension (R = .1)

$$Y = 24254\ X^{-.0829} \qquad [8.1.8\text{-}3]$$

Compression-Compression (R = 10)

$$Y = 12324\ X^{-.0438} \qquad [8.1.8\text{-}4]$$

The derivation of the allowable stress in fatigue parallel to the grain for 4×10^8 cycles is shown in Table 8-61 and is typical of the derivation for other lifetimes. The value for the test mean at R = -1, .1, and 10 is the predicted performance based on the above equations. The average test value at R = 1 tension and R = 1 compression reflects the ultimate static test results since at these stress ratios there is no alternating stress component. The average performance is reduced to account for the test data scatter. Engineering judgement was applied in deriving the standard deviation and the fact that the variability of strength decreases as the volume of the test specimen increases was considered. This behavior is illustrated in Figure 8-72, where standard deviation, expressed as a percent of average static strength, is plotted against stressed volume. The solid line represents a least squares fit of the data. In addition, the variability in tensile properties of wood are greater than in compression, as noted from the static test results shown in Table 8-57. Accordingly, this relationship was maintained in establishing the levels of variability in fatigue. The mean 2σ strength is adjusted to reflect the design wood moisture content of 10%.

A size effect factor is applied to adjust the allowables to reflect the decreased capability at the large stressed volume. The size effect in fatigue was determined by performing tests at stress ratios equal to .1 and -1 with samples with a stressed volume of 4492 in^3 and 7488 in^3 respectively.

Table 8-60 Summary of Parallel to the Grain Fatigue Test Data

	Best Fit Curve Coefficients (1) A	B	Number of Data Points	Failure Stress at 10^6 cycles, psi (2)
Reversed Axial (R=-1)				
Butts	11137	-.0856	10	3415
Scarfs	8176	-.0536	9	3897
Weight Average Slope (3)		(-.0704)		
Tension-Tension (R=.1)				
Butts	21994	-.0897	16	6369
Scarfs	17943	-.0611	5	7716
Weight Average Slope		(-.0829)		
Compression-Compression (R=10)				
Butts	12614	-.0590	18	5586
Scarfs	7180	-.0047	7	6729
Weight Average Slope		(-.0438)		

(1) Best fit curve of the form $Y = AX^B$ where Y equals stress, X equals cycles, and A and B are constants.

(2) Average plus alternating

(3) Weight averaging method

Wt. Avg. $B = B_{butts} - (B_{butts} - B_{scarf})(N_{Butts}/N_{scarf} + N_{scarf})$

Table 8-61 Derivation of Wood Laminae Fatigue Allowable for Stress Parallel to Grain and 4×10^8 Cycles

	Stress Ratio, (R)				
	+1 (T)	.1	-1	+10	+1(C)
Test Mean	11062(1)	4695(4)(5)	2556(4)(6)	-5176(4)(7)	-7583(8)
Standard Deviation, σ(1a)	±885	±376	±128	±207	±295
Mean - 2σ	9292	3944	±2300	-4762	-6993
10% Moisture Factor	1.03	1.0	1.0	1.0	1.113
Size Effect Factor	.65(2)	.44	.58	.89	1.0
Temperature Factor	.98(3)	.98	.94	.90	.90
Load Duration Factor	.53	1.0	1.0	.75	.53
Allowable, psi (Mean plus Alternating)	3200	1700	1300	2900	3700

(1) Predicted ultimate strength at a stressed volume equal to 32 in^3 at moisture content of 12% and 68°F.

(1a) Assumed variation for stressed volume equal to 343,000 in^3.

(2) Static size effect factor corresponding to 343,000 in^3.

(3) Performance factor at 90°F.

(4) Performance at moisture content of 10% and 68°F.

(5) Based on equation [8.1.8-3]

(6) Based on equation [8.1.8-2]

(7) Based on equation [8.1.8-4]

(8) Reflects weighted average of Phase A data for samples without joints with data for scarf-jointed samples at 12% moisture content.

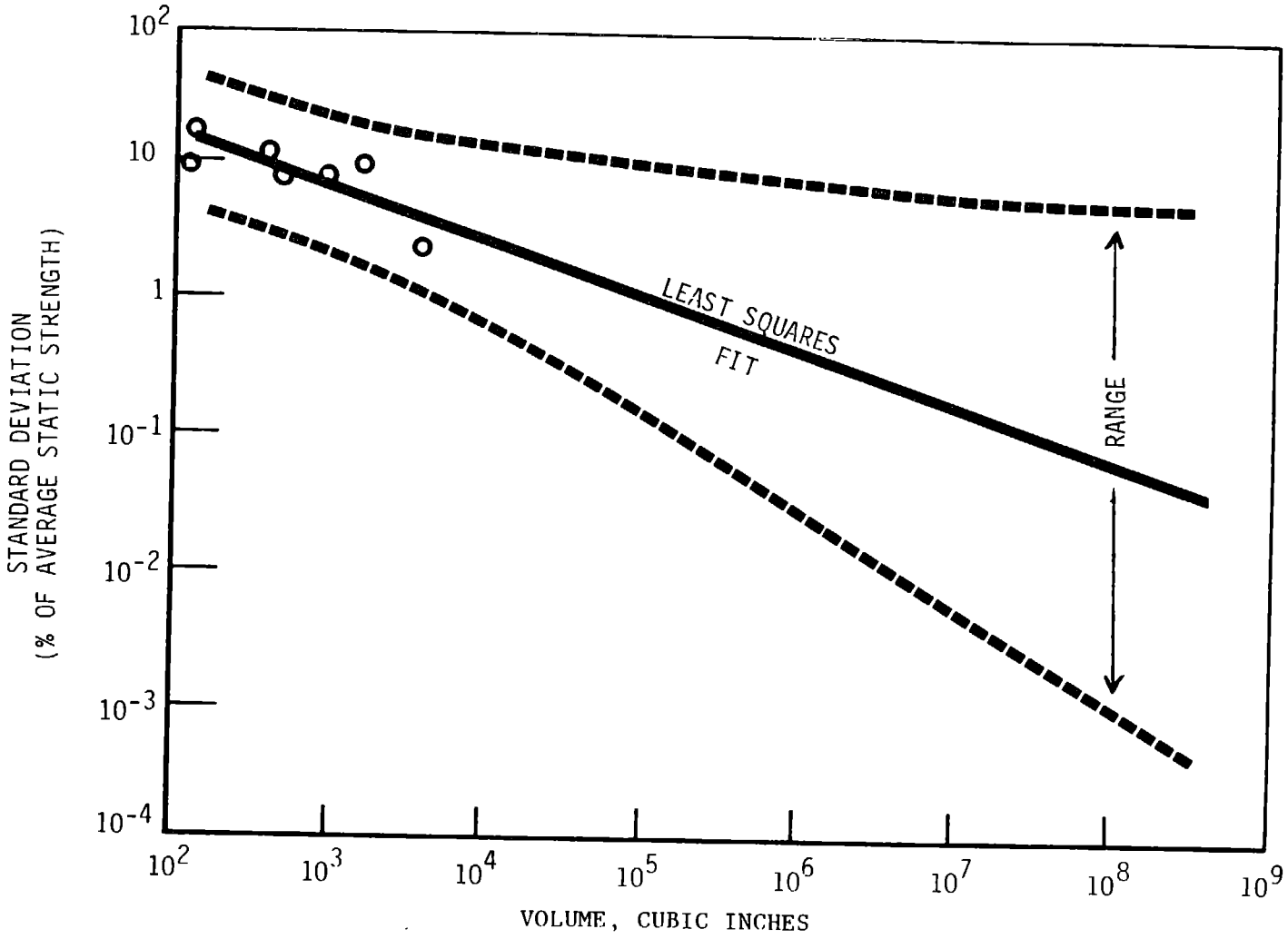

Figure 8-72 Variation of Standard Deviation with Stressed Volume

The results of tests at a load ratio of 0.1 indicate that the large volume samples had nearly the same slope of the S-N curve that the 32 cubic in. test program. The strength of the larger samples was only 61% of the smaller specimens, however. With fully reversed loading, R=-12, the same parallel slope was apparent, as indicated by Tables 8-60 and 8-61. With this load ratio the larger samples had 68% of the smaller specimen strength. In order to extrapolate this effect to the MOD-5A stressed volume the following relationship was used:

$$\frac{\text{Strength at MOD-5A Volume}}{\text{Strength at 32 in}^3} = \frac{\text{Volume of MOD-5A}^n}{32 \text{ in}^3}$$

The exponent n describes the slope of the relationship and can be determined by the results at the volumes tested. Using the strength ratio at 10^6 cycles as typical, "n" is found below:

$$\underline{R = .1} \qquad .61 = \frac{4992^n}{32}$$

Exponent Derivation From Test Data

$$n = -.0985$$

$$\underline{R = -1} \qquad .68 = \frac{7488^n}{32}$$

$$n = -.0698$$

Extrapolated to MOD-5A Volume

$$\frac{343{,}000}{32}^{-.0985} = .40$$

$$\frac{343{,}000}{32}^{-.0698} = .53$$

As shown substituting the stressed volume into the above equations yields strength ratios of .40 and .53 for R = .1 and -1 respectively. These predicted values were increased by 10%, assuming that there would be some asymptotic effect with increasing stressed volume. The assumption is supported by the static test results, in which predictions based on a regression analysis of data limited to stressed volumes of 3200 in^3 underestimated the strength at the MOD-5A volume by 10%, when the analysis was repeated with data at a stressed volume equal to 32000 in^3. The size effect factor versus stress ratio for the MOD-5A is summarized in Figure 8-73. The derivation of the factor for R = 1 (tension) and R = 1 (compression) was described during the discussion for the static allowables. The four data points were connected with a smooth curve, after which the factor at R = 10 was obtained.

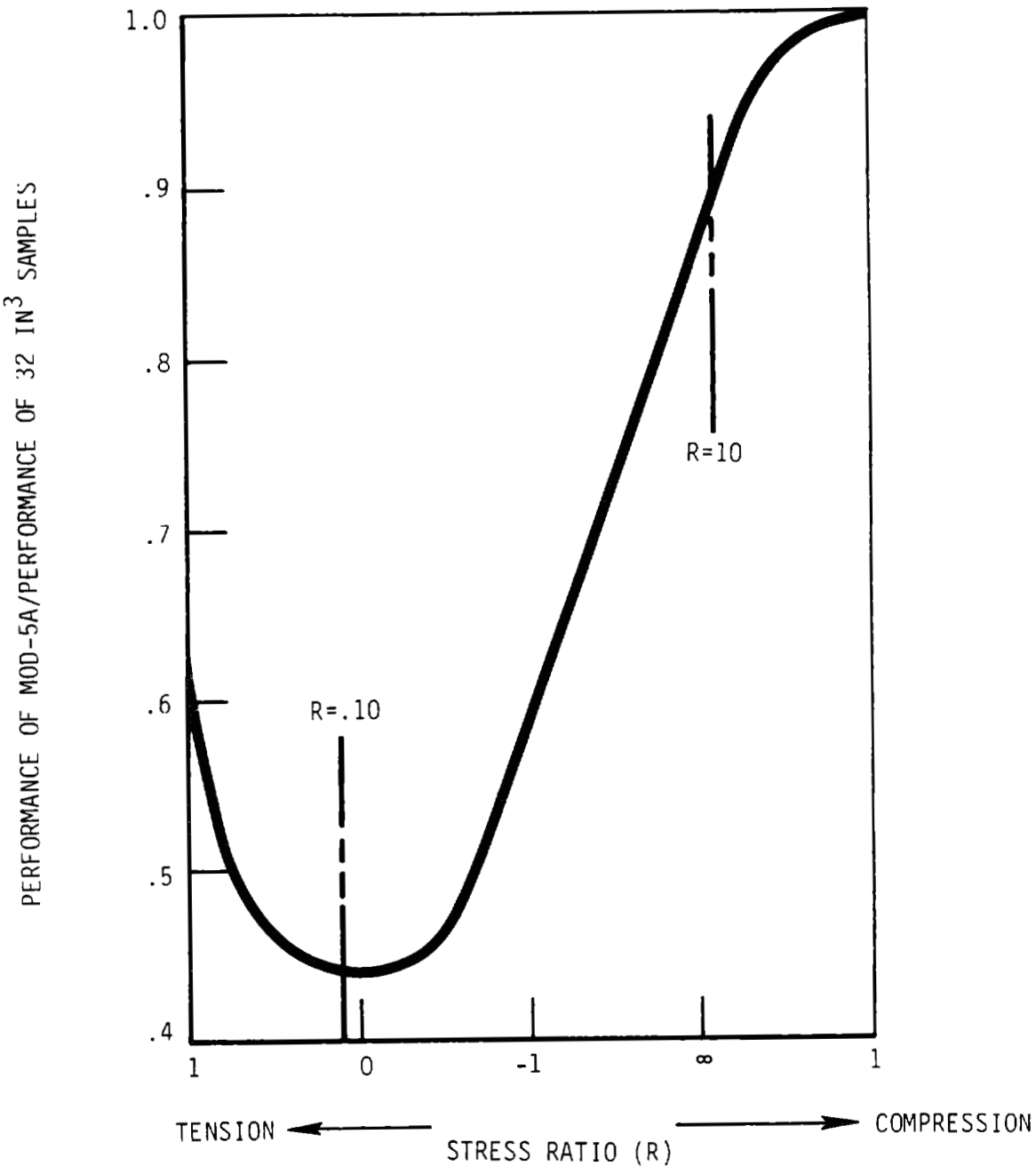

Figure 8-73 Size Effect Factor for Wood Laminae Fatigue Performance

An adjustment was also made for temperature effect, since the strength of wood decreases with increasing temperature. The test results at 68°F are adjusted to reflect the performance of wood at the average operating temperature of 90°F, by applying the temperature factor corresponding to the stress ratio, as shown in Figure 8-74. The strength reduction for tensile and compressive stresses was obtained from data in the wood handbook and in other literature. A linear relationship was assumed between the endpoints of the all tension and all compression stress ratios.

Wood is also affected by the load duration. As the time under load increases, failure will occur with smaller loads. The static ultimate strength of the wood was characterized using a 5 minute load test. Since the wind turbine will accumulate approximately 20 years of operating time, the static strength allowable, represented by a stress ratio equal to 1, must be reduced. Table 8-62 shows the load duration factors corresponding to different periods of life used in the derivation of the R = 1 tension and compression allowables. Likewise, the fatigue test data must be adjusted to represent the rate and, therefore, the time that the turbine accumulates fatigue loads. In the case for R = .1, the test data for the large volume samples was generated at a rate approximately equal to that of the wind turbine, therefore, no load duration effect was included in its derivation of allowables. At R = -1, the mean or constant load equaled 0, hence, the load duration factor equals 1. However, for R = 10, the test rate of 8 Hz would accumulate 4×10^8 cycles in 1.5 years, versus 20 years for the wind turbine, hence a load duration factor of .75 was included. This factor was obtained by interpolating for the 1.5 year and 20 year values of 0.73 and 0.55. The ratio of 0.55 to 0.73 yielded the factor of 0.75 for reducing the compression/compression test results.

The fatigue allowables and their derivation for the other directions of stress are shown in Tables 8-63 and 8-64. These allowables are not design drivers, so they were not verified by test.

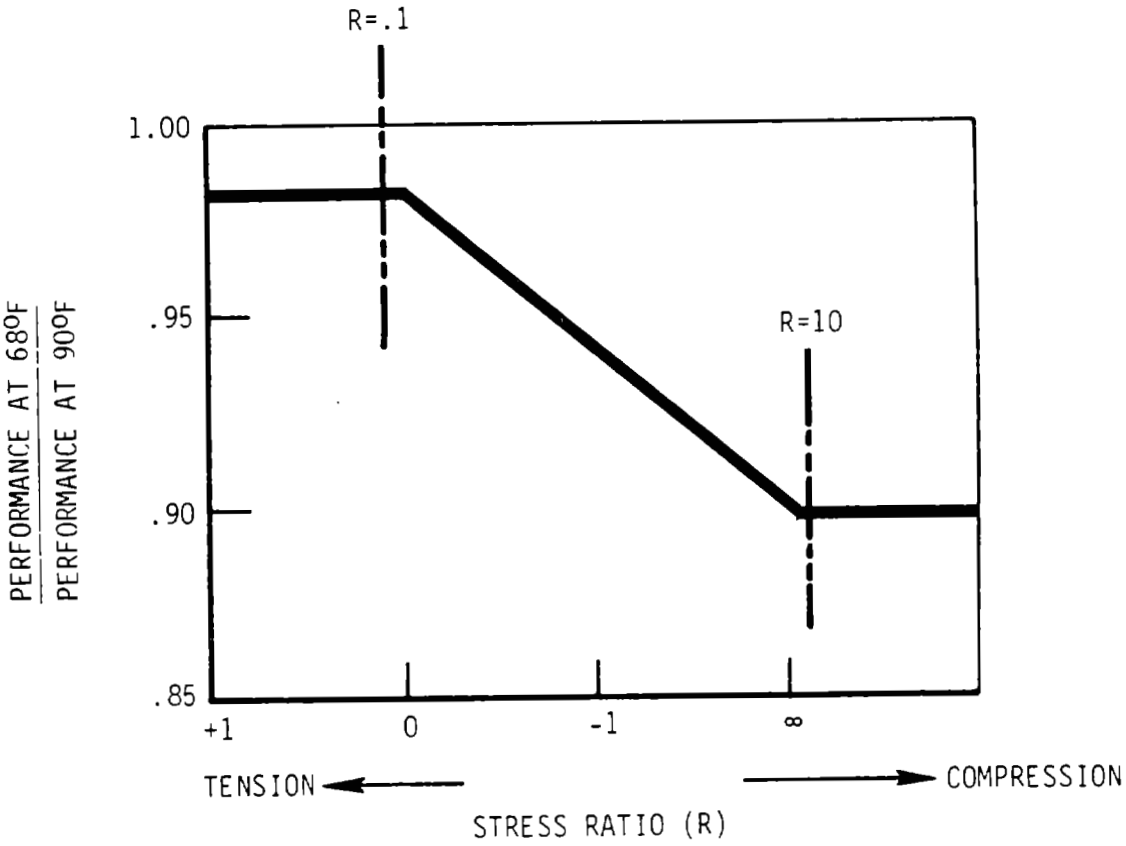

Figure 8-74 Temperature Factor for Wood Laminae Fatigue Performance at 90°F Relative to 68°F

Table 8-62 Load Duration Factors Used With R = 1.0
Wood Laminae Fatigue Allowables

Load Duration Time	Load Duration Factor	Equivalent Number of MOD-5A Cycles (1)
5 hours	.098	10^4
2.1 days	.885	10^5
21 days	.885	10^5
7 months	.789	10^7
23 years	.530	4×10^8

(1) Number of Cycles = 16.8 Rev/Min x 2 Load Cycles/Rev x time in minutes

Table 8-63 Fatigue Allowables for Other Directions of Stress for 4 x 10^8 Load Cycles[1] (Stress Ratio =0.1)

		Cross Grain Tension		Cross Grain Compression		Rolling
	Shear, LT	Radial	Tangential	Radial	Tangential	Shear, RT
Mean, 10% Moisture Content[2]	1608	476	262	-669	-1456	193
Mean - 2σ[2]	1344	280	146	-535	-1165	161
Temperature Factor[3]	.9	.9	.9	.9	.9	.9
Load Duration Factor[3]	.6	.6	.6	.6	.6	.6
Allowable, psi	726	151	79	-289	-629	87

(1) These properties are not design drivers and, therefore, were not verified by test.

(2) See Table 8.1.8-1 for origin of data.

(3) Engineering estimate.

Table 8-64 Fatigue Allowables for Other Directions of Stress for 4×10^8 Load Cycles[1] (Stress Ratio = -1)

		Cross Grain Tension		Cross Grain Compression		Rolling
	Shear, LT	Radial	Tangential	Radial	Tangential	Shear, LT
Mean, 10% Moisture Content[2]	1608	476	262	-669	-1456	193
Mean - 2σ[2]	1344	280	146	-535	-1165	161
Temperature Factor[3]	.9	.9	.9	.9	.9	.9
Strength Ratio	.25	.25	.25	.25	.25	.25
Allowable, psi	±302	±63	±33	±120	±262	±36

(1) These properties are not design drivers, so they were not verified by test.

(2) See Table 8.1.8-1 for origin of data.

(3) Engineering estimate.

(4) Engineering estimate based on extrapolation of data from literature.

8.2 WOOD LAMINATE/EPOXY COMPONENT DEVELOPMENT TESTS

8.2.1 FINGER JOINTS

8.2.1.1 Introduction

The MOD-5A rotor blade consisted of five sections, each 80 ft. long, as shown in Figure 8-75. These elements are mated at the erection site, to facilitate shipping the massive sections. The joint at each interface must have the structural integrity to withstand the high loads expected during operation, and to align properly with adjacent sections. The joints must be fabricated at a reasonable cost and with a reasonably small weight increase.

8.2.1.2 Test Objectives

The finger joint concept is a method of transferring load between sections using a gradual transition from one segment to the other. Several tests provided data on effective joint strength as a function of finger length, finger angle, bond gap thickness, and on augmenting the laminae with glass fiber or Kevlar. The goal was to optimize the joint's efficiency while maintaining a reasonable cost. Such variables as aging effects on the surface of the wood before bonding, full scale joint bonding and the effects of exposing the wood to moisture before bonding were also studied, to prove the validity of the finger joint technique. The objectives of these tests were to demonstrate that the structural integrity was adequate, determine allowable load levels, demonstrate that the joints could be fabricated with the required dimensional accuracy, to prove that the joints could be shipped through various environments without losing their integrity, and to enhance the joint optimization study.

Several alternative joint designs were evaluated but the finger joint was selected as the baseline design for the application. Testing joints with several variations of parameters augmented analytical approaches to the optimization of the finger joint configuration. The testing also provided a means for determining the joint's allowable stresses for both static and fatigue loading.

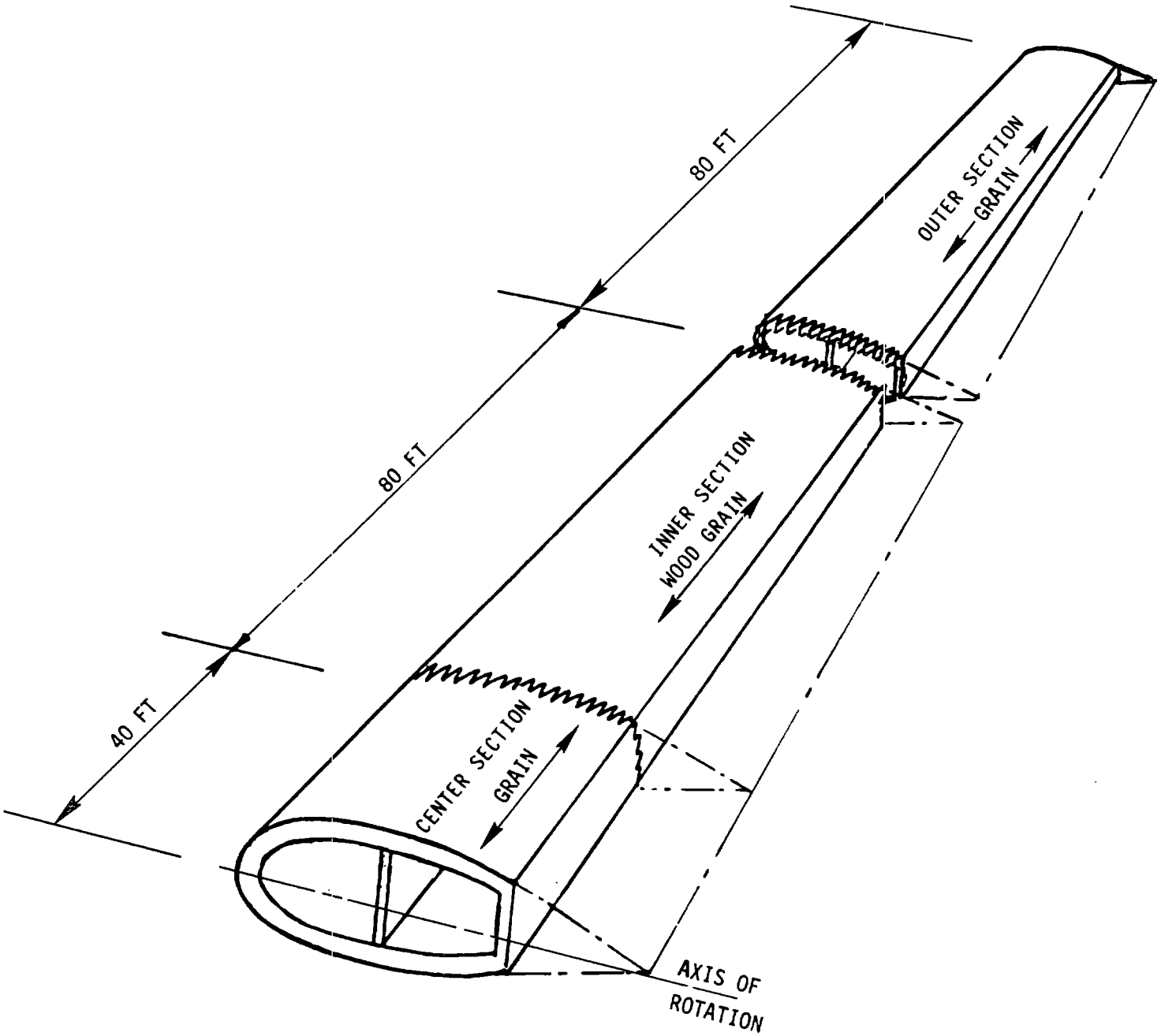

Figure 8-75 MOD-5A Rotor - Field Splice Finger Joint Concept

8.2.1.3 Description

The finger joint test series consisted of five different tests. The length of the finger joints was either 3 in., 6 in., or 10 in. in the test specimens. All of the specimens were fabricated by GBI.

8.2.1.3.1 Static Tension Tests with Various Finger Shapes

Fifty specimens of various geometries were tested, in addition to eight control specimens that were not jointed, which provided basic material strength reference values. Table 8-65 and Figures 8-76 through 8-78 describe the geometry of the joints. The samples were fabricated from 15 layers of 0.10 in. blade grade 1 Douglas fir veneer bonded with West System® epoxy, for a thickness of 1.5 in. They were cut to a width of 2.25 in. and to a length of 92 in., as shown in Figure 8-79. As shown in the table, a finger length of 3 in. with a slope of 1:8, and lengths of 6 in. with slopes of 1:6, 1:8, 1:10 and 1:14 were tested. The testing was conducted by K Consulting Company of Boise, Idaho. A timber testing machine with hydraulically actuated compression grips was used to fail the specimens in one-time load application, using a 5 minute load ramp to failure.

8.2.1.3.2 Static Tension Testing of Aged Joints

A set of ten samples each, of 6 in. and 10 in. finger joints with a 1:10 slope, as shown in Figure 8-80, were tested to failure. Six unjointed static control specimens were also tested. These 26 samples were manufactured and the finger joints were cut eight months before the finger joints were bonded. The testing techniques and facilities were the same as those previously used for tension testing. The intent was to determine if aging the bonding surfaces would affect the strength of the bonded joint. The specimen width was 2.31 in., versus 2.25 in. for previous tension samples (see Figure 8-76). Four of the specimens were bonded with a bond gap of .062 in., versus .015 in. for the other 11 samples, and the previous tension specimens.

Table 8-65 Test Plan, Bonded Finger JointS in Laminated Douglas Fir and Epoxy

Paragraph No.	Augmenting Fiber	Finger Configuration (dimension: in.) Length	Slope	Pitch	Tip Width	Root Width	Bond Gap	Test Specimens Type (1)	Quantity	Type Test Static (Ramp)	Fatigue (2)	Tested By
Static Tests - Variable Finger Geometry												
8.2.1.3.1 and	None	Control - No Joint						A	8	Tens.	---	K Consult.
8.2.1.4.1	None	6.0	1:6	2.125	.062	.062	.015	A	10	Tens.	---	K Consult.
	None	6.0	1:8	1.625	.062	.062	.015	A	10	Tens.	---	K Consult.
	None	6.0	1:10	1.325	.062	.062	.015	A	10	Tens.	---	K Consult.
	None	6.0	1:14	.982	.062	.062	.015	A	10	Tens.	---	K Consult.
	None	3.0	1:8	.875	.062	.062	.015	A	10	Tens.	---	K Consult.
Static Tests - Aged Joints												
8.2.1.3.2 and	None	Control - No Joint						A	6	Tens.	---	K Consult.
8.2.1.4.2	None	6.0	1:10	1.262	.062	.062	.015	A	10	Tens.	---	K Consult.
	None	10.0	1:10	2.344	.156	.188	.015	A	10	Tens.	---	K Consult.
Static Tests - Augmented Joints												
8.2.1.3.3 and	None	Control - No Joint						A	2	Tens.	---	K Consult.
8.2.1.4.3	None	10.0	1:10	2.344	.156	.188	.015	A	1	Tens.	---	K Consult.
	Glass Fiber	10.0	1:10	2.344	.156	.188	.015	A	6	Tens.	---	K Consult.
	None	Control - No Joint						A	2	Tens.	---	K Consult.
	None	10.0	1:10	2.344	.156	.188	.015	A	1	Tens.	---	K Consult.
	Kevlar	10.0	1:10	2.344	.156	.188	.015	A	6	Tens.	---	K Consult.
Fatigue and Static Tests, Narrow and Wide Bond Gaps												
8.2.1.3.4 and	None	6.0	1:10	1.392	.080	.112	.015	B	2	Tens.	---	U. Dayton
8.2.1.4.4	None	6.0	1:10	1.392	.080	.112	.015	B	9	----	Tens.	U. Dayton
	None	6.0	1:10	1.392	.080	.112	.062	B	2	Tens.	---	U. Dayton
	None	6.0	1:10	1.392	.080	.112	.062	B	2	----	Tens.	U. Dayton
	None	Control - No Joint						C	6	Compr.	---	GBI
Fatigue and Static Tests, Augmented Joints												
8.2.1.3.5 and	None	6.0	1:10	1.392	.080	.112	.015	B	2	----	Tens.	GBI
8.2.1.4.5	Glass Fiber	6.0	1:10	1.392	.080	.112	.015	B	3	----	Tens.	GBI
	None	Control - No Joint						C	2	Compr.	---	GBI
	Glass Fiber	Control - No Joint						C	3	Compr.	---	GBIZ

NOTES: (1) A: Rectangular, 1.5 x 2.25 or 2.31 x 92 in.; B: Dogbone; C: Compression, 2 x 2 x 8 in.
(2) R = 0.1

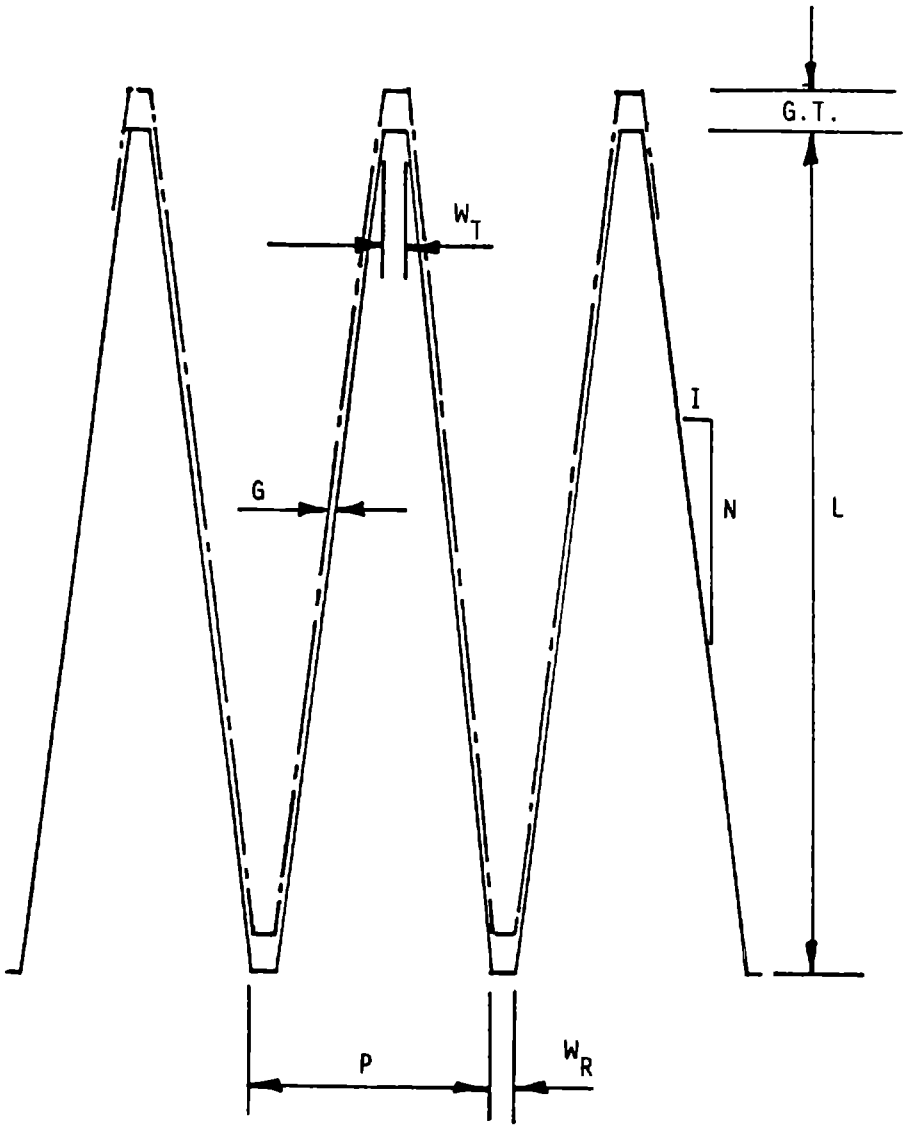

P = PITCH
L = LENGTH
I:N = SLOPE
W_T = TIP WIDTH
W_R = ROOT WIDTH
G = GAP
G.T. = TIP GAP

Figure 8-76 Finger Joint Design Geometry

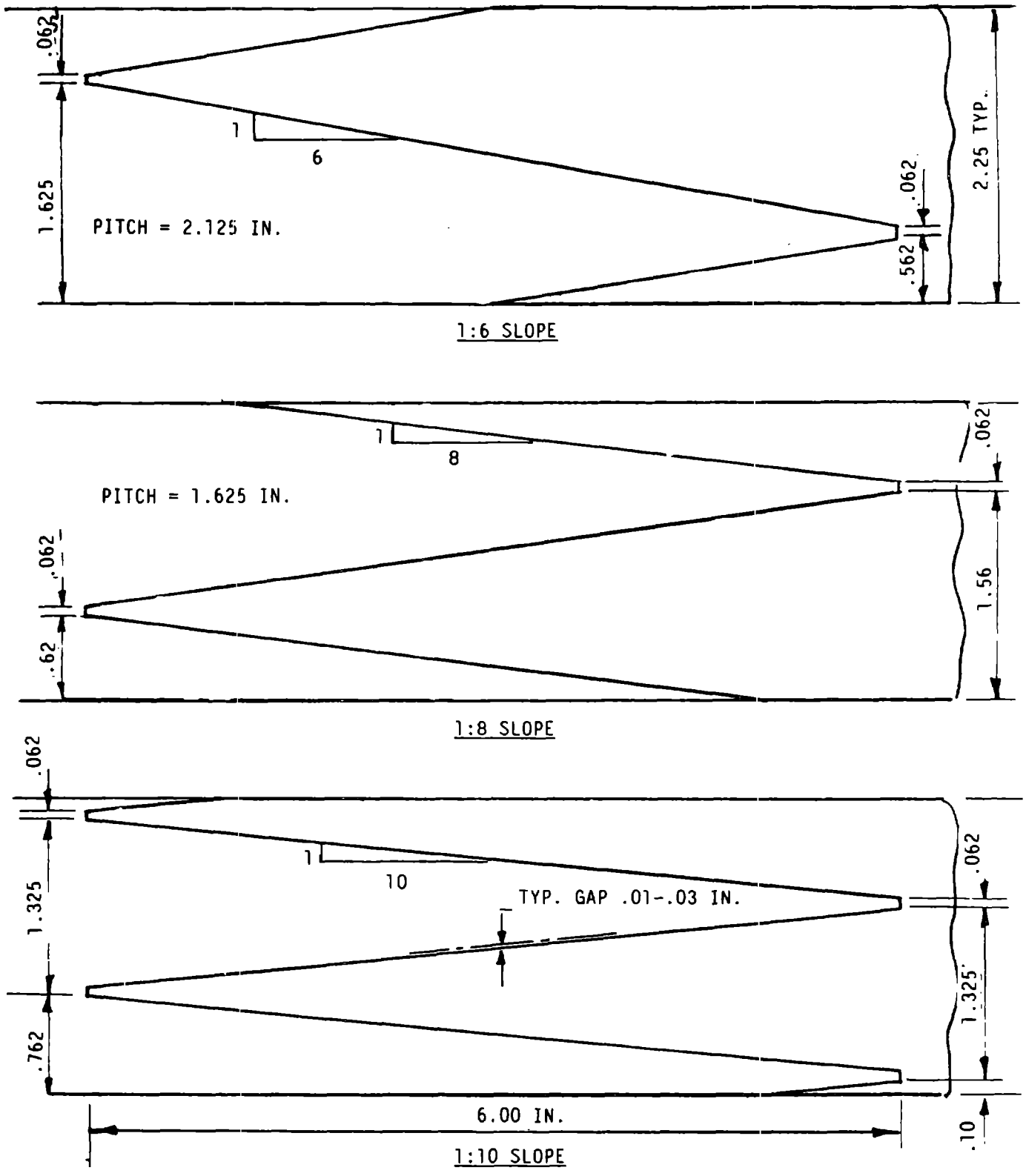

Figure 8-77 Tensile Test Specimens
Details of Machined Fingers, with slopes of 1:6, 1:8, 1:10

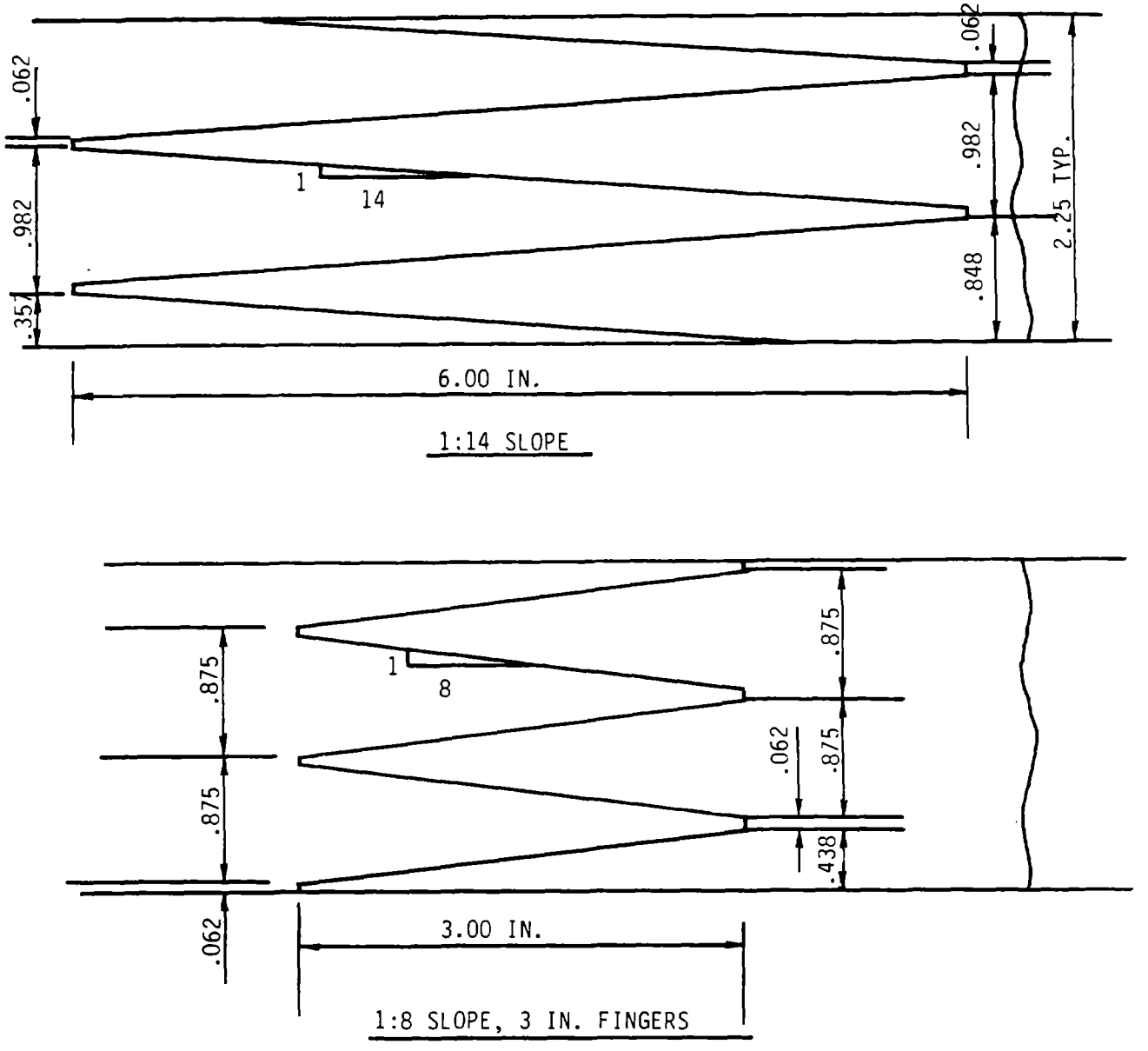

Figure 8-78 3 in. Long Tensile Test Specimens
Details of Machined Fingers, with slopes of 1:14 and 1:8

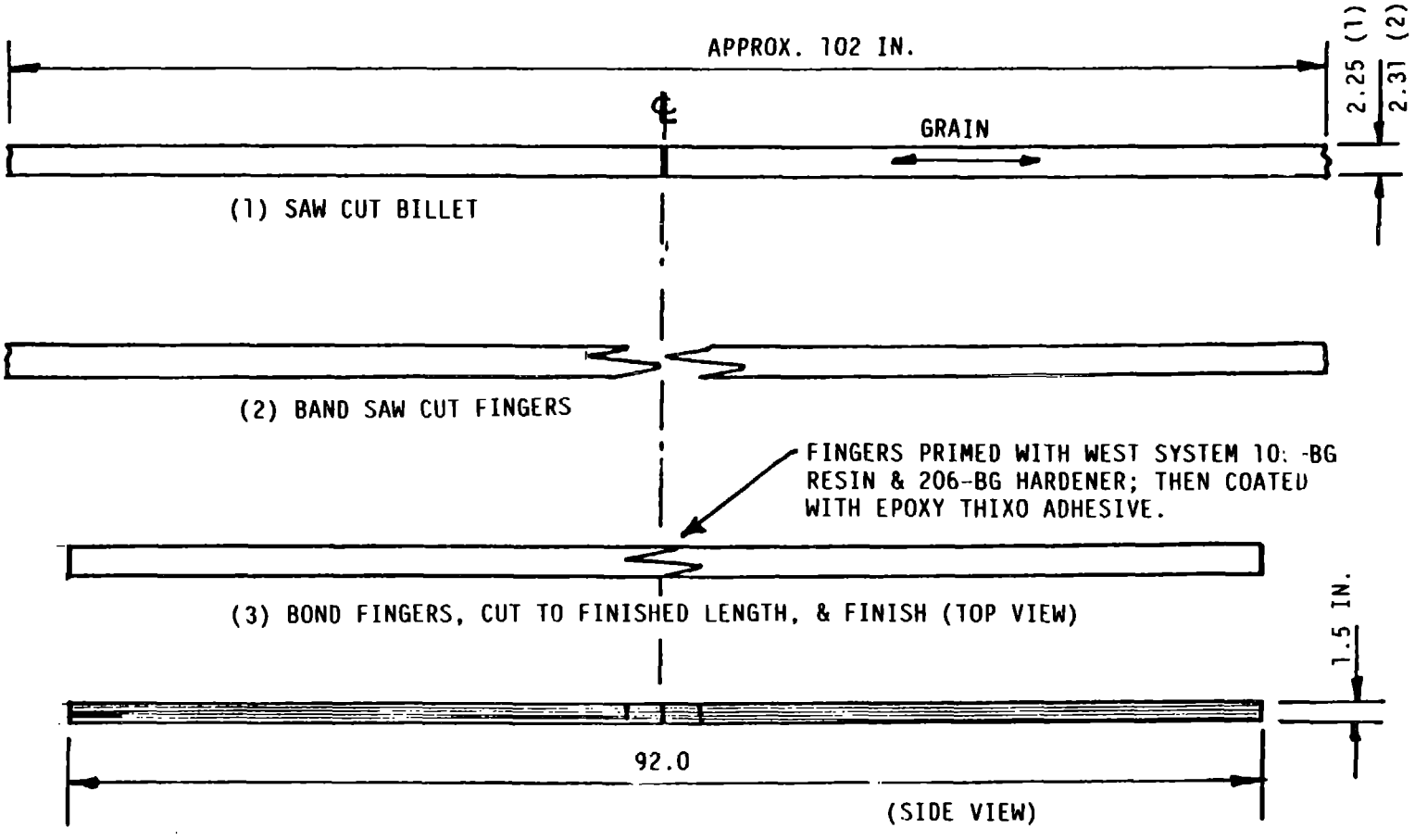

(1) WIDTH OF ALL EXCEPT AUGMENTED LAMINATED AGED SPECIMENS

(2) WIDTH OF AUGMENTED LAMINATE SPECIMENS AND AGED SPECIMENS

Figure 8-79 Fabrication of Finger Joint Tensile Test Specimens

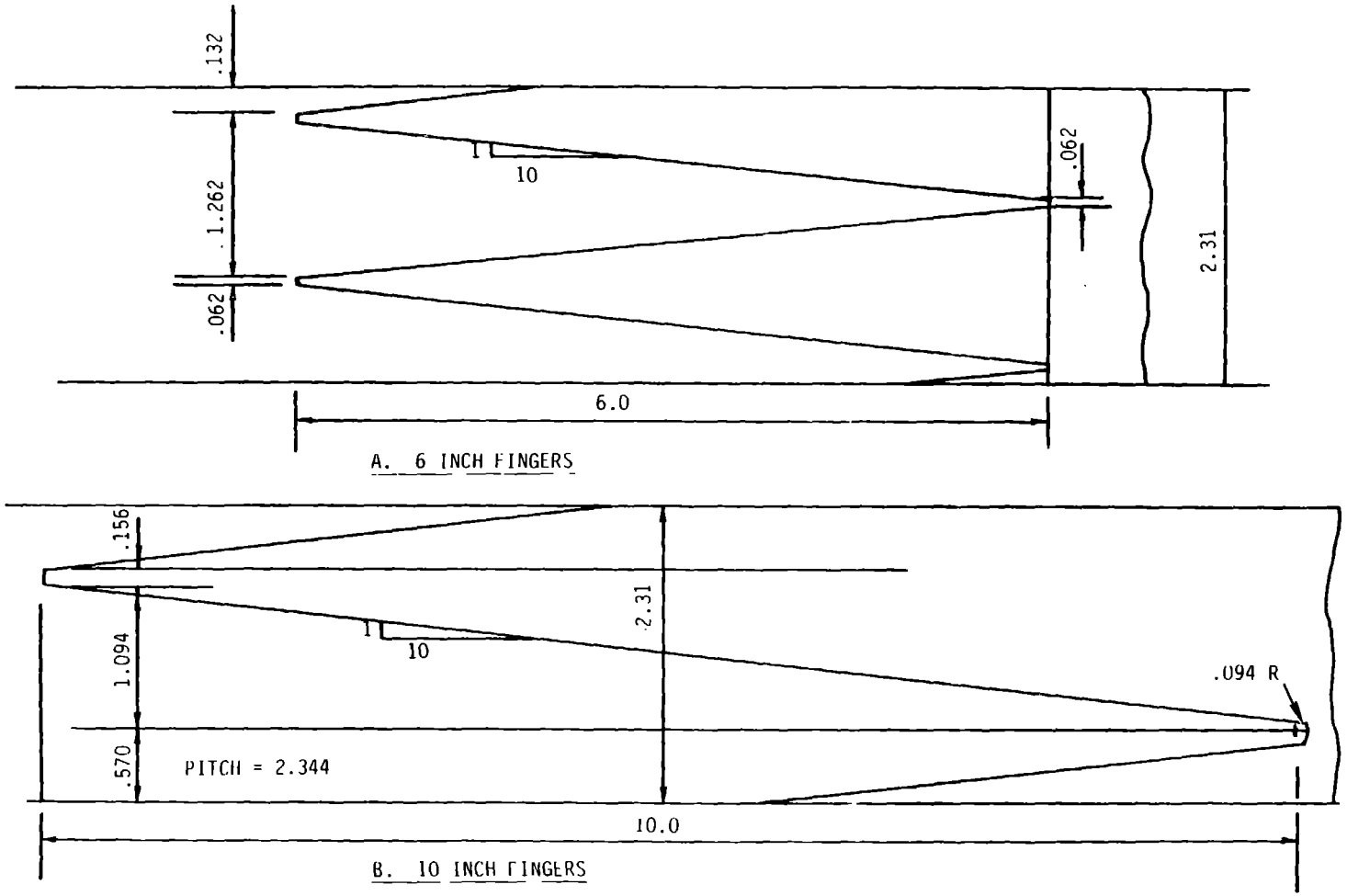

Figure 8-80 Detail of Machined Fingers, Aged Tensile Test Specimens

8.2.1.3.3 Static Tension Testing of Finger-Jointed Augmented Laminae

Six specimens, 2.31 in. wide, were made from laminae augmented with either glass fiber or Kevlar aramid fiber. The billets for each contained unaugmented portions that yielded one jointed sample and two unjointed control specimens. Figure 8-81 shows the configuration of the 10 in. long sample with a 1:10 slope, and details of the augmentation. Figure 8-82 shows the billet configurations. The testing was performed by K Consulting Company using the same equipment and techniques used in previous tests.

8.2.1.3.4 Finger Joint Fatigue Tests

The configuration of specimens for this series of tests was the dogbone shown in Figure 8-83, so that the MTS test machines could be used. The specimens have a button-headed stud bonded into each end for the machine interface. The compression grip timber testing machines are much more expensive to operate than the MTS type, and most do not have cyclic capability. Fifteen of the dogbone samples were fabricated, 11 were fatigue tested at a load ratio of 0.1 and four were static ramp tested in tension. Six control samples, 2 x 2 x 8 in., were made without finger joints, as shown in Figure 8-84. These samples were tested in compression parallel to the grain, using a 5 minute load ramp to failure. All these tests on dogbone specimens were conducted at the University of Dayton Research Institute (UDRI). Compression tests were done at GBI.

All the fingers were 6 in. long in this series, as shown in Figure 8-85. Eleven of the 22 dogbones had a .062 in. gap, and four had a .015 in. bond gap. Two each were subjected to the static ramp to failure.

8.2.1.3.5 Fatigue and Static Tests on Augmented Specimens

With the exception of augmentation, these tests were similar to the tests described above. Each veneer was augmented with one layer of Burlington #7500 fabric. Dogbone specimens, as shown in Figure 8-83, were fabricated for three augmented fatigue specimens and two others from an unaugmented section of the billet. Three augmented and two unaugmented compression samples were fabricated, as shown in Figure 8-85, for control. The testing of the dogbones, which had a bond gap of .015 in., used a load ratio of 0.1. The compression samples were tested using a 5-minute load ramp to failure. All testing was done on an MTS machine by GBI.

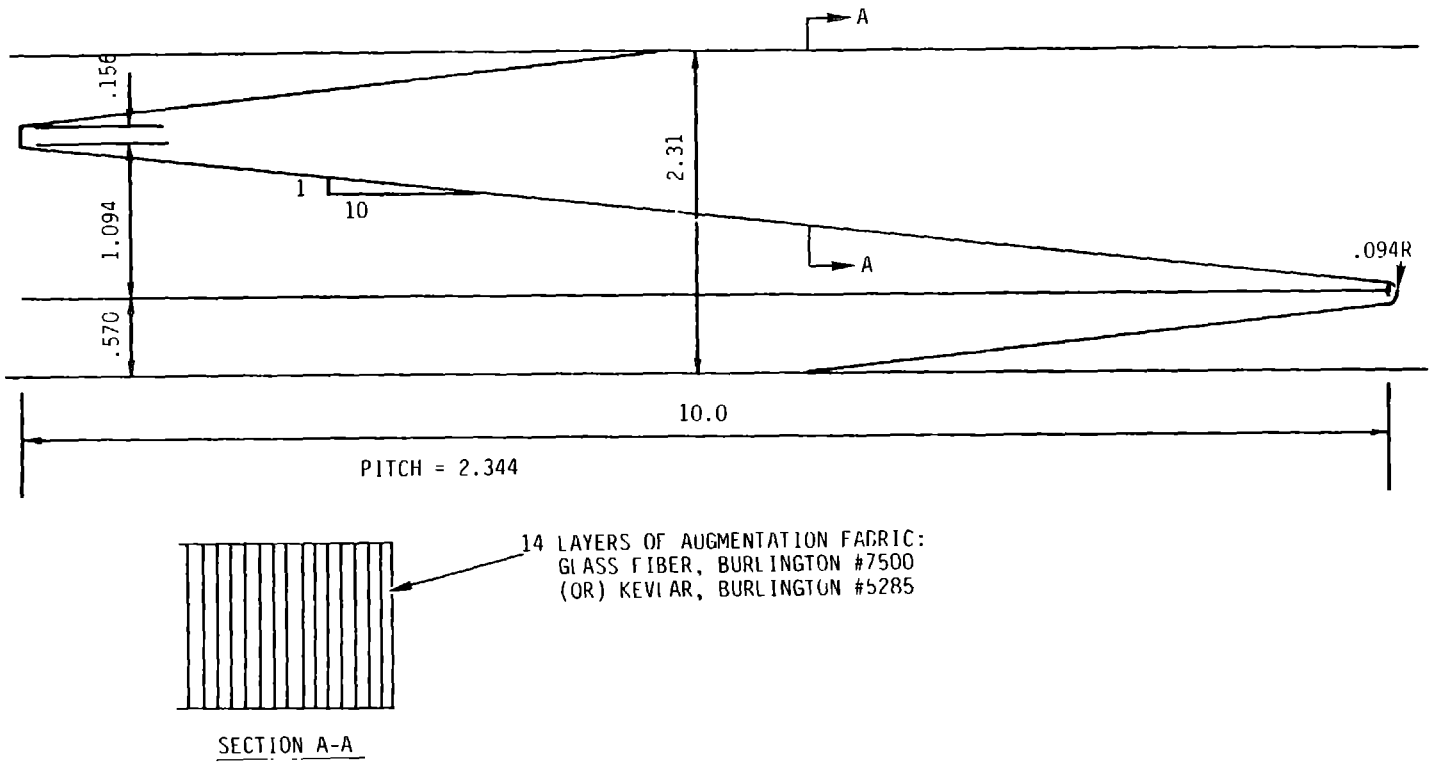

Figure 8-81 Detail of Machined Fingers of Augmented Specimens for Tensile Tests

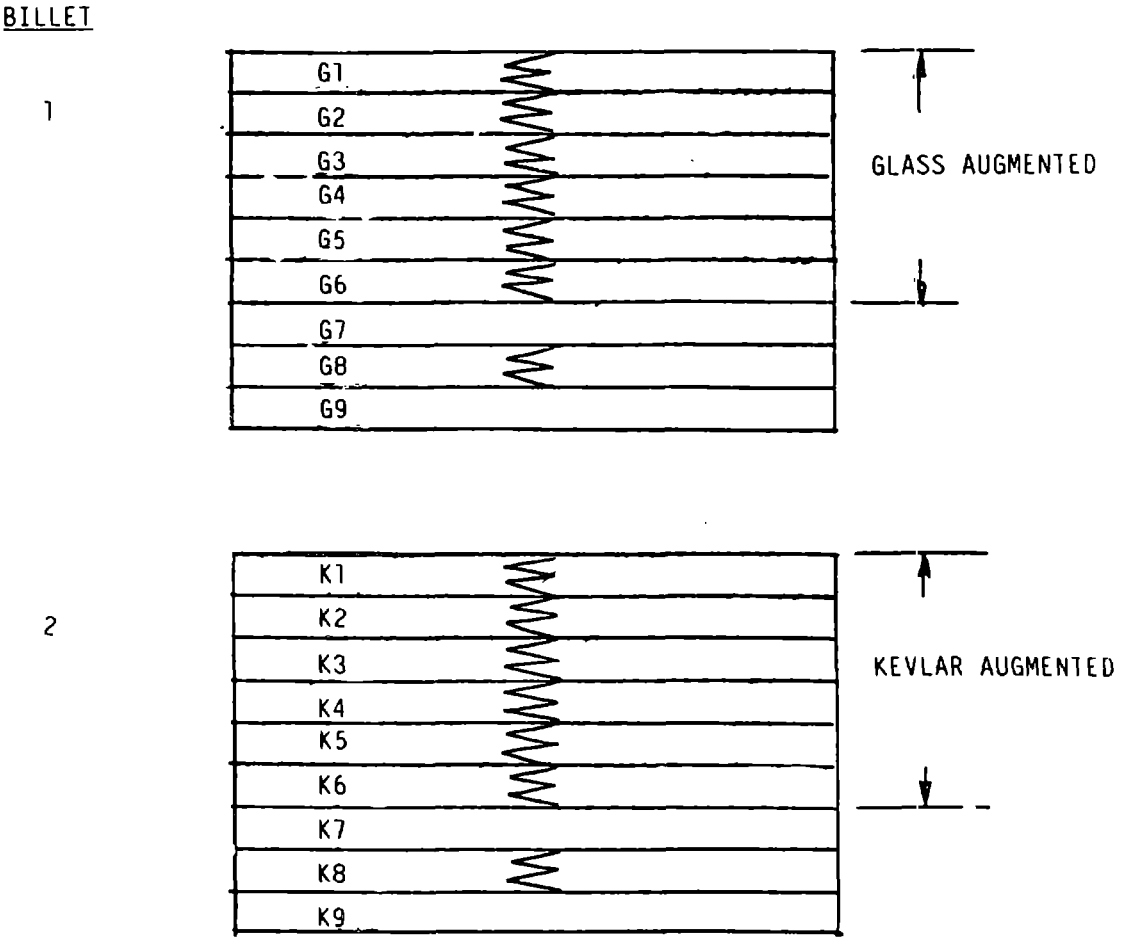

NOTE: ALL FINGERS 10 IN. LONG, WITH 1:10 SLOPE

Figure 8-32 Sectioning of Douglas Fir and Epoxy Laminae Billets with Partial Augmentation, for Finger Joint Tensile Test Specimens

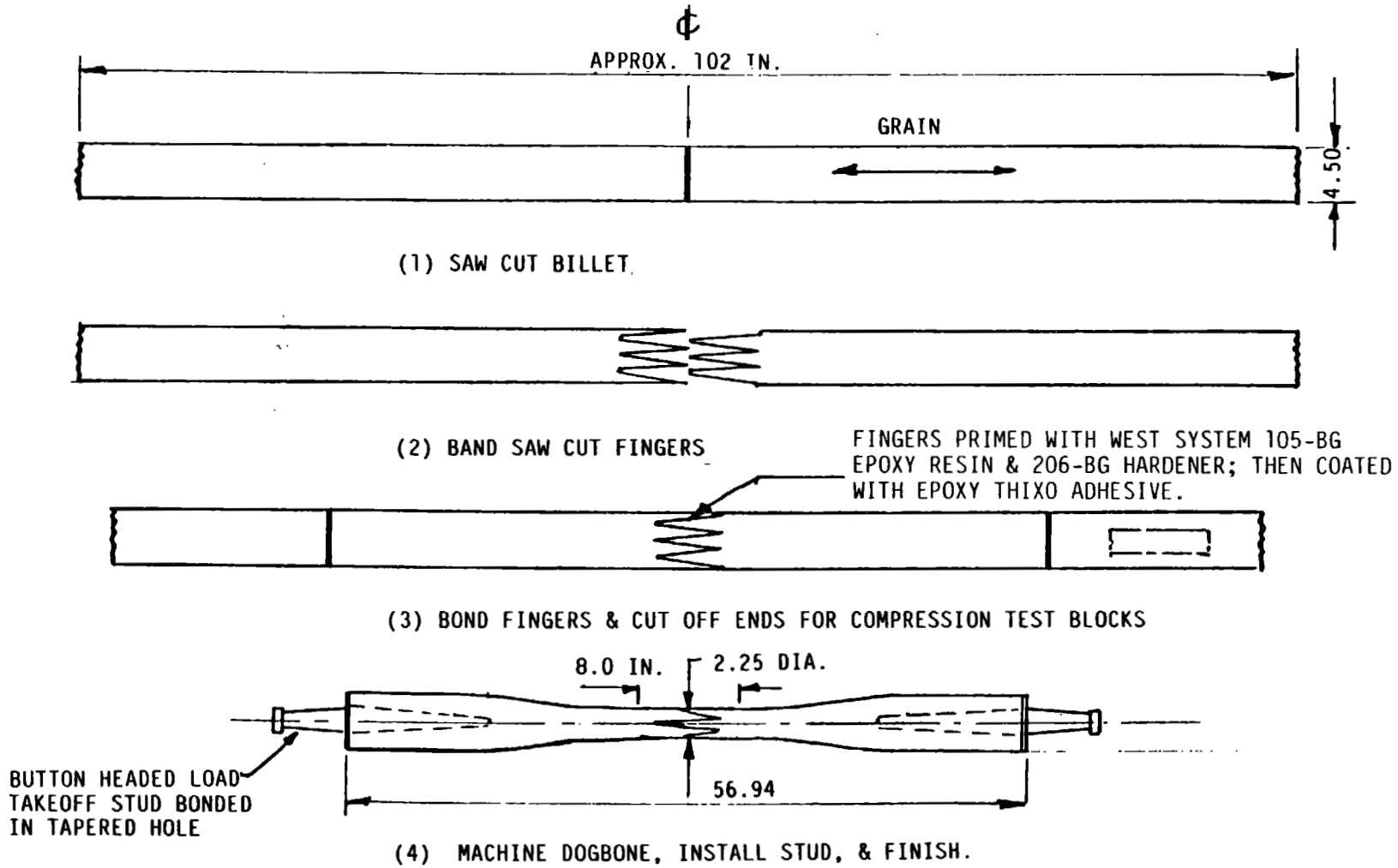

Figure 8-83 Fabrication of Finger Joint, Dogbone Specimens for Fatigue Tests

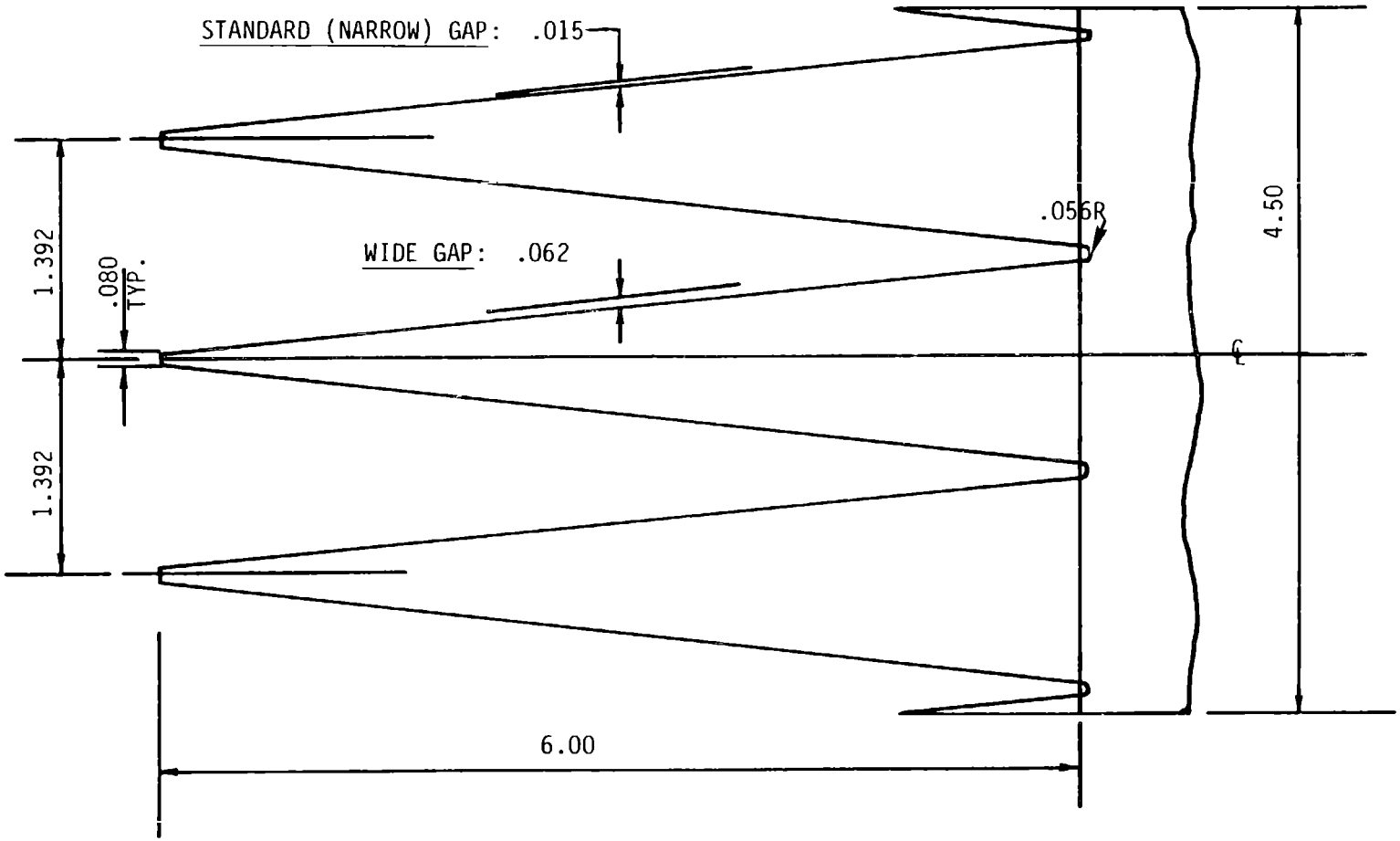

Figure 8-84 Detail of Machined Fingers of Dogbone Specimens for Fatigue Tests

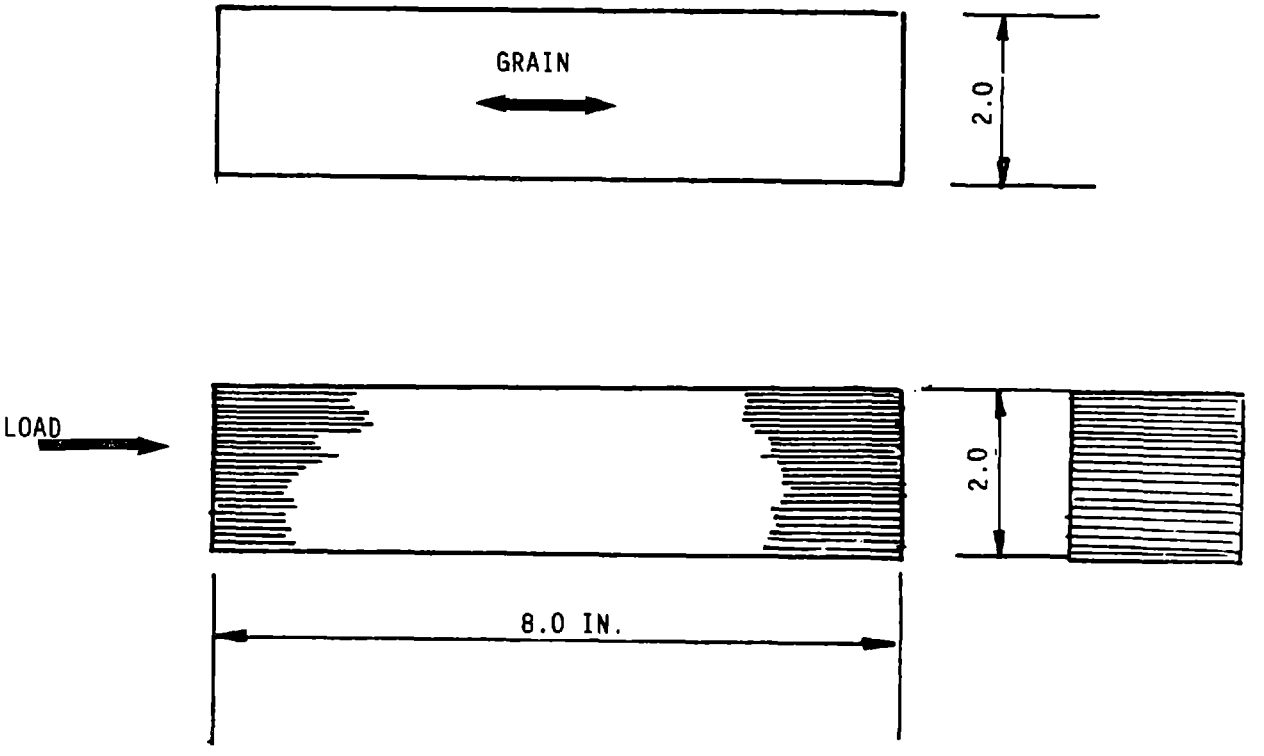

Figure 8-85 Compression Test Specimen

8.2.1.3.6 Full Scale Representation

A full scale representation of a blade joint section was designed and fabricated to prove the techniques and feasibility of the design. This finger joint process demonstration unit is described in section 10.5.5 of Vol. III. The assembly contained joints that were unaugmented, and joints that were augmented with glass fiber or Kevlar. After the full-scale bonding demonstration was completed, the unit was sectioned, and 15 test pieces were removed for static tension testing. The specimens were 2 in. thick, 7 in. wide and 84 in. long. The specimens were cut from areas to provide different joint types and were individually tested to failure in one-time tension using a 5-minute load ramp. The timber testing machine at Washington State University was used for these tests.

8.2.1.4 Results

8.2.1.4.1 Static Tension Tests with Various Finger Shapes

The mean values of tests of various finger sizes and slopes are listed in Table 8-66, section A. Test results are tabulated in Tables 8-67 and 8-68. Table 8-66 also lists mean values corrected to a 12% moisture content, and compares this value to the unjointed control strength for each joint configuration, as a percent of the control's tensile strength. The strength increases as the slope ratio varies from 1:6 to 1:14, with very little difference between the values of 1:10 and 1:14. The 3.0 in. long joint performed slightly better than the 6.0 in. long joint with a comparable slope. The efficiency level of all but the 1:6 slope fingers was above 90%, and shows that this approach for joining wood structures provides an excellent structure.

Based on this data, the slope of 1:10 was selected for all subsequent tests, since its efficiency was 94.1%. The industry standard for much smaller finger joints is also a slope of 1:10.

Table 8-66

Summary - Tensile Strength of Bonded Finger Joints in Laminated Douglas Fir and Epoxy

Test Program: MOD-5A-005 Joint Adhesive: WEST SYSTEM® Epoxy Resin and Hardener, Asbestos-Thickened

Load Direction: Parallel to Wood Grain Test Environment: Approx. 68°F, 50% R.H. Tested By: K Consulting Co.

Total Specimens	Augmentation Material	Finger Geometry Length (in)	Finger Geometry Slope	Nominal Bond Gap (in)	Mean Lam. Moisture Cont.(%)	Mean Tensile Str. (psi) As Tested	Mean Tensile Str. (psi) @12% W.M.C.	Percent of Control T.S.
A. Static Ramp Tests - Variable Finger Geometry								
8	None	------control------		----	6.3	11,565	10,799	100.0
10	None	6.0	1:6	.015	6.5	8,675	8,132	75.3
10	None	6.0	1:8	.015	6.3	10,460	9,767	90.4
10	None	3.0	1:8	.015	6.2	10,619	9,896	91.6
10	None	6.0	1:10	.015	6.4	10,862	10,162	94.1
10	None	6.0	1:14	.015	6.3	10,982	10,254	95.0
B. Static Ramp Tests - Aged Joints								
6	None	------control------		----	5.0	10,050	9,151	100.0
10	None	6.0	1:10	.015	4.5	9,701	8,748	95.6
10	None	10.0	1:10	.015	4.5	8,929	8,052	88.0
C. Static Ramp Tests - Augmented Laminate								
2	None	------control------		----	4.4	14,241	12,817	100.0
1	None	6.0	1:10	.015	3.7	11,299	10,032	78.3
6	Glass Fabric	6.0	1:10	.015	2.9	13,561	11,987	93.5
2	None	------control------		----	4.4	13,650	12,285	100.0
1	None	6.0	1:10	.015	4.1	11,037	9,876	80.4
6	Kevlar Fabric	6.0	1:10	.015	3.6	14,812	13,284	108.1

Table 8-67

Tensile Strength of Finger-Jointed Laminated Douglas Fir and Epoxy

Length of Fingers, 6-in.

A. 1:6 slope of fingers

Specimen #	Moisture Content (%)	Area (in^2)	Failing Load (lbs)	Tensile Strength (psi)	Type of Failure*
600	6.4	3.48	25060	7201	1
601	6.6	3.49	35980	10309	1
602	6.6	3.50	34260	9789	1
603	6.1	3.44	30920	8988	1
604	6.6	3.44	31400	9128	1
605	6.5	3.42	31440	9193	1
606	6.8	3.49	23760	6808	1
607	6.3	3.45	27660	8017	1
608	6.5	3.45	30320	8788	1
609	6.4	3.49	29760	8527	1
$\bar{X}$	6.5			8675	
s				1086	
V				12.5%	

B. 1:8 slope of fingers

800	6.2	3.26	29360	9006	1
801	6.3	3.25	24920	7668	2
802	6.2	3.24	37560	11593	2
803	6.3	3.29	43600	10517	2
804	6.0	3.27	33420	10220	1
805	6.5	3.25	36700	11292	1
806	6.4	3.20	40700	12719	2
807	6.3	3.21	30800	9595	2
808	6.2	3.20	37940	11856	1
809	6.3	3.23	32720	10130	2
$\bar{X}$	6.3			10460	
s				1485	
V				14.2%	

* 1 = failure in joint
2 = failure from joint to some point outside of joint
3 = failure outside of joint

Table 8-67 (Continued)

Tensile Strength of Finger-Jointed Laminated Douglas Fir and Epoxy

Length of Fingers, 6 in. Long

C. 1:10 slope of fingers

Specimen #	Moisture Content (%)	Area (in^2)	Failing Load (lbs)	Tensile Strength (psi)	Type of Failure*
1000	6.3	3.49	35400	10143	2
1001	6.4	3.47	37320	10755	2
1002	6.6	3.46	44280	12798	2
1003	6.5	3.47	40800	11758	2
1004	6.7	3.47	31300	9020	1
1005	6.1	3.44	39100	11366	1
1006	6.3	3.48	37140	10672	3
1007	6.3	3.46	34060	9844	1
1008	6.5	3.44	42140	12250	1
1009	6.1	3.49	34960	10017	3
$\bar{X}$	6.4			10862	
s				1176	
V				10.8%	

D. 1:14 slope of fingers

1400	6.3	3.43	39240	11440	1
1401	6.3	3.47	37520	10813	3
1402	6.6	3.50	30840	8811	2
1403	6.2	3.54	41460	11712	1
1404	6.3	3.47	36900	10634	1
1405	6.1	3.46	45080	13209	1
1406	6.3	3.43	39360	11475	2
1407	6.2	3.46	35060	10133	1
1408	6.1	3.50	40580	11594	1
1409	6.4	3.49	35540	10183	3
$\bar{X}$	6.3			10982	
s				1144	
V				10.4%	

* 1 = failure in joint
2 = failure from joint to some point outside of joint
3 = failure outside of joint

Table 8-68

Tensile Strength of Finger-Jointed Laminated Douglas Fir and Epoxy
Slope of Fingers = 1:8, Length of Fingers = 3 in.

Specimen #	Moisture Content (%)	Area (in^2)	Failing Load (lbs)	Tensile Strength (psi)	Type of Failure*
900	6.2	3.26	34600	10613	3
901	6.4	3.25	36840	11335	1
902	6.3	3.28	36600	11159	1
903	6.2	3.26	38020	11663	1
904	6.2	3.29	36340	11046	1
905	6.2	3.27	30900	9450	2
906	6.3	3.21	29420	9165	2
907	6.0	3.23	33180	10272	1
908	6.1	3.19	35340	11078	1
909	6.4	3.25	33820	10406	1
$\bar{X}$	6.2			10619	
s				812	
V				7.6%	

* 1 = failure in joint
2 = failure from joint to some point outside of joint
3 = failure outside of joint

Tensile strength of veneer composite material without joints

000	6.6	3.47	42500	12248	splintering
001	6.5	3.63	38720	10667	tension
002	6.3	3.44	40760	11849	"
003	6.4	3.45	42960	12452	"
004	6.7	3.44	39840	11581	"
005	6.0	3.48	36100	10374	"
006	6.0	3.25	37520	11545	"
007	6.2	3.27	38600	11804	"
$\bar{X}$	6.3			11565	
s				719	
V				6.2%	

8.2.1.4.2 Aged Joint Static Test Results

Section B of Table 8-66 summarizes the results of joints aged 8 months after cutting and before bonding. The static control mean strength for these joints was approximately 15% lower than that of the previous series, at 12% wood moisture content. The percent of the control tensile strength value for the 6.0 in. fingers was 1.5% higher than that of unaged joints, but the strength of the aged, 10.0 in. finger joint was 7.6% below that of the aged, 6.0 in. joint. Tables 8-69 and 8-70 show the test results for all the aged specimens.

8.2.1.4.3 Augmented Laminae Finger Joint Test Results

Section C of Table 8-66 presents a summary of mean test values for the glass fiber and Kevlar augmented specimens. Both sets of unaugmented, unjointed control samples had very high values: 12,817 and 12,285 psi, at 12% wood moisture content, and relatively low efficiencies for unaugmented finger jointed control samples: 78.3 and 80.4%. The finger joint samples augmented with glass fiber had a strength of 93.5% of the unjointed control, 15.2% greater than the mean of the unaugmented jointed specimen. Kevlar augmentation provided a strength of 108.1%, and the jointed control was at 80.4%. The reason for the high performance of Kevlar augmented joints is probably that the Kevlar fibers are not sheared cleanly during the joint machining operation, so they leave fuzzing beyond the joint face which increases the bonding area.

The test results are tabulated in Tables 8-71 and 8-72.

Table 8-69 Tensile Strength of Finger-Jointed Composite Material.

Fingers Aged Approximately 8 Months Before Bonding.

A. slope of fingers 1:10
length of fingers 6-in.

Specimen #	Moisture Content (%)	Area (in^2)	Failing Load (lbs)	Tensile Strength (psi)	Type of Failure*
1100	4.3	3.47	29260	8432	1
1101	4.5	3.54	32800	9266	1
1102	4.3	3.51	31100	8860	1
1103	4.6	3.41	33800	9912	1
1104	4.5	3.52	33820	9608	2
1105	4.7	3.55	38620	10879	1
1106	4.7	3.48	36460	10477	1
1107	4.3	3.36	30320	9024	2
1108	4.3	3.46	34880	10081	2
1109	5.1	3.50	36660	10474	1
$\bar{X}$	4.5			9701	
s				799	
V				8.2%	

B. slope of fingers 1:10
length of fingers 10-in.

1200	4.6	3.48	29660	8523	1
1201	4.3	3.47	30440	8772	1
1202	4.6	3.48	28580	8213	1
1203	4.9	3.50	29120	8320	1
1204	4.6	3.53	27460	7779	1
1205	4.3	3.51	32240	9185	1
1206	4.6	3.42	27540	8053	1
1207	4.5	3.31	31760	9595	1
1208	4.6	3.32	35200	10602	2
1209	4.4	3.42	35060	10251	1
$\bar{X}$	4.5			8929	
s				956	
V				10.7%	

* 1 = failure in joint
2 = failure from joint to some point outside of joint
3 = failure outside of joint

Table 8-70 Tensile Strength of Composite Material Without Joints.
Material Aged Approximately 8 Months Before Testing.

Specimen #	Moisture Content (%)	Area (in^2)	Failing Load (lbs)	Tensile Strength (psi)	Type of Failure
1300	5.1	3.51	36900	10513	splintering
1301	4.7	3.51	41320	11772	tension
1302	5.4	3.51	26820	7641	"
1303	4.7	3.52	39700	11278	"
1304	5.2	3.32	30660	9235	"
1305	4.7	3.45	34020	9861	"
$\bar{X}$	5.0			10050	
s				1496	
V				14.9%	

Table 8-71 Tensile Strength of Composite Material

A. Augumented finger joint material
with #7500 Burlington glass fiber cloth
slope of fingers 1:10
length of fingers 10-in.

Specimen #	Moisture Content (%)	Area (in^2)	Failing Load (lbs)	Tensile Strength (psi)	Type of Failure*
G 01	3.0	3.90	48860	12528	1
G 02	2.9	3.92	55240	14092	1
G 03	2.6	3.95	54840	13884	1
G 04	3.0	3.86	52020	13477	1
G 05	2.9	3.94	54660	13873	1
G 06	3.2	3.93	55220	14051	1
$\bar{X}$	2.9			13561	

B. Unaugumented finger joint material
slope of fingers 1:10
length of fingers 10-in.

07	3.7	3.51	39660	11299	1

* 1 = failure in joint

C. Unaugumented material without joints

08	4.3	3.52	49520	14068	splintering
09	4.5	3.53	50880	14414	tension
$\bar{X}$	4.4			14241	

Table 8-72 Tensile Strength of Composite Material

A. Augumented finger joint material
with #5285 Burlington Kevlar cloth
slope of fingers 1:10
length of fingers 10-in.

Specimen #	Moisture Content (%)	Area (in^2)	Failing Load (lbs)	Tensile Strength (psi)	Type of Failure*
K 01	3.5	3.83	58160	15185	1
K 02	3.4	3.88	56920	14670	1
K 03	3.8	3.92	57600	14694	1
K 04	3.6	3.92	57000	14541	1
K 05	3.5	3.88	60580	15613	1
K 06	3.8	3.85	54540	14166	1
$\bar{X}$	3.6			14812	

B. Unaugumented finger joint material
slope of fingers 1:10
length of fingers 10-in.

07	4.1	3.55	39180	11037	1

* 1 = failure in joint

C. Unaugumented material without joints

08	4.4	3.53	45860	12992	splintering
09	4.4	3.45	49360	14307	tension
$\bar{X}$	4.4			13650	

8.2.1.4.4 Results of Fatigue Tests on Finger Joints

The results of this test series are listed in Table 8-73, including stress values corrected to 12% wood moisture content. Section A of the table lists the static control tension values. The two wide-gap members had values 12.5% and 16% lower than that of the standard .015 in. bond gap samples from the same billet. The fatigue tests, all with a load ratio of 0.1 (tension-tension), yielded the results shown in section B of the table. The two wide-gap specimens, 15-2 and 16-1, performed poorly, as shown in Figure 8-86. During several of the tests, cracks near the finger's ends were detected before failure, anywhere from 3.3% to 76% of the total cycles. The frequency was 5 Hz for all of the tests, and no problems with overheating occurred.

8.2.1.3.5 Results of Fatigue Tests on Augmented Laminae

The results of this series of tests, corrected to 12% moisture content, are shown in Table 8-74. The testing was conducted at 5 Hz, and no heating problems were noticed. Table 8-75 shows the results of static compression tests conducted by GBI, and indicates a mean stress level of 9,595 psi for "A" blocks and 9,594 psi for "C" blocks. Figure 8-87 is a plot of the fatigue test data, showing the related trend lines.

8.2.1.4.6 Results of Tension Tests on Full Scale Representation Specimens

Table 8-76 presents the data from the 15 specimens. The firgers of samples 1, 2 and 3, were augmented on one side of the longitudinal centerline and Kevlar on the other. The average stress level was 13,000 psi at failure. Samples 4, 5 and 6, which were unaugmented, had an average failure stress of 11,033 psi. Samples 7, 8 and 9, which were augmented with glass fiber, had an average stress level of 9,760 psi, although sample 9 fell well below the others. The joint of sample 9 failed between the epoxy surface and wood face at 6,910 psi, and very little wood was left on the epoxy surface. The specimens augmented with Kevlar performed very well. Numbers 10, 11 and 12 met the machine limit of 13,560 psi without failure. Samples 13, 14 and 15 had an average failure stress of 13,333 psi, 121% of the average strength of the unaugmented control specimen. Figure 8-88 shows the overall FJPDU configuration and defines areas from which samples were removed.

Table 8-73

Tensile Compression Strength and Tension Fatigue Strength of Narrow and Wide Gap Bonded Finger Joints in Unaugmented Douglas Fir Laminae and Epoxy

Test Program: MOD-5A-005 Joint Adhesive: WEST SYSTEM® Epoxy Resin and Hardener, Asbestos-Thickened

Load Direction: Parallel to Wood Grain Test Environment: Approximately 68°F, 50% R.H. Tested By: U.Dayton R.I.

Finger Geometry: Length 10 in.; Slope, 1:10 Fatigue Stress Ratio: 0.1 Cycle Rate: 5 Hz

Specimen Number	Bond Gap (in)	LMC (%)	Tensile Strength (psi) As Tested	Tensile Strength (psi) @12% W.M.C.	Fatigue Strength (psi) As Tested	Fatigue Strength (psi) @12% W.M.C.	No. of Cycles
A. Tensile Ramp Tests							
15-1	.062 (w)	5.07	8,510	7,759	-----	-----	----------
15-4	.015	4.00	9,930	8,868	-----	-----	----------
18-1	.062 (w)	4.61	9,020	8,151	-----	-----	----------
18-2	.015	4.47	10,780	9,715	-----	-----	----------
B. Tension Fatigue Tests							
15-2	.062(w)	4.02	------	-----	4,000	3,574	2,715,700
15-3	.015	4.28	------	-----	4,500	4,041	4,134,300
15-5	.015	4.95	------	-----	4,250	3,866	4,822,500
16-1	.062(w)	5.11	------	-----	4,500	4,106	202,000
16-2	.015	4.95	------	-----	4,500	4,093	5,143,600
16-3	.015	4.87	------	-----	4,250	3,860	13,830,800
16-4	.015	4.70	-----	-----	4,250	3,847	23,319,500
16-5	.015	5.13	-----	-----	5,500	5,021	344,800
18-3	.015	4.65	-----	-----	5,500	4,974	442,700
18-4	.015	4.61	-----	-----	7,000	6,326	31,700
18-5	.015	4.54	-----	-----	6,500	5,866	32,600

Table 8-73 (Continued)
Compressive Strength of Unaugmented Douglas Fir Laminae and Epoxy
Used in Narrow or Wide Gap Finger Joint Tests

Test Program: MOD-5A-005 Test Specimens: 2 in. x 2 in. x 8 in. long
Load Direction: Parallel to Wood Grain (No Finger Joints)
Test Environment: Approximately 68°F, 50% R.H.
Tested By: Gougeon Brothers, Inc.

Specimen Number	LMC (%)	Compressive Strength (psi)(1) As Tested	@12% W.M.C.
15-3C	Est. 5.0	8,898	6,456
15-5C	5.2	8,914	6,576
16-3C	Est. 5.5	9,432	7,074
16-5C	5.8	9,671	7,390
18-1C	5.0	10,473	7,624
18-3C	Est. 5.0	10,061	7,300

NOTES: (1) ASTM Standard 5-Minute Ramp-To-Failure

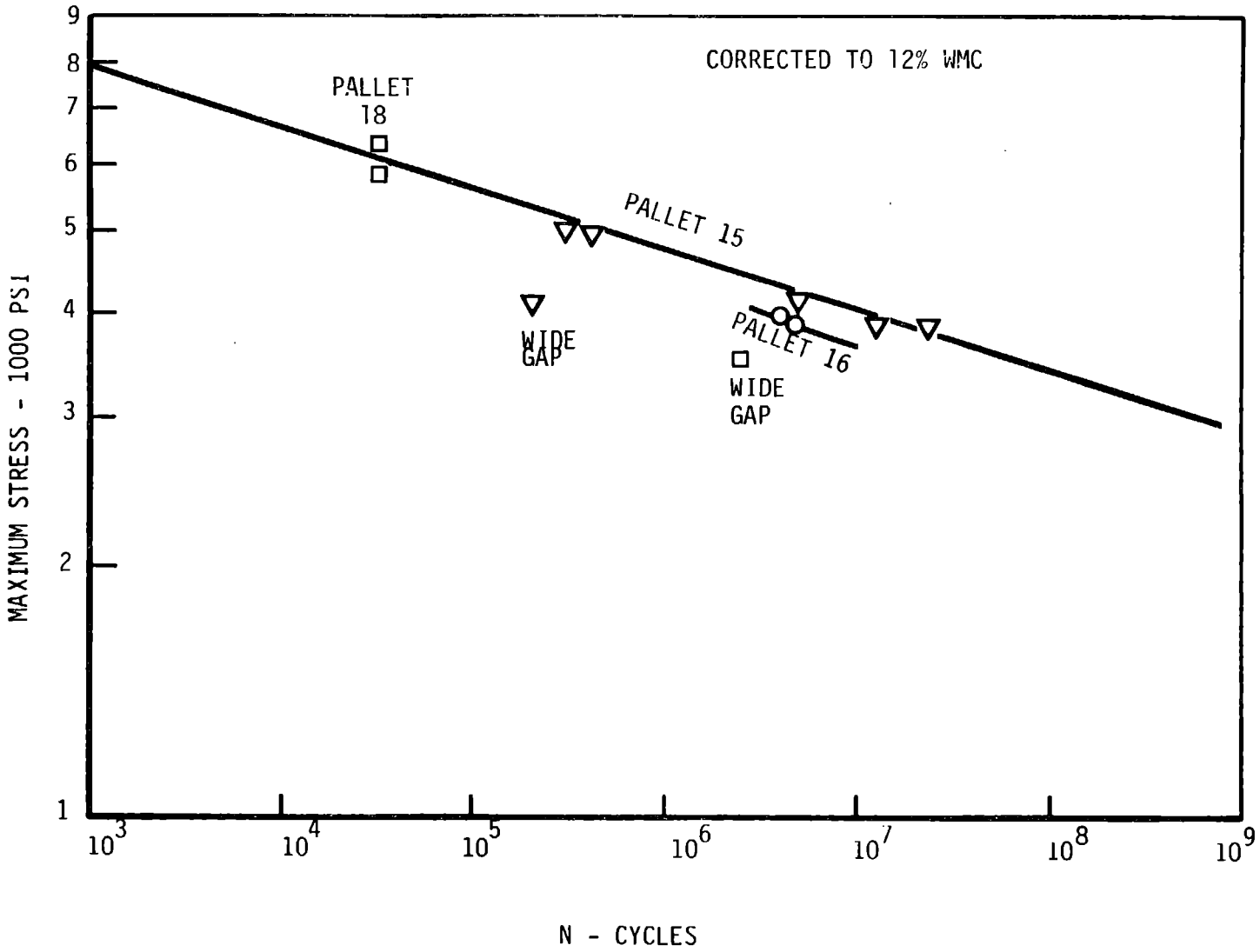

Figure 8-86 Finger Joint Fatigue Test Results

Table 8-74

Tension Fatigue Strength of Bonded Finger Joints in Douglas Fir Laminae and Epoxy Augmented with Glass Fiber

Test Program: MOD-5A-005 Joint Adhesive: WEST SYSTEM® Epoxy Resin and Hardener, Asbestos-Thickened

Finger Joint Geometry: Length - 10 in., Slope - 1:10, Bond Gap - .015in.

Load Direction: Parallel to Wood Grain Fatigue Stress Ratio: 0.1 Cycle Rate: 5 Hz

Test Environment: Approximately 68°F, 50% R.H. Tested By: Gougeon Brothers, Inc.

Specimen Number	Laminae Augmentation	LMC (%)	Fatigue Strength (psi) As Tested	Fatigue Strength (psi) @12% W.M.C.	Number of Cycles
A. Augmented Laminae					
EFJF-1E	Glass	6.15	6,000	5,719	227,800
EFJF-2E	Glass	6.05	7,500	7,132	8,830
EFJF-3E	Glass	6.30	5,125	4,902	493,110
B. Unaugmented Laminae					
EFJF-4S	None	6.50	7,000	6,562	3,900
EFJF-5S	None	6.00	5,500	5,106	207,770

Table 8-75

Compressive Strength of Glass Fiber-Augmented Douglas Fir Laminae and Epoxy Used in Finger Joint Fatigue Tests

Test Program: MOD-5A-005 Test Specimens: 2 in x 2 in x 8 in long

Load Direction: Parallel to wood grain

Test Environment: Approximately 68°F, 50% R.H.

Tested By: Gougeon Brothers, Inc.

Specimen Number	LMC (%)	Compressive Strength (psi)(1)	
		As Tested	@ 12% W.M.C.
EFJF-1E-A	6.0	11,540	9,676
EFJF-2E-A	5.8	11,775	9,718
EFJF-3E-A	5.6	11,562	9,392
EFJF-1E-C	5.6	11,417	9,274
EFJF-2E-C	6.0	11,833	9,922
EFJF-3E-C	5.9	11,525	9,587

NOTES: (1) ASTM Standard 5-Minute Ramp-To-Failure

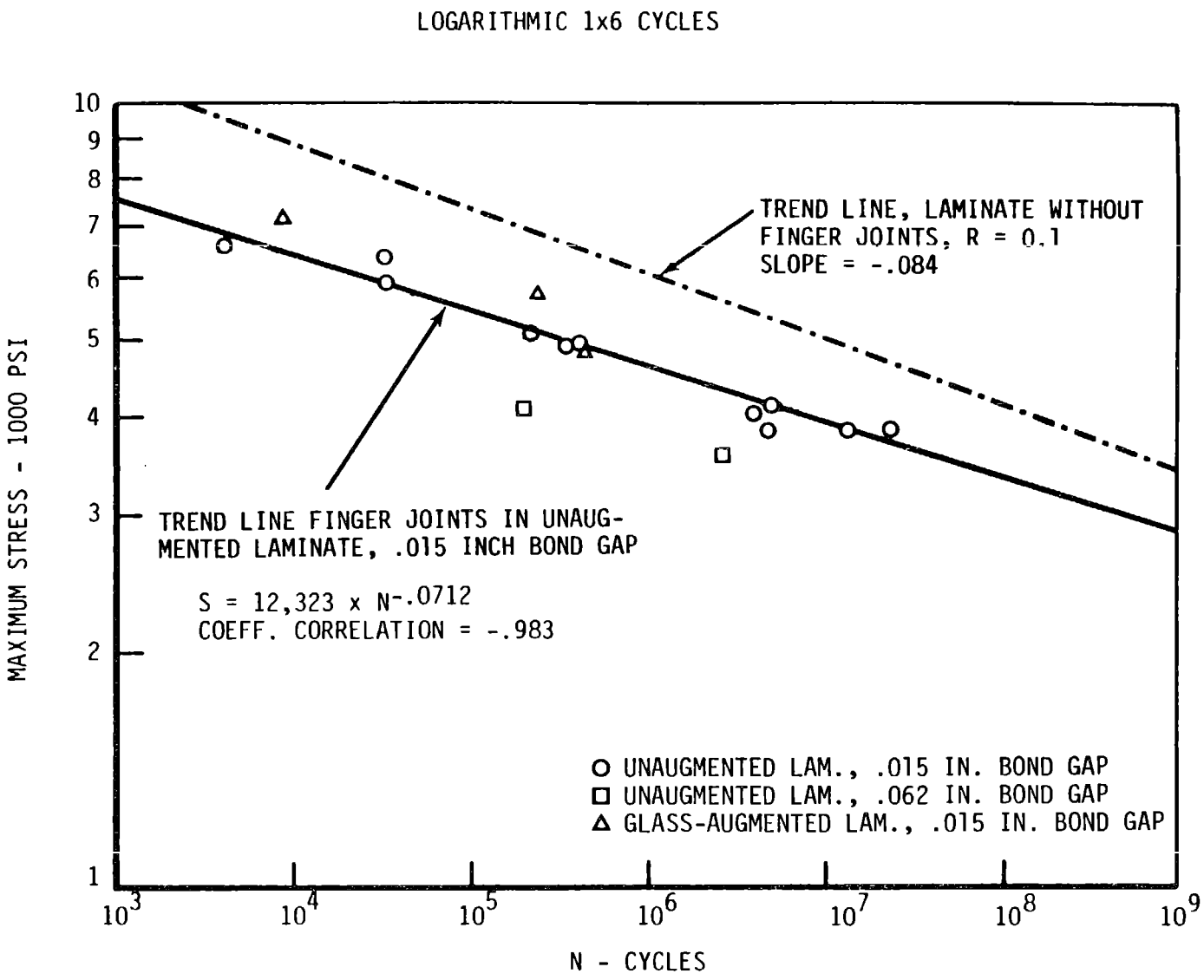

Figure 8-87 Tension Fatigue Test of Douglas Fir and Epoxy Laminae with Bonded Finger Joints

Table 8-76 Full Scale Representation Tension Test Results

Sample Number	Cross Section (in)	Construction	Failure Stress (psi)	Augmentation	Notes
1	2 x 8	Finger Joints	12,810	1/2 end glass, 1/2 Kevlar	
2	2 x 8	Finger Joints	13,500	1/2 end glass, 1/2 Kevlar	
3	2 x 8	Finger Joints	12,690	1/2 end glass, 1/2 Kevlar	
4	2 x 7	Solid-No Joints	11,890	Unaugmented	
5	2 x 7	Solid-No Joints	12,000	Unaugmented	
6	2 x 7	Solid-No Joints	9,210	Unaugmented	
7	2 x 8	Finger Joints	12,560	Glass	
8	2 x 8	Finger Joints	9,810	Glass	
9	2 x 8	Finger Joints	6,910	Glass	Epoxy/Wood Separation
10	2 x 8	Finger Joints	13,560*	Kevlar	
11	2 x 8	Finger Joints	13,560*	Kevlar	
12	2 x 8	Finger Joints	13,560*	Kevlar	
13	2 x 8	Finger Joints	13,500	Kevlar	
14	2 x 8	Finger Joints	12,940	Kevlar	
15	2 x 8	Finger Joints	13,560	Kevlar	

See Figure 8-88 for sample location in Finger Joint Process Demonstration Unit

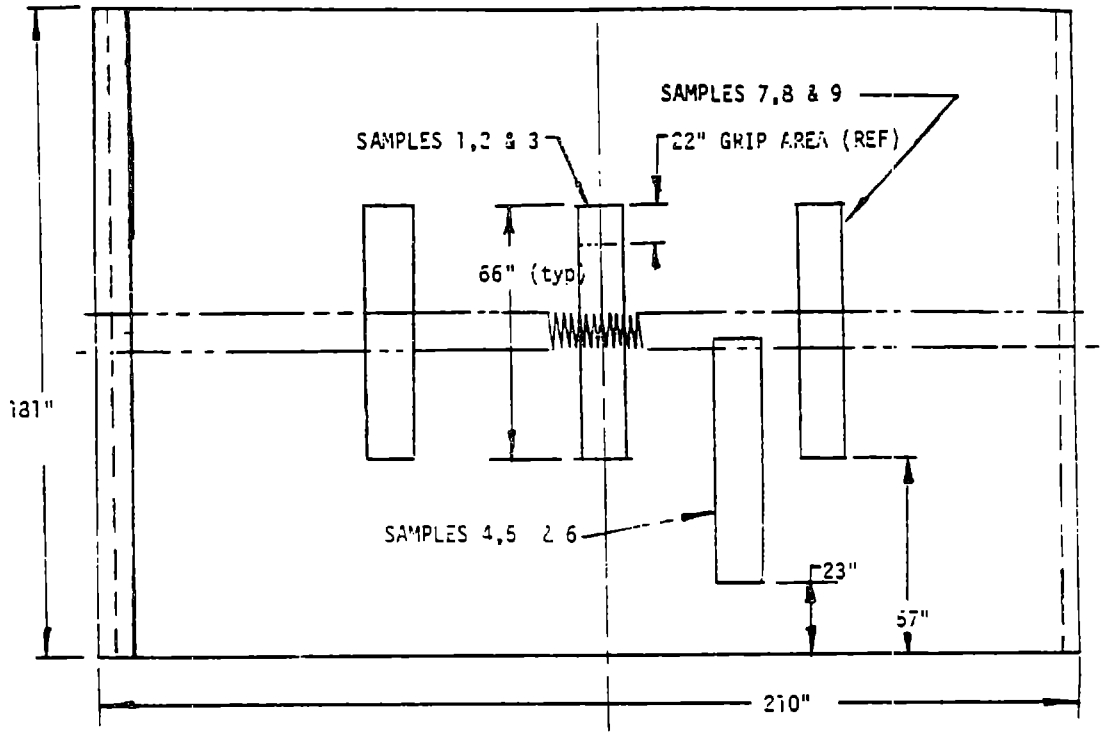

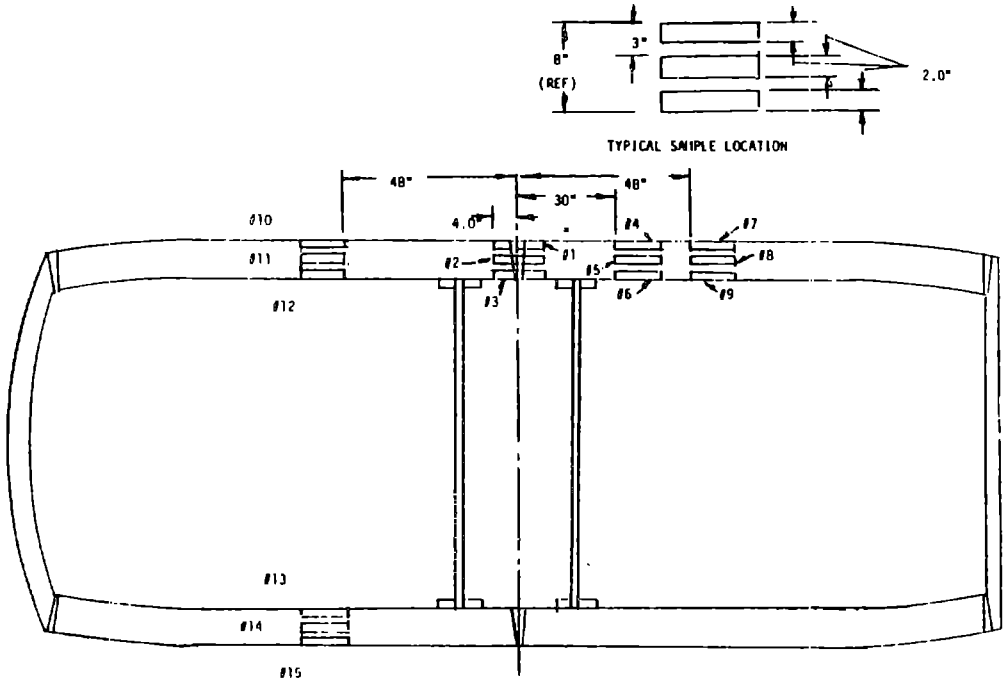

Figure 8-88 Sample Locations in FJPDU.

8.2.2 LONGITUDINAL BONDED JOINTS

8.2.2.1 Introduction

The MOD-5A blade was designed to be made of long, contoured panels of wood veneer and epoxy, as shown in Figure 8-89. These panels are typically 80 ft. long, and are bonded at joints filled with thixotropic epoxy. The early rotor design used a butt joint with faces normal to the surface, as shown in Figure 8-89, detail A. A wood veneer wedge and epoxy-filled joint, as shown in Figure 8-89, detail B evolved later. Both configurations were tested. Since manufacturing defects are possible in a joint of this size, and since inspection is difficult, the effects of typical defects were studied. The joints must be immune to catastrophic propogation of cracks resulting from small defects, so both static and fatigue tests were conducted.

The test results from the two types of joints are not directly comparable. When the first samples were designed no joint configuration change was anticipated. When the change was implemented the configuration of the sample was modified and the bending and shear characteristics were modified.

8.2.2.2 Test Objectives

The objective of this test was to obtain data on the durability of longitudinal bonded joints in Douglas fir veneer and West System® epoxy, which were subjected to static or fatigue loads in a bending test arrangement. The test studied the influence of defects in the bond line of the joint, and of high and low temperatures on the joint. Tables of shear strength, S-N curves and descriptions of failures were recorded.

8.2.2.3 Description

The test program was conducted by the Illinois Institute of Technology Research Institute (IITRI), in Chicago, Illinois. The program lasted one year, and ended in September, 1983.

The configurations of the samples are shown in Figure 8-90. Three point bending loads were imposed on the thick flange I-beam test specimens to

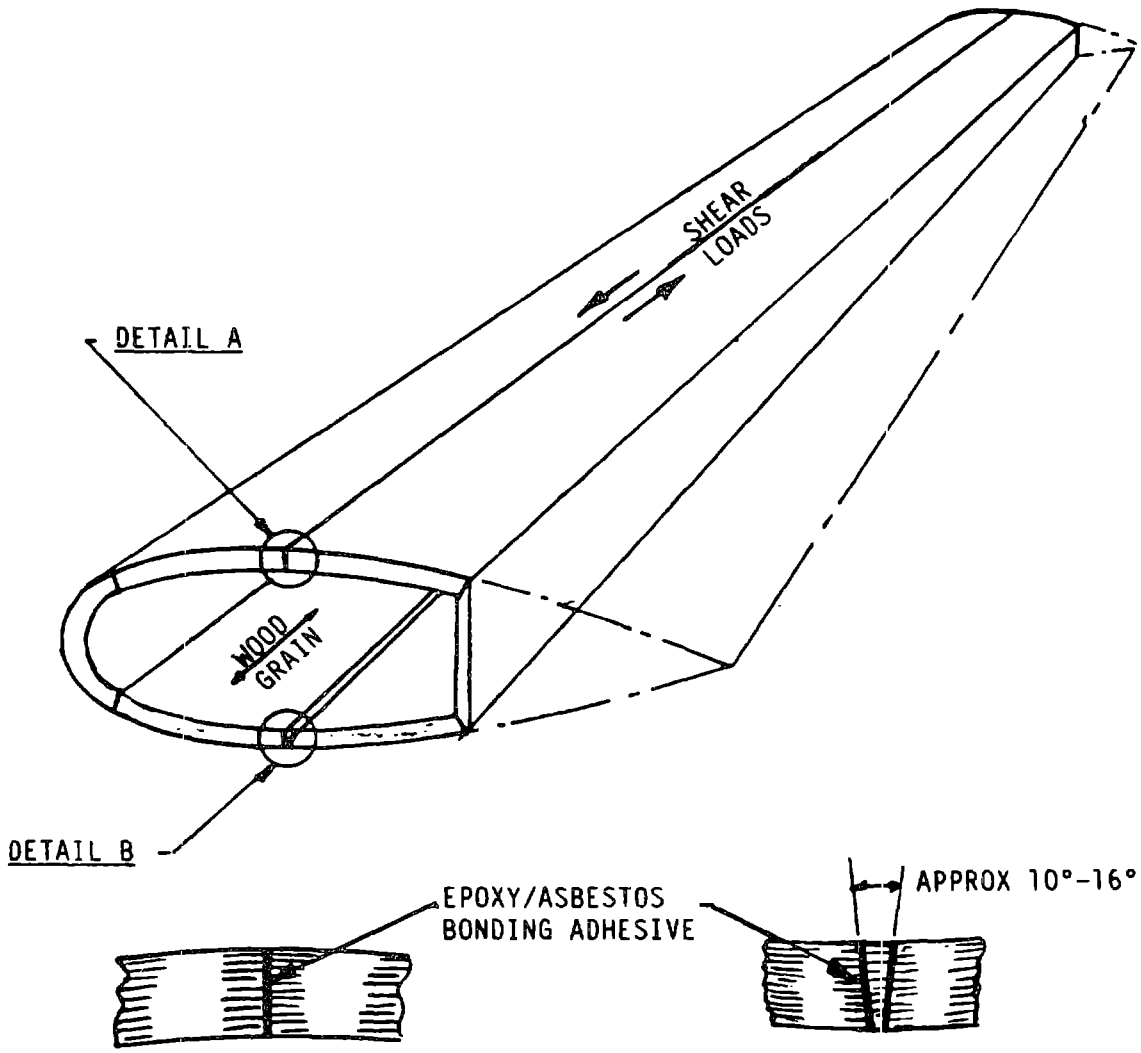

Figure 8-89 MOD-5A Rotor-Panel Assembly-Alternate Joint Concepts

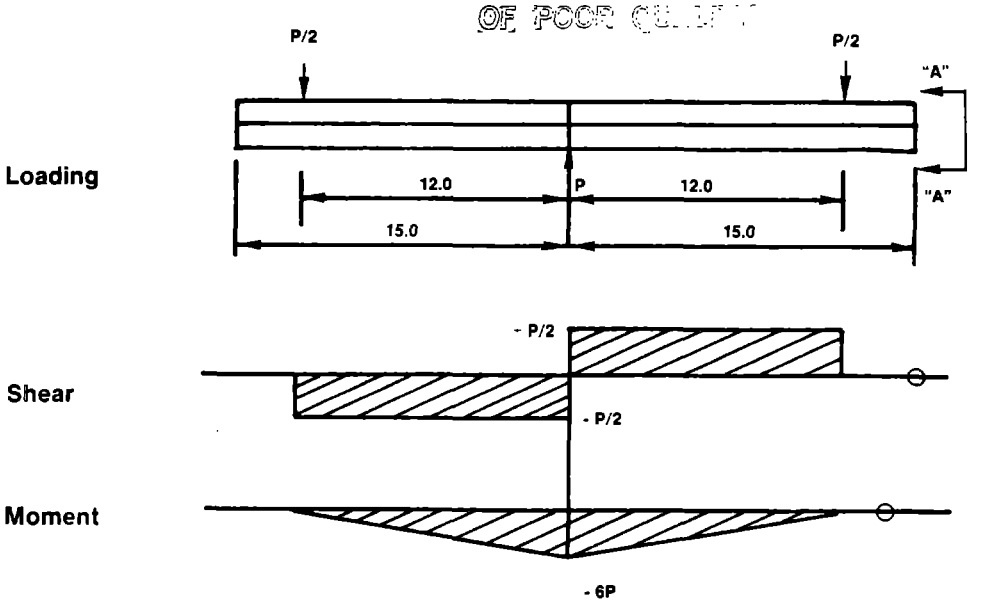

*Ref:
Marks Handbook,
Seventh Ed.,
Pg. 5-23

Longitudinal Butt Joint

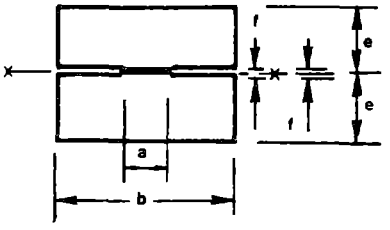

a = 1.0(nom.)
b = 4.0
e = 1.5
f = .062
$v = \frac{P}{2}$

View A-A

Bending Stress

$I_{xx} = \frac{4(3)^3}{12} = 9.0\ in^4$, C = 1.5 in

$S_b = \frac{mc}{I} = \frac{(6P)(1.5)}{9.0} = \underline{\underline{1.0P\ psi}}$

Shear Stress at Centroid*

$S_v\ (Max) = \frac{3v}{4a}\left[\frac{Be^2 - (b-a)f^2}{be^3 - (b-a)f^3}\right]$

$= \frac{3(.5P)}{4(a)}\left[\frac{(4)(1.5)^2 - (3)(.062)^2}{(4)(1.5)^3 - (3)(.062)^3}\right] = \underline{\underline{\frac{.25}{a}\ psi}}$

Longitudinal Wedge Joint

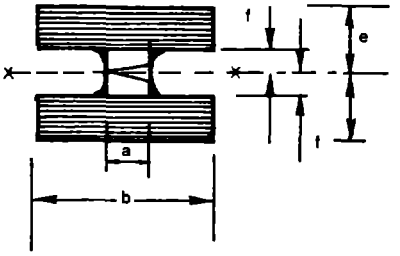

a = 1.0
b = 4.0
e = 1.5
f = 0.5
$v = \frac{P}{2}$

View A-A

Bending Stress

$I_{xx} = \frac{4(3)^3}{12} - \frac{3(1)^3}{12} = 8.75\ in^4$, C = 1.5 in

$S_b = \frac{mc}{I} = \frac{(6P)(1.5)}{8.75} = \underline{\underline{1.025P\ psi}}$

Shear Stress at Centroid*

$S_v\ (Max) = \frac{3v}{4a}\left[\frac{Be^2 - (b-a)f^2}{be^3 - (b-a)f^3}\right]$

$= \frac{3(.5P)}{4(a)}\left[\frac{(4)(1.5)^2 - (3)(.5)^2}{(4)(1.5)^3 - (3)(.5)^3}\right] = \underline{\underline{\frac{.236\ P}{a}\ psi}}$

Figure 8-90 Three-Point Bending Test Specimen Geometry, Loads, and Stresses

simulate snear loading on the longitudinal bonded joint in the web. The figure also relates the calculated beam bending stress and joint shear stress to the beam loading. Figure 8-91 shows the MTS Model 308.01 four-column test machine with the loading frame and a test specimen. This machine had a load capacity of 20,000 lb. The specimen fatigue loading was imposed using stroke control with a sinusoidal loading profile. Load readings were set at the beginning of each test and verified hourly.

Sixty-one butt joint specimens and 24 wedge joint specimens were tested. Table 8-77 describes the test conditions of each of the 85 specimens. Static tests at high and low temperatures were conducted on butt joint samples, with and without defects. Three types of defects, shown in Figure 8-92, were evaluated in the butt joint static test specimens. Square nylon inserts were the only type of defect used in the fatigue tests and in the wedge joint tests. Figure 8-93 describes the layout of butt joint specimens on a typical billet. Each of the four butt joint billets was 4 by 25 by 100 in. and yielded 12 strips, 1.5 by 4 by 96 in. Figure 8-94 shows how each of these 48 strips were cut into three lengths. They were fabricated into the test configuration using asbestos-filled West System® thixotropic epoxy, and coated with unfilled epoxy to retard moisture variation. Wedge joint specimens were made from four billets; three billets augmented with glass fiber yielded 15 caps each. The fourth billet contained a section without glass fiber augmentation, which was used to manufacture the webs. These webs were made of wood veneer and oriented 90° to the flange veneer. They were cut to provide wedge included angles of 16°. The ability to properly locate the wedges was of concern. Poor quality placement was investigated by two wedge positions. The wedges were bonded with asbestos-filled West System® thixotropic epoxy. The centered wedge samples had a 0.12 in. thick bond gap and the shifted wedges had gaps of 0.24 and 0.0 in. The wedge joint samples are shown in Figures 8-95 and 8-96.

8.2.2.4 Test Results

A 5 minute load ramp was used in all static tests using stroke control. Failure generally occurred after approximately one minute. Nineteen specimens were environmentally conditioned in temperatures of -40°F, 70°F, 100°F, and 160°F. All specimens except those at 160°F were tested immediately after they were removed from the environmental chamber.

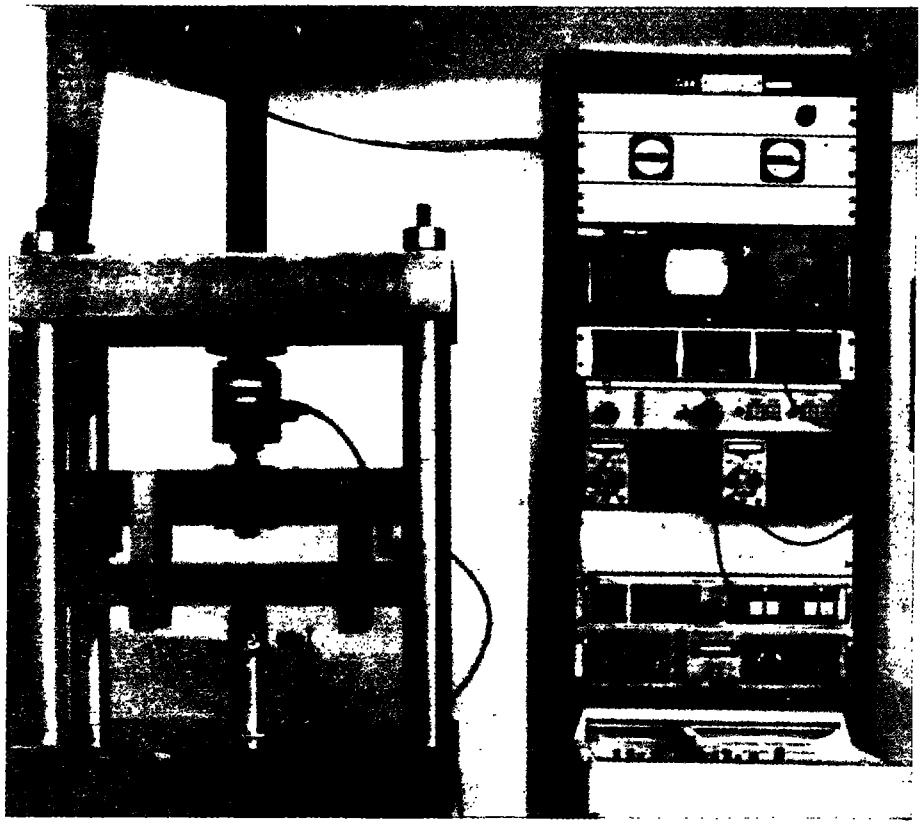

Figure 8-91 MTS Test System IIT Research Institute

Table 8-77 Three Point Bending Test Plan
Longitudinal Bonded Joints

Type Joint	Defect Type	No. of Specimens	Type Test	Temp °F
Butt Joint	None	6	Static Ramp	70
Butt Joint	None	5	Static Ramp	100
Butt Joint	None	4	Static Ramp	160/100(1)
Butt Joint	None	4	Static Ramp	-40
Butt Joint	#1	5	Static Ramp	70
Butt Joint	#2	5	Static Ramp	70
Butt Joint	#3	5	Static Ramp	70
	TOTAL	34		
Butt Joint	None	2	Static Ramp	70
Butt Joint	None	19	Fatigue, R=0.1	70
Butt Joint	#2	6	Fatigue, R=0.1	70
	TOTAL	27		
Centered Wedge	None	2	Static Ramp	70
Shifted Wedge	None	2	Static Ramp	70
Wedge With Defect	#2	2	Static Ramp	70
	TOTAL	6		
Centered Wedge	None	6	Fatigue, R=0.1	70
Shifted Wedge	None	6	Fatigue, R=0.1	70
Wedge With Defect	#2	6	Fatigue, R=0.1	70
	TOTAL	18		

NOTES

1. Specimens were conditioned at 160°F for one hour, then allowed to cool to 100°F before testing, in order to simulate solar heating of a stationary blade, followed by rotation at a moderately elevated temperature.

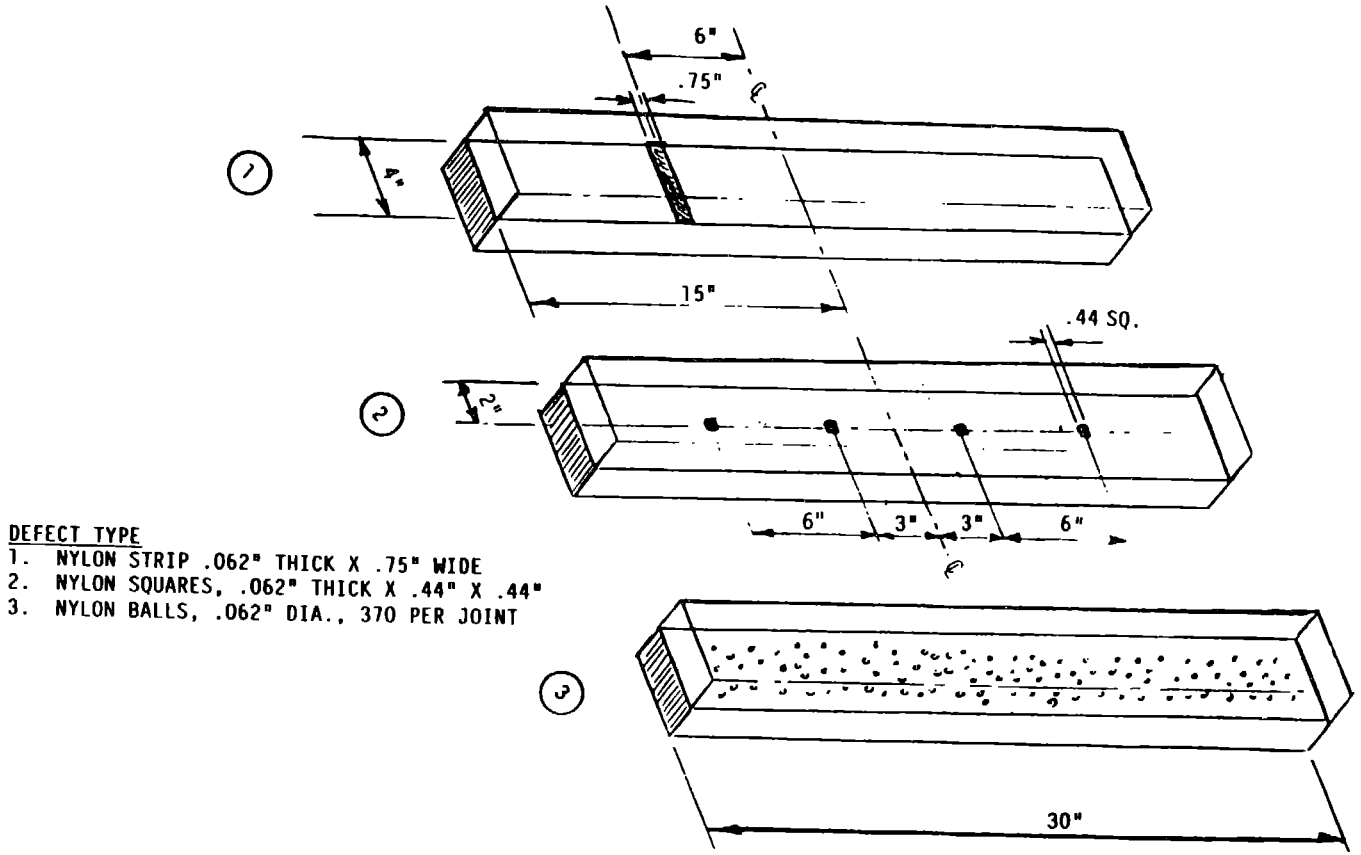

Figure 8-92 Longitudinal Butt Joints Simulated Defects

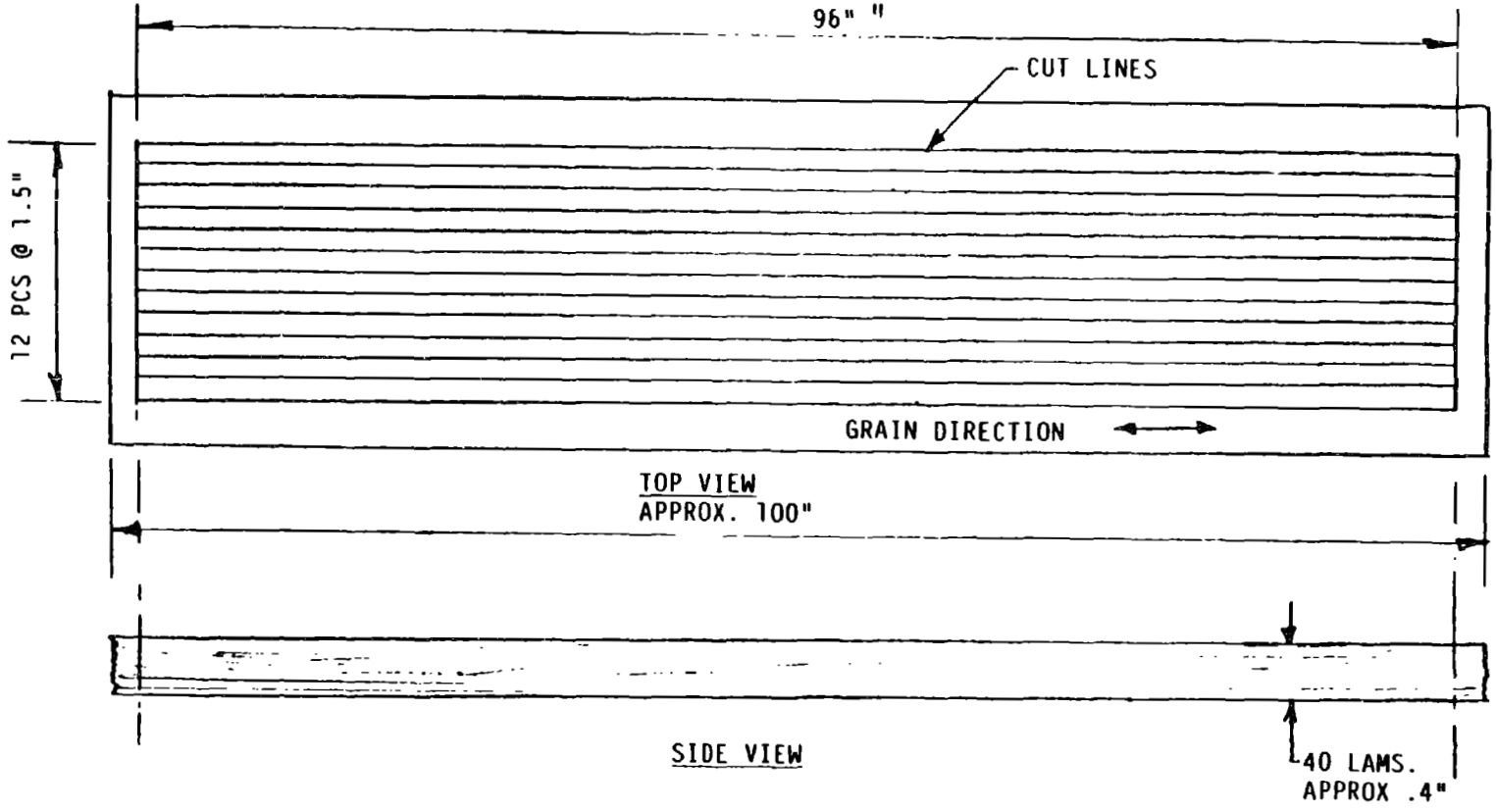

MATERIALS:
DOUGLAS FIR VENEER, 0.1" THICK, BLADE GRADE 2, GMS-001.
WEST SYSTEM 105 EPXOY RESIN/206 HARDENER VACUUM LAMINATED

Figure 8-93 Billet Fabrication, Longitudinal Butt Joint Test Specimens

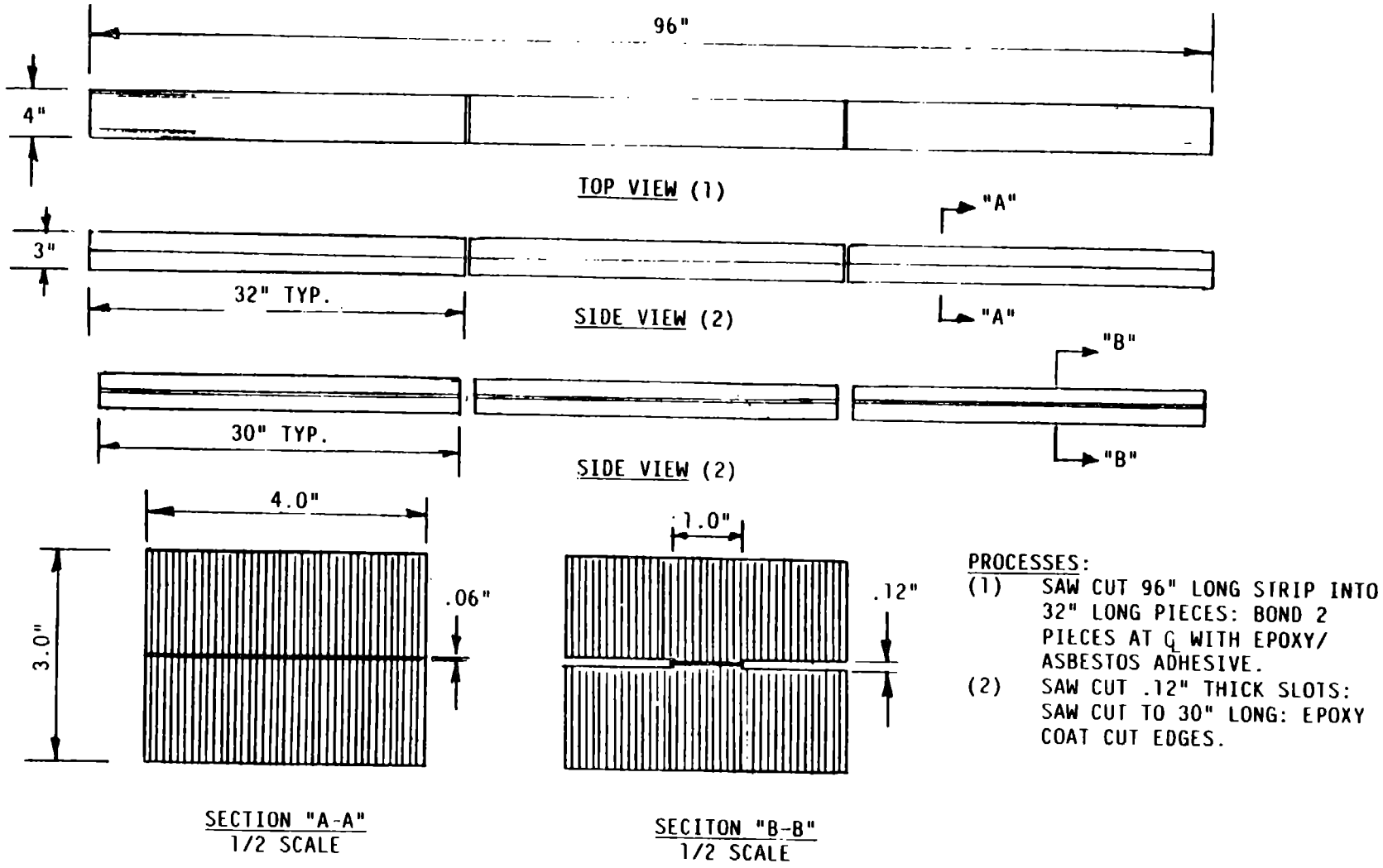

Figure 8-94 Fabrication of Longitudinal Butt Joint Test Specimens

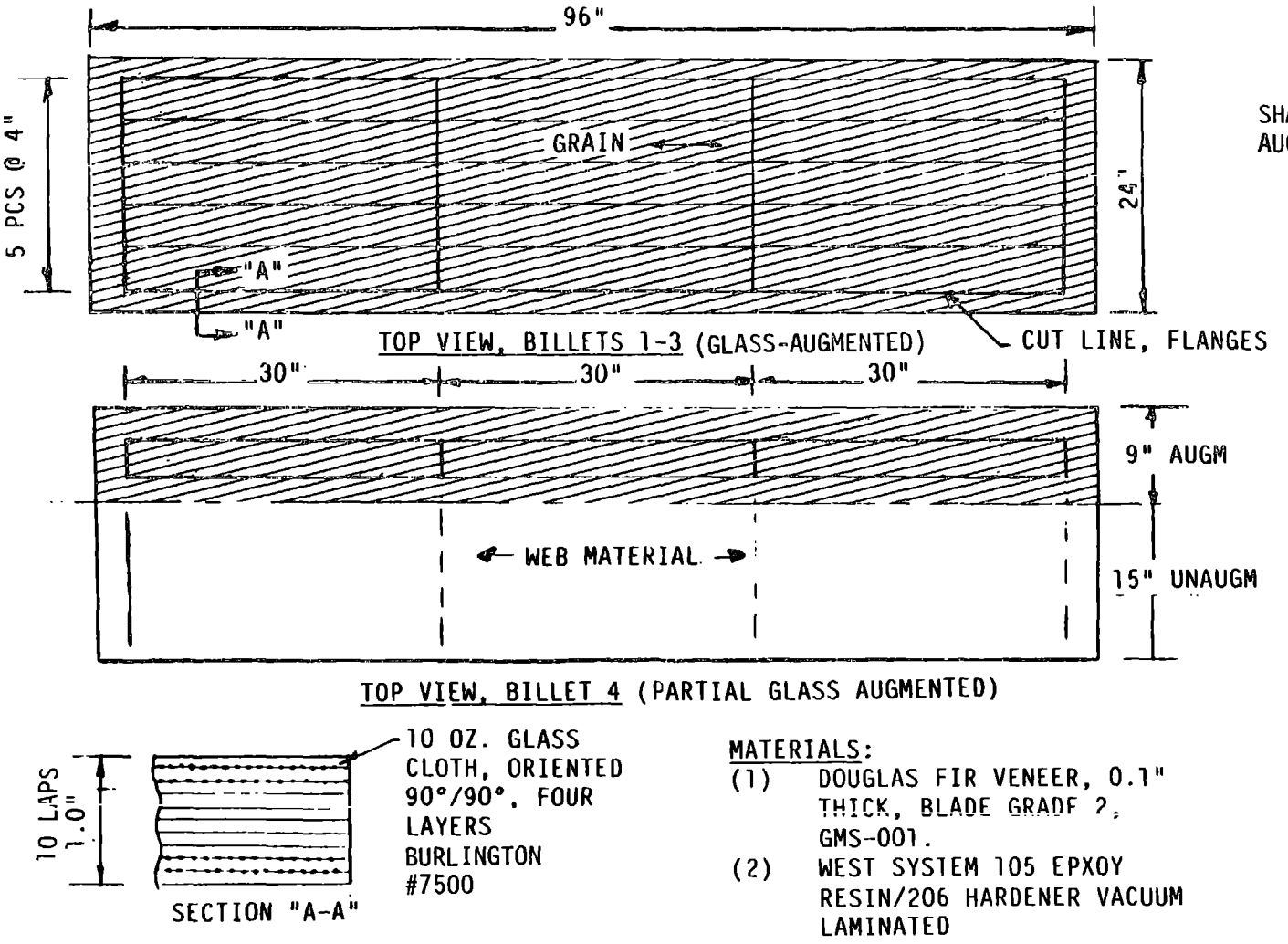

Figure 8-95 Billet Fabrication - Longitudinal Wedge Joint Test Specimens

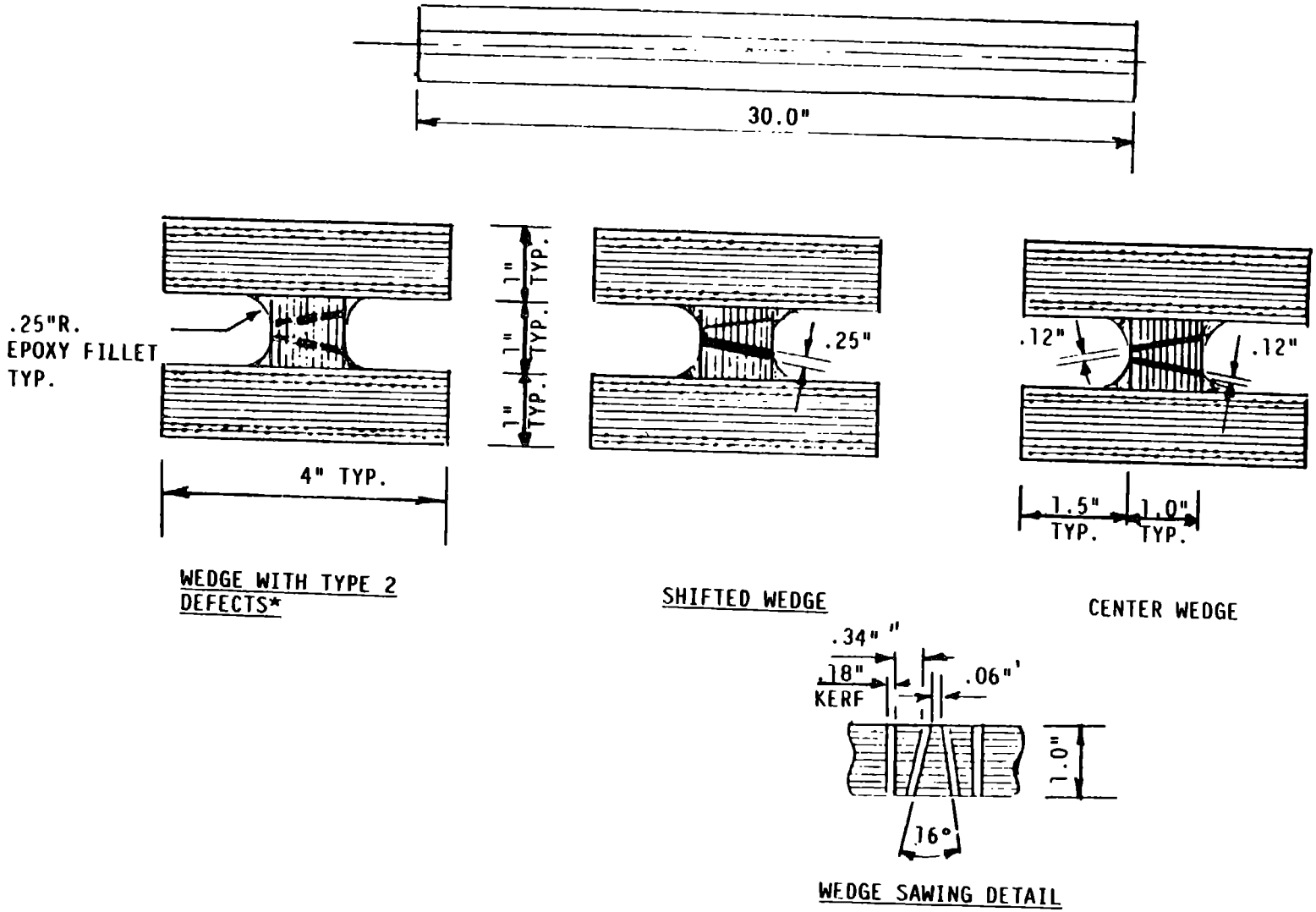

Figure 8-96 Specimen Fabrication - Longitudinal Wedge Joint Test

Those conditioned at 160°F were allowed to cool to 100°F before testing, to simulate the temperature profile of a rotor that is exposed to solar heat while at rest, then stressed at moderately high temperatures while rotating. Anotner 15 samples, tested at 70°F, contained simulated defects in the bond.

For each static ramp test, load vs. time was plotted. A typical plot is shown in Figure 8-97. According to definition, failure took place at the first distinct knee in the curve, when the sample experienced irrevocable damage, even though the load might increase before dropping to zero.

Table 8-78 contains data from the static ramp tests. The beam load at failure was used to calculate the shear stress in the glue line, and the maximum bending stress in the beam outer fibers. The method for calculating stresses is snown in Figure 8-90.

The shear stress was adjusted to a level expected for a moisture content of 12%, according to the practice of the wood industry. The calculation for this adjustment is shown in Table 8-79.

8.2.2.5 Fatigue Load Tests

Twenty-five test specimens with longitudinal butt joints were fatigue-tested in three-point bending. All the specimens were tested at approximately 70°F, 50% relative humidity and cycled at a rate of 5 Hz. The ratio of the minimum to the maximum load used for all tests was 0.1. Six of the 27 specimens contained nylon squares in the bond joint, which is defect type 2, shown in Figure 8-92.

A consistent definition of failure for the fatigue tests was used. The first five specimens were closely monitored at half-hour intervals, to measure crack initiation and propagation, and the delta stroke as described in Figure 8-98. Based on these observations, it appeared that specimens maintained structural integrity in beam bending until joint cracks reached a length of approximately 12 in. Then the specimen behaved like two unconnected beams. The results are shown in Table 8-80.

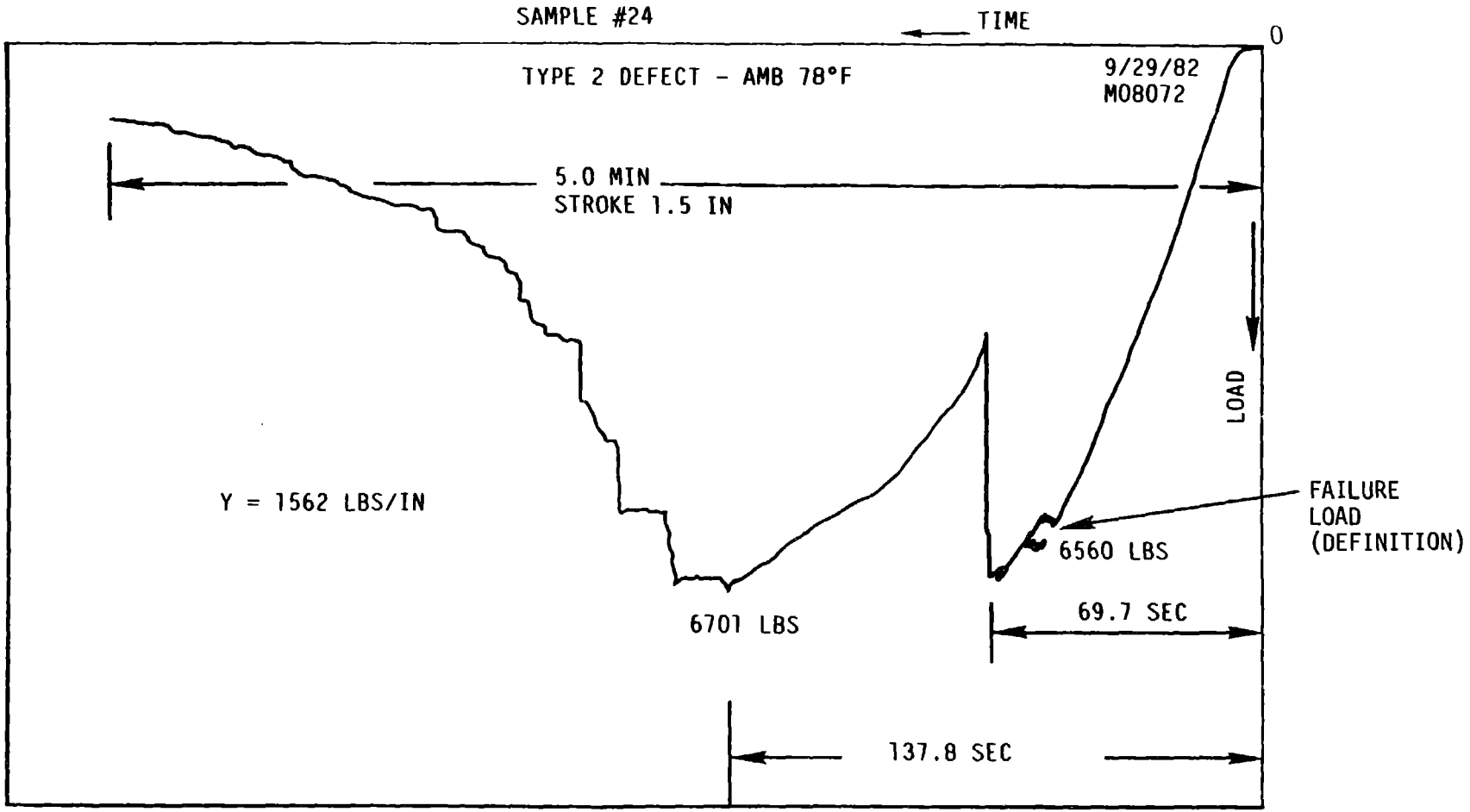

Figure 8-97 Typical Load vs Time Trace Static Ramp Tests

Table 8-78 Three-Point Bending Static Load Tests - Longitudinal Butt Joints

Test Program: MOD-5A
Material: Douglas Fir/Epoxy Laminae, Epoxy/Asbestos Adhesive Joint, .06 in. thick
Test Environment: 70°F, 50% Relative Humidity. Some Specimens Thermally Conditioned As Noted

Sample No	Defect Type (1)	Cond Temp (°F) (2)	Avg. Joint Dim (in) Width	Thick	LMC (%)	Failure Load (lbs) (3)	Max Bending Stress (psi) (4)	Max Shear Stress (psi) (4)	Max Shear (5) Stress @ 12% M.C.	Time To Failure (sec)	Type Failure Wood	Bond
1	None	70	.95	.059	6.0[E]	5,469	5,469	1,439	1,315	155.0	x	
2	"	"	Data not available, test malfunction									
3	"	"	1.00[E]	.042	6.0[E]	5,174	5,174	1,293	1,181	53.6	N.A.	
4	"	"	.98	.047	6.0[E]	4,500	4,500	1,148	1,049	39.8	x	
5	"	"	.85	.055	6.0[E]	4,484	4,484	1,319	1,205	39.9	x	
6	"	"	.95	.065	6.0[E]	6,406	6,406	1,686	1,541	54.2	x	
26	"	"	1.00[E]	.052	6.0[E]	6,530	6,530	1,632	1,491	65.6	N.A.	
Avg	"	"	.96	.053	6.0[E]	5,427	5,427	1,420	1,297	68.0		
7	"	100	1.03	.042	6.0[E]	5,469	5,469	1,327	1,212	57.5	x	
8	"	"	1.00	.048	6.0[E]	5,078	5,078	1,269	1,160	46.7		x
9	"	"	.95	.038	6.0[E]	5,781	5,781	1,521	1,390	49.1	x	
10	"	"	.95	.042	6.0[E]	5,937	5,937	1,562	1,427	61.0	x	
11	"	"	1.03	.045	6.0[E]	6,250	6,250	1,517	1,386	66.0	x	
Avg	"	"	.99	.043	6.0[E]	5,703	5,703	1,439	1,315	56.1		
17	"	160/100	.97	.050	6.1	6,797	6,797	1,752	1,604	76.0	x	
18	"	"	.94	.043	6.1	6,718	6,718	1,787	1,637	77.5	x	
19	"	"	.97	.043	6.1	6,375	6,375	1,643	1,505	66.0	x	
20	"	"	.98	.032	5.8	6,797	6,797	1,734	1,577	68.4	x	
Avg	"	"	.96	.042	6.0	6,672	6,672	1,729	1,581	72.0		

Table 8-78 (Continued) Three-Point Bending Static Load Tests - Longitudinal Butt Joints

Test Program: MOD-5A
Material: Douglas Fir/Epoxy Laminae, Epoxy/Asbestos Adhesive Joint, .06 in. thick
Test Environment: 70°F, 50% Relative Humidity. Some Specimens Thermally Conditioned As Noted

Sample No	Defect Type (1)	Cond Temp (°F) (2)	Avg. Joint Dim (in) Width	Thick	LMC (%)	Failure Load (lbs) (3)	Max Bending Stress (psi) (4)	Max Shear Stress (psi) (4)	Max Shear (5) Stress @ 12% M.C.	Time To Failure (sec)	Type Failure Wood	Bond
32	None	-40	.97	.052	5.6	6,748	6,748	1,739	1,574	55.7	x	
33	"	"	.94	.057	6.0	6,248	6,248	1,662	1,519	49.9	x	
34	"	"	.97	.040	5.8	6,795	6,795	1,751	1,592	59.1	x	
35	"	"	.94	.038	5.8	6,719	6,719	1,787	1,625	68.9	x	
Avg	"	"	.95	.047	5.8	6,627	6,627	1,735	1,577	58.4		
12	1	---	.97	.060	5.8	6,172	6,172	1,590	1,446	56.1	x	
13	1	---	1.00[E]	.055	6.0[E]	6,797	6,797	1,699	1,552	64.3	N.A.	
14	1	---	1.06	.058	5.9	6,875	6,875	1,621	1,478	59.4	x	
15	1	---	.84	.060	5.6	7,344	7,344	2,186	1,979	62.7	x	
16	1	---	1.09	.062	5.8	7,500	7,500	1,720	1,564	64.3	x	
Avg	1	---	.99	.059	5.8	6,938	6,938	1,763	1,604	61.4		
21	2	---	1.06	.060	6.0	7,295	7,295	1,720	1,572	61.1	x	
22	2	---	1.09	.057	6.2	6,139	6,139	1,408	1,293	57.0	x	
23	2	---	1.06	.062	5.5	7,341	7,341	1,731	1,563	72.2	x	
24	2	---	.95	.063	5.8	6,560	6,560	1,726	1,570	69.7	x	
25	2	---	1.15	.062	6.1	7,497	7,497	1,630	1,493	78.7	x	
Avg	2	---	1.06	.061	5.9	6,966	6,966	1,643	1,498	67.7		

Table 8-78 (Continued) Three-Point Bending Static Load Tests - Longitudinal Butt Joints

Test Program: MOD-5A
Material: Douglas Fir/Epoxy Laminae, Epoxy/Asbestos Adhesive Joint, .06 in. thick
Test Environment: 70°F, 50% Relative Humidity. Some Specimens Thermally Conditioned As Noted

Sample No	Defect Type (1)	Cond Temp (°F) (2)	Avg. Joint Dim (In) Width	Thick	EMC (%)	Failure Load (lbs) (3)	Max Bending Stress (psi) (4)	Max Shear Stress (psi) (4)	Max Shear (5) Stress @ 12% M.C.	Time To Failure (sec)	Type Failure Wood	Bond
27	3	-	1.09	.035	5.9	7,732	7,732	1,773	1,616	79.1	x	
28	3	-	1.09	.032	6.0	6,717	6,717	1,540	1,407	72.5	x	
29	3	-	.97	.053	6.0E	6,404	6,404	1,650	1,508	59.3	x	
30	3	-	.97	.030	5.8	7,981	7,981	2,057	1,871	79.1	x	
31	3	-	.97	.037	5.9	7,919	7,919	2,041	1,860	75.8	x	
Avg	3	-	1.02	.037	5.9	7,350	7,350	1,812	1,652	73.2		
F1		-	.96	.062	6.4	6,795	6,795	1,769	1,632	73.3	x	
F2	-	-	1.01	.053	6.2	6,872	6,872	1,701	1,562	67.0	x	
Avg		-	.99	.057	6.3	6,833	6,833	1,735	1,597	70.1		

NOTES:

(1) See Figure 8.2.2-4 for description of defects

(2) Some specimens were conditioned for one hour at the temperature shown, then immediately tested under ambient conditions

(3) Failure load occurs at first "knee" in load/time trace

(4) See Figure 8.2.2-2 for method of calculating stresses

(5) See Table 8.2.2-6 for method of adjusting properties to 12% wood moisture constant level

(6) Test run by mistake under load control

E Estimated value

N/A Specimen not available for examination

Table 8-79 Adjustment of Wood Laminae Mechanical Properties for Moisture Content

From Reference, Pages 4-32 to 4-33:

$$P_M = P_{12} \times \left(\frac{P_{12}}{P_g}\right)^{-\left(\frac{M-12}{M_p-12}\right)}$$

Where:

M = moisture content (%) of wood
P_M = property at wood moisture content M.
P_{12} = property at 12% wood moisture content
P_g = property for all wood moisture contents > M_p
M_p = wood moisture content at which changes in property caused by drying are first observed. (for Douglas fir, M_p = 24%)

$\frac{P_{12}}{P_g}$ = constant K:

K_T = 1.21 (tension)
K_C = 1.92 (compression)
K_S = 1.26 (shear)

If:

M_L = measured moisture content of Douglas fir laminae epoxy
M = wood moisture content = 1.22 x M_L
P_T = physical property as tested

Then:

$$\left(\frac{1.22\ M_L - 12}{12}\right)$$

$P_{12} = P_T \times (K)$

Reference: "Wood Handbook: Wood As An Engineering Material," Agricultural Handbook No. 72, by Forest Products Laboratory, Forest Service, U.S. Department of Agriculture, Madison, Wisconsin

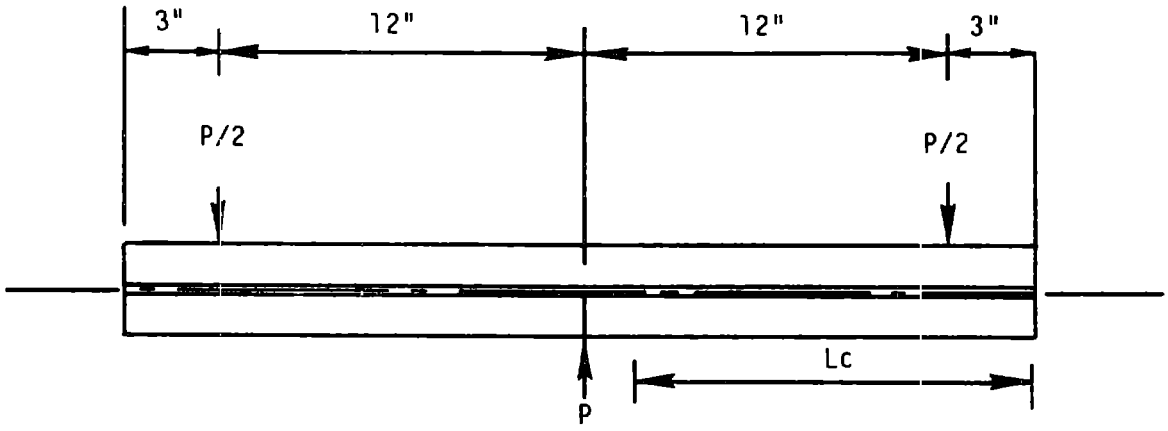

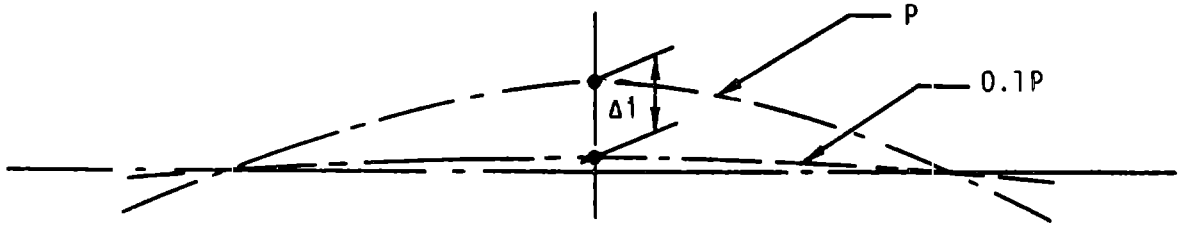

INITIAL DEFLECTIONS

Δi = DELTA STROKE

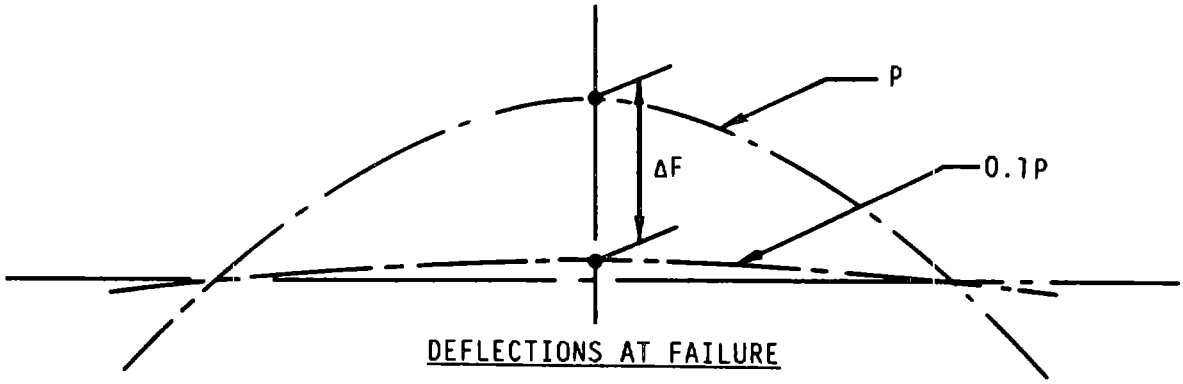

DEFLECTIONS AT FAILURE

AT FAILURE: $\Delta F = 2\Delta i$
CRACK LENGTH $L_C \geq 12.0$ IN.

Figure 8-98 Fatigue Failure Criteria - Three Point Bending Tests (R = 0.1)

Table 8-80 Three-Point Bending Fatigue Tests - Longitudinal Butt Joints

Test Program: MOD-5A
Material: Douglas Fir/Epoxy Laminae, Epoxy/Asbestos Adhesive Joint, .06 in. thick
Test Environment: 70°F, 50% Relative Humidity. Stress Ratio: R = 0.1 Cycle Rate: 5 Hz

Sample No	Defect Type (1)	Avg. Joint Dim (in)		LMC (%)	Failure Load (lbs)		Max Bending Stress (psi) (3)	Max Shear Stress (psi) (3)	Max Shear Stress @ 12% M.C. (4)	Cycles To Failure	Primary Type Failure	
		Width	Thick		Min	Max (2)					Wood	Bond
F3	None	1.00	.045	6.3	500	5,000	5,000	1,250	1,150	134,613		N/A
F4	"	1.05	.050	6.3	500	5,000	5,000	1,190	1,095	302,960		N/A
F5	"	1.03	.056	6.1	450	4,500	4,500	1,092	1,000	191,482		x
F6	"	1.01	.054	6.0	400	4,000	4,000	990	905	513,255		x
F7	"	.95	N/A	5.5[E]	350	3,500	3,500	921	832	301,843		N/A
F8	"	1.01	.064	5.5	350	3,500	3,500	866	782	8,564,236		x
F9	"	1.02	.060	5.7	400	4,000	4,000	980	889	160,000	x	
F10	"	.98	.045	5.7	350	3,500	3,500	893	810	173,192	x	
F11	"	1.00	.062	5.5[E]	350	3,500	3,500	875	790	2,126,614		N/A
F12	"	1.03	.062	5.5[E]	320	3,200	3,200	776	701	10×10^6		N/A
F13	"	.98	.055	5.3	350	3,500	3,500	893	803	8,514,000		N/A
F14	"	.99	.060	5.5	375	3,750	3,750	947	855	5,725,800		N/A
F15	"	1.00	.056	4.7	375	3,750	3,750	937	830	2,827,800		N/A
F16	"	.99	.060	4.6	400	4,000	4,000	1,010	893	$> 10 \times 10^6$		N/A
F17	"	1.03	.065	5.0	400	4,000	4,000	971	867	3,655,000		N/A
F18	"	.96	.060	6.1	607	6,071	6,071	1,581	1,448	28,000	x	
F19	"	1.05	.030	6.2	643	6,428	6,428	1,530	1,405	800	x	
F20	"	.96	.062	6.3	425	4,250	4,250	1,107	1,019	693,000	x	
F21	"	.99	.060	6.9	450	4,500	4,500	1,136	1,060	63,000	x	

Table 8-80 (Continued) Three-Point Bending Fatigue Tests - Longitudinal Butt Joints

Test Program: MOD-5A
Material: Douglas Fir/Epoxy Laminae, Epoxy/Asbestos Adhesive Joint, .06 in. thick
Test Environment: 70°F, 50% Relative Humidity. Stress Ratio: R = 0.1 Cycle Rate: 5 Hz

Sample No	Defect Type (1)	Avg. Joint Dim (in) Width	Thick	LMC (%)	Failure Load (lbs) Min	Max (2)	Max Bending Stress (psi) (3)	Max Shear Stress (psi) (3)	Max Shear Stress @ 12% M.C. (4)	Cycles To Failure	Primary Type Failure Wood	Bond
D2-01	2	1.02	.075	6.9	450	4,500	4,500	1,103	1,029	65,700	x	
D2-02	2	1.01	.070	6.8	400	4,000	4,000	1,114	1,037	586,312	x	
D2-03	2	1.01	.070	7.0	400	4,000	4,000	990	926	279,900	x	
D2-04	2	0.99	.070	6.8	375	3,750	3,750	947	882	1,301,400	x	
D2-05	2	0.99	.063	6.8	375	3,750	3,750	947	882	405,500	x	
D2-06	2	1.01	.076	7.1	350	3,500	3,500	866	812	3,104,800	x	

NOTES:

1. See Figure 8.2.2-4 for description of defects
2. Failure Load is that load at which the difference between maximum and minimum stroke equals 2x the initial stroke difference (See Figure 8.2.2-10)
3. See Figure 8.2.2-2 for method of calculating stresses
4. See Table 8.2.2-6 for method of adjusting properties to 12% wood moisture content level
5. N/A - Test specimens not available for examination

It also appeared that there was a correlation between crack length and delta stroke. When a delta stroke reached twice its initial value, it was accompanied by a failure-inducing crack. All remaining fatigue tests were terminated when the delta stroke reached twice its initial value.

Table 8-80 contains data from the fatigue tests. The beam load at failure was used to calculate the shear stress at the glue line and the maximum bending stress in the beam outer fibers, as shown in Figure 8-90. The shear stress was adjusted to a level expected for a moisture content of 12%, per Table 8-79.

Figure 8-99 is an S-N diagram for the data in Table 8-80. A trend line was fitted to all the data.

Longitudinal butt-jointed static test specimens typically displayed shear failures in the laminated wood near the bond line. The specimen joints contained all the simulated defects shown in Figure 8-92. In all cases, the shear failure extended from the bond line, well into the wood veneer. The shear failure appeared randomly on either the compression side or the tension side of the beam bending axis.

The wood shear failure was usually accompanied by a longitudinal crack, running to the surface of the test specimen. The crack usually ran through the wood rather than in the glue, and formed an approximate semi-circle over the bond zone. This pattern can be accounted for if the cracking was caused by cross-grain tension stresses in the veneer. Such stresses would be induced if the beam loads were applied closer to one edge of the specimen rather than at the centerline, which be caused by stiffness variations across the specimen's width.

Failures in fatigue test specimens were not readily visible after they were removed from the load frame, even though longitudinal cracks in the joints were seen during testing. The specimens were split after testing, to analyze the failures.

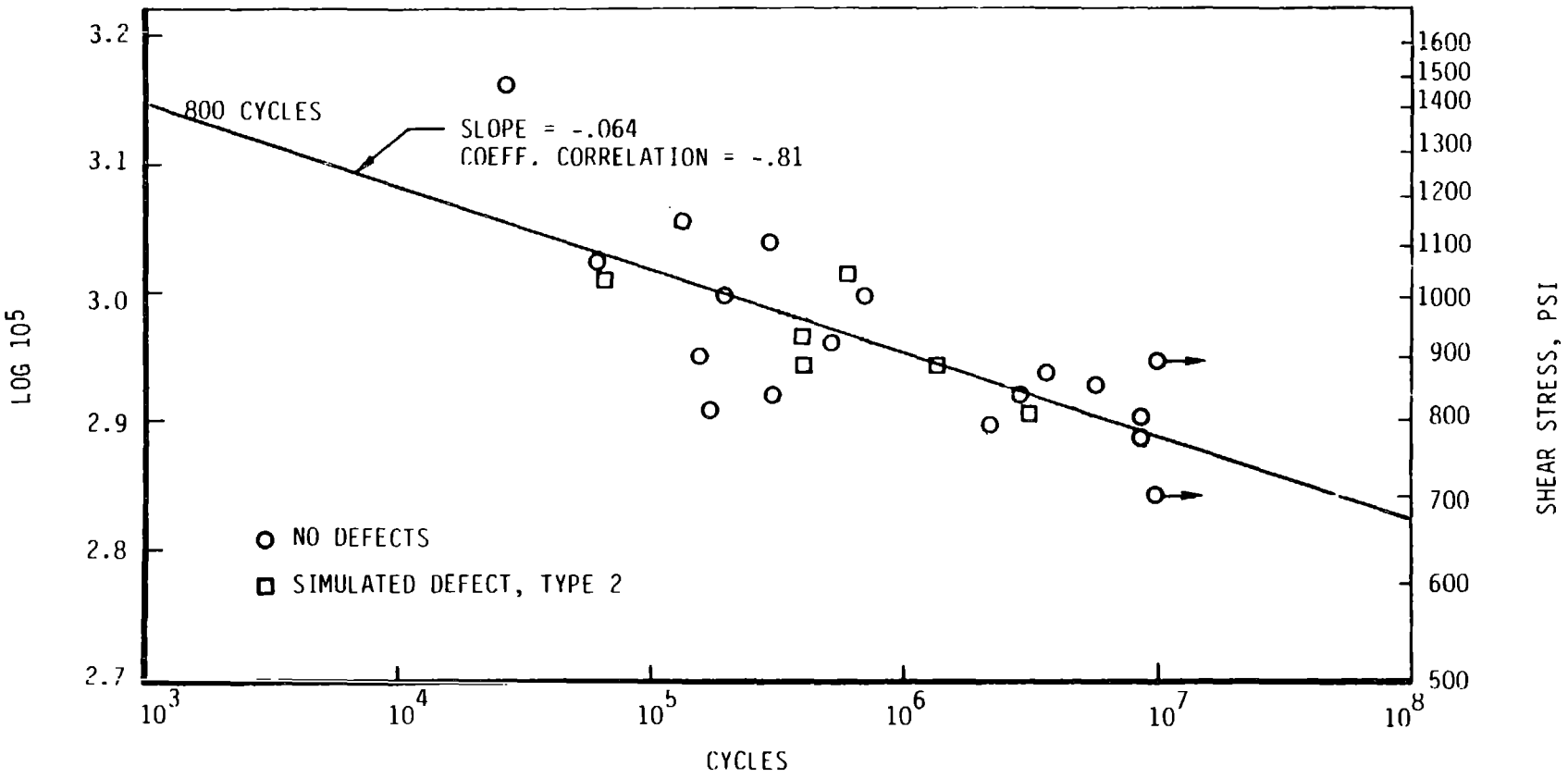

Figure 8-99 S-N Diagram, Longitudinal Butt Joint Shear Stress, Three-Point Bending Tests, Laminated Douglas Fir/Epoxy Room Temperature, R = 0.1, 12% Moisture Content

Most of the failures were in wood shear, adjacent to the butt bond line. One of these specimens displayed a longitudinal crack running to the outer surface of the wood cap along a bond line.

Specimens were split open after testing, to check the condition of the joint bond. In almost all areas, good bonding was achieved, as the predominance of wood shear failures indicated.

Six test specimens with longitudinal wedge joints were tested in three-point bending using an ASTM 5-minute standard ramp to failure, under stroke control. All testing was done at approximately 70°F, 50% relative humidity. Failure was defined as occurring at the first knee in the load/time curve.

Two specimens had centered wedges, two had shifted wedges, and two contained simulated bond line defects. Data from these tests is listed in Table 8-81. The beam load at failure was used to calculate shear and outer fiber bending stresses, as defined in Figure 8-90. Shear stresses were adjusted for 12% moisture content, as calculated in Table 8-79.

Seventeen specimens with longitudinal wedge joints were fatigue-tested in three-point bending at a minimum to maximum stress ratio of R = 0.1. The eighteenth sample was lost because of a malfunction. As in earlier tests, a cycle rate of 5 Hz was used, and tests were conducted at 70°F, 50% relative humidity. Six specimens had centered wedges, six had shifted wedges, and six had the simulated defect in the bond joint shown as type 2 in Figure 8-92.

As in fatigue tests of the butt joint specimens, the criterion for failure was the delta stroke reaching twice its initital value. Data from these fatigue tests is given in Table 8-82. Again, the load at failure was used to calculate stress levels, which were then adjusted for 12% moisture content.

Figure 8-100 is a S-N diagram for the data in Table 8-82. A trend line was fitted to the data, although a low coefficient of correlation was calculated.

Table 8-81 Three-Point Bending Static Load Tests - Longitudinal Wedge Joints

Test Program: MOD-5A
Material: Douglas Fir/Epoxy Laminae, Epoxy/Asbestos Adhesive Joint, Nominal .06 in. thick
Test Environment: 70°F, 50% Relative Humidity

Sample No	Wedge Type (1)	LMC (%)	Failure (2) Load (lbs)	Max (2) Bending Stress (psi)	Max (3) Shear Stress (psi)	Max (4) Shear Stress @ 12% M.C.	Time To Failure (sec)	Primary Type Failure	
								Wood	Bond
CW1	Centered Wedge	5.6	6,543	6,732	1,544	1,398	119.6	Joint	--
CW2	Centered Wedge	5.8	6,144	6,320	1,450	1,391	101.4	Fillet	--
Avg	Centered Wedge	5.7	6,343	6,526	1,497	1,394	110.5		
SW1	Shifted Wedge	6.0	5,905	6,076	1,394	1,273	127.8	Fillet	--
SW2	Shifted Wedge	6.4	5,666	5,830	1,337	1,233	104.0	Joint	--
Avg	Shifted Wedge	6.2	5,785	5,953	1,365	1,253	115.9		
DW1	Wedge with Defect 2	5.7	6,623	6,815	1,563	1,418	109.8	Fillet	-
DW2	Wedge with Defect 2	6.2	6,863	7,062	1,620	1,487	147.1	Fillet	--
Avg	Wedge with Defect 2	6.0	6,743	6,938	1,591	1,452	128.4		

NOTES:

1. See Figure 8.2.2-6 for description of wedge types
2. Failure load occurs at first "knee" in load/time trace
3. See Figure 8.2.2-2 for method of calculating stresses
4. See Table 8.2.2-6 for method of adjusting properties to 12% wood moisture content level

Table 8-82 Three-Point Bending Fatigue Tests - Longitudinal Wedge Joints

Test Program: MOD 5A
Material: Douglas Fir/Epoxy Laminae, Epoxy/Asbestos Adhesive Joint, Nominal .06 in. thick
Test Environment: 70°F, 50% Relative Humidity. Stress Ratio: R = 0.1 Cycle Rate: 5 Hz

Sample No	Wedge Type (1)	LMC (%)	Failure Load (2) (lbs) Min	Failure Load (2) (lbs) Max	Maximum Bending Stress (psi) (3)	Maximum Shear Stress (psi) (3)	Maximum (4) Shear Stress @ 12% M.C.	Cycles To Failure	Primary Type Failure Wood	Primary Type Failure Bond
CW3	Centered Wedge	6.0	425	4,250	4,373	1,003	916	32,400	Joint	--
CW4	Centered Wedge	6.1	375	3,750	3,859	885	811	3,321,000	Joint	--
CW5	Centered Wedge	6.4	325	3,250	3,344	767	707	150,300	Joint	--
CW6	Centered Wedge	6.1	325	3,250	3,344	767	703	1,370,000	Joint	--
CW7	Centered Wedge	6.8	350	3,500	3,601	826	769	1,434,600	Fillet	--
CW8	Centered Wedge	6.3	375	3,750	3,859	885	814	68,400	Joint	--
SW3	Shifted Wedge	6.0	425	4,250	4,373	1,003	917	65,000	Fillet	--
SW4	Shifted Wedge	6.0	425	4,250	4,373	1,003	917	7,000	Joint	-
SW5	Shifted Wedge	6.3	375	3,750	3,859	885	814	27,814	Joint	--
SW6	Shifted Wedge	DATA N/A DUE TO TEST MALFUNCTION								
SW7	Shifted Wedge	6.2	375	3,750	3,859	885	813	17,100		Fillet
SW8	Shifted Wedge	6.8	325	3,250	3,344	767	714	596,700	Fillet	
DW3	Wedge Defect Type 2	6.2	375	3,750	3,859	885	813	77,400	Joint	--
DW4	Wedge Defect Type 2	6.2	350	3,500	3,601	826	758	1,314,000		Fillet
DW5	Wedge Defect Type 2	6.1	375	3,750	3,859	885	811	3,884,400	Joint	
DW6	Wedge Defect Type 2	6.1	400	4,000	4,116	944	865	579,600	Joint	--
DW7	Wedge Defect Type 2	6.1	400	4,000	4,116	944	865	83,700	Joint	--
DW8	Wedge Defect Type 2	6.3	375	3,750	3,859	885	814	1,666,800	Joint	--

NOTES:
1. See Figure 8.2.2-6 for description of wedge types
2. Failure load is that load at which the difference between maximum and minimum stroke equals 2x the initial stroke difference (See Figure 8.2.2-10)
3. See Figure 8.2.2-2 for method of calculating stress
4. See Table 8.2.2 3 for method of adjusting properties to 12% wood moisture content level

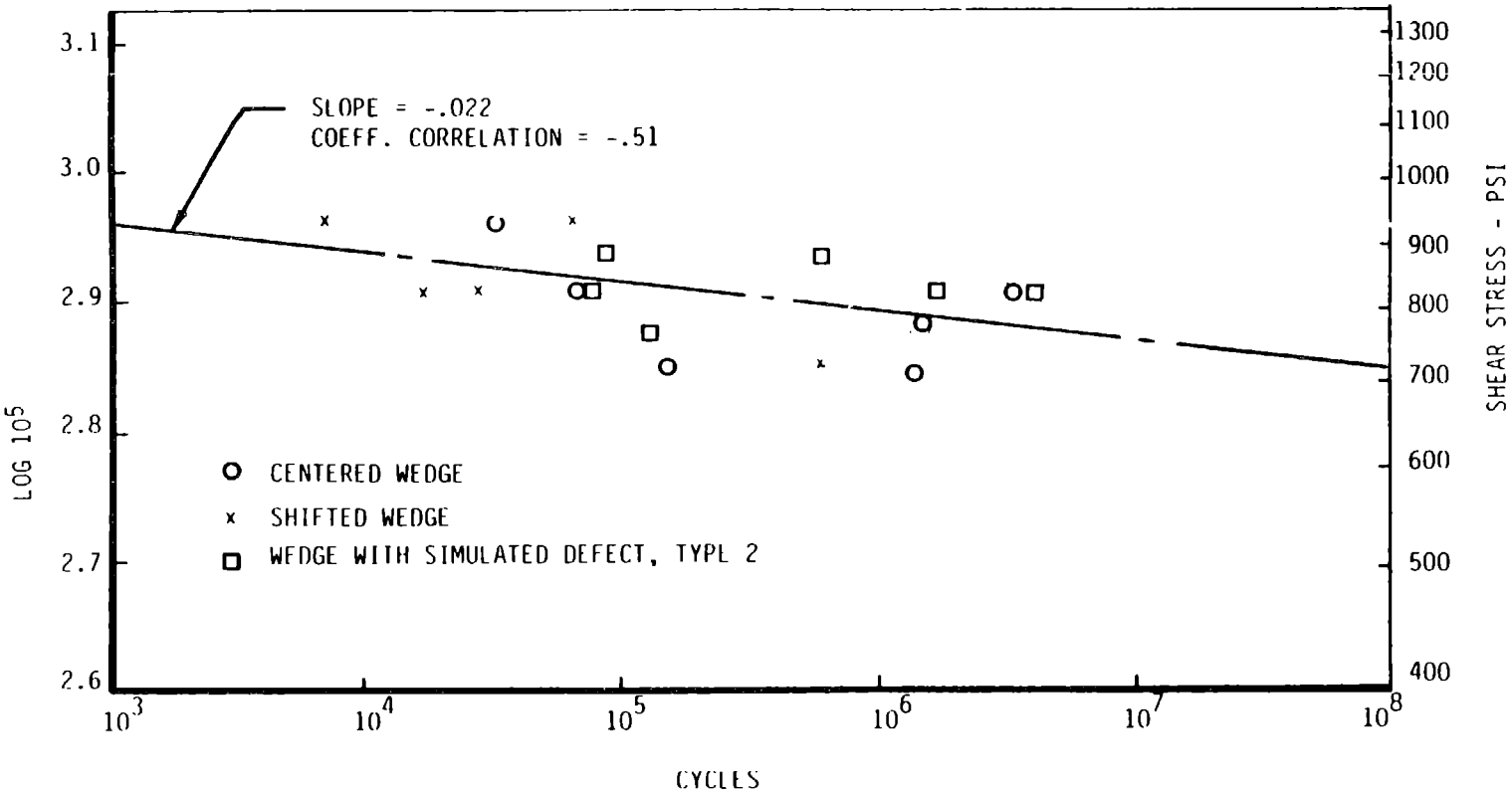

Figure 8-100 S-N Diagram, Longitudinal Wedge Joint Shear Stress, Three-Point Bending Tests, Laminated Douglas Fir/Epoxy, Room Temperature, R= 0.1, 12% M.C.

The six longitudinal wedge joint static test specimens were examined after testing. Two specimens (CW1 and SW2) had shear failure in the wood veneer adjacent to the wedge bond lines. Four specimens (CW2, SW1, DW1, and DW2) showed wood shear failure adjacent to the fillets and the bond line between the I-beam web and flange sections.

The 17 fatigue test specimens also showed these two types of failure. Twelve exhibited shear failure adjacent to the wedge bond lines. Five exhibited shear failure in the fillet area. Three of these involved failure in the wood and two involved failure in the bond line.

Static ramp tests of butt-joint specimens produced an unexpected anomaly. Joints with simulated defects had higher shear strength at room temperature than joints without such defects. From Table 8-78:

8 specimens without defects, - - - - - Avg = 1372 psi
(1, 2, 3, 4, 5, 6, 26, F1, F2)
5 specimens with Type 1 defects, - - - Avg = 1604 psi
5 specimens with Type 2 defects, - - - Avg = 1498 psi
5 specimens with Type 3 defects, - - - Avg = 1652 psi

Destructive inspections of Specimens 1, 2, 4, and 5 revealed poorly bonded areas in the glue joints. The poor bonds could have contributed to the low average static shear strength of the specimens without defects.

The test data does indicate that defect type 2 reduces joint static strength more than the other types.

The test data indicates that conditioning the specimens at a temperature of 100°F reduces joint shear strength slightly. However, conditioning at 160°F before testing at 100°F, may enhance the curing of the asbestos-filled epoxy, increasing the strength of the bond. Exposure to temperatures as low as -40°F did not reduce joint strength under static loads.

Data on the static shear strength of Douglas fir veneer bonded with epoxy were been obtained in the Phase A1 materials test program discussed in section 8.1.1. This data is summarized in Table 8-83, with strength values adjusted for 12% moisture content. Three series of block shear tests were

Table 8-83 Static Block Shear Strength of Douglas Fir/Epoxy Laminae Tested in MOD-5A Phase A1 Program

Reference: "Strength Properties of Rotary-Peeled Douglas Fir Veneer Composite Material for Use in Large Wind Turbine Blades," for Project MOD-5A, R. H. Kunesh, K Consulting Co., Boise, Idaho, January, 1982

From Reference Report tables, block shear strengths were reported as follows, and adjusted to 12% wood moisture levels as noted:

Data	Table 8.1.1-3	Table 8.1.1-3	Table 8.1.1-3	Table 8.1.1-3
Veneer Grade: (2)	A+	C	C	C
No. Specimens:	25	25	25	25
Shear Plane: (3)	Parallel	Parallel	Parallel	Perpendicular
Avg Laminate M.C.:	2.8%	3.6%	11.5%	4.2%
Avg Shear Strength:	1824 psi	1595 psi	1436 psi	2018 psi
Std Deviation:	150 psi	193 psi	100 psi	193 psi
Shear Strength Adj to 12% Wood M.C.: (4)	1347 psi	1413 psi	1465 psi	1879 psi
Average	1546 psi	1357 psi	1493 psi	1767 psi
Minus 1 Std Dev	1419 psi	1193 psi	1389 psi	1598 psi
Plus 1 Std Dev	1673 psi	1521 psi	1597 psi	1937 psi
Average % Wood Failure	79%	91%	89%	100%

NOTES:

1. Veneers laminated with glue spread rate of 60 lbs/MDGL

2. A+ grade veneer is equivalent to Blade Grade 1, Gougeon Materials Specification GMS-001 (commercial A/B grade, with elastic modulus $\geq 2.45 \times 10^6$ psi)
   C grade veneer is commercial C/D grade, with elastic modulus $\geq 2.10 \times 10^6$ psi

3. Relative to laminations. Loads were all parallel to wood grain direction. (See Reference, page 6)

4. See Table 8.2.2-3 for method of adjusting properties to 12% wood moisture content level.

conducted with shear loads parallel to the grain and the plane of the veneer. One series of tests was conducted with shear loads perpendicular to the plane of the veneer and parallel to the grain, producing 100% wood failure. Stress levels from this series of tests were compared with data obtained on laminae with butt joints. After the stress levels were adjusted for 12% moisture content, the data from 25 samples shows:

Average	1767 psi
Minus 1 Standard Deviation:	1598 psi
Plus 1 Standard Deviation:	1937 psi

Longitudinal butt joints with defect type 2 suffer approximately a 15% reduction in static shear strength compared with laminated wood and epoxy with no joints.

The fatigue test data in Figure 8-99 indicates that defects in the bonding material may slightly reduce the shear strength of the joint after more than 1×10^6 cycles. The S-N curve provides a basis for estimating shear stress fatigue allowables for the joint.

It should be pointed out that the design of these butt joint specimens may have introduced stresses that would tend to cause failure sooner than simple shear stresses at the joint.

Note that the machined slots, 0.12 in. thick, as shown in Figure 8-94, produce sharp notches or stress concentrations at the joint. Failed specimens often showed a longitudinal split running from the notch to one surface of the beam.

As shown on Table 8-82, these wedge joint static tests indicate that longitudinal wedge joints are slightly weaker under shear loads than butt joints. When the wedge is not centered in the joint, the reduction in strength is more pronounced. The presence of defect type 2 had no appreciable effect on the strength of the joint.

Fatigue test data, shown in Figure 8-100, indicates that wedge joints are not as strong in shear fatigue as butt joints. The joints with defects were stronger than joints without defects.

The design of the specimens may be responsible for the premature failures of some of the specimens. Examination after the test revealed that five of the 17 specimens (CW7, SW3, SW7, SW8, and DW4) failed in shear between one of the flanges and the web, rather than at the wedge joint. It is apparent that the fillets in this area were not effective in restricting failure to the wedge joint.

Test results provided an insight into the effects of joint design, defects, and temperature on the shear strength of longitudinal joints in Douglas fir veneer and epoxy. The strength data is based on uniform, conservative approaches to determining specimen failure.

Since the blade stress analysis discussed in section 4.3 indicates a very low shear stress condition for the longitudinal bonded joint area, the strength of the wedge joint is currently more than adequate.

Should further structural design analysis indicate that expected shear stresses on the joint will approach the levels obtained in these tests, additional tests would be required to confirm these allowables. These tests should use a specimen that more closely simulates the actual joint design, and that eliminates the inconsistencies noted.

In the fatigue tests, the longitudinal bonded joints appear to tolerate cracks. Small cracks tended to propagate slowly, so periodic inspections for cracks should avoid catastrophic failures.

8.2.3 HOLLOW STUD TESTING

Early in the MOD-5A program, a hollow stud that would attach the partial span control (PSC) flange to the blade was developed. The design was also considered for use in other areas of the blade design. A backup design, consisting of a blade-type stud was also developed, but was never fabricated or tested since the hollow stud was satisfactory.

8.2.3.1 Objectives

The hollow stud tests determined static strength properties in tension and compression and at three temperatures, and fatigue capability at various load ratios. The test loads and ratios were designed to test the stud in the load environment that was predicted for the blade tip attachment. However, the findings of this test could be analytically adapted to other loading combinations. The temperature effects were considered more thoroughly in stud testing since the higher thermal conductivity of the stud of the steel PSC could cause wider diurnal temperature variations at the stud to wood interface than those expected in other areas of the blade. The loading at the PSC interface is primarily axial, and shear loads are relatively small. The testing did not include any shear loading for that reason, but for any further stud applications, shear loading might be more significant.

8.2.3.2 Description

Thirty-seven specimens were fabricated and tested. Nine static tension and five static compression tests were performed at room temperature, two tension tests each were performed at 100°F and -22°F and 19 fatigue tests were performed. The specimens consisted of a block of wood 4 in. square and roughly 50 in. long, with a hollow stud at each end. The specimen is shown in Figure 8-101. For static compression tests the specimens were cut in half to yield two data points per specimen. In the tension and fatigue tests, two studs were simultaneously subjected to loads. The results were somewhat biased, since data was obtained only on the weaker of the two studs, but the sample was designed this way to provide a reliable way to grip both ends on a test machine. GBI used a similar stud approach for fatigue testing wood specimens.

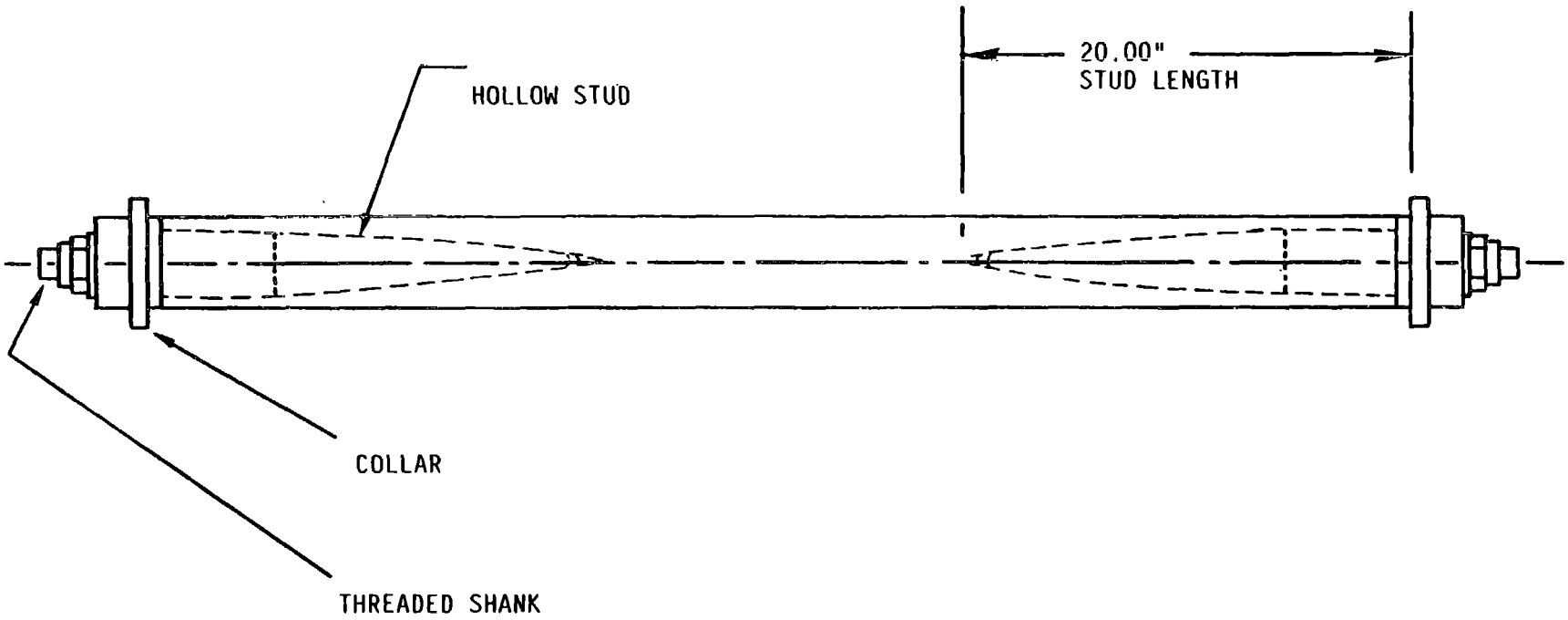

Figure 8-101 Hollow Stud Test Specimen Configuration

Interface fittings that adapted the machine thread to the stud thread were provided to UDRI, where the tests were run. GBI developed the fabrication fixture that was used to align the studs during bonding.

Figure 8-102 shows the setup, which was typical for static tension and fatigue tests. Compression tests were similar, except the half-length specimen reacted against a recessed plate on the actuator end of the MTS test machine. All static test loading ramps were aimed at failure in approximately five minutes.

8.2.3.3 Results

Static testing at room temperature was conducted after allowing two weeks for the West System® thixotropic, asbestos-filled epoxy to cure. A typical load/deflection plot is shown in Figure 8-103. The curve was linear until the load reached approximately 74,000 lbs. A slight step at that point resulted in a softer slope, which appears to be linear until the ultimate load point of 81,000 was reached. The load fell suddenly, to approximately 69,000 lbs, and climbed in a non-linear curve to 81,000 lbs. before trailing off. The initial step at 74,000 lbs. was accompanied by an acoustic report, and most likely indicated the point when the epoxy cracked or separated. On several subsequent tests the trace dropped after the ultimate point without attaining a second load peak. Figure 8-104 contains this type of plot, which also shows more clearly the variation in slope following the initial step. The average value of the first step for the six tests at room temperature was 80,833 lbs., with a sigma of 2,269 lbs. The corresponding ultimate values were 94,633 lbs. and 9,705 lbs. There was a cracking noise, but no indication of stiffness variation was detectable on the traces. Table 8-84 summarizes static test results. Sample reversed D5 was designated for further testing in fatigue.

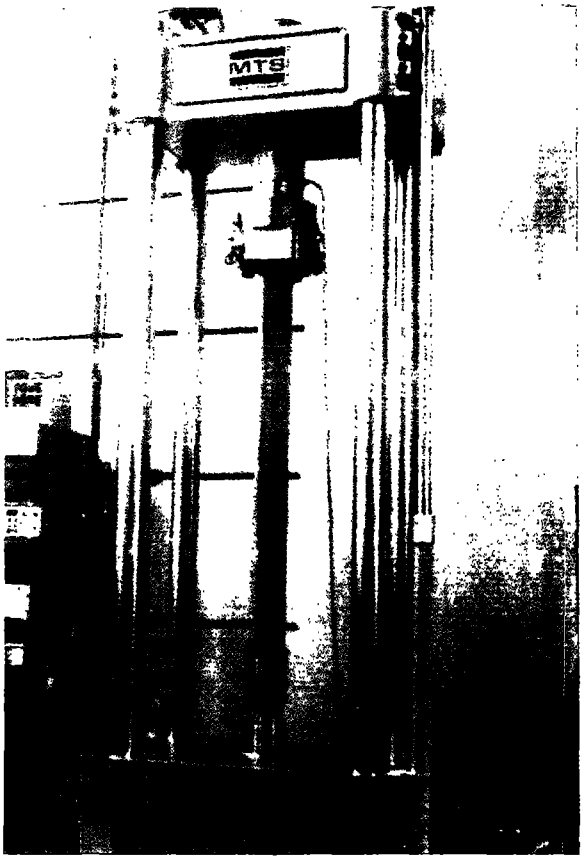

Figure 8-102 Hollow Stud Test Setup

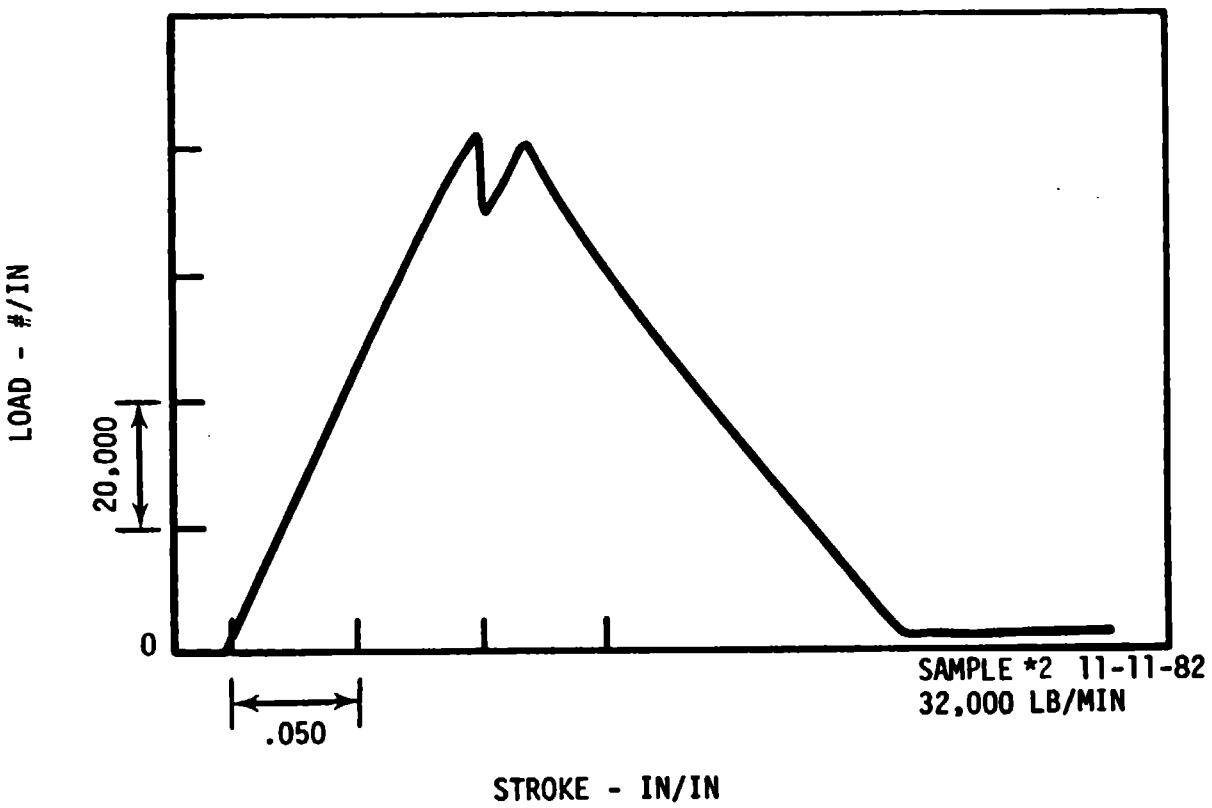

Figure 8-103 Load Deflection Plot, Specimen *2 (Room Temp.)

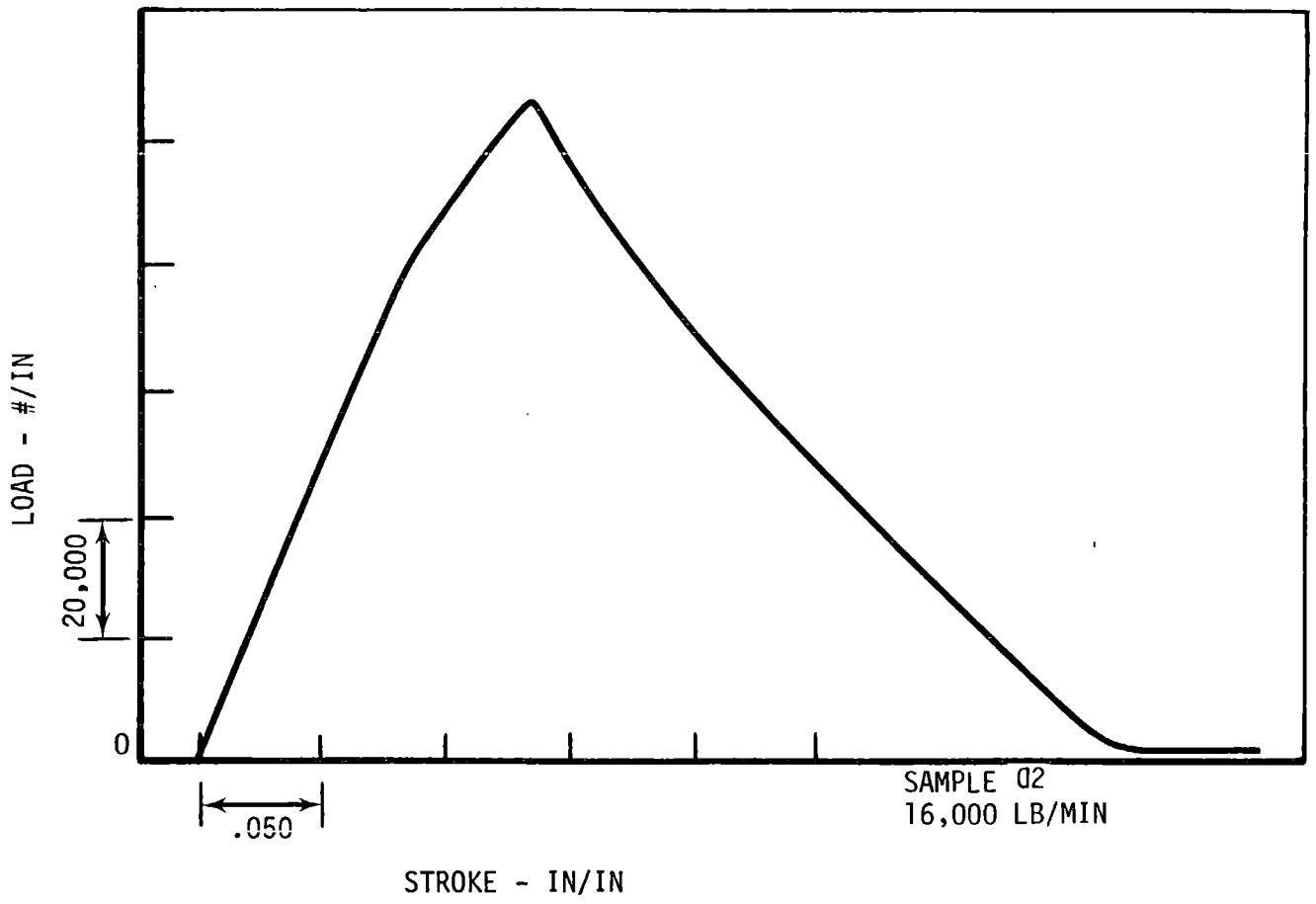

Figure 8-104 Load Deflection Plot, Specimen Q2 (Room Temp.)

Table 8-84 Hollow Stud Static Test Summary

Sample Number	Test Type	Test Temperature	First Offset (lbs.)	Ultimate (lbs.)
Ψ1	Comp	RT		106,400
*1A	Comp	RT		120,410
*1P	Comp	RT		115,000
*3	Tension	-22°F	61,000	80,000
Δ1	Tension	-22°F	55,000	73,800
*4	Tension	100°F		126,000
Δ3	Tension	100°F		125,600
θ1	Tension	RT	84,000	105,900
Ω	Tension	RT	84,000	89,900
Ψ1	Tension	RT	81,000	92,800
π2	Tension	RT	No Data	102,300
Δ2	Tension	RT	74,000	92,300
reversed D2	Tension	RT	87,000	105,900
*2	Tension	RT	75,000	81,000

The tension tests at -22°F produced loads of 72% of the room temperature value at first offset and 81% at ultimate. The load deflection plots for 22°F are very similar to the traces for room temperature. Figure 8-105 shows the trace for sample *3.

The traces for tests at 100°F did not indicate a distinct offset before the ultimate failure. Instead, they were very non-linear.

The ultimate loads at 100°F were approximately 33% higher than for tests at room temperature. Figure 8-106 shows the plot for specimen *4, which had a relatively long, sweeping curve leading to the ultimate load. The head travel

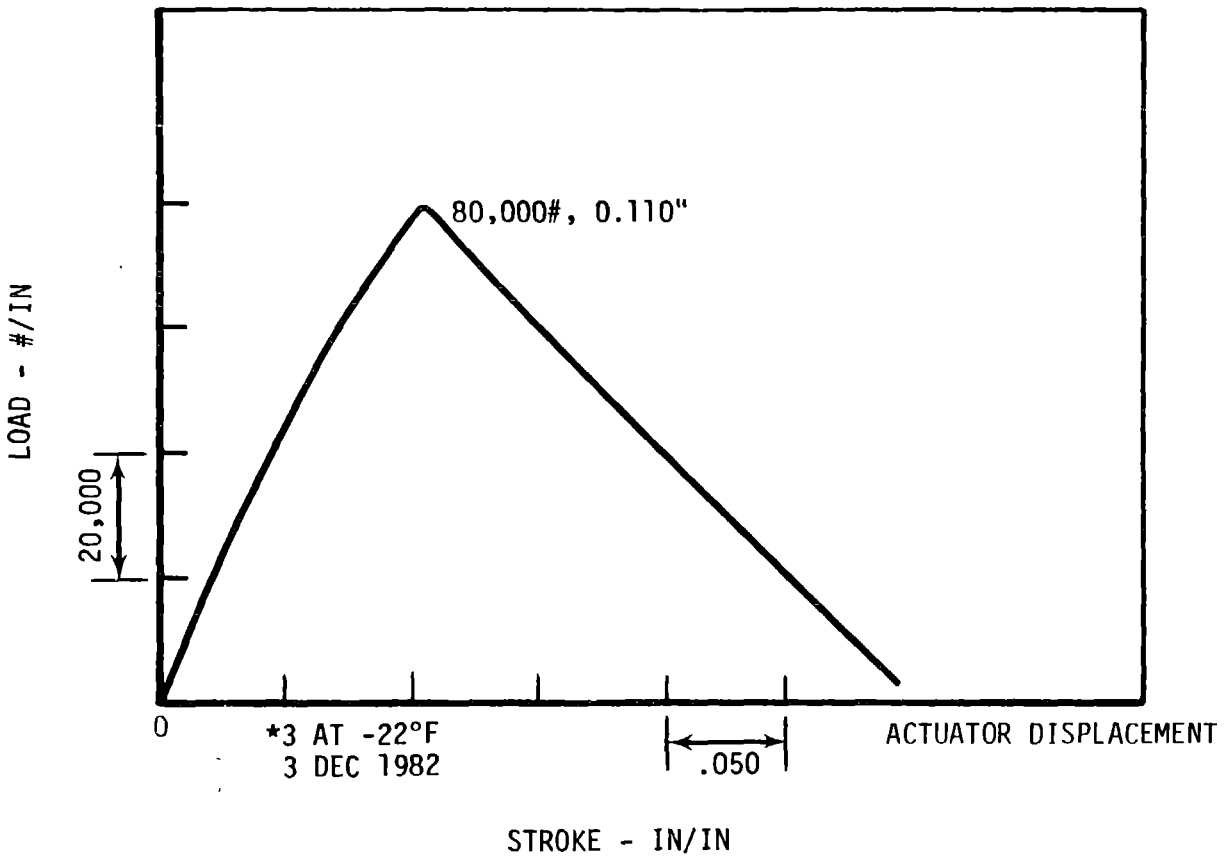

Figure 8-105 Load Deflection Plot, Specimen *3 (-22°F)

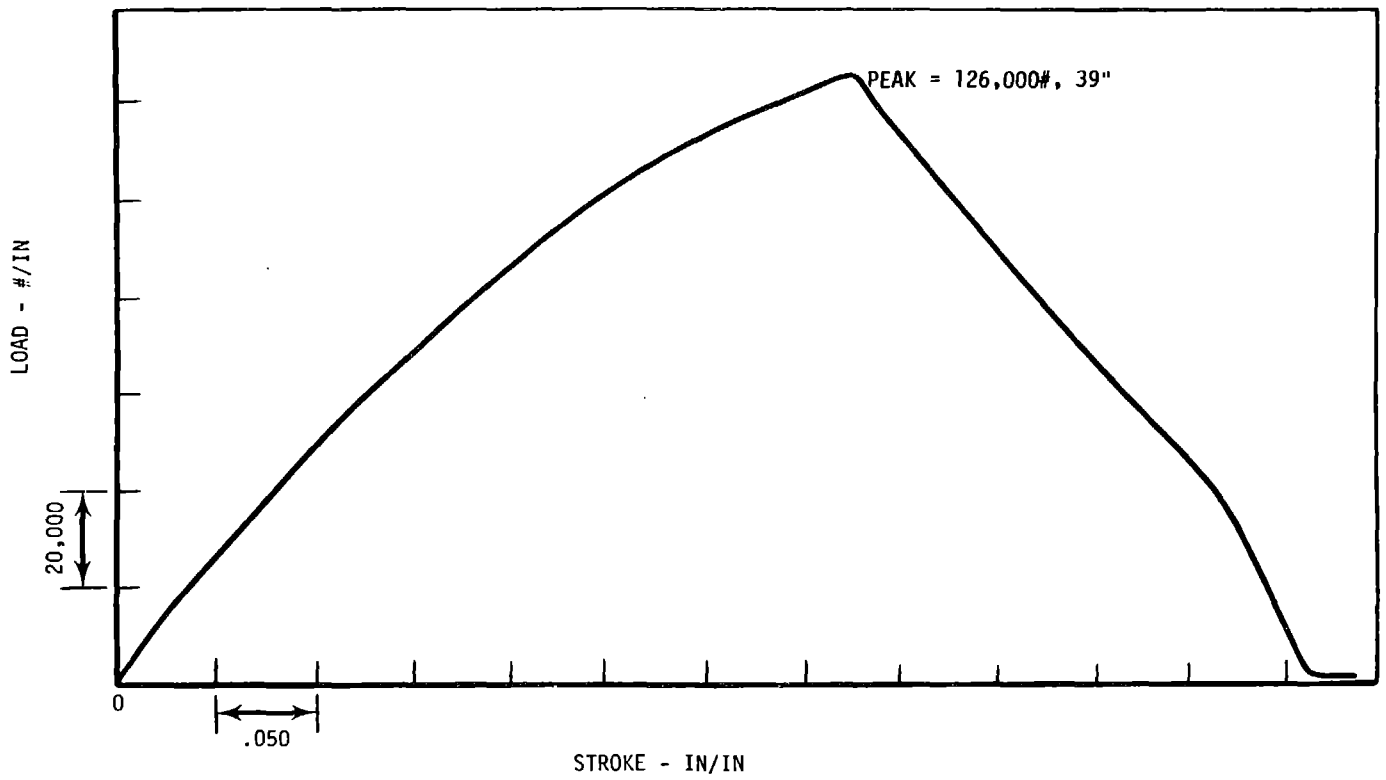

Figure 8-106 Load Deflection Plot, Specimen *4 (100°F)

of 0.39 in. compares with values of approximately 0.125 in. at room temperature and 0.11 in. at -22°F. The results indicate that the epoxy softens at elevated temperatures. Further studies should be conducted before the epoxy is used in applications in which it could be exposed to high temperatures.

Compression tests were performed on two specimens which were identified as *1AM and *1PM. The load deflection traces did not clearly indicate where the initial offset occurred. The trace is linear to above 30,000 lbs., followed by a pair of smooth curves and a second linear trace, with ultimate loads near 115,000. Head travel of approximately 0.15 in. for the half length specimen is signi- ficantly higher than the value of .125 for the full length specimen. Figures 8-107 and 8-108 show the two compression test plots. A third compression test was conducted on specimen Ψ1, which was the undamaged half of a tension test specimen. The result, 106,000 lb., was lower than the two previous results, possibly because of some damage that occurred in the tension test.

Fatigue testing started on December 10, 1982, and used the same equipment as the static tests. Sample reversed D5 was installed in the test machine and prepared for testing. A sequence of load cycles at increasing loads was applied, to determine if permanent damage was being induced at the test loads. Ten cycles were applied at a rate of 0.3 Hz, and load deflection curves were recorded at each of the following load ranges:

+45,000 to -34,000 lbs.
50,000 to -39,000 lbs.
55,000 to -44,000 lbs.
60,000 to -49,000 lbs.
65,000 to -54,000 lbs.

During the first of ten cycle to 45,000 lb, an acoustic output occurred. Forty additional cycles were further accumulated at various load settings. This sample was designated for use only as a "dummy" specimen, which would be used to verify loads.

Specimen reversed D3 was supposed to be fatigue tested at R equal to -.75, from 45,000 lb tension to 34,000 lb compression. During the first cycle the specimen was accidently overloaded to 86,000 lbs. and 72,000 lbs. The specimen was permanently damaged. A significant amount of hysterisis was apparent on the trace.

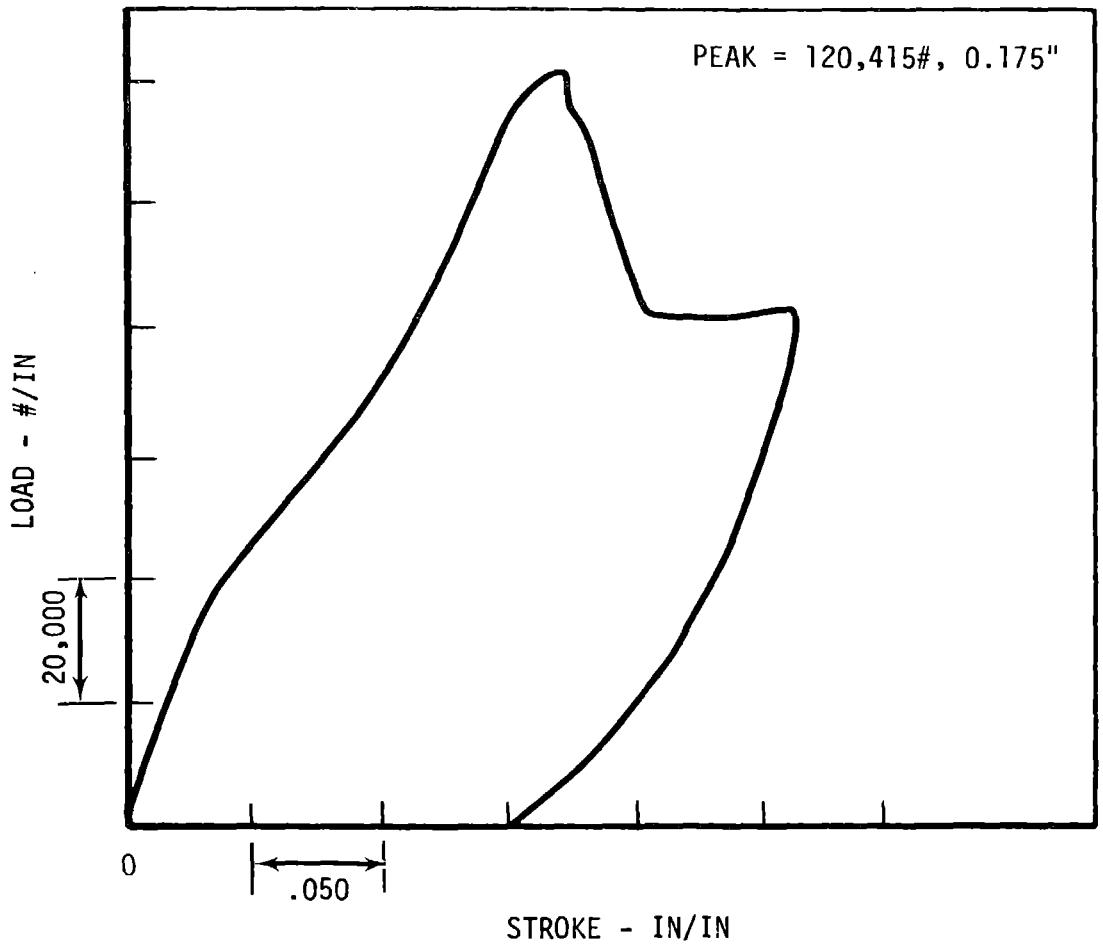

Figure 8-107 Load Deflection Plot, Specimen *1AM (Room Temp. Comp.)

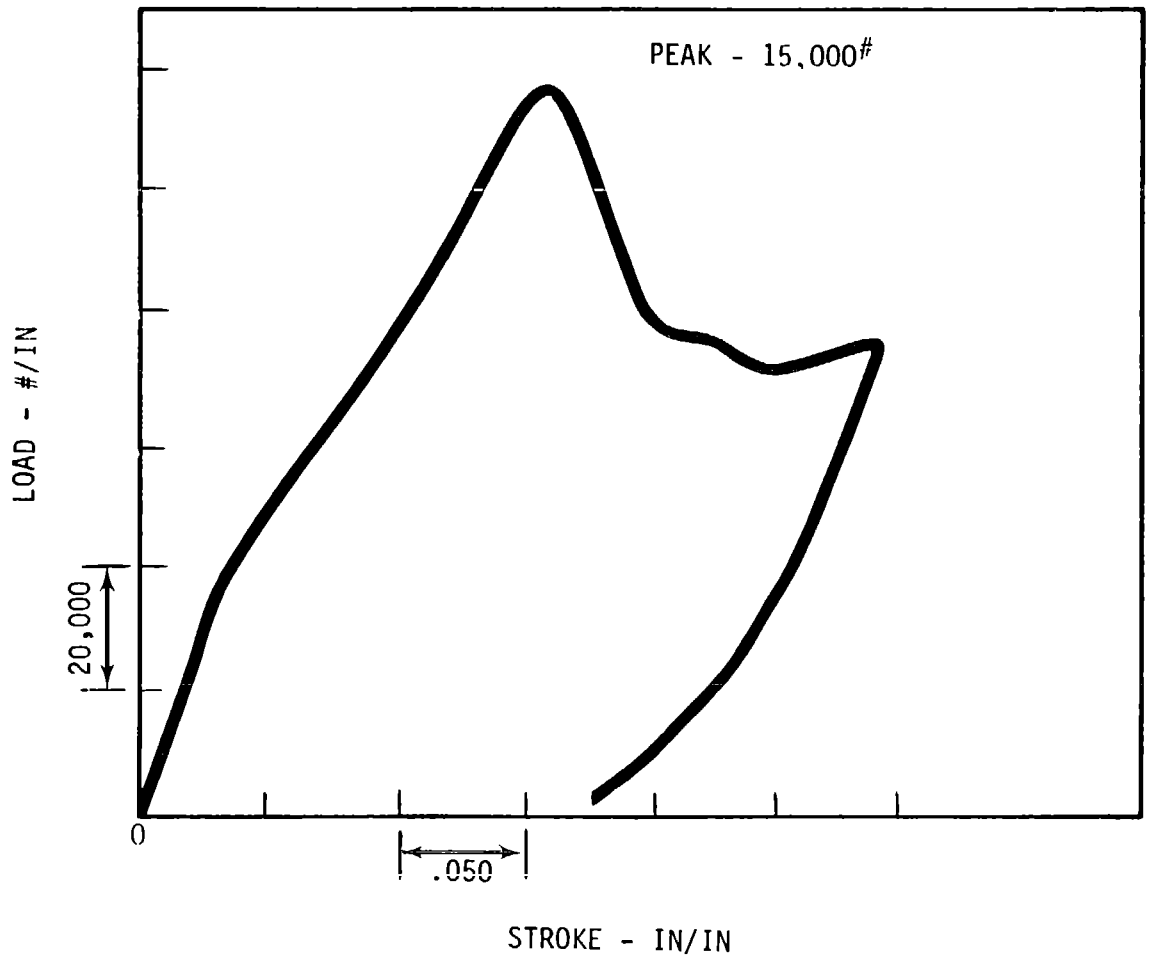

Figure 8-108 **Load Deflection Plot, Specimen *1 PM (Room Temp. Comp.)**

The next specimen tested was reversed D1, with R equal to +0.1 and maximum load of 60,000 lbs. After 1,234,505 cycles, failure occurred when one stud pulled from the sample end. Specimen π5 was tested at the same R and a maximum load of 70,000 lbs., and achieved a life of 43,300 cycles. A third specimen, π3, was also tested at R equal to 0.1 but with a maximum load of 65,000 lbs. It survived 213,600 cycles before it failed. All of these samples were tested at a rate of 3 Hz.

The next group of four specimens was tested at R equal to -1. Sample Θ3 lasted 2,000 cycles at a load of 70,000 lbs., sample reversed D4 survived 27,000 cycles at 55,000 lbs., sample π1 failed after 55,600 cycles at 45,000 lbs., and sample Θ4 was tested and failed after 485,200 cycles at 45,000 lbs. All these samples were tested at a rate of 2 Hz.

Sample Θ2 survived 269,100 cycles when tested at -70,000 lbs. Sample π4 was loaded to -65,000 lbs. also at a load ratio of 10 but it failed after only 216,900 cycles. Both were tested at 5 Hz. Specimens Ω3 and Ψ3 were tested at 5 Hz, at a load of 60,000 lbs and R equal to 0.1 (tension/tension). They failed after 222,000 and 345,800 cycles respectively. The results of tests to this point aroused suspicion that the test rate and the resulting elevated temperature affected fatigue life, so additional tests at both 2 and 5 Hz followed. Samples Δ4 and Ψ4 were tested at 2 Hz, and R equal to -1 and a load of 45,000 lbs. (fully reversed). The specimens failed at 95,100 and 243,800 cycles. These lives were both close to the life of sample π1, which was tested in the same conditions. Specimen Ψ2 was tested in similar conditions but the load was reduced to 39,000 lbs., and the life increased to 521,000 cycles. Sample Ω2 was tested at R equal to 0.1 (tension/tension), a load of 166,700 lbs. and a rate of 2 Hz. The sample failed at 166,700 cycles. Sample Δ5 was subjected to a load of 45,000 lbs. at R equal to 0.1. It lasted 10,000,000 cycles at 5 Hz, when the test halted without failure. The specimens *5 and reversed D5 were tested at R equal to -1.0 (fully reversed) and a load of 35,000 lbs. Sample *5 was tested at 5 Hz and failed after 120,700 cycles; sample reversed D5 survived 10,000,000 cycles at 2 Hz without failure.

The effect of the test rate on the fatigue life is clear. The shorter life at faster rates is probably due to internal heating. The problem is self compounding, since the higher rate of energy dissipation causes the epoxy to lose stiffness, which increases heating by increasing the stroke on each cycle. The degree of temperature increase was not accurately determined, since the measurement cannot be made without creating stress risers by boring holes into the core of the specimen. The stud probably conducts heat away from the epoxy, but the length of the specimen did not allow a significant gradient.

The results of the tests are summarized in Table 8-85. Figures 8-109 through 8-111 summarize the results of a regression analysis, which used the stud test data. The effect of test rate was ignored for this curve fitting evaluation.

The results indicated that the stud strength characteristics were adequate for the MOD-5A application, but additional testing should be conducted for applications where there may be exposure to temperatures above 100°F is indicated. Load duration testing at elevated temperature would also be of interest.

Table 8-85 Test Results

SPECIMEN I.D.	DATE	TYPE OF TEST	P_{MIN}	P_{MAX}	CYCLES AT FAILURE	FREQUENCY HZ	TEMPERATURE °F	COMMENTS
* 2	11/12/82	TENSION		81,000			A *	FAILED AT UPPER STUD
▪ 2	11/12/82	TENSION		102,340			A	NO PLOT
□ 2	11/12/82	TENSION		105,920			A	
Δ 2	11/12/82	TENSION		92,300			A	
* 4	11/18/82	TENSION		126,000			107	
							101	
Δ 3	11/18/82	TENSION		125,600			101	
							97	
* 1 AM	11/23/83	COMPRESSION		-120,410			A	
* 1 PM	11/23/82	COMPRESSION		-115,000			A	
* 3	12/03/82	TENSION		80,000			-22	TEMP = -22°F
Δ 1	12/03/82	TENSION		73,830			-22	TEMP = -22°F
ψ 1	12/07/82	TENSION		92,850			A	
Ω 1	12/07/82	TENSION		89,890			A	ALIGNMENT OFF BY 1/8"
θ 1	12/07/82	TENSION		105,920			A	
□ 5	12/10/82	TENSION						CRACKING ON FIRST QUARTER CYCLE
		COMPRESSION	-54,000	65,000	50	0.3	A	R = -1
α 3	12/10/82	TENSION						FAILURE DUE TO OVERLOAD
		COMPRESSION	-34,000	+ 45,000	10	0.3	A	SETTING OF -72000 to +86000
□ 1	12/16/82	FATIGUE	+ 6,000	+ 60,000	1,234,505	3	A	FAILURE R = 0.1
▪ 5	12/17/82	FATIGUE	+ 7,000	+ 70,000	43,300	3	A	FAILURE-TOP END PULLOUT R = 0.1
ψ 1	12/20/82	COMPRESSION		-106,400		3	A	
▪ 3	12/22/82	FATIGUE	6,500	65,000	213,600	3	A	15" DELAMINATION AT 197,000
								LOAD READJUSTED R = 0.1
θ 3	12/22/82	FATIGUE	-70,000	+ 70,000	2,000	2	A	FAILURE-PULLOUT UPPER END R = -1.0
□ 4	12/22/82	FATIGUE	-55,000	+ 55,000	27,000	2	A	FAILURE-PULLOUT LOWER END R = -1.0
▪ 1	12/28/82	FATIGUE	-45,000	+ 45,000	55,600	2	A	FAILURE-PULLOUT LOWER END R = -1.0

*A = AMBIENT

Table 8-85 (con't) Test Results

SPECIMEN I.D.	DATE	TYPE OF TEST	P_{MIN}	P_{MAX}	CYCLES AT FAILURE	FREQUENCY HZ	TEMPERATURE °F	COMMENTS
θ 4	1/04/83	FATIGUE	-45,000	+ 45,000	485,200	2	A*	FAILURE-PULLOUT LOWER END R = -0.1
θ 5	1/19/83	FATIGUE	- 6,000	- 60,000	2,638,500	5	A	FAILURE-CRACK ON BOTH SIDES FROM END TO CENTER OF SPECIMEN R + 10
θ 2	1/21/83	FATIGUE	- 7,000	- 70,000	269,100	5	A	FAILURE R = 10
¤ 4	1/22/83	FATIGUE	- 6,500	- 65,000	216,900	5	A	FAILURE R = 10
Ω 3	1/22/83	FATIGUE	+ 6,000	+ 60,000	222,000	5	A	FAILURE R = 0.1
ψ 3	1/23/83	FATIGUE	+ 6,000	+ 60,000	345,800	5	A	FAILURE R = 0.1
Δ 4	1/25/83	FATIGUE	-45,000	+ 45,000	95,100	2	A	FAILURE R = -1.0
ψ 4	1/27/83	FATIGUE	-45,000	+ 45,000	243,800	2	A	FAILURE-LARGE CRACK IN 1 IN. FROM SIDE ON TAPER TO CENTER OF SPECIMEN R = -1.0
ψ 2	1/31/83	FATIGUE	-39,000	+ 39,000	521,000	2	A	FAILURE-21" CRACKS ON LOWER END R = -1.0
Ω 2	2/03/83	FATIGUE	+ 5,600	+ 55,600	166,700	2	A	FAILURE R = 0.1
Δ 5	3/03/83	FATIGUE	4,500	45,000	10,000,000	5	A	R = 0.1
* 5	3/07/83	FATIGUE	-35,000	+ 35,000	120,700	5	A	FAILURE-LOWER END PULLOUT, 1/4 IN. SPLIT THROUGH CENTER, R = -1.0
0 5	4/07/83	FATIGUE	-35,000	+ 35,000	10,000,000	2	A	R = -1.0

*A = AMBIENT

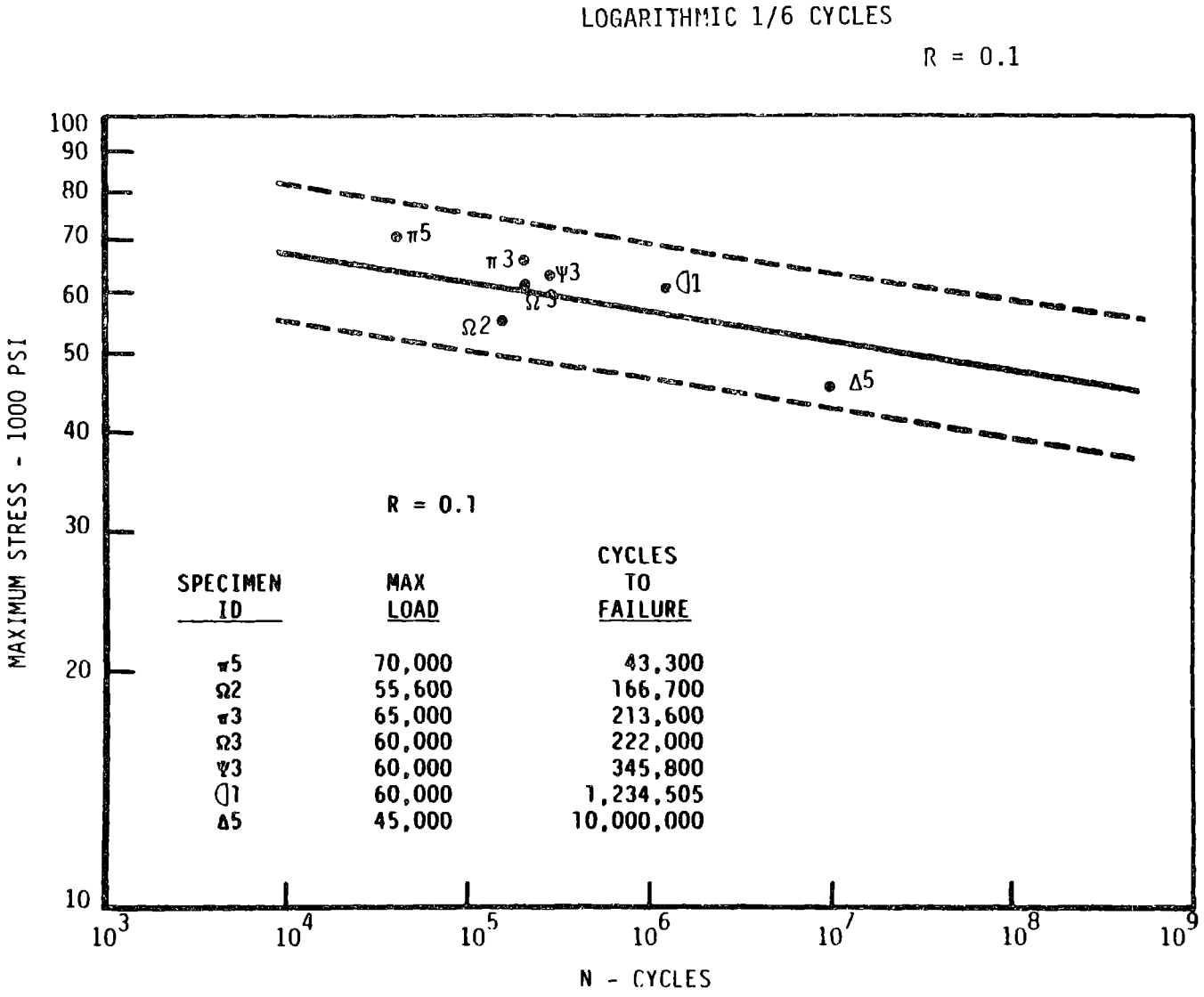

Figure 8-109 MOD-5A Stud Fatigue Tests

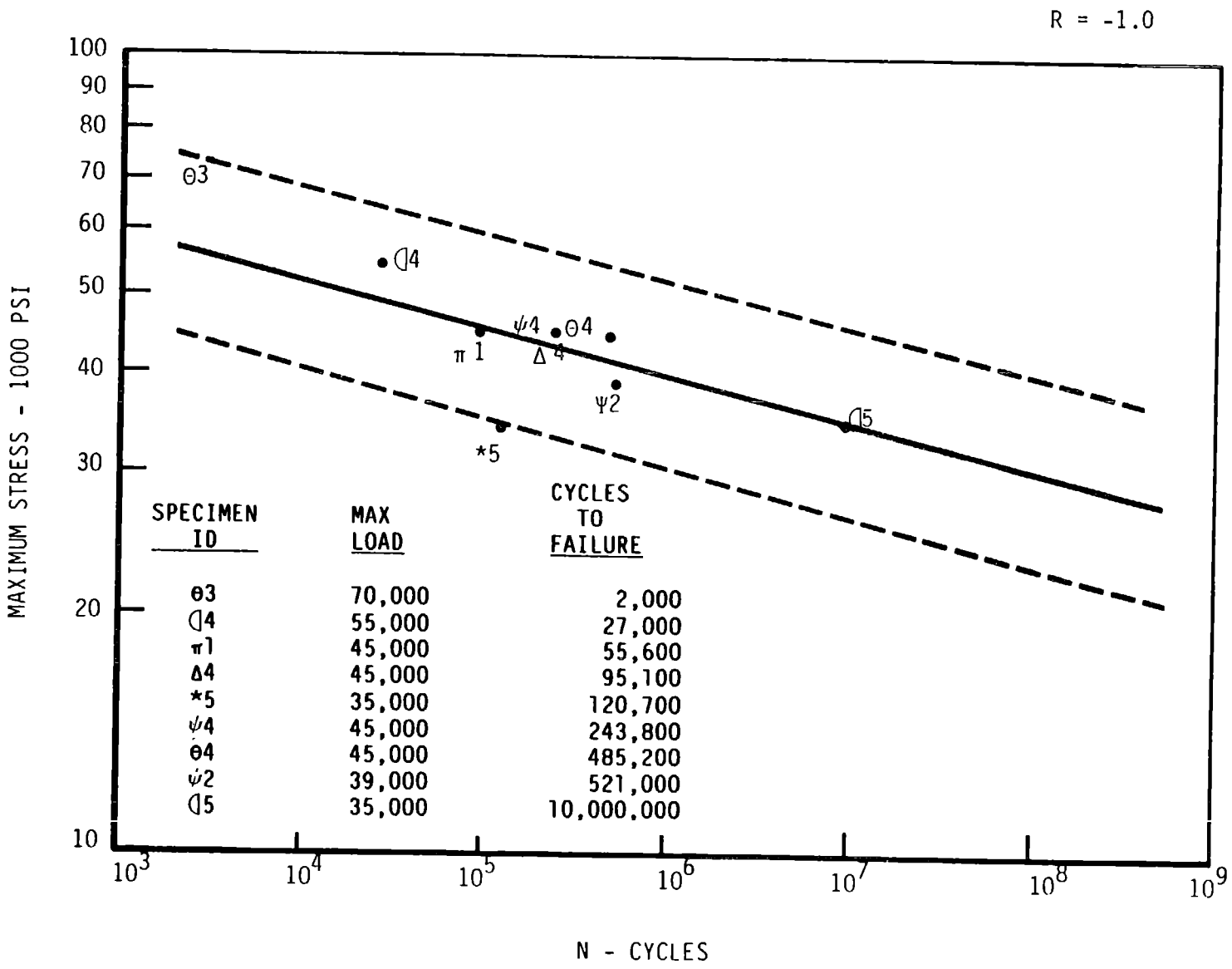

Figure 8-110 MOD-5A Fatigue Tests

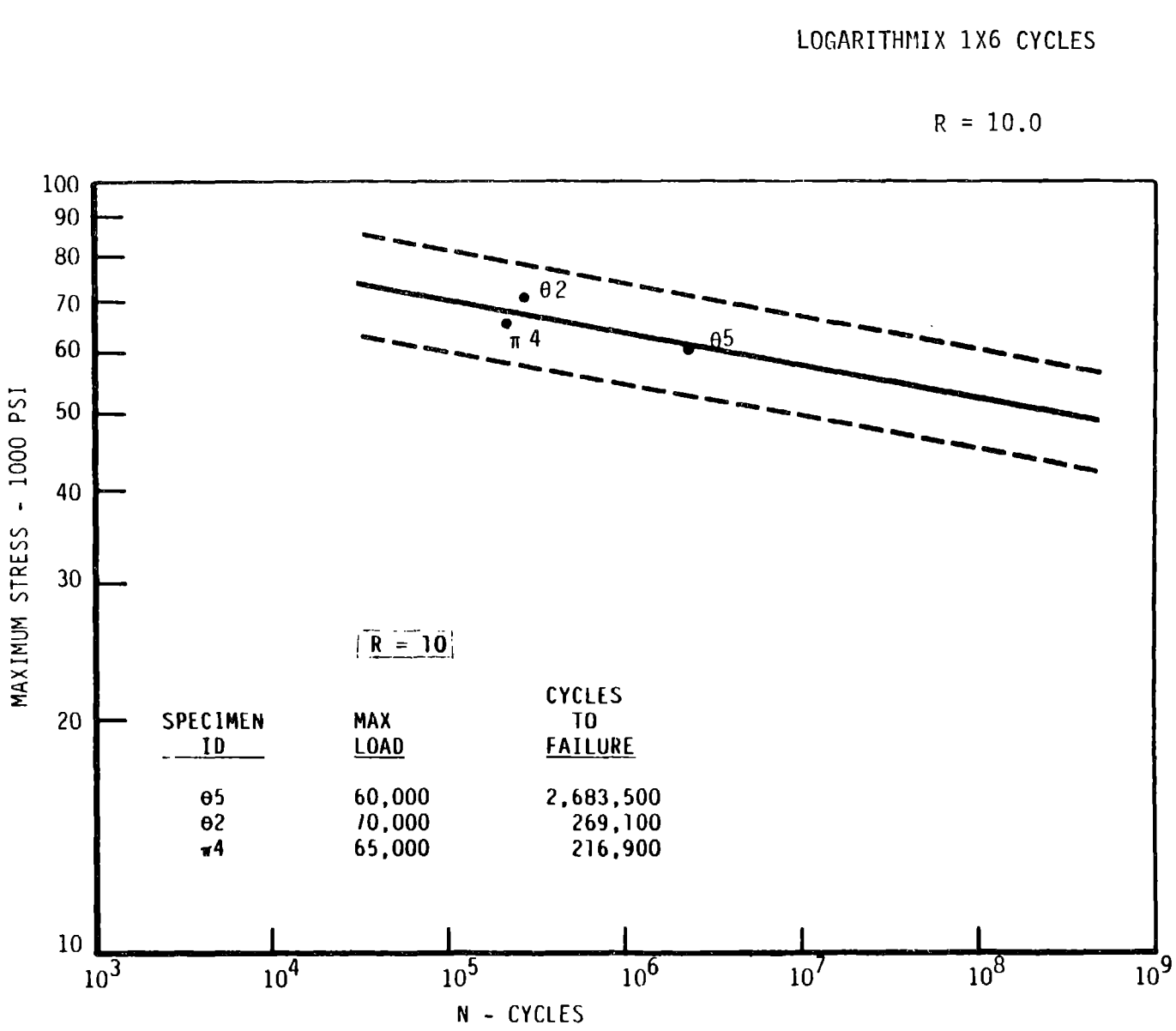

Figure 8-111 MOD-5A Fatigue Tests

8.2.4 BACKUP JOINT TESTING

Large-scale finger joints were developed and tested for joining the blade sections at the site, but other methods of joining the sections were also considered. A loose plate concept had potential advantages. This joint would require only two relatively flat faces to be butted together. Slots would be cut in the field for the loose plates, which would be installed incrementally. This design would eliminate the need for the precisely machined fingers and the bonding of a large surface area. The loose plate could also be used to augment other joints.

8.2.4.1 Objectives

The loose plate joint test evaluated the joint design for use in developing analytical techniques consistent with the failure mode and to permit further refinement of the design if results seemed promising and if the program's needs made it necessary to continue the backup joint design.

The design of the test specimen was not optimum. The design provided a comparison of plates of different stiffnesses.

8.2.4.2 Test Description

The test specimen is shown in Figure 8-112. It is 96 in. long and its cross-section is 1.5 in. by 3 in. It is made of 15 laminations. Ten specimens were tested: four controls made of one piece of wood with no plates, and two each with plates of three different materials. The plate materials initially considered were glass fiber-reinforced plastic (FRP), graphite and a mixture of glass fiber and graphite, but there were difficulties in laminating the graphite material into dense plate materials. Consequently, FRP, aluminum and steel were evaluated. The plates were 3/16 or 0.20 in. thick, and metal faces were sanded just before bonding so that the bond material would adhere well. The testing was done during September, 1983, at Washington State University, using the compression grip timber testing machine.

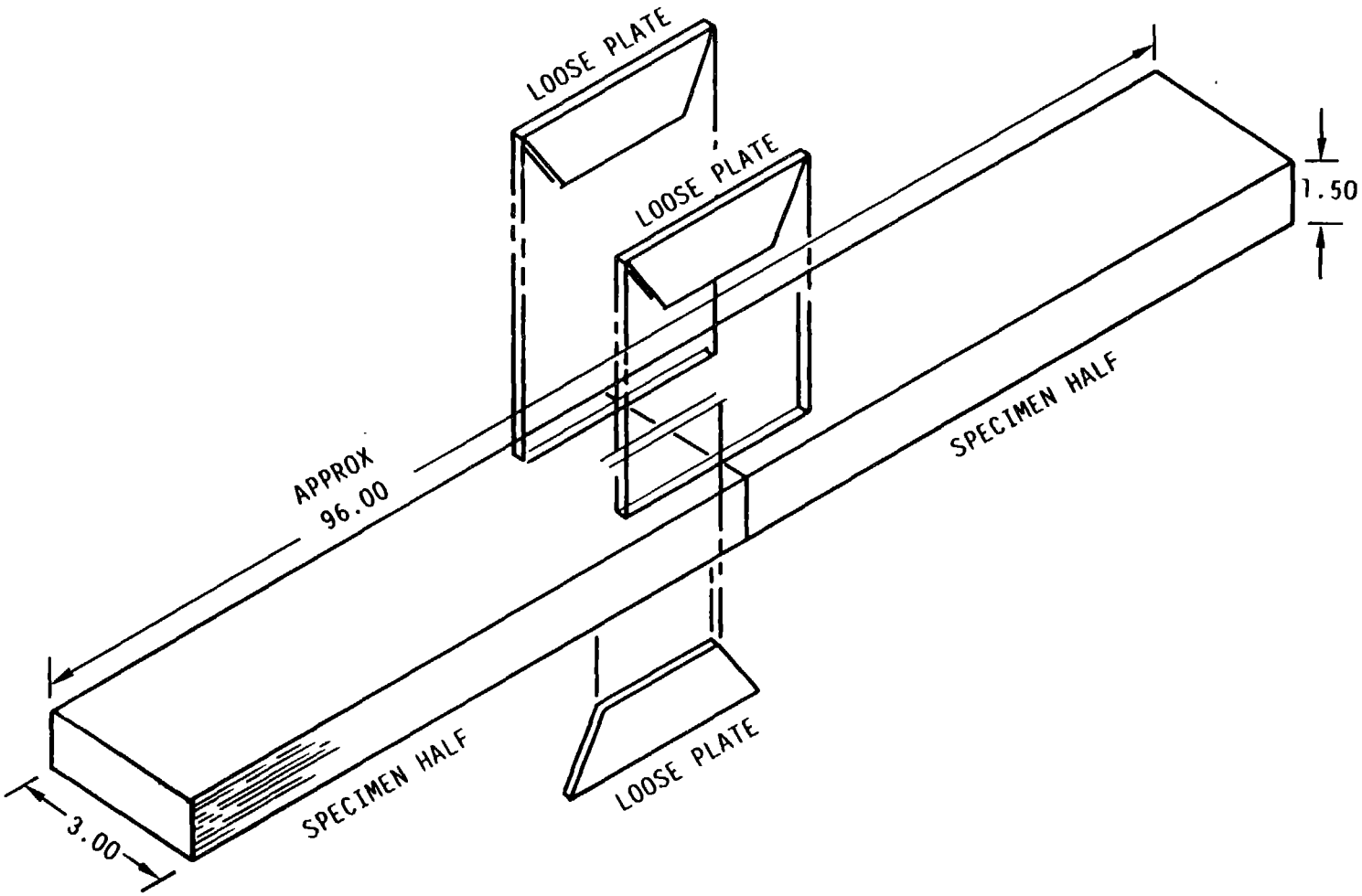

Figure 8-112 Splice Plate Assembly

8.2.4.3 Results

The test results are summarized in Table 8-86. The steel plate samples performed better than the others. The steel reached 56% of the control mean stress at the point of first offset and 88% of the ultimate stress.

Table 8-86 Backup Joint Test Results

Sample No.	Type	Stress Level Ultimate (psi)		Average (psi)	First Offset (psi)		Mean (psi)
2-1C	Control	6710			N/A		
1-1C	Control	8105	----	8486	6362	----	6923
1-7C	Control	10199			7483		
1-7C	Control	8930			N/A		
2-4	Steel	7048	----	7514	3909	----	3885
1-4	Steel	7981			3861		
1-3	Aluminum	4268	----	3805	2838	----	2929
2-3	Aluminum	3343			3020		
1-2	FRP	6356	----	6069	1778	----	1762
2-2	FRP	5781			1747		

The aluminum plate specimen averaged 42% of the first offset, but only 45% of ultimate because the epoxy sheared off the aluminum surface. The glass fiber specimens failed at 25% of the first offset, but since a significant amount of wood failure was involved, the ultimate load reached 71% of the control mean. The point of first offset is actually the meaningful point for blade design, and results indicate that load capacity increases with plate stiffness. These samples did not withstand loads as high as the finger joints withstood, but the design was not optimized. Further improvements to the design and static and fatigue testing would be necessary before a loose plate design could be implemented.

8.2.5 BLADE TEETER AREA TESTS

This test series consists of eight different test sets; each provided data on a particular feature. Table 8-87 summarizes the test program. The sample population was kept small, to minimize expenditures while providing representative data. Typical static tests used three specimens and fatigue tests used four. Unless otherwise specified, the intent of the fatigue test was to have two specimens fail near 10,000 cycles, and two fail near one million cycles, to provide a set of points for extrapolation. Because these materials are very unpredictable, this goal was not met.

8.2.5.1 Shear Tests of Glass Augmented Laminae

8.2.5.1.1 Introduction

Shear tests provides characteristic data for the Douglas fir veneer augmented with #7781 Burlington glass fiber cloth between each layer but not on the outside faces. Each veneer was 0.10 in. thick.

8.2.5.1.2 Objective

The objective of the test was to determine the shear strength of the material in static and fatigue loading cases. The static strength of the individual materials is known, but that of the combination was not then available.

8.2.5.1.3 Description

The test configuration shown in Figure 8-114 was loaded in compression between the actuator and load cell of an MTS test machine at the UDRI. The two shear areas, each 1.0 by 1.5 in. in cross section, were ultimately failed. The lower portion of the test specimen was bonded to a steel plate, to minimize the effect of bending on the shear area.

Static testing was performed on three specimens at room temperature, on three identical specimens at 100°F, and on three identical specimens at 120°F. An Instron oven was placed in the MTS machines for the high temperature tests, and a second oven was used for pre-conditioning the specimens. Two of the three specimens at each temperature were equipped with strain gage rosettes, centered on the shear planes on both sides of the specimens. The center gage read strain normal to the plane, and the other two read on diagonal planes.

Table 8-87 Teeter Area Test Summary

Teeter Test Number	Sub-Section Number	Description	Number and Type of Specimens
1	8.2.5.1	Shear and fatigue strength of glass fibers laminae reinforced with glass fiber	3 shear tests at 75°F, 3 at 100°F and 3 at 120°F 4 fatigue test specimens, R = 20
2	8.2.5.2	Bearing capability of epoxy bushing in various grain directions	3 bearing tests in each of 3 grain directions, at each of 3 temperatures: 75°F, 100°F, and 120°F 4 fatigue test specimens (diagonal grain) at each R value: R = -1.0 and R = 20
3	8.2.5.3	Teeter brake shaft bearing load distribution tests	3 bending specimens 4 fatigue test specimens, R = 0.05
4	8.2.5.4	Flapwise bending test	3 bending specimens 4 fatigue test specimens, R = 0.05
5	8.2.5.5	Chordwise bending tests (tension simulation)	3 tension and 3 compression specimens 4 fatigue specimens, R = -1.0
6	8.2.5.6	Low temperature tension tests	3 tension and 3 compression specimens
7	8.2.5.7	Crossgrain tension testing of augmented laminae	3 static tension specimens 4 fatigue specimens, R = 0.1
8	8.2.5.8	Bolster bending tests (axial simulation	3 each static tension and compression 4 fatigue specimens, R = -1.0

The static samples were tested with the machine stroke rate controlled to provide failure in approximately 5 minutes. The fatigue specimens were tested using the same set-up, but no strain gages were used.

8.2.5.1.4 Results

The static test specimens all failed relatively silently; only sounds of individual glass fibers snapping were heard. No discernable failure could be found visually on most specimens after the test. Table 8-88 lists the failure loads for each specimen, and head travel at maximum load. Figure 8-113 shows the test set-up, and Figure 8-114 shows a photograph of a specimen after its test. Figure 8-115 defines the load deflection plot of a typical static test.

Fatigue testing used the same set-up as that shown in Figure 8-113. It was conducted with a load ratio of 20, and at a frequency of 5 Hz. The first specimen, number 10 SR, was tested with a maximum compression load of 3,800 lbs., about 50% of the mean failure load. Failure occurred at 30,000 cycles. Specimen number 12 SR was tested next, and the loads were reduced to -3,200 lbs. and -160 lbs. The specimen failed after 97,700 cycles. The loads for sample 13 SR were further reduced to -2,900 and -145 lbs., and 252,700 cycles were completed before failure. The last specimen, number 11 SR, lasted 499,100 cycles before failure. It was loaded from -2,700 to -135 psi. The results of these tests are plotted in Figure 8-116, and compare favorably with estimated allowables.

8.2.5.2 Teeter Shaft Bearing Cup Load Bearing Capability Test

8.2.5.2.1 Introduction

The points where concentrated load are introduced to the MOD-5A blade contained metal fittings, primarily because metal has superior wear and bearing capability, compared to wood. The metal inserts were held in place using West System® epoxy in a thixotropic form, and in the case of the teeter shaft cup, a wrapping of glass fiber was used. This is common practice in the boating industry, where masts are fitted into wood hulls. The glass fiber tends to stiffen the epoxy and to reduce the problem of cracking.

Table 8-88 Shear Specimen Static Test Results

Specimen Number	Test Condition	Failure Load (lbs.)	Head Travel (in.)	Calculated Laminae Shear Stress (psi)
2 SR	Room Temperature	6,750	0.0199	2,250
1 SR	Room Temperature	7,610	0.0257	2,537
3 SR	Room Temperature	7,250	0.0215	2,083
4 SR	120°F	4,050	0.0190	1,350
6 SR	120°F	5,000	0.0257	1,667
7 SR	120°F	4,550	0.0230	1,517
5 SR	100°F	5,070	0.0240	1,690
8 SR	100°F	4,740	0.0217	1,580
9 SR	100°F	5,300	0.0222	1,767

Mean Failure Loads

Room Temperature	7,550 lbs.
100°F	5,037 lbs.
120°F	4,533 lbs.

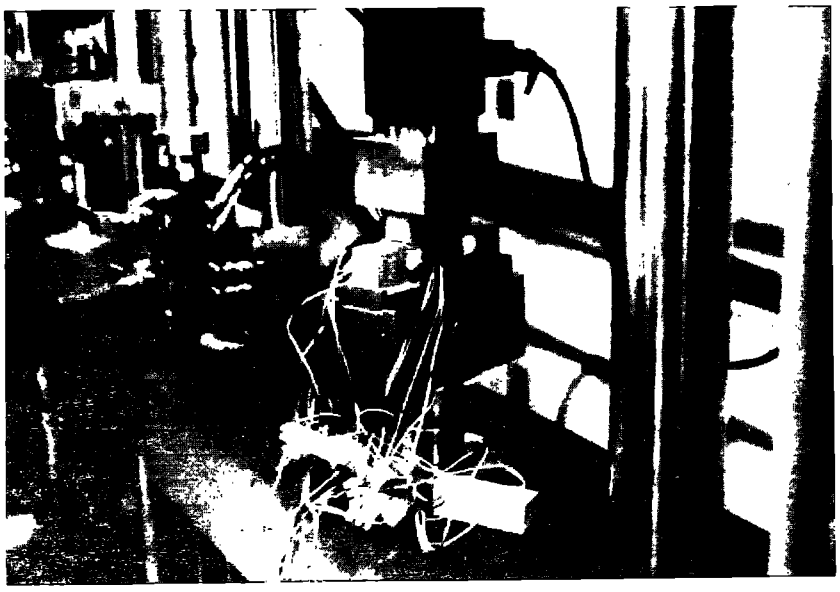

Figure 8-113 Shear Test Setup

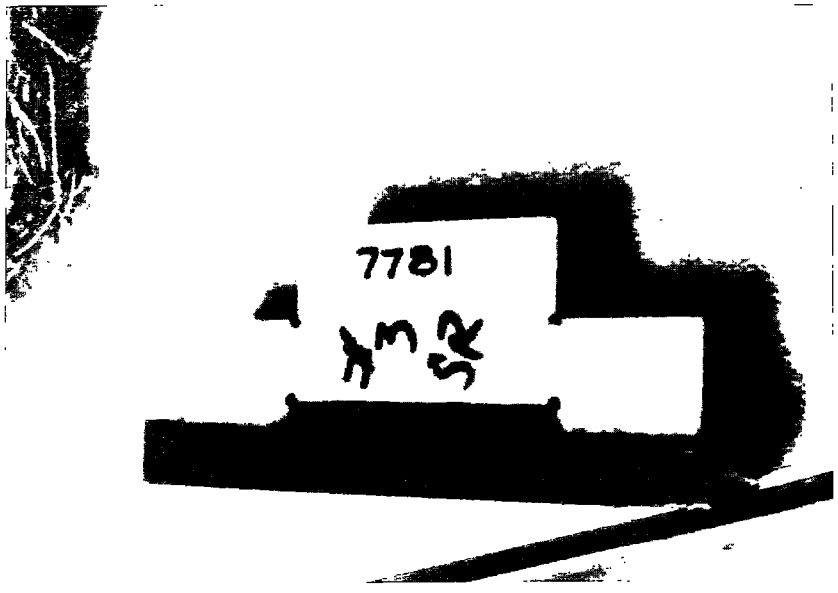

Figure 8-114 Failed Shear Test Specimen

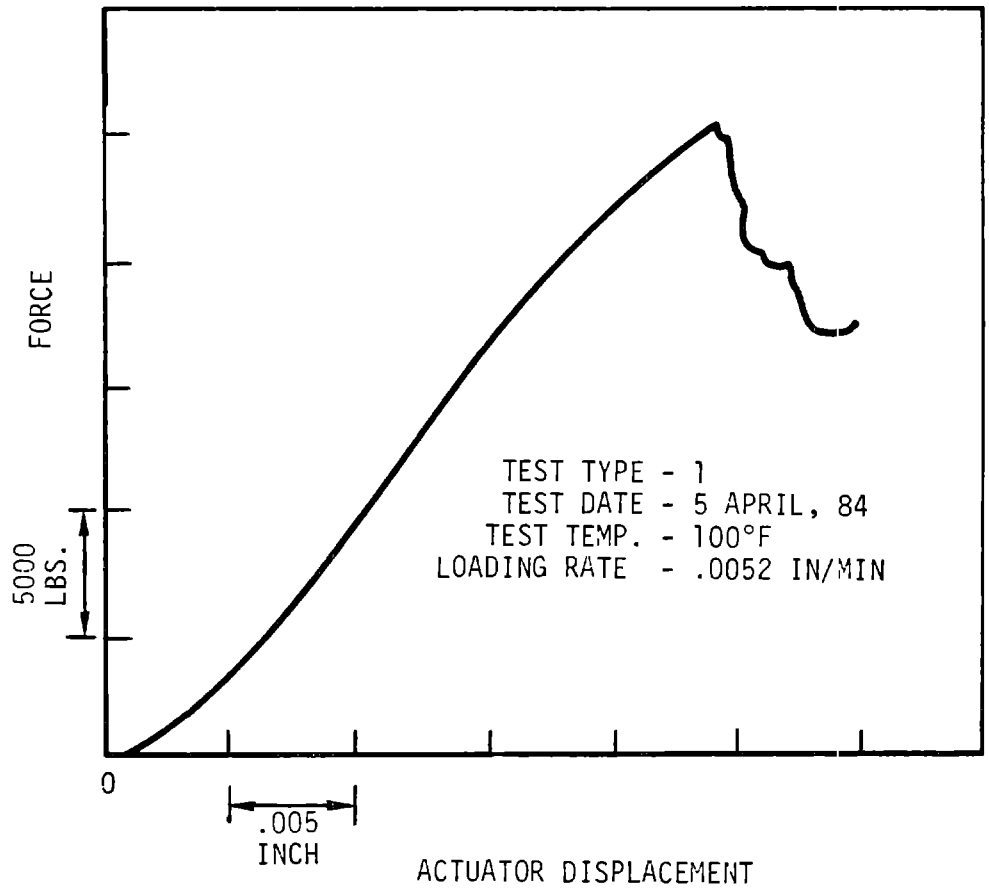

Figure 8-115 Load/Deflection Plot - Shear Test

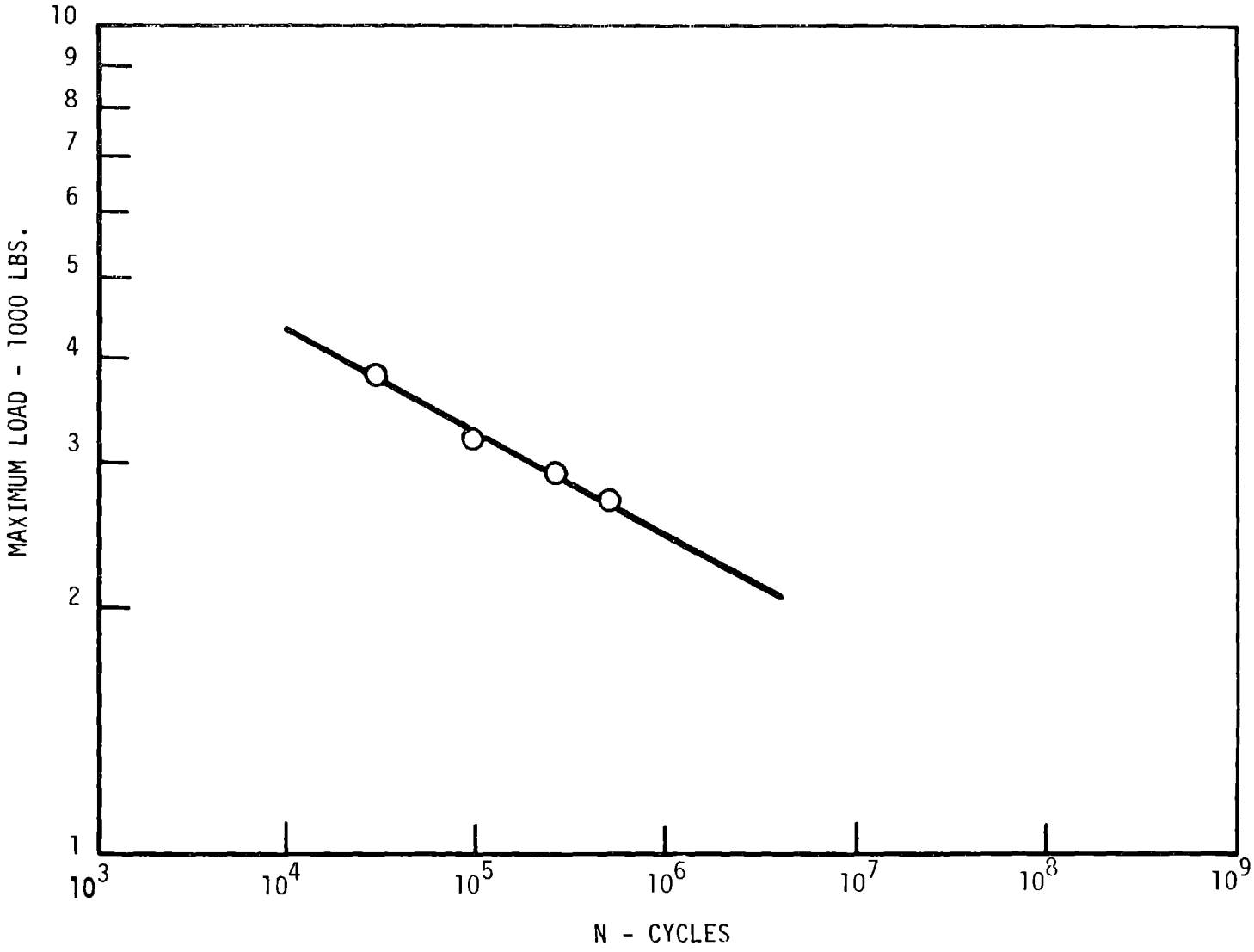

-7-

Figure 8-116 Shear Fatigue Test Results

For the teeter cup application, the glass fiber was 0.125 in. thick, made up of several layers continuously wound in the annulus, with the warp in the direction of the circumference. No data could be found on previous tests of a configuration of this type, so a program was developed to study its static capability at various temperatures and in three different grain directions. Fatigue characteristics in both tension-tension and fully reversed loading conditions were also studied.

8.2.5.2.2 Objectives

The tests provided data on the stress pattern around the circumference, using strain gages. They also determined bearing strength capabilities to permit allowable load limits to be set. Since loading can occur in various directions, because of variations in individual loads, static tests were conducted with the loads parallel to the wood grain, normal to the grain and at 45° to the grain. The high temperature tests were run since the properties of epoxy do change in this range. Fatigue tests were conducted at room temperature only, and only 45° to the grain, since the 45° loading profile was shown to be highest in the MOD-5A blade analysis.

8.2.5.2.3 Description

The test specimens for static testing consisted of a block, 7 in. wide, of ten layers of blade grade 1 Douglas fir veneer with #7781 Burlington glass fiber between each layer. A hole, 4.155 in. diameter, accommodated a hollow steel pin with an outside diameter of 3.875 in. held in place by a single layer wrap of glass fiber and West System® thixotropic epoxy. Figure 8-117 shows a parallel to grain specimen with five rosette strain gages around the pin. Figure 8-118 shows a normal to the grain specimen. The diagonal grain specimen, shown in Figure 8-119, contained eight strain gage rosettes since the loading on the sides of the pin is not symmetrical, because grain induced stiffness paths are not uniform. The test set-up shown in Figure 8-120 was used for all the static specimens. The set-up loaded the wood face on one end while reacting the pin. The MTS machine used for testing controlled the stroke rate to produce failure in approximately 5 minutes. Figure 8-121 shows an Instron oven in place on the MTS machine, the set-up used for all high temperature testing. A second MTS oven was used in a remote location for pre-conditioning the specimens before they were placed in the test machine.

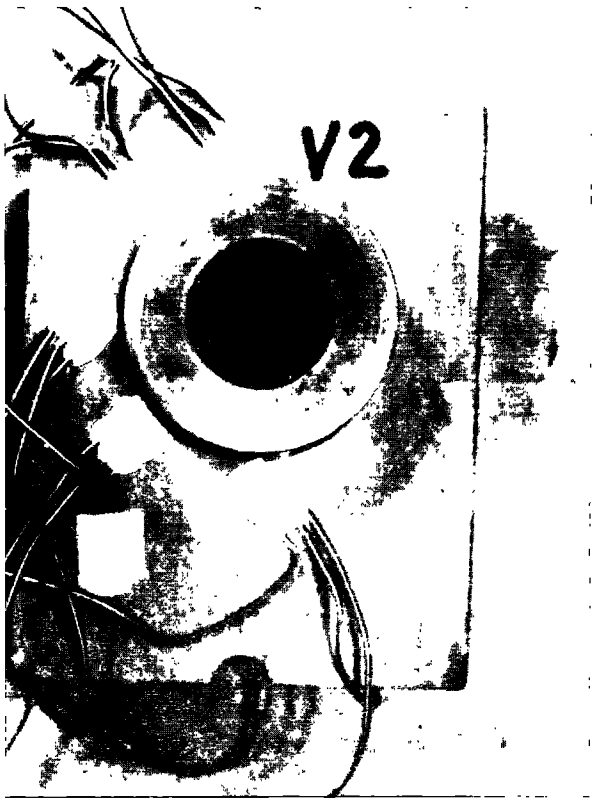

Figure 8-117 Parallel to Grain Static Bearing Test Specimen

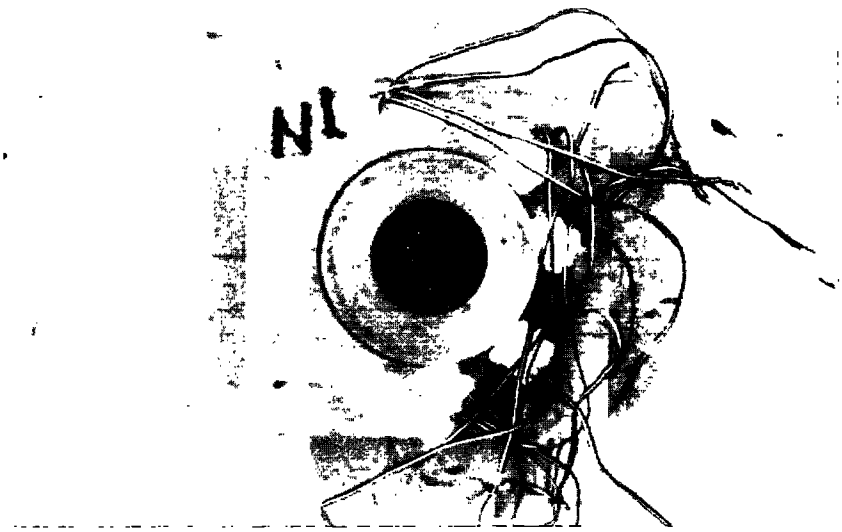

Figure 8-118 Normal to Grain Bearing Test Specimen

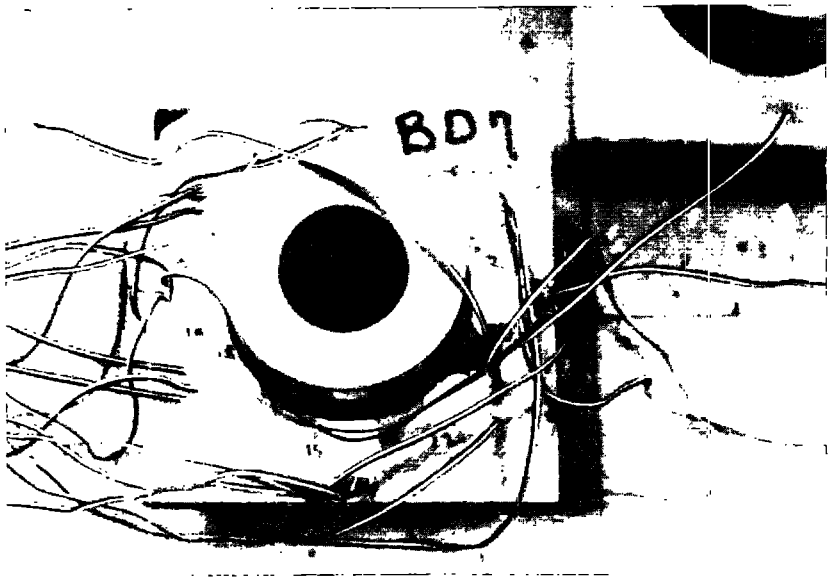

Figure 8-119 Diagonal Grain Bearing Test Specimen

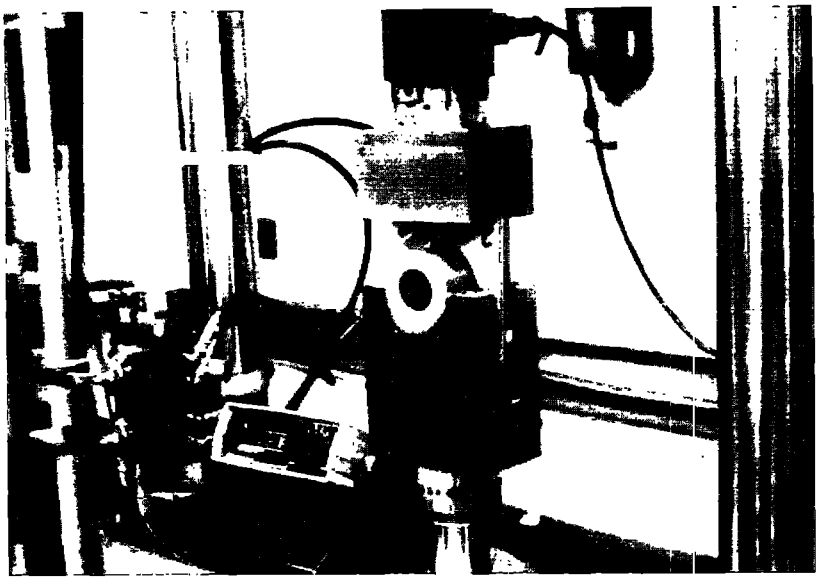

Figure 8-120 Typical Bearing Test Setup for Static and Tension-Tension Fatigue

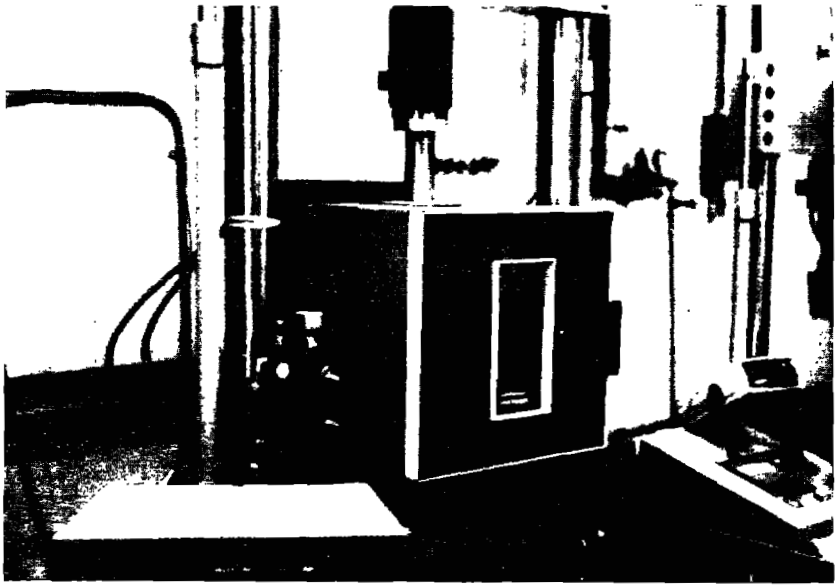

Figure 8-121 Elevated Temperature Bearing Test Setup with Instron Oven

The ovens were used to achieve and maintain temperatures of 100°F or 120°F for testing three static specimens of each of the three grain directions at each temperature.

Two different load ratios were used for fatigue testing. For a load ratio of 10 the diagonal specimen, shown in Figure 8-119, and the static test set-up in Figure 8-120, were used.

For reverse axial testing, it was necessary to use an alternate test specimen as shown in figure 8-122. The (R=-1) test specimen had two steel pins to allow loads to be reacted in both directions. The fixtures are shown in Figure 8-123. The upper end of the specimen was 7 in. wide, the same geometry as the other samples. The lower end was wider and had a larger pin diameter to prevent failure from occurring there. Four specimens of each type (diagonal grain only) were fatigue tested at a frequency of 2 Hz or 5 Hz for R = 20, and 5 Hz for R = -1. The intent was to achieve two failures at 10,000 cycles and two at one million.

8.2.5.2.4 Results

Static test results are shown in Table 8-89, with mean failure loads listed for each set of conditions. Failures were not catastrophic, but were accompanied by cracking sounds. In the parallel to grain and diagonal grain failures, the epoxy separated from the steel pin on the side opposite of the load application (tension in joint). The failure was evidenced by a lower frequency response in the area when the wood was tapped around the pin circumference. The normal to grain specimens at all three temperatures failed by having the wood crush (compression failure) between the load application and pin, as shown in Figure 8-124, and in some cases, bond damage was also detected. On some of the specimens crazing of the epoxy was visible, and on some a gap between the pin and epoxy could be discerned in areas of failure. The temperature effect was significant. In the case of the diagonal grain specimens, heat reduced the mean strength of the specimen tested at 120° by more than 50%. Figures 8-125, 8-126 and 8-127 depict the load versus head travel plots for samples of each type at each temperature.

Fatigue testing of diagonal grain specimens commenced with compression-compression testing of specimen DF1. The machine load setting was inadver-

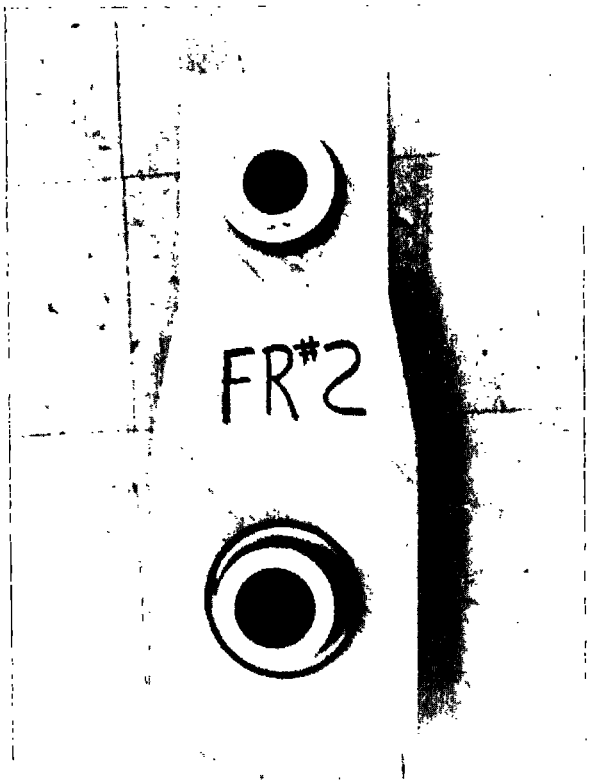

Figure 8-122 Reverse Axial Bearing Fatigue Specimen

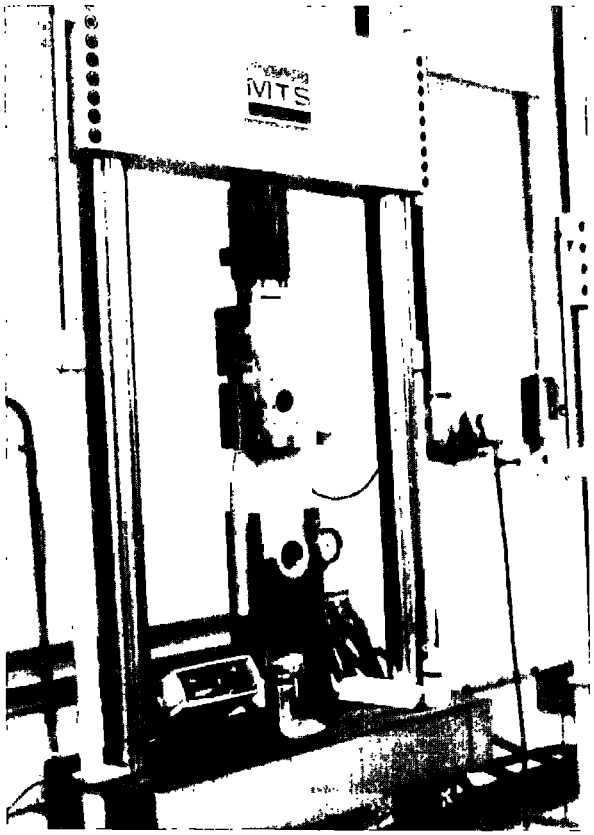

Figure 8-123 Reverse Axial Bearing Fatigue Test Setup

Table 8-89 Bearing Specimen Static Test Results

Room Temperature Tests				100°F Tests				120°F Tests			
Specimen Number	Grain Direction	Failure Load (lbs.)	Head Travel (in.)	Specimen Number	Grain Direction	Failure Load (lbs.)	Head Travel (in.)	Specimen Number	Grain Direction	Failure Load (lbs.)	Head Travel (in.)
V7	Parallel	21,250	0.0280	V4	Parallel	20,700	0.0410	V1	Parallel	21,750	0.0538
V8	Parallel	38,500	0.0530	V5	Parallel	27,750	0.0490	V2	Parallel	21,750	0.0440
V9	Parallel	36,500	0.0478	V6	Parallel	22,250	0.0408	V3	Parallel	22,510	0.0475
	Mean =	32,167			Mean =	23,633			Mean =	22,003	
						(73.5% RT)				(68.4% RT)	
N1	Normal	23,500	0.0463	N4	Normal	18,000	0.0575	N7	Normal	14,000	0.0625
N2	Normal	23,350	0.0438	N5	Normal	19,000	0.0503	N8	Normal	13,600	0.0525
N3	Normal	23,000	0.0432	N6	Normal	17,000	0.0502	N9	Normal	13,850	0.0675
	Mean =	23,288			Mean =	18,000			Mean =	13,817	
						(77.3% RT)				(59.3% RT)	
BD7	Diagonal	32,500	0.0696	BD4	Diagonal	23,250	0.0688	BD1	Diagonal	13,150	0.0633
BD8	Diagonal	30,000	0.0522	BD5	Diagonal	26,850	0.0685	BD2	Diagonal	17,400	0.0720
BD9	Diagonal	30,400	0.0544	BD6	Diagonal	24,250	0.0550	BD3	Diagonal	15,000	0.0660
	Mean =	30,967			Mean =	24,783			Mean =	15,183	
						(80.0% RT)				(49.0% RT)	

Figure 8-124 Static Failure of Normal to Grain Bearing Specimen

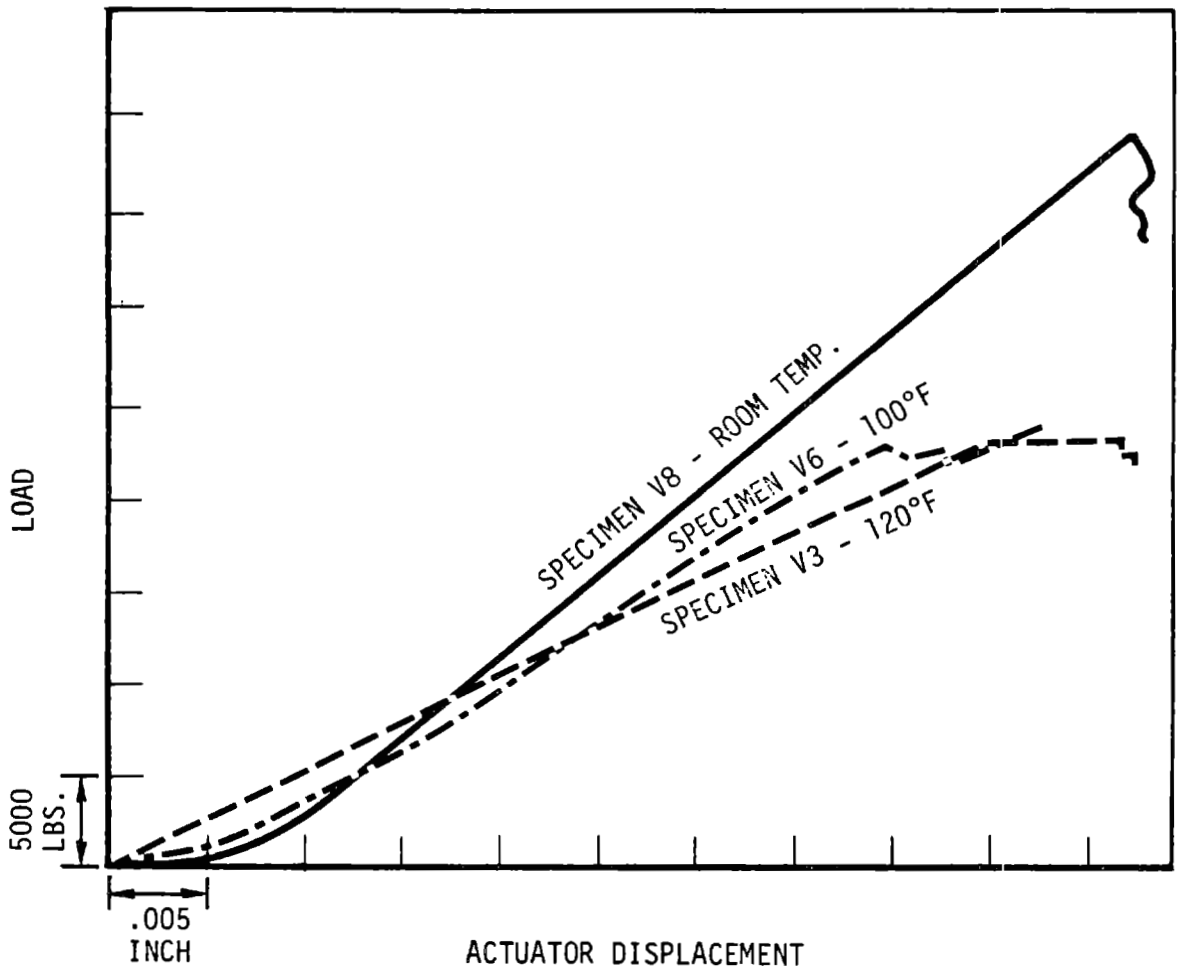

Figure 8-125 Static Bearing Test - Parallel to Grain

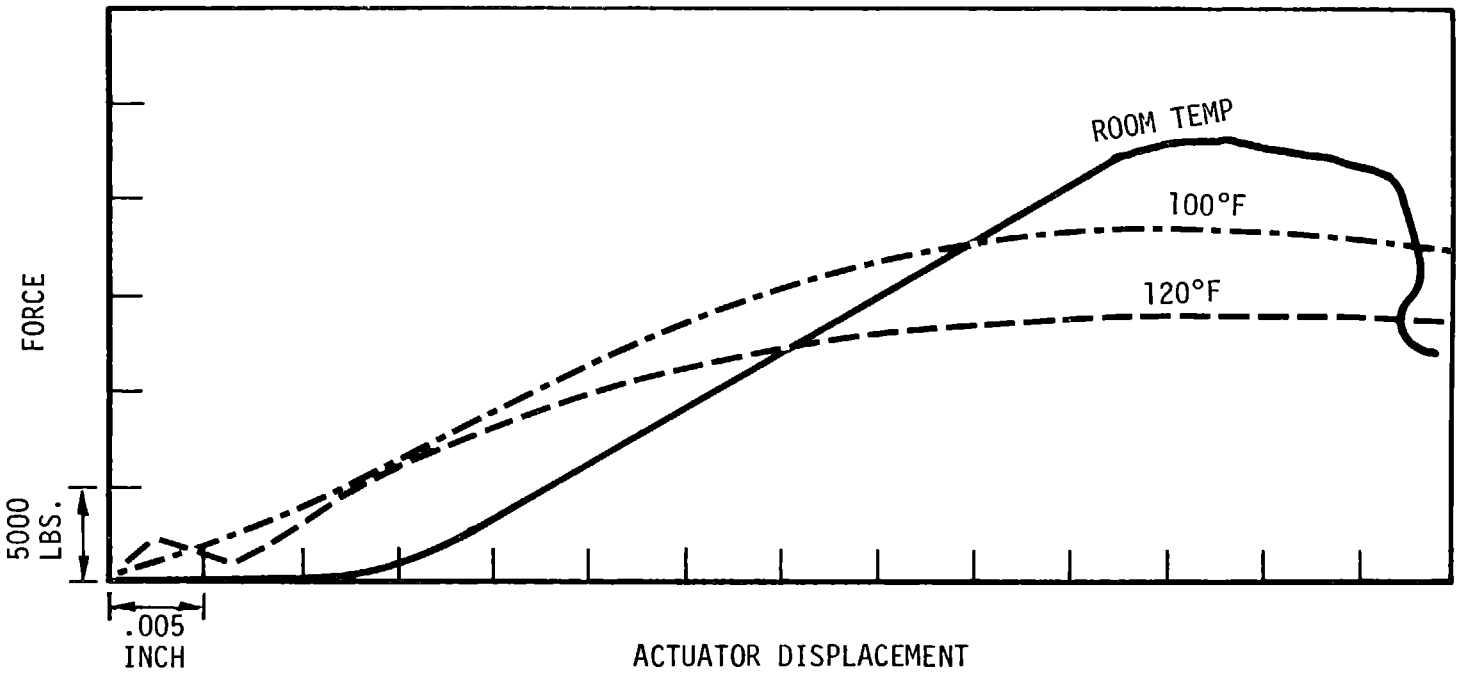

Figure 8-126 Static Bearing Test - Normal to Grain Loading

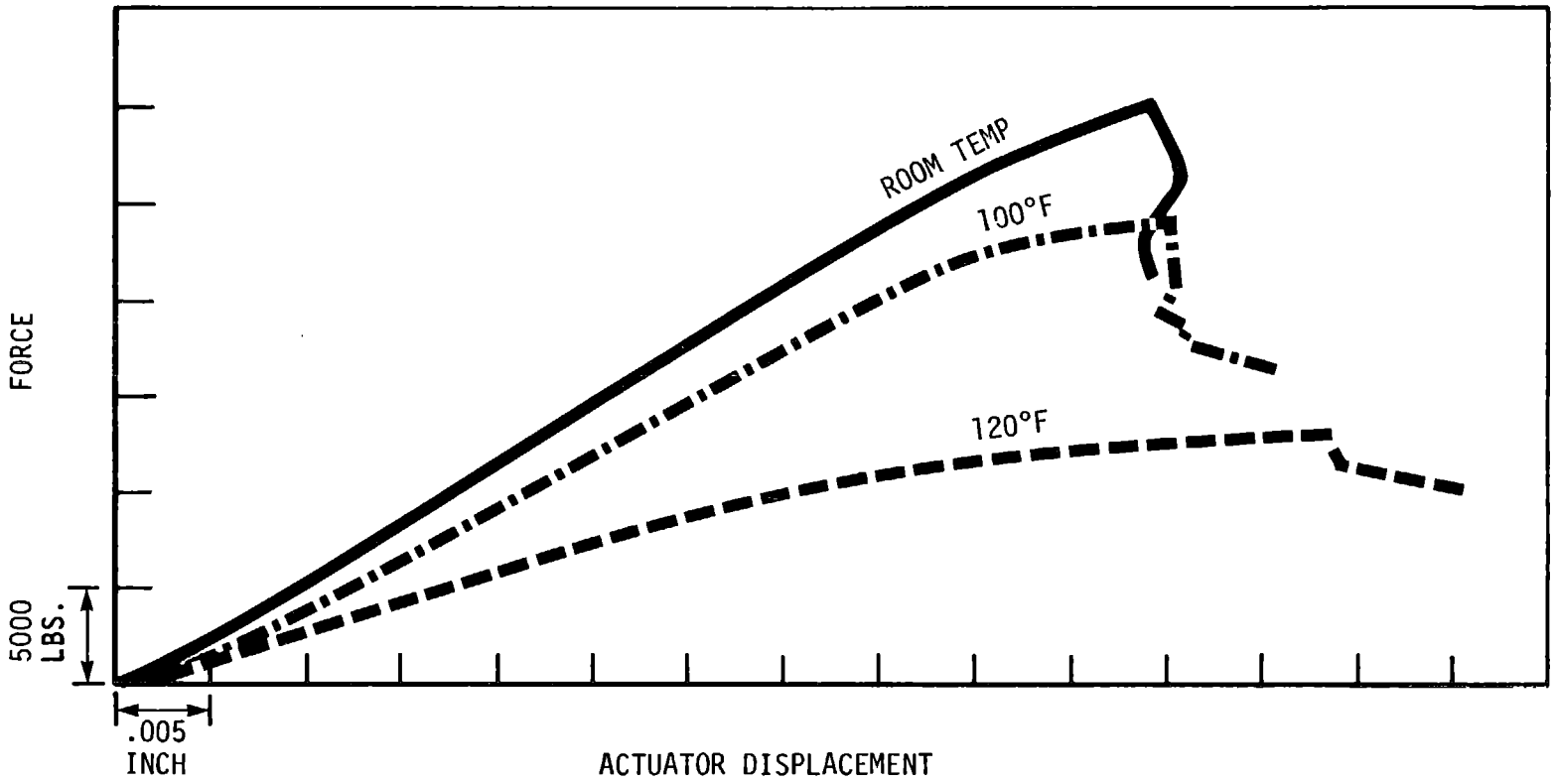

Figure 8-127 Static Bearing Test - Diagonal Grain

tently placed at the range of -15,000 and -1,250 lbs., a load ratio of 12 instead of the intended 20. The sample survived 695,000 cycles at 5 Hz before failing. Specimen DF2 was then tested at the range of -14,500 lbs. and 725 lbs. and at a frequency of 5 Hz. After 902,700 cycles the frequency was decreased to 2 Hz because of accumulating damage, and at 906,900 cycles ultimate failure occurred. Sample DF3 was tested at a higher load: 19,000 to 950 lbs., for failure near 10,000 cycles. The test frequency was set at 5 Hz, and failure occurred after 61,000 cycles. For the last specimen, DF4, the load range was increased to -20,000 and -1,000 lbs. and rate of 2 Hz was maintained for the 27,900 cycle life of this sample.

Fully-reversed fatigue testing was completed next. The load range for specimen number FR1 was set at ±10,000 lbs., but the range was never achieved, because the specimen failed prematurely, as shown in Figure 8-128. The load for sample FR2 was set at ±2,300 lbs. Load versus head travel traces were recorded at frequent intervals, as shown in Figure 8-129. Damage occurred between 5,000 cycles and 55,600 cycles, which resulted in a looseness of the sample. A tapping test revealed that the steel to epoxy joint had failed. The next specimen, FR3, was subjected to a load of ±1,900 lbs. The test was halted after one million cycles with no evidence of ultimate failure. However in the load deflection plot in Figure 8-130, some degree of damage occurred around 5,000 cycles, resulting in a change of slope for the tension side of the load. Only minor changes occurred after that point. Specimen FR4 was tested at the same load: ±1,900 lbs. Between 35,000 and 52,000 cycles a slope change occurred, and after 409,700 cycles a definite offset occurred at the crossover point. Figure 8-131 is a plot of the fatigue test results of specimen FR-4 and Figure 8-132 shows results of all samples.

8.2.5.3 Teeter Brake Shaft Bearing Load Distribution Test

8.2.5.3.1 Introduction

The center section of the MOD-5A blade contained augmented bolsters and interface fittings for the teeter shaft and teeter brake. The relatively complex geometry and the use of composite materials indicated the need for a finite element program to determine stress levels and failure modes.

8.2.5.3.2 Objectives

This test sequence determined the stress field pattern and levels around the teeter brake area when loads are introduced through the brake pins. It also

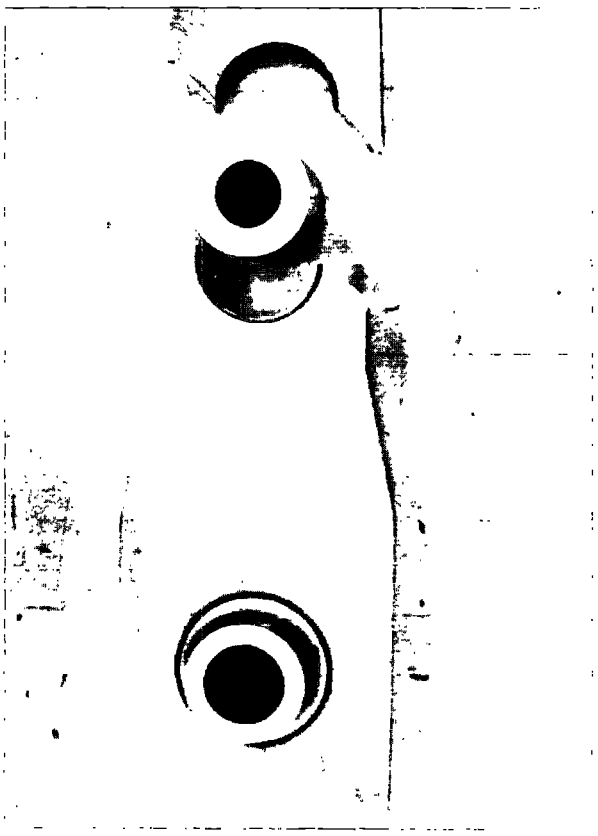

Figure 8-128 Fully Reversed Bearing Fatigue Specimen FR1 Inadvertently Overloaded

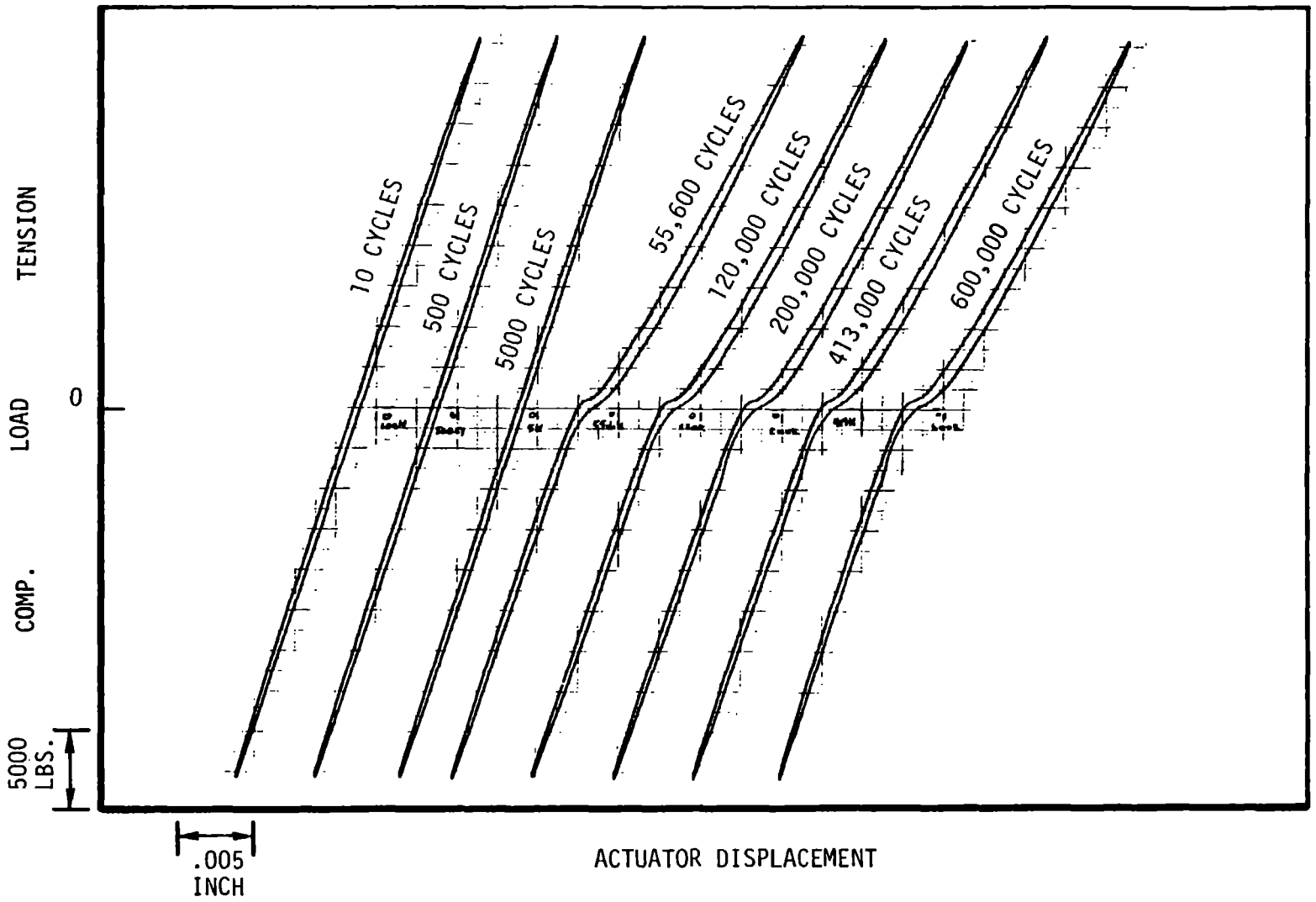

Figure 8-129 Load-Deflection Plot of Fatigue Specimen FR-2

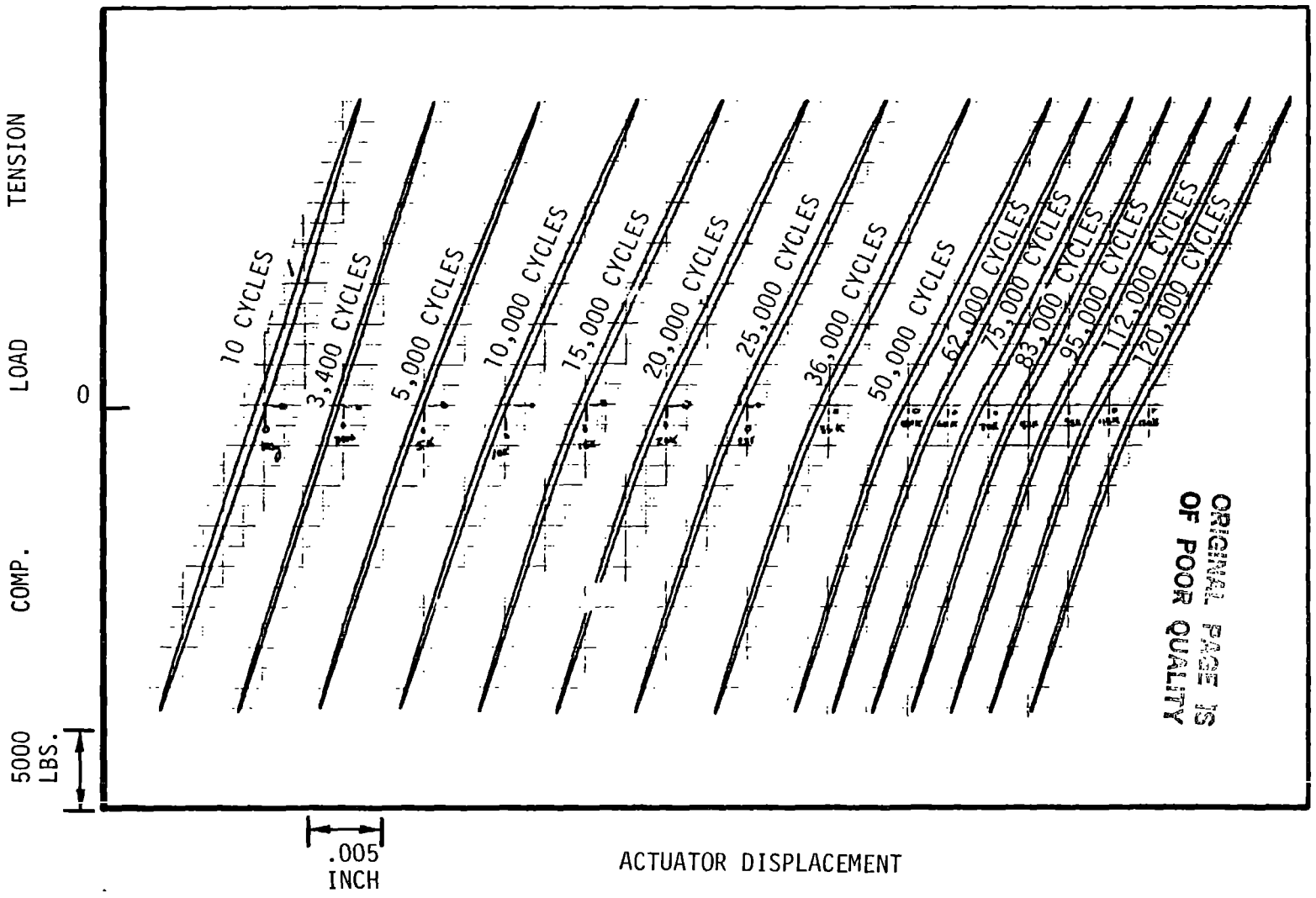

Figure 8-130 Load Deflection Plot of Specimen FR-3

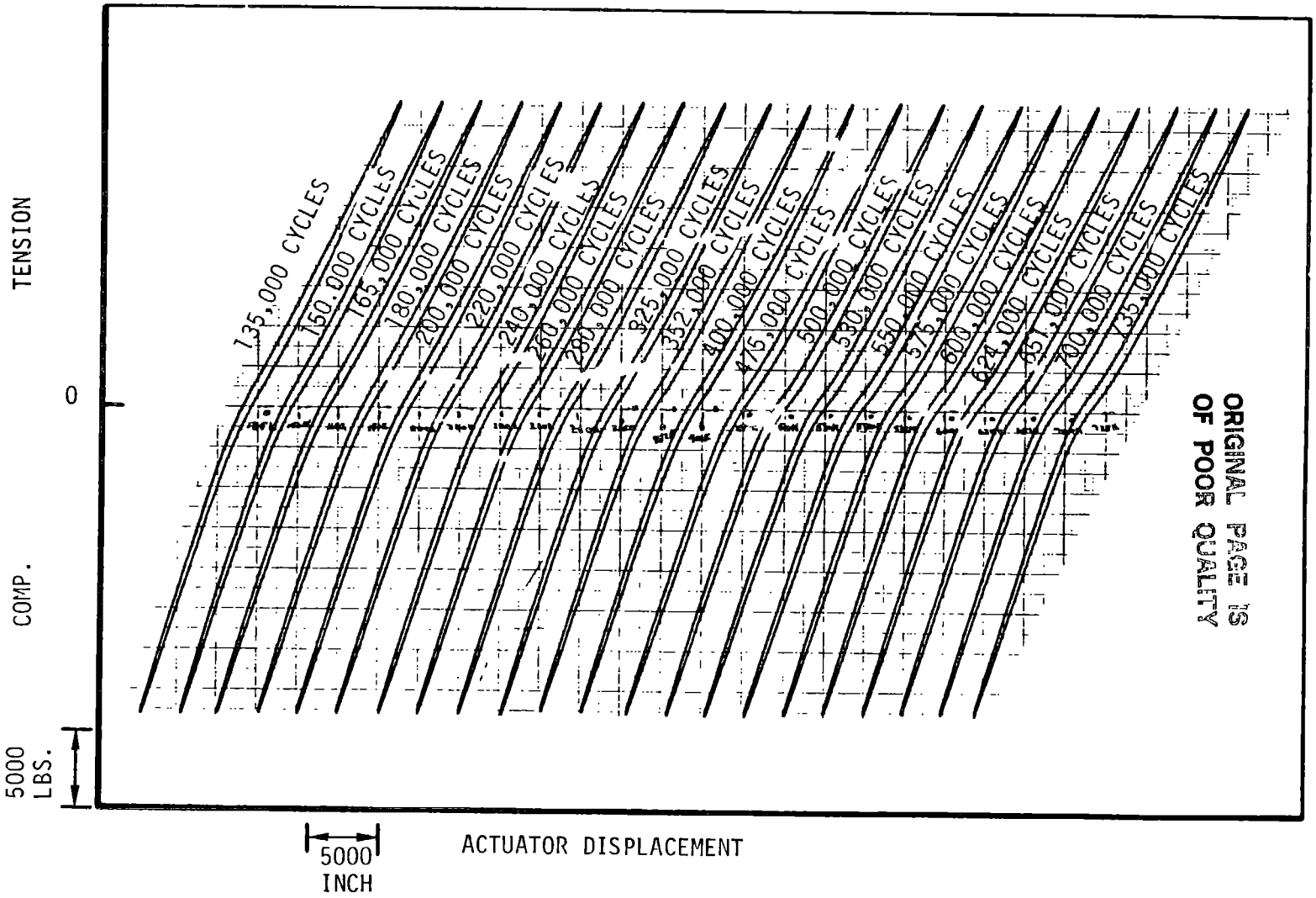

Figure 8-130 Load-Deflection Plot of Specimen FR-3 (Continued)

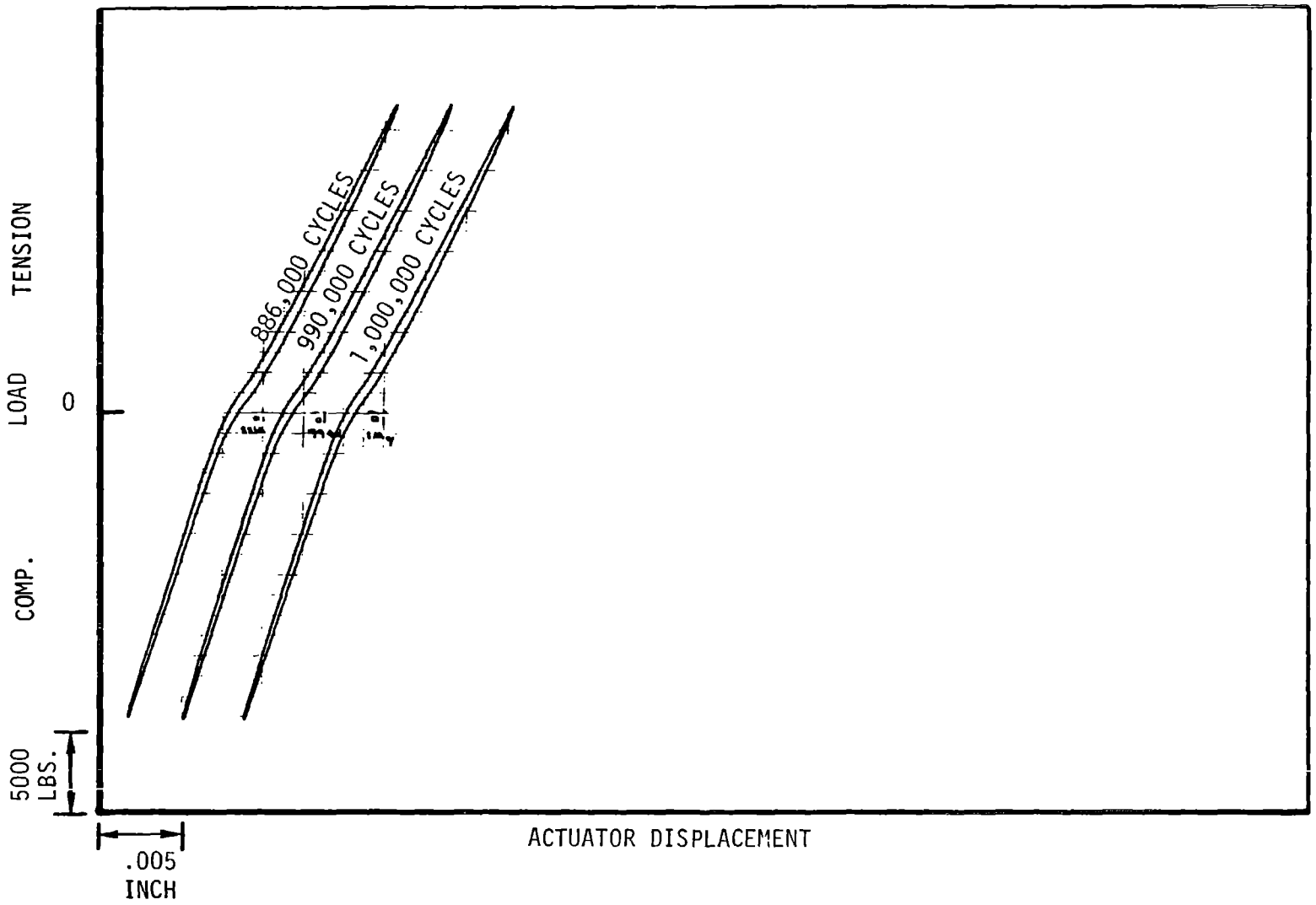

Figure 8-130 Load-Deflection Plot of Specimen FR-3 (Continued)

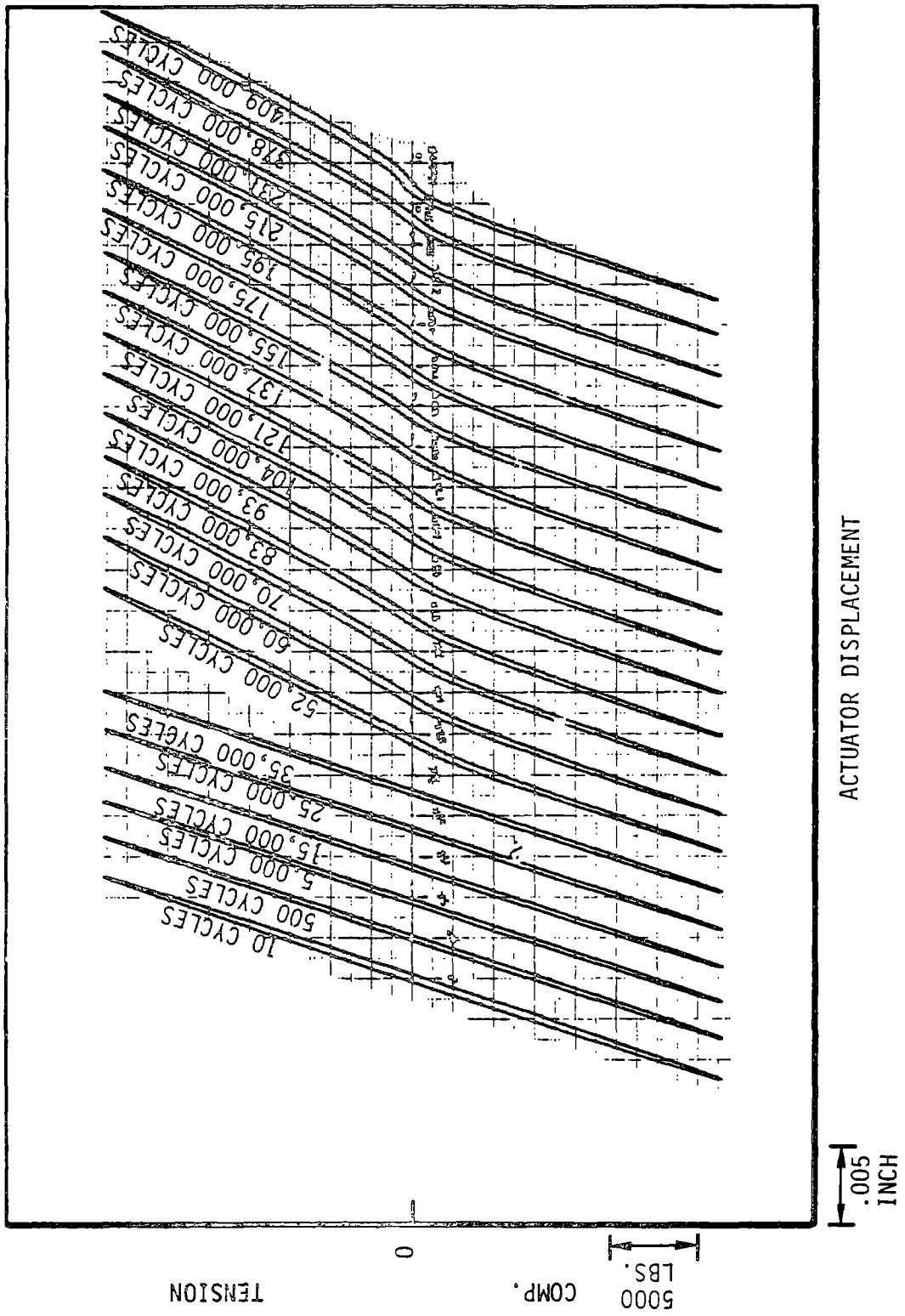

Figure 8-131 Load-Deflection Plot of Specimen FR-4

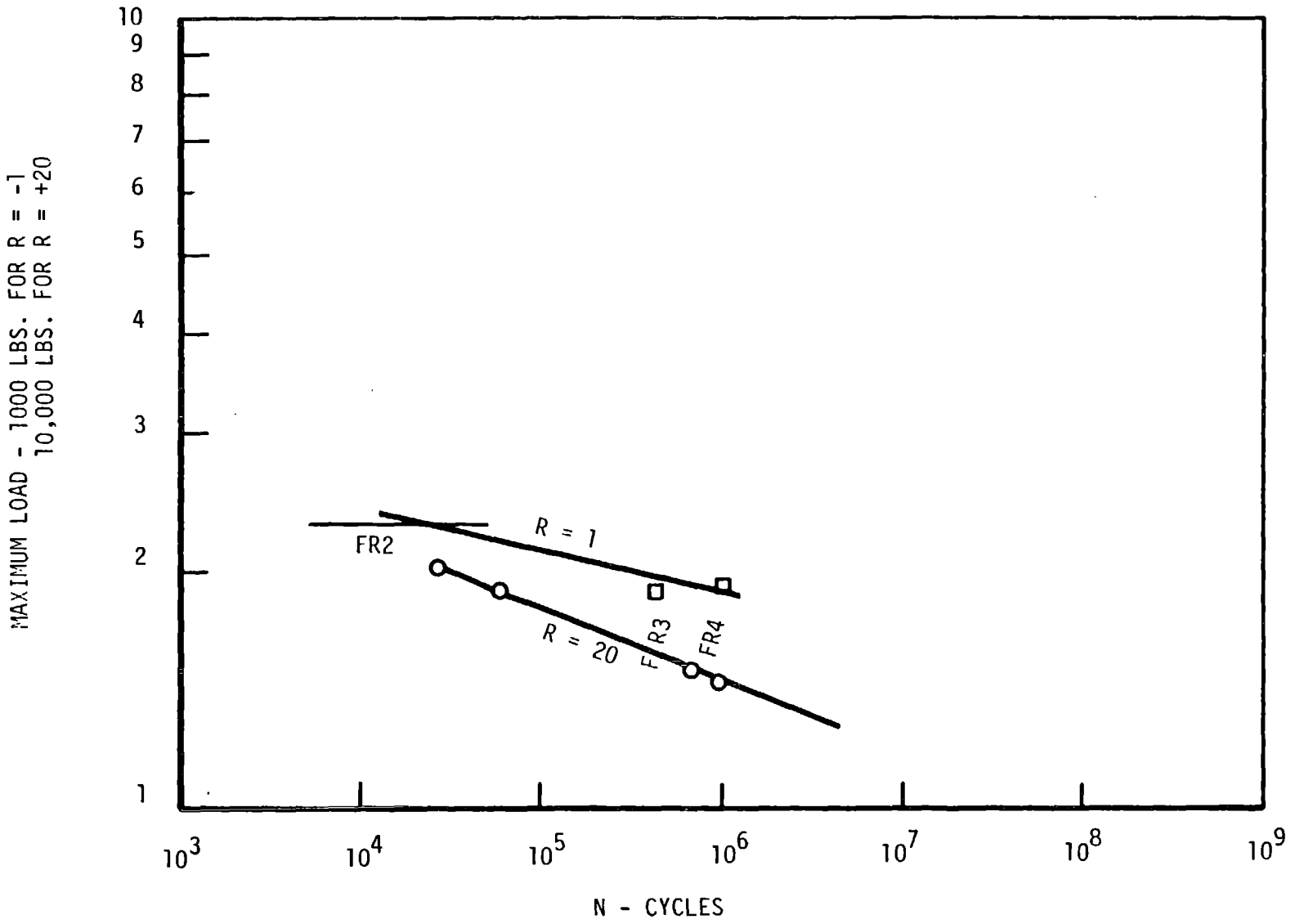

Figure 8-132 Bearing Test Fatigue Data

provided failure mode information, as well as the fatigue life of the simulated blade section. This information will be used to substantiate the finite element model, by creating a program specifically for the test configuration, which will be compared to the test data to verify stress distribution and failure modes.

8.2.5.3.3 Description

The test specimen was 130.8 in. long, representing the center blade area. One end contained the bolster and shaft fittings and the opposite end had a load reaction shaft. The specimen contained model bolsters on a scale of 1/10, and was mounted in a test fixture that interfaced with a four-post MTS test machine. The fixture mounted the specimen at the load reaction point and the outer brake pin fitting, while the load was applied to the inner brake pin fitting through the use of simulated straps and pins. Figure 8-133 shows the specimen, and Figures 8-134 and 8-135 show the test set-up.

The loading pin area was instrumented on two of three static test specimens. Eight strain gage rosettes were used on each side of the specimen, as shown in Figure 8-136. The specimens were loaded in bending, using a 5 minute load ramp to approximately the ultimate load. The brake pin lug exit side of the specimen was in tension (pull on lugs) in all tests.

Following the three static tests, four fatigue test samples were tested using a load ratio of 0.05. No strain gages were used on the fatigue samples.

8.2.5.3.4 Results

The static test specimens all failed in a similar manner: the brake pins bent, the bolsters sheared along the beam interface plane and the beam end cracked. Figure 8-137 shows a bent brake pin after removal with sleeve, Figure 8-138 shows the bolster with crack and Figure 8-139 shows the beam end crack. The loads required to induce failure are listed in Table 8-90, and a typical load deflection plot is shown in Figure 8-140.

Sample number 7 was subjected to the fatigue load range of 16,500 to 825 lbs. with tension on the brake straps. The test was halted after 7,100 cycles at a rate of 1 Hz, when the wood under the brake shaft fitting showed evidence of

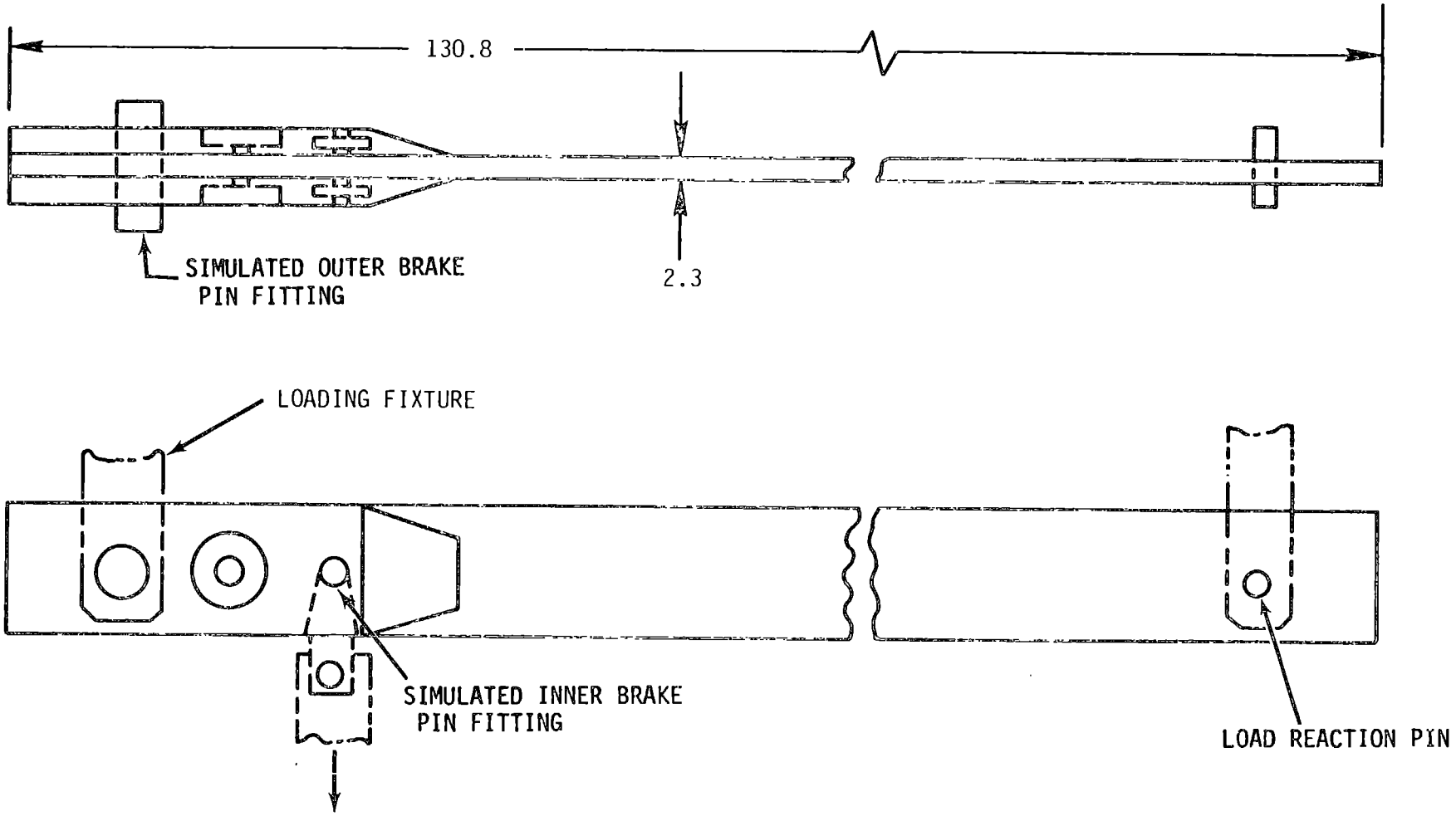

Figure 8-133 Test Specimen #3 (Teeter Brake Load Distribution)

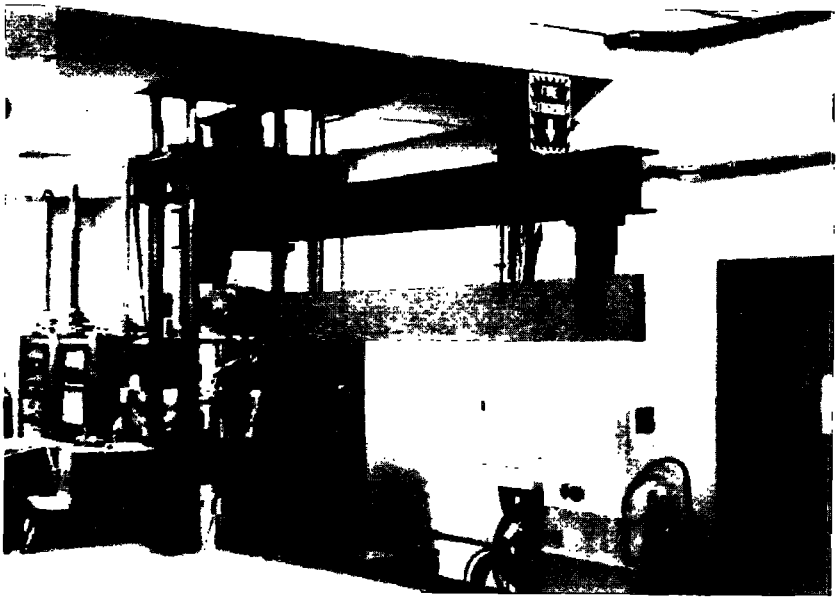

Figure 8-134 Test Setup, Teeter Brake Shaft Load Distribution Test

Figure 8-135 Loading Area of Setup

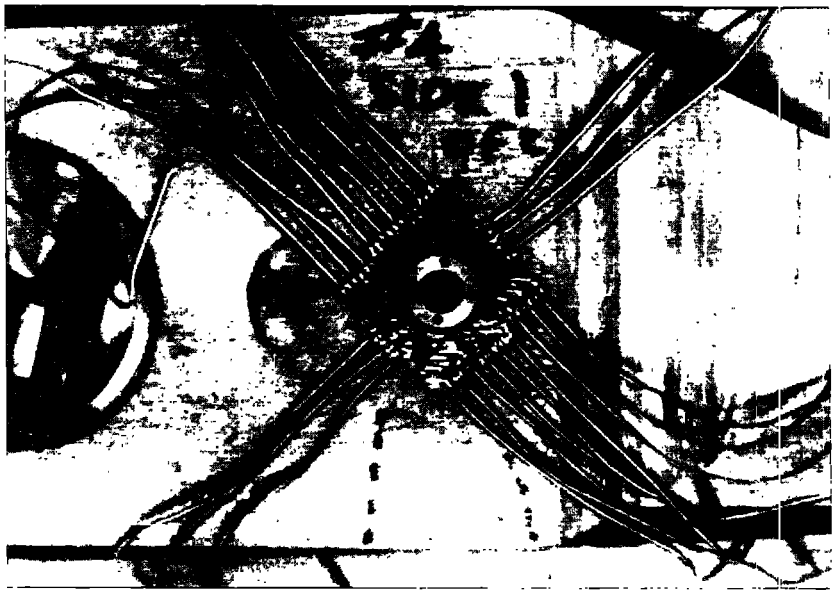

Figure 8-136 Strain Gages Around Teeter Brake Pin

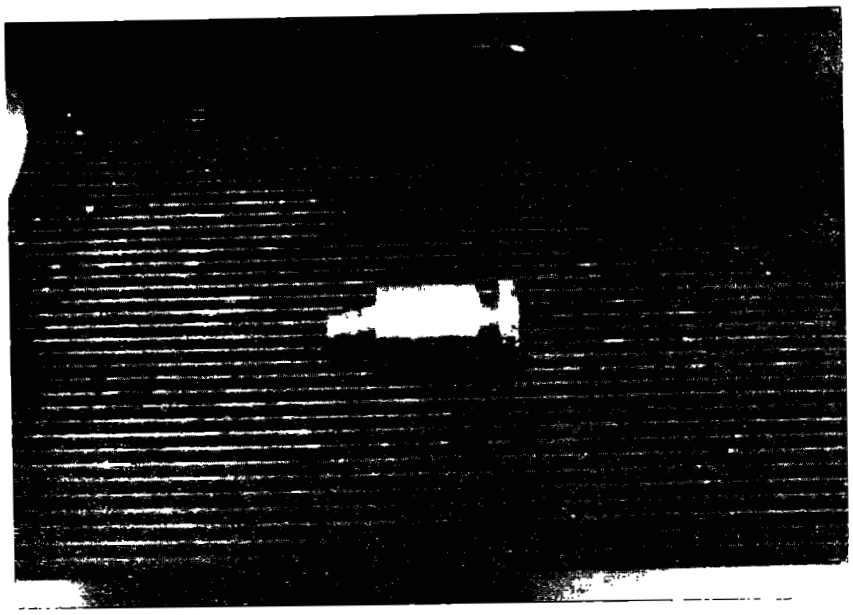

Figure 8-137 Bent Brake Pin and Sleeve

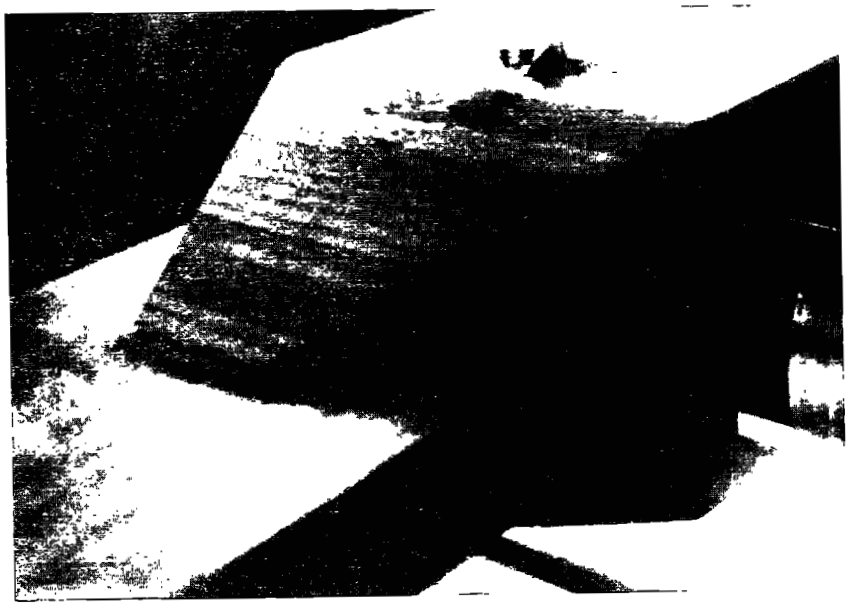

Figure 8-138 Bolster Shear Plane

Figure 8-139 Beam End Failure

Table 8-90 Failure Loads

Specimen Number	Ultimate Load (lbs.)	Load at First Offset (lbs.)
3	27,000	20,000
4	28,000	22,500
5	27,500	20,000
Mean	27,500	20,833

Fatigue

Specimen Number	Load Range (lbs.)	Frequency Hz	Number of Cycles
7	16,500 to 825	1	7,100
6	12,000 to 600	2	207,800
2	10,500 to 500	1	10^6
1	11,000 to 550	2	10^6

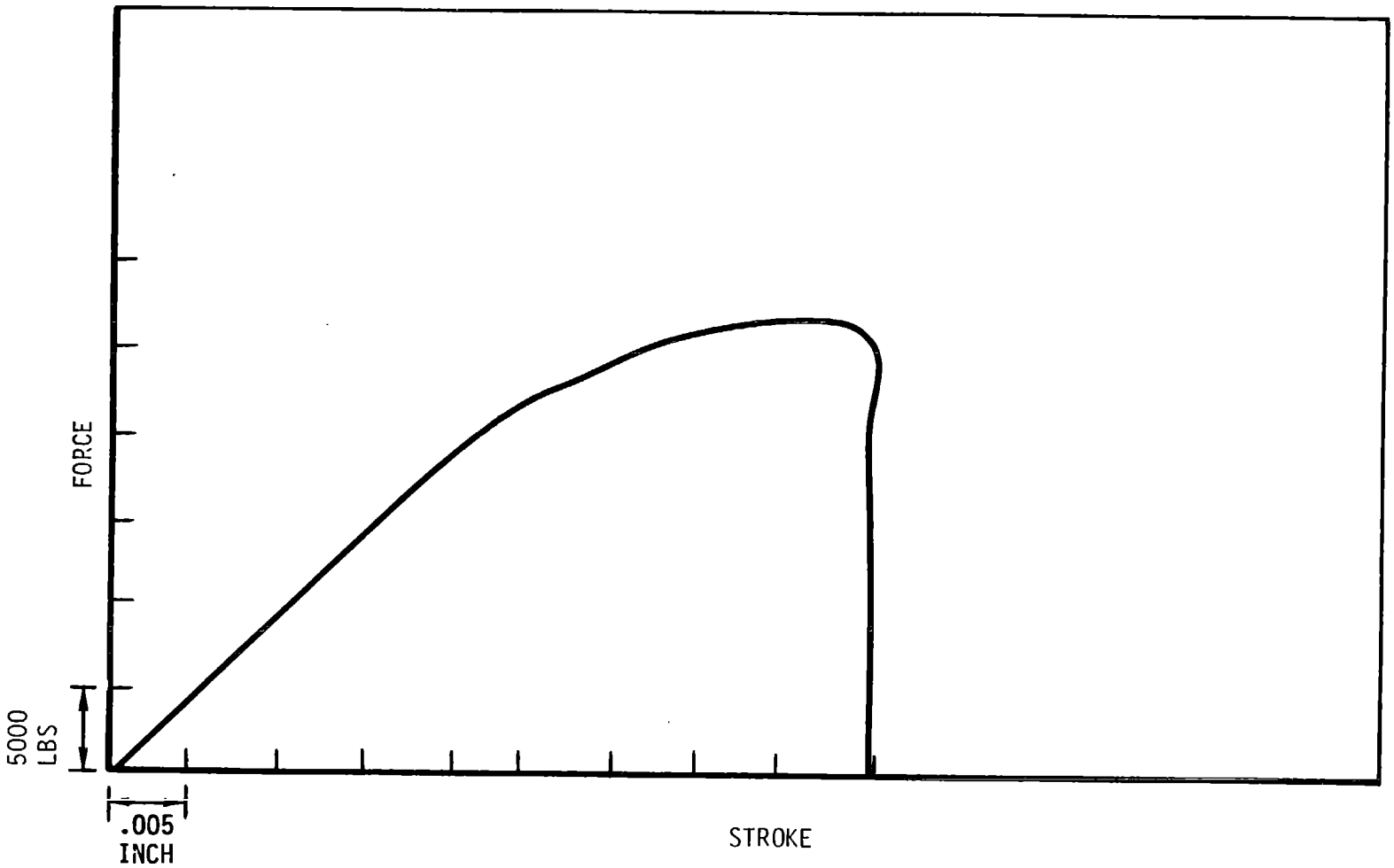

Figure 8-140 Typical Teeter Brake Static Test Load-Deflection Plot Sample Number 3

severe bearing-type failure. Sample 6 was tested next. The test rate was increased to 2 Hz, and the load range decreased to 12,000 to 600 lbs., with a goal of one million cycles. After 207,800 cycles a similar failure became apparent and the test was halted. Specimen 2 then was subjected to the load range of 10,500 to 500 lbs. at a rate of 2 Hz, and it reached one million cycles with no evidence of failure. Testing was halted at that point. A slightly higher load range, 11,000 and 550 lbs., was applied to specimen number 1 at the rate of 2 Hz. This test was stopped after no sign of damage at one million cycles, and the specimen was subjected to a residual static strength test. It reached an ultimate load of 26,000 lbs., and the first offset occurred at 21,000 lbs. The failure was somewhat different from those of the three static tests, in that the beam element cracked in the area of the bolster taper, not at the extreme bolster end. The loads, however, were consistent, and were higher than predicted.

8.2.5.4 Flapwise Bending Tests

8.2.5.4.1 Introduction

This test series also concentrated on load distribution in the center blade area, as did the teeter area brake tests described in previous. The rationale was to test a scaled model on a scale of 1/12, and to compare the results to those of a finite element model developed for the test specimen geometry. The computer program would be similar to the type used for the MOD-5A blade analysis, so the blade analysis technique would be verified by this test. The bolsters were augmented with #7781 Burlington glass fiber cloth, but the center beam section was not. This design made the model more complex.

8.2.5.4.2 Objectives

The objectives of this series of tests were to determine static and fatigue bending strength, failure mode and load distribution data for the center blade area when loads are introduced through the teeter cup.

8.2.5.4.3 Description

The flapwise bending test specimen was 130 in. long as shown in Figure 140A. It contained reaction pins near the ends and a simulated bolster and teeter bearing cup set at the center where loads were imposed. It also had a complement of slots and brake pin fittings so that their effect on load distribution could be studied. Figure 8-141 shows the specimen mounted in

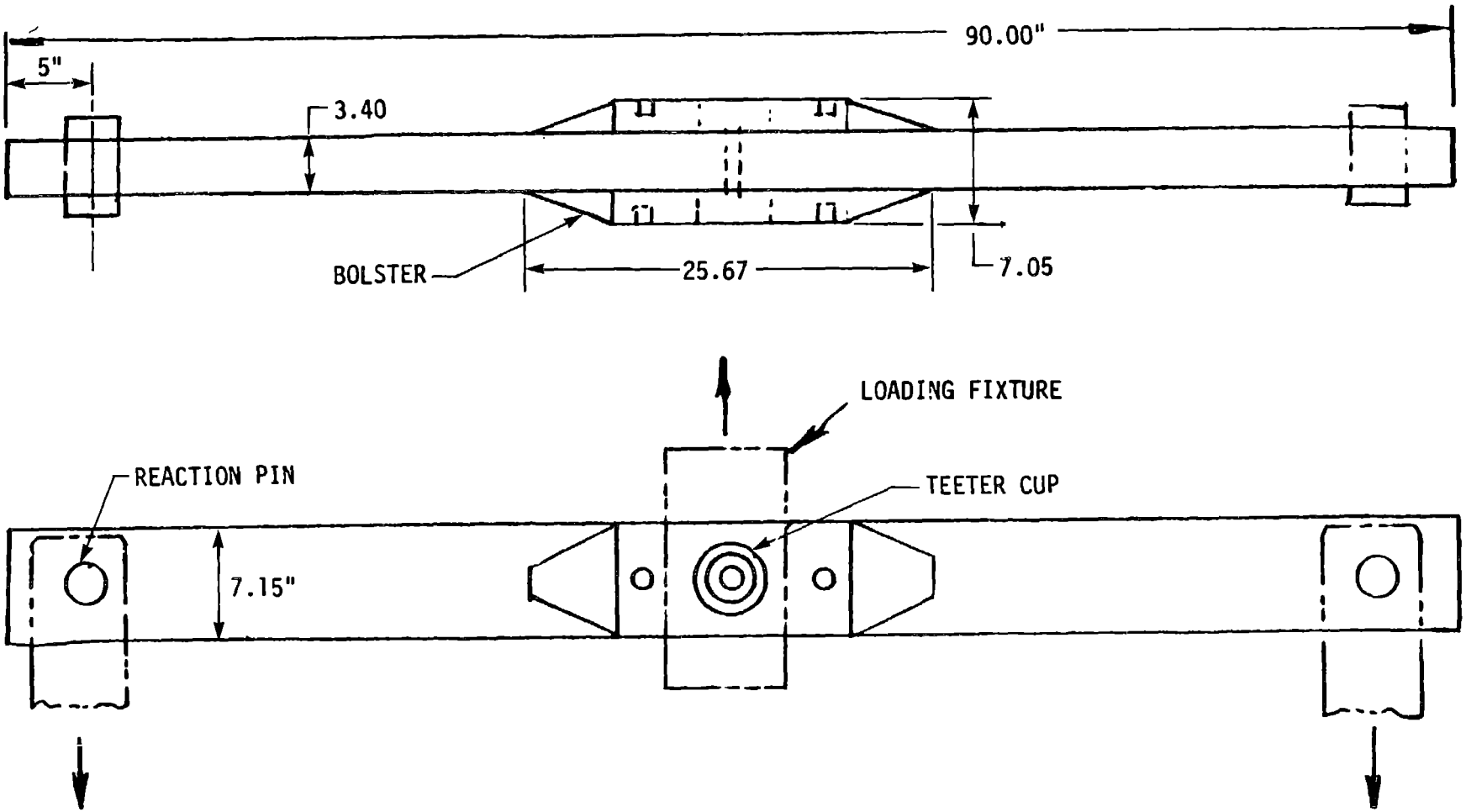

Figure 140A **Flapwise Bending Test Specimen**

Figure 8-141 Flapwise Bending Test Setup

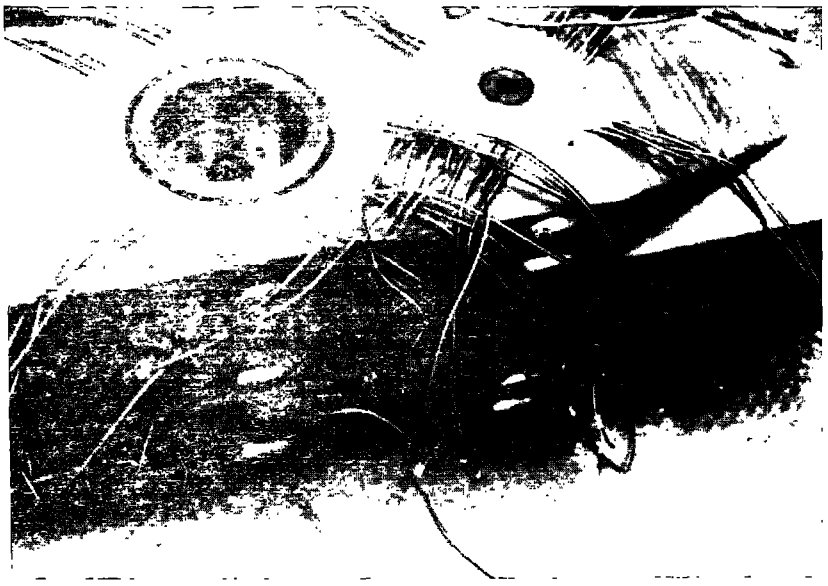

Figure 8-142 Strain Gage Locations

a test fixture that is mounted in an MTS four-post test machine. The actuator imposed a load on the center of the specimen, which was reacted at the end points by fittings mounted to the overhead fixture beam. The load cell was mounted between the actuator rod and the aperture fitting surrounding the sample. On two of the three static test specimens, strain gages were located around the teeter cup, brake pin bushing, and on the edge grain face of the beam. Seven rosettes were used around the teeter cup, eight rosettes surrounded the brake pin fitting and a total of 14 axial gages were used on the edge grain faces, as shown in Figure 8-142. The three static test specimens were tested using an approximate 5 minute load ramp to failure. The edge grain face had teeter brake slots placed in compression.

8.2.5.4.4 Results

The failure mode was consistent for all three static tests. The bolsters were sheared from the center beam section either cleanly, as shown in Figure 8-143, or a few layers of unaugmented wood remained intact, as shown in Figure 8-144. The test results are tabulated in Table 8-91, and Figure 8-145 shows a typical load deflection plot.

Specimen number 5 was subjected to a cyclic load from 8,000 to 400 lbs. (R = 0.05) at a frequency of 1.5 Hz, with the slotted face of the specimen in compression. Some bolster bond line cracking was noticed at 645,000 cycles, but the test ran to 1.05 million cycles and was stopped although no serious damage occurred. Sample number 2 was tested next at 9,600 and 480 lbs., and

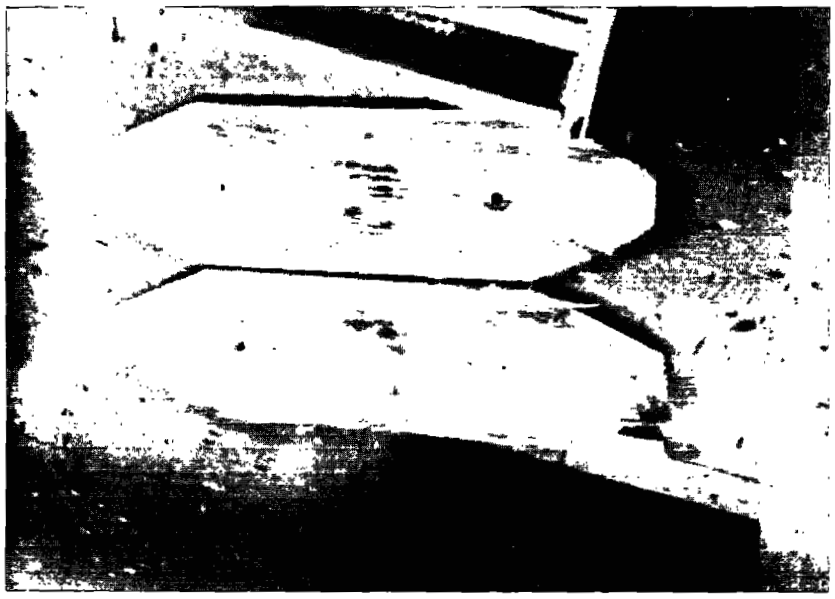

Figure 8-143 Bolsters Sheared from Flapwise Bending Specimen

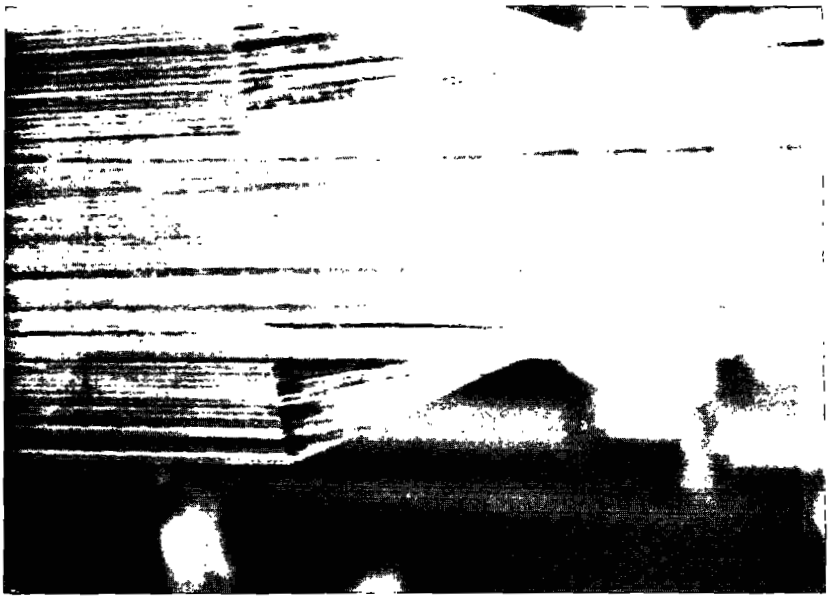

Figure 8-144 Bolster Failure Inside Center Beam

Table 8-91 Flapwise Bending Static Test Results

Specimen Number	Ultimate Load (lbs.)	First Offset (lbs.)
4	19,500	13,000
3	18,250	16,625
1	21,625	16,500
Mean	19,792	15,375

Fatigue Test Results

Specimen Number	Load Range (lbs.)	Test Frequency Hz	Number of Cycles
5	8,000 to 400	1.5	1.05×10^6 1
2	9,600 to 480	1.5	591,400
6	11,400 to 570	1.5	207,000
7	13,000 to 650	1.5	22,600
5*	13,125 to 660	1.5	58,900

* Additional Testing

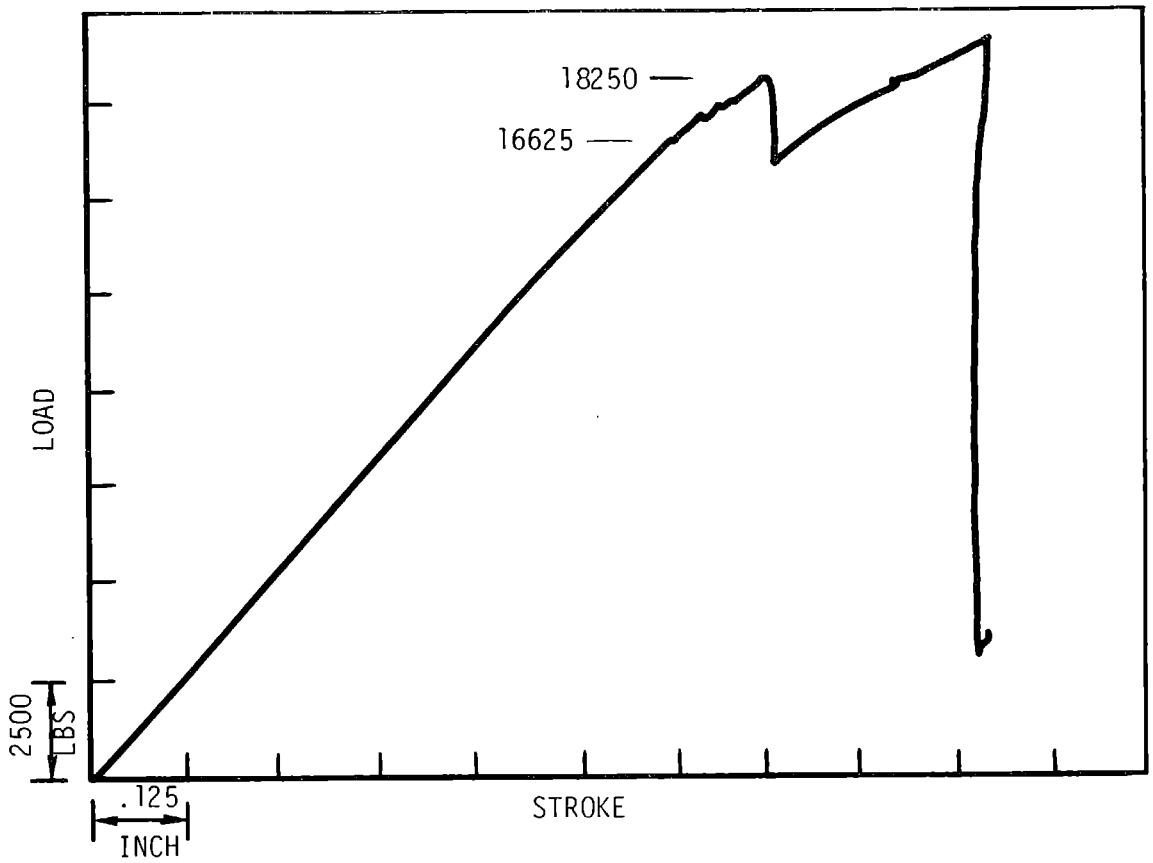

Figure 8-145 Flapwise Bending Static Test
Specimen #3

1.5 Hz. Cracks in the bolster bond gap were noticed at 555,100 cycles. After 591,400 cycles the test was stopped because damage was accumulating. The next specimen tested was number 6, at the rate of 1.5 Hz, with a load range of 11,400 and 570 lbs. Cracks were noticed in the bond gaps at 17,700 cycles, and the test was stopped after 207,000 cycles. Sample 7 was run at the same frequency, but at the load range was increased to 13,000 to 650 lbs. The bond gap cracks occurred after 500 cycles, and at 22,600 cycles one of the bolster ends failed through the bond gap. Residual strength tests were conducted on the unfailed specimens to determine the extent of any damage induced by fatigue. Specimen number 5 was first subjected to 58,900 additional cycles of loading from 13,125 to 660 lbs. The load-deflection hysteresis changed, as shown in Figure 8-146. The subsequent residual strength static test resulted in an ultimate strength of 20,750 lbs. and a first offset load of 16,875 lbs. Thus, the fatigue testing had little, or no effect. Sample 2 was also subjected to a residual strength test, and failed at 20,250 lbs. with a first offset load of about 16,500 lbs., also about full strength. Specimen 6 and 7 also were statically tested, and yielded values the following values:

Sample 6	Ultimate = 21,375 lb.	Offset = 16,875 lb.
Sample 7	Ultimate = 18,750 lb.	Offset = 15,750 lb.

Specimen 7 seemed to be the only specimen that lost static strength. The specimen could have been weakened during the period between 10,000 and 22,600 cycles, as shown on the trace history in Figure 8-147. The slope change indicates a change in beam stiffness, which did not show on other specimens.

The results also exceeded the predictions, but they are difficult to evaluate since the crack initiation time is difficult to pinpoint and it is difficult to define failure.

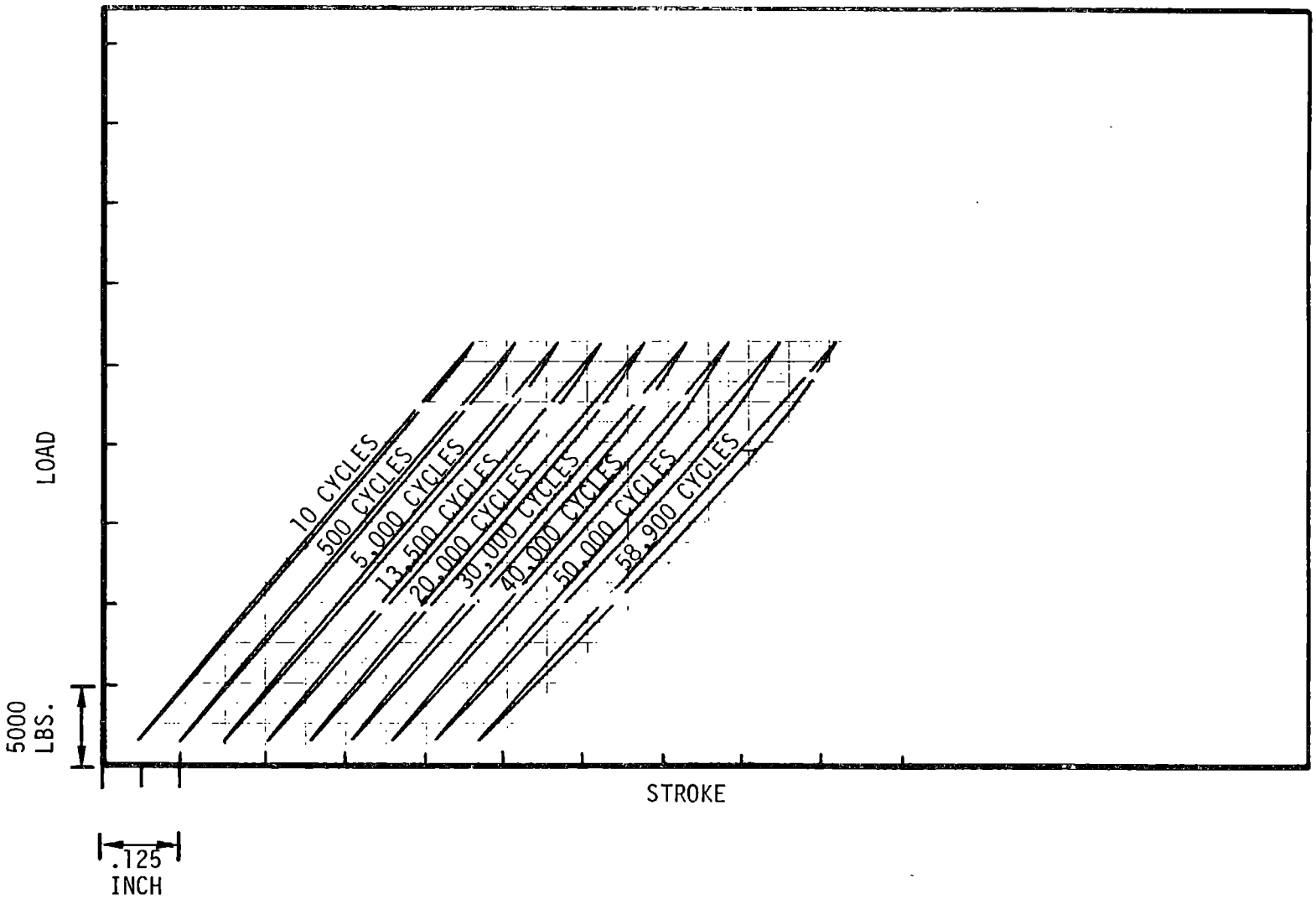

Figure 8-146 Flapwise Bending Test, Sample #5, Accelerated Damage Testing(Previous Testing - 1.06 Million Cycles at 8,000 to 4,000 Pound Load Range)

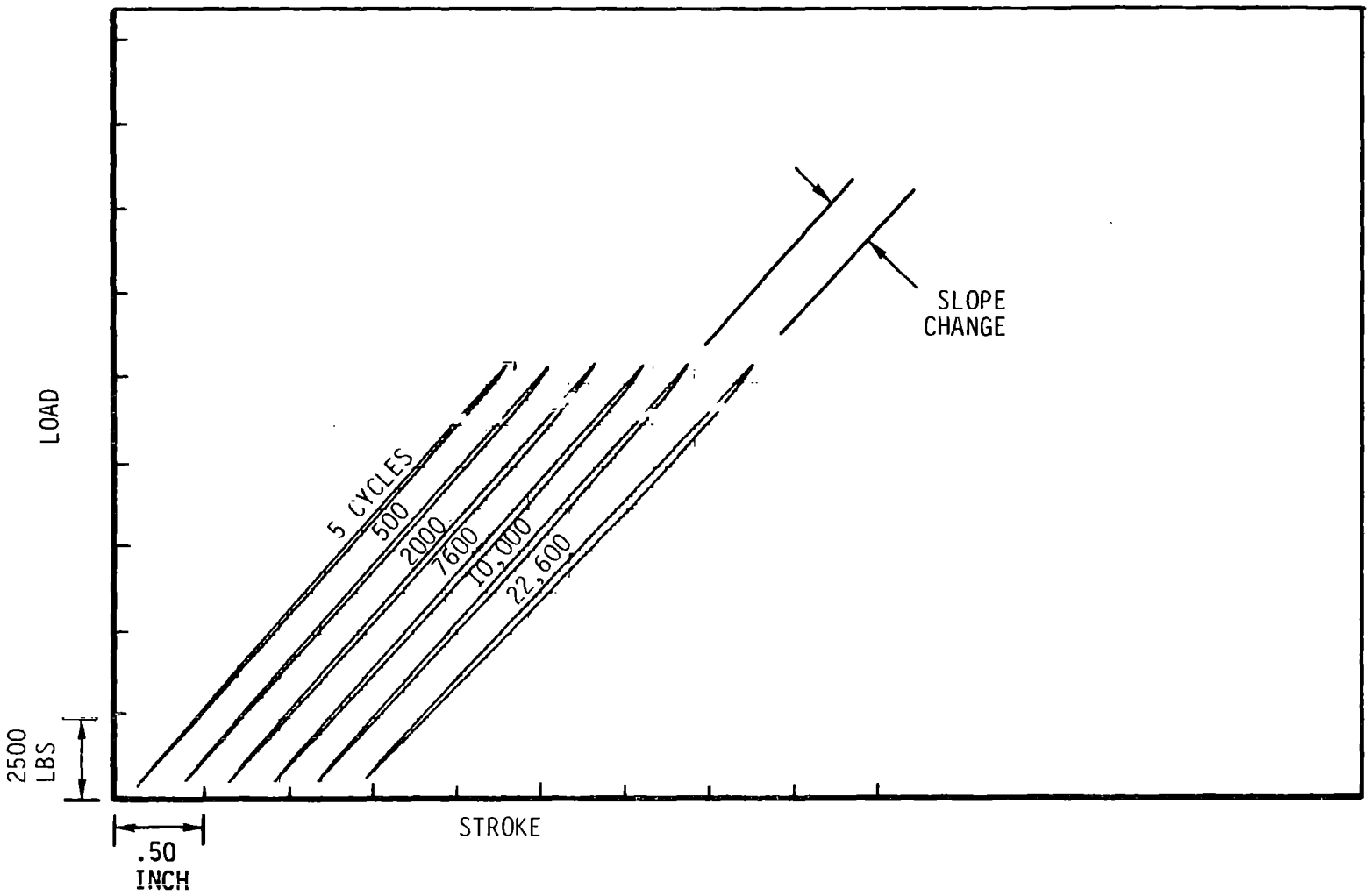

Figure 8-147 Fatigue Hysteresis History
Sample #7

8.2.5.5 Teeter Area Chordwise Bending Tests

8.2.5.5.1 Introduction

The chordwise bending test series was an axially loaded simulation of the center blade area, including bolsters, under chordwise bending loads. A 1/20 scale model of the blade included metal slugs to simulate teeter bearing cups and teeter brake fittings, as well as slots for the brake straps.

8.2.5.5.2 Test Objective

This test series was developed to provide a test base to be compared against a finite element model using the same techniques as the full scale blade model. It is similar to the tests described in sections 8.2.5.2 and 8.2.5.4, but instead of being tested in bending, these specimens were failed in tension and compression. The objective was to prove the ability of the computer analysis to determine the load distribution in the bolster area, and also to disclose the nature of failure modes in the two load directions, and in fatigue loading with fully reversing inputs (R = -1).

8.2.5.5.3 Test Description

The static testing was performed at Washington State University, using their compression grip timber testing machine which had a 200,000 lb capability. The samples were designed with end shapes that compatible with the grips and are shown in Figure 8-148. Three specimens were tested in tension and three in compression, two of each set contained strain gages. Five strain gage rosettes were placed on one side around the simulated teeter shaft insert and five were located around a simulated brake pin slug, as shown in Figure 8-149. Eight axial gages were placed on the edge grain surface on both faces, as shown in Figure 8-150. Figure 8-151 shows the specimen set-up for tension testing with an extensometer with a 12 in. span over the area of interest. The compression test set-up was similar except guide rollers were installed in both perpendicular directions to prevent buckling of the samples under load, as shown in Figure 8-152.

Fatigue testing was performed at the University of Dayton Research Institute using dogbone samples, as shown in Figure 8-153. These dogbones were similar to the static samples, and were made to be compatible with an MTS machine, to expedite testing.

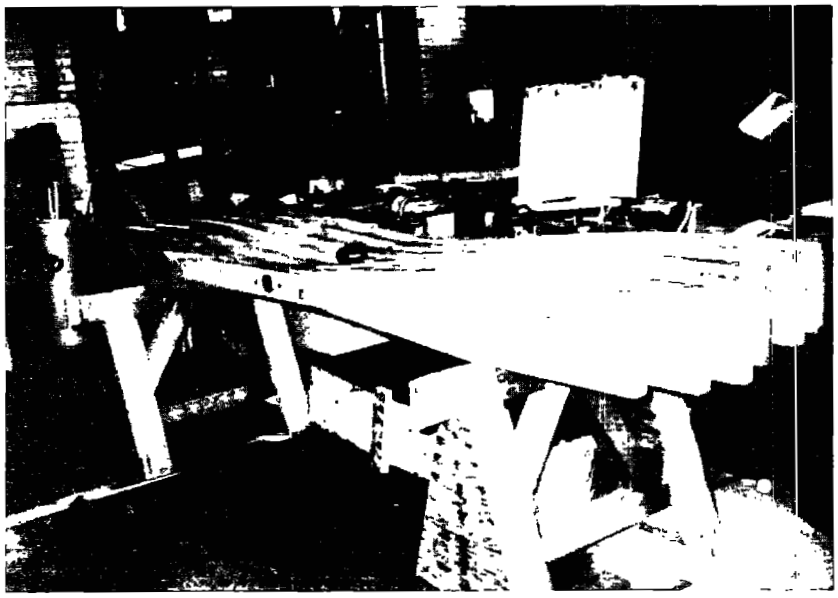

Figure 8-148 Chordwise Bending Static Specimens

Figure 8-149 Chordwise Bending Static Tension Test Setup

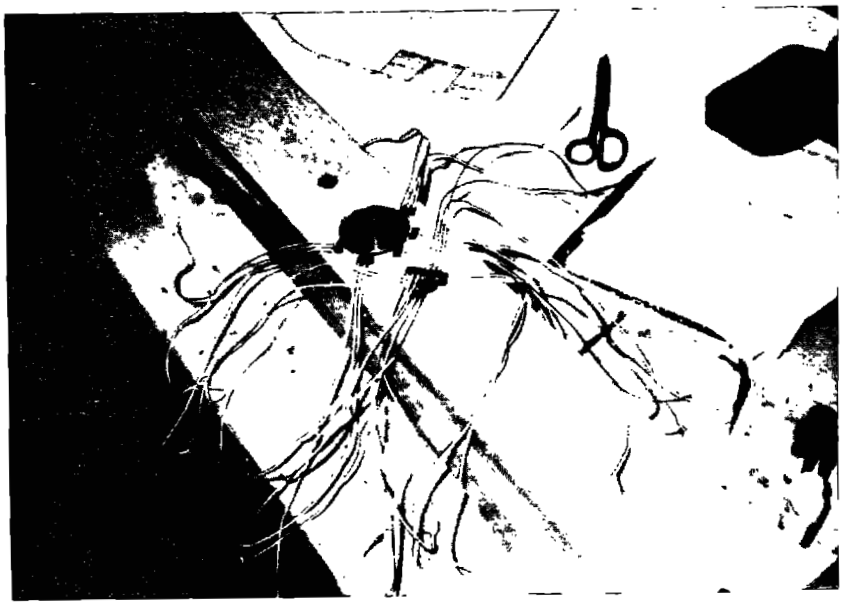

Figure 8-150 Strain Gage Locations Around Steel Inserts

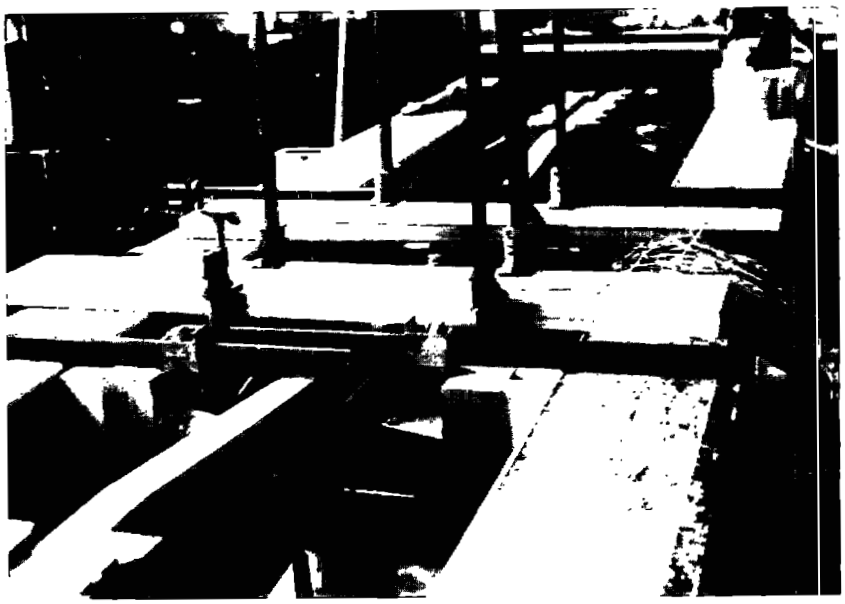

Figure 8-151 Chordwise Bending Static Compression Test Setup

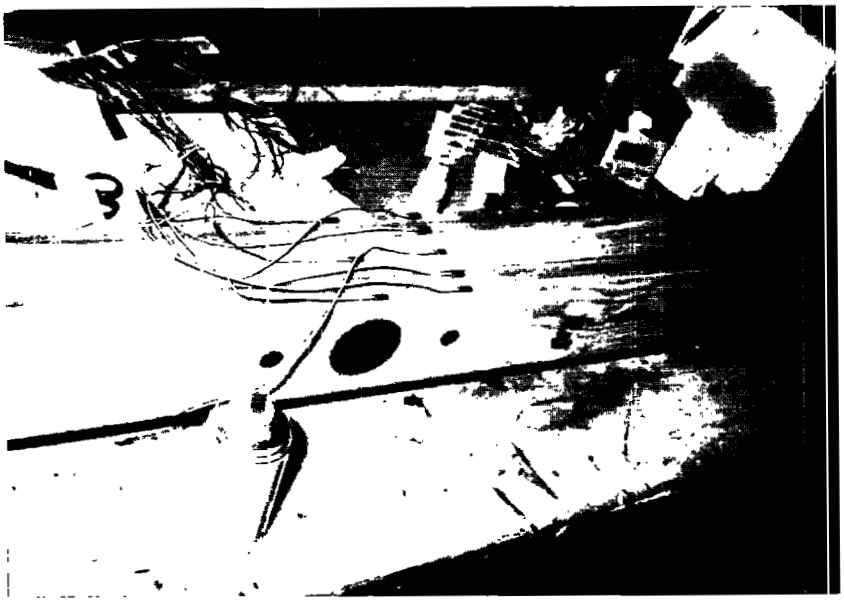

Figure 8-152 Axial Strain Gages on Edge Grain Surface

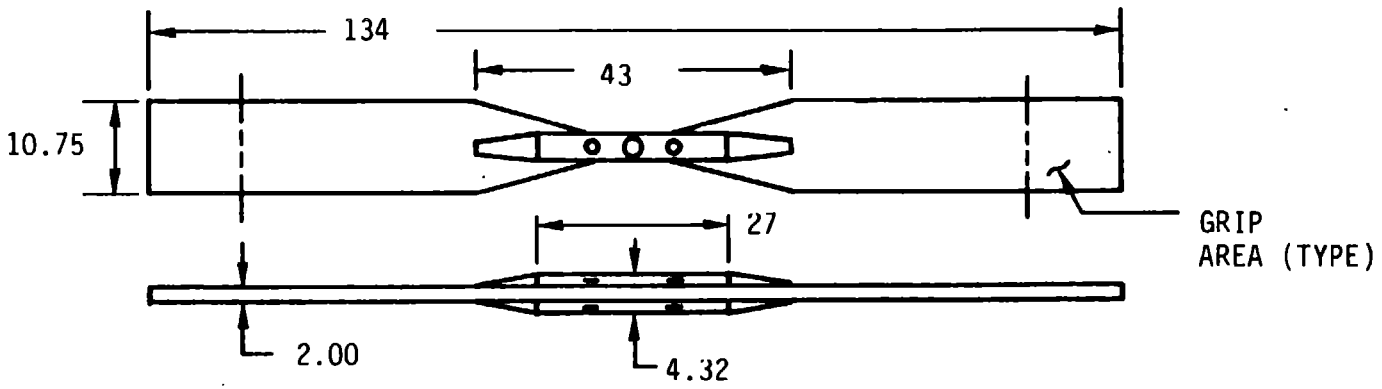

STATIC

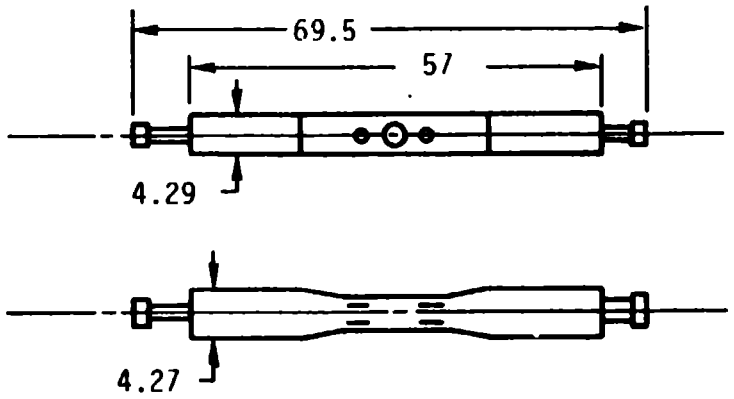

FATIGUE

Figure 8-153 Chordwise Bending Test Specimens

8.2.5.5.4 Test Results

The static tests all used an approximate 5 minute load ramp to ultimate failure. Sample number 6 was tested in tension, and did not contain strain gages. Ultimate failure occurred at 89,500 lbs. The failure mode included a rupture of the 2 in. wide beam center section near steel inserts. The bolster faces sheared free of the center web the entire length of the bolsters, in one direction. Figures 8-154 and 8-155 describe the failure areas. Samples 1 and 4 were fitted with strain gages and were also tested in tension. Their ultimate strengths were 77,500 and 74,700 lbs. Compression tests of samples 3 and 2, both with strain gages, resulted in failure loads of 158,500 and

Figure 8-154 Bolster/Beam Failure

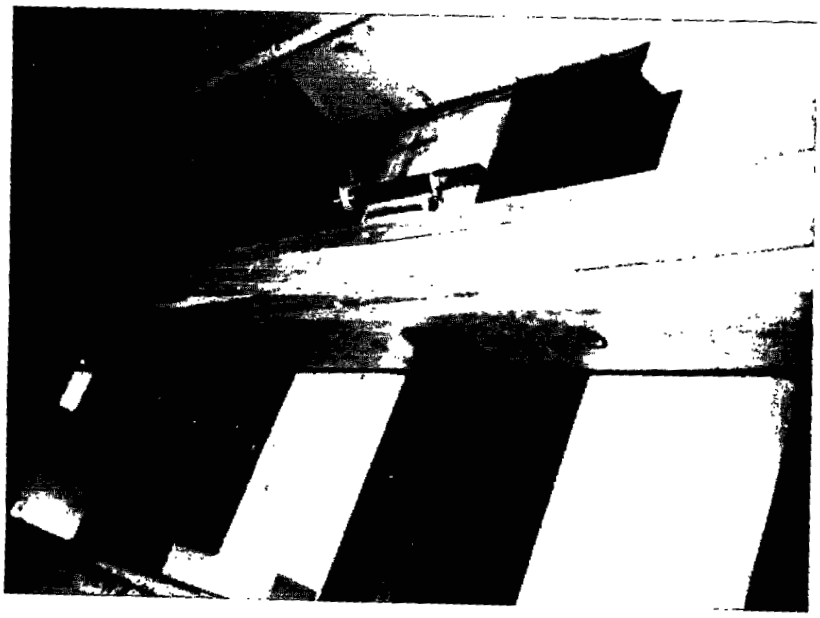

Figure 8-155 Center Beam Failure Area

137,500 lbs. Sample number 5, without strain gages, failed at 146,800 lbs. Both bolsters of sample number 5 separated, and one bolster on samples 3 and 2 buckled, while the other separated. Figures 8-156 and 8-157 show a compression load trace and typical failure. Table 8-92 tabulates the static test results.

Fatigue testing started with sample number 5-5 being tested at ±45,000 lbs. The fully reversed loading test was terminated after 7,600 cycles, when severe cracks propagated along both sides of the dogbone specimen, as shown in Figure 8-158. A crack was detected around the teeter cup epoxy gap after 4,000 cycles, and is shown in Figure 8-159.

Sample number 5-6 was tested next, and the loading was reduced to ± 35,000 lbs. The loading was halted at 232,700 cycles, when the lower half of the specimen showed evidence of delamination as shown in Figure 8-160. Figure 8-161 shows a stiffness trace history indicating essentially no change in slope after 212,000 cycles, but a distinct change at 231,000 cycles. Earlier shifts at the center point after 5,700 and 10,900 cycles were caused by a loose split washer on the machine's rod threads. The loose washer did not affect loading, since the servo uses the load cell output voltage for control determination. Figure 8-162 shows cracks around the large teeter cup pin, which were noticed after 1,000 cycles.

The load for the next test, sample 5-4, was reduced to ±32,000 lbs. The epoxy around the simulated brake pins and teeter cup cracked during the first load cycle as shown in Figure 8-163. The teeter cup began to work out of the hole after 36,000 cycles. No variation in trace shape was apparent through 138,000 cycles, but at 146,500 cycles the upper stud pulled free of the specimen, as shown in Figure 8-164.

The final sample, number 5-3 was tested at ±10,000 lbs. The load deflection trace was unchanged through one million cycles, but some damage to the specimen was visible. After 1,500 cycles an epoxy crack was discovered around the bottom of a simulated brake shaft on the back surface. At 8,500 cycles the epoxy cracked on the lower part of the simulated teeter cup on the front

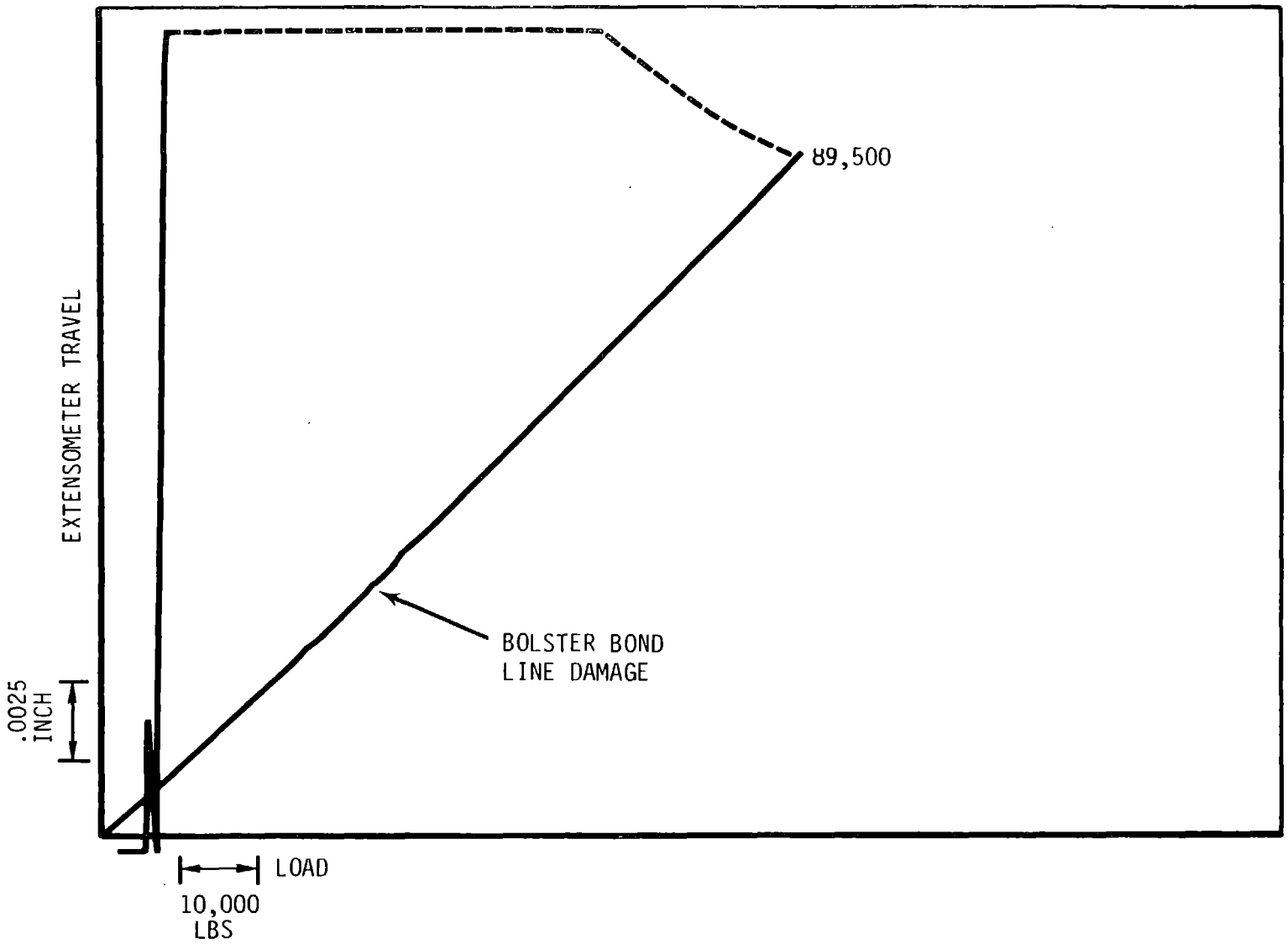

Figure 8-156 Typical Tension Test Load Trace Test #5, Sample #6

Figure 8-157 Compression Induced Failure of Sample #3

Table 8-92 Static Test Results, Chordwise Bending Test

Sample Number		Ultimate Load
6	(tension)	89,500 lbs.
1	(tension)	77,500
4	(tension)	74,700
Mean	(tension)	80,567
5	(compression)	-146,800 lbs.
3	(compression)	-158,500
2	(compression)	-137,500
Mean	(compression)	-147,600

Fatigue

Specimen Number	Load Range (lbs.)	Frequency Hz	Number of Cycles
5	45,000 to -45,000	1	7,600
6	35,000 to -35,000	1	232,700
4	32,000 to -32,000	1	146,500
3	10,000 to -10,000	1	10^6 (No Failure)

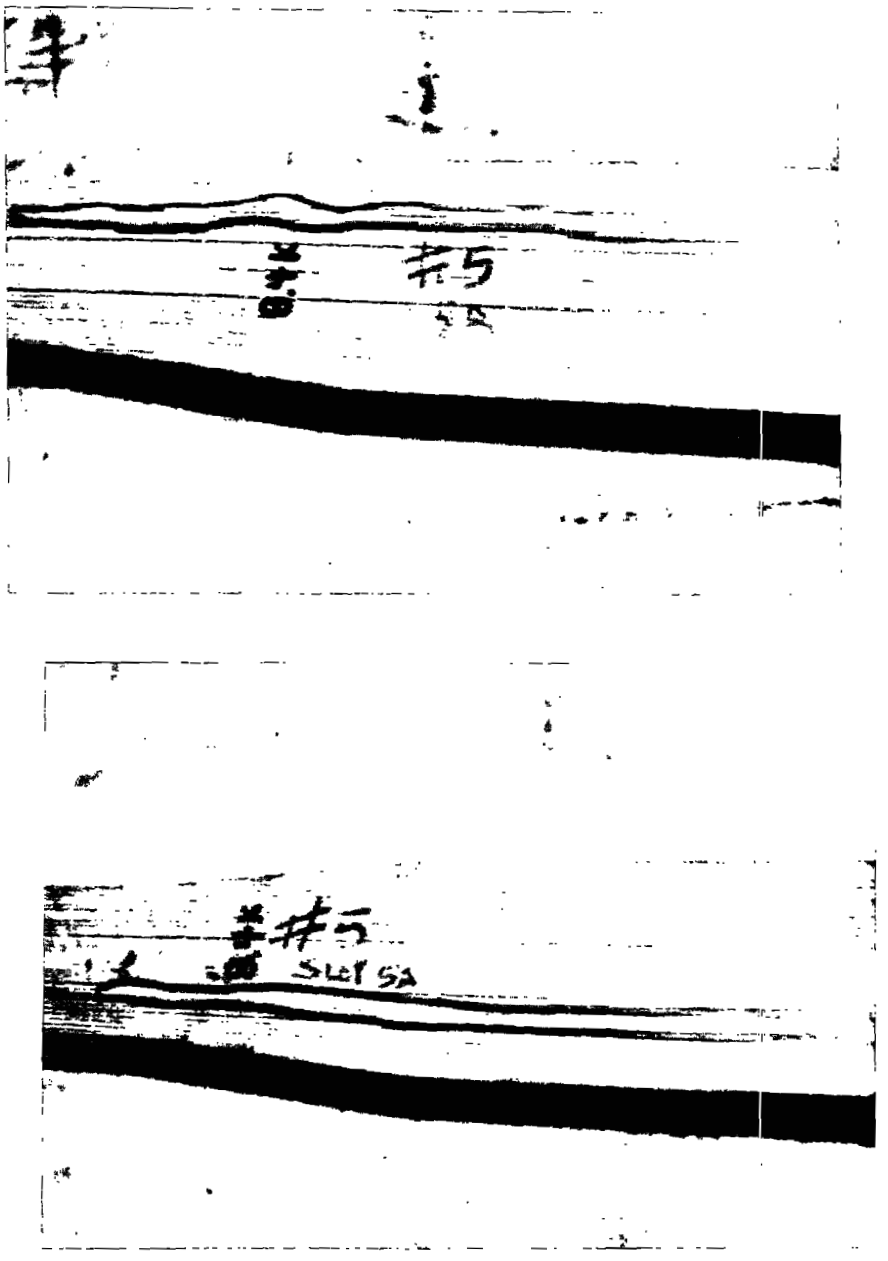

Figure 8-158 Crack Damage to End of Specimen S-5

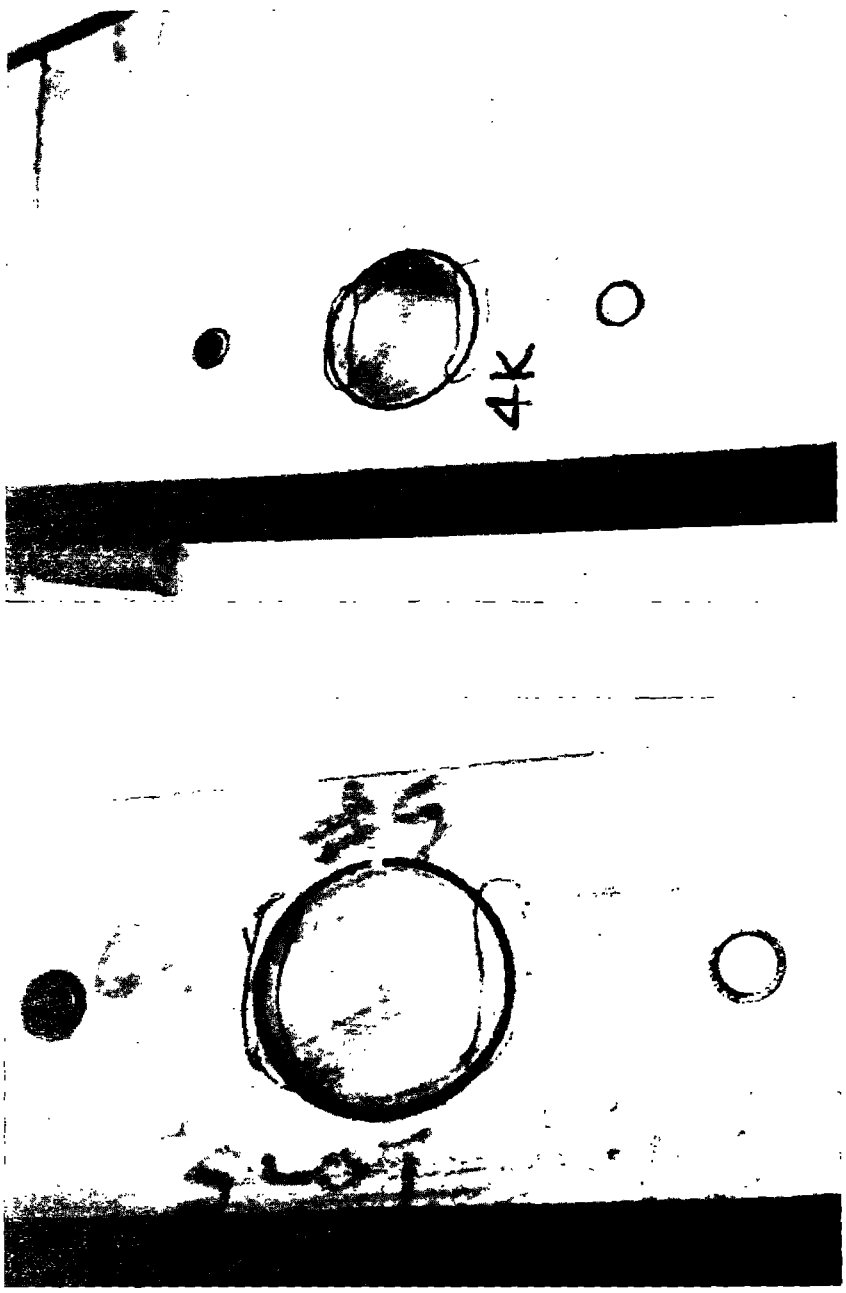

Figure 8-159 Epoxy Damage to Specimen 5-5

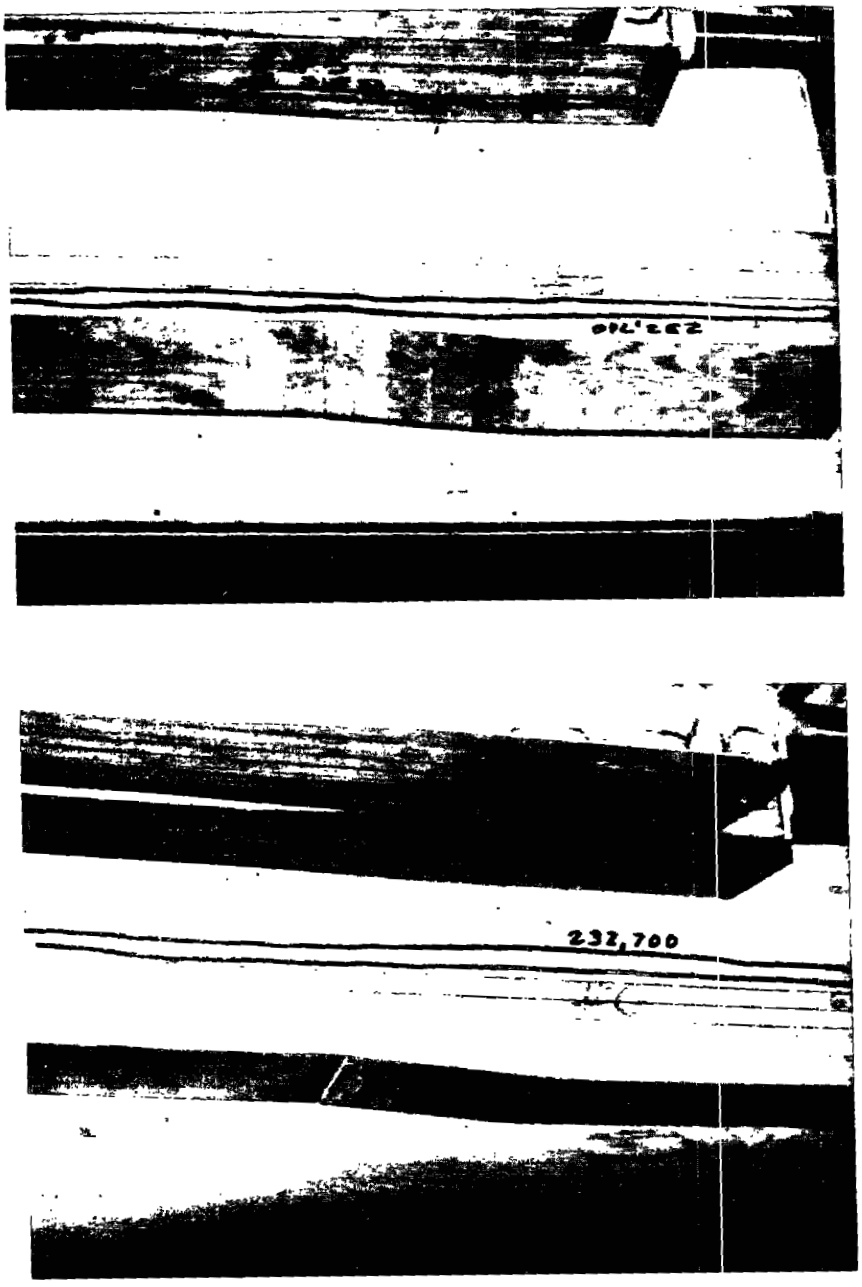

Figure 8-160 End Cracks of Specimen S-6

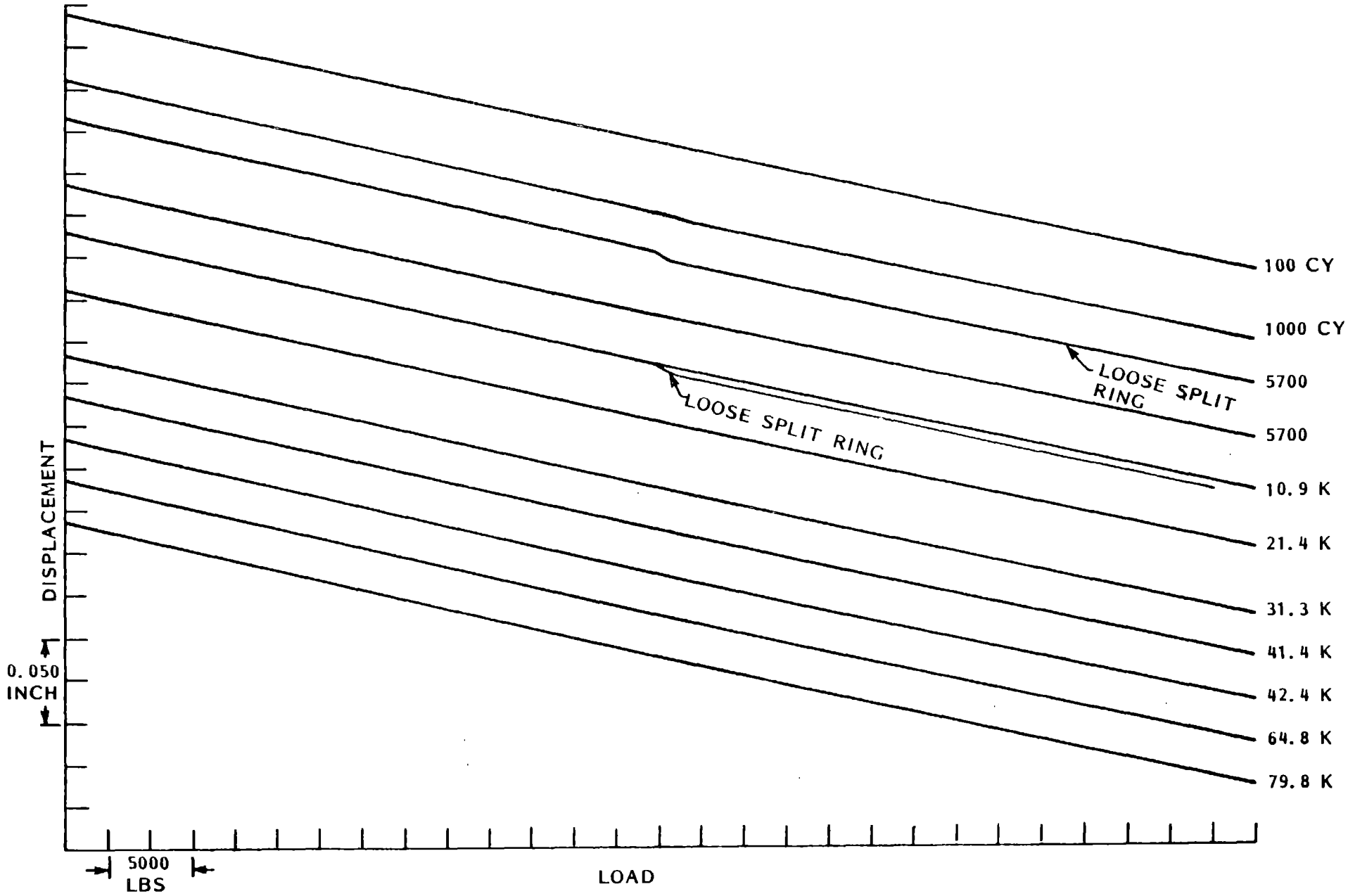

Figure 8-161 Specimen #5-6 - Load = ±35,000 lbs. - Fatigue Test Trace History

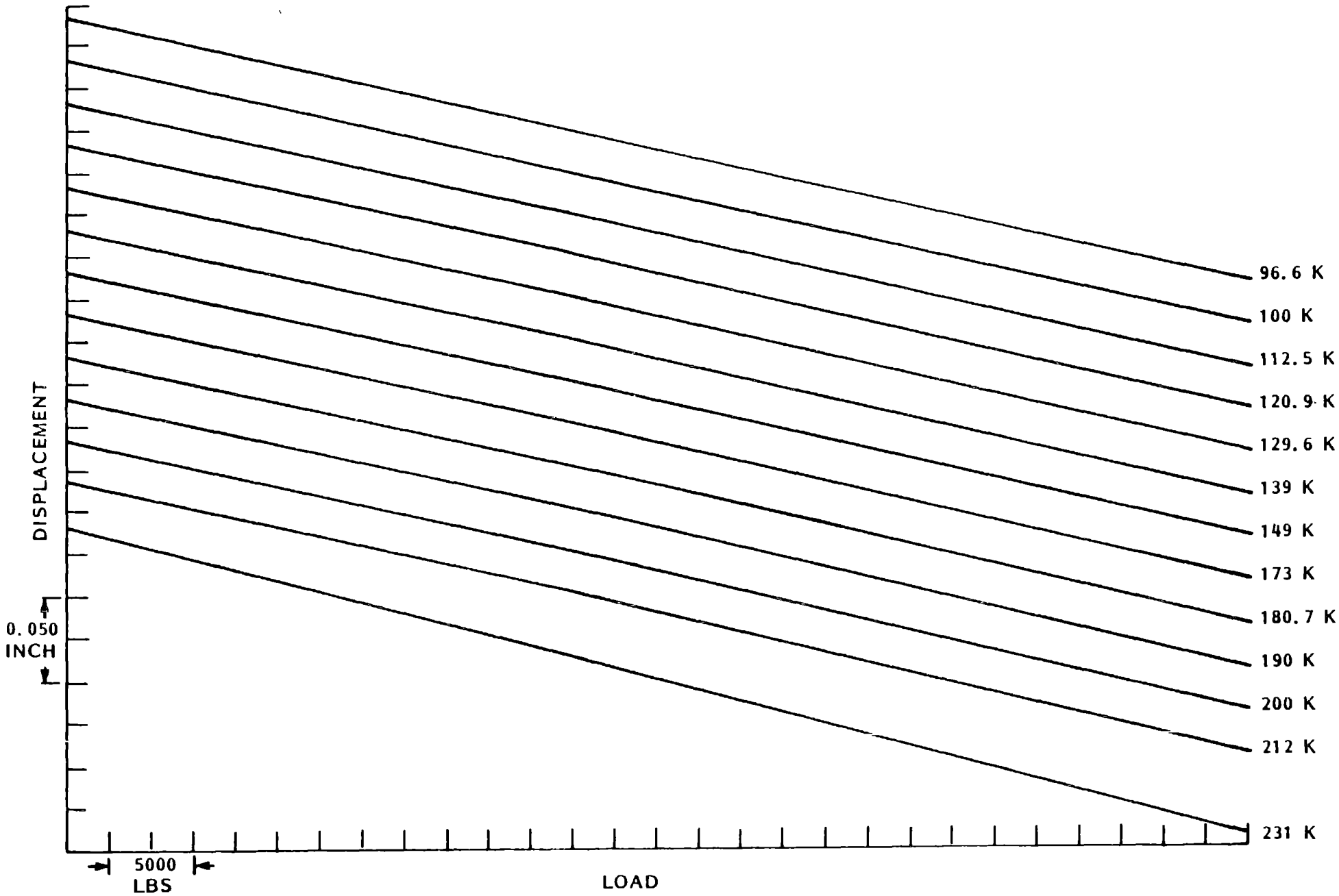

Figure 8-161 (Cont.) - Specimen #5-6 - Load = ±35,000 lbs. - Fatigue Test Trace History

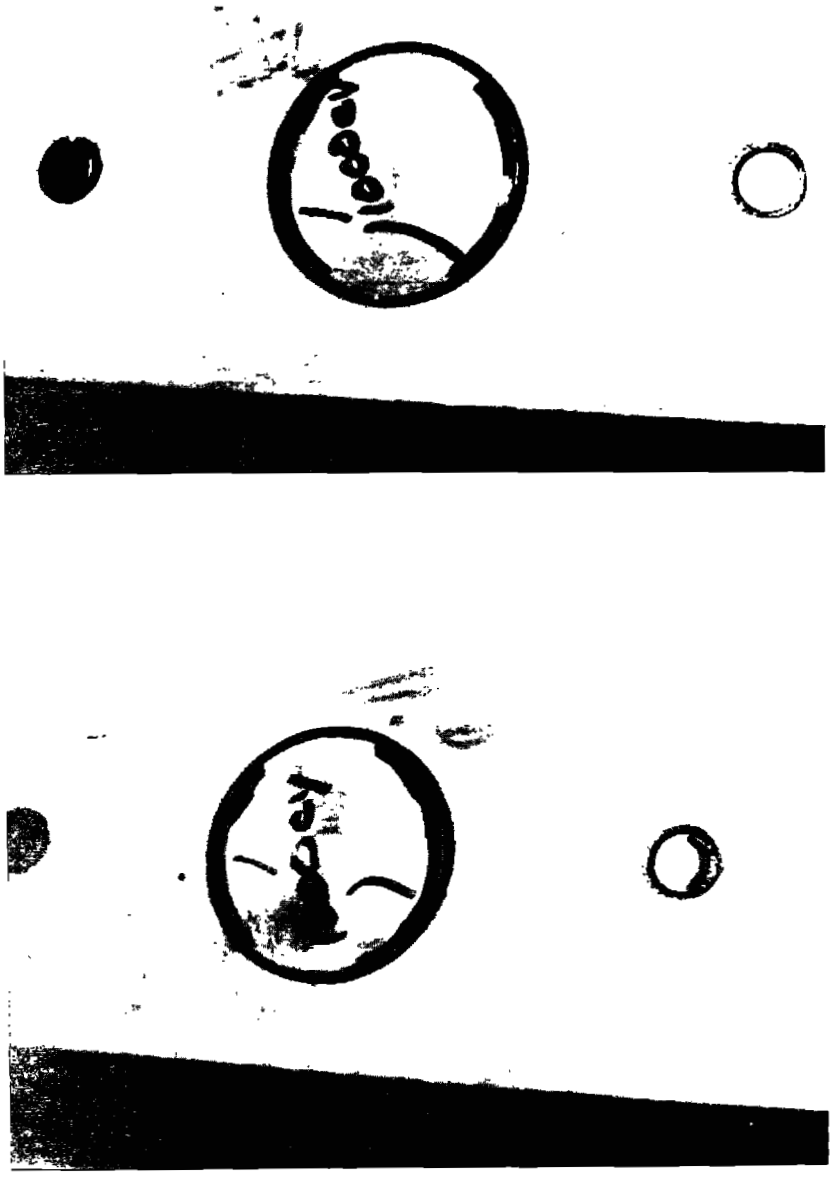

Figure 8-162 Epoxy Cracks in Specimen 5-6

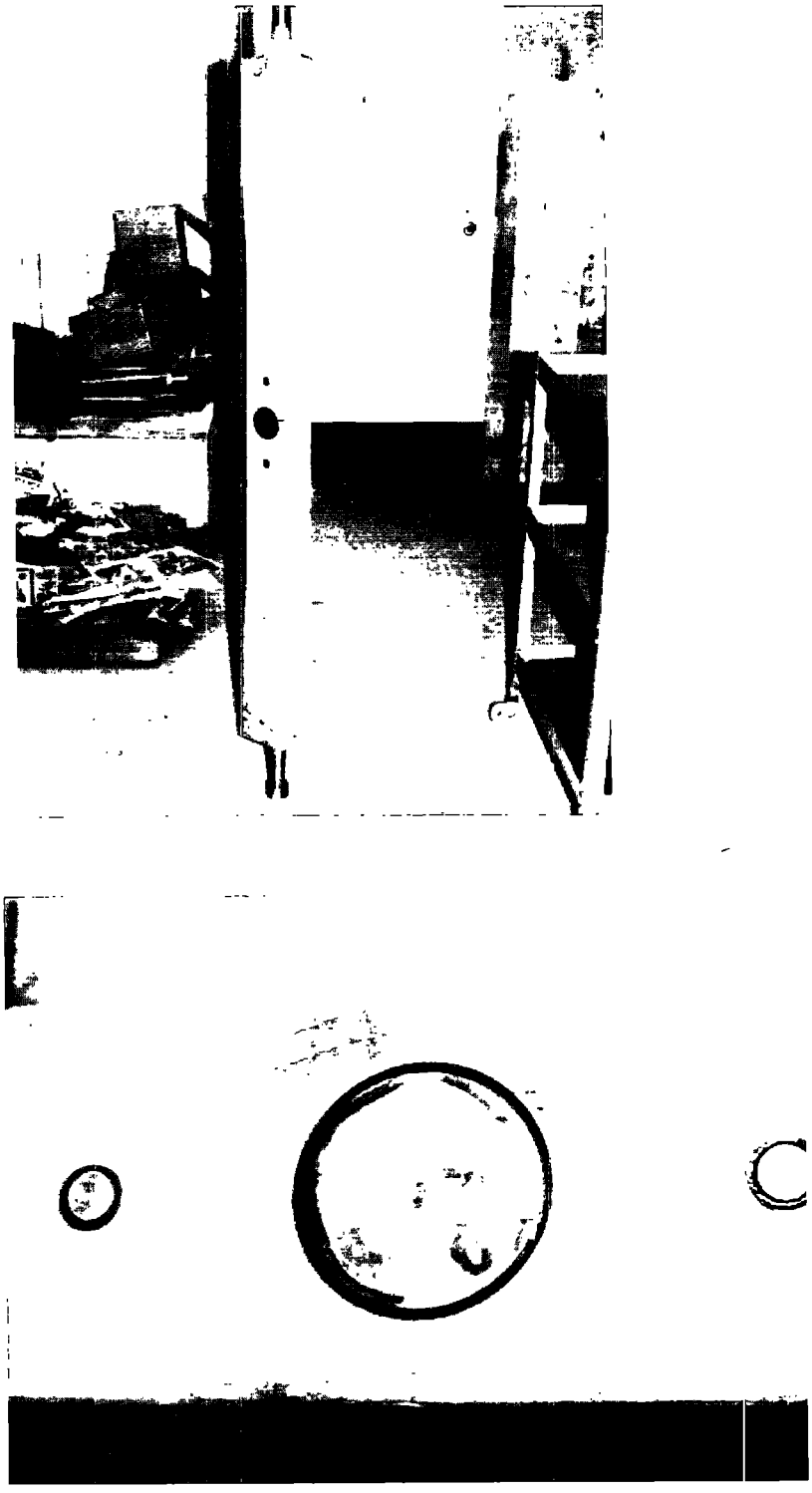

Figure 8-163 Views of Damage to Specimen 5-4

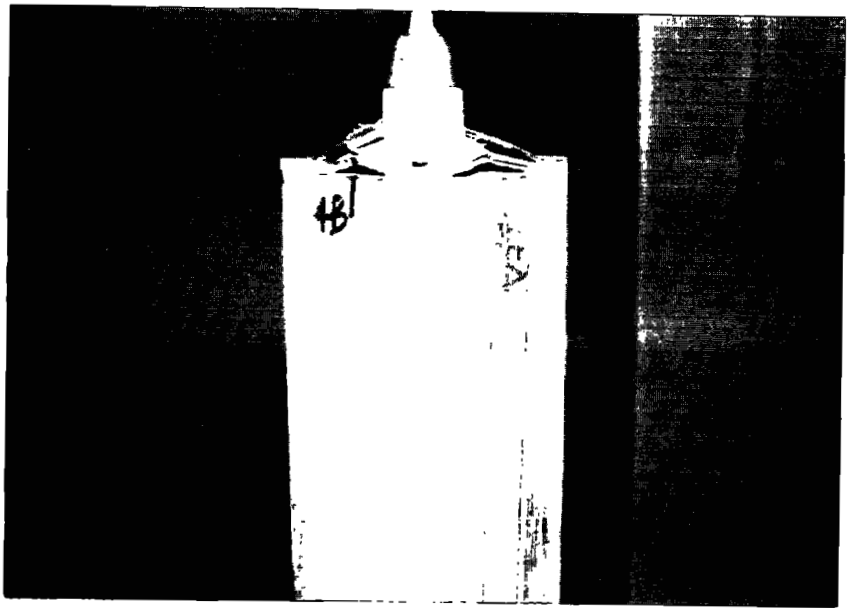

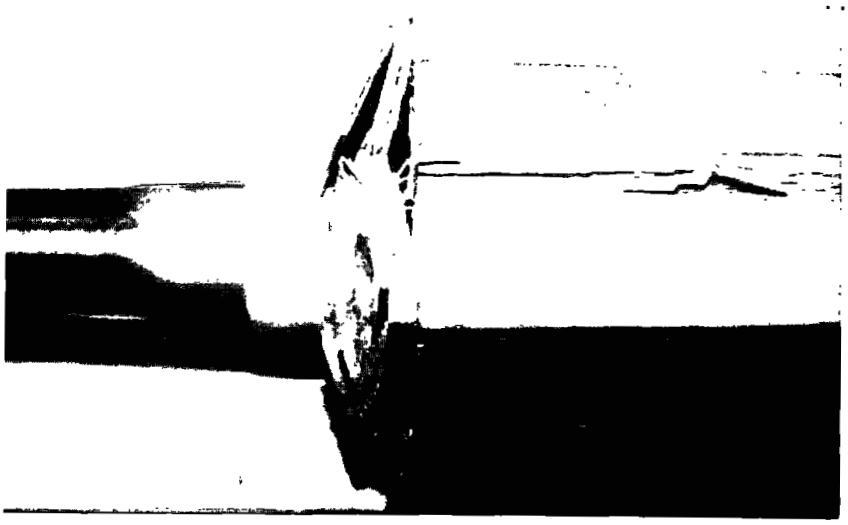

Figure 8-164 Stud Pulled Free of Specimen 5-4

surface. After 10,500 cycles the second brake pin was similarly affected on the back face. At 129,600 cycles, the top side of the teeter cup gap on the back surface cracked. After 216,700 cycles the crack progressed and affected the lower gap as well. Figure 8-165 shows the areas of cracking.

The static tests produced mean ultimate loads of 80,567 and -17,600 in tension and compression. The points at which epoxy cracking occurred in these static samples was not readily monitored. The first fatigue load selection was based on between 50 and 60% of the lower ultimate value, and the failure that occurred in the epoxy was noticed at 4,000 cycles. The ultimate failure occurred in the stud area. The second load was at 44% of ultimate and the failure mode was similar. The third specimen was tested at 25% of ultimate, and stud failure again occurred. The final specimen was tested at 8% of ultimate load to gain on test lifetime.

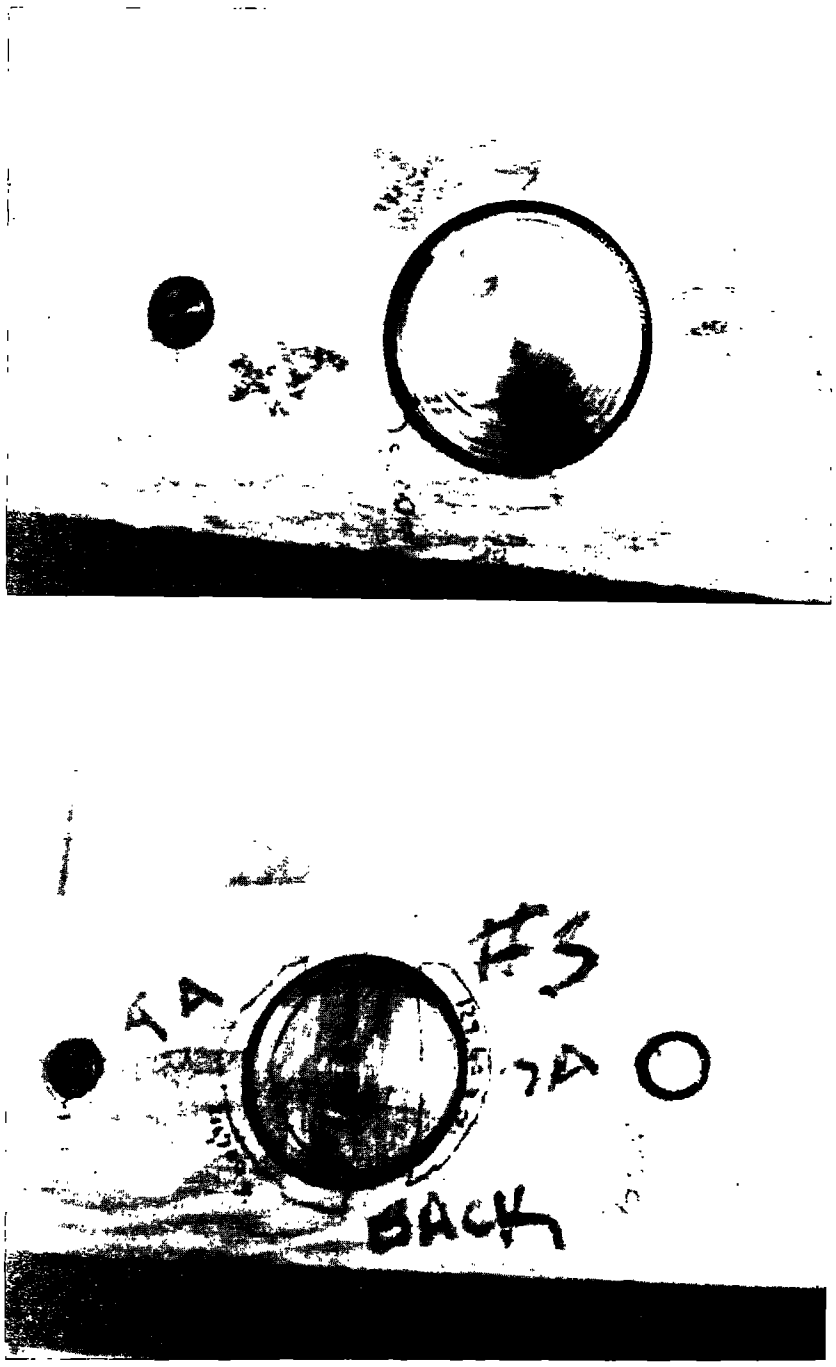

Figure 8-165 Epoxy Damage Areas of Specimen 5-3

8.2.5.6 Low Temperature Static Properties Testing of Laminae

8.2.5.6.1 Introduction

This series of tests provided information on the static strength of blade grade 1 Douglas fir veneer, bonded with West System epoxy at a temperature of -20°F (-29°C). Ideally, all property characterization tests should include maximum and minimum temperature tests, but cost constraints prevented this. However, the results of the temperature tests can be appliec to other test results through conventional analytical techniques.

8.2.5.6.2 Objectives

This simple test series determined the static tension and compression axial strength at the minimum expected exposure temperature. The comparison of these results with room temperature tests indicate whether or not significant changes occur in the strength of laminae at -20°F.

8.2.5.6.3 Description

Three samples were prepared for each test direction. The configurations are shown in Figure 8-166. The samples were 1.5 in. thick by 2.0 in. wide and made of 15 laminations. The samples were designed for use of the timber testing machine or a compression tester at Washington State University. Because the compression test specimen was so short, 6.5 in., no lateral buckling supports were necessary. The testing was conducted on samples that were conditioned to -20°F by immersing them in a freezer room for two days before testing. A foam insulated box was built for transporting the samples from the freezer to the test laboratory, where they were individually removed and tested. A sensing device equipped with a thermocouple verified the temperature of the wood just before testing. A 12 in. long extensometer was used on the tension specimens, which had a stressed volume of 126 cubic in. No head travel data was recorded for the compression specimens, which had a 19.5 cubic in. stressed volume.

8.2.5.6.4 Results

The results of the tests are summarized in Table 8-93. The modulus of elasticity of the tension specimens is quite consistent with room temperature test data. The axial strength values are slightly low, but still fall within

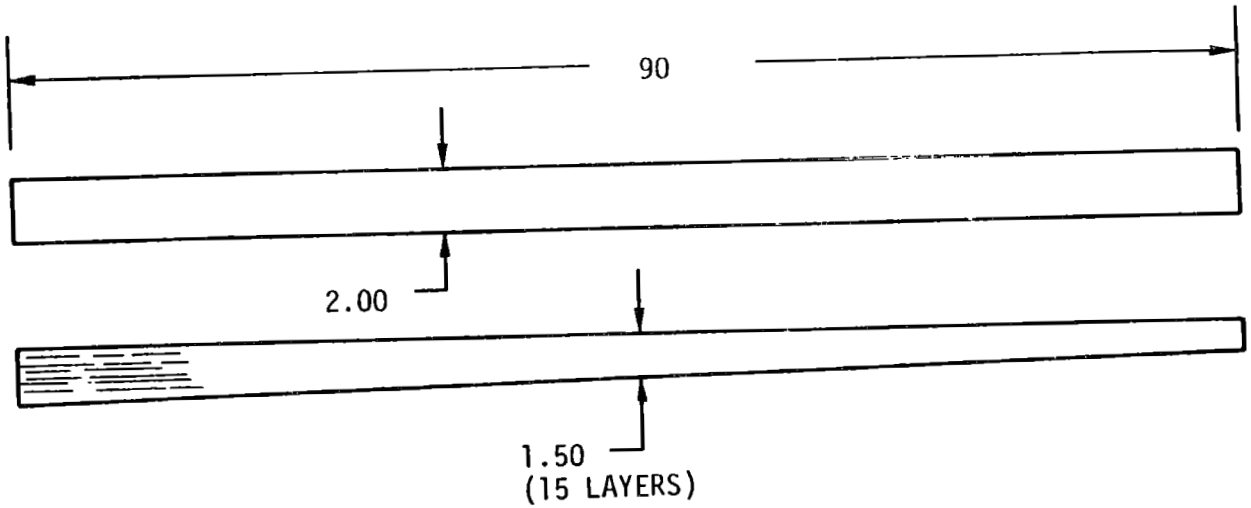

TENSION

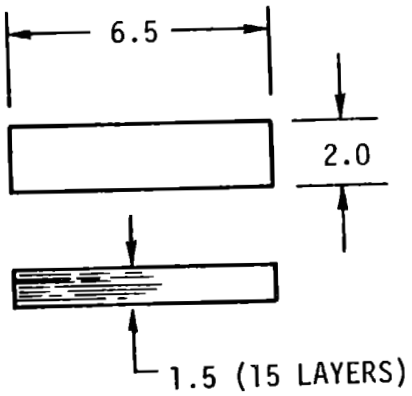

COMPRESSION

Figure 8-166 Low Temperature Test Specimens

Table 8-93 Low Temperature Test Results
(Test Temperature = -20°F)

Tension Tests

Sample Number	Extensometer Travel (in.)	Ultimate Load (lbs.)	Strain (in.)	E (psi)	Stress (psi)
1	0.056	31,800	0.00467	2.27×10^6	10,600
2	0.0413	26,400	0.00343	2.566×10^6	8,800
3	0.0413	25,320	0.00343	2.461×10^6	8,440
Average				2.432×10^6	9,280

Compression Tests

Sample Number	Peak Load (lbs.)	Stress (psi.)
4	33,030	11,010
5	34,010	11,337
6	33,160	11,053
Average		11,133

the room temperature scatter zone. The strength of wood increases with decreasing temperatures for a reasonable range. Whether -20° is low enough to reverse that trend or if the absence of an increase was caused by the epoxy was not known.

8.2.5.7 Crossgrain Tension Properties of Augmented Laminae

8.2.5.7.1 Introduction

The use of glass cloth to augment Douglas fir veneer increases the strength parallel to the grain, and normal to the grain (crossgrain). This test analyzed the crossgrain strength static and fatigue loading.

8.2.5.7.2 Objectives

These tests measured the static and fatigue properties of a Douglas fir, blade grade 1, veneer specimen with a layer of Burlington glass fiber cloth between each veneer. The results defined allowable stress levels based on ultimate loads and failure modes.

8.2.5.7.3 Description

The specimens were all 1.48 in. thick, 2.0 in. wide (parallel to grain) and 50 in. long. They were made of 13 layers. They were tested using Washington State University's timber testing machine. An 11.88 in. long extensometer was used on the static tests. The fatigue tests were all run with an R value of 0.1, to provide tension-tension life values at various loads. The life goals were: to fail two specimens near 10,000 cycles, and to fail two specimens near 300,000 cycles.

Test specimens were made with two different types of glass, Burlington's #7781 and #7500. 7781 was specified, but GBI supplied the latter type without cost, since they had a surplus of the material. 7500 was used earlier in the program, but was eliminated because 7781 provided better results.

8.2.5.7.4 Results

Static tests were started with one sample of 7500 glass, to validate the set-up (#12). Samples 1 through 3 followed. The results are shown in Table 8-94. Figure 8-167 shows the load deflection plots for the last three tests, and Figure 8-168 shows a photograph of the four static specimens after failure, indicating the length of failed area.

C-5

Table 8-94 Crossgrain Tension Test Results

Static Tests

Specimen	Glass Type	Ultimate Load (lbs.)	Ultimate Stress
12	7500	9,000	3,040
1	7781	8,500	2,872
2	7781	8,700	2,939
3	7781	10,000	3,378
Average (1, 2 & 3)		9,067	

Fatigue Tests

Specimen	Glass Type	Load Range	Cycles	Failure
8	7781	4,000 to 400 lbs.	30,000	No (Slope Change)
		3,750 to 375 lbs.	62,000	Yes
10	7781	Accidently failed due to overload		
4	7781	5,000 to 500 lbs.	13,692	Yes
9	7781	5,000 to 500 lbs.	13,850	Yes

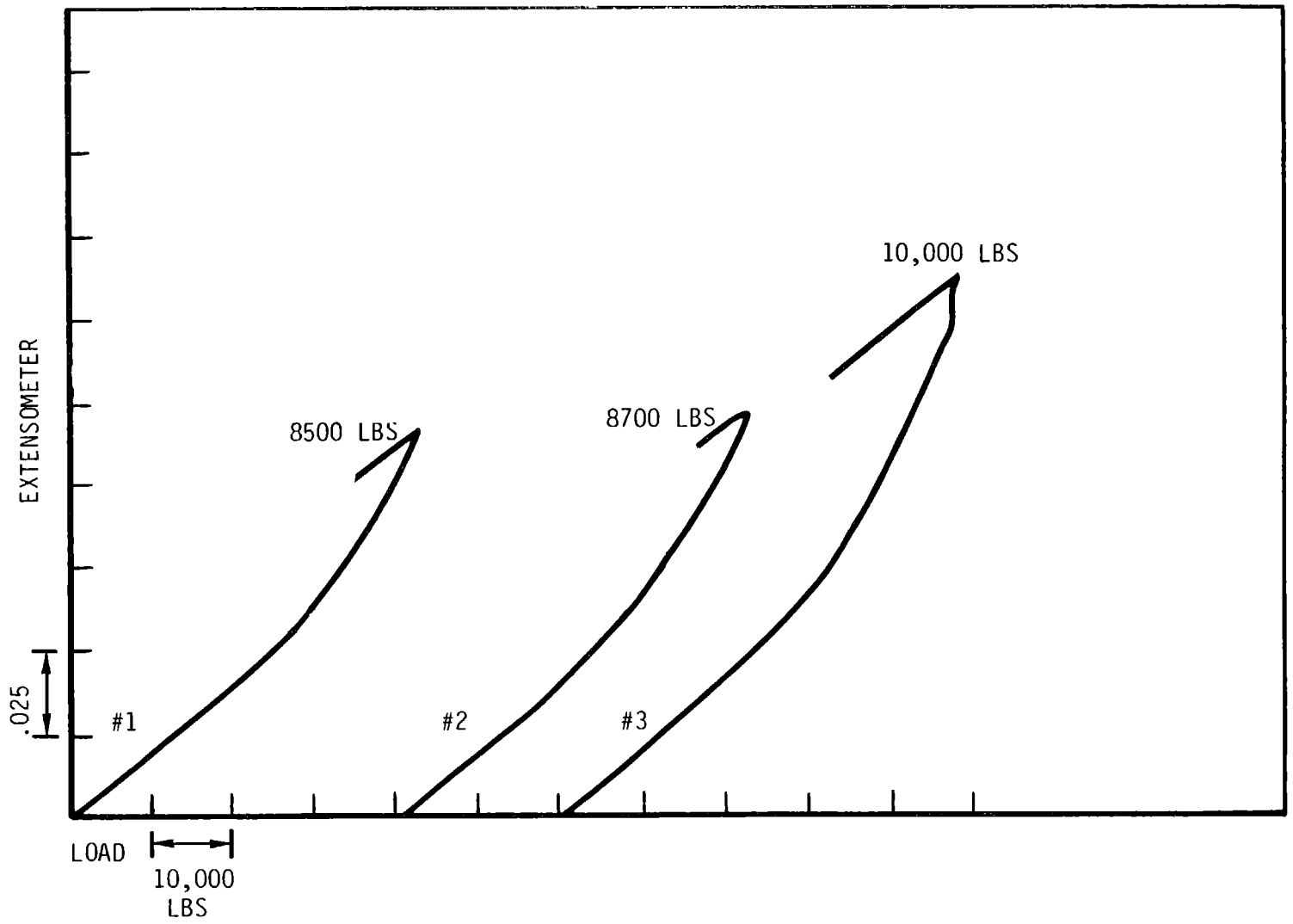

Figure 8-167 Crossgrain Tension Static Test Load-Deflection Plots

Figure 8-168 Crossgrain Fatigue Specimen #7

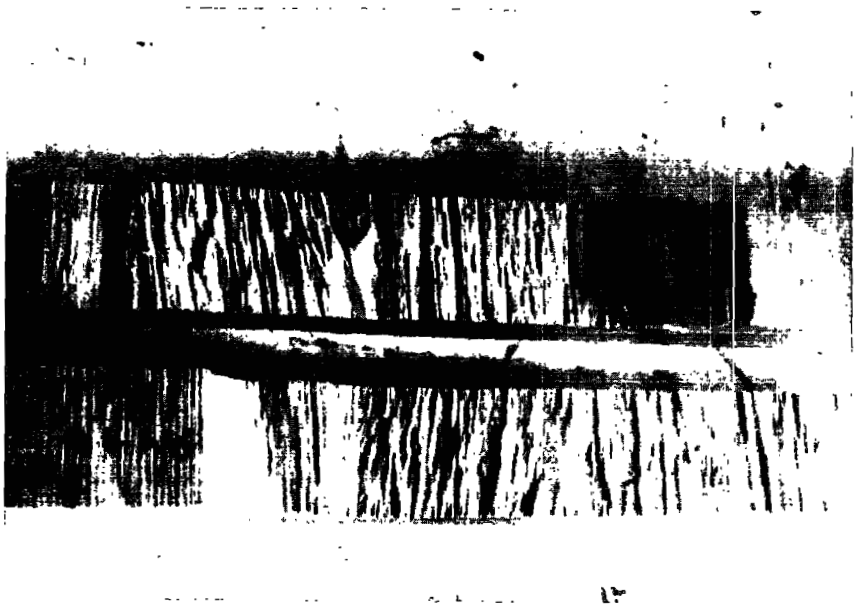

Figure 8-169 Crossgrain Fatigue Specimen #4

Fatigue tests were conducted on four samples. The results are listed in Table 8-94. Failure areas varied from very short to several inches long, as shown in Figures 8-168 and 8-169. Sample 8 was first run at from 4,000 to 400 lbs. for 30,000 cycles and then halted. The test was resumed at a load range between 3,750 and 375 lbs., and ultimate failure occurred after an Additional 62,000 cycles.

8.2.5.8 Bolster Bending Test

8.2.5.8.1 Introduction

The blade center section contains reinforcing bolsters on two sides, which are augmented with glass fiber cloth. The teeter shaft fittings are attached to these bolsters, and spanwise loads must travel from the blade section into the bolsters, to be reacted by the teeter shaft fittings. This test series used a 1/20 scale model of the blade center section bolsters, but did not include metal fittings at the teeter shaft and brake shaft interface points.

Strain gages were used on two static tension samples and two compression samples to provide strain distribution data.

8.2.5.8.2 Objectives

This test series provided data on the yield point and ultimate strength of the bolster to spar joint, and on the distribution of loads along the bolster length. A finite element model comparison was made to verify the analytical techniques used on the blade, similar to the method used in tests described in sections 8.2.5.3, 8.2.5.4 and 8.2.5.5.

8.2.5.8.3 Description

The static test specimens were designed for use of Washington State University's timber testing machine, which has a capacity of 200,000 lbs. Three specimens were tested in tension and three in compression. Two of each set were instrumented with strain gages. Figure 8-170 shows the specimen geometry, and Figure 8-171 shows strain gages on a specimen. The tension test set-up is shown in Figure 8-172, without the extensometer, but with strain

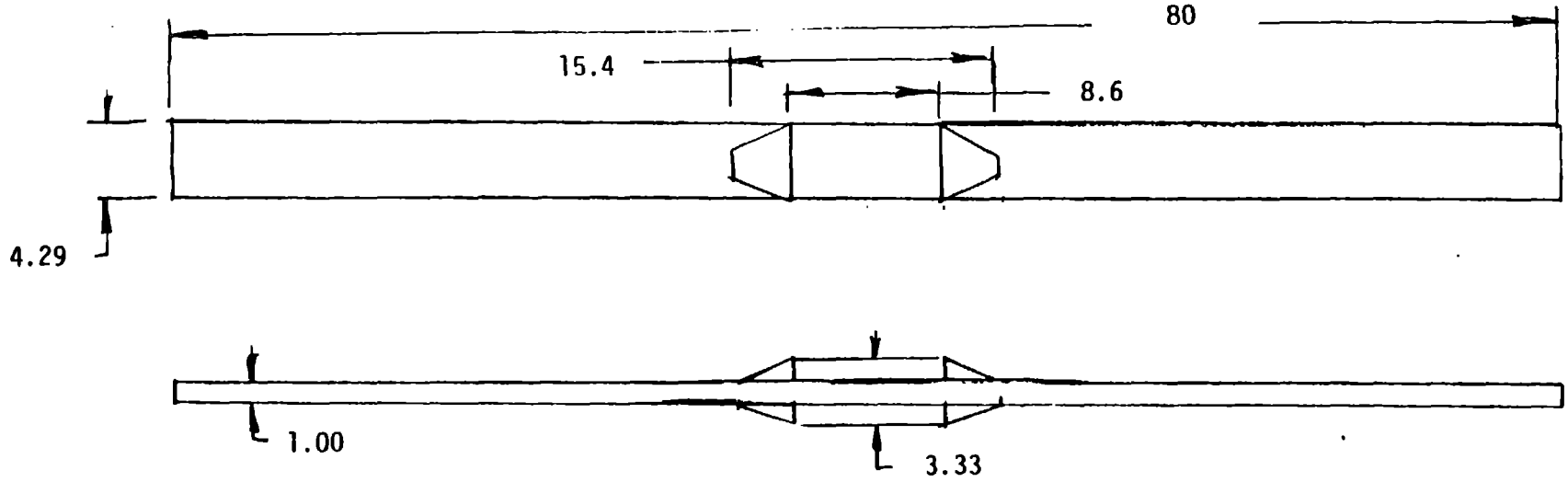

STATIC

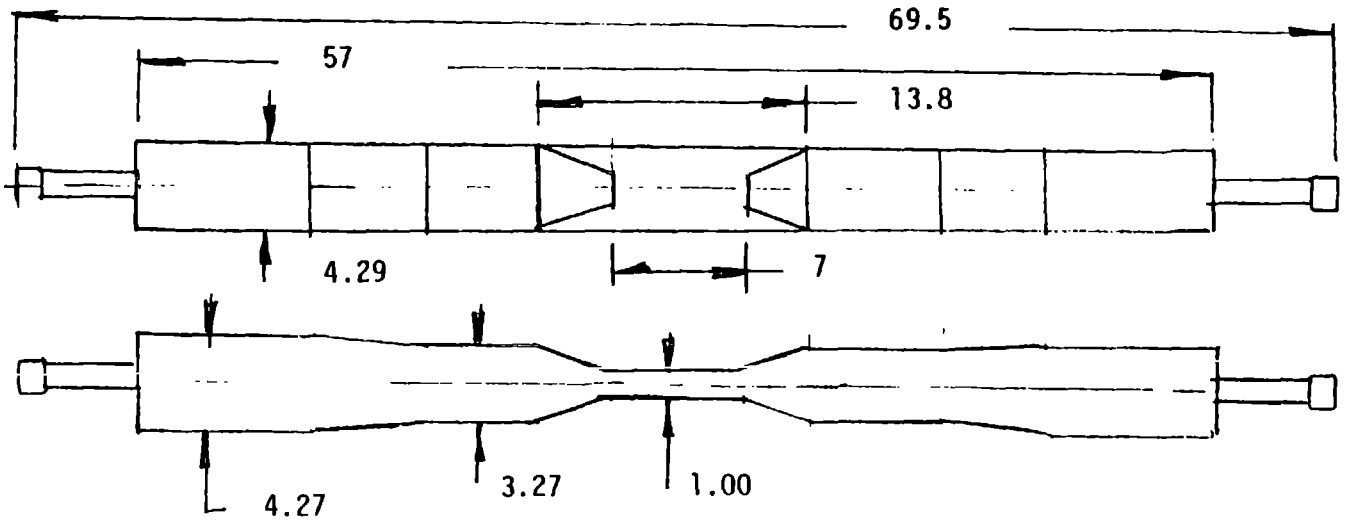

FATIGUE

Figure 8-170 Bolster Test Specimens

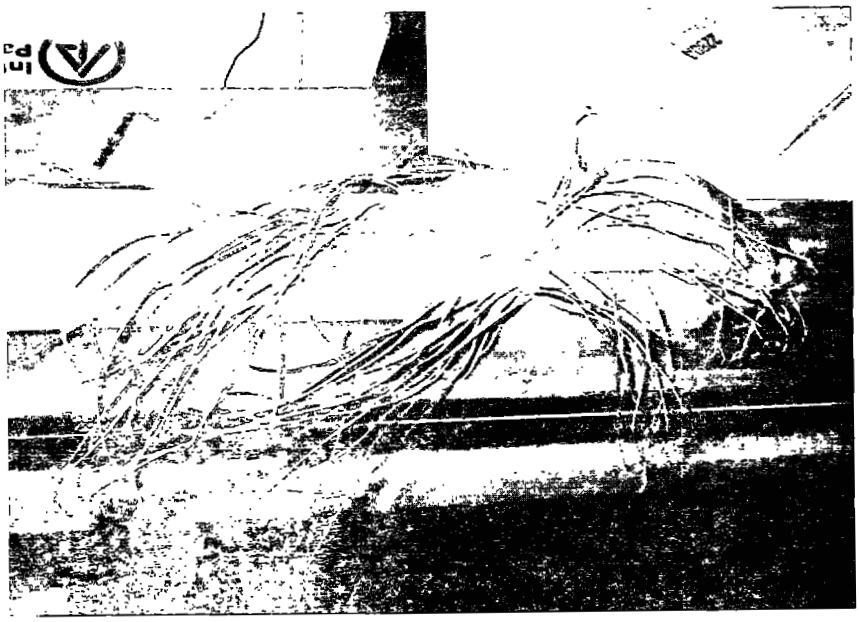

Figure 8-171 Strain Gages on Bolster Test Static Specimens

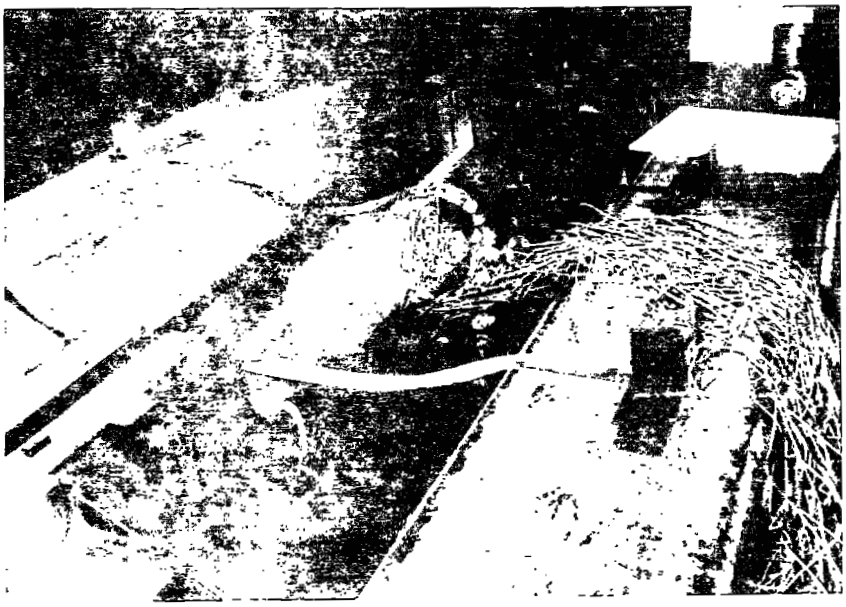

Figure 8-172 Bolster Test Specimen Tension Setup

gages, and Figure 8-173 depicts the compression test set-up with the extensometer. The plywood supports were used to prevent lateral buckling of the test sample.

The machine grips were set 34 in. apart, leaving 23 in. of sample in each grip. The extensometer was set at a gage length of 20 in. centered over the bolster area.

The fatigue test specimen, shown in Figure 8-170, was designed to be compatible with an MTS test machine, and four samples were tested at the University of Dayton Research Institute. The tests were conducted with a load ratio of R = -1, fully reversed loading. Four specimens were tested; two were to last 10,000 cycles and two were to fail near one million cycles.

8.2.5.8.4 Test Results

The tension test specimens failed when one of the bolsters cracked along the bond gap and wood attaching the bolster to the spar. After the crack, a large additional load was required to separate the second bolster, and to reach the ultimate load. The compression test specimen bolsters did not separate from the spar until ultimate failure occurred, which was at an average 73% higher in load than the tension failure. In the compression failure, the bolsters either sheared from the face, forced off by buckling of the spar elements, which created a crossgrain tension load across the bond gap, or they specimen by a compression failure outside the bolster area.

The test results are summarized in Table 8-95, and Figure 8-174 shows a failed tension specimen (#TS8-3). Figure 8-175 shows compression sample TS8-7 after failure, with the buckling forces evident, and Figure 8-176 shows compression specimen TS8-6, which failed outside the bolster area.

The strain gage data was not reduced when this report was written.

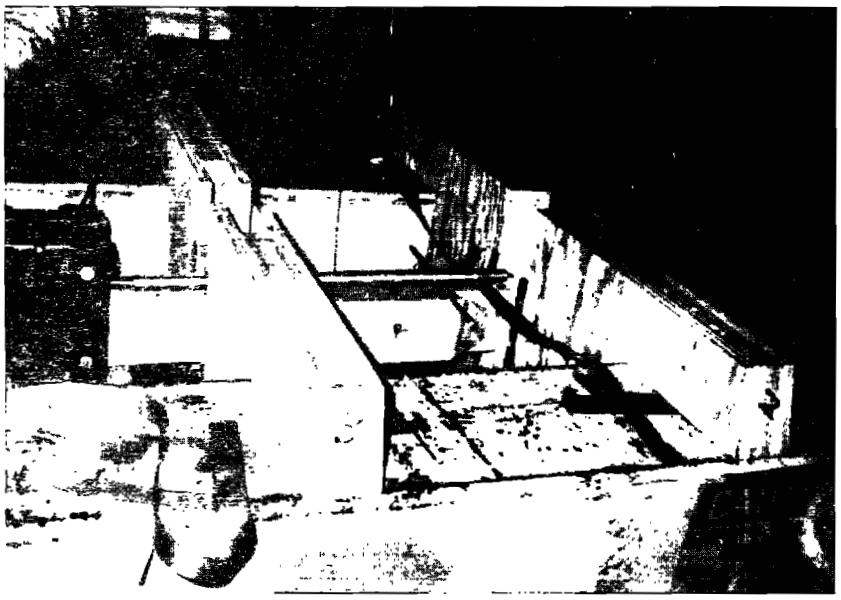

Figure 8-173 Bolster Compression Test Setup

Table 8-95 Bolster Test Results

Static Specimen Number	Load at Bolster Separation (lbs.)	Ultimate Failure Load (lbs.)	Test Type
8-2	28,000	55,000	Tension
8-3	23,800		Tension
8-5	25,600	32,000*	Tension
Tension Mean	25,800		
8-7	43,000	43,000	Compression
8-4	43,500	43,500	Compression
8-6	47,500	47,500	Compression
Compression Mean	44,667		

Fatigue

Specimen Number	Load Range (lbs.)	Frequency Hz	Number of Cycles
7	16,000 to -16,000	1	100
8	12,000 to -12,000	1	6,600
2	10,000 to -10,000	1	66,700
1	7,000 to -7,000	1	$10\ (10)^6$ (No Failure)

* Specimen 8-5 ultimate load occurred during the machine resonance following the bolster separation, so this value is not reliable.

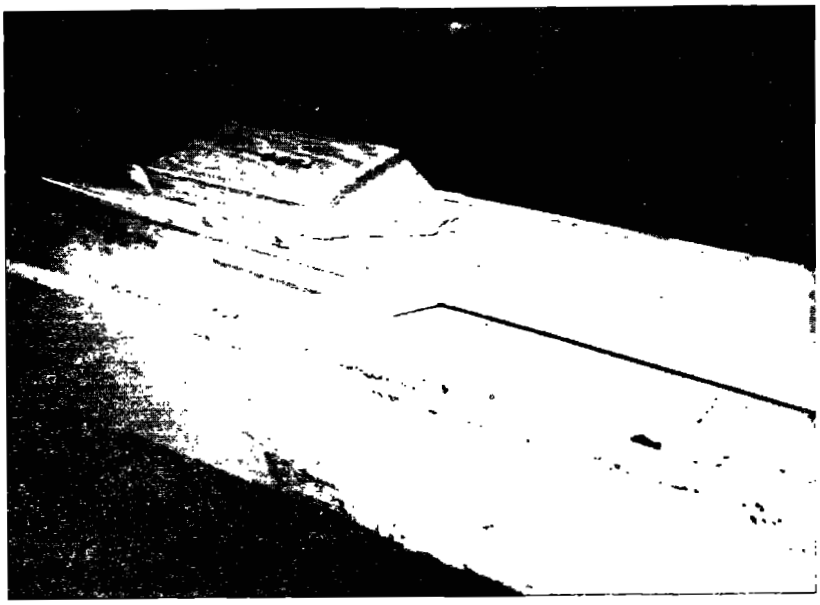

Figure 8-174 Failed Tension Specimen
Number TS8-3

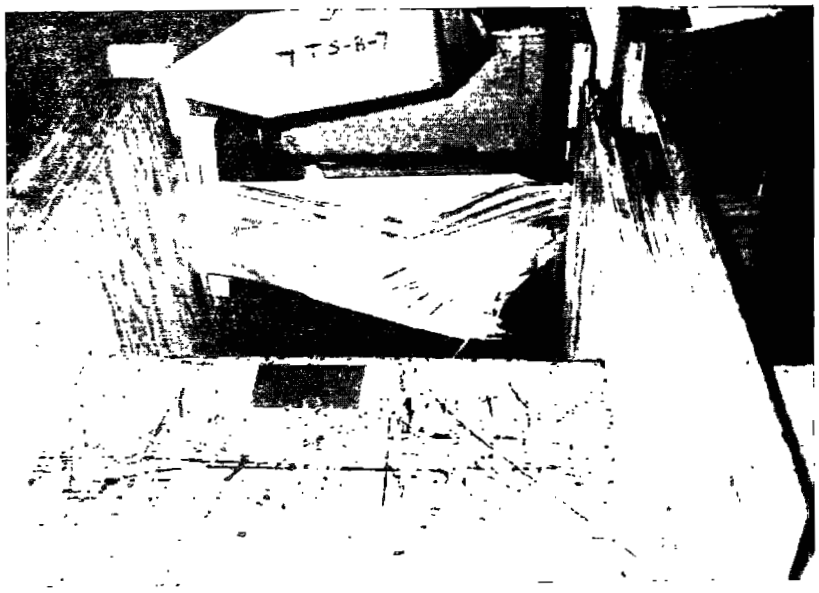

Figure 8-175 Failed Compression Specimen
Number TS8-7

Figure 8-176 Compression Specimen TS8-6

The fatigue testing was conducted at a frequency of 1Hz, and the fully reversed loading was set at 10,000 lbs. for specimen number 8-7. The load deflection trace at the start of testing is shown in Figure 8-177. The test was halted after 100 cycles, when the bolster ends were delaminated. The cracks were between the bolster and the center plank, shown in Figure 8-178, and the overall specimen is shown in Figure 8-179. Testing of specimen 8-8 followed, in the load range of ±12,000 lbs. Figure 8-180 shows load deflection plots after 0 and 1,000 cycles, with no change. The test was halted after 6,600 cycles because the bolsters were severely delaminated. The delamination was first noticed on one face at 600 cycles, and on a second face at 2,600 cycles. Figure 8-181 shows the areas of delamination, and Figure 8-182 shows more detail of the cracked areas.

Specimen 8-2 was tested at a loading of ±10,000 lbs. Load deflection traces are shown in Figure 8-183. After 11,200 cycles, one bolster began to delaminate, and the crack progressed to 9 in. after 27,500 cycles. The test was halted after 66,700 cycles when the crack progressed another 2 in. Figure 8-184 shows details of the crack on two faces of the sample.

The final fatigue specimen number 8-1 was tested at ±7,000 lbs. The lower load level was selected to provide longer term test data. Figure 8-185 defines load-deflection plots, which show virtually no change after 10,000 cycles. A slight delamination of one bolster was noticed after 180,000 cycles, and a second crack appeared after 712,400 cycles. The initial crack grew after 794,000 cycles, but no further damage was noticed when the test ended after 10 million cycles. Figure 8-186 shows the cracked areas.

The failures caused by fatigue loading indicate that when the bolster tip begins to crack, although the load path shifts, the cracks do not propagate as rapidly as would be expected. The initial cracks appear earlier than analyses would indicate, but the progression of failure would require further study before the structural adequacy could be verified.

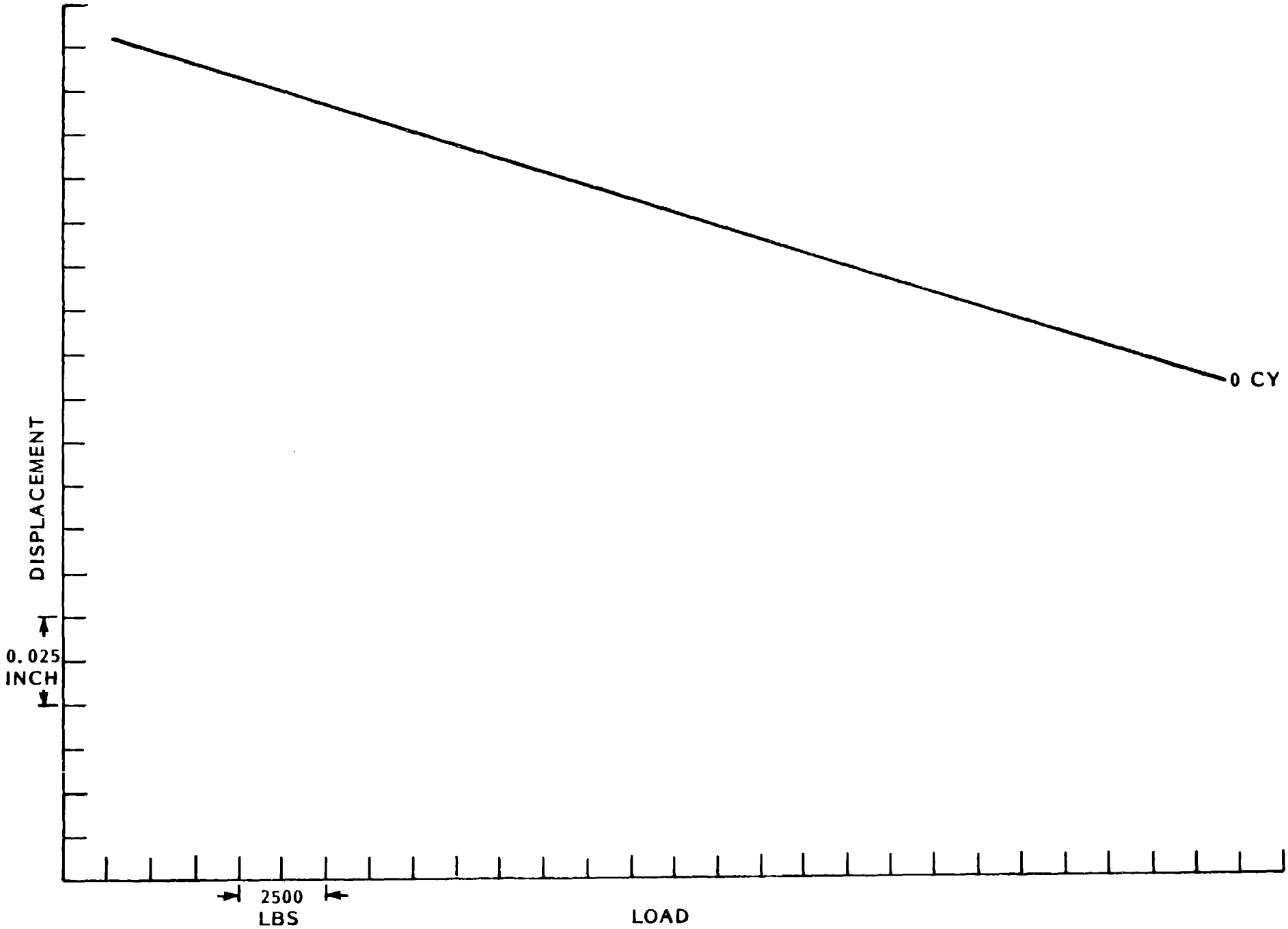

Figure 8-177 Load/Deflection Trace of Fatigue Specimen 8-7 at ±16,000 lbs.

Figure 8-178 Typical Bolster Delamination Crack Area, Specimen 8-7

Figure 8-179 Overall View of Specimen 8-7

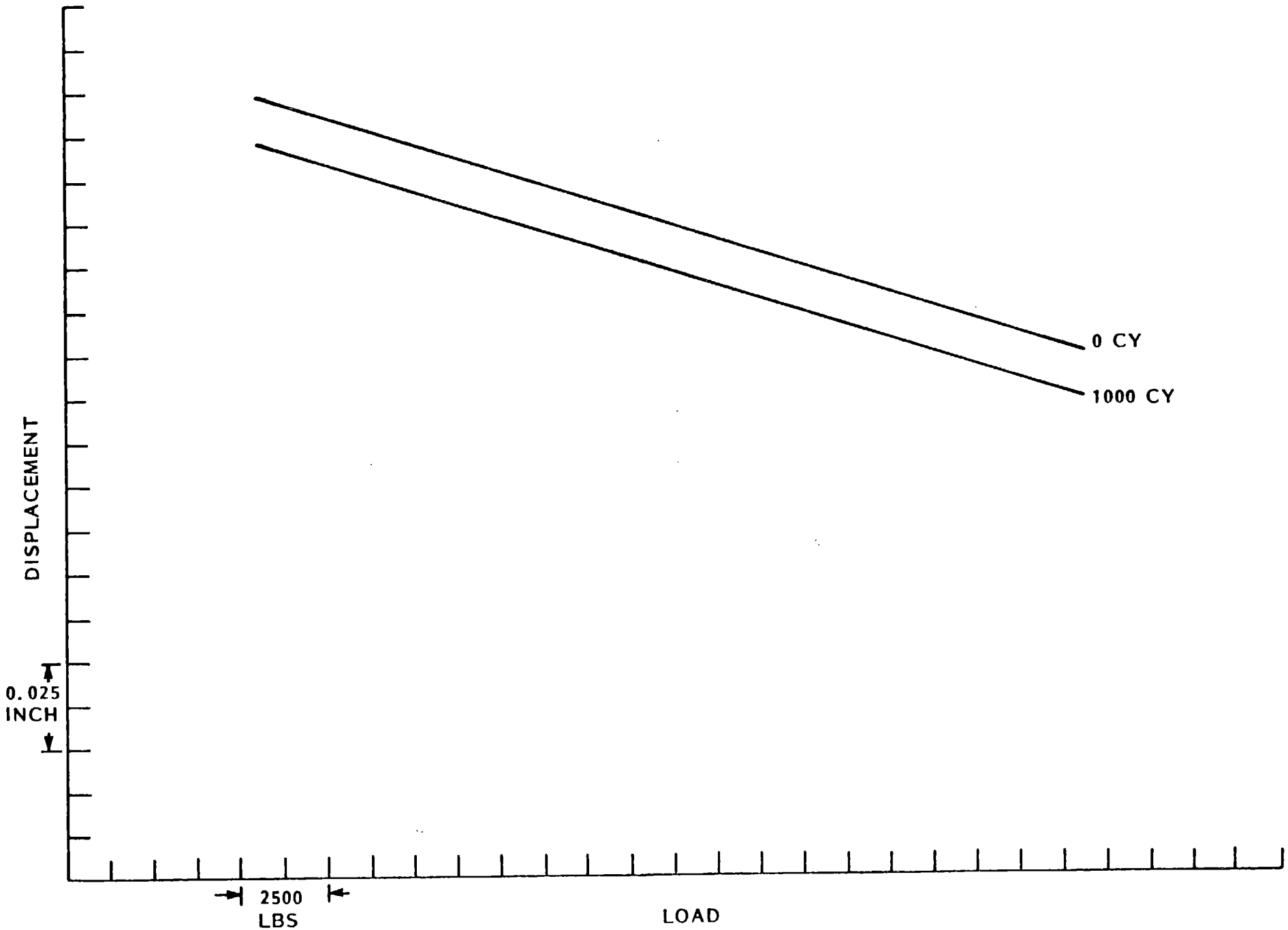

Figure 8-180 Load-Deflection Plots of Specimen 8-8

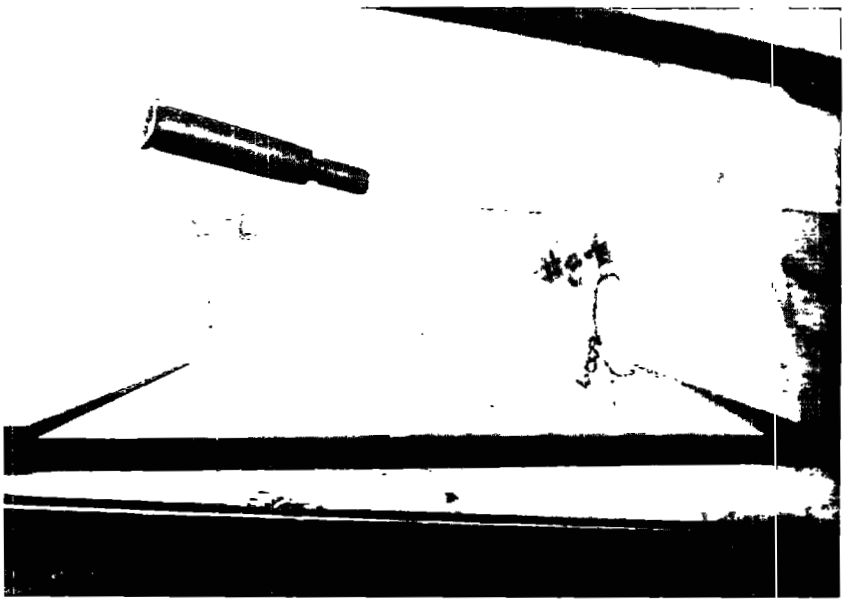

Crack Area After 600 Cycles (right) and 2,600 Cycles (left)

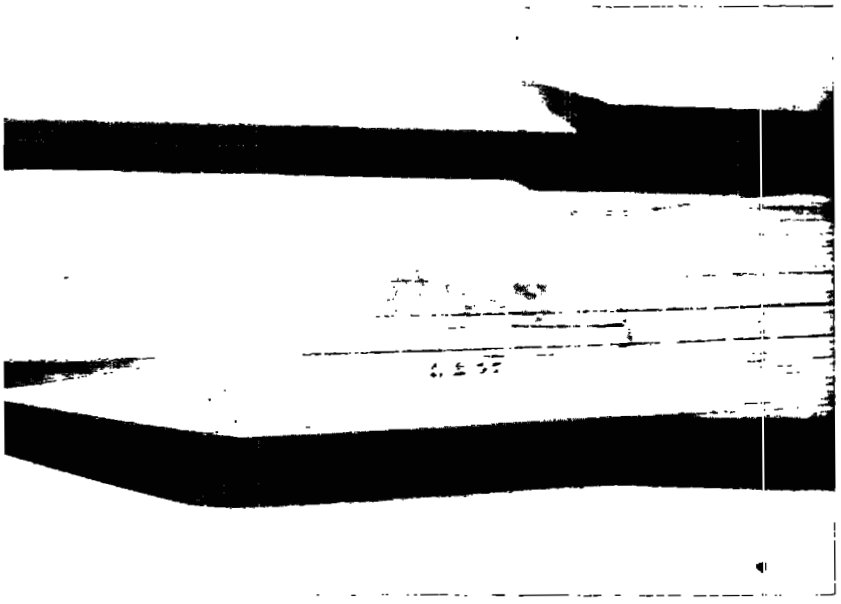

Delamination Area After 6,6000 Cycles

Figure 8-181 Delamination of Specimen 8-8

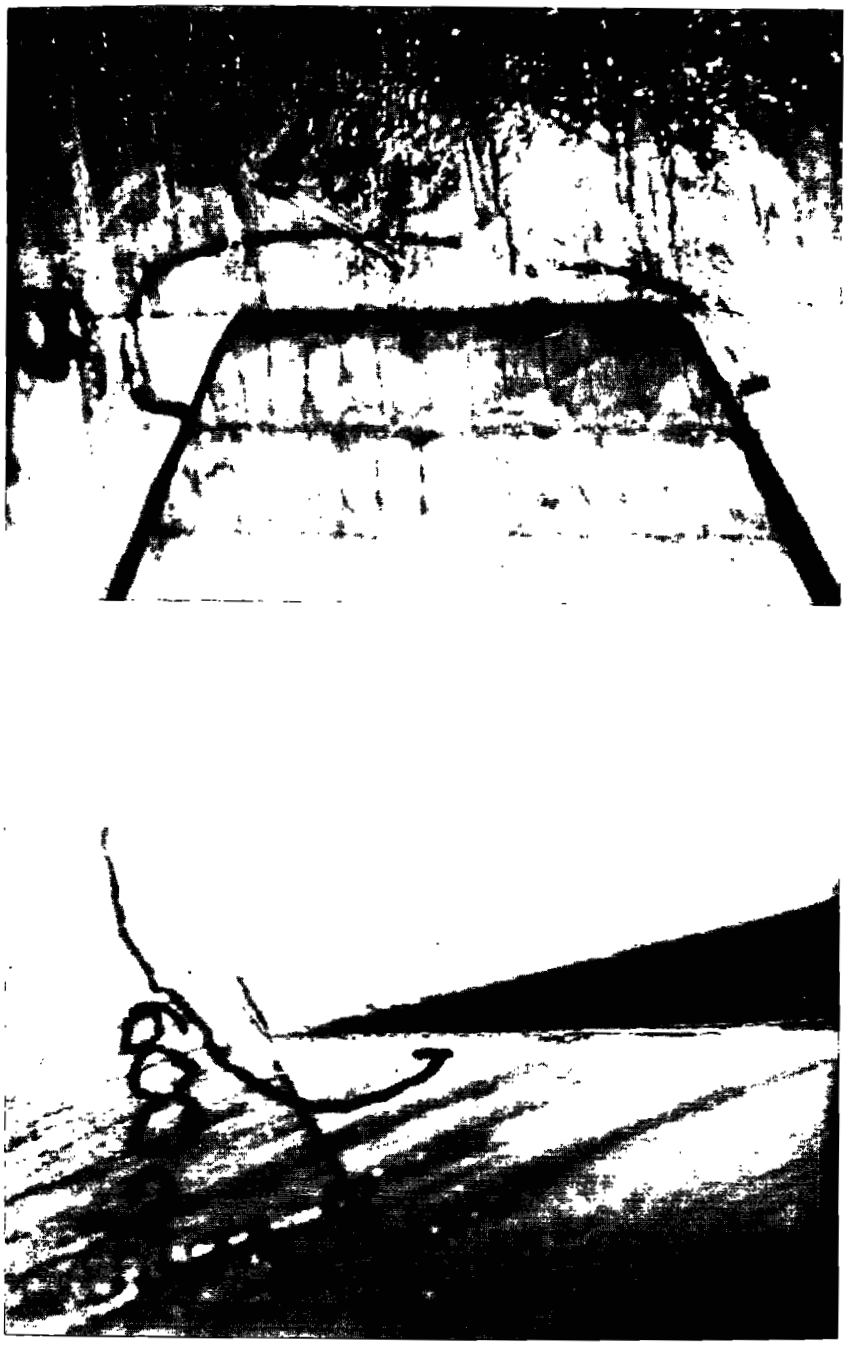

Figure 8-182 Close-up Photographs of Cracks - Specimen 8-8

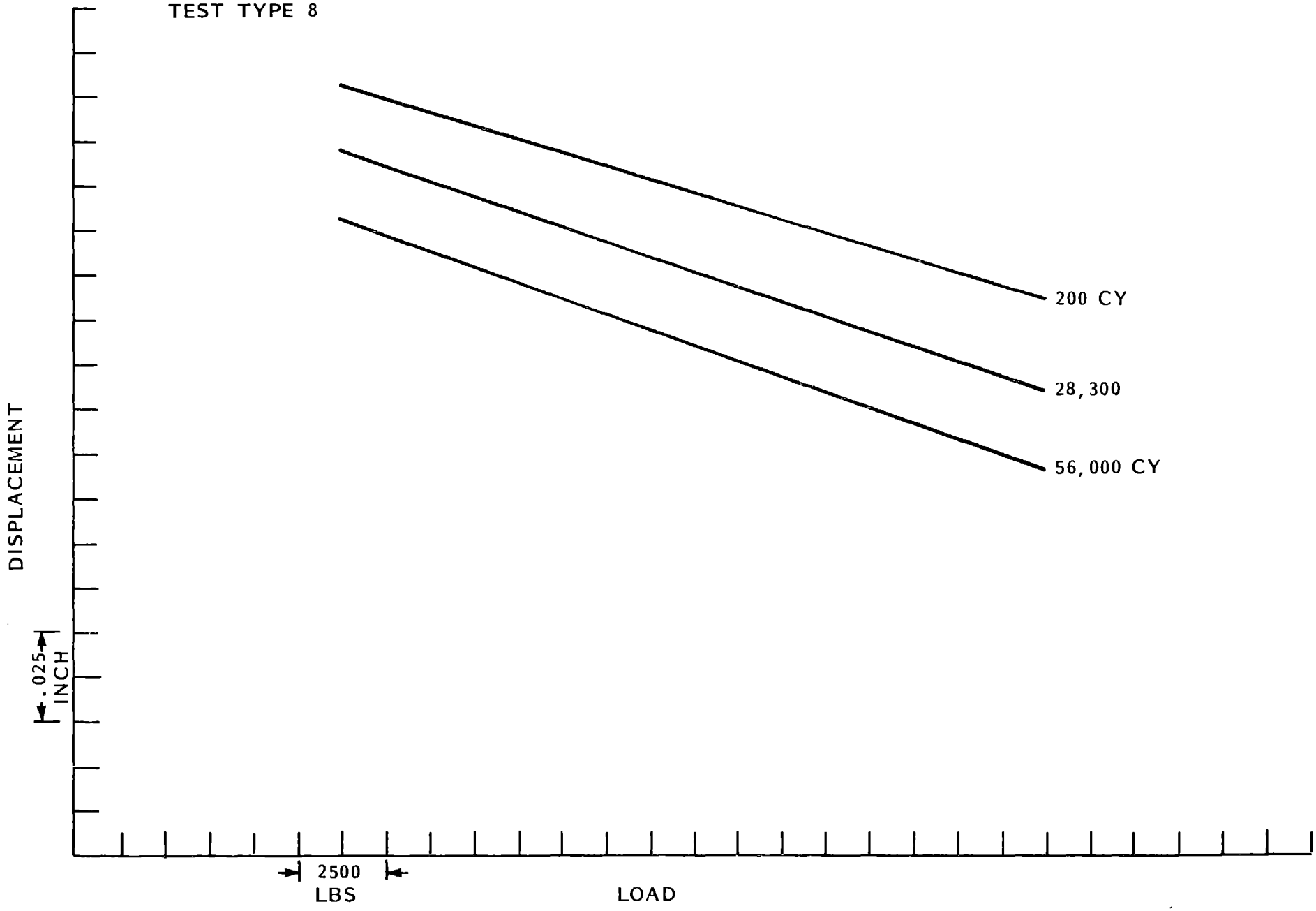

Figure 8-183 Load-Deflection Plots of Specimen 8-2

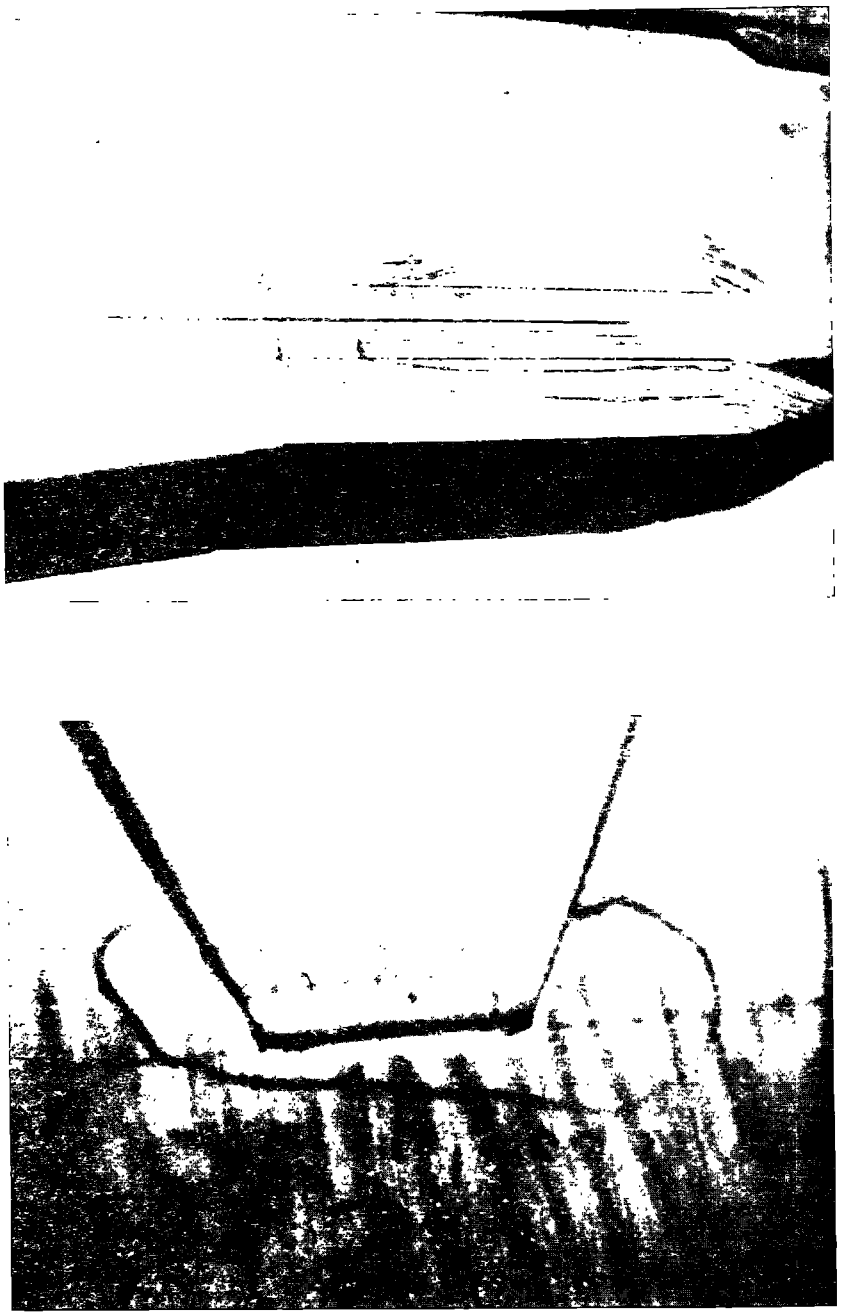

Figure 8-184 Views of Cracks of Sample 8-2

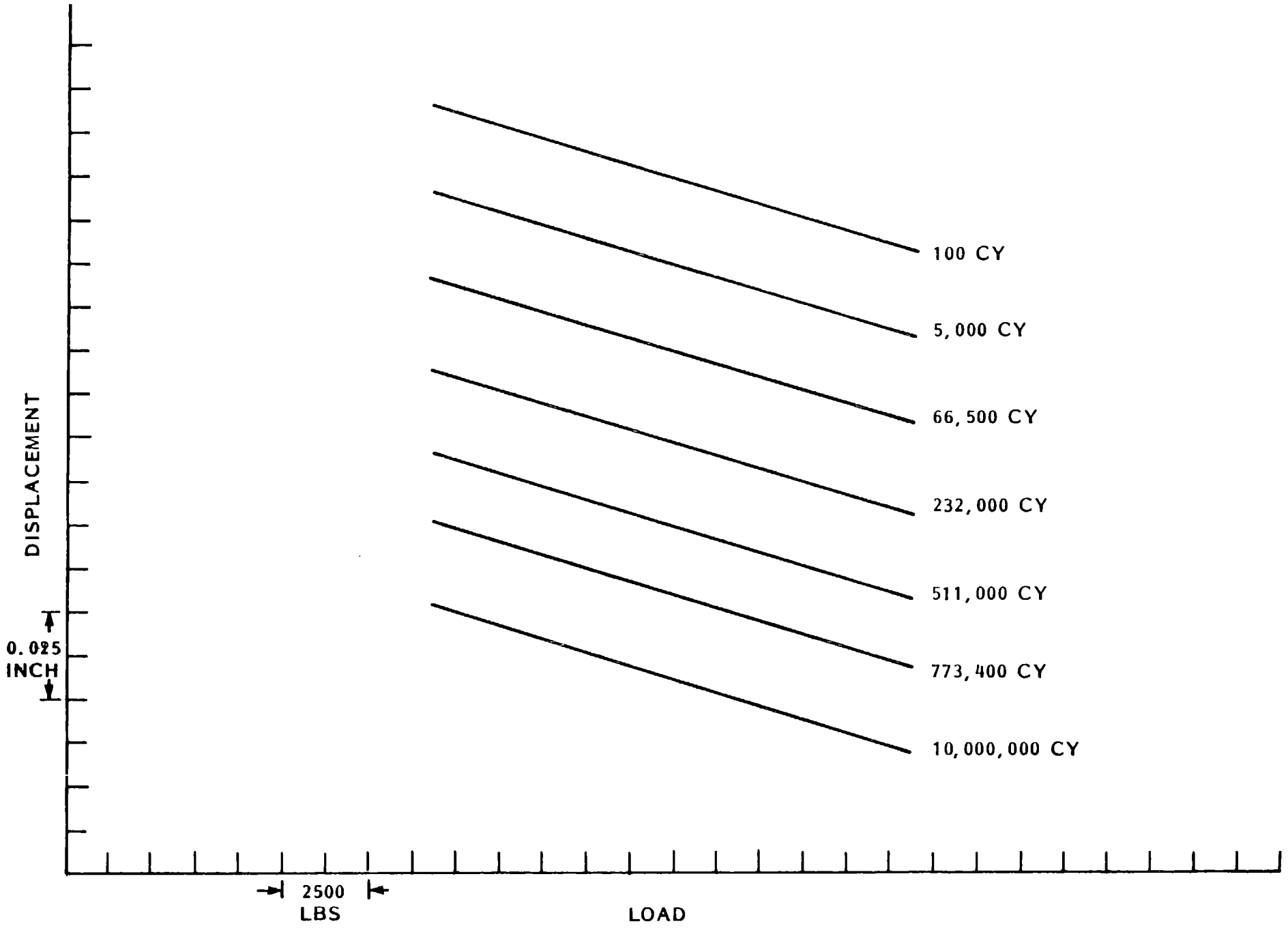

Figure 8-185 Load-Deflection Plots of Sepcimen 8-1

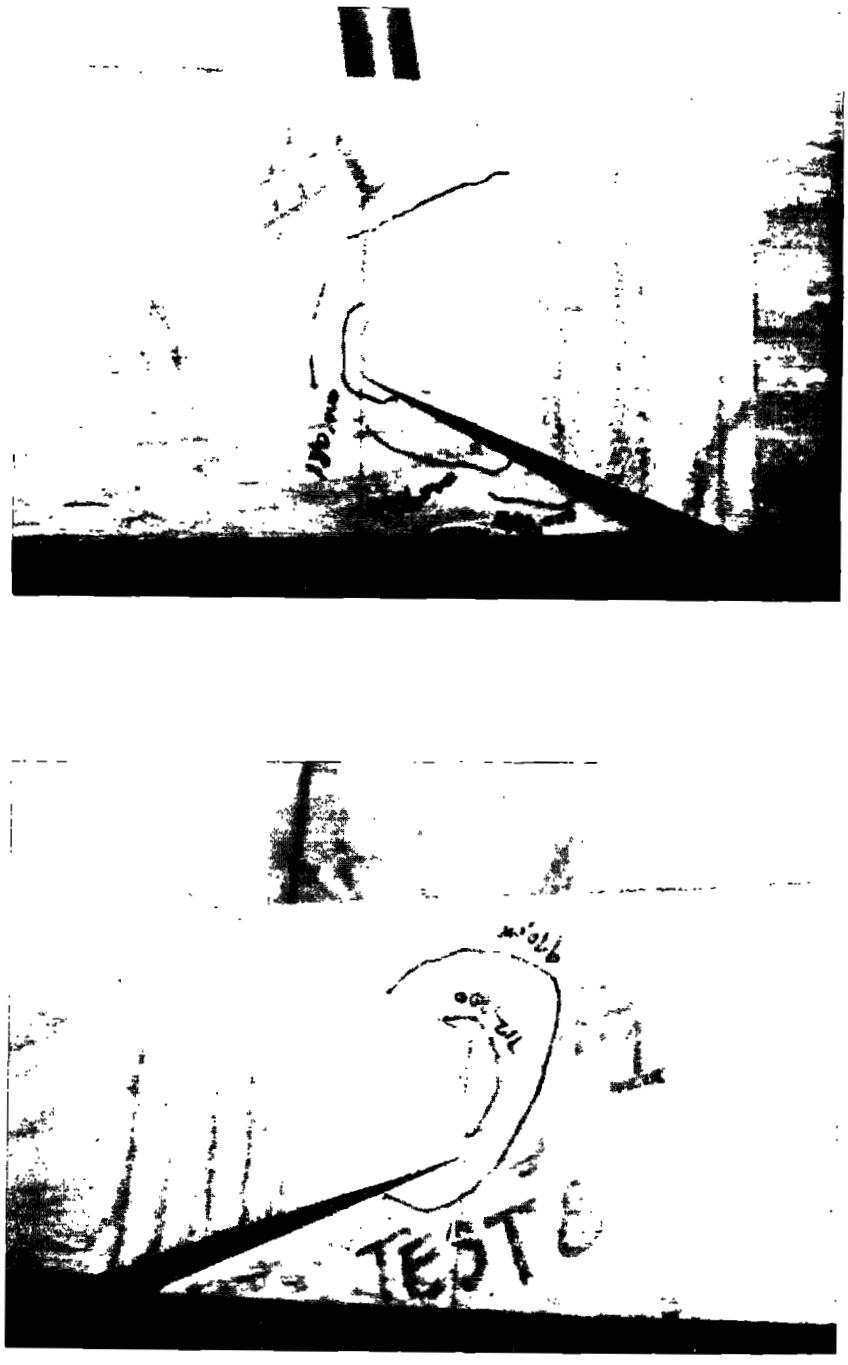

Figure 8-186 Cracked Areas of Specimen Number 8-1

8.3 HYDRAULIC COMPONENT TESTS

The original design for rotor torque control was a partial span control system. In this system the last 25% (50 ft.) of the blade was mounted on a "king post" bearing arrangement, and hydraulic actuators rotated the tip through 90°, to any pitch angle.

The actuator, the controlling servo-valve and an emergency feather valve were located at the interface between the non-pitching and the pitching portions of the blade, 150 ft. from the center of the blade. At high rotational speeds the equipment would experience a high acceleration force. In overspeed conditions, 23 rpm, the acceleration could be as high as 25 g's. To confirm that the actuator and valves would operate properly in the high-g environment, several tests were performed on the actuators and control valves.

8.3.1 PITCH CONTROL ACTUATOR TESTS

The objectives of the actuator test were to simulate the high-g environment the hydraulic actuator would experience, to check the actuator design and performance capability in this environment, and to identify and correct any deficiencies in the design. The rod end bearings, the rod seals and bearings, and the piston rings and seals were the important areas.

The tests were required because GE's suppliers had no experience with the actuator in wind turbine service. Two manafacturers supplied units for testing. The tests were conducted at GE-AEPD's facility in Evendale, Ohio.

8.3.1.1 Test Summary

The rod, rod seal, and rod end bearings were subjected to the loads and strains that they would experience in actual operation. One hydraulic actuator worked against a duplicate actuator, which simulated the axial load, and a small actuator simulated side loads. The test arrangement is illustrated in Figure 8-187 and the hydraulic schematic is shown in Figure 8-188.

The two actuators were axially aligned and connected at their rod ends. The valves and accumulators in the bypass line of the load actuator restricted fluid flow and served as loads in the system. The rod motion was controlled

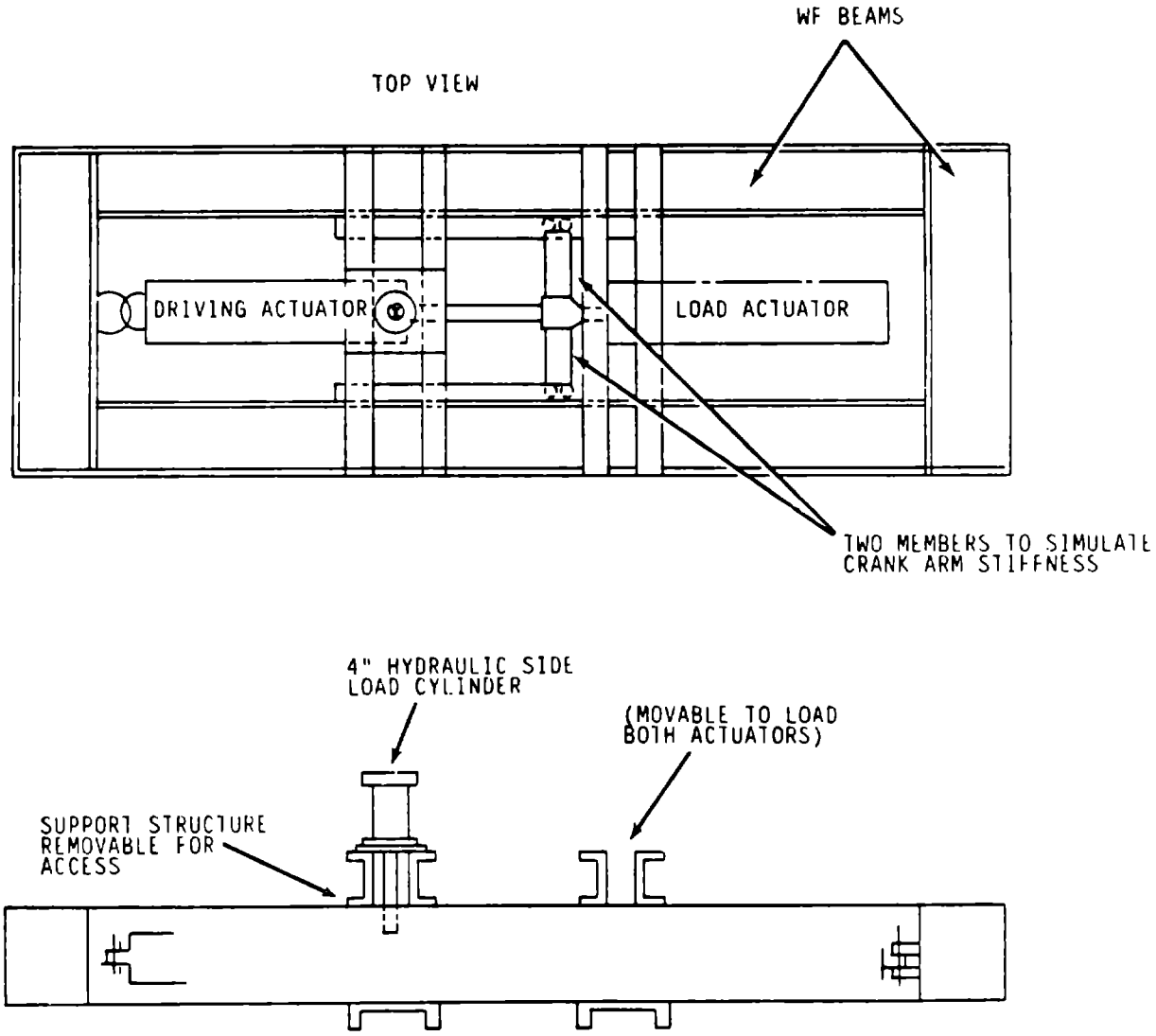

Figure 8-187 Partial Span Control Actuator Test Fixture

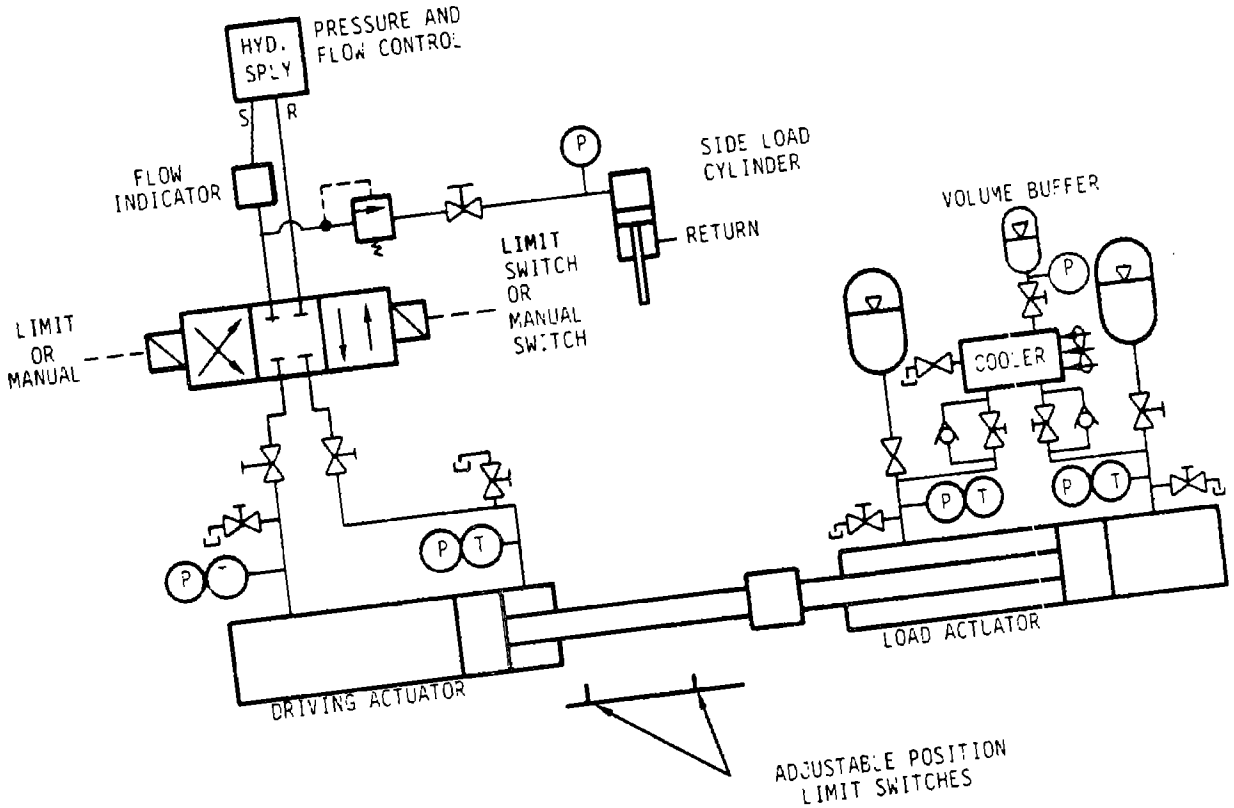

Figure 8-188 Partial Span Control Actuator Test Schematic

by limit switches that alternately operated the solenoids of the directional control valve. A small hydraulic actuator applied a concentrated load to the driving actuator, perpendicular to the rod centerline and along the rod end bearing axes, to simulate a high force on the driving actuator rod seal and bearing. A concentrated load that produced the same bending moment at the rod seals that a transverse acceleration load would produce within the actuator was defined as an "Xg" equivalent side load.

8.3.1.2 Description and Results

An Atlas cylinder model G-82216 and a Milwaukee cylinder model B-6824 were subjected to the lateral g test. Only the test cylinder was subjected to the simulated g load, as illustrated in Figure 8-187.

In the first part of the test, the Atlas cylinder was the test specimen and the Milwaukee unit provided the load. The Atlas unit had been subjected to 30,000 cycles of small oscillation at an equivalent 20 g's when it started leaking. When the leakage rate reached 32 ml/hr, testing was discontinued. The unit was disassembled for failure analysis and it was discovered that the rod and seals were damaged on the circumference, at the point where side loading was simulated. Similar actuators had experienced essentially the same type of damage in MOD-2 operation. The cause of the seal damage was traced to debris shed by wear on the aluminum bronze rod end bearings. The bearings were considerably worn where the load was applied.

The Atlas actuator was refurbished and installed as the load actuator for testing the Milwaukee unit. The Milwaukee unit was subjected to the wear test with the following results: after 54,454 cycles of small oscillation at 20 g's the rod seal leaked at 0.27 ml/hr; after 116,635 cycles, the leakage actually decreased to 0.19 ml/hr; after 136,696 cycles, the leakage was 0.20 ml/hr; and after 161,248 cycles the leakage rate was 0.3 ml/hr. The test continued until 207,449 cycles, when the leakage was too great to continue. A

failure analysis showed wear of the bronze rod bushings, and the resulting debris damaged the Viton rod seals.

According to the design requirements the seals and bearing were to be replaced every five years, or every 600,000 cycles. The test indicated that if the pitch control actuators were to serve successfully without maintenance for five years, the rod seal and bearings would have to be re-designed.

Several approaches were considered: to change the bearing material from bronze to Duralon®, to increase the bearing area and thus lower the pressure on the bearing at the interface, and to design the bearing to self-align with rod deflections. The redesign work was terminated when ailerons replaced partial span control as the torque control system.

8.3.2 PITCH CONTROL VALVE TESTS

The servo, emergency feather and block valves, which control the actuator, are mounted 150 ft from the center of the blade. Consequently, they experience high forces in operating and overspeed conditions. These valves were subjected to a spin test on a centrifuge at an acceleration of 25 g. A complete operation sequence was performed on the valves at accelerations between 5 and 25 g. These tests were conducted at GE-RSD's facility in Philadelphia, PA.

8.3.2.1 Test Summary

The test verified the capability of the emergency feather system and tested the sensitivity of the servo valve in the high-g environment. All the hydraulic equipment mounted on the blade, illustrated in Figure 8-189, performed in accordance with the goals of the design, at accelerations between 0 and 25 g. The maximum acceleration experienced by the valve assembly in operation is 20 g. The baseline data at 0 g was recorded before each series of tests.

When emergency feathering was tested the feather valve showed greater sensitivity to back pressure than was anticipated. The back pressure occurred because the areas of the spool surfaces that experienced pressure were not equal. The performance of this unbalanced spool was unacceptable. A four-way valve with a balanced spool, of the same shear-seal design replaced the tested three-way valve. The construction and configuration of the four-way valve was similar to that of the three-way valve, so little additional testing was required.

The by-pass and servo block valves also required modification. The configuration of these valves is shown in Figure 8-190. The pressure in the valve case, generated by the centrifugal gravity gradient, compressed the inactive pilot spring and caused the spool to float. Holes were drilled in the inactive pilot operator pistons to equalize the pressure across the piston. The vendor was asked to assign a new model number to the modified valve for production.

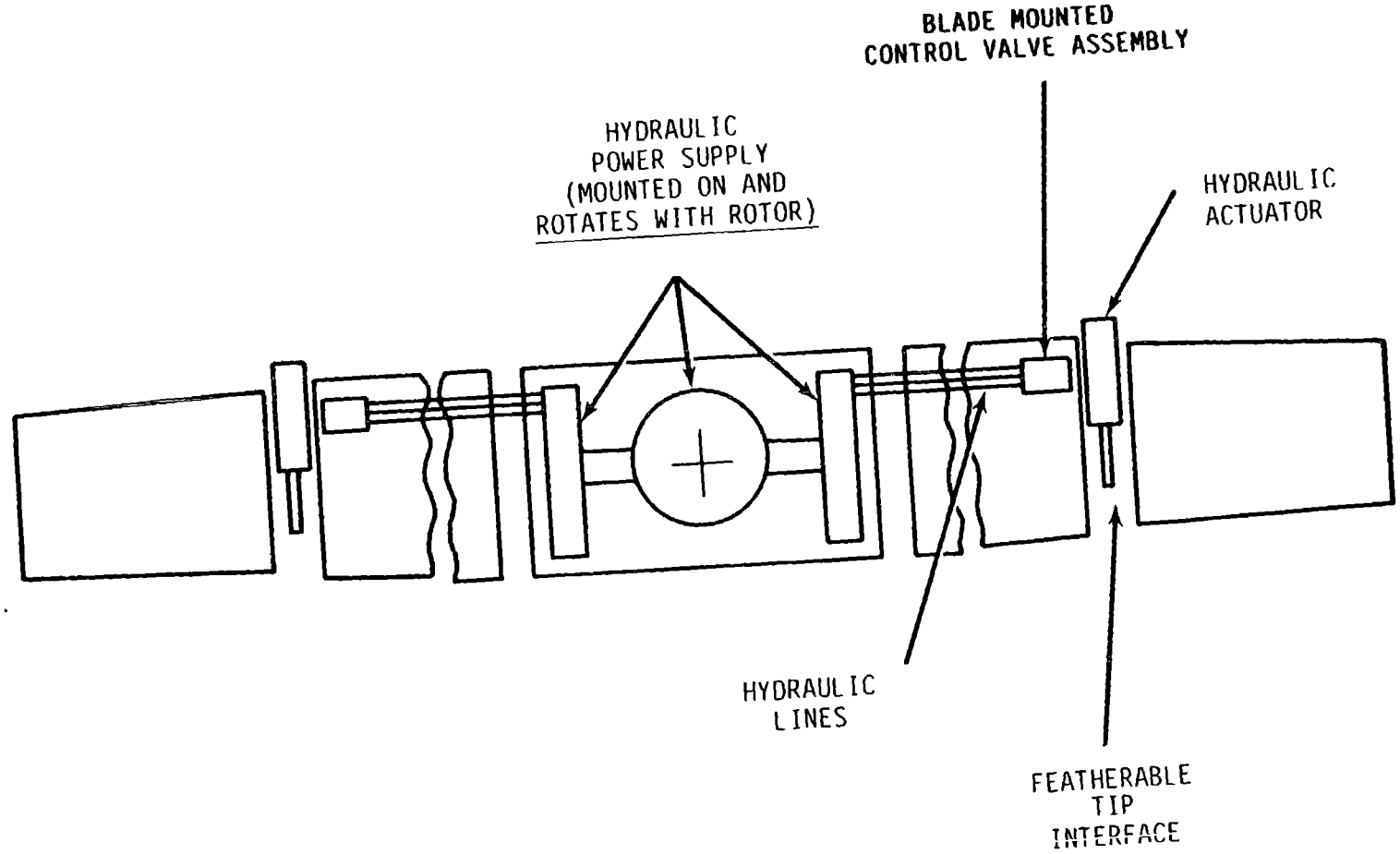

Figure 8-189 Partial Span Control Hydraulic System

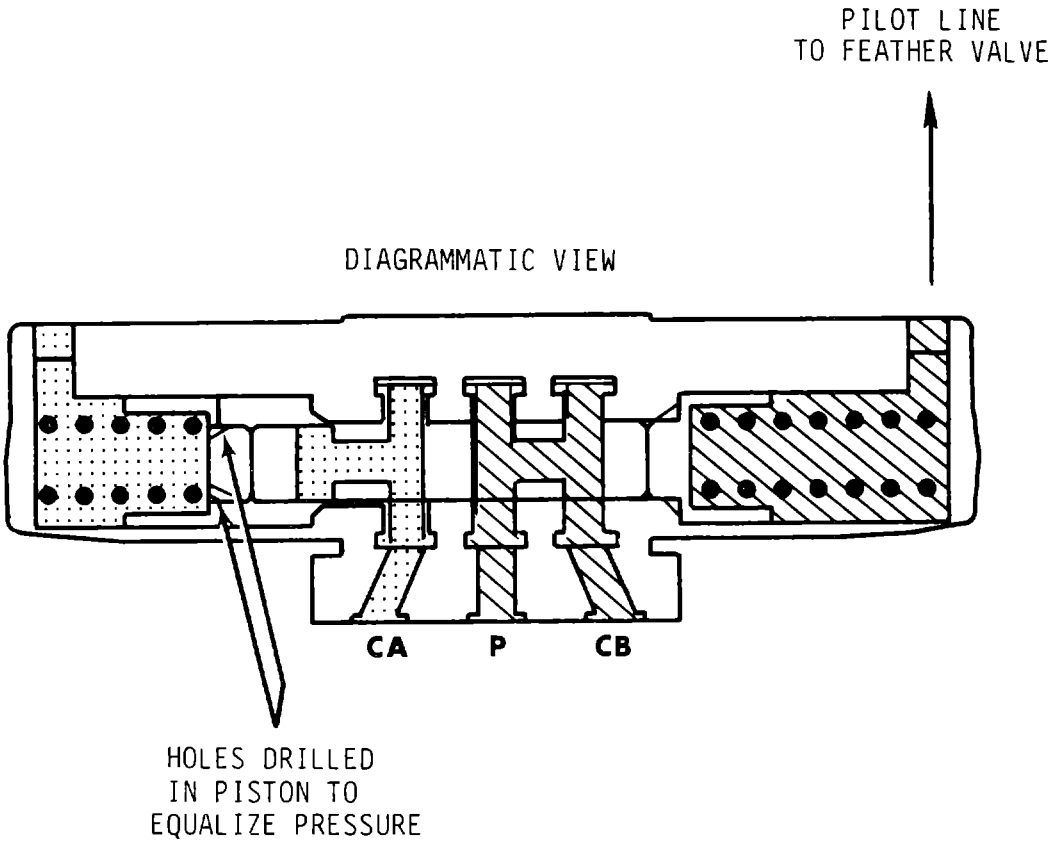

Figure 8-190 By-Pass and Servo Block Valve Modification

The second part of the test compared servo valve sensitivity at various values of g with a constant input current to the servo valve. The results were within ±1.0% of the expected values, as indicated by the flow through the servo valve for various input currents.

8.3.2.2 Test Description and Results

A schematic of the test set-up is shown in Figure 8-191. The hydraulic reservoir, pump, relief valve, flow meter and pressure transducers (P1 and P2) were stationary. All other components were located on the centrifuge.

The first series of tests verified the operation of the emergency feathering system. The flow through the servo valve was established at the beginning of the test, when the centrifuge was not spinning. The feather valve solenoid received a continuous 110 Vac signal, which energized the pilot operation of both the by-pass and servo block valves.

Power to the feather valve was interrupted to simulate the signal calling for emergency feathering. The recorder trace shown in Figure 8-192 indicated that when power was removed the pilot pressure fell to zero and the flow through the servo valve also fell to zero, while both the supply pressure and the signal to the servo valve remained constant, indicating that the servo block valve had closed, as expected. Also, both throttle valve pressures stabilized at the same value, which indicated that the by-pass valve opened.

The centrifuge was rotated at 55 rpm, 78 rpm, and 110 rpm, which simulate 5g, 10g and 20g respectively, with identical results. The same test was conducted later at 25g, with similar satisfactory results.

The trace showed that the flow increased when the by-pass and servo block valve were energized or de-energized, for less than 1 second. The increased flow was due to by-pass and servo block valve overlap. The transient increase in flow was not a problem.

The pilot pressure required to shift the by-pass and servo block valves was determined. The data shows that with 1200 psi supply pressure, at least 1200 psi pilot pressure is required to shift the valve spools fully. The three-way

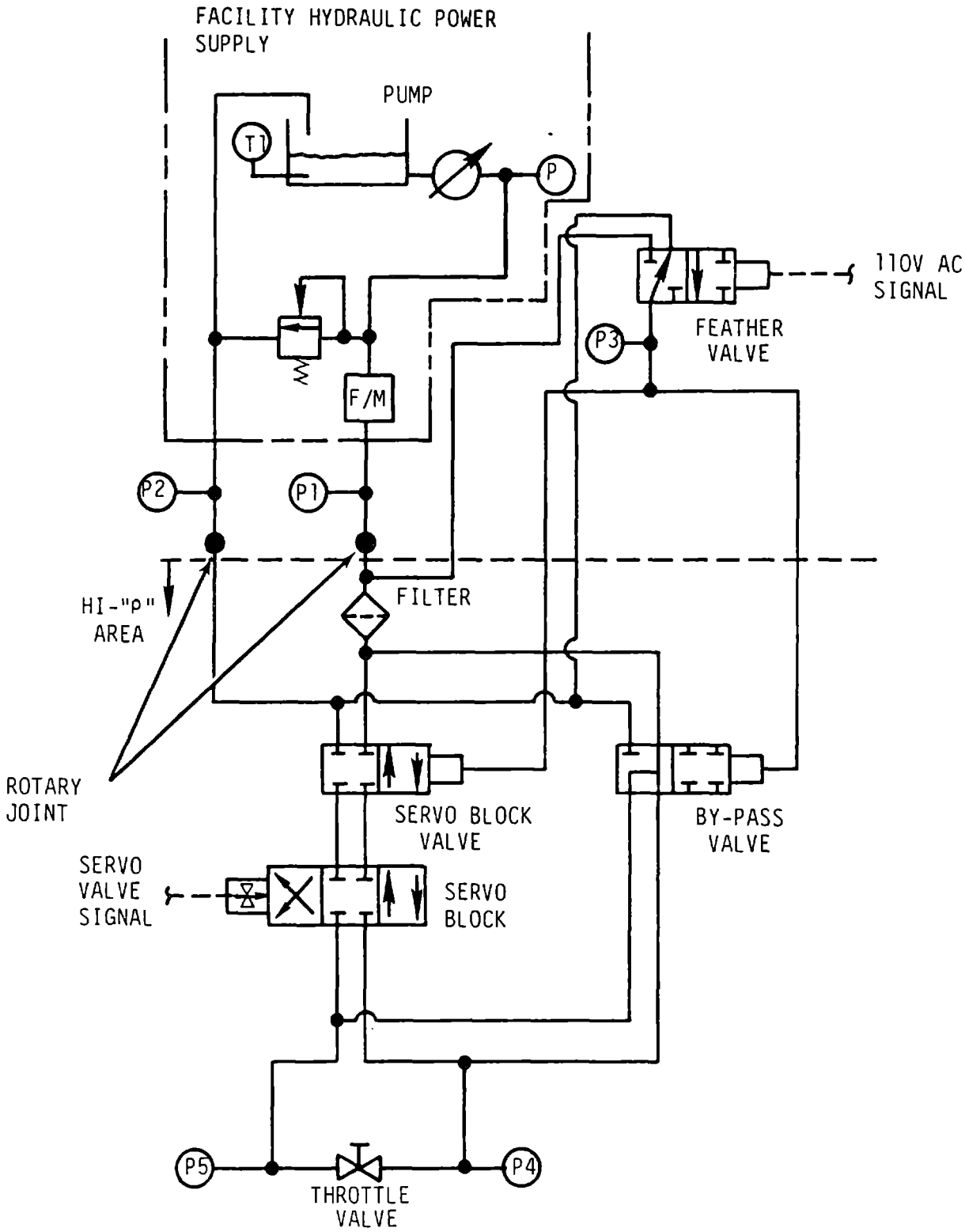

Figure 8-191 Partial Span Control Spin Test Schematic

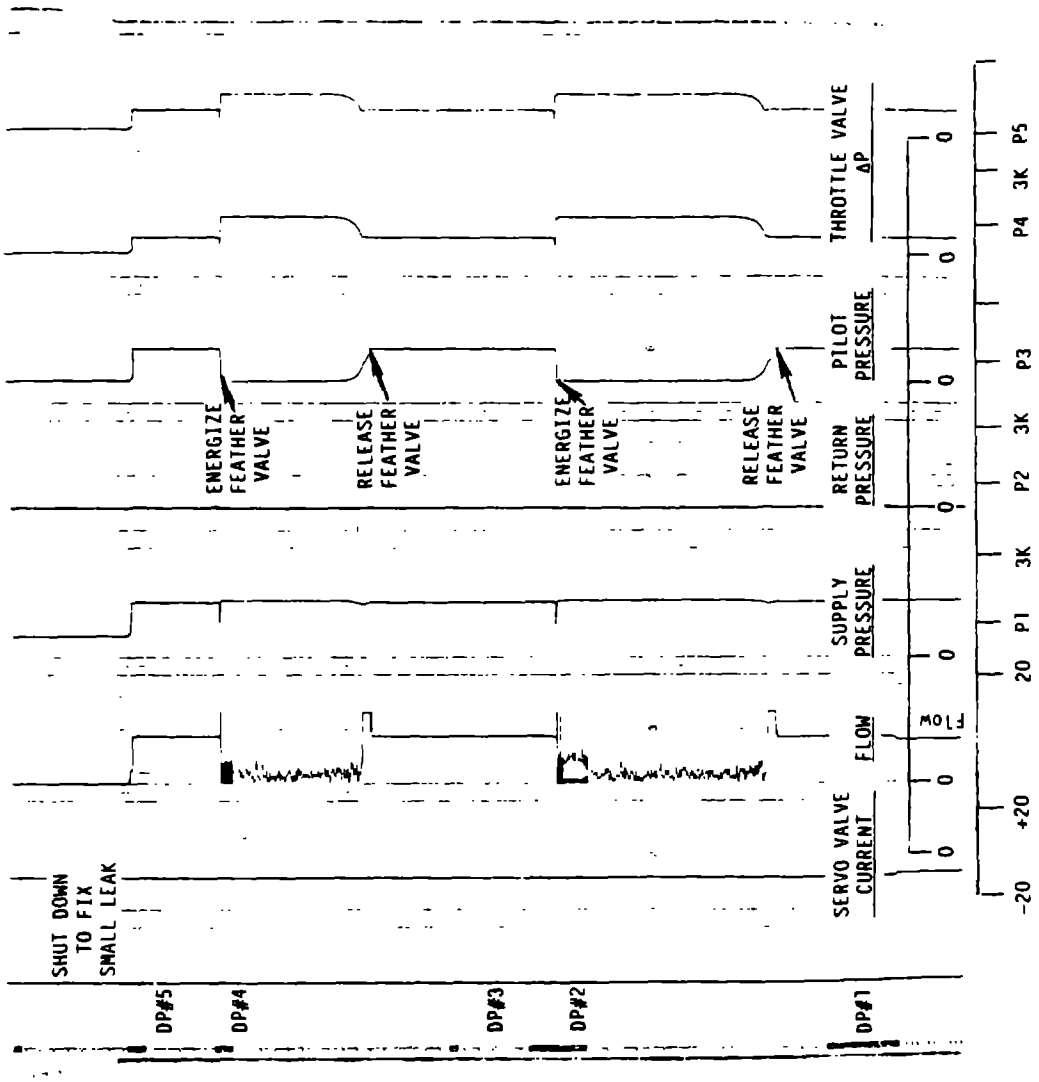

Figure 8-192 Spin Test Traces

and four-way feather valves should be subjected to more testing to furthur determine the characteristics of each.

The test also verified the operation of the valves in emergency feathering at 5 g. The pilot pressure was increased to 1200 psi instantly, rather than gradually, and several runs were made to check that the system operated properly. These emergency feather tests were repeated at 10 g and 20 g.

8.3.2.3 Characteristic Summary

- A minimum pilot pressure of 1200 psi was required for reliable by-pass and servo block valve operation

- With a minimum pilot pressure of 1200 psi, the emergency feathering operation is reliable up to 25 g. The system design provides a minimum pilot pressure of 1800 psi

- When pilot pressure is applied or released there is a transient flow surge for less than one second. This surge will not be a problem because it is a "system leak"; the flow is not translated to actuator motion and will be easily supplied by the accumulators.

8.4 AERODYNAMIC TESTS

8.4.1 AIRFOIL CHARACTERISTICS (WIND TUNNEL TESTS OF BASIC AIRFOILS FOR MOD-5A)

8.4.1.1 Test Objectives

The MOD-5A blade design was based on airfoil sections with varying thickness ratios and a camber derived from the NACA 64XXX airfoils. Design data is available for these airfoil sections with thickness ratios of up to 21%. Little data exists for airfoils with thickness ratios above 21%.

Structural and economic reasons drove the optimum design of the MOD-5A blade toward high thickness ratios. Successive designs led to a blade that was more than 21% thick from 84% of the span and inward. The blade reached 24% thick at 76% of the span and was 28.6% thick at 25% of the span. The wind tunnel test program provided basic aerodynamic data for blades with high thickness ratios and appropriate camber ratios. The program also investigated modifications to the airfoil section that would optimize the airfoil section's characteristics.

8.4.1.2 Test Facilities

In order to provide meaningful data, the test hardware had to be dynamically similar to the full-scale MOD-5A machine. The Reynolds number (R_N) could be 5×10^6 or greater, and the Mach number (M) could not exceed 0.3. The facility selected for these tests was the Transonic Airfoil facility at the Aeronautical and Astronautical Research Laboratory at Ohio State University.

This facility has two wind-tunnels. The large tunnel, 6 in. by 22 in., operates at low pressures and low Reynolds numbers. This tunnel was used for a few ancillary runs, such as flow visualization runs.

The small tunnel, 6 in. by 12 in., provided the main body of data. Models built for use in this tunnel could also be used in the large tunnel. In both tunnels, two dimensional models spanning the test sections were mounted in circular metal windows in the two side walls to provide for adjustable angles of attack. The ceilings and floors of the tunnel test sections were perforated to reduce wave reflection interference. This tunnel could operate at static pressures above 120 psi in the test section, achieving an R_N of 5×10^6 using a model with a 4-in. chord.

Chordwise pressure distributions were obtained from these wind tunnels. The normal force, chordwise force and pitching moment were calculated from the pressure distributions by integration. In addition, a wake survey probe was mounted downstream of the airfoil section model and swept through the wake surveying the wake total pressure defect. The wake survey drag was the main drag measurement for angles of attack at which the wake could be captured by the probe. At higher angles of attack and high drag coefficients, at which the probe could not survey the entire wake, the drag was computed from the chordwise pressure distribution.

The data for low angles of attack from these tests was consistent with data from other facilities.

8.4.1.3 Model Airfoil Sections Tested

All of the models were made of cast epoxy with the pressure taps and associated plumbing cast integrally. The pressure taps were located on the upper and lower surfaces every 2.5% of the chord from the leading edge to 10% of the chord, and at every 5% aft to the trailing edge. Two additional taps were placed at .975% of the chord.

Eleven models were tested. Of these, nine represented airfoil sections of the inner blade and two represented the tip. The inner blade models consisted of seven sections derived from the NACA 64029 airfoil section and two derived from the NACA 64426 section.

The models based on NACA 64029 were devised along three different lines, based on the basic airfoil section. A group of models with a raised trailing edge was derived by raising the upper surface from the maximum thickness point aft to the trailing edge. The geometry of this modification is illustrated in Figure 8-193.

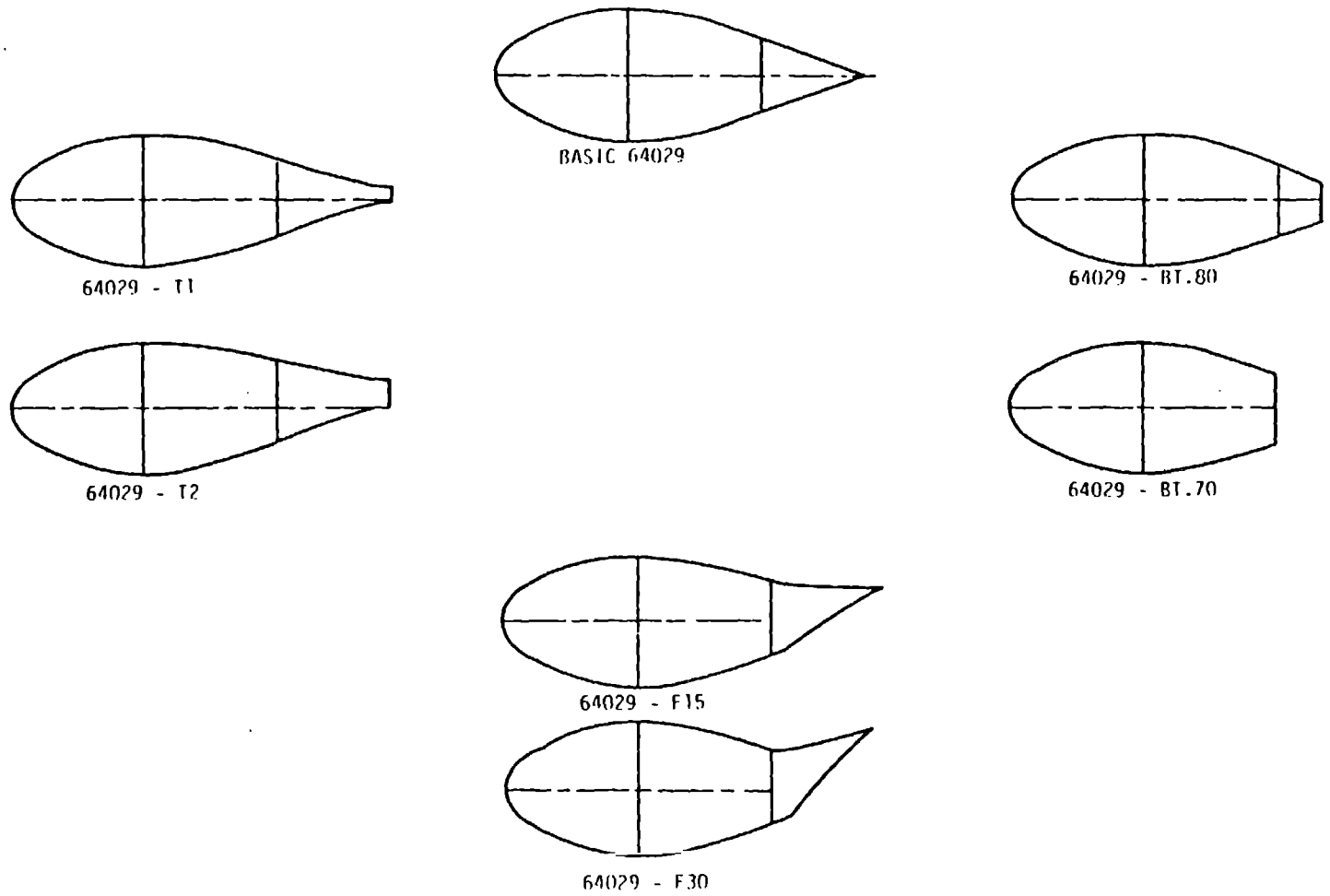

Figure 8-193 Geometry of the Airfoil Sections Tested
a) Inner Blade Sections

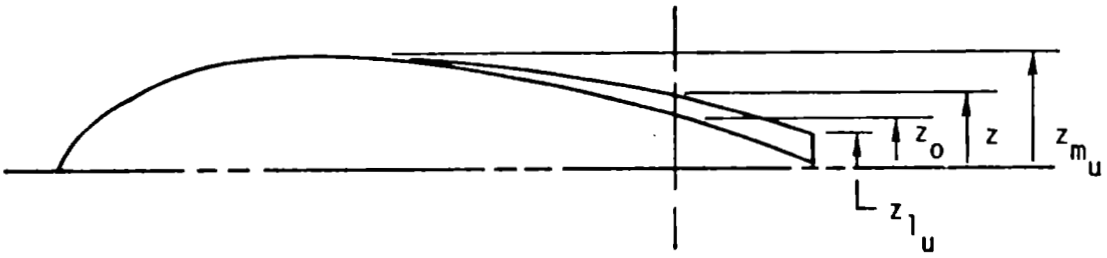

z_{m_u} - the ordinate of the upper surface at the maximum thickness

z_o - the ordinate of the original section

z_{l_u} - the trailing edge ordinate of the modified upper surface

z - the general ordinate of the modified region

$C = \frac{z_{l_u}}{z_{m_u}}$, the trailing edge thickness ratio

$z = z_{m_u} - (z_{m_u} - z_o)(1 - C)$

Figure 8-193 Geometry of the Airfoil Sections Tested (Cont'd.)

THE 64426 FAMILY
(Inner Blade)

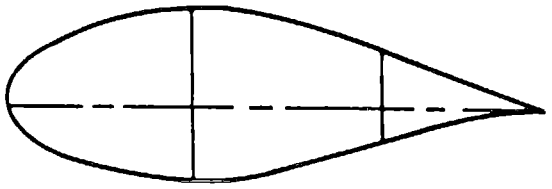

64426

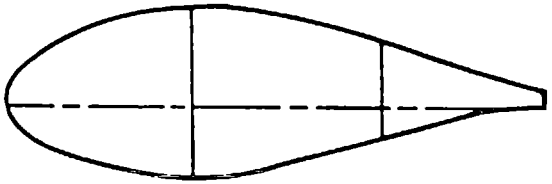

64426 - T1

THE 646XX FAMILY
(PCS Region)

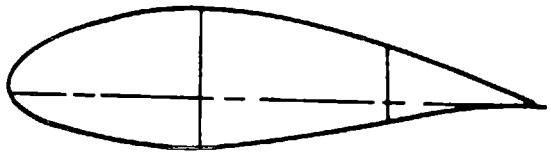

64621

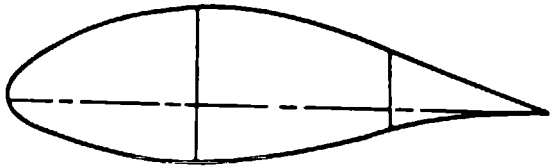

64624

Figure 8-193 Geometry of the Airfoil Sections Tested (Cont'd.) b) Inner and Outer Blade Sections

For simplicity, this modification is called a "raised trailing edge", although the title is not exact.

Model 64029-T1 has the raised trailing edge, with the aft upper surface trailing edge point raised by 20% of the upper surface thickness, or C=0.20. Model 64029-T2 has a configuration with C = 0.40. Models 64029-F15 and 64029-F30 represent an integral plain flap deflected -15° and -30°, respectively. The flap chord was 30% of the model chord.

At the end of the first part of the test, the basic model 64029 was modified by cutting off the trailing edge at, first, 80% chord and then at 70% chord. These two configurations are designated 64029-BT.80 and 64029-BT.70 respectively. All of these configurations are illustrated in Figure 8-193.

The 64426 group consisted of the basic airfoil and an airfoil with the trailing edge raised by 20% of the upper surface thickness, or C = 0.20. The group representing the tip consisted of the NACA 64621 and the NACA 64624 airfoil sections. Both of these groups are shown in Figure 8-193.

8.4.1.4 Results of the Wind Tunnel Tests

In addition to the charts included in this discussion, data from this test is tabulated in Table 8-96 and Table 8-97.

8.4.1.4.1. The 64029 Group

Plots of the basic 64029 characteristics, lift, drag and moment coefficients plotted against angle of attack, are shown in Figure 8-194. The lift curve indicates that the section begins to stall at 6°, where the lift coefficient was less than 0.5. This stall region was detailed by measurements at 7°, 8° and 9° and confirmations of the data at 9°. This early stall is a consequence of the 29% airfoil shape, an unusually thick shape. The jagged shape of the drag curve in the stall and the near past stall region was confirmed by retesting, and is believed to represent the two-dimensional airfoil. The moment coefficient is reported about the quarter chord point. This data is plotted against a smaller scale than was warranted by the accuracy of the data. As a result, the curve contains some noise, about ±.01 at low angles and slightly more at high angles. The faired curve is a probable representation of the moment characteristic.

Table 8-96 Aerodynamic Test Data for the Inner Blade Region

64029

$\alpha°$	C_L	C_D	C_M
-6.0	-.4205	.0572	.0132
0.0	.0159	.0117	-.0137
3.0	.256	.0135	-.0114
6.0	.4409	.0107	.0064
7.0	.456	.0198	-.0224
8.0	.408	.0320	-.0015
9.0	.3807	.0880	.0171
12.0	.5747	.0471	-.0085
15.0	.6731	.0705	.0074
18.0	.8514	.0890	-.0113
21.0	.9037	.1038	-.0060
24.0	.9080	.1523	-.0302

64029 - T1

$\alpha°$	C_L	C_D	C_M
0.0	-.084	.0150	-.0013
3.0	.242	.0156	-.0103
6.0	.572	.0155	-.0227
9.0	.745	.0164	-.0228
11.0	.799	.0249	-.0244
12.0	.695	.0365	-.0003
15.0	.693	.0626	.0119
18.0	.834	.0790	.0018
21.0	.956	.1134	-.0193
24.0	.933	.1917	-.0244

64029 - T2

$\alpha°$	C_L	C_D	C_M
0.0	-.2370	.0248	.0027
6.0	.4410	.0275	-.0144
9.0	.7640	.0208	-.0233
12.0	.9850	.0231	-.0132
13.0	.8030	.0364	.0001
15.0	.9010	.0719	-.0238
18.0	.8070	.1350	.0065
21.0	.9260	.1340	-.0023
24.0	.9930	.2102	-.0289

64029-F15

$\alpha°$	C_L	C_D	C_M
0.0	-.595	.0349	-.1150
3.0	-.326	.0285	-.1131
6.0	-.018	.0324	-.0916
9.0	.088	.0652	-.0778
10.0	.096	.0717	-.0887
12.0	.139	.0785	-.0960
15.0	.158	.0816	-.1193
18.0	.261	.1067	-.1196
0.0	-1.089	.0742	-.1934
6.0	-0.523	.0733	-.1842
12.0	0.212	.0956	-.1047
15.0	0.448	.1309	-.0838

64029 - F30

$\alpha°$	C_L	C_D	C_M
3.0	.2911	.0276	-.0145
9.0	.5252	.0580	.0067
12.0	.6204	.0565	.0342
15.0	.7286	.0723	.0418
18.0	.8625	.0891	.0325
21.0	.9964	.1124	.0225

64029 - BT.70

$\alpha°$	C_L	C_D	C_M
3.0	.110	.0872	.0095
6.0	.469	.0851	-.0202
9.0	.803	.0865	-.0451
12.0	1.153	.0897	-.0715
15.0	1.347	.1028	-.0654
18.0	1.278	.1385	-.0209
21.0	1.310	.1810	-.0088
24.0	1.289	.2118	-.0032

64426

$\alpha°$	C_L	C_D	C_M
-10.5	-.499	.0672	-.0509
- 9.0	-.494	.0426	-.0724
- 6.0	-.344	.0141	-.0597
- 3.0	-.062	.0132	-.0557
0.0	.236	.0130	-.0584
0.0	.284	.0118	-.0733
3.0	.555	.0116	-.0677
6.0	.769	.0109	-.0731
9.0	.813	.0190	-.0814
12.0	.819	.0633	-.0612
15.0	.949	.0696	-.0684

64426 - T1

$\alpha°$	C_L	C_D	C_M
0.0	.157	.0132	-.0636
3.0	.487	.0138	-.0776
6.0	.793	.0151	-.0818
9.0	.926	.0178	-.0666
12.0	.865	.0338	-.0570
15.0	.892	.1242	-.0403

Table 8-97 Aerodynamic Test Data in the PSC Region

64621

α	C_L	C_D	C_M
-39.0	- .940	.861	.187
-36.0	- .947	.791	.166
-33.0	- .944	.727	.148
-30.0	- .829	.291	.113
-27.0	- .729	.272	.0816
-24.0	- .575	.2622	.051
-21.0	- .576	.2405	.048
-18.0	- .358	.2131	.001
-15.0	-1.044	.0772	-.077
-12.0	- .904	.0266	-.086
- 9.0	- .636	.0142	-.0940
- 6.0	- .271	.0117	-.1020
- 3.0	.085	.0103	-.107
0.0	0.470	.0108	-.118
0.0	0.520	.0096	-.136
3.0	0.914	.0112	-.142
6.0	1.237	.0132	-.141
9.0	1.448	.0156	-.135
12.0	1.516	.0214	-.135
15.0	1.513	.0750	-.1175
18.0	1.543	.1148	-.116
21.0	1.527	.1727	-.139

64624

α	C_L	C_D	C_M
11.00	1.08	.0836	-.112
10.00	1.13	.0852	-.122
9.00	1.12	.0390	-.115
6.00	1.07	.0137	-.138
0.00	0.530	0.0105	-.146
- 3.00	0.280	0.0105	-.140
- 6.0	- .210	0.0127	-.120
- 9.0	- .540	0.0189	-.105
-12.0	- .760	0.0505	-.093
-15.0	- .866	0.0867	-.084
-18.0	- .300	0.2138	-.0104
-21.0	- .470	0.2414	.031
-24.0	- .570	0.2692	.054
-27.0	- .650	0.4488	.061
-30.0	- .730	0.5612	.101
-33.0	- .850	0.6850	.142
-36.0	-1.000	0.7811	.163
-39.0	-1.03	0.9356	.225

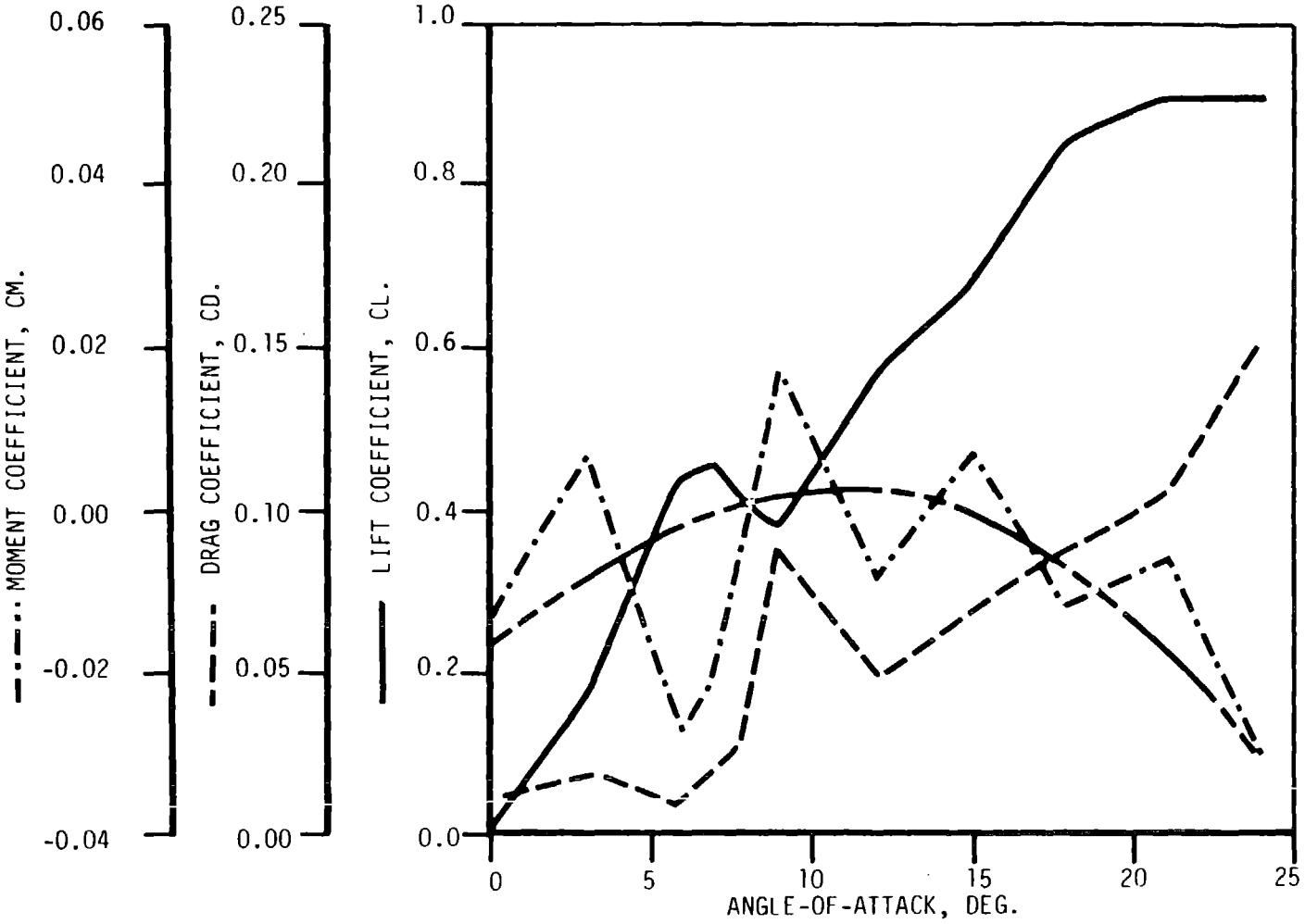

Figure 8-194 Characteristics of the 64029 Airfoil

8.4.1.4.2 Raised Trailing Edge 64029

To improve the performance of these thick sections at higher angles of attack, the upper surface curvature was reduced by raising the upper surface trailing edge by 20% and by 40% of the upper surface thickness. The aerodynamic characteristics of these sections are given in Figures 8-195 and 8-196. The data indicated that the stall was, to some extent, delayed. This improvement can more readily be seen in Figure 8-197, which is a superposition of the three lift curves of this group. The improvement of the lift characteristic at higher angles is apparent. An even more telling comparison is shown in Figure 8-198, which is composed of two charts showing the variation of the three lift-to-drag ratios with both lift coefficient and angle of attack. Raising the trailing edge shifted the maximum lift-to-drag ratio to both higher angles of attack and higher lift coefficients. These results were achieved while increasing the maximum lift-to-drag ratio.

8.4.1.4.3 Flap 64029

One method of reducing the effective angle of attack is to use a flap deflected upward. The affect of this is shown in Figures 8-199 and 8-200, where the lift-to-drag ratio is plotted along with the basic aerodynamic characteristics. The data for the integral plain flap, deflected to δ_f = -15°, is shown in Figure 8-199. This figure shows that the section starts to stall at 6°, which is no improvement over the unflapped case. The loss in lift and the increase in drag, however, produced by the deflected flap reduce the maximum value of the lift-to-drag ratio to less than 3.0. This lower value is no improvement over the basic airfoil. The data for δ_f = -30° is shown in Figure 8-200 with similar, but even less promising results.

8.4.1.4.4 Bob-Tailed 64029

Two sets of tests were run on bob-tailed versions of the 64029 airfoil section. This data was used to evaluate the performance penalties incurred by eliminating or reducing the add-on structure behind the 70% chord span, and as an alternate method of thickening the trailing edge. This data is shown in Figure 8-201 for the section cut off at 80% of the chord and in Figure 8-202 for the section cut off at 70% of the chord. These figures include the

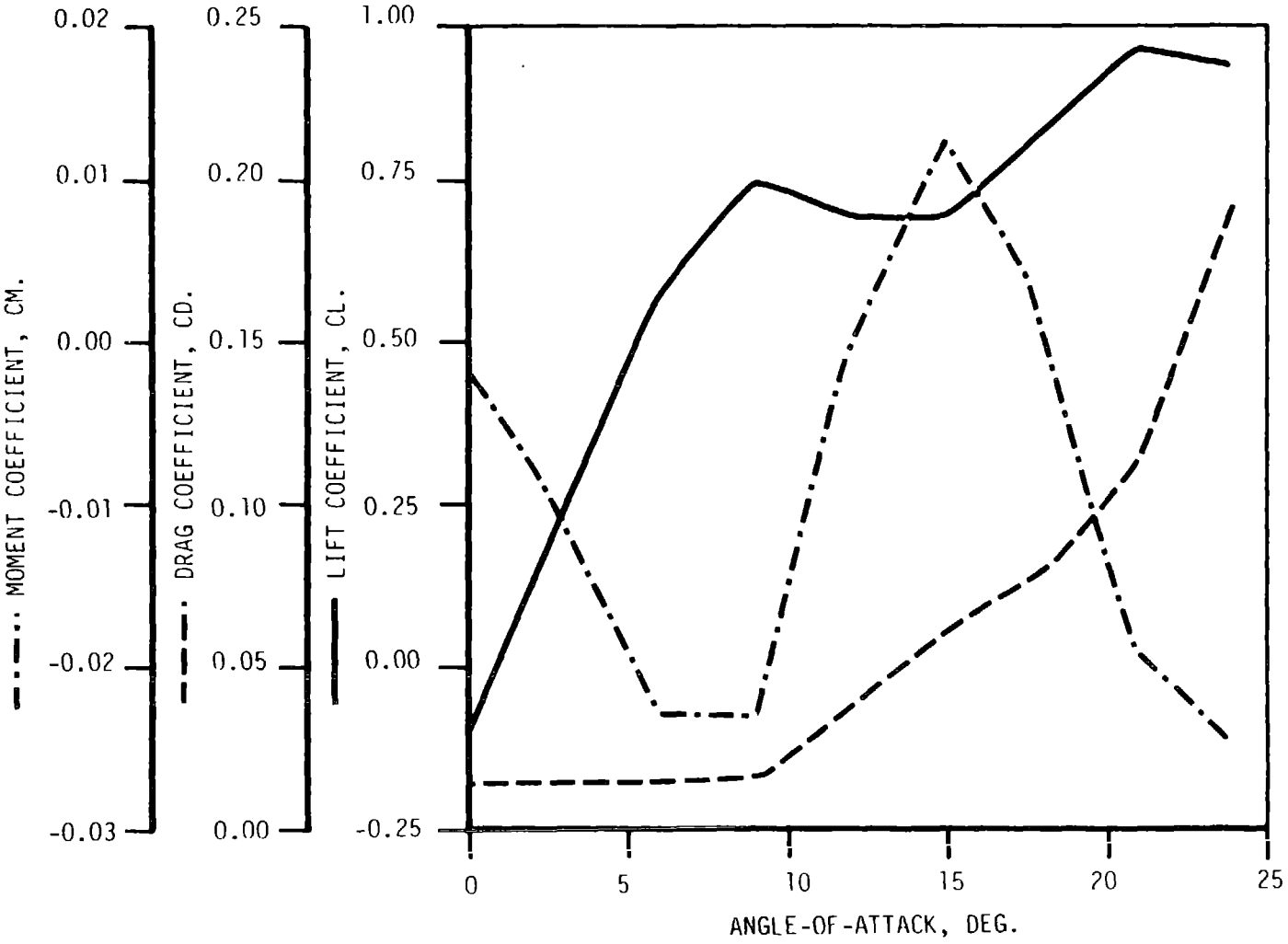

Figure 8-195 Characteristics of the 64029-T1 Airfoil

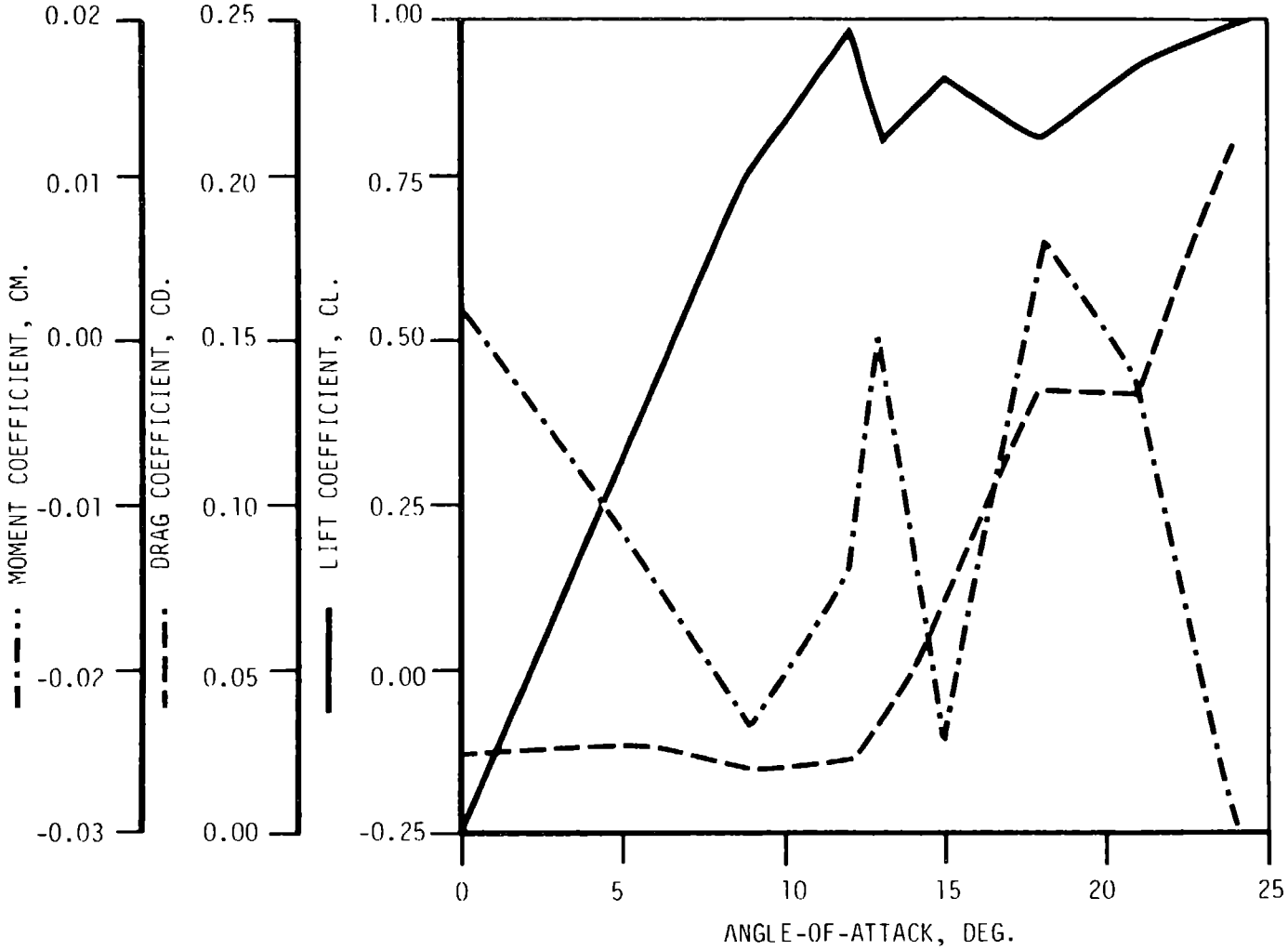

Figure 8-196 Characteristics of Airfoil 64029-T2

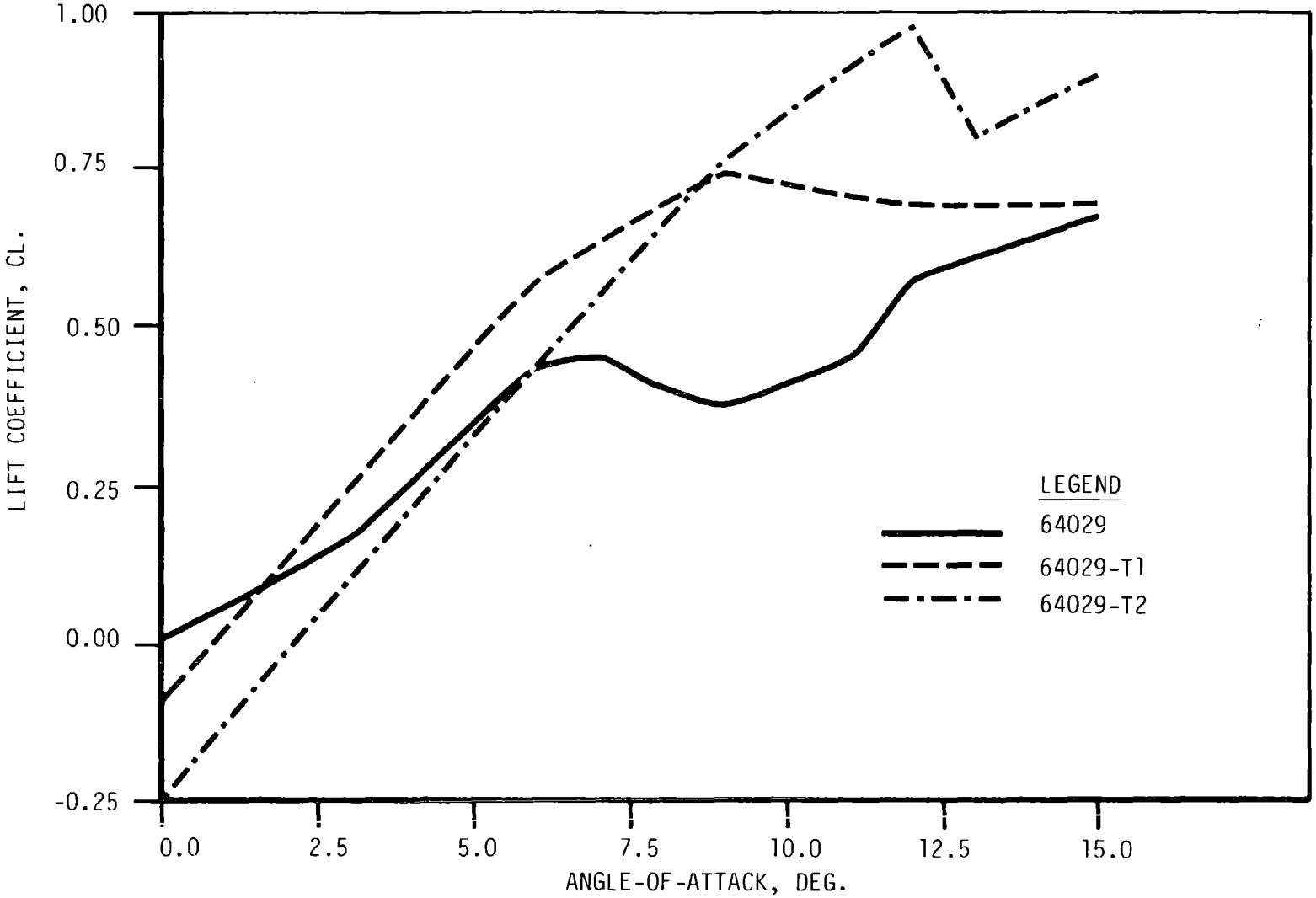

Figure 8-197 Lift Characteristics of Raised Trailing Edges

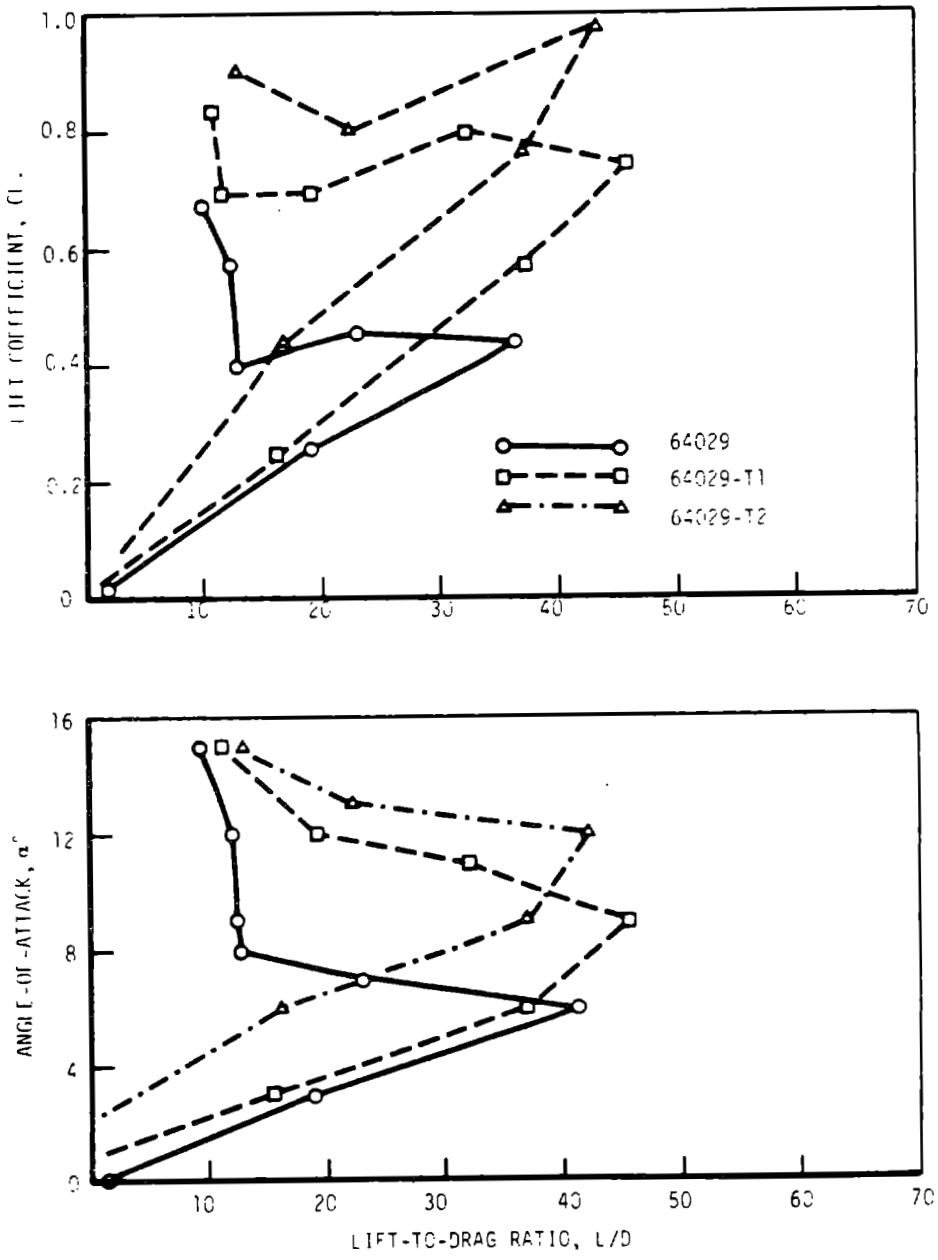

Figure 8-198 Lift/Drag Characteristics of the 64029 Family with Raised Trailing Edges

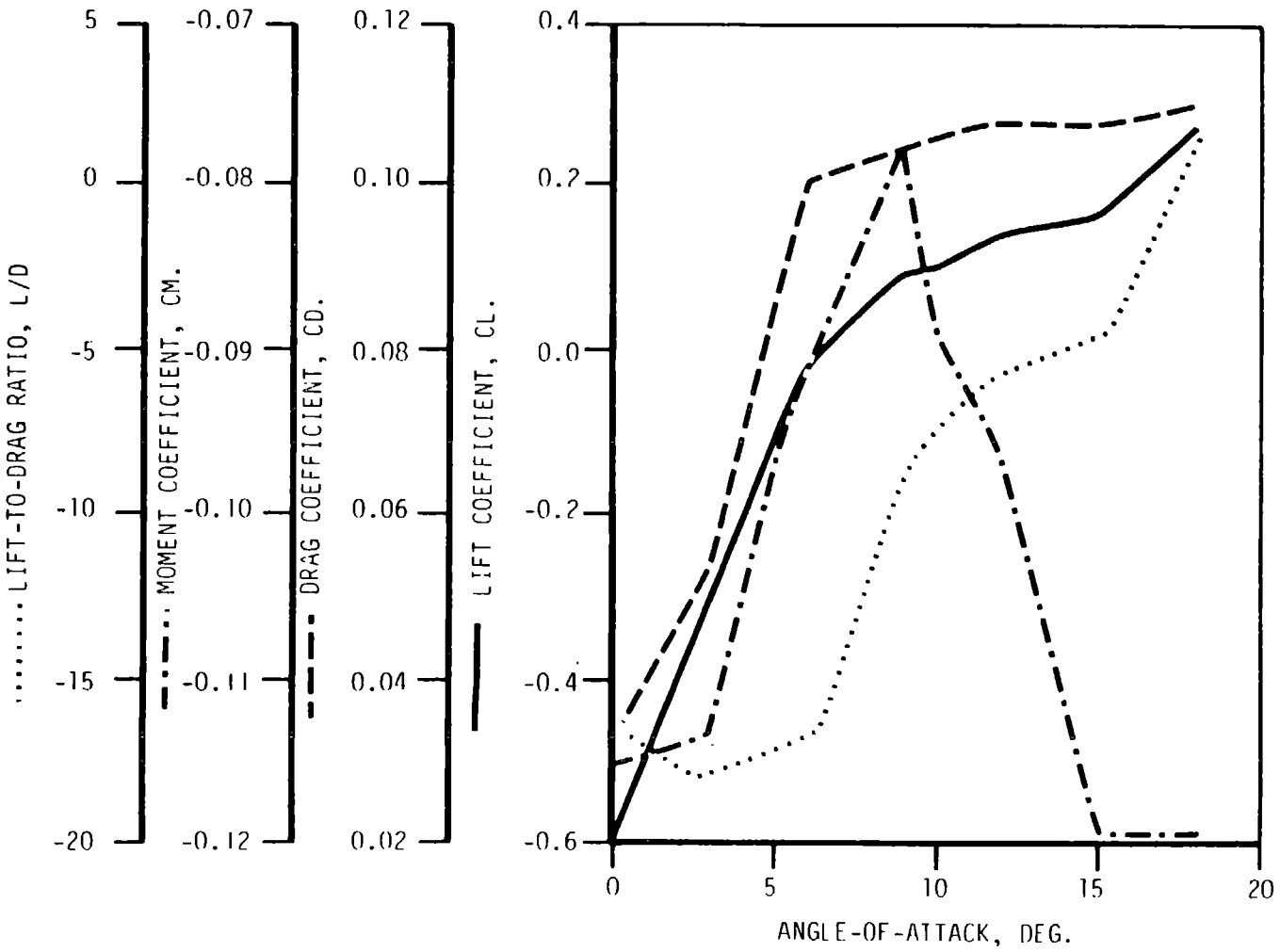

Figure 8-199 Characteristics of the Flapped Configuration (delta = -15 deg.)

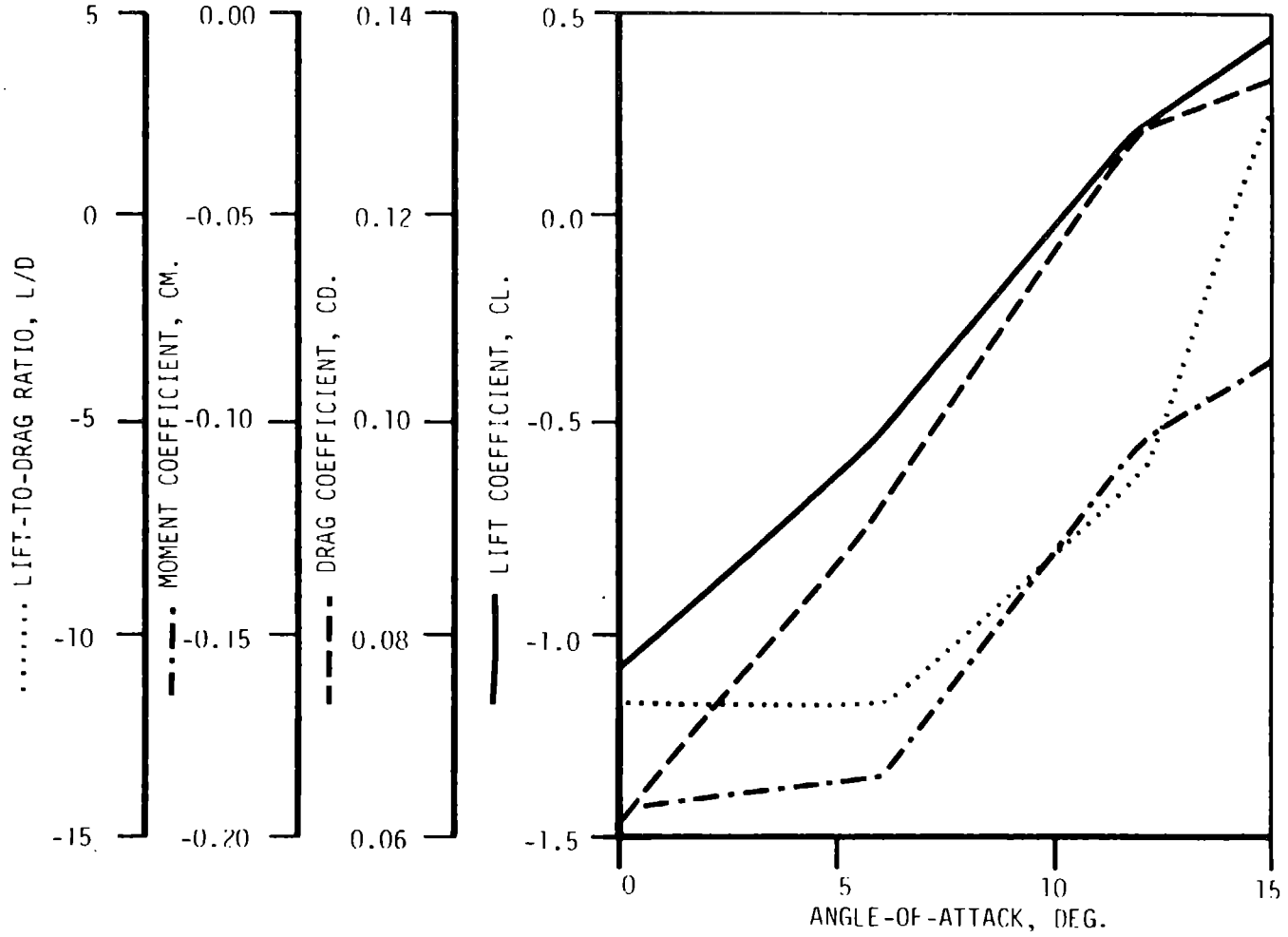

Figure 8-200 Characteristics of the Flapped Configuration (delta = -30 deg.)

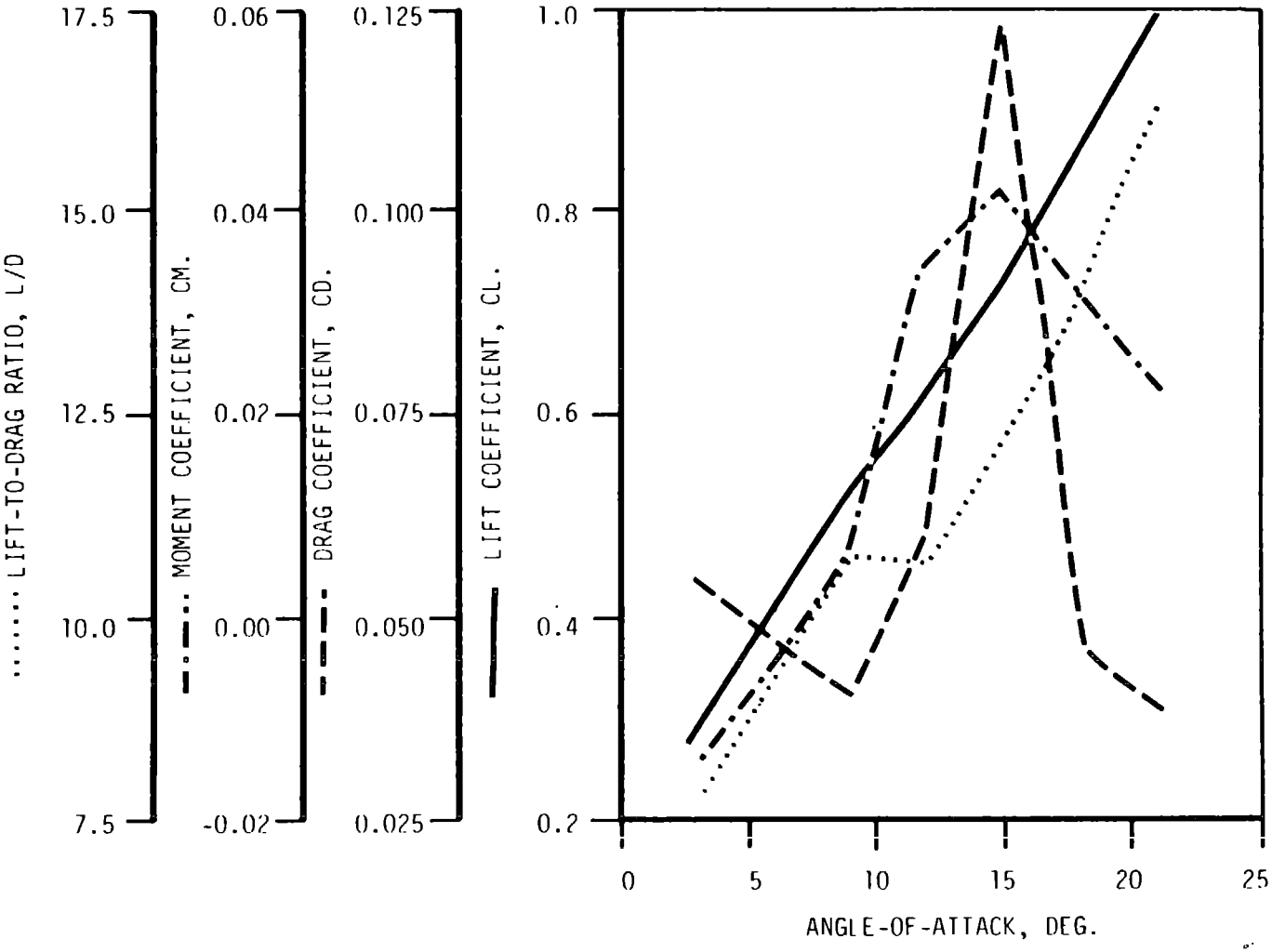

Figure 8-201 Characteristics of the 80% Bob-tailed Configuration

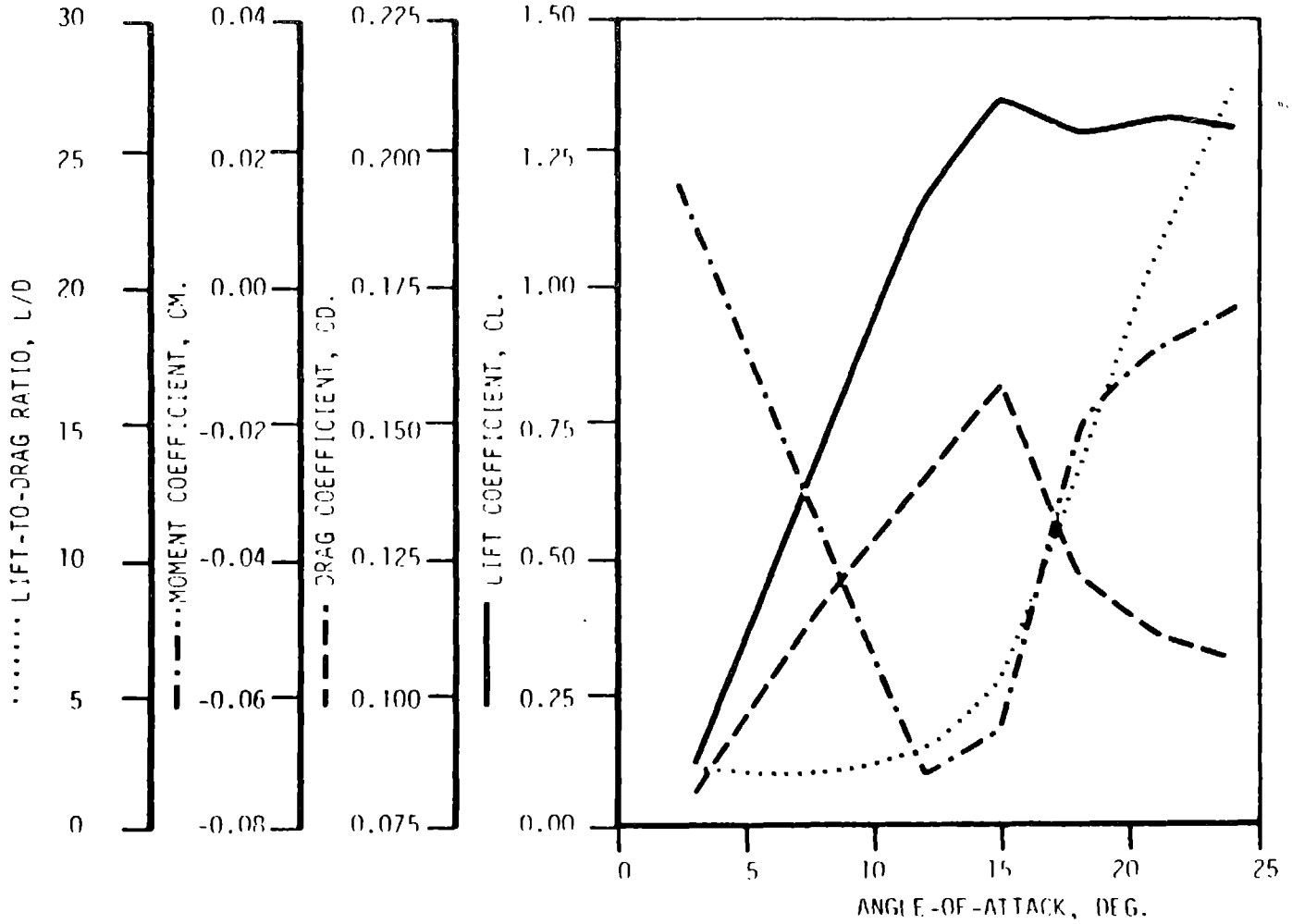

Figure 8-202 Characteristics of the 70% Bob-tailed Configuration

lift-to-drag ratio, and the basic aerodynamic data. The lift-to-drag ratio has been reduced, from approximately 42 for the basic airfoil, to about 17. In both cases, the lift curve was substantially improved over that of the basic airfoil, but the large drag was unacceptable.

8.4.1.4.5 The 64426 Family

The aerodynamic characteristics of the 64426 airfoil section are given in Figure 8-203 for the basic section and in Figure 8-204 for the section with the upper surface trailing edge raised 20%. A comparison of the lift characteristics of the two airfoils is shown in Figure 8-205. The 64029 characteristics are also shown for reference. The two charts of Figure 8-206 show that raising the trailing edge of this section only slightly improves the performance at high angles of attack. The small improvement imposes a loss in the maximum value of the lift-to-drag ratio, from about 70 for the basic section to about 52 for the section with the raised trailing edge.

8.4.1.4.6 Airfoil Sections in the Tip Region

When used in conjunction with a partial span control, the tip sections, in contradistinction to the sections of the inner blade, see large variations in angle of attack, especially in the negative angle region. In this region the variations are caused by control motion. Data was sought here to provide confidence in the design for loads at angles of attack beyond the negative stall point. The data is shown in Figure 8-207 for model 64621, and in Figure 8-208 for model 64624. The data for model 64621 compares well with the data for thinner sections from the NACA TDT tests (see ref. 5). A sharp negative stall is observed for both the 21% and 24% thick sections. This data is consistent with the NACA data on the model 64618.

8.4.1.5 Optimum Airfoil Section Selection

The variation in the geometric characteristics of the blade sections along the MOD-5A radius is shown in Figure 8-209. The variation in the chord and thickness along the span evolved as the optimum configuration through successive designs, considering both economic and structural issues. The twist distribution is constrained by the method of fabrication. To achieve the aerodynamic equivalent of geometric twist, a large amount of camber was used in the outboard region. The camber was decreased sharply from the high value of C_{LD}=0.6 outboard of 75% of the span, to zero at 25% span. This

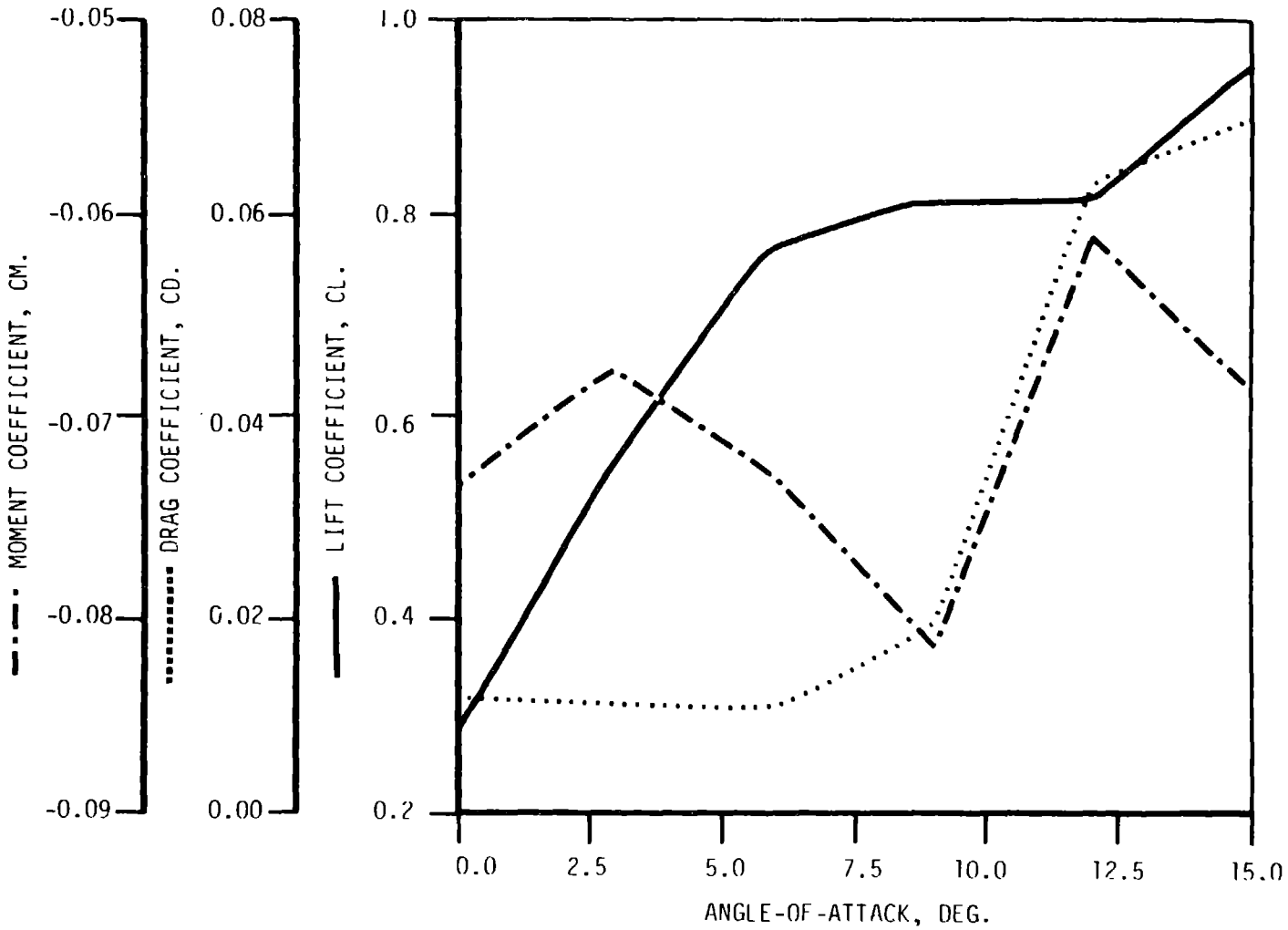

Figure 8-203 Characteristics of the 64426 Airfoil

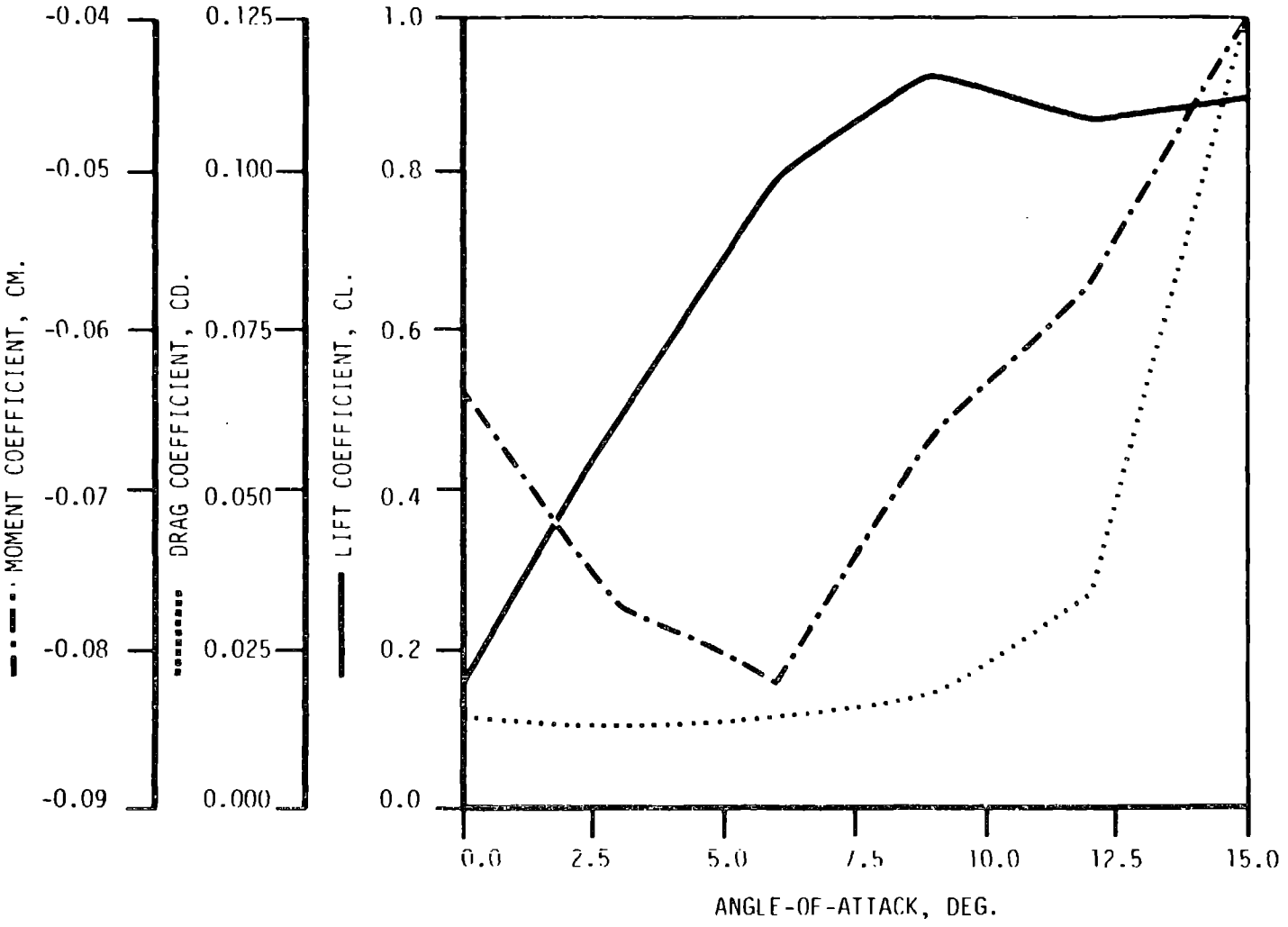

Figure 8-204 Characteristics of the 64426-T1 Airfoil

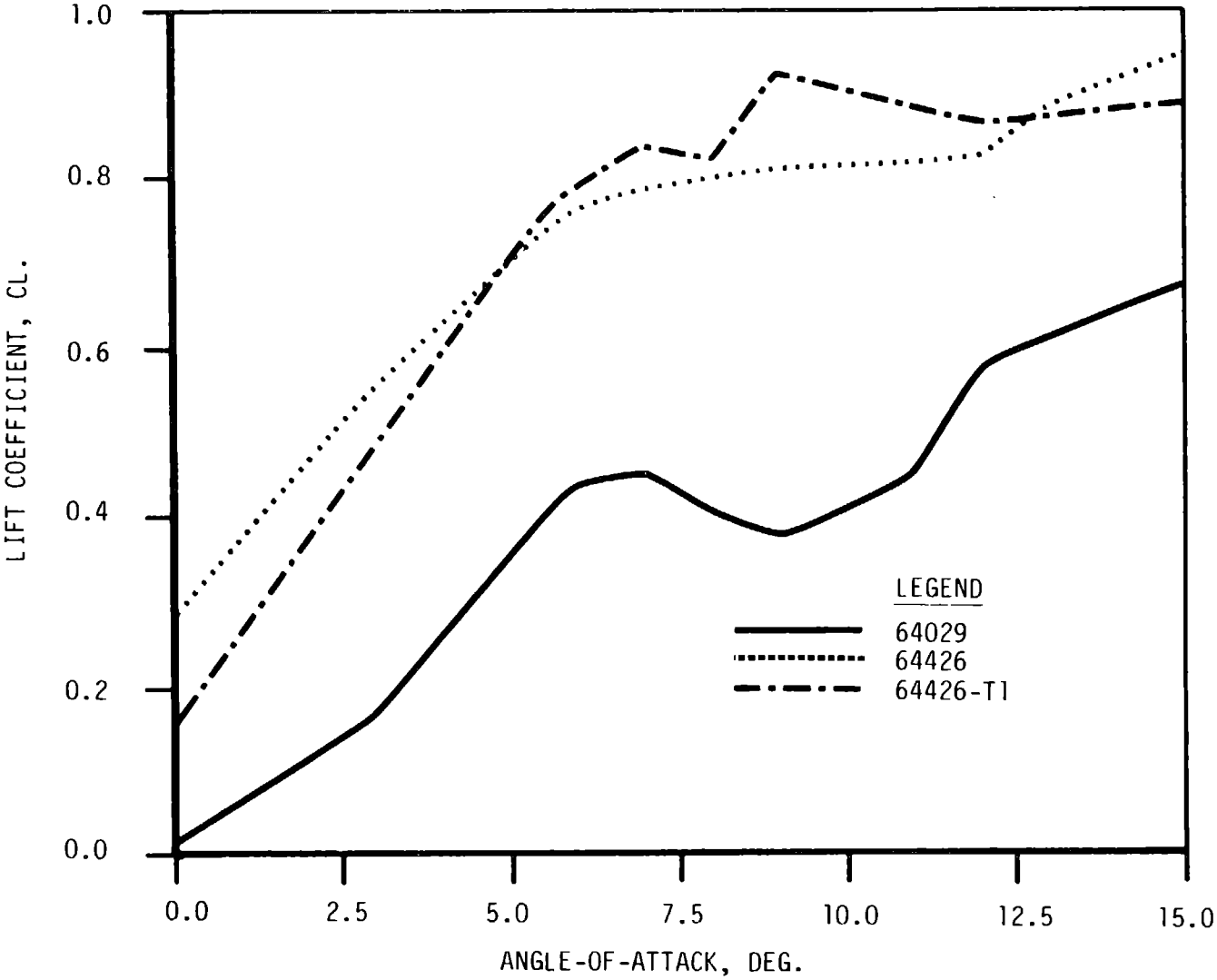

Figure 8-205 Lift Characteristics of the 64426 Family

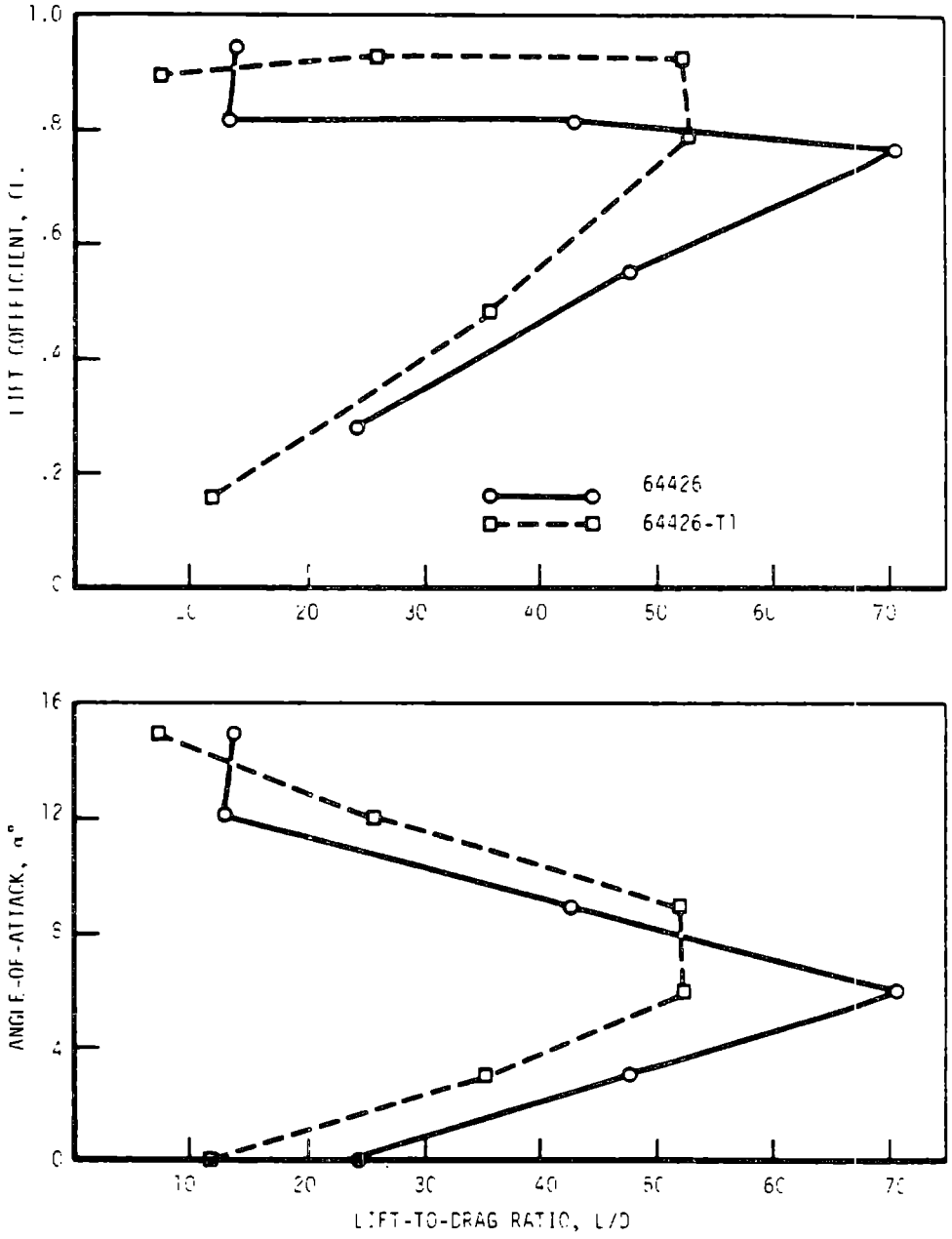

Figure 8-206 Lift/Drag Characteristics of the 64426 Family with Raised Trailing Edges

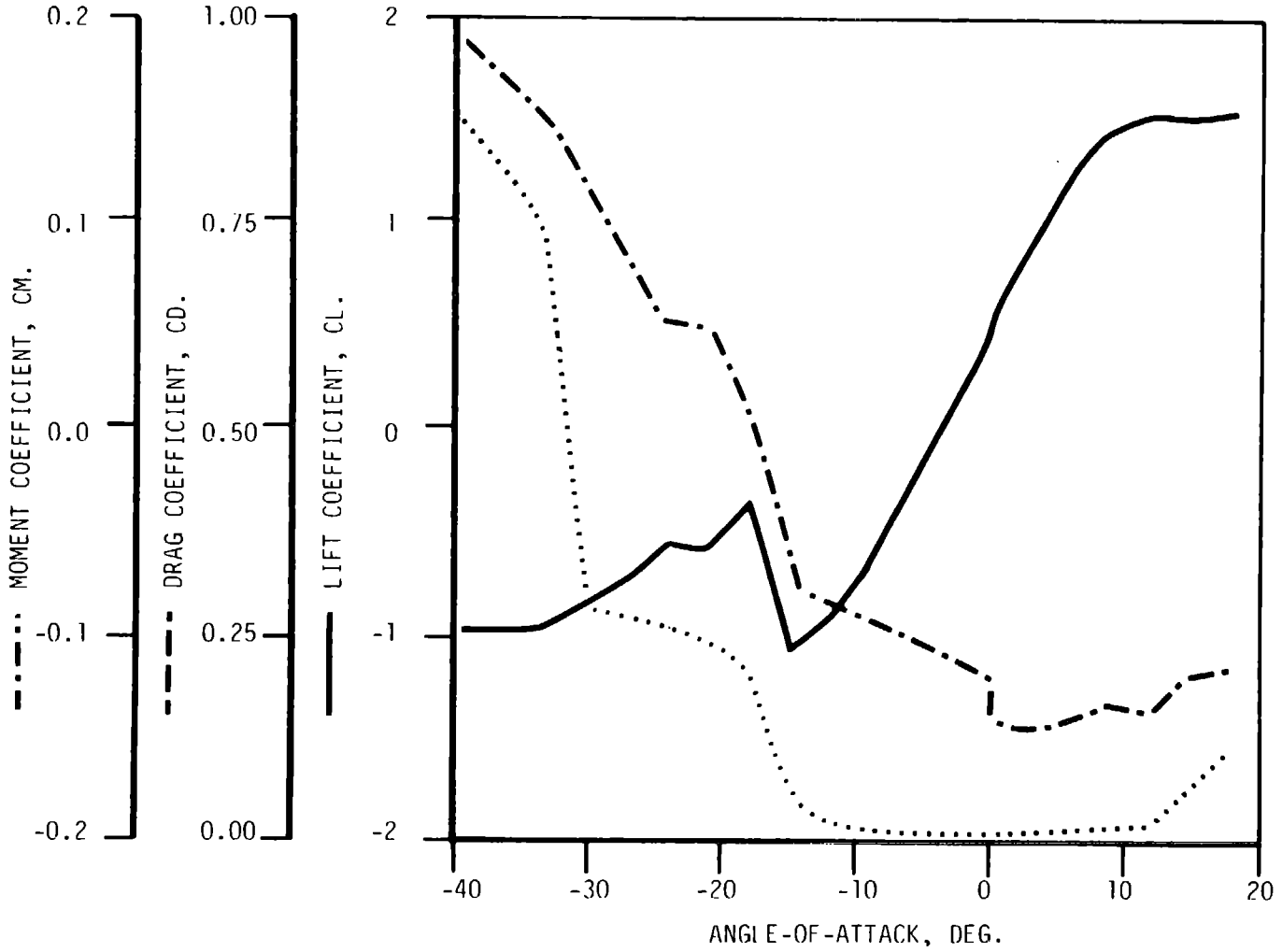

Figure 8-207 Characteristics of the 64621 Airfoil Section

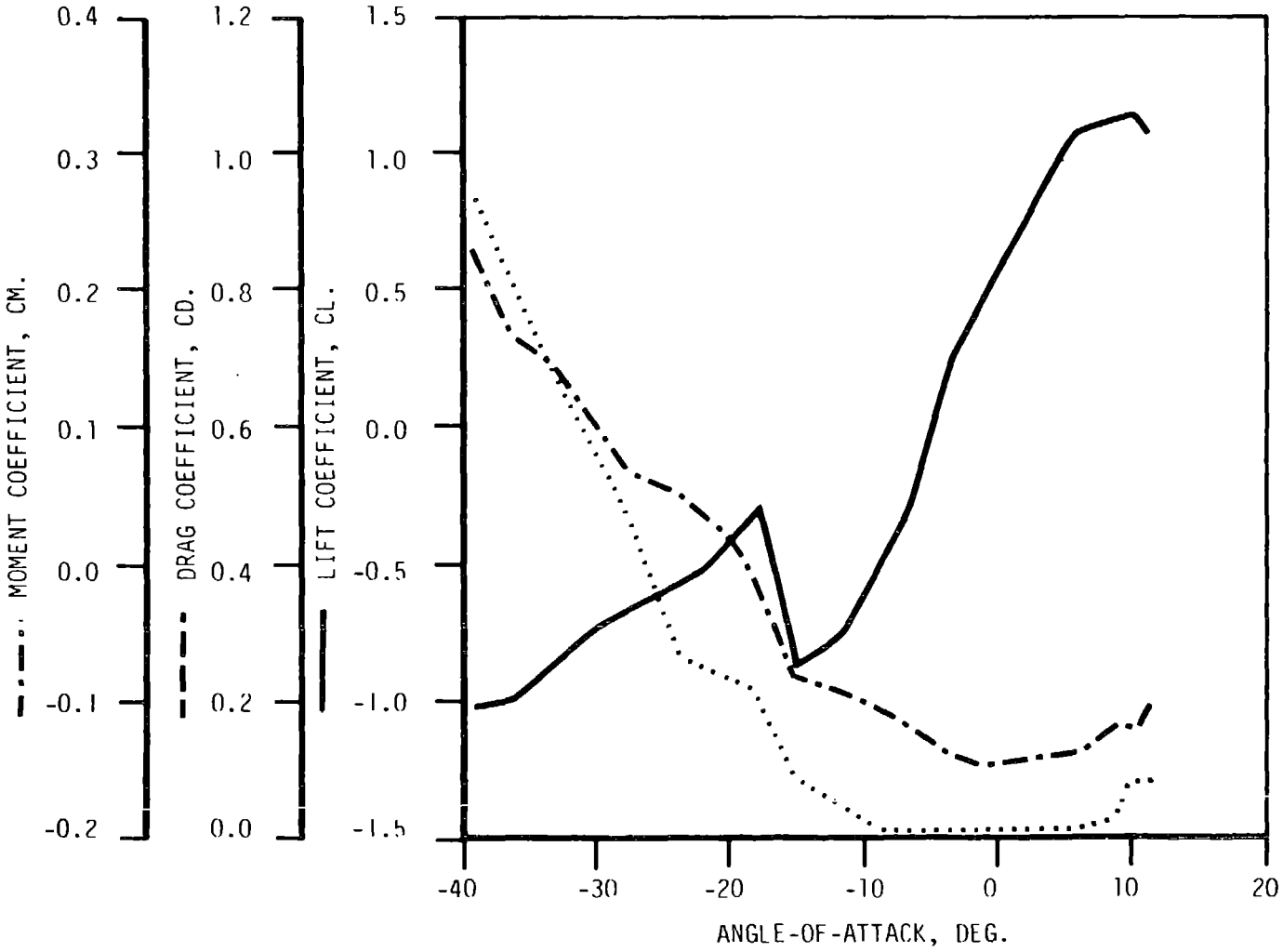

Figure 8-208 Characteristics of the 64624 Airfoil Section

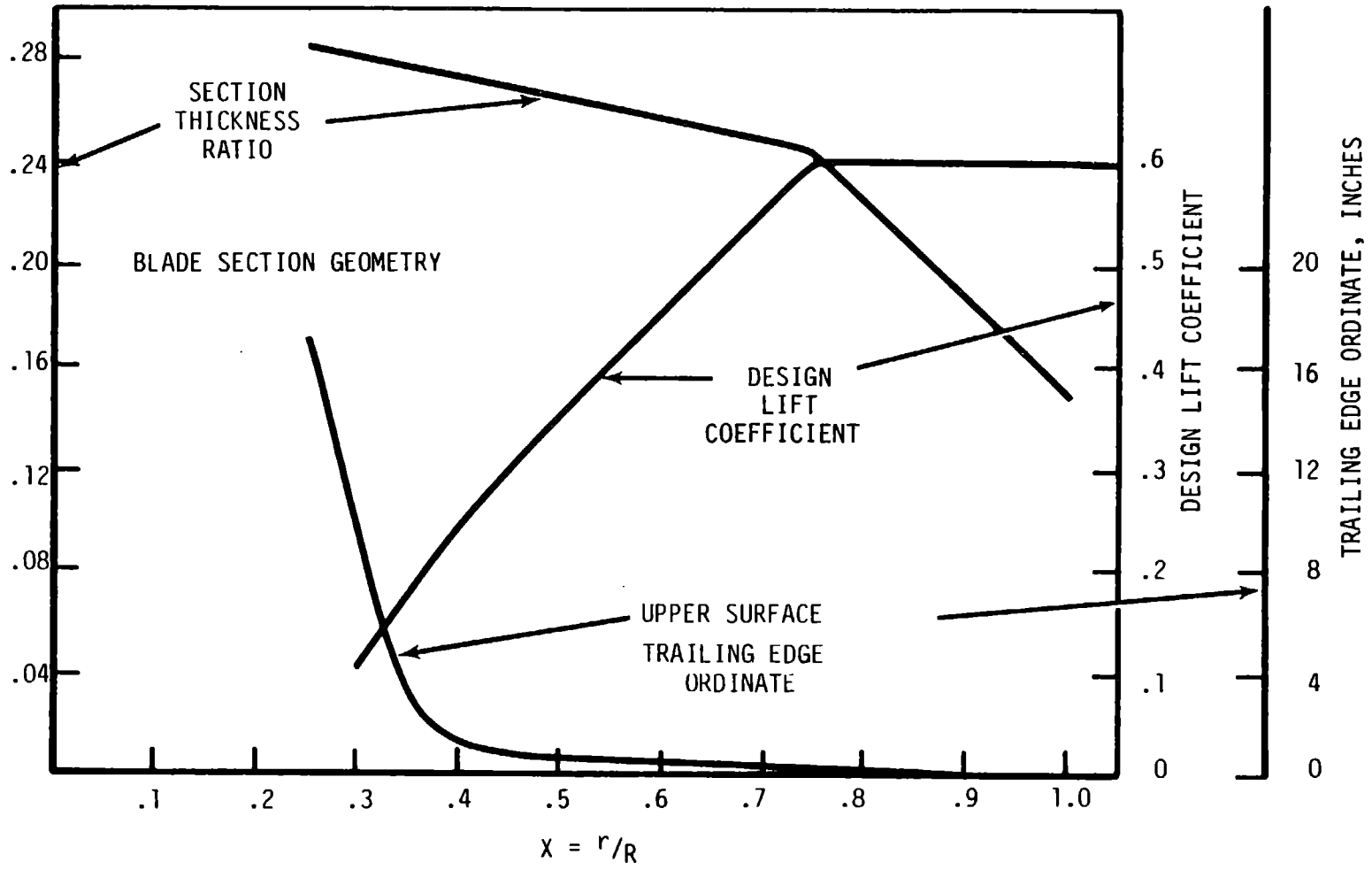

Figure 8-209 Spanwise Geometry of MOD-5A Blade

camber distribution produces the equivalent of an additional 4° of twist in that region of the blade. The amount of trailing edge rise was a maximum of 40% at the 25% span point and decreased to zero at 55% span. This allocation of geometric parameters produced the optimum aerodynamic characteristics within the fabrication constraints of the blade subsystem.

8.4.2 AILERON CHARACTERISTICS (WIND TUNNEL TEST OF AILERONS)

8.4.2.1 General

The design development of the partial span control imposed increasing load, weight and cost penalties on the system. As a result, alternative methods of controlling rotor torque and effecting shut down were explored. Trailing edge flaps emerged from the investigation as the most promising aerodynamic control. These trailing edge flaps have become known as ailerons for this application.

Ailerons are particularly suitable for the MOD-5A rotor control for several reasons. They do not disrupt the structural continuity of the essentially monolithic main blade structure. They could be mounted, in place of the original fixed trailing edge assembly, onto the rear spar of the main blade structure. However, no performance data was available for ailerons on very thick airfoil sections, similar to the MOD-5A blades, or for the high angles of attack to be experienced in high wind shut-downs.

A suitable aileron configuration for application on the wind turbine generator had not been determined and wind-tunnel tests were necessary to develop supporting data. Because wind turbine performance estimates based on two-dimensional wind tunnel data had consistantly under-predicted the maximum rotor torque, it was also necessary to confirm the aileron performance predictions by tests on a suitable wind turbine rotor.

Two test programs were planned to obtain this data. The first was a wind tunnel test designed to obtain the aileron control characteristics on the MOD-5A airfoil section. The second was a test on NASA's MOD-0 wind turbine at Plum Brook Station, Sandusky, Ohio, described in section 8.4.3. This test used outer blades fabricated in the MOD-5A configuration. This configuration is referred to as MOD-0/5A. The test was divided into two phases. Phase I was the screening process and in phase II two designs from Phase I were tested further.

8.4.2.2 Wind Tunnel Test Requirements

The test equipment had to be dynamically similar to the full-scale MOD-5A machine. In particular, the Reynold's number had to equal 5×10^6 or more,

and the Mach number could not exceed 0.3. The range of angles of attack to be tested had to extend from 0° to at least 30,° and aileron deflections had to extend from 0° to -90°. The test data determined the aerodynamic force coefficients as functions of the angle of attack, and of aileron deflection and the load distributions along the chord. These tests were also run in OSU's wind tunnel.

8.4.2.3 Wind Tunnel Tests - Phase I

The objective of these tests was to obtain data characterizing various aileron designs. Aileron configurations would be selected for further testing based on this data.

The span of the aileron airfoil section model was 6 in. and the chord was 4 in., of a construction similar to the models described in section 8.4.1. The 64621 section was the basic airfoil used. This camber was selected because the MOD-5A blade from 75% of the span and outward is designed for a lift coefficient of 0.6. The thickness ratio of 21% was selected because this value represented the geometric mean thickness ratio of the aileron span.

The phase I test models are illustrated in Figure 8-210.

8.4.2.3.1 Results and Discussion - Wind Tunnel Tests - Phase I

The results of phase I are summarized in Figure 8-211. The most critical aileron performance characteristic is the ability to provide a braking force over the operating range of wind velocities and rotor speed. These two variables are conveniently combined into the dimensionless tip speed ratio, $\lambda = \omega R/V$. The tip speed ratio for the 400-ft. rotor and a conceptual aileron configuration extending from 60% to 100% of the span were used to examine the wind tunnel results.

The relationship between the angles of attack at 60% of the span, $\alpha(.6)$, and 100% span, $\alpha(1.0)$ and the tip speed ratio, λ, are shown as two dashed lines in the upper part of the Figure 8-211. These two curves define the angle of attacks seen by the control section of the blade at various tip-speed ratios. For example, for a tip-speed ratio of $\lambda = 2.0$, the angle of attack at $\alpha(1.0)$ is 17° and the angle of attack at $\alpha(0.6)$ is 27°. Consequently, these two lines enable the designer to see what range of angles of attack

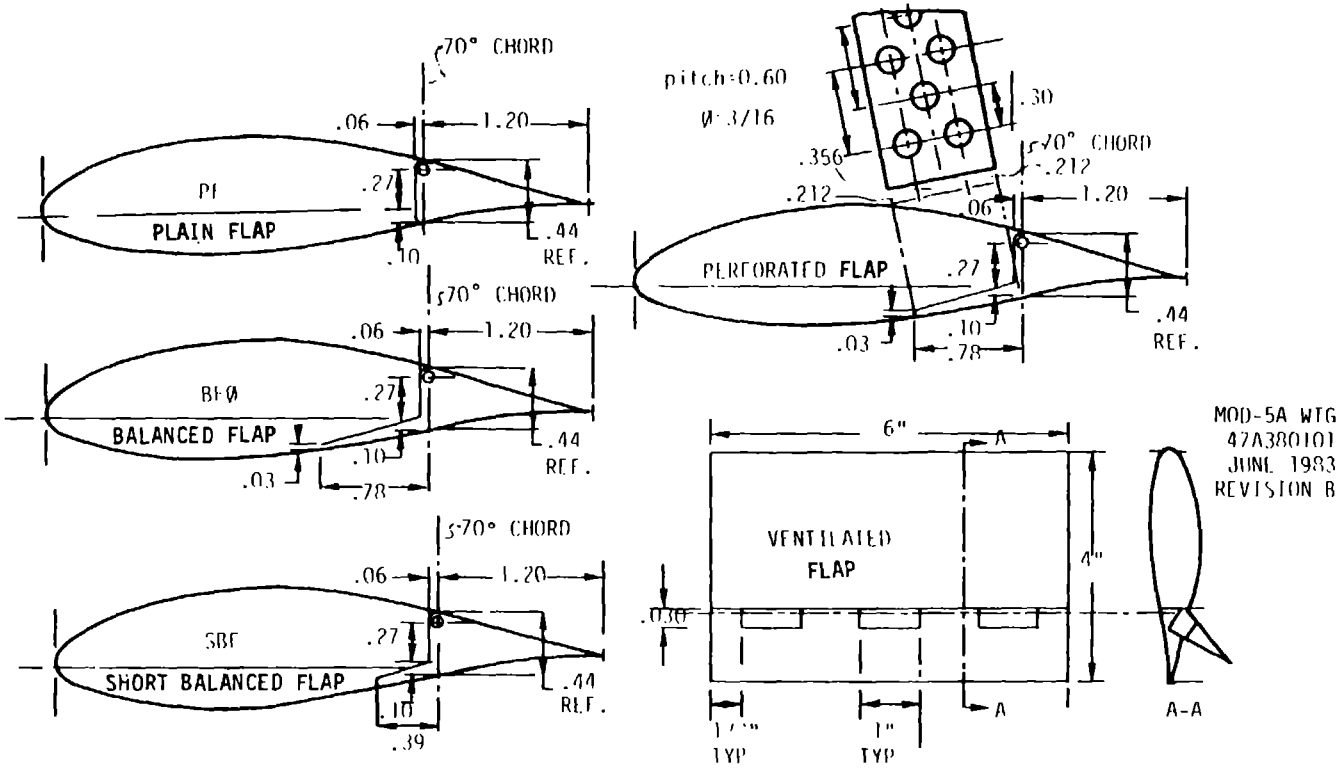

Figure 8-210 Phase I Flap Configurations

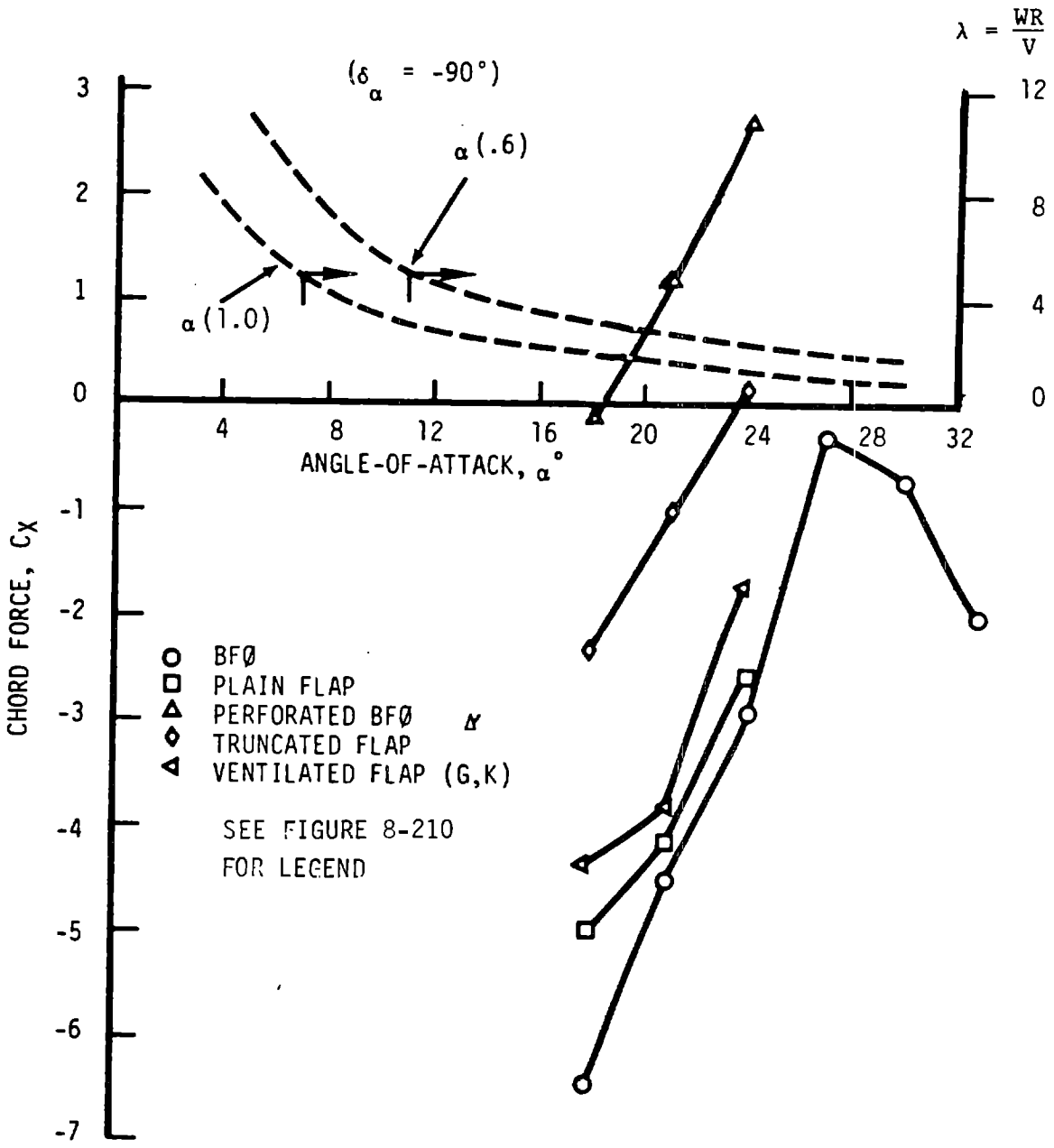

Figure 8-211 Aileron Chordforce Characteristics

exists during any operating condition. The other curves describe the test data in terms of the ability of the various configurations to provide braking force ($C_x<0$) in that range of angles of attack with the aileron deflected to $\delta = -90°$.

The data shows that the 30% chord/50% chord balanced aileron provides large negative values of chord force over most of the significant range and does not leave the negative region. This configuration provides the greatest braking control.

The 30% chord plain aileron shows a similar trend in the range that was tested. This arrangement seemed likely to provide adequate stopping power, but it would have considerably higher hinge moments and would require more actuator capability than the balanced aileron. Furthermore, because of the more positive hinge moments, the plain aileron would be deficient in self-actuation capability, a very desirable characteristic.

The other configurations tested (perforated, truncated and ventilated ailerons) all show either positive chord forces or trends toward positive chord forces, that make them unacceptable for braking. Note that pressure forces on the aileron elements of these three configurations could not be measured directly. The overall lift was measured by using the wind tunnel upper and lower plenum pressure difference correlations. As a result, this data is not as convincing as the data on plain and balanced ailerons, where the pressure forces on the aileron element could be integrated directly from the pressure distribution.

Sound energy was measured during some test runs, for a rough indication of the sound generation properties of deflected ailerons. Unfortunately, reliable sound data could not be obtained. The data qualitatively indicated that the deflected balanced aileron would probably not be a major source of sound energy.

8.4.2.3.2 Wind Tunnel Tests - Phase II

Design work to adapt the aileron control to the MOD-5A blade structure showed that sufficient space was available to the rear of the 60% aft structural spar

to accommodate a 38% chord aileron and the associated actuation mechanisms. Comparison of test results from Wichita State University on a 20% chord aileron with the test results on a 30% chord aileron show that increasing the aileron chord increases the aileron's effectiveness. The 38% chord space was used in designing the two phase II ailerons, as shown in Figures 8-212 and 8-213. Concerns about high noise level from the sharp leading edge of the balanced aileron in the deflected position led to the selection of the plain aileron as the main design, and the balanced configuration as the contingency design.

8.4.2.4 Wind Tunnel Phase II Results - 38% Chord Plain Aileron

The lift and drag coefficients, as functions of the angle of attack, are shown in Figures 8-214 and 8-215. The force extrapolations used in the performance analysis are also shown. These forces are shown in Figures 8-216 and 8-217, projected perpendicular to the chord (the normal force) and parallel to the chord (the chord force). The chord force is defined here as being the negative of the drag force at an angle of attack of 0°. Positive values of this chord force produce power generating torques, and negative values produce retarding or braking torques. The curves of Figure 8-217 show that a control deflection of -90° produces the greatest braking force and that this force goes through zero at an angle of attack of 29°. The increments in lift coefficient (ΔC_L) and drag coefficient (ΔC_D) with respect to the basic 64621 airfoil section data are needed to apply this data to the MOD-5A design calculations. These increments are used in the computation of the air forces on the blade at the appropriate angle of attack and control deflection angle. Table 8-98 is a listing of the increments of lift coefficient. Graphs of these functions are shown in Figures 8-218 through 8-221 with interpolation to 2° increments of control deflection.

Similarly, the increments in drag coefficient are shown in Table 8-99 and in Figures 8-222 through 8-225.

Pitching moment coefficient data, referred to the section quarter chord point, are shown in Figure 8-226.

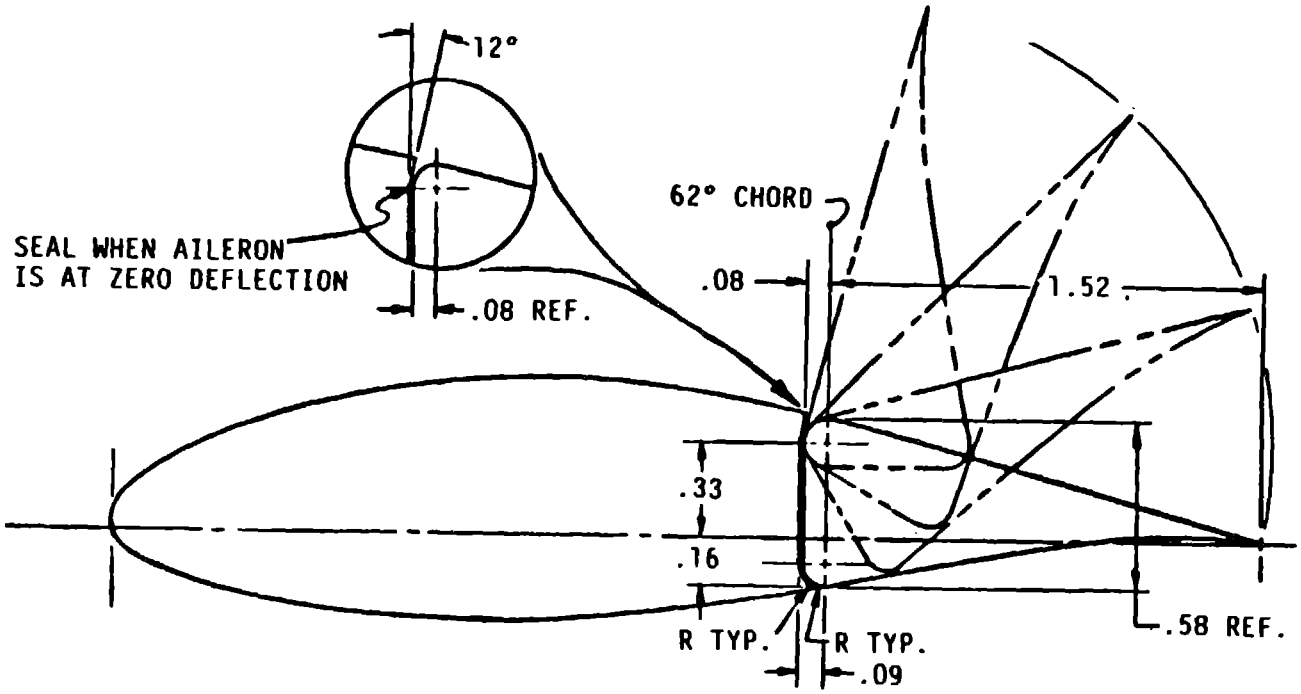

CHORD = 4.00"

Figure 8-212 Plain Aileron Configuration PF 38% Chord

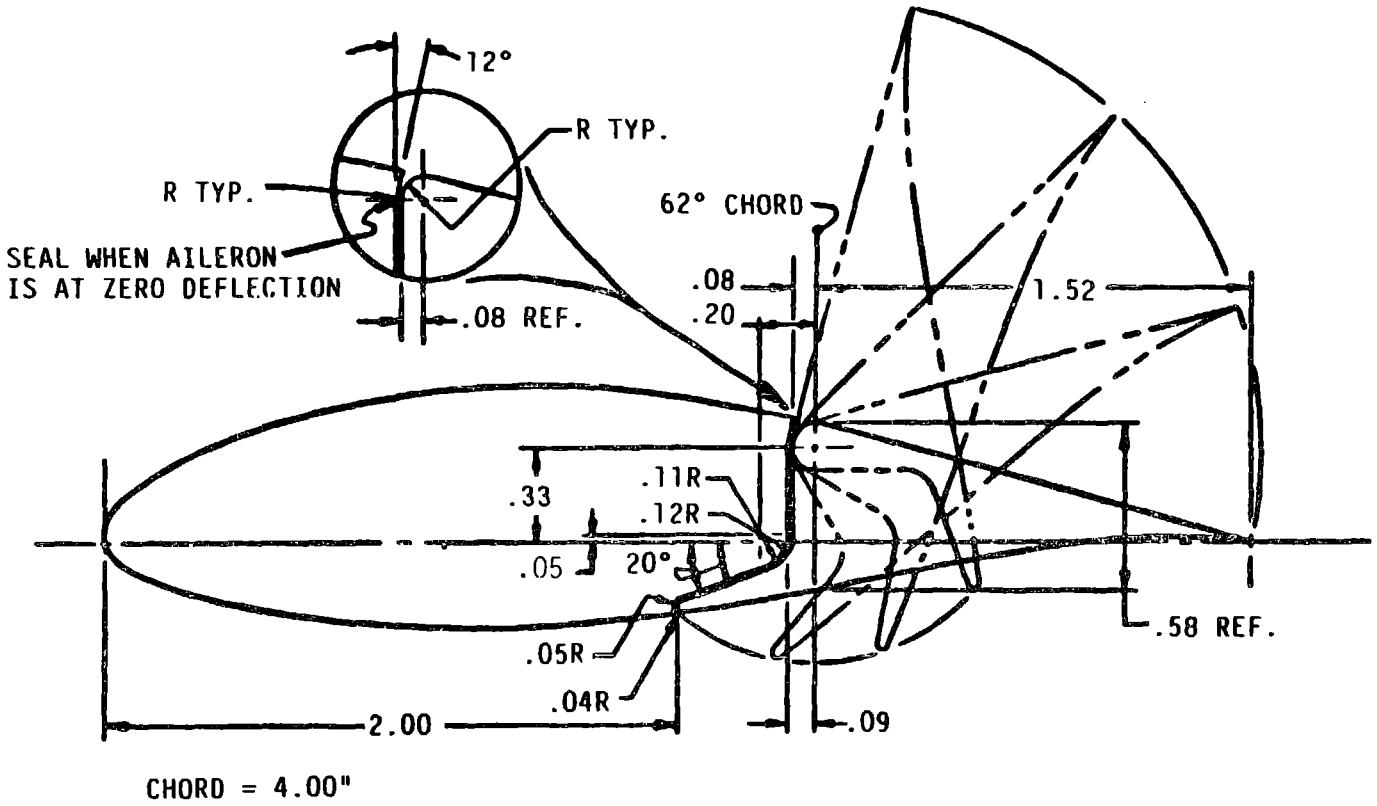

Figure 8-213 Balanced Aileron Configuration BF 38% Chord

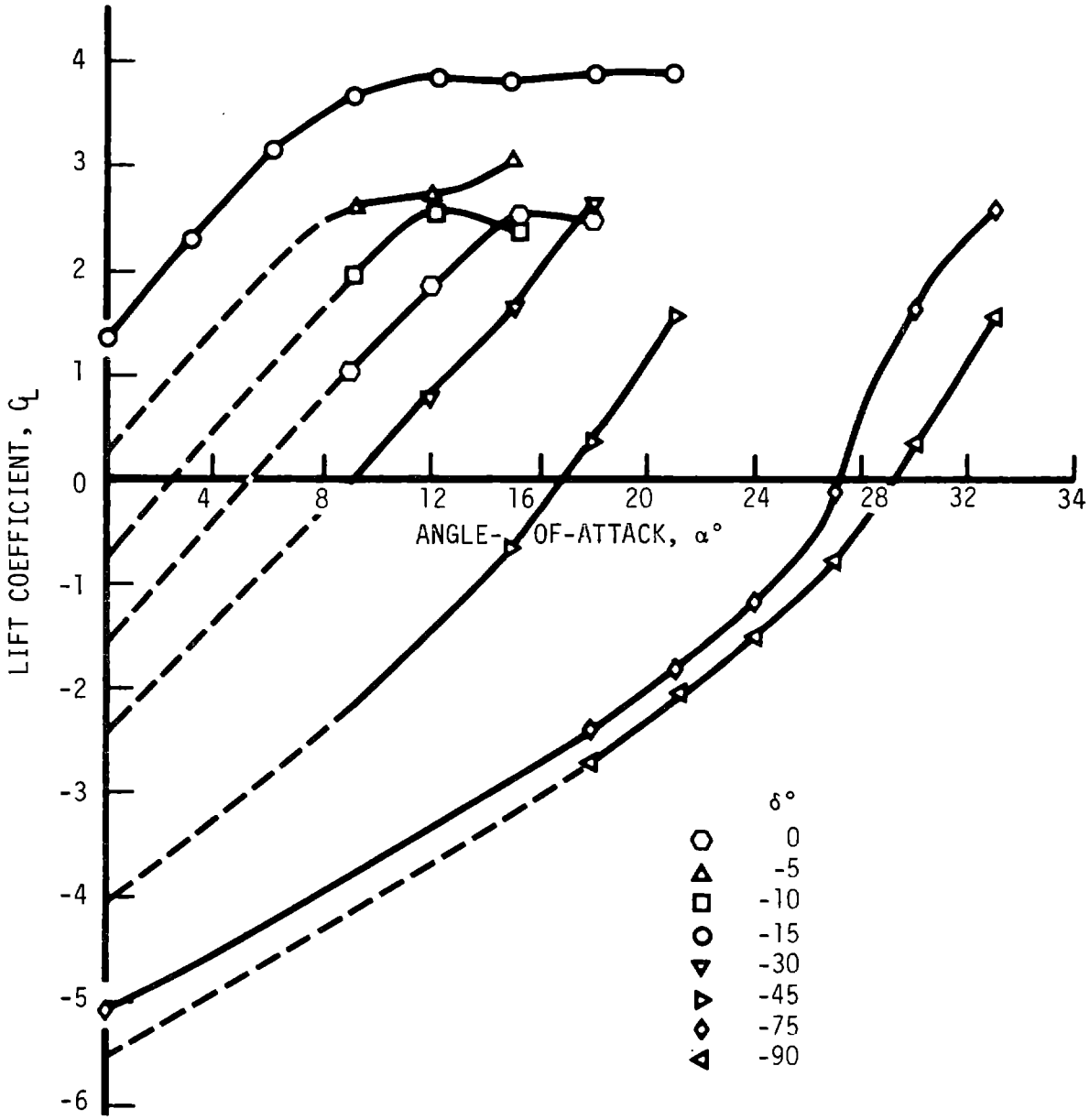

Figure 8-214 Aerodynamic Characteristics of the Plain 38% Chord Aileron

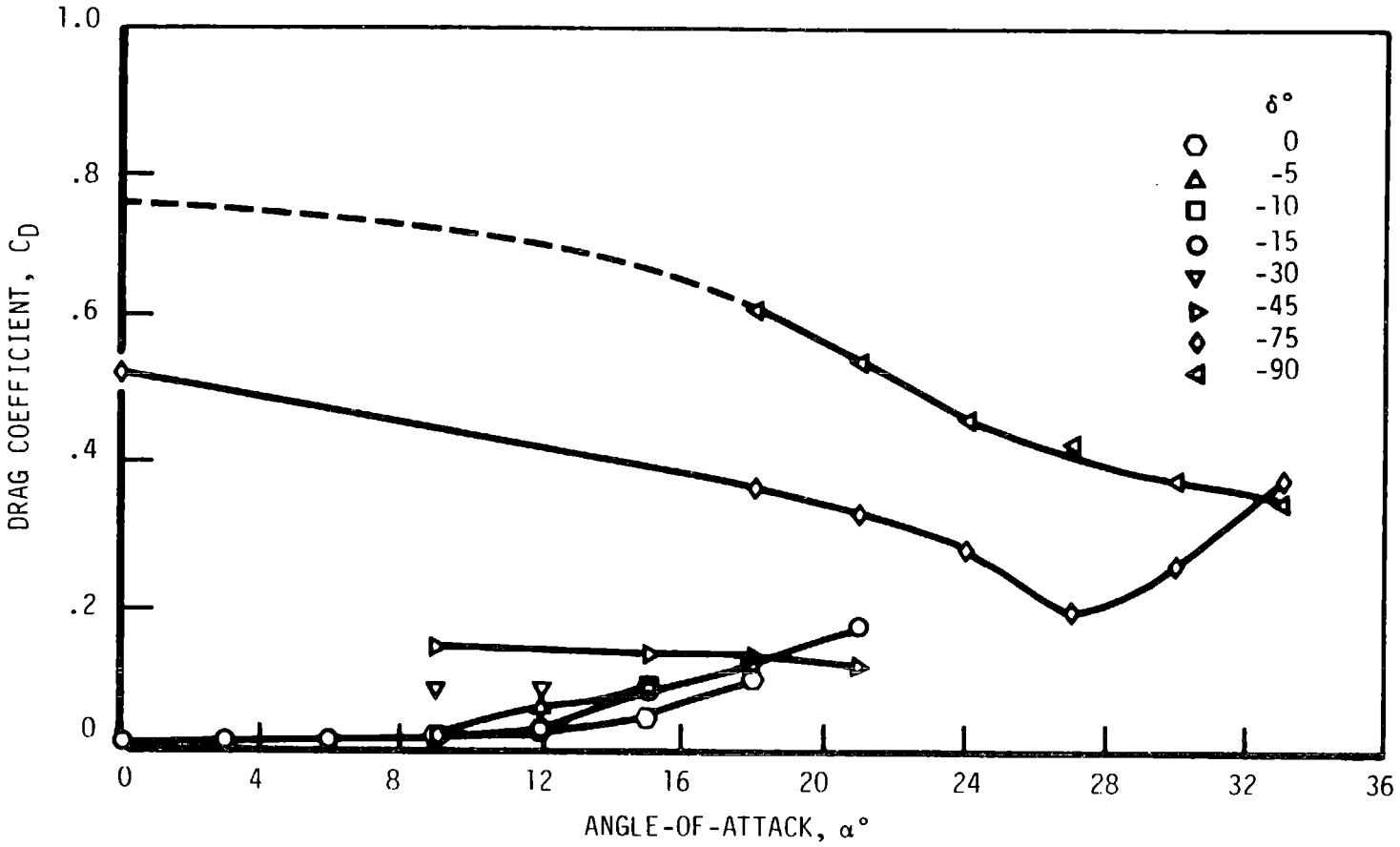

Figure 8-215 Aerodynamic Characteristics of the Plain 38% Chord Aileron

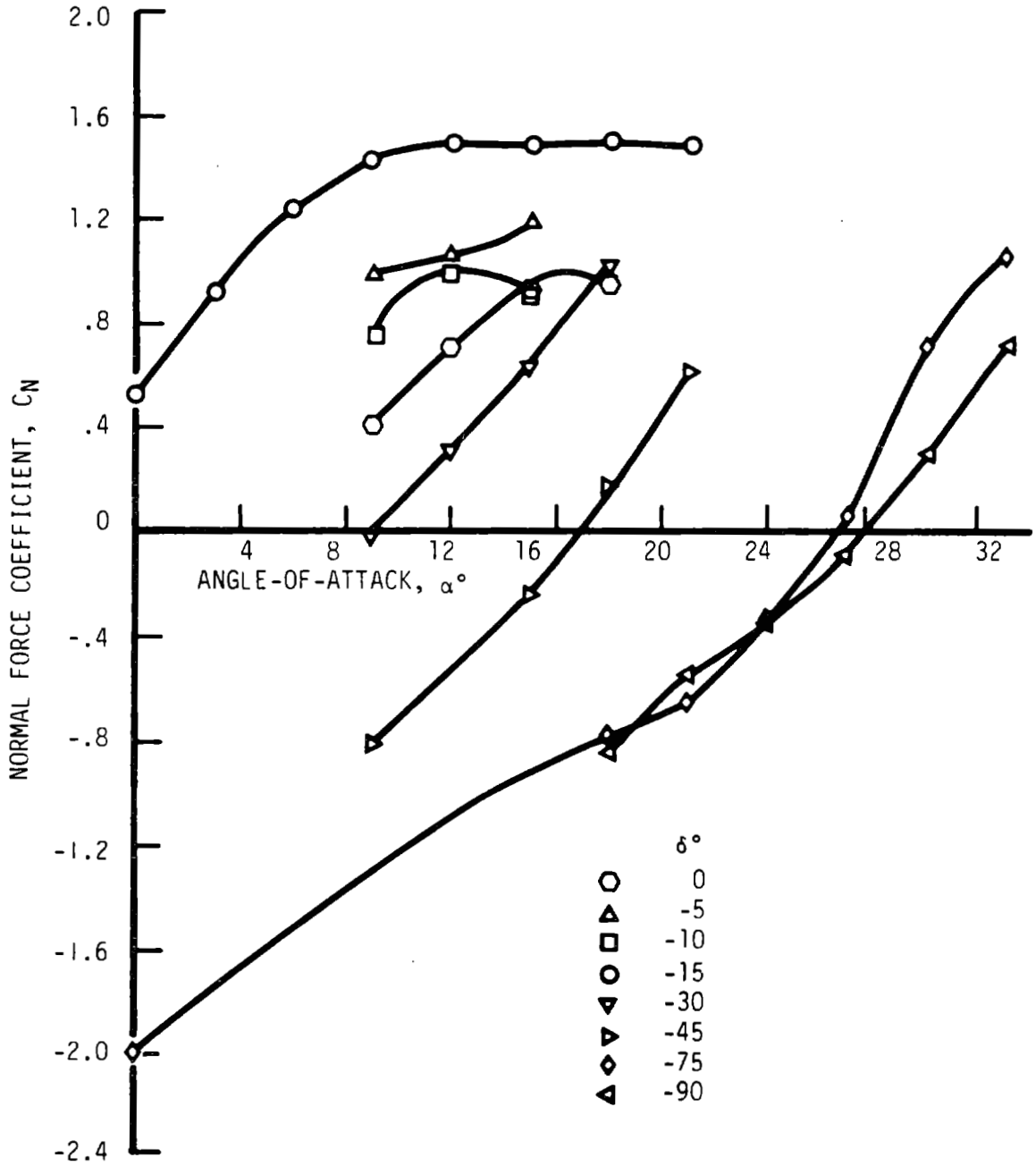

Figure 8-216 Aerodynamic Characteristics of the Plain 38% Chord Aileron

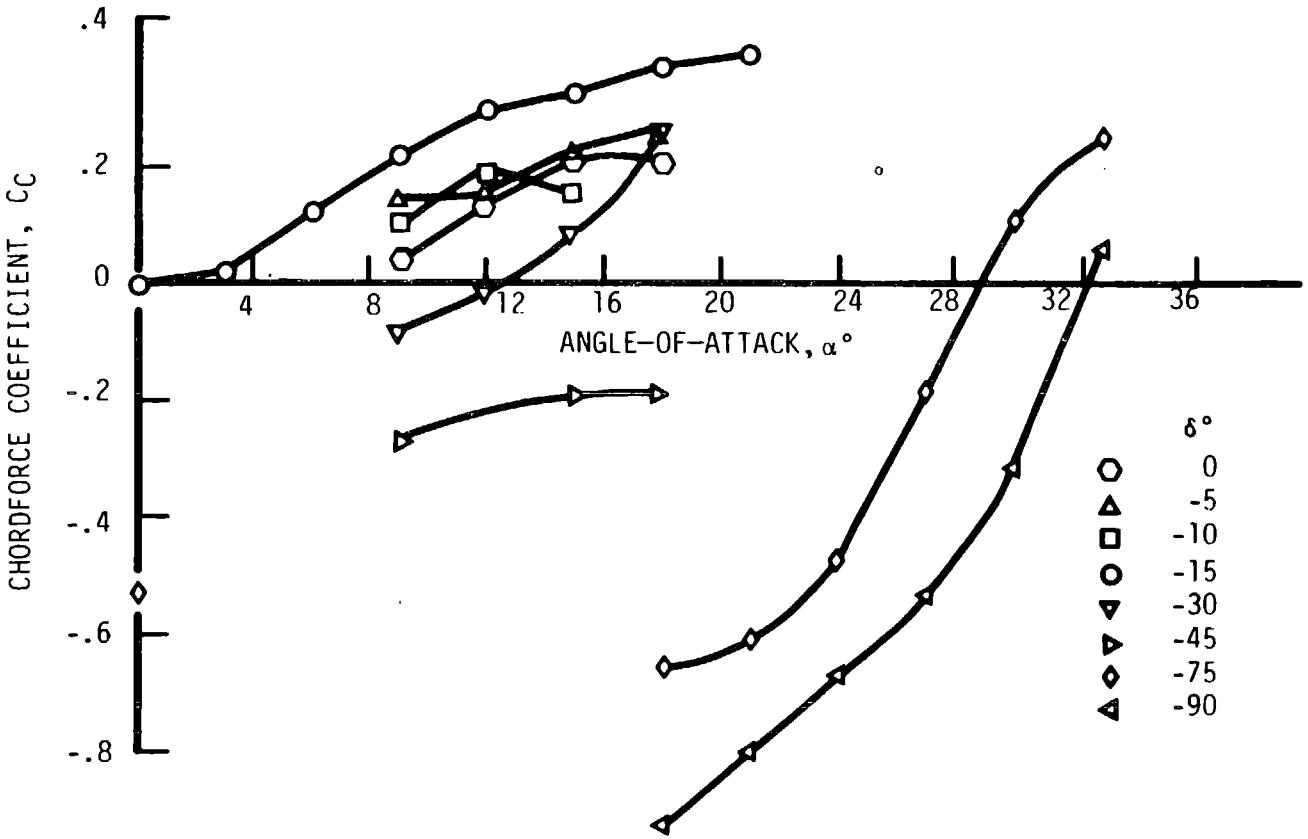

Figure 8-217 Aerodynamic Characteristics of the Plain 38% Chord Aileron

Table 8-98 Incremental Life Coefficient of PF 38% Chord as a Function of Angle of Attack and Aileron Deflection

ALPHA/DELTA	0	5	10	15	20	25	30	35	40	45
0.	0.	-0.340	-0.740	-1.120	-1.310	-1.450	-1.580	-1.890	-2.250	-2.500
6.	0.	-0.340	-0.740	-1.120	-1.310	-1.450	-1.580	-1.890	-2.250	-2.500
9.	0.	-0.450	-0.700	-1.040	-1.240	-1.370	-1.470	-1.650	-1.930	-2.230
12.	0.	-0.400	-0.520	-0.770	-0.930	-1.060	-1.210	-1.360	-1.580	-1.840
15.	0.	-0.300	-0.400	-0.560	-0.720	-0.820	-0.880	-1.010	-1.160	-1.350
18.	0.	-0.250	-0.370	-0.480	-0.540	-0.590	-0.630	-0.690	-0.770	-0.890
21.	0.	-0.190	-0.290	-0.370	-0.400	-0.420	-0.450	-0.490	-0.540	-0.630
24.	0.	-0.110	-0.180	-0.280	-0.310	-0.320	-0.330	-0.360	-0.390	-0.460
27.	0.	-0.050	-0.100	-0.200	-0.215	-0.230	-0.240	-0.250	-0.270	-0.320
30.	0.	-0.030	-0.070	-0.140	-0.155	-0.175	-0.180	-0.180	-0.200	-0.230
33.	0.	-0.010	-0.050	-0.085	-0.100	-0.110	-0.120	-0.125	-0.125	-0.120
36.	0.	-0.005	-0.030	-0.045	-0.055	-0.060	-0.065	-0.066	-0.068	-0.070
40.	0.	-0.121	-0.248	-0.350	-0.317	-0.258	-0.211	-0.159	-0.108	-0.063
45	0.	-0.086	-0.172	-0.250	-0.227	-0.198	-0.174	-0.151	-0.126	-0.102
50	0.	-0.052	-0.100	-0.150	-0.151	-0.140	-0.138	-0.135	-0.132	-0.129
90.	0.	-0.052	-0.100	-0.150	-0.151	-0.140	-0.138	-0.135	-0.132	-0.129

	50	55	60	65	70	75	80	85	90
0.	-2.620	-2.710	-2.760	-2.790	-2.840	-2.880	-2.890	-2.910	-2.920
6.	-2.620	-2.710	-2.760	-2.790	-2.840	-2.880	-2.890	-2.910	-2.920
9.	-2.440	-2.600	-2.710	-2.790	-2.850	-2.910	-2.930	-2.950	-2.970
12.	-2.080	-2.290	-2.450	-2.630	-2.730	-2.830	-2.850	-2.860	-2.880
15.	-1.580	-1.840	-2.130	-2.370	-2.510	-2.640	-2.660	-2.680	-2.700
18.	-1.050	-1.270	-1.560	-1.930	-2.210	-2.480	-2.500	-2.530	-2.550
21.	-0.800	-1.030	-1.320	-1.730	-1.990	-2.250	-2.280	-2.300	-2.330
24.	-0.610	-0.800	-1.070	-1.410	-1.690	-1.970	-2.000	-2.040	-2.070
27.	-0.440	-0.625	-0.870	-1.100	-1.300	-1.440	-1.580	-1.681	-1.760
30.	-0.265	-0.310	-0.381	-0.445	-0.530	-0.740	-0.785	-0.940	-1.260
33.	-0.135	-0.140	-0.165	-0.200	-0.245	-0.300	-0.365	-0.450	-0.700
36.	-0.075	-0.080	-0.105	-0.115	-0.160	-0.200	-0.260	-0.400	-0.500
40.	-0.015	0.033	0.080	0.104	0.129	0.157	0.181	0.206	0.230
45.	-0.077	0.	0.055	-0.030	0.001	0.031	0.061	0.087	0.118
50.	-0.125	-0.123	-0.119	-0.095	-0.046	0.	0.025	0.006	0.037
90.	-0.125	-0.123	-0.119	-0.095	-0.046	-0.025	0.006	0.037	0.070

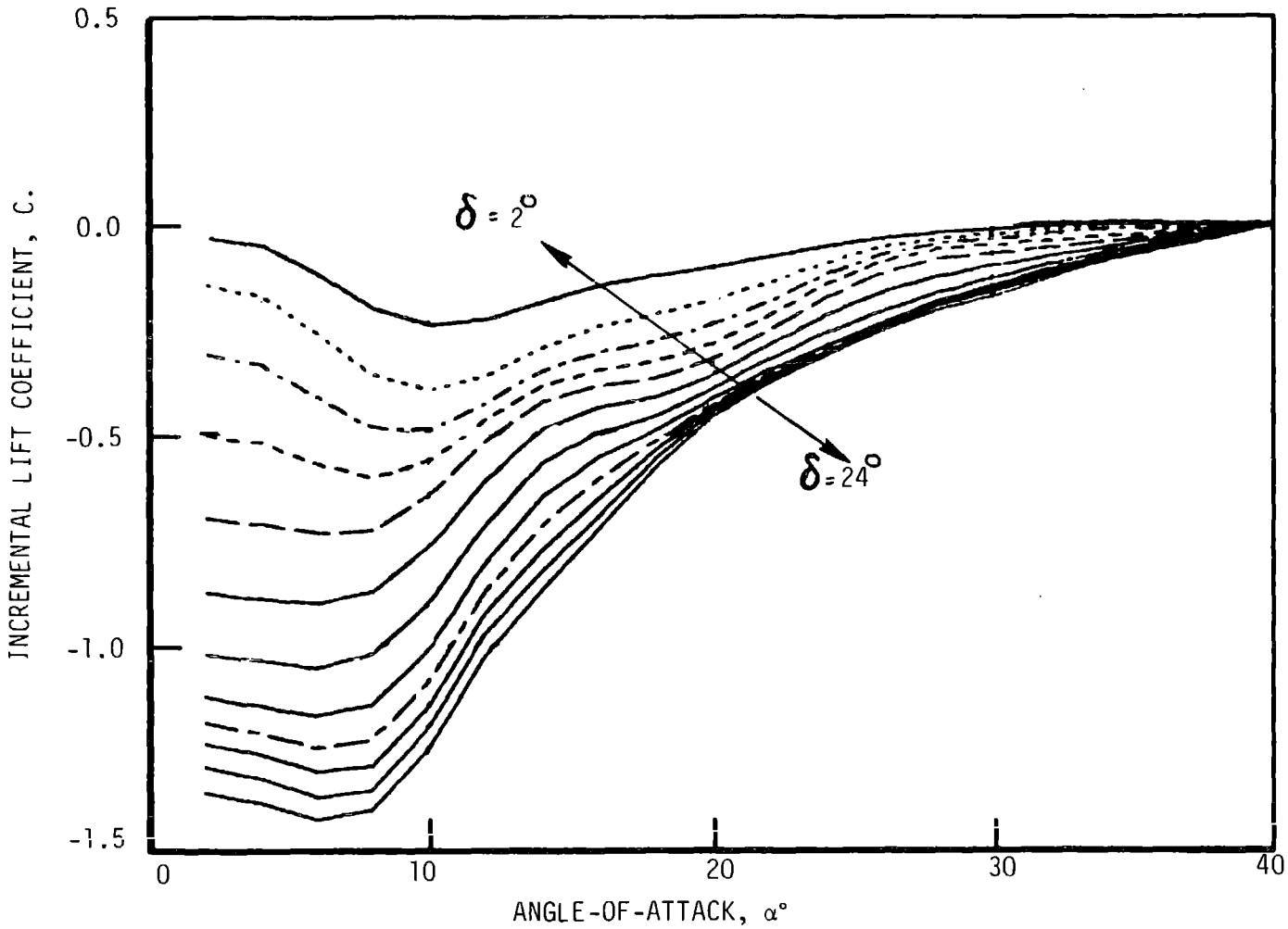

Figure 8-218 Lift Characteristics of the 38% Chord Plain Aileron for Control Deflection Angles from 2^o to 24^o in 2^o Increments

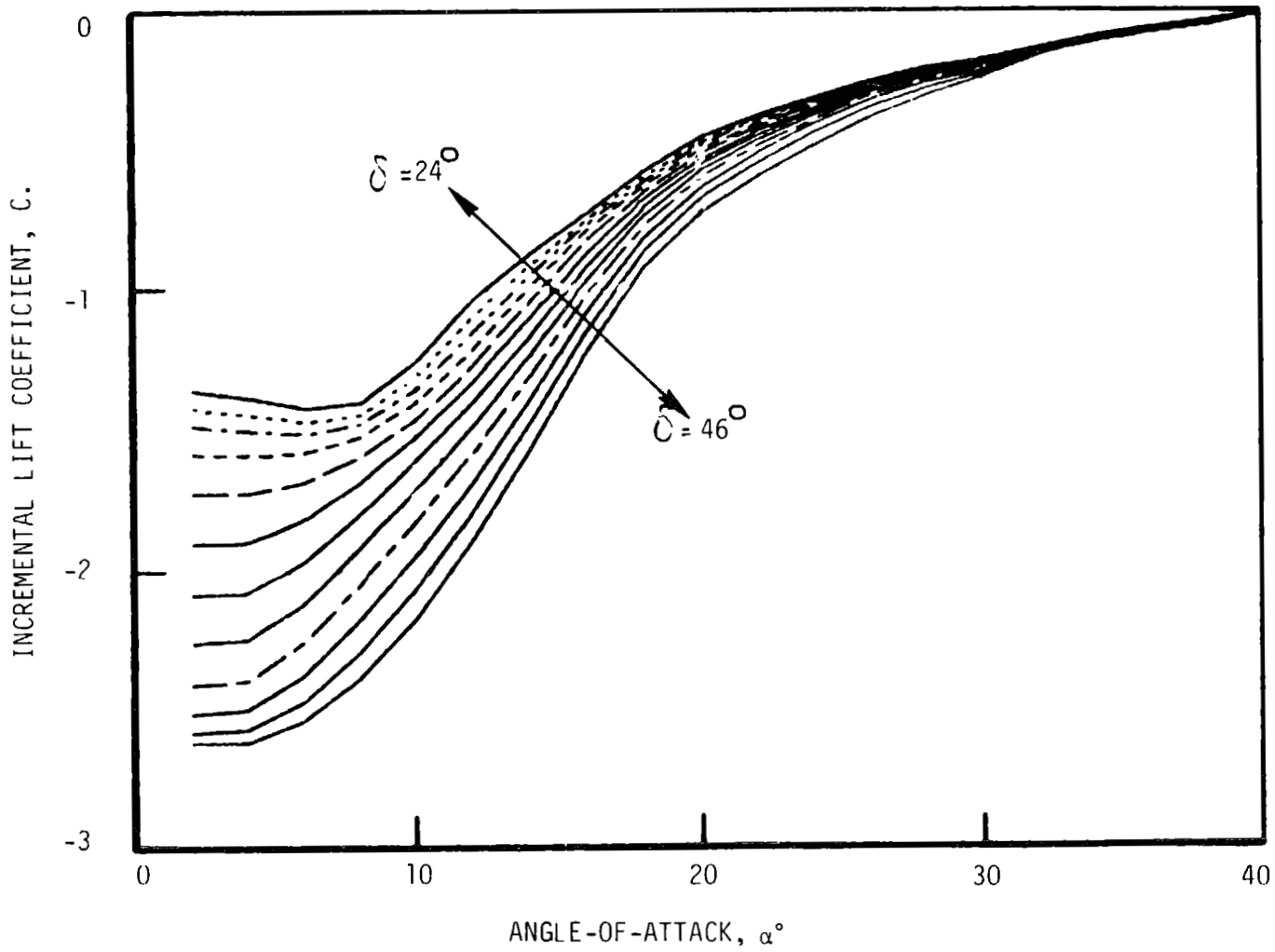

Figure 8-219 Lift Characteristics of the 38% Chord Plain Aileron for Control Deflection Angles from 24^o to 46^o in 2^o Increments

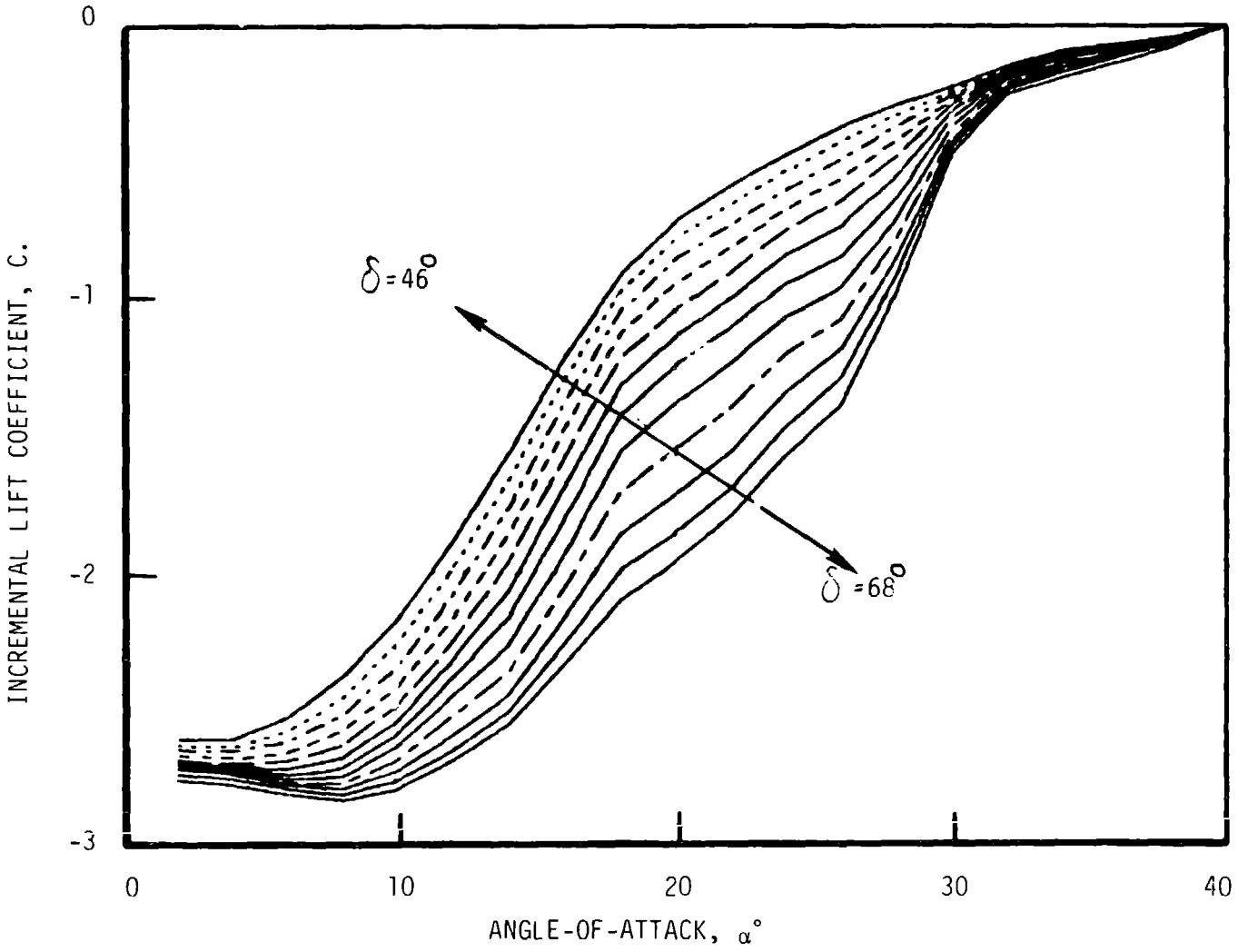

Figure 8-220 Lift Characteristics of the 38% Chord Plain Aileron for Control Deflection Angles from 46^o to 68^o in 2^o Increments

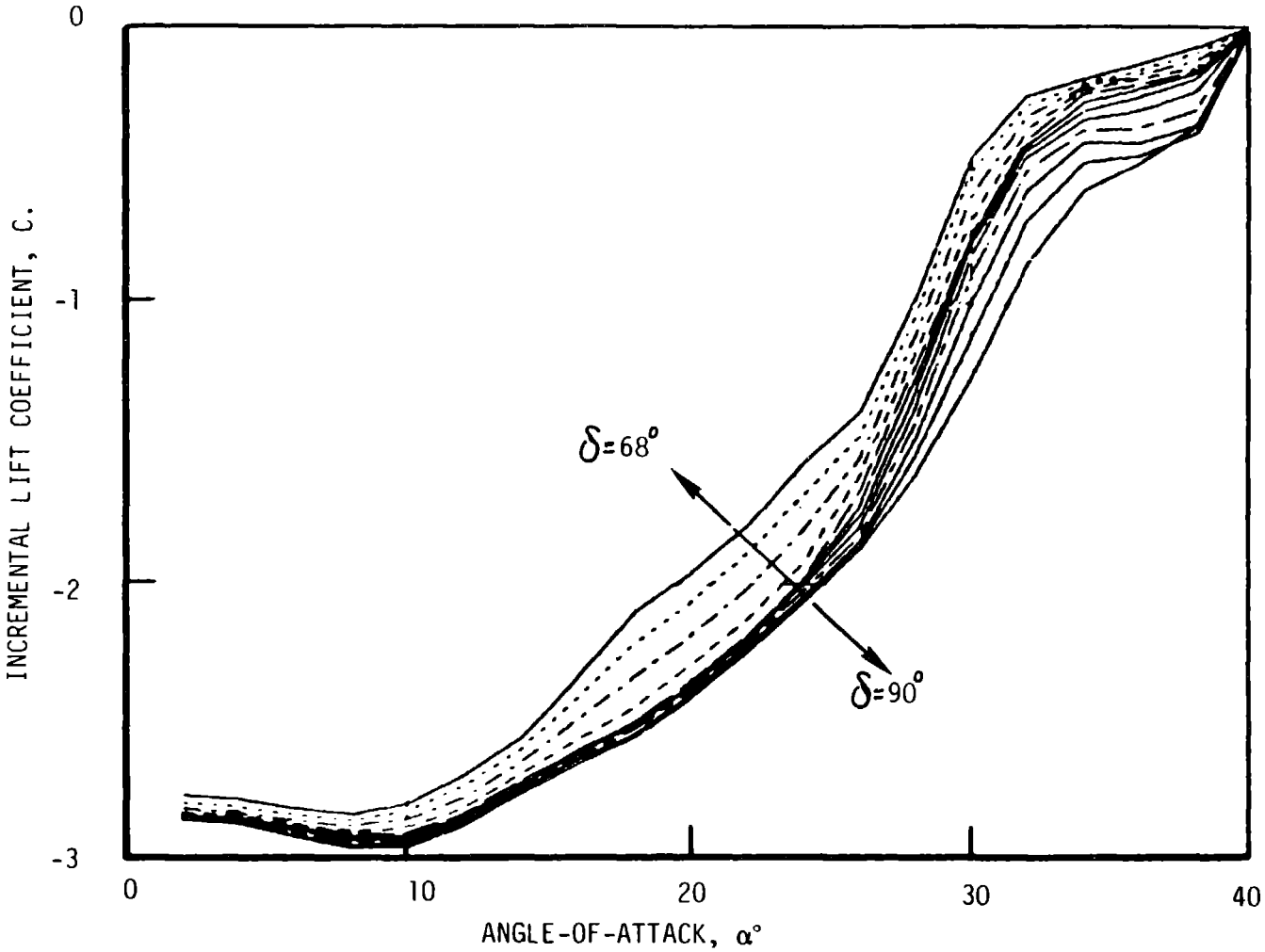

Figure 8-221 Lift Characteristics of the 38% Chord Plain Aileron for Control Deflection Angles from 68° to 80° in 2° Increments

Table 8-99 Incremental Drag Coefficient of PF 38% Chord as a Function of Angle of Attack and Aileron Deflection

ALPHA/DELTA	0	5	10	15	20	25	30	35	40	45
0.	0.	0.	0.005	0.002	0.005	0.079	0.112	0.154	0.196	0.238
6.	0.	0.	0.005	0.002	0.025	0.079	0.112	0.154	0.196	0.238
9.	0.	0.003	0.	0.006	0.035	0.062	0.085	0.132	0.174	0.213
12.	0.	0.040	0.017	0.009	0.030	0.054	0.080	0.116	0.157	0.198
15.	0.	0.025	-0.020	-0.045	-0.018	0.008	0.035	0.069	0.102	0.138
18.	0.	0.015	-0.030	-0.065	-0.043	-0.029	-0.010	0.015	0.048	0.070
21.	0.	0.025	-0.030	-0.065	-0.095	-0.095	-0.077	-0.052	-0.025	0.
24.	0.	0.025	-0.030	-0.065	-0.098	-0.125	-0.162	-0.200	-0.227	-0.257
27.	0.	0.025	-0.030	-0.065	-0.098	-0.125	-0.162	-0.200	-0.267	-0.265
30.	0.	-0.083	-0.182	-0.270	-0.346	-0.419	-0.472	-0.512	-0.538	-0.550
33.	0.	-0.115	-0.228	-0.329	-0.422	-0.491	-0.546	-0.586	-0.614	-0.620
36.	0.	-0.146	-0.288	-0.410	-0.507	-0.585	-0.640	-0.672	-0.696	-0.697
40.	0.	-0.192	-0.370	-0.510	-0.618	-0.700	-0.752	-0.789	-0.801	-0.795
45.	0.	-0.227	-0.420	-0.540	-0.655	-0.720	-0.775	-0.810	-0.860	-0.860
50.	0.	-0.235	-0.435	-0.540	-0.660	-0.745	-0.785	-0.825	-0.870	-0.879
55.	0.	-0.225	-0.415	-0.520	-0.640	-0.720	-0.775	-0.820	-0.860	-0.860
60.	0.	-0.200	-0.370	-0.475	-0.595	-0.690	-0.745	-0.790	-0.820	-0.820
65	0.	-0.167	-0.322	-0.400	-0.530	-0.625	-0.700	-0.745	-0.700	-0.700
70.	0.	-0.133	-0.260	-0.320	-0.460	-0.555	-0.620	-0.695	-0.560	-0.560
75.	0.	-0.100	-0.198	-0.240	-0.380	-0.460	-0.560	-0.620	-0.420	-0.420
80.	0.	-0.067	-0.145	-0.160	-0.270	-0.350	-0.430	-0.500	-0.280	-0.280
85.	0.	-0.033	-0.075	-0.080	-0.130	-0.210	-0.300	-0.350	-0.140	-0.140
90.	0.	0.	0.	0.	0.	0.	0.	0.	0.	0.

	50	55	60	65	70	75	80	85	90
0.	0.280	0.322	0.365	0.405	0.443	0.490	0.597	0.700	0.810
6.	0.280	0.322	0.365	0.405	0.443	0.490	0.597	0.700	0.810
9.	0.255	0.297	0.338	0.379	0.420	0.464	0.562	0.671	0.775
12.	0.235	0.275	0.314	0.353	0.392	0.432	0.527	0.625	0.725
15.	0.174	0.210	0.245	0.281	0.317	0.353	0.440	0.530	0.625
18.	0.102	0.135	0.168	0.200	0.233	0.265	0.346	0.428	0.510
21.	0.030	0.056	0.080	0.106	0.135	0.160	0.220	0.292	0.375
24.	-0.270	-0.275	-0.265	-0.230	-0.180	-0.128	-0.070	0.	0.060
27.	-0.295	-0.335	-0.360	-0.370	-0.350	-0.320	-0.270	-0.210	-0.155
30.	-0.545	-0.530	-0.510	-0.485	-0.454	-0.417	-0.381	-0.352	-0.300
33.	-0.610	-0.592	-0.570	-0.543	-0.519	-0.490	-0.456	-0.422	-0.390
36.	-0.670	-0.645	-0.618	-0.593	-0.566	-0.540	-0.515	-0.488	-0.465
40.	-0.765	-0.738	-0.712	-0.685	-0.659	-0.632	-0.605	-0.577	-0.550
45.	-0.830	-0.780	-0.712	-0.688	-0.667	-0.646	-0.624	-0.602	-0.580
50.	-0.850	-0.820	-0.707	-0.691	-0.667	-0.646	-0.624	-0.602	-0.580
55.	-0.850	-0.820	-0.705	-0.694	-0.684	-0.673	-0.662	-0.651	-0.640
60.	-0.800	-0.780	-0.702	-0.697	-0.692	-0.686	-0.681	-0.675	-0.670
65.	-0.700	-0.700	-0.700	-0.700	-0.700	-0.700	-0.700	-0.700	-0.700
70.	-0.560	-0.560	-0.560	-0.560	-0.560	-0.560	-0.560	-0.560	-0.560
75.	-0.420	-0.420	-0.420	-0.420	-0.420	-0.420	-0.420	-0.420	-0.420
80.	-0.280	-0.280	-0.280	-0.280	-0.280	-0.280	-0.280	-0.280	-0.280
85.	-0.140	-0.140	-0.140	-0.140	-0.140	-0.140	-0.140	-0.140	-0.140
90.	0.	0.	0.	0.	0.	0.	0.	0.	0.

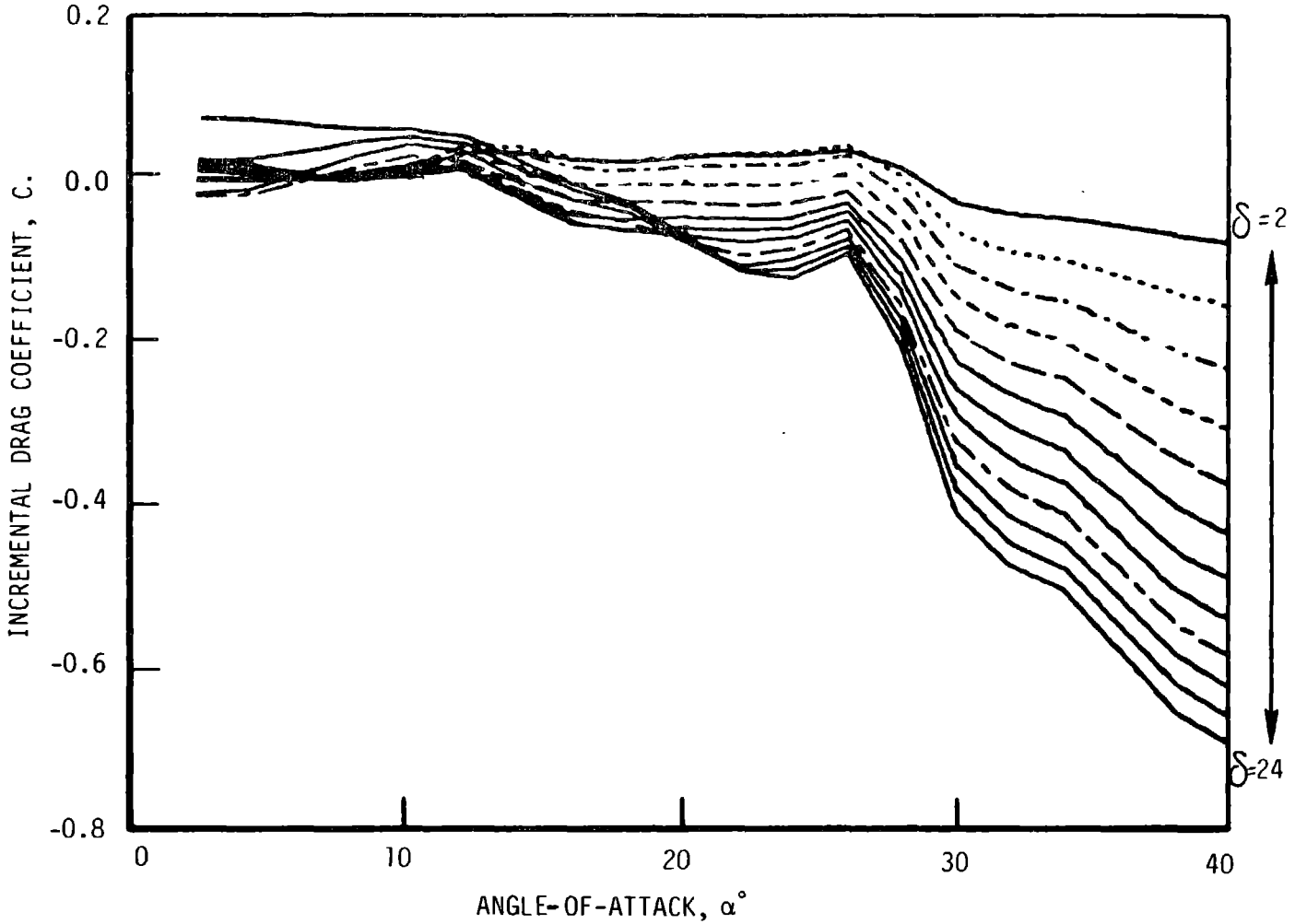

Figure 8-222 Drag Characteristics of the 38% Chord Plain Aileron for Control Deflection Angles from 2^{o} to 24^{o} in 2^{o} Increments

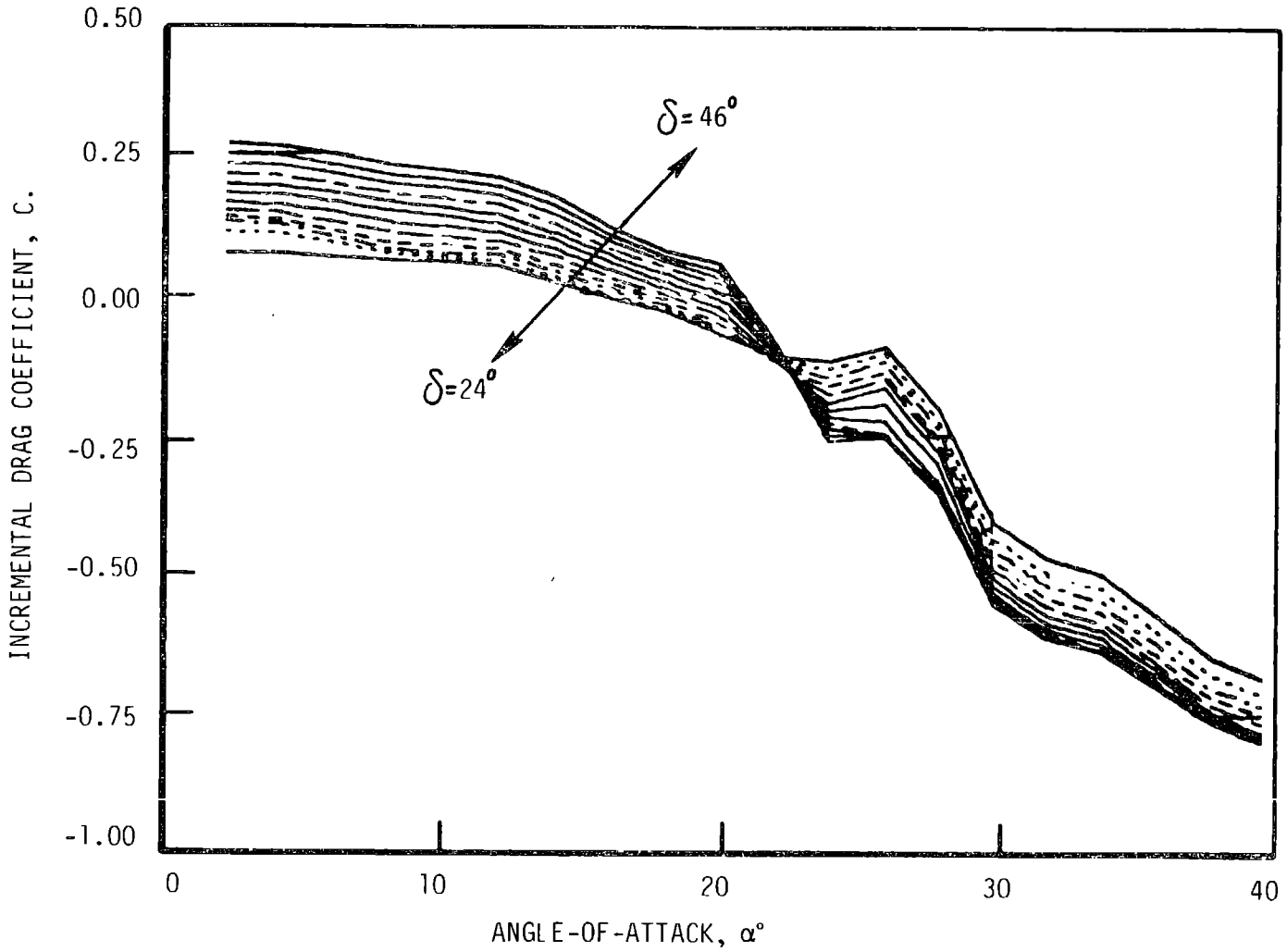

Figure 8-223 Drag Characteristics of the 38% Chord Plain Aileron for Control Deflection Angles from 24° to 46° in 2° Increments

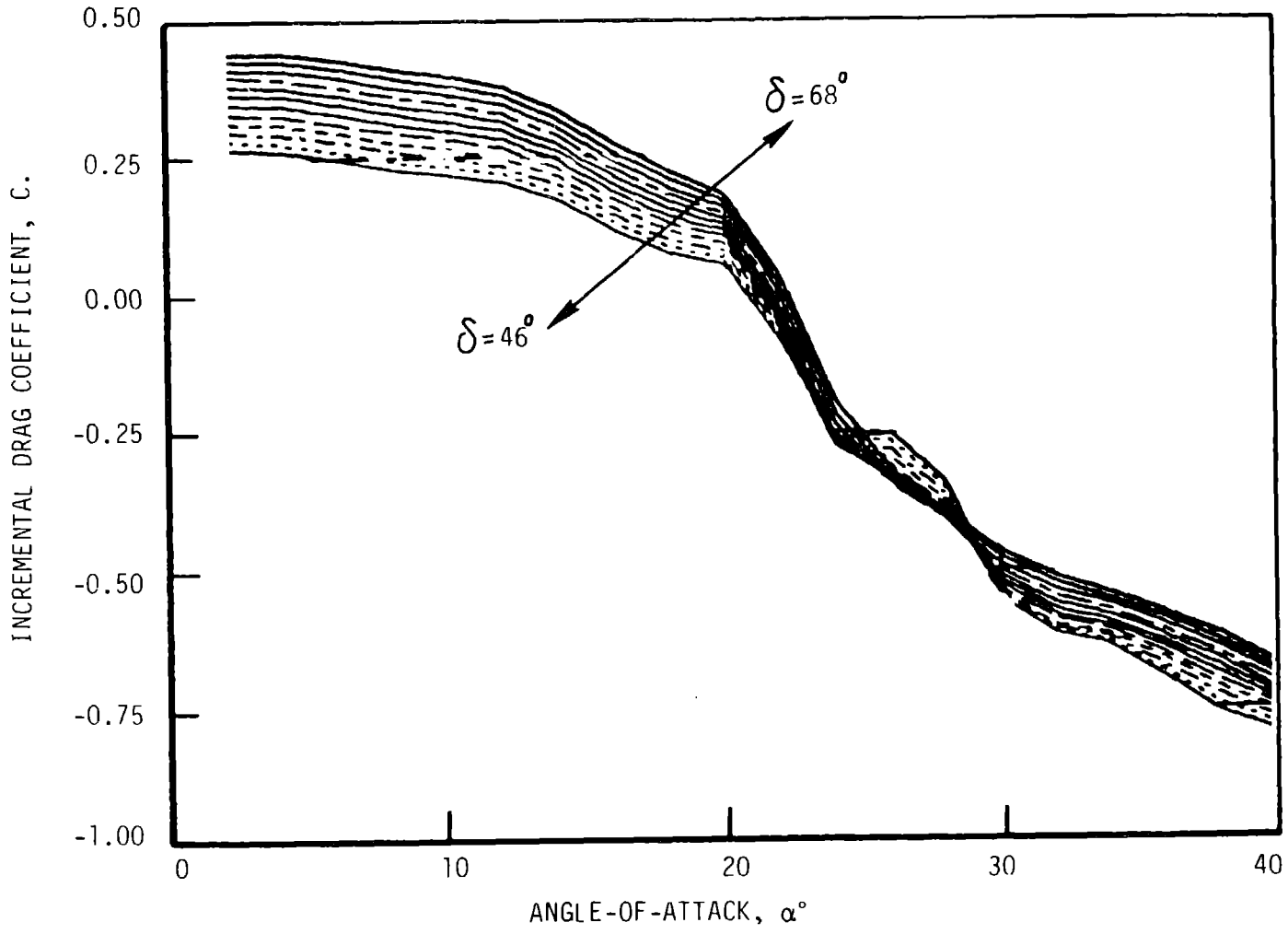

Figure 8-224 Drag Characteristics of the 38% Chord Plain Aileron for Control Deflection Angles from 46^{o} to 68^{o} in 2^{o} Increments

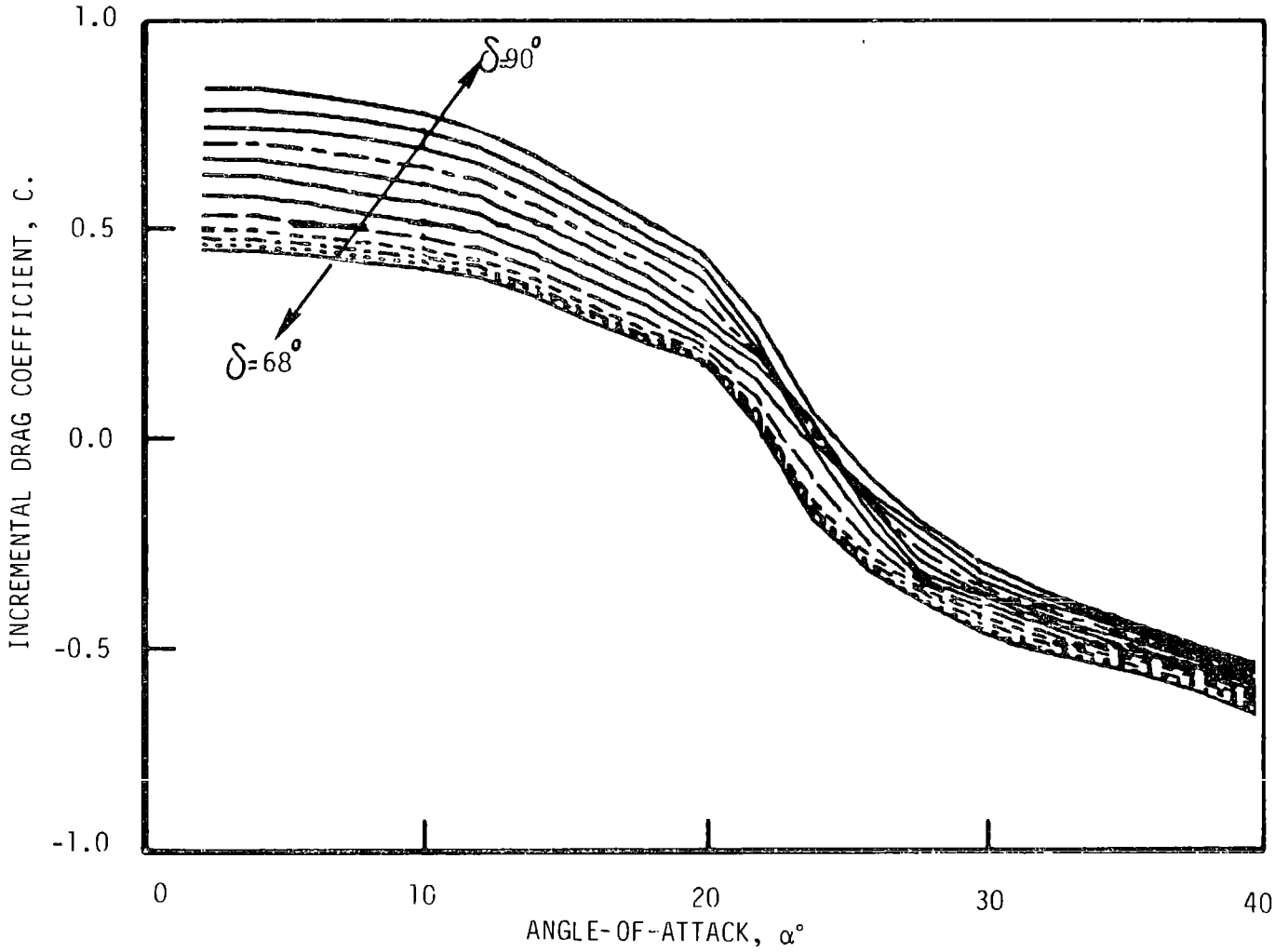

Figure 8-225 Drag Characteristics of the 38% Chord Plain Aileron for Control Deflection Angles from 68^{o} to 90^{o} in 2^{o} Increments

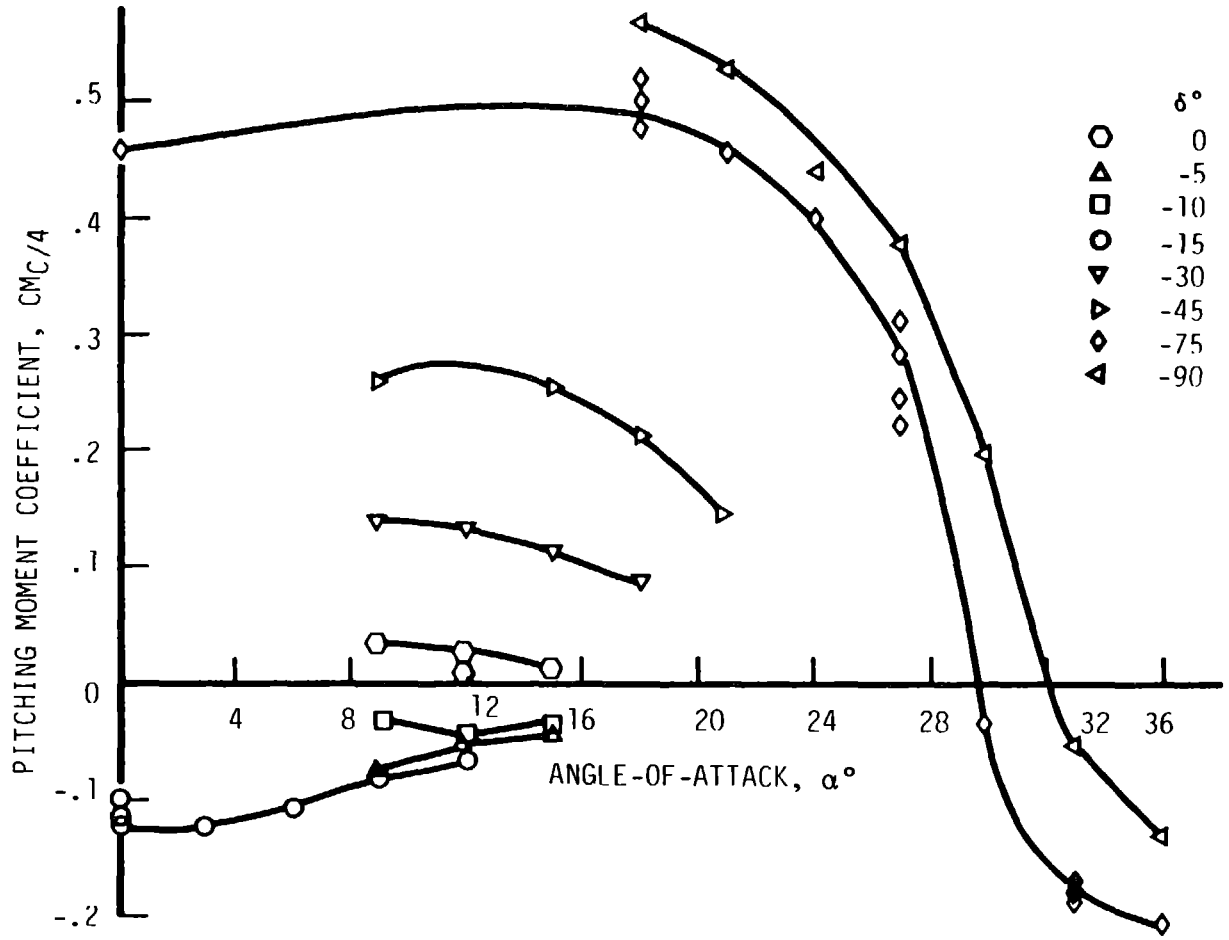

Figure 8-226 Aileron Pitching Moment Characteristics

The hinge moment characteristics of the 38% chord plain aileron are shown in Figure 8-227. Regions of negative hinge moment indicate conditions in which the aileron is self-deploying. The line of zero hinge moment defines the equilibrium conditions for an unrestrained or floating aileron. The hinge moments are based on the aileron chord.

8.4.2.5 Wind Tunnel Test -Phase II Results - 38% Chord Balanced Aileron

The data for the 38% chord, balanced aileron is shown in Figures 8-228 through 8-233 in the same format used for the 38% chord, plain aileron.

The balanced aileron was tested at higher angles of attack than the plain aileron. A remarkable sharp change in characteristics at high angles of attack and control deflection was observed. This phenomenon is clearly shown in Figure 8-231. The curve for normal force, for an aileron deflection of -75° rises with increasing steepness in the range of angles of attack between 18° and 27°. In the range from 27° to 30°, however, an abrupt change takes place and beyond that region the characteristic slopes gently downward. Similar behavior is observed for the -90° deflection. This abrupt change in characteristics was also be observed in the other aerodynamic forces, shown in Figures 8-228 through 8-233.

Pressure distribution data explained these observations, as shown in Figure 8-234. The pressure distribution on the upper surface of the airfoil is shown over the main airfoil element, on the left side of the chart, and over the flap element, on the right, at a deflection angle of -75°. At an angle of attack of 27°, the upper surface pressure over all of the main element and over much of the aileron element is positive, indicating that the flow in this region was retarded to less than stream velocity by the deflected aileron. Increasing the angle of attack to 30° causes the pressure coefficient to drop to C_p = -1.3, which corresponds to a local velocity of 1.5 times the stream velocity. This behavior indicates the region where the upper surface flow "jumps" the deflected aileron. This region does not effectively control the flow at higher angles of attack.

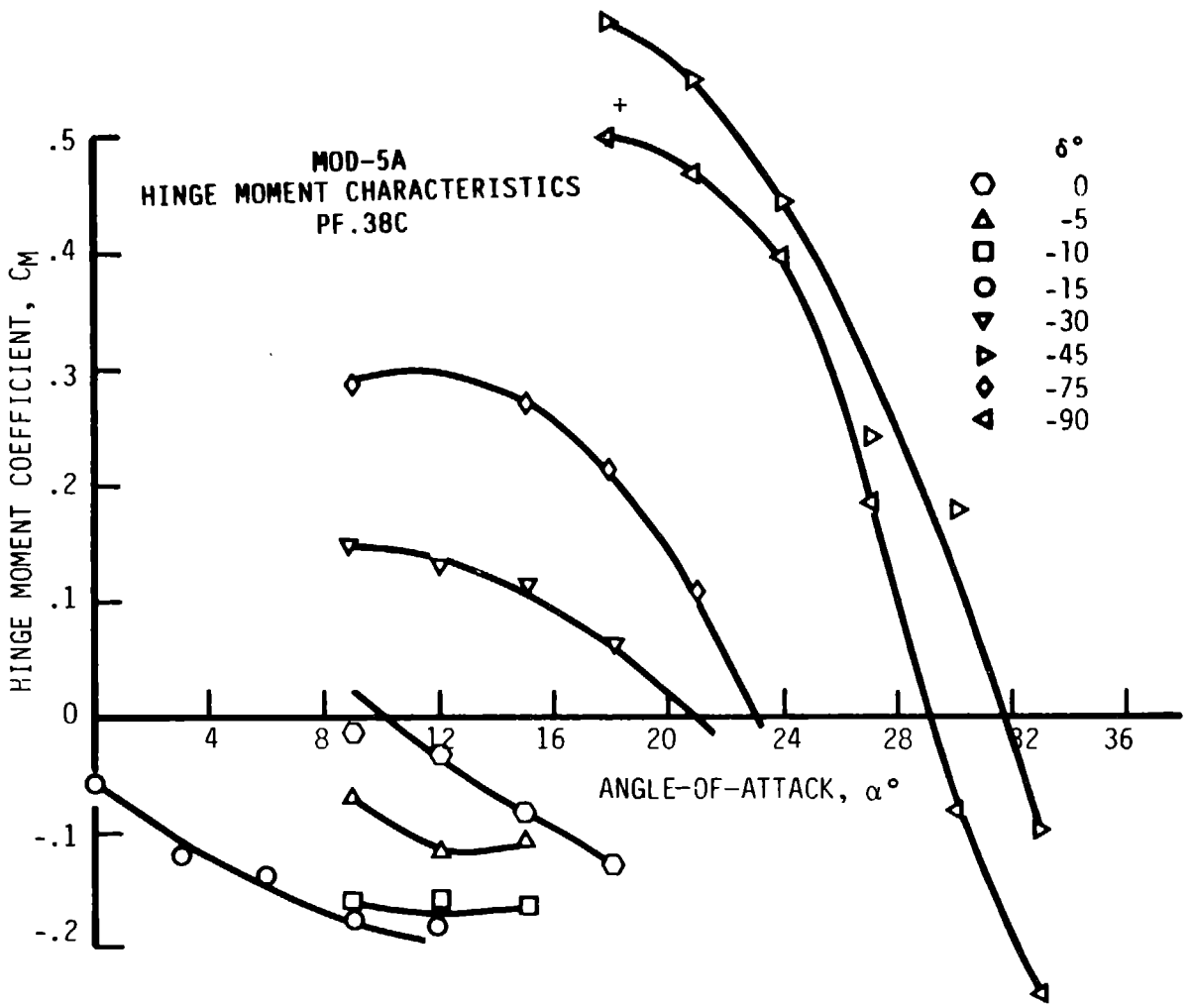

Figure 8-227 Aerodynamic Characteristics of the Plain 38% Chord Aileron Hinge Moment

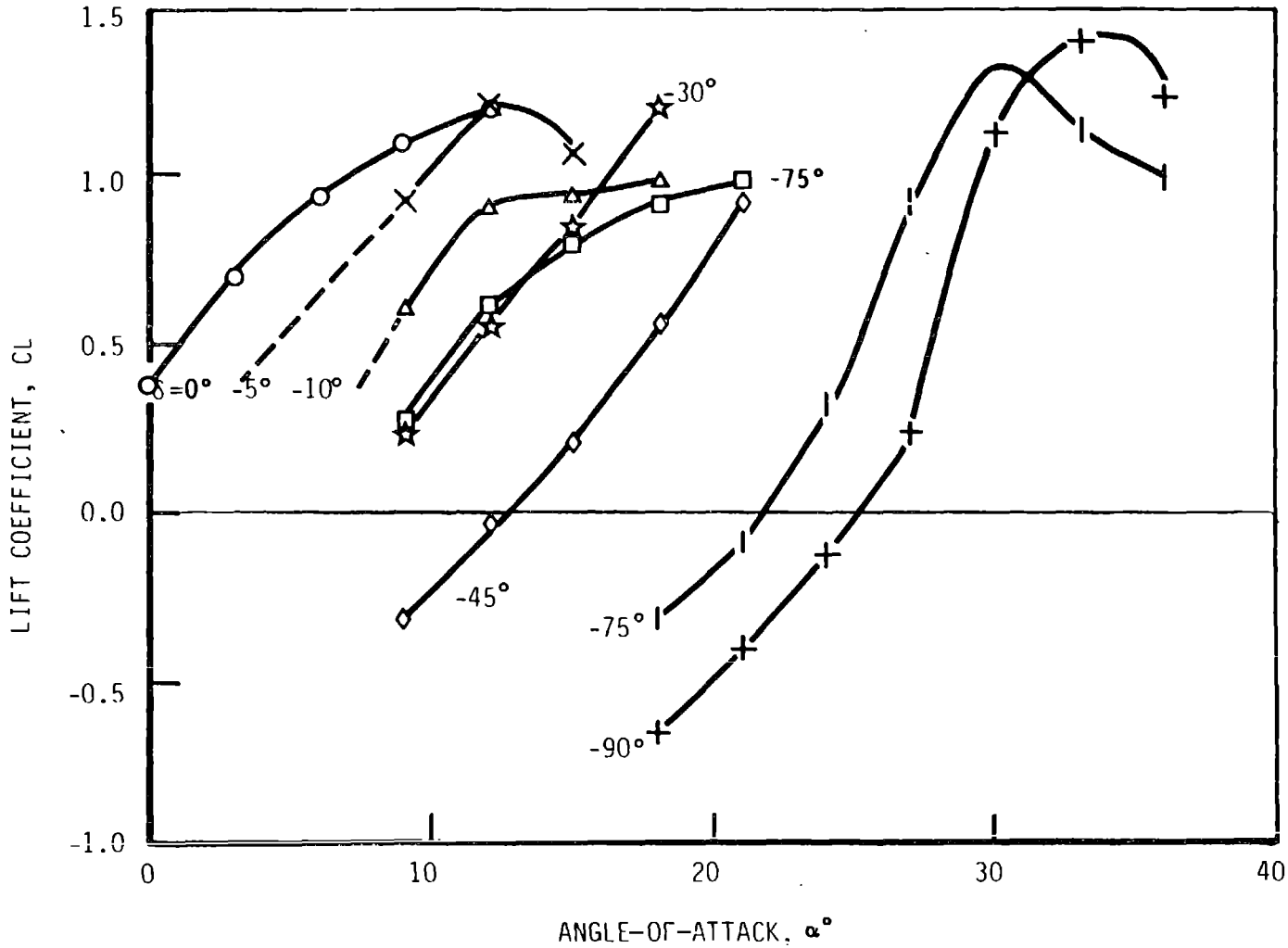

Figure 8-228 Aerodynamic Characteristics of the Balanced 38% Chord Aileron-Lift

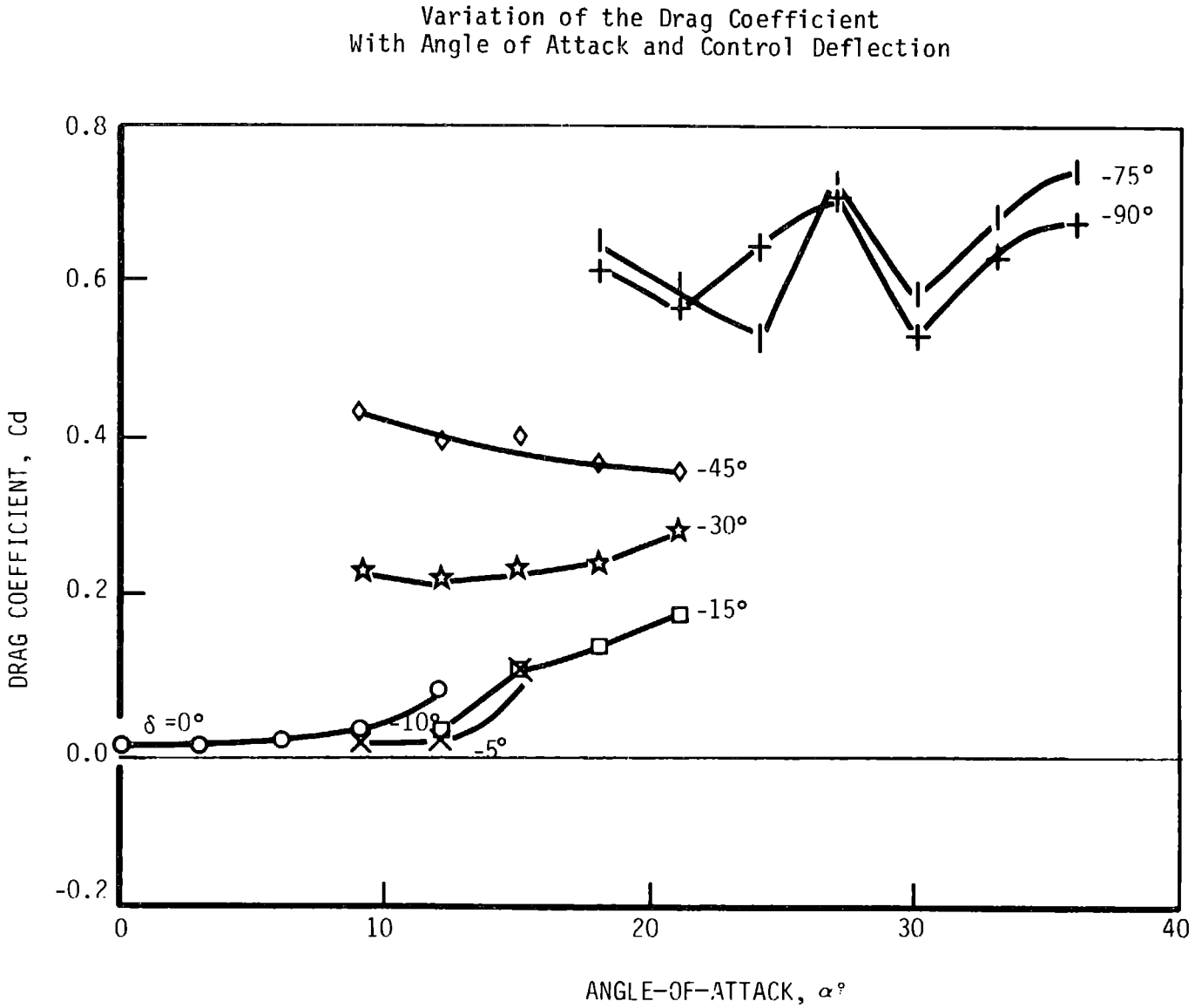

Figure 8-229 Aerodynamic Characteristics of the Balanced 38% Chord Aileron-Drag

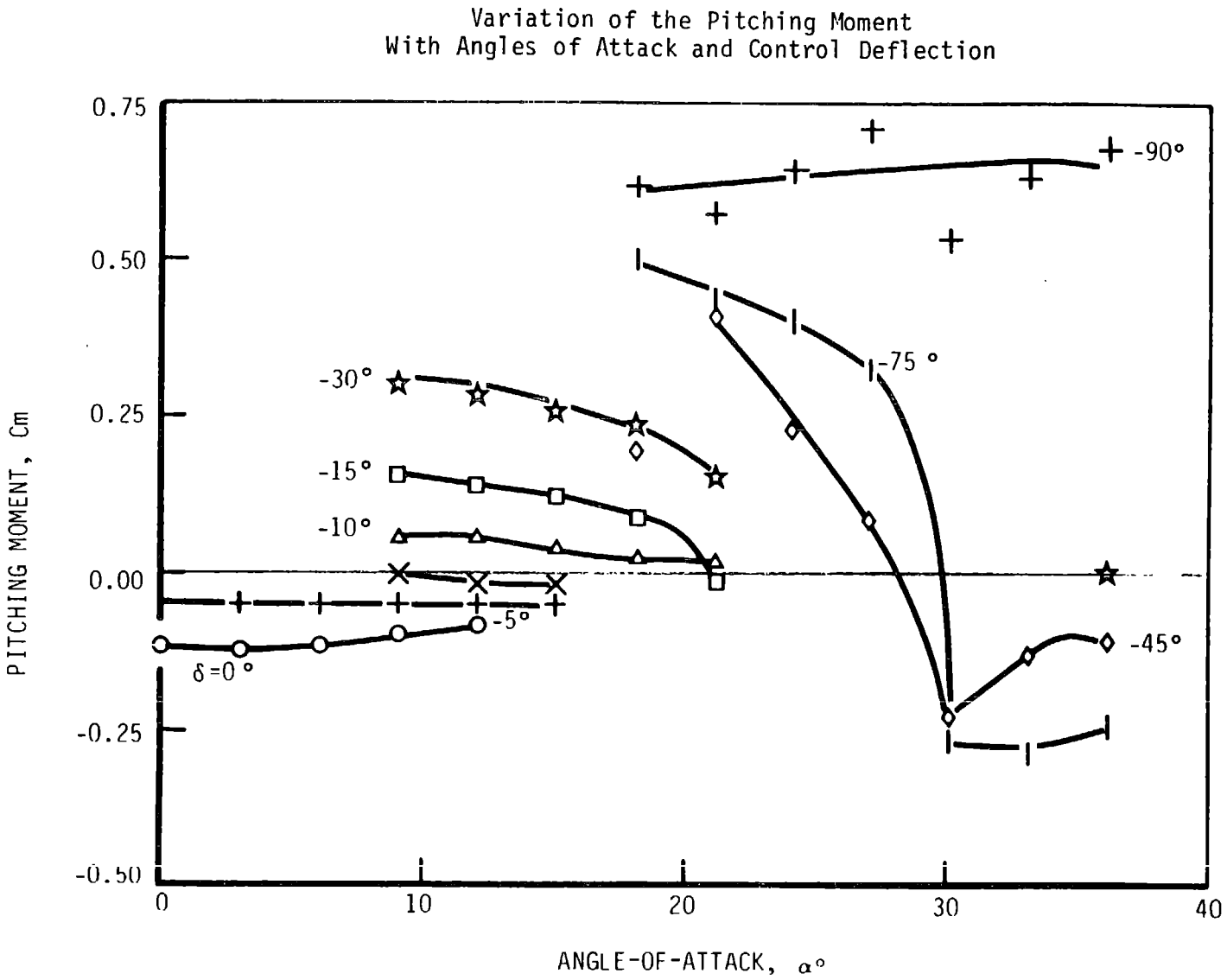

Figure 8-230 Aerodynamic Characteristics of the Balanced 38% Chord Aileron-Pitching Moment

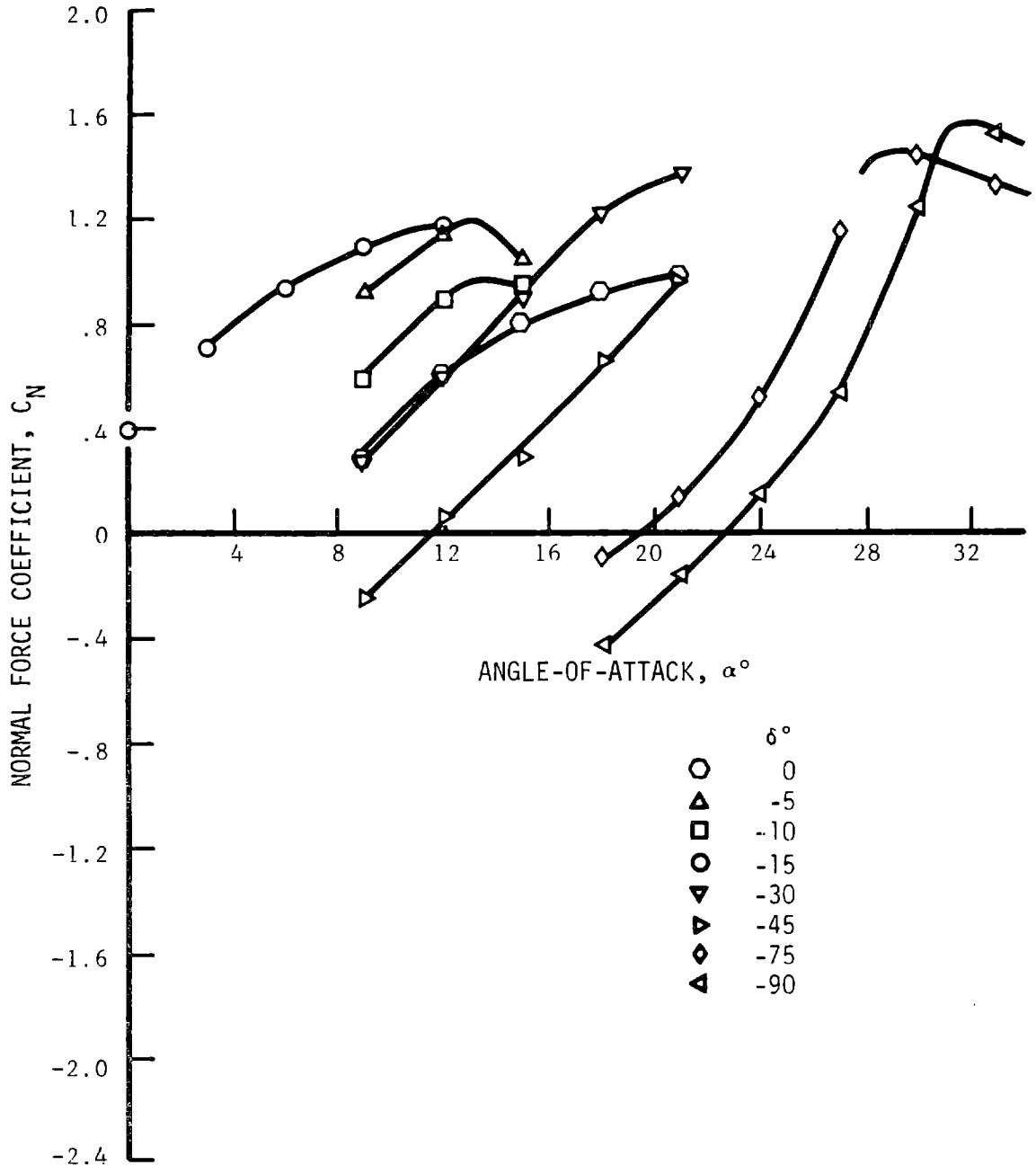

Figure 8-231 Aerodynamic Characteristics of the Balanced 38% Chord Aileron-Normal Force

Variation of the Axial Force Coefficient
With Angle of Attack and Control Deflection

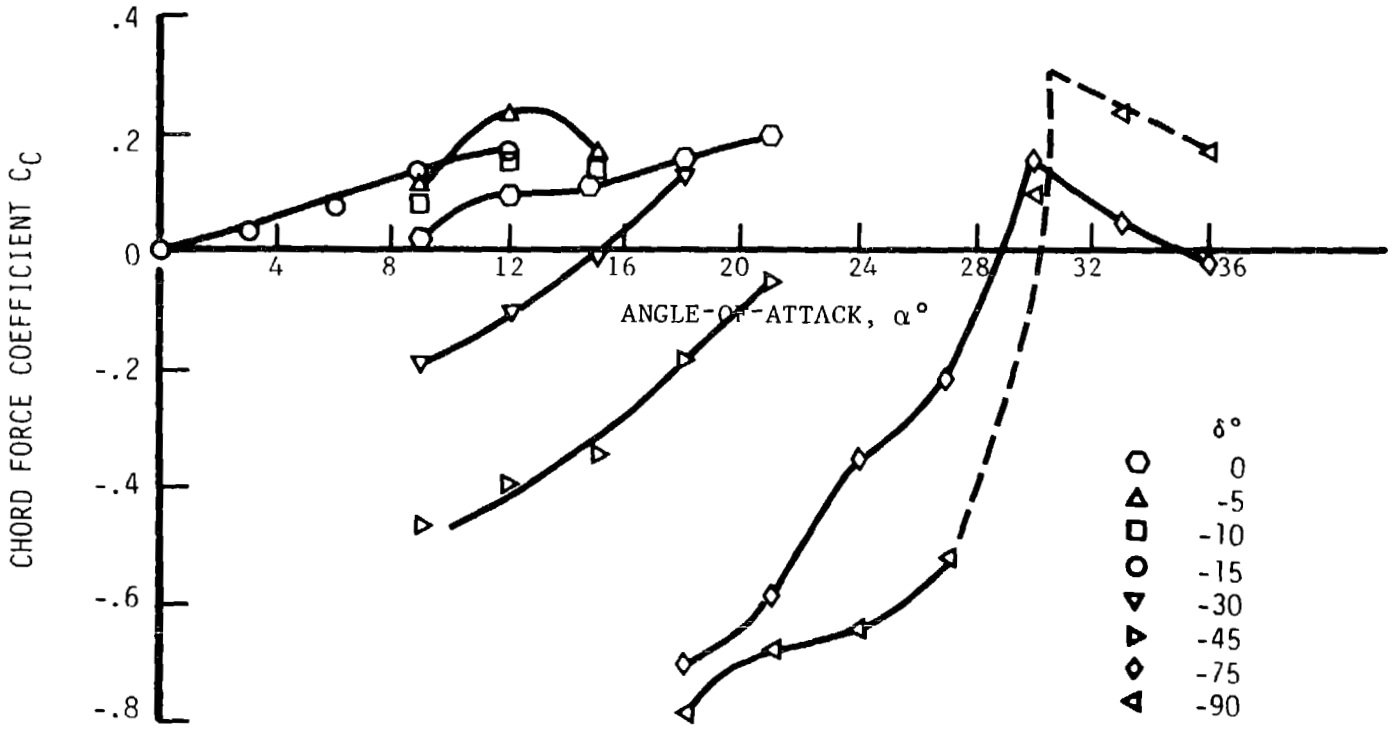

Figure 8-232 Aerodynamic Characteristics of the Balanced 38% Chord Aileron-Axial Force

Variation of the Hinge Moment Coefficient
With Angle of Attack and Control Deflection

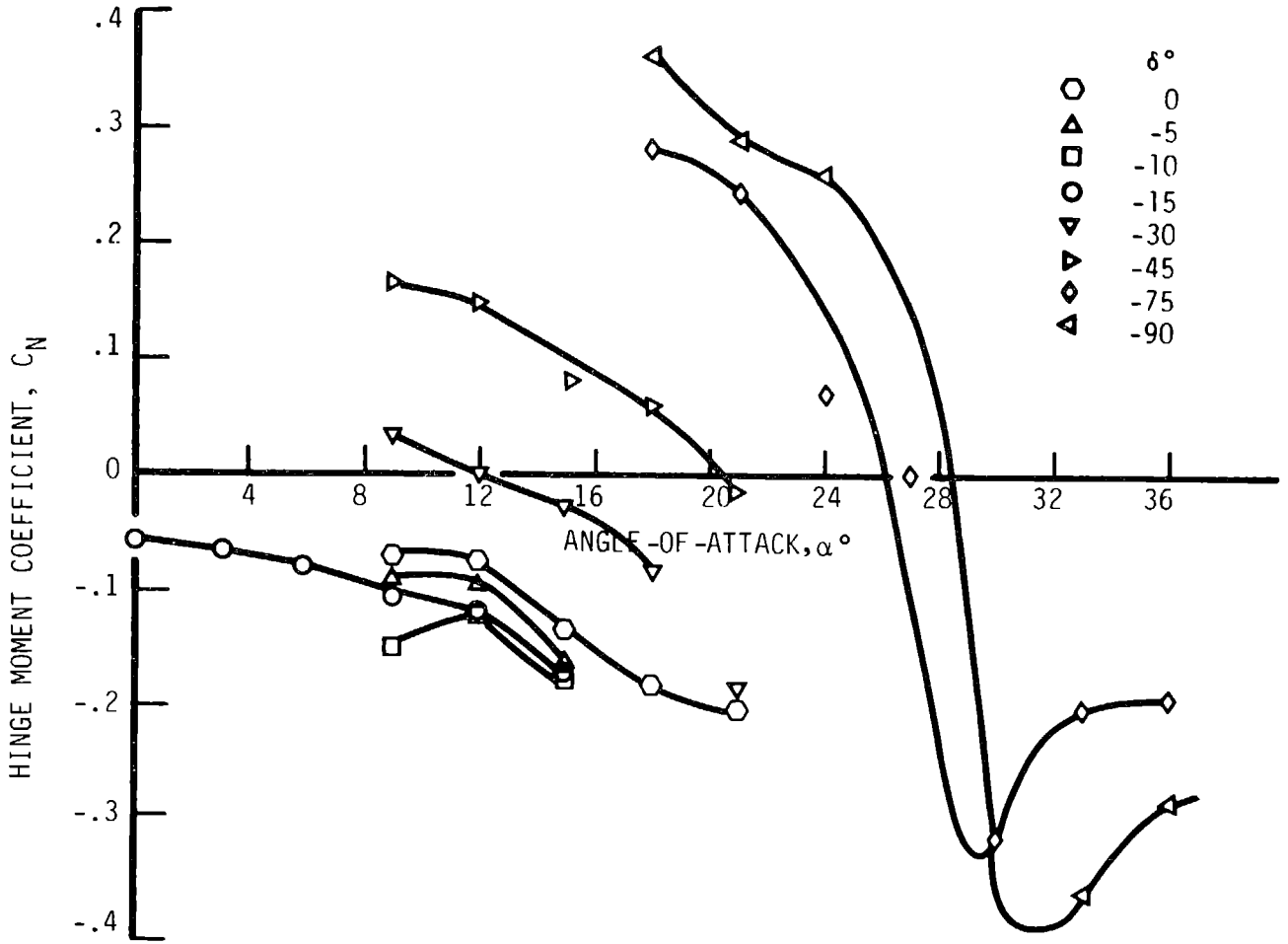

Figure 8-233 Aerodynamic Characteristics of the Balanced 38% Chord Aileron-Hinge Moment

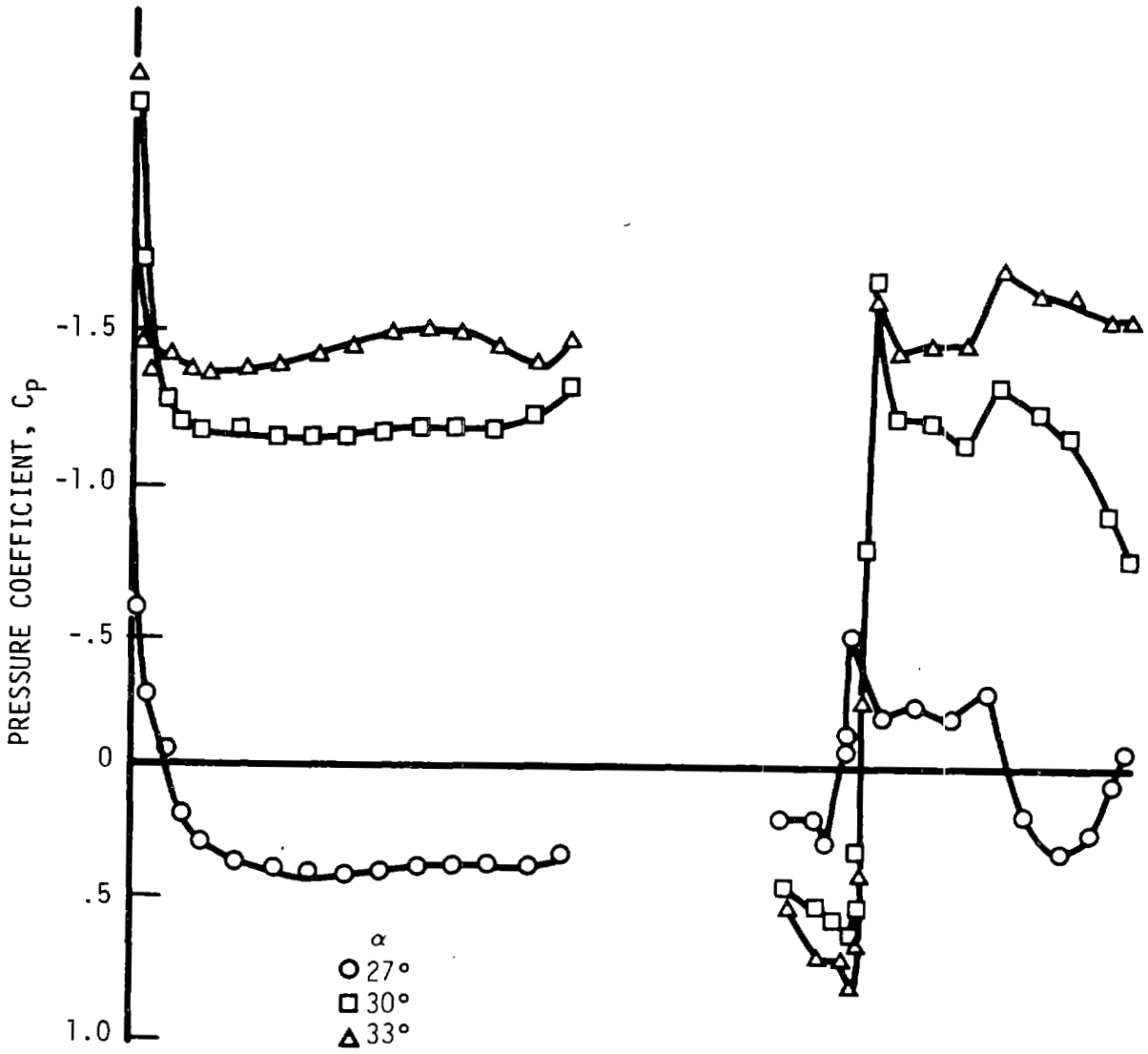

Figure 8-234 Upper Surface Pressure Coefficient for Balanced Aileron, BF 38% Chord at Deflection = -75°

8.4.2.5.1 Wind Tunnel Phase II Results - Aileron Floating Tendency

The floating angle of the two aileron configurations is shown in Figure 8-235. The floating angle is the aileron's equilibrium position under no hinge restraint. The balanced configuration increases the negative hinge moment and as a result the balanced aileron has an equilibrium at a greater floating angle than the plain aileron. The plain aileron would require emergency assistance to ensure automatic shutdown if the hydraulic system fails.

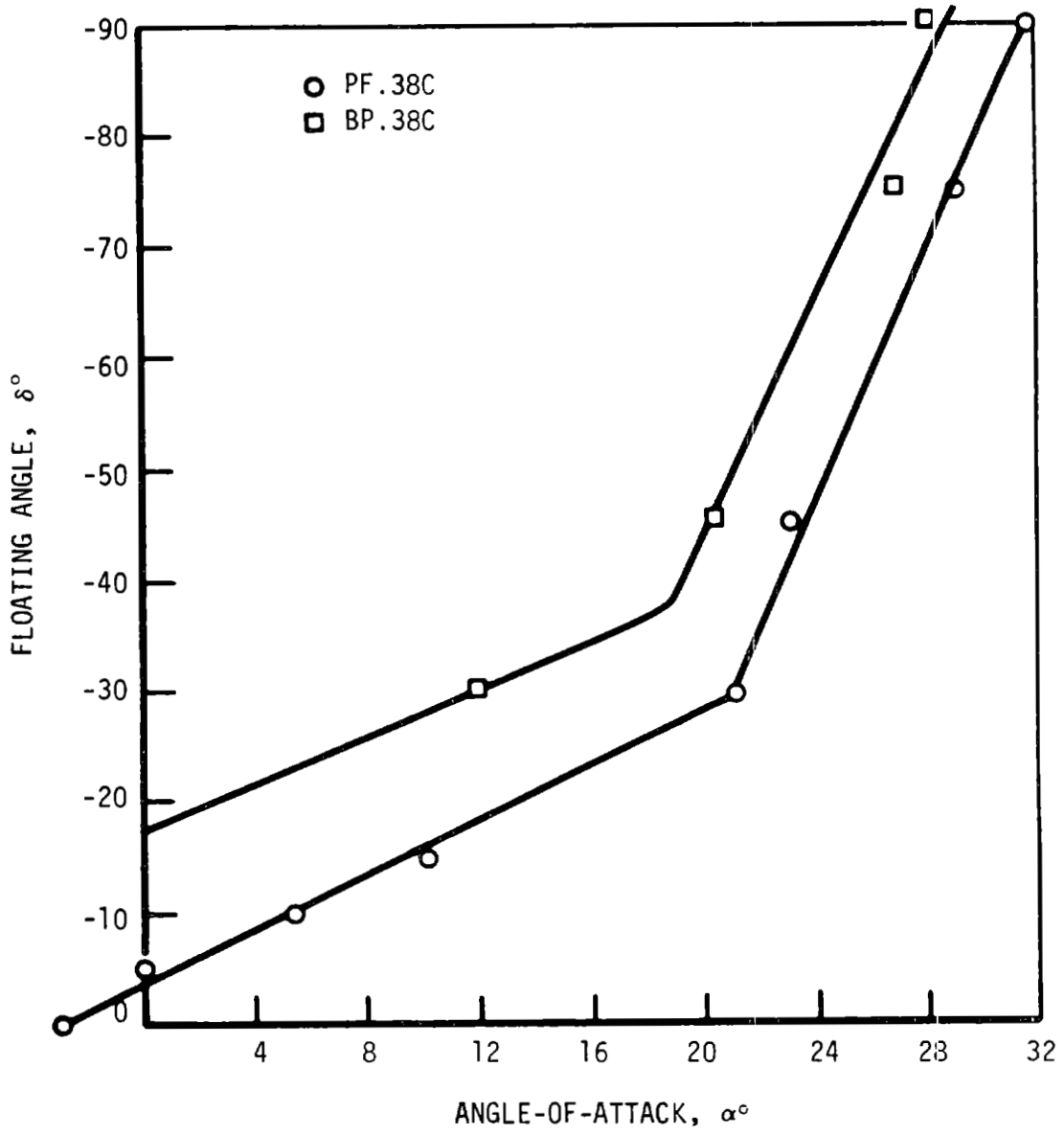

Figure 8-235 MOD-5A Aileron Floating Characteristic

8.4.3 MOD-0/5A AILERON PERFORMANCE TEST

8.4.3.1 General Comments

The MOD-0/5A aileron performance tests were performed on a wind turbine rated at 200 kW, with a 128 ft., aileron controlled rotor. These tests provided more data on the aerodynamic capability of the rotor. This data was used with the two-dimensional wind-tunnel data described in section 8.4.1, to provide further confidence in the models that predicted the performance of the prototype MOD-5A. This test provided larger-scale, three-dimensional data in a rotating field, and also demonstrated the effectiveness of the ailerons on NASA's MOD-0 wind turbine at Plum Brook. This aileron system was designed to validate the MOD-5A technolgy, so the test program was designated the MOD-0/5A aileron performance test.

The dimensions of the MOD-5A wind turbine and the MOD-0/5A test hardware are compared in Figure 8-236. The scale of the MOD-0/5A aileron test tips was 25% to 30% of the corresponding MOD-5A spanwise tip sections. Similar scaling was used for the overall MOD-0 rotor except, that test ailerons were 31% span (the prototype MOD-5A units were 40% span). Because the loads on the MOD-0 and rotor speed of the MOD-0 were limited, the maximum Reynold's number of the tip near the center of the aileron was approximately 2×10^6. The MOD-5A will operate at values approaching 20×10^6 at spanwise locations around the ailerons. The wind tunnel data, which included similar ranges of Reynold's number, was also used to interpret and extend the MOD-0/5A test results, to predict the MOD-5A performance. In addition, a "trip strip" along the leading edge of the test unit's leading edge generated turbulent boundary layer flow.

Although the Reynold's number and rotor sections inboard of the ailerons could not be duplicated, other operational parameters of the MOD-5A were simulated as closely as possible. The airfoil sections, twist and aspect ratio of the test tips, and the 38% chord aileron were designed to simulate, as nearly as possible, the MOD-5A blade. Tests were designed over a range of windspeeds, to duplicate the tip speed ratios and angles of attack of the MOD-5A at the MOD-0 rotor speed of 20 rpm on the MOD-0. Some reduced Reynold's number data was planned at lower rotor speeds. Autorotation data was planned at varying windspeeds up to 40 mph if wind permitted.

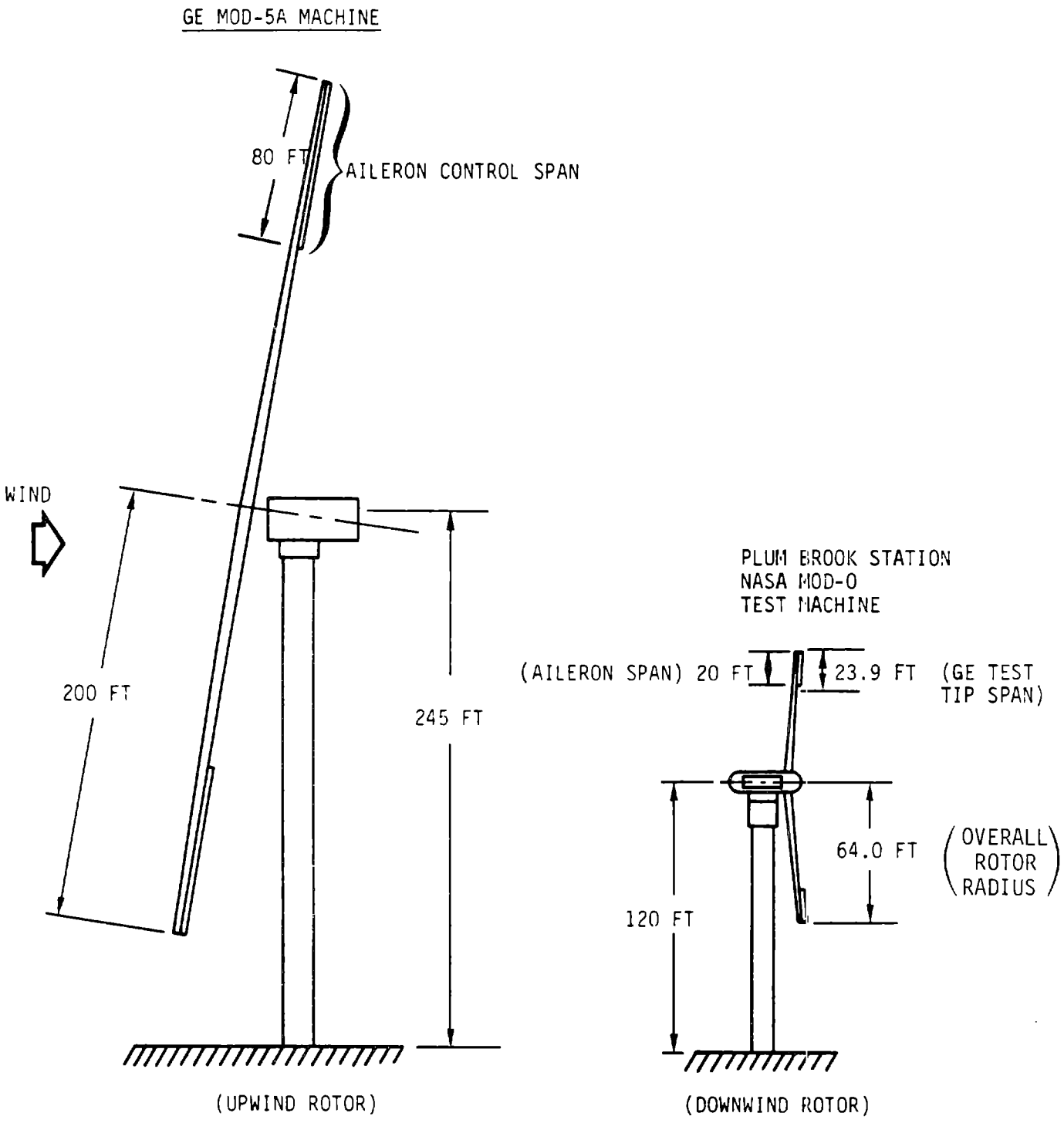

Figure 8-236 Comparison of Dimensions of the MOD-5A and MOD-0/5A Test Machine

C - 6

In order to expedite the design and fabrication of the hardware, and the acquisition of test data, the size, planform and interfaces of the test units closely resembled those used in NASA's previous aileron tests. The test units were designed and fabricated by Schweizer Aircraft Company in Elmira, New York. NASA's concepts and experience were used to define design loads, control system concepts, instrumentation techniques, and structural, hydraulic and electrical interfaces. The MOD-0/5A test units were designed, fabricated, proof-tested and put into operation at Plum Brook Station in only 16 weeks, despite some delay caused by weather during the installation. Preliminary data on aileron stopping performance, autorotation speeds, and power and speed regulation behavior were gathered for the MOD-0/5A aileron configuration before the end of 1983. Testing and data analyses continued into the second quarter of 1984, and indicated that the plain 38% chord aileron configuration would conservatively meet the requirements for aerodynamic rotor control. More detailed descriptions of the MOD-0/5A test, test hardware and results are presented in the following sections. The relevant documentation is listed in section 8.4.3.10.

8.4.3.2 Test Objectives

The objective of this three-dimensional aileron test was to provide data on the performance of the aileron and on its aerodynamic characteristics, for use in the decision to use the aileron controls on the MOD-5A wind turbine generator. (Data from the wind-tunnel tests was also used in this decision). The data was also used to demonstrate the ability of the aileron to control a wind turbine generator under realistic operating conditions.

The two general performance requirements for aerodynamic torque control of the rotor were:

1) The control system must generate enough negative torque to slow the rotor to a safe speed without damage to the rotor in controlled or emergency shutdowns. The aileron control system must also perform satisfactorily with one control surface damaged or mechanically malfunctioning.

2) The control system must provide characteristics of torque vs. control deflection that will provide stable control and regulation for a range of torque values, from at least 10% above rating to at least 10% negative torque, and over an appropriate range of rotor speeds and windspeeds.

The test also provided more basic data on performance characteristics, control characteristics and environmental performance characteristics, which could be correlated with models and predictions based on the wind tunnel data and other modelling analyses.

The MOD-0/5A aileron performance test had 6 specific requirements, to:

1) demonstrate the shutdown capability and overspeed behavior,
2) demonstrate acceptable autorotation equilibrium tip speed ratios (λ_E),
3) regulate power output,
4) regulate rotor speed,
5) evaluate basic aerodynamic parameters,
6) evaluate rotor sound levels.

8.4.3.3 Test Requirements and Success Criteria

The detailed definition of test requirements and success criteria were developed from the test objectives and the performance requirements of the prototype MOD-5A system. Some of the requirements were adjusted to account for differences in MOD-0/5A hardware geometry, size and Reynold's number.

The most significant adjustments were required in shutdown and autorotation parameters, because of the differences in the size of the aileron surfaces, planform differences, tip speeds, of the MOD-5A and MOD-0/5A hardware. Since the full-scale aileron comprises a larger part of the rotor span and area than the MOD-0/5A aileron, the former will be more effective than the latter. Allowable autorotation tip speed ratios for the Plum Brook test hardware were, therefore, estimated to be 50% higher than those specified for the MOD-5A.

The rotational inertia of the MOD-5A rotor is 243 times greater than that of the MOD-0/5A rotor. This factor is approximately offset by the higher aerodynamic loads and rotor torques of the full-scale machine, so that no large scaling factor was required for rotor acceleration-related parameters,

such as overspeed ratios and speed control variations. A small increase in required MOD-0/5A control deflections and rates are anticipated, to account for the difference in size of the aileron surfaces.

Note that some tests were limited to smaller ranges of test parameters or test conditions than originally considered, because of limitations on the test hardware, or weather or schedule constraints. The results from early tests were used to limit the number of configurations and test conditions to those that would meet all the major requirements.

For example, early testing indicated that the unvented, 38% chord, plain aileron would probably meet performance requirements for shutdown and autorotation at deflection angles of -90°, but might not perform as well at lower deflection angles, especially if the aileron were damaged. Therefore, the shutdown tests were limited to -90° deflections.

8.4.3.3.1 Shutdown Demonstration

Undamaged Rotor Shutdown -- With all MOD-5A aileron control surfaces operating, a loss of load shutdown must result in an overspeed of no more than 20% of maximum operating speed and reach an equilibrium tip speed ratio (λ_E = equilibrium rotor tip speed/windspeed) of no more than 1.5. MOD-0/5A control rates in the range from 35° to 10° per second were evaluated, to determine the rate necessary to meet the overspeed limit. Originally, control surface positions of -45°, -60°, -75°, and -95° were planned for evaluation to determine the position necessary to meet the velocity ratio limit. Test wind speeds were selected in three ranges: low ($6 < \lambda$), moderate ($4 < \lambda < 6$), and high ($\lambda < 4$), where λ is the ratio of initial rotor tip speed to windspeed. Three values of initial electrical load, between 0 and 100% of the MOD-0 machine rating, were used.

Normal, controlled shutdowns were planned at low and moderate winds, in which the electrical load was reduced to zero at a controlled rate, and the aileron deployment rate was 5° per second. However, these tests were deleted since the Plum Brook machine utilizes a grid-connected asynchronous generator, with which load cannot be easily reduced, unlike the MOD-5A's variable speed generator.

In defining acceptance criteria for the MOD-0/5A test results, the test hardware performance was scaled to that of the MOD-5A. Adjustments in acceptable values for MOD-0/5A parameters, to account for hardware differences, were incorporated in the following definitions of success criteria for the test.

Acceptance Criteria for MOD-0/5A

a) Overspeed for emergency shutdown of less than 4 rpm at 20 rpm initially for windspeeds between 10 and 20 mph, i.e. 20% of 20 rpm.

b) Stable control characteristics for normal shutdowns

c) Equilibrium rotor speed less than 0.50*windspeed (λ=4.58 N/V_W and λ_E=2.3, where N=rotor speed in rpm and V_W=windspeed in mph) for windspeeds from 15 to 30 mph

Data

a) Standard measurement set, defined in Section 8.4.3.5
b) Minimum aileron deployment rate athat meets overspeed requirement
c) Minimum aileron deployment angle that meets λ_E requirement

Partial Damage Shutdown -- With a minimum of 20% of the effective MOD-5A aileron control surface undeployed in a jammed or damaged condition, a loss of load shutdown must result in an overspeed of no more than 20% of maximum operating speed and must reach an equilibrium velocity ratio of no more than 2.0. Sufficient MOD-0/5A control rates, final control positions, wind speeds, and initial load configurations are selected from values in the previous test to demonstrate by test and analysis the overspeed and equilibrium requirements. The MOD-0/5A performance compatible with the MOD-5A requirements listed above is:

Acceptance Criteria for MOD-0/5A

a) Overspeed for emergency shutdown of less than 4 rpm (20% of 20 rpm) for windspeeds between 10 and 20 mph

b) Stable control characteristics for normal shutdowns

c) Equilibrium rotor speed less than 0.66 * V_W (λ_E=<3.0) for windspeeds from 15 to 30 mph

Data

a) Standard measurement set
b) Aileron deployment rate required with damaged aileron
c) Aileron deployment angle required with damaged aileron

8.4.3.3.2 Stable Regulation Control Demonstration

Speed Regulation -- The MOD-5A rotor speed must be stable and within ±5% of the maximum operating speed around the reference speed. A speed regulating, feedback control loop, with proportional and integral capability, will be used with stable gain settings that use the aileron surface position as the final control element. Full-scale control rate limits of 2° and 5° per second will be simulated by the MOD-0/5A system. Wind speed ranges will be selected from the values required for the basic shutdown tests, to demonstrate the regulation band.

Acceptance Criteria for MOD-0/5A

a) Stable behavior
b) Speed regulation within ±1 rpm (±5% of 20 rpm)

Data

a) Standard measurement set
b) Control rate that meets regulation requirement

Power Regulation -- No control requirement is specified directly on power regulation performance for the MOD-5A. To ensure safe and reliable operation during the test and to demonstrate the ability of the MOD-0/5A aileron to regulate power, MOD-0/5A output power must be stable and within ±20 kW around the reference power when in an active regulating mode. A power regulating feedback control loop with proportional and integral capability will be used with stable gain settings that use the aileron surface position as the final control element. Full-scale control rate limits of 2° and 5° per second will be simulated by the MOD-0/5A system. Sufficient wind speed ranges will be selected from the values required for the basic shutdown tests, to demonstrate the regulation band. Reference power values will be selected to force operation in an active regulating mode for each wind speed range.

Acceptance Criteria for MOD-0/5A

a) Stable behavior
b) Power regulation within ± 20 kW of selected power set points.

Data

a) Standard measurement set
b) Aileron deployment rate that meets regulation requirement

8.4.3.3.3 Sound Level Demonstration

Average sound levels (A-scale weighted) must be no more than 3dBA higher than comparable measurements on a tip-controlled, similarly configured MOD-0. Similarly, noise increments above the zero deflection case caused by aileron deflections required for control must be no more than 3 dB higher than noise caused by deflection of PSC tips for control under similar conditions. Measurements will be recorded at 120-150 ft, and 800-1000 ft or the limit of audibility, and downwind, and in the plane of the rotor. Reliable far-field predictions based on near-field source level measurements and standard acoustic propagation prediction techniques are acceptable. Data will be acquired on rotor positions and control deflection coincident with sound measurements, and analysis will differentiate the effect of tower shadow and control deflection. Broad band measurements from 5 to 20,000 Hz will be recorded to create a data base for spectral analysis.

Acceptance Criteria for MOD-0/5A

a) Average sound must be less than 3dBA above tip-controlled configuration in power control and speed control modes

b) Incremental noise caused by aileron control deflections must be no more than 3 dB above similar PSC control noise increments

c) Acquisition of basic sound level data on MOD-0/5A configuration

Data

a) Standard measurement set, and sound instrumentation
b) Sound recordings in various winds in speed control
c) Sound recordings in various winds in power control
d) Sound recordings in various winds during selected shutdowns
e) Spectral narrow band and 1/3 octave analysis of items b) through d) for representative conditions
f) Qualitative assessment of sound by experienced site operators

8.4.3.3.4 Secondary Effect Demonstration

Stability -- The test unit must show no aerodynamic instability during any speed control, power control, shutdown, or startup operating mode. Aileron hinge line mass balancing may be used to avoid instability.

Acceptance Criteria for MOD-0/5A

a) No aerodynamic instability, indicated by control position or strain measurements

Data

a) Standard measurement set
b) Mass balance weight and location, if any

Aileron Self-Deployment -- The test aileron will deploy when control power is lost. Aerodynamic, centrifugal, or stored energy forces cause smooth, stable motion. This motion may be demonstrated by analysis.

Acceptance Criteria for MOD-0/5A

a) Aileron self-deploys to full deflection when the rotor is not rotating and control power is removed.

b) Aerodynamic and centrifugal forces must be sufficient to drive aileron to approximately 60° or greater deployment. (This criteria may be demonstrated by analysis of measured hinge moments.)

c) Aileron hinge torque or control rod strain versus position at test rotor speeds must produce aerodynamic forces that drive the aileron toward deployment angles required to decelerate the rotor.

Data

a) Standard measurement set

The data and measurements required to quantitatively evaluate the aileron's performance are described in Section 8.4.3.5. This evaluation will determine if an aileron configuration performs acceptably, according to the acceptance criteria.

8.4.3.4 Test Description

Mod-0/5A aileron tests were performed at NASA's Plum Brook Station, in Sandusky, Ohio, from December, 1983 through June, 1984. The tests used NASA's MOD-0 wind turbine test facility and data system. The GE test units, with 38% chord aileron and 64XXX airfoil sections, were installed at the outer ends of the 40 ft. stub inboard blades, as shown in Figure 8-237. The GE tips were aluminum, of aircraft-type construction, 23.9 ft. long and attached to the NASA stub blade ends at station 481 (in). The rotor diameter was 127.9 ft. All hydraulic and electrical lines interfaced with the facility connections through the mating station 481 rib. The tip was mechanically attached by high strength, steel studs .5 in. in diameter. Some dimensions of the rotor are shown in Figure 8-237.

In order to meet the objectives and requirements defined in earlier sections, tests were conducted over a range of wind speeds, between5 mph and more than 35 mph. Data was taken with the plain and the balanced aileron configurations, over a range of aileron deflections, between 0° and approximately -90°. Data was taken with the aileron deflection fixed and with the aileron deflection controlled by the servo system. Data was taken at a selected fixed rotor speed of 20 rpm, and also at lower rotor speeds for autorotation data, speed control data, and shutdown data. Autorotation and shutdown data was taken both with single and double-tip operation to compare undamaged and simulated damaged rotor performance.

During test operations, measurements of various test parameters were made from sets of sensors located at various positions on the tips, on meteorological towers surrounding the site and inside the hub and nacelle. A list of measurement parameters is discussed in a later paragraph. The data was encoded by the standard NASA wind turbine generator data system and transmitted to the control room, where it was processed and recorded on strip charts, digital magnetic tape and FM analog magnetic tape. The on-site monitors evaluated strip chart displays and performed some data manipulation on a Hewlett-Packard HP-85 computer.

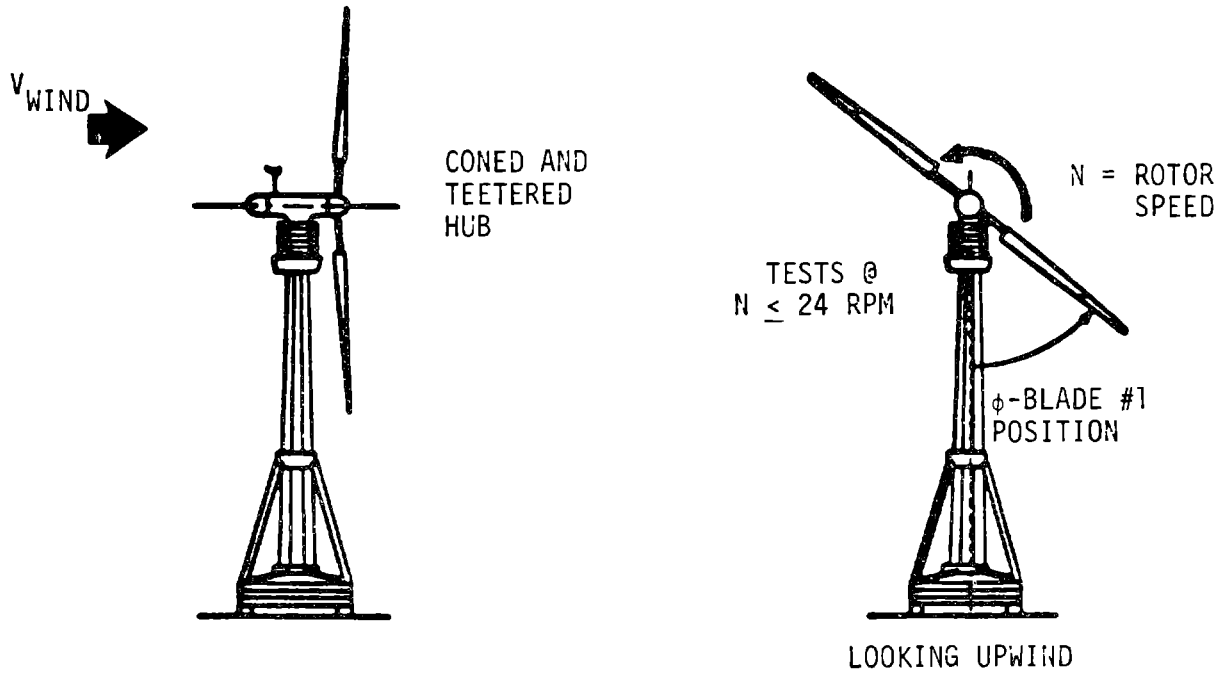

A) NASA'S MOD-0 TEST WIND TURBINE AT THE PLUM BROOK STATION

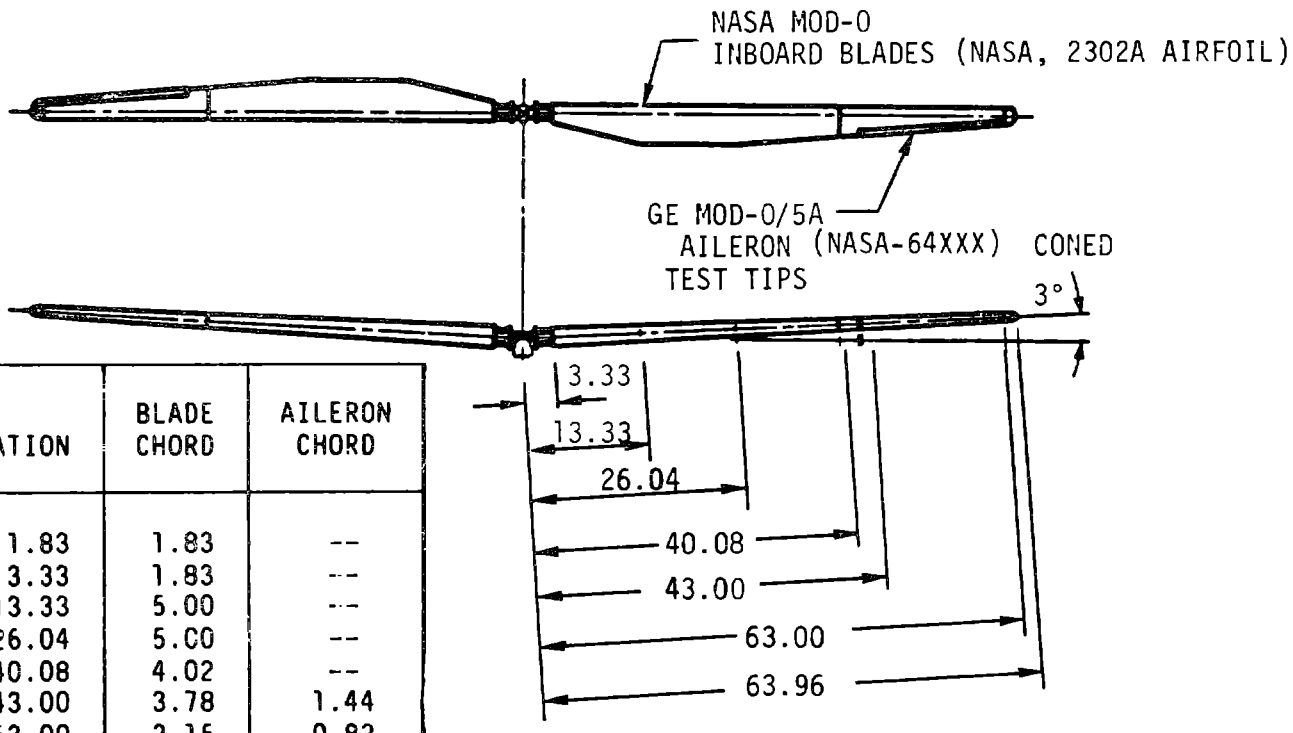

STATION	BLADE CHORD	AILERON CHORD
1.83	1.83	--
3.33	1.83	--
13.33	5.00	--
26.04	5.00	--
40.08	4.02	--
43.00	3.78	1.44
63.00	2.15	0.82
63.96	0.00	--

(ALL DIMENSIONS IN FEET)

B) G.E. MOD-0/5A TEST UNITS AS INSTALLED ON THE NASA MOD-0 WTG

Figure 8-237 MOD-0/5A Test Rotor Arrangement

Post-test data reduction and analysis at NASA's LeRC computer facility in Cleveland, Ohio, used the digital tape, NASA's standard data processing program, and NASA's modified processing program. Shutdown data were reduced by NASA from HP-85 outputs. The reduced data was transmitted to GE on tape, microfiche and in graphic form for the final evaluation and analysis. The analysis results were used in the MOD-5A aileron performance evaluation and prediction program.

More detailed descriptions of the hardware, data measurements and sensors, test operations and on-site evaluations are given in the following paragraphs. Details of post-test processing and final results are presented in sections 8.4.3.7, 8.4.3.8, and 8.4.3.9. NASA's final data analysis report will be published later.

8.4.3.4.1 Description of Test Units and Design Criteria

The test units consist of two aileron-equipped tip sections attached to the outer ends of NASA's 40-ft. wooden stub blades on the MOD-0. The configuration of the test unit can be changed in the air, between plain, balanced, damaged and undamaged configurations. The configurations can also be further modified by removing the aileron surfaces from the rotor for changes on the ground. The test unit's size, planform and actuation system are similar to those of the aileron test units used in earlier experiments on the MOD-0. The basic airfoil section, however, is the NACA 64XXX, which is also used on the GE MOD-5A rotor.

Two basic, unvented aileron configurations were available for test: the plain and the balanced aileron.

Both could be converted to vented configurations in the field, so that four configurations could be evaluated in the MOD-0/5A tests, depending on results of the wind-tunnel test program and the early MOD-0/5A test results. All configurations are hinged at 62% chord on the low pressure side of the airfoil. Balanced aileron configurations extend to the 50% chordline on the high pressure side of the airfoil. All the configurations contained several spanwise aileron sections per blade, so that a jammed control condition or shorter aileron configurations could also be simulated.

Geometric Definition -- GE provided the geometric definition of the test unit. The layout of the test unit, showing the planform and general arrangement of the aileron is shown in Figure 8-238. The planform was the same as that of NASA's aileron control tips, except that the shape at the end of the unit is a scaled-down version of the MOD-5A tip shape. A different spanwise thickness distribution and a twist distribution were incorporated, to better simulate the MOD-5A rotor. The unvented, plain aileron configuration shown in Figure 8-238 illustrates the arrangement of the control actuation system, the hinge line location, and the method of spanwise segmenting of the aileron. The aileron segments can be locked together in the combinations shown on Figure 8-238, to test various spanwise distributions of aileron surface and various damaged conditions. The aileron's deflection range is between 0° for full power, and -90° for full deployment.

A more detailed definition of the aileron test configurations is given in Figures 8-239, -240 and -241. Details of the basic plain aileron are shown in Figure 8-239. This configuration is a typical, unslotted, unvented, 38% chord, trailing edge aileron, hinged at the 62% chord line. The details of the basic balanced aileron and the technique for converting from the plain aileron are shown in Figure 8-240. The balanced configuration consists of a plain aileron at the 38% chord on the low pressure side, augmented by a "spoiler" lip at the 50% chord, which extends from the high pressure side of the airfoil when the aileron is deflected. The entire balanced aileron is hinged at the 62% chord line on the low pressure side of the blade. Figure 8-241 shows the concept for converting the plain aileron to a vented aileron at the site. A similar conversion is available for the balanced aileron. In both cases, the basic ailerons are easily converted to the vented configurations shown in Figure 8-241, by installing doubler plates and drilling vent holes. The amount of venting can be varied by sealing some of the vent holes with tape. Once the aileron has been converted to the vented configuration, it cannot resume the basic configuration. A return to the unvented configuration could be approximated by taping over all vent holes.

POSSIBLE AILERON SEGMENT COMBINATIONS

	AILERON SEGMENT VARIABLE AS UNIT	AILERON SEGMENTS LOCKED FIXED & AS A UNIT
1)	ALL (1-6)	--
2)	1, 2, 3	4, 5, 6
3)	4, 5, 6	1, 2, 3
4)	1, 2	3, 4, 5, 6
5)	3, 4, 5, 6	1, 2

(NOTE: HYDRAULIC TRAVEL @ 6 = 100° MAX)

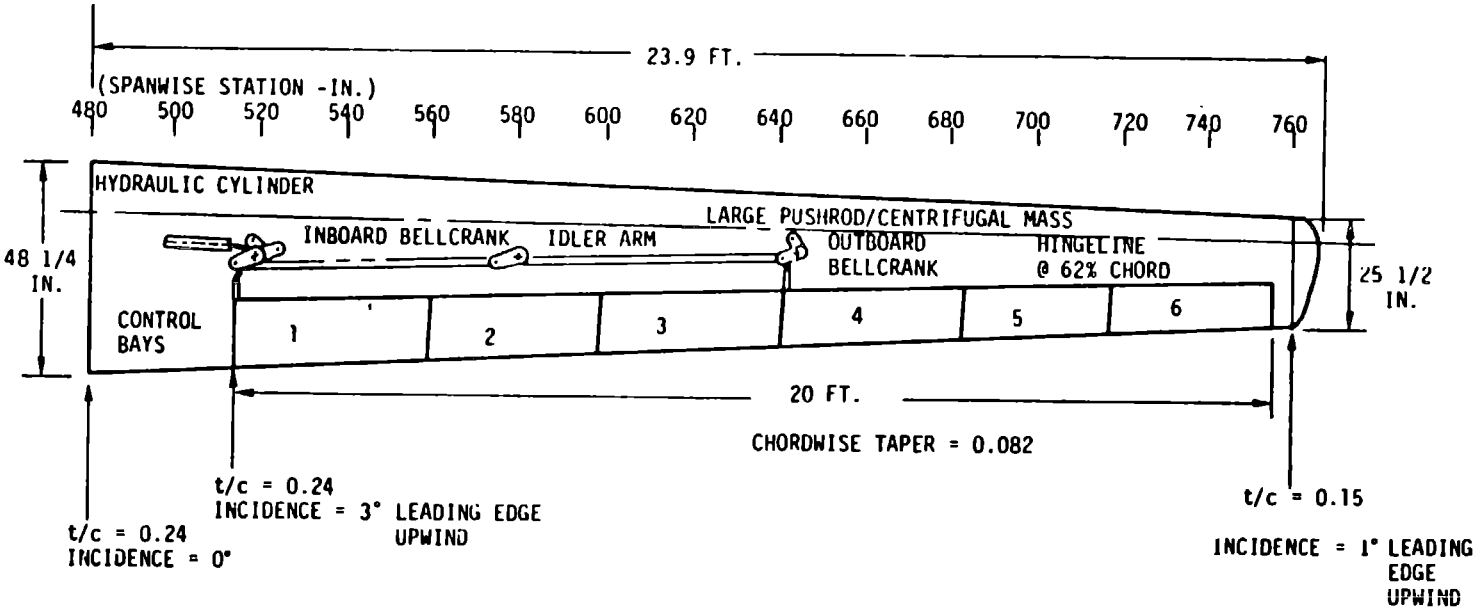

Figure 8-238 General Arrangement of the Test Unit and Control System

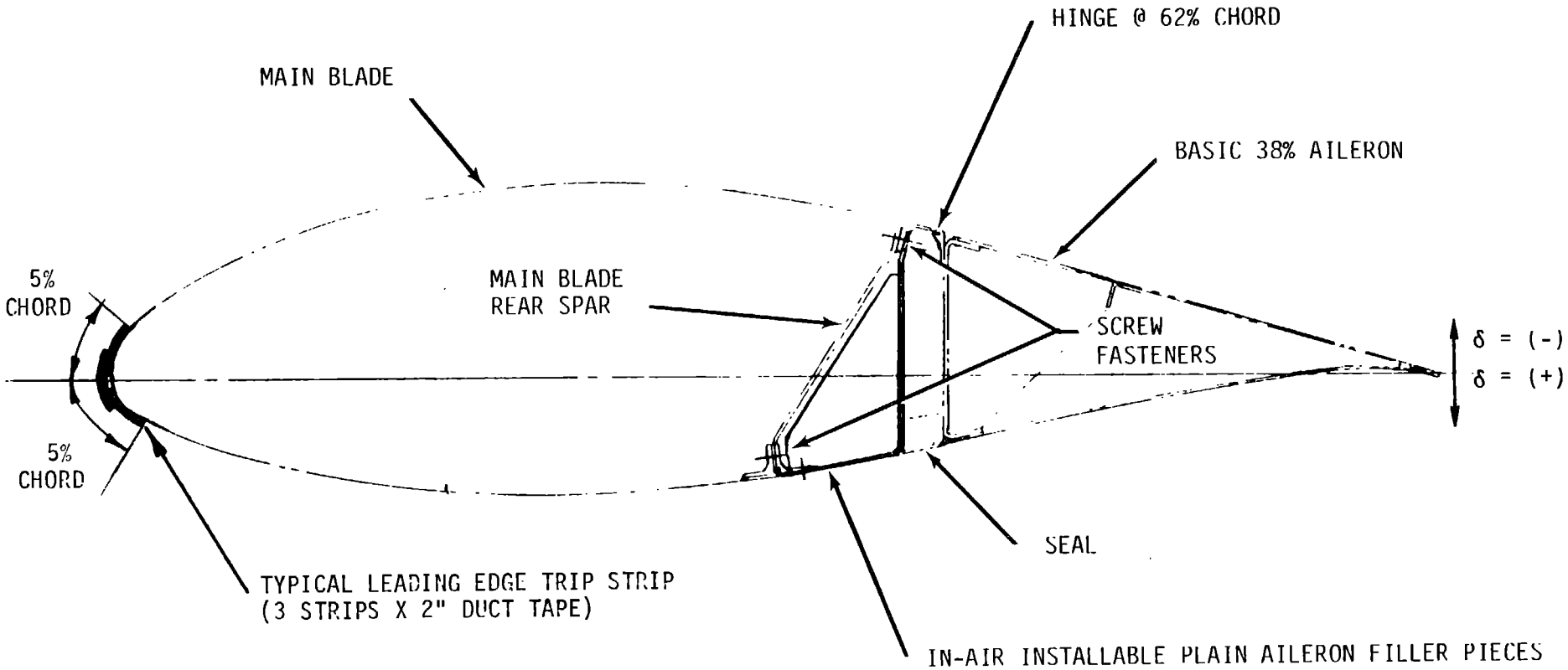

NOTES: - MAXIMUM DEFLECTIONS: $\delta = +10^{0}$ TO $\delta = -105^{0}$
- FILLER PIECES (6 PER BLADE) ARE REMOVED/INSTALLED WITH AILERON DEFLECTED, $\delta = -90^{0}$

Figure 8-239 Plain Aileron Configuration

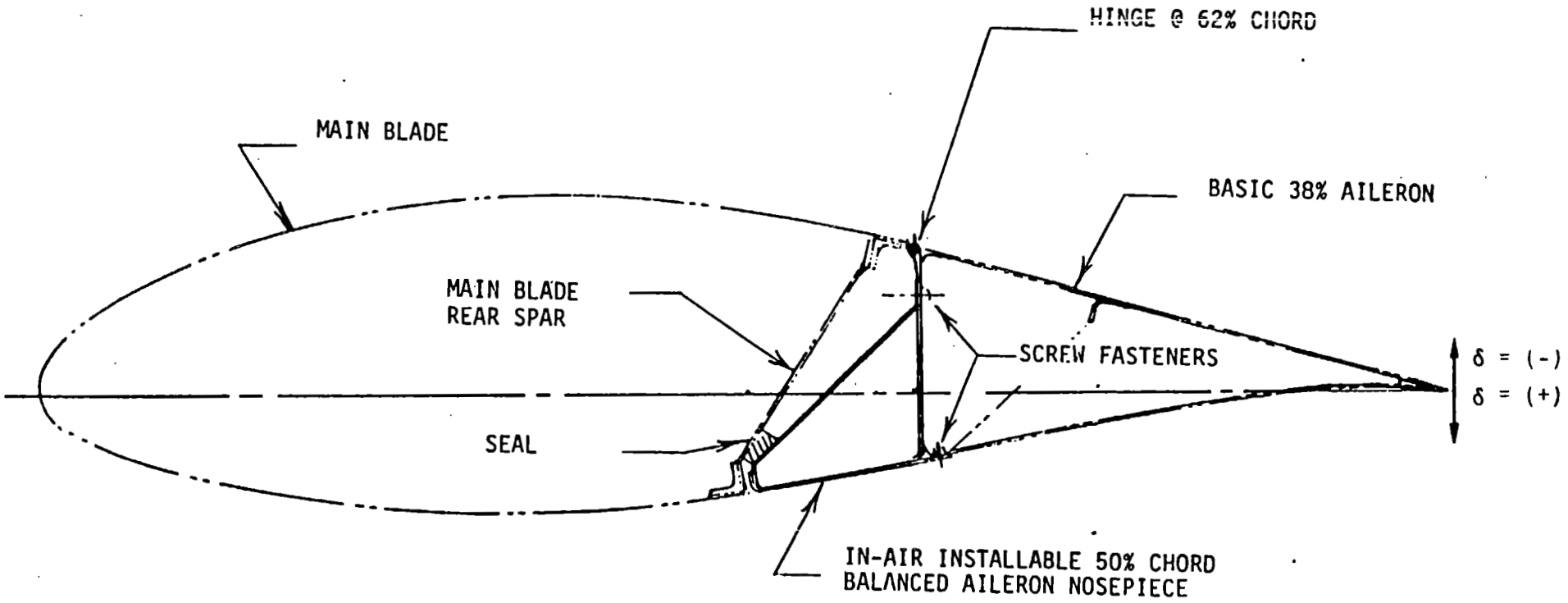

NOTES: - MAXIMUM DEFLECTIONS: $\delta = +10^{o}$ TO $\delta = -105^{o}$
- NOSE PIECES (6 PER BLADE) INSTALLED WITH AILERON $\delta = -90^{o}$ AFTER REMOVAL OF PLAIN AILERON FILLER PIECES (FIGURE 8.4.3-4)

Figure 8-240 Balanced Aileron Configuration

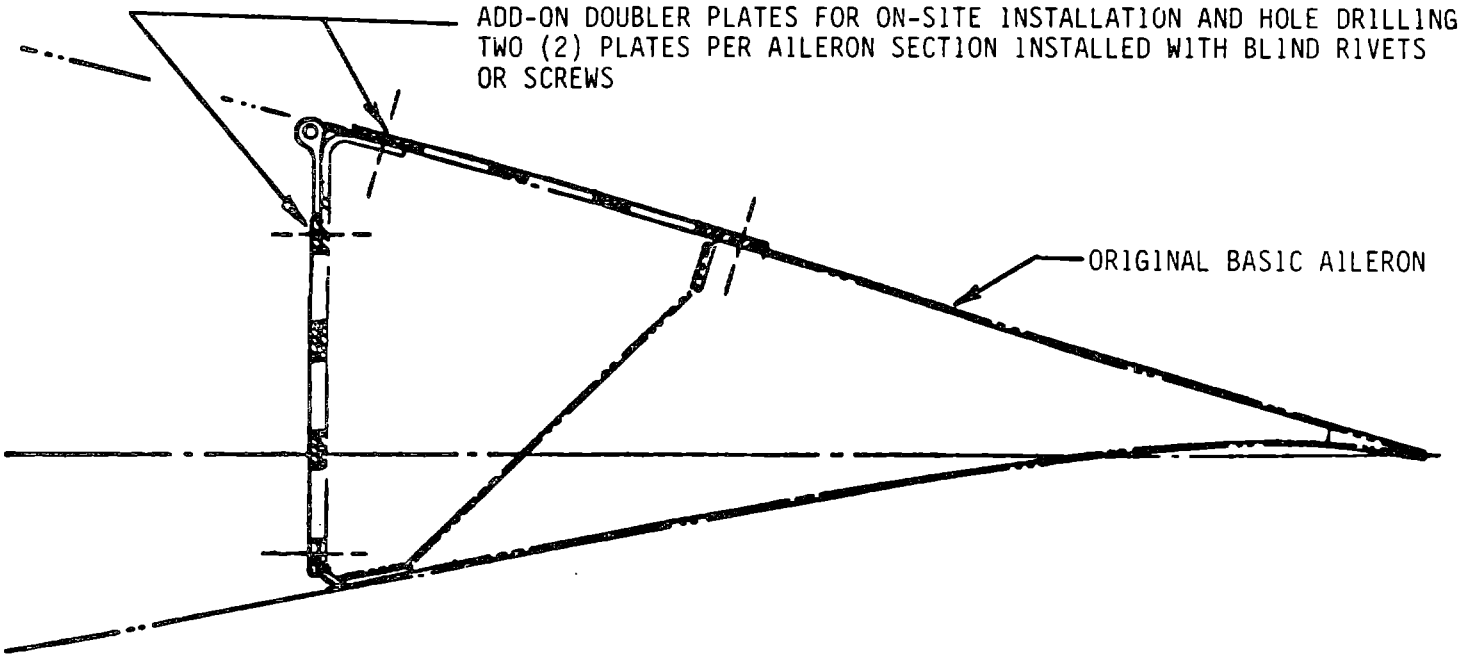

NOTE: SKETCH SHOWS PLAIN AILERON. CONVERSION OF BALANCED CONFIGURATION IS SIMILAR. AILERON SECTIONS TO BE REMOVED FROM BLADE FOR ON-GROUND CONVERSION TO VENTED CONFIGURATION.

Figure 8-241 Field Conversion Concept for Ventilation of Basic Ailerons

Design Criteria -- Details of the design criteria are given in ref 1. The main blade structure was designed for a margin of approximately 1.5, based on material yield strength and maximum design loads. Maximum design loads were based on either the one-time hurricane condition, of 140 mph wind broadside to the planform, which defined the worst case of flapwise bending loads, or the maximum predicted low-cycle operating loads based on a combination of theoretical analysis and loads experience, which defined the worst case of chordwise bending conditions. Although the maximum MOD-0/5A rotor speeds were to be approximately 20 rpm, the loads analysis conservatively assumed 30 rpm, where necessary. The aileron, hinges and actuation system components were designed for a maximum load, assuming that the full 140 mph hurricane wind would be perpendicular to the full aileron planform area, regardless of stowed control deflection angle, as a worst case. The maximum flapwise tip deflection of the test unit under maximum design limit load was restricted to 12 in.

No fatigue life value was specified for the design, but it was specified that good fatigue design practice be employed for a goal of 10^6 cycles. High cycle fatigue loads were also estimated for guidance in development of the design. Schweizer Aircraft performed a stress analysis to calculate the maximum limit loads, low cycle loads and high cycle loads for the various critical structural components and predicted design margins for the three load cases. Proof tests were conducted by Schweizer to verify the acceptability of the hardware.

The GE test units were designed to be compatible with, and to mate directly with, MOD-0 machine interfaces:

- o Mechanical - Studs on the end of the 40 ft. stub blade
- o Hydraulic - 1,500 psi is the maximum actuation pressure requirement (3,000 psi is the maximum system design pressure)
- o Electrical - 110 VAC power, compatible instrumentation and sensor systems.

In order to avoid potential problems caused by the use of unproven components in the rotational environment, this test used the same hydraulic components, electrical connectors and strain-gages that had been used on earlier NASA aileron tips. A different mechanical dual bellcrank system was used, however, because the ailerons were segmented. The long pushrod between the bellcranks, shown in Figure 8-238 also serves as a centrifugal weight to drive the aileron 60° toward full deployment if hydraulic control power is lost. A mechanical system for locking the aileron at full deployment was used, rather than the pneumatic brake system used in the earlier tips. Except for the solenoid-operated, mechanical locks, which required installation of two additional electrical switches, the actuation and data systems of the GE test units were fully compatible with the systems in NASA's facility.

Design and Construction -- A detailed set of hardware performance requirements and interface specifications for the test unit were developed by GE, in ref. 1. The detailed design and the fabrication of the test unit, based on these specifications and requirements, was the responsibility of the subcontractor, Schweizer Aircraft Corp. GE provided technical direction and design approval. Schweizer Aircraft also documented, in Schweizer Aircraft company reports, the stress analyses, structural and operational proof-test data, and flutter parameters which are required by NASA's safety guidelines. GE and NASA assisted in the proof testing that verified the design.

The test units were standard aircraft construction, using an aluminum main box-beam spar with a lighter rear spar, aluminum ribs, and aluminum skins. The ailerons were made with aluminum ribs and skin with an internal web for additional torsional stiffness and strength. The ailerons were attached to the main blade with piano-type hinge segments. Sufficient clearance between the aileron segments and between the hinge segments prevents binding of the ailerons and actuation mechanism under maximum operating loads over the range of operating aileron deflections. The structural components in critical areas were assembled with rivets or light drive-fit bolts or screws. In the areas

where added fatigue life was of concern, components were also bonded with epoxy, to almost double the required design margins. The end tips were made of molded glass fiber to accommodate the complex, double-curved surfaces.

The test unit was attached to the inboard blade studs with a massive root-end fitting, which was machined from a solid block of 7075-T651 aluminum. This fitting was attached to the inboard end of the main spar webs with steel bolts and epoxy. All mating pieces, slots, and bolt holes were precision machined and checked to ensure a hole-filling bolt fit.

The aileron is composed of six segments and is hinged at the 62% chordline on the low-pressure side of the blade. Structural and hinge clearance allows the aileron to move from 10° toward the high pressure side to approximately -105° toward the low pressure side. The aileron is activated by a single hydraulic cylinder driving through a dual bellcrank system, as shown in Figure 8-238. The large pushrod between the two bellcranks transfers cylinder control forces to the outboard bellcrank, and acts as a rotating mass that provides sufficient centrifugal force to drive the aileron to the -60° deployment position if the hydraulic power fails. Flutter characteristics and required control system stiffness for the aileron and blade combination were calculated by GE. Provision was included in the aileron design for approximately 40% mass balance.

The hydraulic control system is diagrammed in ref. 2. The system provides several operational features:

- Standard servo control through the ABEX valve.
- Emergency full-deployment loop that bypasses the servovalve in the event of an electrical failure or emergency-stop command.
- Bypass test loop that removes the hydraulic system from the aileron system to check free-floating and flutter characteristics of the aileron. This loop is provided with a flow-control valve to control rates, damping or both.
- A hydraulic energy storage capacity in an accumulator.

The position of the aileron is sensed by a Durapot transducer that measures the position of the inboard bellcrank.

A solenoid-operated, mechanical lock at the inboard bellcrank location locks the aileron in the maximum deployment position when the rotor is not operating. The lock is engaged when power is shut off and the aileron is deflected to -90 degrees. The lock is disengaged by energizing the solenoid.

Interferences in the filler-piece seals, shown in Figure 8-239, and the actuation mechanism components limit plain aileron travel to 0° to approximately -89°. The range can be changed by adjusting the hydraulic cylinder rod-end fitting and the bellcrank-to-aileron pushrods, and modifying the foam seals.

Tip Instrumentation -- The tip was instrumented to provide data on flapwise and chordwise bending moments, aileron pushrod loads, and aileron deflection angle.

All bending moment and load measurements were implemented by 4-element strain-gage bridges similar to those employed for similar measurements on NASA's aileron tips. 350 Ω strain gages with 10V bridge excitation were compatible with the MOD-0 data multiplexing and transmission system. Bending moments or axial loads were measured at the following locations in the GE test units:

- Flapwise bending - Station 489.5 in., gages mounted on main spar webs.
- Inboard chordwise bending - Station 489.5 in., gages mounted on main spar webs.
- Outboard chordwise bending - Station 524.0 in., gages mounted on inside surfaces of leading edge skin and rear spar.
- Inboard aileron pushrod load - Station 516.0 in., gages mounted on pushrod circumference.
- Outboard aileron pushrod load - Station 642 in., gages mounted on pushrod circumference.

In all locations, two sets of strain gages were installed for 100% gage redundancy. Signal cable limitations, however, did not permit the back-up bridge signals to be telemetered to the control room, except in the flapwise bending case. All strain gage bridges were calibrated as part of the

Schweizer proof-test program. Some discrepancies have been found in the original calibration data. Final calibration values are noted in NASA's final data analysis, which has not yet been published.

A Durapot angular position transducer measured aileron deflection. The transducer reads deflection values through a linkage operated off the inboard bellcrank. The deflection angle transducers were calibrated at Plum Brook after the GE test units were installed on the MOD-0 rotor as part of the pre-test check and system verification procedures. Some nonlinearity, a maximum of about 4° from linear response, was found during these calibrations, probably caused by the drive linkage in the test units. This problem can be corrected in reduced data if required, since actual calibration curves are available. The transducer also supplies control signals for the servo-controlled power and speed regulation modes of operation. No effect of this sensor nonlinearity was expected or noted in the regulation performance data.

Other electrical cabling in the test unit provides power and control signals for the hydraulic control valves and the mechanical latches.

8.4.3.4.2 Summary of Proof Tests

A full set of proof tests and gage calibrations were conducted at the Schweizer Aircraft Plant before the test units were delivered to Plum Brook.

The tests were divided into four parts: 1.) proof test main structural members to design limit loads, 2.) proof test aileron and drive system operation to maximum operational loads, 3.) proof test hydraulic components to specified pressure levels, and 4.) calibrate all strain gage bridges under known loading conditions.

Limit Load Structural Proof Test -- The two test units were subjected to positive and negative flapwise and chordwise loads that exceeded the design limit loads by 2% to 4%. Maximum flapwise and chordwise limit loads were applied independently, since the combined maximum load was too conservative.

Tne deflections at various locations were measured, and skins were examined for buckling under the maximum loads. These tests were conducted before the aileron sections were installed, but all other structural skin sections were in place. Maximum flapwise and chordwise tip deflections under the maximum test loads were 9.25 in. and 4.25 in., respectively. No significant buckling or permanent deformation was noted in any of these tests.

Aileron Operational Proof Test -- One test unit was subjected to maximum predicted operational loads with the aileron near 0° and the other unit was subjected to similar conditions at -90°. In this case, both the main blade and the aileron were loaded with a distribution of loads simulating the maximum chordwise and flapwise loads anticipated for the two operating conditions. The aileron was moved about 10° under the loaded conditions to verify that no binding, or component deformation, would prevent effective operation of the aileron system. No evidence of binding or other problems was noted in either loading case. Structural deformations were monitored to determine the amount of aileron roll-up under load and to verify that the aileron components would not be deformed or buckled permanently. Roll-ups of approximately 0.5° were noted over both the three inboard sections operated by the inboard bellcrank and the three outboard sections operated by the outboard bellcrank. No buckling or permanent deflection was noted.

Hydraulic Pressure Proof Test -- The entire hydraulic system in each tip was proofed by pressurizing it to 4,500 psi, 1.5 times the maximum design operating pressure of the MOD-0 hydraulic system. No failures were noted in any parts of the system, except in a flex-hose end, which was repaired and retested.

Strain Gage Calibrations -- All bending strain gage bridges were calibrated during the structural proof tests. Bridge outputs were monitored and recorded for various steps in the loading schedule to obtain output voltage vs. root bending moment for each of the bridges. During this calibration, the

sensitivity of flapwise bending bridges to chordwise bending, and vice versa, was assessed. It is questionable, however, whether orthogonality of loading directions could be maintained with sufficient accuracy with the proof test loading techniques employed to acquire meaningful crosstalk values, especially for the application of chordwise loadings. Subsequent crosstalk checks with the blades installed on the MOD-0 machine, and calibration data acquired on a third MOD-0/5A blade in NASA's more accurate proof test loading facility indicated that actual values of crosstalk are, in general, much lower than those originally estimated from the Schweizer calibrations.

The aileron pushrod strain-gage bridges were calibrated over the full range of tension and compression values predicted from operational control force estimates. These calibrations were done independently of the bending gage calibrations using separate tensile and compressive test equipment to calibrate each of the pushrods.

8.4.3.5 MOD-0/5A - Plum Brook Facility Interfaces and Checks

Interfaces - Specifications for mating GE's aileron test units to the MOD-0 rotor at Plum Brook were defined by NASA and GE This information is included in ref. 1 and describes the following interfaces:

1. Mechanical interfaces mate with the existing stud pattern on the tips of the stub blades, and match the external airfoil contour of the inboard blade at the interface station, station 481.

2. Hydraulic interfaces mate to supply and return lines at an accessible chordwise location with AN flare connections of the proper size.

3. Electrical interfaces mate the following:
   - 110 Vac supply connections, for operation of controls.
   - Instrumentation connections that interface with servocontrol system signal lines and instrumentation system data lines for strain gages and angle transducer.
   - Interface connection for lightning-strike protection cable.

All these interfaces are accessible for adjustments, repairs, and changes, through removable skins or access hatches in the control bay of the blade.

Pretest Check -- GE's aileron test units were delivered to Plum Brook on 29 Nov. 1983. Both units were subjected to a complete set of system operability checks before they were installed on the MOD-0 rotor. Hydraulic and electrical systems were mated with NASA's test equipment and all control system functions were verified. During this process, it was discovered that the deflection angle transducers were not wired properly for interface with the Plum Brook data system. The Durapot tranducers were rewired and calibrated to verify proper operation. A faulty hydraulic solenoid valve was also replaced during these checks and flow control values in the emergency-feather and bypass loops set for the desired deflection rates.

During this preparation an additional foam seal strip was added to each test unit, to provide better aerodynamic fairing of the high pressure surface with the aileron at 0° deflection. A multi-layered tape "trip strip" was installed along the entire leading edge of each test unit, as shown in Figure 8-239, to help assure turbulent boundary layer flow over the test units, to simulate MOD-5A conditions at the low Reynold's numbers of the MOD-0/5A test.

The test units were installed on the MOD-0 rotor blades and connected to operational hydraulic, electrical and data systems. A series of checks was made to be sure that all systems operated when interfaced with the MOD-0 rotor, nacelle and control room systems. A final deflection-angle transducer calibration was made and the operability and positive or negative sense of all strain gage bridges were determined with the tips attached to the rotor. Then the rotor and nacelle system was lifted to the top of the tower.

The lift and installation on the tower were completed on 13 Dec. 1983. The system was checked and initial data was gathered according to the original GE test matrix the following day. Preliminary data and pretest predictions were used to set up and check data channel and recorder sensitivities during this period. All sensors and data lines from the test units operated properly during these preliminary tests.

Data System and Measurement Parameters -- The MOD-0/5A test used NASA's standard Plum Brook MOD-0 data acquisition system. Table 8-100 lists the parameters that were measured and recorded in the standard data set. The data was multiplexed and transmitted from the nacelle or other sources to the control room, where it was recorded and processed by the following means:

1. Real-time readout on four 8-channel strip charts after demultiplexing.
2. Recorded FM mode on magnetic tape in the composite multiplexed format.
3. Recorded on digital tape after demultiplexing, once-per-revolution sampling and digitizing.
4. Demultiplexed and selectively input to the HP-85 for real-time and near real-time processing and analysis.

The strip chart recorders and the HP-85 were employed on the site to monitor test operations, evaluate the quality of the data, and estimate some preliminary performance characteristics. Most of the data reduction was done at NASA LeRC, using data from the digital tape. Data from the shutdown tests was analyzed from the HP-85 printouts. The FM tape recording was a backup data recording system. Data could be recovered from the FM recording if other systems malfunctioned.

The data channel assignment on the four strip chart recorders is given in Table 8-101. Samples of strip chart data are in Figure 8-242.

The HP-85 output was used to monitor several parameters :

- wind speed history during the test
- rotor speed vs. windspeed during autorotation and speed regulation tests
- power vs. windspeed during basic performance and power regulation tests
- time history during shutdown tests

Some examples of HP-85 printouts are shown in Figure 8-243.

Table 8-100 MOD-0/5A Test Standard Data Set

- Rotor Speed and Position
- Upwind Wind Speed and Direction (corrected for transport lag sensor-to-rotor)
- Power Output or Input
- Shaft Torque
- Nacelle Yaw and Direction
- Aileron Positions from Both Blades (one transducer per blade)
- Aileron Pushrod Loads from Both Blades (two prime, two back-ups per blade) Backup gages will not be recorded if the primary sensors are operational.
- Chordwise Bending moments
- Flapwise Bending Moments

  Both blades, near hub (blade root)
- Chordwise Bending Moment
- Flapwise Bending Moment

  Both blades, Station 489.5 (tip root) (two prime, two back-up per blade)
- Chordwise Bending Moments

  Both blades, Sta 524 (one prime, one back-up per blade)

Table 8-101 Typical MOD-0/5A Strip Chart Recorder Data Channels

	PARAMETER	SCALE* (FULL SCALE VALUES)
Chart #1	Teeter Angle	± 10°
	M_y Shaft Bending	± 100 kNm
	Rotor Position	0-500°
	Rotor Speed	0-25 rpm
	Blade #1 Aileron Deflection	0-100°
	Yaw Angle	± 100°
	Reference Windspeed	0-50 mph
	Generator Power	± 100 kW
Chart #2	Blade #1 Root Flap Bend	± 1.27×10^5 ft. lb.
	Blade #1 Root Chord Bend	± 2.00×10^5 ft. lb.
	Blade #2 Root Flap Bend	± 1.27×10^5 ft. lb.
	Blade #2 Root Chord Bend	± 2.00×10^5 ft. lb.
	Blade #1 Tip Flap Bend	± 1.10×10^4 ft. lb.
	Blade #1 Tip Chord Bend (Sta 489.5)	± 1.00×10^4 ft. lb.
	Blade #2 Tip Flap Bend	± 1.10×10^4 ft. lb.
	Blade #2 Tip Chord Bend (Sta 489.5)	± 1.00×10^4 ft. lb.
Chart #3	Blade #2 Aileron Deflection	0-100°
	Blade #2 Inboard Pushrod Load	± 1,000 lb.
	Blade #2 Outboard Pushrod Load	± 1,000 lb.
	Rotor Speed	0-25 rpm
	Shaft Torque	± 118.6 kNm
	Nacelle Windspeed	0-25 mph
	Generator Power	± 100 kW
	Rotor Position	0-500°
Chart #4	Blade #1 Aileron Deflection	0-100°
	Blade #1 Inboard Pushrod Load	± 1,000 lb.
	Blade #1 Outboard Pushrod Load	± 1,000 lb.
	Blade #1 Tip Chord Bend (Sta 524)	± 1.00×10^4 ft. lb.
	Blade #2 Tip Chord Bend (Sta 524)	± 1.00×10^4 ft. lb.
	Nacelle Windspeed	0-50 mph
	Blade #2 Tip Chord Bend (Sta 489.5)	± 1.00×10^4 ft. lb.
	Blade #2 Tip Flap Bend (backup gages)	± 1.10×10^4 ft. lb.

* The scale sensitivity settings were varied as required for specific test values. The values shown are "average".

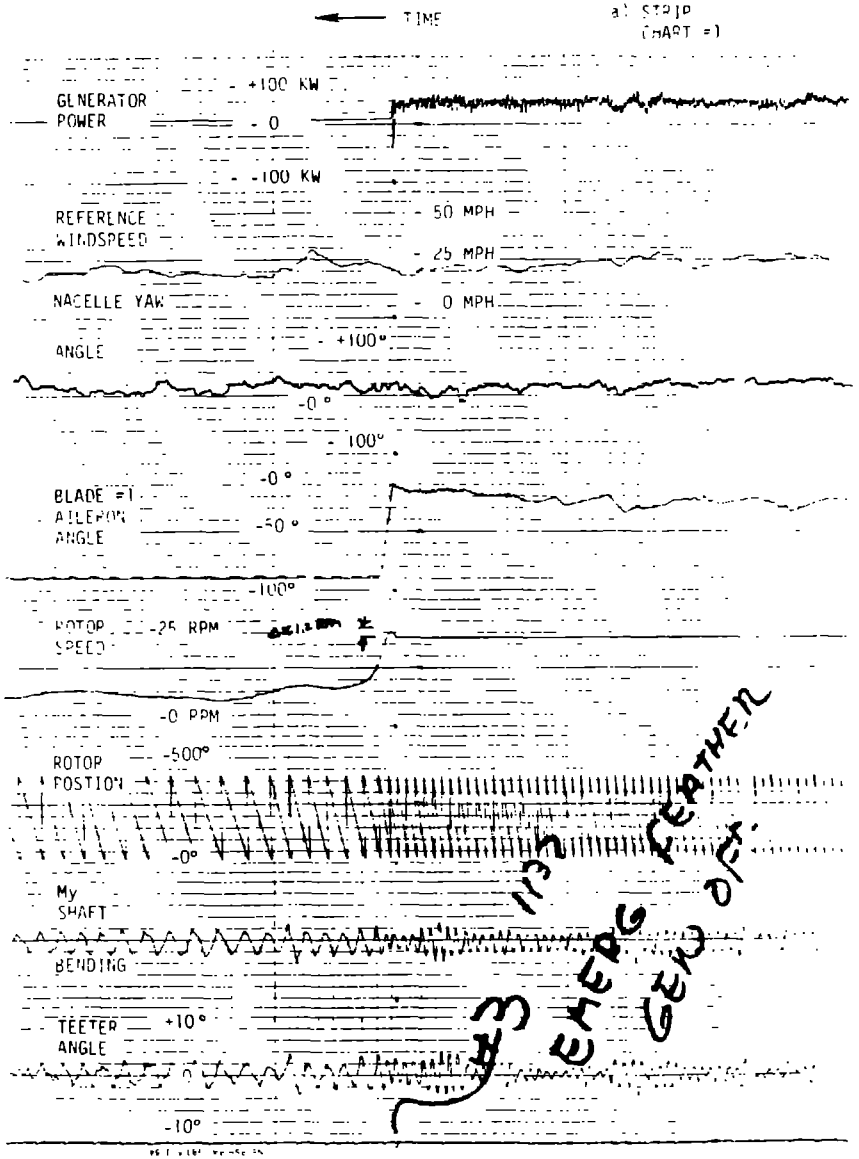

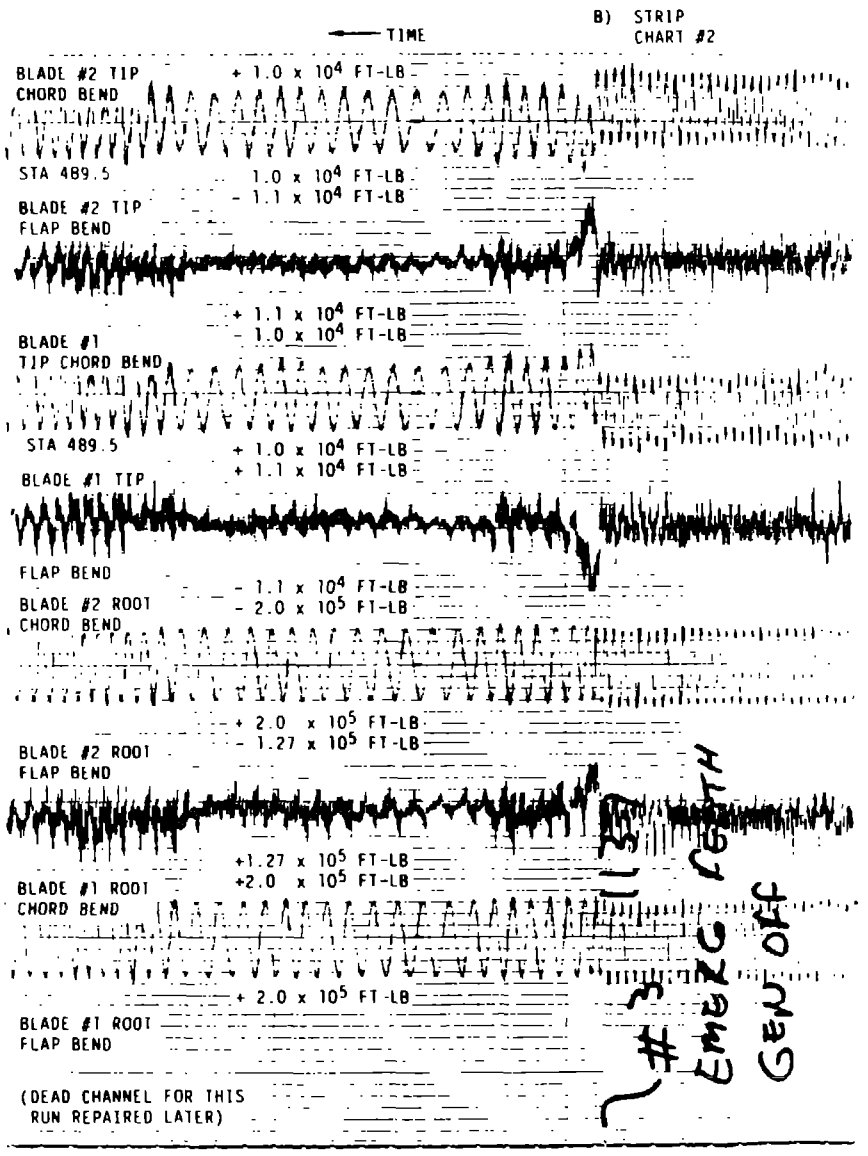

Figure 8-242 Sample Strip Chart Data #1 & #2

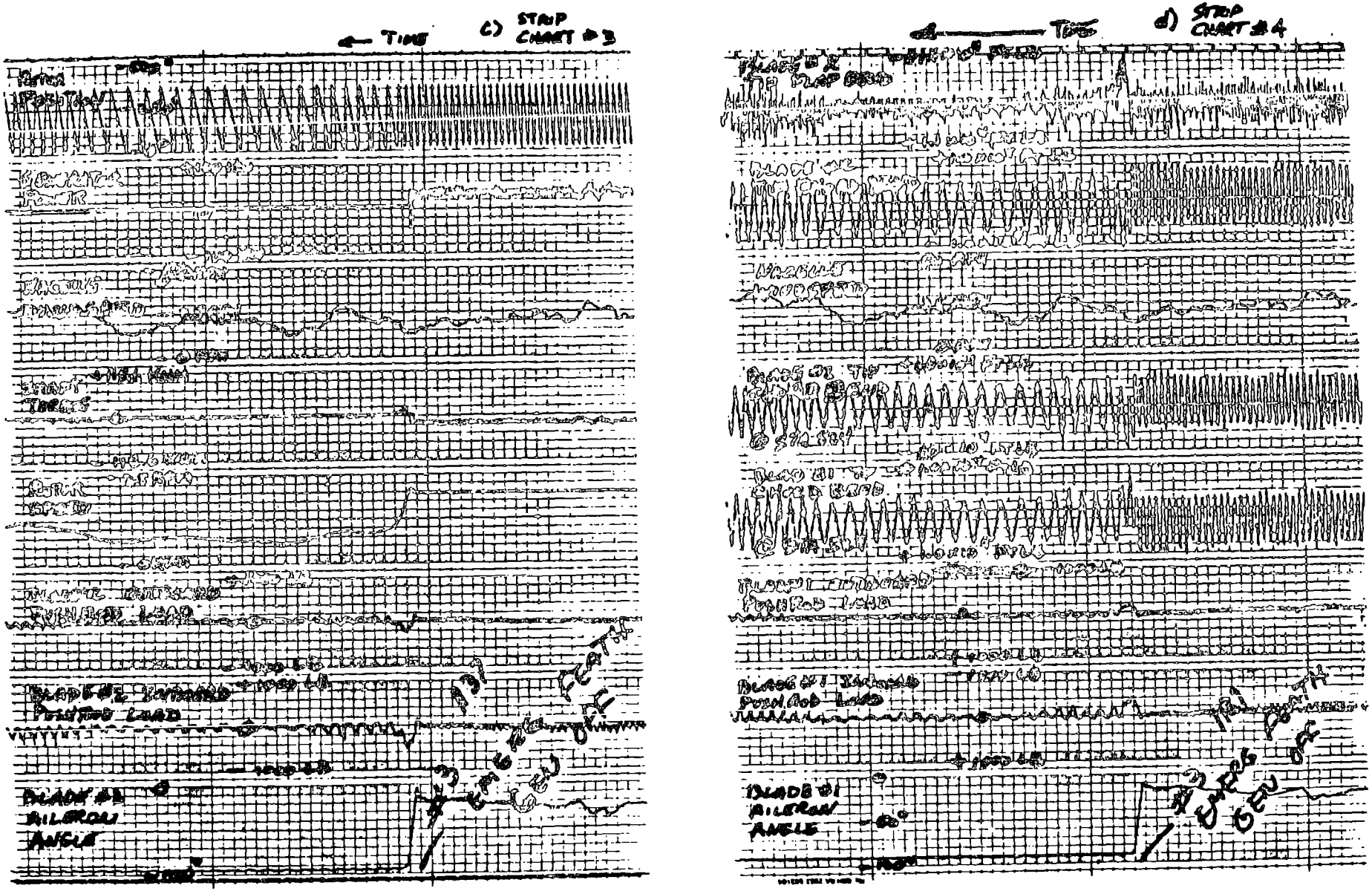

Figure 8-242 Sample Strip Chart Data #3 & #4

A) AUTO-ROTATION TEST

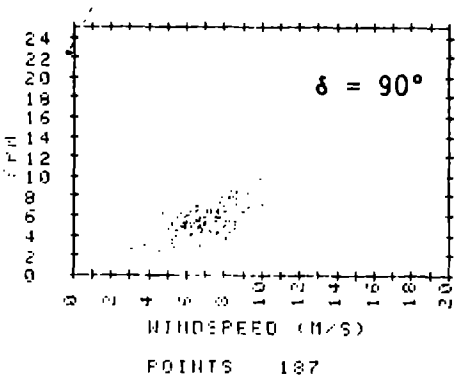

B) SPEED REGULA-TION TEST

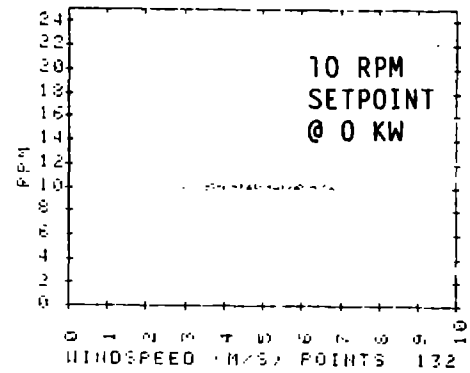

C) POWER REGULA-TION TEST

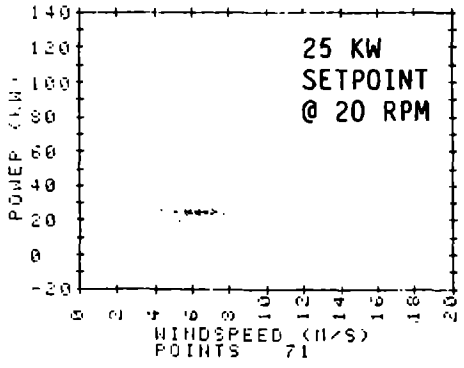

D) BASIC PERF. DATA

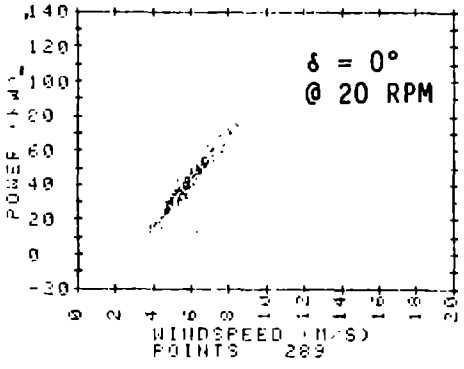

E) WIND SPEED HISTO-GRAM

WINDSPEED (M/S)	TIME (MIN)
0- 2	0
2- 4	0
4- 6	157
6- 8	108
8-10	15
10-12	0
12-14	0
14-16	0
16-18	0
18-20	0

D) SHUTDOWN TEST

- 2 TIPS
- V_{W_0} = 8.5 MPS
- δ = 10°/SEC
- δ_0 = + 1°
- δ_{FINAL} = - 89°
- 1 SEC DELAY

START SHUTDOWN →

MAX RPM →

```
AUTO3  PROGRAM

ITER NUMBER                16
REF WIND SPEED             20
DIGITAL TAPE               NONE

  REMARKS
SHUTDOWN @ 17
10 DEG PER SEC
TWO TIPS

WIND SENSOR @ 2P SELECTED

TAKING DATA WILL STOP AFTER
80  SECONDS OR RPM BELOW  3

JULIAN DAY NO    0 OF 1900
TIME   3 43 11

NO   RPM WIND-SP PITCH-AN TORQUE
 1  20 30   0 45        86  -26314
 2  20 25   0 52        86  -26984
 3  20 25   0 76        86  -25724
 4  20 25   0 71        86  -24425
 5  20 20   0 54        86  -21155
 6  20 20   0 47        86  -21004
 7  20 20   0 50        86  -18889
 8  20 15   0 62        86  -18765
 9  20 20   0 81        86  -18745
10  20 20   0 45        86  -18754
11  20 10   0 58        86  -16759
12  20 20   0 76        86  -16993
13  20 20   0 71        86  -18526
14  20 20   0 54        86  -19470
15  20 20   0 45        86  -20179
16  20 20   0 58        86  -19942
17  20 20   0 67        86  -20886
18  20 15   0 91        86  -19706
19  20 10   0 81        86  -17956
20  20 15   0 49        86  -16166
21  20 45   0 36      - 40  -14750
22  20 60   0 45     -11 54   -9204
23  20 40   0 40     -22 43   -5150
24  19 65   0 18     -33 22   -2241
25  18 60   7 85     -44 10    -110
26  17 30   7 55     -54 98    3714
27  15 75   7 65     -65 96    3854
28  14 65   7 77     -77 02    5192
29  12 90   7 64     -88 17    5782
30  11 75   7 60     -88 89    5546
31  10 95   7 46     -88 44    4484
32  10 10   7 29     -88 17    2959
33   9 40   7 31     -88 26    2596
34   8 85   7 11     -88 89    2124
35   8 40   6 95     -89 70    1410
36   7 95   6 30     -89 61    1062
37   7 60   5 85     -89 16     826
38   7 30   5 54     -88 53     354
39   7 10   5 45     -88 35       0
40   6 75   5 36     -88 35    -118
41   6 50   5 68     -88 44    -118
42   6 45   6 08     -89 52    -118
43   6 25   6 44     -89 70   -1354
44   5 85   6 71     -89 70   -1590
45   5 65   6 91     -89 70    -472
46   5 60   7 37     -89 34
47   5 55   7 38     -88 88   -1062
48   5 50   7 86     -88 44    -826
49   5 45   6 75     -88 35   -1180
50   5 40   6 48     -88 35   -1180
51   5 35   6 44     -88 44    -944
52   5 35   6 53     -88 89   -1180
53   5 30   6 44     -89 61   -1298
54   5 30   6 21     -89 79   -1298
55   5 20   6 08     -89 79   -1180
56   5 15   6 12     -89 79   -1062
57   5 10   6 30     -89 61   -1062
58   5 05   6 21     -89 16   -1062
59   5 10   6 30     -88 71   -1180
60   5 10   6 03     -88 44   -1298
61   5 10   5 99     -88 35   -1416
62   5 10   5 88     -88 35   -1298
63   5 05   6 17     -88 53   -1298
64   5 00   6 30     -88 99   -1298
65   4 85   6 21     -89 61    -944
66   4 60   6 30     -89 79    -826
67   4 70   6 39     -89 79    -944
68   4 65   6 57     -89 79    -708
69   4 60   6 48     -89 70    -708
70   4 55   6 44     -89 35    -708
71   4 55   6 53     -89 35    -708
72   4 50   6 62     -89 44    -708
73   4 45   6 57     -89 44    -708
74   4 40   6 57     -89 35    -708
75   4 35   6 66     -89 35    -944
76   4 25   6 75     -89 44    -944
77   4 20   6 84     -89 30    -708
78   4 15   6 93     -89 43    -944
79   4 10   6 93     -89 61   -1062
THE PITCH RATE  1 D.
```

Figure 8-243 Sample HP-85 Printouts

8.4.3.6 Test Plan and Results

8.4.3.6.1 Test Matrix and Rationale

The tip-speed ratio, λ, was the major simulation parameter. Proper λ simulation provides a spanwise angle of attack distribution over the MOD-0/5A tip, which very nearly duplicates the distribution on the MOD-5A tip under conditions of autorotation, rated windspeed and cutoff windspeed. MOD-0/5A operating windspeed conditions that correspond to the full-scale MOD-5A operating at rated and cutoff windspeeds are V_w=10 mph and V_w=20 mph, respectively. Test conditions in the matrix were selected to duplicate tip-speed ratios over a range that would include these operating points of the MOD-5A as well as autorotation conditions.

The first priority was to assess the acceptability of the aileron configuration that earlier studies had determined to be the optimum for the MOD-5A. Plain ailerons and balanced ailerons were available as basic configurations, and vented plain ailerons and vented balanced ailerons were available as backup configurations.

Wind tunnel data was analyzed before the test. The analysis indicated that the 38% chord, plain aileron met the MOD-5A aileron performance requirements without either balance lip or venting. This configuration was selected as the best configuration for the first testing.

The order of the tests was established so that the most important aileron performance characteristics would be obtained first. The order was:

1.) Autorotation speed/shutdown performance
2.) Autorotation speed/shutdown performance with damaged aileron, in which 25-50% of total rotor aileron surface is locked at full power.
3.) Speed regulation
4.) Power regulation above rated windspeed
5.) Noise level during regulation
6.) Basic aerodynamic performance, for a constant rotor speed at a fixed deflection angle

Tests 1 and 2 were more important since in the regulation tests 3 and 4, significant improvements in undesirable control characteristics can be provided by increasing stability using modern control systems. Data from

earlier tests using 20% - 30% chord ailerons indicated reasonable regulation characteristics.

The noise-level measurements and analyses were conducted by NASA Langley Research Center, employing techniques developed for earlier studies on other wind turbines. The data and analysis results for plain and balanced ailerons will be reported in ref. 3.

The original matrix was designed to follow this priority, to determine quickly whether the plain aileron was acceptable. The availability of high winds did alter the order somewhat, but in general the tests were conducted according to the defined order.

Test Matrix Definition -- The original GE test matrix is defined in detail in ref. 4. The matrix covered test points over the following ranges of independent variables:

1. Windspeed: 5 mph → 35+ mph
2. Rotor Speed: 20 rpm for most testing; lower speeds were used for autorotation, speed regulation tests, initial checks and Reynold's number variation.
3. Aileron Deflection: 0° to approximately 90°
4. Aileron Rates: 2°/sec - 5°/sec for regulation
   15°/sec - 25°/sec for shutdowns
5. Power Outputs: 0-100 kW for various test objectives, negative values for basic data (motoring cases)

The maximum power output, which is achieved with the aileron deflected 0°, as a function of windspeed, for the MOD-0/5A hardware operating at 20 rpm was assumed to be:

P	= 35kW,	V_W	= 10 mph,
	= 70kW,		= 20 mph,
	= 100kW		= 30 mph

These estimates were based on previous experience with the MOD-0 wind turbine, and were employed in initial planning to establish power set points for the regulation and shutdown tests.

The details of the matrix were changed during the testing. The values of parameters and the amount of data recorded changed, but the ranges of variables and the independent parameters did not change significantly. Modifications to the matrix were implemented by mutual agreement between NASA and GE. The changes reflected a shift to more basic development testing. NASA issued a revised matrix in February, 1984, to document these changes.

8.4.3.6.2 Test Operations

Preliminary data at rotor speeds of 13 rpm and 20 rpm was obtained on the plain aileron before the end of 1983. The early data was obtained per the original test matrix. Data was recorded for 10-20 minutes, except for shutdown data, which was only recorded for the duration of the shutdown. This period proved to be too short for the 5-minute data averaging techniques used in NASA's standard data reduction. Significant early results on aileron performance were derived manually from the data sources at Plum Brook, however.

Early problems with malfunctioning servovalves in one of the tips delayed further data acquisition until the second week in January, 1984. The installation of an additional filter in the servovalve supply line solved the problem, and in mid-January the data acquisition proceeded.

Another hardware problem arose during early tests. The outboard pushrod load sensor system on Tip #1 failed. The cause of this problem was not identified, so data acquisition continued without that measurement since the outboard pushrod load data from Tip #2 provided the information. The first few days of testing in December, 1983 were conducted without an operational root flap bending sensor in the Blade #1 spool piece. Data from Blade #2 sensors provided data during this period. This problem was fixed before data acquisition resumed in January, 1984.

Preliminary tests in December 1983 used a solid shaft drive; no clutch system was installed in the drivetrain between the rotor and the generator. This

set-up permitted the rotor to be motored by the generator during low winds. These tests verified the feasibility of the planned tests and provided useful aileron performance data. The standard MOD-0 over-running clutch system was installed for January's tests on autorotation, power and speed regulation, and the basic performance tests, in which windspeed and aileron-angle conditions were consistent with positive power generation. The solid-shaft drive system was reinstalled in early February to permit data acquisition by motoring in low winds at higher aileron angles. In these tests, use of the clutch would have resulted in rotor speeds below the 20 rpm required for most performance tests.

In general, data was taken for a minimum of 60 minutes for each aileron setting in each 2 mps windspeed bin in all tests, except shutdowns. The goal was to take a maximum of 120 minutes of data per bin. The amount of time for each recording was determined by the winds and the constraints on the schedule.

Unusually low winds at Plum Brook during January and February impeded the efficient acquisition of data and caused some delay in the planned test schedule. Very little data was acquired for wind speeds above 18 mph. Periods of wind above 13 mph were infrequent. Several high-wind periods did occur in March, April and May, which permitted acquisition of sufficient data on plain and balanced aileron configurations by early June.

8.4.3.6.3 Preliminary Results

Initially, the strip charts and HP-85 output were used on the site to assess the aileron's performance during the early phases of testing.

Winds during 14-16 December, 1983 varied from less than 10 mph to over 20 mph. Early information on important parameters were estimated from the analog strip chart records for range of windspeeds. Rough performance estimates were made for the plain aileron configuration in: autorotation speed, full-deployment shutdowns, speed regulation, and noise levels.

Autorotation and regulation performance were evaluated by examining strip chart records. Parameters were roughly estimated by averaging the strip chart time histories of windspeed, rotor speed and power output. The averaging

smoothed variations caused by varying windspeeds and rotor dynamics and inertia. Shutdown performance was evaluated from strip chart recordings similiar to the example shown in Figure 8-242, which was obtained on a shutdown test on 16 December, 1983. Noise levels were initially evaluated subjectively. Several experienced observers listened to the rotor noise and compared it with noise of earlier tests. Quantitative sound measurements on the plain aileron were made in late January, 1984.

More elaborate post-test evaluation of HP-85 autorotation data was performed to combine data from similar sets of tests acquired over the test period from January through May 1984 for both plain and balanced ailerons.

The following preliminary analyses and conclusions regarding aileron performance are based on the methods noted above.

1. Shutdown -- The plain aileron will shut the rotor down within the required overspeed specification when the aileron is deflected to -90° at 15-30°/sec. Damaged aileron shutdowns were simulated during the testing by employing only a single tip. Single-tip tests met the requirements at 20°/sec and -90° deflection. Shutdowns at lower deflection angles were not tested.

2. Autorotation -- The autorotation performance was consistent according to the estimates of early strip charts and the later, more detailed analysis of HP-85 outputs. The parameter of interest was the equilibrium tip-speed-ratio, λ_E, which was defined as the ratio of equilibrium rotor tip-speed to windspeed for no load, other than friction in the hub and nacelle.

   Autorotation performance data was taken directly from HP-85 plots and is shown in Figure 8-244 for the plain and balanced ailerons. The shaded areas on these figures were obtained by overlaying autorotation data from various data sets acquired for the same configuration on different days, and illustrate the typical scatter in the on-site autorotation data. Generally, the day-to-day data scatter was no greater than the scatter during a single test run. The plain aileron data of Figure 8-244. also shows the aileron segments on one blade inactive results for deflection angles of -89° and -76°. The dashed lines on these figures represent

a.) PLAIN AILERON

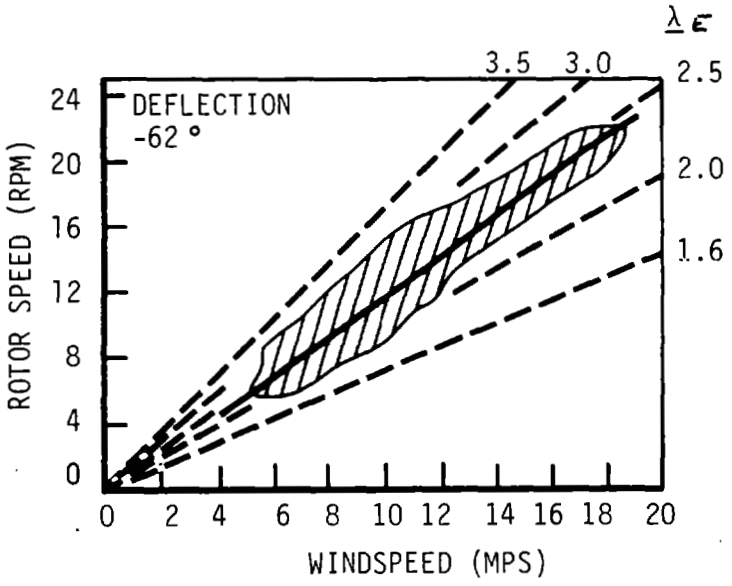

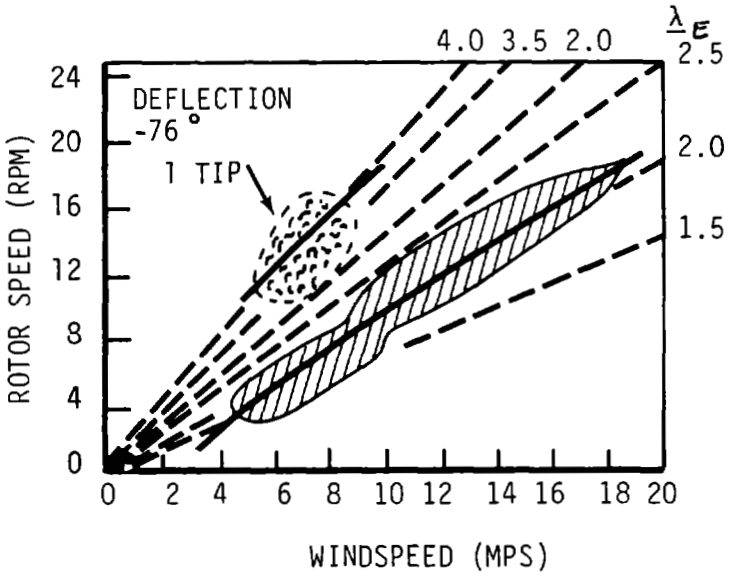

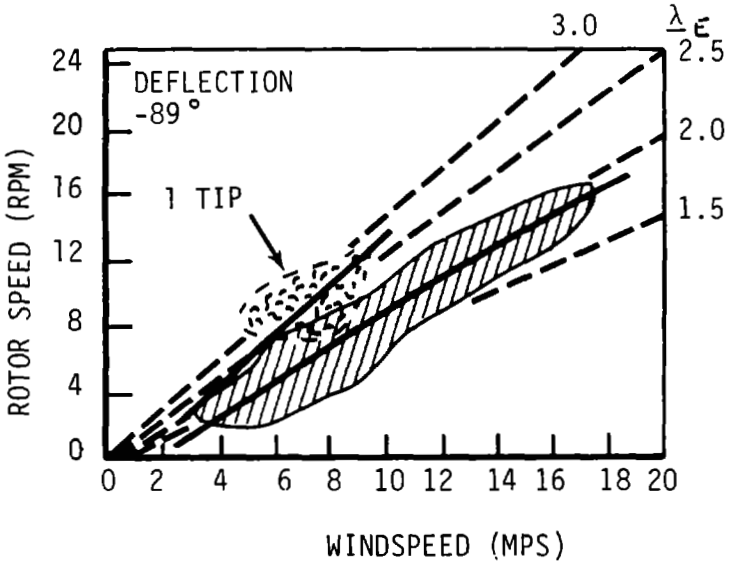

Figure 8-244 On Site Autorotation Data

constant values of tip-speed ratio, λ, while the solid curves drawn through the shaded areas represent estimates of autorotation rotor speed as a function of windspeed for the various test configurations and deflections. These curves were obtained by visually estimating the mean line through the actual data points plotted out by the IIP-85, Figure 8-243A, and are in good agreement with some early results provided by NASA Lewis Research Center from a more elaborate computer analysis. Values of λ_E were estimated from Figure 8-243 at high wind speeds and are summarized in the following table.

Preliminary Autorotation Results

Aileron Deflection Angle (degrees)	MOD-0/5A Equilibrium Tip Speed Ratio (λ_E)		
	Plain Aileron		Balanced Aileron
	Two Tips	One Tip	Two Tips
-89	1.9	2.8	2.2
-76	2.1	4.0	2.5
-62	2.4	-	2.9

These results indicate that the λ_E=2.3, MOD-0/5A autorotation requirement is met by either aileron configuration at -89° deflection and by the plain aileron also at -76° deflection. The MOD-0/5A autorotation requirement for the 20% damaged-rotor case (λ_E=3.0) is also met by the plain aileron at -89° and probably also at -76° if it is assumed that the λ_E value varies linearly with percentage damage since the single tip case represents 50% damage to the control surfaces.

Autorotation performance of the plain and balanced configurations is compared in the data summary of Figure 8-246, where the curves are also the mean curves from Figures 8-244 and 8-245. The superiority of the plain aileron over the balanced configuration for autorotation speed control at high windspeed is easily seen in Figure 8-246 and the λ_E values of the table above.

3. Power and Speed Regulation -- The preliminary evaluation of strip charts and IIP-85 outputs indicates that both the plain aileron and the balanced aileron would meet control and regulation requirements at tested values of

b.) BALANCED AILERON

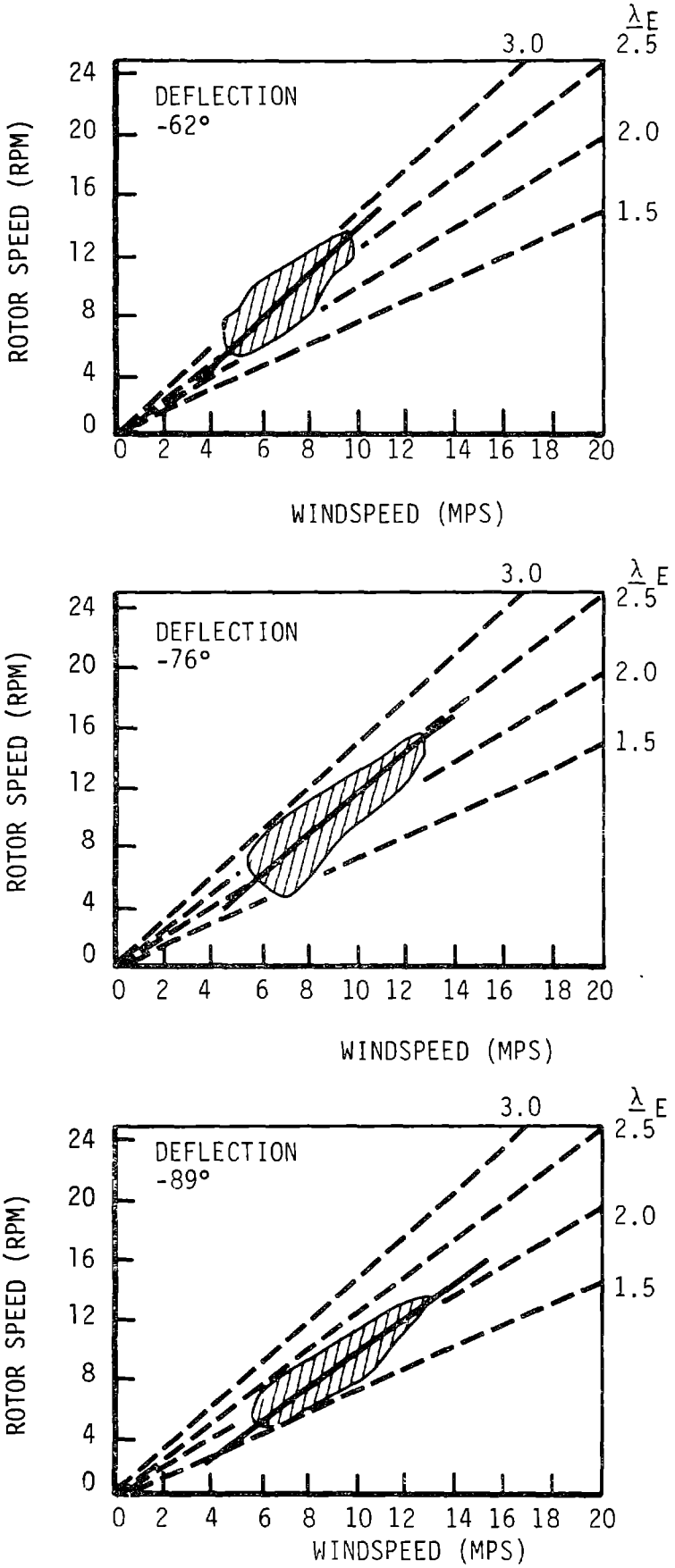

Figure 8-245 On-Site Autorotation Data

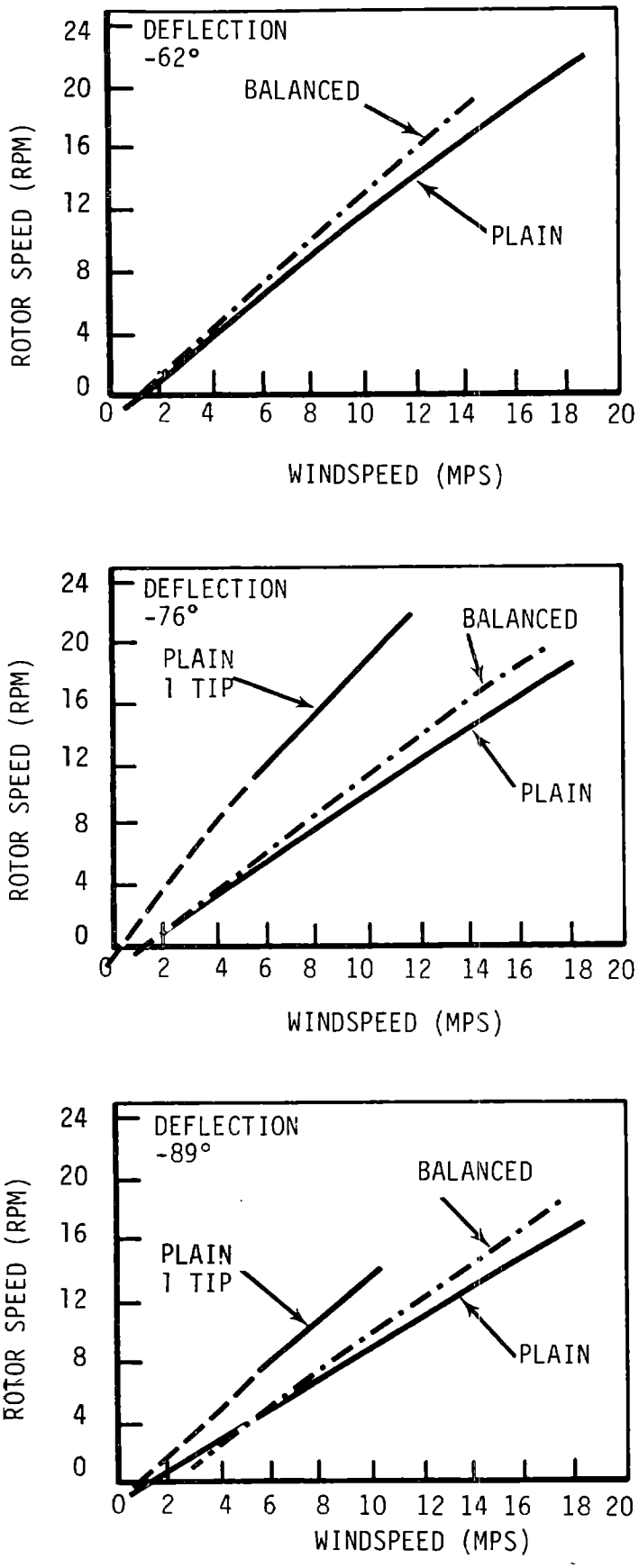

Figure 8-246 On-Site Autorotation Data Summary

maximum control rate between about 2°/second and 30°/second. For winds around 10-20 mph, which was the range encountered during testing, the servosystem rarely called for control angles above - 30° or control rates above 2°/second. Final results on regulation performance require a more detailed analysis of the statistics of parameter variations from the selected set point that will be available from the NASA computer data processing.

4. Sound -- The noise characteristics of the MOD-0/5A plain ailerons were unusual according to previous test experience. The units generated distinctive tonal components for aileron deflections between 0° and 30°. This behavior might have been caused by peculiarities in that configuration of the test unit, such as slots in surfaces for balance weight horns, or cavities. These design features would generate the tonal noise. To verify this hypothesis, some foam filler was forced into various cavities on the test units, and the tonal content of the noise was significantly reduced. More quantitative information on the noise characteristics of the plain aileron was measured and analyzed by NASA Langley. They confirm that the sound, excluding the downwind-rotor tower-shadow effects, is comprised of relatively narrowband tonal components, on top of a lower level broadband spectrum. The latter is more typical of other wind turbine noise. When the configuration was converted to the balanced aileron, the tonals were not evident. This configuration does not have the slots and gaps associated with the plain aileron. Their data and analysis for aileron noise will be presented in ref. 3.

The HP-85 outputs and strip charts were monitored to estimate the quality of the data from the amount of scatter in the points and to verify the quantitative magnitude of the measurement parameters. All force and moment data, however, was obtained from the final LERC computer data reduction.

Final evaluation, results and recommendations were based on the detailed reduction and analysis, at NASA-LeRC, Cleveland and at GE, which is discussed in the following sections.

8.4.3.7 Data Reduction and Analysis

There were basic problems in the application of the MOD-0/5A test data to the MOD-5A wind turbine that arise from the nature of wind turbine testing. The wind speed was always changing and was, therefore, an uncontrollable independent variable. Fluctuation in the wind speeds imposed a "noisy" environment on the test and made the basic data difficult to interpret. Furthermore, the wind-speed instrumentation could not be located at the turbine because power extraction by the turbine imposed a significant change in the local speed at the rotor from the uninfluenced, remote wind. As a result, the wind speed measured at a given instant by the anemometer was not necessarily the wind speed affecting the rotor at that time. Furthermore, the geometry of the MOD-0/5A, the best representation that the test bed could provide, differed in some important particulars from the MOD-5A. Finally, there were differences in Reynolds number. The data reduction and analysis had to deal with these problems, to maximize the utility of the test data in characterizing the MOD-5A wind turbine.

8.4.3.7.1 Reduction of the Basic MOD-0/5A Data

All of the basic data were taken as analog data and converted to digital data of the maximum and minimum of each rotor cycle for each transducer. The sum and differences of these two readings were used to compute the average steady load and the cyclical component during the period of the rotor, 3 seconds in the case of 20 rpm. This "per cycle" data were the beginnings of the data reduction and analysis. A typical test run took, for example, 3 hours, during which 3,600 data points for each of many sensors was recorded. The individual data set can be considered a two-dimensional array in which each row consists of the following array:

Time interval, seconds
Reference Wind Speed, M/S
Flap primary bending moment blade #1 N-m
Chord primary bending moment blade #2 N-m
Flap primary bending moment blade #1 N-m
Chord primary bending moment blade #2 N-m
Tip 1 flap primary bending moment N-m
Tip 1 chord primary bending moment N-m
Tip 2 flap primary bending moment N-m
Tip 2 chord primary bending moment N-m
Tip 1 inboard link control force N
Tip 1 outboard link control force N
Tip 2 inboard link control force N
Tip 2 outboard link control force N

Inspection of the data reveals that there was considerable high frequency fluctuation of the wind data for which little corresponding correlation of force data could be seen. Therefore, the data was filtered to remove high frequency data by using a truncated Fourier transform. The data was cut off at periods less than 30 sec., or a frequency greater than 1/30 Hz. Therefore, we retained 512 terms in the Fourier transform to smooth out the unwanted fluctuations. All of the data was passed through this smoothing filter to obtain an array of smoothed data. With the smoothed wind data, the instantaneous transport delay, or the time required for the measured wind to reach the turbine, could be computed. The wind speed was locally shifted along the time scale by the transport delay to provide a new array in which only the velocity has been reconstructed to correspond in time to the measured data. All of these processes were carried out for data sorted on control deflection, so that each array was for a single control deflection angle.

At this point, a "matrix sort" operation was carried out so that the velocities were sorted in ascending order. In this operation, each transducer output initially associated with a shifted wind speed remained associated with that wind speed. The new array no longer had a meaningful time, but each row represented a velocity point with all of the dependent variables corresponding to that velocity.

The velocity range provided by the data was then divided into suitable bins and the average value of each of the variables and other statistical measures were computed. This arrangement provided a set of experimental relationships between the wind speed and all of the dependent variables. At this point, the statistical properties of the binned data could be analyzed and revisions to the binning made as necessary, completing the data reduction phase.

8.4.3.7.2

Analysis of Basic Performance Data

Using measurements of the bending moment in the plane of rotation at two different stations, the increment in chord force, Δx, caused by aileron deflection, was inferred from the data as a function of tip speed ratio for each control deflection angle. Next, the effective incremental chord force

coefficient as a function of angle of attack was inferred. Then, the effective chord force coefficient, $\bar{C}_X$, was calculated from equations 8.4.3-1 and -2, in which all of the terms were known:

$$\bar{C}_X = \Delta X/(\frac{1}{2}\rho\omega^2R^2 * R^2 * I_1) \qquad [8.4.3\text{-}1]$$

$$I_1 = \int_{x_i}^{x_o} \frac{c}{R}(x)(x^2 + \lambda^2)\,dx \qquad [8.4.3\text{-}2]$$

Where ΔX is the increment in chord force (lbs. or N.)

ρ is the air density (slugs or kg)

ω is the rotor speed (radius/s)

x is the ratio of the radii of the MOD-5A and MOD-0/5A, V/R

c/R is the ratio of the local chord to the blade radius

λ is the tip-speed ratio and the subscript i, and o refer the inner and outer radial boundaries of the aileron

Similarly, the effective normal force coefficient, $\bar{C}_N$, and its location, Δr_n, can be computed from analogous data.

The angle of attack, $\bar{\alpha}$, is computed from equations 8.4.3-3 through -6, where the barred symbols refer to the effective or "average" value of the variables that represent the aileron as a whole:

$$\bar{\alpha} = \phi_o - \phi_i - \bar{\Theta} \qquad [8.4.3\text{-}3]$$

$$\phi_o = \tan^{-1}(1/(\lambda\,\bar{x})) \qquad [8.4.3\text{-}4]$$

$$\bar{x} = x_i + \frac{\Delta r}{R} \qquad [8.4.3\text{-}5]$$

$$\phi_i = ((\bar{c}/R) \times \bar{C}_N)/4\pi\bar{x}\,\kappa \qquad [8.4.3\text{-}6]$$

ϕ_o is the "2-D" air angle whose tangent is $\frac{1}{\lambda x}$

ϕ_i is the induced air angle

Θ is the local blade pitch angle

Δr is the spanwise location of the incremented chord force measured outboard from the inner end of the aileron

C_N is the local normal force coefficient, and

κ is the Goldstein induction factor

Using the measured force data from the aileron control links, the hinge moments on the aileron were inferred and transformed into a non-dimensional hinge moment by the formula

$$\bar{C}_H = \frac{F_H \cdot k}{\frac{1}{2}\rho\omega^2 R^2 * c^2 R\ (x_o - x_i)}$$

Where F_H is the force in the link

k is moment arm of the force (i.e., $F_H \cdot k = M_H$)

M_H is the hinge moment of the aileron

These data analysis steps provide experimental values of the effective generalized performance of the MOD-0/5A ailerons as functions of control deflection angle, tip-speed ratio and angle of attack for each wind speed bin.

8.4.3.7.3 Application of the Data to the MOD-5A

The experimental coefficients derived in section 8.4.3.7.2 from the MOD-0/5A were essentially properties of the tested airfoil sections. They represented the corresponding airfoil section properties of the MOD-5A. This data was applied to the MOD-5A by direct quadratures using the MOD-5A geometry.

As a typical example, the increment in rotor torque caused by aileron deflection was calculated from equations 8.4.3-7 and -8, in which all the terms are known:

$$\Delta Q = \frac{1}{2}\rho V^2 \pi R^3 * \Delta C_Q \qquad [8.4.3\text{-}7]$$

$$\Delta C_Q = \frac{\Delta C_X}{\pi} \int_{x_i}^{x_o} (1 + \lambda^2 x^2) \frac{c}{R} x\, dx \qquad [8.4.3\text{-}8]$$

ΔQ is the increment in rotor torque produced by the aileron.

V is the wind speed and the other terms are as defined above.

These calculations can then be compared with the predictions based on wind-tunnel data. This process of data reduction, analysis and application will be published by GE in September, 1984 in a final report documenting the MOD-0/5A tests.

8.4.3.7.4 Extrapolation of MOD-0/5A Autorotation Test Results to MOD-5A Aileron Geometry

There was an intrinsic and important difference between the aileron control power as tested on the MOD-0/5A and as designed on the MOD-5A. This difference arises because of unavoidable differences in geometry between the two configurations. The MOD-0/5A aileron extended from 67% to 93.5% of span, while the MOD-5A extended from 60% to 99%. There are also planform differences. These geometric differences were analyzed by using the expression for the elementary torque coefficient represented by equation 8.4.3-9:

$$dC_Q = \frac{2}{\pi} c \times C_X \, dx * \frac{U^2}{V^2} \qquad [8.4.3\text{-}9]$$

where U is the resultant velocity at the section, V is the wind velocity, c is the dimensionless chord, x is the ratio of the radii, and C_x is the aerodynamic force in the plane of the rotor, the "torque force". The contribution to the torque coefficient of the portion of the blade extending from x=a to x=b, is given by the integral between the limits a and b. Or, if C_x is replaced by its average value in the interval a<x<b, $\overline{C}_{ab}$:

$$\Delta\overline{C}_\chi = C_\chi \frac{2}{\pi} \int_{\chi i}^{\chi o} \frac{U}{V}^2 c(x) \chi \, dx \qquad [8.4.3\text{-}10]$$

V is the resultant velocity at the station χ and the remainder of the terms are defined above.

The square of the velocity ratio is:

$$\frac{U^2}{V^2} = \frac{\omega^2 R^2 x^2 + V_w^2 + V_i^2}{V_w^2} = \lambda^2 x^2 + 1 + \frac{V_i}{V_w}^2 \qquad [8.4.3\text{-}11]$$

The last term is usually of little importance, so

$$\frac{U^2}{V^2} = 1 + \lambda^2 x^2 \text{ , approximately, and} \qquad [8.4.3\text{-}12]$$

$$\Delta C_Q = \overline{C}_\chi \frac{2}{\pi} \int_{\chi i}^{\chi o} (1 + \lambda^2 x^2) c(x) \chi dx = \overline{C}_\chi \frac{2}{\pi} P \qquad [8.4.3\text{-}13]$$

P is the constant geometric, kinematic parameter resulting from the integration.

which can be evaluated directly. Equation 8.4.3-13 states that the torque produced by a blade region is proportional to the product of an aerodynamic factor C_X and a geometric/kinematic factor P. Figures 8-247, -249, -251 and -253 show the integral of equation 8.4.3-13 while Figures 8-248, -250 -252 and -254 provide the indefinite integrand of this function for both the MOD-5A and the MOD-0/5A blades and λ = 1, 2, 3 and 4. The term P is called the geometric parameter. The relative power of the two aileron systems was determined by first evaluating P_A, the integrated aileron torque geometric parameter taken from the outboard to the inboard end of the aileron. Next P_I was computed in the same manner from the inboard end of the aileron to the blade root. The ratio of these two quantities

$$R = {}^{P_A}/_{P_I} \qquad [8.4.3\text{-}14]$$

is a measure of the geometry-related power effectiveness of the aileron portion of the blade relative to that of the inboard sections of the blade. This value was calculated for four values of the tip speed ratio (λ) as displayed in Table 8-102.

Table 8-102 Relative Torque Parameters of the MOD-5A and the MOD-0/5A Blades

λ	P_A	P_I	R_{5A}	P_A	P_I	$R_{0/5A}$
1	.0280	.0212	1.32	.0208	.0193	1.075
2	.0605	.0305	1.95	.0463	.0302	1.53
3	.1145	.0461	2.48	.0889	.0482	1.85
4	.1905	.0680	2.80	.1486	.0733	2.03

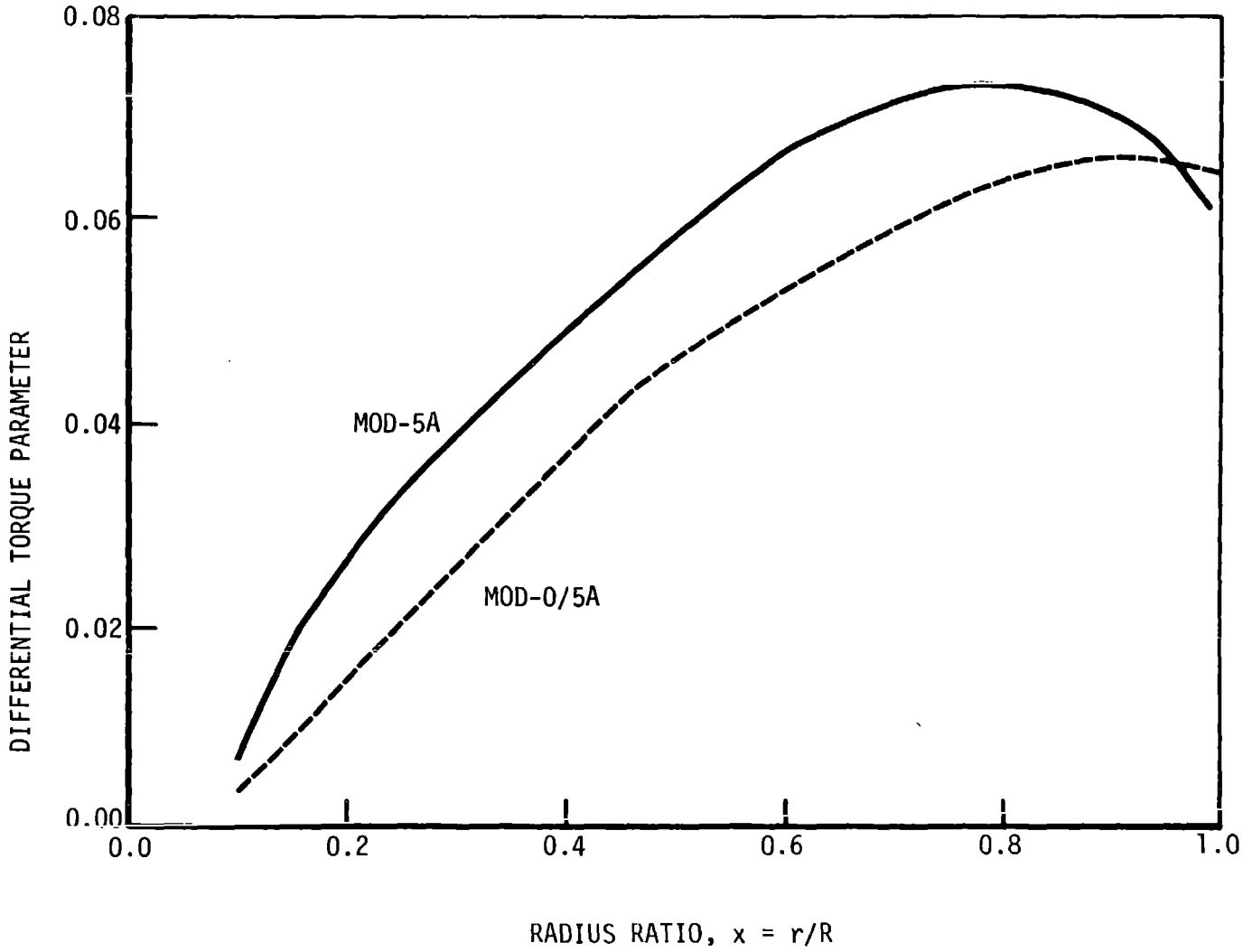

Figure 8-247 Differential Torque Parameter Versus Span for $\lambda = 1.0$

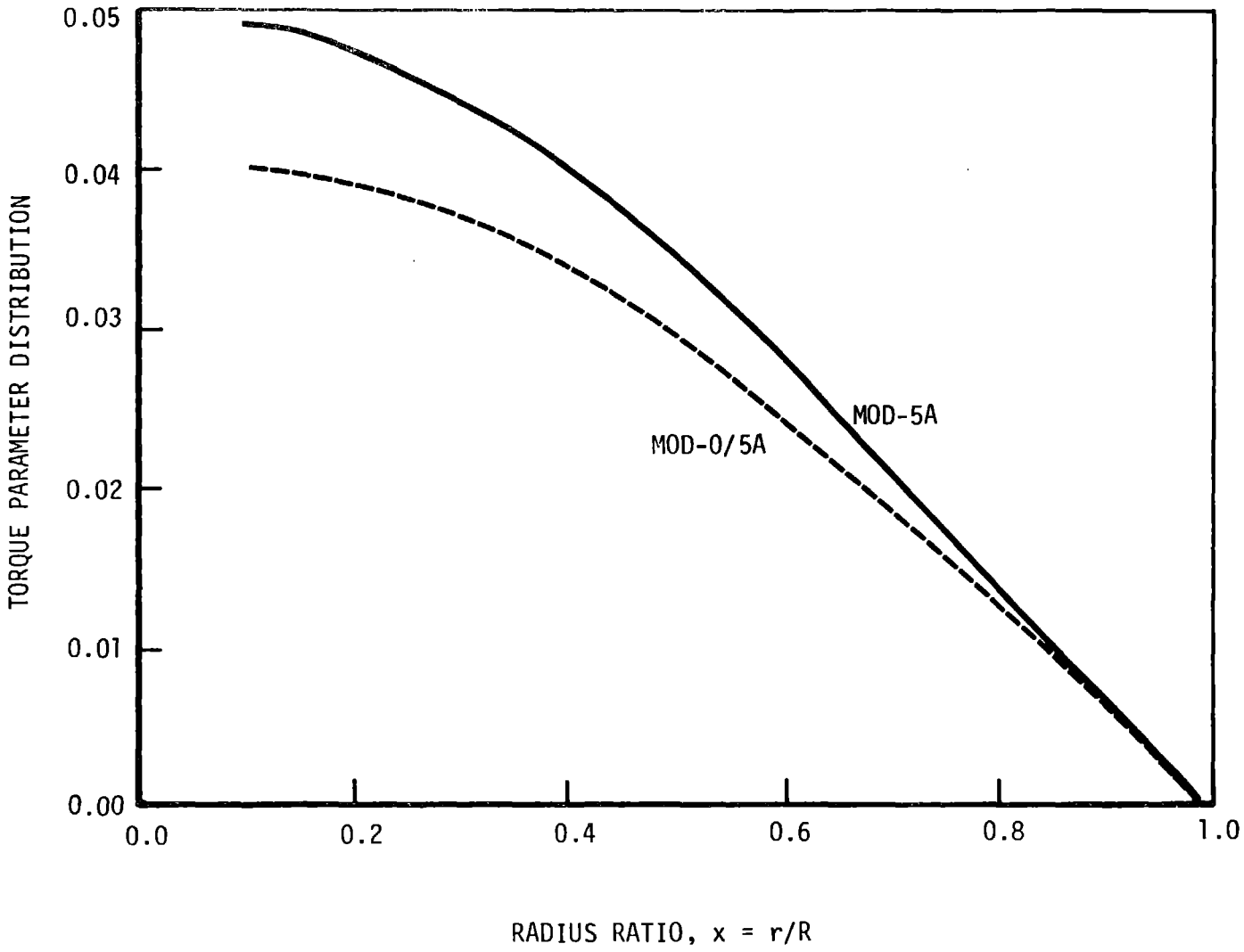

Figure 8-248 Torque Parameter Versus Span for $\lambda = 1.0$

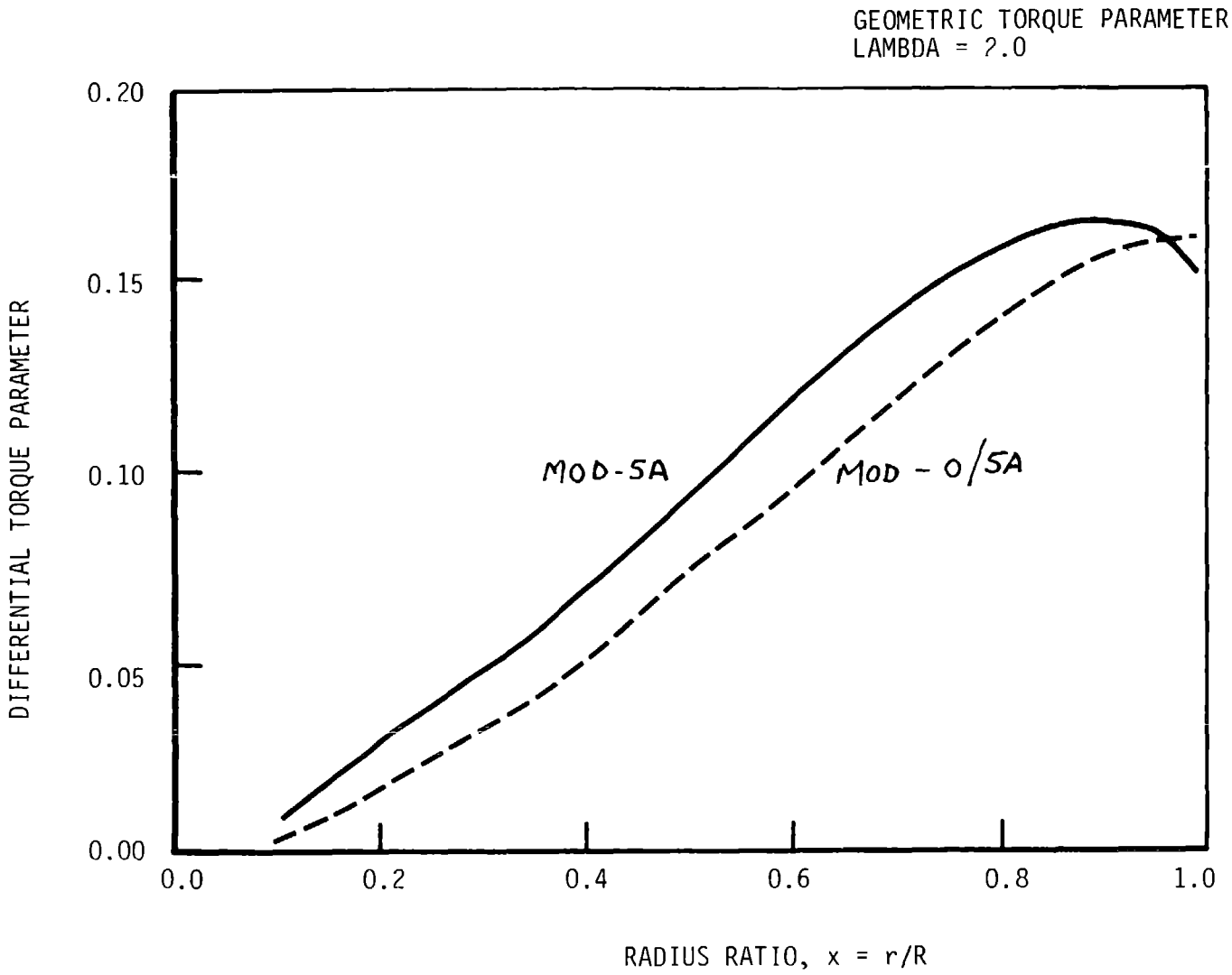

Figure 8-249 Differential Torque Parameter Versus Span for λ = 2.0

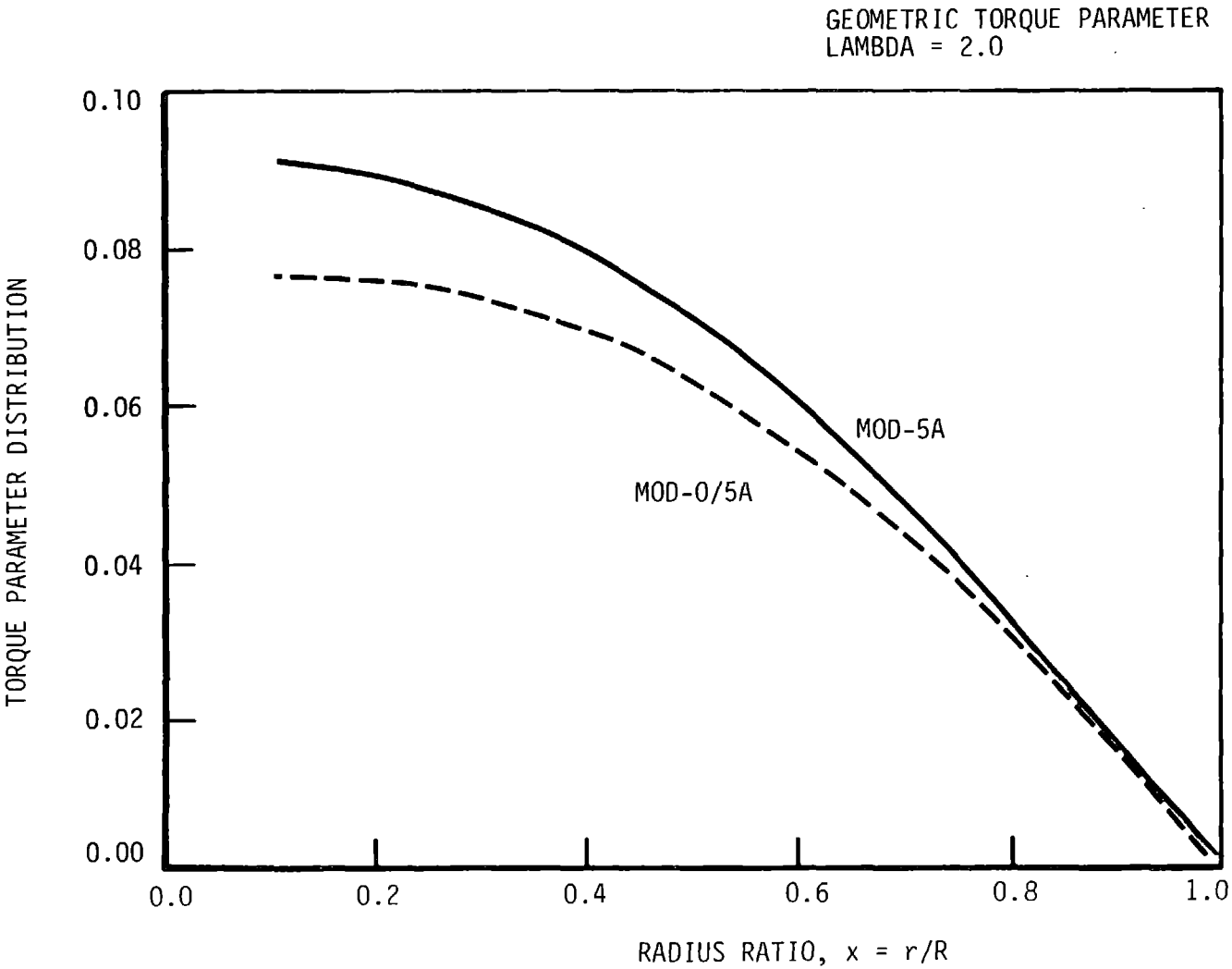

Figure 8-250 Torque Parameter versus Span for λ = 2.0

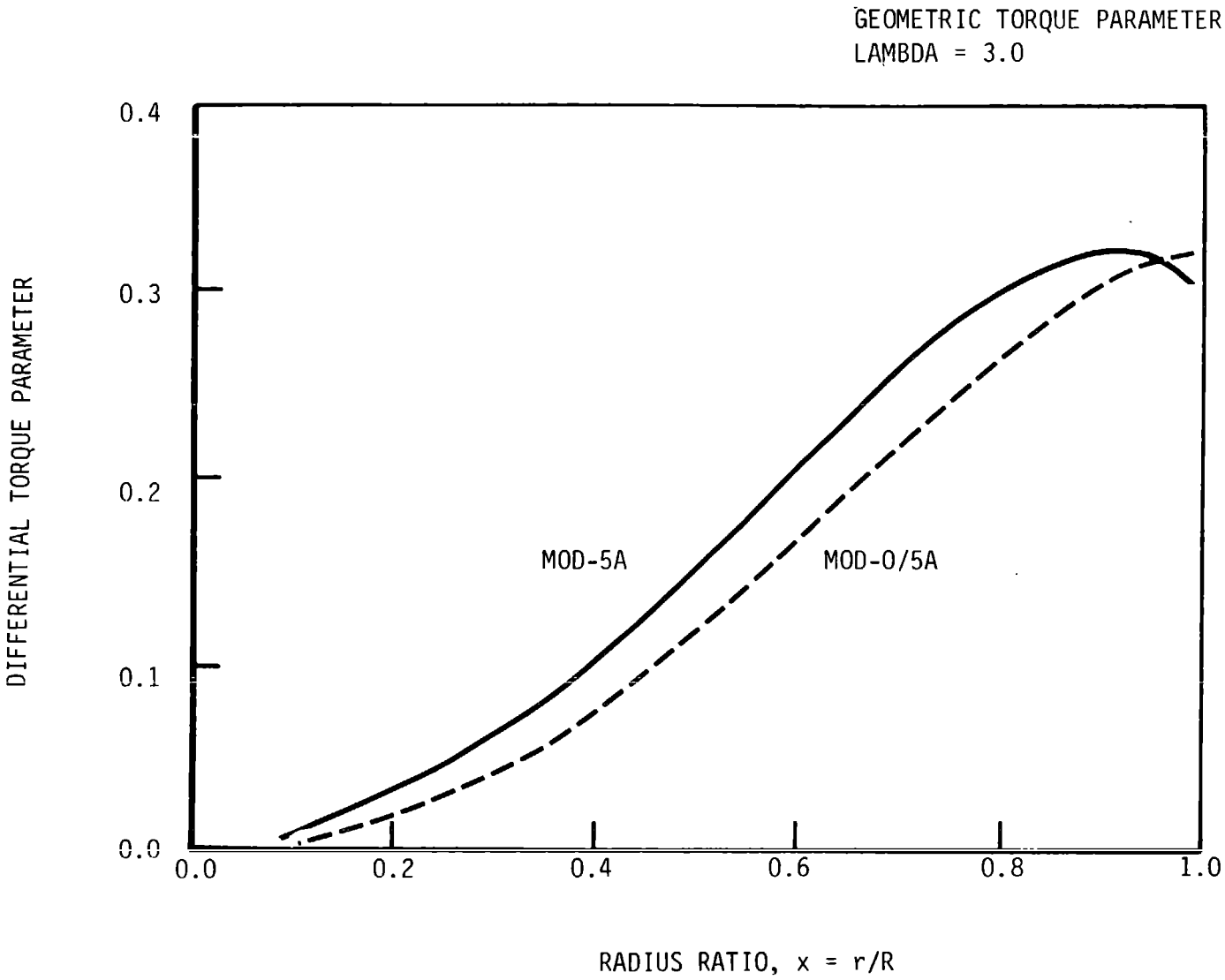

Figure 8-251 Differential Torque Parameter Versus Span for λ = 3.0

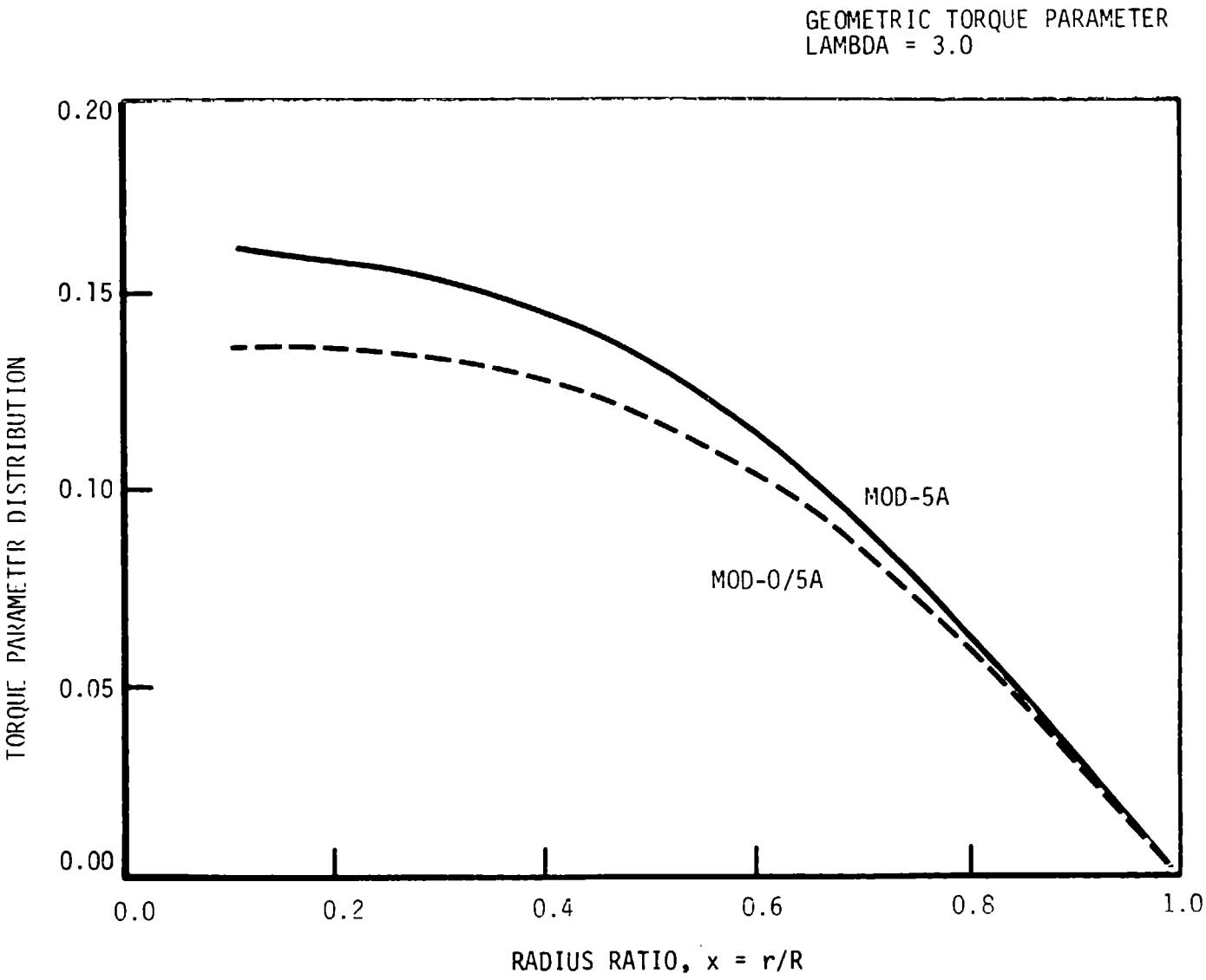

Figure 8-252 Torque Parameter Versus Span for λ = 3.0

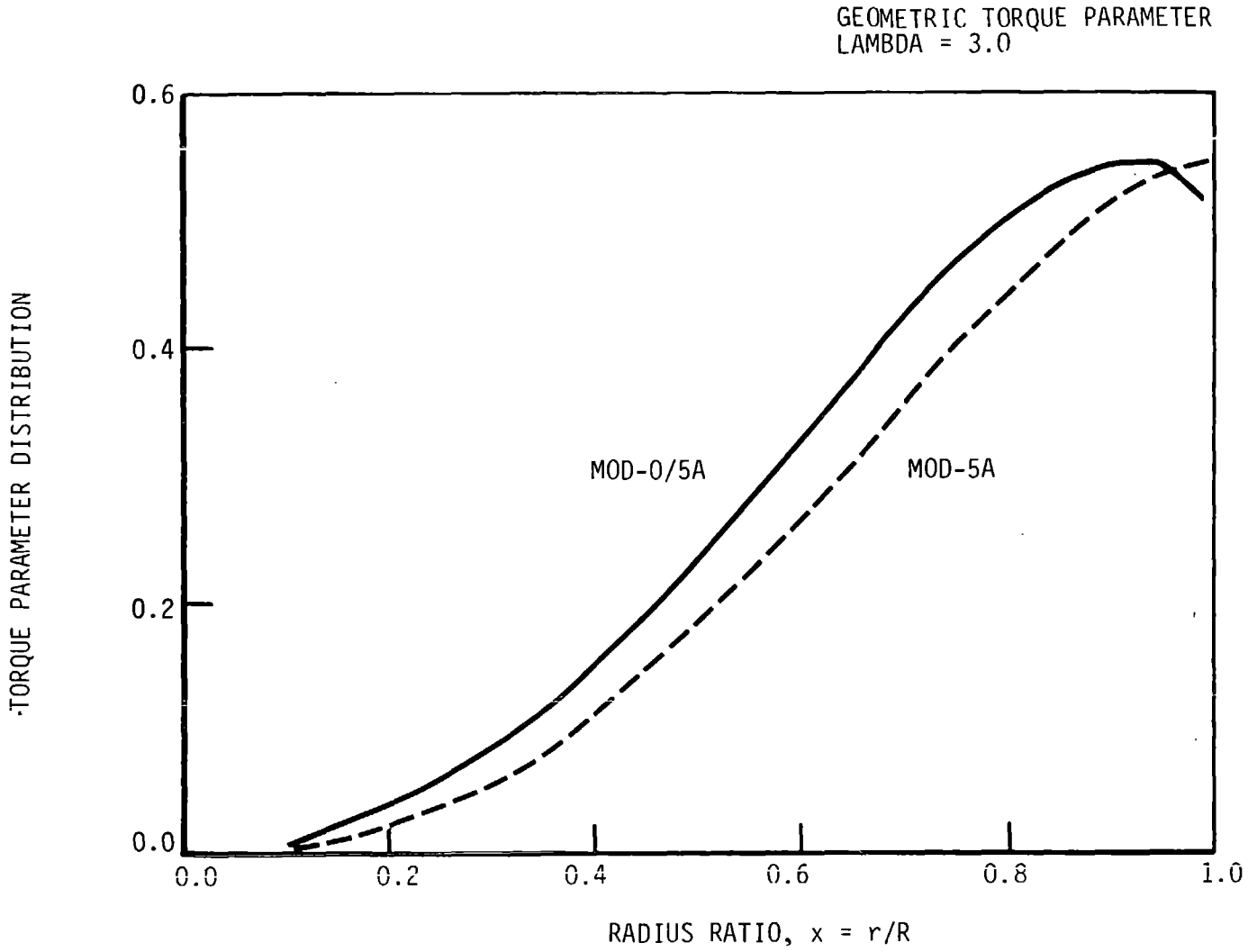

Figure 8-253 Differential Torque Parameter Versus Span for λ = 4.0

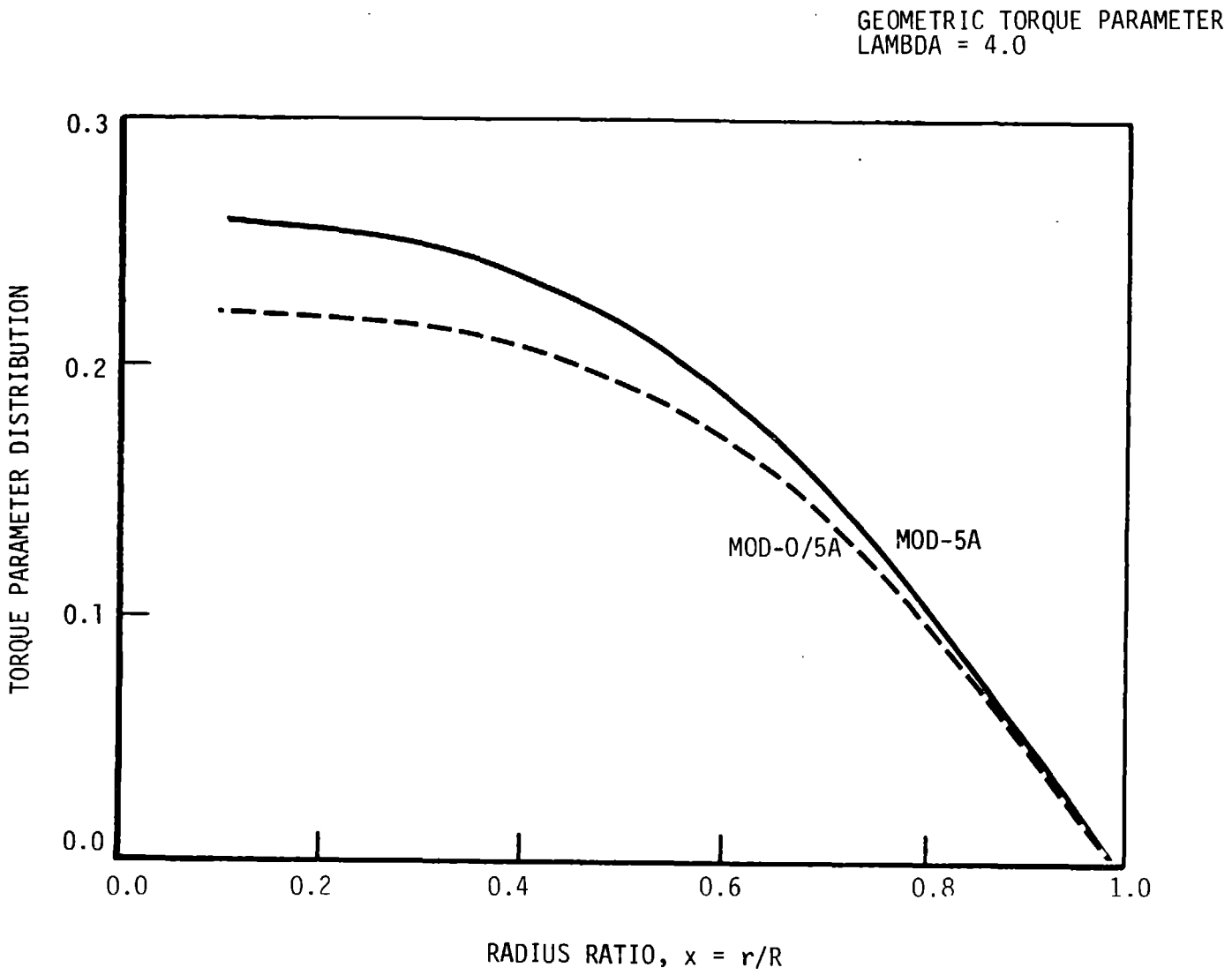

Figure 8-254 Torque Parameter Versus Span for λ = 4.0

The ratio of the relative aileron power effectiveness of the MOD-5A to that of the MOD-0/5A is illustrated in Figure 8-255.

This figure shows that the relative power effectiveness of the aileron geometry of the MOD-5A to the MOD-0/5A increases with increasing tip-speed ratio for low tip-speed ratios. In the region of interest ($\lambda \simeq 1.5$), the geometry of the MOD-5A is about 25% more effective than that of the MOD-0/5A configuration.

A useful extension of this approach was finding an equivalence between the observed equilibrium tip-speed of the MOD-0/5A tests and the corresponding prediction for the MOD-5A. At equilibrium, neglecting the shaft friction, there is no net torque and:

$$Q_I = -Q_A \qquad [8.4.3\text{-}15]$$

that is, in the no-load equilibrium condition, the inboard and outboard torques are equal and opposite. The outboard region torque is the aileron region torque.

Using the notation of equation 8.4.3-13, equation 8.4.3-14 was rearranged as:

$$P_I \cdot \bar{C}_{XI} = - P_A \cdot \bar{C}_{XA} \qquad [8.4.3\text{-}16]$$

$$\frac{\bar{C}_{XI}}{\bar{C}_{XA}} = - \frac{P_A}{P_I} = - R \qquad [8.4.3\text{-}17]$$

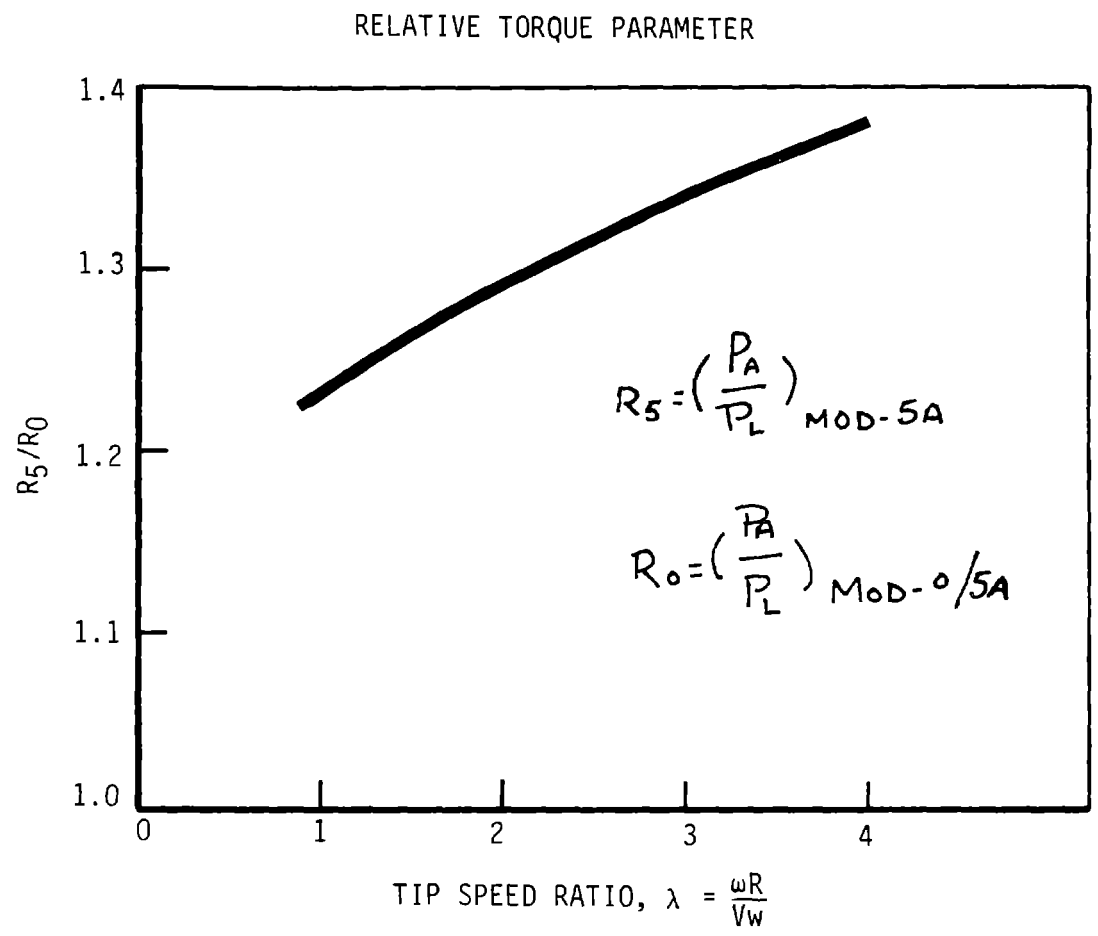

Figure 8-255 Relative Aileron Power

EXTRAPOLATION CHART

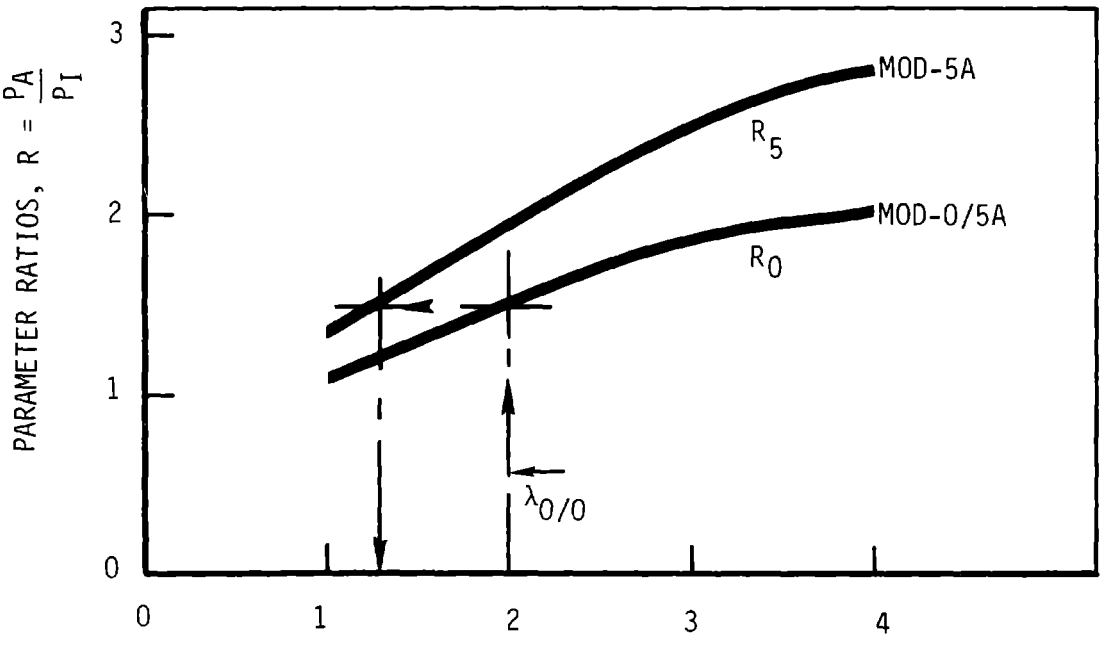

Figure 8-256 Autorotation Extrapolation from MOD-0/5A to MOD-5A

Equation 8.4.3-17 indicates that at no load equilibrium, the relative aerodynamic effectiveness of the inboard region to the aileron region can be evaluated as the negative of the inverse geometric parameter ratios.

Experimental data show that for high angles of attack from 25° to more than 50°, the chordwise force coefficients for clean (δ = 0°) and deflected (δ = -90°) airfoils is nearly constant. It is not a function of angle of attack.

This analysis approach enabled application of test results from the MOD-0/5A geometric configuration to the MOD-5A configuration by assuming that the ratio $\bar{C}_{XI}/\bar{C}_{XA}$ does not change with small changes in tip-speed ratio, or angle of attack. The further assumption that the aerodynamic characteristics of the MOD-0/5A represent those of the MOD-5A is implicit in the basic test program.

Figure 8-255 shows the relative torque parameter ratios of the MOD-0/5A and MOD-5A aileron configuration plotted against tip-speed ratio. In Figure 8-256 the parameters R_5 and R_0 are plotted against tip-speed ratio. The equilibrium tip-speed ratio, $\lambda_{\%}$, measured on the MOD-0/5A at δ = -90°, is shown in Figure 8-256, where $\lambda_{\%}$ = 2.0.

The value of the parameter ratio R = PA/PI corresponding to the measured equilibrium tip speed ratio as indicated on Figure 8-256 at the intersection of the $\lambda_{\%}$ line with the MOD-0/5A line (R ≃ 1.5). The MOD-5A will come to equilibrium at the same value of R. The construction lines on the figure indicate that the MOD-5A will have an equilibrium tip speed ratio of λ = 1.27.

The extrapolation curve shown in Figure 8-257 was constructed from the curves shown in Figure 8-256. This chart may be used to determine the autorotation tip speed ratio predicted for MOD-5A from measured data on MOD-0/5A.

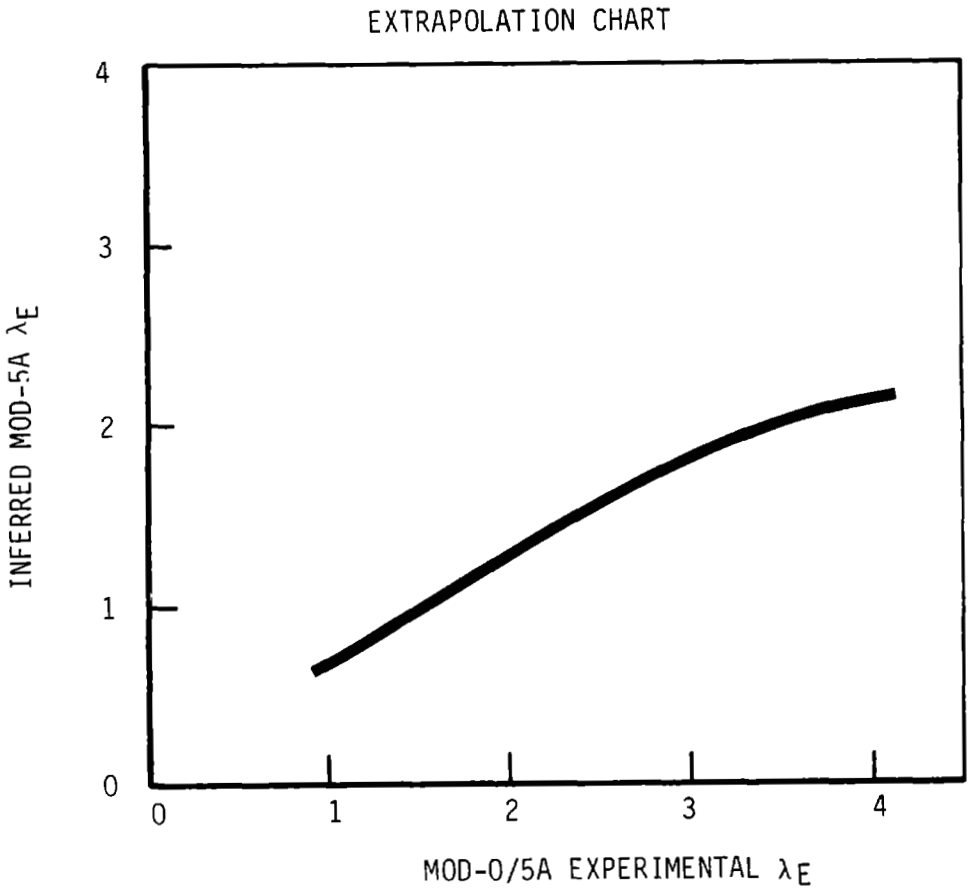

Figure 8-257 MOD-5A Autorotation Speed Versus MOD-0/5A Autorotation Measurements

8.4.3.8 Results and Conclusions

The results of these tests will not be available until the data reduction and analysis discussed in 8.4.3.7 above is complete. When this analyzed data becomes available, the results will be presented and discussed in the final test report.

8.4.3.9 Recommendations

Techniques should be developed for improving the performance of aileron controls in the high wind shutdowns and for failsafe performance.

In the area of high wind shutdowns, high angle-of-attack performance of controls needs more attention. Specifically, the optimization of aileron configuration for high angle-of-attack is a promising area. In a comparison of the two balanced ailerons tested in OSU's wind tunnel, one with 30% chord flap and 20% chord balance was definitely superior to the 38% chord flap with 10% balance. This superiority includes not only the ability to maintain a negative chordforce throughout the angle-of-attack range tested (which BF.38C could not) but also a higher float angle.

The spanwise load distribution at low tip-speed-ratios should also be researched, since it effects not only shutdown performance, but also other wind turbine design quantities.

Devices for providing higher floating angles should also be pursued.

Further recommendations will have to await completion of the work described in 8.4.3.7.

8.5 ELECTRICAL COMPONENT TESTS

8.5.1 CONTROLLER COMPONENT TEST

An EPIAK 700 system was put into operation in March, 1982 to support the controller software development. Approximately 2,000 hours of operation have been accumulated with only one failure. In July, 1982 an analog output module, CP 756, failed during the first operation of the module. This failure would be considered an infant mortality.

In production, a complete check and burn-in test would be performed on the controller. This test would detect any infant mortality failures and repair them before shipment.

8.5.2 CABLE TWIST

8.5.2.1 Test Description

Because of the cost and size of the slipring, another design for transmitting signals and power between the rotating nacelle and the stationary tower was considered. The design positioned all cables around the center of rotation beneath the nacelle and allowed them to twist ±360° over approximately 200 ft. between the nacelle and the ground.

The objective of the test was to demonstrate that the 5 kV power cable and the flexible conduit could survive the reverse bending and the reverse twisting of a simulated, accelerated life cycle without mechanical failure or deterioration of the insulation.

The test used a 20 ft. length of GE #SI-58140-MV-90, 5 kV, 350 MCM cable and a 10 ft. length of Anaconda LA helical conduit with an outer diameter of 2.5 in., which was insulated against liquid. The cable and conduit were mounted to simulate the worst loads. The top ends of the test pieces were clamped to a fixed beam and the bottom ends were clamped to a pivoted beam. The clamps and the pivot points were separated by 12 in. The test set-up is shown in Figure 8-258.

The pivoted beam was oscillated through ±50°, simultaneously subjecting the cables and conduit to twist and to a lateral displacement of ±10.47 in. over the unrestrained length. The test was run for more than 3×10^4 cycles with no visible evidence of a gross failure. The maximum cyclic rate was 10 cycles per minute. All testing was conducted at room temperature, estimated to vary between 65°F and 80°F.

The 5 kV cable was clamped through the insulation, so that the two ends were vertically aligned as they were laterally displaced. In addition, the conductor was clamped as closely as possible to the insulation clamps so that the conductor did in fact twist through the ±50° angle, and did not rotate inside the insulation layer.

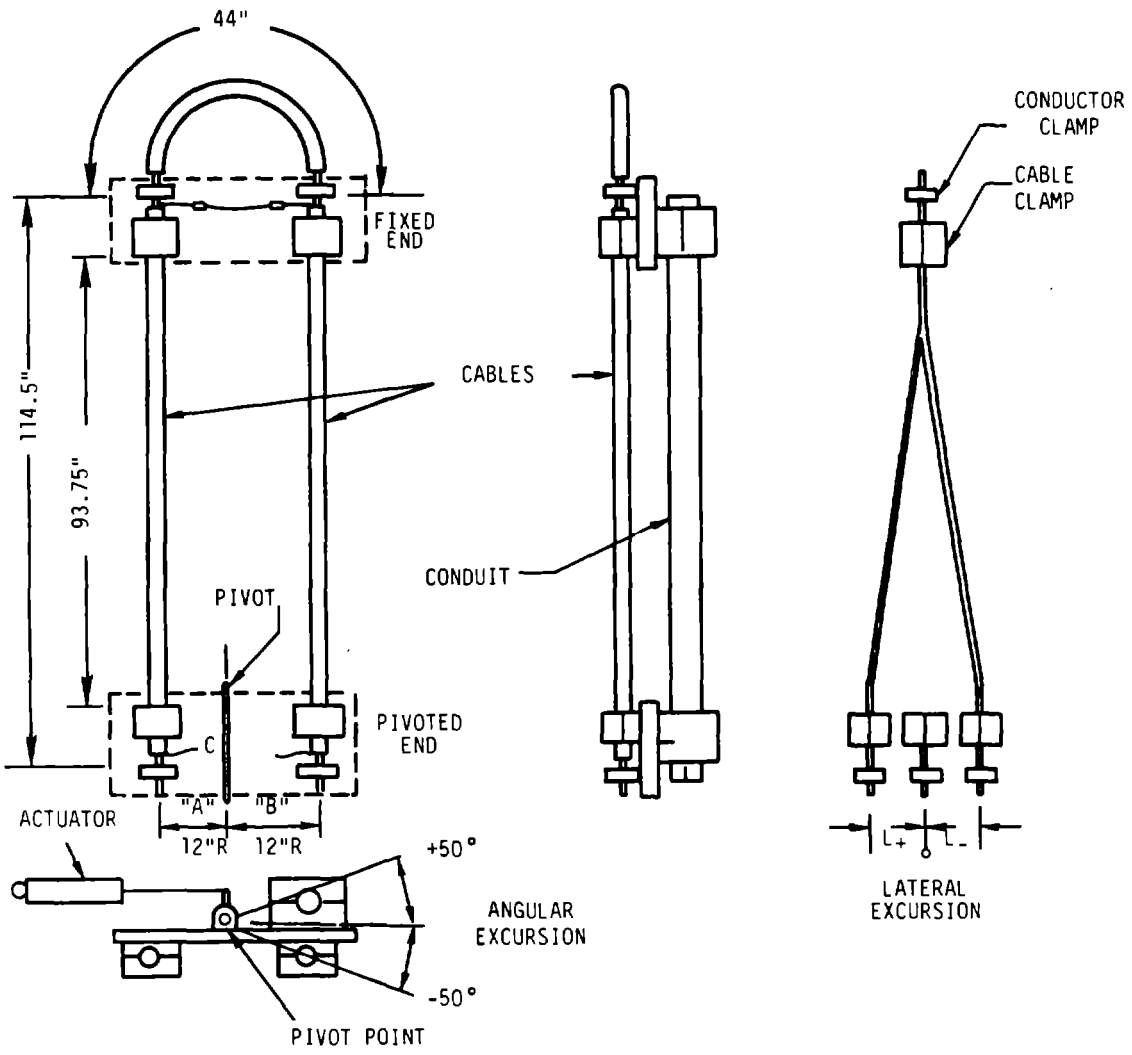

Figure 8-258 Test Set-up

The fatigue test was stopped every 7 or 8 hours to run a 3 kV insulation leakage test from conductor to shield to verify the integrity of the insulation. A resistance measurement was made at the same time to verify the integrity of the conductor.

At the end of the test, the cable was carefully dissected and examined for broken strands or cracked insulation, which would be evidence of mechanical failure.

The flexible conduit was clamped so that the two ends were vertically aligned as they were laterally displaced, and to impart a ±50° twist over the unrestrained length. No wires were pulled through the conduit because the number of conductors and the gage sizes were undefined at the time.

The flexible conduit was visually inspected every 7 to 8 hours for signs of fatigue. It showed no signs of gross failure over during the test.

Cable voltage drop was measured at a constant 10.0 Vdc between points A & B approximately every 7-8 hours, as shown in Figure 8-259. This measurement verified the integrity of the conductor during the test. The data seemed to show an trend towards increasing resistance. However, post test analysis and additional measurements indicated that the variation was caused by fluctuations in the contact resistance caused by changes in clamping pressure at the current leads.

Insulation leakage measurements were made at 3 kVdc between the conductor and shield wires points A&C in Figure 8-259. No measurement exceeded the 1 μA minimum resolution of the leakage tester before, during, or after testing.

The 5 kV power cable was dissected after the test. The inspection looked for broken conductor strands, cracked or failed insulation, and examined the condition of the shield wires. There was no deterioration of the conductor or insulation 4 cable ends, where maximum bending combined with cable twist. The shield wires of 3 out of 4 cable ends just inboard of the clamping area were twisted, displaced, and broken.

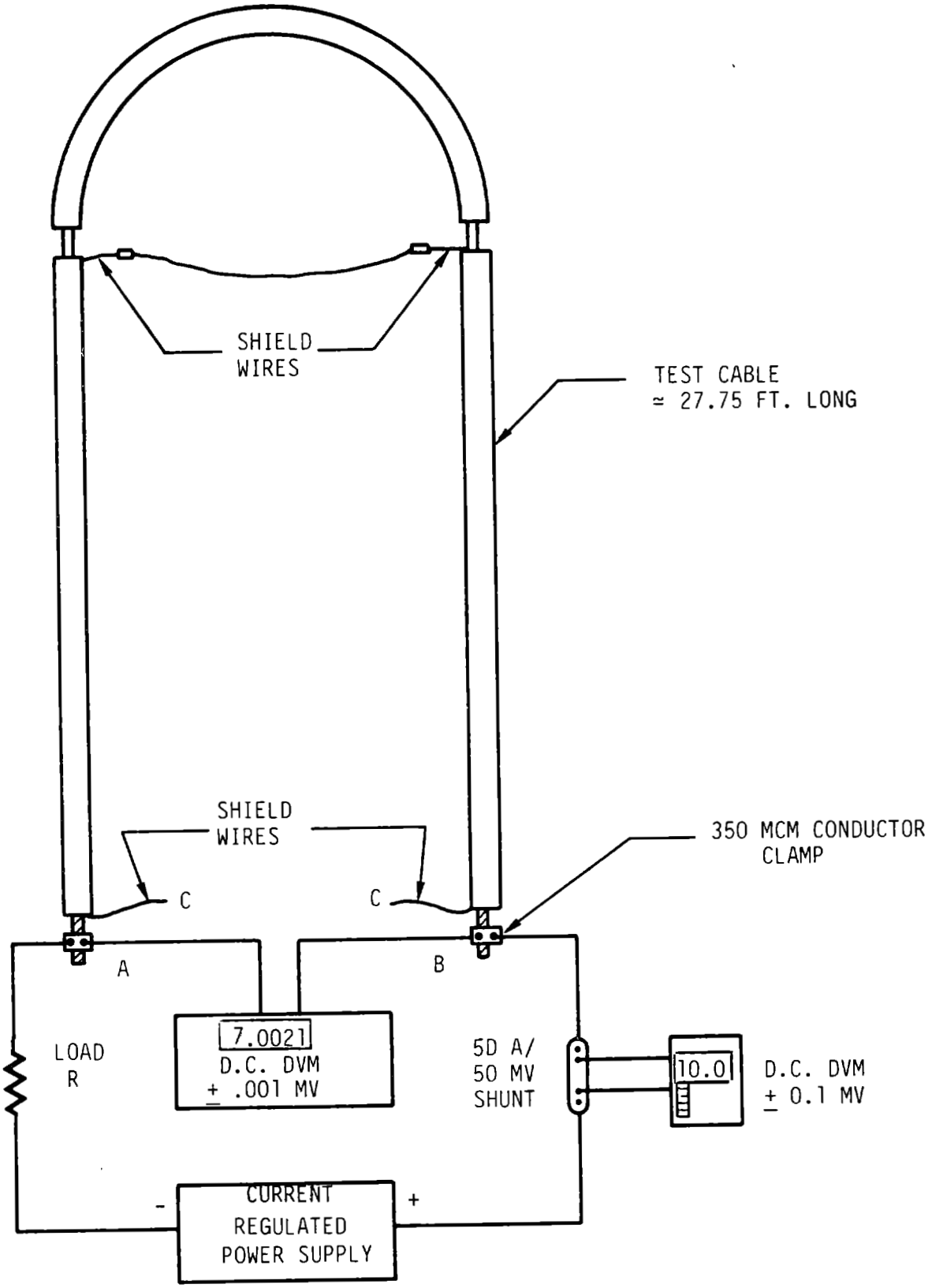

Figure 8-259 Method for Measuring the Resistance

The flexible conduit was dissected after the test. The inspection looked for evidence of mechanical failure, broken or cracked convulitions, or other evidence of fatigue failure.

1) Thermoplastic Jacket:

   There was no difference in the appearance of the outer diameter of the thermoplastic cover jacket before and after the test.

   A fine black powder coated the inner diameter of the jacket just inboard from the clamping location, where the most flexing occurred.

2) Galvanized Steel Core:

   There was no evidence of cracking or failure of the core after removal of the jacket.

8.5.2.2 Conclusions

1) The 350 MCM cable conductor and insulation survived 30,222 cycles with a ±50° twist without visible evidence of damage.

2) Attempts to measure changes in resistance vs. number of cycles were inconclusive, because of changes in contact resistance. The resistance varied between .000096 ohms and .000340 ohms, however, the calculated cable resistance was only .000676 ohms at 20°C.

3) The cable shield wires were displaced, deformed and broken in 3 of the 4 clamping areas.

4) Measurements made before during, and after the tests indicated no measurable current between the conductor and shield at 3 kVdc.

Discussions with a manufacturer of high voltage power cables indicated that a partial discharge or corona test would be a more definitive test for insulation deterioration. Equipment for performing a partial discharge test is available from such companies as James Biddle Co. It is recommended that more conclusive test results could be obtained with this type of test equipment before implementing a cable twist design.

References

1. "GE MOD-0/5A Aileron Test Unit Technical Specification", GE Technical Specification No. 47A380114, Rev A, dated August 1983. (Includes GE Dwg. No. 47J382316, Rev A titled "GE MOD-0/5A Aileron Test Unit).

2. "Aileron Control Schematic - MOD-0/5A", GE Drawing No. 47D382347, Rev A, dated February 1984.

3. "Effects of Aileron Angle on the Noise from the MOD-0/5A," by Kevin P. Shepherd and Harvey H. Hubbard, NASA Contractor Report, to be published.

4. "Test Plan for the MOD-0/5A Aileron Development Test Program", GE Test Plan No. 47A380107 dated November 1983 (transmitted in final form 1/6/84).

5. Abbott, Ira H., von Doenhoff, Albert E., Stivers, Louis S., Jr., Summary of Airfoil Data, NACA FR #824, Washington D.C., 1945.

9.0 DESIGN CRITERIA

9.0 DESIGN CRITERIA

The first MOD-5A specification issued was the "Structural Design Criteria for MOD-5A Wind Turbine Generator". This document defines terminology and procedures that should achieve good structural integrity. Allowable stress values that were developed from the testing of laminated wood have been added to the document. Both structural and dynamic criteria are included in this specification.

The Structural Design Criteria main text is included as Sections 9.1 through 9.6 of this section. It contains detailed definitions of terminology, tables of factors and allowables and a description of the Margin of Safety formula that makes use of factors in the referenced tables. Comments on the criteria are in Section 9.7.

9.1 STRUCTURAL DESIGN CRITERIA

9.1.1 PURPOSE

This document presents the Structural Design Criteria and interpretive information to be utilized for structural design of the MOD-5A Wind Turbine Generator (WTG). Specifically, the objectives of this document are:

- To ensure the structural integrity of the WTG hardware end items.
- To accomplish design and development of the WTG to satisfy this structural integrity with lowest practical cost of energy (COE) and life cycle cost. Specifically, these parameters may be quantified, for the MOD-5A WTG, as the following:

  COE less than 3.75 cents per KWH (1980 Dollars)

  life greater than 30 years (approximately 4×10^8 cycles)

Structural design criteria presented in this document concentrates on the strength, stiffness, and structural performance aspects of the design. It is intended to supplement and expand on general structural design requirements specified in the Statement of Work for the MOD-5A WTG.

It is the intent of this document to establish the requirements for structural design by:

a) Defining the basic design philosophy governing the structural design of the WTG for structural integrity objectives.

b) Defining the criteria or standards that the design structural integrity is based on.

c) Providing the basic design data necessary to perform the structural design.

Structural design criteria presented in this document also establish requirements for the structural analysis documentation and signature approval of formally controlled structural drawings issued through the print control system. The structural analysis approval signature on the drawing signifies the drawing complies with all criteria contained in this document.

9.1.2 SCOPE

This document presents the basic requirements and information governing the strength, stiffness, and structural performance aspects of the structural design for the MOD-5A WTG.

9.2 APPLICABLE DOCUMENTS

The following documents apply to the structural design to the extent specified herein. In case of conflict between this criteria and the documents listed below, the criteria shall take precedence.

1. MIL-HDBK-5C
2. 1980 Structural Welding Code (AWS)
3. 1976 Uniform Building Code (UBC)
4. Specifications of the American Association of State Highway and Transportation Officials (AASHTO)
5. American Concrete Institute Code (ACI) 318-77
6. Manual of Steel Construction, American Institute of Steel Construction (AISC), 8th Edition, 1978
7. Specifications of the American Society of Mechanical Engineers (ASME)
8. Design and Construction of Steel Chimney Liners, American Society of Civil Engineers (ASCE).
9. Specifications of the American Society for Testing Materials (ASTM)
10. Wood Handbook, U.S. Department of Agriculture Forest Products Laboratory

11. Design of Wood Aircraft Structures, ANC-18, June 1951

12. Joining of Advanced Composites, Engineering Design Handbook, DARCOMP 706-316

13. Detection and Repair of Fatigue Damage in Welded Highway Bridges, NCHRP Report 206

9.3 DEFINITION OF TERMS

For purposes of interpreting this document and to achieve unambiguous criteria the following definitions will apply:

9.3.1 GENERAL

Buckling - An instability phenomenon in a column, plate or shell where an infinitesimal increase in the external loading produces a sucden, large, non-linear deformation in the structure.

Creep - A time dependent deformation under load and thermal environments that results in cumulative permanent deformation.

Crippling - A local inelastic deformation (i.e., collapse) of a structural element, plate or shell, substantially reducing the ability of the structure to withstand loads.

Critical - The extreme value of a load or stress, or the most severe environmental condition imposed on a structure during its service life. The design of the structure is based on an appropriate combination of such critical loads, stresses, and conditions.

Design Load Factors - A multiplying factor applied to load (or pressure) to obtain design load (or pressure). Refer to Table 9-1 through 9-4. The application of such factors is defined by the flow chart in Figure 9-1.

Design Gross Weight - For design purposes, the maximum system weight the foundation will be designed to support.

Detrimental Deformations - Deformations, either elastic or inelastic, resulting from the application of loads and temperatures that prevent any portion of the WTG structure from performing its intended function. Examples include structural deformations, deflections, or displacements that: (1) Cause unintentional contact, misalignment, or divergence between adjacent components; (2) Cause a component to exceed its established dynamic space envelope; (3) Reduce the strength or related life of the structure below specified levels; (4) Reduce the effectiveness of thermal protection coatings or shields; (5) Jeopardize the proper functioning of equipment.

Failure Rupture, collapse, seizure, yielding, or any other phenomenon resulting in an inability to sustain design loads, pressures, or environments without detrimental deformation.

Pressure Vessel - A container designed primarily to carry fluids or gases at sustained internal pressure, which may also carry some structural loads.

Structure - All components and assemblies designed to sustain loads or pressures, provide stiffness and stability, or provide support or containment.

9.3.2 LOADS

See paragraph 9.3.7 for definition of terms uniquely related to fatigue.

Limit Load - The maximum anticipated static or quasi-static load on a structure resulting from an expected operating environment.

Design Load - The product of the predicted load and the design load factors.

Allowable Load - The maximum load that can be permitted in a structure for a given design condition. See also paragraph 9.3.4.

Predicted Load - The load expected by best estimate from mathematical models of the transient and steady dynamic response of the WTG mechanical system (including control system interaction, if necessary) in operation, starting, stopping, parked, in storms, caused by seismic response, and also best estimate from models of thermal distortion or moisture distortion.

Proof Test Load - The product of the limit load and the proof test design factor.

Quasi-Steady Load - Maximum expected load factors expressed in gravity units (g) that are intended to generate static loads in the structure equivalent to the worst case of combined effects caused by rigid body and elastic accelerations.

9.3.3 PRESSURES

9.3.3.1 Design Pressures for Pressure Vessels

Limit Pressure - The maximum differential pressure that can be anticipated to occur while the pressure vessel is in service in the expected operating environments. Limit pressures include combinations of such pressures as maximum operating pressure, transient pressure, and head pressure.

Design Pressure - The product of the limit pressure and the design factors.

9.3.3.2 Operating Pressures

Nominal Operating Pressure - The maximum pressure applied to a pressure vessel by the pressurizing system with the pressure regulators and relief valves at their nominal settings and with nominal fluid flow rate.

Maximum Operating Pressure - The maximum pressure applied to a pressure vessel by the pressurizing system with the pressure regulators and relief valves at their upper limit and with the maximum fluid flow rate.

9.3.3.3 Test Pressures

Proof Test Pressure - The product of the limit pressure and the proof factor.

Burst Test Pressure - The pressure at which a pressurized component shall not rupture. The product of the limit pressure and the burst factor.

9.3.4 STRENGTH

Proportional Limit Strength - The stress level at which the material stress-strain relation ceases to be linear. This level is especially applicable to wood and some man-made composites in compression.

Yield Strength - Corresponds to the tensile load or stress in a structure or material at which a permanent set of 0.2% occurs. Not applicable to wood laminae.

Ultimate Strength - Corresponds to the maximum load or stress that a structure or material can withstand without incurring rupture or collapse.

9.3.5 STRESSES

See paragraph 9.3.7 for the definition of stress terms uniquely relating to fatigue.

Allowable Stress - The maximum stress that can be permitted in a material for a given design condition. See also paragraph 9.3.4.

Applied Stress - The structural stress induced by a given applied load and environment.

Design Stress - The structural stress induced by the applied design load.

Predicted Stress - The structural stress induced by the applied predicted load.

Residual Stress - A stress that remains in a structure caused by local yielding or creep after processing, fabrication, assembly, testing, or operation.

Thermal Stress - The structural stress arising from temperature gradients and differential thermal expansion in or between structural components, assemblies, or systems.

9.3.6 MARGIN OF SAFETY

The margin by which the allowable load (or stress) exceeds the design load (or stress) for a specific design condition when all design factors (see paragraph 9.3.1) have been taken into account. Acceptable calculations for margins of safety are defined in paragraph 9.4.2.3.

9.3.7 FATIGUE

Refer to Figures 9-5 through 9-9 for illustrative definitions and symbols pertaining to the following nomenclature.

Fatigue Loads - An applied load, or spectrum of loads, many repetitions of which result in a tendency for a material to fail at considerably less than its ultimate static strength.

Fatigue Stresses - The structural stresses induced by application of fatigue loads, as above defined, and including all stress concentration factors.

Stress Cycle - The smallest division of the stress-time function that is repeated.

Maximum Stress - The highest algebraic value of stress in the stress cycle.

Minimum Stress - The lowest algebraic value of stress in the stress cycle.

Mid-Range Stress - The algebraic mean of the maximum and minimum stress in a cycle.

Stress Range - The algebraic difference between the maximum and the minimum stress.

Alternating Stress - Half the stress range.

Stress Ratio, "R" - The algebraic ratio of the minimum stress to the maximum stress.

Cycles Endured - The number of cycles, at a given stress level, that a part has endured at any time during loading.

Fatigue Strength - The maximum stress that a material can withstand for a given number of stress cycles.

Fatigue Life - The number of cycles that a part can sustain at a given stress level, after which damage or failure is likely.

S-N Curve - A plot of stress vs. cycles to failure.

Endurance Limit - The maximum material stress that can be reversed an indefinitely large number of times without producing fracture. Some materials have no endurance limit and the S-N data must be extrapolated to encompass the number of cycles expected to be applied to the design.

Goodman Diagram. A graphic expression of empirical formula for the endurance limit, alternating stress vs. mean stress.

Constant Life Fatigue Diagram - Similar to the Goodman diagram, but relating the fatigue strength for any given number of cycles to any given range of stress variation.

Stress Intensity Factor - The parameter that characterizes the fundamental concept of linear-elastic fracture mechanics. This parameter, related to both the stress level and the flaw size, defines the stress field ahead of a sharp crack for flat crack propagation. When a particular combination of stress and flaw size leads to a critical value of the intensity factor, unstable crack growth occurs.

Flaw - A crystal imperfection, dislocation, microcrack, lack of weld penetration, etc., resulting from a material imperfection or fabrication technique, such as welding. A conservative approach to fatigue failure prevention is to assume the presence of an initial flaw, dependent on the quality of fabrication and inspection, and analyze the fatigue-crack-growth behavior of the structural member.

Crack Growth Threshold (CGT) - A stress level below which flaw propagation is extremely slow or absent. Important variables include initial flaw size, location of the flaw, shape of flaw, stress distribution, stress intensity range threshold factor, and the arrangement of parts being joined, especially in weldment. Flaw growth occurs when applied stress range exceeds the CGT. When the flaw reaches a critical size, failure is likely.

9.4 GENERAL DESIGN CRITERIA AND PROCEDURES

9.4.1 GENERAL DESIGN PHILOSOPHY

The structure design shall serve to provide the necessary structural support and housing to effectively and efficiently position and environmentally protect the system and subsystem components. The mechanical design shall provide structural integrity with strength and rigidity characteristics adequate to withstand all operational and environmental constraints, and to

withstand all pre-operational environments such as manufacture, ground handling, transportation, and erection, and to achieve minimum practical weight, within the constraints of obtaining a minimum cost of energy.

The WTG structure shall be designed and analyzed to satisfy the stiffness requirements of paragraph 9.4.2.2 and for the loads that result from the critical design conditions and any qualification test levels. The qualification test levels will be intended to demonstrate a structural design of the applicable subsystems that is sufficiently conservative to give a high level of confidence in the reliability of the structure.

Pre-operational conditions and environments shall influence the structural design to the minimum extent possible. Where practicable, means shall be devised for assembling, handling, transporting, and erecting that do not require an increase in the WTG weight over that required for the operational conditions.

9.4.2 GENERAL DESIGN CRITERIA

9.4.2.1 Strength Requirements

At design load, the structure shall have sufficient strength to withstand simultaneously the design loads and the other applicable environments of the design condition without experiencing detrimental deformations (as defined in paragraph 9.3.1), a plastic deformation of 0.2%, or loss of functional capability.

Strength is assessed analytically by comparing design loads (or stresses) with allowable loads (or stresses). See paragraph 9.4.2.3.

9.4.2.2 Stiffness Requirements

When subjected to design loads, the structure or any component thereof shall not experience detrimental distortions. The fulfillment of the strength requirements of paragraph 9.4.2.1 shall not be deemed sufficient in itself to satisfy this requirement.

Resonant frequency requirements will be used to control the dynamic response of the rotor, shaft, drive system, and components and to preclude dynamic interactions with the nacelle, yaw system, or tower. These resonant frequencies will be specified for the primary structure and for critical secondary support structure. The primary structure for any subassembly shall be designed independent of any potential stiffening effect provided by any subsystem component installations. These modules and components will be treated as mass items only and their inertial loads applied to the basic WTG substructures.

9.4.2.3 Margin of Safety

The margin of safety shall be determined at design load levels versus allowable levels, and at the temperatures expected for all critical conditions. A high margin of safety shall not be used as a substitute for the appropriate design factor.

For minimum-weight design, the margin of safety shall be the smallest practicable equal to or greater than zero. The margin of safety shall be calculated by the following equation:

$$MS\ (design) = \frac{\text{Allowable Design Load (or Stress)}}{\text{Design Load (or Stress)}} - 1$$

At the location of minimum margin of safety versus allowable load or stress in each stress analysis of a substructure, the margin of safety between the predicted stress and the material yield strength or proportional limit shall also be reported.

9.4.2.4 Design Load Factors

Design load factors shall be used to account for uncertainties in design that cannot be analyzed or otherwise accounted for in a rational manner. Design factors shall be applied to limit loads and pressures and to the stresses arising from temperature differences and gradients, but not to the temperatures and temperature differences. These factors, as defined below, are to be combined for margin of safety calculations as prescribed by the flow chart of Figure 9-1.

The design load factors shown in Table 9-1 shall be used to obtain the design loads.

The pressure vessel design factors shown in Table 9-2 shall be applied to maximum expected operating pressures to obtain design pressures for all pressure vessels, lines, and fittings.

The configuration design factors shown in Table 9-3 are used to account for uncertainties in load or stress distributions in fittings and joints and variations in the control of welding and bonding processes. The contingency load factors shown in Table 9-4 are used to account for the degree of confidence in the predicted loads.

*DESIGN LOAD = PREDICTED LOAD

X *DESIGN LOAD FACTOR
(TABLE 9-1)

X *CONFIGURATION DESIGN FACTOR
(TABLE 9-3)

X CONTINGENCY LOAD FACTOR
(TABLE 9-4)

$$MS = \frac{\text{ALLOWABLE *DESIGN LOAD}}{\text{*DESIGN LOAD}} - 1.$$

Notes:

* 1. The following may be substituted for the word "DESIGN": "FATIGUE," "PROOF TEST," or "BURST." The more critical of these shall govern the Margin of Safety calculation (see paragraph 9.4.2.3).

2. The following may be substituted for the word "LOAD": "PRESSURE" or "STRESS."

3. For pressure vessels, substitute Table 9-2 for Table 9-1.

Figure 9-1 Design Load Factor Flow Chart

Table 9-1 Design Load Factors

LOAD CONDITION	DESIGN LOAD FACTOR FATIGUE	STATIC
Maximum Wind Loading	---	1.00
Operational Loads	1.00	1.00
System Qualification Test	---	1.00
Transportation, Hoisting & Handling Fittings:		
Hazardous to Personnel	---	4.00
Not Hazardous to Personnel	---	3.00
WTG Structure Critical to Alignment	---	1.15
Tower Overturning (see 9.4.3.3.3 and 9.4.3.4.2)	1.00	1.00

Table 9-2 Pressure Vessel Design Factors

PRESSURE CONTAINER	DESIGN	PROOF TEST	BURST
Hydraulic Systems	1.00	1.50	2.00
Pneumatic Systems	1.00	2.00	3.00

Table 9-3 Minimum Configuration Design Factors

(Not to replace consideration of stress concentrations, eccentricities, etc., that are to be used in estimating the predicted load or stress)

ITEM	FATIGUE*	STATIC**
Fittings	1.00	1.15
Welded Joints	1.00	1.00
Bonded Joints	1.00	1.25
Shear Fasteners	1.00	1.15
Tension Fasteners	1.00	1.25
Stud Capacity in Wood	1.00	1.25
Castings	1.00	1.50
All Others	1.00	1.00
Buckling critical		
Verified by test	1.25	1.25
Analytical only	1.50	1.50

*Subject to AISC Range Stress Limitations, which are based on critical crack-growth thresholds relating to specific stress concentration conditions.

**When two or more configuration factors apply, use the more severe factor, but not both.

Table 9-4 Contingency Load Factors

LOAD TYPE	CRITERIA FOR SELECTION OF LOAD TYPE	CONTINGENCY FACTOR
A	Specified loads derived from analysis in which a high degree of confidence exists because the structural characteristics used in an analysis of the coupled substructures have been based on experimental data obtained from MOD-5A or similar machines.	1.00
B	Loads derived from an analysis that involves complex methods and makes use of detailed structural drawings. The design is frozen, so there will only be small changes in structural details.	1.15
C	Loads derived from analysis that makes use of a simplified mathematical model representative of the structure. Structural sketches or layouts are used to generate the mathematical model. The design is in a state of evolution and there is a high likelihood of changes in structural details.	1.25
D	Loads derived by direct estimates.	*As assigned by Load Analyst
E	Hurricane, Seismic, Maximum overspeed, FMEA	1.0

*Dependent on degree of confidence and design importance of load.

NOTE: MORE SPECIFICALLY, THE LOAD TYPE MAY BE ASSIGNED, BASED ON MOD-5A WTG PROGRAM PLANNING, AS FOLLOWS:

(a) Conceptual Design Phase - Load Types "C" and "D".

(b) Preliminary Design Phase and Final Design - Load Type "B".

(c) After field data available (2nd MOD-5A WTG, or later) - Load Type "A".

9.4.2.5 External Loads

External loads shall be determined by conservative analysis of the design environment, or with appropriate load contingency factors.

9.4.2.5.1 Dynamic Loads

Dynamic loads shall be determined for quasi-static and transient phenomena expected in each design environment. The calculation of all dynamic loads shall include the effects of WTG structural flexibilities and damping, and coupling of structural dynamics with the actuation and braking systems and the external environment. Control system interaction with structural modes shall be included in the determination of the predicted loads.

Iterations of the dynamic loads calculations shall be performed as necessary to reflect design changes and mathematical model refinements. The final set of dynamic loads shall be determined with the use of experimental values of dynamic characteristics as obtained from appropriate tests and modal surveys.

9.4.2.5.2 Contingency Load Factors

The basis for the assignment of the contingency load factor to each load condition is given in Table 9-4.

9.4.3 DESIGN PROCEDURES

9.4.3.1 Reference Axes

Loads are oriented with respect to the coordinate axes shown in Figure 9-2.

9.4.3.2 Symbols

Standard symbols as per the Manual of Steel Construction, AISC, will be employed, unless specifically noted to the contrary. Symbols utilized only in the discussion in paragraph 9.4.3.6.2 on fatigue are per the MIL-HDBK-5C or reference 9-2, paragraph C13.6.

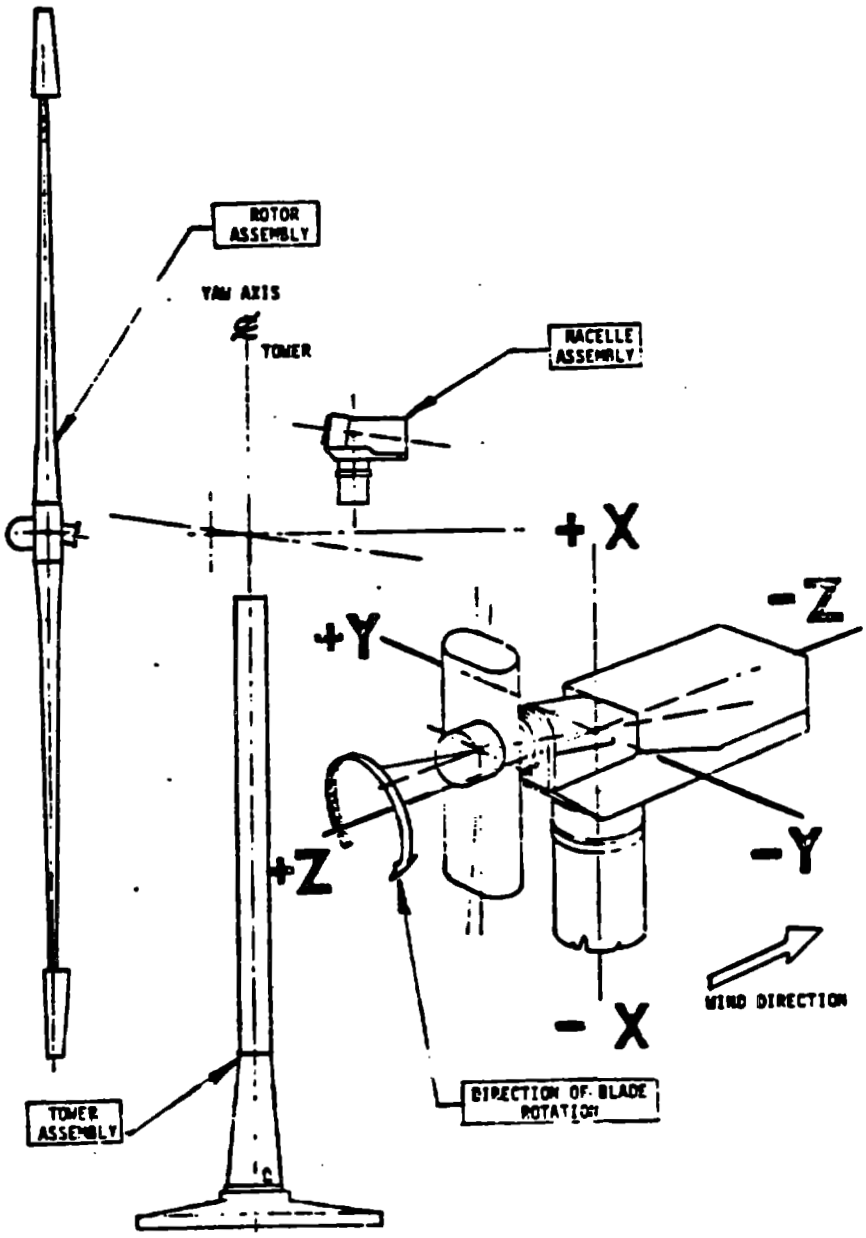

Figure 9-2 Coordinate Axes of MOD-5A WTG

9.4.3.3 Material Static Properties

(See paragraph 9.4.3.6 for Fatigue Material Properties)

9.4.3.3.1 Allowable Mechanical Properties

Values for allowable mechanical properties of structure and joints in their design environment shall be taken from approved sources. The Wood Handbook and ANC 18 shall be used for the wood blade properties, until test data is made available. When values for mechanical properties of materials or joints are not available because they are new or used in a new environment, they shall be determined by approved analytical or test methods. A sufficient number of tests shall be conducted to establish values for the mechanical properties on a statistical basis. The effects of temperature, thermal cycling and gradients shall be accounted for in defining allowable mechanical properties.

In general, the following guidelines apply, subject to modification by the stress analyst.

Steel Static Design Allowables (See AISC Manual of Steel Construction)

The entire AISC specification for the design of structural steel for buildings is helpful as a mature and successful procedure for design allowables in steel. Some important values are listed here.

- Tension and compression: .60 yield
- Shear: .40 yield
- Simple bearing: .90 yield
- Fasteners, bending, buckling and combined stress per the appropriate AISC specification
- For very infrequent or "one time" loads, such as seismic or hurricane, with the permission of the Project Structural Analysis Engineer, the allowable stresses may be increased by .33 as long as minimum yield is not exceeded and no stability criteria are exceeded. Limit loads normally fall in this catagory except when determined by peak fatigue loads, which are "frequent".
  For buckling, the safety factors shall be reduced to 1.15 and 1.35 for test and analysis respectively in lieu of an increased allowable.

Wood Laminae Static Design Allowables - Based on no more than 80% of minimum tested value, where minimum is defined as the lower 2 sigma value of the scatter band, and as documented by the responsible engineer. The effects of size, temperature, rate and duration of load, and moisture content shall be used in converting the minimum test article strength to the design allowable strength for normal operating loads. See paragraphs 9.4.3.6.3 and 9.4.3.6.4 for static and fatigue design allowable stresses. See load Type E in Table 9-4 for abnormal conditions.

Suitable laminae analysis shall be performed in a composite of layers of anisotropic materials at different orientations to one another, or of multiple materials having different moduli. The laminae stresses or strains shall be compared to allowable stresses or strains.

9.4.3.3.2 Component Allowables

Component structural allowables shall be based on applicable component test data or analyses.

9.4.3.3.3 Foundation Properties

The foundation shall be of reinforced concrete design conforming with specifications of the Uniform Building Code 1976 and the ACI Code (documents 3 and 5). Concrete shall have a minimum 3000 psi compressive strength at 28 days. Constituents shall conform to or exceed the following specifications:

ASTM C 150 type I Portland cement
ASTM C 33 concrete aggregates
ASTM A615 Grade 60 (reinforcing steel)

If designed for yielding soils, the foundation shall use a net allowable soil bearing value substantiated by an adequate soils investigation. Expected settlements and the effects of cyclic loading must be addressed in the soils investigation.

The net allowable soil pressure will have a factor of safety of 3.0 against bearing capacity failure. After site selection the actual soil capacity will be measured and the allowable pressure set at 1/3 of the actual static capacity. The preliminary design soil allowable pressure of 4000 lb/sq. ft. is 1/3 of the expected soil static bearing capacity.

Under normal operating loads, the maximum toe pressure from applied loads shall not exceed the assumed 4000 lb/sq. ft. net allowable bearing value of the soil. The net toe pressure includes weight of structure, and overturning moment caused by normal operating loads. No uplift is allowed under normal loading conditions.

The foundation must have sufficient fatigue strength to withstand normal operating loads. See references 9-8 and 9-9. The maximum toe pressure shall not exceed 1.33 the assumed net allowable bearing value of the soil (4000 lb/sq. ft.) under very infrequent operating loads. The net toe pressure includes the weight of the structure, and overturning moment caused by abnormal operating loads. Very infrequent loading is considered non-cyclic in nature with occurrence spaced years apart.

9.4.3.4 Buckling, Crippling, and Other Instabilities

9.4.3.4.1 Buckling and Crippling

Structural components loaded in compression that are subject to buckling (primary instability) or crippling (local instability) shall not fail under design load. Nor shall deformation from design loads reduce the functioning of any system or produce changes in loading that are not accounted for. Maximum crippling stresses are cut off at the material compressive yield strength unless test results are obtained to substantiate the use of higher crippling stresses. Usage of the AISC criteria for "Compact Sections" (per section 2 of document 8 (see section 9.2) and Specification paragraph 1.5.1.4 will generally preclude the necessity for calculating local crippling allowables for sections normally used as columns or beams.

Structural panels or webs loaded in compression or shear shall not undergo initial compression or shear buckling at design load. References 9-1, 9-2, or 9-3, and document 10 (see section 9.2) provide acceptable criteria for calculating panel buckling allowables.

9.4.3.4.2 Tower Overturning

The foundation shall be designed so that no uplift occurs at any point on the base for normal design load condition, when the structure is founded on a yielding base. All base materials except solid rock and hard shale shall be considered as yielding. The soil dead weight directly above the foundation slab and structural weight, both inside and outside the ringwall can be used to resist the uplift.

With very infrequent loading, such as a hurricane, the point of zero soil pressure is allowed to be as much as 1/3 the diameter measured radially inward from the circumference of a spread footing or tangent to the ringwall, whichever provides less uplift. The maximum toe pressure shall not exceed 1.33 x the allowable soil pressure (as determined by in situ or laboratory measurements or both) under these very infrequent conditions. Very infrequent loading is considered non-cyclic in nature with occurrence spaced years apart.

9.4.3.5 Structural Non-Linearities

The structure shall possess "linearity" to a degree that will allow accurate prediction of its behavior at any time. Important types of non-linearities that should be avoided or minimized are adverse non-linearities in energy dissipating mechanisms, mechanical backlash, and to a certain degree, elastic shear buckling in structural elements.

9.4.3.6 Fatigue Material Properties

Consideration shall be given in the design of the WTG structure to ensure good fatigue design characteristics. Caution shall be exercised to reduce residual stresses, and stress concentrations, and to avoid poor surface finishes. Post-weld heat treatments (PWHT) shall be used wherever practical for all weldments. Materials and structural details utilized shall exhibit satisfactory fatigue characteristics, with allowables below the crack growth threshold (CGT) as the preferred approach. Since fatigue design will probably be the design driver for the rotor, hub and drivetrain, and to some extent, certain areas of the nacelle, bedplate and the yaw system, the following fatigue design guidelines shall be followed:

1. Use steels with adequate notch toughness (see paragraph 9.4.3.6.1 and Table 9-5).

2. Use CGT fatigue allowables based on AISC fatigue allowables for "Condition 4", if the part receives a PWHT, otherwise use the root-mean-cubed (RMC) method.

3. Assume a maximum permissable flaw size approximating 0.100 in. in all welded joints, and call out appropriate inspection requirements to reject flaws larger than 0.100 in.

4. Use material development tests to establish fatigue allowables in materials other than steels.

9.4.3.6.1 Fatigue Allowables - Steels

To ensure adequate fracture toughness and fatigue resistance for steels utilized in the WTG design, they shall initially meet the Charpy Vee-Notch (CVN) test requirements of the American Association of State Highway and Transportation Officials (AASHTO) specifications of Table 9-5. The WTG operating regime (-40°F to +120°F) corresponds to Zone 3 of the AASHTO Specification, and most steels are anticipated to be in the low to medium strength ranges. These CVN requirements should be met or exceed in qualification of base metal and weld joints. Test samples taken from weld joints should include weld metal and the heat affected zone.

The AASHTO CVN requirements are based on empirical data that implies that the Nil-ductility transition (NDT) temperature for intermediate strain rates (10^{-3} sec^{-1}) will be about 50-120°F below the AASHTO test temperature. This rate is consistent with WTG operational loading. Steels selected on this basis should also meet additional requirements as listed in Table 9-5.

9.4.3.6.1.1 Steel Weldments With PWHT

Allowable stress ranges, derived from test data and supported by linear elastic fracture mechanics analysis, applicable to base metal and various welded joint configurations are defined by the 1978 AISC Specification Appendix B of document 6, and are outlined in Table 9-6. Figure 9-3 is included to illustrate various joint configurations.

Examples of welded joint configurations to be avoided are as follows:

1. Don't attempt to carry a tensile load through a material thickness in the development of a rigid welded joint. This configuration of load and joint may result in a laminar tear in the material thickness.

2. Don't weld closure members (ribs or bulkheads, for instance) in a closed cell section. Weld shrinkage in this case may result in dimpling the skin of the closed cell, precipitating an early buckling failure, laminar tearing or both.

Illustrative examples appear in Figure 9-4.

Table 9-5 AASHTO Notch-Toughness Specifications for Bridge Steels

ASTM Designation**	Thickness (in)	CVN Impact Value, ft lb		
		Zone 1*	Zone 2*	Zone 3*
A36		15 @ 70°F	15 @ 40°F	15 @ 10°F
A572	Up to 4 in. mechanically fastened	15 @ 70°F	15 @ 40°F	15 @ 10°F
	Up to 2 in. welded	15 @ 70°F	15 @ 40°F	15 @ 10°F
A440		15 @ 70°F	15 @ 40°F	15 @ 10°F
A441		15 @ 70°F	15 @ 40°F	15 @ 10°F
A242		15 @ 70°F	15 @ 40°F	15 @ 10°F
A588	Up to 4 in. mechanically fastened	15 @ 70°F	15 @ 40°F	15 @ 10°F
	Up to 2 in. welded	15 @ 70°F	15 @ 40°F	15 @ 10°F
	Over 2 in. welded	20 @ 70°	20 @ 40°F	20 @ 10°F
A514	Up to 4 in. mechanically fastened	25 @ 30°F	25 @ 0°F	25 @ -30°F
	Up to 2.5 in. welded	25 @ 30°F	25 @ 0°F	25 @ -30°F
	Between 2.5 - 4 in. welded	35 @ 30°F	35 @ 0°F	35 @ -30°F

* Zone 1: minimum service temperature 0°F and above.
Zone 2: minimum service temperature from -1°F to -30°F.
Zone 3: minimum service temperature from -31°F to -60°F.

** If the yield point of the material exceeds 65 ksi, the temperature for the CVN value for acceptability shall be reduced by 15°F for each increment of 10 ksi above 65 ksi.

Additional Parameters Recommended For Any Candidate Steel

1) Intermediate strain rate ($10^{-3}sec^{-1}$) NDT temperature shall be less than -40°F.

2) Stress corrosion cracking stress intensity threshold (K_{ISCC}) should exceed 50 ksi $\sqrt{IN}$ at room temperature (most steels with a minimum tensile yield point greater than 150 ksi are prohibited by the above requirements)

3) K_{IC} (ASTM Method E399) or K_c should exceed 100 ksi $\sqrt{IN}$ or [Tensile Yield Point (Method E8)] times $\left[\frac{\text{plate thickness}}{2.5}\right]^2$

whichever is greater

Table 9-6 Allowable Stress Range Related to AISC Code (1978 Edition)
For Configuration with PWHT

CATEGORY [NOTE (1)]	ALLOWABLE MAXIMUM FATIGUE STRESS RANGE				
	R<0.1 S_r(ksi) RANGE	R=0.2 S_r	R=0.4 S_r	R=0.6 S_r	R=0.8 S_r
A	24	21.05	16.74	12.42	8.12
B	16	14.04	11.16	8.28	5.41
C	10	8.77	6.97	5.17	3.38
C*	12	10.53	8.37	6.21	4.06
D	7	6.14	4.88	3.62	2.36
E	5	4.39	3.99	2.09	1.69
F	8	7.02	5.58	4.14	2.72

NOTES:

1) "Categories" conform to Appendix B Manual of Steel Construction, 8th Edition. Configurations not conforming shall be individually evaluated.

2) R = Minimum Stress/Maximum Stress

3) The flaw detection size requirement shall be smaller than the size related to S_r, by fracture mechanics formulae, considering the local stress state and the propagation threshold versus R

4) S_r is Maximum Stress - Minimum Stress even if part of the time history is compressive

5) Post weld heat treatment is required to assure applicability of these allowables

6) C*: Permitted if stiffener is less than the thickness of main sheet or flange. Otherwise revert to C.

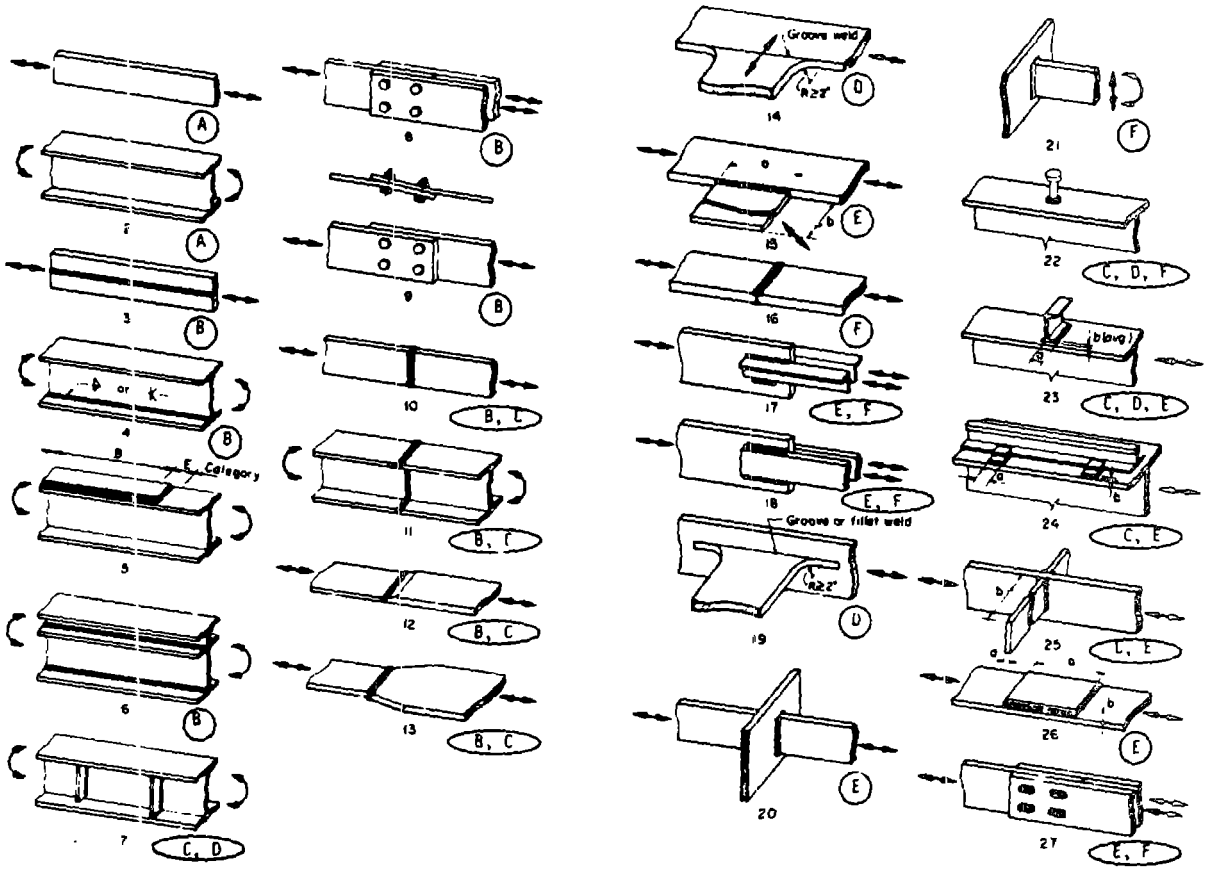

See AISC Code (Document 6) Table B2 and Document 13 for further description of weld categories

Figure 9-3 Illustrative Examples

Case 1 Rigid Weldment

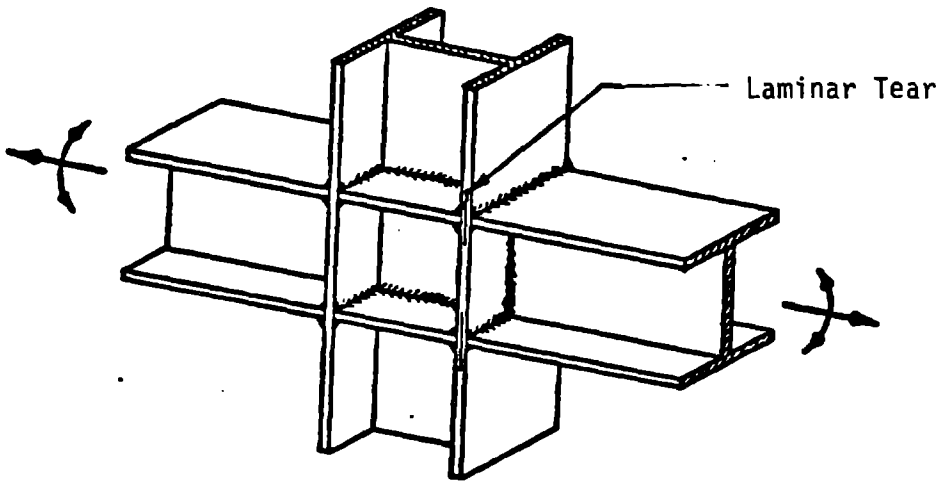

Case 2 Closed Cell

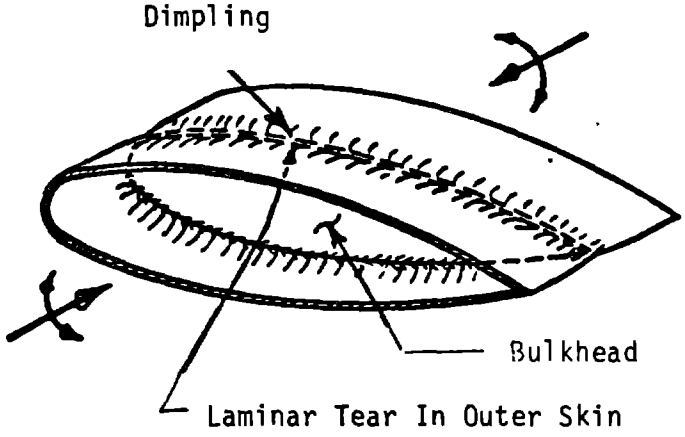

Notes: 1) Avoid intersecting welds as much as possible (coping helps).

2) Avoid details subject to displacement induced cracking such as local attachments to webs

3) Avoid the use of backing bars.

Figure 9-4 Illustrative Examples of Joints to be Avoided

9.4.3.6.1.2 Steel Weldments Without PWHT

Table 9-7 provides allowable stress criteria based on the RMC method for weldments without PWHT that conform to configuration categories defined in the AISC Specification. Other configurations will be considered individually.

9.4.3.6.2 Fatigue Allowables for Multiple Environments

WTG designs must be concerned with two types of interrelated failures: brittle failure and fatigue, which is normally related to welded joints. Generally speaking, as stated in reference 9-4, if a design for fatigue is adequate, brittle fracture considerations are often secondary; therefore, adequate fatigue analysis is mandatory for the multiple loading environments experienced by a WTG. Avoidance of brittle fracture away from welds at stress below strength allowables does require adequate toughness and separate design consideration. Dynamic analyses will be performed evaluating these multiple loading systems, with the output as loading histograms. From these will be developed stress histograms relating summaries of stress levels versus their respective numbers of occurrences. An assessment of the R value to be used in setting fatigue allowables will be made by the stress analyst.

References 9-4 and 9-5 present a LEFM approach, in which a known initial flaw size is assumed to be 0.100 in., and a crack growth threshold determined.

Fatigue characteristics and terminology are discussed in paragraph 9.3.7. Figure 9-5 illustrates the construction of a modified Goodman diagram for subsequent usage in the preferred fatigue analysis. This technique is outlined by Figure 9-6. Figure 9-7 illustrates S-N curves from the AISC code that are applicable to the MOD-5A WTG.

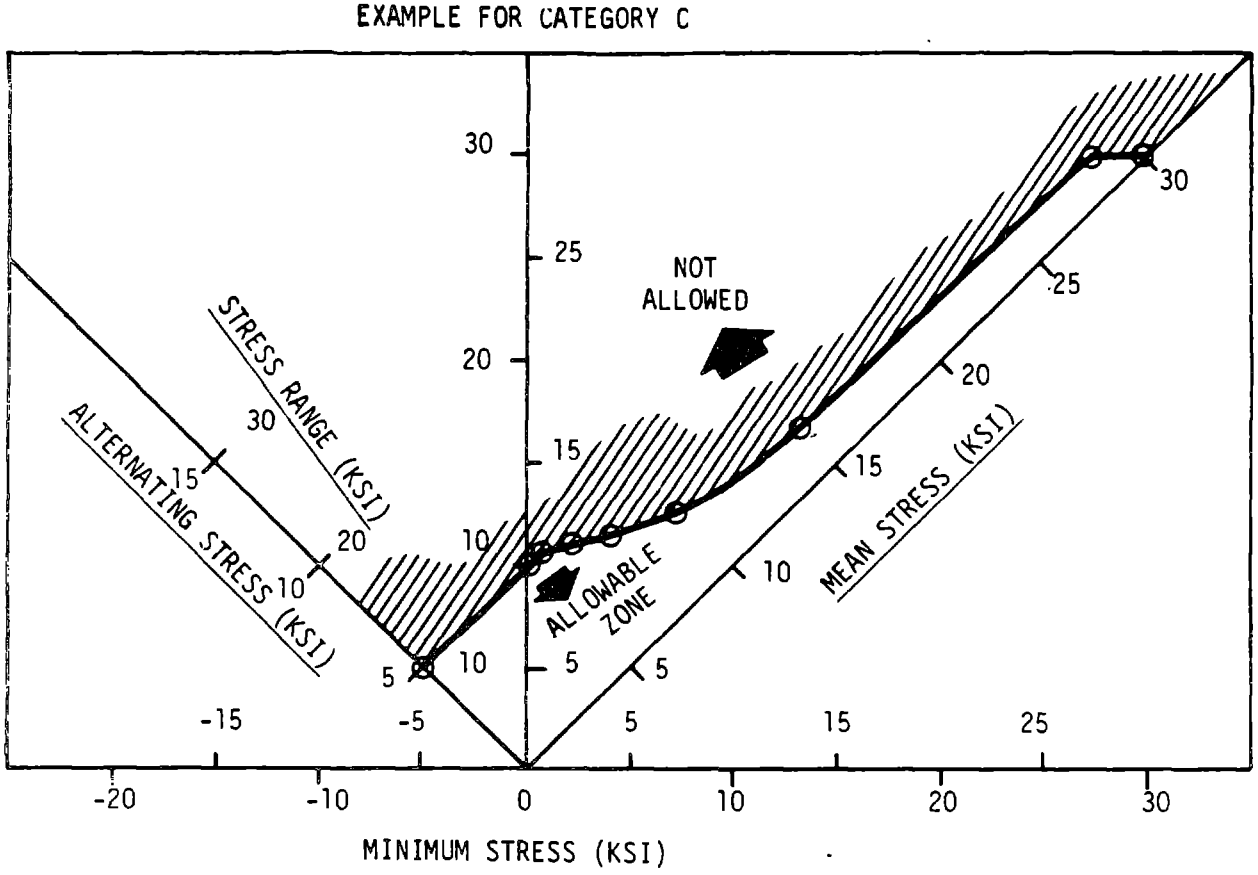

Figure 9-5 Allowable Stress Diagrams For Bridge Construction Steel Alloys (Table 9-5)

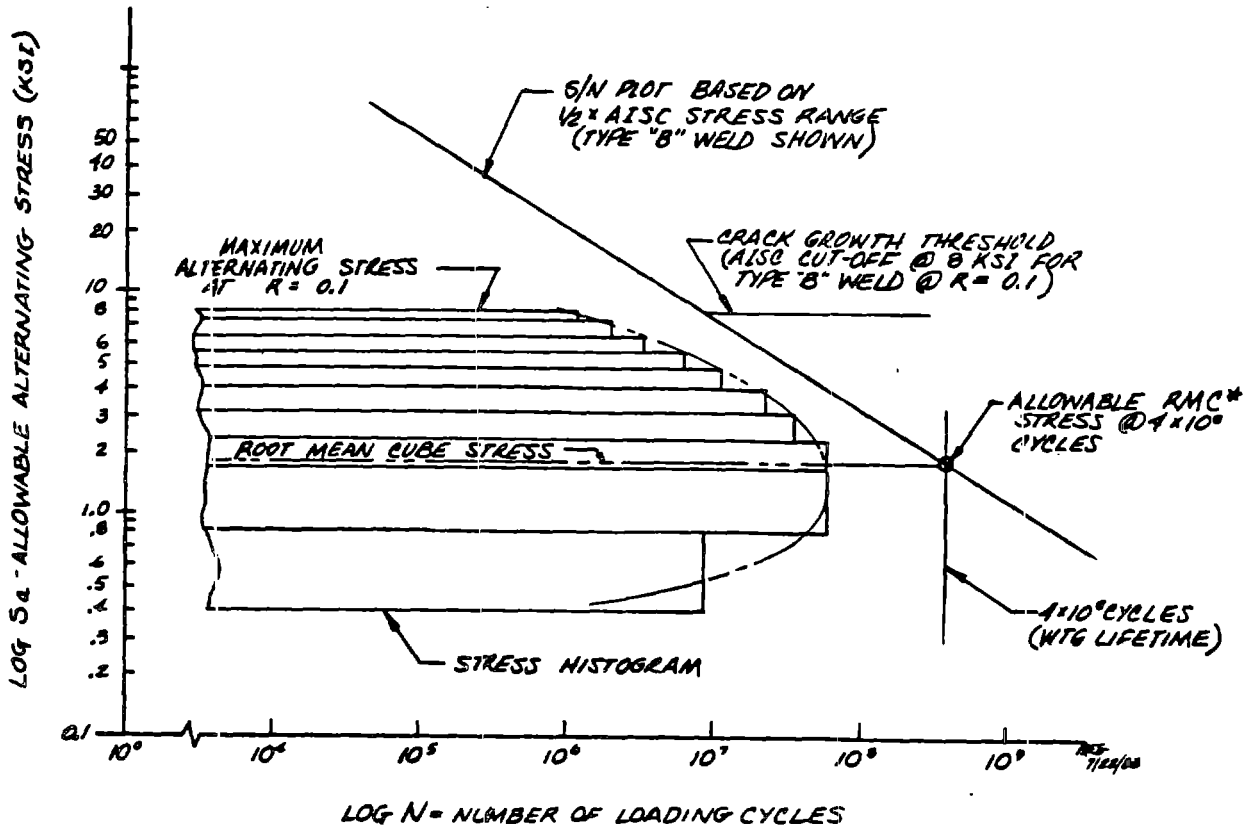

NOTES:

1. S-N Curve and Crack Growth Threshold allowables are dependent on S_{min}/S_{max} ratio.

2. All cycles of the stress histogram must lie below the Crack Growth Threshold. The CGT has been previously derived from a Linear-Elastic Fracture Mechanics Analysis (LEFM), assuming an initial flaw size (2a) of 0.100 in. See Table 9-6 for CGT allowables versus R value. If some stress cycles are above the Crack Growth Threshold, then follow note 3.

3. The root mean cube of the stress histogram must lie below the extrapolated S-N Curve if the stress range exceeds the CGT or if no PWHT is used. This assumes the RMC stress is an equivalent constant amplitude stress. This criteria only applies if note 2 is not met. RMC procedure is equivalent to Palmgren-Miner cycle ratio summation, being less than 1 when the S-N curve has a slope of -3.

Figure 9-6 Effect of Fatigue Spectrum

Table 9-7. Allowable RMC Stresses in ksi without PWHT for Fatigue Life Longer than 4 X 10^8 Cycles

CATEGORY (NOTE 2)	Allowable Alternating CIS At Various A- Values A = 1 (R = 0)	A=0.5 (R=0.33)	A=0.1 (R=0.818)
A	2.07	1.99	1.51
B	1.58	1.53	1.23
C, C*	1.124	1.10	0.935
D	0.868	0.854	0.751
E	0.692	0.683	0.616
F	0.934	0.917	0.800

Notes:

(1) The RMC Design alternating stress must not exceed the above values if there is no PWHT

(2) Categories are defined by AISC Manual of Steel Construction, 8th Edition

(3) Configurations not defined by note (2) shall be considered individually

(4) CIS = Total Cycle Intercept Stress found by extrapolation of S-N data to the number of cycles in the applied stress histogram

(5) $A = \frac{\text{RMC alternating stress}}{\text{average mean stress}}$

(6) $RMC = [\Sigma(s_{a_i}^3 n_i)/\Sigma n_i]^{1/3}$

(7) The maximum stress range in the histogram must be compared to the CGT allowables of Table 9-6. Flaw growth analysis shall be used to evaluate stresses in excess of CGT, Table 9-6.

(8) Table 9-7 is not effected by parent material yield point

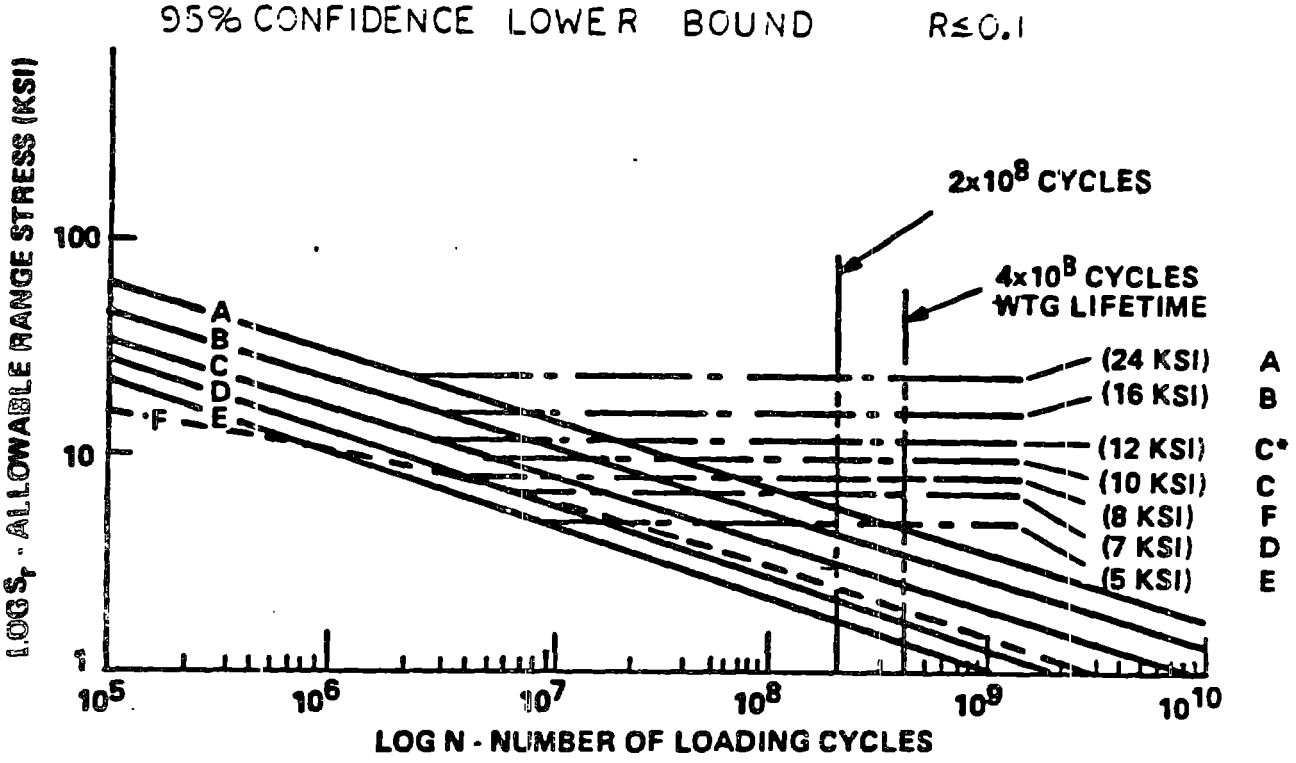

See Table 9-6 for extrapolation to other R-values

Figure 9-7 S-N Curves For Various Weld Categories

C - 7

9.4.3.6.3 Wood Allowable Stresses

Each component of stress caused by the combined design loading must be less than the allowable values in Table 9-8 and Figure 9-8. In conceptual design the 99.9th percentile of the histogram of operating stress should be below the fatigue test data strength extrapolation for 4 x 10^8 cycles considering the MOD-5A moisture content, temperature, size, R-value, and duration of load versus those parameters in the material test program. Miner's ratio may be used with S-N data including stress ratio effects for detailed analysis of fatigue in the Final Design.

For a stud bonded in a prepared hole parallel to the grain, allowable loads are given in Figure 9-9. The compressive mean side does not have reflective symmetry with the tensile mean side of Figure 9-9.

9.4.3.6.4 Glass Fiber Reinforced Plastic Allowable Stresses

Each component of stress caused by the combined design maximum or limit loading must be less than the strength reported in MIL-H-17 by the proportions listed in Table 9-9, until more applicable data is available.

The 99.9th percentile maximum stress in the fatigue stress histogram should, for conceptual design, lie within the boundaries in Figure 9-10, which were derived by extrapolation of data in MIL-H-17. Damage accumulation methods considering the effect of stress ratio may be used during detailed analysis. Duration of load data shows that if the maximum steady stress is less than 60% of proportional limit stress, or of ultimate in tension, then no creep should occur.

If room temperature curing resins are used, allowables shall be based on applicable test data.

Table 9-8 Douglas Fir (Coastal) Laminated Veneer Allowables at 10% Moisture Content, Blade Grade 1*

	Allowable Stress (psi)		
Parallel To Grain	Working	Fatigue at 4×10^8 Cycles	
		R = -1	R=+1
Tension	4100	±1280	3200
Compression	-4430	±1280	-3710
Shear LT	900	±300	730
Shear LR	1139	±300	730
Perpendicular To Grain			
Tension R	190	±60	150
Tension T	100	±30	75
Compression R	-230	-120**	-200
Compression T	-440	-260**	-330
Shear RT	110	±40	90

* Blade Grade 1 is selected ultrasonically for modulus greater than 2.45×10^6, and is used for the more highly stressed applications. The allowables for Blade Grade 2 are to be determined.

Failure modes and effects studies may use stress levels for full-scale minimum proportional limit or ultimate strength, depending on orientation of stress, which are approximately 1.5 times the "working" allowable maximum stresses.

**These values are for the noted compressive minimum stress and a zero maximum stress.

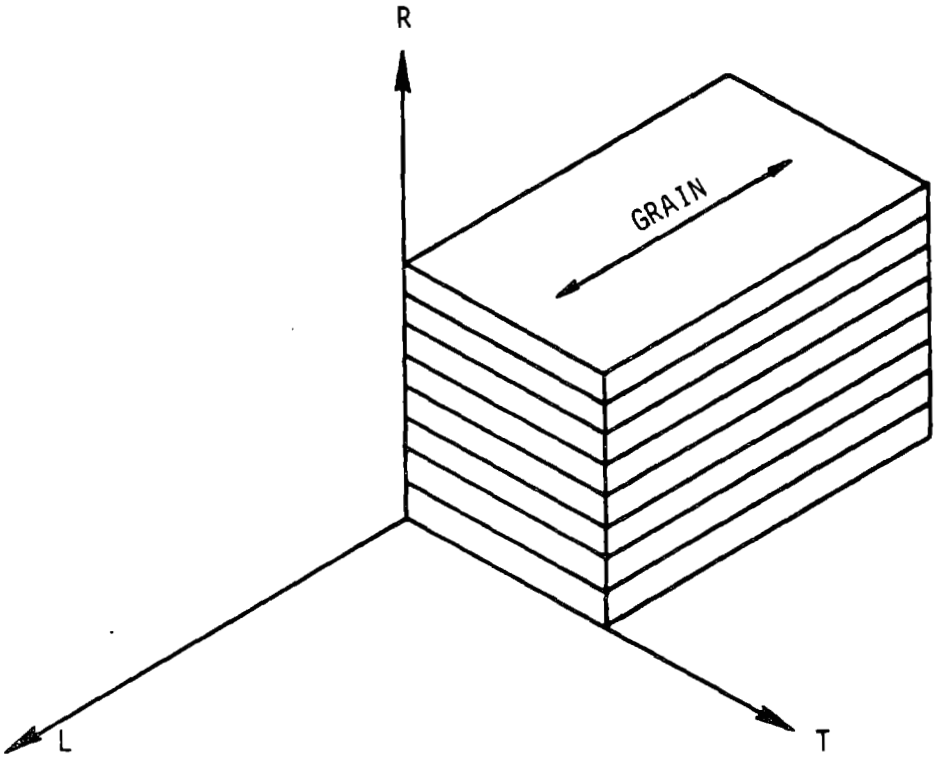

L = LONGITUDINAL
R = RADIAL
T = TANGENTIAL

a) Nomenclature

Veneers are tangential slices from timber by peeling 1/10 inch layer from rotating log.

Laminations are composed of veneers which are in the LT plane.

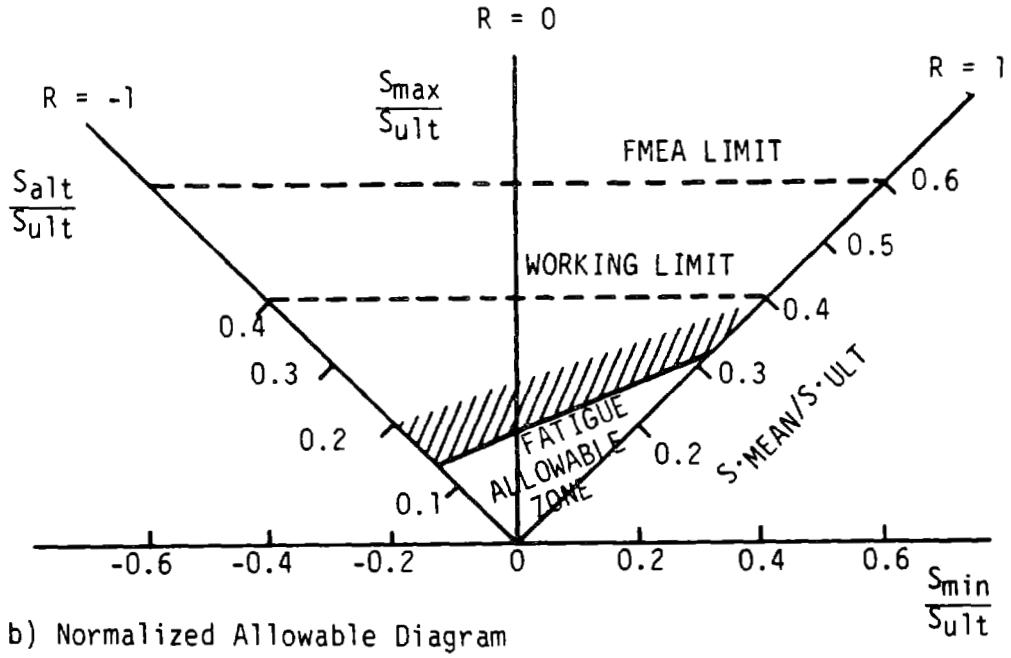

b) Normalized Allowable Diagram

Figure 9-8 Wood Nomenclature and Normalized Goodman Diagram

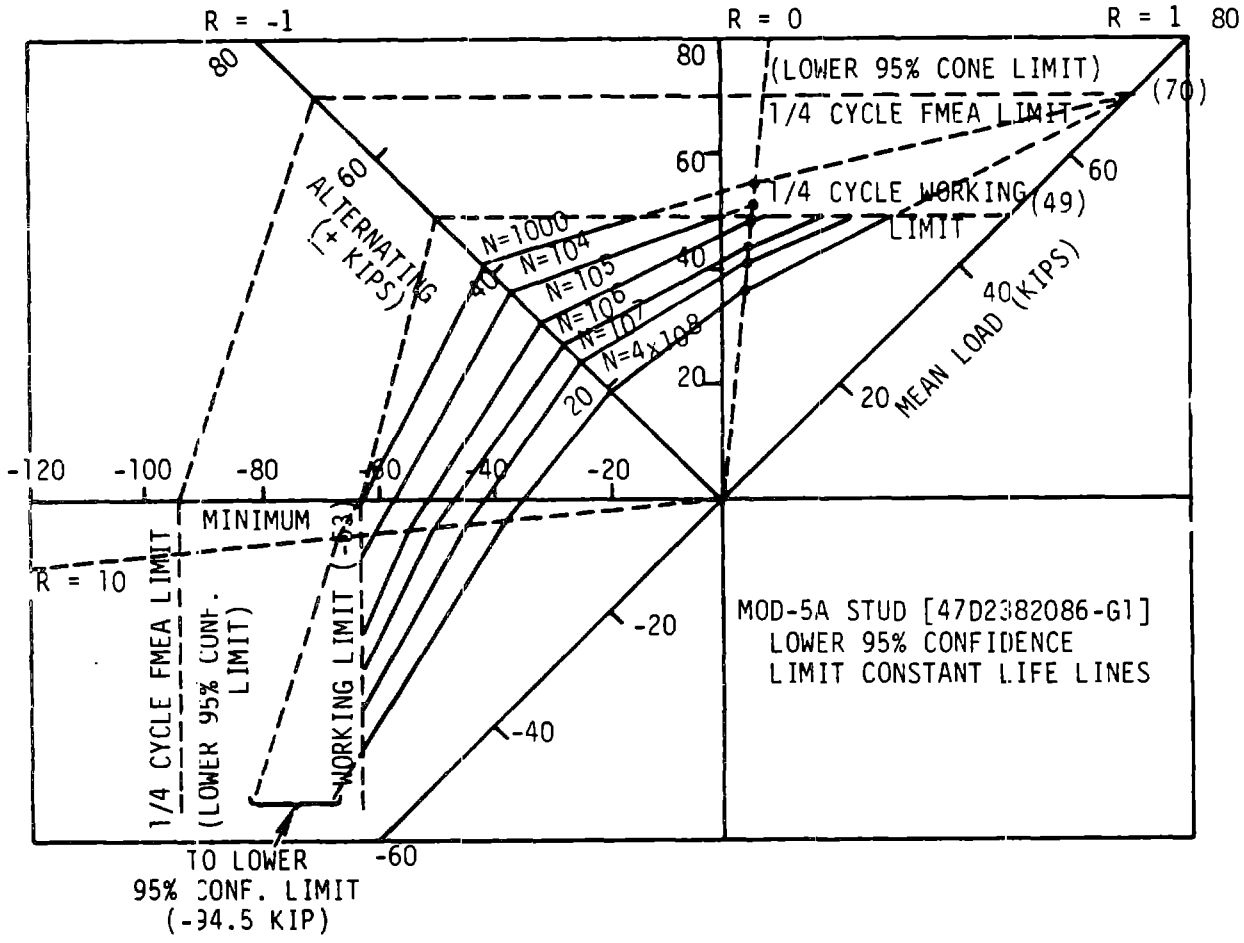

Figure 9-9 Stud Design Allowable

Table 9-9 Glass Fiber Composite Static Strength
Factor of Safety Requirements
(All Temperatures)

$\frac{\text{Ultimate Strength}}{\text{Maximum Design Stress}}$	> 3.0
$\frac{\text{Proportional Limit Stress}}{\text{Maximum Design Stress}}$	> 2.0

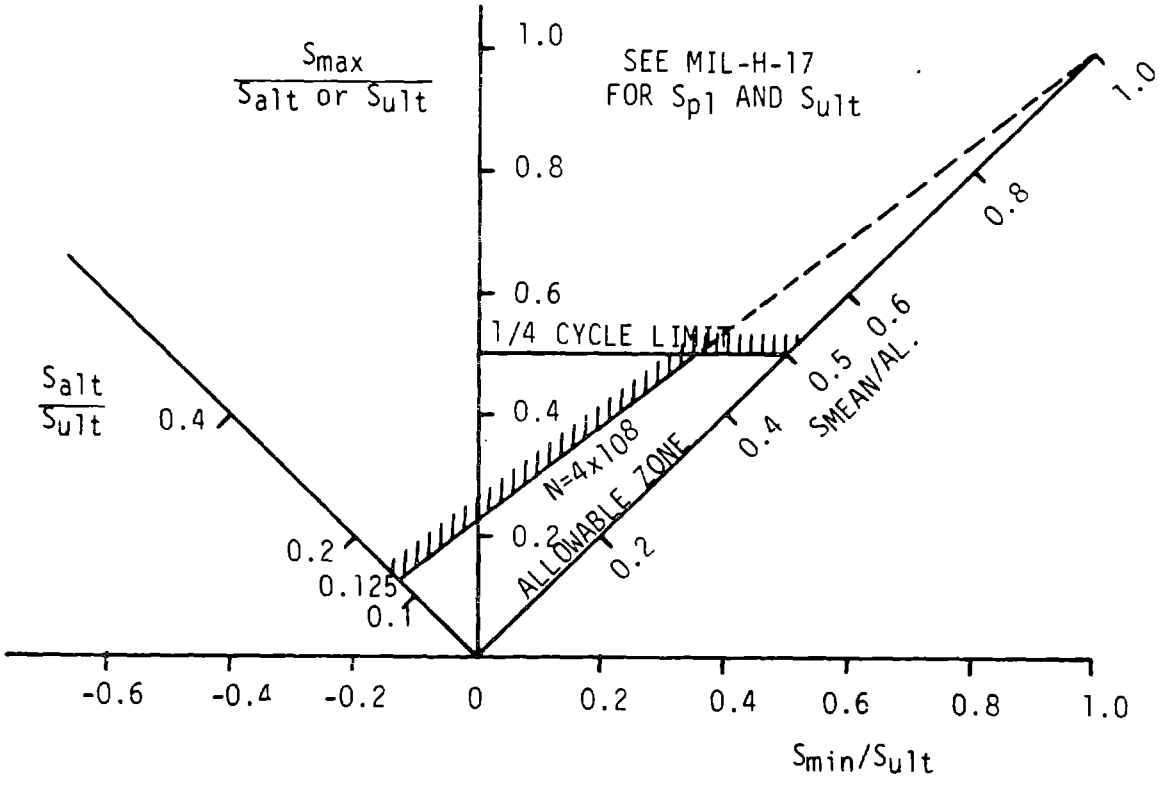

Figure 9-10 Glass Fiber Composite Fatigue Allowable Stress
For Conceptual Design

9.4.3.7 Alignment

The WTG structure shall be designed to meet mechanical and thermal alignment requirements within established error budget allocations. These requirements shall be met after exposure to all environments to which the WTG could be subjected throughout its design life.

Mechanical alignment includes consideration of load deflections during operation, maximum wind conditions, maneuvering, hysteresis effects, mechanical adjustment uncertainties, and manufacturing assembly tolerances.

Thermal alignment shall include distortion of equipment mounts and local supporting structure caused by the thermal environment, overall thermal distortion of the primary structure, and thermal creep effects.

9.4.3.8 Thermal Effects

Consideration shall be given to thermal effects on the structure, including temperatures, temperature gradients, thermal stresses, thermal deformations, and mechanical and physical material property changes. Mating of materials with widely varying coefficients of expansion in areas susceptible to large temperature variations shall be avoided. Temperature distributions shall be derived by rational analyses, considering the steady state and transient thermal environments.

The structural design shall account for: (1) Temperature distributions that vary with time, (2) Deflections caused by creep or short term applied loads and temperatures, and (3) compatibility of strains and deformations induced by differential thermal expansion and contraction of elements of the structure.

9.4.3.9 Welding

Welded joints shall be in accordance with applicable welding specifications, as provided by the AISC Specification and the "Structural Welding Code" of the AWS (detailed specifications for MOD-5A to be determined). Full penetration weld call-outs are strongly recommended for joints in the primary load path. Other welds, such as fillet welds, may be considered on an individual basis.

9.4.3.10 Fasteners

9.4.3.10.1 Bolted Joints

Bolted fasteners shall adhere to paragraph 9.1.4.4 of the AISC Specification, which recommends conformity to the latest edition of one of the following specifications:

> High Strength Bolts for Structural Steel Joints, Including Suitable Nuts and Plain Hardened Washers, ASTM A325, or special bolts from a reputable supplier.
>
> Quenched and Tempered Alloy Steel Bolts for Structural Steel Joints, ASTM A490 with additional specifications that maximum hardness be less than 36 on Rockwell C scale, threads shall be cold-rolled after heat treatment.
>
> Other bolts shall conform to the Specification for Low-Carbon Steel Externally and Internally Threaded Standard Fasteners, ASTM A307, latest edition, hereinafter designed as A307 bolts.

Manufacturer's certification shall constitute sufficient evidence of conformity with the specifications.

All threaded fasteners intended for fatigue application must have the thread form cold-rolled after heat treatment. Fasteners with hardness greater than Rockwell C 36 require certification for stress corrosion resistance. All fasteners should be zinc coated.

The shanks of all structural bolts in shear shall have no threads in bearing in sheet or fittings equal to or less than .093 in. thick. In thicker sheet or fittings, a maximum of two threads, including thread runout, is permitted in bearing when based on the maximum joint thickness and minimum bolt grip. However, not more than 25% of the minimum thickness of the sheet or fitting shall have threads in bearing. Structural bolts in primary load paths shall have a minimum diameter of .75 in., except as approved by the Manager of Engineering.

Bolt and screw applications shall be pre-stressed as recommended for tension applications, to obtain tight joints with minimum hysteresis effects. An hydraulic bolt tensioner is recommended for pre-tensioning.

Residual preload after tightening should be verified by a test simulating the joint. All joints in which preload is required to achieve satisfactory structural integrity shall be checked for tightness at assembly and rechecked after 50 to 100 hours of WTG operation. Positive mechanical approaches should be used to preserve tightness. A paint stripe should be applied after tightning to indicate the tight position of studs, bolts and washers with respect to the parts being held, on critical bolts.

Bolt design load estimates shall include the effects of eccentric design load paths and joint flexibility.

Residual preload shall be sufficient to preclude joint opening under maximum joint tension amplified by prying action. The maximum recommended residual preload is 75% of the bolt material yield point calculated with the reduced or "stress area" of the fastener. In order to achieve beneficial fastener flexibility in clamping together stiff flanges, the actual geometry and loading must be evaluated as in reference 9-7.

9.4.3.10.2 Torque Carrying Bolted Joints

The design of flanged joints that carry torque and bending through the joint must consider the combination of both types of loads in establishing the margin of safety. The bending portion involves design with bolts in tension for which good guidance can be found in reference 9-7. The design for the torque load path must include some assumptions for the value of the coefficient of friction and the number of bolts simultaneously sharing the load in single shear. Close tolerance holes are mandatory, so that bolt bending is minimal if the friction torque capability is overcome. Line-to-line or interference fit shear pins and keys may be required.

Table 9-10 summarizes some recommended values and assumptions. Shear forces from torque and all loads transverse to the tube axis must be combined with any bending and axial loads by the use of a suitable interaction formula.

Table 9-10 Recommended Parameters for Bolted Joint Design

Maximum Residual Preload of Bolts	75% of Yield
Maximum Fraction of Bolts Carrying Torque via Single Shear (Close Tolerance Design)	34%
Coefficient of Static Friction Steel to Steel, surfaces grit blast cleaned, degreased	0.2
Coefficient of Static Friction with Thin Copper Shim	0.3
Minimum Torque Capability of Only the Bolts (34%) in Shear	1.5 x Maximum Torque
Minimum Torque Capability of Only the Friction (no loss of preload)	2.25 x Maximum
Minimum Grip Length Divided by Diameter	6.0
Embedment Factor to Estimate Residual Preload	0.8

9.4.3.11 Venting

Consideration shall be given to providing adequate venting of each structural component in order to prevent significant loadings caused by the ambient pressure differentials encountered during the WTG service life. A structure without satisfactory venting will be designed for an internal pressure of 5 psi, unless otherwise specified. The final design shall provide a blade venting arrangement that results in a blade internal gauge pressure (caused by centrifugal gradients) of less than ±0.5 psi.

All airfoil cells and honeycomb shall be vented to preclude overpressure resulting from shipment by air cargo in an unpressurized cabin or bay.

9.4.3.12 Misalignment and Dimensional Tolerances

The effects of allowable structural misalignments, deflections and other permissable and expected dimensional tolerances shall be included in the analysis of all loads, load distribution, and allowable loads.

9.5 DESIGN CONDITIONS

9.5.1 GENERAL CONDITIONS

All static and dynamic loads and pressures (external and internal) that may affect structural integrity or influence design shall be defined and accounted for. The effects of thermally and mechanically induced structural deflections, allowable structural misalignments, and structural offsets and dimensional tolerances shall be included in analysis of loads, load distributions, and structural adequacy. Limit loads shall be determined for the WTG in all configurations for the design conditions identified in this document.

Loads shall be distributed throughout the structure by analyses that study the effects of structural non-linearities and temperature. Analysis of dynamic loads shall account for all significant changes in WTG mass properties with time, and all significant structural flexibilities, damping, and load spectra. The analysis shall also account for coupling of the various components and subassemblies of the WTG, including the rotor system (blades, hub, teeter bearings, stops, etc.), drive system (shafts, gearbox, brake, generator, and associated equipment), nacelle, yaw system, tower, foundation, and soil stiffness.

9.5.2 DESIGN CONDITIONS AND ENVIRONMENT

This section presents the operational, non-operational, and environmental loading conditions that are considered significant to the structural design of the WTG.

9.5.2.1 Operational Loading Conditions

9.5.2.1.1 Critical Environments

The WTG will be designed to survive, with adequate margin, the loads and environments associated with all phases of operation, including steady winds, gusts, maximum winds, shutdowns, startups, maneuvering, and braking.

9.5.2.1.2 Primary Structure

The primary structure may be defined as the structure that provides the system major load paths from the points of initiation of the loads to the loads to the system reaction point. In this case, the loads result from steady and cyclic loads on the rotor blades, rotational loads on the rotor system and drive system, and the gross weights of the major subassemblies that constitute the primary structure. The reaction point in this case is the tower foundation. The items constituting the primary structure of the WTG system are: the rotor blades, hub, teeter bearing, drivetrain, nacelle and bedplate, yaw system, tower, and foundation.

9.5.2.1.2.1 Critical Loading Conditions

For initial sizing of primary structure components, maximum quasi-static limit applied loads and static weights distribution are used. These loads apply to areas where fatigue from cyclic loads is not expected to be the design driving force. These forces and weights are subject to the design load factors of paragraph 9.4.2.4. Checks for fatigue will be made again as loading histograms are derived.

For areas in which fatigue design is probably the design driver (the rotor, hub and drivetrain), a dynamic analysis evaluating combinations of oscillatory and steady state effects will provide loadings.

9.5.2.1.2.2 Minimum Resonant Frequencies

The primary structure shall provide adequate stiffness to satisfy the system requirement for resonant frequency. The design selected for the MOD-5A WTG represents a "soft" tower approach with the first cantilevered bending mode frequency chosen, well below the predominant exciting frequency of 2P at normal rotor speed, and with sufficient separation at reduced rotor speed. The resulting loads alleviation provides roughly a 50% reduction of cyclic and seismic loading.

The placement of the coupled tower/foundation resonant frequency is complicated by the two-speed operation of the WTG, since the system natural frequencies should not coincide with the 1, 2 or 3 per revolution (P), etc., forcing frequencies. A frequency separation of 0.5P from the forcing frequency is recommended, but smaller separations may be permitted if verified by systems dynamic analysis.

Resonant frequencies for other WTG system subassemblies should be sufficiently separated from the tower/foundation resonant frequency to preclude coupling between components.

9.5.2.1.3 Secondary Structure

For the purposes of WTG development, the secondary structure may be defined as the structure that constitutes and locally supports the various equipment modules or components; it also includes the operating panels, and other component support bracketry of a non-structural nature. Major items, such as the gearbox, generator, brake, etc., are essentially load-carrying, and do not fall into this category.

9.5.2.1.3.1 Critical Loading Conditions

The general loads requirements for secondary structure, brackets, and components contained in the nacelle and bedplate or the tower are as follows:

Vertically (X-Axis) ± 2 g
Laterally (Y or Z-Axes) ± 5 g
Note: Axis definition is established in Figure 9-2.

These load levels may be superseded by dynamic forced response analysis, considering the mounting as excited by the predicted vibration of the primary structure.

For secondary structures, contained in the rotating portion of the WTG outboard of the nacelle rotor bearing interface (rotor blades and hub), the effects of centrifugal force and gyroscopic moments must be considered.

These g factors are to be used for design and stress analysis of components and their attachments to the structure. Loads, calculated by the g factor times weight, shall be applied separately for each of the three principal axes. These loads are the result of the vibration environment, and are subject to the factors of paragraph 9-4. Transportation, operational and thermal loads shall be considered separately.

9.5.2.1.3.2 Resonant Frequencies

Individual components, when mounted to their secondary support structure, shall be designed to meet a design goal of 20 Hz or more in all directions.

9.5.2.2 Non-Operational Loading Conditions

The structural design shall include consideration of all non-operational environments to which the subassemblies and their component parts are exposed during manufacture, ground handling, transportation and erection. Except for local areas at handling attachment points, the non-operational loads shall govern design of the structure to the minimum extent possible. Environments of MIL-STD-810B are deemed applicable to supplement information that follows:

9.5.2.2.1 Manufacturing

Fabrication and assembly operations effects on the structural design shall be evaluated for (1) material handling, forming, stretching or other processing; (2) misfit and misalignments; (3) welding, bonding and brazing; (4) heat treatment; and (5) checking and acceptance operations including pressurization cycles.

9.5.2.2.2 Transportation and Ground Handling

During transportation and ground handling, the effects of natural and induced environments on the WTG structure shall be evaluated.

9.5.2.2.3 Transportation Limit Load Factors

Limit load factors for transportation of the WTG are as follows:

Longitudinal	±3.0	(truck)
	±9.0	(rail)
Lateral	±1.0	
Vertical	+3.0	

These load factors include the maximum expected quasi-steady accelerations expected from truck or rail transportation and are to be applied separately as equivalent static loads. The directional terms are with respect to the transport vehicle axes. The component effective weight shall be the design gross weight, plus the weight of any non-operational equipment supported by the component, during ground handling operations.

9.5.2.2.4 Hoisting Limit Load Factors

The limit load factor for hoisting the WTG components and subassemblies shall be applied upward in any direction within 20° of vertical. The hoisting weight shall be the design weight of the applicable component or subassembly plus any attached weights.

9.5.2.2.5 Mating and Erecting Limit Load Factors

Limit load factors for vertical mating and erecting of the WTG subassemblies shall be determined before the erection. The subassembly shall be within the attitude envelope established for erecting and mating. The effective weight shall be the component design weight plus any attached weights.

9.5.2.2.6 Storage

Loads and environments that the structural components may experience during storage shall be accounted for or the structure shall be protected against them. At least the following shall be considered:

1. Pressure-differential loads, including the effects of venting.

2. Natural and induced environments.

3. Environments and loads from stored fluids, considering pressure, temperature, and chemical and physical effects on structural materials and adhesives.

4. Changes in moisture content of wood.

9.5.2.3 Environmental Considerations

9.5.2.3.1 Temperature

The WTG shall be capable of survival in ambient temperatures from -40°C to +49°C (-40°F to +120°F), and operation in ambient temperatures of -30°C to +40°C (-22°F to +104°F).

9.5.2.3.2 Seismic

The WTG, excluding the foundation, shall be designed to the seismic requirements characteristic of Zone 3 per the Uniform Building Code. The foundation shall be designed to seismic environments and soil conditions appropriate to the site. Before the site selection, the foundation design shall be based on Zone 3 seismic requirements assuming firm soil conditions having a bearing design strength of 4000 lb/sq. ft. (12000 lb/sq. ft. static bearing capacity).

9.5.2.3.3 Precipitation

The WTG shall be subjected to the following precipitation environments after installation, per paragraphs 9.3.4 and 9.3.5, of the Statement of Work.

Rain:	4 in./hour
Hail:	1.0 in. diameter, 50 lb/cu. ft., 66.6 ft/sec terminal velocity (for horizontal and vertical surfaces)
Ice:	2.0 in., 60 lb/cu. ft. on all external surfaces non-operating
Snow:	Blade: 21 lb/sq. ft. Nacelle: 41 lb/sq. ft.

9.5.2.3.4 Lightning

The WTG shall be subjected to lightning strikes as defined in Figure B-1 of the NASA Statement of Work for the MOD-5A WTG.

9.5.2.3.5 Projectile Impact

The WTG shall be subjected to impact of 4 lb. birds moving at 35 mph, on surfaces above 150 ft. Failures are not permitted, but local yielding is allowed.

9.5.2.3.6 Corrosion

Steel alloys should be selected with a stress corrosion cracking stress intensity threshold (K_{ISCC}) of more than 50 ksi $\sqrt{IN}$. Protective coatings will be used and maintained on a schedule related to the durability of the coating.

9.6 PROOF OF DESIGN

Proof of structural adequacy of the design under all critical combinations of design loads and environmental conditions shall be provided by analysis, tests, or both, all of which shall be documented.

9.6.1 ANALYSIS DOCUMENTATION

Reports shall be prepared on analysis made to verify structural adequacy in compliance with criteria contained in this document.

9.6.1.1 Dynamic Analysis

A dynamic analysis of the coupled WTG component assemblies, including the foundation and soil stiffness, will be performed. The mathematical model of the WTG system will be a linear, lumped-parameter, coupled system with up to six degrees of freedom per mass element.

This analysis will:

1. Support and verify the design of the WTG system to the fundamental frequency requirements.
2. Furnish the analytical model for operational loads and dynamic deflections analysis.

9.6.1.2 Internal Loads Analysis

From the design loads and associated environments, the critical loads and critical combinations of loads on the structure shall be used in loads analysis to obtain the internal loads in the primary structure. The interactions of the various structural components shall be considered in this loads analysis.

Structural loads induced by ground handling, including hoisting, transportation, and erection of the WTG components shall be determined.

9.6.1.3 Structural Analysis

A structural analysis of the major components of the WTG assembly will be performed evaluating stresses and deflections resulting from critical loads, environments, and temperatures anticipated during its 30 year service life. For the purposes of this document, the major components of the WTG assembly will be limited to the rotor assembly (blades, ailerons and hub), the nacelle and bedplate, the tower, the foundation, and all secondary structures contained by those components above the ground level deemed necessary. This analysis shall define the critical loads and design conditions, and determine stress levels and margins of safety.

9.6.2 DOCUMENTATION FORMAT

Documentation of structural analyses in support of the WTG development shall follow a consistent format. The following general format was suggested for documentation of these structural analyses:

1.0	Introduction	(a)	Objective
		(b)	Approach
		(c)	Background
2.0	Results	(a)	Tables: Margins of Safety Natural Frequencies, if pertinent Fatigue results
		(b)	Other pertinent summary data
3.0	Conclusions & Recommendations	(a)	Are criteria, requirements, goals met?
		(b)	Recommended changes, additional analysis
4.0	Substantiating Data	(a)	Scope of Analysis
		(b)	Approach, methods, models
		(c)	Sample analysis, notes.

The objective of Sections 1.0 through 3.0 is to briefly describe the problem, the resulting data, and what it means. Section 4.0 will describe in greater detail the scope and methods of analysis, computer models, materials, assumptions, and limitations. Pertinent notes and critical element analyses should be attached.

The WEPO Outline for Structural Analysis Reports, per reference 9-6, is presented as a guide to more formal documentation, such as final reports, and also forms a logical guide to the organization of structural analysis work.

9.7 COMMENTARY ON STRUCTURAL DESIGN CRITERIA

9.7.1 WOOD AND STEEL FATIGUE ALLOWABLE STRESS

The RMC allowable for steel weld category E is less than the allowable for wood at the same number of cycles. Category E is a weldment with significant stress concentrations. The allowable for E and other categories is for the unconcentrated stress adjacent to, or at, the weld detail. The wood allowable should be compared to weld category B for similarity of unconcentrated stress. Then, steel does have a higher allowable than wood in the Miner's approach, which is the RMC method in steel, despite the severe slope of steel weld S-N data if the CGT is exceeded. Lacking a CGT in wood, only Miner's approach was used. The low density of wood was influential in the choice for the rotor.

9.7.2 FATIGUE CRITERIA FOR STEEL

The MOD-5A Structural Design Criteria follows the AISC Manual of Steel Construction for strength and stability, but expands AISC fatigue criteria. The AISC fatigue criteria identifies various stress levels for various categories of welded and bolted details for over two million cycles. The origin of these allowables was researched with the help of consultants at Lehigh University, where a lot of testing had been done for the National Cooperative Highway Research Program. These tests led directly to the AISC and AASHTO allowable stress criteria. Because the wind turbine generator should accumulate four hundred million cycles of variable amplitude stress in 30 years, the test data and stress criteria were very important.

Some of the S-N data (reference 9-10) on steel fatigue is shown in Figure 9-11 for as-rolled beams and weldments without residual stress relief. The lowest stress level tested in each category is above the allowable for over two million cycles and some data points with arrows are runouts or no failure at ten million cycles. The data suggest that these full-scale test articles may have a true endurance limit stress, and that below this limit a very long fatigue life is likely. Such endurance limits behavior has been found for the same alloys in small laboratory specimens, but usually at somewhat higher stress levels tnan for full size parts.

Fracture mechanics data for crack propagation has also shown behavior analogous to an endurance limit. As shown in Figure 9-12, there are three regions (reference 9-11). Region I shows an extremely slow propagation rate with a distinctly different slope than Region II. Consideration of the crack size and applied stress range are the major parameters in calculating the stress intensity range, that is related to crack growth rate as illustrated in Figure 9-12. When the growth rate is less than 10^{-9} in. per cycle and the slope is properly different than Region II, then the corresponding stress intensity range is called the CGT. Given a flaw size assumed to be a crack, a stress range can be calculated that will produce a stress intensity range below the CGT, and the specimen will endure the stress cycles for an indefinitely large number of cycles. This stress range is also called the CGT allowable because it is directly proportional to the stress intensity range.

As shown in Figure 9-13, the CGT has a lower bound in the alloys popular for large structures (reference 9-11). The MOD-5A design intended to use such steels, and further consideration of the flaw size aspect was made.

The flaw size in the finished part must not be larger than a design value, or the CGT will be exceeded for the desired design allowable stress range. Conversely, the stress range in service must never exceed the CGT for whatever flaw size is left in the finished part. Either circumstance will cause crack propagation at a rate that can be predicted from knowledge of the stress range variable amplitude spectrum, stress distribution, crack description, crack growth data, and fracture mechanics formulae.

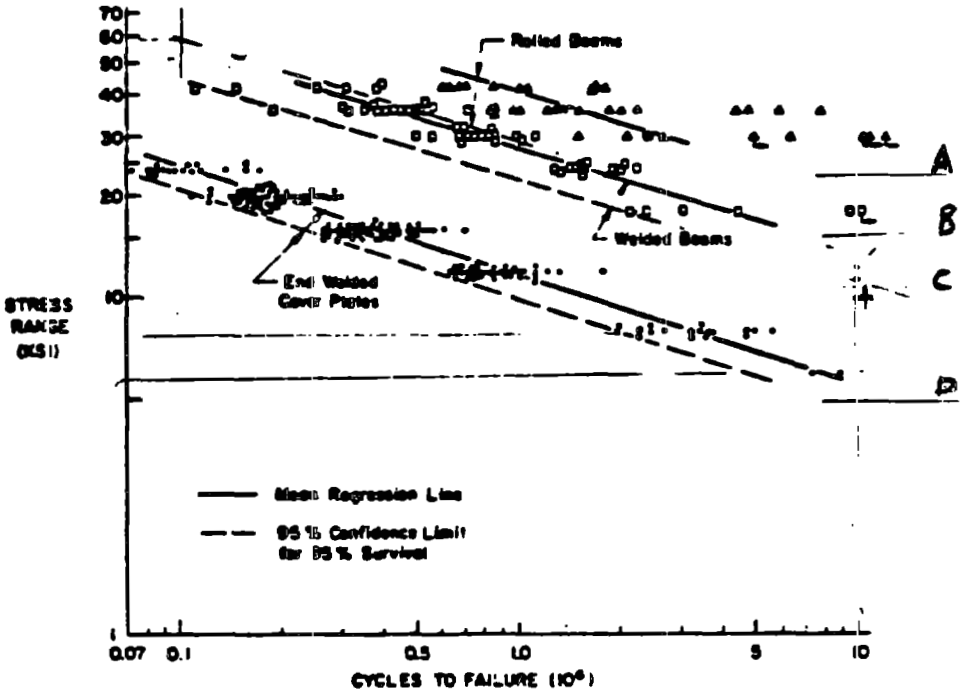

Mean fatigue strength and 95 percent confidence limits for rolled, welded, and cover-plated beams.

Figure 9-11 Fatigue Strength of Beams

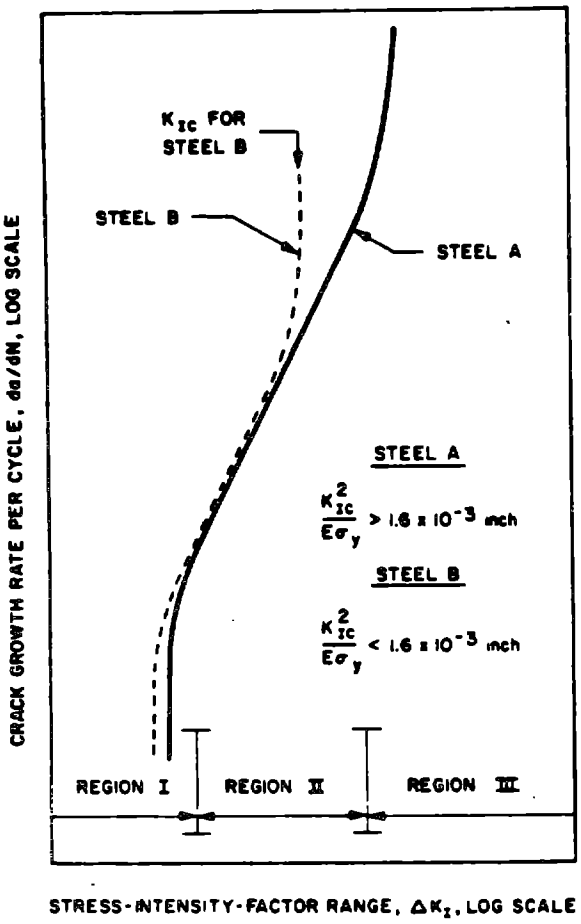

(a)

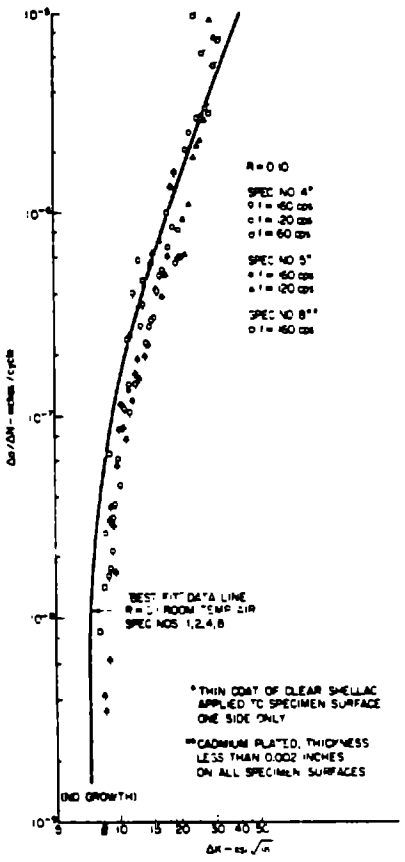

(b)

Figure 9-12 Fatigue Crack Growth

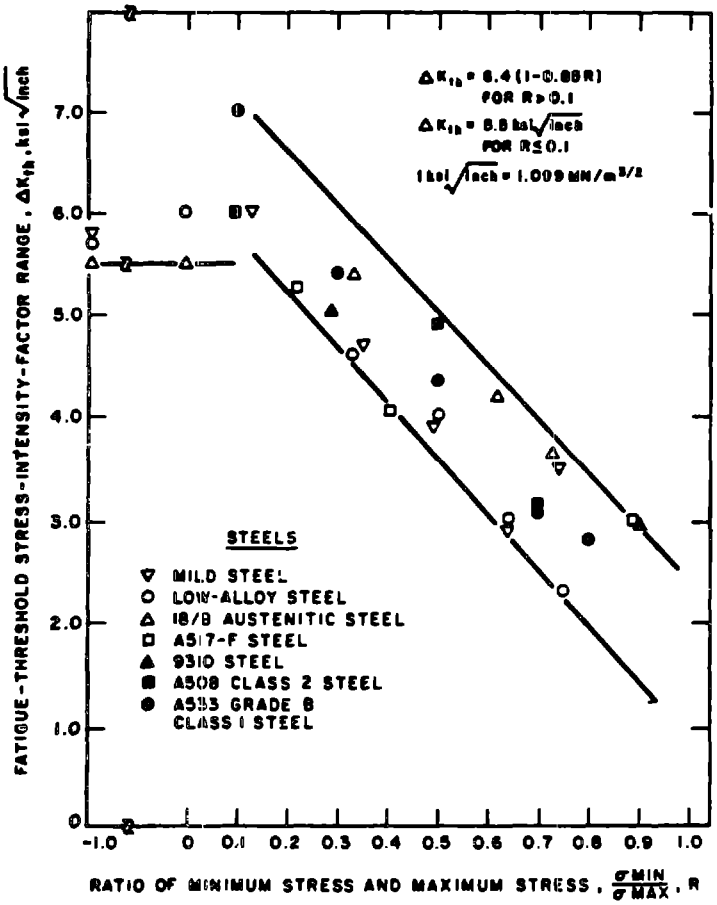

Figure 9-13 Dependence of Fatigue-Threshold Stress-Intensity-Factor Range on Stress Ratio

The flaw size that can be reliably detected was found to be small enough to satisfy fracture mechanics criteria for the CGT using the AISC stress range allowables for over two million cycles. However, the residual stress and applied stress ratio must be low to clearly defend the AISC stress range allowables for four hundred million cycles for the flaw sizes that may remain. Although some inspection shops can detect surface indications as small as 0.02 in. deep and 0.04 in. long with non-destructive examinations, values of 0.05 in. deep and 0.10 in. long were chosen as reliably detectable (reference 9-12). Not only must the weld specification require this, as the MOD-5A specification does, but the weldment drawing should direct the inspector to the critical zone.

PWHT was required to minimize residual tensile stresses in the welds, where flaws are most likely. In order to minimize warping, the weldment and manufacturing process must be carefully defined and the PWHT should be done on the entire finished product in a furnace.

Residual stress after PWHT should be less than 20% of the tensile yield point. Without PWHT the residual tensile stress is expected to be at the yield point. Consideration of the residual stress, applied stress range and applied mean stress defines the stress ratio with which Figure 9-13 can be used.

As shown in Figure 9-13, the CGT stress intensity range is reduced if the stress ratio is over 0.1. This directly led to a reduction of the AISC stress range allowables for stress ratios over 0.1, as identified in the Structural Design Criteria, Table 9-6, and Figures 9-3 and 9-5. There is some margin for human error in the non-destructive examination and analytic approximations in the use of these allowables.

The amount of forgiveness of the MOD-5A steel fatigue CGT allowable stress criteria can only be estimated. An example is a Category B weld that is ground flush, well inspected and has no geometric stress riser. At stress ratios below 0.1, the allowable stress range is 16 ksi. A semi-circular

surface flaw as large as 0.09 in. deep should produce a stress intensity below the CGT. Therefore, the non-destructive examination has a size factor of safety of 1.8 over the MOD-5A specification, to repair all surface indications over 0.05 in. deep by 0.10 in. long. Furthermore, if the indication is 0.1 in. long and less than 0.05 in. deep the stress intensity range is less severe. Also, if the largest surface indication is a semicircular flaw 0.05 in. deep, a stress range of 21.8 ksi is needed to exceed the CGT below a 0.1 stress ratio. Therefore, the stress factor of safety to the CGT is 1.36. Other weld categories have different degrees of forgiveness.

Another procedure, which depends neither on the existence of an endurance limit nor on a stress intensity range CGT, is specified in the Structural Design Criteria. The slope of the data in Figure 9-11 equals 3. The data is linearized by the two logarithmic scales, and it fits an equation of stress cubed times the number of cycles, which equals a constant. The RMC of the applied variable amplitude spectrum is an equivalent constant amplitude design stress. The RMC stress should be less than the total cycle intercept stress (CIS) for the relevant S-N data. The CIS is the stress level of the fatigue data equation for the total number of cycles in the applied spectrum. When the RMC stress is equal to the CIS, Miner's cycle ratio summation is 1.0 (reference 9-13). This is a modification of the original Palmgrin-Miner Hypothesis, since no endurance limit is used and the S-N data is the lower bound of the 95% scatter band with 95% confidence.

The allowable CIS levels are shown in Table 9-7. In keeping with the general appearance of constant life lines in MIL-HNDBK-5C (reference 9-19) the allowable CIS is reduced at higher stress ratios. The approximation method was to use the data of Figure 9-11 and other data to set the CIS for 4×10^8 cycles at a stress ratio of 0.1, and then linearly reduce the allowable CIS to zero as the mean stress approaches the tensile yield point.

9.7.3 WOOD DESIGN CRITERIA

The design criteria for wood considered a great deal of test data and the anisotropy of the material. The MOD-5A program conducted testing on the rotary peeled veneer assembled with the process and adhesive used for the actual wind turbone generator. This data, described in section 8, Volume II,

agreed fairly well with older data (reference 9-14) on clear-grained, small pieces of lumber. With this reassurance, factors were considered for temperature, moisture content, load duration, rate of loading, and the effect of size on strength. The allowable stress is considerably below the lower bound of the 95% scatter band, suggesting low risk of failure when the wind turbine generator is first put into service and a good chance of reaching the 30-year design life. The allowable stresses are less than those recommended for manned wooden aircraft (reference 9-15) primarily because of size, the 30-year design life and the functional requirement for unattended operation.

Anisotropic stress analysis using planar and three dimensional theory is required by the Structural Design Criteria. Stress analysis for laminae (reference 9-16), the Finite Element Method (reference 9-17), and stress interaction theories of failure (reference 9-16) were all used during the design process.

9.7.4 INSPECTION INTERVAL DETERMINATION

The relation between the design stress spectrum and the test data for the yoke location with the minimum margin is shown in Figure 9-14. Fracture mechanics data for the flaw growth threshold and the vendor's ability to detect flaws were used to determine the acceptable flaw size. A semi-circular surface flaw with a 0.05 in. radius is acceptable for this stress spectrum. In the fracture mechanics assumptions, tensile stress reduction credit was taken for the compressive pre-stress of about -4000 psi at the critical location, which would be caused by reaction to the elastomeric thrust teeter bearing preload. This approach is conservative by an undetermined amount. If the preload were lost, the yoke weldment should be able to sustain the design alternating stress level for 30 years, using the full stress range of 10.8 ksi, even though some of that range should be in compression.

An inspection interval of 3 months for the yoke was determined for a range of possibilities in which the flaw growth threshold may be exceeded. The possibilities include flaws larger than allowed in the weld specification, the absence of a threshold size, or a threshold stress intensity much lower than expected.

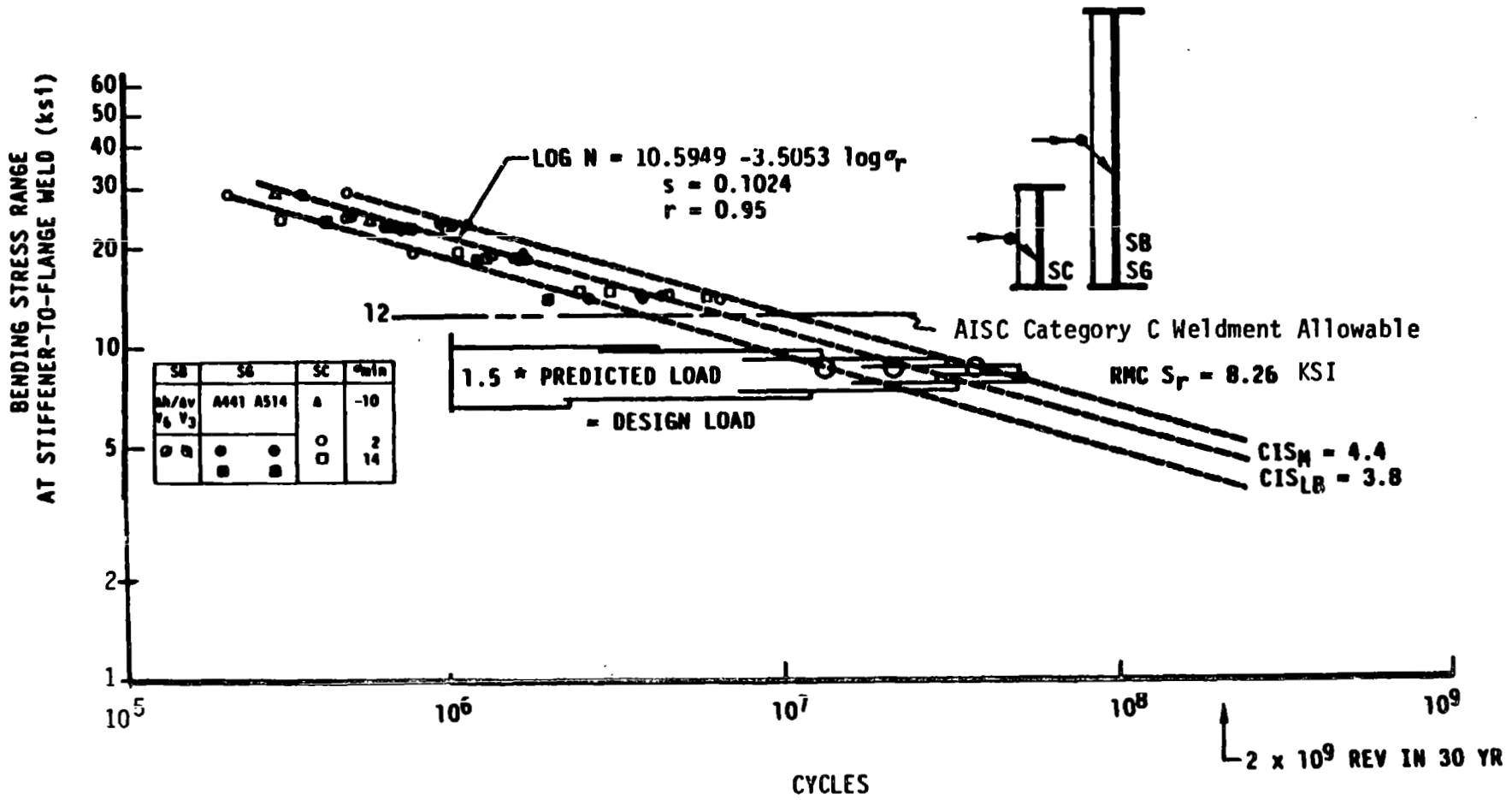

Figure 9-14 Relation of Yoke Design Stress Histogram and Relevant test Data

Two methods of analysis were used to determine inspection interval. One method extended the S-N data with no change in slope, and then calculated the number of rotor revolutions necessary to initiate a visible crack. The other method used fracture mechanics to estimate the number of revolutions necessary to grow the initial flaw to various visible final flaws.

In Figure 9-14, the 30-year histogram RMC stress crosses the extension of the S-N curve adjusted to the 95% confidence level, at 1.3×10^7 cycles and crosses the mean regression fit for the S-N data at 2.5×10^7 cycles. At 16.8 rpm and 7000 hours of operation per year, 2×10^8 yoke cycles of stress are expected. A Miner's cycle ratio summation of 1.0 occurs for 2.1 years of operation to the lower bound and for 3.3 years of operation to the mean S-N line. The S-N statistics were compared with the histogram of predicted stress. A 10% coefficient of variance was assumed for both stress and applied cycles. This led to a 45-month life, with a 97.7% probability of survival, and a Miner's sum of 1.04 to the mean S-N curve if the curve does not change slope. Failure would be highly probable in 12.3 years if the expected endurance limit of 12 ksi does not exist.

The time required for an initial flaw to reach a transition size, after which there is danger of rupture, was calculated from fracture mechanics formulae. The formula for Region II growth rate, which has a constant exponent, in ferritic-perlitic steel, corrected for stress ratio, was used to find the number of cycles required to reach a stress intensity of 50.0 ksi $(IN)^{0.5}$. This is a through-crack under a uniform 10.0 ksi stress field with a 2a dimension of 8 in. The crack shape was assumed to be initially semicircular, and coefficients were changed according to proximity of the free back surface and stress gradient. After penetrating to 75% of the plate thickness, the coefficients representing a through-crack were used. Although shop inspections should detect 0.1 in. long surface indications, reports on field inspection of bridges reveal that cracks are often unnoticed until they reach 1 to 2 in.

The results of the flaw growth study are shown in Figure 9-15 for the inside corner of the yoke elbow. It takes a long time for a small flaw to penetrate

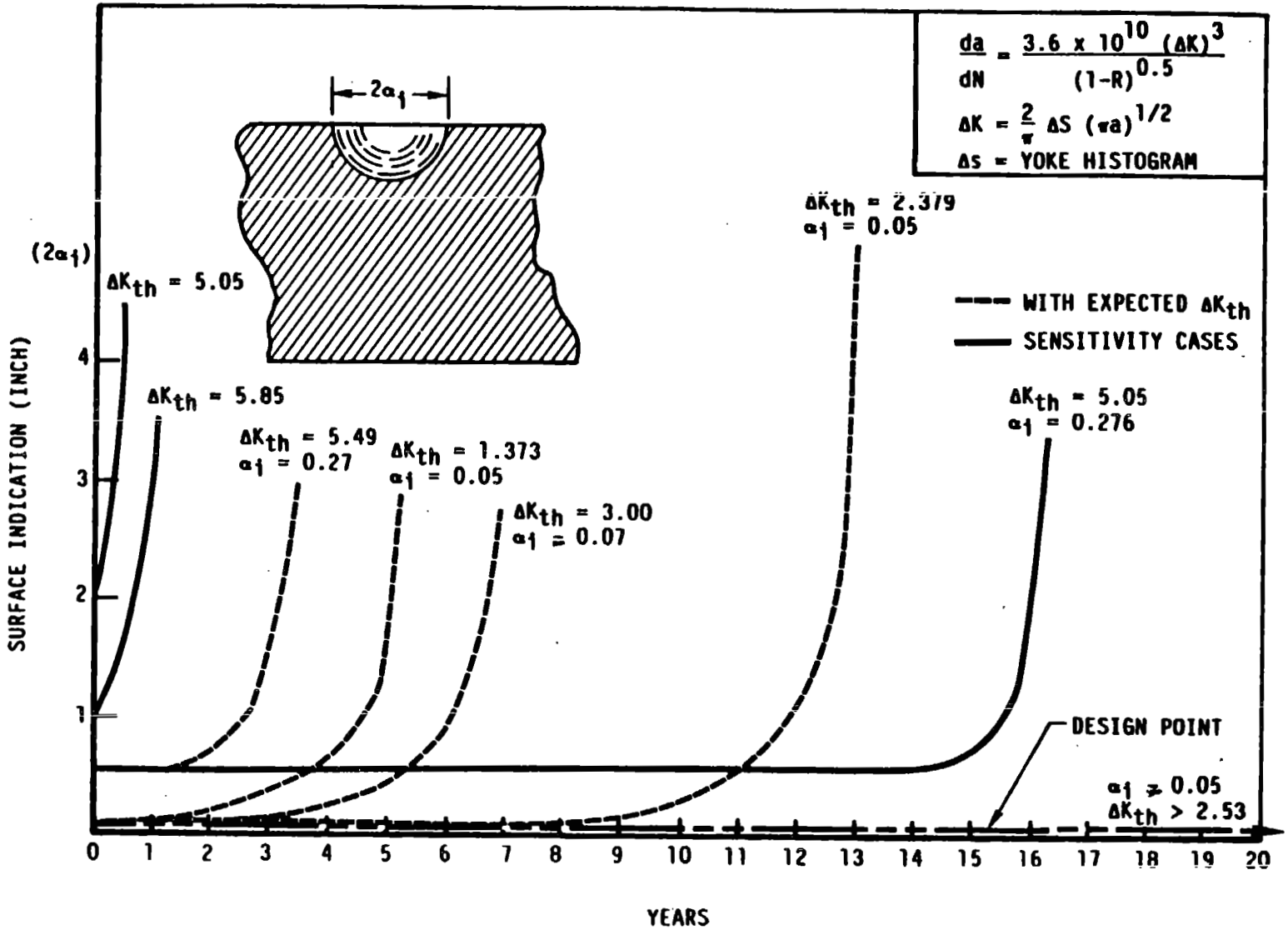

Figure 9- 15 Flaw Growth Study for Yoke Inspection Interval

the thickness of the 2 in. plate. Once the crack does penetrate the full thickness, the rate of growth is 2.34 in. per month. Therefore, the inspection interval should detect the flaw before it grows to 2 in. on the surface, or through 50% of the plate.

The lower bound of the stress intensity range threshold has little effect on the time it takes for the surface dimension to grow from 1 in. to 2 in. In Figure 9-15, the solid curves were computed with respect to the expected lower bound threshold of 5.85 ksi $(IN)^{0.5}$. The dashed curves were computed with lower thresholds, as noted. In each case, at least 6 months was predicted for the diameter of the semi-circular surface crack to grow from 1.0 in. to 2.0 in., which penetrates 50% of the 2 in. plate. Therefore, the recommended inspection interval for the yoke is 3.0 months, which should provide a safe margin for human error or faster growth rates.

The flaw growth calculations are consistent with the Miner's summation prediction of a 4 to 12 year life in the case with no endurance limit. This case corresponds to a low threshold stress intensity range for propagation. In Figure 9-15, the dashed lines and the solid line with an initial radius of 0.276 in. bound the possibilities. It was considered unlikely that a surface indication as large as 0.552 in. could escape detection in the shop, but this size is necessary if the yoke's maximum stress range were to cause a stress intensity over the expected lower bound threshold for propagation. However, to estimate sensitivity if the prototype fails to comply with data on threshold, the cases described by dashed lines were postulated.

The use of the Region II growth equation for the entire life is conservative. When the flaw is small, the predicted growth rate is much faster than the growth rate observed in laboratory testing. If the maximum stress range is 10 ksi and the flaw radius is 0.1 in., then the predicted Region II growth rate is 1.64×10^{-8} in. per cycle. Data for growth at 3.57 ksi $(IN)^{0.5}$ shows imperceptable growth for low stress ratios and 10^{-9} in. per cycle for a stress ratio of 0.5, which is much worse than expected for the yoke, since furnace post-weld heat treatment is included for stress relief. Since most of the life is spent on the initial growth, the Region II equation should underestimate total life. This fact has been confirmed by various tests.

Other locations in the MOD-5A wind turbine were less sensitive to fatigue than the yoke. The design stress histograms for the gearbox mount are more widely dispersed. The design placed the maximum stress range below the crack growth threshold in most cases, as was done in the yoke. However, if there is no crack growth threshold, the broader histograms are much less damaging, with a 30-year Miner's summation of 1.0 or less, considering the S-N data adjusted to the 95% confidence level. The gearbox mount RMC stress, for example, indicates satisfactory fatigue life as shown in Figure 9-14. Annual inspections were recommended for all structures except the yoke.

9.7.5 REFERENCES

The following references are relevant to the extend noted in Section 9.2.

9-1 Baker, E.H., et al, "Structural Analysis of Shells," McGraw-Hill Book Co., 1972

9-2 Bruhn, E.F., "Analysis and Design of Flight Vehicle Structures," Tri-State Offset Co., Cincinnati, Ohio 45202, 1965

9-3 Roark, R.J., "Formulas for Stress and Strain," Fourth Edition, McGraw-Hill Book Co., 1965.

9-4 Rolf, S.T., and Barsom, J.M., "Fracture and Fatigue Control in Structures, Applications of Fracture Mechanics," Prentice-Hall, Mc., Englewood Cliffs, NJ 07632, 1977.

9-5 Rolf, S.T., "Fracture and Fatigue Control in Steel Structures," Engineering Journal, American Institute of Steel Construction, First Quarter, 1977

9-6 WEPO PIR No. 71, "Outline for Structural Analysis Reports," Spera/Finnegan to Distribution, dated 09/22/78.

9-7 Aaronson, S. F., "Analyzing Critical Joints", Machine Design, January 21, 1982.

9-8 Hanson, J. M., et al, "Considerations for Design of Concrete Structures Subjected to Fatigue Loading", ACI 215R-74, revised 1981.

9-9 Helgason, T., et al, "Fatigue Strength of High-Yield Reinforcing Bars", NCHRP report 164, Portland Cement Association.

9-10 J.W. Fisher et al, "Effect of Weldments on the Fatigue Strength of Steel Beams," National Cooperative Highway Research Program (NCHRP) Report 102, Lehigh University for Highway Research Board, NAS, Washington, DC, 1970.

9-11 S.T. Rolfe and J.M. Barsom, Fracture and Fatigue Control in Structures, Application of Fracture Mechanics, Prentice Hall Inc., Englewood, Cliffs, NJ 07632, 1977.

9-12 "Assessment of NDE Reliability Data," NASA CR-134991, October 1976.

9-13 J.M. Medaglia, "Design for Long Life in Random Vibration Environment", Proceedings of Institute of Environmental Science, March 25-26, 1982, Library of Congress Catalog Card Number 62-38584.

9-14 Wood Handbook: Wood as an Engineering Material, U.S. Forest Products Laboratory, 1974 - (USDA Agr Handb. 72, rev.), Library of Congress Catalog Card No. 73-600335.

9-15 "Design of Wood Aircraft Structures," ANC-18, June 1951.

9-16 R.M. Jones, Mechanics of Composite Materials, Scripta Book Co., 1975.

9-17 MSC/NASTRAN, The MacNeal-Schwendler Corporation, 815 Colorado Boulevard, Los Angeles, CA 90041.

9-18 "Plastics for Flight Vehicles, Part I, Reinforced Plastics," MIL-HDBK-17, Rev. A and Rev. H.

9-19) "Metallic Materials and Elements for Aerospace Vehicle Structures," MIL-HDBK-5C.

9-20) S. F. Aaronson, "Analyzing Critical Joints", Machine Design, January 21, 1982.

APPENDIX A
SYSTEM SPECIFICATION

REVISIONS

A | ISSUED DOC NOW UNDER CONFIG. CONT. 4/27/84

SYSTEM SPECIFICATION

FOR THE

MOD-5A WIND TURBINE GENERATOR

November 1983

SYSTEMS ENGINEERING — DATE: 3 JAN 1984

CHIEF ENGINEER — DATE: 12 JAN 1984

QUALITY ASSURANCE — DATE: 24 Jan, 1984

INTEGRATION & TEST — DATE: 23 JAN, 1984

PROGRAM OFFICE — DATE:

TOTAL NUMBER OF PAGES 99

WTG 503

PRINTS TO

REVISION LOG

This log identifies those portions of this document which have been revised since original issue. Revised portions of each page, for the current revisions only, are identified by marginal striping or text notes.

Revision	Page No.	Paragraph Number(s) Affected	Rev. Date	Approval
A	ALL	ISSUED; DOCUMENT NOW UNDER CONFIGURATION CONTROL	NOV-83	

TABLE OF CONTENTS

TABLE OF CONTENTS

TABLE OF CONTENTS

TABLE OF CONTENTS

TABLE OF CONTENTS

TABLE OF CONTENTS

TABLE OF CONTENTS

TABLE OF CONTENTS

SECTION 1.0

SCOPE

This specification establishes performance, design, development and test requirements for the Model 304.2 MOD-5A Wind Turbine Generator (WTG).

SECTION 2.0
APPLICABLE DOCUMENTS

This specification incorporates the following documents, of exact issue date shown, to the extent referenced. In the event of conflict in document requirements, the detail content of Section 3 and following shall supercede the documents noted in this section.

2.1 GOVERNMENT DOCUMENTS

Contract DEN 3-153 (April 11, 1983)
FAA-Circular 70/7460-1F "Obstruction Marking and Lighting"
MIL-STD-210 Climactic Extremes
MIL-STD-1472 Human Engineering Design Criteria, Military

2.2 NON-GOVERNMENT DOCUMENTS

AGMA Aircraft Specification
AFBMA Section #11, Load Ratings Method
AWS D1.1-76 Structural Welding Code
SSPC-SPI0-63T Structural Steel Painting Council
NEMA MG-1, MG2 Motor and Generator Standards
ANSI C50.10, C57.12 Machine, Transformer Standard
NFPA 70-1980 National Electrical Code
ANSI Y14.1 Drawings

IEEE 519 Guide for Harmonic Control, etc, of Static Power Converters

47A380013 Control System Specification

47E387080 One-line System Diagram

47A380094 Variable Speed Subsystem Specification (Scherbiustat)

47A380115 Variable Speed Subsystem Specification (Generic)

47A387005 Signal & Command List

47A380002 Structural Design Criteria

ANSI C114.1 Grounding

47A380020 RAM Plan for MOD-5A

2.3 OTHER DOCUMENTS

NASA TP 1359 Engineering Handbook on the Atmospheric Environmental Guidelines for use in Wind Turbine General Development, W. Frost, B.H. Long, R.E. Turner, December 1978.

SECTION 3.0

REQUIREMENTS

The MOD-5A WTG system shall be designed in accordance with NASA requirements defined in Contract DEN 3-153 Statement of Work and attached exhibits. The MOD-5A WTG system shall also be designed in accordance with good commercial and General Electric Company practice. As specified in the following paragraphs, the MOD-5A WTG system shall be designed to accomplish specific functions, include specific characteristics, meet design, construction and maintenance requirements and be operated in a specific manner.

The MOD-5A WTG system shall be primarily designed for a single unit installation. Multiple installations or clusters of units shall be accomplished by interconnecting several single unit installation type WTG's at a distribution or sub-transmission voltage level.

Primary program requirements are that cost of energy (COE) at the electrical system grid interface be less than 3.75 cents per kilowatt-hour (1980 dollars) in a 14 mph mean wind regime with acceptable design risk. COE shall be computed in accordance with DEN 3-153, Exhibit E, summarized as follows:

$$COE = \frac{\text{Levelized Annual Cost (1980 \$)}}{\text{Available Annual Energy}}$$

Where Levelized Annual Cost (LAC) =

$$(IIC) \times (EFCR) + (LC) \times (LFCR) + (PRC) \times (PLF) + (AOM) \times (ALF)$$

and

IIC = Initial installed cost - turnkey
EFCR = Equipment fixed charge rate = .18
LC = Land cost = $750/acre
LFCR = Land fixed charge rate = .15
PRC = Periodic replacement cost
PLF = Periodic levelizing factor = $CRF\ ((C1+e)/(1+r))^i$
AOM = Annual operation and maintenance costs, average

ALF = Annual levelizing factor = 2.0
CRF = Capitol recovery factor = 0.089
e = Price escalation rate = 0.06
r = Discount rate = 0.08
i = Years after installation that PRC cost is incurred

and

Available Annual Energy (AAE) = (AKWH) x (AF)

where

AKWH = Annual grid Kwh energy based on the wind speed duration regime specified in Section 3.2.3.1.3, the system efficiency specified in Section 3.2.1.3, and 100% availability.

AF = Availability factor, based on the allocated values specified in Section 3.2.2.9.

For cluster installations, the per WTG pro-rata cost and efficiency of cluster equipment shall be included in the appropriate COE equation categories.

All tradeoffs shall be responsive to the goals of achieving COE below 3.75 cents per kilowatt-hour (1980 dollars) and minimizing COE with commercially acceptable risk.

3.1 SYSTEM DEFINITION

The MOD-5A WTG design shall be based on the description of Paragraph 3.1.1, for the purpose of Paragraph 3.1.2 when installed per Paragraph 3.1.3, defined per paragraph 3.1.4, and compatible with interfaces per Paragraph 3.1.5. The WTG system shall utilize customer furnished elements per Paragraph 3.1.6, and be capable of operating in the modes described in Paragraph 3.1.7.

3.1.1 SYSTEM DESCRIPTION

The WTG shall be a large, two bladed rotor, horizontal axis, propellor type wind turbine producing electrical energy. It will be designed for operation while electrically connected to an energized conventional 60 Hertz alternating

current utility system. The rotor will be mounted on a tower and be capable of maintaining upwind orientation relative to the tower. The WTG will be designed for unattended, fully automatic, failsafe operation for a 30 year operational service life, and be compatible with electric utility company operating, interface, maintenance and equipment requirements.

The WTG system is comprised of the following equipment and elements:

a) Foundation and site
b) Ground electrical equipment
c) Operation and maintenance
d) Rotor assembly (control surfaces, blades, yoke, hydraulics)
e) Drivetrain assembly (gearbox, shafting, generator)
f) Nacelle assembly (structure for rotor and drivetrain support)
g) Tower assembly
h) Control subsystem
i) Reliability, availability, maintainability and spares

3.1.2 PURPOSE

Terms used in this section are defined and specified in Paragraph 3.2.1 and following subparagraphs.

The WTG shall generate 60 Hz electrical power while connected to an energized utility network in rated sea level air density wind speeds from low (wind) cut-out (VLCO) to high cut-out (VHCO) wind speeds. Startup for generation shall be accomplished in rated air density wind speeds from low cut-in (VLCI)

to high cut-in (VHCI). The WTG shall generate rated power output at the utility network side of the WTG site step-up transformer when wind speeds are between rated wind speed and VHCO wind speed.

3.1.3 INSTALLATON

The WTG shall be capable of installation at a site accessible to conventional rail and/or truck surface transportation. Transportation and erection limitations on weight, size and availability of equipment shall be considered in the definition of system transportable assemblies.

3.1.4 DRAWINGS

The WTG and its components shall be defined by drawings and specifications. All engineering drawings shall conform to American National Standard ANSI Y 14.1 (drawing sheet size and format). The set of drawings shall provide the necessary design, engineering, manufacturing and quality support information directly or by reference to enable the procurement, without additional design effort or recourse to the original design activity, of an item that duplicates the physical and performance characteristics of the original design. These drawings shall not provide manufacturing process information unless this information is essential to accomplish manufacture of an identical item by other than the original source.

3.1.5 INTERFACE

The WTG shall be operated by and interface with an electrical utility company. An interface control document shall be prepared by GE that clearly defines necessary interfaces and responsibilities. GE will maintain the document and obtain mutual agreement to its contents by GE and the utility company. Major interfaces are as follows.

3.1.5.1 Electrical Network Interface

The WTG will feed its net output of up to 7300 KW into a 60 Hz, 3-phase utility network. Nominal connection to the network is at the terminals of a fused manual disconnect switch with visible break at the high voltage side of the site step-up transformer via overhead or underground circuit. The utility line shall provide between 0.05 and 0.45 per unit impedance per phase to an infinite bus equivalent on a 4.16 KV 7.5 MVA base and operate at no less than 11 KV and no more than 80 KV L-L. Automatic reclosing devices on the utility circuit shall be provided with voltage blocks or their equivalent to prevent asynchronous reclosing. Loads may be served by tapping the tie line between the WTG and the utility transformer substation, but may be subject to more than 3% voltage fluctuation. The nominal WTG output at the connection will deliver variable average real power from zero to 7300 KW and constant reactive (lagging) power at up to 1500 KVAR (0.98 Pf at 7300 KV). Operation in a constant voltage mode with fluctuating vars shall be a selectable option. Auxiliary power requirements of the WTG when not generating shall be supplied by the utility at the connection per Paragraph 3.1.6.4. The connection point at the transformer will be located about 200 ft from the WTG support tower to avoid interference with maintenance and erection operations.

3.1.5.2 Communication and Control Interface

Telephone circuits defined per Paragraph 3.1.6.2 shall be provided for voice and data communication between the WTG and the utility operator/dispatcher (nominally located up to 50 miles away). The WTG control system as a minimum will enable the utility operator/dispatcher to:

a) Receive WTG status information
b) Enable automatic WTG operation.
c) Disable automatic WTG operation, causing a normal shutdown if generating.
d) Alter maximum power set point to below rating.

3.1.5.3 Operating and Maintenance Interface

The Operation and Maintenance Manuals and training materials shall provide documentation of the utility and other service and operation personnel interfaces with the WTG.

3.1.6 CUSTOMER FURNISHED OR SPECIFIED ITEMS

The WTG design shall be compatible with customer furnished or specified items in contract DEN 3-153 or elsewhere. The term customer identifies either NASA or the WTG owner or user.

3.1.6.1 Location

The site shall be consistent with Paragraph 3.1.3. For design purposes, the assumed site is in the Cleveland, Ohio, area. The site is located on generally flat terrain with a substrate presenting no unusual or adverse features. Soil to a depth of 15 feet is assumed to consist of a very stiff to hard brown sandy, silty clay with gravel and shale fragments. Split spoon penetrations of 20 to 60 blows per foot are assumed, increasing with depth. Minimum allowable bearing pressures of 4000 psf are asssumed. No drainage problems are assumed. A soil minimum effective modulus of elasticity of 5000 psi is assumed.

3.1.6.1.1 Area

The nominal design site area required for construction and operation of a single WTG shall be 400 feet by 480 feet, (192,000 square feet = 4.41 acres). Permanent land use during operation may be limited to a 100 feet by 300 feet

strip (1.45 acres) with limited air rights and maintenance equipment access rights on adjacent land.

3.1.6.1.2 Access

An access road shall be provided from the nearest public road to the WTG site with the following characteristics:

a) Twenty-four foot wide all-weather roadbed or eighteen foot wide with turnoffs with one time maximum load capability of 300,000 lbs gross weight, nominal maximum load capability of 180,000 lbs gross weight and 4,000 lb per wheel.

b) Right-of-way as required to accommodate a 100 foot long load around corners with a 70 foot axle distance.

c) Eleven percent maximum grade.

d) Twenty foot minimum overhead clearance.

e) Seventy-five foot minimum turn radius measured to inside of roadbed.

3.1.6.1.3 Approvals

The customer will furnish all necessary Federal, State and local government approvals, including any FAA approvals or Environmental Impact Statement(s) (EIS) related to WTG installation and operation. Permits and licenses for construction will be the responsibility of the contractor.

3.1.6.2 Communication

The customer shall provide at least two dedicated voice grade unswitched telephone circuits between the WTG site and the utility's operator/dispatcher site compatible with Bell 103/113 modem/data set operating characteristics to be used for transmission of information specified in Paragraph 3.1.5.2 and voice communication. Optionally, the customer shall provide for transmission of parallel signals instead of the standard serial signals on one circuit.

3.1.6.3 Distribution Line

The customer shall furnish a distribution line from the WTG with the interface and characteristics specified in Paragraph 3.1.5.1 to carry power to the utility when the WTG is generating and supply auxiliary power when the WTG is not generating. A source of construction power shall also be provided.

3.1.6.4 Electrical Power Requirements

The customer shall provide the following power requirements at the interface of Paragraph 3.1.5.1:

a) 80 KVA, 0.8 power factor 60 Hz ± 1% for continuous consumption while the WTG is not generating, which includes power for the mobile data acquisition system.

b) 1000 KVA, 0.9 power factor, 60 Hz ± 1% for periods of up to 5 minutes for startup, auxiliaries, and unloaded generator motoring during low wind conditions.

c) 200 KVA, 0.8 power factor, 60 Hz, ± 1% at 480 VAC ± 10%, 3-phase temporary construction power.

d) 0.1 KVA, 0.8 power factor, 60 Hz ± 1%, at 120 VAC ± 10%, 1-phase at the utility operator/dispatcher location to power the remote control equipment.

3.1.6.5 Color and Markings

The customer shall specify the WTG color and marking scheme. The assumed color of the system is white with aviation red double bands at the blade extremities and on the tower for daytime hazard warning. Assumed FAA hazard lighting consists of a white flashing dusk/night duty lamp located only on the nacelle.

3.1.6.6 Mobile Data Acquisition System

The customer shall provide the contractor with the use of a Mobile Data Acquisition System as defined in Contract DEN 3-153, Exhibit B, Paragraph 2.5.3, including skilled operation and maintenance personnel, during WTG checkout, acceptance and initial operation testing.

3.1.6.7 Utility Control and Storage Space

The customer shall provide, at the utility's facilities, the following space requirements:

a) At the utility operator/dispatcher location, an office environment area of 8 feet by 6 feet, including a standard desk and chair shall be provided for installation and operation of the remote control interface.

b) At a utility substation or storage location near the WTG site, an area approximately 8 feet by 20 feet by 8 feet high shall be provided for storage of WTG spares and maintenance equipment.

3.1.7 SYSTEM MODES

The WTG system shall have automatic and manual operational modes.

3.1.7.1 Automatic Modes

The WTG automatic sequence modes shall be as follows:

a) Lockout
b) Standby
c) Startup
d) Generating
e) Normal Shutdown
f) Emergency Shutdown

Mode interactions and major entry and exit conditions shall be as shown in Table 3.1-1.

3.1.7.2 Manual Modes

The WTG shall have manual modes under control at the site only, with capability to:

a) Initiate a shutdown to lockout.

b) Initiate a transition from lockout to standby when the lockout causing condition has been removed.

c) Initiate specific control of subsystems, within the constraints of the automatic mode operating limits, to:

1) Operate the yaw drive

2) Operate the rotor control surfaces

3) Operate the WTG rotor at less than 1 RPM for rotor positioning.

4) Operate system commands individually

TABLE 3.1-1
AUTOMATIC MODE INTERACTIONS

MODE	ENTRY	EXIT
Lockout	From power-up, manual mode, standby, or shutdown on sensor change or command established as lockout condition	To standby on removal of lockout causing condition and site manual entry
Standby (Ready for operation with wind in operating range and enabled)	From normal shutdown or lockout on manual entry	To startup on satisfactory wind conditions, with enable. To lockout on sensor change or command established as lockout condition.
Startup (Wind in operating range and procedure to get to generating speed)	From standby on operating wind conditions present	To normal shutdown or emergency shutdown on sensor change or command established as shutdown. To generating mode after synchronized
Generating (Delivery of power to grid)	From startup after synchronized	To normal shutdown or emergency shutdown on sensor change or command established as shutdown
Normal shutdown (orderly disconnect from grid and slow stop of rotation)	From startup or generating on sensor change or command established as shutdown. From emergency shutdown where appropriate to change type.	To standby on completion of shutdown sequence. To emergency shutdown where appropriate to change type.
Emergency shutdown (Rapid, limited control feathering and disconnect from grid)	From startup, generating, or normal shutdown on sensor change or command	To normal shutdown or lockout depending on type of sensor change or command.

3.2 CHARACTERISTICS

The WTG shall meet the following system and subsystem design requirements and characteristics.

3.2.1 SYSTEM REQUIREMENTS

3.2.1.1 System Power Output

The WTG shall provide a rated electrical output at the utility interface defined in paragraph 3.1.5.1 of 7300 KW at up to 1500 KVAR (0.98 PF at 7300 KW) at 69 KV line to line, 60 hertz, 3 phase. A specific utility distribution line voltage, between 11 KV and 80 KV, may be utilized instead of 69 KV. For cluster application, the rated output is defined at the cluster tie to the utility network and is an average unit rating. The rated power output shall be produced in wind speeds from rated wind speed (VRAT) to high cut out wind speed (VHCO) at sea level air density and for ambient temperatures defined in paragraph 3.2.3.2.1. Less than rated output shall be provided at all prescribed ambient conditions for wind speeds between cut-in wind speed and rated wind speed. The general relation of power output to wind speed at sea level and 7000 feet for standard atmospheric conditions is illustrated in Figure 3.2-1. Power varies directly as the atmospheric density ratio for wind speeds below rated power. Power quality at the utility tie shall meet IEEE 519 guidelines.

3.2.1.2 Design Wind Speed Values

The WTG shall be designed for operation at the hub height wind speeds defined in Table 3.2-1 for sea level air density of 0.0763 pcf., and 250 ft. hub height above grade.

ORIGINAL PAGE IS
OF POOR QUALITY

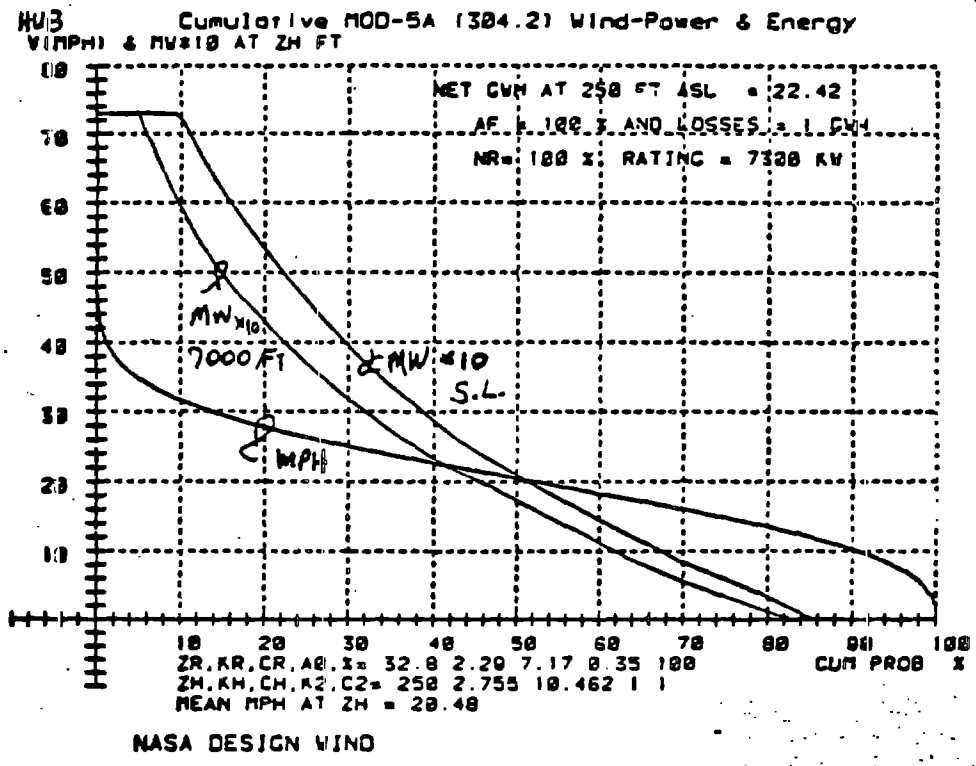

FIGURE 3.2-1

OUTPUT POWER VS. WIND SPEED

(1561A)

TABLE 3.2-1 DESIGN WIND SPEED VALUES

REFERENCE	DESCRIPTION	HUB WIND SPEED (MPH)
VLCO	Low cut-out wind speed where light motoring at low RPM can just be sustained and shut-down cycle begins as wind speed falls	12.0
VLCI	Low cut-in wind speed where acceleration to normal low RPM can be made in less than 15 minutes and startup cycle begins as average wind speed rises	14.0
VRAT	Nominal rated wind speed where WTG produces rated power output	32.0
VHCI	High cut-in wind speed where startup cycle begins as average wind speed falls	55.0
VHCO	High cut-out wind speed where shutdown cycle begins as average wind speed rises	60.0

3.2.1.3 Design Efficiency

The system design shall be based on the following maximum losses, expressed as percent of rated input such that component efficiency is equal to

1 - (% loss/100)

Fixed drivetrain loss	1.5%
Variable drivetrain loss	1.5% at rating
Fixed Electrical loss	1.5%
Variable Electrical loss	3% at rating
Miscellaneous loss	4.2% below rating

Rotor aerodynamic efficiency shall be based on the data in Figure 3.2-2. Miscellaneous losses consist of changes in rotor aerodynamic efficiency due to tilt, teeter, wind turbulance, and heading error. Auxiliary power consumption and startup time losses based on 35,000 starts in 30 years shall be included separately in energy capture calculations.

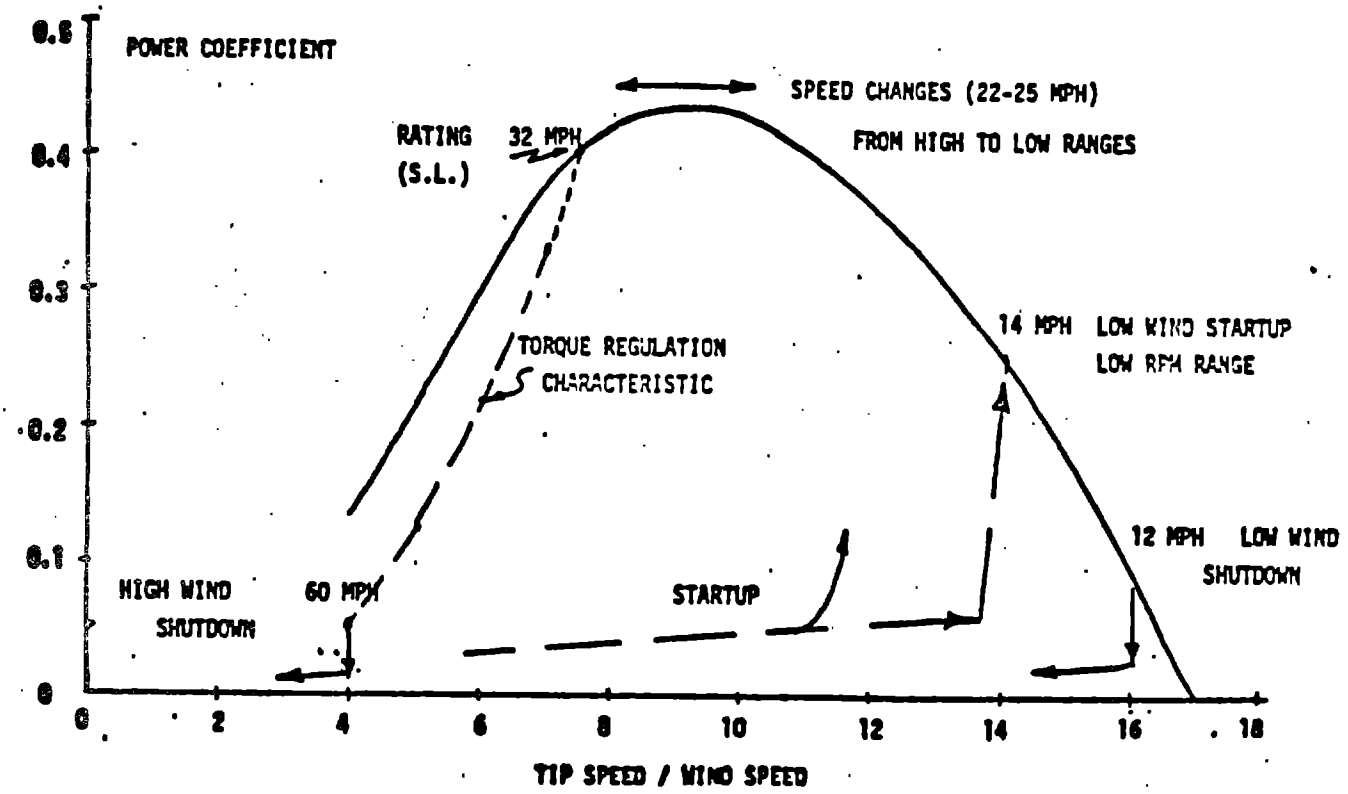

FIGURE 3.2-2
ROTOR DESIGN PERFORMANCE

(1561A)

3.2.1.4 Design Life

The WTG design service life shall be 30 years. Periodic replacement of components shall be used to meet this requirement if lower cost of energy can be calculated per paragraph 3.0. Life shall be based on 220 million rotor revolutions and 35,000 start-stop cycles.

3.2.1.5 Frequency Placement

The WTG system frequencies and operating speeds shall be located to avoid load amplification at integer multiples of the operating speeds. Specific frequencies to avoid shall include, but not be limited, to:

a) Tower bending and all integer multiples
b) Blade flapwise bending and even integer multiples
c) Blade chordwise bending and odd integer multiples
d) Drivetrain torsion and all integer multiples

3.2.1.6 Wind Characteristics

3.2.1.6.1 Design Wind

The design wind regime is defined in section 3.2.3.1.

3.2.1.6.2 Site Specific Wind

Wind regimes with characteristics other than the design wind regime shall be considered with respect to the system effects of at least:

a) Altitude/air density effects on cooling and dielectric strength.

b) Turbulence effects on loads, number of starts, high wind cut-out and cut-in.

c) Duration effects on load/life.

Where appropriate, rating revision shall be utilized to accommodate the site specific data.

3.2.2 SUBSYSTEM REQUIREMENTS

The WTG includes the subsystems and elements in paragraph 3.1.5. Performance and design requirements for these are defined in the following paragraphs.

3.2.2.1 Foundation and Site

The foundation and site elements consist of the tower foundation, ground electrical equipment foundation, grounding, fencing, maintenance tie downs, erection area preparation and grading.

3.2.2.1.1 Tower Foundation

The tower foundation shall be designed to carry the steady and cyclic loads due to WTG weight, rotor thrust and wind forces, and also carry the infrequently occurring limit loads due to seismic disturbance, extreme wind speeds and rotor overspeed. Soil pressures in accordance with paragraph 3.1.6.1 shall be considered in the design. The design shall provide anchor bolts or other suitable anchor provisions to carry tower loads at the tower interface. The design shall provide for conduits for power and signal wiring from the tower interior to the ground equipment location using below grade

routing. The design shall provide for the grounding system of paragraph 3.2.2.1.3. The design shall include blade tether and hoist tie down points. The general foundation design shall be modifiable to accommodate site specific soil conditions.

3.2.2.1.2 Ground Electrical Equipment Foundation (GEEF)

The GEEF shall be located about 200 feet from the tower base and provide a level support surface for the weight and limit wind and seismic loads of the ground electrical equipment (GEE) of paragraph 3.2.2.2. The design shall provide for conduits for power and signal wiring from the GEE to the tower foundation using below grade routing. The design shall provide for grounding conductors from at least four points on the GEE equipment base to the grounding system of paragraph 3.2.2.1.3. The design shall provide anchor studs to secure the GEE.

3.2.2.1.3 Grounding

The WTG shall have a grounding system that provides less than five ohms effective resistance to earth as measured at both the tower base and the GEE base. Connection methods and measurement techniques shall conform to section 4 of IEEE Standard 142 (Green Book)/ANSI C114.1 "IEEE Recommended Practice for Grounding of Industrial and Commercial Power Systems". The grounding system shall be adequate to accommodate the transient currents due to the lightning definition of paragraph 3.2.3.2. Test wells shall be provided by each foundation. All foundations shall be electrically connected together by the grounding system.

3.2.2.1.4 Fencing

A utility type galvanized fence with lockable gates shall be provided around at least the ground electrical equipment (GEE) described in paragraph 3.2.2.2. A fence may be provided around the tower base. The fencing shall be located at least 15 feet from the structure and shall be at least 8 feet high. The fencing shall be connected to the grounding system.

3.2.2.1.5 Grading

A crushed rock fill surface shall be provided within the fencing confines. A suitable surface for light vehicle parking and movement around the WTG tower base and the GEE installation shall be provided. If necessary, provision shall be made for drainage away from foundation to soil interfaces.

3.2.2.1.6 Maintenance and Access

Foundation and site equipment shall be substantially maintenance-free. The fencing shall have site security alarm sensors for unauthorized intruder detection.

3.2.2.2 Ground Electrical Equipment (GEE)

The GEE consists of the site step-up transformer, switchgear, converter, filters, capacitors, UPS, auxiliary power supply, battery power supply, switchboard, and ground control interface. The GEE shall be installed on the foundation of paragraph 3.2.2.1.2, as factory subassembled and wired units. Items and accessories shall be provided as shown on single line drawing 47D387080 and the following. Indoor rated equipment shall either be provided with a protected aisle enclosure or be housed in a site fabricated building.

3.2.2.2.1 Step-up Transformer

An outdoor oil filled transformer, rated 7450 KVA for 65 C oil rise with forced air cooling shall provide step-up of 4,160 volt generator output to a nominal 69,000 volt electrical network as described in paragraph 3.1.5.1. A high voltage visible break fused disconnect switch shall be provided either as part of the transformer assembly or mounted on the first distribution line pole.

3.2.2.2.2 Switchgear Assembly

A switchgear assembly shall be connected to the transformer and house or provide for mounting of the following.

3.2.2.2.2.1 Circuit Breakers

Circuit breakers shall be suitable for starting, switching and fault protection at 7450 KVA, 4160 volt. Interrupting rating shall be suitable to clear generator or network fed faults.

3.2.2.2.2.2 Converter

The converter portion of the variable speed generator system defined in specification 47D380094 or 47D380115 shall convert from generator variable speed frequency to 60 hertz grid frequency at 4160 volts.

3.2.2.2.2.3 Filters

Harmonic filters shall be provided as required to limit voltage fluctuations at the grid connection to IEEE 519 guidelines, when the WTG is operating.

Site specific requirements may require filtering in excess of IEEE 519 guidelines on a requisition-only basis.

3.2.2.2.2.4 Capacitors

Power factor correction capacitors, including the 60 hertz effect of filters, shall be provided as necessary to operate in a controlled Var mode at greater than 0.98 power factor.

3.2.2.2.2.5 UPS

An uninterruptable power supply at 120 VAC shall be provided with suitable rating to operate the control system for a minimum of 30 minutes, including sensors and actuators.

3.2.2.2.2.6 Accessory Power

Air insulated transformers and protective devices rated to provide 300 KVA, 480 volt, 3 phase and 208Y/120 volt, 3 phase multiple circuit accessory power by step-down from the 4,160 volt system shall be provided.

3.2.2.2.2.7 Battery Power

A DC stationary battery and charger system shall be provided for switchgear control system operation. Temperature control, voltage drop and venting shall be considered in the battery system and connection design.

3.2.2.2.2.8 Switchboard

A switchboard shall be provided with electrical protective relaying, transducers, and meters. Instrument transformers and connection areas shall

be located in metalclad bays as part of the overall assembly.

3.2.2.2.2.9 Enclosure

The equipment enclosure shall have anti-condensation heaters provided in insulation areas. Two lockable doors with security system sensors shall be provided, with panic-bar type inside latch releases. A means shall be provided for observing the WTG from inside the enclosure. Fluorescent interior lighting and convenience outlets shall be provided in the aisle area. Rodent and insect barriers shall be included in the design. Exterior area lighting shall be provided. Inlet air shall be mechanically filtered to remove airborne particulates.

3.2.2.2.3 Interlocks

Key interlocks or tamper-proof hardware shall be provided on equipment access doors, to mechanically prevent door opening while equipment is energized.

3.2.2.2.4 Ground Control Equipment

The ground level control system site interface defined in paragraph 3.2.2.8.2 shall be installed as part of the GEE.

3.2.2.2.5 Interfaces

The GEE equipment has interfaces with the WTG per paragraph 3.2.2.1.2 and with the utility per paragraph 3.1.5.1.

3.2.2.2.6 Lightning Protection

Lightning protection shall be provided such that the lightning model of paragraph 3.2.3.2 will not cause damage to the GEE enclosure or equipment.

Station class lightning arrestors shall be applied at the utility grid connection and elsewhere to avoid over voltages.

3.2.2.2.7 Instrumentation

3.2.2.2.7.1 Operational Instrumentation

The GEE shall provide for sensors, controls and wiring per 47A387005, Signal and Command List.

3.2.2.2.7.2 Engineering Data Instrumentation

GEE Engineering Data Instrumentation shall be per 47A387005. This instrumentation is required on initial units and is a requisition option for volume production. A GEE mounted multiplexor capable of handling at least 32 channels simultaneously shall be used with the Engineering Data Instrumentation.

3.2.2.2.8 Maintenance and Access

GEE equipment shall be substantially maintenance free. Periodic inspection of insulation, contact surfaces, and moving parts shall be simplified with drawout type construction with adequate access space. Provision shall be made for at least two voice telephone circuits and a monitor for closed circuit nacelle video display.

3.2.2.3 Operation and Maintenance

MOD-5A WTG operation and maintenance functions shall be eased by equipment design features and personnel training.

3.2.2.3.1 Personnel

The WTG shall be designed for operation and maintenance by trained technicians having electrician, machinist, and mechanic qualifications. Operation of the WTG, from either the site or remote control locations, shall only require a single technician. Maintenance shall be based on a crew of two technicians for most operations. All operation and maintenance personnel shall have completed the training of paragraph 3.2.2.3.5.

3.2.2.3.2 Site Operation

Site operation shall consist of the automatic and manual modes of paragraph 3.1.7. A portable maintenance input/output device may be used to provide site control of these modes.

3.2.2.3.3 Remote Operation

Remote operation shall consist of the automatic modes of paragraph 3.1.7.1 using the interface of paragraph 3.1.5.2.

3.2.2.3.4 Scheduled Maintenance

Periodic scheduled maintenance shall be used in the design of the WTG, totaling an allocated number of hours per year per section 3.2.2.9 for a volume production WTG. Periodic maintenance shall be used for servicing and lubrication functions that do not require automatic operation and for detection and repair of non-critical failures such as lamp burnout and minor leakage. The nominal interval shall be 90 days between inspections, with maintenance only as required.

3.2.2.3.5 Training

The contractor shall provide a training course for utility operation and maintenance personnel, based on the operation and maintenance manuals of paragraph 3.2.2.3.6. Training shall consist of classroom and on-the-job sessions as appropriate to the subject matter and be completed within one month of acceptance.

3.2.2.3.6 Manuals

The contractor shall prepare operation and maintenance manuals containing material of sufficient depth and scope to enable personnel of the skills level of paragraph 3.2.2.3.1 to perform all work related to the manual descriptive title.

3.2.2.4 Rotor Subsystem

The rotor subsystem consists of all WTG elements that rotate with the rotor and are located on the rotor side of the drivetrain to rotor interface of paragraph 3.2.2.4.7 as follows. The rotor shall be capable of operation at a 7 degree tilt from 16.2 to 16.8 RPM and from 13.2 to 13.8 RPM. Design overspeed shall be 21 RPM (1.25 x 16.8). Survival overspeed shall be 25 RPM.

3.2.2.4.1 Yoke Assembly

The yoke assembly consists of the yoke, teeter, brake, bearing assembly, and rotor hydraulic assembly.

3.2.2.4.1.1 Yoke

The yoke shall support the rotor and react all rotor loads through bearings into a rotor support spindle. It shall accommodate installation of the assembled rotor on the nacelle mechanically and electrically and provide for routing of wiring. The yoke shall accommodate installation of a rotor stopping brake assembly.

3.2.2.4.1.2 Teeter Assembly

The teeter assembly shall provide for up to +/- 9 degrees of teeter motion of the blade longitudinal axis about an axis normal to the hub shaft axis. Compliant stops or energy dissipating means shall be provided at the limits of teeter travel to limit reaction loads to non-design driver levels. A teeter motion restricting means shall be provided capable of being controllably released and applied. The teeter assembly shall carry blade loads into the yoke.

3.2.2.4.1.3 Rotor Hydraulic Assembly

The rotor hydraulic assembly shall consist of motor, pump, reservoir, accumulator, piping, valving, and environmental protection devices necessary to provide normal and emergency hydraulic pressure and flow to operate the aerodynamic control of paragraph 3.2.2.4.3 and rotor mounted hydraulic device needs. The rotor hydraulic assembly shall be a packaged subassembly design suitable for mounting on the yoke.

3.2.2.4.2 Blades

The blades shall consist of a structural/airfoil geometry optimized for low cost and weight and high performance. The reference configuration shall be

the NACA 64XXX airfoil series rotating clockwise when observed from upwind. All blade loads shall be carried into the yoke. A means for one time field joining of spanwise sections of the blade shall be provided. A means for field joining non-structural chordwise (trailing edge) sections of blade to extend beyond transportation dimensions shall be provided. The blades shall consist of a center 100 ft. section, two inner sections and two outer sections. The outer 80 ft. of each blade shall incorporate a means for aerodynamic torque control. The blades shall provide a means for adjusting static mass balance to within 7000 ft. lb. on the complete rotor about the teeter axis. Nominal blade performance shall be per paragraph 3.2.1.3.

3.2.2.4.3 Aerodynamic Control (Ailerons)

The aerodynamic control shall be a multiple section, hydraulically powered, electrically controlled device for changing the position of the trailing edge portion of the outer blade. The range shall be from aligned with the leading edge portion of the blade to at least 75 degrees toward the low pressure (down wind) side of the airfoil.

3.2.2.4.3.1 Configuration

The aerodynamic control shall have at least three mechanically independent sections on each blade. Each section shall be provided with an actuating means with position servocontroller and energy storage means that provides motion to full deflection on loss control power and/or main blade hydraulics. A spring applied, hydraulically released mechanical latch shall be provided to secure the control surfaces in the deflected position in the absence of hydraulic power. The hydraulic and structural interface with the leading edge portion of the blade and the mechanical properties and support of the control surfaces shall prevent any aerodynamic instability. The control surface

design and actuation means shall produce retarding torque with one surface jammed in an aligned position for a hub wind speed of 1.25 times high cut-out (VHCO). The aerodynamic control shall slow the rotor to an equilibrium velocity ratio (tip speed/wind speed) of 1.5 or less with all surfaces operating or 2.0 or less with one surface jammed.

3.2.2.4.3.2 Rates and Storage Requirements

The aerodynamic control and the hydraulic supply of paragraph 3.2.2.4.1.4 shall have the following rate and storage capabilities.

a) Accumulator Recharge - The pump capacity shall be adequate to charge hydraulic accumulators within 6 minutes from a no-fluid condition.

b) Continuous Operation - The pump capacity shall be adequate for up to 2 degree/second motion of all control surfaces. Flow will be distributed between control motion and operating accumulator recovery. Operating accumulators shall be sized for 120 degrees of motion of all control surfaces. The continuous operating servo system shall be adequate for a peak rate of 5 degrees per second.

c) Emergency Feather - The actuator stored energy and control shall provide for full control motion per blade. A passive means for scheduling emergency feather rate from 1 to 10 degrees per second shall be provided.

3.2.2.4.4 Lightning Protection

Lightning protection shall be provided such that the lightning model of paragraph 3.2.3.2 will not cause damage to the rotor structure, bearings, hydraulic lines and devices, or electrical lines and devices. Lightning

conductors shall be added in a manner to minimize electromagnetic reflecting area. Shunt current paths shall be provided around bearings.

3.2.2.4.5 Ice Detection

The rotor shall have provisions for installation and wiring of an aircraft type icing detector on each blade. The detector location shall be accessible from the yoke.

3.2.2.4.6 Instrumentation

The rotor shall have provision for operational and engineering data instrumentations and wiring as follows.

3.2.2.4.6.1 Operational Instrumentation

Rotor operational sensors, and controls shall be per 47A387005, Signal and Command List.

3.2.2.4.6.2 Engineering Data Instrumentation

Rotor Engineering Data sensors and controls shall be per 47A387005. This instrumentation is required on initial units and is a requisition option for volume production. A rotor mounted multiplexor capable of handling at least 32 channels simultaneously shall be used with the Engineering Data instrumentation.

3.2.2.4.6.3 Wiring

Rotor operational wiring shall be routed in continuous metallic conduit, with appropriate surge protection installed at the conduit entry. Rotor

Engineering Data Wiring from strain gages shall be surface routed with environmental protection up to conduit entry points then routed similarly to operational wiring.

3.2.2.4.7 Interfaces

The rotor subsystem shall interface mechanically with the rotor support spindle bearings, stopping brake and drivetrain low speed shaft. Rotor thrust and gravity loads shall be transferred to the spindle and rotor torque loads shall be transferred to the low speed shaft during operation and through the stopping brake and spindle support while stopping and parked. Electrical signal and power leads shall be connectable on the yoke structure and be routed both across the teeter axis to the blade and to the low speed shaft interior.

3.2.2.4.8 Maintenance and Access

Access and support features shall be provided on the rotor subsystem to minimize inspection and maintenance life cycle costs. Minimum requirements are as follows.

a) Blade tether points shall be provided near the outer end of the main blade for restraining blade position in either a horizontal or a vertical position, for tethering to foundation.

b) The blade and aerodynamic control design shall provide for removal of control sections and actuators with minimum equipment while the rotor is oriented, restrained and tethered.

c) The aerodynamic control design shall provide for hardware, seal, sensor and bearing inspection access and minimize disassembly for repair.

d) The rotor hydraulic assembly shall provide for inspection access and have provisions for the securing of test devices and for attaching rigging for handling components.

e) The rotor shall have provision for manually positioning and restraining teeter angle at either limit of travel.

f) The rotor assembly shall be capable of being slowly manually positioned in rotation and restrained (locked) in either the vertical or horizontal blade orientations by drivetrain devices.

g) The teeter assembly shall have provisions for bearing removal and replacement while the rotor assembly is mounted on the drivetrain and restrained and tethered in a horizontal blade orientation.

h) The yoke shall have provision for personnel access to the rotor hydraulic assembly, teeter assembly and provide attachment points for rigging of blade inspection and maintenance devices.

3.2.2.5 Drive Subsystem

The drivetrain subsystem consists of all WTG elements that rotate when the rotor is turning and their principal accessories. The main elements are the low speed shaft, gearbox, high speed shafting, and the generator.

3.2.2.5.1 Low Speed Shaft

The low speed shaft shall transmit torque from the rotor yoke to the gearbox. A hollow shaft shall be used to provide for a rotating wiring conduit to the rotor. The shaft shall have floating ends to accommodate misalignment and differential expansion.

3.2.2.5.2 Gearbox

The gearbox shall provide for single ratio speed increase from the rotor speed to the generator speed, static torque reaction, lubrication and mounting of accessory devices.

3.2.2.5.2 1 Operating Characteristics

Nominal gearbox characteristics shall be:

a) Rated output speed: 1380 RPM

b) Rated input speed: 16.8 RPM

c) Rated input torque: 3.39 million ft. lb.

d) Static limit torque: 2 times rated torque

e) Operating limit torque: 1.3 times rating for 1.35 percent of life

f) Operating life: 220 million input revolutions over 30 years.

g) Rotation: CW input when viewed from input shaft end

3.2.2.5.2.2 Lubrication

The gearbox shall provide for both auxiliary shaft driven and motor driven lubrication pumps. The WTG nacelle subsystem shall provide heating and cooling functions for the lubrication system. The lubrication system shall provide the proper lubrication of all gearbox bearings, while the WTG is operating within the design environmental conditions. The lubrication system shall provide for bringing the gearbox input from rated RPM to a stop, unloaded, without electric power available and for one complete rotation of the input shaft unloaded at .2 RPM without lubricant flow.

3.2.2.5.2.3 Accessories

The gearbox shall provide for mounting of sensors, railings, holding brake caliper, rotor manual positioner, and attachment and rigging points for maintenance. A continuously engaged shaft shall be provided for mounting of a holding brake disk. A rotating wiring conduit shall be provided concentric with the input shaft. Mounting for a mating slip ring shall be provided on the gearbox opposite the rotor end. The slipring shall provide for continuous rotation of electrical circuits between the nacelle and the rotor.

3.2.2.5.3 High Speed Shafting

The high speed shafting shall transfer torque from the gearbox to the generator and provide floating ends for alignment compensation.

3.2.2.5.4 Generator

The generator shall be part of a variable speed subsystem as defined in specifications 47D380094 or 47D380115 with the following characteristics.

a) Rated output: 7300 KW, 0.98 pf.

b) Rated voltage: 4160 V L-L 3-phase, 60 hertz

c) Speed: 0 - 300 RPM motoring, 960 - 1440 RPM generating, rotation either direction.

d) Temperature: class F insulation and class F rated rise at rated output.

e) Cooling: shaft fans, ducted outlet.

f) Bearings: two, oil ring and flood lubricated, thrust and external load capability at drive end.

g) Ambient: ANSI standard ratings. System derating for temperature and altitude as appropriate.

h) Protection and Accessories: per drawing 47D387080 (electrical single line diagram).

3.2.2.5.5 Rotor Stopping Brake

The rotor stopping brake operating on the rotor yoke shall be hydraulically powered from the yaw hydraulic assembly. The design shall provide for 100 hours of engagement without hydraulic pump operation. The rotor brake holding torque shall be two million ft. lb. and the design shall thermally provide for stopping the rotor inertia from a speed of 12 RPM. The rotor stopping brake shall be capable of being manually applied for rotor locking.

3.2.2.5.6 Rotor Positioner

The rotor positioner shall provide for manual and automatic control of rotor orientation. Operation shall be at no more than 2 degrees per second average rate at a torque level of no more than 0.15 of rated gearbox torque. Intermittent drive motion is acceptable.

3.2.2.5.7 Lightning Protection

Lightning protection shall be provided such that the lightning model of paragraph 3.2.3.2 will not cause damage to the gearing, structure, bearings, hydraulic lines and devices or electrical lines and devices. Shunt current paths (around bearings), surge capacitors, and voltage limiting devices shall be provided where necessary.

3.2.2.5.8 Instrumentation

3.2.2.5.8.1 Operational Instrumentation

Drivetrain operational instrumentation sensors and controls shall be per 47D387005, Signal and Command List.

3.2.2.5.8.2 Engineering Data Instrumentation

Drivetrain engineering data instrumentation sensors and controls shall be per 47D387005. This instrumentation is required on initial units and is a requisition option for volume production. Rotor and nacelle mounted multiplexors shall be used to transmit data.

3.2.2.5.9 Interfaces

The drivetrain subsystem mechanically interfaces with the rotor subsystem at the yoke and brake and with the nacelle subsystem at the gearbox and generator mounting locations. All interfaces shall provide for interchangeable connection of hydraulic lines and electrical power and signal circuits.

3.2.2.5.10 Maintenance and Access

Access and support features shall be provided on the drivetrain subsystem to minimize inspection and maintenance life cycle costs. Minimum requirements are as follows.

a) The gearbox and generator structure shall have provision for personnel access to inspection and service locations and provide attachment points for rigging of maintenance devices and safety lines.

b) The lubrication system shall have provision with a filter for connection of a portable pump for manual filling, draining, and circulation of lubricant.

c) Grease lubricated seals and couplings shall be provided with accessible lubrication fittings.

d) Generator bearings shall be replaceable without generator rotor removal.

e) Valving and fittings shall be provided for connection of a manual pumping device to the rotor stopping brake.

f) Gearbox covers and high speed stage design shall provide for major maintenance operations without gearbox removal from the nacelle.

g) Replaceable element filters, delta pressure indicators, access openings, sample valves, sight gages and similar devices shall be provided in the lubrication system.

3.2.2.6 Nacelle Subsystem

The nacelle subsystem consists of the rotor support structure bedplate structure, fairing, yaw subsystem, hydraulic assembly, lubrication system components, control system assembly, maintenance hoist and accessories. The nacelle subsystem supports the rotor and drivetrain.

3.2.2.6.1 Bedplate and Rotor Support

The bedplate and rotor support shall provide structural support for the rotor spindle and drivetrain subsystems, and carry all reaction loads through the yaw bearing into the tower. The bedplate shall provide for mounting of all items in section 3.2.2.6, accessories and accessible routing of hydraulic and electrical circuits. Minimum access and work spaces shall be provided using MIL-STD-1472 as a guide. The bedplate shall have attachment points for assembled nacelle lifting. Metal containers shall be secured to the bedplate for storage of standard tools. A lube oil subsystem shall be field mounted underneath the bedplate. The rotor support spindle shall support the yoke of paragraph 3.2.2.4.1 using a rolling element bearing assembly capable of reacting weight, thrust and dynamic loads.

3.2.2.6.2 Fairing

The fairing shall provide an enclosed space around nacelle mounted WTG items and reduce environmental exposure for these items and maintenance personnel.

The fairing structure shall provide for: mounting of two wind sensor supports at the end opposite the rotor; mounting of generator cooling exhaust ducting; mounting of maintenance lighting fixtures; mounting of convenience outlet and conduit runs; mounting of a fire protection system; mounting of aircraft hazard lighting; mounting of personnel access openings and safety fittings for access to the rotor and fairing mounted items; mounting of openings for major maintenance access by external crane or hoist; mounting of lube oil cooler.

3.2.2.6.2.1 Wind Sensor Mounting

The two wind sensor mountings shall locate the sensors at a minimum of 30 feet apart parallel to the rotor plane, and with sufficient vertical height above the rotor axis to prevent simultaneous rotor blockage of both sensors. The mountings shall provide for sensor servicing from the nacelle.

3.2.2.6.2.2 Air Flow and Ducting

Generator cooling air shall be drawn from within the fairing and the heated exhaust air shall be ducted. The exhaust ducting shall provide a temperature controlled means of directing exhaust air to either inside or outside the fairing. Air entrance to the fairing shall be mechanically filtered to remove airborn particulates with louvers for controlled shutoff.

3.2.2.6.2.3 Fire Protection

The fire protection system shall provide for releasing a non-toxic fire extinguishing agent within the nacelle and for control system sensor inputs indicating that fire conditions are sensed and that the agent has been released.

3.2.2.6.2.4 Maintenance Hoist

A boom type maintenance hoist shall be installable on top of the rotor support structure. The hoist shall be capable of raising 10,000 lb. from the ground. The hoist shall be maneuverable to reach fairing access hatches and yoke equipment and be usable for rotor inspection and maintenance.

3.2.2.6.2.5 Maintenance Light and Power

a) Maintenance lighting shall provide for illumination of at least 10 foot candles in all accessible areas and at least 50 foot candles in maintenance working areas using fixed and moveable sources.

b) Maintenance power outlets shall provide GFI protected 120 volt, 15 ampere, 60 hertz service and be located 20 feet apart around the interior of the fairing. Each end of the nacelle shall also contain protected outlets for two 208 volt, and two 480 volts, 3 phase circuits, each rated at 15 amperes. Nacelle power shall be supplied from one feeder 480 volt, 3 phase circuit with step-down and circuit protection provided in the nacelle.

3.2.2.6.2.6 Hazard Lighting

The fairing shall provide for mounting of FAA approved white flashing dusk/dark hazard lighting fixtures. The lighting shall comply with the requirements of DOT, FAA Advisory Circular 70/7460 - 1F "Obstruction Marking and Lighting".

3.2.2.6.3 Yaw Subsystem

The yaw subsystem shall carry all bedplate loads into the tower, provide for controlled continuous rotation in either direction, provide personnel access from the tower to the nacelle, and provide for electrical circuit continuity.

3.2.2.6.3.1 Yaw Drive Assembly

The yaw drive assembly shall consist of the yaw bearing assembly, drive actuators and grippers, holding brakes, a nacelle mounted hydraulic supply, and controls. The drive shall be capable of rotating the nacelle at an average rate of at least 0.250 degrees per second in either direction. The holding brakes shall provide sufficient torque to lock yaw in all operating conditions. Yaw drive stiffness and damping in both driving and non-driving modes shall minimize system response to periodic excitations. The hydraulic supply shall be designed to supply the yaw drive and the rotor stopping brake flow and pressure requirements.

3.2.2.6.3 2 Slip Ring

The yaw slipring shall provide continous rotation capability for circuits between the nacelle and tower.

3.2.2.6.4 Lightning Protection

Lightning protection shall be provided such that the lightning model of paragraph 3.2.3.2 will not cause damage to structure, bearings, hydraulic lines and devices, or electrical lines and devices. Shunt current paths around bearings and voltage limiting devices shall be provided where necessary.

3.2.2.6.5 Instrumentation

3.2.2.6.5.1 Operational Instrumentation

Nacelle operational instrumentation sensors, controls and wiring shall be per 47D387005, Signal and Command List.

3.2.2.6.5.2 Engineering Data Instrumentation

Nacelle engineering data instrumentation sensors, controls and wiring shall be per 47D387005. This instrumentation is required on initial units and is a requisition option for volume production. A nacelle mounted multiplexor shall provide for at least 32 data channels.

3.2.2.6.6 Interfaces

The nacelle subsystem interfaces with the rotor subsystem at the support spindle, with the drivetrain subsystem at the gearbox and generator mounting locations and with the tower subsystem below the yaw structure. All interfaces shall provide for connection of hydraulic lines and electrical power and signal circuits.

3.2.2.6.7 Maintenance and Access

Access and support features shall be provided on the nacelle subsystem to minimize inspection and maintenance life cycle costs. Minimum requirements are as follows; in addition to requirements shown in other paragraphs of this section.

a) The nacelle and yaw areas shall have modular jacks located by maintenance areas and wiring for telephone communication on at least two circuits.

b) The nacelle shall have provision for mounting and wiring of a closed circuit video monitor.

c) Valving and fittings shall be provided for connection of a portable pumping device to the yaw drive hydraulic system.

d) The yaw area shall have suitable attachment points for removal and servicing of the slipring and yaw drive components.

3.2.2.7 Tower Subsystem

The tower subsystem consists of the tower structure, nacelle access device, tower lighting and tower wiring.

3.2.2.7.1 Tower Structure

The tower structure shall carry its own and all nacelle reaction loads into the tower foundation, and provide for personnel access into the tower base by means of a lockable metallic door. The top of the tower shall provide for anchoring and servicing of the nacelle access device and provide for personnel access from the tower into the nacelle. The tower shall locate the rotor axis for blade clearance of 50 feet above the local grade. For operating loads, the absolute wind azimuth can be assumed to vary in a Gaussian manner with 30 degree standard deviation.

3.2.2.7.2 Nacelle Access Device

The tower shall provide an internally mounted 480 volt, electrically powered nacelle access device capable of moving up to 650 pounds of personnel and equipment from the ground to nacelle level in less than 4 minutes one way. Control of device movement shall be provided on the device, at ground level, and at the top of the tower. A means of descending the tower from any access device elevation without the use of electrical power shall be provided. A protected landing platform shall be provided at the top of the tower. Access device power shall be interruptable from the Ground Electrical Equipment enclosure.

3.2.2.7.3 Tower Lighting and Power

Tower interior lighting shall provide for illumination of at least 10 foot candles when switched on at either the top or bottom of the tower. Maintenance power outlets shall provide weatherproof GFI protected 120 volt, 15 ampere, 60 hertz service and be located at the tower base and at the nacelle access device and landings. A weatherproof 480 volt, 3 phase outlet shall be provided at the tower base and at the nacelle access device landings.

3.2.2.7.4 Tower Wiring

The access device installation shall provide for supporting and protecting power and signal wiring from the yaw slipring to the tower foundation conduiting.

3.2.2.7.5 Lightning Protection

Lightning protection shall be provided such that the lightning model of paragraph 3.2.3.2 will not cause damage to the structure or electrical lines and devices. Lightning currents shall be transferred from at least three points at the tower base into the grounding system specified in paragraph 3.2.2.1.1.

3.2.2.7.6 Interfaces

The tower subsystem interfaces with the nacelle subsystem at the yaw bearing and with the tower foundation anchors. The tower structure shall provide suitable bearing and anchor reaction features to carry tower loads into the foundation. All interfaces shall provide for connection of electrical power and signal circuits.

3.2.2.7.7 Instrumentation

3.2.2.7.7.1 Engineering Data Instrumentation

Tower engineering data sensors shall be per 47D387005, Signal and Command List. This instrumentation is required on initial units and is a requisition option for volume production. The ground mounted multiplexer shall be used for data transmission.

3.2.2.7.8 Maintenance and Access

The tower shall be designed for low maintenance and provide features that minimize inspection and maintenance life cycle costs. Minimum requirements are:

a) The tower base, nacelle access device, and access device landings shall have modular jacks and wiring for telephone communications on at least two circuits.

b) The tower shall provide for rigging points for interior and exterior access to all surfaces for inspection and refinishing.

c) The tower shall provide for controlling condensation runoff on interior surfaces if necessary to avoid corrosion acceleration.

d) The tower door and nacelle access device and landing gates shall have site security system sensors for intruder detection.

3.2.2.8 Control Subsystem

The control subsystem consists of the equipment necessary to sense and manipulate data from WTG operational sensors and controls; perform decision logical processes; perform computations; generate operational and maintenance commands; store data windows of WTG performance both before and after shutdown initiation fault occurrance; and maintain communication for transmittal of data and commands between elements of the WTG, the local control interface, and the remote control interface specified in paragraph 3.1.5.2. The control subsystem shall provide for operation in the modes of paragraph 3.1.7 with continually operating data collection, communication and fault monitoring functions.

3.2.2.8.1 Controller

The controller equipment shall consist of an enclosed rack located in the nacelle which senses and controls all WTG functions. The controller equipment shall as a minimum provide for: connection and signal conditioning of sensor inputs and command outputs; dynamic control of blade and generator control elements failsafe electronics; real time generation; data window memory; non-volatile memory; watchdog electronics; and ports. The controller equipment shall be powered by the uninterruptable power supply defined in section 3.2.2.2.2.5.

3.2.2.8.2 Site Interface

The site interface shall consist of a display panel and a terminal. The panel shall provide: discrete mode indication; limited data indication of blade control position, RPM, power, wind speed and wind direction; key switch control over WTG mode; port for connecting the terminal; port and modem for connecting link to remote interface per paragraph 3.1.6.2; connection to controller. The terminal shall provide the functions generally available on a printing data terminal including alphanumeric display and keyboard entry.

3.2.2.8.3 Remote Interface

3.2.2.8.3.1 Standard Remote Interface

The standard remote interface shall consist of a modem and a terminal that provides the functions generally available on a printing terminal including alphanumeric display and keyboard entry.

3.2.2.8.3.2 Site Specific Remote Interface

Where user requirements are for parallel rather than serial signals, the user shall provide for signal handling of standard WTG signals at the site interface.

3.2.2.8.4 Supervisory Control Priority

The controller of paragraph 3.2.2.8.1 shall be capable of failsafe automatic WTG operating control after enabled by the site and remote interfaces. Continuous interface communication shall not be required to maintain automatic operation. The remote interface shall be able to enable and disable automatic mode, alter maximum power setting, alter reactive power setting, and transfer control to the other interface. The site interface shall be able to do all remote interface functions plus enter manual control functions of paragraph 3.1.7.2, and read out information stored in the data window. Lockout conditions occurring during automatic operation shall require site interface operation in order to enforce on-site inspection.

3.2.2.8.5 Control Functions

The controller shall provide control of sequencing between the automatic modes of paragraph 3.1.7.1 and the following control functions.

3.2.2.8.5.1 Yaw Position Control

The yaw position control function shall provide for:

a) Averaging wind azimuth error.

b) Generating commands to the yaw drive to position the rotor axis upwind of the tower within an average wind azimuth error of +/- 8 degrees for rotational modes.

c) Generating commands to the yaw drive for directional rotation of the nacelle in manual mode.

d) Monitoring of drive operation for fault detection.

e) Local control of drive components for coordination and sequencing.

3.2.2.8.3.2 Rotor Torque Control

The rotor torque control function shall provide for:

a) Sending position reference signals to pairs of control surface position servoactuators.

b) Electrical adjustment of individual control surface position reference offset relative to a single collective position reference.

c) Generating an initial position reference and a speed reference command ramp for startup to achieve operating speed in a reasonable time with respect to wind conditions.

d) Generating position reference commands for speed control with a goal to maintain +/- 1.0 RPM to a speed reference from 3 to 17 RPM at the rotor.

e) Generating a speed reference command ramp for shutdown.

f) Monitoring of differential control angle and command mismatch for fault detection.

g) Closed loop control of each control surface position in response to position reference commands (incorporated with actuation of paragraph 3.2.2.4.3.1.

h) Generating a speed reference command to maximize subrated wind power output.

i) Generating position reference commands for limited position control in manual mode.

3.2.2.8.5.3 Hydraulic Systems Control

The hydraulic systems control function shall provide for:

a) Generating commands to enable and disable the rotor, yaw and lubrication hydraulic systems for automatic and manual modes.

b) Monitoring pressure, flow, level and temperature conditions as appropriate for fault detection.

c) Local control of accumulator pressure, flow, cooling and heating as appropriate to system operation.

3.2.2.8.5.4 Electrical System Control

The electrical system control function shall provide for:

a) Generating commands to enable operation of the generator as a variable speed drive to accelerate the wind rotor from zero to approximately 4 RPM.

b) Generating commands to synchronize the generator to the utility at wind rotor speeds anywhere between 12 and 17 RPM.

c) Generating airgap torque commands as a function of speed and maximum user power set point to provide no more than 120% of rated torque and an effective dynamic airgap characteristic of 160% +/- 20% rated torque per RPM at the wind rotor. The converter of paragraph 3.2.2.2.2.2 shall follow the command.

d) Generating reactive power reference commands or optionally voltage reference commands as a function of user set point. The converter of paragraph 3.2.2.2.2.2 shall follow the commands and provide for a manual selection of reactive power or voltage control mode.

e) Monitoring voltage, power position and temperature conditions as appropriate for fault detection and command mismatch.

3.2.2.8.5.5 Teeter Restrictor Control

The teeter restrictor control function shall provide for applying the restrictor at rotor speeds below 11 RPM and releasing the restrictor at rotor speeds above 11 RPM. Local control of the restrictor shall be used to apply light damping restriction.

3.2.2.8.5.6 Rotor Stopping Brake Control

The rotor brake control shall provide for:

a) Generating a command to release the brake for startup.

b) Generating a command to apply the brake on shutdown for rotor speed less than 8 RPM or after aerodynamic control surfaces are deployed.

c) Generator commands to release and apply the brake for rotor positioning and manual modes.

3.2.2.8.5.7 Rotor Positioning Control

The rotor positioning control shall provide for:

a) Generating commands to the rotor positioning device of paragraph 3.2.2.5.6 for rotation of the rotor.

b) Generating coordination commands for the rotor stopping brake of paragraph 3.2.2.8.5.6 during positioning operation.

3.2.2.8.5.8 Failsafe Emergency Shutdown Control

The failsafe control function shall provide for separate hardware to initiate an emergency shutdown in response to critical backup sensor anomaly, manual input, controller command, controller malfunction or loss of control power. An emergency shutdown shall consist as a minimum of aerodynamic control surface operation at the emergency feather rate of paragraph 3.2.2.4.3.3 and application of the rotor stopping brake after a time delay. When the

aerodynamic controls are fully feathered, an emergency shutdown shall lead to a normal shutdown sequence if the controller is active and power is available.

3.2.2.8.5.9 Fault Monitor Control

The fault monitor control function shall provide for:

a) Comparing all sensor values to expected state and alarm reference values.

b) Generating commands for mode transfer or shutdown on value mismatches.

3.2.2.8.5.10 Manual Control

The manual control function shall provide for site interface controlled operation in the manual modes of paragraph 3.1.7.2.

3.2.2.8.5.11 Data Window

The data window function shall provide for:

a) Retention of all sensor and critical average values time sampled and tagged at 1.0 second intervals for up to 120 seconds prior to any fault indication.

b) Retention of all sensor and critical average values sampled and time tagged at 1.0 second intervals for up to 180 seconds following the last fault indication.

c) Selectable display of retained values at the site interface in engineering units. Display shall be required prior to exit from a lockout mode.

3.2.2.8.5.12 Operating Accumulation

The operation accumulation function shall provide hardware and software for:

a) Accumulation of total time and hours when average wind is: less than VLCI, from VLCI to VRAT, from VRAT to VHCI, and greater than VHCI as defined in paragraph 3.2.1.2 and based on one minute average wind speeds, and hours when output is positive.

b) Accumulation of unavailable time when system mode is manual or lockout and user commanded unavailability in standby inhibit mode.

c) Accumulation of daily KW-hours based on a one minute average and overall total KW-hours.

d) Accumulation of rotor revolutions.

e) Display of selected software accumulated values periodically at the site or remote interface.

3.2.2.8.5.13 Data Display

The data display function shall provide for display of time tagged sensor, average and command values in engineering units with automatic updating at approximately 15 minute intervals or on change of mode at the site and remote interface.

3.2.2.8.6 Instrumentation

3.2.2.8.6.1 Operational Instrumentation

Operational instrumentation sensors, controls, device range, resolution, accuracy and other parameters shall be per 47D387005, Signal and Command List. Signal conditioning shall be supplied as needed.

3.2.2.8.6.2 Engineering Data Instrumentation

Engineering data instrumentation sensors, controls, device ranges, resolution, accuracy and other parameters shall be per 47D387005, Signal and Command List. This instrumentation is required on initial units and is a requisition option for volume production.

The control subsystem shall provide signal conditioning and multiplexing of Engineering Instrumentation System (EIS) sensors. Each data channel shall be frequency modulated into a band of +/- 125 Hz about a center frequency of from 1000 to 8500 Hz in 500 Hz increments. The resulting 16 data channels plus a 9500 Hz reference frequency shall be multiplexed and be capable of driving 2000 ft. of 75 ohm coaxial cable with BNC connector termination. A triple conductor calibration line shall interconnect all signal conditioners.

Up to six multiplexed lines shall be provided per WTG for a total of 96 data channels. Interface information provided by GE to the customer furnished recording and processing function shall include channel assignments, calibration data, and display requirements.

3.2.2.8.6.3 User Instrumentation

User instrumentation shall be provided as necessary to meet the reasonable needs of the connected utility for maintenance and operating data collecton. Initial device ranges, resolution accuracy and other parameters shall be per 47D387005, Signal and Command List.

3.2.2.8.6.4 Wiring

Control system wiring external to the controller cabinet shall be routed in continuous metallic conduit.

3.2.2.8.7 Lightning Protection

Lightning protection shall be provided such that the lightning model of parargraph 3.2.3.2 will not cause damage to the control system. Shielding and voltage limiting devices shall be provided where necessary. Strain gages mounted on the rotor may be expendable.

3.2.2.8.8 Interfaces

The control subsystem interfaces with the nacelle, rotor, drivetrain, tower and site equipment for mechanical and electrical installation. The network interface is per paragraph 3.1.5.2. Site and remote operator interfaces are described in paragraphs 3.2.2.8.1 through 3.2.2.8.5.

3.2.2.8.9 Maintenance and Access

Control system hardware shall be provided with features to minimize WTG inspection and maintenance life cycle costs. Minimum requirements are as follows:

a) Diagnostic functions shall be built into the controller.

b) No lower than board level replacement shall be used for maintenance.

c) All electrical connections at major devices shall be keyed to ease assembly, test and replacement.

d) All sensor and command lines shall have test points where they leave the controller for single location maintenance checks.

e) A sensor simulator and connection shall be available for major checkouts. This is a non-deliverable simulator for use on installation.

f) The site and remote interfaces shall have the capability to drive either hard copy or non-hard copy terminal devices.

g) All motor control circuits shall have local/automatic and local start/stop switches on controllers located near the motor.

3.2.2.9 Reliability, Availability, Maintainability, Spares

3.2.2.9.1 Reliability, Availability, Maintainability

The WTG reliability shall be consistent with the requirement that availability shall not be less than 92 percent when wind is between VLCO and VHCO as defined in paragraph 3.2.1.2 over a 30 year operational life for volume production in single or cluster installations.

3.2.2.9.2 Reliability

Reliability allocations shall be as shown in Table 3.2.2.9-1.

System Mean Time Between Failures (SMTBF) are for the duty cycle of paragraph 3.2.1.1 and the wind characteristic of paragraph 3.2.1.2 on an annualized basis. A mature system (after infant mortality) is assumed.

Reliability methodology shall be per document 47A380020 "Reliability, Availability, Maintainability and Failure Modes and Effects Analysis Plan".

3.2.2.9.3 Availability

System availability allocations shall be as shown in Table 3.2.2.9-1.

Average Annual Outage (AAO) time is the sum of scheduled and unscheduled times.

Availability methodology shall be per document 47A380020.

3.2.2.9.4 Maintainability

System maintainability allocations shall be as shown in Table 3.2.2.9-1.

Mean Time To Repair (MTTR) hours per system failure assume a full spares and on-site maintenance crew availability. Single unit installations and first units have higher MTTR reflected due to experience.

Maintainability methodology shall be per document 47A380020.

TABLE 3.2.2.9-1
RAM ALLOCATIONS

Installation	Mature Volume Production	Cluster	Cluster	Single	First
Subsystem	SMTBF	MTTR	AAO	AAO	AAO
Rotor	2731	28	89.8	197.7	250
Drivetrain	3063	19.8	56.6	124.5	141
Nacelle & Tower	3650	15.0	35.5	68.0	110
Controls, Instrumentation & Switchgear	1460	6.4	38.6	85.1	120
Cluster (Per WTG)	105,162	48.0	4.0	--	--
Unscheduled	602		224.5	475.3	621
Scheduled AAO			90.0	120.0	180.0
Total AAO			314.5	595.5	801.0
Availability			.964	.932	.908

(1561A)

3.2.2.9.5 Maintainability Features

The WTG shall have the maintainability and access features described in the subsystem requirements paragraph of this Section 3.2.2. General shop facilities shall be assumed for off-site work. MIL-STD-1472 shall be used as a guide for access. Single person lifting requirements shall not exceed 40 lb. Commercially available test equipment and tools shall be used as much as possible.

3.2.2.9.6 Spares

The WTG design shall include a listing of spare parts required to meet the availability goals of paragraph 3.2.2.9.3 based on the reliability allocations of paragraph 3.2.2.9.2. Separate listings shall be prepared for 1st, 2nd, 3rd, single and cluster installations.

3.2.2.9.7 Maintenance Personnel

Cluster installation maintenance and repair manpower shall be based on a dedicated crew and single installation maintenance and repair manpower shall be based on a per-job basis contract or general crew. Crews shall be trained per paragraph 3.2.2.3 in order to meet the maintainability goals of paragraph 3.2.2.9.4

3.2.3 Environment

3.2.3.1 Design Wind Environment

The WTG shall be designed for optimum cost-of-energy computed per paragraph 3.0 in a mean wind environment of 14 miles per hour (6.3 mps) measured at 32.8 feet (10m) above ground level.

3.2.3.1.1 Extreme Wind

The WTG shall be designed to survive a maximum design wind of 120 miles per hour (53.6 mps) measured at 32.8 feet (10m) above ground level. Loads shall be computed for no turbulence (zero gusts) and a vertical gradient exponent of 0.04 as used in paragraph 3.2.3.1.2.

3.2.3.1.2 Design Vertical Wind Gradient

The steady wind speed varies with vertical distance above ground level dependent on wind speed and surface roughness as:

$$\text{Log } (VZ/VR) = A \times \log (Z/ZR)$$

$$A = AO \times (1 - (\text{Log}(VR/2.237)/\text{Log}(VH/2.237)))$$

Where VZ = Steady wind at elevation Z, mph

VR = Steady wind at reference elevation ZR, mph

A = Vertical gradient exponent

Z = Elevation of interest, feet

ZR = Reference elevation, 32.8 feet (10m)

AO = Surface roughness exponent, 0.35

VH = Homogeneous wind speed for A = 0, 150 mph (67 mps)

3.2.3.1.3 Design Annual Wind Duration

The steady wind speed varies annually in accordance with a Weibull distribution as:

$$H = 8760 \times EXP [- (V/CR) ** KR]$$

Where H = Annual time that VR is greater or equal to V, hours

V = Wind speed at reference elevation ZR, mph

CR = Weibull scale factor at ZR, 16.04 mph (7.17 mps)

KR = Weibull shape factor at ZR, 2.29

** = denotes operation of raising to a power

The above defines a mean wind of 14 mph at ZR = 32.8 feet. Weibull parameters for elevations other than ZR may be derived in accordance with the method of Exhibit B, 3.1.2, Contract DEN 3-153.

3.2.3.1.4 Design Wind Turbulence

Wind turbulence is characterized as a Gaussian random process around the steady wind speed at reference elevation with standard deviations of:

$$SD(R,X) = VR/(\ln((ZR/ZO) + 1))$$
$$SD(R,Y) = 0.8 \times SD(R,X)$$
$$SD(R,Z) = 0.5 \times SD(R,X)$$

Where SD(R,X) = Turbulence standard deviation associated with VR, mps
VR = Reference elevation steady wind speed, mps
ZR = Reference elevation, 32.8 feet (10m)
ZO = Surface roughness length, 0.0162 feet (0.053 m)
X = denotes longitudinal directional
Y = denotes lateral direction
Z = denotes vertical direction

3.2.3.1.4.1 Spectrum

The spectrum of turbulence is characterized by:

$$FX(N,Z,V) = (((SD(R,X))^{**}2.)/n) \times ((0.164 \times FIX)/(1 + 0.164 \times (FIX^{**}(5/3))))$$

Where FX (n,z,v) = average annual spectrum for longitudinal component of wind turbulence, MPS x MPS x Sec., for frequency n, at height Z, and wind speed V.

n = circular frequency, hz

FIX = N/NOX

N = reduced frequency = NZ/V, dimensionless

NOX = constant for X direction = 0.0144, dimensionless using similar equations, lateral and vertical components are characterized with:

NOY = constant for Y direction = 0.0265

NOZ = constant for Z direction = 0.0962

The turbulence longitudinal standard deviation, SDX, for use in determining gust amplitude is obtained from the square foot of the integral of FX(N,Z,V) x dn over the frequencies from n(min) to n(max) where the limits are representative of the WTG response characteristics. Gust amplitude probability is determined by use of the standard deviation in a Gaussian random process as:

$$P(AX) = (0.299/SDX) \times EXP\ (-(0.5) \times (0.75 \times AX/SDX)^{**2})$$

Where P(AX) = probability density function of longitudinal gust amplitude, AX

AX = longitudinal gust amplitude, mps

SDX = longitudinal direction gust standard deviation from integral evaluation, mps

This probability model is valid to AX = 2*SDX. For larger amplitudes, a Rayleigh filtered distribution should be used to fit measured data. The above model produces conservatively large amplitude probabilities for AX greater than 2*SDX. The P(AX) expression is based on NASA WEPO PIR #151 which utilizes a 4/3 multiplier on SDX instead of the Contract DEN 3-153, Exhibit B, section 3.1.3 multiplier of 1.

3.2.3.1.4.2 Time History Gust Model

A first estimate of gust model shape is:

$$VX(t) = +/- (AX/2) \times (1 - \cos(6.283 \times t/TX))$$

Where VX(t) = longitudinal gust amplitude with time relative to steady wind, mps

AX = longitudinal gust amplitude, mps

TX = gust period, sec

The gust period may be selected at the modal periods of the WTG for worst case response. The most probable period is:

$$TAX(50\%) = .74 \times (ST/SA) \times AX$$

Where TAX = longitudinal period of amplitude AX, sec

ST = (4/3) x TM

SA = (4/3) x SDX

TM = .5 x square root of
((integral of FX(N Z,V) x dn)/(integral of n*n*FX(N,Z,V) x dn)) with integrals evaluated from n(min) to n(max) as in paragraph 3.2.2.1.4.1

Similar relationships apply in the y and z directions. The above amplitude is based on NASA WEPO PIR #151 which is half the amplitude in Contract DEN 3-153, Exhibit B, section 3.1.3.

3.2.3.2 Other Environmental Conditions

3.2.3.2.1 Temperature

The WTG shall be designed to survive in ambient temperatures from -40° C to +52° C (-40° F to +125° F). The WTG shall be designed to operate in ambient temperatures from -18° C to +40°C (0° F to +104° F).

3.2.3.2.2 Seismic

The WTG shall be capable of withstanding Zone 3 siesmic intensity as defined in the Uniform Building Code of issue date in effect on April 2, 1982.

3.2.3.2.3 Moisture

The WTG shall be designed to withstand exposure to precipitation and ambient humidity conditions of:

Rain - 4 inches/hour

Hail - 1 inch diameter, 50 lb/cu.ft., 66.6 ft/sec impact velocity on horizontal and vertical surfaces

Ice - 2 inch thickness, 60 lb/cu.ft. non-operating on all external surfaces

Snow - 21 lb/sq.ft. blades, 41 lb/sq.ft. other horizontal surfaces

Humidity - Exposure equivalent to MIL STD 210 B.

3.2.3.2.4 Lightning

Direct and nearby strikes with current-time histories per Figure 3.2.3-1 shall be considered in the design of lightning protection details. The WTG shall withstand such strikes and provide for a discharge path to earth.

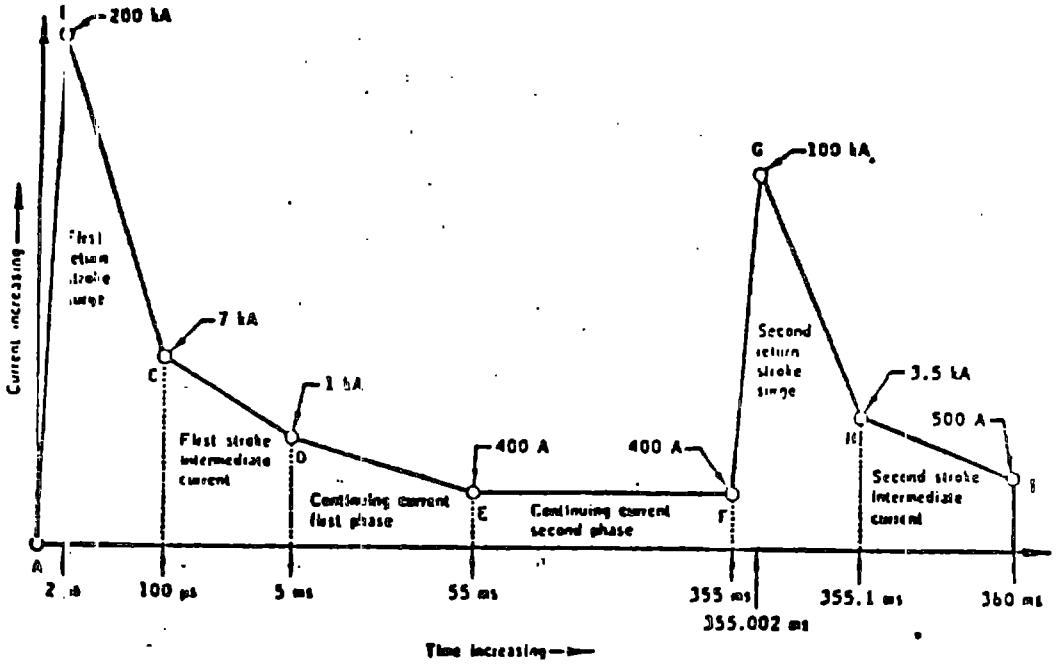

- DIAGRAMMATIC REPRESENTATION OF LIGHTNING MODEL
(Note that the diagram is not to scale.)

FIGURE 3.2.3-1
LIGHTNING CURRENT VS. TIME

(1561A)

3.2.3.2.5 Impact

The WTG shall be designed to sustain impact of a 4 lb. bird moving at 51.3 ft/sec into the rotor plane. Small arms projectiles shall be deflected or absorbed without structural degradation.

3.2.3.2.6 Intruders

Unauthorized personnel are considered as an environmental condition. The WTG design shall consider vandalism and prevent entry to secured areas.

3.2.3.2.7 Altitude

The WTG shall be designed for application at altitudes from sea level to 7000 feet. Derating of cooling and insulation characteristics dependent on air density may be utilized for application above 3300 feet.

3.2.3.2.8 Miscellaneous

Design sand, dust, salt spray, and fungus exposure shall be equivalent to MIL STD 210 B. Solar radiation shall be 363 BTU/sq.ft.-hr for 4 hours per day. Other environmental data shall be per NASA Technical Paper 1359.

3.2.4 Transportation

The WTG shall be designed for both rail and truck transport. Elements that exceed general truck limitations shall be rail transportable to a site rail-head then transferred to the site on the access roadway defined in paragraph 3.1.6.1.2. General constraints are as follows:

Item	Rail	Truck
Maximum weight	260,000 lb.	70,000 lb. (200,000 lb.)
Maximum length	85 ft. (120 ft.)	50 ft. (150 ft.)
Maximum width	Figure 3.2.4-1	12 ft. (14 ft.)
Maximum height	Figure 3.2.4-1	10 ft. (12 ft.)

Values in parenthesis are possible at added cost due to special routing, escorts and permits. Rail limits are more severe in the Northeast.

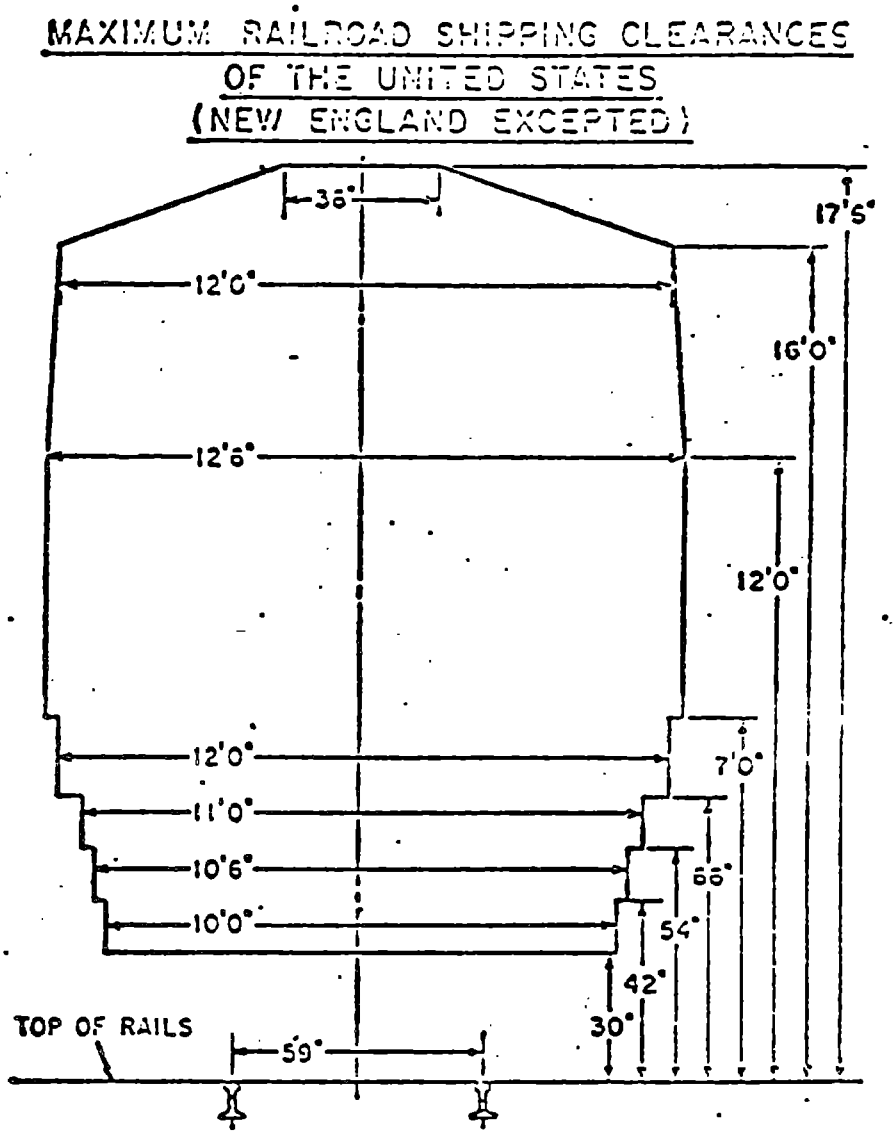

FIGURE 3.2.4-1
RAIL SIZE LIMITS

3.2.5 Design Loads

Design loads shall be computed with an analytical model representative of the transient dynamic behavior of the wind turbine structure, control system and wind.

3.2.5.1 Normal Operating Loads

Normal operating loads shall be based on the conditions of Table 3.2.5-1.

3.2.5.2 Abnormal Operating Loads

Abnormal operating loads shall be based on the conditions of Table 3.2.5-2. Abnormal operating loads are infrequently occurring and produce limit load conditions or define extent of survivable damage.

3.2.5.3 Handling Loads

Handling loads are those resulting from shop operations, shipping, erection, and repair activities. Attachment points and rigging lines of action shall be considered in addition to wind, temperature, shock and vibration loads. Section 5.2.2 of 47A38002, Structural Design Criteria, provides definition of handling load factors with respect to weight.

TABLE 3.2.5-1 NORMAL OPERATING LOAD CONDITIONS

	Environment (See Temperature Note)								
	Wind			Shock		Impact		Weight	
	10-60 MPH Mean	Gust	120 MPH Extreme	Seismic	Vibration	Hail	Fauna	Ice	Snow
Parked			x	x	x	x		x	x
Startup/Shutdown	x	x			x				
Motoring	x	x			x				
Generating	x	x		x	x	x	x	x	
Loss of Load	x	x							

The survival temperature range shall be considered in the parked condition and the operating temperature range shall be considered in other normal operating conditions.

TABLE 3.2.5-2 ABNORMAL OPERATING LOAD CONDITIONS

	Environment								
	Wind			Shock		Impact		Weight	
	10-60 MPH Mean	Gust	120 MPH Extreme	Seismic	Vibration	Hail	Fauna	Ice	Snow
Partial Control Jam (one surface stuck)	x	x							
Control Malfunction (hard over to maximum torque)	x	x							
Overspeed (50% survival)	x				x				
Brakes On (application while generating)	x				x				
Partial Blade Failure	x				x				
Generator Malfunction (bad sync)	x				x				

SECTION 4.0
VERIFICATION

4.1 Verification Methods and Requirements

Verification that the WTG complies with the requirements of Section 3.0 shall be accomplished by the methods of inspection, analysis, demonstration, and test.

4.1.1 Inspection Method

The inspection method consists of visual observation or measurement of drawings, items or higher level assemblies to establish compliance with requirements.

4.1.2 Analysis Method

The analysis method consists of calculations and evaluation using mathematical models, extrapolation of data from similar units, hand or computer methods, and drawing review to predict performance or establish compliance with requirements.

4.1.3 Demonstration Method

The demonstration method consists of performing an observed activity where the observer qualifications and/or the activity procedure permit establishing compliance with requirements by opinion.

4.1.4 Test Method

The test method consists of performing an activity with calibrated instrumentation or special equipment, following a detailed procedure, to acquire data establishing compliance with requirements or definition of performance.

4.1.5 Verification Requirements

The requirements of Section 3 shall be verified in accordance with Table 4.1-1.

TABLE 4.1-1

of

VERIFICATION REQUIREMENTS

REQUIREMENT PARAGRAPH	ITEM	VERIFICATION LEVEL
		N = NONE SY = SYSTEM SS = SUBSYSTEM I = INSPECTION A = ANALYSIS D = DEMONSTRATION T = TEST
3.0	REQUIREMENTS	N
3.1	System Definition	N
3.1.1	System Description	N
3.1.2	Purpose	T,SY
3.1.3	Installation	D,SY
3.1.4	Drawings	I,SY
3.1.5	Interface	N
3.1.5.1	Electrical Network Interface	A,SY
3.1.5.2	Communication and Control Interface	T,SY
3.1.5.3	Operating and Maintenance Interface	N
3.1.6	Customer Furnished or Specified Items	N
3.1.6.1	Location	I
3.1.6.1.1	Area	I
3.1.6.1.2	Access	A
3.1.6.1.3	Approvals	N
3.1.6.2	Communication	I
3.1.6.3	Distribution Line	I,SY
3.1.6.4	Electrical Power Requirements	T,SY
3.1.6.5	Color and Markings	I,SY
3.1.6.6	Mobile Data Acquisition System	I
3.1.6.7	Utility Control and Storage Space	I
3.1.7	System Modes	T,SY
3.1.7.1	Automatic Modes	T,SS,SY
3.1.7.2	Manual Modes	T,SS,SY
3.2	Characteristics	N
3.2.1	System Requirements	N
3.2.1.1	System Power Output	T,SY
3.2.1.2	Design Wind Speed Values	A,T,SY
3.2.1.3	Design Efficiency	A,T,SS
3.2.1.4	Design Life	A,SS,SY
3.2.1.5	Frequency Placement	A,T,SY
3.2.1.6	Wind Characteristics	A
3.2.1.6.1	Design Wind	A
3.2.1.6.2	Site Specific Wind	A
3.2.2	Subsystem Requirements	N
3.2.2.1	Foundation and Site	N

REQUIREMENT PARAGRAPH	ITEM	VERIFICATION LEVEL N = NONE SY = SYSTEM SS = SUBSYSTEM I = INSPECTION A = ANALYSIS D = DEMONSTRATION T = TEST
3.2.2.1.1	Tower Foundation	I,A,SS
3.2.2.1.2	Ground Electrical Equipment Foundation (GEEF)	I,SS
3.2.2.1.3	Grounding	I,A,T,SS
3.2.2.1.4	Fencing	I
3.2.2.1.5	Grading	I
3.2.2.1.6	Maintenance and Access	I
3.2.2.2	Ground Electrical Equipment (GEE)	N
3.2.2.2.1	Step-up Transformer	A,SY
3.2.2.2.2	Switchgear Assembly	A,SS
3.2.2.2.2.1	Circuit Breakers	A,SY
3.2.2.2.2.2	Converter	A,T,SS,SY
3.2.2.2.2.3	Filters	A,T,SY
3.2.2.2.2.4	Capacitors	A,T,SY
3.2.2.2.2.5	UPS	A,D,SS
3.2.2.2.2.6	Accessory Power	A,D,SY
3.2.2.2.2.7	Battery Power	A,D,SS
3.2.2.2.2.8	Switchboard	A,D,SY
3.2.2.2.2.9	Enclosure	I,T,SS
3.2.2.2.3	Interlocks	I,SS
3.2.2.2.4	Ground Control Equipment	I,SS
3.2.2.2.5	Interfaces	A,SS,SY
3.2.2.2.6	Lightning Protection	A,SS,SY
3.2.2.2.7	Instrumentation	N
3.2.2.2.7.1	Operational Instrumentation	I,SS,SY
3.2.2.2.7.2	Engineering Data Instrumentation	I,T,SS
3.2.2.2.8	Maintenance and Access	I
3.2.2.3	Operation and Maintenance	N
3.2.2.3.1	Personnel	N
3.2.2.3.2	Site Operation	D,SY
3.2.2.3.3	Remote Operation	D,SY
3.2.2.3.4	Scheduled Maintenance	N
3.2.2.3.5	Training	D
3.2.2.3.6	Manuals	I
3.2.2.4	Rotor Subsystem	N
3.2.2.4.1	Yoke Assembly	A
3.2.2.4.1.1	Yoke	A,SS,SY
3.2.2.4.1.2	Teeter Assembly	A,SS,SY
3.2.2.4.1.3	Rotor Hydraulic Assembly	A,SS,SY
3.2.2.4.2	Blades	A,T,SS,SY
3.2.2.4.3	Aerodynamic Control (Ailerons)	A,T,SS,SY
3.2.2.4.3.1	Configuration	A,T,SS
3.2.2.4.3.2	Rates and Storage Requirements	A,T,SS

REQUIREMENT PARAGRAPH	ITEM	VERIFICATION LEVEL N = NONE SY = SYSTEM SS = SUBSYSTEM I = INSPECTION A = ANALYSIS D = DEMONSTRATION T = TEST
3.2.2.4.4	Lightning Protection	A,SY
3.2.2.4.5	Ice Detection	A,T,SS
3.2.2.4.6	Instrumentation	N
3.2.2.4.6.1	Operational Instrumentation	A,I,T
3.2.2.4.6.2	Engineering Data Instrumentation	I,T,SS
3.2.2.4.6.3	Wiring	I,SY
3.2.2.4.7	Interfaces	D,SY
3.2.2.4.8	Maintenance and Access	I,A,SS
3.2.2.5	Drive Subsystem	N
3.2.2.5.1	Low Speed Shaft	A,T,SS,SY
3.2.2.5.2	Gearbox	A,T
3.2.2.5.2.1	Operating Characteristics	A,T,SY
3.2.2.5.2.2	Lubrication	A,T,SS
3.2.2.5.2.3	Accessories	I,T,SS
3.2.2.5.3	High Speed Shafting	A,T,SS
3.2.2.5.4	Generator	A,T,SS,SY
3.2.2.5.5	Rotor Stopping Brake	A,T,SY
3.2.2.5.6	Rotor Positioner	A,T,SY
3.2.2.5.7	Lightning Protection	A,SY
3.2.2.5.8	Instrumentation	N
3.2.2.5.8.1	Operational Instrumentation	A,I,T
3.2.2.5.8.2	Engineering Data Instrumentation	I,T,SS
3.2.2.5.9	Interfaces	D,SY
3.2.2.5.10	Maintenance and Access	I,A,SS
3.2.2.6	Nacelle Subsystem	N
3.2.2.6.1	Bedplate and Rotor Support	A,I,SY
3.2.2.6.2	Fairing	I,SS,SY
3.2.2.6.2.1	Wind Sensor Mounting	I,SS
3.2.2.6.2.2	Air Flow and Ducting	A,T,SY
3.2.2.6.2.3	Fire Protection	A,T,SS
3.2.2.6.2.4	Maintenance Hoist	A,T,SS
3.2.2.6.2.5	Maintenance Light and Power	A,D,SS
3.2.2.6.2.6	Hazard Lighting	A,T,SS
3.2.2.6.3	Yaw Subsystem	N
3.2.2.6.3.1	Yaw Drive Assembly	A,T,SS
3.2.2.6.3.2	Slip Ring	A,T,SY
3.2.2.6.4	Lightning Protection	A,SY
3.2.2.6.5	Instrumentation	N
3.2.2.6.5.1	Operational Instrumentation	A,I,T
3.2.2.6.5.2	Engineering Data Instrumentation	I,T,SS
3.2.2.6.6	Interfaces	D,SY
3.2.2.6.7	Maintenance and Access	I,A,SS

REQUIREMENT PARAGRAPH	ITEM	VERIFICATION LEVEL N = NONE SY = SYSTEM SS = SUBSYSTEM I = INSPECTION A = ANALYSIS D = DEMONSTRATION T = TEST
3.2.2.7	Tower Subsystem	N
3.2.2.7.1	Tower Structure	A,T,SY
3.2.2.7.2	Nacelle Access Device	A,T,SS
3.2.2.7.3	Tower Lighting and Power	A,T,SS
3.2.2.7.4	Tower Wiring	A,I
3.2.2.7.5	Lightning Protection	A,SY
3.2.2.7.6	Interfaces	D,SY
3.2.2.7.7	Instrumentation	N
3.2.2.7.7.1	Engineering Data Instrumentation	I,T,SS
3.2.2.7.8	Maintenance and Access	I,A,SS
3.2.2.8	Control Subsystem	N
3.2.2.8.1	Controller	A,T,SS,SY
3.2.2.8.2	Site Interface	A,T,SS
3.2.2.8.3	Remote Interface	N
3.2.2.8.3.1	Standard Remote Interface	A,T,SY
3.2.2.8.3.2	Site Specific Remote Interface	A,T,SY
3.2.2.8.4	Supervisory Control Priority	A,T,SS
3.2.2.8.5	Control Functions	N
3.2.2.8.5.1	Yaw Position Control	T,SS,SY
3.2.2.8.5.2	Rotor Torque Control	T,SS,SY
3.2.2.8.5.3	Hydraulic System Control	T,SS,SY
3.2.2.8.5.4	Electrical System Control	A,T,SS,SY
3.2.2.8.5.5	Teeter Restrictor Control	A,T,SS,SY
3.2.2.8.5.6	Rotor Stopping Brake Control	T,SS,SY
3.2.2.8.5.7	Rotor Positioning Control	T,SS,SY
3.2.2.8.5.8	Failsafe Emergency Shutdown Control	T,SS,SY
3.2.2.8.5.9	Fault Monitor Control	T,SS,SY
3.2.2.8.5.10	Manual Control	T,SS,SY
3.2.2.8.5.11	Data Window	T,SS,SY
3.2.2.8.5.12	Operating Accumulation	T,SS,SY
3.2.2.8.5.13	Data Display	T,SS,SY
3.2.2.8.6	Instrumentation	N
3.2.2.8.6.1	Operational Instrumentation	I,T,SS
3.2.2.8.6.2	Engineering Data Instrumentation	I,T,SY
3.2.2.8.6.3	User Instrumentation	I,T,SY
3.2.2.8.6.4	Wiring	I
3.2.2.8.7	Lightning Protection	A,SY
3.2.2.8.8	Interfaces	D,SY
3.2.2.8.9	Maintenance and Access	I,A,SS
3.2.2.9	Reliability, Availability, Maintainability, Spares	N
3.2.2.9.1	Reliability, Availability, Maintainability	N

PARAGRAPH	REQUIREMENT ITEM	VERIFICATION LEVEL
		N = NONE SY = SYSTEM SS = SUBSYSTEM I = INSPECTION A = ANALYSIS D = DEMONSTRATION T = TEST
3.2.2.3.2	Reliability	A,SY
3.2.2.3.3	Availability	A,SY
3.2.2.3.4	Maintainability	A,SY
3.2.2.3.5	Maintainability Features	A.I
3.2.2.3.6	Spares	A,I
3.2.2.3.7	Maintenance Personnel	N
3.2.3	Environment	N
3.2.3.1	Design Wind Environment	N
3.2.3.1.1	Extreme Wind	A,SY
3.2.3.1.2	Design Vertical Wind Gradient	A,SY
3.2.3.1.3	Design Annual Wind Duration	A,SY
3.2.3.1.4	Design Wind Turbulence	A
3.2.3.1.4.1	Spectrum	A
3.2.3.1.4.2	Time History Gust Model	A
3.2.3.2	Other Environmental Conditions	N
3.2.3.2.1	Temperature	A,SY
3.2.3.2.2	Seismic	A,SY
3.2.3.2.3	Moisture	A,SY
3.2.3.2.4	Lightning	I,A,SY
3.2.3.2.5	Impact	A,SS
3.2.3.2.6	Intruders	A,SS
3.2.3.2.7	Altitude	A,SY
3.2.3.2.8	Miscellaneous	A,SY
3.2.4	Transporation	A,D,SS
3.2.5	Design Loads	N
3.2.5.1	Normal Operating Loads	A,SY
3.2.5.2	Abnormal Operating Loads	A,SY
3.2.5.3	Handling Loads	A,SS

4.2 Test,Types Requirements

In addition to requirements verification tests of Section 4.1, tests shall be conducted for the purposes of item, assembly, or system acceptance, integration, functional verification and design development.

4.2.1 Acceptance Tests

Acceptance tests are conducted as formal demonstration of performance or function with customer witnesses and in accordance with a mutually approved test procedure. Test results shall be approved by the witnesses as a prerequisite to delivery of the item, assembly or system.

4.2.2 Integration Tests

Integration tests verify interface compatibility between an item and a mating item or assembly. Physical and functional integration of all WTG subsystems is required.

4.2.3 Functional Tests

Functional tests verify the item or assembly function or performance (including structural integrity) and ability to operate at design capability or within design limits.

4.2.4 DEVELOPMENT TESTS

Development tests provide substantiation for a design concept, material configuration, allowable load level or manufacturing process prior to final release of production drawings. WTG development testing is expected in the design of the rotor and drivetrain.

4.2.5 Test Requirements

WTG items, assemblies and systems shall be tested in accordance with Table 4.2-1.

TABLE 4.2-1

Test Requirements

Paragraph	Item	Test Category A = Acceptance I = Integration F = Functional D = Development
3.1.3.2.1	SYSTEM	A (Customer)
3.1.7	System Modes	A,I,F (Local & Remote)
3.2.1.1	Power Output	A,I,F (Rating, P vs V)
3.2.1.2	Design Wind Speed	I,F (Cut-in, Rating)
3.2.1.5	Frequency Placement	I,F (Measurements)
3.2.2.1	Foundation & Site	A
3.2.2.1.1	Tower Foundation	A,I (Tower)
3.2.2.1.2	GEE Foundation	A,I (GEE)
3.2.2.1.3	Grounding	I,F (Check Resistance)
3.2.2.1.4	Fencing	I (Grounding, Security)
3.2.2.2	Ground Electrical Equipment	A
3.2.2.2	All Items	A,I,F,D (Variable Speed Subsystem)
3.2.2.4	Rotor Subsystem	A
3.2.2.4.1	Yoke Assembly	A,I,F (All Subsystems)
3.2.2.4.2	Blades	A,I,F (Proof), D (Properties)
3.2.2.4.3	Aerodynamic Control	A,I,F (Actuators & Surface), D (Actuators)
3.2.2.4.5	Ice Detection	I,F
3.2.2.4.6	Instrumentation	I,F (Calibration)
3.2.2.5	Drivetrain	A
3.2.2.5.1	Low Speed Shaft	I,F (Alignment)
3.2.2.5.2	Gearbox	A,I,F (Ratio, Sensors, Lube)
3.2.2.5.3	Highspeed Shafting	I,F
3.2.2.5.4	Generator	A,I,F,D (Variable Speed Subsystem, Tilt)
3.2.2.5.5	Stopping Brake	I,F (Yoke/Nacelle)
3.2.2.5.6	Rotor Positioner	F
3.2.2.5.8	Instrumentation	I,F (Calibration)

Paragraph	Item	Test Category A = Acceptance I = Integration F = Functional D = Development
3.2.2.6	Nacelle	A
3.2.2.6.1	Bedplate & Rotor Support	I (Rotor & Drivetrain)
3.2.2.6.2	Fairing	I,F
3.2.2.6.2.1	Wind Sensor Mounting	I,F
3.2.2.6.2.2	Air Flow & Ducting	I,F (Filtration)
3.2.2.6.2.3	Fire Protection	I,F (Alarm, Sealing)
3.2.2.6.2.4	Maintenance Hoist	I,F (Accessibility)
3.2.2.6.2.5	Light & Power	F
3.2.2.6.2.6	Hazard Lighting	I,F (Control)
3.2.2.6.3.1	Yaw Drive ASM	I,F (Rates, Control)
3.2.2.6.3.2	Slipring	A,I,F (Resistance)
3.2.2.6.4	Lightning Protection	I
3.2.2.6.5	Instrumentation	I,F (Calibration)
3.2.2.7	Tower Subsystem	A
3.2.2.7.1	Structure	A,I
3.2.2.7.2	Access Device	A,I,F (Weight, Rate)
3.2.2.7.3	Lighting & Power	F
3.2.2.7.4	Wiring	I,F
3.2.2.7.5	Lightning Protection	I
3.2.2.7.7	Instrumentation	I,F (Calibration)
3.2.2.8	Control Subsystem	A,I,D (Software)
3.2.2.8.1	Controller	A,I,F
3.2.2.8.2	Site Interface Device	I,F
3.2.2.8.3	Remote Interface Device	A,I,F (Customer)
3.2.2.8.4	Supervisory Control Priority	I,F,D
3.2.2.8.5	Control Functions (All)	I,F,D (Interaction, Software Development)
3.2.2.8.6	Instrumentation	I,F (Calibration, EIS)
3.2.2.8.7	Lightning Protection	I

SECTION 5.0

PREPARATION FOR DELIVERY

The contractor shall provide control of the delivery requirements of all deliverable items in order to assure quality and prevent damage, loss, deterioriz ation or unauthorized substitution. Procedures for packaging, packing, marking and shipping shall be established and maintained, in compliance with Interstate Commerce Commission rules and regulations, in order to provide secure transport and clear identification at the destination and during erection.

APPENDIX B
DESIGN LOAD TABLES

Appendix B Design Load Tables

Contents

TABLE H- 1
CUMMULATIVE FATIGUE HISTOGRAM OUTPUT

0. R BLADE VX

NO. CYCLES IN 30 YEARS (TYPES 1+2)	CUM PROB	HALF-RANGE FATIGUE LOADS: LOAD LEVELS	HALF-RANGE FATIGUE LOADS: NORMALIZED LOAD LEVELS	HALF-RANGE FATIGUE LOADS: LOAD/50% AT RATED	MID-RANGE MEAN
0.180E 08	0.05000	0. - 0.142E 06	0. - 0.81	0. - 0.94	0.691E 06
0.180E 08	0.10000	0.142E 06 - 0.145E 06	0.81 - 0.82	0.94 - 0.96	0.682E 06
0.180E 08	0.15000	0.145E 06 - 0.146E 06	0.82 - 0.83	0.96 - 0.97	0.669E 06
0.179E 08	0.20000	0.146E 06 - 0.148E 06	0.83 - 0.84	0.97 - 0.98	0.655E 06
0.180E 08	0.25000	0.148E 06 - 0.149E 06	0.84 - 0.85	0.98 - 0.99	0.641E 06
0.180E 08	0.30000	0.149E 06 - 0.150E 06	0.85 - 0.85	0.99 - 1.00	0.626E 06
0.180E 08	0.35000	0.150E 06 - 0.151E 06	0.85 - 0.86	1.00 - 1.00	0.611E 06
0.179E 08	0.40000	0.151E 06 - 0.152E 06	0.86 - 0.86	1.00 - 1.01	0.596E 06
0.180E 08	0.45000	0.152E 06 - 0.152E 06	0.86 - 0.87	1.01 - 1.01	0.584E 06
0.180E 08	0.50000	0.152E 06 - 0.153E 06	0.87 - 0.87	1.01 - 1.02	0.579E 06
0.179E 08	0.55000	0.153E 06 - 0.154E 06	0.87 - 0.88	1.02 - 1.02	0.576E 06
0.180E 08	0.60000	0.154E 06 - 0.155E 06	0.88 - 0.88	1.02 - 1.03	0.570E 06
0.179E 08	0.65000	0.155E 06 - 0.156E 06	0.88 - 0.89	1.03 - 1.04	0.564E 06
0.180E 08	0.70000	0.156E 06 - 0.157E 06	0.89 - 0.89	1.04 - 1.04	0.554E 06
0.179E 08	0.75000	0.157E 06 - 0.158E 06	0.89 - 0.90	1.04 - 1.05	0.541E 06
0.179E 08	0.80000	0.158E 06 - 0.159E 06	0.90 - 0.90	1.05 - 1.06	0.532E 06
0.180E 08	0.85000	0.159E 06 - 0.160E 06	0.90 - 0.91	1.06 - 1.06	0.529E 06
0.179E 08	0.90000	0.160E 06 - 0.162E 06	0.91 - 0.92	1.06 - 1.08	0.524E 06
0.180E 08	0.95000	0.162E 06 - 0.164E 06	0.92 - 0.93	1.08 - 1.09	0.514E 06
0.718E 07	0.97000	0.164E 06 - 0.166E 06	0.93 - 0.94	1.09 - 1.10	0.508E 06
0.718E 07	0.99000	0.166E 06 - 0.169E 06	0.94 - 0.96	1.10 - 1.12	0.499E 06
0.323E 07	0.99900	0.169E 06 - 0.174E 06	0.96 - 0.99	1.12 - 1.16	0.478E 06
0.323E 06	0.99990	0.174E 06 - 0.176E 06	0.99 - 1.00	1.16 - 1.17	0.488E 06

TOTAL CYCLES = 0.359E 09

ROOT MEAN CUBED IS 0.152E 06 AVERAGE MEAN IS 0.587E 06

TABLE H- 2
CUMMULATIVE FATIGUE HISTOGRAM OUTPUT

0. R BLADE VY

NO. CYCLES IN 30 YEARS (TYPES 1+2)	CUM PROB	HALF-RANGE FATIGUE LOADS: LOAD LEVELS	HALF-RANGE FATIGUE LOADS: NORMALIZED LOAD LEVELS	HALF-RANGE FATIGUE LOADS: LOAD/50% AT RATED	MID-RANGE MEAN
0.180E 08	0.05000	0. - 0.154E 06	0. - 0.78	0. - 0.93	0.424E 04
0.180E 08	0.10000	0.154E 06 - 0.156E 06	0.78 - 0.80	0.93 - 0.94	0.445E 04
0.180E 08	0.15000	0.156E 06 - 0.158E 06	0.80 - 0.81	0.94 - 0.95	0.452E 04
0.179E 08	0.20000	0.158E 06 - 0.159E 06	0.81 - 0.81	0.95 - 0.96	0.452E 04
0.180E 08	0.25000	0.159E 06 - 0.160E 06	0.81 - 0.82	0.96 - 0.96	0.448E 04
0.180E 08	0.30000	0.160E 06 - 0.161E 06	0.82 - 0.82	0.96 - 0.97	0.443E 04
0.180E 08	0.35000	0.161E 06 - 0.162E 06	0.82 - 0.83	0.97 - 0.98	0.435E 04
0.179E 08	0.40000	0.162E 06 - 0.163E 06	0.83 - 0.83	0.98 - 0.98	0.426E 04
0.180E 08	0.45000	0.163E 06 - 0.164E 06	0.83 - 0.84	0.98 - 0.99	0.415E 04
0.180E 08	0.50000	0.164E 06 - 0.165E 06	0.84 - 0.84	0.99 - 0.99	0.403E 04
0.179E 08	0.55000	0.165E 06 - 0.166E 06	0.84 - 0.85	0.99 - 1.00	0.389E 04
0.180E 08	0.60000	0.166E 06 - 0.167E 06	0.85 - 0.85	1.00 - 1.00	0.375E 04
0.179E 08	0.65000	0.167E 06 - 0.167E 06	0.85 - 0.85	1.00 - 1.01	0.360E 04
0.180E 08	0.70000	0.167E 06 - 0.168E 06	0.85 - 0.86	1.01 - 1.01	0.344E 04
0.179E 08	0.75000	0.168E 06 - 0.169E 06	0.86 - 0.86	1.01 - 1.02	0.344E 04
0.179E 08	0.80000	0.169E 06 - 0.170E 06	0.86 - 0.87	1.02 - 1.02	0.356E 04
0.180E 08	0.85000	0.170E 06 - 0.172E 06	0.87 - 0.88	1.02 - 1.03	0.354E 04
0.179E 08	0.90000	0.172E 06 - 0.174E 06	0.88 - 0.89	1.03 - 1.05	0.341E 04
0.180E 08	0.95000	0.174E 06 - 0.176E 06	0.89 - 0.90	1.05 - 1.06	0.330E 04
0.718E 07	0.97000	0.176E 06 - 0.178E 06	0.90 - 0.91	1.06 - 1.07	0.324E 04
0.718E 07	0.99000	0.178E 06 - 0.182E 06	0.91 - 0.93	1.07 - 1.09	0.310E 04
0.323E 07	0.99900	0.182E 06 - 0.187E 06	0.93 - 0.96	1.09 - 1.13	0.299E 04
0.323E 06	0.99990	0.187E 06 - 0.196E 06	0.96 - 1.00	1.13 - 1.18	-0.122E 04

TOTAL CYCLES = 0.359E 09

ROOT MEAN CUBED IS 0.163E 06 AVERAGE MEAN IS 0.392E 04

TABLE H- 3
CUMMULATIVE FATIGUE HISTOGRAM OUTPUT

0. R BLADE VZ

NO. CYCLES IN 30 YEARS (TYPES 1+2)	CUM PROB	HALF-RANGE FATIGUE LOADS: LOAD LEVELS	NORMALIZED LOAD LEVELS	LOAD/50% AT RATED	MID-RANGE MEAN
0.180E 08	0.05000	0. - 0.455E 04	0. - 0.08	0. - 0.43	-0.795E 05
0.180E 08	0.10000	0.455E 04 - 0.527E 04	0.08 - 0.09	0.43 - 0.50	-0.827E 05
0.180E 08	0.15000	0.527E 04 - 0.582E 04	0.09 - 0.10	0.50 - 0.55	-0.853E 05
0.179E 08	0.20000	0.582E 04 - 0.629E 04	0.10 - 0.11	0.55 - 0.60	-0.875E 05
0.180E 08	0.25000	0.629E 04 - 0.674E 04	0.11 - 0.11	0.60 - 0.64	-0.895E 05
0.180E 08	0.30000	0.674E 04 - 0.716E 04	0.11 - 0.12	0.64 - 0.68	-0.913E 05
0.180E 08	0.35000	0.716E 04 - 0.758E 04	0.12 - 0.13	0.68 - 0.72	-0.930E 05
0.179E 08	0.40000	0.758E 04 - 0.800E 04	0.13 - 0.13	0.72 - 0.76	-0.946E 05
0.180E 08	0.45000	0.800E 04 - 0.843E 04	0.13 - 0.14	0.76 - 0.80	-0.960E 05
0.180E 08	0.50000	0.843E 04 - 0.887E 04	0.14 - 0.15	0.80 - 0.84	-0.974E 05
0.179E 08	0.55000	0.887E 04 - 0.934E 04	0.15 - 0.16	0.84 - 0.89	-0.988E 05
0.180E 08	0.60000	0.934E 04 - 0.984E 04	0.16 - 0.17	0.89 - 0.93	-0.100E 06
0.179E 08	0.65000	0.984E 04 - 0.104E 05	0.17 - 0.17	0.93 - 0.98	-0.102E 06
0.180E 08	0.70000	0.104E 05 - 0.110E 05	0.17 - 0.19	0.98 - 1.04	-0.103E 06
0.179E 08	0.75000	0.110E 05 - 0.117E 05	0.19 - 0.20	1.04 - 1.11	-0.104E 06
0.179E 08	0.80000	0.117E 05 - 0.126E 05	0.20 - 0.21	1.11 - 1.19	-0.105E 06
0.180E 08	0.85000	0.126E 05 - 0.136E 05	0.21 - 0.23	1.19 - 1.29	-0.106E 06
0.179E 08	0.90000	0.136E 05 - 0.151E 05	0.23 - 0.25	1.29 - 1.43	-0.107E 06
0.180E 08	0.95000	0.151E 05 - 0.176E 05	0.25 - 0.30	1.43 - 1.67	-0.111E 06
0.718E 07	0.97000	0.176E 05 - 0.194E 05	0.30 - 0.33	1.67 - 1.84	-0.114E 06
0.718E 07	0.99000	0.194E 05 - 0.235E 05	0.33 - 0.40	1.84 - 2.24	-0.118E 06
0.323E 07	0.99300	0.235E 05 - 0.314E 05	0.40 - 0.53	2.24 - 2.98	-0.124E 06
0.323E 06	0.99990	0.314E 05 - 0.593E 05	0.53 - 1.00	2.98 - 5.63	-0.121E 06

TOTAL CYCLES = 0.359E 09

ROOT MEAN CUBED IS 0.117E 05 AVERAGE MEAN IS -0.976E 05

TABLE H- 4
CUMMULATIVE FATIGUE HISTOGRAM OUTPUT

0. R BLADE MX

NO. CYCLES IN 30 YEARS (TYPES 1+2)	CUM PROB	HALF-RANGE FATIGUE LOADS: LOAD LEVELS	NORMALIZED LOAD LEVELS	LOAD/50% AT RATED	MID-RANGE MEAN
0.180E 08	0.05000	0. - 0.674E 05	0. - 0.40	0. - 0.49	-0.879E 05
0.180E 08	0.10000	0.674E 05 - 0.697E 05	0.40 - 0.41	0.49 - 0.51	-0.879E 05
0.180E 08	0.15000	0.697E 05 - 0.712E 05	0.41 - 0.42	0.51 - 0.52	-0.878E 05
0.179E 08	0.20000	0.712E 05 - 0.725E 05	0.42 - 0.43	0.52 - 0.53	-0.878E 05
0.180E 08	0.25000	0.725E 05 - 0.736E 05	0.43 - 0.43	0.53 - 0.54	-0.878E 05
0.180E 08	0.30000	0.736E 05 - 0.857E 05	0.43 - 0.50	0.54 - 0.63	-0.872E 05
0.180E 08	0.35000	0.857E 05 - 0.882E 05	0.50 - 0.52	0.63 - 0.64	-0.869E 05
0.179E 08	0.40000	0.882E 05 - 0.906E 05	0.52 - 0.53	0.64 - 0.66	-0.865E 05
0.180E 08	0.45000	0.906E 05 - 0.931E 05	0.53 - 0.55	0.66 - 0.68	-0.860E 05
0.180E 08	0.50000	0.931E 05 - 0.959E 05	0.55 - 0.56	0.68 - 0.70	-0.864E 05
0.179E 08	0.55000	0.959E 05 - 0.100E 06	0.56 - 0.59	0.70 - 0.73	-0.915E 05
0.180E 08	0.60000	0.100E 06 - 0.105E 06	0.59 - 0.62	0.73 - 0.76	-0.996E 05
0.179E 08	0.65000	0.105E 06 - 0.108E 06	0.62 - 0.64	0.76 - 0.79	-0.105E 06
0.180E 08	0.70000	0.108E 06 - 0.112E 06	0.64 - 0.66	0.79 - 0.82	-0.110E 06
0.179E 08	0.75000	0.112E 06 - 0.117E 06	0.66 - 0.69	0.82 - 0.86	-0.115E 06
0.179E 08	0.80000	0.117E 06 - 0.125E 06	0.69 - 0.74	0.86 - 0.91	-0.115E 06
0.180E 08	0.85000	0.125E 06 - 0.131E 06	0.74 - 0.77	0.91 - 0.95	-0.115E 06
0.179E 08	0.90000	0.131E 06 - 0.137E 06	0.77 - 0.81	0.95 - 1.00	-0.119E 06
0.180E 08	0.95000	0.137E 06 - 0.141E 06	0.81 - 0.83	1.00 - 1.03	-0.119E 06
0.718E 07	0.97000	0.141E 06 - 0.143E 06	0.83 - 0.84	1.03 - 1.04	-0.119E 06
0.718E 07	0.99000	0.143E 06 - 0.146E 06	0.84 - 0.86	1.04 - 1.07	-0.119E 06
0.323E 07	0.99300	0.146E 06 - 0.152E 06	0.86 - 0.90	1.07 - 1.11	-0.119E 06
0.323E 06	0.99990	0.152E 06 - 0.170E 06	0.90 - 1.00	1.11 - 1.24	-0.180E 06

TOTAL CYCLES = 0.359E 09

ROOT MEAN CUBED IS 0.105E 06 AVERAGE MEAN IS -0.990E 05

TABLE H- 5
CUMMULATIVE FATIGUE HISTOGRAM OUTPUT

0. R BLADE MY

NO. CYCLES IN 30 YEARS (TYPES 1+2)	CUM PROB	HALF-RANGE FATIGUE LOADS: LOAD LEVELS	NORMALIZED LOAD LEVELS	LOAD/50% AT RATED	MID-RANGE MEAN
0.180E 08	0.05000	0. - 0.674E 06	0. - 0.10	0. - 0.45	0.865E 07
0.180E 08	0.10000	0.674E 06 - 0.776E 06	0.10 - 0.12	0.45 - 0.52	0.894E 07
0.180E 08	0.15000	0.776E 06 - 0.854E 06	0.12 - 0.13	0.52 - 0.57	0.918E 07
0.179E 08	0.20000	0.854E 06 - 0.922E 06	0.13 - 0.14	0.57 - 0.62	0.937E 07
0.180E 08	0.25000	0.922E 06 - 0.985E 06	0.14 - 0.15	0.62 - 0.66	0.954E 07
0.180E 08	0.30000	0.985E 06 - 0.104E 07	0.15 - 0.16	0.66 - 0.70	0.970E 07
0.180E 08	0.35000	0.104E 07 - 0.110E 07	0.16 - 0.17	0.70 - 0.74	0.984E 07
0.179E 08	0.40000	0.110E 07 - 0.116E 07	0.17 - 0.18	0.74 - 0.78	0.998E 07
0.180E 08	0.45000	0.116E 07 - 0.122E 07	0.18 - 0.19	0.78 - 0.82	0.101E 08
0.180E 08	0.50000	0.122E 07 - 0.129E 07	0.19 - 0.20	0.82 - 0.87	0.102E 08
0.179E 08	0.55000	0.129E 07 - 0.135E 07	0.20 - 0.20	0.87 - 0.91	0.103E 08
0.180E 08	0.60000	0.135E 07 - 0.142E 07	0.20 - 0.22	0.91 - 0.96	0.104E 08
0.179E 08	0.65000	0.142E 07 - 0.150E 07	0.22 - 0.23	0.96 - 1.01	0.105E 08
0.180E 08	0.70000	0.150E 07 - 0.159E 07	0.23 - 0.24	1.01 - 1.07	0.106E 08
0.179E 08	0.75000	0.159E 07 - 0.169E 07	0.24 - 0.26	1.07 - 1.13	0.107E 08
0.179E 08	0.80000	0.169E 07 - 0.180E 07	0.26 - 0.27	1.13 - 1.21	0.108E 08
0.180E 08	0.85000	0.180E 07 - 0.195E 07	0.27 - 0.29	1.21 - 1.31	0.110E 08
0.179E 08	0.90000	0.195E 07 - 0.214E 07	0.29 - 0.32	1.31 - 1.44	0.112E 08
0.180E 08	0.95000	0.214E 07 - 0.249E 07	0.32 - 0.38	1.44 - 1.67	0.115E 08
0.718E 07	0.97000	0.249E 07 - 0.274E 07	0.38 - 0.42	1.67 - 1.84	0.118E 08
0.718E 07	0.99000	0.274E 07 - 0.329E 07	0.42 - 0.50	1.84 - 2.21	0.122E 08
0.323E 07	0.99900	0.329E 07 - 0.433E 07	0.50 - 0.66	2.21 - 2.91	0.127E 08
0.323E 06	0.99990	0.433E 07 - 0.660E 07	0.66 - 1.00	2.91 - 4.44	0.112E 08

TOTAL CYCLES = 0.359E 09

ROOT MEAN CUBED IS 0.165E 07 AVERAGE MEAN IS 0.102E 08

TABLE H- 6
CUMMULATIVE FATIGUE HISTOGRAM OUTPUT

0. R BLADE MZ

NO. CYCLES IN 30 YEARS (TYPES 1+2)	CUM PROB	HALF-RANGE FATIGUE LOADS: LOAD LEVELS	NORMALIZED LOAD LEVELS	LOAD/50% AT RATED	MID-RANGE MEAN
0.180E 08	0.05000	0. - 0.775E 07	0. - 0.89	0. - 1.05	-0.896E 06
0.180E 08	0.10000	0.775E 07 - 0.790E 07	0.89 - 0.91	1.05 - 1.07	-0.942E 06
0.180E 08	0.15000	0.790E 07 - 0.800E 07	0.91 - 0.92	1.07 - 1.08	-0.965E 06
0.179E 08	0.20000	0.800E 07 - 0.808E 07	0.92 - 0.93	1.08 - 1.09	-0.979E 06
0.180E 08	0.25000	0.808E 07 - 0.815E 07	0.93 - 0.94	1.09 - 1.10	-0.989E 06
0.180E 08	0.30000	0.815E 07 - 0.821E 07	0.94 - 0.94	1.10 - 1.11	-0.995E 06
0.180E 08	0.35000	0.821E 07 - 0.827E 07	0.94 - 0.95	1.11 - 1.12	-0.100E 07
0.179E 08	0.40000	0.827E 07 - 0.832E 07	0.95 - 0.96	1.12 - 1.13	-0.100E 07
0.180E 08	0.45000	0.832E 07 - 0.838E 07	0.96 - 0.96	1.13 - 1.14	-0.100E 07
0.180E 08	0.50000	0.838E 07 - 0.843E 07	0.96 - 0.97	1.14 - 1.14	-0.100E 07
0.179E 08	0.55000	0.843E 07 - 0.849E 07	0.97 - 0.97	1.14 - 1.15	-0.100E 07
0.180E 08	0.60000	0.849E 07 - 0.854E 07	0.97 - 0.98	1.15 - 1.16	-0.104E 07
0.179E 08	0.65000	0.854E 07 - 0.860E 07	0.98 - 0.99	1.16 - 1.17	-0.110E 07
0.180E 08	0.70000	0.860E 07 - 0.867E 07	0.99 - 1.00	1.17 - 1.18	-0.113E 07
0.179E 08	0.75000	0.867E 07 - 0.874E 07	1.00 - 1.00	1.18 - 1.18	-0.112E 07
0.179E 08	0.80000	0.874E 07 - 0.878E 07	1.00 - 1.01	1.18 - 1.19	-0.113E 07
0.180E 08	0.85000	0.878E 07 - 0.886E 07	1.01 - 1.02	1.19 - 1.20	-0.114E 07
0.179E 08	0.90000	0.886E 07 - 0.899E 07	1.02 - 1.03	1.20 - 1.22	-0.115E 07
0.180E 08	0.95000	0.899E 07 - 0.918E 07	1.03 - 1.05	1.22 - 1.24	-0.118E 07
0.718E 07	0.97000	0.918E 07 - 0.930E 07	1.05 - 1.07	1.24 - 1.26	-0.120E 07
0.718E 07	0.99000	0.930E 07 - 0.954E 07	1.07 - 1.10	1.26 - 1.29	-0.124E 07
0.323E 07	0.99900	0.954E 07 - 0.987E 07	1.10 - 1.13	1.29 - 1.34	-0.116E 07
0.323E 06	0.99990	0.987E 07 - 0.100E 08	1.13 - 1.15	1.34 - 1.36	-0.164E 07

TOTAL CYCLES = 0.359E 09

ROOT MEAN CUBED IS 0.838E 07 AVERAGE MEAN IS -0.105E 07

TABLE H- 7
CUMMULATIVE FATIGUE HISTOGRAM OUTPUT

0.100R BLADE VX

NO. CYCLES IN 30 YEARS (TYPES 1+2)	CUM PROB	HALF-RANGE FATIGUE LOADS: LOAD LEVELS	NORMALIZED LOAD LEVELS	LOAD/50% AT RATED	MID-RANGE MEAN
0.180E 08	0.05000	0. - 0.989E 05	0. - 0.80	0. - 0.97	0.668E 06
0.180E 08	0.10000	0.989E 05 - 0.101E 06	0.80 - 0.81	0.97 - 0.98	0.648E 06
0.180E 08	0.15000	0.101E 06 - 0.102E 06	0.81 - 0.82	0.98 - 0.99	0.629E 06
0.179E 08	0.20000	0.102E 06 - 0.103E 06	0.82 - 0.83	0.99 - 1.00	0.611E 06
0.180E 08	0.25000	0.103E 06 - 0.104E 06	0.83 - 0.83	1.00 - 1.01	0.593E 06
0.180E 08	0.30000	0.104E 06 - 0.104E 06	0.83 - 0.84	1.01 - 1.02	0.578E 06
0.180E 08	0.35000	0.104E 06 - 0.105E 06	0.84 - 0.85	1.02 - 1.03	0.568E 06
0.179E 08	0.40000	0.105E 06 - 0.106E 06	0.85 - 0.85	1.03 - 1.03	0.561E 06
0.180E 08	0.45000	0.106E 06 - 0.106E 06	0.85 - 0.86	1.03 - 1.04	0.554E 06
0.180E 08	0.50000	0.106E 06 - 0.107E 06	0.86 - 0.86	1.04 - 1.04	0.549E 06
0.179E 08	0.55000	0.107E 06 - 0.108E 06	0.86 - 0.87	1.04 - 1.05	0.544E 06
0.180E 08	0.60000	0.108E 06 - 0.108E 06	0.87 - 0.87	1.05 - 1.06	0.540E 06
0.179E 08	0.65000	0.108E 06 - 0.109E 06	0.87 - 0.88	1.06 - 1.06	0.535E 06
0.180E 08	0.70000	0.109E 06 - 0.109E 06	0.88 - 0.88	1.06 - 1.07	0.530E 06
0.179E 08	0.75000	0.109E 06 - 0.110E 06	0.88 - 0.89	1.07 - 1.08	0.523E 06
0.179E 08	0.80000	0.110E 06 - 0.111E 06	0.89 - 0.89	1.08 - 1.08	0.515E 06
0.180E 08	0.85000	0.111E 06 - 0.112E 06	0.89 - 0.90	1.08 - 1.09	0.510E 06
0.179E 08	0.90000	0.112E 06 - 0.113E 06	0.90 - 0.91	1.09 - 1.10	0.508E 06
0.180E 08	0.95000	0.113E 06 - 0.115E 06	0.91 - 0.92	1.10 - 1.12	0.503E 06
0.718E 07	0.97000	0.115E 06 - 0.116E 06	0.92 - 0.93	1.12 - 1.13	0.501E 06
0.718E 07	0.99000	0.116E 06 - 0.118E 06	0.93 - 0.95	1.13 - 1.15	0.495E 06
0.323E 07	0.99900	0.118E 06 - 0.121E 06	0.95 - 0.98	1.15 - 1.18	0.488E 06
0.323E 06	0.99990	0.121E 06 - 0.124E 06	0.98 - 1.00	1.18 - 1.21	0.612E 06

TOTAL CYCLES = 0.359E 09

ROOT MEAN CUBED IS 0.106E 06 AVERAGE MEAN IS 0.558E 06

TABLE H- 8
CUMMULATIVE FATIGUE HISTOGRAM OUTPUT

0.100R BLADE VY

NO. CYCLES IN 30 YEARS (TYPES 1+2)	CUM PROB	HALF-RANGE FATIGUE LOADS: LOAD LEVELS	NORMALIZED LOAD LEVELS	LOAD/50% AT RATED	MID-RANGE MEAN
0.180E 08	0.05000	0. - 0.108E 06	0. - 0.77	0. - 0.91	0.729E 04
0.180E 08	0.10000	0.108E 06 - 0.110E 06	0.77 - 0.79	0.91 - 0.93	0.736E 04
0.180E 08	0.15000	0.110E 06 - 0.111E 06	0.79 - 0.80	0.93 - 0.94	0.740E 04
0.179E 08	0.20000	0.111E 06 - 0.112E 06	0.80 - 0.80	0.94 - 0.95	0.743E 04
0.180E 08	0.25000	0.112E 06 - 0.113E 06	0.80 - 0.81	0.95 - 0.96	0.744E 04
0.180E 08	0.30000	0.113E 06 - 0.114E 06	0.81 - 0.82	0.96 - 0.97	0.745E 04
0.180E 08	0.35000	0.114E 06 - 0.115E 06	0.82 - 0.82	0.97 - 0.97	0.746E 04
0.179E 08	0.40000	0.115E 06 - 0.116E 06	0.82 - 0.83	0.97 - 0.98	0.747E 04
0.180E 08	0.45000	0.116E 06 - 0.117E 06	0.83 - 0.83	0.98 - 0.99	0.747E 04
0.180E 08	0.50000	0.117E 06 - 0.117E 06	0.83 - 0.84	0.99 - 0.99	0.746E 04
0.179E 08	0.55000	0.117E 06 - 0.118E 06	0.84 - 0.84	0.99 - 1.00	0.745E 04
0.180E 08	0.60000	0.118E 06 - 0.119E 06	0.84 - 0.85	1.00 - 1.00	0.744E 04
0.179E 08	0.65000	0.119E 06 - 0.119E 06	0.85 - 0.85	1.00 - 1.01	0.731E 04
0.180E 08	0.70000	0.119E 06 - 0.120E 06	0.85 - 0.86	1.01 - 1.02	0.714E 04
0.179E 08	0.75000	0.120E 06 - 0.121E 06	0.86 - 0.87	1.02 - 1.02	0.709E 04
0.179E 08	0.80000	0.121E 06 - 0.122E 06	0.87 - 0.88	1.02 - 1.03	0.719E 04
0.180E 08	0.85000	0.122E 06 - 0.123E 06	0.88 - 0.88	1.03 - 1.04	0.712E 04
0.179E 08	0.90000	0.123E 06 - 0.125E 06	0.88 - 0.89	1.04 - 1.05	0.705E 04
0.180E 08	0.95000	0.125E 06 - 0.127E 06	0.89 - 0.91	1.05 - 1.07	0.704E 04
0.718E 07	0.97000	0.127E 06 - 0.129E 06	0.91 - 0.92	1.07 - 1.09	0.701E 04
0.718E 07	0.99000	0.129E 06 - 0.132E 06	0.92 - 0.94	1.09 - 1.11	0.694E 04
0.323E 07	0.99900	0.132E 06 - 0.137E 06	0.94 - 0.98	1.11 - 1.16	0.723E 04
0.323E 06	0.99990	0.137E 06 - 0.140E 06	0.98 - 1.00	1.16 - 1.19	0.360E 04

TOTAL CYCLES = 0.359E 09

ROOT MEAN CUBED IS 0.116E 06 AVERAGE MEAN IS 0.730E 04

TABLE M- 9
CUMMULATIVE FATIGUE HISTOGRAM OUTPUT

0.100R BLADE VZ

NO. CYCLES IN 30 YEARS (TYPES 1+2)	CUM PROB	HALF-RANGE FATIGUE LOADS: LOAD LEVELS	NORMALIZED LOAD LEVELS	LOAD/50% AT RATED	MID-RANGE MEAN
0.180E 08	0.05000	0. - 0.601E 04	0. - 0.10	0. - 0.57	-0.753E 05
0.180E 08	0.10000	0.601E 04 - 0.676E 04	0.10 - 0.11	0.57 - 0.64	-0.784E 05
0.180E 08	0.15000	0.676E 04 - 0.733E 04	0.11 - 0.12	0.64 - 0.70	-0.808E 05
0.179E 08	0.20000	0.733E 04 - 0.783E 04	0.12 - 0.13	0.70 - 0.75	-0.827E 05
0.180E 08	0.25000	0.783E 04 - 0.828E 04	0.13 - 0.14	0.75 - 0.79	-0.844E 05
0.180E 08	0.30000	0.828E 04 - 0.872E 04	0.14 - 0.15	0.79 - 0.83	-0.859E 05
0.180E 08	0.35000	0.872E 04 - 0.915E 04	0.15 - 0.15	0.83 - 0.87	-0.874E 05
0.179E 08	0.40000	0.915E 04 - 0.958E 04	0.15 - 0.16	0.87 - 0.91	-0.888E 05
0.180E 08	0.45000	0.958E 04 - 0.100E 05	0.16 - 0.17	0.91 - 0.96	-0.901E 05
0.180E 08	0.50000	0.100E 05 - 0.105E 05	0.17 - 0.18	0.96 - 1.00	-0.912E 05
0.179E 08	0.55000	0.105E 05 - 0.110E 05	0.18 - 0.18	1.00 - 1.04	-0.923E 05
0.180E 08	0.60000	0.110E 05 - 0.115E 05	0.18 - 0.19	1.04 - 1.09	-0.935E 05
0.179E 08	0.65000	0.115E 05 - 0.120E 05	0.19 - 0.20	1.09 - 1.15	-0.948E 05
0.180E 08	0.70000	0.120E 05 - 0.127E 05	0.20 - 0.21	1.15 - 1.21	-0.958E 05
0.179E 08	0.75000	0.127E 05 - 0.134E 05	0.21 - 0.22	1.21 - 1.27	-0.967E 05
0.179E 08	0.80000	0.134E 05 - 0.142E 05	0.22 - 0.24	1.27 - 1.36	-0.975E 05
0.180E 08	0.85000	0.142E 05 - 0.153E 05	0.24 - 0.26	1.36 - 1.46	-0.980E 05
0.179E 08	0.90000	0.153E 05 - 0.168E 05	0.26 - 0.28	1.46 - 1.60	-0.994E 05
0.180E 08	0.93000	0.168E 05 - 0.193E 05	0.28 - 0.32	1.60 - 1.84	-0.103E 06
0.718E 07	0.97000	0.193E 05 - 0.211E 05	0.32 - 0.35	1.84 - 2.01	-0.105E 06
0.718E 07	0.99000	0.211E 05 - 0.251E 05	0.35 - 0.42	2.01 - 2.39	-0.109E 06
0.323E 07	0.99900	0.251E 05 - 0.328E 05	0.42 - 0.55	2.39 - 3.13	-0.116E 06
0.323E 06	0.99990	0.328E 05 - 0.612E 05	0.55 - 1.03	3.13 - 5.83	-0.115E 06

TOTAL CYCLES = 0.359E 09

ROOT MEAN CUBED IS 0.130E 05 AVERAGE MEAN IS -0.912E 05

TABLE M-10
CUMMULATIVE FATIGUE HISTOGRAM OUTPUT

0.100R BLADE MX

NO. CYCLES IN 30 YEARS (TYPES 1+2)	CUM PROB	HALF-RANGE FATIGUE LOADS: LOAD LEVELS	NORMALIZED LOAD LEVELS	LOAD/50% AT RATED	MID-RANGE MEAN
0.180E 08	0.05000	0. - 0.576E 05	0. - 0.38	0. - 0.53	-0.884E 05
0.180E 08	0.10000	0.576E 05 - 0.582E 05	0.38 - 0.39	0.53 - 0.54	-0.884E 05
0.180E 08	0.15000	0.582E 05 - 0.585E 05	0.39 - 0.39	0.54 - 0.54	-0.883E 05
0.179E 08	0.20000	0.585E 05 - 0.611E 05	0.39 - 0.41	0.54 - 0.57	-0.883E 05
0.180E 08	0.25000	0.611E 05 - 0.640E 05	0.41 - 0.43	0.57 - 0.59	-0.890E 05
0.180E 08	0.30000	0.640E 05 - 0.694E 05	0.43 - 0.46	0.59 - 0.64	-0.905E 05
0.180E 08	0.35000	0.694E 05 - 0.729E 05	0.46 - 0.49	0.64 - 0.67	-0.923E 05
0.179E 08	0.40000	0.729E 05 - 0.756E 05	0.49 - 0.50	0.67 - 0.70	-0.929E 05
0.180E 08	0.45000	0.756E 05 - 0.776E 05	0.50 - 0.52	0.70 - 0.72	-0.919E 05
0.180E 08	0.50000	0.776E 05 - 0.796E 05	0.52 - 0.53	0.72 - 0.74	-0.907E 05
0.179E 08	0.55000	0.796E 05 - 0.821E 05	0.53 - 0.55	0.74 - 0.76	-0.902E 05
0.180E 08	0.60000	0.821E 05 - 0.848E 05	0.55 - 0.57	0.76 - 0.78	-0.906E 05
0.179E 08	0.65000	0.848E 05 - 0.885E 05	0.57 - 0.59	0.78 - 0.82	-0.983E 05
0.180E 08	0.70000	0.885E 05 - 0.925E 05	0.59 - 0.62	0.82 - 0.86	-0.111E 06
0.179E 08	0.75000	0.925E 05 - 0.961E 05	0.62 - 0.64	0.86 - 0.89	-0.114E 06
0.179E 08	0.80000	0.961E 05 - 0.101E 06	0.64 - 0.67	0.89 - 0.93	-0.114E 06
0.180E 08	0.85000	0.101E 06 - 0.105E 06	0.67 - 0.70	0.93 - 0.97	-0.114E 06
0.179E 08	0.90000	0.105E 06 - 0.110E 06	0.70 - 0.73	0.97 - 1.02	-0.115E 06
0.180E 08	0.95000	0.110E 06 - 0.113E 06	0.73 - 0.75	1.02 - 1.04	-0.115E 06
0.718E 07	0.97000	0.113E 06 - 0.114E 06	0.75 - 0.76	1.04 - 1.06	-0.115E 06
0.718E 07	0.99000	0.114E 06 - 0.117E 06	0.76 - 0.78	1.06 - 1.08	-0.115E 06
0.323E 07	0.99900	0.117E 06 - 0.122E 06	0.78 - 0.81	1.08 - 1.13	-0.115E 06
0.323E 06	0.99990	0.122E 06 - 0.150E 06	0.81 - 1.00	1.13 - 1.39	-0.182E 06

TOTAL CYCLES = 0.359E 09

ROOT MEAN CUBED IS 0.853E 05 AVERAGE MEAN IS -0.989E 05

TABLE H-11
CUMMULATIVE FATIGUE HISTOGRAM OUTPUT

0.100R BLADE MY

NO. CYCLES IN 30 YEARS (TYPES 1+2)	CUM PROB	HALF-RANGE FATIGUE LOADS: LOAD LEVELS	NORMALIZED LOAD LEVELS	LOAD/50% AT RATED	MID-RANGE MEAN
0.180E 08	0.00000	0. - 0.625E 06	0. - 0.11	0. - 0.50	0.727E 07
0.180E 08	0.10000	0.625E 06 - 0.712E 06	0.11 - 0.12	0.50 - 0.57	0.752E 07
0.180E 08	0.10000	0.712E 06 - 0.778E 06	0.12 - 0.13	0.57 - 0.62	0.772E 07
0.179E 08	0.20000	0.778E 06 - 0.836E 06	0.13 - 0.14	0.62 - 0.67	0.787E 07
0.180E 08	0.20000	0.836E 06 - 0.889E 06	0.14 - 0.15	0.67 - 0.71	0.801E 07
0.180E 08	0.30000	0.889E 06 - 0.939E 06	0.15 - 0.16	0.71 - 0.75	0.814E 07
0.180E 08	0.30000	0.939E 06 - 0.988E 06	0.16 - 0.17	0.75 - 0.79	0.825E 07
0.179E 08	0.40000	0.988E 06 - 0.104E 07	0.17 - 0.18	0.79 - 0.83	0.836E 07
0.180E 08	0.45000	0.104E 07 - 0.109E 07	0.18 - 0.19	0.83 - 0.87	0.847E 07
0.180E 08	0.50000	0.109E 07 - 0.114E 07	0.19 - 0.20	0.87 - 0.92	0.857E 07
0.179E 08	0.55000	0.114E 07 - 0.120E 07	0.20 - 0.21	0.92 - 0.96	0.864E 07
0.180E 08	0.60000	0.120E 07 - 0.126E 07	0.21 - 0.22	0.96 - 1.01	0.872E 07
0.179E 08	0.65000	0.126E 07 - 0.132E 07	0.22 - 0.23	1.01 - 1.06	0.882E 07
0.180E 08	0.70000	0.132E 07 - 0.139E 07	0.23 - 0.24	1.06 - 1.12	0.892E 07
0.179E 08	0.75000	0.139E 07 - 0.148E 07	0.24 - 0.25	1.12 - 1.18	0.900E 07
0.179E 08	0.80000	0.148E 07 - 0.157E 07	0.25 - 0.27	1.18 - 1.26	0.907E 07
0.180E 08	0.85000	0.157E 07 - 0.170E 07	0.27 - 0.29	1.26 - 1.36	0.914E 07
0.179E 08	0.90000	0.170E 07 - 0.187E 07	0.29 - 0.32	1.36 - 1.50	0.933E 07
0.180E 08	0.95000	0.187E 07 - 0.215E 07	0.32 - 0.37	1.50 - 1.73	0.965E 07
0.718E 07	0.97000	0.215E 07 - 0.237E 07	0.37 - 0.41	1.73 - 1.90	0.986E 07
0.718E 07	0.99000	0.237E 07 - 0.284E 07	0.41 - 0.49	1.90 - 2.28	0.103E 08
0.323E 07	0.99300	0.284E 07 - 0.376E 07	0.49 - 0.65	2.28 - 3.02	0.110E 08
0.323E 06	0.99990	0.376E 07 - 0.589E 07	0.65 - 1.01	3.02 - 4.72	0.915E 07

TOTAL CYCLES = 0.359E 09

ROOT MEAN CUBED IS 0.144E 07 AVERAGE MEAN IS 0.858E 07

TABLE H-12
CUMMULATIVE FATIGUE HISTOGRAM OUTPUT

0.100R BLADE MZ

NO. CYCLES IN 30 YEARS (TYPES 1+2)	CUM PROB	HALF-RANGE FATIGUE LOADS: LOAD LEVELS	NORMALIZED LOAD LEVELS	LOAD/50% AT RATED	MID-RANGE MEAN
0.180E 08	0.05000	0. - 0.560E 07	0. - 0.89	0. - 1.05	-0.752E 06
0.180E 08	0.10000	0.560E 07 - 0.570E 07	0.89 - 0.91	1.05 - 1.07	-0.787E 06
0.180E 08	0.15000	0.570E 07 - 0.578E 07	0.91 - 0.92	1.07 - 1.08	-0.803E 06
0.179E 08	0.20000	0.578E 07 - 0.584E 07	0.92 - 0.93	1.08 - 1.09	-0.811E 06
0.180E 08	0.25000	0.584E 07 - 0.589E 07	0.93 - 0.94	1.09 - 1.10	-0.814E 06
0.180E 08	0.30000	0.589E 07 - 0.594E 07	0.94 - 0.95	1.10 - 1.11	-0.814E 06
0.180E 08	0.35000	0.594E 07 - 0.598E 07	0.95 - 0.95	1.11 - 1.12	-0.812E 06
0.179E 08	0.40000	0.598E 07 - 0.602E 07	0.95 - 0.96	1.12 - 1.13	-0.808E 06
0.180E 08	0.45000	0.602E 07 - 0.606E 07	0.96 - 0.97	1.13 - 1.13	-0.803E 06
0.180E 08	0.50000	0.606E 07 - 0.610E 07	0.97 - 0.97	1.13 - 1.14	-0.796E 06
0.179E 08	0.55000	0.610E 07 - 0.614E 07	0.97 - 0.98	1.14 - 1.15	-0.795E 06
0.180E 08	0.60000	0.614E 07 - 0.618E 07	0.98 - 0.99	1.15 - 1.16	-0.817E 06
0.179E 08	0.65000	0.618E 07 - 0.623E 07	0.99 - 0.99	1.16 - 1.16	-0.843E 06
0.180E 08	0.70000	0.623E 07 - 0.627E 07	0.99 - 1.00	1.16 - 1.17	-0.864E 06
0.179E 08	0.75000	0.627E 07 - 0.632E 07	1.00 - 1.01	1.17 - 1.18	-0.875E 06
0.179E 08	0.80000	0.632E 07 - 0.637E 07	1.01 - 1.01	1.18 - 1.19	-0.884E 06
0.180E 08	0.85000	0.637E 07 - 0.644E 07	1.01 - 1.03	1.19 - 1.20	-0.891E 06
0.179E 08	0.90000	0.644E 07 - 0.652E 07	1.03 - 1.04	1.20 - 1.22	-0.894E 06
0.180E 08	0.95000	0.652E 07 - 0.666E 07	1.04 - 1.06	1.22 - 1.24	-0.901E 06
0.718E 07	0.97000	0.666E 07 - 0.675E 07	1.06 - 1.08	1.24 - 1.26	-0.905E 06
0.718E 07	0.99000	0.675E 07 - 0.691E 07	1.08 - 1.10	1.26 - 1.29	-0.924E 06
0.323E 07	0.99300	0.691E 07 - 0.719E 07	1.10 - 1.14	1.29 - 1.34	-0.814E 06
0.323E 06	0.99990	0.719E 07 - 0.729E 07	1.14 - 1.16	1.34 - 1.36	-0.135E 07

TOTAL CYCLES = 0.359E 09

ROOT MEAN CUBED IS 0.606E 07 AVERAGE MEAN IS -0.833E 06

TABLE M-13
CUMULATIVE FATIGUE HISTOGRAM OUTPUT

0.200R BLADE VX

NO. CYCLES IN 30 YEARS (TYPES 1+2)	CUM PROB	HALF-RANGE FATIGUE LOADS: LOAD LEVELS	NORMALIZED LOAD LEVELS	LOAD/50% AT RATED	MID-RANGE MEAN
0.180E 08	0.05000	0. - 0.699E 05	0. - 0.78	0. - 0.97	0.625E 06
0.180E 08	0.10000	0.699E 05 - 0.712E 05	0.78 - 0.79	0.97 - 0.98	0.603E 06
0.180E 08	0.15000	0.712E 05 - 0.721E 05	0.79 - 0.80	0.98 - 1.00	0.584E 06
0.179E 08	0.20000	0.721E 05 - 0.728E 05	0.80 - 0.81	1.00 - 1.01	0.566E 06
0.180E 08	0.25000	0.728E 05 - 0.734E 05	0.81 - 0.82	1.01 - 1.01	0.549E 06
0.180E 08	0.30000	0.734E 05 - 0.739E 05	0.82 - 0.82	1.01 - 1.02	0.535E 06
0.180E 08	0.35000	0.739E 05 - 0.744E 05	0.82 - 0.83	1.02 - 1.03	0.527E 06
0.179E 08	0.40000	0.744E 05 - 0.748E 05	0.83 - 0.83	1.03 - 1.03	0.522E 06
0.180E 08	0.45000	0.748E 05 - 0.753E 05	0.83 - 0.84	1.03 - 1.04	0.516E 06
0.180E 08	0.50000	0.753E 05 - 0.758E 05	0.84 - 0.84	1.04 - 1.05	0.509E 06
0.179E 08	0.55000	0.758E 05 - 0.762E 05	0.84 - 0.85	1.05 - 1.05	0.503E 06
0.180E 08	0.60000	0.762E 05 - 0.767E 05	0.85 - 0.85	1.05 - 1.06	0.498E 06
0.179E 08	0.65000	0.767E 05 - 0.771E 05	0.85 - 0.86	1.06 - 1.07	0.494E 06
0.180E 08	0.70000	0.771E 05 - 0.776E 05	0.86 - 0.86	1.07 - 1.07	0.490E 06
0.179E 08	0.75000	0.776E 05 - 0.781E 05	0.86 - 0.87	1.07 - 1.08	0.485E 06
0.179E 08	0.80000	0.781E 05 - 0.787E 05	0.87 - 0.88	1.08 - 1.09	0.477E 06
0.180E 08	0.85000	0.787E 05 - 0.793E 05	0.88 - 0.88	1.09 - 1.10	0.471E 06
0.179E 08	0.90000	0.793E 05 - 0.802E 05	0.88 - 0.89	1.10 - 1.11	0.468E 06
0.180E 08	0.95000	0.802E 05 - 0.814E 05	0.89 - 0.91	1.11 - 1.13	0.464E 06
0.718E 07	0.97000	0.814E 05 - 0.822E 05	0.91 - 0.92	1.13 - 1.14	0.462E 06
0.718E 07	0.99000	0.822E 05 - 0.838E 05	0.92 - 0.93	1.14 - 1.16	0.457E 06
0.323E 07	0.99900	0.838E 05 - 0.861E 05	0.93 - 0.96	1.16 - 1.19	0.455E 06
0.323E 06	0.99990	0.861E 05 - 0.897E 05	0.96 - 1.00	1.19 - 1.24	0.640E 06

TOTAL CYCLES = 0.359E 09

ROOT MEAN CUBED IS 0.751E 05 AVERAGE MEAN IS 0.517E 06

TABLE M-14
CUMULATIVE FATIGUE HISTOGRAM OUTPUT

0.200R BLADE VY

NO. CYCLES IN 30 YEARS (TYPES 1+2)	CUM PROB	HALF-RANGE FATIGUE LOADS: LOAD LEVELS	NORMALIZED LOAD LEVELS	LOAD/50% AT RATED	MID-RANGE MEAN
0.180E 08	0.05000	0. - 0.774E 05	0. - 0.75	0. - 0.91	0.877E 04
0.180E 08	0.10000	0.774E 05 - 0.790E 05	0.75 - 0.77	0.91 - 0.92	0.877E 04
0.180E 08	0.15000	0.790E 05 - 0.801E 05	0.77 - 0.78	0.92 - 0.94	0.880E 04
0.179E 08	0.20000	0.801E 05 - 0.810E 05	0.78 - 0.79	0.94 - 0.95	0.884E 04
0.180E 08	0.25000	0.810E 05 - 0.817E 05	0.79 - 0.79	0.95 - 0.96	0.888E 04
0.180E 08	0.30000	0.817E 05 - 0.824E 05	0.79 - 0.80	0.96 - 0.97	0.892E 04
0.180E 08	0.35000	0.824E 05 - 0.831E 05	0.80 - 0.81	0.97 - 0.97	0.897E 04
0.179E 08	0.40000	0.831E 05 - 0.837E 05	0.81 - 0.81	0.97 - 0.98	0.902E 04
0.180E 08	0.45000	0.837E 05 - 0.843E 05	0.81 - 0.82	0.98 - 0.99	0.908E 04
0.180E 08	0.50000	0.843E 05 - 0.849E 05	0.82 - 0.82	0.99 - 0.99	0.913E 04
0.179E 08	0.55000	0.849E 05 - 0.855E 05	0.82 - 0.83	0.99 - 1.00	0.917E 04
0.180E 08	0.60000	0.855E 05 - 0.862E 05	0.83 - 0.84	1.00 - 1.01	0.922E 04
0.179E 08	0.65000	0.862E 05 - 0.868E 05	0.84 - 0.84	1.01 - 1.02	0.910E 04
0.180E 08	0.70000	0.868E 05 - 0.874E 05	0.84 - 0.85	1.02 - 1.02	0.892E 04
0.179E 08	0.75000	0.874E 05 - 0.882E 05	0.85 - 0.86	1.02 - 1.04	0.884E 04
0.179E 08	0.80000	0.882E 05 - 0.889E 05	0.86 - 0.87	1.04 - 1.05	0.888E 04
0.180E 08	0.85000	0.889E 05 - 0.901E 05	0.87 - 0.87	1.05 - 1.06	0.880E 04
0.179E 08	0.90000	0.901E 05 - 0.910E 05	0.87 - 0.88	1.06 - 1.07	0.878E 04
0.180E 08	0.95000	0.910E 05 - 0.934E 05	0.88 - 0.91	1.07 - 1.09	0.879E 04
0.718E 07	0.97000	0.934E 05 - 0.946E 05	0.91 - 0.92	1.09 - 1.11	0.877E 04
0.718E 07	0.99000	0.946E 05 - 0.971E 05	0.92 - 0.94	1.11 - 1.14	0.877E 04
0.323E 07	0.99900	0.971E 05 - 0.102E 06	0.94 - 0.99	1.14 - 1.19	0.931E 04
0.323E 06	0.99990	0.102E 06 - 0.104E 06	0.99 - 1.01	1.19 - 1.22	0.567E 04

TOTAL CYCLES = 0.359E 09

ROOT MEAN CUBED IS 0.845E 05 AVERAGE MEAN IS 0.892E 04

TABLE H-15
CUMMULATIVE FATIGUE HISTOGRAM OUTPUT

0.200R BLADE VZ

NO. CYCLES IN 30 YEARS (TYPES 1+2)	CUM PROB	HALF-RANGE FATIGUE LOADS: LOAD LEVELS	NORMALIZED LOAD LEVELS	LOAD/50% AT RATED	MID-RANGE MEAN
0.180E 08	0.05000	0. - 0.649E 04	0. - 0.11	0. - 0.64	-0.719E 05
0.180E 08	0.10000	0.649E 04 - 0.724E 04	0.11 - 0.13	0.64 - 0.71	-0.745E 05
0.180E 08	0.15000	0.724E 04 - 0.781E 04	0.13 - 0.14	0.71 - 0.77	-0.765E 05
0.179E 08	0.20000	0.781E 04 - 0.831E 04	0.14 - 0.14	0.77 - 0.81	-0.780E 05
0.180E 08	0.25000	0.831E 04 - 0.877E 04	0.14 - 0.15	0.81 - 0.86	-0.794E 05
0.180E 08	0.30000	0.877E 04 - 0.920E 04	0.15 - 0.16	0.86 - 0.90	-0.806E 05
0.180E 08	0.35000	0.920E 04 - 0.963E 04	0.16 - 0.17	0.90 - 0.94	-0.817E 05
0.179E 08	0.40000	0.963E 04 - 0.101E 05	0.17 - 0.17	0.94 - 0.99	-0.828E 05
0.180E 08	0.45000	0.101E 05 - 0.105E 05	0.17 - 0.18	0.99 - 1.03	-0.839E 05
0.180E 08	0.50000	0.105E 05 - 0.110E 05	0.18 - 0.19	1.03 - 1.07	-0.848E 05
0.179E 08	0.55000	0.110E 05 - 0.114E 05	0.19 - 0.20	1.07 - 1.12	-0.855E 05
0.180E 08	0.60000	0.114E 05 - 0.120E 05	0.20 - 0.21	1.12 - 1.17	-0.865E 05
0.179E 08	0.65000	0.120E 05 - 0.125E 05	0.21 - 0.22	1.17 - 1.23	-0.875E 05
0.180E 08	0.70000	0.125E 05 - 0.131E 05	0.22 - 0.23	1.23 - 1.29	-0.883E 05
0.179E 08	0.75000	0.131E 05 - 0.139E 05	0.23 - 0.24	1.29 - 1.36	-0.890E 05
0.179E 08	0.80000	0.139E 05 - 0.147E 05	0.24 - 0.25	1.36 - 1.44	-0.895E 05
0.180E 08	0.85000	0.147E 05 - 0.157E 05	0.25 - 0.27	1.44 - 1.54	-0.899E 05
0.179E 08	0.90000	0.157E 05 - 0.172E 05	0.27 - 0.30	1.54 - 1.69	-0.913E 05
0.180E 08	0.95000	0.172E 05 - 0.197E 05	0.30 - 0.34	1.69 - 1.94	-0.942E 05
0.718E 07	0.97000	0.197E 05 - 0.215E 05	0.34 - 0.37	1.94 - 2.11	-0.962E 05
0.718E 07	0.99000	0.215E 05 - 0.255E 05	0.37 - 0.44	2.11 - 2.50	-0.100E 06
0.323E 07	0.99900	0.255E 05 - 0.326E 05	0.44 - 0.56	2.50 - 3.19	-0.106E 06
0.323E 06	0.99990	0.326E 05 - 0.601E 05	0.56 - 1.04	3.19 - 5.89	-0.108E 06

TOTAL CYCLES = 0.359E 09

ROOT MEAN CUBED IS 0.134E 05 AVERAGE MEAN IS -0.848E 05

TABLE H-16
CUMMULATIVE FATIGUE HISTOGRAM OUTPUT

0.200R BLADE MX

NO. CYCLES IN 30 YEARS (TYPES 1+2)	CUM PROB	HALF-RANGE FATIGUE LOADS: LOAD LEVELS	NORMALIZED LOAD LEVELS	LOAD/50% AT RATED	MID-RANGE MEAN
0.180E 08	0.05000	0. - 0.468E 05	0. - 0.40	0. - 0.54	-0.881E 05
0.180E 08	0.10000	0.468E 05 - 0.465E 05	0.40 - 0.39	0.54 - 0.53	-0.881E 05
0.180E 08	0.15000	0.465E 05 - 0.467E 05	0.39 - 0.39	0.53 - 0.53	-0.883E 05
0.179E 08	0.20000	0.467E 05 - 0.495E 05	0.39 - 0.42	0.53 - 0.57	-0.884E 05
0.180E 08	0.25000	0.495E 05 - 0.525E 05	0.42 - 0.44	0.57 - 0.60	-0.889E 05
0.180E 08	0.30000	0.525E 05 - 0.553E 05	0.44 - 0.47	0.60 - 0.63	-0.889E 05
0.180E 08	0.35000	0.553E 05 - 0.586E 05	0.47 - 0.50	0.63 - 0.67	-0.905E 05
0.179E 08	0.40000	0.586E 05 - 0.609E 05	0.50 - 0.51	0.67 - 0.70	-0.913E 05
0.180E 08	0.45000	0.609E 05 - 0.623E 05	0.51 - 0.53	0.70 - 0.71	-0.905E 05
0.180E 08	0.50000	0.623E 05 - 0.638E 05	0.53 - 0.54	0.71 - 0.73	-0.891E 05
0.179E 08	0.55000	0.638E 05 - 0.650E 05	0.54 - 0.55	0.73 - 0.74	-0.867E 05
0.180E 08	0.60000	0.650E 05 - 0.669E 05	0.55 - 0.57	0.74 - 0.77	-0.865E 05
0.179E 08	0.65000	0.669E 05 - 0.703E 05	0.57 - 0.59	0.77 - 0.80	-0.971E 05
0.180E 08	0.70000	0.703E 05 - 0.736E 05	0.59 - 0.62	0.80 - 0.84	-0.110E 06
0.179E 08	0.75000	0.736E 05 - 0.761E 05	0.62 - 0.64	0.84 - 0.87	-0.113E 06
0.179E 08	0.80000	0.761E 05 - 0.788E 05	0.64 - 0.67	0.87 - 0.90	-0.113E 06
0.180E 08	0.85000	0.788E 05 - 0.817E 05	0.67 - 0.69	0.90 - 0.93	-0.113E 06
0.179E 08	0.90000	0.817E 05 - 0.855E 05	0.69 - 0.72	0.93 - 0.98	-0.111E 06
0.180E 08	0.95000	0.855E 05 - 0.875E 05	0.72 - 0.74	0.98 - 1.00	-0.111E 06
0.718E 07	0.97000	0.875E 05 - 0.887E 05	0.74 - 0.75	1.00 - 1.01	-0.111E 06
0.718E 07	0.99000	0.887E 05 - 0.910E 05	0.75 - 0.77	1.01 - 1.04	-0.111E 06
0.323E 07	0.99900	0.910E 05 - 0.947E 05	0.77 - 0.80	1.04 - 1.08	-0.111E 06
0.323E 06	0.99990	0.947E 05 - 0.118E 06	0.80 - 1.00	1.08 - 1.35	-0.162E 06

TOTAL CYCLES = 0.359E 09

ROOT MEAN CUBED IS 0.574E 05 AVERAGE MEAN IS -0.973E 05

TABLE H-17
CUMMULATIVE FATIGUE HISTOGRAM OUTPUT

0.200R BLADE MY

NO. CYCLES IN 30 YEARS (TYPES 1+2)	CUM PROB	HALF-RANGE FATIGUE LOADS: LOAD LEVELS	NORMALIZED LOAD LEVELS	LOAD/50% AT RATED	MID-RANGE MEAN
0.180E 08	0.05000	0. - 0.537E 06	0. - 0.11	0. - 0.53	0.606E 07
0.180E 08	0.10000	0.537E 06 - 0.609E 06	0.11 - 0.13	0.53 - 0.60	0.624E 07
0.180E 08	0.15000	0.609E 06 - 0.663E 06	0.13 - 0.14	0.60 - 0.65	0.638E 07
0.179E 08	0.20000	0.663E 06 - 0.710E 06	0.14 - 0.15	0.65 - 0.70	0.649E 07
0.180E 08	0.25000	0.710E 06 - 0.753E 06	0.15 - 0.16	0.70 - 0.74	0.659E 07
0.180E 08	0.30000	0.753E 06 - 0.794E 06	0.16 - 0.17	0.74 - 0.78	0.668E 07
0.180E 08	0.35000	0.794E 06 - 0.835E 06	0.17 - 0.17	0.78 - 0.82	0.676E 07
0.179E 08	0.40000	0.835E 06 - 0.876E 06	0.17 - 0.18	0.82 - 0.86	0.684E 07
0.180E 08	0.45000	0.876E 06 - 0.918E 06	0.18 - 0.19	0.86 - 0.90	0.691E 07
0.180E 08	0.50000	0.918E 06 - 0.962E 06	0.19 - 0.20	0.90 - 0.94	0.698E 07
0.179E 08	0.55000	0.962E 06 - 0.101E 07	0.20 - 0.21	0.94 - 0.99	0.704E 07
0.180E 08	0.60000	0.101E 07 - 0.106E 07	0.21 - 0.22	0.99 - 1.04	0.710E 07
0.179E 08	0.65000	0.106E 07 - 0.110E 07	0.22 - 0.23	1.04 - 1.08	0.716E 07
0.180E 08	0.70000	0.110E 07 - 0.116E 07	0.23 - 0.24	1.08 - 1.14	0.723E 07
0.179E 08	0.75000	0.116E 07 - 0.123E 07	0.24 - 0.26	1.14 - 1.21	0.728E 07
0.179E 08	0.80000	0.123E 07 - 0.131E 07	0.26 - 0.27	1.21 - 1.29	0.733E 07
0.180E 08	0.85000	0.131E 07 - 0.142E 07	0.27 - 0.29	1.29 - 1.39	0.737E 07
0.179E 08	0.90000	0.142E 07 - 0.155E 07	0.29 - 0.32	1.39 - 1.52	0.751E 07
0.180E 08	0.95000	0.155E 07 - 0.179E 07	0.32 - 0.37	1.52 - 1.75	0.778E 07
0.718E 07	0.97000	0.179E 07 - 0.197E 07	0.37 - 0.41	1.75 - 1.93	0.794E 07
0.718E 07	0.99000	0.197E 07 - 0.235E 07	0.41 - 0.49	1.93 - 2.31	0.829E 07
0.323E 07	0.99900	0.235E 07 - 0.312E 07	0.49 - 0.65	2.31 - 3.06	0.886E 07
0.323E 06	0.99990	0.312E 07 - 0.490E 07	0.65 - 1.02	3.06 - 4.81	0.733E 07

TOTAL CYCLES = 0.359E 09

ROOT MEAN CUBED IS 0.120E 07 AVERAGE MEAN IS 0.700E 07

TABLE H-18
CUMMULATIVE FATIGUE HISTOGRAM OUTPUT

0.200R BLADE MZ

NO. CYCLES IN 30 YEARS (TYPES 1+2)	CUM PROB	HALF-RANGE FATIGUE LOADS: LOAD LEVELS	NORMALIZED LOAD LEVELS	LOAD/50% AT RATED	MID-RANGE MEAN
0.180E 08	0.05000	0. - 0.391E 07	0. - 0.89	0. - 1.07	-0.614E 06
0.180E 08	0.10000	0.391E 07 - 0.398E 07	0.89 - 0.91	1.07 - 1.09	-0.643E 06
0.180E 08	0.15000	0.398E 07 - 0.404E 07	0.91 - 0.92	1.09 - 1.10	-0.653E 06
0.179E 08	0.20000	0.404E 07 - 0.408E 07	0.92 - 0.93	1.10 - 1.11	-0.657E 06
0.180E 08	0.25000	0.408E 07 - 0.412E 07	0.93 - 0.94	1.11 - 1.12	-0.656E 06
0.180E 08	0.30000	0.412E 07 - 0.415E 07	0.94 - 0.95	1.12 - 1.13	-0.652E 06
0.180E 08	0.35000	0.415E 07 - 0.418E 07	0.95 - 0.95	1.13 - 1.14	-0.646E 06
0.179E 08	0.40000	0.418E 07 - 0.422E 07	0.95 - 0.96	1.14 - 1.15	-0.639E 06
0.180E 08	0.45000	0.422E 07 - 0.424E 07	0.96 - 0.97	1.15 - 1.16	-0.630E 06
0.180E 08	0.50000	0.424E 07 - 0.427E 07	0.97 - 0.97	1.16 - 1.17	-0.619E 06
0.179E 08	0.55000	0.427E 07 - 0.430E 07	0.97 - 0.98	1.17 - 1.18	-0.616E 06
0.180E 08	0.60000	0.430E 07 - 0.433E 07	0.98 - 0.99	1.18 - 1.18	-0.622E 06
0.179E 08	0.65000	0.433E 07 - 0.436E 07	0.99 - 0.99	1.18 - 1.19	-0.628E 06
0.180E 08	0.70000	0.436E 07 - 0.439E 07	0.99 - 1.00	1.19 - 1.20	-0.641E 06
0.179E 08	0.75000	0.439E 07 - 0.443E 07	1.00 - 1.01	1.20 - 1.21	-0.662E 06
0.179E 08	0.80000	0.443E 07 - 0.447E 07	1.01 - 1.02	1.21 - 1.22	-0.674E 06
0.180E 08	0.85000	0.447E 07 - 0.452E 07	1.02 - 1.03	1.22 - 1.24	-0.679E 06
0.179E 08	0.90000	0.452E 07 - 0.458E 07	1.03 - 1.05	1.24 - 1.25	-0.677E 06
0.180E 08	0.95000	0.458E 07 - 0.468E 07	1.05 - 1.07	1.25 - 1.28	-0.672E 06
0.718E 07	0.97000	0.468E 07 - 0.474E 07	1.07 - 1.08	1.28 - 1.30	-0.671E 06
0.718E 07	0.99000	0.474E 07 - 0.486E 07	1.08 - 1.11	1.30 - 1.33	-0.673E 06
0.323E 07	0.99900	0.486E 07 - 0.507E 07	1.11 - 1.16	1.33 - 1.38	-0.674E 06
0.323E 06	0.99990	0.507E 07 - 0.521E 07	1.16 - 1.19	1.38 - 1.42	-0.114E 07

TOTAL CYCLES = 0.359E 09

ROOT MEAN CUBED IS 0.425E 07 AVERAGE MEAN IS -0.647E 06

TABLE M-19
CUMMULATIVE FATIGUE HISTOGRAM OUTPUT

0.250R BLADE VX

NO. CYCLES IN 30 YEARS (TYPES 1+2)	CUM PROB	HALF-RANGE FATIGUE LOADS: LOAD LEVELS	NORMALIZED LOAD LEVELS	LOAD/50% AT RATED	MID-RANGE MEAN
0.180E 08	0.(5000	C. - 0.619E 05	0. - 0.77	0. - 0.96	0.593E 06
0.180E 08	0.:0000	0.619E 05 - 0.630E 05	0.77 - 0.79	0.96 - 0.98	0.574E 06
0.180E 08	0.:5000	0.630E 05 - 0.637E 05	0.79 - 0.79	0.98 - 0.99	0.557E 06
0.179E 08	0.:0000	0.637E 05 - 0.643E 05	0.79 - 0.80	0.99 - 1.00	0.542E 06
0.180E 08	0.:5000	0.643E 05 - 0.648E 05	0.80 - 0.81	1.00 - 1.01	0.527E 06
0.180E 08	0.:0000	0.648E 05 - 0.653E 05	0.81 - 0.81	1.01 - 1.02	0.514E 06
0.180E 08	0.:5000	0.653E 05 - 0.657E 05	0.81 - 0.82	1.02 - 1.02	0.506E 06
0.179E 08	0.:0000	0.657E 05 - 0.661E 05	0.82 - 0.83	1.02 - 1.03	0.499E 06
0.180E 08	0.:5000	0.661E 05 - 0.666E 05	0.83 - 0.83	1.03 - 1.04	0.492E 06
0.180E 08	0.:0000	0.666E 05 - 0.670E 05	0.83 - 0.84	1.04 - 1.04	0.484E 06
0.179E 08	0.:5000	0.670E 05 - 0.674E 05	0.84 - 0.84	1.04 - 1.05	0.477E 06
0.180E 08	0.:0000	0.674E 05 - 0.678E 05	0.84 - 0.85	1.05 - 1.05	0.471E 06
0.179E 08	0.:5000	0.678E 05 - 0.682E 05	0.85 - 0.85	1.05 - 1.06	0.466E 06
0.180E 08	0.:0000	0.682E 05 - 0.687E 05	0.85 - 0.86	1.06 - 1.07	0.462E 06
0.179E 08	0.:5000	0.687E 05 - 0.691E 05	0.86 - 0.86	1.07 - 1.07	0.456E 06
0.179E 08	0.:0000	0.691E 05 - 0.696E 05	0.86 - 0.87	1.07 - 1.08	0.448E 06
0.180E 08	0.:5000	0.696E 05 - 0.702E 05	0.87 - 0.88	1.08 - 1.09	0.441E 06
0.179E 08	0.:0000	0.702E 05 - 0.710E 05	0.88 - 0.89	1.09 - 1.10	0.436E 06
0.180E 08	0.:5000	0.710E 05 - 0.720E 05	0.89 - 0.90	1.10 - 1.12	0.431E 06
0.718E 07	0.:7000	0.720E 05 - 0.728E 05	0.90 - 0.91	1.12 - 1.13	0.429E 06
0.718E 07	0.:9000	0.728E 05 - 0.742E 05	0.91 - 0.93	1.13 - 1.15	0.423E 06
0.323E 07	0.:9900	0.742E 05 - 0.763E 05	0.93 - 0.95	1.15 - 1.19	0.420E 06
0.323E 06	0.:9990	0.763E 05 - 0.802E 05	0.95 - 1.00	1.19 - 1.25	0.610E 06

TOTAL CYCLES = 0.35:E 09

ROOT MEAN CUBED IS 0.664E 05 AVERAGE MEAN IS 0.490E 06

TABLE M-20
CUMMULATIVE FATIGUE HISTOGRAM OUTPUT

0.250R BLADE VY

NO. CYCLES IN 30 YEARS (TYPES 1+2)	CUM PROB	HALF-RANGE FATIGUE LOADS: LOAD LEVELS	NORMALIZED LOAD LEVELS	LOAD/50% AT RATED	MID-RANGE MEAN
0.180E 08	0.05000	0. - 0.689E 05	0. - 0.74	0. - 0.91	0.888E 04
0.180E 08	0.10000	0.689E 05 - 0.702E 05	0.74 - 0.75	0.91 - 0.92	0.887E 04
0.180E 08	0.15000	0.702E 05 - 0.712E 05	0.75 - 0.76	0.92 - 0.94	0.890E 04
0.179E 08	0.20000	0.712E 05 - 0.720E 05	0.76 - 0.77	0.94 - 0.95	0.894E 04
0.180E 08	0.25000	0.720E 05 - 0.727E 05	0.77 - 0.78	0.95 - 0.96	0.898E 04
0.180E 08	0.30000	0.727E 05 - 0.734E 05	0.78 - 0.79	0.96 - 0.97	0.903E 04
0.180E 08	0.35000	0.734E 05 - 0.740E 05	0.79 - 0.79	0.97 - 0.97	0.908E 04
0.179E 08	0.40000	0.740E 05 - 0.745E 05	0.79 - 0.80	0.97 - 0.98	0.913E 04
0.180E 08	0.45000	0.745E 05 - 0.751E 05	0.80 - 0.80	0.98 - 0.99	0.919E 04
0.180E 08	0.50000	0.751E 05 - 0.756E 05	0.80 - 0.81	0.99 - 0.99	0.925E 04
0.179E 08	0.55000	0.756E 05 - 0.762E 05	0.81 - 0.82	0.99 - 1.00	0.930E 04
0.180E 08	0.60000	0.762E 05 - 0.768E 05	0.82 - 0.82	1.00 - 1.01	0.933E 04
0.179E 08	0.65000	0.768E 05 - 0.773E 05	0.82 - 0.83	1.01 - 1.02	0.922E 04
0.180E 08	0.70000	0.773E 05 - 0.779E 05	0.83 - 0.84	1.02 - 1.03	0.904E 04
0.179E 08	0.75000	0.779E 05 - 0.788E 05	0.84 - 0.84	1.03 - 1.04	0.895E 04
0.179E 08	0.80000	0.788E 05 - 0.797E 05	0.84 - 0.85	1.04 - 1.05	0.896E 04
0.180E 08	0.85000	0.797E 05 - 0.804E 05	0.85 - 0.86	1.05 - 1.06	0.890E 04
0.179E 08	0.90000	0.804E 05 - 0.813E 05	0.86 - 0.87	1.06 - 1.07	0.889E 04
0.180E 08	0.95000	0.813E 05 - 0.833E 05	0.87 - 0.89	1.07 - 1.10	0.890E 04
0.718E 07	0.97000	0.833E 05 - 0.845E 05	0.89 - 0.91	1.10 - 1.11	0.889E 04
0.718E 07	0.99000	0.845E 05 - 0.868E 05	0.91 - 0.93	1.11 - 1.14	0.893E 04
0.323E 07	0.99900	0.868E 05 - 0.908E 05	0.93 - 0.97	1.14 - 1.19	0.947E 04
0.323E 06	0.99990	0.908E 05 - 0.945E 05	0.97 - 1.01	1.19 - 1.24	0.552E 04

TOTAL CYCLES = 0.359E 09

ROOT MEAN CUBED IS 0.753E 05 AVERAGE MEAN IS 0.903E 04

TABLE H-21
CUMMULATIVE FATIGUE HISTOGRAM OUTPUT

0.25OR BLADE VZ

NO. CYCLES IN 30 YEARS (TYPES 1+2)	CUM PROB	HALF-RANGE FATIGUE LOADS: LOAD LEVELS	NORMALIZED LOAD LEVELS	LOAD/50% AT RATED	MID-RANGE MEAN
0.180E 08	0.05000	0. - 0.649E 04	0. - 0.12	0. - 0.65	-0.702E 05
0.180E 08	0.10000	0.649E 04 - 0.723E 04	0.12 - 0.13	0.65 - 0.73	-0.725E 05
0.180E 08	0.15000	0.723E 04 - 0.779E 04	0.13 - 0.14	0.73 - 0.78	-0.742E 05
0.179E 08	0.20000	0.779E 04 - 0.828E 04	0.14 - 0.15	0.78 - 0.83	-0.756E 05
0.180E 08	0.25000	0.828E 04 - 0.873E 04	0.15 - 0.16	0.83 - 0.88	-0.768E 05
0.180E 08	0.30000	0.873E 04 - 0.916E 04	0.16 - 0.16	0.88 - 0.92	-0.778E 05
0.180E 08	0.35000	0.916E 04 - 0.959E 04	0.16 - 0.17	0.92 - 0.96	-0.788E 05
0.179E 08	0.40000	0.959E 04 - 0.100E 05	0.17 - 0.18	0.96 - 1.01	-0.797E 05
0.180E 08	0.45000	0.100E 05 - 0.104E 05	0.18 - 0.19	1.01 - 1.05	-0.806E 05
0.180E 08	0.50000	0.104E 05 - 0.109E 05	0.19 - 0.19	1.05 - 1.09	-0.814E 05
0.179E 08	0.55000	0.109E 05 - 0.114E 05	0.19 - 0.20	1.09 - 1.14	-0.820E 05
0.180E 08	0.60000	0.114E 05 - 0.119E 05	0.20 - 0.21	1.14 - 1.19	-0.828E 05
0.179E 08	0.65000	0.119E 05 - 0.125E 05	0.21 - 0.22	1.19 - 1.25	-0.837E 05
0.180E 08	0.70000	0.125E 05 - 0.131E 05	0.22 - 0.23	1.25 - 1.31	-0.844E 05
0.179E 08	0.75000	0.131E 05 - 0.138E 05	0.23 - 0.24	1.31 - 1.38	-0.850E 05
0.179E 08	0.80000	0.138E 05 - 0.146E 05	0.24 - 0.26	1.38 - 1.47	-0.855E 05
0.180E 08	0.85000	0.146E 05 - 0.156E 05	0.26 - 0.28	1.47 - 1.57	-0.858E 05
0.179E 08	0.90000	0.156E 05 - 0.171E 05	0.28 - 0.30	1.57 - 1.72	-0.871E 05
0.180E 08	0.95000	0.171E 05 - 0.196E 05	0.30 - 0.35	1.72 - 1.97	-0.899E 05
0.718E 07	0.97000	0.196E 05 - 0.216E 05	0.35 - 0.38	1.97 - 2.15	-0.919E 05
0.718E 07	0.99000	0.216E 05 - 0.252E 05	0.38 - 0.45	2.15 - 2.54	-0.958E 05
0.323E 07	0.99900	0.252E 05 - 0.320E 05	0.45 - 0.57	2.54 - 3.21	-0.100E 06
0.323E 06	0.99990	0.320E 05 - 0.588E 05	0.57 - 1.04	3.21 - 5.91	-0.104E 06

TOTAL CYCLES = 0.359E 09

ROOT MEAN CUBED IS 0.133E 05 AVERAGE MEAN IS -0.815E 05

TABLE H-22
CUMMULATIVE FATIGUE HISTOGRAM OUTPUT

0.25OR BLADE HX

NO. CYCLES IN 30 YEARS (TYPES 1+2)	CUM PROB	HALF-RANGE FATIGUE LOADS: LOAD LEVELS	NORMALIZED LOAD LEVELS	LOAD/50% AT RATED	MID-RANGE MEAN
0.180E 08	0.05000	0. - 0.411E 05	0. - 0.42	0. - 0.53	-0.873E 05
0.180E 08	0.10000	0.411E 05 - 0.407E 05	0.42 - 0.41	0.53 - 0.52	-0.873E 05
0.180E 08	0.15000	0.407E 05 - 0.413E 05	0.41 - 0.42	0.52 - 0.53	-0.878E 05
0.179E 08	0.20000	0.413E 05 - 0.437E 05	0.42 - 0.44	0.53 - 0.56	-0.879E 05
0.180E 08	0.25000	0.437E 05 - 0.461E 05	0.44 - 0.47	0.56 - 0.59	-0.881E 05
0.180E 08	0.30000	0.461E 05 - 0.492E 05	0.47 - 0.50	0.59 - 0.63	-0.861E 05
0.180E 08	0.35000	0.492E 05 - 0.520E 05	0.50 - 0.53	0.63 - 0.67	-0.867E 05
0.179E 08	0.40000	0.520E 05 - 0.537E 05	0.53 - 0.54	0.67 - 0.69	-0.873E 05
0.180E 08	0.45000	0.537E 05 - 0.550E 05	0.54 - 0.56	0.69 - 0.71	-0.868E 05
0.180E 08	0.50000	0.550E 05 - 0.561E 05	0.56 - 0.57	0.71 - 0.72	-0.859E 05
0.179E 08	0.55000	0.561E 05 - 0.572E 05	0.57 - 0.58	0.72 - 0.74	-0.843E 05
0.180E 08	0.60000	0.572E 05 - 0.590E 05	0.58 - 0.60	0.74 - 0.76	-0.865E 05
0.179E 08	0.65000	0.590E 05 - 0.621E 05	0.60 - 0.63	0.76 - 0.80	-0.983E 05
0.180E 08	0.70000	0.621E 05 - 0.647E 05	0.63 - 0.66	0.80 - 0.83	-0.109E 06
0.179E 08	0.75000	0.647E 05 - 0.668E 05	0.66 - 0.68	0.83 - 0.86	-0.112E 06
0.179E 08	0.80000	0.668E 05 - 0.690E 05	0.68 - 0.70	0.86 - 0.89	-0.113E 06
0.180E 08	0.85000	0.690E 05 - 0.715E 05	0.70 - 0.72	0.89 - 0.92	-0.113E 06
0.179E 08	0.90000	0.715E 05 - 0.747E 05	0.72 - 0.76	0.92 - 0.96	-0.110E 06
0.180E 08	0.95000	0.747E 05 - 0.765E 05	0.76 - 0.77	0.96 - 0.98	-0.110E 06
0.718E 07	0.97000	0.765E 05 - 0.775E 05	0.77 - 0.79	0.98 - 1.00	-0.110E 06
0.718E 07	0.99000	0.775E 05 - 0.795E 05	0.79 - 0.80	1.00 - 1.02	-0.110E 06
0.323E 07	0.99900	0.795E 05 - 0.825E 05	0.80 - 0.84	1.02 - 1.06	-0.110E 06
0.323E 06	0.99990	0.825E 05 - 0.988E 05	0.84 - 1.00	1.06 - 1.27	-0.142E 06

TOTAL CYCLES = 0.359E 09

ROOT MEAN CUBED IS 0.591E 05 AVERAGE MEAN IS -0.959E 05

TABLE H-23
CUMMULATIVE FATIGUE HISTOGRAM OUTPUT

0.250R BLADE MY

NO. CYCLES IN 30 YEARS (TYPES 1+2)	CUM PROB	HALF-RANGE FATIGUE LOADS: LOAD LEVELS	NORMALIZED LOAD LEVELS	LOAD/50% AT RATED	MID-RANGE MEAN
0.180E 08	0.0[illegible]000	0. - 0.483E 06	0. - 0.11	0. - 0.54	0.550E 07
0.180E 08	0.1[illegible]000	0.483E 06 - 0.547E 06	0.11 - 0.13	0.54 - 0.61	0.565E 07
0.180E 08	0.1[illegible]000	0.547E 06 - 0.595E 06	0.13 - 0.14	0.61 - 0.66	0.576E 07
0.179E 08	0.2[illegible]000	0.595E 06 - 0.637E 06	0.14 - 0.15	0.66 - 0.71	0.584E 07
0.180E 08	0.2[illegible]000	0.637E 06 - 0.675E 06	0.15 - 0.16	0.71 - 0.75	0.592E 07
0.180E 08	0.3[illegible]000	0.675E 06 - 0.712E 06	0.16 - 0.17	0.75 - 0.79	0.599E 07
0.180E 08	0.3[illegible]000	0.712E 06 - 0.749E 06	0.17 - 0.18	0.79 - 0.83	0.606E 07
0.179E 08	0.4[illegible]000	0.749E 06 - 0.786E 06	0.18 - 0.19	0.83 - 0.87	0.612E 07
0.180E 08	0.4[illegible]000	0.786E 06 - 0.823E 06	0.19 - 0.19	0.87 - 0.91	0.617E 07
0.180E 08	0.5[illegible]000	0.823E 06 - 0.862E 06	0.19 - 0.20	0.91 - 0.96	0.622E 07
0.179E 08	0.5[illegible]000	0.862E 06 - 0.904E 06	0.20 - 0.21	0.96 - 1.00	0.627E 07
0.180E 08	0.6[illegible]000	0.904E 06 - 0.946E 06	0.21 - 0.22	1.00 - 1.05	0.632E 07
0.179E 08	0.6[illegible]000	0.946E 06 - 0.990E 06	0.22 - 0.23	1.05 - 1.10	0.636E 07
0.180E 08	0.7[illegible]000	0.990E 06 - 0.104E 07	0.23 - 0.25	1.10 - 1.16	0.641E 07
0.179E 08	0.7[illegible]000	0.104E 07 - 0.111E 07	0.25 - 0.26	1.16 - 1.23	0.645E 07
0.179E 08	0.8[illegible]000	0.111E 07 - 0.118E 07	0.26 - 0.28	1.23 - 1.31	0.648E 07
0.180E 08	0.8[illegible]000	0.118E 07 - 0.127E 07	0.28 - 0.30	1.31 - 1.41	0.652E 07
0.179E 08	0.9[illegible]000	0.127E 07 - 0.139E 07	0.30 - 0.33	1.41 - 1.55	0.664E 07
0.180E 08	0.9[illegible]000	0.139E 07 - 0.160E 07	0.33 - 0.38	1.55 - 1.78	0.686E 07
0.718E 07	0.9[illegible]000	0.160E 07 - 0.176E 07	0.38 - 0.42	1.78 - 1.96	0.700E 07
0.718E 07	0.9[illegible]000	0.176E 07 - 0.211E 07	0.42 - 0.50	1.96 - 2.34	0.732E 07
0.323E 07	0.9[illegible]900	0.211E 07 - 0.279E 07	0.50 - 0.66	2.34 - 3.09	0.785E 07
0.323E 06	0.9[illegible]990	0.279E 07 - 0.432E 07	0.66 - 1.02	3.09 - 4.80	0.649E 07

TOTAL CYCLES = 0.[illegible]59E 09

ROOT MEAN CUBE[illegible] IS 0.108E 07 AVERAGE MEAN IS 0.624E 07

TABLE H-24
CUMMULATIVE FATIGUE HISTOGRAM OUTPUT

0.250R BLADE MZ

NO. CYCLES IN 30 YEARS (TYPES 1+2)	CUM PROB	HALF-RANGE FATIGUE LOADS: LOAD LEVELS	NORMALIZED LOAD LEVELS	LOAD/50% AT RATED	MID-RANGE MEAN
0.180E 08	0.0[illegible]000	0. - 0.320E 07	0. - 0.87	0. - 1.06	-0.532E 06
0.180E 08	0.1[illegible]000	0.320E 07 - 0.326E 07	0.87 - 0.88	1.06 - 1.08	-0.558E 06
0.180E 08	0.1[illegible]000	0.326E 07 - 0.331E 07	0.88 - 0.89	1.08 - 1.09	-0.567E 06
0.179E 08	0.2[illegible]000	0.331E 07 - 0.334E 07	0.89 - 0.90	1.09 - 1.10	-0.569E 06
0.180E 08	0.2[illegible]000	0.334E 07 - 0.337E 07	0.90 - 0.91	1.10 - 1.11	-0.567E 06
0.180E 08	0.3[illegible]000	0.337E 07 - 0.340E 07	0.91 - 0.92	1.11 - 1.12	-0.562E 06
0.180E 08	0.3[illegible]000	0.340E 07 - 0.343E 07	0.92 - 0.93	1.12 - 1.13	-0.555E 06
0.179E 08	0.4[illegible]000	0.343E 07 - 0.345E 07	0.93 - 0.93	1.13 - 1.14	-0.547E 06
0.180E 08	0.4[illegible]000	0.345E 07 - 0.348E 07	0.93 - 0.94	1.14 - 1.15	-0.537E 06
0.180E 08	0.5[illegible]000	0.348E 07 - 0.350E 07	0.94 - 0.95	1.15 - 1.16	-0.526E 06
0.179E 08	0.5[illegible]000	0.350E 07 - 0.353E 07	0.95 - 0.95	1.16 - 1.16	-0.522E 06
0.180E 08	0.6[illegible]000	0.353E 07 - 0.355E 07	0.95 - 0.96	1.16 - 1.17	-0.521E 06
0.179E 08	0.6[illegible]000	0.355E 07 - 0.357E 07	0.96 - 0.97	1.17 - 1.18	-0.521E 06
0.180E 08	0.7[illegible]000	0.357E 07 - 0.360E 07	0.97 - 0.97	1.18 - 1.19	-0.531E 06
0.179E 08	0.7[illegible]000	0.360E 07 - 0.363E 07	0.97 - 0.98	1.19 - 1.20	-0.554E 06
0.179E 08	0.8[illegible]000	0.363E 07 - 0.367E 07	0.98 - 0.99	1.20 - 1.21	-0.567E 06
0.180E 08	0.8[illegible]000	0.367E 07 - 0.371E 07	0.99 - 1.00	1.21 - 1.22	-0.570E 06
0.179E 08	0.9[illegible]000	0.371E 07 - 0.376E 07	1.00 - 1.02	1.22 - 1.24	-0.567E 06
0.180E 08	0.9[illegible]000	0.376E 07 - 0.384E 07	1.02 - 1.04	1.24 - 1.27	-0.562E 06
0.718E 07	0.9[illegible]000	0.384E 07 - 0.389E 07	1.04 - 1.05	1.27 - 1.29	-0.562E 06
0.718E 07	0.9[illegible]000	0.389E 07 - 0.399E 07	1.05 - 1.08	1.29 - 1.32	-0.558E 06
0.323E 07	0.9[illegible]900	0.399E 07 - 0.417E 07	1.08 - 1.13	1.32 - 1.38	-0.477E 06
0.323E 06	0.9[illegible]990	0.417E 07 - 0.434E 07	1.13 - 1.17	1.38 - 1.43	-0.104E 07

TOTAL CYCLES = 0.[illegible]59E 09

ROOT MEAN CUBE[illegible] IS 0.348E 07 AVERAGE MEAN IS -0.549E 06

TABLE H-25
CUMULATIVE FATIGUE HISTOGRAM OUTPUT

0.3COR BLADE VX

NO. CYCLES IN 30 YEARS (TYPES 1+2)	CUM PROB	HALF-RANGE FATIGUE LOADS: LOAD LEVELS	NORMALIZED LOAD LEVELS	LOAD/50% AT RATED	MID-RANGE MEAN
0.180E 08	0.05000	0. - 0.560E 05	0. - 0.77	0. - 0.96	0.556E 06
0.180E 08	0.10000	0.560E 05 - 0.570E 05	0.77 - 0.78	0.96 - 0.97	0.542E 06
0.180E 08	0.15000	0.570E 05 - 0.577E 05	0.78 - 0.79	0.97 - 0.98	0.528E 06
0.179E 08	0.20000	0.577E 05 - 0.532E 05	0.79 - 0.80	0.98 - 0.99	0.515E 06
0.180E 08	0.25000	0.582E 05 - 0.587E 05	0.80 - 0.80	0.99 - 1.00	0.502E 06
0.180E 08	0.30000	0.587E 05 - 0.591E 05	0.80 - 0.81	1.00 - 1.01	0.491E 06
0.180E 08	0.35000	0.591E 05 - 0.595E 05	0.81 - 0.81	1.01 - 1.02	0.481E 06
0.179E 08	0.40000	0.595E 05 - 0.598E 05	0.81 - 0.82	1.02 - 1.02	0.472E 06
0.180E 08	0.45000	0.598E 05 - 0.602E 05	0.82 - 0.82	1.02 - 1.03	0.464E 06
0.180E 08	0.50000	0.602E 05 - 0.606E 05	0.82 - 0.83	1.03 - 1.04	0.455E 06
0.179E 08	0.55000	0.606E 05 - 0.610E 05	0.83 - 0.83	1.04 - 1.04	0.448E 06
0.180E 08	0.60000	0.610E 05 - 0.614E 05	0.83 - 0.84	1.04 - 1.05	0.441E 06
0.179E 08	0.65000	0.614E 05 - 0.618E 05	0.84 - 0.84	1.05 - 1.05	0.435E 06
0.180E 08	0.70000	0.618E 05 - 0.622E 05	0.84 - 0.85	1.05 - 1.06	0.429E 06
0.179E 08	0.75000	0.622E 05 - 0.626E 05	0.85 - 0.86	1.06 - 1.07	0.422E 06
0.179E 08	0.80000	0.626E 05 - 0.631E 05	0.86 - 0.86	1.07 - 1.08	0.414E 06
0.180E 08	0.85000	0.631E 05 - 0.636E 05	0.86 - 0.87	1.08 - 1.09	0.406E 06
0.179E 08	0.90000	0.636E 05 - 0.643E 05	0.87 - 0.88	1.09 - 1.10	0.400E 06
0.180E 08	0.95000	0.643E 05 - 0.653E 05	0.88 - 0.89	1.10 - 1.11	0.393E 06
0.718E 07	0.97000	0.653E 05 - 0.659E 05	0.89 - 0.90	1.11 - 1.13	0.391E 06
0.718E 07	0.99000	0.659E 05 - 0.672E 05	0.90 - 0.92	1.13 - 1.15	0.385E 06
0.323E 07	0.99900	0.672E 05 - 0.694E 05	0.92 - 0.95	1.15 - 1.18	0.379E 06
0.323E 06	0.99990	0.694E 05 - 0.732E 05	0.95 - 1.00	1.18 - 1.25	0.563E 06

TOTAL CYCLES = 0.359E 09

ROOT MEAN CUBED IS 0.601E 05 AVERAGE MEAN IS 0.459E 06

TABLE H-26
CUMULATIVE FATIGUE HISTOGRAM OUTPUT

0.300R BLADE VY

NO. CYCLES IN 30 YEARS (TYPES 1+2)	CUM PROB	HALF-RANGE FATIGUE LOADS: LOAD LEVELS	NORMALIZED LOAD LEVELS	LOAD/50% AT RATED	MID-RANGE MEAN
0.180E 08	0.05000	0. - 0.628E 05	0. - 0.73	0. - 0.91	0.734E 04
0.180E 08	0.10000	0.628E 05 - 0.640E 05	0.73 - 0.74	0.91 - 0.92	0.730E 04
0.180E 08	0.15000	0.640E 05 - 0.649E 05	0.74 - 0.75	0.92 - 0.94	0.729E 04
0.179E 08	0.20000	0.649E 05 - 0.655E 05	0.75 - 0.76	0.94 - 0.95	0.730E 04
0.180E 08	0.25000	0.655E 05 - 0.662E 05	0.76 - 0.77	0.95 - 0.96	0.733E 04
0.180E 08	0.30000	0.662E 05 - 0.668E 05	0.77 - 0.77	0.96 - 0.97	0.736E 04
0.180E 08	0.35000	0.668E 05 - 0.673E 05	0.77 - 0.78	0.97 - 0.97	0.739E 04
0.179E 08	0.40000	0.673E 05 - 0.678E 05	0.78 - 0.79	0.97 - 0.98	0.743E 04
0.180E 08	0.45000	0.678E 05 - 0.683E 05	0.79 - 0.79	0.98 - 0.99	0.747E 04
0.180E 08	0.50000	0.683E 05 - 0.688E 05	0.79 - 0.80	0.99 - 0.99	0.751E 04
0.179E 08	0.55000	0.688E 05 - 0.693E 05	0.80 - 0.80	0.99 - 1.00	0.755E 04
0.180E 08	0.60000	0.693E 05 - 0.698E 05	0.80 - 0.81	1.00 - 1.01	0.755E 04
0.179E 08	0.65000	0.698E 05 - 0.703E 05	0.81 - 0.82	1.01 - 1.02	0.742E 04
0.180E 08	0.70000	0.703E 05 - 0.709E 05	0.82 - 0.82	1.02 - 1.02	0.725E 04
0.179E 08	0.75000	0.709E 05 - 0.716E 05	0.82 - 0.83	1.02 - 1.03	0.715E 04
0.179E 08	0.80000	0.716E 05 - 0.723E 05	0.83 - 0.84	1.03 - 1.05	0.713E 04
0.180E 08	0.85000	0.723E 05 - 0.730E 05	0.84 - 0.85	1.05 - 1.06	0.707E 04
0.179E 08	0.90000	0.730E 05 - 0.740E 05	0.85 - 0.86	1.06 - 1.07	0.705E 04
0.180E 08	0.95000	0.740E 05 - 0.757E 05	0.86 - 0.88	1.07 - 1.09	0.702E 04
0.718E 07	0.97000	0.757E 05 - 0.768E 05	0.88 - 0.89	1.09 - 1.11	0.699E 04
0.718E 07	0.99000	0.768E 05 - 0.789E 05	0.89 - 0.91	1.11 - 1.14	0.700E 04
0.323E 07	0.99900	0.789E 05 - 0.823E 05	0.91 - 0.95	1.14 - 1.19	0.741E 04
0.323E 06	0.99990	0.823E 05 - 0.874E 05	0.95 - 1.01	1.19 - 1.26	0.287E 04

TOTAL CYCLES = 0.359E 09

ROOT MEAN CUBED IS 0.685E 05 AVERAGE MEAN IS 0.729E 04

TABLE H-27
CUMMULATIVE FATIGUE HISTOGRAM OUTPUT

0.300R BLADE VZ

NO. CYCLES IN 30 YEARS (TYPES 1+2)	CUM PROB	HALF-RANGE FATIGUE LOADS: LOAD LEVELS	NORMALIZED LOAD LEVELS	LOAD/50% AT RATED	MID-RANGE MEAN
0.180E 08	0.(5000	0. - 0.602E 04	0. - 0.11	0. - 0.62	-0.683E 05
0.180E 08	0.10000	0.602E 04 - 0.674E 04	0.11 - 0.12	0.62 - 0.69	-0.703E 05
0.180E 08	0.15000	0.674E 04 - 0.728E 04	0.12 - 0.13	0.69 - 0.75	-0.718E 05
0.179E 08	0.(0000	0.728E 04 - 0.776E 04	0.13 - 0.14	0.75 - 0.80	-0.729E 05
0.180E 08	0.(5000	0.776E 04 - 0.820E 04	0.14 - 0.15	0.80 - 0.85	-0.739E 05
0.180E 08	0.(0000	0.820E 04 - 0.862E 04	0.15 - 0.16	0.85 - 0.89	-0.749E 05
0.180E 08	0.(5000	0.862E 04 - 0.903E 04	0.16 - 0.16	0.89 - 0.93	-0.757E 05
0.179E 08	0.(0000	0.903E 04 - 0.945E 04	0.16 - 0.17	0.93 - 0.97	-0.765E 05
0.180E 08	0.(5000	0.945E 04 - 0.987E 04	0.17 - 0.18	0.97 - 1.02	-0.773E 05
0.180E 08	0.(0000	0.987E 04 - 0.103E 05	0.18 - 0.19	1.02 - 1.06	-0.780E 05
0.179E 08	0.(5000	0.103E 05 - 0.108E 05	0.19 - 0.20	1.06 - 1.11	-0.785E 05
0.180E 08	0.(0000	0.108E 05 - 0.113E 05	0.20 - 0.20	1.11 - 1.16	-0.792E 05
0.179E 08	0.(5000	0.113E 05 - 0.118E 05	0.20 - 0.21	1.16 - 1.22	-0.800E 05
0.180E 08	0.(0000	0.118E 05 - 0.124E 05	0.21 - 0.23	1.22 - 1.28	-0.806E 05
0.179E 08	0.(5000	0.124E 05 - 0.131E 05	0.23 - 0.24	1.28 - 1.35	-0.811E 05
0.179E 08	0.(0000	0.131E 05 - 0.140E 05	0.24 - 0.25	1.35 - 1.44	-0.816E 05
0.180E 08	0.(5000	0.140E 05 - 0.150E 05	0.25 - 0.27	1.44 - 1.55	-0.819E 05
0.179E 08	0.(0000	0.150E 05 - 0.164E 05	0.27 - 0.30	1.55 - 1.69	-0.831E 05
0.180E 08	0.(5000	0.164E 05 - 0.189E 05	0.30 - 0.34	1.69 - 1.95	-0.858E 05
0.718E 07	0.(7000	0.189E 05 - 0.207E 05	0.34 - 0.37	1.95 - 2.13	-0.878E 05
0.718E 07	0.(9000	0.207E 05 - 0.244E 05	0.37 - 0.44	2.13 - 2.52	-0.918E 05
0.323E 07	0.(9900	0.244E 05 - 0.308E 05	0.44 - 0.56	2.52 - 3.18	-0.952E 05
0.323E 06	0.(9990	0.308E 05 - 0.574E 05	0.56 - 1.04	3.18 - 5.91	-0.970E 05

TOTAL CYCLES = 0.359E 09

ROOT MEAN CUBED IS 0.127E 05 AVERAGE MEAN IS -0.781E 05

TABLE H-28
CUMMULATIVE FATIGUE HISTOGRAM OUTPUT

0.300R BLADE MX

NO. CYCLES IN 30 YEARS (TYPES 1+2)	CUM PROB	HALF-RANGE FATIGUE LOADS: LOAD LEVELS	NORMALIZED LOAD LEVELS	LOAD/50% AT RATED	MID-RANGE MEAN
0.180E 08	0.(5000	0. - 0.353E 05	0. - 0.44	0. - 0.53	-0.860E 05
0.180E 08	0.(0000	0.353E 05 - 0.351E 05	0.44 - 0.44	0.53 - 0.52	-0.861E 05
0.180E 08	0.(5000	0.351E 05 - 0.361E 05	0.44 - 0.45	0.52 - 0.54	-0.868E 05
0.179E 08	0.(0000	0.361E 05 - 0.379E 05	0.45 - 0.48	0.54 - 0.57	-0.869E 05
0.180E 08	0.(5000	0.379E 05 - 0.397E 05	0.48 - 0.50	0.57 - 0.59	-0.867E 05
0.180E 08	0.(0000	0.397E 05 - 0.434E 05	0.50 - 0.55	0.59 - 0.65	-0.828E 05
0.180E 08	0.(5000	0.434E 05 - 0.455E 05	0.55 - 0.57	0.65 - 0.68	-0.823E 05
0.179E 08	0.(0000	0.455E 05 - 0.468E 05	0.57 - 0.59	0.68 - 0.70	-0.826E 05
0.180E 08	0.(5000	0.468E 05 - 0.478E 05	0.59 - 0.60	0.70 - 0.71	-0.825E 05
0.180E 08	0.(0000	0.478E 05 - 0.487E 05	0.60 - 0.61	0.71 - 0.73	-0.824E 05
0.179E 08	0.(5000	0.487E 05 - 0.497E 05	0.61 - 0.63	0.73 - 0.74	-0.821E 05
0.180E 08	0.(0000	0.497E 05 - 0.516E 05	0.63 - 0.65	0.74 - 0.77	-0.871E 05
0.179E 08	0.(5000	0.516E 05 - 0.542E 05	0.65 - 0.68	0.77 - 0.81	-0.994E 05
0.180E 08	0.(0000	0.542E 05 - 0.562E 05	0.68 - 0.71	0.81 - 0.84	-0.107E 06
0.179E 08	0.(5000	0.562E 05 - 0.580E 05	0.71 - 0.73	0.84 - 0.86	-0.111E 06
0.179E 08	0.(0000	0.580E 05 - 0.599E 05	0.73 - 0.75	0.86 - 0.89	-0.113E 06
0.180E 08	0.(5000	0.599E 05 - 0.620E 05	0.75 - 0.78	0.89 - 0.92	-0.112E 06
0.179E 08	0.(0000	0.620E 05 - 0.647E 05	0.78 - 0.81	0.92 - 0.97	-0.108E 06
0.180E 08	0.(5000	0.647E 05 - 0.663E 05	0.81 - 0.83	0.97 - 0.99	-0.108E 06
0.718E 07	0.(7000	0.663E 05 - 0.672E 05	0.83 - 0.85	0.99 - 1.00	-0.108E 06
0.718E 07	0.(9000	0.672E 05 - 0.688E 05	0.85 - 0.87	1.00 - 1.03	-0.108E 06
0.323E 07	0.(9900	0.688E 05 - 0.714E 05	0.87 - 0.90	1.03 - 1.07	-0.108E 06
0.323E 06	0.(9990	0.714E 05 - 0.794E 05	0.90 - 1.00	1.07 - 1.19	-0.122E 06

TOTAL CYCLES = 0.359E 09

ROOT MEAN CUBED IS 0.514E 05 AVERAGE MEAN IS -0.940E 05

TABLE H-29
CUMMULATIVE FATIGUE HISTOGRAM OUTPUT

0.300R BLADE MY

NO. CYCLES IN 30 YEARS (TYPES 1+2)	CUM PROB	HALF-RANGE FATIGUE LOADS: LOAD LEVELS	HALF-RANGE FATIGUE LOADS: NORMALIZED LOAD LEVELS	HALF-RANGE FATIGUE LOADS: LOAD/50% AT RATED	MID-RANGE MEAN
0.180E 08	0.05000	0. - 0.413E 06	0. - 0.11	0. - 0.53	0.494E 07
0.180E 08	0.10000	0.413E 06 - 0.469E 06	0.11 - 0.13	0.53 - 0.60	0.505E 07
0.180E 08	0.15000	0.469E 06 - 0.511E 06	0.13 - 0.14	0.60 - 0.65	0.513E 07
0.179E 08	0.20000	0.511E 06 - 0.548E 06	0.14 - 0.15	0.65 - 0.70	0.520E 07
0.180E 08	0.25000	0.548E 06 - 0.582E 06	0.15 - 0.16	0.70 - 0.74	0.526E 07
0.180E 08	0.30000	0.582E 06 - 0.615E 06	0.16 - 0.17	0.74 - 0.79	0.531E 07
0.180E 08	0.35000	0.615E 06 - 0.647E 06	0.17 - 0.18	0.79 - 0.83	0.536E 07
0.179E 08	0.40000	0.647E 06 - 0.680E 06	0.18 - 0.18	0.83 - 0.87	0.540E 07
0.180E 08	0.45000	0.680E 06 - 0.713E 06	0.18 - 0.19	0.87 - 0.91	0.545E 07
0.180E 08	0.50000	0.713E 06 - 0.748E 06	0.19 - 0.20	0.91 - 0.96	0.549E 07
0.179E 08	0.55000	0.748E 06 - 0.785E 06	0.20 - 0.21	0.96 - 1.00	0.552E 07
0.180E 08	0.60000	0.785E 06 - 0.823E 06	0.21 - 0.22	1.00 - 1.05	0.555E 07
0.179E 08	0.65000	0.823E 06 - 0.864E 06	0.22 - 0.23	1.05 - 1.10	0.558E 07
0.180E 08	0.70000	0.864E 06 - 0.911E 06	0.23 - 0.25	1.10 - 1.16	0.561E 07
0.179E 08	0.75000	0.911E 06 - 0.966E 06	0.25 - 0.26	1.16 - 1.23	0.564E 07
0.179E 08	0.80000	0.966E 06 - 0.103E 07	0.26 - 0.28	1.23 - 1.32	0.567E 07
0.180E 08	0.85000	0.103E 07 - 0.111E 07	0.28 - 0.30	1.32 - 1.42	0.571E 07
0.179E 08	0.90000	0.111E 07 - 0.122E 07	0.30 - 0.33	1.42 - 1.56	0.580E 07
0.180E 08	0.95000	0.122E 07 - 0.141E 07	0.33 - 0.38	1.56 - 1.80	0.598E 07
0.718E 07	0.97000	0.141E 07 - 0.155E 07	0.38 - 0.42	1.80 - 1.98	0.610E 07
0.718E 07	0.99000	0.155E 07 - 0.186E 07	0.42 - 0.50	1.98 - 2.37	0.639E 07
0.323E 07	0.99900	0.186E 07 - 0.245E 07	0.50 - 0.66	2.37 - 3.13	0.686E 07
0.323E 06	0.99990	0.245E 07 - 0.377E 07	0.66 - 1.02	3.13 - 4.81	0.560E 07

TOTAL CYCLES = 0.359E 09

ROOT MEAN CUBED IS 0.944E 06 AVERAGE MEAN IS 0.550E 07

TABLE H-30
CUMMULATIVE FATIGUE HISTOGRAM OUTPUT

0.300R BLADE MZ

NO. CYCLES IN 30 YEARS (TYPES 1+2)	CUM PROB	HALF-RANGE FATIGUE LOADS: LOAD LEVELS	HALF-RANGE FATIGUE LOADS: NORMALIZED LOAD LEVELS	HALF-RANGE FATIGUE LOADS: LOAD/50% AT RATED	MID-RANGE MEAN
0.180E 08	0.05000	0. - 0.262E 07	0. - 0.84	0. - 1.04	-0.549E 06
0.180E 08	0.10000	0.262E 07 - 0.267E 07	0.84 - 0.86	1.04 - 1.06	-0.575E 06
0.180E 08	0.15000	0.267E 07 - 0.271E 07	0.86 - 0.87	1.06 - 1.07	-0.584E 06
0.179E 08	0.20000	0.271E 07 - 0.274E 07	0.87 - 0.88	1.07 - 1.08	-0.587E 06
0.180E 08	0.25000	0.274E 07 - 0.276E 07	0.88 - 0.89	1.08 - 1.09	-0.585E 06
0.180E 08	0.30000	0.276E 07 - 0.278E 07	0.89 - 0.89	1.09 - 1.10	-0.581E 06
0.180E 08	0.35000	0.278E 07 - 0.281E 07	0.89 - 0.90	1.10 - 1.11	-0.575E 06
0.179E 08	0.40000	0.281E 07 - 0.283E 07	0.90 - 0.91	1.11 - 1.12	-0.568E 06
0.180E 08	0.45000	0.283E 07 - 0.285E 07	0.91 - 0.91	1.12 - 1.13	-0.559E 06
0.180E 08	0.50000	0.285E 07 - 0.287E 07	0.91 - 0.92	1.13 - 1.14	-0.548E 06
0.179E 08	0.55000	0.287E 07 - 0.289E 07	0.92 - 0.93	1.14 - 1.14	-0.543E 06
0.180E 08	0.60000	0.289E 07 - 0.290E 07	0.93 - 0.93	1.14 - 1.15	-0.539E 06
0.179E 08	0.65000	0.290E 07 - 0.292E 07	0.93 - 0.94	1.15 - 1.16	-0.534E 06
0.180E 08	0.70000	0.292E 07 - 0.295E 07	0.94 - 0.94	1.16 - 1.17	-0.544E 06
0.179E 08	0.75000	0.295E 07 - 0.297E 07	0.94 - 0.95	1.17 - 1.18	-0.566E 06
0.179E 08	0.80000	0.297E 07 - 0.300E 07	0.95 - 0.96	1.18 - 1.19	-0.581E 06
0.180E 08	0.85000	0.300E 07 - 0.304E 07	0.96 - 0.97	1.19 - 1.20	-0.581E 06
0.179E 08	0.90000	0.304E 07 - 0.308E 07	0.97 - 0.99	1.20 - 1.22	-0.580E 06
0.180E 08	0.95000	0.308E 07 - 0.315E 07	0.99 - 1.01	1.22 - 1.25	-0.581E 06
0.718E 07	0.97000	0.315E 07 - 0.319E 07	1.01 - 1.02	1.25 - 1.26	-0.585E 06
0.718E 07	0.99000	0.319E 07 - 0.327E 07	1.02 - 1.05	1.26 - 1.30	-0.582E 06
0.323E 07	0.99900	0.327E 07 - 0.341E 07	1.05 - 1.09	1.30 - 1.35	-0.531E 06
0.323E 06	0.99990	0.341E 07 - 0.359E 07	1.09 - 1.15	1.35 - 1.42	-0.106E 07

TOTAL CYCLES = 0.359E 09

ROOT MEAN CUBED IS 0.285E 07 AVERAGE MEAN IS -0.567E 06

TABLE H-31
CUMMULATIVE FATIGUE HISTOGRAM OUTPUT

0.400R BLADE VX

NO. CYCLES IN 30 YEARS (TYPES 1+2)	CUM PROB	HALF-RANGE FATIGUE LOADS: LOAD LEVELS	NORMALIZED LOAD LEVELS	LOAD/50% AT RATED	MID-RANGE MEAN
0.180E 08	0.05000	0. - 0.449E 05	0. - 0.76	0. - 0.95	0.473E 06
0.180E 08	0.10000	0.449E 05 - 0.456E 05	0.76 - 0.77	0.95 - 0.96	0.466E 06
0.180E 08	0.15000	0.456E 05 - 0.461E 05	0.77 - 0.78	0.96 - 0.98	0.457E 06
0.179E 08	0.20000	0.461E 05 - 0.466E 05	0.78 - 0.79	0.98 - 0.98	0.448E 06
0.180E 08	0.25000	0.466E 05 - 0.469E 05	0.79 - 0.79	0.98 - 0.99	0.438E 06
0.180E 08	0.30000	0.469E 05 - 0.473E 05	0.79 - 0.80	0.99 - 1.00	0.428E 06
0.180E 08	0.35000	0.473E 05 - 0.476E 05	0.80 - 0.80	1.00 - 1.01	0.416E 06
0.179E 08	0.40000	0.476E 05 - 0.478E 05	0.80 - 0.81	1.01 - 1.01	0.404E 06
0.180E 08	0.45000	0.478E 05 - 0.481E 05	0.81 - 0.81	1.01 - 1.02	0.394E 06
0.180E 08	0.50000	0.481E 05 - 0.484E 05	0.81 - 0.82	1.02 - 1.02	0.387E 06
0.179E 08	0.55000	0.484E 05 - 0.488E 05	0.82 - 0.82	1.02 - 1.03	0.379E 06
0.180E 08	0.60000	0.488E 05 - 0.491E 05	0.82 - 0.83	1.03 - 1.04	0.371E 06
0.179E 08	0.65000	0.491E 05 - 0.494E 05	0.83 - 0.83	1.04 - 1.04	0.362E 06
0.180E 08	0.70000	0.494E 05 - 0.497E 05	0.83 - 0.84	1.04 - 1.05	0.354E 06
0.179E 08	0.75000	0.497E 05 - 0.501E 05	0.84 - 0.85	1.05 - 1.06	0.345E 06
0.179E 08	0.80000	0.501E 05 - 0.505E 05	0.85 - 0.85	1.06 - 1.07	0.337E 06
0.180E 08	0.85000	0.505E 05 - 0.510E 05	0.85 - 0.86	1.07 - 1.08	0.329E 06
0.179E 08	0.90000	0.510E 05 - 0.515E 05	0.86 - 0.87	1.08 - 1.09	0.322E 06
0.180E 08	0.95000	0.515E 05 - 0.523E 05	0.87 - 0.88	1.09 - 1.11	0.316E 06
0.718E 07	0.97000	0.523E 05 - 0.529E 05	0.88 - 0.89	1.11 - 1.12	0.312E 06
0.718E 07	0.99000	0.529E 05 - 0.539E 05	0.89 - 0.91	1.12 - 1.14	0.307E 06
0.323E 07	0.99900	0.539E 05 - 0.559E 05	0.91 - 0.94	1.14 - 1.18	0.302E 06
0.323E 06	0.99990	0.559E 05 - 0.592E 05	0.94 - 1.00	1.18 - 1.25	0.451E 06

TOTAL CYCLES = 0.359E 09

ROOT MEAN CUBED IS 0.481E 05 AVERAGE MEAN IS 0.387E 06

TABLE H-32
CUMMULATIVE FATIGUE HISTOGRAM OUTPUT

0.400R BLADE VY

NO. CYCLES IN 30 YEARS (TYPES 1+2)	CUM PROB	HALF-RANGE FATIGUE LOADS: LOAD LEVELS	NORMALIZED LOAD LEVELS	LOAD/50% AT RATED	MID-RANGE MEAN
0.180E 08	0.05000	0. - 0.512E 05	0. - 0.72	0. - 0.91	0.456E 04
0.180E 08	0.10000	0.512E 05 - 0.521E 05	0.72 - 0.73	0.91 - 0.92	0.447E 04
0.180E 08	0.15000	0.521E 05 - 0.528E 05	0.73 - 0.74	0.92 - 0.94	0.443E 04
0.179E 08	0.20000	0.528E 05 - 0.533E 05	0.74 - 0.75	0.94 - 0.94	0.443E 04
0.180E 08	0.25000	0.533E 05 - 0.538E 05	0.75 - 0.75	0.94 - 0.95	0.444E 04
0.180E 08	0.30000	0.538E 05 - 0.542E 05	0.75 - 0.76	0.95 - 0.96	0.446E 04
0.180E 08	0.35000	0.542E 05 - 0.546E 05	0.76 - 0.76	0.96 - 0.97	0.448E 04
0.179E 08	0.40000	0.546E 05 - 0.550E 05	0.76 - 0.77	0.97 - 0.97	0.452E 04
0.180E 08	0.45000	0.550E 05 - 0.553E 05	0.77 - 0.77	0.97 - 0.98	0.455E 04
0.180E 08	0.50000	0.553E 05 - 0.557E 05	0.77 - 0.78	0.98 - 0.99	0.459E 04
0.179E 08	0.55000	0.557E 05 - 0.561E 05	0.78 - 0.79	0.99 - 0.99	0.461E 04
0.180E 08	0.60000	0.561E 05 - 0.564E 05	0.79 - 0.79	0.99 - 1.00	0.458E 04
0.179E 08	0.65000	0.564E 05 - 0.569E 05	0.79 - 0.80	1.00 - 1.01	0.448E 04
0.180E 08	0.70000	0.569E 05 - 0.573E 05	0.80 - 0.80	1.01 - 1.02	0.436E 04
0.179E 08	0.75000	0.573E 05 - 0.577E 05	0.80 - 0.81	1.02 - 1.02	0.427E 04
0.179E 08	0.80000	0.577E 05 - 0.582E 05	0.81 - 0.81	1.02 - 1.03	0.423E 04
0.180E 08	0.85000	0.582E 05 - 0.588E 05	0.81 - 0.82	1.03 - 1.04	0.419E 04
0.179E 08	0.90000	0.588E 05 - 0.597E 05	0.82 - 0.84	1.04 - 1.06	0.416E 04
0.180E 08	0.95000	0.597E 05 - 0.608E 05	0.84 - 0.85	1.06 - 1.08	0.415E 04
0.718E 07	0.97000	0.608E 05 - 0.617E 05	0.85 - 0.86	1.08 - 1.09	0.413E 04
0.718E 07	0.99000	0.617E 05 - 0.633E 05	0.86 - 0.89	1.09 - 1.12	0.414E 04
0.323E 07	0.99900	0.633E 05 - 0.657E 05	0.89 - 0.92	1.12 - 1.16	0.440E 04
0.323E 06	0.99990	0.657E 05 - 0.723E 05	0.92 - 1.01	1.16 - 1.28	-0.173E 04

TOTAL CYCLES = 0.359E 09

ROOT MEAN CUBED IS 0.554E 05 AVERAGE MEAN IS 0.44DE 04

TABLE H-33
CUMMULATIVE FATIGUE HISTOGRAM OUTPUT

0.400R BLADE VZ

NO. CYCLES IN 30 YEARS (TYPES 1+2)	CUM PROB	HALF-RANGE FATIGUE LOADS: LOAD LEVELS	NORMALIZED LOAD LEVELS	LOAD/50% AT RATED	MID-RANGE MEAN
0.180E 08	0.05000	0. - 0.505E 04	0. - 0.09	0. - 0.54	-0.616E 05
0.180E 08	0.10000	0.505E 04 - 0.572E 04	0.09 - 0.10	0.54 - 0.61	-0.633E 05
0.180E 08	0.15000	0.572E 04 - 0.623E 04	0.10 - 0.11	0.61 - 0.67	-0.645E 05
0.179E 08	0.20000	0.623E 04 - 0.668E 04	0.11 - 0.12	0.67 - 0.72	-0.655E 05
0.180E 08	0.25000	0.668E 04 - 0.710E 04	0.12 - 0.13	0.72 - 0.76	-0.664E 05
0.180E 08	0.30000	0.710E 04 - 0.750E 04	0.13 - 0.13	0.76 - 0.80	-0.672E 05
0.180E 08	0.35000	0.750E 04 - 0.789E 04	0.13 - 0.14	0.80 - 0.84	-0.680E 05
0.179E 08	0.40000	0.789E 04 - 0.829E 04	0.14 - 0.15	0.84 - 0.89	-0.687E 05
0.180E 08	0.45000	0.829E 04 - 0.870E 04	0.15 - 0.16	0.89 - 0.93	-0.694E 05
0.180E 08	0.50000	0.870E 04 - 0.912E 04	0.16 - 0.16	0.93 - 0.98	-0.700E 05
0.179E 08	0.55000	0.912E 04 - 0.957E 04	0.16 - 0.17	0.98 - 1.02	-0.705E 05
0.180E 08	0.60000	0.957E 04 - 0.100E 05	0.17 - 0.18	1.02 - 1.08	-0.711E 05
0.179E 08	0.65000	0.100E 05 - 0.106E 05	0.18 - 0.19	1.08 - 1.13	-0.718E 05
0.180E 08	0.70000	0.106E 05 - 0.112E 05	0.19 - 0.20	1.13 - 1.19	-0.724E 05
0.179E 08	0.75000	0.112E 05 - 0.118E 05	0.20 - 0.21	1.19 - 1.27	-0.730E 05
0.179E 08	0.80000	0.118E 05 - 0.126E 05	0.21 - 0.23	1.27 - 1.35	-0.734E 05
0.180E 08	0.85000	0.126E 05 - 0.136E 05	0.23 - 0.24	1.35 - 1.46	-0.738E 05
0.179E 08	0.90000	0.136E 05 - 0.150E 05	0.24 - 0.27	1.46 - 1.61	-0.749E 05
0.180E 08	0.95000	0.150E 05 - 0.174E 05	0.27 - 0.31	1.61 - 1.86	-0.777E 05
0.718E 07	0.97000	0.174E 05 - 0.190E 05	0.31 - 0.34	1.86 - 2.04	-0.797E 05
0.718E 07	0.99000	0.190E 05 - 0.226E 05	0.34 - 0.40	2.04 - 2.42	-0.835E 05
0.323E 07	0.99900	0.226E 05 - 0.287E 05	0.40 - 0.51	2.42 - 3.07	-0.869E 05
0.323E 06	0.99990	0.287E 05 - 0.573E 05	0.51 - 1.02	3.07 - 6.13	-0.746E 05

TOTAL CYCLES = 0.359E 09

ROOT MEAN CUBED IS 0.116E 05 AVERAGE MEAN IS -0.703E 05

TABLE H-34
CUMMULATIVE FATIGUE HISTOGRAM OUTPUT

0.400R BLADE MX

NO. CYCLES IN 30 YEARS (TYPES 1+2)	CUM PROB	HALF-RANGE FATIGUE LOADS: LOAD LEVELS	NORMALIZED LOAD LEVELS	LOAD/50% AT RATED	MID-RANGE MEAN
0.180E 08	0.05000	0. - 0.246E 05	0. - 0.49	0. - 0.55	-0.817E 05
0.180E 08	0.10000	0.246E 05 - 0.249E 05	0.49 - 0.49	0.55 - 0.56	-0.817E 05
0.180E 08	0.15000	0.249E 05 - 0.263E 05	0.49 - 0.52	0.56 - 0.59	-0.822E 05
0.179E 08	0.20000	0.263E 05 - 0.272E 05	0.52 - 0.54	0.59 - 0.61	-0.821E 05
0.180E 08	0.25000	0.272E 05 - 0.280E 05	0.54 - 0.55	0.61 - 0.63	-0.815E 05
0.180E 08	0.30000	0.280E 05 - 0.317E 05	0.55 - 0.63	0.63 - 0.71	-0.770E 05
0.180E 08	0.35000	0.317E 05 - 0.327E 05	0.63 - 0.65	0.71 - 0.73	-0.756E 05
0.179E 08	0.40000	0.327E 05 - 0.334E 05	0.65 - 0.66	0.73 - 0.75	-0.758E 05
0.180E 08	0.45000	0.334E 05 - 0.341E 05	0.66 - 0.67	0.75 - 0.76	-0.767E 05
0.180E 08	0.50000	0.341E 05 - 0.349E 05	0.67 - 0.69	0.76 - 0.78	-0.781E 05
0.179E 08	0.55000	0.349E 05 - 0.357E 05	0.69 - 0.71	0.78 - 0.80	-0.800E 05
0.180E 08	0.60000	0.357E 05 - 0.374E 05	0.71 - 0.74	0.80 - 0.84	-0.872E 05
0.179E 08	0.65000	0.374E 05 - 0.391E 05	0.74 - 0.77	0.84 - 0.87	-0.974E 05
0.180E 08	0.70000	0.391E 05 - 0.401E 05	0.77 - 0.79	0.87 - 0.90	-0.101E 06
0.179E 08	0.75000	0.401E 05 - 0.414E 05	0.79 - 0.82	0.90 - 0.92	-0.105E 06
0.179E 08	0.80000	0.414E 05 - 0.429E 05	0.82 - 0.85	0.92 - 0.96	-0.108E 06
0.180E 08	0.85000	0.429E 05 - 0.444E 05	0.85 - 0.88	0.96 - 0.99	-0.108E 06
0.179E 08	0.90000	0.444E 05 - 0.463E 05	0.88 - 0.91	0.99 - 1.03	-0.104E 06
0.180E 08	0.95000	0.463E 05 - 0.477E 05	0.91 - 0.94	1.03 - 1.07	-0.104E 06
0.718E 07	0.97000	0.477E 05 - 0.486E 05	0.94 - 0.96	1.07 - 1.09	-0.104E 06
0.718E 07	0.99000	0.486E 05 - 0.501E 05	0.96 - 0.99	1.09 - 1.12	-0.103E 06
0.323E 07	0.99900	0.501E 05 - 0.522E 05	0.99 - 1.03	1.12 - 1.17	-0.103E 06
0.323E 06	0.99990	0.522E 05 - 0.506E 05	1.03 - 1.00	1.17 - 1.13	-0.963E 05

TOTAL CYCLES = 0.359E 09

ROOT MEAN CUBED IS 0.369E 05 AVERAGE MEAN IS -0.895E 05

TABLE H-35
CUMMULATIVE FATIGUE HISTOGRAM OUTPUT

0.400R BLADE MY

NO. CYCLES IN 30 YEARS (TYPES 1+2)	CUM PROB	HALF-RANGE FATIGUE LOADS: LOAD LEVELS	NORMALIZED LOAD LEVELS	LOAD/50% AT RATED	MID-RANGE MEAN
0.180E 08	0.05000	0. - 0.290E 06	0. - 0.10	0. - 0.50	0.372E 07
0.180E 08	0.10000	0.290E 06 - 0.332E 06	0.10 - 0.11	0.50 - 0.57	0.380E 07
0.180E 08	0.15000	0.332E 06 - 0.365E 06	0.11 - 0.12	0.57 - 0.63	0.385E 07
0.179E 08	0.20000	0.365E 06 - 0.393E 06	0.12 - 0.13	0.63 - 0.68	0.389E 07
0.180E 08	0.25000	0.393E 06 - 0.419E 06	0.13 - 0.14	0.68 - 0.72	0.393E 07
0.180E 08	0.30000	0.419E 06 - 0.444E 06	0.14 - 0.15	0.72 - 0.77	0.397E 07
0.180E 08	0.35000	0.444E 06 - 0.470E 06	0.15 - 0.16	0.77 - 0.81	0.400E 07
0.179E 08	0.40000	0.470E 06 - 0.495E 06	0.16 - 0.17	0.81 - 0.85	0.403E 07
0.180E 08	0.45000	0.495E 06 - 0.521E 06	0.17 - 0.18	0.85 - 0.90	0.406E 07
0.180E 08	0.50000	0.521E 06 - 0.549E 06	0.18 - 0.19	0.90 - 0.95	0.409E 07
0.179E 08	0.55000	0.549E 06 - 0.577E 06	0.19 - 0.19	0.95 - 0.99	0.412E 07
0.180E 08	0.60000	0.577E 06 - 0.607E 06	0.19 - 0.21	0.99 - 1.05	0.413E 07
0.179E 08	0.65000	0.607E 06 - 0.641E 06	0.21 - 0.22	1.05 - 1.10	0.415E 07
0.180E 08	0.70000	0.641E 06 - 0.678E 06	0.22 - 0.23	1.10 - 1.17	0.417E 07
0.179E 08	0.75000	0.678E 06 - 0.721E 06	0.23 - 0.24	1.17 - 1.24	0.420E 07
0.179E 08	0.80000	0.721E 06 - 0.771E 06	0.24 - 0.26	1.24 - 1.33	0.422E 07
0.180E 08	0.85000	0.771E 06 - 0.835E 06	0.26 - 0.28	1.33 - 1.44	0.426E 07
0.179E 08	0.90000	0.835E 06 - 0.924E 06	0.28 - 0.31	1.44 - 1.59	0.432E 07
0.180E 08	0.95000	0.924E 06 - 0.107E 07	0.31 - 0.36	1.59 - 1.85	0.443E 07
0.718E 07	0.97000	0.107E 07 - 0.119E 07	0.36 - 0.40	1.85 - 2.05	0.452E 07
0.718E 07	0.99000	0.119E 07 - 0.143E 07	0.40 - 0.48	2.05 - 2.46	0.471E 07
0.323E 07	0.99900	0.143E 07 - 0.191E 07	0.48 - 0.64	2.46 - 3.29	0.501E 07
0.323E 06	0.99990	0.191E 07 - 0.299E 07	0.64 - 1.01	3.29 - 5.16	0.354E 07

TOTAL CYCLES = 0.359E 09

ROOT MEAN CUBED IS 0.712E 06 AVERAGE MEAN IS 0.410E 07

TABLE H-36
CUMMULATIVE FATIGUE HISTOGRAM OUTPUT

0.400R BLADE MZ

NO. CYCLES IN 30 YEARS (TYPES 1+2)	CUM PROB	HALF-RANGE FATIGUE LOADS: LOAD LEVELS	NORMALIZED LOAD LEVELS	LOAD/50% AT RATED	MID-RANGE MEAN
0.180E 08	0.05000	0. - 0.164E 07	0. - 0.77	0. - 0.94	-0.527E 06
0.180E 08	0.10000	0.164E 07 - 0.167E 07	0.77 - 0.78	0.94 - 0.96	-0.545E 06
0.180E 08	0.15000	0.167E 07 - 0.169E 07	0.78 - 0.79	0.96 - 0.97	-0.551E 06
0.179E 08	0.20000	0.169E 07 - 0.171E 07	0.79 - 0.80	0.97 - 0.98	-0.552E 06
0.180E 08	0.25000	0.171E 07 - 0.172E 07	0.80 - 0.81	0.98 - 0.99	-0.550E 06
0.180E 08	0.30000	0.172E 07 - 0.174E 07	0.81 - 0.82	0.99 - 1.00	-0.546E 06
0.180E 08	0.35000	0.174E 07 - 0.175E 07	0.82 - 0.82	1.00 - 1.01	-0.541E 06
0.179E 08	0.40000	0.175E 07 - 0.176E 07	0.82 - 0.83	1.01 - 1.02	-0.534E 06
0.180E 08	0.45000	0.176E 07 - 0.178E 07	0.83 - 0.83	1.02 - 1.02	-0.526E 06
0.180E 08	0.50000	0.178E 07 - 0.179E 07	0.83 - 0.84	1.02 - 1.03	-0.517E 06
0.179E 08	0.55000	0.179E 07 - 0.180E 07	0.84 - 0.84	1.03 - 1.04	-0.510E 06
0.180E 08	0.60000	0.180E 07 - 0.181E 07	0.84 - 0.85	1.04 - 1.04	-0.503E 06
0.179E 08	0.65000	0.181E 07 - 0.182E 07	0.85 - 0.86	1.04 - 1.05	-0.496E 06
0.180E 08	0.70000	0.182E 07 - 0.184E 07	0.86 - 0.86	1.05 - 1.06	-0.501E 06
0.179E 08	0.75000	0.184E 07 - 0.185E 07	0.86 - 0.87	1.06 - 1.07	-0.516E 06
0.179E 08	0.80000	0.185E 07 - 0.187E 07	0.87 - 0.88	1.07 - 1.08	-0.529E 06
0.180E 08	0.85000	0.187E 07 - 0.189E 07	0.88 - 0.89	1.08 - 1.09	-0.526E 06
0.179E 08	0.90000	0.189E 07 - 0.192E 07	0.89 - 0.90	1.09 - 1.10	-0.526E 06
0.180E 08	0.95000	0.192E 07 - 0.196E 07	0.90 - 0.92	1.10 - 1.13	-0.529E 06
0.718E 07	0.97000	0.196E 07 - 0.198E 07	0.92 - 0.93	1.13 - 1.14	-0.533E 06
0.718E 07	0.99000	0.198E 07 - 0.204E 07	0.93 - 0.96	1.14 - 1.17	-0.533E 06
0.323E 07	0.99900	0.204E 07 - 0.212E 07	0.96 - 0.99	1.17 - 1.22	-0.527E 06
0.323E 06	0.99990	0.212E 07 - 0.227E 07	0.99 - 1.07	1.22 - 1.31	-0.993E 06

TOTAL CYCLES = 0.359E 09

ROOT MEAN CUBED IS 0.178E 07 AVERAGE MEAN IS -0.528E 06

TABLE H-37
CUMMULATIVE FATIGUE HISTOGRAM OUTPUT

0.500R BLADE VX

NO. CYCLES IN 30 YEARS (TYPES 1+2)	CUM PROB	HALF-RANGE FATIGUE LOADS: LOAD LEVELS	NORMALIZED LOAD LEVELS	LOAD/50% AT RATED	MID-RANGE MEAN
0.180E 08	0.05000	0. - 0.316E 05	0. - 0.75	0. - 0.95	0.379E 06
0.180E 08	0.10000	0.316E 05 - 0.322E 05	0.75 - 0.76	0.95 - 0.96	0.375E 06
0.180E 08	0.15000	0.322E 05 - 0.326E 05	0.76 - 0.77	0.96 - 0.98	0.369E 06
0.179E 08	0.20000	0.326E 05 - 0.329E 05	0.77 - 0.78	0.98 - 0.99	0.361E 06
0.180E 08	0.25000	0.329E 05 - 0.332E 05	0.78 - 0.78	0.99 - 0.99	0.353E 06
0.180E 08	0.30000	0.332E 05 - 0.334E 05	0.78 - 0.79	0.99 - 1.00	0.344E 06
0.180E 08	0.35000	0.334E 05 - 0.337E 05	0.79 - 0.80	1.00 - 1.01	0.333E 06
0.179E 08	0.40000	0.337E 05 - 0.339E 05	0.80 - 0.80	1.01 - 1.02	0.322E 06
0.180E 08	0.45000	0.339E 05 - 0.341E 05	0.80 - 0.81	1.02 - 1.02	0.313E 06
0.180E 08	0.50000	0.341E 05 - 0.343E 05	0.81 - 0.81	1.02 - 1.03	0.306E 06
0.179E 08	0.55000	0.343E 05 - 0.346E 05	0.81 - 0.82	1.03 - 1.04	0.298E 06
0.180E 08	0.60000	0.346E 05 - 0.348E 05	0.82 - 0.82	1.04 - 1.04	0.288E 06
0.179E 08	0.65000	0.348E 05 - 0.351E 05	0.82 - 0.83	1.04 - 1.05	0.278E 06
0.180E 08	0.70000	0.351E 05 - 0.354E 05	0.83 - 0.84	1.05 - 1.06	0.270E 06
0.179E 08	0.75000	0.354E 05 - 0.357E 05	0.84 - 0.84	1.06 - 1.07	0.262E 06
0.179E 08	0.80000	0.357E 05 - 0.360E 05	0.84 - 0.85	1.07 - 1.08	0.255E 06
0.180E 08	0.85000	0.360E 05 - 0.363E 05	0.85 - 0.86	1.08 - 1.09	0.249E 06
0.179E 08	0.90000	0.363E 05 - 0.367E 05	0.86 - 0.87	1.09 - 1.10	0.245E 06
0.180E 08	0.95000	0.367E 05 - 0.374E 05	0.87 - 0.88	1.10 - 1.12	0.242E 06
0.718E 07	0.97000	0.374E 05 - 0.378E 05	0.88 - 0.89	1.12 - 1.13	0.239E 06
0.718E 07	0.99000	0.378E 05 - 0.385E 05	0.89 - 0.91	1.13 - 1.15	0.237E 06
0.323E 07	0.99900	0.385E 05 - 0.399E 05	0.91 - 0.94	1.15 - 1.20	0.238E 06
0.323E 06	0.99990	0.399E 05 - 0.423E 05	0.94 - 1.00	1.20 - 1.27	0.335E 06

TOTAL CYCLES = 0.359E 09

ROOT MEAN CUBED IS 0.341E 05 AVERAGE MEAN IS 0.304E 06

TABLE H-38
CUMMULATIVE FATIGUE HISTOGRAM OUTPUT

0.500R BLADE VY

NO. CYCLES IN 30 YEARS (TYPES 1+2)	CUM PROB	HALF-RANGE FATIGUE LOADS: LOAD LEVELS	NORMALIZED LOAD LEVELS	LOAD/50% AT RATED	MID-RANGE MEAN
0.180E 08	0.05000	0. - 0.374E 05	0. - 0.71	0. - 0.91	0.263E 04
0.180E 08	0.10000	0.374E 05 - 0.380E 05	0.71 - 0.72	0.91 - 0.93	0.254E 04
0.180E 08	0.15000	0.380E 05 - 0.385E 05	0.72 - 0.73	0.93 - 0.94	0.252E 04
0.179E 08	0.20000	0.385E 05 - 0.389E 05	0.73 - 0.74	0.94 - 0.95	0.253E 04
0.180E 08	0.25000	0.389E 05 - 0.392E 05	0.74 - 0.74	0.95 - 0.96	0.255E 04
0.180E 08	0.30000	0.392E 05 - 0.395E 05	0.74 - 0.75	0.96 - 0.96	0.259E 04
0.180E 08	0.35000	0.395E 05 - 0.397E 05	0.75 - 0.75	0.96 - 0.97	0.263E 04
0.179E 08	0.40000	0.397E 05 - 0.400E 05	0.75 - 0.76	0.97 - 0.98	0.268E 04
0.180E 08	0.45000	0.400E 05 - 0.402E 05	0.76 - 0.76	0.98 - 0.98	0.274E 04
0.180E 08	0.50000	0.402E 05 - 0.405E 05	0.76 - 0.77	0.98 - 0.99	0.279E 04
0.179E 08	0.55000	0.405E 05 - 0.408E 05	0.77 - 0.77	0.99 - 0.99	0.281E 04
0.180E 08	0.60000	0.408E 05 - 0.410E 05	0.77 - 0.78	0.99 - 1.00	0.280E 04
0.179E 08	0.65000	0.410E 05 - 0.413E 05	0.78 - 0.78	1.00 - 1.01	0.278E 04
0.180E 08	0.70000	0.413E 05 - 0.416E 05	0.78 - 0.79	1.01 - 1.01	0.274E 04
0.179E 08	0.75000	0.416E 05 - 0.419E 05	0.79 - 0.79	1.01 - 1.02	0.270E 04
0.179E 08	0.80000	0.419E 05 - 0.422E 05	0.79 - 0.80	1.02 - 1.03	0.267E 04
0.180E 08	0.85000	0.422E 05 - 0.427E 05	0.80 - 0.81	1.03 - 1.04	0.263E 04
0.179E 08	0.90000	0.427E 05 - 0.433E 05	0.81 - 0.82	1.04 - 1.06	0.262E 04
0.180E 08	0.95000	0.433E 05 - 0.441E 05	0.82 - 0.83	1.06 - 1.07	0.271E 04
0.718E 07	0.97000	0.441E 05 - 0.446E 05	0.83 - 0.84	1.07 - 1.09	0.276E 04
0.718E 07	0.99000	0.446E 05 - 0.458E 05	0.84 - 0.87	1.09 - 1.12	0.280E 04
0.323E 07	0.99900	0.458E 05 - 0.475E 05	0.87 - 0.90	1.12 - 1.16	0.300E 04
0.323E 06	0.99990	0.475E 05 - 0.533E 05	0.90 - 1.01	1.16 - 1.30	-0.317E 04

TOTAL CYCLES = 0.359E 09

ROOT MEAN CUBED IS 0.403E 05 AVERAGE MEAN IS 0.267E 04

TABLE H-39
CUMMULATIVE FATIGUE HISTOGRAM OUTPUT

0.500R BLADE VZ

NO. CYCLES IN 30 YEARS (TYPES 1+2)	CUM PROB	HALF-RANGE FATIGUE LOADS: LOAD LEVELS	NORMALIZED LOAD LEVELS	LOAD/50% AT RATED	MID-RANGE MEAN
0.180E 08	0.05000	0. - 0.421E 04	0. - 0.08	0. - 0.46	-0.514E 05
0.180E 08	0.10000	0.421E 04 - 0.484E 04	0.08 - 0.09	0.46 - 0.53	-0.530E 05
0.180E 08	0.15000	0.484E 04 - 0.533E 04	0.09 - 0.10	0.53 - 0.58	-0.542E 05
0.179E 08	0.20000	0.533E 04 - 0.575E 04	0.10 - 0.11	0.58 - 0.63	-0.553E 05
0.180E 08	0.25000	0.575E 04 - 0.614E 04	0.11 - 0.11	0.63 - 0.67	-0.562E 05
0.180E 08	0.30000	0.614E 04 - 0.652E 04	0.11 - 0.12	0.67 - 0.71	-0.570E 05
0.180E 08	0.35000	0.652E 04 - 0.689E 04	0.12 - 0.13	0.71 - 0.75	-0.578E 05
0.179E 08	0.40000	0.689E 04 - 0.727E 04	0.13 - 0.13	0.75 - 0.80	-0.586E 05
0.180E 08	0.45000	0.727E 04 - 0.766E 04	0.13 - 0.14	0.80 - 0.84	-0.594E 05
0.180E 08	0.50000	0.766E 04 - 0.806E 04	0.14 - 0.15	0.84 - 0.88	-0.600E 05
0.179E 08	0.55000	0.806E 04 - 0.848E 04	0.15 - 0.16	0.88 - 0.93	-0.605E 05
0.180E 08	0.60000	0.848E 04 - 0.894E 04	0.16 - 0.16	0.93 - 0.98	-0.612E 05
0.179E 08	0.65000	0.894E 04 - 0.943E 04	0.16 - 0.17	0.98 - 1.03	-0.618E 05
0.180E 08	0.70000	0.943E 04 - 0.998E 04	0.17 - 0.18	1.03 - 1.09	-0.625E 05
0.179E 08	0.75000	0.998E 04 - 0.106E 05	0.18 - 0.20	1.09 - 1.16	-0.632E 05
0.179E 08	0.80000	0.106E 05 - 0.114E 05	0.20 - 0.21	1.16 - 1.25	-0.638E 05
0.180E 08	0.85000	0.114E 05 - 0.123E 05	0.21 - 0.23	1.25 - 1.35	-0.642E 05
0.179E 08	0.90000	0.123E 05 - 0.136E 05	0.23 - 0.25	1.35 - 1.50	-0.653E 05
0.180E 08	0.95000	0.136E 05 - 0.158E 05	0.25 - 0.29	1.50 - 1.73	-0.681E 05
0.718E 07	0.97000	0.158E 05 - 0.174E 05	0.29 - 0.32	1.73 - 1.90	-0.699E 05
0.718E 07	0.99000	0.174E 05 - 0.206E 05	0.32 - 0.38	1.90 - 2.25	-0.729E 05
0.323E 07	0.99900	0.206E 05 - 0.269E 05	0.38 - 0.49	2.25 - 2.94	-0.778E 05
0.323E 06	0.99990	0.269E 05 - 0.549E 05	0.49 - 1.01	2.94 - 6.02	-0.526E 05

TOTAL CYCLES = 0.359E 09

ROOT MEAN CUBED IS 0.105E 05 AVERAGE MEAN IS -0.603E 05

TABLE H-40
CUMMULATIVE FATIGUE HISTOGRAM OUTPUT

0.500R BLADE MX

NO. CYCLES IN 30 YEARS (TYPES 1+2)	CUM PROB	HALF-RANGE FATIGUE LOADS: LOAD LEVELS	NORMALIZED LOAD LEVELS	LOAD/50% AT RATED	MID-RANGE MEAN
0.180E 08	0.05000	0. - 0.159E 05	0. - 0.43	0. - 0.55	-0.745E 05
0.180E 08	0.10000	0.159E 05 - 0.166E 05	0.43 - 0.44	0.55 - 0.57	-0.743E 05
0.180E 08	0.15000	0.166E 05 - 0.175E 05	0.44 - 0.47	0.57 - 0.60	-0.743E 05
0.179E 08	0.20000	0.175E 05 - 0.182E 05	0.47 - 0.49	0.60 - 0.63	-0.740E 05
0.180E 08	0.25000	0.182E 05 - 0.189E 05	0.49 - 0.51	0.63 - 0.65	-0.737E 05
0.180E 08	0.30000	0.189E 05 - 0.204E 05	0.51 - 0.55	0.65 - 0.70	-0.723E 05
0.180E 08	0.35000	0.204E 05 - 0.211E 05	0.55 - 0.57	0.70 - 0.73	-0.717E 05
0.179E 08	0.40000	0.211E 05 - 0.218E 05	0.57 - 0.58	0.73 - 0.75	-0.724E 05
0.180E 08	0.45000	0.218E 05 - 0.224E 05	0.58 - 0.60	0.75 - 0.77	-0.739E 05
0.180E 08	0.50000	0.224E 05 - 0.231E 05	0.60 - 0.62	0.77 - 0.80	-0.759E 05
0.179E 08	0.55000	0.231E 05 - 0.238E 05	0.62 - 0.64	0.80 - 0.82	-0.784E 05
0.180E 08	0.60000	0.238E 05 - 0.247E 05	0.64 - 0.66	0.82 - 0.85	-0.815E 05
0.179E 08	0.65000	0.247E 05 - 0.255E 05	0.66 - 0.68	0.85 - 0.88	-0.847E 05
0.180E 08	0.70000	0.255E 05 - 0.263E 05	0.68 - 0.70	0.88 - 0.91	-0.876E 05
0.179E 08	0.75000	0.263E 05 - 0.272E 05	0.70 - 0.73	0.91 - 0.94	-0.903E 05
0.179E 08	0.80000	0.272E 05 - 0.282E 05	0.73 - 0.75	0.94 - 0.97	-0.928E 05
0.180E 08	0.85000	0.282E 05 - 0.292E 05	0.75 - 0.78	0.97 - 1.01	-0.947E 05
0.179E 08	0.90000	0.292E 05 - 0.305E 05	0.78 - 0.82	1.01 - 1.05	-0.961E 05
0.180E 08	0.95000	0.305E 05 - 0.321E 05	0.82 - 0.86	1.05 - 1.11	-0.959E 05
0.718E 07	0.97000	0.321E 05 - 0.330E 05	0.86 - 0.88	1.11 - 1.14	-0.954E 05
0.718E 07	0.99000	0.330E 05 - 0.348E 05	0.88 - 0.93	1.14 - 1.20	-0.950E 05
0.323E 07	0.99900	0.348E 05 - 0.374E 05	0.93 - 1.00	1.20 - 1.29	-0.947E 05
0.323E 06	0.99990	0.374E 05 - 0.373E 05	1.00 - 1.00	1.29 - 1.29	-0.903E 05

TOTAL CYCLES = 0.359E 09

ROOT MEAN CUBED IS 0.244E 05 AVERAGE MEAN IS -0.825E 05

TABLE H-41
CUMMULATIVE FATIGUE HISTOGRAM OUTPUT

0.500R BLADE MY

NO. CYCLES IN 30 YEARS (TYPES 1+2)	CUM PROB	HALF-RANGE FATIGUE LOADS: LOAD LEVELS	NORMALIZED LOAD LEVELS	LOAD/50% AT RATED	MID-RANGE MEAN
0.180E 08	0.05000	0. - 0.195E 06	0. - 0.08	0. - 0.43	0.248E 07
0.180E 08	0.10000	0.195E 06 - 0.226E 06	0.08 - 0.09	0.43 - 0.50	0.254E 07
0.180E 08	0.15000	0.226E 06 - 0.250E 06	0.09 - 0.10	0.50 - 0.55	0.260E 07
0.179E 08	0.20000	0.250E 06 - 0.271E 06	0.10 - 0.11	0.55 - 0.60	0.264E 07
0.180E 08	0.25000	0.271E 06 - 0.290E 06	0.11 - 0.12	0.60 - 0.64	0.268E 07
0.180E 08	0.30000	0.290E 06 - 0.310E 06	0.12 - 0.12	0.64 - 0.68	0.272E 07
0.180E 08	0.35000	0.310E 06 - 0.329E 06	0.12 - 0.13	0.68 - 0.73	0.275E 07
0.179E 08	0.40000	0.329E 06 - 0.348E 06	0.13 - 0.14	0.73 - 0.77	0.279E 07
0.180E 08	0.45000	0.348E 06 - 0.368E 06	0.14 - 0.15	0.77 - 0.81	0.282E 07
0.180E 08	0.50000	0.368E 06 - 0.388E 06	0.15 - 0.16	0.81 - 0.86	0.285E 07
0.179E 08	0.55000	0.388E 06 - 0.410E 06	0.16 - 0.16	0.86 - 0.91	0.288E 07
0.180E 08	0.60000	0.410E 06 - 0.433E 06	0.16 - 0.17	0.91 - 0.96	0.291E 07
0.179E 08	0.65000	0.433E 06 - 0.459E 06	0.17 - 0.18	0.96 - 1.02	0.294E 07
0.180E 08	0.70000	0.459E 06 - 0.488E 06	0.18 - 0.19	1.02 - 1.08	0.297E 07
0.179E 08	0.75000	0.488E 06 - 0.521E 06	0.19 - 0.21	1.08 - 1.15	0.300E 07
0.179E 08	0.80000	0.521E 06 - 0.560E 06	0.21 - 0.22	1.15 - 1.24	0.303E 07
0.180E 08	0.85000	0.560E 06 - 0.611E 06	0.22 - 0.24	1.24 - 1.35	0.306E 07
0.179E 08	0.90000	0.611E 06 - 0.680E 06	0.24 - 0.27	1.35 - 1.50	0.309E 07
0.180E 08	0.95000	0.680E 06 - 0.797E 06	0.27 - 0.32	1.50 - 1.76	0.318E 07
0.718E 07	0.97000	0.797E 06 - 0.886E 06	0.32 - 0.35	1.76 - 1.96	0.324E 07
0.718E 07	0.99000	0.886E 06 - 0.108E 07	0.35 - 0.43	1.96 - 2.39	0.329E 07
0.323E 07	0.99900	0.108E 07 - 0.150E 07	0.43 - 0.60	2.39 - 3.32	0.334E 07
0.323E 06	0.99990	0.150E 07 - 0.251E 07	0.60 - 1.00	3.32 - 5.56	0.155E 07

TOTAL CYCLES = 0.359E 09

ROOT MEAN CUBED IS 0.526E 06 AVERAGE MEAN IS 0.286E 07

TABLE H-42
CUMMULATIVE FATIGUE HISTOGRAM OUTPUT

0.500R BLADE MZ

NO. CYCLES IN 30 YEARS (TYPES 1+2)	CUM PROB	HALF-RANGE FATIGUE LOADS: LOAD LEVELS	NORMALIZED LOAD LEVELS	LOAD/50% AT RATED	MID-RANGE MEAN
0.180E 08	0.05000	0. - 0.952E 06	0. - 0.72	0. - 0.88	-0.484E 06
0.180E 08	0.10000	0.952E 06 - 0.967E 06	0.72 - 0.73	0.88 - 0.90	-0.490E 06
0.180E 08	0.15000	0.967E 06 - 0.979E 06	0.73 - 0.74	0.90 - 0.91	-0.491E 06
0.179E 08	0.20000	0.979E 06 - 0.989E 06	0.74 - 0.75	0.91 - 0.92	-0.489E 06
0.180E 08	0.25000	0.989E 06 - 0.998E 06	0.75 - 0.76	0.92 - 0.92	-0.486E 06
0.180E 08	0.30000	0.998E 06 - 0.101E 07	0.76 - 0.76	0.92 - 0.93	-0.482E 06
0.180E 08	0.35000	0.101E 07 - 0.101E 07	0.76 - 0.77	0.93 - 0.94	-0.477E 06
0.179E 08	0.40000	0.101E 07 - 0.102E 07	0.77 - 0.77	0.94 - 0.95	-0.471E 06
0.180E 08	0.45000	0.102E 07 - 0.103E 07	0.77 - 0.78	0.95 - 0.95	-0.464E 06
0.180E 08	0.50000	0.103E 07 - 0.103E 07	0.78 - 0.78	0.95 - 0.96	-0.457E 06
0.179E 08	0.55000	0.103E 07 - 0.104E 07	0.78 - 0.79	0.96 - 0.96	-0.451E 06
0.180E 08	0.60000	0.104E 07 - 0.105E 07	0.79 - 0.79	0.96 - 0.97	-0.443E 06
0.179E 08	0.65000	0.105E 07 - 0.105E 07	0.79 - 0.80	0.97 - 0.98	-0.435E 06
0.180E 08	0.70000	0.105E 07 - 0.106E 07	0.80 - 0.80	0.98 - 0.98	-0.438E 06
0.179E 08	0.75000	0.106E 07 - 0.107E 07	0.80 - 0.81	0.98 - 0.99	-0.444E 06
0.179E 08	0.80000	0.107E 07 - 0.108E 07	0.81 - 0.82	0.99 - 1.00	-0.451E 06
0.180E 08	0.85000	0.108E 07 - 0.109E 07	0.82 - 0.82	1.00 - 1.01	-0.449E 06
0.179E 08	0.90000	0.109E 07 - 0.110E 07	0.82 - 0.83	1.01 - 1.02	-0.448E 06
0.180E 08	0.95000	0.110E 07 - 0.113E 07	0.83 - 0.85	1.02 - 1.04	-0.444E 06
0.718E 07	0.97000	0.113E 07 - 0.114E 07	0.85 - 0.86	1.04 - 1.06	-0.443E 06
0.718E 07	0.99000	0.114E 07 - 0.117E 07	0.86 - 0.89	1.06 - 1.08	-0.444E 06
0.323E 07	0.99900	0.117E 07 - 0.122E 07	0.89 - 0.92	1.08 - 1.13	-0.457E 06
0.323E 06	0.99990	0.122E 07 - 0.131E 07	0.92 - 0.99	1.13 - 1.21	-0.827E 06

TOTAL CYCLES = 0.359E 09

ROOT MEAN CUBED IS 0.103E 07 AVERAGE MEAN IS -0.462E 06

TABLE H-43
CUMMULATIVE FATIGUE HISTOGRAM OUTPUT

0.600R BLADE VX

NO. CYCLES IN 30 YEARS (TYPES 1+2)	CUM PROB	HALF-RANGE FATIGUE LOADS: LOAD LEVELS	HALF-RANGE FATIGUE LOADS: NORMALIZED LOAD LEVELS	HALF-RANGE FATIGUE LOADS: LOAD/50% AT RATED	MID-RANGE: MEAN
0.180E 08	0.05000	0. - 0.196E 05	0. - 0.72	0. - 0.95	0.267E 06
0.180E 08	0.10000	0.196E 05 - 0.200E 05	0.72 - 0.73	0.95 - 0.97	0.266E 06
0.180E 08	0.15000	0.200E 05 - 0.203E 05	0.73 - 0.74	0.97 - 0.98	0.263E 06
0.179E 08	0.20000	0.203E 05 - 0.205E 05	0.74 - 0.75	0.98 - 0.99	0.260E 06
0.180E 08	0.25000	0.205E 05 - 0.207E 05	0.75 - 0.76	0.99 - 1.00	0.257E 06
0.180E 08	0.30000	0.207E 05 - 0.210E 05	0.76 - 0.76	1.00 - 1.01	0.253E 06
0.180E 08	0.35000	0.210E 05 - 0.212E 05	0.76 - 0.77	1.01 - 1.03	0.248E 06
0.179E 08	0.40000	0.212E 05 - 0.214E 05	0.77 - 0.78	1.03 - 1.04	0.242E 06
0.180E 08	0.45000	0.214E 05 - 0.217E 05	0.78 - 0.79	1.04 - 1.05	0.230E 06
0.180E 08	0.50000	0.217E 05 - 0.220E 05	0.79 - 0.80	1.05 - 1.07	0.212E 06
0.179E 08	0.55000	0.220E 05 - 0.222E 05	0.80 - 0.81	1.07 - 1.08	0.200E 06
0.180E 08	0.60000	0.222E 05 - 0.225E 05	0.81 - 0.82	1.08 - 1.09	0.190E 06
0.179E 08	0.65000	0.225E 05 - 0.227E 05	0.82 - 0.83	1.09 - 1.10	0.184E 06
0.180E 08	0.70000	0.227E 05 - 0.229E 05	0.83 - 0.83	1.10 - 1.11	0.179E 06
0.179E 08	0.75000	0.229E 05 - 0.231E 05	0.83 - 0.84	1.11 - 1.12	0.176E 06
0.179E 08	0.80000	0.231E 05 - 0.233E 05	0.84 - 0.85	1.12 - 1.13	0.173E 06
0.180E 08	0.85000	0.233E 05 - 0.235E 05	0.85 - 0.86	1.13 - 1.14	0.171E 06
0.179E 08	0.90000	0.235E 05 - 0.238E 05	0.86 - 0.87	1.14 - 1.15	0.170E 06
0.180E 08	0.95000	0.238E 05 - 0.242E 05	0.87 - 0.88	1.15 - 1.17	0.169E 06
0.718E 07	0.97000	0.242E 05 - 0.245E 05	0.88 - 0.89	1.17 - 1.18	0.168E 06
0.718E 07	0.99000	0.245E 05 - 0.250E 05	0.89 - 0.91	1.18 - 1.21	0.168E 06
0.323E 07	0.99900	0.250E 05 - 0.257E 05	0.91 - 0.94	1.21 - 1.24	0.170E 06
0.323E 06	0.99990	0.257E 05 - 0.274E 05	0.94 - 1.00	1.24 - 1.33	0.202E 06

TOTAL CYCLES = 0.359E 09

ROOT MEAN CUBED IS 0.218E 05 AVERAGE MEAN IS 0.214E 06

TABLE H-44
CUMMULATIVE FATIGUE HISTOGRAM OUTPUT

0.600R BLADE VY

NO. CYCLES IN 30 YEARS (TYPES 1+2)	CUM PROB	HALF-RANGE FATIGUE LOADS: LOAD LEVELS	HALF-RANGE FATIGUE LOADS: NORMALIZED LOAD LEVELS	HALF-RANGE FATIGUE LOADS: LOAD/50% AT RATED	MID-RANGE: MEAN
0.180E 08	0.05000	0. - 0.243E 05	0. - 0.64	0. - 0.90	0.147E 04
0.180E 08	0.10000	0.243E 05 - 0.249E 05	0.64 - 0.66	0.90 - 0.92	0.148E 04
0.180E 08	0.15000	0.249E 05 - 0.252E 05	0.66 - 0.67	0.92 - 0.94	0.150E 04
0.179E 08	0.20000	0.252E 05 - 0.256E 05	0.67 - 0.68	0.94 - 0.95	0.152E 04
0.180E 08	0.25000	0.256E 05 - 0.258E 05	0.68 - 0.68	0.95 - 0.96	0.156E 04
0.180E 08	0.30000	0.258E 05 - 0.261E 05	0.68 - 0.69	0.96 - 0.97	0.159E 04
0.180E 08	0.35000	0.261E 05 - 0.263E 05	0.69 - 0.70	0.97 - 0.98	0.163E 04
0.179E 08	0.40000	0.263E 05 - 0.265E 05	0.70 - 0.70	0.98 - 0.98	0.167E 04
0.180E 08	0.45000	0.265E 05 - 0.267E 05	0.70 - 0.71	0.98 - 0.99	0.171E 04
0.180E 08	0.50000	0.267E 05 - 0.270E 05	0.71 - 0.71	0.99 - 1.00	0.175E 04
0.179E 08	0.55000	0.270E 05 - 0.272E 05	0.71 - 0.72	1.00 - 1.01	0.177E 04
0.180E 08	0.60000	0.272E 05 - 0.274E 05	0.72 - 0.72	1.01 - 1.02	0.180E 04
0.179E 08	0.65000	0.274E 05 - 0.276E 05	0.72 - 0.73	1.02 - 1.02	0.183E 04
0.180E 08	0.70000	0.276E 05 - 0.278E 05	0.73 - 0.74	1.02 - 1.03	0.185E 04
0.179E 08	0.75000	0.278E 05 - 0.281E 05	0.74 - 0.74	1.03 - 1.04	0.186E 04
0.179E 08	0.80000	0.281E 05 - 0.283E 05	0.74 - 0.75	1.04 - 1.05	0.183E 04
0.180E 08	0.85000	0.283E 05 - 0.287E 05	0.75 - 0.76	1.05 - 1.06	0.179E 04
0.179E 08	0.90000	0.287E 05 - 0.291E 05	0.76 - 0.77	1.06 - 1.08	0.183E 04
0.180E 08	0.95000	0.291E 05 - 0.298E 05	0.77 - 0.79	1.08 - 1.11	0.193E 04
0.718E 07	0.97000	0.298E 05 - 0.303E 05	0.79 - 0.80	1.11 - 1.12	0.197E 04
0.718E 07	0.99000	0.303E 05 - 0.311E 05	0.80 - 0.82	1.12 - 1.15	0.202E 04
0.323E 07	0.99900	0.311E 05 - 0.325E 05	0.82 - 0.86	1.15 - 1.21	0.210E 04
0.323E 06	0.99990	0.325E 05 - 0.379E 05	0.86 - 1.00	1.21 - 1.41	0.217E 03

TOTAL CYCLES = 0.359E 09

ROOT MEAN CUBED IS 0.268E 05 AVERAGE MEAN IS 0.172E 04

TABLE H-45
CUMMULATIVE FATIGUE HISTOGRAM OUTPUT

0.600R BLADE VZ

NO. CYCLES IN 30 YEARS (TYPES 1+2)	CUM PROB	HALF-RANGE FATIGUE LOADS: LOAD LEVELS	NORMALIZED LOAD LEVELS	LOAD/50% AT RATED	MID-RANGE MEAN
0.180E 08	0.05000	0. - 0.356E 04	0. - 0.10	0. - 0.43	-0.406E 05
0.180E 08	0.10000	0.356E 04 - 0.413E 04	0.10 - 0.11	0.43 - 0.49	-0.420E 05
0.180E 08	0.15000	0.413E 04 - 0.456E 04	0.11 - 0.13	0.49 - 0.54	-0.429E 05
0.179E 08	0.20000	0.456E 04 - 0.494E 04	0.13 - 0.14	0.54 - 0.59	-0.437E 05
0.180E 08	0.25000	0.494E 04 - 0.530E 04	0.14 - 0.15	0.59 - 0.63	-0.445E 05
0.180E 08	0.30000	0.530E 04 - 0.564E 04	0.15 - 0.16	0.63 - 0.67	-0.451E 05
0.180E 08	0.35000	0.564E 04 - 0.598E 04	0.16 - 0.17	0.67 - 0.71	-0.458E 05
0.179E 08	0.40000	0.598E 04 - 0.632E 04	0.17 - 0.17	0.71 - 0.75	-0.464E 05
0.180E 08	0.45000	0.632E 04 - 0.667E 04	0.17 - 0.18	0.75 - 0.80	-0.470E 05
0.180E 08	0.50000	0.667E 04 - 0.703E 04	0.18 - 0.19	0.80 - 0.84	-0.474E 05
0.179E 08	0.55000	0.703E 04 - 0.741E 04	0.19 - 0.20	0.84 - 0.88	-0.478E 05
0.180E 08	0.60000	0.741E 04 - 0.782E 04	0.20 - 0.22	0.88 - 0.93	-0.483E 05
0.179E 08	0.65000	0.782E 04 - 0.826E 04	0.22 - 0.23	0.93 - 0.99	-0.488E 05
0.180E 08	0.70000	0.826E 04 - 0.875E 04	0.23 - 0.24	0.99 - 1.04	-0.493E 05
0.179E 08	0.75000	0.875E 04 - 0.931E 04	0.24 - 0.26	1.04 - 1.11	-0.498E 05
0.179E 08	0.80000	0.931E 04 - 0.998E 04	0.26 - 0.28	1.11 - 1.19	-0.503E 05
0.180E 08	0.85000	0.998E 04 - 0.108E 05	0.28 - 0.30	1.19 - 1.29	-0.510E 05
0.179E 08	0.90000	0.108E 05 - 0.120E 05	0.30 - 0.33	1.29 - 1.43	-0.519E 05
0.180E 08	0.95000	0.120E 05 - 0.138E 05	0.33 - 0.38	1.43 - 1.65	-0.537E 05
0.718E 07	0.97000	0.138E 05 - 0.152E 05	0.38 - 0.42	1.65 - 1.81	-0.547E 05
0.718E 07	0.99000	0.152E 05 - 0.181E 05	0.42 - 0.50	1.81 - 2.16	-0.562E 05
0.323E 07	0.99900	0.181E 05 - 0.243E 05	0.50 - 0.67	2.16 - 2.90	-0.586E 05
0.323E 06	0.99990	0.243E 05 - 0.363E 05	0.67 - 1.00	2.90 - 4.33	-0.571E 05

TOTAL CYCLES = 0.359E 09

ROOT MEAN CUBED IS 0.913E 04 AVERAGE MEAN IS -0.476E 05

TABLE H-46
CUMMULATIVE FATIGUE HISTOGRAM OUTPUT

0.600R BLADE MX

NO. CYCLES IN 30 YEARS (TYPES 1+2)	CUM PROB	HALF-RANGE FATIGUE LOADS: LOAD LEVELS	NORMALIZED LOAD LEVELS	LOAD/50% AT RATED	MID-RANGE MEAN
0.180E 08	0.05000	0. - 0.959E 04	0. - 0.30	0. - 0.49	-0.633E 05
0.180E 08	0.10000	0.959E 04 - 0.104E 05	0.30 - 0.33	0.49 - 0.53	-0.634E 05
0.180E 08	0.15000	0.104E 05 - 0.110E 05	0.33 - 0.35	0.53 - 0.56	-0.635E 05
0.179E 08	0.20000	0.110E 05 - 0.115E 05	0.35 - 0.36	0.56 - 0.59	-0.636E 05
0.180E 08	0.25000	0.115E 05 - 0.120E 05	0.36 - 0.38	0.59 - 0.61	-0.638E 05
0.180E 08	0.30000	0.120E 05 - 0.124E 05	0.38 - 0.39	0.61 - 0.63	-0.643E 05
0.180E 08	0.35000	0.124E 05 - 0.129E 05	0.39 - 0.41	0.63 - 0.66	-0.647E 05
0.179E 08	0.40000	0.129E 05 - 0.134E 05	0.41 - 0.42	0.66 - 0.69	-0.655E 05
0.180E 08	0.45000	0.134E 05 - 0.139E 05	0.42 - 0.44	0.69 - 0.71	-0.665E 05
0.180E 08	0.50000	0.139E 05 - 0.144E 05	0.44 - 0.45	0.71 - 0.74	-0.678E 05
0.179E 08	0.55000	0.144E 05 - 0.149E 05	0.45 - 0.47	0.74 - 0.76	-0.691E 05
0.180E 08	0.60000	0.149E 05 - 0.153E 05	0.47 - 0.48	0.76 - 0.79	-0.703E 05
0.179E 08	0.65000	0.153E 05 - 0.158E 05	0.48 - 0.50	0.79 - 0.81	-0.719E 05
0.180E 08	0.70000	0.158E 05 - 0.164E 05	0.50 - 0.52	0.81 - 0.84	-0.739E 05
0.179E 08	0.75000	0.164E 05 - 0.170E 05	0.52 - 0.54	0.84 - 0.87	-0.755E 05
0.179E 08	0.80000	0.170E 05 - 0.177E 05	0.54 - 0.56	0.87 - 0.90	-0.770E 05
0.180E 08	0.85000	0.177E 05 - 0.185E 05	0.56 - 0.58	0.90 - 0.95	-0.782E 05
0.179E 08	0.90000	0.185E 05 - 0.195E 05	0.58 - 0.61	0.95 - 1.00	-0.792E 05
0.180E 08	0.95000	0.195E 05 - 0.210E 05	0.61 - 0.66	1.00 - 1.07	-0.799E 05
0.718E 07	0.97000	0.210E 05 - 0.220E 05	0.66 - 0.69	1.07 - 1.12	-0.799E 05
0.718E 07	0.99000	0.220E 05 - 0.240E 05	0.69 - 0.76	1.12 - 1.23	-0.800E 05
0.323E 07	0.99900	0.240E 05 - 0.275E 05	0.76 - 0.87	1.23 - 1.41	-0.801E 05
0.323E 06	0.99990	0.275E 05 - 0.317E 05	0.87 - 1.00	1.41 - 1.62	-0.844E 05

TOTAL CYCLES = 0.359E 09

ROOT MEAN CUBED IS 0.155E 05 AVERAGE MEAN IS -0.701E 05

TABLE H-47
CUMMULATIVE FATIGUE HISTOGRAM OUTPUT

0.600R BLADE MY

NO. CYCLES IN 30 YEARS (TYPES 1+2)	CUM PROB	HALF-RANGE FATIGUE LOADS: LOAD LEVELS	NORMALIZED LOAD LEVELS	LOAD/50% AT RATED	MID-RANGE MEAN
0.180E 08	0.05000	0. - 0.120E 06	0. - 0.07	0. - 0.36	0.153E 07
0.180E 08	0.10000	0.120E 06 - 0.140E 06	0.07 - 0.08	0.36 - 0.42	0.158E 07
0.180E 08	0.15000	0.140E 06 - 0.155E 06	0.08 - 0.09	0.42 - 0.47	0.162E 07
0.179E 08	0.20000	0.155E 06 - 0.169E 06	0.09 - 0.10	0.47 - 0.51	0.166E 07
0.180E 08	0.25000	0.169E 06 - 0.183E 06	0.10 - 0.11	0.51 - 0.55	0.169E 07
0.180E 08	0.30000	0.183E 06 - 0.195E 06	0.11 - 0.11	0.55 - 0.58	0.173E 07
0.180E 08	0.35000	0.195E 06 - 0.208E 06	0.11 - 0.12	0.58 - 0.62	0.176E 07
0.179E 08	0.40000	0.208E 06 - 0.221E 06	0.12 - 0.13	0.62 - 0.66	0.180E 07
0.180E 08	0.45000	0.221E 06 - 0.235E 06	0.13 - 0.14	0.66 - 0.70	0.183E 07
0.180E 08	0.50000	0.235E 06 - 0.249E 06	0.14 - 0.15	0.70 - 0.74	0.186E 07
0.179E 08	0.55000	0.249E 06 - 0.264E 06	0.15 - 0.16	0.74 - 0.79	0.189E 07
0.180E 08	0.60000	0.264E 06 - 0.280E 06	0.16 - 0.16	0.79 - 0.84	0.192E 07
0.179E 08	0.65000	0.280E 06 - 0.298E 06	0.16 - 0.17	0.84 - 0.89	0.195E 07
0.180E 08	0.70000	0.298E 06 - 0.318E 06	0.17 - 0.19	0.89 - 0.95	0.198E 07
0.179E 08	0.75000	0.318E 06 - 0.342E 06	0.19 - 0.20	0.95 - 1.02	0.200E 07
0.179E 08	0.80000	0.342E 06 - 0.370E 06	0.20 - 0.22	1.02 - 1.11	0.202E 07
0.180E 08	0.85000	0.370E 06 - 0.405E 06	0.22 - 0.24	1.11 - 1.21	0.204E 07
0.179E 08	0.90000	0.405E 06 - 0.455E 06	0.24 - 0.27	1.21 - 1.36	0.206E 07
0.180E 08	0.95000	0.455E 06 - 0.540E 06	0.27 - 0.32	1.36 - 1.62	0.210E 07
0.718E 07	0.97000	0.540E 06 - 0.604E 06	0.32 - 0.36	1.62 - 1.81	0.209E 07
0.718E 07	0.99000	0.604E 06 - 0.753E 06	0.36 - 0.44	1.81 - 2.25	0.202E 07
0.323E 07	0.99900	0.753E 06 - 0.109E 07	0.44 - 0.64	2.25 - 3.27	0.190E 07
0.323E 06	0.99990	0.109E 07 - 0.170E 07	0.64 - 1.00	3.27 - 5.09	0.756E 06

TOTAL CYCLES = 0.359E 09

ROOT MEAN CUBED IS 0.354E 06 AVERAGE MEAN IS 0.185E 07

TABLE H-48
CUMMULATIVE FATIGUE HISTOGRAM OUTPUT

0.600R BLADE MZ

NO. CYCLES IN 30 YEARS (TYPES 1+2)	CUM PROB	HALF-RANGE FATIGUE LOADS: LOAD LEVELS	NORMALIZED LOAD LEVELS	LOAD/50% AT RATED	MID-RANGE MEAN
0.180E 08	0.05000	0. - 0.505E 06	0. - 0.60	0. - 0.84	-0.492E 06
0.180E 08	0.10000	0.505E 06 - 0.515E 06	0.60 - 0.61	0.84 - 0.85	-0.491E 06
0.180E 08	0.15000	0.515E 06 - 0.523E 06	0.61 - 0.62	0.85 - 0.87	-0.490E 06
0.179E 08	0.20000	0.523E 06 - 0.530E 06	0.62 - 0.63	0.87 - 0.88	-0.487E 06
0.180E 08	0.25000	0.530E 06 - 0.536E 06	0.63 - 0.64	0.88 - 0.89	-0.485E 06
0.180E 08	0.30000	0.536E 06 - 0.541E 06	0.64 - 0.64	0.89 - 0.90	-0.482E 06
0.180E 08	0.35000	0.541E 06 - 0.546E 06	0.64 - 0.65	0.90 - 0.90	-0.479E 06
0.179E 08	0.40000	0.546E 06 - 0.550E 06	0.65 - 0.65	0.90 - 0.91	-0.476E 06
0.180E 08	0.45000	0.550E 06 - 0.555E 06	0.65 - 0.66	0.91 - 0.92	-0.473E 06
0.180E 08	0.50000	0.555E 06 - 0.559E 06	0.66 - 0.67	0.92 - 0.93	-0.469E 06
0.179E 08	0.55000	0.559E 06 - 0.564E 06	0.67 - 0.67	0.93 - 0.93	-0.465E 06
0.180E 08	0.60000	0.564E 06 - 0.568E 06	0.67 - 0.68	0.93 - 0.94	-0.460E 06
0.179E 08	0.65000	0.568E 06 - 0.573E 06	0.68 - 0.68	0.94 - 0.95	-0.454E 06
0.180E 08	0.70000	0.573E 06 - 0.577E 06	0.68 - 0.69	0.95 - 0.96	-0.452E 06
0.179E 08	0.75000	0.577E 06 - 0.582E 06	0.69 - 0.69	0.96 - 0.96	-0.453E 06
0.179E 08	0.80000	0.582E 06 - 0.588E 06	0.69 - 0.70	0.96 - 0.97	-0.458E 06
0.180E 08	0.85000	0.588E 06 - 0.595E 06	0.70 - 0.71	0.97 - 0.99	-0.462E 06
0.179E 08	0.90000	0.595E 06 - 0.604E 06	0.71 - 0.72	0.99 - 1.00	-0.462E 06
0.180E 08	0.95000	0.604E 06 - 0.619E 06	0.72 - 0.74	1.00 - 1.03	-0.457E 06
0.718E 07	0.97000	0.619E 06 - 0.628E 06	0.74 - 0.75	1.03 - 1.04	-0.457E 06
0.718E 07	0.99000	0.628E 06 - 0.648E 06	0.75 - 0.77	1.04 - 1.07	-0.462E 06
0.323E 07	0.99900	0.648E 06 - 0.675E 06	0.77 - 0.80	1.07 - 1.12	-0.474E 06
0.323E 06	0.99990	0.675E 06 - 0.774E 06	0.80 - 0.92	1.12 - 1.28	-0.633E 06

TOTAL CYCLES = 0.359E 09

ROOT MEAN CUBED IS 0.557E 06 AVERAGE MEAN IS -0.471E 06

TABLE H-49
CUMMULATIVE FATIGUE HISTOGRAM OUTPUT

0.700R BLADE VX

NO. CYCLES IN 30 YEARS (TYPES 1+2)	CUM PROB	HALF-RANGE FATIGUE LOADS: LOAD LEVELS	NORMALIZED LOAD LEVELS	LOAD/50% AT RATED	MID-RANGE MEAN
0.180E 08	0.05000	0. - 0.109E 05	0. - 0.66	0. - 0.96	0.154E 06
0.180E 08	0.10000	0.109E 05 - 0.111E 05	0.66 - 0.67	0.96 - 0.98	0.154E 06
0.180E 08	0.15000	0.111E 05 - 0.113E 05	0.67 - 0.68	0.98 - 1.00	0.154E 06
0.179E 08	0.20000	0.113E 05 - 0.114E 05	0.68 - 0.69	1.00 - 1.01	0.154E 06
0.180E 08	0.25000	0.114E 05 - 0.116E 05	0.69 - 0.69	1.01 - 1.02	0.155E 06
0.180E 08	0.30000	0.116E 05 - 0.117E 05	0.69 - 0.70	1.02 - 1.03	0.155E 06
0.180E 08	0.35000	0.117E 05 - 0.119E 05	0.70 - 0.71	1.03 - 1.05	0.155E 06
0.179E 08	0.40000	0.119E 05 - 0.121E 05	0.71 - 0.73	1.05 - 1.06	0.151E 06
0.180E 08	0.45000	0.121E 05 - 0.123E 05	0.73 - 0.74	1.06 - 1.09	0.141E 06
0.180E 08	0.50000	0.123E 05 - 0.126E 05	0.74 - 0.75	1.09 - 1.11	0.125E 06
0.179E 08	0.55000	0.126E 05 - 0.128E 05	0.75 - 0.77	1.11 - 1.13	0.111E 06
0.180E 08	0.60000	0.128E 05 - 0.129E 05	0.77 - 0.78	1.13 - 1.14	0.102E 06
0.179E 08	0.65000	0.129E 05 - 0.131E 05	0.78 - 0.79	1.14 - 1.15	0.990E 05
0.180E 08	0.70000	0.131E 05 - 0.132E 05	0.79 - 0.79	1.15 - 1.16	0.979E 05
0.179E 08	0.75000	0.132E 05 - 0.134E 05	0.79 - 0.80	1.16 - 1.18	0.969E 05
0.179E 08	0.80000	0.134E 05 - 0.135E 05	0.80 - 0.81	1.18 - 1.19	0.968E 05
0.180E 08	0.85000	0.135E 05 - 0.137E 05	0.81 - 0.82	1.19 - 1.21	0.980E 05
0.179E 08	0.90000	0.137E 05 - 0.139E 05	0.82 - 0.83	1.21 - 1.22	0.983E 05
0.180E 08	0.95000	0.139E 05 - 0.141E 05	0.83 - 0.85	1.22 - 1.24	0.986E 05
0.718E 07	0.97000	0.141E 05 - 0.143E 05	0.85 - 0.86	1.24 - 1.26	0.987E 05
0.718E 07	0.99000	0.143E 05 - 0.146E 05	0.86 - 0.88	1.26 - 1.29	0.990E 05
0.323E 07	0.99900	0.146E 05 - 0.151E 05	0.88 - 0.91	1.29 - 1.34	0.993E 05
0.323E 06	0.99990	0.151E 05 - 0.166E 05	0.91 - 1.00	1.34 - 1.47	0.924E 05

TOTAL CYCLES = 0.359E 09

ROOT MEAN CUBED IS 0.125E 05 AVERAGE MEAN IS 0.125E 06

TABLE H-50
CUMMULATIVE FATIGUE HISTOGRAM OUTPUT

0.700R BLADE VY

NO. CYCLES IN 30 YEARS (TYPES 1+2)	CUM PROB	HALF-RANGE FATIGUE LOADS: LOAD LEVELS	NORMALIZED LOAD LEVELS	LOAD/50% AT RATED	MID-RANGE MEAN
0.180E 08	0.05000	0. - 0.137E 05	0. - 0.55	0. - 0.86	0.563E 03
0.180E 08	0.10000	0.137E 05 - 0.142E 05	0.55 - 0.57	0.86 - 0.89	0.598E 03
0.180E 08	0.15000	0.142E 05 - 0.145E 05	0.57 - 0.58	0.89 - 0.91	0.625E 03
0.179E 08	0.20000	0.145E 05 - 0.148E 05	0.58 - 0.59	0.91 - 0.92	0.650E 03
0.180E 08	0.25000	0.148E 05 - 0.150E 05	0.59 - 0.60	0.92 - 0.94	0.665E 03
0.180E 08	0.30000	0.150E 05 - 0.153E 05	0.60 - 0.61	0.94 - 0.96	0.678E 03
0.180E 08	0.35000	0.153E 05 - 0.155E 05	0.61 - 0.62	0.96 - 0.97	0.693E 03
0.179E 08	0.40000	0.155E 05 - 0.157E 05	0.62 - 0.63	0.97 - 0.98	0.705E 03
0.180E 08	0.45000	0.157E 05 - 0.159E 05	0.63 - 0.64	0.98 - 1.00	0.713E 03
0.180E 06	0.50000	0.159E 05 - 0.161E 05	0.64 - 0.65	1.00 - 1.01	0.730E 03
0.179E 08	0.55000	0.161E 05 - 0.163E 05	0.65 - 0.65	1.01 - 1.02	0.757E 03
0.180E 08	0.60000	0.163E 05 - 0.165E 05	0.65 - 0.66	1.02 - 1.03	0.791E 03
0.179E 08	0.65000	0.165E 05 - 0.167E 05	0.66 - 0.67	1.03 - 1.04	0.824E 03
0.180E 08	0.70000	0.167E 05 - 0.169E 05	0.67 - 0.68	1.04 - 1.06	0.828E 03
0.179E 08	0.75000	0.169E 05 - 0.171E 05	0.68 - 0.69	1.06 - 1.07	0.779E 03
0.179E 08	0.80000	0.171E 05 - 0.175E 05	0.69 - 0.70	1.07 - 1.09	0.765E 03
0.180E 08	0.85000	0.175E 05 - 0.178E 05	0.70 - 0.72	1.09 - 1.12	0.787E 03
0.179E 08	0.90000	0.178E 05 - 0.183E 05	0.72 - 0.73	1.12 - 1.15	0.821E 03
0.180E 08	0.95000	0.183E 05 - 0.189E 05	0.73 - 0.76	1.15 - 1.19	0.865E 03
0.718E 07	0.97000	0.189E 05 - 0.194E 05	0.76 - 0.78	1.19 - 1.22	0.886E 03
0.718E 07	0.99000	0.194E 05 - 0.203E 05	0.78 - 0.81	1.22 - 1.27	0.938E 03
0.323E 07	0.99900	0.203E 05 - 0.218E 05	0.81 - 0.88	1.27 - 1.37	0.104E 04
0.323E 06	0.99990	0.218E 05 - 0.249E 05	0.88 - 1.00	1.37 - 1.56	0.169E 04

TOTAL CYCLES = 0.359E 09

ROOT MEAN CUBED IS 0.162E 05 AVERAGE MEAN IS 0.739E 03

TABLE M-51
CUMMULATIVE FATIGUE HISTOGRAM OUTPUT

0.700R BLADE VZ

NO. CYCLES IN 30 YEARS (TYPES 1+2)	CUM PROB	HALF-RANGE FATIGUE LOADS: LOAD LEVELS	HALF-RANGE FATIGUE LOADS: NORMALIZED LOAD LEVELS	HALF-RANGE FATIGUE LOADS: LOAD/50% AT RATED	MID-RANGE: MEAN
0.180E 08	0.05000	0. - 0.283E 04	0. - 0.13	0. - 0.49	-0.288E 05
0.180E 08	0.10000	0.283E 04 - 0.328E 04	0.13 - 0.15	0.49 - 0.57	-0.293E 05
0.180E 08	0.15000	0.328E 04 - 0.362E 04	0.15 - 0.17	0.57 - 0.63	-0.296E 05
0.179E 08	0.20000	0.362E 04 - 0.391E 04	0.17 - 0.18	0.63 - 0.68	-0.299E 05
0.180E 08	0.25000	0.391E 04 - 0.418E 04	0.18 - 0.20	0.68 - 0.73	-0.300E 05
0.180E 08	0.30000	0.418E 04 - 0.444E 04	0.20 - 0.21	0.73 - 0.77	-0.301E 05
0.180E 08	0.35000	0.444E 04 - 0.470E 04	0.21 - 0.22	0.77 - 0.82	-0.303E 05
0.179E 08	0.40000	0.470E 04 - 0.496E 04	0.22 - 0.23	0.82 - 0.86	-0.305E 05
0.180E 08	0.45000	0.496E 04 - 0.523E 04	0.23 - 0.25	0.86 - 0.91	-0.306E 05
0.180E 08	0.50000	0.523E 04 - 0.550E 04	0.25 - 0.26	0.91 - 0.96	-0.306E 05
0.179E 08	0.55000	0.550E 04 - 0.579E 04	0.26 - 0.27	0.96 - 1.00	-0.307E 05
0.180E 08	0.60000	0.579E 04 - 0.609E 04	0.27 - 0.29	1.00 - 1.06	-0.307E 05
0.179E 08	0.65000	0.609E 04 - 0.642E 04	0.29 - 0.30	1.06 - 1.11	-0.308E 05
0.180E 08	0.70000	0.642E 04 - 0.678E 04	0.30 - 0.32	1.11 - 1.18	-0.309E 05
0.179E 08	0.75000	0.678E 04 - 0.720E 04	0.32 - 0.34	1.18 - 1.25	-0.310E 05
0.179E 08	0.80000	0.720E 04 - 0.768E 04	0.34 - 0.36	1.25 - 1.33	-0.312E 05
0.180E 08	0.85000	0.768E 04 - 0.828E 04	0.36 - 0.39	1.33 - 1.44	-0.315E 05
0.179E 08	0.90000	0.828E 04 - 0.910E 04	0.39 - 0.43	1.44 - 1.58	-0.319E 05
0.180E 08	0.95000	0.910E 04 - 0.104E 05	0.43 - 0.49	1.58 - 1.81	-0.324E 05
0.718E 07	0.97000	0.104E 05 - 0.115E 05	0.49 - 0.54	1.81 - 1.99	-0.326E 05
0.718E 07	0.99000	0.115E 05 - 0.136E 05	0.54 - 0.64	1.99 - 2.37	-0.332E 05
0.323E 07	0.99900	0.136E 05 - 0.175E 05	0.64 - 0.82	2.37 - 3.04	-0.351E 05
0.323E 06	0.99990	0.175E 05 - 0.212E 05	0.82 - 1.00	3.04 - 3.69	-0.331E 05

TOTAL CYCLES = 0.359E 09

ROOT MEAN CUBED IS 0.693E 04 AVERAGE MEAN IS -0.307E 05

TABLE M-52
CUMMULATIVE FATIGUE HISTOGRAM OUTPUT

0.700R BLADE MX

NO. CYCLES IN 30 YEARS (TYPES 1+2)	CUM PROB	HALF-RANGE FATIGUE LOADS: LOAD LEVELS	HALF-RANGE FATIGUE LOADS: NORMALIZED LOAD LEVELS	HALF-RANGE FATIGUE LOADS: LOAD/50% AT RATED	MID-RANGE: MEAN
0.180E 08	0.05000	0. - 0.381E 04	0. - 0.16	0. - 0.49	-0.450E 05
0.180E 08	0.10000	0.381E 04 - 0.422E 04	0.16 - 0.18	0.49 - 0.54	-0.453E 05
0.180E 08	0.15000	0.422E 04 - 0.453E 04	0.18 - 0.19	0.54 - 0.58	-0.457E 05
0.179E 08	0.20000	0.453E 04 - 0.479E 04	0.19 - 0.20	0.58 - 0.61	-0.461E 05
0.180E 08	0.25000	0.479E 04 - 0.501E 04	0.20 - 0.21	0.61 - 0.64	-0.465E 05
0.180E 08	0.30000	0.501E 04 - 0.524E 04	0.21 - 0.22	0.64 - 0.67	-0.470E 05
0.180E 08	0.35000	0.524E 04 - 0.546E 04	0.22 - 0.23	0.67 - 0.70	-0.475E 05
0.179E 08	0.40000	0.546E 04 - 0.568E 04	0.23 - 0.24	0.70 - 0.73	-0.482E 05
0.180E 08	0.45000	0.568E 04 - 0.591E 04	0.24 - 0.25	0.73 - 0.76	-0.490E 05
0.180E 08	0.50000	0.591E 04 - 0.616E 04	0.25 - 0.26	0.76 - 0.79	-0.499E 05
0.179E 08	0.55000	0.616E 04 - 0.643E 04	0.26 - 0.27	0.79 - 0.82	-0.508E 05
0.180E 08	0.60000	0.643E 04 - 0.671E 04	0.27 - 0.28	0.82 - 0.86	-0.519E 05
0.179E 08	0.65000	0.671E 04 - 0.701E 04	0.28 - 0.30	0.86 - 0.90	-0.532E 05
0.180E 08	0.70000	0.701E 04 - 0.733E 04	0.30 - 0.31	0.90 - 0.94	-0.547E 05
0.179E 08	0.75000	0.733E 04 - 0.770E 04	0.31 - 0.33	0.94 - 0.99	-0.561E 05
0.179E 08	0.80000	0.770E 04 - 0.815E 04	0.33 - 0.34	0.99 - 1.05	-0.572E 05
0.180E 08	0.85000	0.815E 04 - 0.870E 04	0.34 - 0.37	1.05 - 1.12	-0.584E 05
0.179E 08	0.90000	0.870E 04 - 0.944E 04	0.37 - 0.40	1.12 - 1.21	-0.594E 05
0.180E 08	0.95000	0.944E 04 - 0.106E 05	0.40 - 0.45	1.21 - 1.36	-0.611E 05
0.718E 07	0.97000	0.106E 05 - 0.115E 05	0.45 - 0.48	1.36 - 1.47	-0.621E 05
0.718E 07	0.99000	0.115E 05 - 0.132E 05	0.48 - 0.56	1.47 - 1.69	-0.633E 05
0.323E 07	0.99900	0.132E 05 - 0.166E 05	0.56 - 0.70	1.69 - 2.13	-0.649E 05
0.323E 06	0.99990	0.166E 05 - 0.237E 05	0.70 - 1.00	2.13 - 3.03	-0.703E 05

TOTAL CYCLES = 0.359E 09

ROOT MEAN CUBED IS 0.730E 04 AVERAGE MEAN IS -0.518E 05

TABLE H-53
CUMMULATIVE FATIGUE HISTOGRAM OUTPUT

0.700R BLADE MY

NO. CYCLES IN 30 YEARS (TYPES 1+2)	CUM PROB	HALF-RANGE FATIGUE LOADS: LOAD LEVELS	NORMALIZED LOAD LEVELS	LOAD/50% AT RATED	MID-RANGE MEAN
0.180E 08	0.05000	0. - 0.603E 05	0. - 0.06	0. - 0.37	0.776E 06
0.180E 08	0.10000	0.603E 05 - 0.710E 05	0.06 - 0.07	0.37 - 0.43	0.810E 06
0.180E 08	0.15000	0.710E 05 - 0.795E 05	0.07 - 0.08	0.43 - 0.48	0.839E 06
0.179E 08	0.20000	0.795E 05 - 0.872E 05	0.08 - 0.09	0.48 - 0.53	0.865E 06
0.180E 08	0.25000	0.872E 05 - 0.944E 05	0.09 - 0.10	0.53 - 0.57	0.890E 06
0.180E 08	0.30000	0.944E 05 - 0.101E 06	0.10 - 0.11	0.57 - 0.62	0.916E 06
0.180E 08	0.35000	0.101E 06 - 0.108E 06	0.11 - 0.11	0.62 - 0.66	0.941E 06
0.179E 08	0.40000	0.108E 06 - 0.116E 06	0.11 - 0.12	0.66 - 0.70	0.964E 06
0.180E 08	0.45000	0.116E 06 - 0.123E 06	0.12 - 0.13	0.70 - 0.75	0.984E 06
0.180E 08	0.50000	0.123E 06 - 0.131E 06	0.13 - 0.14	0.75 - 0.79	0.100E 07
0.179E 08	0.55000	0.131E 06 - 0.140E 06	0.14 - 0.15	0.79 - 0.85	0.102E 07
0.180E 08	0.60000	0.140E 06 - 0.148E 06	0.15 - 0.16	0.85 - 0.90	0.104E 07
0.179E 08	0.65000	0.148E 06 - 0.158E 06	0.16 - 0.17	0.90 - 0.96	0.106E 07
0.180E 08	0.70000	0.158E 06 - 0.170E 06	0.17 - 0.18	0.96 - 1.03	0.107E 07
0.179E 08	0.75000	0.170E 06 - 0.183E 06	0.18 - 0.19	1.03 - 1.11	0.108E 07
0.179E 08	0.80000	0.183E 06 - 0.199E 06	0.19 - 0.21	1.11 - 1.21	0.109E 07
0.180E 08	0.85000	0.199E 06 - 0.220E 06	0.21 - 0.23	1.21 - 1.33	0.110E 07
0.179E 08	0.90000	0.220E 06 - 0.248E 06	0.23 - 0.26	1.33 - 1.51	0.110E 07
0.180E 08	0.95000	0.248E 06 - 0.296E 06	0.26 - 0.31	1.51 - 1.80	0.108E 07
0.718E 07	0.97000	0.296E 06 - 0.334E 06	0.31 - 0.35	1.80 - 2.03	0.103E 07
0.718E 07	0.99000	0.334E 06 - 0.425E 06	0.35 - 0.45	2.03 - 2.58	0.905E 06
0.323E 07	0.99900	0.425E 06 - 0.664E 06	0.45 - 0.70	2.58 - 4.04	0.698E 06
0.323E 06	0.99990	0.664E 06 - 0.949E 06	0.70 - 1.00	4.04 - 5.76	0.567E 06

TOTAL CYCLES = 0.359E 09

ROOT MEAN CUBED IS 0.196E 06 AVERAGE MEAN IS 0.977E 06

TABLE H-54
CUMMULATIVE FATIGUE HISTOGRAM OUTPUT

0.700R BLADE MZ

NO. CYCLES IN 30 YEARS (TYPES 1+2)	CUM PROB	HALF-RANGE FATIGUE LOADS: LOAD LEVELS	NORMALIZED LOAD LEVELS	LOAD/50% AT RATED	MID-RANGE MEAN
0.180E 08	0.05000	0. - 0.200E 06	0. - 0.43	0. - 0.69	-0.245E 06
0.180E 08	0.10000	0.200E 06 - 0.208E 06	0.43 - 0.45	0.69 - 0.72	-0.242E 06
0.180E 08	0.15000	0.208E 06 - 0.213E 06	0.45 - 0.46	0.72 - 0.74	-0.241E 06
0.179E 08	0.20000	0.213E 06 - 0.218E 06	0.46 - 0.47	0.74 - 0.75	-0.239E 06
0.180E 08	0.25000	0.218E 06 - 0.222E 06	0.47 - 0.48	0.75 - 0.77	-0.238E 06
0.180E 08	0.30000	0.222E 06 - 0.225E 06	0.48 - 0.49	0.77 - 0.78	-0.236E 06
0.180E 08	0.35000	0.225E 06 - 0.228E 06	0.49 - 0.49	0.78 - 0.79	-0.235E 06
0.179E 08	0.40000	0.228E 06 - 0.231E 06	0.49 - 0.50	0.79 - 0.80	-0.233E 06
0.180E 08	0.45000	0.231E 06 - 0.234E 06	0.50 - 0.51	0.80 - 0.81	-0.232E 06
0.180E 08	0.50000	0.234E 06 - 0.237E 06	0.51 - 0.51	0.81 - 0.82	-0.230E 06
0.179E 08	0.55000	0.237E 06 - 0.240E 06	0.51 - 0.52	0.82 - 0.83	-0.228E 06
0.180E 08	0.60000	0.240E 06 - 0.243E 06	0.52 - 0.52	0.83 - 0.84	-0.225E 06
0.179E 08	0.65000	0.243E 06 - 0.245E 06	0.52 - 0.53	0.84 - 0.85	-0.222E 06
0.180E 08	0.70000	0.245E 06 - 0.249E 06	0.53 - 0.54	0.85 - 0.86	-0.220E 06
0.179E 08	0.75000	0.249E 06 - 0.252E 06	0.54 - 0.55	0.86 - 0.87	-0.222E 06
0.179E 08	0.80000	0.252E 06 - 0.257E 06	0.55 - 0.56	0.87 - 0.89	-0.225E 06
0.180E 08	0.85000	0.257E 06 - 0.262E 06	0.56 - 0.57	0.89 - 0.91	-0.227E 06
0.179E 08	0.90000	0.262E 06 - 0.269E 06	0.57 - 0.58	0.91 - 0.93	-0.227E 06
0.180E 08	0.95000	0.269E 06 - 0.279E 06	0.58 - 0.60	0.93 - 0.97	-0.226E 06
0.718E 07	0.97000	0.279E 06 - 0.286E 06	0.60 - 0.62	0.97 - 0.99	-0.228E 06
0.718E 07	0.99000	0.286E 06 - 0.299E 06	0.62 - 0.65	0.99 - 1.03	-0.235E 06
0.323E 07	0.99900	0.299E 06 - 0.320E 06	0.65 - 0.69	1.03 - 1.11	-0.247E 06
0.323E 06	0.99990	0.320E 06 - 0.377E 06	0.69 - 0.82	1.11 - 1.31	-0.242E 06

TOTAL CYCLES = 0.359E 09

ROOT MEAN CUBED IS 0.238E 06 AVERAGE MEAN IS -0.231E 06

TABLE H-55
CUMMULATIVE FATIGUE HISTOGRAM OUTPUT

0.80CR BLADE VX

NO. CYCLES IN 30 YEARS (TYPES 1+2)	CUM PROB	HALF-RANGE FATIGUE LOADS: LOAD LEVELS	NORMALIZED LOAD LEVELS	LOAD/50% AT RATED	MID-RANGE MEAN
0.180E 08	0.05000	0. - 0.461E 04	0. - 0.69	0. - 0.96	0.778E 05
0.180E 08	0.10000	0.451E 04 - 0.459E 04	0.69 - 0.70	0.96 - 0.98	0.769E 05
0.180E 08	0.15000	0.459E 04 - 0.465E 04	0.70 - 0.71	0.98 - 0.99	0.757E 05
0.179E 08	0.20000	0.465E 04 - 0.469E 04	0.71 - 0.71	0.99 - 1.00	0.744E 05
0.180E 08	0.25000	0.469E 04 - 0.473E 04	0.71 - 0.72	1.00 - 1.01	0.730E 05
0.180E 08	0.30000	0.473E 04 - 0.477E 04	0.72 - 0.73	1.01 - 1.02	0.714E 05
0.180E 08	0.35000	0.477E 04 - 0.481E 04	0.73 - 0.73	1.02 - 1.02	0.697E 05
0.179E 08	0.40000	0.481E 04 - 0.484E 04	0.73 - 0.74	1.02 - 1.03	0.680E 05
0.180E 08	0.45000	0.484E 04 - 0.488E 04	0.74 - 0.74	1.03 - 1.04	0.662E 05
0.180E 08	0.50000	0.488E 04 - 0.491E 04	0.74 - 0.75	1.04 - 1.05	0.646E 05
0.179E 08	0.55000	0.491E 04 - 0.494E 04	0.75 - 0.75	1.05 - 1.05	0.630E 05
0.180E 08	0.60000	0.494E 04 - 0.498E 04	0.75 - 0.76	1.05 - 1.06	0.614E 05
0.179E 08	0.65000	0.498E 04 - 0.502E 04	0.76 - 0.76	1.06 - 1.07	0.597E 05
0.180E 08	0.70000	0.502E 04 - 0.505E 04	0.76 - 0.77	1.07 - 1.08	0.579E 05
0.179E 08	0.75000	0.505E 04 - 0.509E 04	0.77 - 0.77	1.08 - 1.08	0.565E 05
0.179E 08	0.80000	0.509E 04 - 0.513E 04	0.77 - 0.78	1.08 - 1.09	0.549E 05
0.180E 08	0.85000	0.513E 04 - 0.518E 04	0.78 - 0.79	1.09 - 1.10	0.534E 05
0.179E 08	0.90000	0.518E 04 - 0.525E 04	0.79 - 0.80	1.10 - 1.12	0.521E 05
0.180E 08	0.95000	0.525E 04 - 0.534E 04	0.80 - 0.81	1.12 - 1.14	0.512E 05
0.718E 07	0.97000	0.534E 04 - 0.540E 04	0.81 - 0.82	1.14 - 1.15	0.510E 05
0.718E 07	0.99000	0.540E 04 - 0.553E 04	0.82 - 0.84	1.15 - 1.18	0.513E 05
0.323E 07	0.99900	0.553E 04 - 0.578E 04	0.84 - 0.88	1.18 - 1.23	0.544E 05
0.323E 06	0.99990	0.578E 04 - 0.657E 04	0.88 - 1.00	1.23 - 1.40	0.754E 05

TOTAL CYCLES = 0.359E 09

ROOT MEAN CUBED IS 0.488E 04 AVERAGE MEAN IS 0.640E 05

TABLE H-56
CUMMULATIVE FATIGUE HISTOGRAM OUTPUT

0.80OR BLADE VY

NO. CYCLES IN 30 YEARS (TYPES 1+2)	CUM PROB	HALF-RANGE FATIGUE LOADS: LOAD LEVELS	NORMALIZED LOAD LEVELS	LOAD/50% AT RATED	MID-RANGE MEAN
0.180E 08	0.05000	0. - 0.455E 04	0. - 0.55	0. - 0.85	0.672E 03
0.180E 08	0.10000	0.455E 04 - 0.474E 04	0.55 - 0.57	0.85 - 0.88	0.739E 03
0.180E 08	0.15000	0.474E 04 - 0.488E 04	0.57 - 0.59	0.88 - 0.91	0.763E 03
0.179E 08	0.20000	0.488E 04 - 0.499E 04	0.59 - 0.60	0.91 - 0.93	0.786E 03
0.180E 08	0.25000	0.499E 04 - 0.509E 04	0.60 - 0.62	0.93 - 0.95	0.810E 03
0.180E 08	0.30000	0.509E 04 - 0.518E 04	0.62 - 0.63	0.95 - 0.96	0.833E 03
0.180E 08	0.35000	0.518E 04 - 0.526E 04	0.63 - 0.64	0.96 - 0.98	0.856E 03
0.179E 08	0.40000	0.526E 04 - 0.534E 04	0.64 - 0.65	0.98 - 0.99	0.880E 03
0.180E 08	0.45000	0.534E 04 - 0.542E 04	0.65 - 0.66	0.99 - 1.01	0.903E 03
0.180E 08	0.50000	0.542E 04 - 0.549E 04	0.66 - 0.67	1.01 - 1.02	0.931E 03
0.179E 08	0.55000	0.549E 04 - 0.557E 04	0.67 - 0.67	1.02 - 1.04	0.963E 03
0.180E 08	0.60000	0.557E 04 - 0.564E 04	0.67 - 0.68	1.04 - 1.05	0.998E 03
0.179E 08	0.65000	0.564E 04 - 0.572E 04	0.68 - 0.69	1.05 - 1.06	0.101E 04
0.180E 08	0.70000	0.572E 04 - 0.581E 04	0.69 - 0.70	1.06 - 1.08	0.101E 04
0.179E 08	0.75000	0.581E 04 - 0.590E 04	0.70 - 0.72	1.08 - 1.10	0.100E 04
0.179E 08	0.80000	0.590E 04 - 0.601E 04	0.72 - 0.73	1.10 - 1.12	0.101E 04
0.180E 08	0.85000	0.601E 04 - 0.614E 04	0.73 - 0.74	1.12 - 1.14	0.102E 04
0.179E 08	0.90000	0.614E 04 - 0.632E 04	0.74 - 0.77	1.14 - 1.17	0.102E 04
0.180E 08	0.95000	0.632E 04 - 0.658E 04	0.77 - 0.80	1.17 - 1.22	0.103E 04
0.718E 07	0.97000	0.658E 04 - 0.676E 04	0.80 - 0.82	1.22 - 1.26	0.104E 04
0.718E 07	0.99000	0.676E 04 - 0.710E 04	0.82 - 0.86	1.26 - 1.32	0.997E 03
0.323E 07	0.99900	0.710E 04 - 0.769E 04	0.86 - 0.93	1.32 - 1.43	0.669E 03
0.323E 06	0.99990	0.769E 04 - 0.824E 04	0.93 - 1.00	1.43 - 1.53	0.119E 04

TOTAL CYCLES = 0.359E 09

ROOT MEAN CUBED IS 0.555E 04 AVERAGE MEAN IS 0.909E 03

TABLE H-57
CUMMULATIVE FATIGUE HISTOGRAM OUTPUT

0.800R BLADE VZ

NO. CYCLES IN 30 YEARS (TYPES 1+2)	CUM PROB	HALF-RANGE FATIGUE LOADS: LOAD LEVELS	NORMALIZED LOAD LEVELS	LOAD/50% AT RATED	MID-RANGE MEAN
0.180E 08	0.05000	0. - 0.116E 04	0. - 0.05	0. - 0.35	-0.158E 05
0.180E 08	0.10000	0.116E 04 - 0.136E 04	0.05 - 0.06	0.35 - 0.41	-0.165E 05
0.180E 08	0.15000	0.136E 04 - 0.152E 04	0.06 - 0.07	0.41 - 0.46	-0.171E 05
0.179E 08	0.20000	0.152E 04 - 0.167E 04	0.07 - 0.08	0.46 - 0.51	-0.176E 05
0.180E 08	0.25000	0.167E 04 - 0.181E 04	0.08 - 0.09	0.51 - 0.55	-0.182E 05
0.180E 08	0.30000	0.181E 04 - 0.194E 04	0.09 - 0.09	0.55 - 0.59	-0.187E 05
0.180E 08	0.35000	0.194E 04 - 0.208E 04	0.09 - 0.10	0.59 - 0.63	-0.193E 05
0.179E 08	0.40000	0.208E 04 - 0.222E 04	0.10 - 0.11	0.63 - 0.68	-0.198E 05
0.180E 08	0.45000	0.222E 04 - 0.237E 04	0.11 - 0.11	0.68 - 0.72	-0.203E 05
0.180E 08	0.50000	0.237E 04 - 0.251E 04	0.11 - 0.12	0.72 - 0.77	-0.208E 05
0.179E 08	0.55000	0.251E 04 - 0.267E 04	0.12 - 0.13	0.77 - 0.81	-0.212E 05
0.180E 08	0.60000	0.267E 04 - 0.285E 04	0.13 - 0.14	0.81 - 0.87	-0.217E 05
0.179E 08	0.65000	0.285E 04 - 0.304E 04	0.14 - 0.14	0.87 - 0.93	-0.221E 05
0.180E 08	0.70000	0.304E 04 - 0.326E 04	0.14 - 0.15	0.93 - 0.99	-0.225E 05
0.179E 08	0.75000	0.326E 04 - 0.351E 04	0.15 - 0.17	0.99 - 1.07	-0.229E 05
0.179E 08	0.80000	0.351E 04 - 0.381E 04	0.17 - 0.18	1.07 - 1.16	-0.231E 05
0.180E 08	0.85000	0.381E 04 - 0.419E 04	0.18 - 0.20	1.16 - 1.28	-0.233E 05
0.179E 08	0.90000	0.419E 04 - 0.473E 04	0.20 - 0.22	1.28 - 1.44	-0.233E 05
0.180E 08	0.95000	0.473E 04 - 0.564E 04	0.22 - 0.27	1.44 - 1.72	-0.236E 05
0.718E 07	0.97000	0.564E 04 - 0.632E 04	0.27 - 0.30	1.72 - 1.92	-0.236E 05
0.718E 07	0.99000	0.632E 04 - 0.794E 04	0.30 - 0.38	1.92 - 2.42	-0.228E 05
0.323E 07	0.99900	0.794E 04 - 0.134E 05	0.38 - 0.63	2.42 - 4.07	-0.168E 05
0.323E 06	0.99990	0.134E 05 - 0.210E 05	0.63 - 1.00	4.07 - 6.40	-0.139E 05

TOTAL CYCLES = 0.359E 09

ROOT MEAN CUBED IS 0.378E 04 AVERAGE MEAN IS -0.205E 05

TABLE H-58
CUMMULATIVE FATIGUE HISTOGRAM OUTPUT

0.800R BLADE MX

NO. CYCLES IN 30 YEARS (TYPES 1+2)	CUM PROB	HALF-RANGE FATIGUE LOADS: LOAD LEVELS	NORMALIZED LOAD LEVELS	LOAD/50% AT RATED	MID-RANGE MEAN
0.180E 08	0.05000	0. - 0.127E 04	0. - 0.12	0. - 0.43	-0.249E 05
0.180E 08	0.10000	0.127E 04 - 0.141E 04	0.12 - 0.13	0.43 - 0.48	-0.251E 05
0.180E 08	0.15000	0.141E 04 - 0.152E 04	0.13 - 0.14	0.48 - 0.52	-0.254E 05
0.179E 08	0.20000	0.152E 04 - 0.162E 04	0.14 - 0.15	0.52 - 0.55	-0.257E 05
0.180E 08	0.25000	0.162E 04 - 0.170E 04	0.15 - 0.16	0.55 - 0.58	-0.260E 05
0.180E 08	0.30000	0.170E 04 - 0.178E 04	0.16 - 0.16	0.58 - 0.61	-0.263E 05
0.180E 08	0.35000	0.178E 04 - 0.186E 04	0.16 - 0.17	0.61 - 0.64	-0.267E 05
0.179E 08	0.40000	0.186E 04 - 0.195E 04	0.17 - 0.18	0.64 - 0.67	-0.272E 05
0.180E 08	0.45000	0.195E 04 - 0.204E 04	0.18 - 0.19	0.67 - 0.70	-0.278E 05
0.180E 08	0.50000	0.204E 04 - 0.213E 04	0.19 - 0.19	0.70 - 0.73	-0.285E 05
0.179E 08	0.55000	0.213E 04 - 0.224E 04	0.19 - 0.20	0.73 - 0.77	-0.294E 05
0.180E 08	0.60000	0.224E 04 - 0.235E 04	0.20 - 0.21	0.77 - 0.80	-0.303E 05
0.179E 08	0.65000	0.235E 04 - 0.247E 04	0.21 - 0.22	0.80 - 0.84	-0.314E 05
0.180E 08	0.70000	0.247E 04 - 0.260E 04	0.22 - 0.24	0.84 - 0.89	-0.324E 05
0.179E 08	0.75000	0.260E 04 - 0.275E 04	0.24 - 0.25	0.89 - 0.94	-0.334E 05
0.179E 08	0.80000	0.275E 04 - 0.294E 04	0.25 - 0.27	0.94 - 1.01	-0.345E 05
0.180E 08	0.85000	0.294E 04 - 0.318E 04	0.27 - 0.29	1.01 - 1.09	-0.353E 05
0.179E 08	0.90000	0.318E 04 - 0.350E 04	0.29 - 0.32	1.09 - 1.20	-0.359E 05
0.180E 08	0.95000	0.350E 04 - 0.405E 04	0.32 - 0.37	1.20 - 1.39	-0.371E 05
0.718E 07	0.97000	0.405E 04 - 0.445E 04	0.37 - 0.41	1.39 - 1.52	-0.379E 05
0.718E 07	0.99000	0.445E 04 - 0.524E 04	0.41 - 0.48	1.52 - 1.80	-0.391E 05
0.323E 07	0.99900	0.524E 04 - 0.688E 04	0.48 - 0.63	1.80 - 2.35	-0.407E 05
0.323E 06	0.99990	0.688E 04 - 0.110E 05	0.63 - 1.00	2.35 - 3.75	-0.442E 05

TOTAL CYCLES = 0.359E 09

ROOT MEAN CUBED IS 0.270E 04 AVERAGE MEAN IS -0.301E 05

TABLE M-59
CUMMULATIVE FATIGUE HISTOGRAM OUTPUT

0.800R BLADE MY

NO. CYCLES IN 30 YEARS (TYPES 1+2)	CUM PROB	HALF-RANGE FATIGUE LOADS: LOAD LEVELS	HALF-RANGE FATIGUE LOADS: NORMALIZED LOAD LEVELS	HALF-RANGE FATIGUE LOADS: LOAD/50% AT RATED	MID-RANGE MEAN
0.180E 08	0.05000	0. - 0.229E 05	0. - 0.06	0. - 0.35	0.292E 06
0.180E 08	0.10000	0.229E 05 - 0.270E 05	0.06 - 0.07	0.35 - 0.41	0.305E 06
0.180E 08	0.15000	0.270E 05 - 0.302E 05	0.07 - 0.07	0.41 - 0.46	0.316E 06
0.179E 08	0.20000	0.302E 05 - 0.332E 05	0.07 - 0.08	0.46 - 0.51	0.328E 06
0.180E 08	0.25000	0.332E 05 - 0.360E 05	0.08 - 0.09	0.51 - 0.55	0.339E 06
0.180E 08	0.30000	0.360E 05 - 0.386E 05	0.09 - 0.09	0.55 - 0.59	0.349E 06
0.180E 08	0.35000	0.386E 05 - 0.413E 05	0.09 - 0.10	0.59 - 0.63	0.360E 06
0.179E 08	0.40000	0.413E 05 - 0.441E 05	0.10 - 0.11	0.63 - 0.68	0.370E 06
0.180E 08	0.45000	0.441E 05 - 0.470E 05	0.11 - 0.12	0.68 - 0.72	0.379E 06
0.180E 08	0.50000	0.470E 05 - 0.500E 05	0.12 - 0.12	0.72 - 0.77	0.389E 06
0.179E 08	0.55000	0.500E 05 - 0.532E 05	0.12 - 0.13	0.77 - 0.82	0.398E 06
0.180E 08	0.60000	0.532E 05 - 0.568E 05	0.13 - 0.14	0.82 - 0.87	0.407E 06
0.179E 08	0.65000	0.568E 05 - 0.606E 05	0.14 - 0.15	0.87 - 0.93	0.415E 06
0.180E 08	0.70000	0.606E 05 - 0.650E 05	0.15 - 0.16	0.93 - 1.00	0.423E 06
0.179E 08	0.75000	0.650E 05 - 0.699E 05	0.16 - 0.17	1.00 - 1.07	0.430E 06
0.179E 08	0.80000	0.699E 05 - 0.759E 05	0.17 - 0.19	1.07 - 1.16	0.435E 06
0.180E 08	0.85000	0.759E 05 - 0.835E 05	0.19 - 0.20	1.16 - 1.28	0.439E 06
0.179E 08	0.90000	0.835E 05 - 0.940E 05	0.20 - 0.23	1.28 - 1.44	0.440E 06
0.180E 08	0.95000	0.940E 05 - 0.112E 06	0.23 - 0.27	1.44 - 1.71	0.445E 06
0.718E 07	0.97000	0.112E 06 - 0.125E 06	0.27 - 0.31	1.71 - 1.91	0.444E 06
0.718E 07	0.99000	0.125E 06 - 0.157E 06	0.31 - 0.38	1.91 - 2.40	0.429E 06
0.323E 07	0.99900	0.157E 06 - 0.259E 06	0.38 - 0.64	2.40 - 3.98	0.309E 06
0.323E 06	0.99990	0.259E 06 - 0.408E 06	0.64 - 1.00	3.98 - 6.26	0.247E 06

TOTAL CYCLES = 0.359E 09

ROOT MEAN CUBED IS 0.746E 05 AVERAGE MEAN IS 0.383E 06

TABLE M-60
CUMMULATIVE FATIGUE HISTOGRAM OUTPUT

0.800R BLADE MZ

NO. CYCLES IN 30 YEARS (TYPES 1+2)	CUM PROB	HALF-RANGE FATIGUE LOADS: LOAD LEVELS	HALF-RANGE FATIGUE LOADS: NORMALIZED LOAD LEVELS	HALF-RANGE FATIGUE LOADS: LOAD/50% AT RATED	MID-RANGE MEAN
0.180E 08	0.05000	0. - 0.585E 05	0. - 0.35	0. - 0.58	-0.513E 05
0.180E 08	0.10000	0.585E 05 - 0.610E 05	0.35 - 0.36	0.58 - 0.61	-0.503E 05
0.180E 08	0.15000	0.610E 05 - 0.628E 05	0.36 - 0.37	0.61 - 0.63	-0.495E 05
0.179E 08	0.20000	0.628E 05 - 0.642E 05	0.37 - 0.38	0.63 - 0.64	-0.488E 05
0.180E 08	0.25000	0.642E 05 - 0.654E 05	0.38 - 0.39	0.64 - 0.65	-0.482E 05
0.180E 08	0.30000	0.654E 05 - 0.666E 05	0.39 - 0.40	0.65 - 0.66	-0.475E 05
0.180E 08	0.35000	0.666E 05 - 0.676E 05	0.40 - 0.40	0.66 - 0.68	-0.469E 05
0.179E 08	0.40000	0.676E 05 - 0.687E 05	0.40 - 0.41	0.68 - 0.69	-0.463E 05
0.180E 08	0.45000	0.687E 05 - 0.697E 05	0.41 - 0.41	0.69 - 0.70	-0.457E 05
0.180E 08	0.50000	0.697E 05 - 0.706E 05	0.41 - 0.42	0.70 - 0.71	-0.450E 05
0.179E 08	0.55000	0.706E 05 - 0.716E 05	0.42 - 0.43	0.71 - 0.72	-0.442E 05
0.180E 08	0.60000	0.716E 05 - 0.726E 05	0.43 - 0.43	0.72 - 0.73	-0.433E 05
0.179E 08	0.65000	0.726E 05 - 0.737E 05	0.43 - 0.44	0.73 - 0.74	-0.428E 05
0.180E 08	0.70000	0.737E 05 - 0.749E 05	0.44 - 0.44	0.74 - 0.75	-0.426E 05
0.179E 08	0.75000	0.749E 05 - 0.761E 05	0.44 - 0.45	0.75 - 0.76	-0.427E 05
0.179E 08	0.80000	0.761E 05 - 0.775E 05	0.45 - 0.46	0.76 - 0.77	-0.426E 05
0.180E 08	0.85000	0.775E 05 - 0.791E 05	0.46 - 0.47	0.77 - 0.79	-0.423E 05
0.179E 08	0.90000	0.791E 05 - 0.813E 05	0.47 - 0.48	0.79 - 0.81	-0.422E 05
0.180E 08	0.95000	0.813E 05 - 0.847E 05	0.48 - 0.50	0.81 - 0.85	-0.421E 05
0.718E 07	0.97000	0.847E 05 - 0.870E 05	0.50 - 0.52	0.85 - 0.87	-0.420E 05
0.718E 07	0.99000	0.870E 05 - 0.915E 05	0.52 - 0.54	0.87 - 0.91	-0.424E 05
0.323E 07	0.99900	0.915E 05 - 0.992E 05	0.54 - 0.59	0.91 - 0.99	-0.494E 05
0.323E 06	0.99990	0.992E 05 - 0.116E 06	0.59 - 0.69	0.99 - 1.16	-0.613E 05

TOTAL CYCLES = 0.359E 09

ROOT MEAN CUBED IS 0.714E 05 AVERAGE MEAN IS -0.454E 05

TABLE H-61
CUMMULATIVE FATIGUE HISTOGRAM OUTPUT

0.900R BLADE VX

NO. CYCLES IN 30 YEARS (TYPES 1+2)	CUM PROB	HALF-RANGE FATIGUE LOADS: LOAD LEVELS	NORMALIZED LOAD LEVELS	LOAD/50% AT RATED	MID-RANGE MEAN
0.180E 08	0.05000	0. - 0.152E 04	0. - 0.68	0. - 1.12	0.262E 05
0.180E 08	0.10000	0.152E 04 - 0.155E 04	0.68 - 0.70	1.12 - 1.14	0.258E 05
0.180E 08	0.15000	0.155E 04 - 0.157E 04	0.70 - 0.71	1.14 - 1.15	0.254E 05
0.179E 08	0.20000	0.157E 04 - 0.158E 04	0.71 - 0.71	1.15 - 1.16	0.249E 05
0.180E 08	0.25000	0.158E 04 - 0.160E 04	0.71 - 0.72	1.16 - 1.17	0.244E 05
0.180E 08	0.30000	0.160E 04 - 0.161E 04	0.72 - 0.72	1.17 - 1.18	0.239E 05
0.180E 08	0.35000	0.161E 04 - 0.162E 04	0.72 - 0.73	1.18 - 1.19	0.233E 05
0.179E 08	0.40000	0.162E 04 - 0.163E 04	0.73 - 0.73	1.19 - 1.19	0.229E 05
0.180E 08	0.45000	0.163E 04 - 0.164E 04	0.73 - 0.74	1.19 - 1.20	0.224E 05
0.180E 08	0.50000	0.164E 04 - 0.165E 04	0.74 - 0.74	1.20 - 1.21	0.218E 05
0.179E 08	0.55000	0.165E 04 - 0.166E 04	0.74 - 0.74	1.21 - 1.21	0.214E 05
0.180E 08	0.60000	0.166E 04 - 0.167E 04	0.74 - 0.75	1.21 - 1.22	0.209E 05
0.179E 08	0.65000	0.167E 04 - 0.168E 04	0.75 - 0.75	1.22 - 1.23	0.204E 05
0.180E 08	0.70000	0.168E 04 - 0.169E 04	0.75 - 0.76	1.23 - 1.24	0.199E 05
0.179E 08	0.75000	0.169E 04 - 0.170E 04	0.76 - 0.77	1.24 - 1.25	0.195E 05
0.179E 08	0.80000	0.170E 04 - 0.172E 04	0.77 - 0.77	1.25 - 1.26	0.191E 05
0.180E 08	0.85000	0.172E 04 - 0.174E 04	0.77 - 0.78	1.26 - 1.27	0.186E 05
0.179E 08	0.90000	0.174E 04 - 0.176E 04	0.78 - 0.79	1.27 - 1.29	0.182E 05
0.180E 08	0.95000	0.176E 04 - 0.179E 04	0.79 - 0.80	1.29 - 1.31	0.177E 05
0.718E 07	0.97000	0.179E 04 - 0.181E 04	0.80 - 0.81	1.31 - 1.33	0.176E 05
0.718E 07	0.99000	0.181E 04 - 0.186E 04	0.81 - 0.83	1.33 - 1.36	0.176E 05
0.323E 07	0.99900	0.186E 04 - 0.195E 04	0.83 - 0.88	1.36 - 1.43	0.196E 05
0.323E 06	0.99990	0.195E 04 - 0.222E 04	0.88 - 1.00	1.43 - 1.63	0.251E 05

TOTAL CYCLES = 0.359E 09

ROOT MEAN CUBED IS 0.164E 04 AVERAGE MEAN IS 0.217E 05

TABLE H-62
CUMMULATIVE FATIGUE HISTOGRAM OUTPUT

0.900R BLADE VY

NO. CYCLES IN 30 YEARS (TYPES 1+2)	CUM PROB	HALF-RANGE FATIGUE LOADS: LOAD LEVELS	NORMALIZED LOAD LEVELS	LOAD/50% AT RATED	MID-RANGE MEAN
0.180E 08	0.05000	0. - 0.160E 04	0. - 0.52	0. - 1.00	0.611E 02
0.180E 08	0.10000	0.160E 04 - 0.166E 04	0.52 - 0.55	1.00 - 1.04	0.651E 02
0.180E 08	0.15000	0.166E 04 - 0.171E 04	0.55 - 0.56	1.04 - 1.07	0.740E 02
0.179E 08	0.20000	0.171E 04 - 0.175E 04	0.56 - 0.57	1.07 - 1.10	0.816E 02
0.180E 08	0.25000	0.175E 04 - 0.179E 04	0.57 - 0.59	1.10 - 1.12	0.891E 02
0.180E 08	0.30000	0.179E 04 - 0.182E 04	0.59 - 0.60	1.12 - 1.14	0.967E 02
0.180E 08	0.35000	0.182E 04 - 0.185E 04	0.60 - 0.61	1.14 - 1.16	0.104E 03
0.179E 08	0.40000	0.185E 04 - 0.188E 04	0.61 - 0.62	1.16 - 1.18	0.110E 03
0.180E 08	0.45000	0.188E 04 - 0.191E 04	0.62 - 0.62	1.18 - 1.19	0.117E 03
0.180E 08	0.50000	0.191E 04 - 0.193E 04	0.62 - 0.63	1.19 - 1.21	0.123E 03
0.179E 08	0.55000	0.193E 04 - 0.196E 04	0.63 - 0.64	1.21 - 1.23	0.128E 03
0.180E 08	0.60000	0.196E 04 - 0.199E 04	0.64 - 0.65	1.23 - 1.24	0.139E 03
0.179E 08	0.65000	0.199E 04 - 0.201E 04	0.65 - 0.66	1.24 - 1.26	0.149E 03
0.180E 08	0.70000	0.201E 04 - 0.204E 04	0.66 - 0.67	1.26 - 1.28	0.155E 03
0.179E 08	0.75000	0.204E 04 - 0.208E 04	0.67 - 0.68	1.28 - 1.30	0.154E 03
0.179E 08	0.80000	0.208E 04 - 0.212E 04	0.68 - 0.69	1.30 - 1.32	0.152E 03
0.180E 08	0.85000	0.212E 04 - 0.216E 04	0.69 - 0.71	1.32 - 1.35	0.154E 03
0.179E 08	0.90000	0.216E 04 - 0.223E 04	0.71 - 0.73	1.35 - 1.39	0.156E 03
0.180E 08	0.95000	0.223E 04 - 0.232E 04	0.73 - 0.76	1.39 - 1.45	0.157E 03
0.718E 07	0.97000	0.232E 04 - 0.238E 04	0.76 - 0.78	1.45 - 1.49	0.159E 03
0.718E 07	0.99000	0.238E 04 - 0.250E 04	0.78 - 0.82	1.49 - 1.56	0.149E 03
0.323E 07	0.99900	0.250E 04 - 0.270E 04	0.82 - 0.88	1.56 - 1.69	0.503E 02
0.323E 06	0.99990	0.270E 04 - 0.305E 04	0.88 - 1.00	1.69 - 1.91	0.235E 03

TOTAL CYCLES = 0.359E 09

ROOT MEAN CUBED IS 0.195E 04 AVERAGE MEAN IS 0.121E 03

TABLE H-63
CUMMULATIVE FATIGUE HISTOGRAM OUTPUT

0.900R BLADE VZ

NO. CYCLES IN 30 YEARS (TYPES 1+2)	CUM PROB	HALF-RANGE FATIGUE LOADS: LOAD LEVELS	NORMALIZED LOAD LEVELS	LOAD/50% AT RATED	MID-RANGE MEAN
0.180E 08	0.05000	0. - 0.529E 03	0. - 0.05	0. - 0.38	-0.680E 04
0.180E 08	0.10000	0.529E 03 - 0.626E 03	0.05 - 0.06	0.38 - 0.45	-0.709E 04
0.180E 08	0.15000	0.626E 03 - 0.704E 03	0.06 - 0.07	0.45 - 0.51	-0.740E 04
0.179E 08	0.20000	0.704E 03 - 0.771E 03	0.07 - 0.08	0.51 - 0.56	-0.766E 04
0.180E 08	0.25000	0.771E 03 - 0.832E 03	0.08 - 0.09	0.56 - 0.60	-0.791E 04
0.180E 08	0.30000	0.832E 03 - 0.897E 03	0.09 - 0.09	0.60 - 0.65	-0.817E 04
0.180E 08	0.35000	0.897E 03 - 0.961E 03	0.09 - 0.10	0.65 - 0.69	-0.840E 04
0.179E 08	0.40000	0.961E 03 - 0.103E 04	0.10 - 0.11	0.69 - 0.74	-0.861E 04
0.180E 08	0.45000	0.103E 04 - 0.109E 04	0.11 - 0.11	0.74 - 0.79	-0.881E 04
0.180E 08	0.50000	0.109E 04 - 0.117E 04	0.11 - 0.12	0.79 - 0.84	-0.905E 04
0.179E 08	0.55000	0.117E 04 - 0.124E 04	0.12 - 0.13	0.84 - 0.89	-0.926E 04
0.180E 08	0.60000	0.124E 04 - 0.132E 04	0.13 - 0.14	0.89 - 0.95	-0.943E 04
0.179E 08	0.65000	0.132E 04 - 0.141E 04	0.14 - 0.14	0.95 - 1.02	-0.962E 04
0.180E 08	0.70000	0.141E 04 - 0.152E 04	0.14 - 0.16	1.02 - 1.09	-0.979E 04
0.179E 08	0.75000	0.152E 04 - 0.164E 04	0.16 - 0.17	1.09 - 1.18	-0.993E 04
0.179E 08	0.80000	0.164E 04 - 0.178E 04	0.17 - 0.18	1.18 - 1.28	-0.101E 05
0.180E 08	0.85000	0.178E 04 - 0.196E 04	0.18 - 0.20	1.28 - 1.41	-0.102E 05
0.179E 08	0.90000	0.196E 04 - 0.221E 04	0.20 - 0.23	1.41 - 1.59	-0.102E 05
0.180E 08	0.95000	0.221E 04 - 0.262E 04	0.23 - 0.27	1.59 - 1.89	-0.104E 05
0.718E 07	0.97000	0.262E 04 - 0.293E 04	0.27 - 0.30	1.89 - 2.11	-0.104E 05
0.718E 07	0.99000	0.293E 04 - 0.370E 04	0.30 - 0.38	2.11 - 2.67	-0.101E 05
0.323E 07	0.99900	0.370E 04 - 0.618E 04	0.38 - 0.63	2.67 - 4.46	-0.730E 04
0.323E 06	0.99990	0.618E 04 - 0.975E 04	0.63 - 1.00	4.46 - 7.03	-0.554E 04

TOTAL CYCLES = 0.359E 09

ROOT MEAN CUBED IS 0.176E 04 AVERAGE MEAN IS -0.892E 04

TABLE H-64
CUMMULATIVE FATIGUE HISTOGRAM OUTPUT

0.900R BLADE MX

NO. CYCLES IN 30 YEARS (TYPES 1+2)	CUM PROB	HALF-RANGE FATIGUE LOADS: LOAD LEVELS	NORMALIZED LOAD LEVELS	LOAD/50% AT RATED	MID-RANGE MEAN
0.180E 08	0.05000	0. - 0.378E 03	0. - 0.11	0. - 0.52	-0.940E 04
0.180E 08	0.10000	0.378E 03 - 0.418E 03	0.11 - 0.12	0.52 - 0.58	-0.948E 04
0.180E 08	0.15000	0.418E 03 - 0.447E 03	0.12 - 0.13	0.58 - 0.62	-0.956E 04
0.179E 08	0.20000	0.447E 03 - 0.473E 03	0.13 - 0.13	0.62 - 0.65	-0.970E 04
0.180E 08	0.25000	0.473E 03 - 0.497E 03	0.13 - 0.14	0.65 - 0.69	-0.983E 04
0.180E 08	0.30000	0.497E 03 - 0.521E 03	0.14 - 0.15	0.69 - 0.72	-0.996E 04
0.180E 08	0.35000	0.521E 03 - 0.543E 03	0.15 - 0.15	0.72 - 0.75	-0.101E 05
0.179E 08	0.40000	0.543E 03 - 0.563E 03	0.15 - 0.16	0.75 - 0.78	-0.102E 05
0.180E 08	0.45000	0.563E 03 - 0.588E 03	0.16 - 0.17	0.78 - 0.81	-0.104E 05
0.180E 08	0.50000	0.588E 03 - 0.612E 03	0.17 - 0.17	0.81 - 0.85	-0.107E 05
0.179E 08	0.55000	0.612E 03 - 0.637E 03	0.17 - 0.18	0.85 - 0.88	-0.110E 05
0.180E 08	0.60000	0.637E 03 - 0.664E 03	0.18 - 0.19	0.88 - 0.92	-0.113E 05
0.179E 08	0.65000	0.664E 03 - 0.695E 03	0.19 - 0.20	0.92 - 0.96	-0.117E 05
0.180E 08	0.70000	0.695E 03 - 0.732E 03	0.20 - 0.21	0.96 - 1.01	-0.121E 05
0.179E 08	0.75000	0.732E 03 - 0.775E 03	0.21 - 0.22	1.01 - 1.07	-0.126E 05
0.179E 08	0.80000	0.775E 03 - 0.827E 03	0.22 - 0.24	1.07 - 1.15	-0.130E 05
0.180E 08	0.85000	0.827E 03 - 0.898E 03	0.24 - 0.26	1.15 - 1.24	-0.133E 05
0.179E 08	0.90000	0.898E 03 - 0.995E 03	0.26 - 0.28	1.24 - 1.38	-0.135E 05
0.180E 08	0.95000	0.995E 03 - 0.120E 04	0.28 - 0.34	1.38 - 1.66	-0.143E 05
0.718E 07	0.97000	0.120E 04 - 0.136E 04	0.34 - 0.39	1.66 - 1.88	-0.148E 05
0.718E 07	0.99000	0.136E 04 - 0.169E 04	0.39 - 0.48	1.88 - 2.34	-0.145E 05
0.323E 07	0.99900	0.169E 04 - 0.225E 04	0.48 - 0.64	2.34 - 3.12	-0.148E 05
0.323E 06	0.99990	0.225E 04 - 0.350E 04	0.64 - 1.00	3.12 - 4.85	-0.170E 05

TOTAL CYCLES = 0.359E 09

ROOT MEAN CUBED IS 0.800E 03 AVERAGE MEAN IS -0.114E 05

TABLE H-65
CUMMULATIVE FATIGUE HISTOGRAM OUTPUT

0.900R BLADE MY

NO. CYCLES IN 30 YEARS (TYPES 1+2)	CUM PROB	HALF-RANGE FATIGUE LOADS: LOAD LEVELS	HALF-RANGE FATIGUE LOADS: NORMALIZED LOAD LEVELS	HALF-RANGE FATIGUE LOADS: LOAD/50% AT RATED	MID-RANGE MEAN
0.180E 08	0.05000	0. - 0.640E 04	0. - 0.06	0. - 0.39	0.806E 05
0.180E 08	0.10000	0.640E 04 - 0.754E 04	0.06 - 0.07	0.39 - 0.46	0.839E 05
0.180E 08	0.15000	0.754E 04 - 0.847E 04	0.07 - 0.07	0.46 - 0.51	0.866E 05
0.179E 08	0.20000	0.847E 04 - 0.930E 04	0.07 - 0.08	0.51 - 0.56	0.894E 05
0.180E 08	0.25000	0.930E 04 - 0.101E 05	0.08 - 0.09	0.56 - 0.61	0.925E 05
0.180E 08	0.30000	0.101E 05 - 0.109E 05	0.09 - 0.09	0.61 - 0.66	0.956E 05
0.180E 08	0.35000	0.109E 05 - 0.117E 05	0.09 - 0.10	0.66 - 0.70	0.986E 05
0.179E 08	0.40000	0.117E 05 - 0.125E 05	0.10 - 0.11	0.70 - 0.75	0.101E 06
0.180E 08	0.45000	0.125E 05 - 0.133E 05	0.11 - 0.12	0.75 - 0.80	0.104E 06
0.180E 08	0.50000	0.133E 05 - 0.142E 05	0.12 - 0.12	0.80 - 0.86	0.106E 06
0.179E 08	0.55000	0.142E 05 - 0.151E 05	0.12 - 0.13	0.86 - 0.91	0.109E 06
0.180E 08	0.60000	0.151E 05 - 0.162E 05	0.13 - 0.14	0.91 - 0.98	0.112E 06
0.179E 08	0.65000	0.162E 05 - 0.173E 05	0.14 - 0.15	0.98 - 1.04	0.114E 06
0.180E 08	0.70000	0.173E 05 - 0.185E 05	0.15 - 0.16	1.04 - 1.12	0.117E 06
0.179E 08	0.75000	0.185E 05 - 0.199E 05	0.16 - 0.17	1.12 - 1.20	0.119E 06
0.179E 08	0.80000	0.199E 05 - 0.216E 05	0.17 - 0.19	1.20 - 1.31	0.121E 06
0.180E 08	0.85000	0.216E 05 - 0.238E 05	0.19 - 0.21	1.31 - 1.44	0.122E 06
0.179E 08	0.90000	0.238E 05 - 0.269E 05	0.21 - 0.23	1.44 - 1.63	0.123E 06
0.180E 08	0.95000	0.269E 05 - 0.320E 05	0.23 - 0.28	1.63 - 1.93	0.125E 06
0.718E 07	0.97000	0.320E 05 - 0.358E 05	0.28 - 0.31	1.93 - 2.16	0.125E 06
0.718E 07	0.99000	0.358E 05 - 0.450E 05	0.31 - 0.39	2.16 - 2.72	0.122E 06
0.323E 07	0.99900	0.450E 05 - 0.730E 05	0.39 - 0.63	2.72 - 4.41	0.881E 05
0.323E 06	0.99990	0.730E 05 - 0.115E 06	0.63 - 1.00	4.41 - 6.97	0.664E 05

TOTAL CYCLES = 0.359E 09

ROOT MEAN CUBED IS 0.213E 05 AVERAGE MEAN IS 0.106E 06

TABLE H-66
CUMMULATIVE FATIGUE HISTOGRAM OUTPUT

0.900R BLADE MZ

NO. CYCLES IN 30 YEARS (TYPES 1+2)	CUM PROB	HALF-RANGE FATIGUE LOADS: LOAD LEVELS	HALF-RANGE FATIGUE LOADS: NORMALIZED LOAD LEVELS	HALF-RANGE FATIGUE LOADS: LOAD/50% AT RATED	MID-RANGE MEAN
0.180E 08	0.05000	0. - 0.110E 05	0. - 0.25	0. - 0.50	-0.181E 05
0.180E 08	0.10000	0.110E 05 - 0.115E 05	0.25 - 0.26	0.50 - 0.52	-0.179E 05
0.180E 08	0.15000	0.115E 05 - 0.118E 05	0.26 - 0.26	0.52 - 0.53	-0.178E 05
0.179E 08	0.20000	0.118E 05 - 0.121E 05	0.26 - 0.27	0.53 - 0.55	-0.177E 05
0.180E 08	0.25000	0.121E 05 - 0.123E 05	0.27 - 0.28	0.55 - 0.56	-0.175E 05
0.180E 08	0.30000	0.123E 05 - 0.125E 05	0.28 - 0.28	0.56 - 0.57	-0.174E 05
0.180E 08	0.35000	0.125E 05 - 0.128E 05	0.28 - 0.29	0.57 - 0.58	-0.173E 05
0.179E 08	0.40000	0.128E 05 - 0.129E 05	0.29 - 0.29	0.58 - 0.58	-0.172E 05
0.180E 08	0.45000	0.129E 05 - 0.131E 05	0.29 - 0.29	0.58 - 0.59	-0.171E 05
0.180E 08	0.50000	0.131E 05 - 0.133E 05	0.29 - 0.30	0.59 - 0.60	-0.170E 05
0.179E 08	0.55000	0.133E 05 - 0.135E 05	0.30 - 0.30	0.60 - 0.61	-0.168E 05
0.180E 08	0.60000	0.135E 05 - 0.137E 05	0.30 - 0.31	0.61 - 0.62	-0.166E 05
0.179E 08	0.65000	0.137E 05 - 0.139E 05	0.31 - 0.31	0.62 - 0.63	-0.165E 05
0.180E 08	0.70000	0.139E 05 - 0.141E 05	0.31 - 0.31	0.63 - 0.64	-0.164E 05
0.179E 08	0.75000	0.141E 05 - 0.143E 05	0.31 - 0.32	0.64 - 0.65	-0.164E 05
0.179E 08	0.80000	0.143E 05 - 0.146E 05	0.32 - 0.33	0.65 - 0.66	-0.164E 05
0.180E 08	0.85000	0.146E 05 - 0.149E 05	0.33 - 0.33	0.66 - 0.67	-0.164E 05
0.179E 08	0.90000	0.149E 05 - 0.153E 05	0.33 - 0.34	0.67 - 0.69	-0.164E 05
0.180E 08	0.95000	0.153E 05 - 0.159E 05	0.34 - 0.36	0.69 - 0.72	-0.164E 05
0.718E 07	0.97000	0.159E 05 - 0.164E 05	0.36 - 0.37	0.72 - 0.74	-0.164E 05
0.718E 07	0.99000	0.164E 05 - 0.173E 05	0.37 - 0.39	0.74 - 0.78	-0.167E 05
0.323E 07	0.99900	0.173E 05 - 0.186E 05	0.39 - 0.42	0.78 - 0.84	-0.171E 05
0.323E 06	0.99990	0.186E 05 - 0.225E 05	0.42 - 0.50	0.84 - 1.02	-0.202E 05

TOTAL CYCLES = 0.359E 09

ROOT MEAN CUBED IS 0.134E 05 AVERAGE MEAN IS -0.170E 05

TABLE H- 67
CUMULATIVE FATIGUE HISTOGRAM OUTPUT

TEETER BRNG VX

NO. CYCLES IN 30 YEARS (TYPES 1+2)	CUM PROB	HALF-RANGE FATIGUE LOADS: LOAD LEVELS	NORMALIZED LOAD LEVELS	LOAD/50% AT RATED	CORRESPONDING MID-RANGE LOAD DISTRIBUTION: MEAN	STANDARD DEVIATION	MAXIMUM	MINIMUM
0.	0.	0. - 0.227E 05	0. - 0.06	0. - 0.08	0.	0.	0.	0.
0.	0.	0.227E 05 - 0.454E 05	0.06 - 0.12	0.08 - 0.15	0.	0.	0.	0.
0.	0.	0.454E 05 - 0.681E 05	0.12 - 0.18	0.15 - 0.23	0.	0.	0.	0.
0.	0.	0.681E 05 - 0.908E 05	0.18 - 0.24	0.23 - 0.31	0.	0.	0.	0.
0.	0.	0.908E 05 - 0.114E 06	0.24 - 0.30	0.31 - 0.38	0.	0.	0.	0.
0.	0.	0.114E 06 - 0.136E 06	0.30 - 0.36	0.38 - 0.46	0.	0.	0.	0.
0.	0.	0.136E 06 - 0.159E 06	0.36 - 0.42	0.46 - 0.54	0.	0.	0.	0.
0.	0.	0.159E 06 - 0.182E 06	0.42 - 0.48	0.54 - 0.62	0.	0.	0.	0.
0.	0.	0.182E 06 - 0.204E 06	0.48 - 0.54	0.62 - 0.69	0.	0.	0.	0.
0.	0.	0.204E 06 - 0.227E 06	0.54 - 0.60	0.69 - 0.77	0.	0.	0.	0.
0.	0.	0.227E 06 - 0.250E 06	0.60 - 0.66	0.77 - 0.85	0.	0.	0.	0.
0.537E 07	0.01495	0.250E 06 - 0.272E 06	0.66 - 0.72	0.85 - 0.92	-0.108E 01	0.203E 03	0.575E 03	-0.288E 03
0.134E 09	0.38890	0.272E 06 - 0.295E 06	0.72 - 0.78	0.92 - 1.00	-0.303E 02	0.201E 03	0.575E 03	-0.288E 03
0.829E 08	0.61987	0.295E 06 - 0.301E 06	0.78 - 0.80	1.00 - 1.02	-0.453E 02	0.192E 03	0.575E 03	-0.322E 03
0.590E 08	0.78478	0.301E 06 - 0.308E 06	0.80 - 0.82	1.02 - 1.04	-0.547E 02	0.196E 03	0.575E 03	-0.288E 03
0.401E 08	0.89601	0.308E 06 - 0.314E 06	0.82 - 0.83	1.04 - 1.06	-0.619E 02	0.194E 03	0.575E 03	-0.288E 03
0.219E 08	0.95708	0.314E 06 - 0.320E 06	0.83 - 0.85	1.06 - 1.09	-0.666E 02	0.194E 03	0.575E 03	-0.288E 03
0.980E 07	0.98438	0.320E 06 - 0.327E 06	0.85 - 0.87	1.09 - 1.11	-0.662E 02	0.199E 03	0.575E 03	-0.288E 03
0.370E 07	0.99468	0.327E 06 - 0.333E 06	0.87 - 0.88	1.11 - 1.13	-0.502E 02	0.218E 03	0.575E 03	-0.288E 03
0.129E 07	0.99826	0.333E 06 - 0.339E 06	0.88 - 0.90	1.13 - 1.15	-0.261E 01	0.253E 03	0.575E 03	-0.288E 03
0.445E 06	0.99940	0.339E 06 - 0.345E 06	0.90 - 0.92	1.15 - 1.17	0.109E 03	0.318E 03	0.575E 03	-0.288E 03
0.753E 05	0.99971	0.345E 06 - 0.352E 06	0.92 - 0.93	1.17 - 1.19	0.431E 03	0.	0.431E 03	0.431E 03
0.405E 05	0.99983	0.352E 06 - 0.358E 06	0.93 - 0.95	1.19 - 1.21	0.431E 03	0.442E-01	0.431E 03	0.431E 03
0.183E 05	0.99988	0.358E 06 - 0.364E 06	0.95 - 0.97	1.21 - 1.23	0.431E 03	0.	0.431E 03	0.431E 03
0.704E 04	0.99990	0.364E 06 - 0.371E 06	0.97 - 0.98	1.23 - 1.26	0.431E 03	0.	0.431E 03	0.431E 03
0.231E 04	0.99990	0.371E 06 - 0.377E 06	0.98 - 1.00	1.26 - 1.28	0.431E 03	0.	0.431E 03	0.431E 03

TOTAL CYCLES = 0.359E 09

ROOT MEAN CUBED IS 0.298E 06 AVERAGE MEAN IS -0.438E 02

TABLE H- 68
CUMULATIVE FATIGUE HISTOGRAM OUTPUT

TEETER BRNG VY

NO. CYCLES IN 30 YEARS (TYPES 1+2)	CUM PROB	HALF-RANGE FATIGUE LOADS: LOAD LEVELS	NORMALIZED LOAD LEVELS	LOAD/50% AT RATED	CORRESPONDING MID-RANGE LOAD DISTRIBUTION: MEAN	STANDARD DEVIATION	MAXIMUM	MINIMUM
0.	0.	0. - 0.246E 05	0. - 0.06	0. - 0.08	0.	0.	0.	0.
0.	0.	0.246E 05 - 0.491E 05	0.06 - 0.12	0.08 - 0.15	0.	0.	0.	0.
0.	0.	0.491E 05 - 0.737E 05	0.12 - 0.18	0.15 - 0.23	0.	0.	0.	0.
0.	0.	0.737E 05 - 0.982E 05	0.18 - 0.24	0.23 - 0.31	0.	0.	0.	0.
0.	0.	0.982E 05 - 0.123E 06	0.24 - 0.30	0.31 - 0.38	0.	0.	0.	0.
0.	0.	0.123E 06 - 0.147E 06	0.30 - 0.36	0.38 - 0.46	0.	0.	0.	0.
0.	0.	0.147E 06 - 0.172E 06	0.36 - 0.42	0.46 - 0.54	0.	0.	0.	0.
0.	0.	0.172E 06 - 0.196E 06	0.42 - 0.48	0.54 - 0.62	0.	0.	0.	0.
0.	0.	0.196E 06 - 0.221E 06	0.48 - 0.54	0.62 - 0.69	0.	0.	0.	0.
0.	0.	0.221E 06 - 0.246E 06	0.54 - 0.60	0.69 - 0.77	0.	0.	0.	0.
0.	0.	0.246E 06 - 0.270E 06	0.60 - 0.66	0.77 - 0.85	0.	0.	0.	0.
0.145E 08	0.04027	0.270E 06 - 0.295E 06	0.66 - 0.72	0.85 - 0.92	-0.472E 03	0.138E 03	-0.288E 03	-0.575E 03
0.192E 09	0.57602	0.295E 06 - 0.319E 06	0.72 - 0.78	0.92 - 1.00	-0.479E 03	0.149E 03	0.165E 03	-0.575E 03
0.684E 08	0.76643	0.319E 06 - 0.326E 06	0.78 - 0.80	1.00 - 1.02	-0.508E 03	0.121E 03	-0.288E 03	-0.575E 03
0.435E 08	0.88755	0.326E 06 - 0.333E 06	0.80 - 0.81	1.02 - 1.04	-0.509E 03	0.121E 03	-0.288E 03	-0.575E 03
0.238E 08	0.95390	0.333E 06 - 0.340E 06	0.81 - 0.83	1.04 - 1.06	-0.516E 03	0.116E 03	-0.288E 03	-0.575E 03
0.105E 08	0.98321	0.340E 06 - 0.347E 06	0.83 - 0.85	1.06 - 1.09	-0.522E 03	0.111E 03	-0.288E 03	-0.575E 03
0.387E 07	0.99399	0.347E 06 - 0.354E 06	0.85 - 0.87	1.09 - 1.11	-0.530E 03	0.105E 03	-0.288E 03	-0.575E 03
0.137E 07	0.99780	0.354E 06 - 0.361E 06	0.87 - 0.88	1.11 - 1.13	-0.533E 03	0.101E 03	-0.288E 03	-0.575E 03
0.428E 06	0.99899	0.361E 06 - 0.367E 06	0.88 - 0.90	1.13 - 1.15	-0.575E 03	0.	-0.575E 03	-0.575E 03
0.179E 06	0.99949	0.367E 06 - 0.374E 06	0.90 - 0.92	1.15 - 1.17	-0.575E 03	0.884E-01	-0.575E 03	-0.575E 03
0.776E 05	0.99971	0.374E 06 - 0.381E 06	0.92 - 0.93	1.17 - 1.19	-0.575E 03	0.	-0.575E 03	-0.575E 03
0.418E 05	0.99982	0.381E 06 - 0.388E 06	0.93 - 0.95	1.19 - 1.22	-0.575E 03	0.	-0.575E 03	-0.575E 03
0.189E 05	0.99988	0.388E 06 - 0.395E 06	0.95 - 0.97	1.22 - 1.24	-0.575E 03	0.	-0.575E 03	-0.575E 03
0.720E 04	0.99990	0.395E 06 - 0.402E 06	0.97 - 0.98	1.24 - 1.26	-0.575E 03	0.	-0.575E 03	-0.575E 03
0.235E 04	0.99990	0.402E 06 - 0.409E 06	0.98 - 1.00	1.26 - 1.28	-0.575E 03	0.	-0.575E 03	-0.575E 03

TOTAL CYCLES = 0.359E 09

ROOT MEAN CUBED IS 0.316E 06 AVERAGE MEAN IS -0.492E 03

TABLE H- 69
CUMULATIVE FATIGUE HISTOGRAM OUTPUT

TEETER BRNG VZ

NO. CYCLES IN 30 YEARS (TYPES 1+2)	CUM PROB	HALF-RANGE FATIGUE LOADS: LOAD LEVELS	NORMALIZED LOAD LEVELS	LOAD/50% AT RATED	CORRESPONDING MID-RANGE LOAD DISTRIBUTION: MEAN	STANDARD DEVIATION	MAXIMUM	MINIMUM
0.	0.	0. - 0.127E 04	0. - 0.01	0. - 0.08	0.	0.	0.	0.
0.	0.	0.127E 04 - 0.254E 04	0.01 - 0.03	0.08 - 0.15	0.	0.	0.	0.
0.194E 06	0.00054	0.254E 04 - 0.381E 04	0.03 - 0.04	0.15 - 0.23	-0.118E 06	0.113E 02	-0.118E 06	-0.118E 06
0.225E 07	0.00680	0.381E 04 - 0.508E 04	0.04 - 0.05	0.23 - 0.31	-0.136E 06	0.291E 05	-0.118E 06	-0.224E 06
0.790E 07	0.02881	0.508E 04 - 0.635E 04	0.05 - 0.07	0.31 - 0.38	-0.145E 06	0.402E 05	-0.118E 06	-0.268E 06
0.164E 08	0.07444	0.635E 04 - 0.762E 04	0.07 - 0.08	0.38 - 0.46	-0.152E 06	0.439E 05	-0.118E 06	-0.268E 06
0.250E 08	0.14413	0.762E 04 - 0.888E 04	0.08 - 0.09	0.46 - 0.54	-0.160E 06	0.474E 05	-0.118E 06	-0.268E 06
0.314E 08	0.23148	0.888E 04 - 0.102E 05	0.09 - 0.11	0.54 - 0.62	-0.167E 06	0.500E 05	-0.118E 06	-0.268E 06
0.345E 08	0.32746	0.102E 05 - 0.114E 05	0.11 - 0.12	0.62 - 0.69	-0.174E 06	0.517E 05	-0.118E 06	-0.268E 06
0.346E 08	0.42378	0.114E 05 - 0.127E 05	0.12 - 0.13	0.69 - 0.77	-0.180E 06	0.527E 05	-0.117E 06	-0.268E 06
0.327E 08	0.51480	0.127E 05 - 0.140E 05	0.13 - 0.15	0.77 - 0.85	-0.186E 06	0.532E 05	-0.116E 06	-0.268E 06
0.295E 08	0.59707	0.140E 05 - 0.152E 05	0.15 - 0.16	0.85 - 0.92	-0.191E 06	0.534E 05	-0.114E 06	-0.268E 06
0.257E 08	0.66853	0.152E 05 - 0.165E 05	0.16 - 0.17	0.92 - 1.00	-0.195E 06	0.531E 05	-0.113E 06	-0.268E 06
0.749E 08	0.87715	0.165E 05 - 0.225E 05	0.17 - 0.24	1.00 - 1.36	-0.204E 06	0.521E 05	-0.109E 06	-0.268E 06
0.280E 08	0.95510	0.225E 05 - 0.285E 05	0.24 - 0.30	1.36 - 1.73	-0.214E 06	0.497E 05	-0.103E 06	-0.268E 06
0.975E 07	0.98225	0.285E 05 - 0.346E 05	0.30 - 0.36	1.73 - 2.09	-0.219E 06	0.476E 05	-0.974E 05	-0.268E 06
0.364E 07	0.99239	0.346E 05 - 0.406E 05	0.36 - 0.43	2.09 - 2.46	-0.225E 06	0.410E 05	-0.925E 05	-0.268E 06
0.147E 07	0.99648	0.406E 05 - 0.466E 05	0.43 - 0.49	2.46 - 2.82	-0.232E 06	0.342E 05	-0.120E 06	-0.268E 06
0.764E 06	0.99860	0.466E 05 - 0.526E 05	0.49 - 0.56	2.82 - 3.19	-0.235E 06	0.304E 05	-0.120E 06	-0.268E 06
0.269E 06	0.99935	0.526E 05 - 0.586E 05	0.56 - 0.62	3.19 - 3.55	-0.228E 06	0.275E 05	-0.121E 06	-0.264E 06
0.126E 06	0.99971	0.586E 05 - 0.646E 05	0.62 - 0.68	3.55 - 3.92	-0.230E 06	0.234E 05	-0.167E 06	-0.267E 06
0.580E 05	0.99987	0.646E 05 - 0.707E 05	0.68 - 0.75	3.92 - 4.28	-0.224E 06	0.977E 04	-0.167E 06	-0.231E 06
0.707E 04	0.99989	0.707E 05 - 0.767E 05	0.75 - 0.81	4.28 - 4.65	-0.219E 06	0.153E 05	-0.168E 06	-0.231E 06
0.308E 04	0.99990	0.767E 05 - 0.827E 05	0.81 - 0.87	4.65 - 5.01	-0.224E 06	0.226E 02	-0.224E 06	-0.224E 06
0.143E 04	0.99990	0.827E 05 - 0.887E 05	0.87 - 0.94	5.01 - 5.38	-0.224E 06	0.	-0.224E 06	-0.224E 06
0.944E 03	0.99990	0.887E 05 - 0.947E 05	0.94 - 1.00	5.38 - 5.74	-0.224E 06	0.	-0.224E 06	-0.224E 06

TOTAL CYCLES = 0.359E 09

ROOT MEAN CUBED IS 0.185E 05 AVERAGE MEAN IS -0.186E 06

TABLE H- 70
CUMULATIVE FATIGUE HISTOGRAM OUTPUT

TEETER BRNG HX

NO. CYCLES IN 30 YEARS (TYPES 1+2)	CUM PROB	HALF-RANGE FATIGUE LOADS: LOAD LEVELS	HALF-RANGE FATIGUE LOADS: NORMALIZED LOAD LEVELS	HALF-RANGE FATIGUE LOADS: LOAD/50% AT RATED	CORRESPONDING MID-RANGE LOAD DISTRIBUTION: MEAN	STANDARD DEVIATION	MAXIMUM	MINIMUM
0.	0.	0. - 0.209E 05	0. - 0.07	0. - 0.08	0.	0.	0.	0.
0.	0.	0.209E 05 - 0.418E 05	0.07 - 0.14	0.08 - 0.15	0.	0.	0.	0.
0.	0.	0.418E 05 - 0.626E 05	0.14 - 0.20	0.15 - 0.23	0.	0.	0.	0.
0.	0.	0.626E 05 - 0.835E 05	0.20 - 0.27	0.23 - 0.31	0.	0.	0.	0.
0.	0.	0.835E 05 - 0.104E 06	0.27 - 0.34	0.31 - 0.38	0.	0.	0.	0.
0.229E 08	0.06365	0.104E 06 - 0.125E 06	0.34 - 0.41	0.38 - 0.46	0.690E 05	0.	0.690E 05	0.690E 05
0.731E 08	0.26712	0.125E 06 - 0.146E 06	0.41 - 0.47	0.46 - 0.54	0.690E 05	0.800E 01	0.690E 05	0.690E 05
0.130E 08	0.30322	0.146E 06 - 0.167E 06	0.47 - 0.54	0.54 - 0.62	0.693E 05	0.425E 02	0.693E 05	0.690E 05
0.855E 08	0.54129	0.167E 06 - 0.188E 06	0.54 - 0.61	0.62 - 0.69	0.692E 05	0.191E 03	0.694E 05	0.684E 05
0.228E 08	0.60481	0.188E 06 - 0.209E 06	0.61 - 0.68	0.69 - 0.77	0.687E 05	0.403E 03	0.696E 05	0.684E 05
0.512E 08	0.74747	0.209E 06 - 0.230E 06	0.68 - 0.75	0.77 - 0.85	0.690E 05	0.111E 03	0.698E 05	0.684E 05
0.222E 08	0.80942	0.230E 06 - 0.251E 06	0.75 - 0.81	0.85 - 0.92	0.690E 05	0.720E 02	0.701E 05	0.688E 05
0.327E 08	0.90056	0.251E 06 - 0.271E 06	0.81 - 0.88	0.92 - 1.00	0.690E 05	0.226E 02	0.702E 05	0.689E 05
0.911E 07	0.92591	0.271E 06 - 0.274E 06	0.88 - 0.89	1.00 - 1.01	0.690E 05	0.113E 02	0.690E 05	0.690E 05
0.615E 07	0.94305	0.274E 06 - 0.277E 06	0.89 - 0.90	1.01 - 1.02	0.690E 05	0.	0.690E 05	0.690E 05
0.558E 07	0.95804	0.277E 06 - 0.280E 06	0.90 - 0.91	1.02 - 1.03	0.690E 05	0.	0.690E 05	0.690E 05
0.444E 07	0.97040	0.280E 06 - 0.283E 06	0.91 - 0.92	1.03 - 1.04	0.690E 05	0.	0.690E 05	0.690E 05
0.345E 07	0.98002	0.283E 06 - 0.285E 06	0.92 - 0.93	1.04 - 1.05	0.690E 05	0.	0.690E 05	0.690E 05
0.254E 07	0.98710	0.285E 06 - 0.288E 06	0.93 - 0.94	1.05 - 1.06	0.690E 05	0.	0.690E 05	0.690E 05
0.178E 07	0.99205	0.288E 06 - 0.291E 06	0.94 - 0.95	1.06 - 1.07	0.690E 05	0.	0.690E 05	0.690E 05
0.118E 07	0.99532	0.291E 06 - 0.294E 06	0.95 - 0.95	1.07 - 1.08	0.690E 05	0.	0.690E 05	0.690E 05
0.740E 06	0.99738	0.294E 06 - 0.297E 06	0.95 - 0.96	1.08 - 1.09	0.690E 05	0.	0.690E 05	0.690E 05
0.443E 06	0.99861	0.297E 06 - 0.300E 06	0.96 - 0.97	1.09 - 1.10	0.690E 05	0.	0.690E 05	0.690E 05
0.253E 06	0.99932	0.300E 06 - 0.302E 06	0.97 - 0.98	1.10 - 1.11	0.690E 05	0.	0.690E 05	0.690E 05
0.138E 06	0.99970	0.302E 06 - 0.305E 06	0.98 - 0.99	1.11 - 1.12	0.690E 05	0.	0.690E 05	0.690E 05
0.718E 05	0.99990	0.305E 06 - 0.308E 06	0.99 - 1.00	1.12 - 1.13	0.690E 05	0.	0.690E 05	0.690E 05

TOTAL CYCLES = 0.359E 09

ROOT MEAN CUBED IS 0.206E 06 AVERAGE MEAN IS 0.691E 05

TABLE H- 71
CUMULATIVE FATIGUE HISTOGRAM OUTPUT

TEETER BRNG MY

NO. CYCLES IN 30 YEARS (TYPES 1+2)	CUM PROB	HALF-RANGE FATIGUE LOADS: LOAD LEVELS	HALF-RANGE FATIGUE LOADS: NORMALIZED LOAD LEVELS	HALF-RANGE FATIGUE LOADS: LOAD/50% AT RATED	CORRESPONDING MID-RANGE LOAD DISTRIBUTION: MEAN	STANDARD DEVIATION	MAXIMUM	MINIMUM
0.	0.	0. - 0.529E 04	0. - 0.02	0. - 0.08	0.	0.	0.	0.
0.	0.	0.529E 04 - 0.106E 05	0.02 - 0.04	0.08 - 0.15	0.	0.	0.	0.
0.	0.	0.106E 05 - 0.159E 05	0.04 - 0.06	0.15 - 0.23	0.	0.	0.	0.
0.339E 05	0.00009	0.159E 05 - 0.212E 05	0.06 - 0.09	0.23 - 0.31	0.694E 05	0.115E 03	0.694E 05	0.687E 05
0.121E 07	0.00346	0.212E 05 - 0.265E 05	0.09 - 0.11	0.31 - 0.38	0.694E 05	0.729E 02	0.695E 05	0.687E 05
0.357E 07	0.01340	0.265E 05 - 0.318E 05	0.11 - 0.13	0.38 - 0.46	0.694E 05	0.720E 02	0.695E 05	0.687E 05
0.797E 07	0.03558	0.318E 05 - 0.371E 05	0.13 - 0.15	0.46 - 0.54	0.694E 05	0.697E 02	0.695E 05	0.687E 05
0.136E 08	0.07354	0.371E 05 - 0.424E 05	0.15 - 0.17	0.54 - 0.62	0.694E 05	0.693E 02	0.695E 05	0.687E 05
0.194E 08	0.12753	0.424E 05 - 0.476E 05	0.17 - 0.19	0.62 - 0.69	0.694E 05	0.674E 02	0.695E 05	0.687E 05
0.242E 08	0.19484	0.476E 05 - 0.529E 05	0.19 - 0.21	0.69 - 0.77	0.694E 05	0.660E 02	0.695E 05	0.687E 05
0.273E 08	0.27097	0.529E 05 - 0.582E 05	0.21 - 0.23	0.77 - 0.85	0.694E 05	0.640E 02	0.695E 05	0.687E 05
0.291E 08	0.35204	0.582E 05 - 0.635E 05	0.23 - 0.26	0.85 - 0.92	0.694E 05	0.645E 02	0.695E 05	0.687E 05
0.289E 08	0.43260	0.635E 05 - 0.688E 05	0.26 - 0.28	0.92 - 1.00	0.694E 05	0.660E 02	0.695E 05	0.687E 05
0.782E 08	0.65039	0.688E 05 - 0.826E 05	0.28 - 0.33	1.00 - 1.20	0.694E 05	0.577E 02	0.695E 05	0.687E 05
0.500E 08	0.78974	0.826E 05 - 0.964E 05	0.33 - 0.39	1.20 - 1.40	0.694E 05	0.936E 02	0.698E 05	0.687E 05
0.312E 08	0.87658	0.964E 05 - 0.110E 06	0.39 - 0.44	1.40 - 1.60	0.694E 05	0.593E 02	0.701E 05	0.687E 05
0.189E 08	0.92926	0.110E 06 - 0.124E 06	0.44 - 0.50	1.60 - 1.80	0.694E 05	0.560E 02	0.703E 05	0.687E 05
0.110E 08	0.95999	0.124E 06 - 0.138E 06	0.50 - 0.56	1.80 - 2.00	0.694E 05	0.543E 02	0.706E 05	0.687E 05
0.629E 07	0.97752	0.138E 06 - 0.151E 06	0.56 - 0.61	2.00 - 2.20	0.694E 05	0.512E 02	0.695E 05	0.687E 05
0.355E 07	0.98740	0.151E 06 - 0.165E 06	0.61 - 0.67	2.20 - 2.40	0.694E 05	0.518E 02	0.695E 05	0.687E 05
0.199E 07	0.99295	0.165E 06 - 0.179E 06	0.67 - 0.72	2.40 - 2.60	0.694E 05	0.487E 02	0.695E 05	0.687E 05
0.112E 07	0.99607	0.179E 06 - 0.193E 06	0.72 - 0.78	2.60 - 2.80	0.694E 05	0.473E 02	0.695E 05	0.687E 05
0.641E 06	0.99785	0.193E 06 - 0.207E 06	0.78 - 0.83	2.80 - 3.00	0.694E 05	0.525E 02	0.695E 05	0.687E 05
0.485E 06	0.99920	0.207E 06 - 0.220E 06	0.83 - 0.89	3.00 - 3.20	0.694E 05	0.512E 02	0.695E 05	0.694E 05
0.189E 06	0.99973	0.220E 06 - 0.234E 06	0.89 - 0.94	3.20 - 3.40	0.694E 05	0.179E 02	0.694E 05	0.694E 05
0.627E 05	0.99990	0.234E 06 - 0.248E 06	0.94 - 1.00	3.40 - 3.60	0.694E 05	0.	0.694E 05	0.694E 05

TOTAL CYCLES = 0.359E 09

ROOT MEAN CUBED IS 0.884E 05 AVERAGE MEAN IS 0.694E 05

TABLE H- 72
CUMULATIVE FATIGUE HISTOGRAM OUTPUT

TEETER BRNG MZ

NO. CYCLES IN 30 YEARS (TYPES 1+2)	CUM PROB	HALF-RANGE FATIGUE LOADS: LOAD LEVELS	NORMALIZED LOAD LEVELS	LOAD/50% AT RATED	CORRESPONDING MID-RANGE LOAD DISTRIBUTION: MEAN	STANDARD DEVIATION	MAXIMUM	MINIMUM
0.	0.	0. - 0.127E 05	0. - 0.01	0. - 0.08	0.	0.	0.	0.
0.	0.	0.127E 05 - 0.255E 05	0.01 - 0.01	0.08 - 0.15	0.	0.	0.	0.
0.	0.	0.255E 05 - 0.382E 05	0.01 - 0.02	0.15 - 0.23	0.	0.	0.	0.
0.	0.	0.382E 05 - 0.510E 05	0.02 - 0.02	0.23 - 0.31	0.	0.	0.	0.
0.104E 07	0.00290	0.510E 05 - 0.637E 05	0.02 - 0.03	0.31 - 0.38	-0.200E 07	0.141E 07	-0.631E 06	-0.396E 07
0.310E 07	0.01154	0.637E 05 - 0.764E 05	0.03 - 0.03	0.38 - 0.46	-0.203E 07	0.138E 07	-0.631E 06	-0.396E 07
0.706E 07	0.03120	0.764E 05 - 0.892E 05	0.03 - 0.04	0.46 - 0.54	-0.203E 07	0.136E 07	-0.631E 06	-0.396E 07
0.123E 08	0.06543	0.892E 05 - 0.102E 06	0.04 - 0.05	0.54 - 0.62	-0.203E 07	0.133E 07	-0.631E 06	-0.396E 07
0.178E 08	0.11494	0.102E 06 - 0.115E 06	0.05 - 0.05	0.62 - 0.69	-0.204E 07	0.131E 07	-0.631E 06	-0.396E 07
0.225E 08	0.17761	0.115E 06 - 0.127E 06	0.05 - 0.06	0.69 - 0.77	-0.204E 07	0.129E 07	-0.631E 06	-0.396E 07
0.258E 08	0.24956	0.127E 06 - 0.140E 06	0.06 - 0.06	0.77 - 0.85	-0.205E 07	0.127E 07	-0.631E 06	-0.396E 07
0.276E 08	0.32630	0.140E 06 - 0.153E 06	0.06 - 0.07	0.85 - 0.92	-0.205E 07	0.126E 07	-0.631E 06	-0.396E 07
0.278E 08	0.40363	0.153E 06 - 0.166E 06	0.07 - 0.08	0.92 - 1.00	-0.206E 07	0.124E 07	-0.631E 06	-0.396E 07
0.181E 09	0.90779	0.166E 06 - 0.321E 06	0.08 - 0.15	1.00 - 1.94	-0.208E 07	0.120E 07	-0.552E 06	-0.396E 07
0.233E 08	0.97281	0.321E 06 - 0.477E 06	0.15 - 0.22	1.94 - 2.88	-0.205E 07	0.113E 07	-0.476E 06	-0.396E 07
0.480E 07	0.98618	0.477E 06 - 0.632E 06	0.22 - 0.29	2.88 - 3.82	-0.209E 07	0.102E 07	-0.555E 06	-0.396E 07
0.185E 07	0.99133	0.632E 06 - 0.788E 06	0.29 - 0.36	3.82 - 4.76	-0.237E 07	0.926E 06	-0.644E 06	-0.393E 07
0.101E 07	0.99415	0.788E 06 - 0.944E 06	0.36 - 0.43	4.76 - 5.70	-0.255E 07	0.800E 06	-0.709E 06	-0.328E 07
0.696E 06	0.99609	0.944E 06 - 0.110E 07	0.43 - 0.50	5.70 - 6.64	-0.268E 07	0.692E 06	-0.739E 06	-0.312E 07
0.462E 06	0.99737	0.110E 07 - 0.125E 07	0.50 - 0.57	6.64 - 7.58	-0.268E 07	0.574E 06	-0.125E 07	-0.297E 07
0.319E 06	0.99826	0.125E 07 - 0.141E 07	0.57 - 0.64	7.58 - 8.52	-0.266E 07	0.393E 06	-0.134E 07	-0.282E 07
0.223E 06	0.99888	0.141E 07 - 0.157E 07	0.64 - 0.72	8.52 - 9.46	-0.259E 07	0.226E 06	-0.149E 07	-0.273E 07
0.149E 06	0.99930	0.157E 07 - 0.172E 07	0.72 - 0.79	9.46 - 10.40	-0.247E 07	0.126E 06	-0.160E 07	-0.256E 07
0.101E 06	0.99958	0.172E 07 - 0.188E 07	0.79 - 0.86	10.40 - 11.34	-0.233E 07	0.257E 05	-0.224E 07	-0.237E 07
0.724E 05	0.99978	0.188E 07 - 0.203E 07	0.86 - 0.93	11.34 - 12.28	-0.218E 07	0.702E 04	-0.215E 07	-0.218E 07
0.449E 05	0.99990	0.203E 07 - 0.219E 07	0.93 - 1.00	12.28 - 13.22	-0.209E 07	0.116E 05	-0.202E 07	-0.209E 07

TOTAL CYCLES = 0.359E 09

ROOT MEAN CUBED IS 0.320E 06 AVERAGE MEAN IS -0.207E 07

TABLE H- 73
CUMULATIVE FATIGUE HISTOGRAM OUTPUT

ROTOR-CL-STA YX

NO. CYCLES IN 30 YEARS (TYPES 1+2)	CUM PROB	HALF-RANGE FATIGUE LOADS: LOAD LEVELS	NORMALIZED LOAD LEVELS	LOAD/50% AT RATED	CORRESPONDING MID-RANGE LOAD DISTRIBUTION: MEAN	STANDARD DEVIATION	MAXIMUM	MINIMUM
0.	0.	0. - 0.111E 04	0. - 0.05	0. - 0.08	0.	0.	0.	0.
0.	0.	0.111E 04 - 0.221E 04	0.05 - 0.10	0.08 - 0.15	0.	0.	0.	0.
0.	0.	0.221E 04 - 0.332E 04	0.10 - 0.16	0.15 - 0.23	0.	0.	0.	0.
0.	0.	0.332E 04 - 0.442E 04	0.16 - 0.21	0.23 - 0.31	0.	0.	0.	0.
0.	0.	0.442E 04 - 0.553E 04	0.21 - 0.26	0.31 - 0.38	0.	0.	0.	0.
0.134E 07	0.00374	0.553E 04 - 0.663E 04	0.26 - 0.31	0.38 - 0.46	-0.307E 06	0.128E 03	-0.307E 06	-0.307E 06
0.242E 08	0.07103	0.663E 04 - 0.774E 04	0.31 - 0.37	0.46 - 0.54	-0.307E 06	0.143E 03	-0.307E 06	-0.307E 06
0.778E 08	0.28758	0.774E 04 - 0.885E 04	0.37 - 0.42	0.54 - 0.62	-0.307E 06	0.139E 03	-0.307E 06	-0.307E 06
0.671E 08	0.47452	0.885E 04 - 0.995E 04	0.42 - 0.47	0.62 - 0.69	-0.307E 06	0.181E 03	-0.307E 06	-0.308E 06
0.230E 08	0.53848	0.995E 04 - 0.111E 05	0.47 - 0.52	0.69 - 0.77	-0.307E 06	0.197E 03	-0.307E 06	-0.309E 06
0.146E 08	0.57925	0.111E 05 - 0.122E 05	0.52 - 0.57	0.77 - 0.85	-0.308E 06	0.283E 03	-0.307E 06	-0.309E 06
0.293E 08	0.66096	0.122E 05 - 0.133E 05	0.57 - 0.63	0.85 - 0.92	-0.308E 06	0.229E 03	-0.307E 06	-0.309E 06
0.441E 08	0.78374	0.133E 05 - 0.144E 05	0.63 - 0.68	0.92 - 1.00	-0.308E 06	0.231E 03	-0.307E 06	-0.309E 06
0.216E 08	0.84389	0.144E 05 - 0.149E 05	0.68 - 0.70	1.00 - 1.04	-0.308E 06	0.229E 03	-0.307E 06	-0.309E 06
0.172E 08	0.89173	0.149E 05 - 0.154E 05	0.70 - 0.73	1.04 - 1.07	-0.308E 06	0.262E 03	-0.307E 06	-0.309E 06
0.129E 08	0.92765	0.154E 05 - 0.159E 05	0.73 - 0.75	1.07 - 1.11	-0.308E 06	0.252E 03	-0.307E 06	-0.310E 06
0.947E 07	0.95402	0.159E 05 - 0.165E 05	0.75 - 0.78	1.11 - 1.15	-0.308E 06	0.256E 03	-0.307E 06	-0.309E 06
0.650E 07	0.97211	0.165E 05 - 0.170E 05	0.78 - 0.80	1.15 - 1.18	-0.308E 06	0.260E 03	-0.307E 06	-0.309E 06
0.420E 07	0.98380	0.170E 05 - 0.175E 05	0.80 - 0.83	1.18 - 1.22	-0.308E 06	0.260E 03	-0.307E 06	-0.309E 06
0.257E 07	0.99095	0.175E 05 - 0.180E 05	0.83 - 0.85	1.22 - 1.26	-0.308E 06	0.268E 03	-0.307E 06	-0.309E 06
0.149E 07	0.99512	0.180E 05 - 0.186E 05	0.85 - 0.88	1.26 - 1.29	-0.308E 06	0.268E 03	-0.307E 06	-0.309E 06
0.831E 06	0.99743	0.186E 05 - 0.191E 05	0.88 - 0.90	1.29 - 1.33	-0.308E 06	0.272E 03	-0.307E 06	-0.309E 06
0.444E 06	0.99867	0.191E 05 - 0.196E 05	0.90 - 0.93	1.33 - 1.36	-0.308E 06	0.272E 03	-0.307E 06	-0.309E 06
0.269E 06	0.99942	0.196E 05 - 0.201E 05	0.93 - 0.95	1.36 - 1.40	-0.308E 06	0.256E 03	-0.307E 06	-0.309E 06
0.135E 06	0.99979	0.201E 05 - 0.207E 05	0.95 - 0.98	1.40 - 1.44	-0.308E 06	0.292E 03	-0.307E 06	-0.309E 06
0.396E 05	0.99990	0.207E 05 - 0.212E 05	0.98 - 1.00	1.44 - 1.47	-0.308E 06	0.	-0.308E 06	-0.308E 06

TOTAL CYCLES = 0.359E 09

ROOT MEAN CUBED IS 0.121E 05 AVERAGE MEAN IS -0.307E 06

TABLE H- 74
CUMULATIVE FATIGUE HISTOGRAM OUTPUT

ROTOR-CL-STA VY

NO. CYCLES IN 30 YEARS (TYPES 1+2)	CUM PROB	HALF-RANGE FATIGUE LOADS: LOAD LEVELS	NORMALIZED LOAD LEVELS	LOAD/50% AT RATED	CORRESPONDING MID-RANGE LOAD DISTRIBUTION: MEAN	STANDARD DEVIATION	MAXIMUM	MINIMUM
0.	0.	0. - 0.630E 03	0. - 0.05	0. - 0.08	0.	0.	0.	0.
0.	0.	0.630E 03 - 0.126E 04	0.05 - 0.10	0.08 - 0.15	0.	0.	0.	0.
0.	0.	0.126E 04 - 0.189E 04	0.10 - 0.15	0.15 - 0.23	0.	0.	0.	0.
0.313E 08	0.08710	0.189E 04 - 0.252E 04	0.15 - 0.20	0.23 - 0.31	0.427E 03	0.163E 03	0.713E 03	0.334E 03
0.127E 09	0.44192	0.252E 04 - 0.315E 04	0.20 - 0.25	0.31 - 0.38	0.520E 03	0.191E 03	0.789E 03	0.193E 03
0.350E 08	0.53933	0.315E 04 - 0.378E 04	0.25 - 0.30	0.38 - 0.46	0.639E 03	0.192E 03	0.110E 04	0.334E 03
0.145E 07	0.54337	0.378E 04 - 0.441E 04	0.30 - 0.35	0.46 - 0.54	0.680E 03	0.139E 03	0.139E 04	0.334E 03
0.	0.54337	0.441E 04 - 0.504E 04	0.35 - 0.40	0.54 - 0.62	0.	0.	0.	0.
0.122E 06	0.54371	0.504E 04 - 0.567E 04	0.40 - 0.45	0.62 - 0.69	0.496E 03	0.442E-01	0.496E 03	0.496E 03
0.220E 07	0.54983	0.567E 04 - 0.630E 04	0.45 - 0.49	0.69 - 0.77	0.618E 03	0.184E 03	0.897E 03	0.496E 03
0.115E 08	0.58180	0.630E 04 - 0.693E 04	0.49 - 0.54	0.77 - 0.85	0.640E 03	0.190E 03	0.897E 03	0.496E 03
0.286E 08	0.66155	0.693E 04 - 0.756E 04	0.54 - 0.59	0.85 - 0.92	0.665E 03	0.195E 03	0.897E 03	0.496E 03
0.425E 08	0.78001	0.756E 04 - 0.819E 04	0.59 - 0.64	0.92 - 1.00	0.682E 03	0.193E 03	0.897E 03	0.450E 03
0.234E 08	0.84504	0.819E 04 - 0.854E 04	0.64 - 0.67	1.00 - 1.04	0.723E 03	0.186E 03	0.897E 03	0.496E 03
0.183E 08	0.89591	0.854E 04 - 0.889E 04	0.67 - 0.70	1.04 - 1.09	0.728E 03	0.184E 03	0.897E 03	0.496E 03
0.142E 08	0.93546	0.889E 04 - 0.924E 04	0.70 - 0.73	1.09 - 1.13	0.741E 03	0.174E 03	0.113E 04	0.496E 03
0.924E 07	0.96120	0.924E 04 - 0.959E 04	0.73 - 0.75	1.13 - 1.17	0.749E 03	0.171E 03	0.897E 03	0.496E 03
0.596E 07	0.97779	0.959E 04 - 0.994E 04	0.75 - 0.78	1.17 - 1.21	0.760E 03	0.162E 03	0.897E 03	0.496E 03
0.361E 07	0.98784	0.994E 04 - 0.103E 05	0.78 - 0.81	1.21 - 1.26	0.769E 03	0.152E 03	0.897E 03	0.496E 03
0.207E 07	0.99360	0.103E 05 - 0.106E 05	0.81 - 0.84	1.26 - 1.30	0.776E 03	0.141E 03	0.897E 03	0.496E 03
0.113E 07	0.99675	0.106E 05 - 0.110E 05	0.84 - 0.86	1.30 - 1.34	0.782E 03	0.130E 03	0.897E 03	0.496E 03
0.637E 06	0.99852	0.110E 05 - 0.113E 05	0.86 - 0.89	1.34 - 1.38	0.766E 03	0.137E 03	0.897E 03	0.496E 03
0.322E 06	0.99942	0.113E 05 - 0.117E 05	0.89 - 0.92	1.38 - 1.43	0.835E 03	0.536E 02	0.897E 03	0.628E 03
0.100E 06	0.99970	0.117E 05 - 0.120E 05	0.92 - 0.95	1.43 - 1.47	0.791E 03	0.216E 02	0.794E 03	0.628E 03
0.494E 05	0.99984	0.120E 05 - 0.124E 05	0.95 - 0.97	1.47 - 1.51	0.794E 03	0.	0.794E 03	0.794E 03
0.236E 05	0.99990	0.124E 05 - 0.127E 05	0.97 - 1.00	1.51 - 1.55	0.794E 03	0.	0.794E 03	0.794E 03

TOTAL CYCLES = 0.359E 09

ROOT MEAN CUBED IS 0.651E 04 AVERAGE MEAN IS 0.607E 03

TABLE H- 75
CUMULATIVE FATIGUE HISTOGRAM OUTPUT

ROTOR-CL-STA VZ

NO. CYCLES IN 30 YEARS (TYPES 1+2)	CUM PROB	HALF-RANGE FATIGUE LOADS: LOAD LEVELS	NORMALIZED LOAD LEVELS	LOAD/50% AT RATED	CORRESPONDING MID-RANGE LOAD DISTRIBUTION: MEAN	STANDARD DEVIATION	MAXIMUM	MINIMUM
0.	0.	0. - 0.115E 04	0. - 0.01	0. - 0.08	0.	0.	0.	0.
0.	0.	0.115E 04 - 0.231E 04	0.01 - 0.02	0.08 - 0.15	0.	0.	0.	0.
0.243E 06	0.00068	0.231E 04 - 0.346E 04	0.02 - 0.04	0.15 - 0.23	-0.115E 06	0.113E 02	-0.115E 06	-0.115E 06
0.253E 07	0.00771	0.346E 04 - 0.462E 04	0.04 - 0.05	0.23 - 0.31	-0.130E 06	0.261E 05	-0.115E 06	-0.217E 06
0.855E 07	0.03152	0.462E 04 - 0.577E 04	0.05 - 0.06	0.31 - 0.38	-0.140E 06	0.389E 05	-0.115E 06	-0.266E 06
0.171E 08	0.07918	0.577E 04 - 0.692E 04	0.06 - 0.07	0.38 - 0.46	-0.147E 06	0.430E 05	-0.115E 06	-0.266E 06
0.255E 08	0.15022	0.692E 04 - 0.808E 04	0.07 - 0.09	0.46 - 0.54	-0.155E 06	0.471E 05	-0.115E 06	-0.266E 06
0.314E 08	0.23779	0.808E 04 - 0.923E 04	0.09 - 0.10	0.54 - 0.62	-0.163E 06	0.501E 05	-0.115E 06	-0.266E 06
0.342E 08	0.33301	0.923E 04 - 0.104E 05	0.10 - 0.11	0.62 - 0.69	-0.171E 06	0.520E 05	-0.115E 06	-0.266E 06
0.341E 08	0.42800	0.104E 05 - 0.115E 05	0.11 - 0.12	0.69 - 0.77	-0.178E 06	0.530E 05	-0.114E 06	-0.266E 06
0.321E 08	0.51750	0.115E 05 - 0.127E 05	0.12 - 0.14	0.77 - 0.85	-0.184E 06	0.534E 05	-0.113E 06	-0.266E 06
0.290E 08	0.59830	0.127E 05 - 0.138E 05	0.14 - 0.15	0.85 - 0.92	-0.189E 06	0.535E 05	-0.112E 06	-0.266E 06
0.252E 08	0.66846	0.138E 05 - 0.150E 05	0.15 - 0.16	0.92 - 1.00	-0.194E 06	0.530E 05	-0.111E 06	-0.266E 06
0.777E 08	0.88493	0.150E 05 - 0.210E 05	0.16 - 0.23	1.00 - 1.40	-0.203E 06	0.515E 05	-0.107E 06	-0.266E 06
0.268E 08	0.95952	0.210E 05 - 0.270E 05	0.23 - 0.29	1.40 - 1.80	-0.214E 06	0.486E 05	-0.101E 06	-0.266E 06
0.875E 07	0.98389	0.270E 05 - 0.329E 05	0.29 - 0.36	1.80 - 2.20	-0.217E 06	0.467E 05	-0.951E 05	-0.266E 06
0.321E 07	0.99283	0.329E 05 - 0.389E 05	0.36 - 0.42	2.20 - 2.59	-0.221E 06	0.414E 05	-0.901E 05	-0.266E 06
0.140E 07	0.99672	0.389E 05 - 0.449E 05	0.42 - 0.48	2.59 - 2.99	-0.226E 06	0.347E 05	-0.117E 06	-0.266E 06
0.641E 06	0.99851	0.449E 05 - 0.509E 05	0.48 - 0.55	2.99 - 3.39	-0.230E 06	0.321E 05	-0.118E 06	-0.266E 06
0.284E 06	0.99930	0.509E 05 - 0.568E 05	0.55 - 0.61	3.39 - 3.79	-0.225E 06	0.277E 05	-0.118E 06	-0.261E 06
0.136E 06	0.99968	0.568E 05 - 0.628E 05	0.61 - 0.68	3.79 - 4.19	-0.225E 06	0.254E 05	-0.165E 06	-0.265E 06
0.608E 05	0.99985	0.628E 05 - 0.688E 05	0.68 - 0.74	4.19 - 4.59	-0.227E 06	0.125E 05	-0.165E 06	-0.233E 06
0.149E 05	0.99989	0.688E 05 - 0.748E 05	0.74 - 0.81	4.59 - 4.99	-0.217E 06	0.121E 05	-0.166E 06	-0.228E 06
0.314E 04	0.99990	0.748E 05 - 0.808E 05	0.81 - 0.87	4.99 - 5.38	-0.222E 06	0.	-0.222E 06	-0.222E 06
0.145E 04	0.99990	0.808E 05 - 0.867E 05	0.87 - 0.94	5.38 - 5.78	-0.222E 06	0.	-0.222E 06	-0.222E 06
0.950E 03	0.99990	0.867E 05 - 0.927E 05	0.94 - 1.00	5.78 - 6.18	-0.222E 06	0.	-0.222E 06	-0.222E 06

TOTAL CYCLES = 0.359E 09

ROOT MEAN CUBED IS 0.171E 05 AVERAGE MEAN IS -0.184E 06

TABLE H- 76
CUMULATIVE FATIGUE HISTOGRAM OUTPUT

ROTOR-CL-STA MX

NO. CYCLES IN 30 YEARS (TYPES 1+2)	CUM PROB	HALF-RANGE FATIGUE LOADS: LOAD LEVELS	NORMALIZED LOAD LEVELS	LOAD/50% AT RATED	CORRESPONDING MID-RANGE LOAD DISTRIBUTION: MEAN	STANDARD DEVIATION	MAXIMUM	MINIMUM
0.	0.	0. - 0.129E 05	0. - 0.05	0. - 0.08	0.	0.	0.	0.
0.	0.	0.129E 05 - 0.257E 05	0.05 - 0.11	0.08 - 0.15	0.	0.	0.	0.
0.	0.	0.257E 05 - 0.386E 05	0.11 - 0.16	0.15 - 0.23	0.	0.	0.	0.
0.125E 07	0.00349	0.386E 05 - 0.515E 05	0.16 - 0.22	0.23 - 0.31	0.225E 05	0.200E 01	0.225E 05	0.225E 05
0.366E 08	0.10531	0.515E 05 - 0.644E 05	0.22 - 0.27	0.31 - 0.38	0.225E 05	0.	0.225E 05	0.225E 05
0.509E 08	0.24699	0.644E 05 - 0.772E 05	0.27 - 0.33	0.38 - 0.46	0.225E 05	0.241E 03	0.229E 05	-0.168E 04
0.201E 08	0.30286	0.772E 05 - 0.901E 05	0.33 - 0.38	0.46 - 0.54	0.225E 05	0.261E 04	0.230E 05	-0.173E 04
0.432E 08	0.42302	0.901E 05 - 0.103E 06	0.38 - 0.43	0.54 - 0.62	0.213E 05	0.556E 04	0.230E 05	-0.174E 04
0.508E 08	0.56438	0.103E 06 - 0.116E 06	0.43 - 0.49	0.62 - 0.69	0.178E 05	0.820E 04	0.229E 05	-0.293E 04
0.449E 08	0.68928	0.116E 06 - 0.129E 06	0.49 - 0.54	0.69 - 0.77	0.137E 05	0.785E 04	0.229E 05	-0.173E 04
0.312E 08	0.77621	0.129E 06 - 0.142E 06	0.54 - 0.60	0.77 - 0.85	0.118E 05	0.611E 04	0.229E 05	-0.173E 04
0.230E 08	0.84024	0.142E 06 - 0.154E 06	0.60 - 0.65	0.85 - 0.92	0.949E 04	0.465E 04	0.229E 05	-0.173E 04
0.210E 08	0.89865	0.154E 06 - 0.167E 06	0.65 - 0.71	0.92 - 1.00	0.729E 04	0.274E 04	0.225E 05	-0.173E 04
0.102E 08	0.92698	0.167E 06 - 0.173E 06	0.71 - 0.73	1.00 - 1.03	0.655E 04	0.142E 04	0.224E 05	-0.173E 04
0.674E 07	0.94575	0.173E 06 - 0.178E 06	0.73 - 0.75	1.03 - 1.06	0.650E 04	0.116E 04	0.224E 05	0.633E 04
0.564E 07	0.96145	0.178E 06 - 0.183E 06	0.75 - 0.77	1.06 - 1.10	0.648E 04	0.107E 04	0.139E 05	0.633E 04
0.435E 07	0.97356	0.183E 06 - 0.189E 06	0.77 - 0.80	1.10 - 1.13	0.633E 04	0.	0.633E 04	0.633E 04
0.323E 07	0.98257	0.189E 06 - 0.194E 06	0.80 - 0.82	1.13 - 1.16	0.633E 04	0.	0.633E 04	0.633E 04
0.228E 07	0.98892	0.194E 06 - 0.200E 06	0.82 - 0.84	1.16 - 1.19	0.633E 04	0.	0.633E 04	0.633E 04
0.153E 07	0.99319	0.200E 06 - 0.205E 06	0.84 - 0.86	1.19 - 1.22	0.633E 04	0.	0.633E 04	0.633E 04
0.986E 06	0.99594	0.205E 06 - 0.210E 06	0.86 - 0.89	1.22 - 1.26	0.633E 04	0.	0.633E 04	0.633E 04
0.609E 06	0.99763	0.210E 06 - 0.216E 06	0.89 - 0.91	1.26 - 1.29	0.633E 04	0.	0.633E 04	0.633E 04
0.362E 06	0.99864	0.216E 06 - 0.221E 06	0.91 - 0.93	1.29 - 1.32	0.633E 04	0.	0.633E 04	0.633E 04
0.208E 06	0.99922	0.221E 06 - 0.226E 06	0.93 - 0.95	1.32 - 1.35	0.633E 04	0.707E 00	0.633E 04	0.633E 04
0.116E 06	0.99954	0.226E 06 - 0.232E 06	0.95 - 0.98	1.35 - 1.38	0.633E 04	0.	0.633E 04	0.633E 04
0.129E 06	0.99990	0.232E 06 - 0.237E 06	0.98 - 1.00	1.38 - 1.42	0.633E 04	0.	0.633E 04	0.633E 04

TOTAL CYCLES = 0.359E 09

ROOT MEAN CUBED IS 0.124E 06 AVERAGE MEAN IS 0.163E 05

TABLE H- 77
CUMULATIVE FATIGUE HISTOGRAM OUTPUT

ROTOR-CL-STA MY

NO. CYCLES IN 30 YEARS (TYPES 1+2)	CUM PROB	HALF-RANGE FATIGUE LOADS: LOAD LEVELS	NORMALIZED LOAD LEVELS	LOAD/50% AT RATED	CORRESPONDING MID-RANGE LOAD DISTRIBUTION: MEAN	STANDARD DEVIATION	MAXIMUM	MINIMUM
0.	0.	0. - 0.140E 05	0. - 0.05	0. - 0.08	0.	0.	0.	0.
0.	0.	0.140E 05 - 0.280E 05	0.05 - 0.11	0.08 - 0.15	0.	0.	0.	0.
0.	0.	0.280E 05 - 0.420E 05	0.11 - 0.16	0.15 - 0.23	0.	0.	0.	0.
0.348E 07	0.00970	0.420E 05 - 0.560E 05	0.16 - 0.22	0.23 - 0.31	0.793E 05	0.	0.793E 05	0.793E 05
0.522E 08	0.15507	0.560E 05 - 0.700E 05	0.22 - 0.27	0.31 - 0.38	0.793E 05	0.113E 02	0.798E 05	0.793E 05
0.391E 08	0.26398	0.700E 05 - 0.840E 05	0.27 - 0.33	0.38 - 0.46	0.805E 05	0.462E 04	0.124E 06	0.793E 05
0.241E 08	0.33120	0.840E 05 - 0.980E 05	0.33 - 0.38	0.46 - 0.54	0.985E 05	0.784E 04	0.124E 06	0.793E 05
0.464E 08	0.46037	0.980E 05 - 0.112E 06	0.38 - 0.43	0.54 - 0.62	0.103E 06	0.408E 04	0.124E 06	0.990E 05
0.401E 08	0.57212	0.112E 06 - 0.126E 06	0.43 - 0.49	0.62 - 0.69	0.108E 06	0.804E 04	0.124E 06	0.102E 06
0.373E 08	0.67593	0.126E 06 - 0.140E 06	0.49 - 0.54	0.69 - 0.77	0.116E 06	0.706E 04	0.143E 06	0.102E 06
0.333E 08	0.76858	0.140E 06 - 0.154E 06	0.54 - 0.60	0.77 - 0.85	0.121E 06	0.857E 04	0.143E 06	0.102E 06
0.247E 08	0.83749	0.154E 06 - 0.168E 06	0.60 - 0.65	0.85 - 0.92	0.130E 06	0.122E 05	0.143E 06	0.116E 06
0.218E 08	0.89818	0.168E 06 - 0.182E 06	0.65 - 0.71	0.92 - 1.00	0.139E 06	0.920E 04	0.143E 06	0.116E 06
0.103E 08	0.92681	0.182E 06 - 0.188E 06	0.71 - 0.73	1.00 - 1.03	0.142E 06	0.510E 04	0.143E 06	0.116E 06
0.682E 07	0.94580	0.188E 06 - 0.194E 06	0.73 - 0.75	1.03 - 1.06	0.143E 06	0.448E 04	0.143E 06	0.116E 06
0.568E 07	0.96163	0.194E 06 - 0.200E 06	0.75 - 0.77	1.06 - 1.10	0.143E 06	0.402E 04	0.143E 06	0.119E 06
0.435E 07	0.97374	0.200E 06 - 0.205E 06	0.77 - 0.80	1.10 - 1.13	0.143E 06	0.	0.143E 06	0.143E 06
0.323E 07	0.98275	0.205E 06 - 0.211E 06	0.80 - 0.82	1.13 - 1.16	0.143E 06	0.	0.143E 06	0.143E 06
0.228E 07	0.98910	0.211E 06 - 0.217E 06	0.82 - 0.84	1.16 - 1.19	0.143E 06	0.	0.143E 06	0.143E 06
0.153E 07	0.99337	0.217E 06 - 0.223E 06	0.84 - 0.86	1.19 - 1.22	0.143E 06	0.	0.143E 06	0.143E 06
0.986E 06	0.99612	0.223E 06 - 0.229E 06	0.86 - 0.89	1.22 - 1.26	0.143E 06	0.226E 02	0.143E 06	0.143E 06
0.609E 06	0.99782	0.229E 06 - 0.235E 06	0.89 - 0.91	1.26 - 1.29	0.143E 06	0.	0.143E 06	0.143E 06
0.362E 06	0.99882	0.235E 06 - 0.240E 06	0.91 - 0.93	1.29 - 1.32	0.143E 06	0.	0.143E 06	0.143E 06
0.208E 06	0.99940	0.240E 06 - 0.246E 06	0.93 - 0.95	1.32 - 1.35	0.143E 06	0.	0.143E 06	0.143E 06
0.116E 06	0.99973	0.246E 06 - 0.252E 06	0.95 - 0.98	1.35 - 1.38	0.143E 06	0.	0.143E 06	0.143E 06
0.627E 05	0.99990	0.252E 06 - 0.258E 06	0.98 - 1.00	1.38 - 1.42	0.143E 06	0.160E 02	0.143E 06	0.143E 06

TOTAL CYCLES = 0.359E 09

ROOT MEAN CUBED IS 0.135E 06 AVERAGE MEAN IS 0.108E 06

TABLE H- 78
CUMULATIVE FATIGUE HISTOGRAM OUTPUT

ROTOR-CL-STA MZ

NO. CYCLES IN 30 YEARS (TYPES 1+2)	CUM PROB	HALF-RANGE FATIGUE LOADS: LOAD LEVELS	NORMALIZED LOAD LEVELS	LOAD/50% AT RATED	CORRESPONDING MID-RANGE LOAD DISTRIBUTION: MEAN	STANDARD DEVIATION	MAXIMUM	MINIMUM
0.	0.	0. - 0.127E 05	0. - 0.01	0. - 0.08	0.	0.	0.	0.
0.	0.	0.127E 05 - 0.255E 05	0.01 - 0.01	0.08 - 0.15	0.	0.	0.	0.
0.	0.	0.255E 05 - 0.382E 05	0.01 - 0.02	0.15 - 0.23	0.	0.	0.	0.
0.	0.	0.382E 05 - 0.510E 05	0.02 - 0.02	0.23 - 0.31	0.	0.	0.	0.
0.117E 07	0.00325	0.510E 05 - 0.637E 05	0.02 - 0.03	0.31 - 0.38	-0.207E 07	0.136E 07	-0.630E 06	-0.396E 07
0.346E 07	0.01287	0.637E 05 - 0.764E 05	0.03 - 0.03	0.38 - 0.46	-0.207E 07	0.133E 07	-0.630E 06	-0.396E 07
0.785E 07	0.03473	0.764E 05 - 0.892E 05	0.03 - 0.04	0.46 - 0.54	-0.207E 07	0.131E 07	-0.630E 06	-0.396E 07
0.136E 08	0.07256	0.892E 05 - 0.102E 06	0.04 - 0.05	0.54 - 0.62	-0.207E 07	0.130E 07	-0.630E 06	-0.396E 07
0.195E 08	0.12678	0.102E 06 - 0.115E 06	0.05 - 0.05	0.62 - 0.69	-0.207E 07	0.128E 07	-0.630E 06	-0.396E 07
0.244E 08	0.19471	0.115E 06 - 0.127E 06	0.05 - 0.06	0.69 - 0.77	-0.207E 07	0.127E 07	-0.630E 06	-0.396E 07
0.277E 08	0.27174	0.127E 05 - 0.140E 06	0.06 - 0.06	0.77 - 0.85	-0.207E 07	0.126E 07	-0.630E 06	-0.396E 07
0.291E 08	0.35281	0.140E 06 - 0.153E 06	0.06 - 0.07	0.85 - 0.92	-0.207E 07	0.125E 07	-0.630E 06	-0.396E 07
0.289E 08	0.43337	0.153E 06 - 0.166E 06	0.07 - 0.08	0.92 - 1.00	-0.208E 07	0.124E 07	-0.630E 06	-0.396E 07
0.175E 09	0.92035	0.166E 06 - 0.321E 06	0.08 - 0.15	1.00 - 1.94	-0.207E 07	0.121E 07	-0.552E 06	-0.396E 07
0.196E 08	0.97485	0.321E 06 - 0.476E 06	0.15 - 0.22	1.94 - 2.88	-0.195E 07	0.112E 07	-0.476E 06	-0.396E 07
0.423E 07	0.98668	0.476E 06 - 0.631E 06	0.22 - 0.29	2.88 - 3.81	-0.203E 07	0.100E 07	-0.554E 06	-0.396E 07
0.175E 07	0.99157	0.631E 06 - 0.787E 06	0.29 - 0.36	3.81 - 4.75	-0.237E 07	0.918E 06	-0.644E 06	-0.346E 07
0.932E 06	0.99430	0.787E 06 - 0.942E 06	0.36 - 0.43	4.75 - 5.69	-0.258E 07	0.808E 06	-0.705E 06	-0.328E 07
0.678E 06	0.99619	0.942E 06 - 0.110E 07	0.43 - 0.50	5.69 - 6.63	-0.269E 07	0.699E 06	-0.732E 06	-0.312E 07
0.447E 06	0.99743	0.110E 07 - 0.125E 07	0.50 - 0.57	6.63 - 7.56	-0.268E 07	0.582E 06	-0.125E 07	-0.296E 07
0.314E 06	0.99831	0.125E 07 - 0.141E 07	0.57 - 0.64	7.56 - 8.50	-0.266E 07	0.397E 06	-0.134E 07	-0.281E 07
0.218E 06	0.99891	0.141E 07 - 0.156E 07	0.64 - 0.72	8.50 - 9.44	-0.259E 07	0.231E 06	-0.149E 07	-0.271E 07
0.144E 06	0.99932	0.156E 07 - 0.172E 07	0.72 - 0.79	9.44 - 10.38	-0.247E 07	0.125E 06	-0.159E 07	-0.255E 07
0.979E 05	0.99959	0.172E 07 - 0.187E 07	0.79 - 0.86	10.38 - 11.32	-0.234E 07	0.271E 05	-0.224E 07	-0.237E 07
0.688E 05	0.99978	0.187E 07 - 0.203E 07	0.86 - 0.93	11.32 - 12.25	-0.219E 07	0.824E 04	-0.215E 07	-0.219E 07
0.442E 05	0.99990	0.203E 07 - 0.218E 07	0.93 - 1.00	12.25 - 13.19	-0.209E 07	0.126E 05	-0.202E 07	-0.209E 07

TOTAL CYCLES = 0.359E 09

ROOT MEAN CUBED IS 0.314E 06 AVERAGE MEAN IS -0.207E 07

TABLE H- 79
CUMULATIVE FATIGUE HISTOGRAM OUTPUT

ROTOR-NAC VX

NO. CYCLES IN 30 YEARS (TYPES 1+2)	CUM PROB	HALF-RANGE FATIGUE LOADS: LOAD LEVELS	NORMALIZED LOAD LEVELS	LOAD/50% AT RATED	CORRESPONDING MID-RANGE LOAD DISTRIBUTION: MEAN	STANDARD DEVIATION	MAXIMUM	MINIMUM
0.	0.	0. - 0.124E 04	0. - 0.05	0. - 0.08	0.	0.	0.	0.
0.	0.	0.124E 04 - 0.248E 04	0.05 - 0.11	0.08 - 0.15	0.	0.	0.	0.
0.	0.	0.248E 04 - 0.372E 04	0.11 - 0.16	0.15 - 0.23	0.	0.	0.	0.
0.	0.	0.372E 04 - 0.495E 04	0.16 - 0.22	0.23 - 0.31	0.	0.	0.	0.
0.153E 06	0.00043	0.495E 04 - 0.619E 04	0.22 - 0.27	0.31 - 0.38	-0.590E 06	0.	-0.590E 06	-0.590E 06
0.990E 07	0.02799	0.619E 04 - 0.743E 04	0.27 - 0.33	0.38 - 0.46	-0.590E 06	0.905E 02	-0.590E 06	-0.590E 06
0.598E 08	0.15455	0.743E 04 - 0.867E 04	0.33 - 0.38	0.46 - 0.54	-0.590E 06	0.157E 03	-0.590E 06	-0.590E 06
0.817E 08	0.42218	0.867E 04 - 0.991E 04	0.38 - 0.43	0.54 - 0.62	-0.590E 06	0.143E 03	-0.589E 06	-0.590E 06
0.357E 08	0.52156	0.991E 04 - 0.111E 05	0.43 - 0.49	0.62 - 0.69	-0.590E 06	0.181E 03	-0.589E 06	-0.590E 06
0.117E 08	0.55426	0.111E 05 - 0.124E 05	0.49 - 0.54	0.69 - 0.77	-0.590E 06	0.351E 03	-0.590E 06	-0.591E 06
0.181E 08	0.60470	0.124E 05 - 0.136E 05	0.54 - 0.60	0.77 - 0.85	-0.590E 06	0.293E 03	-0.590E 06	-0.591E 06
0.260E 08	0.70501	0.136E 05 - 0.149E 05	0.60 - 0.65	0.85 - 0.92	-0.590E 06	0.333E 03	-0.590E 06	-0.591E 06
0.425E 08	0.82325	0.149E 05 - 0.161E 05	0.65 - 0.71	0.92 - 1.00	-0.590E 06	0.379E 03	-0.590E 06	-0.591E 06
0.183E 08	0.87424	0.161E 05 - 0.166E 05	0.71 - 0.73	1.00 - 1.03	-0.590E 06	0.405E 03	-0.590E 06	-0.592E 06
0.128E 08	0.90981	0.166E 05 - 0.171E 05	0.73 - 0.75	1.03 - 1.06	-0.590E 06	0.415E 03	-0.590E 06	-0.592E 06
0.998E 07	0.93759	0.171E 05 - 0.176E 05	0.75 - 0.77	1.06 - 1.10	-0.590E 06	0.429E 03	-0.590E 06	-0.592E 06
0.748E 07	0.95842	0.176E 05 - 0.182E 05	0.77 - 0.80	1.10 - 1.13	-0.590E 06	0.439E 03	-0.590E 06	-0.591E 06
0.534E 07	0.97328	0.182E 05 - 0.187E 05	0.80 - 0.82	1.13 - 1.16	-0.590E 06	0.443E 03	-0.590E 06	-0.591E 06
0.363E 07	0.98340	0.187E 05 - 0.192E 05	0.82 - 0.84	1.16 - 1.19	-0.590E 06	0.453E 03	-0.590E 06	-0.591E 06
0.237E 07	0.99000	0.192E 05 - 0.197E 05	0.84 - 0.86	1.19 - 1.22	-0.590E 06	0.453E 03	-0.590E 06	-0.591E 06
0.149E 07	0.99415	0.197E 05 - 0.202E 05	0.86 - 0.89	1.22 - 1.26	-0.590E 06	0.462E 03	-0.590E 06	-0.591E 06
0.950E 06	0.99665	0.202E 05 - 0.207E 05	0.89 - 0.91	1.26 - 1.29	-0.590E 06	0.470E 03	-0.590E 06	-0.591E 06
0.576E 06	0.99826	0.207E 05 - 0.213E 05	0.91 - 0.93	1.29 - 1.32	-0.590E 06	0.448E 03	-0.590E 06	-0.591E 06
0.271E 06	0.99901	0.213E 05 - 0.218E 05	0.93 - 0.95	1.32 - 1.35	-0.590E 06	0.492E 03	-0.590E 06	-0.591E 06
0.151E 06	0.99943	0.218E 05 - 0.223E 05	0.95 - 0.98	1.35 - 1.38	-0.590E 06	0.487E 03	-0.590E 06	-0.591E 06
0.168E 06	0.99990	0.223E 05 - 0.228E 05	0.98 - 1.00	1.38 - 1.42	-0.590E 06	0.487E 03	-0.590E 06	-0.591E 06

TOTAL CYCLES = 0.359E 09

ROOT MEAN CUBED IS 0.131E 05 AVERAGE MEAN IS -0.590E 06

TABLE H- 80
CUMULATIVE FATIGUE HISTOGRAM OUTPUT

ROTOR-NAC VY

NO. CYCLES IN 30 YEARS (TYPES 1+2)	CUM PROB	HALF-RANGE FATIGUE LOADS: LOAD LEVELS	NORMALIZED LOAD LEVELS	LOAD/50% AT RATED	CORRESPONDING MID-RANGE LOAD DISTRIBUTION: MEAN	STANDARD DEVIATION	MAXIMUM	MINIMUM
0.	0.	0. - 0.265E 03	0. - 0.05	0. - 0.08	0.	0.	0.	0.
0.	0.	0.265E 03 - 0.530E 03	0.05 - 0.11	0.08 - 0.15	0.	0.	0.	0.
0.	0.	0.530E 03 - 0.794E 03	0.11 - 0.16	0.15 - 0.23	0.	0.	0.	0.
0.	0.	0.794E 03 - 0.106E 04	0.16 - 0.22	0.23 - 0.31	0.	0.	0.	0.
0.	0.	0.106E 04 - 0.132E 04	0.22 - 0.27	0.31 - 0.38	0.	0.	0.	0.
0.	0.	0.132E 04 - 0.159E 04	0.27 - 0.33	0.38 - 0.46	0.	0.	0.	0.
0.	0.	0.159E 04 - 0.185E 04	0.33 - 0.38	0.46 - 0.54	0.	0.	0.	0.
0.379E 06	0.00105	0.185E 04 - 0.212E 04	0.38 - 0.43	0.54 - 0.62	0.624E 03	0.664E 02	0.709E 03	0.572E 03
0.567E 07	0.01685	0.212E 04 - 0.238E 04	0.43 - 0.49	0.62 - 0.69	0.626E 03	0.669E 02	0.709E 03	0.572E 03
0.283E 08	0.09567	0.238E 04 - 0.265E 04	0.49 - 0.54	0.69 - 0.77	0.626E 03	0.102E 03	0.983E 03	0.357E 03
0.631E 08	0.27131	0.265E 04 - 0.291E 04	0.54 - 0.60	0.77 - 0.85	0.623E 03	0.139E 03	0.983E 03	0.357E 03
0.812E 08	0.49743	0.291E 04 - 0.318E 04	0.60 - 0.65	0.85 - 0.92	0.626E 03	0.191E 03	0.983E 03	0.357E 03
0.768E 08	0.71129	0.318E 04 - 0.344E 04	0.65 - 0.70	0.92 - 1.00	0.619E 03	0.241E 03	0.983E 03	0.350E 03
0.292E 08	0.79263	0.344E 04 - 0.355E 04	0.70 - 0.73	1.00 - 1.03	0.647E 03	0.268E 03	0.983E 03	0.324E 03
0.217E 08	0.85315	0.355E 04 - 0.366E 04	0.73 - 0.75	1.03 - 1.06	0.622E 03	0.274E 03	0.983E 03	0.284E 03
0.164E 08	0.89883	0.366E 04 - 0.378E 04	0.75 - 0.77	1.06 - 1.10	0.631E 03	0.280E 03	0.983E 03	0.245E 03
0.121E 08	0.93260	0.378E 04 - 0.389E 04	0.77 - 0.80	1.10 - 1.13	0.639E 03	0.283E 03	0.983E 03	0.205E 03
0.864E 07	0.95667	0.389E 04 - 0.400E 04	0.80 - 0.82	1.13 - 1.16	0.644E 03	0.286E 03	0.983E 03	0.183E 03
0.590E 07	0.97311	0.400E 04 - 0.411E 04	0.82 - 0.84	1.16 - 1.19	0.647E 03	0.288E 03	0.983E 03	0.357E 03
0.395E 07	0.98411	0.411E 04 - 0.422E 04	0.84 - 0.86	1.19 - 1.23	0.651E 03	0.286E 03	0.983E 03	0.357E 03
0.238E 07	0.99073	0.422E 04 - 0.433E 04	0.86 - 0.89	1.23 - 1.26	0.654E 03	0.293E 03	0.983E 03	0.357E 03
0.144E 07	0.99475	0.433E 04 - 0.444E 04	0.89 - 0.91	1.26 - 1.29	0.657E 03	0.293E 03	0.983E 03	0.357E 03
0.846E 06	0.99710	0.444E 04 - 0.455E 04	0.91 - 0.93	1.29 - 1.32	0.660E 03	0.293E 03	0.983E 03	0.357E 03
0.478E 06	0.99844	0.455E 04 - 0.467E 04	0.93 - 0.95	1.32 - 1.36	0.663E 03	0.293E 03	0.983E 03	0.357E 03
0.262E 06	0.99917	0.467E 04 - 0.478E 04	0.95 - 0.98	1.36 - 1.39	0.666E 03	0.293E 03	0.983E 03	0.357E 03
0.264E 06	0.99990	0.478E 04 - 0.489E 04	0.98 - 1.00	1.39 - 1.42	0.670E 03	0.302E 03	0.983E 03	0.357E 03

TOTAL CYCLES = 0.359E 09

ROOT MEAN CUBED IS 0.326E 04 AVERAGE MEAN IS 0.627E 03

TABLE H- 81
CUMULATIVE FATIGUE HISTOGRAM OUTPUT

ROTOR-NAC VZ

NO. CYCLES IN 30 YEARS (TYPES 1+2)	CUM PROB	HALF-RANGE FATIGUE LOADS: LOAD LEVELS	NORMALIZED LOAD LEVELS	LOAD/50% AT RATED	CORRESPONDING MID-RANGE LOAD DISTRIBUTION: MEAN	STANDARD DEVIATION	MAXIMUM	MINIMUM
0.	0.	0. - 0.692E 03	0. - 0.01	0. - 0.08	0.	0.	0.	0.
0.	0.	0.692E 03 - 0.138E 04	0.01 - 0.02	0.08 - 0.15	0.	0.	0.	0.
0.	0.	0.138E 04 - 0.208E 04	0.02 - 0.02	0.15 - 0.23	0.	0.	0.	0.
0.928E 06	0.00258	0.208E 04 - 0.277E 04	0.02 - 0.03	0.23 - 0.31	-0.180E 06	0.374E 05	-0.152E 06	-0.252E 06
0.423E 07	0.01436	0.277E 04 - 0.346E 04	0.03 - 0.04	0.31 - 0.38	-0.194E 06	0.486E 05	-0.152E 06	-0.301E 06
0.106E 08	0.04390	0.346E 04 - 0.415E 04	0.04 - 0.05	0.38 - 0.46	-0.198E 06	0.493E 05	-0.152E 06	-0.301E 06
0.188E 08	0.09633	0.415E 04 - 0.485E 04	0.05 - 0.06	0.46 - 0.54	-0.202E 06	0.507E 05	-0.152E 06	-0.301E 06
0.265E 08	0.17004	0.485E 04 - 0.554E 04	0.06 - 0.06	0.54 - 0.62	-0.207E 06	0.517E 05	-0.152E 06	-0.301E 06
0.318E 08	0.25847	0.554E 04 - 0.623E 04	0.06 - 0.07	0.62 - 0.69	-0.211E 06	0.525E 05	-0.152E 06	-0.301E 06
0.341E 08	0.35336	0.623E 04 - 0.692E 04	0.07 - 0.08	0.69 - 0.77	-0.214E 06	0.531E 05	-0.152E 06	-0.301E 06
0.337E 08	0.44730	0.692E 04 - 0.762E 04	0.08 - 0.09	0.77 - 0.85	-0.217E 06	0.535E 05	-0.152E 06	-0.301E 06
0.315E 08	0.53491	0.762E 04 - 0.831E 04	0.09 - 0.10	0.85 - 0.92	-0.220E 06	0.538E 05	-0.151E 06	-0.301E 06
0.281E 08	0.61308	0.831E 04 - 0.900E 04	0.10 - 0.10	0.92 - 1.00	-0.223E 06	0.539E 05	-0.150E 06	-0.301E 06
0.112E 09	0.92494	0.900E 04 - 0.150E 05	0.10 - 0.17	1.00 - 1.67	-0.230E 06	0.542E 05	-0.147E 06	-0.301E 06
0.183E 08	0.97580	0.150E 05 - 0.210E 05	0.17 - 0.24	1.67 - 2.34	-0.236E 06	0.550E 05	-0.141E 06	-0.301E 06
0.474E 07	0.98898	0.210E 05 - 0.271E 05	0.24 - 0.31	2.34 - 3.01	-0.229E 06	0.534E 05	-0.135E 06	-0.301E 06
0.198E 07	0.99450	0.271E 05 - 0.331E 05	0.31 - 0.38	3.01 - 3.67	-0.237E 06	0.482E 05	-0.129E 06	-0.301E 06
0.992E 06	0.99726	0.331E 05 - 0.391E 05	0.38 - 0.45	3.67 - 4.34	-0.246E 06	0.412E 05	-0.125E 06	-0.289E 06
0.504E 06	0.99866	0.391E 05 - 0.451E 05	0.45 - 0.52	4.34 - 5.01	-0.254E 06	0.349E 05	-0.153E 06	-0.290E 06
0.257E 06	0.99938	0.451E 05 - 0.511E 05	0.52 - 0.59	5.01 - 5.68	-0.256E 06	0.302E 05	-0.153E 06	-0.296E 06
0.121E 06	0.99972	0.511E 05 - 0.571E 05	0.59 - 0.66	5.68 - 6.35	-0.259E 06	0.253E 05	-0.153E 06	-0.300E 06
0.511E 05	0.99986	0.571E 05 - 0.632E 05	0.66 - 0.72	6.35 - 7.02	-0.257E 06	0.131E 05	-0.200E 06	-0.263E 06
0.106E 05	0.99989	0.632E 05 - 0.692E 05	0.72 - 0.79	7.02 - 7.69	-0.249E 06	0.159E 05	-0.200E 06	-0.263E 06
0.320E 04	0.99990	0.692E 05 - 0.752E 05	0.79 - 0.86	7.69 - 8.35	-0.257E 06	0.	-0.257E 06	-0.257E 06
0.147E 04	0.99990	0.752E 05 - 0.812E 05	0.86 - 0.93	8.35 - 9.02	-0.257E 06	0.320E 02	-0.257E 06	-0.257E 06
0.613E 03	0.99990	0.812E 05 - 0.872E 05	0.93 - 1.00	9.02 - 9.69	-0.257E 06	0.	-0.257E 06	-0.257E 06

TOTAL CYCLES = 0.359E 09

ROOT MEAN CUBED IS 0.121E 05 AVERAGE MEAN IS -0.220E 06

TABLE H- 82
CUMULATIVE FATIGUE HISTOGRAM OUTPUT

ROTOR-HAC MX

NO. CYCLES IN 30 YEARS (TYPES 1+2)	CUM PROB	HALF-RANGE FATIGUE LOADS: LOAD LEVELS	NORMALIZED LOAD LEVELS	LOAD/50% AT RATED	CORRESPONDING MID-RANGE LOAD DISTRIBUTION: MEAN	STANDARD DEVIATION	MAXIMUM	MINIMUM
0.	0.	0. - 0.916E 04	0. - 0.05	0. - 0.08	0.	0.	0.	0.
0.	0.	0.916E 04 - 0.183E 05	0.05 - 0.11	0.08 - 0.15	0.	0.	0.	0.
0.	0.	0.183E 05 - 0.275E 05	0.11 - 0.16	0.15 - 0.23	0.	0.	0.	0.
0.	0.	0.275E 05 - 0.366E 05	0.16 - 0.22	0.23 - 0.31	0.	0.	0.	0.
0.118E 04	0.00000	0.366E 05 - 0.458E 05	0.22 - 0.27	0.31 - 0.38	-0.707E 04	0.	-0.707E 04	-0.707E 04
0.357E 07	0.00995	0.458E 05 - 0.549E 05	0.27 - 0.33	0.38 - 0.46	0.634E 04	0.133E 05	0.170E 05	-0.103E 05
0.311E 08	0.09649	0.549E 05 - 0.641E 05	0.33 - 0.38	0.46 - 0.54	0.994E 04	0.117E 05	0.170E 05	-0.103E 05
0.607E 08	0.26556	0.641E 05 - 0.732E 05	0.38 - 0.43	0.54 - 0.62	0.116E 05	0.963E 04	0.170E 05	-0.103E 05
0.532E 08	0.41364	0.732E 05 - 0.824E 05	0.43 - 0.49	0.62 - 0.69	0.101E 05	0.737E 04	0.170E 05	-0.103E 05
0.480E 08	0.54736	0.824E 05 - 0.916E 05	0.49 - 0.54	0.69 - 0.77	0.948E 04	0.579E 04	0.170E 05	-0.103E 05
0.471E 08	0.67852	0.916E 05 - 0.101E 06	0.54 - 0.60	0.77 - 0.85	0.112E 05	0.622E 04	0.170E 05	-0.108E 05
0.405E 08	0.79164	0.101E 06 - 0.110E 06	0.60 - 0.65	0.85 - 0.92	0.930E 04	0.816E 04	0.153E 05	-0.476E 04
0.324E 08	0.88162	0.110E 06 - 0.119E 06	0.65 - 0.71	0.92 - 1.00	0.504E 04	0.888E 04	0.153E 05	-0.379E 04
0.127E 08	0.91688	0.119E 06 - 0.123E 06	0.71 - 0.73	1.00 - 1.03	0.115E 04	0.748E 04	0.153E 05	-0.288E 04
0.833E 07	0.94007	0.123E 06 - 0.127E 06	0.73 - 0.75	1.03 - 1.06	0.846E 03	0.725E 04	0.153E 05	-0.288E 04
0.654E 07	0.95830	0.127E 06 - 0.130E 06	0.75 - 0.77	1.06 - 1.10	-0.131E 03	0.640E 04	0.153E 05	-0.288E 04
0.492E 07	0.97200	0.130E 06 - 0.134E 06	0.77 - 0.80	1.10 - 1.13	-0.854E 03	0.559E 04	0.153E 05	-0.288E 04
0.354E 07	0.98187	0.134E 06 - 0.138E 06	0.80 - 0.82	1.13 - 1.16	-0.138E 04	0.485E 04	0.153E 05	-0.288E 04
0.253E 07	0.98892	0.138E 06 - 0.142E 06	0.82 - 0.84	1.16 - 1.19	-0.117E 04	0.518E 04	0.153E 05	-0.288E 04
0.157E 07	0.99328	0.142E 06 - 0.146E 06	0.84 - 0.86	1.19 - 1.22	-0.259E 04	0.199E 04	0.111E 05	-0.288E 04
0.100E 07	0.99607	0.146E 06 - 0.150E 06	0.86 - 0.89	1.22 - 1.26	-0.264E 04	0.178E 04	0.107E 05	-0.288E 04
0.618E 06	0.99779	0.150E 06 - 0.153E 06	0.89 - 0.91	1.26 - 1.29	-0.268E 04	0.158E 04	0.103E 05	-0.288E 04
0.367E 06	0.99882	0.153E 06 - 0.157E 06	0.91 - 0.93	1.29 - 1.32	-0.272E 04	0.140E 04	0.992E 04	-0.288E 04
0.212E 06	0.99940	0.157E 06 - 0.161E 06	0.93 - 0.95	1.32 - 1.35	-0.267E 04	0.158E 04	0.963E 04	-0.288E 04
0.116E 06	0.99973	0.161E 06 - 0.165E 06	0.95 - 0.98	1.35 - 1.38	-0.288E 04	0.	-0.288E 04	-0.288E 04
0.627E 05	0.99990	0.165E 06 - 0.169E 06	0.98 - 1.00	1.38 - 1.42	-0.288E 04	0.	-0.288E 04	-0.288E 04

TOTAL CYCLES = 0.359E 09

ROOT MEAN CUBED IS 0.956E 05 AVERAGE MEAN IS 0.861E 04

TABLE H- 83
CUMULATIVE FATIGUE HISTOGRAM OUTPUT

ROTOR-HAC MY

NO. CYCLES IN 30 YEARS (TYPES 1+2)	CUM PROB	HALF-RANGE FATIGUE LOADS: LOAD LEVELS	NORMALIZED LOAD LEVELS	LOAD/50% AT RATED	CORRESPONDING MID-RANGE LOAD DISTRIBUTION: MEAN	STANDARD DEVIATION	MAXIMUM	MINIMUM
0.	0.	0. - 0.442E 04	0. - 0.04	0. - 0.08	0.	0.	0.	0.
0.	0.	0.442E 04 - 0.885E 04	0.04 - 0.07	0.08 - 0.15	0.	0.	0.	0.
0.	0.	0.885E 04 - 0.133E 05	0.07 - 0.11	0.15 - 0.23	0.	0.	0.	0.
0.	0.	0.133E 05 - 0.177E 05	0.11 - 0.14	0.23 - 0.31	0.	0.	0.	0.
0.	0.	0.177E 05 - 0.221E 05	0.14 - 0.18	0.31 - 0.38	0.	0.	0.	0.
0.561E 07	0.01562	0.221E 05 - 0.265E 05	0.18 - 0.22	0.38 - 0.46	-0.495E 07	0.	-0.495E 07	-0.495E 07
0.343E 08	0.11119	0.265E 05 - 0.310E 05	0.22 - 0.25	0.46 - 0.54	-0.495E 07	0.162E 04	-0.495E 07	-0.497E 07
0.430E 08	0.23098	0.310E 05 - 0.354E 05	0.25 - 0.29	0.54 - 0.62	-0.495E 07	0.631E 04	-0.495E 07	-0.497E 07
0.329E 08	0.32265	0.354E 05 - 0.398E 05	0.29 - 0.33	0.62 - 0.69	-0.496E 07	0.114E 05	-0.494E 07	-0.497E 07
0.387E 08	0.43051	0.398E 05 - 0.442E 05	0.33 - 0.36	0.69 - 0.77	-0.497E 07	0.148E 05	-0.488E 07	-0.497E 07
0.356E 08	0.52967	0.442E 05 - 0.487E 05	0.36 - 0.40	0.77 - 0.85	-0.495E 07	0.312E 05	-0.488E 07	-0.497E 07
0.378E 08	0.63494	0.487E 05 - 0.531E 05	0.40 - 0.43	0.85 - 0.92	-0.493E 07	0.370E 05	-0.488E 07	-0.498E 07
0.443E 08	0.75823	0.531E 05 - 0.575E 05	0.43 - 0.47	0.92 - 1.00	-0.491E 07	0.314E 05	-0.488E 07	-0.498E 07
0.435E 08	0.87924	0.575E 05 - 0.625E 05	0.47 - 0.51	1.00 - 1.09	-0.491E 07	0.290E 05	-0.488E 07	-0.498E 07
0.254E 08	0.94986	0.625E 05 - 0.675E 05	0.51 - 0.55	1.09 - 1.17	-0.491E 07	0.282E 05	-0.488E 07	-0.499E 07
0.105E 08	0.97917	0.675E 05 - 0.724E 05	0.55 - 0.59	1.17 - 1.26	-0.491E 07	0.277E 05	-0.488E 07	-0.499E 07
0.386E 07	0.98990	0.724E 05 - 0.774E 05	0.59 - 0.63	1.26 - 1.35	-0.491E 07	0.265E 05	-0.488E 07	-0.499E 07
0.174E 07	0.99475	0.774E 05 - 0.824E 05	0.63 - 0.67	1.35 - 1.43	-0.492E 07	0.248E 05	-0.488E 07	-0.499E 07
0.873E 06	0.99718	0.824E 05 - 0.874E 05	0.67 - 0.71	1.43 - 1.52	-0.492E 07	0.207E 05	-0.490E 07	-0.496E 07
0.525E 06	0.99864	0.874E 05 - 0.923E 05	0.71 - 0.76	1.52 - 1.61	-0.493E 07	0.181E 05	-0.491E 07	-0.496E 07
0.243E 06	0.99932	0.923E 05 - 0.973E 05	0.76 - 0.80	1.61 - 1.69	-0.493E 07	0.163E 05	-0.491E 07	-0.497E 07
0.117E 06	0.99964	0.973E 05 - 0.102E 06	0.80 - 0.84	1.69 - 1.78	-0.494E 07	0.132E 05	-0.492E 07	-0.497E 07
0.582E 05	0.99981	0.102E 06 - 0.107E 06	0.84 - 0.88	1.78 - 1.87	-0.494E 07	0.113E 05	-0.492E 07	-0.497E 07
0.236E 05	0.99987	0.107E 06 - 0.112E 06	0.88 - 0.92	1.87 - 1.95	-0.494E 07	0.595E 04	-0.493E 07	-0.494E 07
0.911E 04	0.99990	0.112E 06 - 0.117E 06	0.92 - 0.96	1.95 - 2.04	-0.494E 07	0.431E 04	-0.493E 07	-0.494E 07
0.193E 04	0.99990	0.117E 06 - 0.122E 06	0.96 - 1.00	2.04 - 2.13	-0.494E 07	0.	-0.494E 07	-0.494E 07

TOTAL CYCLES = 0.359E 09

ROOT MEAN CUBED IS 0.507E 05 AVERAGE MEAN IS -0.494E 07

TABLE H- 84
CUMULATIVE FATIGUE HISTOGRAM OUTPUT

ROTOR-NAC MZ

NO. CYCLES IN 30 YEARS (TYPES 1+2)	CUM PROB	HALF-RANGE FATIGUE LOADS: LOAD LEVELS	NORMALIZED LOAD LEVELS	LOAD/50% AT RATED	CORRESPONDING MID-RANGE LOAD DISTRIBUTION: MEAN	STANDARD DEVIATION	MAXIMUM	MINIMUM
0.	0.	0. - 0.127E 05	0. - 0.01	0. - 0.08	0.	0.	0.	0.
0.	0.	0.127E 05 - 0.255E 05	0.01 - 0.01	0.08 - 0.15	0.	0.	0.	0.
0.	0.	0.255E 05 - 0.382E 05	0.01 - 0.02	0.15 - 0.23	0.	0.	0.	0.
0.	0.	0.382E 05 - 0.510E 05	0.02 - 0.02	0.23 - 0.31	0.	0.	0.	0.
0.117E 07	0.00325	0.510E 05 - 0.637E 05	0.02 - 0.03	0.31 - 0.38	-0.207E 07	0.136E 07	-0.630E 06	-0.396E 07
0.346E 07	0.01287	0.637E 05 - 0.764E 05	0.03 - 0.03	0.38 - 0.46	-0.207E 07	0.133E 07	-0.630E 06	-0.396E 07
0.785E 07	0.03473	0.764E 05 - 0.892E 05	0.03 - 0.04	0.46 - 0.54	-0.207E 07	0.131E 07	-0.630E 06	-0.396E 07
0.136E 08	0.07256	0.892E 05 - 0.102E 06	0.04 - 0.05	0.54 - 0.62	-0.207E 07	0.130E 07	-0.630E 06	-0.396E 07
0.195E 08	0.12678	0.102E 06 - 0.115E 06	0.05 - 0.05	0.62 - 0.69	-0.207E 07	0.128E 07	-0.630E 06	-0.396E 07
0.244E 08	0.19471	0.115E 06 - 0.127E 06	0.05 - 0.06	0.69 - 0.77	-0.207E 07	0.127E 07	-0.630E 06	-0.396E 07
0.277E 08	0.27174	0.127E 06 - 0.140E 06	0.06 - 0.06	0.77 - 0.85	-0.207E 07	0.126E 07	-0.630E 06	-0.396E 07
0.291E 08	0.35281	0.140E 06 - 0.153E 06	0.06 - 0.07	0.85 - 0.92	-0.207E 07	0.125E 07	-0.630E 06	-0.396E 07
0.289E 08	0.43337	0.153E 06 - 0.166E 06	0.07 - 0.08	0.92 - 1.00	-0.208E 07	0.124E 07	-0.630E 06	-0.396E 07
0.175E 09	0.92035	0.166E 06 - 0.321E 06	0.08 - 0.15	1.00 - 1.94	-0.207E 07	0.121E 07	-0.552E 06	-0.396E 07
0.196E 08	0.97485	0.321E 06 - 0.476E 06	0.15 - 0.22	1.94 - 2.88	-0.195E 07	0.112E 07	-0.476E 06	-0.396E 07
0.425E 07	0.98668	0.476E 06 - 0.631E 06	0.22 - 0.29	2.88 - 3.81	-0.203E 07	0.100E 07	-0.554E 06	-0.396E 07
0.176E 07	0.99157	0.631E 06 - 0.787E 06	0.29 - 0.36	3.81 - 4.75	-0.237E 07	0.918E 06	-0.644E 06	-0.346E 07
0.982E 06	0.99430	0.787E 06 - 0.942E 06	0.36 - 0.43	4.75 - 5.69	-0.258E 07	0.808E 06	-0.705E 06	-0.328E 07
0.678E 06	0.99619	0.942E 06 - 0.110E 07	0.43 - 0.50	5.69 - 6.63	-0.269E 07	0.699E 06	-0.732E 06	-0.312E 07
0.447E 06	0.99743	0.110E 07 - 0.125E 07	0.50 - 0.57	6.63 - 7.56	-0.268E 07	0.582E 06	-0.125E 07	-0.296E 07
0.314E 06	0.99831	0.125E 07 - 0.141E 07	0.57 - 0.64	7.56 - 8.50	-0.266E 07	0.397E 06	-0.134E 07	-0.281E 07
0.218E 06	0.99891	0.141E 07 - 0.156E 07	0.64 - 0.72	8.50 - 9.44	-0.259E 07	0.231E 06	-0.149E 07	-0.271E 07
0.144E 06	0.99932	0.156E 07 - 0.172E 07	0.72 - 0.79	9.44 - 10.38	-0.247E 07	0.125E 06	-0.159E 07	-0.255E 07
0.979E 05	0.99959	0.172E 07 - 0.187E 07	0.79 - 0.86	10.38 - 11.32	-0.234E 07	0.271E 05	-0.224E 07	-0.237E 07
0.688E 05	0.99978	0.187E 07 - 0.203E 07	0.86 - 0.93	11.32 - 12.25	-0.219E 07	0.824E 04	-0.215E 07	-0.219E 07
0.442E 05	0.99990	0.203E 07 - 0.218E 07	0.93 - 1.00	12.25 - 13.19	-0.209E 07	0.126E 05	-0.202E 07	-0.209E 07

TOTAL CYCLES = 0.359E 09

ROOT MEAN CUBED IS 0.314E 06 AVERAGE MEAN IS -0.207E 07

TABLE H- 85
CUMULATIVE FATIGUE HISTOGRAM OUTPUT

YAW BRNG VX

NO. CYCLES IN 30 YEARS (TYPES 1+2)	CUM PROB	HALF-RANGE FATIGUE LOADS: LOAD LEVELS	NORMALIZED LOAD LEVELS	LOAD/50% AT RATED	CORRESPONDING MID-RANGE LOAD DISTRIBUTION: MEAN	STANDARD DEVIATION	MAXIMUM	MINIMUM
0.	0.	0. - 0.133E 04	0. - 0.05	0. - 0.08	0.	0.	0.	0.
0.	0.	0.133E 04 - 0.265E 04	0.05 - 0.11	0.08 - 0.15	0.	0.	0.	0.
0.	0.	0.265E 04 - 0.398E 04	0.11 - 0.16	0.15 - 0.23	0.	0.	0.	0.
0.	0.	0.398E 04 - 0.531E 04	0.16 - 0.22	0.23 - 0.31	0.	0.	0.	0.
0.186E 07	0.00519	0.531E 04 - 0.663E 04	0.22 - 0.27	0.31 - 0.38	-0.119E 07	0.287E 04	-0.119E 07	-0.119E 07
0.426E 08	0.12392	0.663E 04 - 0.796E 04	0.27 - 0.33	0.38 - 0.46	-0.119E 07	0.287E 04	-0.119E 07	-0.119E 07
0.984E 08	0.39791	0.796E 04 - 0.929E 04	0.33 - 0.38	0.46 - 0.54	-0.119E 07	0.291E 04	-0.119E 07	-0.120E 07
0.455E 08	0.52452	0.929E 04 - 0.106E 05	0.38 - 0.43	0.54 - 0.62	-0.119E 07	0.400E 04	-0.119E 07	-0.120E 07
0.221E 08	0.58598	0.106E 05 - 0.119E 05	0.43 - 0.49	0.62 - 0.69	-0.120E 07	0.655E 04	-0.119E 07	-0.120E 07
0.270E 08	0.66128	0.119E 05 - 0.133E 05	0.49 - 0.54	0.69 - 0.77	-0.120E 07	0.173E 04	-0.119E 07	-0.121E 07
0.254E 08	0.73211	0.133E 05 - 0.146E 05	0.54 - 0.60	0.77 - 0.85	-0.121E 07	0.169E 04	-0.120E 07	-0.121E 07
0.238E 08	0.79841	0.146E 05 - 0.159E 05	0.60 - 0.65	0.85 - 0.92	-0.121E 07	0.202E 04	-0.120E 07	-0.121E 07
0.252E 08	0.86864	0.159E 05 - 0.172E 05	0.65 - 0.71	0.92 - 1.00	-0.121E 07	0.119E 04	-0.120E 07	-0.121E 07
0.133E 08	0.90561	0.172E 05 - 0.178E 05	0.71 - 0.73	1.00 - 1.03	-0.121E 07	0.627E 03	-0.120E 07	-0.121E 07
0.869E 07	0.92982	0.178E 05 - 0.184E 05	0.73 - 0.75	1.03 - 1.06	-0.121E 07	0.496E 03	-0.120E 07	-0.121E 07
0.728E 07	0.95008	0.184E 05 - 0.189E 05	0.75 - 0.77	1.06 - 1.10	-0.121E 07	0.496E 03	-0.120E 07	-0.121E 07
0.566E 07	0.96585	0.189E 05 - 0.195E 05	0.77 - 0.80	1.10 - 1.13	-0.121E 07	0.128E 03	-0.121E 07	-0.121E 07
0.421E 07	0.97757	0.195E 05 - 0.200E 05	0.80 - 0.82	1.13 - 1.16	-0.121E 07	0.181E 03	-0.121E 07	-0.121E 07
0.297E 07	0.98584	0.200E 05 - 0.206E 05	0.82 - 0.84	1.16 - 1.19	-0.121E 07	0.	-0.121E 07	-0.121E 07
0.200E 07	0.99140	0.206E 05 - 0.211E 05	0.84 - 0.86	1.19 - 1.22	-0.121E 07	0.181E 03	-0.121E 07	-0.121E 07
0.128E 07	0.99498	0.211E 05 - 0.217E 05	0.86 - 0.89	1.22 - 1.26	-0.121E 07	0.181E 03	-0.121E 07	-0.121E 07
0.793E 06	0.99719	0.217E 05 - 0.222E 05	0.89 - 0.91	1.26 - 1.29	-0.121E 07	0.128E 03	-0.121E 07	-0.121E 07
0.472E 06	0.99850	0.222E 05 - 0.228E 05	0.91 - 0.93	1.29 - 1.32	-0.121E 07	0.181E 03	-0.121E 07	-0.121E 07
0.271E 06	0.99925	0.228E 05 - 0.233E 05	0.93 - 0.95	1.32 - 1.35	-0.121E 07	0.128E 03	-0.121E 07	-0.121E 07
0.151E 06	0.99968	0.233E 05 - 0.239E 05	0.95 - 0.98	1.35 - 1.38	-0.121E 07	0.	-0.121E 07	-0.121E 07
0.817E 05	0.99990	0.239E 05 - 0.244E 05	0.98 - 1.00	1.38 - 1.42	-0.121E 07	0.128E 03	-0.121E 07	-0.121E 07

TOTAL CYCLES = 0.359E 09

ROOT MEAN CUBED IS 0.130E 05 AVERAGE MEAN IS -0.120E 07

TABLE H- 88
CUMULATIVE FATIGUE HISTOGRAM OUTPUT

YAW BRNG MX

NO. CYCLES IN 30 YEARS (TYPES 1+2)	CUM PROB	HALF-RANGE FATIGUE LOADS: LOAD LEVELS	NORMALIZED LOAD LEVELS	LOAD/50% AT RATED	CORRESPONDING MID-RANGE LOAD DISTRIBUTION: MEAN	STANDARD DEVIATION	MAXIMUM	MINIMUM
0.	0.	0. - 0.646E 04	0. - 0.01	0. - 0.08	0.	0.	0.	0.
0.	0.	0.646E 04 - 0.129E 05	0.01 - 0.03	0.08 - 0.15	0.	0.	0.	0.
0.	0.	0.129E 05 - 0.194E 05	0.03 - 0.04	0.15 - 0.23	0.	0.	0.	0.
0.	0.	0.194E 05 - 0.258E 05	0.04 - 0.06	0.23 - 0.31	0.	0.	0.	0.
0.	0.	0.258E 05 - 0.323E 05	0.06 - 0.07	0.31 - 0.38	0.	0.	0.	0.
0.	0.	0.323E 05 - 0.387E 05	0.07 - 0.09	0.38 - 0.46	0.	0.	0.	0.
0.278E 05	0.00008	0.387E 05 - 0.452E 05	0.09 - 0.10	0.46 - 0.54	-0.527E 06	0.	-0.527E 06	-0.527E 06
0.165E 07	0.00468	0.452E 05 - 0.517E 05	0.10 - 0.12	0.54 - 0.62	-0.398E 06	0.106E 06	-0.311E 06	-0.527E 06
0.116E 08	0.03711	0.517E 05 - 0.581E 05	0.12 - 0.13	0.62 - 0.69	-0.375E 06	0.108E 06	-0.650E 05	-0.531E 06
0.302E 08	0.12112	0.581E 05 - 0.646E 05	0.13 - 0.15	0.69 - 0.77	-0.345E 06	0.121E 06	-0.650E 05	-0.531E 06
0.427E 08	0.24014	0.646E 05 - 0.710E 05	0.15 - 0.16	0.77 - 0.85	-0.298E 06	0.156E 06	-0.650E 05	-0.531E 06
0.498E 08	0.37875	0.710E 05 - 0.775E 05	0.16 - 0.17	0.85 - 0.92	-0.258E 06	0.190E 06	-0.650E 05	-0.531E 06
0.517E 08	0.52258	0.775E 05 - 0.840E 05	0.17 - 0.19	0.92 - 1.00	-0.254E 06	0.207E 06	-0.631E 05	-0.534E 06
0.141E 09	0.91431	0.840E 05 - 0.112E 06	0.19 - 0.25	1.00 - 1.33	-0.238E 06	0.165E 06	-0.475E 05	-0.545E 06
0.244E 08	0.98216	0.112E 06 - 0.139E 06	0.25 - 0.31	1.33 - 1.66	-0.202E 06	0.721E 05	-0.250E 05	-0.531E 06
0.341E 07	0.99165	0.139E 06 - 0.167E 06	0.31 - 0.38	1.66 - 1.99	-0.287E 06	0.145E 06	-0.845E 05	-0.531E 06
0.138E 07	0.99548	0.167E 06 - 0.195E 06	0.38 - 0.44	1.99 - 2.32	-0.361E 06	0.129E 06	-0.946E 05	-0.531E 06
0.735E 06	0.99753	0.195E 06 - 0.222E 06	0.44 - 0.50	2.32 - 2.65	-0.412E 06	0.119E 06	-0.197E 06	-0.531E 06
0.402E 06	0.99865	0.222E 06 - 0.250E 06	0.50 - 0.56	2.65 - 2.98	-0.458E 06	0.948E 05	-0.174E 06	-0.531E 06
0.227E 06	0.99928	0.250E 06 - 0.278E 06	0.56 - 0.63	2.98 - 3.31	-0.476E 06	0.695E 05	-0.157E 06	-0.531E 06
0.120E 06	0.99962	0.278E 06 - 0.305E 06	0.63 - 0.69	3.31 - 3.64	-0.483E 06	0.494E 05	-0.243E 06	-0.531E 06
0.595E 05	0.99978	0.305E 06 - 0.333E 06	0.69 - 0.75	3.64 - 3.97	-0.483E 06	0.428E 05	-0.292E 06	-0.531E 06
0.268E 05	0.99986	0.333E 06 - 0.361E 06	0.75 - 0.81	3.97 - 4.30	-0.479E 06	0.445E 05	-0.436E 06	-0.531E 06
0.113E 05	0.99989	0.361E 06 - 0.388E 06	0.81 - 0.88	4.30 - 4.63	-0.475E 06	0.495E 05	-0.426E 06	-0.531E 06
0.463E 04	0.99990	0.388E 06 - 0.416E 06	0.88 - 0.94	4.63 - 4.96	-0.456E 06	0.528E 05	-0.417E 06	-0.531E 06
0.767E 03	0.99990	0.416E 06 - 0.444E 06	0.94 - 1.00	4.96 - 5.29	-0.527E 06	0.129E 04	-0.527E 06	-0.531E 06

TOTAL CYCLES = 0.359E 09

ROOT MEAN CUBED IS 0.935E 05 AVERAGE MEAN IS -0.264E 06

TABLE H- 89
CUMULATIVE FATIGUE HISTOGRAM OUTPUT

YAW BRNG MY

NO. CYCLES IN 30 YEARS (TYPES 1+2)	CUM PROB	HALF-RANGE FATIGUE LOADS: LOAD LEVELS	NORMALIZED LOAD LEVELS	LOAD/50% AT RATED	CORRESPONDING MID-RANGE LOAD DISTRIBUTION: MEAN	STANDARD DEVIATION	MAXIMUM	MINIMUM
0.	0.	0. - 0.215E 05	0. - 0.02	0. - 0.08	0.	0.	0.	0.
0.	0.	0.215E 05 - 0.431E 05	0.02 - 0.03	0.08 - 0.15	0.	0.	0.	0.
0.	0.	0.431E 05 - 0.646E 05	0.03 - 0.05	0.15 - 0.23	0.	0.	0.	0.
0.	0.	0.646E 05 - 0.862E 05	0.05 - 0.06	0.23 - 0.31	0.	0.	0.	0.
0.834E 05	0.00023	0.862E 05 - 0.108E 06	0.06 - 0.08	0.31 - 0.38	-0.753E 07	0.102E 04	-0.753E 07	-0.753E 07
0.173E 07	0.00505	0.108E 06 - 0.129E 06	0.08 - 0.10	0.38 - 0.46	-0.822E 07	0.979E 06	-0.659E 07	-0.940E 07
0.558E 07	0.02060	0.129E 06 - 0.151E 06	0.10 - 0.11	0.46 - 0.54	-0.819E 07	0.979E 06	-0.659E 07	-0.940E 07
0.130E 08	0.05674	0.151E 06 - 0.172E 06	0.11 - 0.13	0.54 - 0.62	-0.818E 07	0.989E 06	-0.659E 07	-0.940E 07
0.224E 08	0.11912	0.172E 06 - 0.194E 06	0.13 - 0.14	0.62 - 0.69	-0.817E 07	0.997E 06	-0.659E 07	-0.940E 07
0.312E 08	0.20608	0.194E 06 - 0.215E 06	0.14 - 0.16	0.69 - 0.77	-0.816E 07	0.100E 07	-0.659E 07	-0.940E 07
0.372E 08	0.30960	0.215E 06 - 0.237E 06	0.16 - 0.17	0.77 - 0.85	-0.815E 07	0.101E 07	-0.659E 07	-0.940E 07
0.393E 08	0.41900	0.237E 06 - 0.258E 06	0.17 - 0.19	0.85 - 0.92	-0.814E 07	0.102E 07	-0.659E 07	-0.940E 07
0.379E 08	0.52454	0.258E 06 - 0.280E 06	0.19 - 0.21	0.92 - 1.00	-0.813E 07	0.102E 07	-0.659E 07	-0.940E 07
0.104E 09	0.81500	0.280E 06 - 0.301E 06	0.21 - 0.27	1.00 - 1.30	-0.812E 07	0.103E 07	-0.659E 07	-0.945E 07
0.424E 08	0.93309	0.301E 06 - 0.323E 06	0.27 - 0.33	1.30 - 1.59	-0.811E 07	0.104E 07	-0.659E 07	-0.953E 07
0.145E 08	0.97335	0.323E 06 - 0.344E 06	0.33 - 0.39	1.59 - 1.89	-0.812E 07	0.104E 07	-0.659E 07	-0.962E 07
0.532E 07	0.98816	0.344E 06 - 0.366E 06	0.39 - 0.45	1.89 - 2.18	-0.810E 07	0.999E 06	-0.659E 07	-0.970E 07
0.241E 07	0.99488	0.366E 06 - 0.387E 06	0.45 - 0.51	2.18 - 2.48	-0.801E 07	0.945E 06	-0.659E 07	-0.978E 07
0.109E 07	0.99791	0.387E 06 - 0.409E 06	0.51 - 0.57	2.48 - 2.77	-0.774E 07	0.804E 06	-0.692E 07	-0.986E 07
0.358E 06	0.99890	0.409E 06 - 0.430E 06	0.57 - 0.63	2.77 - 3.07	-0.797E 07	0.733E 06	-0.713E 07	-0.938E 07
0.182E 06	0.99941	0.430E 06 - 0.452E 06	0.63 - 0.69	3.07 - 3.36	-0.786E 07	0.679E 06	-0.721E 07	-0.937E 07
0.935E 05	0.99967	0.452E 06 - 0.473E 06	0.69 - 0.76	3.36 - 3.66	-0.780E 07	0.608E 06	-0.729E 07	-0.937E 07
0.441E 05	0.99979	0.473E 06 - 0.495E 06	0.76 - 0.82	3.66 - 3.95	-0.774E 07	0.526E 06	-0.735E 07	-0.937E 07
0.249E 05	0.99986	0.495E 06 - 0.516E 06	0.82 - 0.88	3.95 - 4.25	-0.772E 07	0.412E 06	-0.746E 07	-0.854E 07
0.100E 05	0.99989	0.516E 06 - 0.538E 06	0.88 - 0.94	4.25 - 4.54	-0.773E 07	0.355E 06	-0.754E 07	-0.854E 07
0.486E 04	0.99990	0.538E 06 - 0.559E 06	0.94 - 1.00	4.54 - 4.84	-0.783E 07	0.365E 06	-0.761E 07	-0.853E 07

TOTAL CYCLES = 0.359E 09

ROOT MEAN CUBED IS 0.329E 06 AVERAGE MEAN IS -0.813E 07

TABLE H- 90
CUMULATIVE FATIGUE HISTOGRAM OUTPUT

YAW BRNG MZ

NO. CYCLES IN 30 YEARS (TYPES 1+2)	CUM PROB	HALF-RANGE FATIGUE LOADS: LOAD LEVELS	NORMALIZED LOAD LEVELS	LOAD/50% AT RATED	CORRESPONDING MID-RANGE LOAD DISTRIBUTION: MEAN	STANDARD DEVIATION	MAXIMUM	MINIMUM
0.	0.	0. - 0.141E 05	0. - 0.01	0. - 0.08	0.	0.	0.	0.
0.	0.	0.141E 05 - 0.283E 05	0.01 - 0.01	0.08 - 0.15	0.	0.	0.	0.
0.	0.	0.283E 05 - 0.424E 05	0.01 - 0.02	0.15 - 0.23	0.	0.	0.	0.
0.	0.	0.424E 05 - 0.565E 05	0.02 - 0.02	0.23 - 0.31	0.	0.	0.	0.
0.183E 06	0.00051	0.565E 05 - 0.707E 05	0.02 - 0.03	0.31 - 0.38	-0.256E 07	0.622E 06	-0.227E 07	-0.389E 07
0.124E 07	0.00396	0.707E 05 - 0.848E 05	0.03 - 0.04	0.38 - 0.46	-0.302E 07	0.815E 06	-0.227E 07	-0.392E 07
0.354E 07	0.01382	0.848E 05 - 0.989E 05	0.04 - 0.04	0.46 - 0.54	-0.297E 07	0.834E 06	-0.160E 07	-0.392E 07
0.755E 07	0.03484	0.989E 05 - 0.113E 06	0.04 - 0.05	0.54 - 0.62	-0.290E 07	0.942E 06	-0.617E 06	-0.392E 07
0.123E 08	0.06896	0.113E 06 - 0.127E 06	0.05 - 0.05	0.62 - 0.69	-0.287E 07	0.978E 06	-0.617E 06	-0.392E 07
0.169E 08	0.11616	0.127E 06 - 0.141E 06	0.05 - 0.06	0.69 - 0.77	-0.280E 07	0.104E 07	-0.617E 06	-0.392E 07
0.208E 08	0.17414	0.141E 06 - 0.155E 06	0.06 - 0.07	0.77 - 0.85	-0.271E 07	0.111E 07	-0.617E 06	-0.392E 07
0.235E 08	0.23958	0.155E 06 - 0.170E 06	0.07 - 0.07	0.85 - 0.92	-0.259E 07	0.116E 07	-0.617E 06	-0.392E 07
0.250E 08	0.30913	0.170E 06 - 0.184E 06	0.07 - 0.08	0.92 - 1.00	-0.246E 07	0.121E 07	-0.617E 06	-0.392E 07
0.201E 09	0.86800	0.184E 06 - 0.350E 06	0.08 - 0.15	1.00 - 1.91	-0.184E 07	0.118E 07	-0.574E 06	-0.392E 07
0.365E 08	0.96970	0.350E 06 - 0.517E 06	0.15 - 0.22	1.91 - 2.81	-0.125E 07	0.794E 06	-0.448E 06	-0.392E 07
0.617E 07	0.98687	0.517E 06 - 0.684E 06	0.22 - 0.29	2.81 - 3.72	-0.159E 07	0.101E 07	-0.424E 06	-0.387E 07
0.201E 07	0.99246	0.684E 06 - 0.850E 06	0.29 - 0.36	3.72 - 4.63	-0.219E 07	0.105E 07	-0.523E 06	-0.373E 07
0.101E 07	0.99527	0.850E 06 - 0.102E 07	0.36 - 0.43	4.63 - 5.53	-0.267E 07	0.931E 06	-0.670E 06	-0.357E 07
0.607E 06	0.99696	0.102E 07 - 0.118E 07	0.43 - 0.50	5.53 - 6.44	-0.287E 07	0.798E 06	-0.698E 06	-0.340E 07
0.396E 06	0.99806	0.118E 07 - 0.135E 07	0.50 - 0.57	6.44 - 7.35	-0.294E 07	0.624E 06	-0.117E 07	-0.323E 07
0.265E 06	0.99880	0.135E 07 - 0.152E 07	0.57 - 0.65	7.35 - 8.25	-0.292E 07	0.413E 06	-0.123E 07	-0.307E 07
0.172E 06	0.99927	0.152E 07 - 0.168E 07	0.65 - 0.72	8.25 - 9.16	-0.283E 07	0.261E 06	-0.136E 07	-0.290E 07
0.106E 06	0.99957	0.168E 07 - 0.185E 07	0.72 - 0.79	9.16 - 10.07	-0.269E 07	0.134E 06	-0.224E 07	-0.276E 07
0.609E 05	0.99974	0.185E 07 - 0.202E 07	0.79 - 0.86	10.07 - 10.98	-0.254E 07	0.100E 06	-0.214E 07	-0.257E 07
0.348E 05	0.99984	0.202E 07 - 0.218E 07	0.86 - 0.93	10.98 - 11.88	-0.239E 07	0.680E 05	-0.202E 07	-0.245E 07
0.233E 05	0.99990	0.218E 07 - 0.235E 07	0.93 - 1.00	11.88 - 12.79	-0.224E 07	0.805E 04	-0.223E 07	-0.226E 07

TOTAL CYCLES = 0.359E 09

ROOT MEAN CUBED IS 0.347E 06 AVERAGE MEAN IS -0.205E 07

TABLE H- 91
CUMULATIVE FATIGUE HISTOGRAM OUTPUT

TOWER 185 VX

NO. CYCLES IN 30 YEARS (TYPES 1+2)	CUM PROB	HALF-RANGE FATIGUE LOADS: LOAD LEVELS	NORMALIZED LOAD LEVELS	LOAD/50% AT RATED	CORRESPONDING MID-RANGE LOAD DISTRIBUTION: MEAN	STANDARD DEVIATION	MAXIMUM	MINIMUM
0.	0.	0. - 0.133E 04	0. - 0.05	0. - 0.08	0.	0.	0.	0.
0.	0.	0.133E 04 - 0.265E 04	0.05 - 0.11	0.08 - 0.15	0.	0.	0.	0.
0.	0.	0.265E 04 - 0.398E 04	0.11 - 0.16	0.15 - 0.23	0.	0.	0.	0.
0.	0.	0.398E 04 - 0.531E 04	0.16 - 0.22	0.23 - 0.31	0.	0.	0.	0.
0.186E 07	0.00519	0.531E 04 - 0.663E 04	0.22 - 0.27	0.31 - 0.38	-0.122E 07	0.288E 04	-0.122E 07	-0.123E 07
0.426E 08	0.12392	0.663E 04 - 0.796E 04	0.27 - 0.33	0.38 - 0.46	-0.122E 07	0.287E 04	-0.122E 07	-0.123E 07
0.984E 08	0.39791	0.796E 04 - 0.929E 04	0.33 - 0.38	0.46 - 0.54	-0.122E 07	0.290E 04	-0.122E 07	-0.124E 07
0.455E 08	0.52452	0.929E 04 - 0.106E 05	0.38 - 0.43	0.54 - 0.62	-0.122E 07	0.400E 04	-0.122E 07	-0.124E 07
0.221E 08	0.58598	0.106E 05 - 0.119E 05	0.43 - 0.49	0.62 - 0.69	-0.123E 07	0.655E 04	-0.122E 07	-0.124E 07
0.270E 08	0.66128	0.119E 05 - 0.133E 05	0.49 - 0.54	0.69 - 0.77	-0.124E 07	0.173E 04	-0.122E 07	-0.124E 07
0.254E 08	0.73211	0.133E 05 - 0.146E 05	0.54 - 0.60	0.77 - 0.85	-0.124E 07	0.169E 04	-0.124E 07	-0.124E 07
0.238E 08	0.79841	0.146E 05 - 0.159E 05	0.60 - 0.65	0.85 - 0.92	-0.124E 07	0.201E 04	-0.124E 07	-0.124E 07
0.252E 08	0.86864	0.159E 05 - 0.172E 05	0.65 - 0.71	0.92 - 1.00	-0.124E 07	0.121E 04	-0.124E 07	-0.124E 07
0.133E 08	0.90561	0.172E 05 - 0.178E 05	0.71 - 0.73	1.00 - 1.03	-0.124E 07	0.572E 03	-0.124E 07	-0.124E 07
0.869E 07	0.92982	0.178E 05 - 0.184E 05	0.73 - 0.75	1.03 - 1.06	-0.124E 07	0.512E 03	-0.124E 07	-0.124E 07
0.728E 07	0.95008	0.184E 05 - 0.189E 05	0.75 - 0.77	1.06 - 1.10	-0.124E 07	0.462E 03	-0.124E 07	-0.124E 07
0.566E 07	0.96585	0.189E 05 - 0.195E 05	0.77 - 0.80	1.10 - 1.13	-0.124E 07	0.181E 03	-0.124E 07	-0.124E 07
0.421E 07	0.97757	0.195E 05 - 0.200E 05	0.80 - 0.82	1.13 - 1.16	-0.124E 07	0.	-0.124E 07	-0.124E 07
0.297E 07	0.98584	0.200E 05 - 0.206E 05	0.82 - 0.84	1.16 - 1.19	-0.124E 07	0.	-0.124E 07	-0.124E 07
0.200E 07	0.99140	0.206E 05 - 0.211E 05	0.84 - 0.86	1.19 - 1.22	-0.124E 07	0.128E 03	-0.124E 07	-0.124E 07
0.128E 07	0.99498	0.211E 05 - 0.217E 05	0.86 - 0.89	1.22 - 1.26	-0.124E 07	0.	-0.124E 07	-0.124E 07
0.793E 06	0.99719	0.217E 05 - 0.222E 05	0.89 - 0.91	1.26 - 1.29	-0.124E 07	0.	-0.124E 07	-0.124E 07
0.472E 06	0.99850	0.222E 05 - 0.228E 05	0.91 - 0.93	1.29 - 1.32	-0.124E 07	0.	-0.124E 07	-0.124E 07
0.271E 06	0.99925	0.228E 05 - 0.233E 05	0.93 - 0.95	1.32 - 1.35	-0.124E 07	0.128E 03	-0.124E 07	-0.124E 07
0.151E 06	0.99968	0.233E 05 - 0.239E 05	0.95 - 0.98	1.35 - 1.38	-0.124E 07	0.181E 03	-0.124E 07	-0.124E 07
0.817E 05	0.99990	0.239E 05 - 0.244E 05	0.98 - 1.00	1.38 - 1.42	-0.124E 07	0.222E 03	-0.124E 07	-0.124E 07

TOTAL CYCLES = 0.359E 09

ROOT MEAN CUBED IS 0.130E 05 AVERAGE MEAN IS -0.123E 07

TABLE H- 92
CUMULATIVE FATIGUE HISTOGRAM OUTPUT

TOWER 185 VY

NO. CYCLES IN 30 YEARS (TYPES 1+2)	CUM PROB	HALF-RANGE FATIGUE LOADS: LOAD LEVELS	NORMALIZED LOAD LEVELS	LOAD/50% AT RATED	CORRESPONDING MID-RANGE LOAD DISTRIBUTION: MEAN	STANDARD DEVIATION	MAXIMUM	MINIMUM
0.	0.	0. - 0.666E 03	0. - 0.03	0. - 0.08	0.	0.	0.	0.
0.	0.	0.666E 03 - 0.133E 04	0.03 - 0.06	0.08 - 0.15	0.	0.	0.	0.
0.	0.	0.133E 04 - 0.200E 04	0.06 - 0.10	0.15 - 0.23	0.	0.	0.	0.
0.	0.	0.200E 04 - 0.266E 04	0.10 - 0.13	0.23 - 0.31	0.	0.	0.	0.
0.	0.	0.266E 04 - 0.333E 04	0.13 - 0.16	0.31 - 0.38	0.	0.	0.	0.
0.	0.	0.333E 04 - 0.399E 04	0.16 - 0.19	0.38 - 0.46	0.	0.	0.	0.
0.	0.	0.399E 04 - 0.466E 04	0.19 - 0.23	0.46 - 0.54	0.	0.	0.	0.
0.	0.	0.466E 04 - 0.533E 04	0.23 - 0.26	0.54 - 0.62	0.	0.	0.	0.
0.	0.	0.533E 04 - 0.599E 04	0.26 - 0.29	0.62 - 0.69	0.	0.	0.	0.
0.665E 06	0.00185	0.599E 04 - 0.666E 04	0.29 - 0.32	0.69 - 0.77	0.239E 04	0.	0.239E 04	0.239E 04
0.488E 07	0.01544	0.666E 04 - 0.732E 04	0.32 - 0.36	0.77 - 0.85	0.223E 04	0.336E 03	0.239E 04	0.149E 04
0.159E 08	0.05976	0.732E 04 - 0.799E 04	0.36 - 0.39	0.85 - 0.92	0.215E 04	0.386E 03	0.239E 04	0.149E 04
0.301E 08	0.14370	0.799E 04 - 0.866E 04	0.39 - 0.42	0.92 - 1.00	0.204E 04	0.420E 03	0.239E 04	0.149E 04
0.537E 08	0.29335	0.866E 04 - 0.957E 04	0.42 - 0.46	1.00 - 1.11	0.191E 04	0.416E 03	0.239E 04	0.125E 04
0.399E 08	0.40439	0.957E 04 - 0.105E 05	0.46 - 0.51	1.11 - 1.21	0.174E 04	0.421E 03	0.239E 04	0.704E 03
0.235E 08	0.46986	0.105E 05 - 0.114E 05	0.51 - 0.55	1.21 - 1.32	0.152E 04	0.407E 03	0.239E 04	0.172E 03
0.255E 08	0.54083	0.114E 05 - 0.123E 05	0.55 - 0.60	1.32 - 1.42	0.122E 04	0.330E 03	0.239E 04	0.704E 03
0.355E 08	0.63959	0.123E 05 - 0.132E 05	0.60 - 0.64	1.42 - 1.53	0.107E 04	0.275E 03	0.192E 04	0.704E 03
0.435E 08	0.76086	0.132E 05 - 0.142E 05	0.64 - 0.69	1.53 - 1.64	0.101E 04	0.271E 03	0.192E 04	0.704E 03
0.394E 08	0.87056	0.142E 05 - 0.151E 05	0.69 - 0.73	1.64 - 1.74	0.894E 03	0.271E 03	0.174E 04	0.562E 03
0.239E 08	0.93716	0.151E 05 - 0.160E 05	0.73 - 0.78	1.74 - 1.85	0.863E 03	0.266E 03	0.125E 04	0.258E 03
0.130E 08	0.97333	0.160E 05 - 0.169E 05	0.78 - 0.82	1.85 - 1.95	0.831E 03	0.231E 03	0.125E 04	0.704E 03
0.603E 07	0.99014	0.169E 05 - 0.178E 05	0.82 - 0.87	1.95 - 2.06	0.797E 03	0.205E 03	0.125E 04	0.704E 03
0.240E 07	0.99684	0.178E 05 - 0.188E 05	0.87 - 0.91	2.06 - 2.17	0.771E 03	0.180E 03	0.125E 04	0.704E 03
0.859E 06	0.99923	0.188E 05 - 0.197E 05	0.91 - 0.96	2.17 - 2.27	0.765E 03	0.173E 03	0.125E 04	0.704E 03
0.243E 06	0.99990	0.197E 05 - 0.206E 05	0.96 - 1.00	2.27 - 2.38	0.704E 03	0.625E-01	0.704E 03	0.704E 03

TOTAL CYCLES = 0.359E 09

ROOT MEAN CUBED IS 0.124E 05 AVERAGE MEAN IS 0.140E 04

TABLE H- 93
CUMULATIVE FATIGUE HISTOGRAM OUTPUT

TOWER 185 VZ

NO. CYCLES IN 30 YEARS (TYPES 1+2)	CUM PROB	HALF-RANGE FATIGUE LOADS: LOAD LEVELS	NORMALIZED LOAD LEVELS	LOAD/50% AT RATED	CORRESPONDING MID-RANGE LOAD DISTRIBUTION: MEAN	STANDARD DEVIATION	MAXIMUM	MINIMUM
0.	0.	0. - 0.846E 03	0. - 0.01	0. - 0.08	0.	0.	0.	0.
0.	0.	0.846E 03 - 0.169E 04	0.01 - 0.02	0.08 - 0.15	0.	0.	0.	0.
0.	0.	0.169E 04 - 0.254E 04	0.02 - 0.03	0.15 - 0.23	0.	0.	0.	0.
0.897E 05	0.00025	0.254E 04 - 0.338E 04	0.03 - 0.04	0.23 - 0.31	-0.178E 06	0.160E 02	-0.178E 06	-0.178E 06
0.875E 06	0.00269	0.338E 04 - 0.423E 04	0.04 - 0.04	0.31 - 0.38	-0.196E 06	0.234E 05	-0.178E 06	-0.228E 06
0.314E 07	0.01143	0.423E 04 - 0.508E 04	0.04 - 0.05	0.38 - 0.46	-0.177E 06	0.437E 05	-0.767E 05	-0.228E 06
0.666E 07	0.02998	0.508E 04 - 0.592E 04	0.05 - 0.06	0.46 - 0.54	-0.177E 06	0.451E 05	-0.767E 05	-0.228E 06
0.114E 08	0.06165	0.592E 04 - 0.677E 04	0.06 - 0.07	0.54 - 0.62	-0.172E 06	0.480E 05	-0.767E 05	-0.228E 06
0.163E 08	0.10703	0.677E 04 - 0.762E 04	0.07 - 0.08	0.62 - 0.69	-0.168E 06	0.504E 05	-0.767E 05	-0.228E 06
0.206E 08	0.16439	0.762E 04 - 0.846E 04	0.08 - 0.09	0.69 - 0.77	-0.164E 06	0.522E 05	-0.767E 05	-0.228E 06
0.238E 08	0.23052	0.846E 04 - 0.931E 04	0.09 - 0.10	0.77 - 0.85	-0.160E 06	0.535E 05	-0.767E 05	-0.228E 06
0.256E 08	0.30169	0.931E 04 - 0.102E 05	0.10 - 0.11	0.85 - 0.92	-0.156E 06	0.544E 05	-0.767E 05	-0.228E 06
0.261E 08	0.37431	0.102E 05 - 0.110E 05	0.11 - 0.12	0.92 - 1.00	-0.152E 06	0.550E 05	-0.767E 05	-0.228E 06
0.148E 09	0.78652	0.110E 05 - 0.175E 05	0.12 - 0.18	1.00 - 1.59	-0.140E 06	0.549E 05	-0.759E 05	-0.228E 06
0.519E 08	0.93117	0.175E 05 - 0.240E 05	0.18 - 0.25	1.59 - 2.18	-0.124E 06	0.502E 05	-0.730E 05	-0.228E 06
0.155E 08	0.97444	0.240E 05 - 0.305E 05	0.25 - 0.32	2.18 - 2.78	-0.120E 06	0.482E 05	-0.683E 05	-0.228E 06
0.531E 07	0.98921	0.305E 05 - 0.370E 05	0.32 - 0.39	2.78 - 3.37	-0.128E 06	0.503E 05	-0.630E 05	-0.228E 06
0.218E 07	0.99529	0.370E 05 - 0.436E 05	0.39 - 0.46	3.37 - 3.96	-0.139E 06	0.506E 05	-0.577E 05	-0.228E 06
0.819E 06	0.99757	0.436E 05 - 0.501E 05	0.46 - 0.52	3.96 - 4.55	-0.176E 06	0.434E 05	-0.543E 05	-0.228E 06
0.433E 06	0.99877	0.501E 05 - 0.566E 05	0.52 - 0.59	4.55 - 5.14	-0.188E 06	0.371E 05	-0.777E 05	-0.228E 06
0.221E 06	0.99939	0.566E 05 - 0.631E 05	0.59 - 0.66	5.14 - 5.74	-0.198E 06	0.290E 05	-0.779E 05	-0.228E 06
0.107E 06	0.99969	0.631E 05 - 0.696E 05	0.66 - 0.73	5.74 - 6.33	-0.203E 06	0.269E 05	-0.123E 06	-0.228E 06
0.476E 05	0.99982	0.696E 05 - 0.761E 05	0.73 - 0.80	6.33 - 6.92	-0.209E 06	0.225E 05	-0.123E 06	-0.228E 06
0.192E 05	0.99987	0.761E 05 - 0.826E 05	0.80 - 0.86	6.92 - 7.51	-0.213E 06	0.194E 05	-0.184E 06	-0.228E 06
0.795E 04	0.99989	0.826E 05 - 0.891E 05	0.86 - 0.93	7.51 - 8.10	-0.212E 06	0.201E 05	-0.184E 06	-0.228E 06
0.339E 04	0.99990	0.891E 05 - 0.956E 05	0.93 - 1.00	8.10 - 8.69	-0.215E 06	0.198E 05	-0.184E 06	-0.228E 06

TOTAL CYCLES = 0.359E 09

ROOT MEAN CUBED IS 0.175E 05 AVERAGE MEAN IS -0.145E 06

TABLE H- 94
CUMULATIVE FATIGUE HISTOGRAM OUTPUT

TOWER 185 MX

NO. CYCLES IN 30 YEARS (TYPES 1+2)	CUM PROB	HALF-RANGE FATIGUE LOADS: LOAD LEVELS	NORMALIZED LOAD LEVELS	LOAD/50% AT RATED	CORRESPONDING MID-RANGE LOAD DISTRIBUTION: MEAN	STANDARD DEVIATION	MAXIMUM	MINIMUM
0.	0.	0. - 0.646E 04	0. - 0.01	0. - 0.08	0.	0.	0.	0.
0.	0.	0.646E 04 - 0.129E 05	0.01 - 0.03	0.08 - 0.15	0.	0.	0.	0.
0.	0.	0.129E 05 - 0.194E 05	0.03 - 0.04	0.15 - 0.23	0.	0.	0.	0.
0.	0.	0.194E 05 - 0.258E 05	0.04 - 0.06	0.23 - 0.31	0.	0.	0.	0.
0.	0.	0.258E 05 - 0.323E 05	0.06 - 0.07	0.31 - 0.38	0.	0.	0.	0.
0.	0.	0.323E 05 - 0.387E 05	0.07 - 0.09	0.38 - 0.46	0.	0.	0.	0.
0.278E 05	0.00008	0.387E 05 - 0.452E 05	0.09 - 0.10	0.46 - 0.54	-0.527E 06	0.	-0.527E 06	-0.527E 06
0.165E 07	0.00468	0.452E 05 - 0.517E 05	0.10 - 0.12	0.54 - 0.62	-0.398E 06	0.106E 06	-0.311E 06	-0.527E 06
0.116E 08	0.03711	0.517E 05 - 0.581E 05	0.12 - 0.13	0.62 - 0.69	-0.375E 06	0.108E 06	-0.650E 05	-0.531E 06
0.302E 08	0.12112	0.581E 05 - 0.646E 05	0.13 - 0.15	0.69 - 0.77	-0.345E 06	0.121E 06	-0.650E 05	-0.531E 06
0.427E 08	0.24014	0.646E 05 - 0.710E 05	0.15 - 0.16	0.77 - 0.85	-0.298E 06	0.156E 06	-0.650E 05	-0.531E 06
0.498E 08	0.37875	0.710E 05 - 0.775E 05	0.16 - 0.17	0.85 - 0.92	-0.258E 06	0.190E 06	-0.650E 05	-0.531E 06
0.517E 08	0.52258	0.775E 05 - 0.840E 05	0.17 - 0.19	0.92 - 1.00	-0.254E 06	0.207E 06	-0.631E 05	-0.534E 06
0.141E 09	0.91431	0.840E 05 - 0.112E 06	0.19 - 0.25	1.00 - 1.33	-0.238E 06	0.165E 06	-0.475E 05	-0.545E 06
0.244E 08	0.98216	0.112E 06 - 0.139E 06	0.25 - 0.31	1.33 - 1.66	-0.202E 06	0.721E 05	-0.250E 05	-0.531E 06
0.341E 07	0.99165	0.139E 06 - 0.167E 06	0.31 - 0.38	1.66 - 1.99	-0.287E 06	0.145E 06	-0.845E 05	-0.531E 06
0.138E 07	0.99548	0.167E 06 - 0.195E 06	0.38 - 0.44	1.99 - 2.32	-0.361E 06	0.129E 06	-0.946E 05	-0.531E 06
0.735E 06	0.99753	0.195E 06 - 0.222E 06	0.44 - 0.50	2.32 - 2.65	-0.412E 06	0.119E 06	-0.197E 06	-0.531E 06
0.402E 06	0.99865	0.222E 06 - 0.250E 06	0.50 - 0.56	2.65 - 2.98	-0.458E 06	0.948E 05	-0.174E 06	-0.531E 06
0.227E 06	0.99928	0.250E 06 - 0.278E 06	0.56 - 0.63	2.98 - 3.31	-0.476E 06	0.695E 05	-0.157E 06	-0.531E 06
0.120E 06	0.99962	0.278E 06 - 0.305E 06	0.63 - 0.69	3.31 - 3.64	-0.483E 06	0.494E 05	-0.243E 06	-0.531E 06
0.595E 05	0.99978	0.305E 06 - 0.333E 06	0.69 - 0.75	3.64 - 3.97	-0.483E 06	0.428E 05	-0.292E 06	-0.531E 06
0.268E 05	0.99986	0.333E 06 - 0.361E 06	0.75 - 0.81	3.97 - 4.30	-0.479E 06	0.445E 05	-0.436E 06	-0.531E 06
0.113E 05	0.99989	0.361E 06 - 0.388E 06	0.81 - 0.88	4.30 - 4.63	-0.475E 06	0.495E 05	-0.426E 06	-0.531E 06
0.463E 04	0.99990	0.388E 06 - 0.416E 06	0.88 - 0.94	4.63 - 4.96	-0.456E 06	0.528E 05	-0.417E 06	-0.531E 06
0.767E 03	0.99990	0.416E 06 - 0.444E 06	0.94 - 1.00	4.96 - 5.29	-0.527E 06	0.129E 04	-0.527E 06	-0.531E 06

TOTAL CYCLES = 0.359E 09

ROOT MEAN CUBED IS 0.935E 05 AVERAGE MEAN IS -0.264E 06

TABLE H- 95
CUMULATIVE FATIGUE HISTOGRAM OUTPUT

TOWER 185 MY

NO. CYCLES IN 30 YEARS (TYPES 1+2)	CUM PROB	HALF-RANGE FATIGUE LOADS: LOAD LEVELS	NORMALIZED LOAD LEVELS	LOAD/50% AT RATED	CORRESPONDING MID-RANGE LOAD DISTRIBUTION: MEAN	STANDARD DEVIATION	MAXIMUM	MINIMUM
0.	0.	0. - 0.525E 05	0. - 0.01	0. - 0.08	0.	0.	0.	0.
0.	0.	0.525E 05 - 0.105E 06	0.01 - 0.02	0.08 - 0.15	0.	0.	0.	0.
0.	0.	0.105E 06 - 0.158E 06	0.02 - 0.03	0.15 - 0.23	0.	0.	0.	0.
0.	0.	0.158E 06 - 0.210E 06	0.03 - 0.03	0.23 - 0.31	0.	0.	0.	0.
0.449E 06	0.00125	0.210E 06 - 0.263E 06	0.03 - 0.04	0.31 - 0.38	0.482E 06	0.129E 07	0.257E 07	-0.372E 06
0.211E 07	0.00714	0.263E 06 - 0.315E 06	0.04 - 0.05	0.38 - 0.46	-0.602E 06	0.262E 07	0.257E 07	-0.631E 07
0.552E 07	0.02252	0.315E 06 - 0.368E 06	0.05 - 0.06	0.46 - 0.54	-0.678E 06	0.273E 07	0.257E 07	-0.631E 07
0.108E 08	0.05266	0.368E 06 - 0.420E 06	0.06 - 0.07	0.54 - 0.62	-0.913E 06	0.289E 07	0.257E 07	-0.631E 07
0.170E 08	0.10002	0.420E 06 - 0.473E 06	0.07 - 0.08	0.62 - 0.69	-0.115E 07	0.302E 07	0.257E 07	-0.631E 07
0.228E 08	0.16352	0.473E 06 - 0.525E 06	0.08 - 0.08	0.69 - 0.77	-0.138E 07	0.311E 07	0.257E 07	-0.631E 07
0.272E 08	0.23928	0.525E 06 - 0.578E 06	0.08 - 0.09	0.77 - 0.85	-0.161E 07	0.318E 07	0.257E 07	-0.631E 07
0.297E 08	0.32202	0.578E 06 - 0.630E 06	0.09 - 0.10	0.85 - 0.92	-0.182E 07	0.322E 07	0.257E 07	-0.631E 07
0.303E 08	0.40647	0.630E 06 - 0.683E 06	0.10 - 0.11	0.92 - 1.00	-0.202E 07	0.325E 07	0.257E 07	-0.631E 07
0.160E 09	0.85129	0.683E 06 - 0.111E 07	0.11 - 0.18	1.00 - 1.62	-0.263E 07	0.323E 07	0.257E 07	-0.631E 07
0.360E 08	0.95159	0.111E 07 - 0.153E 07	0.18 - 0.25	1.62 - 2.24	-0.345E 07	0.300E 07	0.257E 07	-0.643E 07
0.924E 07	0.97731	0.153E 07 - 0.196E 07	0.25 - 0.32	2.24 - 2.87	-0.364E 07	0.302E 07	0.257E 07	-0.687E 07
0.410E 07	0.98872	0.196E 07 - 0.238E 07	0.32 - 0.38	2.87 - 3.49	-0.344E 07	0.288E 07	0.257E 07	-0.757E 07
0.204E 07	0.99440	0.238E 07 - 0.281E 07	0.38 - 0.45	3.49 - 4.11	-0.223E 07	0.266E 07	0.257E 07	-0.626E 07
0.109E 07	0.99744	0.281E 07 - 0.323E 07	0.45 - 0.52	4.11 - 4.73	-0.120E 07	0.244E 07	0.257E 07	-0.624E 07
0.500E 06	0.99884	0.323E 07 - 0.366E 07	0.52 - 0.59	4.73 - 5.35	-0.137E 06	0.215E 07	0.257E 07	-0.623E 07
0.215E 06	0.99943	0.366E 07 - 0.408E 07	0.59 - 0.66	5.35 - 5.98	0.818E 06	0.174E 07	0.257E 07	-0.360E 07
0.970E 05	0.99971	0.408E 07 - 0.451E 07	0.66 - 0.73	5.98 - 6.60	0.135E 07	0.138E 07	0.257E 07	-0.359E 07
0.440E 05	0.99983	0.451E 07 - 0.493E 07	0.73 - 0.79	6.60 - 7.22	0.156E 07	0.117E 07	0.257E 07	-0.372E 06
0.173E 05	0.99988	0.493E 07 - 0.536E 07	0.79 - 0.86	7.22 - 7.84	0.173E 07	0.110E 07	0.257E 07	0.978E 04
0.697E 04	0.99990	0.536E 07 - 0.578E 07	0.86 - 0.93	7.84 - 8.46	0.166E 07	0.113E 07	0.257E 07	0.978E 04
0.260E 04	0.99990	0.578E 07 - 0.621E 07	0.93 - 1.00	8.46 - 9.09	0.194E 07	0.110E 07	0.257E 07	0.978E 04

TOTAL CYCLES = 0.359E 09

ROOT MEAN CUBED IS 0.106E 07 AVERAGE MEAN IS -0.229E 07

TABLE H- 96
CUMULATIVE FATIGUE HISTOGRAM OUTPUT

TOWER 185 MZ

ORIGINAL PAGE IS
OF POOR QUALITY

NO. CYCLES IN 30 YEARS (TYPES 1+2)	CUM PROB	HALF-RANGE FATIGUE LOADS: LOAD LEVELS	NORMALIZED LOAD LEVELS	LOAD/50% AT RATED	CORRESPONDING MID-RANGE LOAD DISTRIBUTION: MEAN	STANDARD DEVIATION	MAXIMUM	MINIMUM
0.	0.	0. - 0.419E 05	0. - 0.02	0. - 0.08	0.	0.	0.	0.
0.	0.	0.419E 05 - 0.838E 05	0.02 - 0.03	0.08 - 0.15	0.	0.	0.	0.
0.	0.	0.838E 05 - 0.126E 06	0.03 - 0.05	0.15 - 0.23	0.	0.	0.	0.
0.	0.	0.126E 06 - 0.168E 06	0.05 - 0.06	0.23 - 0.31	0.	0.	0.	0.
0.	0.	0.168E 06 - 0.209E 06	0.06 - 0.08	0.31 - 0.38	0.	0.	0.	0.
0.736E 05	0.00020	0.209E 06 - 0.251E 06	0.08 - 0.09	0.38 - 0.46	-0.382E 07	0.362E 03	-0.382E 07	-0.382E 07
0.840E 06	0.00254	0.251E 06 - 0.293E 06	0.09 - 0.11	0.46 - 0.54	-0.314E 07	0.792E 06	-0.221E 07	-0.382E 07
0.270E 07	0.01005	0.293E 06 - 0.335E 06	0.11 - 0.12	0.54 - 0.62	-0.317E 07	0.787E 06	-0.221E 07	-0.382E 07
0.640E 07	0.02787	0.335E 06 - 0.377E 06	0.12 - 0.14	0.62 - 0.69	-0.312E 07	0.812E 06	-0.155E 07	-0.382E 07
0.114E 08	0.05971	0.377E 06 - 0.419E 06	0.14 - 0.15	0.69 - 0.77	-0.306E 07	0.873E 06	-0.593E 06	-0.382E 07
0.165E 08	0.10574	0.419E 06 - 0.461E 06	0.15 - 0.17	0.77 - 0.85	-0.299E 07	0.911E 06	-0.593E 06	-0.382E 07
0.207E 08	0.16349	0.461E 06 - 0.503E 06	0.17 - 0.18	0.85 - 0.92	-0.289E 07	0.975E 06	-0.593E 06	-0.382E 07
0.235E 08	0.22893	0.503E 06 - 0.545E 06	0.18 - 0.20	0.92 - 1.00	-0.276E 07	0.105E 07	-0.593E 06	-0.382E 07
0.983E 08	0.50279	0.545E 06 - 0.712E 06	0.20 - 0.26	1.00 - 1.31	-0.229E 07	0.117E 07	-0.593E 06	-0.382E 07
0.800E 08	0.72561	0.712E 06 - 0.880E 06	0.26 - 0.32	1.31 - 1.62	-0.161E 07	0.104E 07	-0.589E 06	-0.382E 07
0.534E 08	0.87438	0.880E 06 - 0.105E 07	0.32 - 0.38	1.62 - 1.92	-0.125E 07	0.815E 06	-0.588E 06	-0.382E 07
0.274E 08	0.95058	0.105E 07 - 0.122E 07	0.38 - 0.45	1.92 - 2.23	-0.114E 07	0.704E 06	-0.578E 06	-0.382E 07
0.111E 08	0.98148	0.122E 07 - 0.138E 07	0.45 - 0.51	2.23 - 2.54	-0.115E 07	0.737E 06	-0.582E 06	-0.381E 07
0.403E 07	0.99269	0.138E 07 - 0.155E 07	0.51 - 0.57	2.54 - 2.85	-0.125E 07	0.884E 06	-0.593E 06	-0.353E 07
0.149E 07	0.99683	0.155E 07 - 0.172E 07	0.57 - 0.63	2.85 - 3.16	-0.147E 07	0.105E 07	-0.593E 06	-0.337E 07
0.631E 06	0.99858	0.172E 07 - 0.189E 07	0.63 - 0.69	3.16 - 3.46	-0.180E 07	0.111E 07	-0.593E 06	-0.320E 07
0.270E 06	0.99934	0.189E 07 - 0.205E 07	0.69 - 0.75	3.46 - 3.77	-0.202E 07	0.116E 07	-0.593E 06	-0.303E 07
0.991E 05	0.99961	0.205E 07 - 0.222E 07	0.75 - 0.82	3.77 - 4.08	-0.279E 07	0.220E 06	-0.161E 07	-0.288E 07
0.547E 05	0.99976	0.222E 07 - 0.239E 07	0.82 - 0.88	4.08 - 4.39	-0.266E 07	0.155E 06	-0.204E 07	-0.269E 07
0.320E 05	0.99985	0.239E 07 - 0.256E 07	0.88 - 0.94	4.39 - 4.70	-0.251E 07	0.102E 06	-0.192E 07	-0.259E 07
0.177E 05	0.99990	0.256E 07 - 0.273E 07	0.94 - 1.00	4.70 - 5.00	-0.236E 07	0.174E 05	-0.236E 07	-0.242E 07

TOTAL CYCLES = 0.359E 09

ROOT MEAN CUBED IS 0.839E 06 AVERAGE MEAN IS -0.199E 07

TABLE H- 97
CUMULATIVE FATIGUE HISTOGRAM OUTPUT

TOWER 117 VX

NO. CYCLES IN 30 YEARS (TYPES 1+2)	CUM PROB	HALF-RANGE FATIGUE LOADS: LOAD LEVELS	NORMALIZED LOAD LEVELS	LOAD/50% AT RATED	CORRESPONDING MID-RANGE LOAD DISTRIBUTION: MEAN	STANDARD DEVIATION	MAXIMUM	MINIMUM
0.	0.	0. - 0.133E 04	0. - 0.05	0. - 0.08	0.	0.	0.	0.
0.	0.	0.133E 04 - 0.265E 04	0.05 - 0.11	0.08 - 0.15	0.	0.	0.	0.
0.	0.	0.265E 04 - 0.398E 04	0.11 - 0.16	0.15 - 0.23	0.	0.	0.	0.
0.	0.	0.398E 04 - 0.531E 04	0.16 - 0.22	0.23 - 0.31	0.	0.	0.	0.
0.186E 07	0.00519	0.531E 04 - 0.663E 04	0.22 - 0.27	0.31 - 0.38	-0.144E 07	0.288E 04	-0.143E 07	-0.144E 07
0.426E 08	0.12392	0.663E 04 - 0.796E 04	0.27 - 0.33	0.38 - 0.46	-0.144E 07	0.287E 04	-0.143E 07	-0.144E 07
0.984E 08	0.39791	0.796E 04 - 0.929E 04	0.33 - 0.38	0.46 - 0.54	-0.144E 07	0.289E 04	-0.143E 07	-0.145E 07
0.455E 08	0.52452	0.929E 04 - 0.106E 05	0.38 - 0.43	0.54 - 0.62	-0.144E 07	0.399E 04	-0.143E 07	-0.145E 07
0.221E 08	0.58598	0.106E 05 - 0.119E 05	0.43 - 0.49	0.62 - 0.69	-0.144E 07	0.655E 04	-0.143E 07	-0.145E 07
0.270E 08	0.66128	0.119E 05 - 0.133E 05	0.49 - 0.54	0.69 - 0.77	-0.145E 07	0.175E 04	-0.143E 07	-0.145E 07
0.254E 08	0.73211	0.133E 05 - 0.146E 05	0.54 - 0.60	0.77 - 0.85	-0.145E 07	0.169E 04	-0.145E 07	-0.145E 07
0.238E 08	0.79841	0.146E 05 - 0.159E 05	0.60 - 0.65	0.85 - 0.92	-0.145E 07	0.200E 04	-0.145E 07	-0.145E 07
0.252E 08	0.86864	0.159E 05 - 0.172E 05	0.65 - 0.71	0.92 - 1.00	-0.145E 07	0.119E 04	-0.145E 07	-0.145E 07
0.133E 08	0.90561	0.172E 05 - 0.178E 05	0.71 - 0.73	1.00 - 1.03	-0.145E 07	0.543E 03	-0.145E 07	-0.145E 07
0.869E 07	0.92982	0.178E 05 - 0.184E 05	0.73 - 0.75	1.03 - 1.06	-0.145E 07	0.528E 03	-0.145E 07	-0.145E 07
0.728E 07	0.95008	0.184E 05 - 0.189E 05	0.75 - 0.77	1.06 - 1.10	-0.145E 07	0.462E 03	-0.145E 07	-0.145E 07
0.566E 07	0.96585	0.189E 05 - 0.195E 05	0.77 - 0.80	1.10 - 1.13	-0.145E 07	0.222E 03	-0.145E 07	-0.145E 07
0.421E 07	0.97757	0.195E 05 - 0.200E 05	0.80 - 0.82	1.13 - 1.16	-0.145E 07	0.128E 03	-0.145E 07	-0.145E 07
0.297E 07	0.98584	0.200E 05 - 0.206E 05	0.82 - 0.84	1.16 - 1.19	-0.145E 07	0.	-0.145E 07	-0.145E 07
0.200E 07	0.99140	0.206E 05 - 0.211E 05	0.84 - 0.86	1.19 - 1.22	-0.145E 07	0.128E 03	-0.145E 07	-0.145E 07
0.128E 07	0.99498	0.211E 05 - 0.217E 05	0.86 - 0.89	1.22 - 1.26	-0.145E 07	0.	-0.145E 07	-0.145E 07
0.793E 06	0.99719	0.217E 05 - 0.222E 05	0.89 - 0.91	1.26 - 1.29	-0.145E 07	0.128E 03	-0.145E 07	-0.145E 07
0.472E 06	0.99850	0.222E 05 - 0.228E 05	0.91 - 0.93	1.29 - 1.32	-0.145E 07	0.	-0.145E 07	-0.145E 07
0.271E 06	0.99925	0.228E 05 - 0.233E 05	0.93 - 0.95	1.32 - 1.35	-0.145E 07	0.128E 03	-0.145E 07	-0.145E 07
0.151E 06	0.99968	0.233E 05 - 0.239E 05	0.95 - 0.98	1.35 - 1.38	-0.145E 07	0.128E 03	-0.145E 07	-0.145E 07
0.817E 05	0.99990	0.239E 05 - 0.244E 05	0.98 - 1.00	1.38 - 1.42	-0.145E 07	0.128E 03	-0.145E 07	-0.145E 07

TOTAL CYCLES = 0.359E 09

ROOT MEAN CUBED IS 0.130E 05 AVERAGE MEAN IS -0.144E 07

TABLE H- 98
CUMULATIVE FATIGUE HISTOGRAM OUTPUT

TOWER 117 VY

NO. CYCLES IN 30 YEARS (TYPES 1+2)	CUM PROB	HALF-RANGE FATIGUE LOADS: LOAD LEVELS	NORMALIZED LOAD LEVELS	LOAD/50% AT RATED	CORRESPONDING MID-RANGE LOAD DISTRIBUTION: MEAN	STANDARD DEVIATION	MAXIMUM	MINIMUM
0.	0.	0. - 0.761E 03	0. - 0.03	0. - 0.08	0.	0.	0.	0.
0.	0.	0.761E 03 - 0.152E 04	0.03 - 0.07	0.08 - 0.15	0.	0.	0.	0.
0.	0.	0.152E 04 - 0.228E 04	0.07 - 0.10	0.15 - 0.23	0.	0.	0.	0.
0.	0.	0.228E 04 - 0.304E 04	0.10 - 0.14	0.23 - 0.31	0.	0.	0.	0.
0.	0.	0.304E 04 - 0.380E 04	0.14 - 0.17	0.31 - 0.38	0.	0.	0.	0.
0.	0.	0.380E 04 - 0.457E 04	0.17 - 0.20	0.38 - 0.46	0.	0.	0.	0.
0.	0.	0.457E 04 - 0.533E 04	0.20 - 0.24	0.46 - 0.54	0.	0.	0.	0.
0.	0.	0.533E 04 - 0.609E 04	0.24 - 0.27	0.54 - 0.62	0.	0.	0.	0.
0.	0.	0.609E 04 - 0.685E 04	0.27 - 0.30	0.62 - 0.69	0.	0.	0.	0.
0.737E 06	0.00205	0.685E 04 - 0.761E 04	0.30 - 0.34	0.69 - 0.77	0.240E 04	0.279E 03	0.249E 04	0.155E 04
0.490E 07	0.01570	0.761E 04 - 0.837E 04	0.34 - 0.37	0.77 - 0.85	0.232E 04	0.355E 03	0.249E 04	0.155E 04
0.162E 08	0.06086	0.837E 04 - 0.913E 04	0.37 - 0.41	0.85 - 0.92	0.222E 04	0.411E 03	0.249E 04	0.155E 04
0.306E 08	0.14614	0.913E 04 - 0.989E 04	0.41 - 0.44	0.92 - 1.00	0.211E 04	0.442E 03	0.249E 04	0.155E 04
0.506E 08	0.28717	0.989E 04 - 0.109E 05	0.44 - 0.48	1.00 - 1.10	0.198E 04	0.437E 03	0.249E 04	0.128E 04
0.408E 08	0.40080	0.109E 05 - 0.118E 05	0.48 - 0.53	1.10 - 1.20	0.179E 04	0.454E 03	0.249E 04	0.725E 03
0.285E 08	0.48011	0.118E 05 - 0.128E 05	0.53 - 0.57	1.20 - 1.29	0.154E 04	0.446E 03	0.249E 04	0.167E 03
0.306E 08	0.56521	0.128E 05 - 0.138E 05	0.57 - 0.61	1.29 - 1.39	0.124E 04	0.361E 03	0.249E 04	0.725E 03
0.396E 08	0.67543	0.138E 05 - 0.147E 05	0.61 - 0.66	1.39 - 1.49	0.110E 04	0.297E 03	0.249E 04	0.725E 03
0.403E 08	0.78767	0.147E 05 - 0.157E 05	0.66 - 0.70	1.49 - 1.59	0.100E 04	0.278E 03	0.197E 04	0.725E 03
0.357E 08	0.88714	0.157E 05 - 0.167E 05	0.70 - 0.74	1.59 - 1.68	0.902E 03	0.273E 03	0.175E 04	0.578E 03
0.208E 08	0.94499	0.167E 05 - 0.176E 05	0.74 - 0.78	1.68 - 1.78	0.881E 03	0.260E 03	0.128E 04	0.314E 03
0.112E 08	0.97631	0.176E 05 - 0.186E 05	0.78 - 0.83	1.78 - 1.88	0.847E 03	0.231E 03	0.128E 04	0.725E 03
0.525E 07	0.99092	0.186E 05 - 0.196E 05	0.83 - 0.87	1.88 - 1.98	0.815E 03	0.205E 03	0.128E 04	0.725E 03
0.221E 07	0.99707	0.196E 05 - 0.205E 05	0.87 - 0.91	1.98 - 2.08	0.810E 03	0.201E 03	0.128E 04	0.725E 03
0.694E 06	0.99901	0.205E 05 - 0.215E 05	0.91 - 0.96	2.08 - 2.17	0.725E 03	0.	0.725E 03	0.725E 03
0.321E 06	0.99990	0.215E 05 - 0.225E 05	0.96 - 1.00	2.17 - 2.27	0.725E 03	0.	0.725E 03	0.725E 03

TOTAL CYCLES = 0.359E 09

ROOT MEAN CUBED IS 0.137E 05 AVERAGE MEAN IS 0.145E 04

TABLE H- 99
CUMULATIVE FATIGUE HISTOGRAM OUTPUT

TOWER 117 VZ

NO. CYCLES IN 30 YEARS (TYPES 1+2)	CUM PROB	HALF-RANGE FATIGUE LOADS: LOAD LEVELS	NORMALIZED LOAD LEVELS	LOAD/50% AT RATED	CORRESPONDING MID-RANGE LOAD DISTRIBUTION: MEAN	STANDARD DEVIATION	MAXIMUM	MINIMUM
0.	0.	0. - 0.923E 03	0. - 0.01	0. - 0.08	0.	0.	0.	0.
0.	0.	0.923E 03 - 0.185E 04	0.01 - 0.02	0.08 - 0.15	0.	0.	0.	0.
0.	0.	0.185E 04 - 0.277E 04	0.02 - 0.03	0.15 - 0.23	0.	0.	0.	0.
0.	0.	0.277E 04 - 0.369E 04	0.03 - 0.04	0.23 - 0.31	0.	0.	0.	0.
0.823E 06	0.00229	0.369E 04 - 0.462E 04	0.04 - 0.05	0.31 - 0.38	-0.197E 06	0.238E 05	-0.178E 06	-0.228E 06
0.280E 07	0.01008	0.462E 04 - 0.554E 04	0.05 - 0.06	0.38 - 0.46	-0.178E 06	0.453E 05	-0.763E 05	-0.228E 06
0.608E 07	0.02702	0.554E 04 - 0.646E 04	0.06 - 0.07	0.46 - 0.54	-0.177E 06	0.464E 05	-0.763E 05	-0.228E 06
0.106E 08	0.05654	0.646E 04 - 0.738E 04	0.07 - 0.08	0.54 - 0.62	-0.173E 06	0.490E 05	-0.763E 05	-0.228E 06
0.154E 08	0.09953	0.738E 04 - 0.831E 04	0.08 - 0.09	0.62 - 0.69	-0.169E 06	0.512E 05	-0.763E 05	-0.228E 06
0.198E 08	0.15461	0.831E 04 - 0.923E 04	0.09 - 0.10	0.69 - 0.77	-0.164E 06	0.528E 05	-0.763E 05	-0.228E 06
0.231E 08	0.21886	0.923E 04 - 0.102E 05	0.10 - 0.11	0.77 - 0.85	-0.160E 06	0.540E 05	-0.763E 05	-0.228E 06
0.251E 08	0.28866	0.102E 05 - 0.111E 05	0.11 - 0.11	0.85 - 0.92	-0.156E 06	0.547E 05	-0.763E 05	-0.228E 06
0.258E 08	0.36050	0.111E 05 - 0.120E 05	0.11 - 0.12	0.92 - 1.00	-0.152E 06	0.552E 05	-0.763E 05	-0.228E 06
0.142E 09	0.75556	0.120E 05 - 0.185E 05	0.12 - 0.19	1.00 - 1.54	-0.141E 06	0.549E 05	-0.756E 05	-0.228E 06
0.574E 08	0.91552	0.185E 05 - 0.250E 05	0.19 - 0.26	1.54 - 2.09	-0.126E 06	0.505E 05	-0.730E 05	-0.228E 06
0.191E 08	0.96869	0.250E 05 - 0.315E 05	0.26 - 0.33	2.09 - 2.63	-0.121E 06	0.480E 05	-0.685E 05	-0.228E 06
0.674E 07	0.98747	0.315E 05 - 0.380E 05	0.33 - 0.39	2.63 - 3.17	-0.125E 06	0.494E 05	-0.631E 05	-0.228E 06
0.244E 07	0.99426	0.380E 05 - 0.446E 05	0.39 - 0.46	3.17 - 3.71	-0.135E 06	0.497E 05	-0.578E 05	-0.228E 06
0.117E 07	0.99752	0.446E 05 - 0.511E 05	0.46 - 0.53	3.71 - 4.26	-0.153E 06	0.519E 05	-0.542E 05	-0.228E 06
0.443E 06	0.99875	0.511E 05 - 0.576E 05	0.53 - 0.60	4.26 - 4.80	-0.187E 06	0.376E 05	-0.774E 05	-0.228E 06
0.228E 06	0.99938	0.576E 05 - 0.641E 05	0.60 - 0.66	4.80 - 5.34	-0.196E 06	0.314E 05	-0.775E 05	-0.228E 06
0.109E 06	0.99969	0.641E 05 - 0.706E 05	0.66 - 0.73	5.34 - 5.88	-0.202E 06	0.276E 05	-0.122E 06	-0.228E 06
0.479E 05	0.99982	0.706E 05 - 0.771E 05	0.73 - 0.80	5.88 - 6.43	-0.208E 06	0.229E 05	-0.122E 06	-0.228E 06
0.192E 05	0.99987	0.771E 05 - 0.836E 05	0.80 - 0.87	6.43 - 6.97	-0.213E 06	0.198E 05	-0.184E 06	-0.228E 06
0.795E 04	0.99989	0.836E 05 - 0.901E 05	0.87 - 0.93	6.97 - 7.51	-0.211E 06	0.205E 05	-0.184E 06	-0.228E 06
0.305E 04	0.99990	0.901E 05 - 0.966E 05	0.93 - 1.00	7.51 - 8.05	-0.218E 06	0.178E 05	-0.184E 06	-0.228E 06

TOTAL CYCLES = 0.359E 09

ROOT MEAN CUBED IS 0.189E 05 AVERAGE MEAN IS -0.145E 06

TABLE H-100
CUMULATIVE FATIGUE HISTOGRAM OUTPUT

TOWER 117 MX

NO. CYCLES IN 30 YEARS (TYPES 1+2)	CUM PROB	HALF-RANGE FATIGUE LOADS: LOAD LEVELS	NORMALIZED LOAD LEVELS	LOAD/50% AT RATED	CORRESPONDING MID-RANGE LOAD DISTRIBUTION: MEAN	STANDARD DEVIATION	MAXIMUM	MINIMUM
0.	0.	0. - 0.646E 04	0. - 0.01	0. - 0.08	0.	0.	0.	0.
0.	0.	0.646E 04 - 0.129E 05	0.01 - 0.03	0.08 - 0.15	0.	0.	0.	0.
0.	0.	0.129E 05 - 0.194E 05	0.03 - 0.04	0.15 - 0.23	0.	0.	0.	0.
0.	0.	0.194E 05 - 0.258E 05	0.04 - 0.06	0.23 - 0.31	0.	0.	0.	0.
0.	0.	0.258E 05 - 0.323E 05	0.06 - 0.07	0.31 - 0.38	0.	0.	0.	0.
0.	0.	0.323E 05 - 0.387E 05	0.07 - 0.09	0.38 - 0.46	0.	0.	0.	0.
0.278E 05	0.00008	0.387E 05 - 0.452E 05	0.09 - 0.10	0.46 - 0.54	-0.527E 06	0.	-0.527E 06	-0.527E 06
0.165E 07	0.00468	0.452E 05 - 0.517E 05	0.10 - 0.12	0.54 - 0.62	-0.398E 06	0.106E 06	-0.311E 06	-0.527E 06
0.116E 08	0.03711	0.517E 05 - 0.581E 05	0.12 - 0.13	0.62 - 0.69	-0.375E 06	0.108E 06	-0.650E 05	-0.531E 06
0.302E 08	0.12112	0.581E 05 - 0.646E 05	0.13 - 0.15	0.69 - 0.77	-0.345E 06	0.121E 06	-0.650E 05	-0.531E 06
0.427E 08	0.24014	0.646E 05 - 0.710E 05	0.15 - 0.16	0.77 - 0.85	-0.298E 06	0.156E 06	-0.650E 05	-0.531E 06
0.498E 08	0.37875	0.710E 05 - 0.775E 05	0.16 - 0.17	0.85 - 0.92	-0.258E 06	0.190E 06	-0.650E 05	-0.531E 06
0.517E 08	0.52258	0.775E 05 - 0.840E 05	0.17 - 0.19	0.92 - 1.00	-0.254E 06	0.207E 06	-0.631E 05	-0.534E 06
0.141E 09	0.91431	0.840E 05 - 0.112E 06	0.19 - 0.25	1.00 - 1.33	-0.238E 06	0.165E 06	-0.475E 05	-0.545E 06
0.244E 08	0.98216	0.112E 06 - 0.139E 06	0.25 - 0.31	1.33 - 1.66	-0.202E 06	0.721E 05	-0.250E 05	-0.531E 06
0.341E 07	0.99165	0.139E 06 - 0.167E 06	0.31 - 0.38	1.66 - 1.99	-0.287E 06	0.145E 06	-0.845E 05	-0.531E 06
0.138E 07	0.99548	0.167E 06 - 0.195E 06	0.38 - 0.44	1.99 - 2.32	-0.361E 06	0.129E 06	-0.946E 05	-0.531E 06
0.735E 06	0.99753	0.195E 06 - 0.222E 06	0.44 - 0.50	2.32 - 2.65	-0.412E 06	0.119E 06	-0.197E 06	-0.531E 06
0.402E 06	0.99865	0.222E 06 - 0.250E 06	0.50 - 0.56	2.65 - 2.98	-0.458E 06	0.948E 05	-0.174E 06	-0.531E 06
0.227E 06	0.99928	0.250E 06 - 0.278E 06	0.56 - 0.63	2.98 - 3.31	-0.476E 06	0.695E 05	-0.157E 06	-0.531E 06
0.120E 06	0.99962	0.278E 06 - 0.305E 06	0.63 - 0.69	3.31 - 3.64	-0.483E 06	0.494E 05	-0.243E 06	-0.531E 06
0.595E 05	0.99978	0.305E 06 - 0.333E 06	0.69 - 0.75	3.64 - 3.97	-0.483E 06	0.428E 05	-0.292E 06	-0.531E 06
0.268E 05	0.99986	0.333E 06 - 0.361E 06	0.75 - 0.81	3.97 - 4.30	-0.479E 06	0.445E 05	-0.436E 06	-0.531E 06
0.113E 05	0.99989	0.361E 06 - 0.388E 06	0.81 - 0.88	4.30 - 4.63	-0.475E 06	0.495E 05	-0.426E 06	-0.531E 06
0.463E 04	0.99990	0.388E 06 - 0.416E 06	0.88 - 0.94	4.63 - 4.96	-0.456E 06	0.528E 05	-0.417E 06	-0.531E 06
0.767E 03	0.99990	0.416E 06 - 0.444E 06	0.94 - 1.00	4.96 - 5.29	-0.527E 06	0.129E 04	-0.527E 06	-0.531E 06

TOTAL CYCLES = 0.359E 09

ROOT MEAN CUBED IS 0.935E 05 AVERAGE MEAN IS -0.264E 06

TABLE H-101
CUMULATIVE FATIGUE HISTOGRAM OUTPUT

TOWER 117 MY

NO. CYCLES IN 30 YEARS (TYPES 1+2)	CUM PROB	HALF-RANGE FATIGUE LOADS: LOAD LEVELS	NORMALIZED LOAD LEVELS	LOAD/50% AT RATED	CORRESPONDING MID-RANGE LOAD DISTRIBUTION: MEAN	STANDARD DEVIATION	MAXIMUM	MINIMUM
0.	0.	0. - 0.115E 06	0. - 0.01	0. - 0.08	0.	0.	0.	0.
0.	0.	0.115E 06 - 0.231E 06	0.01 - 0.02	0.08 - 0.15	0.	0.	0.	0.
0.	0.	0.231E 06 - 0.346E 06	0.02 - 0.03	0.15 - 0.23	0.	0.	0.	0.
0.	0.	0.346E 06 - 0.462E 06	0.03 - 0.04	0.23 - 0.31	0.	0.	0.	0.
0.730E 06	0.00203	0.462E 06 - 0.577E 06	0.04 - 0.05	0.31 - 0.38	0.136E 08	0.280E 07	0.181E 08	0.118E 08
0.283E 07	0.00992	0.577E 06 - 0.692E 06	0.05 - 0.05	0.38 - 0.46	0.112E 08	0.570E 07	0.181E 08	-0.108E 07
0.651E 07	0.02806	0.692E 06 - 0.808E 06	0.05 - 0.06	0.46 - 0.54	0.111E 08	0.589E 07	0.181E 08	-0.108E 07
0.117E 08	0.06076	0.808E 06 - 0.923E 06	0.06 - 0.07	0.54 - 0.62	0.106E 08	0.624E 07	0.181E 08	-0.108E 07
0.174E 08	0.10925	0.923E 06 - 0.104E 07	0.07 - 0.08	0.62 - 0.69	0.101E 08	0.651E 07	0.181E 08	-0.108E 07
0.224E 08	0.17174	0.104E 07 - 0.115E 07	0.08 - 0.09	0.69 - 0.77	0.961E 07	0.672E 07	0.181E 08	-0.108E 07
0.261E 08	0.24441	0.115E 07 - 0.127E 07	0.09 - 0.10	0.77 - 0.85	0.913E 07	0.686E 07	0.181E 08	-0.108E 07
0.281E 08	0.32261	0.127E 07 - 0.138E 07	0.10 - 0.11	0.85 - 0.92	0.867E 07	0.696E 07	0.181E 08	-0.108E 07
0.285E 08	0.40189	0.138E 07 - 0.150E 07	0.11 - 0.12	0.92 - 1.00	0.824E 07	0.702E 07	0.181E 08	-0.108E 07
0.149E 09	0.81617	0.150E 07 - 0.237E 07	0.12 - 0.19	1.00 - 1.58	0.695E 07	0.700E 07	0.181E 08	-0.108E 07
0.440E 08	0.93871	0.237E 07 - 0.323E 07	0.19 - 0.25	1.58 - 2.15	0.520E 07	0.655E 07	0.181E 08	-0.145E 07
0.128E 08	0.97443	0.323E 07 - 0.410E 07	0.25 - 0.32	2.15 - 2.73	0.448E 07	0.639E 07	0.181E 08	-0.266E 07
0.490E 07	0.98807	0.410E 07 - 0.496E 07	0.32 - 0.39	2.73 - 3.31	0.514E 07	0.625E 07	0.181E 08	-0.426E 07
0.229E 07	0.99444	0.496E 07 - 0.583E 07	0.39 - 0.46	3.31 - 3.89	0.718E 07	0.575E 07	0.181E 08	-0.108E 07
0.107E 07	0.99743	0.583E 07 - 0.669E 07	0.46 - 0.52	3.89 - 4.46	0.102E 08	0.512E 07	0.181E 08	-0.961E 06
0.491E 06	0.99880	0.669E 07 - 0.756E 07	0.52 - 0.59	4.46 - 5.04	0.125E 08	0.447E 07	0.181E 08	-0.931E 06
0.219E 06	0.99941	0.756E 07 - 0.843E 07	0.59 - 0.66	5.04 - 5.62	0.144E 08	0.364E 07	0.181E 08	0.475E 07
0.102E 06	0.99969	0.843E 07 - 0.929E 07	0.66 - 0.73	5.62 - 6.19	0.154E 08	0.315E 07	0.181E 08	0.479E 07
0.464E 05	0.99982	0.929E 07 - 0.102E 08	0.73 - 0.80	6.19 - 6.77	0.159E 08	0.253E 07	0.181E 08	0.118E 08
0.187E 05	0.99987	0.102E 08 - 0.110E 08	0.80 - 0.86	6.77 - 7.35	0.163E 08	0.240E 07	0.181E 08	0.126E 08
0.773E 04	0.99989	0.110E 08 - 0.119E 08	0.86 - 0.93	7.35 - 7.93	0.161E 08	0.249E 07	0.181E 08	0.126E 08
0.329E 04	0.99990	0.119E 08 - 0.128E 08	0.93 - 1.00	7.93 - 8.50	0.165E 08	0.253E 07	0.181E 08	0.126E 08

TOTAL CYCLES = 0.359E 09

ROOT MEAN CUBED IS 0.231E 07 AVERAGE MEAN IS 0.761E 07

TABLE H-102
CUMULATIVE FATIGUE HISTOGRAM OUTPUT

TOWER 117 MZ

NO. CYCLES IN 30 YEARS (TYPES 1+2)	CUM PROB	HALF-RANGE FATIGUE LOADS: LOAD LEVELS	NORMALIZED LOAD LEVELS	LOAD/50% AT RATED	CORRESPONDING MID-RANGE LOAD DISTRIBUTION: MEAN	STANDARD DEVIATION	MAXIMUM	MINIMUM
0.	0.	0. - 0.917E 05	0. - 0.03	0. - 0.08	0.	0.	0.	0.
0.	0.	0.917E 05 - 0.183E 06	0.03 - 0.05	0.08 - 0.15	0.	0.	0.	0.
0.	0.	0.183E 06 - 0.275E 06	0.05 - 0.08	0.15 - 0.23	0.	0.	0.	0.
0.	0.	0.275E 06 - 0.367E 06	0.08 - 0.11	0.23 - 0.31	0.	0.	0.	0.
0.	0.	0.367E 06 - 0.458E 06	0.11 - 0.13	0.31 - 0.38	0.	0.	0.	0.
0.	0.	0.458E 06 - 0.550E 06	0.13 - 0.16	0.38 - 0.46	0.	0.	0.	0.
0.	0.	0.550E 06 - 0.642E 06	0.16 - 0.18	0.46 - 0.54	0.	0.	0.	0.
0.472E 06	0.00131	0.642E 06 - 0.734E 06	0.18 - 0.21	0.54 - 0.62	-0.326E 07	0.671E 06	-0.211E 07	-0.369E 07
0.212E 07	0.00721	0.734E 06 - 0.825E 06	0.21 - 0.24	0.62 - 0.69	-0.320E 07	0.706E 06	-0.211E 07	-0.369E 07
0.632E 07	0.02480	0.825E 06 - 0.917E 06	0.24 - 0.26	0.69 - 0.77	-0.314E 07	0.730E 06	-0.211E 07	-0.369E 07
0.130E 08	0.06098	0.917E 06 - 0.101E 07	0.26 - 0.29	0.77 - 0.85	-0.307E 07	0.759E 06	-0.146E 07	-0.369E 07
0.201E 08	0.11693	0.101E 07 - 0.110E 07	0.29 - 0.32	0.85 - 0.92	-0.300E 07	0.800E 06	-0.543E 06	-0.369E 07
0.251E 08	0.18688	0.110E 07 - 0.119E 07	0.32 - 0.34	0.92 - 1.00	-0.290E 07	0.846E 06	-0.543E 06	-0.369E 07
0.541E 08	0.33760	0.119E 07 - 0.137E 07	0.34 - 0.39	1.00 - 1.15	-0.270E 07	0.968E 06	-0.543E 06	-0.369E 07
0.497E 08	0.47591	0.137E 07 - 0.155E 07	0.39 - 0.44	1.15 - 1.30	-0.216E 07	0.108E 07	-0.543E 06	-0.369E 07
0.466E 08	0.60570	0.155E 07 - 0.172E 07	0.44 - 0.49	1.30 - 1.44	-0.161E 07	0.980E 06	-0.543E 06	-0.369E 07
0.428E 08	0.72491	0.172E 07 - 0.190E 07	0.49 - 0.54	1.44 - 1.59	-0.126E 07	0.779E 06	-0.543E 06	-0.369E 07
0.381E 08	0.83112	0.190E 07 - 0.208E 07	0.54 - 0.59	1.59 - 1.74	-0.108E 07	0.629E 06	-0.479E 06	-0.369E 07
0.281E 08	0.90943	0.208E 07 - 0.225E 07	0.59 - 0.65	1.74 - 1.89	-0.961E 06	0.541E 06	-0.328E 06	-0.369E 07
0.161E 08	0.95424	0.225E 07 - 0.243E 07	0.65 - 0.70	1.89 - 2.04	-0.910E 06	0.494E 06	-0.151E 06	-0.369E 07
0.852E 07	0.97798	0.243E 07 - 0.261E 07	0.70 - 0.75	2.04 - 2.19	-0.860E 06	0.448E 06	-0.329E 05	-0.247E 07
0.431E 07	0.98999	0.261E 07 - 0.278E 07	0.75 - 0.80	2.19 - 2.33	-0.825E 06	0.431E 06	-0.497E 06	-0.236E 07
0.205E 07	0.99570	0.278E 07 - 0.296E 07	0.80 - 0.85	2.33 - 2.48	-0.795E 06	0.415E 06	-0.543E 06	-0.197E 07
0.925E 06	0.99828	0.296E 07 - 0.314E 07	0.85 - 0.90	2.48 - 2.63	-0.768E 06	0.398E 06	-0.543E 06	-0.184E 07
0.449E 06	0.99953	0.314E 07 - 0.331E 07	0.90 - 0.95	2.63 - 2.78	-0.823E 06	0.424E 06	-0.543E 06	-0.173E 07
0.134E 06	0.99990	0.331E 07 - 0.349E 07	0.95 - 1.00	2.78 - 2.93	-0.543E 06	0.	-0.543E 06	-0.543E 06

TOTAL CYCLES = 0.359E 09

ROOT MEAN CUBED IS 0.175E 07 AVERAGE MEAN IS -0.189E 07

TABLE H-103
CUMULATIVE FATIGUE HISTOGRAM OUTPUT

TOWER 51 YX

NO. CYCLES IN 30 YEARS (TYPES 1+2)	CUM PROB	HALF-RANGE FATIGUE LOADS: LOAD LEVELS	NORMALIZED LOAD LEVELS	LOAD/50% AT RATED	CORRESPONDING MID-RANGE LOAD DISTRIBUTION: MEAN	STANDARD DEVIATION	MAXIMUM	MINIMUM
0.	0.	0. - 0.133E 04	0. - 0.05	0. - 0.08	0.	0.	0.	0.
0.	0.	0.133E 04 - 0.265E 04	0.05 - 0.11	0.08 - 0.15	0.	0.	0.	0.
0.	0.	0.265E 04 - 0.398E 04	0.11 - 0.16	0.15 - 0.23	0.	0.	0.	0.
0.	0.	0.398E 04 - 0.531E 04	0.16 - 0.22	0.23 - 0.31	0.	0.	0.	0.
0.186E 07	0.00519	0.531E 04 - 0.663E 04	0.22 - 0.27	0.31 - 0.38	-0.162E 07	0.288E 04	-0.162E 07	-0.162E 07
0.426E 08	0.12392	0.663E 04 - 0.796E 04	0.27 - 0.33	0.38 - 0.46	-0.162E 07	0.287E 04	-0.162E 07	-0.162E 07
0.984E 08	0.39791	0.796E 04 - 0.929E 04	0.33 - 0.38	0.46 - 0.54	-0.162E 07	0.291E 04	-0.162E 07	-0.163E 07
0.455E 08	0.52452	0.929E 04 - 0.106E 05	0.38 - 0.43	0.54 - 0.62	-0.162E 07	0.398E 04	-0.162E 07	-0.163E 07
0.221E 08	0.58598	0.106E 05 - 0.119E 05	0.43 - 0.49	0.62 - 0.69	-0.163E 07	0.656E 04	-0.162E 07	-0.163E 07
0.270E 08	0.66128	0.119E 05 - 0.133E 05	0.49 - 0.54	0.69 - 0.77	-0.163E 07	0.175E 04	-0.162E 07	-0.164E 07
0.254E 08	0.73211	0.133E 05 - 0.146E 05	0.54 - 0.60	0.77 - 0.85	-0.164E 07	0.167E 04	-0.163E 07	-0.164E 07
0.238E 08	0.79841	0.146E 05 - 0.159E 05	0.60 - 0.65	0.85 - 0.92	-0.164E 07	0.202E 04	-0.163E 07	-0.164E 07
0.252E 08	0.86864	0.159E 05 - 0.172E 05	0.65 - 0.71	0.92 - 1.00	-0.164E 07	0.119E 04	-0.163E 07	-0.164E 07
0.133E 08	0.90561	0.172E 05 - 0.178E 05	0.71 - 0.73	1.00 - 1.03	-0.164E 07	0.479E 03	-0.163E 07	-0.164E 07
0.869E 07	0.92982	0.178E 05 - 0.184E 05	0.73 - 0.75	1.03 - 1.06	-0.164E 07	0.512E 03	-0.163E 07	-0.164E 07
0.728E 07	0.95008	0.184E 05 - 0.189E 05	0.75 - 0.77	1.06 - 1.10	-0.164E 07	0.443E 03	-0.163E 07	-0.164E 07
0.566E 07	0.96585	0.189E 05 - 0.195E 05	0.77 - 0.80	1.10 - 1.13	-0.164E 07	0.	-0.164E 07	-0.164E 07
0.421E 07	0.97757	0.195E 05 - 0.200E 05	0.80 - 0.82	1.13 - 1.16	-0.164E 07	0.	-0.164E 07	-0.164E 07
0.297E 07	0.98584	0.200E 05 - 0.206E 05	0.82 - 0.84	1.16 - 1.19	-0.164E 07	0.	-0.164E 07	-0.164E 07
0.200E 07	0.99140	0.206E 05 - 0.211E 05	0.84 - 0.86	1.19 - 1.22	-0.164E 07	0.256E 03	-0.164E 07	-0.164E 07
0.128E 07	0.99498	0.211E 05 - 0.217E 05	0.86 - 0.89	1.22 - 1.26	-0.164E 07	0.	-0.164E 07	-0.164E 07
0.793E 06	0.99719	0.217E 05 - 0.222E 05	0.89 - 0.91	1.26 - 1.29	-0.164E 07	0.181E 03	-0.164E 07	-0.164E 07
0.472E 06	0.99850	0.222E 05 - 0.228E 05	0.91 - 0.93	1.29 - 1.32	-0.164E 07	0.256E 03	-0.164E 07	-0.164E 07
0.271E 06	0.99925	0.228E 05 - 0.233E 05	0.93 - 0.95	1.32 - 1.35	-0.164E 07	0.181E 03	-0.164E 07	-0.164E 07
0.151E 06	0.99968	0.233E 05 - 0.239E 05	0.95 - 0.98	1.35 - 1.38	-0.164E 07	0.181E 03	-0.164E 07	-0.164E 07
0.817E 05	0.99990	0.239E 05 - 0.244E 05	0.98 - 1.00	1.38 - 1.42	-0.164E 07	0.181E 03	-0.164E 07	-0.164E 07

TOTAL CYCLES = 0.359E 09

ROOT MEAN CUBED IS 0.130E 05 AVERAGE MEAN IS -0.163E 07

TABLE H-104
CUMULATIVE FATIGUE HISTOGRAM OUTPUT

TOWER 51 VY

NO. CYCLES IN 30 YEARS (TYPES 1+2)	CUM PROB	HALF-RANGE FATIGUE LOADS: LOAD LEVELS	NORMALIZED LOAD LEVELS	LOAD/50% AT RATED	CORRESPONDING MID-RANGE LOAD DISTRIBUTION: MEAN	STANDARD DEVIATION	MAXIMUM	MINIMUM
0.	0.	0. - 0.793E 03	0. - 0.03	0. - 0.08	0.	0.	0.	0.
0.	0.	0.793E 03 - 0.159E 04	0.03 - 0.07	0.08 - 0.15	0.	0.	0.	0.
0.	0.	0.159E 04 - 0.238E 04	0.07 - 0.10	0.15 - 0.23	0.	0.	0.	0.
0.	0.	0.238E 04 - 0.317E 04	0.10 - 0.14	0.23 - 0.31	0.	0.	0.	0.
0.	0.	0.317E 04 - 0.397E 04	0.14 - 0.17	0.31 - 0.38	0.	0.	0.	0.
0.	0.	0.397E 04 - 0.476E 04	0.17 - 0.21	0.38 - 0.46	0.	0.	0.	0.
0.	0.	0.476E 04 - 0.555E 04	0.21 - 0.24	0.46 - 0.54	0.	0.	0.	0.
0.	0.	0.555E 04 - 0.635E 04	0.24 - 0.27	0.54 - 0.62	0.	0.	0.	0.
0.	0.	0.635E 04 - 0.714E 04	0.27 - 0.31	0.62 - 0.69	0.	0.	0.	0.
0.740E 06	0.00206	0.714E 04 - 0.793E 04	0.31 - 0.34	0.69 - 0.77	0.243E 04	0.289E 03	0.252E 04	0.157E 04
0.493E 07	0.01578	0.793E 04 - 0.873E 04	0.34 - 0.38	0.77 - 0.85	0.234E 04	0.365E 03	0.252E 04	0.157E 04
0.163E 08	0.06120	0.873E 04 - 0.952E 04	0.38 - 0.41	0.85 - 0.92	0.225E 04	0.421E 03	0.252E 04	0.157E 04
0.308E 08	0.14688	0.952E 04 - 0.103E 05	0.41 - 0.45	0.92 - 1.00	0.214E 04	0.451E 03	0.252E 04	0.157E 04
0.498E 08	0.28562	0.103E 05 - 0.113E 05	0.45 - 0.49	1.00 - 1.10	0.200E 04	0.447E 03	0.252E 04	0.128E 04
0.413E 08	0.40072	0.113E 05 - 0.123E 05	0.49 - 0.53	1.10 - 1.19	0.180E 04	0.469E 03	0.252E 04	0.730E 03
0.303E 08	0.48506	0.123E 05 - 0.133E 05	0.53 - 0.57	1.19 - 1.29	0.154E 04	0.461E 03	0.252E 04	0.161E 03
0.322E 08	0.57485	0.133E 05 - 0.142E 05	0.57 - 0.62	1.29 - 1.38	0.124E 04	0.371E 03	0.252E 04	0.730E 03
0.402E 08	0.68687	0.142E 05 - 0.152E 05	0.62 - 0.66	1.38 - 1.48	0.110E 04	0.299E 03	0.252E 04	0.730E 03
0.394E 08	0.79670	0.152E 05 - 0.162E 05	0.66 - 0.70	1.48 - 1.57	0.998E 03	0.274E 03	0.199E 04	0.730E 03
0.345E 08	0.89293	0.162E 05 - 0.172E 05	0.70 - 0.74	1.57 - 1.67	0.897E 03	0.269E 03	0.199E 04	0.565E 03
0.197E 08	0.94784	0.172E 05 - 0.182E 05	0.74 - 0.79	1.67 - 1.76	0.881E 03	0.251E 03	0.128E 04	0.294E 03
0.107E 08	0.97760	0.182E 05 - 0.192E 05	0.79 - 0.83	1.76 - 1.86	0.846E 03	0.223E 03	0.128E 04	0.730E 03
0.499E 07	0.99151	0.192E 05 - 0.201E 05	0.83 - 0.87	1.86 - 1.95	0.815E 03	0.198E 03	0.128E 04	0.730E 03
0.212E 07	0.99740	0.201E 05 - 0.211E 05	0.87 - 0.91	1.95 - 2.05	0.811E 03	0.194E 03	0.128E 04	0.730E 03
0.674E 06	0.99928	0.211E 05 - 0.221E 05	0.91 - 0.96	2.05 - 2.14	0.730E 03	0.	0.730E 03	0.730E 03
0.224E 06	0.99990	0.221E 05 - 0.231E 05	0.96 - 1.00	2.14 - 2.24	0.730E 03	0.	0.730E 03	0.730E 03

TOTAL CYCLES = 0.359E 09

ROOT MEAN CUBED IS 0.141E 05 AVERAGE MEAN IS 0.146E 04

TABLE H-105
CUMULATIVE FATIGUE HISTOGRAM OUTPUT

TOWER 51 VZ

NO. CYCLES IN 30 YEARS (TYPES 1+2)	CUM PROB	HALF-RANGE FATIGUE LOADS: LOAD LEVELS	NORMALIZED LOAD LEVELS	LOAD/50% AT RATED	CORRESPONDING MID-RANGE LOAD DISTRIBUTION: MEAN	STANDARD DEVIATION	MAXIMUM	MINIMUM
0.	0.	0. - 0.962E 03	0. - 0.01	0. - 0.08	0.	0.	0.	0.
0.	0.	0.962E 03 - 0.192E 04	0.01 - 0.02	0.08 - 0.15	0.	0.	0.	0.
0.	0.	0.192E 04 - 0.288E 04	0.02 - 0.03	0.15 - 0.23	0.	0.	0.	0.
0.	0.	0.288E 04 - 0.385E 04	0.03 - 0.04	0.23 - 0.31	0.	0.	0.	0.
0.818E 06	0.00228	0.385E 04 - 0.481E 04	0.04 - 0.05	0.31 - 0.38	-0.197E 06	0.238E 05	-0.177E 06	-0.227E 06
0.286E 07	0.01025	0.481E 04 - 0.577E 04	0.05 - 0.06	0.38 - 0.46	-0.176E 06	0.467E 05	-0.760E 05	-0.227E 06
0.621E 07	0.02754	0.577E 04 - 0.673E 04	0.06 - 0.07	0.46 - 0.54	-0.175E 06	0.474E 05	-0.760E 05	-0.227E 06
0.108E 08	0.05771	0.673E 04 - 0.769E 04	0.07 - 0.08	0.54 - 0.62	-0.171E 06	0.499E 05	-0.760E 05	-0.227E 06
0.158E 08	0.10165	0.769E 04 - 0.865E 04	0.08 - 0.09	0.62 - 0.69	-0.166E 06	0.517E 05	-0.760E 05	-0.227E 06
0.202E 08	0.15792	0.865E 04 - 0.962E 04	0.09 - 0.10	0.69 - 0.77	-0.162E 06	0.531E 05	-0.760E 05	-0.227E 06
0.235E 08	0.22345	0.962E 04 - 0.106E 05	0.10 - 0.11	0.77 - 0.85	-0.158E 06	0.541E 05	-0.760E 05	-0.227E 06
0.255E 08	0.29450	0.106E 05 - 0.115E 05	0.11 - 0.12	0.85 - 0.92	-0.155E 06	0.548E 05	-0.760E 05	-0.227E 06
0.262E 08	0.36740	0.115E 05 - 0.125E 05	0.12 - 0.13	0.92 - 1.00	-0.151E 06	0.551E 05	-0.760E 05	-0.227E 06
0.138E 09	0.75216	0.125E 05 - 0.190E 05	0.13 - 0.20	1.00 - 1.52	-0.141E 06	0.548E 05	-0.753E 05	-0.227E 06
0.576E 08	0.91256	0.190E 05 - 0.255E 05	0.20 - 0.26	1.52 - 2.04	-0.127E 06	0.510E 05	-0.727E 05	-0.227E 06
0.197E 08	0.96743	0.255E 05 - 0.320E 05	0.26 - 0.33	2.04 - 2.56	-0.122E 06	0.486E 05	-0.682E 05	-0.227E 06
0.697E 07	0.98685	0.320E 05 - 0.385E 05	0.33 - 0.40	2.56 - 3.08	-0.125E 06	0.489E 05	-0.629E 05	-0.227E 06
0.261E 07	0.99412	0.385E 05 - 0.450E 05	0.40 - 0.46	3.08 - 3.60	-0.137E 06	0.511E 05	-0.576E 05	-0.227E 06
0.122E 07	0.99751	0.450E 05 - 0.514E 05	0.46 - 0.53	3.60 - 4.12	-0.150E 06	0.520E 05	-0.540E 05	-0.227E 06
0.443E 06	0.99874	0.514E 05 - 0.579E 05	0.53 - 0.60	4.12 - 4.63	-0.186E 06	0.374E 05	-0.770E 05	-0.227E 06
0.228E 06	0.99938	0.579E 05 - 0.644E 05	0.60 - 0.67	4.63 - 5.15	-0.195E 06	0.313E 05	-0.772E 05	-0.227E 06
0.109E 06	0.99968	0.644E 05 - 0.709E 05	0.67 - 0.73	5.15 - 5.67	-0.202E 06	0.276E 05	-0.122E 06	-0.227E 06
0.480E 05	0.99982	0.709E 05 - 0.774E 05	0.73 - 0.80	5.67 - 6.19	-0.208E 06	0.229E 05	-0.122E 06	-0.227E 06
0.192E 05	0.99987	0.774E 05 - 0.839E 05	0.80 - 0.87	6.19 - 6.71	-0.212E 06	0.198E 05	-0.183E 06	-0.227E 06
0.800E 04	0.99989	0.839E 05 - 0.904E 05	0.87 - 0.93	6.71 - 7.23	-0.211E 06	0.205E 05	-0.183E 06	-0.227E 06
0.341E 04	0.99990	0.904E 05 - 0.969E 05	0.93 - 1.00	7.23 - 7.75	-0.215E 06	0.198E 05	-0.183E 06	-0.227E 06

TOTAL CYCLES = 0.359E 09

ROOT MEAN CUBED IS 0.193E 05 AVERAGE MEAN IS -0.144E 06

TABLE H-106
CUMULATIVE FATIGUE HISTOGRAM OUTPUT

TOWER 51 MX

NO. CYCLES IN 30 YEARS (TYPES 1+2)	CUM PROB	HALF-RANGE FATIGUE LOADS: LOAD LEVELS	NORMALIZED LOAD LEVELS	LOAD/50% AT RATED	CORRESPONDING MID-RANGE LOAD DISTRIBUTION: MEAN	STANDARD DEVIATION	MAXIMUM	MINIMUM
0.	0.	0. - 0.646E 04	0. - 0.01	0. - 0.08	0.	0.	0.	0.
0.	0.	0.646E 04 - 0.129E 05	0.01 - 0.03	0.08 - 0.15	0.	0.	0.	0.
0.	0.	0.129E 05 - 0.194E 05	0.03 - 0.04	0.15 - 0.23	0.	0.	0.	0.
0.	0.	0.194E 05 - 0.258E 05	0.04 - 0.06	0.23 - 0.31	0.	0.	0.	0.
0.	0.	0.258E 05 - 0.323E 05	0.06 - 0.07	0.31 - 0.38	0.	0.	0.	0.
0.	0.	0.323E 05 - 0.387E 05	0.07 - 0.09	0.38 - 0.46	0.	0.	0.	0.
0.278E 05	0.00008	0.387E 05 - 0.452E 05	0.09 - 0.10	0.46 - 0.54	-0.527E 06	0.	-0.527E 06	-0.527E 06
0.165E 07	0.00468	0.452E 05 - 0.517E 05	0.10 - 0.12	0.54 - 0.62	-0.398E 06	0.106E 06	-0.311E 06	-0.527E 06
0.116E 08	0.03711	0.517E 05 - 0.581E 05	0.12 - 0.13	0.62 - 0.69	-0.375E 06	0.108E 06	-0.650E 05	-0.531E 06
0.302E 08	0.12112	0.581E 05 - 0.646E 05	0.13 - 0.15	0.69 - 0.77	-0.345E 06	0.121E 06	-0.650E 05	-0.531E 06
0.427E 08	0.24014	0.646E 05 - 0.710E 05	0.15 - 0.16	0.77 - 0.85	-0.298E 06	0.156E 06	-0.650E 05	-0.531E 06
0.498E 08	0.37875	0.710E 05 - 0.775E 05	0.16 - 0.17	0.85 - 0.92	-0.258E 06	0.190E 06	-0.650E 05	-0.531E 06
0.517E 08	0.52258	0.775E 05 - 0.840E 05	0.17 - 0.19	0.92 - 1.00	-0.254E 06	0.207E 06	-0.631E 05	-0.534E 06
0.141E 09	0.91431	0.840E 05 - 0.112E 06	0.19 - 0.25	1.00 - 1.33	-0.238E 06	0.165E 06	-0.475E 05	-0.545E 06
0.244E 08	0.98216	0.112E 06 - 0.139E 06	0.25 - 0.31	1.33 - 1.66	-0.202E 06	0.721E 05	-0.250E 05	-0.531E 06
0.341E 07	0.99165	0.139E 06 - 0.167E 06	0.31 - 0.38	1.66 - 1.99	-0.287E 06	0.145E 06	-0.845E 05	-0.531E 06
0.138E 07	0.99548	0.167E 06 - 0.195E 06	0.38 - 0.44	1.99 - 2.32	-0.361E 06	0.129E 06	-0.946E 05	-0.531E 06
0.735E 06	0.99753	0.195E 06 - 0.222E 06	0.44 - 0.50	2.32 - 2.65	-0.412E 06	0.119E 06	-0.197E 06	-0.531E 06
0.402E 06	0.99865	0.222E 06 - 0.250E 06	0.50 - 0.56	2.65 - 2.98	-0.458E 06	0.948E 05	-0.174E 06	-0.531E 06
0.227E 06	0.99928	0.250E 06 - 0.278E 06	0.56 - 0.63	2.98 - 3.31	-0.476E 06	0.695E 05	-0.157E 06	-0.531E 06
0.120E 06	0.99962	0.278E 06 - 0.305E 06	0.63 - 0.69	3.31 - 3.64	-0.483E 06	0.494E 05	-0.243E 06	-0.531E 06
0.595E 05	0.99978	0.305E 06 - 0.333E 06	0.69 - 0.75	3.64 - 3.97	-0.483E 06	0.428E 05	-0.292E 06	-0.531E 06
0.268E 05	0.99986	0.333E 06 - 0.361E 06	0.75 - 0.81	3.97 - 4.30	-0.479E 06	0.445E 05	-0.436E 06	-0.531E 06
0.113E 05	0.99989	0.361E 06 - 0.388E 06	0.81 - 0.88	4.30 - 4.63	-0.475E 06	0.495E 05	-0.426E 06	-0.531E 06
0.463E 04	0.99990	0.388E 06 - 0.416E 06	0.88 - 0.94	4.63 - 4.96	-0.456E 06	0.528E 05	-0.417E 06	-0.531E 06
0.767E 03	0.99990	0.416E 06 - 0.444E 06	0.94 - 1.00	4.96 - 5.29	-0.527E 06	0.129E 04	-0.527E 06	-0.531E 06

TOTAL CYCLES = 0.359E 09

ROOT MEAN CUBED IS 0.935E 05 AVERAGE MEAN IS -0.264E 06

TABLE H-107
CUMULATIVE FATIGUE HISTOGRAM OUTPUT

TOWER 51 MY

NO. CYCLES IN 30 YEARS (TYPES 1+2)	CUM PROB	HALF-RANGE FATIGUE LOADS: LOAD LEVELS	NORMALIZED LOAD LEVELS	LOAD/50% AT RATED	CORRESPONDING MID-RANGE LOAD DISTRIBUTION: MEAN	STANDARD DEVIATION	MAXIMUM	MINIMUM
0.	0.	0. - 0.177E 06	0. - 0.01	0. - 0.08	0.	0.	0.	0.
0.	0.	0.177E 06 - 0.354E 06	0.01 - 0.02	0.08 - 0.15	0.	0.	0.	0.
0.	0.	0.354E 06 - 0.531E 06	0.02 - 0.03	0.15 - 0.23	0.	0.	0.	0.
0.942E 05	0.00026	0.531E 06 - 0.708E 06	0.03 - 0.04	0.23 - 0.31	0.237E 08	0.509E 06	0.247E 08	0.234E 08
0.828E 06	0.00257	0.708E 06 - 0.885E 06	0.04 - 0.05	0.31 - 0.38	0.272E 08	0.455E 07	0.331E 08	0.234E 08
0.324E 07	0.01160	0.885E 06 - 0.106E 07	0.05 - 0.06	0.38 - 0.46	0.225E 08	0.908E 07	0.331E 08	0.393E 07
0.687E 07	0.03074	0.106E 07 - 0.124E 07	0.06 - 0.06	0.46 - 0.54	0.225E 08	0.922E 07	0.331E 08	0.393E 07
0.118E 08	0.06363	0.124E 07 - 0.142E 07	0.06 - 0.07	0.54 - 0.62	0.217E 08	0.966E 07	0.331E 08	0.393E 07
0.170E 08	0.11091	0.142E 07 - 0.159E 07	0.07 - 0.08	0.62 - 0.69	0.209E 08	0.100E 08	0.331E 08	0.393E 07
0.215E 08	0.17069	0.159E 07 - 0.177E 07	0.08 - 0.09	0.69 - 0.77	0.202E 08	0.103E 08	0.331E 08	0.393E 07
0.247E 08	0.23947	0.177E 07 - 0.195E 07	0.09 - 0.10	0.77 - 0.85	0.195E 08	0.104E 08	0.331E 08	0.393E 07
0.265E 08	0.31320	0.195E 07 - 0.212E 07	0.10 - 0.11	0.85 - 0.92	0.188E 08	0.106E 08	0.331E 08	0.393E 07
0.269E 08	0.38802	0.212E 07 - 0.230E 07	0.11 - 0.12	0.92 - 1.00	0.182E 08	0.106E 08	0.331E 08	0.393E 07
0.143E 09	0.78734	0.230E 07 - 0.359E 07	0.12 - 0.19	1.00 - 1.56	0.163E 08	0.106E 08	0.331E 08	0.393E 07
0.496E 08	0.92533	0.359E 07 - 0.489E 07	0.19 - 0.26	1.56 - 2.12	0.137E 08	0.100E 08	0.331E 08	0.334E 07
0.160E 08	0.96991	0.489E 07 - 0.618E 07	0.26 - 0.32	2.12 - 2.69	0.124E 08	0.966E 07	0.331E 08	0.143E 07
0.611E 07	0.98693	0.618E 07 - 0.747E 07	0.32 - 0.39	2.69 - 3.25	0.133E 08	0.943E 07	0.331E 08	-0.107E 07
0.268E 07	0.99438	0.747E 07 - 0.876E 07	0.39 - 0.46	3.25 - 3.81	0.153E 08	0.873E 07	0.331E 08	0.393E 07
0.108E 07	0.99740	0.876E 07 - 0.101E 08	0.46 - 0.53	3.81 - 4.37	0.211E 08	0.770E 07	0.331E 08	0.410E 07
0.495E 06	0.99878	0.101E 08 - 0.113E 08	0.53 - 0.59	4.37 - 4.93	0.246E 08	0.674E 07	0.331E 08	0.415E 07
0.223E 06	0.99940	0.113E 08 - 0.126E 08	0.59 - 0.66	4.93 - 5.50	0.273E 08	0.553E 07	0.331E 08	0.128E 08
0.103E 06	0.99969	0.126E 08 - 0.139E 08	0.66 - 0.73	5.50 - 6.06	0.288E 08	0.485E 07	0.331E 08	0.128E 08
0.473E 05	0.99982	0.139E 08 - 0.152E 08	0.73 - 0.80	6.06 - 6.62	0.295E 08	0.416E 07	0.331E 08	0.128E 08
0.189E 05	0.99987	0.152E 08 - 0.165E 08	0.80 - 0.86	6.62 - 7.18	0.303E 08	0.370E 07	0.331E 08	0.247E 08
0.783E 04	0.99989	0.165E 08 - 0.178E 08	0.86 - 0.93	7.18 - 7.74	0.300E 08	0.384E 07	0.331E 08	0.247E 08
0.334E 04	0.99990	0.178E 08 - 0.191E 08	0.93 - 1.00	7.74 - 8.31	0.306E 08	0.382E 07	0.331E 08	0.247E 08

TOTAL CYCLES = 0.359E 09

ROOT MEAN CUBED IS 0.360E 07 AVERAGE MEAN IS 0.171E 08

TABLE H-108
CUMULATIVE FATIGUE HISTOGRAM OUTPUT

TOWER 51 MZ

NO. CYCLES IN 30 YEARS (TYPES 1+2)	CUM PROB	HALF-RANGE FATIGUE LOADS: LOAD LEVELS	NORMALIZED LOAD LEVELS	LOAD/50% AT RATED	CORRESPONDING MID-RANGE LOAD DISTRIBUTION: MEAN	STANDARD DEVIATION	MAXIMUM	MINIMUM
0.	0.	0. - 0.137E 06	0. - 0.03	0. - 0.08	0.	0.	0.	0.
0.	0.	0.137E 06 - 0.275E 06	0.03 - 0.06	0.08 - 0.15	0.	0.	0.	0.
0.	0.	0.275E 06 - 0.412E 06	0.06 - 0.09	0.15 - 0.23	0.	0.	0.	0.
0.	0.	0.412E 06 - 0.549E 06	0.09 - 0.12	0.23 - 0.31	0.	0.	0.	0.
0.	0.	0.549E 06 - 0.687E 06	0.12 - 0.15	0.31 - 0.38	0.	0.	0.	0.
0.	0.	0.687E 06 - 0.824E 06	0.15 - 0.18	0.38 - 0.46	0.	0.	0.	0.
0.	0.	0.824E 06 - 0.961E 06	0.18 - 0.21	0.46 - 0.54	0.	0.	0.	0.
0.	0.	0.961E 06 - 0.110E 07	0.21 - 0.24	0.54 - 0.62	0.	0.	0.	0.
0.	0.	0.110E 07 - 0.124E 07	0.24 - 0.28	0.62 - 0.69	0.	0.	0.	0.
0.766E 06	0.00213	0.124E 07 - 0.137E 07	0.28 - 0.31	0.69 - 0.77	-0.329E 07	0.500E 06	-0.200E 07	-0.348E 07
0.517E 07	0.01652	0.137E 07 - 0.151E 07	0.31 - 0.34	0.77 - 0.85	-0.319E 07	0.597E 06	-0.200E 07	-0.357E 07
0.171E 08	0.06424	0.151E 07 - 0.165E 07	0.34 - 0.37	0.85 - 0.92	-0.306E 07	0.673E 06	-0.200E 07	-0.357E 07
0.321E 08	0.15351	0.165E 07 - 0.179E 07	0.37 - 0.40	0.92 - 1.00	-0.293E 07	0.722E 06	-0.200E 07	-0.357E 07
0.563E 08	0.31032	0.179E 07 - 0.199E 07	0.40 - 0.44	1.00 - 1.12	-0.278E 07	0.756E 06	-0.138E 07	-0.357E 07
0.401E 08	0.42203	0.199E 07 - 0.220E 07	0.44 - 0.49	1.12 - 1.23	-0.249E 07	0.849E 06	-0.495E 06	-0.357E 07
0.308E 08	0.50768	0.220E 07 - 0.241E 07	0.49 - 0.54	1.23 - 1.35	-0.175E 07	0.896E 06	-0.495E 06	-0.357E 07
0.402E 08	0.61959	0.241E 07 - 0.262E 07	0.54 - 0.58	1.35 - 1.47	-0.120E 07	0.628E 06	-0.495E 06	-0.357E 07
0.479E 08	0.75285	0.262E 07 - 0.282E 07	0.58 - 0.63	1.47 - 1.58	-0.101E 07	0.525E 06	-0.495E 06	-0.357E 07
0.433E 08	0.87341	0.282E 07 - 0.303E 07	0.63 - 0.68	1.58 - 1.70	-0.885E 06	0.490E 06	-0.422E 06	-0.357E 07
0.271E 08	0.94889	0.303E 07 - 0.324E 07	0.68 - 0.72	1.70 - 1.82	-0.772E 06	0.467E 06	-0.246E 06	-0.357E 07
0.119E 08	0.98212	0.324E 07 - 0.345E 07	0.72 - 0.77	1.82 - 1.93	-0.711E 06	0.446E 06	-0.377E 05	-0.357E 07
0.446E 07	0.99454	0.345E 07 - 0.366E 07	0.77 - 0.81	1.93 - 2.05	-0.669E 06	0.429E 06	0.670E 05	-0.357E 07
0.146E 07	0.99860	0.366E 07 - 0.386E 07	0.81 - 0.86	2.05 - 2.16	-0.660E 06	0.452E 06	-0.495E 06	-0.357E 07
0.357E 06	0.99959	0.386E 07 - 0.407E 07	0.86 - 0.91	2.16 - 2.28	-0.567E 06	0.447E 06	-0.495E 06	-0.357E 07
0.110E 06	0.99990	0.407E 07 - 0.428E 07	0.91 - 0.95	2.28 - 2.40	-0.571E 06	0.476E 06	-0.495E 06	-0.357E 07
0.115E 04	0.99990	0.428E 07 - 0.449E 07	0.95 - 1.00	2.40 - 2.51	-0.355E 07	0.507E 04	-0.355E 07	-0.357E 07

TOTAL CYCLES = 0.359E 09

ROOT MEAN CUBED IS 0.251E 07 AVERAGE MEAN IS -0.180E 07

TABLE H-109
CUMULATIVE FATIGUE HISTOGRAM OUTPUT

TOWER BASE VX

NO. CYCLES IN 30 YEARS (TYPES 1+2)	CUM PROB	HALF-RANGE FATIGUE LOADS: LOAD LEVELS	NORMALIZED LOAD LEVELS	LOAD/50% AT RATED	CORRESPONDING MID-RANGE LOAD DISTRIBUTION: MEAN	STANDARD DEVIATION	MAXIMUM	MINIMUM
0.	0.	0. - 0.133E 04	0. - 0.05	0. - 0.08	0.	0.	0.	0.
0.	0.	0.133E 04 - 0.265E 04	0.05 - 0.11	0.08 - 0.15	0.	0.	0.	0.
0.	0.	0.265E 04 - 0.398E 04	0.11 - 0.16	0.15 - 0.23	0.	0.	0.	0.
0.	0.	0.398E 04 - 0.531E 04	0.16 - 0.22	0.23 - 0.31	0.	0.	0.	0.
0.186E 07	0.00519	0.531E 04 - 0.663E 04	0.22 - 0.27	0.31 - 0.38	-0.184E 07	0.287E 04	-0.184E 07	-0.184E 07
0.426E 08	0.12392	0.663E 04 - 0.796E 04	0.27 - 0.33	0.38 - 0.46	-0.184E 07	0.287E 04	-0.184E 07	-0.184E 07
0.984E 08	0.39791	0.796E 04 - 0.929E 04	0.33 - 0.38	0.46 - 0.54	-0.184E 07	0.293E 04	-0.184E 07	-0.185E 07
0.455E 08	0.52452	0.929E 04 - 0.106E 05	0.38 - 0.43	0.54 - 0.62	-0.184E 07	0.400E 04	-0.184E 07	-0.185E 07
0.221E 08	0.58598	0.106E 05 - 0.119E 05	0.43 - 0.49	0.62 - 0.69	-0.185E 07	0.655E 04	-0.184E 07	-0.185E 07
0.270E 08	0.66128	0.119E 05 - 0.133E 05	0.49 - 0.54	0.69 - 0.77	-0.185E 07	0.173E 04	-0.184E 07	-0.186E 07
0.254E 08	0.73211	0.133E 05 - 0.146E 05	0.54 - 0.60	0.77 - 0.85	-0.185E 07	0.169E 04	-0.185E 07	-0.186E 07
0.238E 08	0.79841	0.146E 05 - 0.159E 05	0.60 - 0.65	0.85 - 0.92	-0.186E 07	0.200E 04	-0.185E 07	-0.186E 07
0.252E 08	0.86864	0.159E 05 - 0.172E 05	0.65 - 0.71	0.92 - 1.00	-0.186E 07	0.116E 04	-0.185E 07	-0.186E 07
0.133E 08	0.90561	0.172E 05 - 0.178E 05	0.71 - 0.73	1.00 - 1.03	-0.186E 07	0.724E 03	-0.185E 07	-0.186E 07
0.869E 07	0.92982	0.178E 05 - 0.184E 05	0.73 - 0.75	1.03 - 1.06	-0.186E 07	0.512E 03	-0.185E 07	-0.186E 07
0.728E 07	0.95008	0.184E 05 - 0.189E 05	0.75 - 0.77	1.06 - 1.10	-0.186E 07	0.443E 03	-0.185E 07	-0.186E 07
0.566E 07	0.96585	0.189E 05 - 0.195E 05	0.77 - 0.80	1.10 - 1.13	-0.186E 07	0.256E 03	-0.186E 07	-0.186E 07
0.421E 07	0.97757	0.195E 05 - 0.200E 05	0.80 - 0.82	1.13 - 1.16	-0.186E 07	0.256E 03	-0.186E 07	-0.186E 07
0.297E 07	0.98584	0.200E 05 - 0.206E 05	0.82 - 0.84	1.16 - 1.19	-0.186E 07	0.181E 03	-0.186E 07	-0.186E 07
0.200E 07	0.99140	0.206E 05 - 0.211E 05	0.84 - 0.86	1.19 - 1.22	-0.186E 07	0.181E 03	-0.186E 07	-0.186E 07
0.128E 07	0.99498	0.211E 05 - 0.217E 05	0.86 - 0.89	1.22 - 1.26	-0.186E 07	0.256E 03	-0.186E 07	-0.186E 07
0.793E 06	0.99719	0.217E 05 - 0.222E 05	0.89 - 0.91	1.26 - 1.29	-0.186E 07	0.256E 03	-0.186E 07	-0.186E 07
0.472E 06	0.99850	0.222E 05 - 0.228E 05	0.91 - 0.93	1.29 - 1.32	-0.186E 07	0.181E 03	-0.186E 07	-0.186E 07
0.271E 06	0.99925	0.228E 05 - 0.233E 05	0.93 - 0.95	1.32 - 1.35	-0.186E 07	0.181E 03	-0.186E 07	-0.186E 07
0.151E 06	0.99968	0.233E 05 - 0.239E 05	0.95 - 0.98	1.35 - 1.38	-0.186E 07	0.181E 03	-0.186E 07	-0.186E 07
0.817E 05	0.99990	0.239E 05 - 0.244E 05	0.98 - 1.00	1.38 - 1.42	-0.186E 07	0.181E 03	-0.186E 07	-0.186E 07

TOTAL CYCLES = 0.359E 09

ROOT MEAN CUBED IS 0.130E 05 AVERAGE MEAN IS -0.185E 07

TABLE H-110
CUMULATIVE FATIGUE HISTOGRAM OUTPUT

TOWER BASE VY

NO. CYCLES IN 30 YEARS (TYPES 1+2)	CUM PROB	HALF-RANGE FATIGUE LOADS: LOAD LEVELS	NORMALIZED LOAD LEVELS	LOAD/50% AT RATED	CORRESPONDING MID-RANGE LOAD DISTRIBUTION: MEAN	STANDARD DEVIATION	MAXIMUM	MINIMUM
0.	0.	0. - 0.796E 03	0. - 0.03	0. - 0.08	0.	0.	0.	0.
0.	0.	0.796E 03 - 0.159E 04	0.03 - 0.07	0.08 - 0.15	0.	0.	0.	0.
0.	0.	0.159E 04 - 0.239E 04	0.07 - 0.10	0.15 - 0.23	0.	0.	0.	0.
0.	0.	0.239E 04 - 0.318E 04	0.10 - 0.14	0.23 - 0.31	0.	0.	0.	0.
0.	0.	0.318E 04 - 0.398E 04	0.14 - 0.17	0.31 - 0.38	0.	0.	0.	0.
0.	0.	0.398E 04 - 0.477E 04	0.17 - 0.21	0.38 - 0.46	0.	0.	0.	0.
0.	0.	0.477E 04 - 0.557E 04	0.21 - 0.24	0.46 - 0.54	0.	0.	0.	0.
0.	0.	0.557E 04 - 0.636E 04	0.24 - 0.27	0.54 - 0.62	0.	0.	0.	0.
0.	0.	0.636E 04 - 0.716E 04	0.27 - 0.31	0.62 - 0.69	0.	0.	0.	0.
0.740E 06	0.00206	0.716E 04 - 0.796E 04	0.31 - 0.34	0.69 - 0.77	0.243E 04	0.287E 03	0.252E 04	0.157E 04
0.492E 07	0.01576	0.796E 04 - 0.875E 04	0.34 - 0.38	0.77 - 0.85	0.235E 04	0.363E 03	0.252E 04	0.157E 04
0.163E 08	0.06110	0.875E 04 - 0.955E 04	0.38 - 0.41	0.85 - 0.92	0.225E 04	0.418E 03	0.252E 04	0.157E 04
0.307E 08	0.14666	0.955E 04 - 0.103E 05	0.41 - 0.45	0.92 - 1.00	0.214E 04	0.448E 03	0.252E 04	0.157E 04
0.498E 08	0.28524	0.103E 05 - 0.113E 05	0.45 - 0.49	1.00 - 1.10	0.201E 04	0.445E 03	0.252E 04	0.129E 04
0.413E 08	0.40024	0.113E 05 - 0.123E 05	0.49 - 0.53	1.10 - 1.19	0.181E 04	0.466E 03	0.252E 04	0.753E 03
0.302E 08	0.48445	0.123E 05 - 0.133E 05	0.53 - 0.57	1.19 - 1.29	0.155E 04	0.455E 03	0.252E 04	0.165E 03
0.322E 08	0.57409	0.133E 05 - 0.143E 05	0.57 - 0.62	1.29 - 1.38	0.126E 04	0.366E 03	0.252E 04	0.753E 03
0.402E 08	0.68599	0.143E 05 - 0.153E 05	0.62 - 0.66	1.38 - 1.48	0.112E 04	0.296E 03	0.252E 04	0.753E 03
0.395E 08	0.79603	0.153E 05 - 0.163E 05	0.66 - 0.70	1.48 - 1.57	0.102E 04	0.271E 03	0.200E 04	0.753E 03
0.347E 08	0.89261	0.163E 05 - 0.172E 05	0.70 - 0.74	1.57 - 1.67	0.916E 03	0.270E 03	0.200E 04	0.554E 03
0.197E 08	0.94748	0.172E 05 - 0.182E 05	0.74 - 0.79	1.67 - 1.76	0.905E 03	0.248E 03	0.129E 04	0.253E 03
0.107E 08	0.97730	0.182E 05 - 0.192E 05	0.79 - 0.83	1.76 - 1.86	0.869E 03	0.222E 03	0.129E 04	0.753E 03
0.500E 07	0.99124	0.192E 05 - 0.202E 05	0.83 - 0.87	1.86 - 1.95	0.838E 03	0.197E 03	0.129E 04	0.753E 03
0.212E 07	0.99714	0.202E 05 - 0.212E 05	0.87 - 0.91	1.95 - 2.05	0.834E 03	0.193E 03	0.129E 04	0.753E 03
0.674E 06	0.99902	0.212E 05 - 0.222E 05	0.91 - 0.96	2.05 - 2.14	0.753E 03	0.	0.753E 03	0.753E 03
0.317E 06	0.99990	0.222E 05 - 0.232E 05	0.96 - 1.00	2.14 - 2.24	0.753E 03	0.	0.753E 03	0.753E 03

TOTAL CYCLES = 0.359E 09

ROOT MEAN CUBED IS 0.142E 05 AVERAGE MEAN IS 0.147E 04

TABLE H-111
CUMULATIVE FATIGUE HISTOGRAM OUTPUT

TOWER BASE VZ

NO. CYCLES IN 30 YEARS (TYPES 1+2)	CUM PROB	HALF-RANGE FATIGUE LOADS: LOAD LEVELS	NORMALIZED LOAD LEVELS	LOAD/50% AT RATED	CORRESPONDING MID-RANGE LOAD DISTRIBUTION: MEAN	STANDARD DEVIATION	MAXIMUM	MINIMUM
0.	0.	0. - 0.962E 03	0. - 0.01	0. - 0.08	0.	0.	0.	0.
0.	0.	0.962E 03 - 0.192E 04	0.01 - 0.02	0.08 - 0.15	0.	0.	0.	0.
0.	0.	0.192E 04 - 0.288E 04	0.02 - 0.03	0.15 - 0.23	0.	0.	0.	0.
0.	0.	0.288E 04 - 0.385E 04	0.03 - 0.04	0.23 - 0.31	0.	0.	0.	0.
0.818E 06	0.00228	0.385E 04 - 0.481E 04	0.04 - 0.05	0.31 - 0.38	-0.197E 06	0.238E 05	-0.177E 06	-0.227E 06
0.286E 07	0.01024	0.481E 04 - 0.577E 04	0.05 - 0.06	0.38 - 0.46	-0.176E 06	0.466E 05	-0.760E 05	-0.227E 06
0.620E 07	0.02751	0.577E 04 - 0.673E 04	0.06 - 0.07	0.46 - 0.54	-0.175E 06	0.474E 05	-0.760E 05	-0.227E 06
0.108E 08	0.05764	0.673E 04 - 0.769E 04	0.07 - 0.08	0.54 - 0.62	-0.171E 06	0.498E 05	-0.760E 05	-0.227E 06
0.158E 08	0.10153	0.769E 04 - 0.865E 04	0.08 - 0.09	0.62 - 0.69	-0.167E 06	0.517E 05	-0.760E 05	-0.227E 06
0.202E 08	0.15774	0.865E 04 - 0.962E 04	0.09 - 0.10	0.69 - 0.77	-0.162E 06	0.531E 05	-0.760E 05	-0.227E 06
0.235E 08	0.22320	0.962E 04 - 0.106E 05	0.10 - 0.11	0.77 - 0.85	-0.158E 06	0.541E 05	-0.760E 05	-0.227E 06
0.255E 08	0.29418	0.106E 05 - 0.115E 05	0.11 - 0.12	0.85 - 0.92	-0.155E 06	0.548E 05	-0.760E 05	-0.227E 06
0.262E 08	0.36703	0.115E 05 - 0.125E 05	0.12 - 0.13	0.92 - 1.00	-0.151E 06	0.551E 05	-0.760E 05	-0.227E 06
0.138E 09	0.75175	0.125E 05 - 0.190E 05	0.13 - 0.20	1.00 - 1.52	-0.141E 06	0.548E 05	-0.753E 05	-0.227E 06
0.577E 08	0.91234	0.190E 05 - 0.255E 05	0.20 - 0.26	1.52 - 2.04	-0.127E 06	0.510E 05	-0.727E 05	-0.227E 06
0.198E 08	0.96734	0.255E 05 - 0.320E 05	0.26 - 0.33	2.04 - 2.56	-0.122E 06	0.486E 05	-0.682E 05	-0.227E 06
0.699E 07	0.98682	0.320E 05 - 0.385E 05	0.33 - 0.40	2.56 - 3.08	-0.125E 06	0.489E 05	-0.629E 05	-0.227E 06
0.262E 07	0.99411	0.385E 05 - 0.450E 05	0.40 - 0.46	3.08 - 3.60	-0.136E 06	0.511E 05	-0.576E 05	-0.227E 06
0.122E 07	0.99751	0.450E 05 - 0.514E 05	0.46 - 0.53	3.60 - 4.12	-0.150E 06	0.521E 05	-0.540E 05	-0.227E 06
0.443E 06	0.99874	0.514E 05 - 0.579E 05	0.53 - 0.60	4.12 - 4.63	-0.186E 06	0.375E 05	-0.770E 05	-0.227E 06
0.228E 06	0.99938	0.579E 05 - 0.644E 05	0.60 - 0.67	4.63 - 5.15	-0.195E 06	0.314E 05	-0.771E 05	-0.227E 06
0.109E 06	0.99968	0.644E 05 - 0.709E 05	0.67 - 0.73	5.15 - 5.67	-0.202E 06	0.276E 05	-0.122E 06	-0.227E 06
0.480E 05	0.99982	0.709E 05 - 0.774E 05	0.73 - 0.80	5.67 - 6.19	-0.208E 06	0.229E 05	-0.122E 06	-0.227E 06
0.192E 05	0.99987	0.774E 05 - 0.839E 05	0.80 - 0.87	6.19 - 6.71	-0.212E 06	0.198E 05	-0.183E 06	-0.227E 06
0.800E 04	0.99989	0.839E 05 - 0.904E 05	0.87 - 0.93	6.71 - 7.23	-0.211E 06	0.205E 05	-0.183E 06	-0.227E 06
0.341E 04	0.99990	0.904E 05 - 0.969E 05	0.93 - 1.00	7.23 - 7.75	-0.215E 06	0.198E 05	-0.183E 06	-0.227E 06

TOTAL CYCLES = 0.359E 09

ROOT MEAN CUBED IS 0.194E 05 AVERAGE MEAN IS -0.144E 06

TABLE H-112
CUMULATIVE FATIGUE HISTOGRAM OUTPUT

TOWER BASE MX

NO. CYCLES IN 30 YEARS (TYPES 1+2)	CUM PROB	HALF-RANGE FATIGUE LOADS: LOAD LEVELS	NORMALIZED LOAD LEVELS	LOAD/50% AT RATED	CORRESPONDING MID-RANGE LOAD DISTRIBUTION: MEAN	STANDARD DEVIATION	MAXIMUM	MINIMUM
0.	0.	0. - 0.646E 04	0. - 0.01	0. - 0.08	0.	0.	0.	0.
0.	0.	0.646E 04 - 0.129E 05	0.01 - 0.03	0.08 - 0.15	0.	0.	0.	0.
0.	0.	0.129E 05 - 0.194E 05	0.03 - 0.04	0.15 - 0.23	0.	0.	0.	0.
0.	0.	0.194E 05 - 0.258E 05	0.04 - 0.06	0.23 - 0.31	0.	0.	0.	0.
0.	0.	0.258E 05 - 0.323E 05	0.06 - 0.07	0.31 - 0.38	0.	0.	0.	0.
0.	0.	0.323E 05 - 0.387E 05	0.07 - 0.09	0.38 - 0.46	0.	0.	0.	0.
0.278E 05	0.00008	0.387E 05 - 0.452E 05	0.09 - 0.10	0.46 - 0.54	-0.527E 06	0.	-0.527E 06	-0.527E 06
0.165E 07	0.00468	0.452E 05 - 0.517E 05	0.10 - 0.12	0.54 - 0.62	-0.398E 06	0.106E 06	-0.311E 06	-0.527E 06
0.116E 08	0.03711	0.517E 05 - 0.581E 05	0.12 - 0.13	0.62 - 0.69	-0.375E 06	0.108E 06	-0.650E 05	-0.531E 06
0.302E 08	0.12112	0.581E 05 - 0.646E 05	0.13 - 0.15	0.69 - 0.77	-0.345E 06	0.121E 06	-0.650E 05	-0.531E 06
0.427E 08	0.24014	0.646E 05 - 0.710E 05	0.15 - 0.16	0.77 - 0.85	-0.298E 06	0.156E 06	-0.650E 05	-0.531E 06
0.498E 08	0.37875	0.710E 05 - 0.775E 05	0.16 - 0.17	0.85 - 0.92	-0.258E 06	0.190E 06	-0.650E 05	-0.531E 06
0.517E 08	0.52258	0.775E 05 - 0.840E 05	0.17 - 0.19	0.92 - 1.00	-0.254E 06	0.207E 06	-0.631E 05	-0.534E 06
0.141E 09	0.91431	0.840E 05 - 0.112E 06	0.19 - 0.25	1.00 - 1.33	-0.238E 06	0.165E 06	-0.475E 05	-0.545E 06
0.244E 08	0.98216	0.112E 06 - 0.139E 06	0.25 - 0.31	1.33 - 1.66	-0.202E 06	0.721E 05	-0.250E 05	-0.531E 06
0.341E 07	0.99165	0.139E 06 - 0.167E 06	0.31 - 0.38	1.66 - 1.99	-0.287E 06	0.145E 06	-0.845E 05	-0.531E 06
0.138E 07	0.99548	0.167E 06 - 0.195E 06	0.38 - 0.44	1.99 - 2.32	-0.361E 06	0.129E 06	-0.946E 05	-0.531E 06
0.735E 06	0.99753	0.195E 06 - 0.222E 06	0.44 - 0.50	2.32 - 2.65	-0.412E 06	0.119E 06	-0.197E 06	-0.531E 06
0.402E 06	0.99865	0.222E 06 - 0.250E 06	0.50 - 0.56	2.65 - 2.98	-0.458E 06	0.948E 05	-0.174E 06	-0.531E 06
0.227E 06	0.99928	0.250E 06 - 0.278E 06	0.56 - 0.63	2.98 - 3.31	-0.476E 06	0.695E 05	-0.157E 06	-0.531E 06
0.120E 06	0.99962	0.278E 06 - 0.305E 06	0.63 - 0.69	3.31 - 3.64	-0.483E 06	0.494E 05	-0.243E 06	-0.531E 06
0.595E 05	0.99978	0.305E 06 - 0.333E 06	0.69 - 0.75	3.64 - 3.97	-0.483E 06	0.428E 05	-0.292E 06	-0.531E 06
0.268E 05	0.99986	0.333E 06 - 0.361E 06	0.75 - 0.81	3.97 - 4.30	-0.479E 06	0.445E 05	-0.436E 06	-0.531E 06
0.113E 05	0.99989	0.361E 06 - 0.388E 06	0.81 - 0.88	4.30 - 4.63	-0.475E 06	0.495E 05	-0.426E 06	-0.531E 06
0.463E 04	0.99990	0.388E 06 - 0.416E 06	0.88 - 0.94	4.63 - 4.96	-0.456E 06	0.528E 05	-0.417E 06	-0.531E 06
0.767E 03	0.99990	0.416E 06 - 0.444E 06	0.94 - 1.00	4.96 - 5.29	-0.527E 06	0.129E 04	-0.527E 06	-0.531E 06

TOTAL CYCLES = 0.359E 09

ROOT MEAN CUBED IS 0.935E 05 AVERAGE MEAN IS -0.264E 06

TABLE H-113
CUMULATIVE FATIGUE HISTOGRAM OUTPUT

TOWER BASE MY

NO. CYCLES IN 30 YEARS (TYPES 1+2)	CUM PROB	HALF-RANGE FATIGUE LOADS: LOAD LEVELS	NORMALIZED LOAD LEVELS	LOAD/50% AT RATED	CORRESPONDING MID-RANGE LOAD DISTRIBUTION: MEAN	STANDARD DEVIATION	MAXIMUM	MINIMUM
0.	0.	0. - 0.223E 06	0. - 0.01	0. - 0.08	0.	0.	0.	0.
0.	0.	0.223E 06 - 0.446E 06	0.01 - 0.02	0.08 - 0.15	0.	0.	0.	0.
0.	0.	0.446E 06 - 0.669E 06	0.02 - 0.03	0.15 - 0.23	0.	0.	0.	0.
0.769E 05	0.00021	0.669E 06 - 0.892E 06	0.03 - 0.04	0.23 - 0.31	0.325E 08	0.290E 04	0.325E 08	0.325E 08
0.832E 06	0.00253	0.892E 06 - 0.112E 07	0.04 - 0.05	0.31 - 0.38	0.372E 08	0.577E 07	0.447E 08	0.325E 08
0.309E 07	0.01112	0.112E 07 - 0.134E 07	0.05 - 0.06	0.38 - 0.46	0.320E 08	0.112E 08	0.447E 08	0.779E 07
0.659E 07	0.02946	0.134E 07 - 0.156E 07	0.06 - 0.06	0.46 - 0.54	0.318E 08	0.115E 08	0.447E 08	0.779E 07
0.113E 08	0.06106	0.156E 07 - 0.178E 07	0.06 - 0.07	0.54 - 0.62	0.308E 08	0.121E 08	0.447E 08	0.779E 07
0.163E 08	0.10658	0.178E 07 - 0.201E 07	0.07 - 0.08	0.62 - 0.69	0.298E 08	0.126E 08	0.447E 08	0.779E 07
0.207E 08	0.16435	0.201E 07 - 0.223E 07	0.08 - 0.09	0.69 - 0.77	0.288E 08	0.130E 08	0.447E 08	0.779E 07
0.240E 08	0.23111	0.223E 07 - 0.245E 07	0.09 - 0.10	0.77 - 0.85	0.278E 08	0.132E 08	0.447E 08	0.779E 07
0.258E 08	0.30302	0.245E 07 - 0.268E 07	0.10 - 0.11	0.85 - 0.92	0.269E 08	0.134E 08	0.447E 08	0.779E 07
0.264E 08	0.37640	0.268E 07 - 0.290E 07	0.11 - 0.12	0.92 - 1.00	0.260E 08	0.135E 08	0.447E 08	0.779E 07
0.144E 09	0.77665	0.290E 07 - 0.453E 07	0.12 - 0.19	1.00 - 1.56	0.235E 08	0.134E 08	0.447E 08	0.779E 07
0.518E 08	0.92087	0.453E 07 - 0.616E 07	0.19 - 0.26	1.56 - 2.12	0.200E 08	0.125E 08	0.447E 08	0.704E 07
0.171E 08	0.96841	0.616E 07 - 0.778E 07	0.26 - 0.32	2.12 - 2.68	0.183E 08	0.120E 08	0.447E 08	0.458E 07
0.648E 07	0.98644	0.778E 07 - 0.941E 07	0.32 - 0.39	2.68 - 3.25	0.194E 08	0.117E 08	0.447E 08	0.137E 07
0.262E 07	0.99374	0.941E 07 - 0.110E 08	0.39 - 0.46	3.25 - 3.81	0.225E 08	0.110E 08	0.447E 08	0.779E 07
0.131E 07	0.99739	0.110E 08 - 0.127E 08	0.46 - 0.53	3.81 - 4.37	0.269E 08	0.109E 08	0.447E 08	0.779E 07
0.499E 06	0.99878	0.127E 08 - 0.143E 08	0.53 - 0.59	4.37 - 4.93	0.339E 08	0.852E 07	0.447E 08	0.808E 07
0.223E 06	0.99940	0.143E 08 - 0.159E 08	0.59 - 0.66	4.93 - 5.49	0.373E 08	0.704E 07	0.447E 08	0.191E 06
0.103E 06	0.99969	0.159E 08 - 0.176E 08	0.66 - 0.73	5.49 - 6.05	0.392E 08	0.621E 07	0.447E 08	0.191E 08
0.469E 05	0.99982	0.176E 08 - 0.192E 08	0.73 - 0.80	6.05 - 6.61	0.402E 08	0.537E 07	0.447E 08	0.192E 08
0.187E 05	0.99987	0.192E 08 - 0.208E 08	0.80 - 0.86	6.61 - 7.18	0.411E 08	0.472E 07	0.447E 08	0.341E 08
0.772E 04	0.99989	0.208E 08 - 0.224E 08	0.86 - 0.93	7.18 - 7.74	0.408E 08	0.490E 07	0.447E 08	0.341E 08
0.328E 04	0.99990	0.224E 08 - 0.241E 08	0.93 - 1.00	7.74 - 8.30	0.415E 08	0.487E 07	0.447E 08	0.341E 08

TOTAL CYCLES = 0.359E 09

ROOT MEAN CUBED IS 0.460E 07 AVERAGE MEAN IS 0.245E 08

TABLE H-114
CUMULATIVE FATIGUE HISTOGRAM OUTPUT

TOWER BASE MZ

NO. CYCLES IN 30 YEARS (TYPES 1+2)	CUM PROB	HALF-RANGE FATIGUE LOADS: LOAD LEVELS	NORMALIZED LOAD LEVELS	LOAD/50% AT RATED	CORRESPONDING MID-RANGE LOAD DISTRIBUTION: MEAN	STANDARD DEVIATION	MAXIMUM	MINIMUM
0.	0.	0. - 0.178E 06	0. - 0.03	0. - 0.08	0.	0.	0.	0.
0.	0.	0.178E 06 - 0.357E 06	0.03 - 0.07	0.08 - 0.15	0.	0.	0.	0.
0.	0.	0.357E 06 - 0.535E 06	0.07 - 0.10	0.15 - 0.23	0.	0.	0.	0.
0.	0.	0.535E 06 - 0.713E 06	0.10 - 0.14	0.23 - 0.31	0.	0.	0.	0.
0.	0.	0.713E 06 - 0.891E 06	0.14 - 0.17	0.31 - 0.38	0.	0.	0.	0.
0.	0.	0.891E 06 - 0.107E 07	0.17 - 0.20	0.38 - 0.46	0.	0.	0.	0.
0.	0.	0.107E 07 - 0.125E 07	0.20 - 0.24	0.46 - 0.54	0.	0.	0.	0.
0.	0.	0.125E 07 - 0.143E 07	0.24 - 0.27	0.54 - 0.62	0.	0.	0.	0.
0.	0.	0.143E 07 - 0.160E 07	0.27 - 0.30	0.62 - 0.69	0.	0.	0.	0.
0.764E 06	0.00213	0.160E 07 - 0.178E 07	0.30 - 0.34	0.69 - 0.77	-0.317E 07	0.480E 06	-0.192E 07	-0.335E 07
0.516E 07	0.01650	0.178E 07 - 0.196E 07	0.34 - 0.37	0.77 - 0.85	-0.307E 07	0.574E 06	-0.192E 07	-0.347E 07
0.171E 08	0.06416	0.196E 07 - 0.214E 07	0.37 - 0.41	0.85 - 0.92	-0.295E 07	0.649E 06	-0.192E 07	-0.347E 07
0.320E 08	0.15338	0.214E 07 - 0.232E 07	0.41 - 0.44	0.92 - 1.00	-0.282E 07	0.698E 06	-0.192E 07	-0.347E 07
0.482E 08	0.28771	0.232E 07 - 0.254E 07	0.44 - 0.48	1.00 - 1.10	-0.269E 07	0.733E 06	-0.131E 07	-0.347E 07
0.390E 08	0.39639	0.254E 07 - 0.277E 07	0.48 - 0.53	1.10 - 1.20	-0.248E 07	0.798E 06	-0.457E 06	-0.347E 07
0.278E 08	0.47380	0.277E 07 - 0.300E 07	0.53 - 0.57	1.20 - 1.29	-0.196E 07	0.905E 06	-0.457E 06	-0.347E 07
0.302E 08	0.55802	0.300E 07 - 0.322E 07	0.57 - 0.61	1.29 - 1.39	-0.134E 07	0.743E 06	-0.457E 06	-0.347E 07
0.377E 08	0.66305	0.322E 07 - 0.345E 07	0.61 - 0.66	1.39 - 1.49	-0.105E 07	0.560E 06	-0.457E 06	-0.347E 07
0.414E 08	0.77822	0.345E 07 - 0.368E 07	0.66 - 0.70	1.49 - 1.59	-0.937E 06	0.486E 06	-0.337E 06	-0.347E 07
0.364E 08	0.87972	0.368E 07 - 0.391E 07	0.70 - 0.74	1.59 - 1.69	-0.793E 06	0.441E 06	-0.135E 06	-0.347E 07
0.228E 08	0.94334	0.391E 07 - 0.413E 07	0.74 - 0.78	1.69 - 1.78	-0.703E 06	0.419E 06	-0.155E 06	-0.347E 07
0.117E 08	0.97582	0.413E 07 - 0.436E 07	0.78 - 0.83	1.78 - 1.88	-0.659E 06	0.384E 06	0.394E 05	-0.347E 07
0.537E 07	0.99076	0.436E 07 - 0.459E 07	0.83 - 0.87	1.88 - 1.98	-0.613E 06	0.347E 06	-0.284E 06	-0.347E 07
0.217E 07	0.99679	0.459E 07 - 0.481E 07	0.87 - 0.91	1.98 - 2.08	-0.575E 06	0.309E 06	-0.457E 06	-0.347E 07
0.797E 06	0.99901	0.481E 07 - 0.504E 07	0.91 - 0.96	2.08 - 2.17	-0.569E 06	0.303E 06	-0.457E 06	-0.347E 07
0.322E 06	0.99990	0.504E 07 - 0.527E 07	0.96 - 1.00	2.17 - 2.27	-0.457E 06	0.453E 02	-0.457E 06	-0.457E 06

TOTAL CYCLES = 0.359E 09

ROOT MEAN CUBED IS 0.322E 07 AVERAGE MEAN IS -0.172E 07

TABLE III-1

TYPE III HALF-RANGE LOADS

INTERFACE	Vx	Vy	Vz	Mx	My	Mz
	lb			ft-lb		
	$X10^{-5}$	$X10^{-5}$	$X10^{-5}$	$X10^{-6}$	$X10^{-6}$	$X10^{-6}$
BLADE .90R	.171	.0188	.120	.0090	.165	.0265
.80R	.500	.0618	.220	.0212	.525	.124
.70R	1.04	.133	.316	.0423	1.08	.479
.60R	1.74	.232	.401	.0588	1.77	1.14
.50R	2.47	.321	.482	.0711	2.60	1.99
.40R	3.19	.501	.557	.0815	3.65	3.87
.30R	3.84	.675	.613	.0923	4.72	4.48
.25R	4.15	.774	.637	.0985	5.40	5.29
.20R	4.46	.868	.652	.105	6.03	6.20
.10R	5.03	1.06	.666	.120	7.25	8.37
OR	5.65	1.58	.650	.136	8.23	11.67
TEETER BRGS.	3.08	3.24	1.31	.253	.183	2.18
ROTOR CL	.196	.143	1.29	.195	.205	2.18
ROTOR/NACELLE	.190	.184	1.50	.247	.159	2.18
YAW BEARING	.233	.327	1.26	.618	2.42	2.65
TOWER 185	.233	.342	1.27	.618	7.44	3.91
TOWER 117	.233	.363	1.27	.618	16.1	6.17
TOWER 51	.233	.371	1.27	.618	24.5	8.39
TOWER BASE	.233	.371	1.27	.618	31.0	10.1

NOTE: There are 35,000 Type III cycles in 30 years.

TABLE III-2

TYPE III MID-RANGE LOADS

INTERFACE	Vx	Vy	Vz	Mx	My	Mz
	lb			ft-lb		
	$X10^{-5}$		$X10^{-5}$	$X10^{-6}$	$X10^{-6}$	$X10^{-6}$
BLADE .90R	.154	199.	-.025	-.0078	.0317	-.0342
.80R	.447	884.	-.080	-.0190	.110	-.0683
.70R	.920	1437.	-.230	-.0297	.265	-.255
.60R	1.52	1785.	-.347	-.0468	.942	-.374
.50R	2.14	2550.	-.465	-.0591	1.73	-.476
.40R	2.73	3910.	-.555	-.0690	2.90	-.629
.30R	3.23	6410.	-.633	-.0786	4.30	-.850
.25R	3.46	7922.	-.669	-.0844	5.05	-.950
.20R	3.67	7905.	-.705	-.0907	5.75	-1.10
.10R	4.01	3735.	-.772	-.104	7.20	-1.46
OR	4.11	3842.	-.833	-.119	8.67	-1.94
TEETER BRGS.	-.0613	-3420.	-1.63	.0828	-.0301	-1.88
ROTOR CL	-3.12	-2280.	-1.57	-.0247	.116	-1.88
ROTOR/NACELLE	-5.87	-.102E5	-1.58	-.1340	-4.97	-1.88
YAW BEARING	-12.0	-.171E5	-1.18	.0170	-8.60	-1.48
TOWER 185	-12.3	-.175E5	-1.18	.0170	-3.87	-.635
TOWER 117	-13.7	-.181E5	-1.19	.0170	4.22	.852
TOWER 51	-14.5	-.183E5	-1.19	.0170	12.0	2.37
TOWER BASE	-15.6	-.183E5	-1.19	.0170	18.0	3.48

NOTE: There are 35,000 Type III cycles in 30 years.

TABLE L-1. 50% OVERSPEED @ 47 MPH
(SURVIVAL CONDITION)

INTERFACE	Vx lb	Vy	Vz	Mx ft-lb	My	Mz
BLADE .90R	.0707E6	-.120E5	-.390E5	-.047E6	.550E6	-.188E6
.80R	.207E6	-.181E5	-.780E5	-.131E6	1.75E6	-.566E6
.70R	.426E6	-.240E5	-1.18E5	-.223E6	3.80E6	-.851E6
.60R	.705E6	-.290E5	-1.58E5	-.290E6	6.50E6	-1.25E6
.50R	.996E6	-.360E5	-1.93E5	-.308E6	10.0E6	-1.89E6
.40R	1.28E6	-.472E5	-2.24E5	-.317E6	14.0E6	-2.69E6
.30R	1.52E6	-.610E5	-2.50E5	-.324E6	18.5E6	-4.08E6
.25R	1.62E6	-.695E5	-2.66E5	-.327E6	20.9E6	-4.88E6
.20R	1.74E6	-.824E5	-2.77E5	-.329E6	23.5E6	-5.77E6
.10R	1.91E6	-1.10E5	-2.98E5	-.353E6	28.8E6	-8.00E6
0R	2.00E6	-1.72E5	-3.00E5	-.411E6	35.0E6	-10.8E6
TEETER BRGS.	±.305E6	±.362E6	-.591E6	±.506E6	±.309E6	-4.30E6
ROTOR CL	-.267E6	±.0291E6	-.595E6	±.396E6	±.521E6	-4.29E6
ROTOR/NACELLE	-.540E6	±.0296E6	-.633E6	±.322E6	-4.46E6	-4.29E6
YAW BEARING	-1.28E6	±.0558E6	-.562E6	±.892E6	-.403E6	-4.31E6
TOWER 185	-1.37E6	±.0580E6	-.565E6	±.892E6	2.21E7	-4.48E6
TOWER 117	-1.53E6	±.0613E6	-.569E6	±.892E6	6.06E7	-4.91E6
TOWER 51	-1.73E6	±.0624E6	-.572E6	±.892E6	9.83E7	-8.06E6
TOWER BASE	-1.93E6	±.0626E6	-.572E6	±.892E6	1.28E8	-11.2E6

TABLE L-2a EXTREME WIND CONDITION 130 MPH BLADES UPWIND

INTERFACE	Vx lb	Vy	Vz	Mx ft-lb	My	Mz
	X10^{-5}	X10^{-5}	X10^{-5}	X10^{-6}	X10^{-6}	X10^{-6}
BLADE .90R	0.	±.0147	-.0987	-.0167	.0930	±.0138
.80R	0.	±.0460	-.233	-.0515	.419	±.0719
.70R	0.	±.103	-.403	-.0961	1.05	±.220
.60R	0.	±.186	-.610	-.160	2.06	±.509
.50R	0.	±.287	-.852	-.246	3.52	±1.00
.40R	0.	±.402	-1.13	-.357	5.49	±1.71
.30R	0.	±.531	-1.44	-.498	8.06	±2.66
.25R	0.	±.604	-1.61	-.579	9.59	±3.24
.20R	0.	±.686	-1.79	-.661	11.29	±3.90
.10R	0.	±.887	-2.11	-.750	15.21	±5.48
0R	0.	±1.34	-2.36	-.750	19.64	±7.44
TEETER BRGS.	0.	±2.68	-4.72	0.	0.	0.
ROTOR CL	-3.21	0.	-4.72	0.	0.	0.
ROTOR/NACELLE	-5.67	0.	-5.02	0.	-4.39	0.
YAW BEARING	-10.8	0.	-4.36	0.	-1.89	0.
TOWER 185	-11.5	0.	-4.36	0.	15.7	0.
TOWER 117	-12.9	0.	-4.36	0.	45.3	0.
TOWER 51	-14.7	0.	-4.36	0.	74.1	0.
TOWER BASE	-16.4	0.	-4.36	0.	96.4	0.

TABLE L-2b EXTREME WIND CONDITION 130 MPH BLADES DOWNWIND

INTERFACE	Vx lb	Vy	Vz	Mx ft-lb	My	Mz
	$\times 10^{-5}$	$\times 10^{-5}$	$\times 10^{-5}$	$\times 10^{-6}$	$\times 10^{-6}$	$\times 10^{-6}$
BLADE .90R	0.	±.0147	.0951	.0167	-.0897	±.0138
.80R	0.	±.0460	.222	.0515	-.401	±.0719
.70R	0.	±.103	.378	.0961	-.995	±.220
.60R	0.	±.186	.565	.160	-1.93	±.509
.50R	0.	±.287	.782	.246	-3.27	±1.00
.40R	0.	±.402	1.03	.357	-5.08	±1.71
.30R	0.	±.531	1.31	.498	-7.41	±2.66
.25R	0.	±.604	1.46	.579	-8.80	±3.24
.20R	0.	±.686	1.62	.661	-10.34	±3.90
.10R	0.	±.887	1.89	.750	-13.87	±5.48
0R	0.	±1.34	2.03	.750	-17.83	±7.44
TEETER BRGS.	0.	±2.68	4.06	0.	0.	0.
ROTOR CL	-2.14	0.	4.0[illegible]		0.	0.
ROTOR/NACELLE	-4.61	0.	3.77	0.	4.39	0.
YAW BEARING	-9.74	0.	4.36	0.	17.0	0.
TOWER 185	-10.5	0.	4.36	0.	34.5	0.
TOWER 117	-11.9	0.	4.36	0.	64.2	0.
TOWER 51	-13.6	0.	4.36	0.	93.0	0.
TOWER BASE	-15.4	0.	4.36	0.	115.	0.

TABLE L-2c

LIMIT LOADS DUE TO EXTREME WIND CONDITIONS
(130 MPH)
TOWER WIND PRESSURES

HEIGHT (FT)	V (MPH)	PRESSURE (LB/FT
0.	0.12294931E 03	0.29010523E 02
0.20000000E 02	0.12580250E 03	0.30372594E 02
0.40000000E 02	0.12686095E 03	0.30885827E 02
0.60000000E 02	0.12752764E 03	0.31211311E 02
0.80000000E 02	0.12801623E 03	0.31450922E 02
0.10000000E 03	0.12840239E 03	0.31640955E 02
0.12000000E 03	0.12872190E 03	0.31798617E 02
0.14000000E 03	0.12899451E 03	0.31933448E 02
0.16000000E 03	0.12923231E 03	0.32051295E 02
0.18000000E 03	0.12944324E 03	0.32156005E 02
0.20000000E 03	0.12963278E 03	0.32250247E 02
0.22000000E 03	0.12980491E 03	0.32335948E 02
0.24000000E 03	0.12996257E 03	0.32414544E 02

TO BE ADDED TO LOAD IN
TABLE L-2a or TABLE L-2b

TABLE L-3. CONTROL MALFUNCTION @ 60 MPH
(AILERONS IN POWER POSITION -0°)

INTERFACE	Vx lb	Vy	Vz	Mx ft-lb	My	Mz
BLADE .90R	.0355E6	-.095E5	-.345E6	-.0140E6	.417E6	-.107E6
.80R	.0948E6	-.163E5	-.720E6	-.0311E6	1.59E5	-.370E6
.70R	.215E6	-.181E5	-1.08E6	-.0403E6	3.71E6	-.805E6
.60R	.356E6	-.295E5	-1.38E6	-.0460E6	6.50E6	-1.30E6
.50R	.505E6	-.375E5	-1.68E6	-.0874E6	9.58E6	-1.97E6
.40R	.647E6	-.541E5	-1.95E6	-.155E6	13.3E6	-2.93E6
.30R	.774E6	-.732E5	-2.16E6	-.233E6	17.0E6	-4.25E6
.25R	.833E6	-.833E5	-2.25E6	-.271E6	19.0E6	-5.07E6
.20R	.889E6	-.950E5	-2.32E6	-.309E6	21.3E6	-6.02E6
.10R	.987E6	-1.21E5	-2.42E6	-.373E6	26.2E6	-8.30E6
0R	1.06E6	-1.65E5	-2.45E6	-.426E6	30.4E6	-11.1E6
TEETER BRGS.	2.97E5	3.30E5	-4.82E5	3.82E5	1.82E5	-4.72E6
ROTOR CL	-3.30E5	1.38E4	-4.80E5	3.88E5	4.70E5	-4.70E6
ROTOR/NACELLE	-6.17E5	7.57E3	-5.18E5	2.31E5	-5.06E6	-4.70E6
YAW BEARING	-1.26E6	1.28E4	-4.28E5	-7.72E5	-3.07E6	-4.73E6
TOWER 185	-1.34E6	1.38E4	-4.28E5	-7.72E5	14.0E6	-4.90E6
TOWER 117	-1.51E6	1.54E4	-4.27E5	-7.72E5	43.2E6	-5.30E6
TOWER 51	-1.71E6	1.59E4	-4.27E5	-7.72E5	71.4E6	-5.76E6
TOWER BASE	-1.91E6	1.60E4	-4.27E5	-7.72E5	93.1E6	-6.13E6

TABLE L-4. 99.99%'ILE GUST AT RATED (32-48 MPH) FOLLOWED BY DESYCHRONIZATION, 25% OVERSPEED, AND SHUTDOWN

INTERFACE	Vx	Vy	Vz	Mx	My	Mz
	lb				ft-lb	
BLADE .90R	.0504E6		.130E5	-.345E5	-.345E5	.410E6	.121E6
.80R	.147E6		.262E5	-.730E5	-.874E5	1.56E6	.533E6
.70R	.314E6		.435E5	-1.09E5	-1.48E5	3.30E6	1.29E6
.60R	.515E6		.624E5	-1.43E5	-1.85E5	5.70E6	2.44E6
.50R	.712E6		.695E5	-1.67E5	-2.02E5	8.70E6	3.91E6
.40R	.912E6		.840E5	-1.90E5	-2.14E5	12.0E6	5.56E6
.30R	1.09E6		.969E5	-2.08E5	-2.40E5	15.8E6	7.41E6
.25R	1.17E6		1.04E5	-2.15E5	-2.62E5	17.8E6	8.42E6
.20R	1.25E6		1.12E5	-2.22E5	-2.84E5	19.9E6	9.58E6
.10R	1.38E6		1.32E5	-2.34E5	-3.30E5	24.3E6	12.3E6
0R	1.46E6		1.78E5	-2.38E5	-3.80E5	29.0E6	15.6E6
TEETER BRGS.	±2.92E5		±3.42E5	-4.75E5	±4.27E5	±.214E6	-4.22E6
ROTOR CL	-2.75E5		±2.30E4	-4.73E5	±3.66E5	±.500E6	-4.29E6
ROTOR/NACELLE	-5.52E5		±2.96E4	-5.13E5	±3.29E5	-4.66E6	-4.29E6
YAW BEARING	-1.26E6		±5.58E4	-4.28E5	±8.92E5	-3.59E6	-4.31E6
TOWER 185	-1.34E6		±5.80E4	-4.29E5	±8.92E5	14.1E6	-4.48E6
TOWER 117	-1.51E6		±6.13E4	-4.30E5	±8.92E5	43.4E6	-4.86E6
TOWER 51	-1.71E6		±6.24E4	-4.30E5	±8.92E5	71.8E6	-8.06E6
TOWER BASE	-1.91E6		±6.26E4	-4.30E5	±8.92E5	93.8E6	-11.2E6

NOTES: Vy & Mz (of blade) are subsequent to feather.

Vz & My May have opposite sign & equal magnitudes as shown above for blade stations outboard of .60R.

TABLE L-5 CYCLOCONVERTER MISHAP

DRIVE TRAIN TORQUE-MZ = 5.87E6 FT-LB

- CAN OCCUR IN CONJUNCTION WITH ANY OTHER LOAD CONDITION EXCEPT HURRICANE (TABLE L-2)

- TO BE APPLIED AT INTERFACES BELOW
  - TEETER BEARING
  - ROTOR CENTERLINE
  - YAW BEARING
  - ALL TOWER

TABLE L-6 TEETER BRAKE APPLICATION

BRAKE MOMENT = ± 2.76E6 FT-LB

- o TO BE ADDED TO NORMAL OPERATING LOADS AT
  - BLADE ROOT My (1/2 LOAD PER BLADE)
  - TEETER BEARINGS My
  - ROTOR CENTER LINE Mx OR My
  - ROTOR/NACELLE Mx OR My
  - YAW BEARING My

- o NORMAL OPERATING LOADS TO BE USED WITH THE ABOVE ARE:

  AVE MEAN LOAD ± ROOT MEAN CUBED LOAD

  WHICH APPEAR IN TABLES H-1 THROUGH H-114.

ABBREVIATIONS

A	Amperes
AAO	average annual outage time
AASHTO	American Association of State Highway and Transportation Officials
ac	alternating current
ACI	American Concrete Institute
A/C	aircraft
AGMA	American Gear Manufacturers Association
AILSTAB	Aileron Stability Analysis
AISC	American Institute of Steel Construction
ASCE	American Society of Civil Engineers
ASCII	American Standard for Computer Information Interchange
ASTER	a computer program
ASTM	American Society for Testing Materials
AWG	American Wire Gauge
AWS	American Welding Society
baud	the rate of transmission of data from one part of computer to another
BESD	backup emergency shutdown
CBI	Chicago Bridge and Iron
CD	coefficient of drag
CDS	controls data system
CEC	control electronics cabinet
ccw	counterclockwise
cfm	cubic feet per minute
CGT	crack growth threshold
CI	cut-in
CIS	cycle intercept stress
CMD	command
COE	cost of energy
COV	coefficient of variation
CPU	central processing unit
CRT	cathode ray tube
CVN	Charpy V-notch test
dc	direct current
DOE	Department of Energy

ECL	Eptak control language
EHD	elastohydrodynamic
EMC	equivalent moisture content
ES	engineering instrumentation system
EPTAK	trade name for controller from Eagle Signal Division of Gulf and Western Industries
EMI	electromagnetic interference
ESD	emergency shutdown
FMEA	failure modes effects analysis
fpm	feet per minute
fpy	failures per year
FRP	glass fiber-reinforced plastic
ft.	feet
g	a unit of acceleration, equal to 32 ft/sec or 9.8 m/sec
G	giga, a prefix meaning one billion
gal.	gallons
GBI	Gougeon Brothers Incorporatedde
GETSS	GE Turbine System Analysis
GETSTAB	a computer program
gpm	gallons per minute
Hz.	Hertz
IITRI	Illinois Institute of Technology, Research Institute
I/O	input/output
in.	inch
ISM	input signal manager
k	kilo, a prefix meaning 1000
kips	a unit of force or weight, kilopounds, or 1000 pounds
ksi	a unit of stress, kips per square inch, or 1000 psi
kV	kiloVolts, or 1000 Volts
kW	kiloWatt or 1000 Watts
kWh	kiloWatt-hours, or 1000 Watt-hours
lbs.	pounds
lb/MDGL	pounds per 1000 square feet of double glue line
LEFM	linear elastic fracture mechanics
LMC	laminae moisture content
LVDT	linear variable differential transformer

m	milli, a prefix meaning .001
M	mega, a prefix meaning 1,000,000
mA	milliAmperes, or .001 of an Ampere
MC	moisture content
ml	milliliter
mpn	miles per hour
mps	meters per second
MTBF	mean time between failures
MTTR	mean time to repair
MS	structural margin of safety
m/sec	meters per second
mps	meters per second
MUX	multiplexer
MW	megaWatt, or one million Watts
MWA	megaWatt-Amperes, or a million Watt-Amperes
N	Newton, the unit of force in the metric system
NASA	National Aeronautics and Space Administration
NASTRAN	a computer program
NDT	Nil-ductility transition
NEMA	National Electrical Manufacturers Association
N-m	Newton-meter, the unit of moment in the metric system
NSD	normal shutdown
O&M	operating and maintenance
OIS	operational information system
OSM	output signal manager
P	per revolution
PCS	pitch change system
PGC	Philadelphia Gear Corporation
PSC	partial span control
PIR	progarm information report
PLV	pitch line velocity
ppm	parts per million
PROM	programmable read only memory
psf	pounds per square feet
psi	pounds per square inch
PWHT	post-weld heat treatment
QAERO	a computer program

R	ratio of actual stress to allowable stress, or minimum fatigue stress cycle to maximum fatigue stress cycle
rad/sec	radians per second
RAM	random access memory
RAM	reliability, availability, and maintainability
RFP	request for proposal
RMC	root mean cubed
ROM	read only memory
rpm	revolutions per minute
RT	room temperature
SCAMP	Stiffness Coupling Approach Modal-Synthesis Program
SCI	Structural Composites, Incorporated
SIM-5A	a computer code for control system analysis
S_{min}	minimum stress
S_{max}	maximum stress
S-N	stress vs. number of cycles
SOW	Statement of Work
STRAP	Static Row Analysis Program
ssu	Saybolt univeral seconds
TBD	to be determined
TBR	to be resolved
TFT	transverse filament tape
TRAC	Transient Rotor Analysis Code
tty	teletype
TVI	television interference
UBC	Uniform Building Code
UPS	uninterruptible power supply
UDRI	University of Dayton Research Institute
V	Volts
Vac	alternating voltage
Vdc	constant voltage
W	Watts
WEPO	Wind Energy Project Office
WTG	wind turbine generator
WT	weight
WINDLD	a computer program
WINDOPT	a computer program

1. Report No.	2. Government Accession No.	3. Recipient's Catalog No.
NASA CR-174735		

4. Title and Subtitle	5. Report Date
MOD-5A Wind Turbine Generator Program Design Report Volume II - Conceptual and Preliminary Design Book 2	August, 1984
	6. Performing Organization Code
7. Author(s)	8. Performing Organization Report No.
	10. Work Unit No.
9. Performing Organization Name and Address General Electric Company Advanced Energy Programs Department P.O. Box 527 King of Prussia, PA 19406	11. Contract or Grant No. DEN 3-153
	13. Type of Report and Period Covered Contractor Report
12. Sponsoring Agency Name and Address U.S. Department of Energy Conservation and Renewable Energy Division of Wind Energy Technology Washington, D.C. 20545	14. Sponsoring Agency Code DOE/NASA/0153-2

15. Supplementary Notes

Final report. Prepared under Interagency Agreement DE-AI01-79ET20305. Project Manager, T.P. Cahill, Wind Energy Project Office, NASA Lewis Research Center, Cleveland, Ohio 44135

16. Abstract

This report documents the design, development and analysis of the 7.3MW MOD-5A wind turbine generator covering work performed between July 1980 and June 1984. The report is divided into four volumes: Volume I summarizes the entire MOD-5A program, Volume II discusses the conceptual and preliminary design phases, Volume III describes the final design of the MOD-5A, and Volume IV contains the drawings and specifications developed for the final design.

In Volume II, Conceptual and Preliminary Design, the requirements and criteria for the design are presented. The conceptual design studies, which defined a baseline configuration and determined the weights, costs and sizes of each subsystem, are described. The development and optimization of the wind turbine generator are presented through the description of the ten intermediate configurations between the conceptual and final designs. The development tests, which determined or characterized many of the materials and components of the wind turbine generator, are described. Analyses of the system's loads and dynamics are presented.

17. Key Words (Suggested by Author(s))	18. Distribution Statement
Renewable energy; Wind energy Wind power; Variable speed generator Wind turbine design; Wind turbine system; Wood rotor blades; Large scale wind turbine	Unclassified - unlimited STAR Category - 44 DOE Category - UC-60

19. Security Classif. (of this report)	20. Security Classif. (of this page)	21. No. of pages	22. Price*
Unclassified	Unclassified		

*For sale by the National Technical Information Service, Springfield, Virginia 22161

1. Report No.	2. Government Accession No.	3. Recipient's Catalog No.
NASA CR-174735		

4. Title and Subtitle	5. Report Date
MOD-5A Wind Turbine Generator Program Design Report Volume II - Conceptual and Preliminary Design Book 2	August, 1984
	6. Performing Organization Code
7. Author(s)	8. Performing Organization Report No.
	10. Work Unit No.
9. Performing Organization Name and Address General Electric Company Advanced Energy Programs Department P.O. Box 527 King of Prussia, PA 19406	11. Contract or Grant No. DEN 3-153
	13. Type of Report and Period Covered Contractor Report
12. Sponsoring Agency Name and Address U.S. Department of Energy Conservation and Renewable Energy Division of Wind Energy Technology Washington, D.C. 20545	14. Sponsoring Agency Code DOE/NASA/0153-2

15. Supplementary Notes

Final report. Prepared under Interagency Agreement DE-AI01-79ET20305. Project Manager, T.P. Cahill, Wind Energy Project Office, NASA Lewis Research Center, Cleveland, Ohio 44135

16. Abstract

This report documents the design, development and analysis of the 7.3MW MOD-5A wind turbine generator covering work performed between July 1980 and June 1984. The report is divided into four volumes: Volume I summarizes the entire MOD-5A program, Volume II discusses the conceptual and preliminary design phases, Volume III describes the final design of the MOD-5A, and Volume IV contains the drawings and specifications developed for the final design.

In Volume II, Conceptual and Preliminary Design, the requirements and criteria for the design are presented. The conceptual design studies, which defined a baseline configuration and determined the weights, costs and sizes of each subsystem, are described. The development and optimization of the wind turbine generator are presented through the description of the ten intermediate configurations between the conceptual and final designs. The development tests, which determined or characterized many of the materials and components of the wind turbine generator, are described. Analyses of the system's loads and dynamics are presented.

17. Key Words (Suggested by Author(s))	18. Distribution Statement
Renewable energy; Wind energy Wind power; Variable speed generator Wind turbine design; Wind turbine system; Wood rotor blades; Large scale wind turbine	Unclassified - unlimited STAR Category - 44 DOE Category - UC-60

19. Security Classif. (of this report)	20. Security Classif. (of this page)	21. No. of pages	22. Price*
Unclassified	Unclassified		

*For sale by the National Technical Information Service, Springfield, Virginia 22161